Institute of High Current Electronics SB RAS
Tomsk Scientific Center SB RAS
National Research Tomsk Polytechnic University
Chongqing University of Arts and Sciences

7th International Congress on Energy Fluxes and Radiation Effects (EFRE-2020 online)

Abstracts

September 14–25, 2020

Tomsk, Russia

Tomsk
Publishing House of IAO SB RAS
2020

IEEE NPSS NUCLEAR & PLASMA SCIENCES SOCIETY

ISBN 978-5-94458-182-2

7th International Congress on Energy Fluxes and Radiation Effects (EFRE-2020 online): Abstracts. — Tomsk: Publishing House of IAO SB RAS, 2020. — 635 pp. 1 CD-ROM. – System requirements: PC Pentium 1 or higher; Acrobat Reader 4.0 or higher.

Signed to use June 5, 2020
Publishing House of IAO SB RAS, 634055, Tomsk, pl. Akademika Zueva, 1.
Phone: 8-3822-492384

This book comprises the abstracts of the reports (presentations) for the oral and poster sessions of VII International Congress on Energy Fluxes and Radiation Effects (EFRE-2020 online). Due to the unfavorable epidemiological situation associated with the COVID-19 pandemic, the Congress was held in a remote format using modern information technologies. The Congress incorporated together four international meetings: International Symposium on High-Current Electronics, International Conference on Modification of Materials with Particle Beams and Plasma Flows, International Conference on Radiation Physics and Chemistry of Condensed Matter, and International Conference on New Materials and High Technologies. It will be a good platform for researchers to discuss a wide range of scientific, engineering, and technical problems in the fields of pulsed power technologies; ion and electron beams; high power microwaves; plasma and particle beam sources; modification of material properties; pulsed power applications in chemistry, biology, and medicine; physical and chemical nonlinear processes excited in inorganic dielectrics by particle and photon beams; physical principles of radiation-related and additive technologies; self-propagating high-temperature synthesis; and combustion waves in heterogeneous systems.

OC Microsoft Windows; Adobe Acrobat.
Published in author's version.
Composed by Valery Shklyaev and Pavel Kiziridi

General Chairman of the Congress

Gennady Mesyats
Russian Academy of Sciences

Co-Chairmen of the Congress

Nikolay Ratakhin
Institute of High Current Electronics SB RAS
Andrey Yakovlev
National Research Tomsk Polytechnic University

Local Organizing Committee

Chairman

Dr. Maxim Vorobyov	Institute of High Current Electronics SB RAS, Tomsk, Russia

Co-Chairman

Valery Shklyaev	Institute of High Current Electronics SB RAS, Tomsk, Russia
E. Petrikova	Institute of High Current Electronics SB RAS, Tomsk, Russia
Yu. Akhmadeev	Institute of High Current Electronics SB RAS, Tomsk, Russia
L. Avdeeva	Institute of High Current Electronics SB RAS, Tomsk, Russia
A. Batrakov	Institute of High Current Electronics SB RAS, Tomsk, Russia
G. Bleikher	National Research Tomsk Polytechnic University, Tomsk, Russia
E. Chudinova	Institute of High Current Electronics SB RAS, Tomsk, Russia
E. Dubrovskaya	Institute of High Current Electronics SB RAS, Tomsk, Russia
I. Egorov	National Research Tomsk Polytechnic University, Tomsk, Russia
V. Frolova	Institute of High Current Electronics SB RAS, Tomsk, Russia
D. Genin	Institute of High Current Electronics SB RAS, Tomsk, Russia
O. Ivanova	National Research Tomsk Polytechnic University, Tomsk, Russia
P. Kiziridi	Institute of High Current Electronics SB RAS, Tomsk, Russia
K. Kostikov	National Research Tomsk Polytechnic University, Tomsk, Russia
N. Labetskaya	Institute of High Current Electronics SB RAS, Tomsk, Russia
A. Maznoy	National Research Tomsk Polytechnic University, Tomsk, Russia
O. Nozdrina	National Research Tomsk Polytechnic University, Tomsk, Russia
S. Onischenko	Institute of High Current Electronics SB RAS, Tomsk, Russia
I. Pegel	Institute of High Current Electronics SB RAS, Tomsk, Russia
N. Prokopenko	Institute of High Current Electronics SB RAS, Tomsk, Russia
A. Schneider	Institute of High Current Electronics SB RAS, Tomsk, Russia
A. Shipilova	Institute of High Current Electronics SB RAS, Tomsk, Russia
D. Sorokin	Institute of High Current Electronics SB RAS, Tomsk, Russia
M. Zaytseva	National Research Tomsk Polytechnic University, Tomsk, Russia

Conferences

21st International Symposium on High-Current Electronics
15th International Conference on Modification of Materials with Particle Beams and Plasma Flows
19th International Conference on Radiation Physics and Chemistry of Condensed Matter
4th International Conference on New Materials and High Technologies

RFBR RUSSIAN FOUNDATION FOR BASIC RESEARCH

CONTENTS

EFRE-2020 online
Plenary Lectures

ON THE NATURE OF NANOSECOND DIFFUSION-CHANNEL DISCHARGES IN AIR[1]

G. A. Mesyats

P.N.Lebedev Physical Institute of the Russian Academy of Sciences, Moscow, Russia

When a single-electron-initiated discharge operates in a gap with a uniform electric field under high (double, triple, or more severe) overvoltage, a diffuse (volume) glow pierced by several plasma channels is observed [1–6]. This occurs on the nanosecond scale in gaps of millimeter and smaller spacing. The discharge pattern indicates that it exhibits simultaneously the features of Townsend and streamer discharges. There is still no complete understanding of the phenomena occurring in discharges of this type; so, let us see what happens in them.

The surface of a metal cathode always contains microprotrusions at the tips of which there occurs an enhancement of the electric field. These tips are sites at which electron avalanches are initiated. As the drift velocity of electrons is many times greater than the velocity of their diffusion front, an electron avalanche develops at a plasma tip whose radius is much smaller than its length. This results in a tenfold enhancement of the electric field in the avalanche head, which suffices for the generation of runaway electrons and the initiation of x-ray emission from the anode. Let us consider how discharge channels are formed and why a diffuse glow appears between the cathode and the anode.

An electron avalanche, having developed to a critical size, transforms into a streamer. For a nanosecond diffusion-channel discharge, this transformation process is very peculiar. For instance, a classical avalanche (which develops in air at atmospheric pressure in a centimeter gap overvolted by no more than 10%) contains 10^8 electrons, whereas an avalanche developing at atmospheric air pressure in a nanosecond diffusion-channel discharge contains 10^6 electrons even when the electric-field-to-pressure ration is equal to or greater than 150 V/(cm·Torr). The critical avalanche length in such a discharge is $14\cdot10^{-3}$ cm; that is, in a 0.2-cm discharge gap, almost 15 avalanches of critical size fit along the gap spacing. That is why the avalanche-to-streamer transition occurs at the cathode rather than in the anode region. The electron density in an avalanche transforming into a streamer is of the order of 10^{14} cm^{-3}. Such a streamer, reaching the anode, forms a plasma column with very low conductivity. As the streamer develops, it emits runaway electrons, just like an avalanche, due to the high electric field at its tip.

The runaway electrons and x-rays ionize the gas, that is, produce a plasma and excite the gas molecules. This makes the discharge diffuse in structure. The plasma plays a supporting part. It is a source of seed electrons initiating an auxiliary discharge, which is similar to a multielectron-initiated nanosecond volume discharge. An indication of this similarity is that the maximum rate of current rise is nearly the same for nanosecond diffuse-channel and classical multielectron-initiated discharges. This is an indisputable fact in the physics of nanosecond pulsed discharges in gases.

While the auxiliary discharge is developing, there occurs a redistribution of the electric field in the gap with its sharp increase at the cathode. This leads to an increase in the field emission current from the cathode microprotrusions, initiation of explosive electron emission, and formation of a cathode spot [7, 8]. In essence, this is a process similar to the transition of an anomalous glow discharge to an arc.

REFERENCES

[1] G. A. Mesyats, Study on the Generation of Nanosecond High-Power Pulses, D. Sci. Thesis, Tomsk, 1966 (in Russian).

[2] G. A. Mesyats and Yu. I. Bychkov, "Statistical investigation of the delay in breakdown of short gas gaps with superhigh electric fields on the nanosecond scale", Zh. Tekh. Fiz., vol. 37, p. 1712, 1967.

[3] G. A. Mesyats, Yu. I. Bychkov, and A. M. Iskoldskii, "The formation time of a discharge in a short air gap on the nanosecond scale ", Zh. Tekh. Fiz., vol. 38, p. 1281, 1968.

[4] G. A. Mesyats, Yu. I. Bychkov, and V. V. Kremnev, "Nanosecond pulsed electrical discharges in gases ", Usp. Fiz. Nauk , vol. 107, p. 201, 1972.

[5] Yu. D. Korolev and G. A. Mesyats, Field Emission and Explosive Processes in Gas Discharges, Nauka, Novosibirsk,1982 (in Russian).

[6] Yu. D. Korolev and G. A. Mesyats, Physics of Pulsed Breakdown of Gases, Nauka, Moscow, 1991 (in Russian).

[7] G. A. Mesyats, Pulsed Power, Kluwer Academic/Plenum, New York, 2004.

[8] G. A. Mesyats, Explosive Electron Emission, Fizmatlit, Moscow, 2011 (in Russian).

[1] This work was supported in part by the Russian Science Foundation (project No. 19-79-30086).

COMPUTER MODELLING OF RADIATION-INDUCED PROCESSES IN OXIDE SOLIDS

E.A. KOTOMIN, V.N. KUZOVKOV, A.I. POPOV, D. GRYAZNOV, A. PLATONENKO

Institute of Solid State Physics, University of Latvia, Riga, Latvia

The radiation-resistant oxide insulators (Al_2O_3, $Y_3Al_5O_{12}$, $MgAl_2O_4$) are important materials for application in fusion reactors, e.g. as optical windows. It is very important to predict/simulate a long-time defect structure evolution including thermal defect annealing after irradiation. For further prediction of the radiation stability of materials, it is also necessary to determine main kinetic parameters - interstitial migration energy E_a and diffusion pre-exponent D_0.

In this talk, we discuss the latest results of the defect computer simulations combining the first principles calculation of the atomic, electronic, magnetic structure and optical properties of defective oxides with the kinetics of defect recombination upon annealing. Primary radiation defects in ionic solids consist of Frenkel defects—pairs of anion vacancies with trapped electrons (F-type centers) and interstitial ions. Their thermal annealing is controlled by the interstitial ion migration, whose mobility is much higher than that of the F centers. The basic theory (how to extract from experimental data the migration energy of interstitials and pre-exponential factor of diffusion) was developed and applied to irradiated insulators in our recent study [1,2]. It was showed that the correlation of these two parameters in strongly irradiated oxides satisfies the so-called Meyer–Neldel rule (MNR) [2] observed more than once earlier in glasses, liquids, and disordered materials, but not in radiation physics.

We performed large scale computer calculations of basic defects and analyzed available experimental kinetics of the F-type electronic and V-type hole center annealing for three different ionic solids: neutron/ion-irradiated Al_2O_3 (sapphire) [1-3], ion-irradiated $Y_3Al_5O_{12}$ (YAG) [4,5] and $MgAl_2O_4$ spinel [6] -- all three wide gap insulating materials but with different crystalline structures. We demonstrated that in sapphire upon an increase of radiation fluence, both the migration energy and pre-exponent are decreasing, irrespective of the type of irradiation. This is MNR with normal dose dependence. For YAG and spinel we have confirmed MNR, but the dose dependence is inverse. We discuss the cause of this phenomenon.

Thus, in this study, we demonstrated that the dependence of defect migration parameters on the radiation fluence plays an important role in the quantitative analysis of the radiation damage of real materials and should not be neglected.

REFERENCES

[1] V.Kuzovkov, E.Kotomin, A.Popov, R.Villa, Nucl. Inst. Meth. B 374, 107 (2016).

[2] E.Kotomin, V.Kuzovkov, A.Popov, J.Maier, R.Vila, J.Phys.Chem.A, 22, 28 (2018).

[3] A. Platonenko, D. Gryaznov, Yu. Zhukovskii, E.A. Kotomin, Nucl. Inst. Meth. B 435, 74 (2018).

[4] A. Lushchik et al, Scientific Reports (2020), in press

[5] M. Izerrouken, A. Meftah, M. Nekkab, Nucl. Instr. Meth. B 258, 395 (2007).

[6] A.Platonenko, D.Gryaznov, Yu. Zhukovskii, E.A. Kotomin, Phys Stat Sol B 256, 1800282 (2019)

ENERGY AND MOMENTUM FLUXES IN PLASMA PROCESSING

H. KERSTEN, T. TROTTENBERG, A. SPETHMANN, M. KLETTE, L. HANSEN

[1]*Institute for Experimental and Applied Physics, Kiel University, Kiel, Germany*

For an optimization of plasma-based processes as thin film deposition, suitable diagnostics are required. In addition to well-established plasma diagnostic methods (e.g. optical emission spectroscopy, mass spectrometry, Langmuir probes, etc.) we perform examples of “non-conventional” low-cost diagnostics, which are applicable in technological plasma processes. Examples are the determination of energy fluxes by calorimetric probes [1,2] and the measurement of momentum transfer due to sputtered particles or changes of plasma pressure by force probes [3,4].

The total energy influx from the plasma to a substrate can be measured by special calorimetric sensors [1]. One method is the passive thermal probe (PTP) [2] based on the determination of the temporal slope of the substrate surface temperature (heating, cooling) in the course of the plasma process. By knowing the calibrated heat capacity of the sensor, the difference of the time derivatives yields the integral energy influx to the surface. Simultaneously, the electrical current to the substrate can be obtained and by variation of the bias voltage the energetic contribution of charge carriers can be determined. By comparison with model assumptions on the involved plasma-surface mechanisms the different energetic contributions to the total energy influx can be separated.

Furthermore, for thin film deposition by sputtering it is essential to determine the sputtering yield as well as the angular distribution of sputtered atoms. In addition to model calculations (TRIM, TRIDYN etc.), an experimental determination of the related quantities is highly demanded. For this purpose, we developed an interferometric force probe [3]. Such a quite sensitive probe bends a few µm due to momentum transfer by the bombarding and released particles, i.e. sputtered target atoms and recoiled ions [4]. By knowing the material properties of the cantilever and by measuring its deflection, the transferred momentum, e.g. the force in µN range, can be determined experimentally. In the present study, measurements are compared with TRIM simulations for different experimental discharge conditions.

[1] Kersten, H., Deutsch, H., Steffen, H., Kroesen G.M.W., Hippler, R., “The energy balance at substrates during plasma processing”, Vacuum, 63, 385-431, 2001.

[2] Gauter, S., Haase, F., Kersten, H., “Experimental unraveling the energy flux originating from a DC magnetron sputtering source”, Thin Solid Films, 669, 8-18, 2019.

[3] Trottenberg, T., Spethmann, A., Kersten, H., “An interferometric force probe for beam diagnostics and the study of sputtering”, Eur. Phys. J. TI, 5, 3, 2018.

[4] Klette, M., Maas, M., Trottenberg, T., Kersten, H., „Directionally resolved measurements of momentum transport in sputter plumes as a critical test for simulations”, J. Vac. Sci. Technol. A, 38, 033013, 2020.

OPTICAL DIAGNOSTICS OF VACUUM ARC DISCHARGES FOR SWITCHING APPLICATIONS

S. GORTSCHAKOW

Leibniz Institute for Plasma Science and Technology, Greifswald, Germany

Vacuum switching devices provides environmentally compatible and emission-free solutions for power grids. A high number of operations under standard load conditions, safe and reproducible short-circuit current interruption capability, and maintenance-free operation are few examples of advantages of vacuum interrupters. Further development of such devices requires fundamental knowledge about the switching process and interaction of materials used with the working medium – the vacuum arc plasma. The optical diagnostics offers numerous methods for the characterization of the arc plasma and surrounding components, like e.g. electrodes and chamber walls. Studies of plasma and electrode phenomena by combination of optical and electrical diagnostics allow for material qualification, choice of design and arc extinguishing control methods.

The contribution gives an overview over optical diagnostics methods, which are used for determination of such important parameters as arc plasma temperature, anode surface temperature, densities of plasma species during the current pulse and after current termination. Especially, the influence of the anode activity (various high-current anode modes) on the properties of vacuum arc plasma has been studied. The vacuum arcs have been investigated under typical switching conditions - ignition by CuCr contact separation during the AC current flow at several kA magnitude. High-speed cinematography was used for observation of arc dynamics and characterization of the anode activity. Optical emission spectroscopy (imaging and high-speed) has been applied for determination of temporal dynamics of copper spectral lines from various plasma species – atoms, single and double charged ions during the active phase, as well as for determination of plasma temperature and electron density. Several methods have been used at the experimental facility (Fig. 1) for quantitative characterization of the anode surface temperature: NIR spectroscopy, pyrometry and high-speed camera techniques enhanced by narrow-band filters. Advantages and drawbacks of each method will be discussed. The temporal evolution of the surface temperature for different anode modes will be analysed. Broad band absorption spectroscopy is a suitable techniques for determination of the vapour density close to the current zero crossing and in the early post-arc phase. The temporal evolution of the Cr ground state density will be presented and discussed.

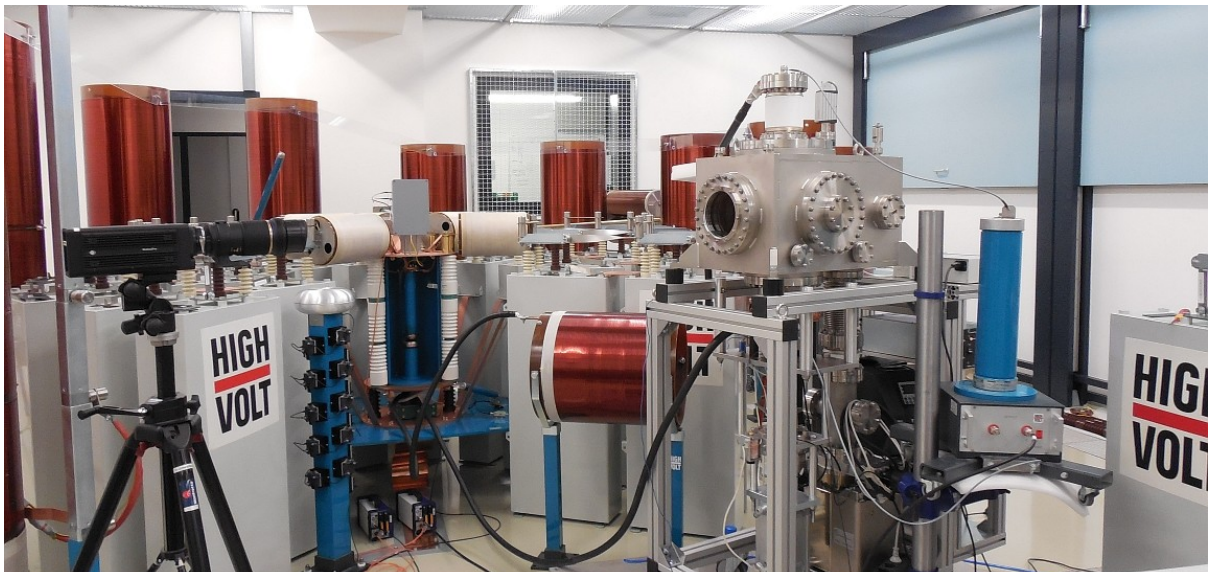

Fig. 1. Experimental facility for studying interruption of high current is vacuum.

21st International Symposium on High-Current Electronics

Chairman	Nikolay Ratakhin,	Institute of High Current Electronics, Tomsk, Russia
Co-Chairman	Gennady Remnev,	National Research Tomsk Polytechnic University, Tomsk, Russia
Program Chairman	Alexander Batrakov,	Institute of High Current Electronics, Tomsk, Russia
Program Co-Chairman	Gennady Remnev,	National Research Tomsk Polytechnic University, Tomsk, Russia

Program Committee

Efim OKS	Institute of High Current Electronics SB RAS, Tomsk, Russia
Alexander SHISHLOV	Institute of High Current Electronics SB RAS, Tomsk, Russia
Vladimir KOSHELEV	Institute of High Current Electronics SB RAS, Tomsk, Russia
Eduard ABDULLIN	Institute of High Current Electronics SB RAS, Tomsk, Russia
Gennady REMNEV	National Research Tomsk Polytechnic University, Tomsk, Russia
Victor TARASENKO	Institute of High Current Electronics SB RAS, Tomsk, Russia
Igor PEGEL	Institute of High Current Electronics SB RAS, Tomsk, Russia

International Advisory Committee

Stanislav CHAYKOVSKY	Institute of Electrophysics UB RAS, Ekaterinburg, Russia
Vasily GLUKHIKH	D.V. Efremov Scientific Research Institute of Electrophysical Apparatus, St. Petersburg, Russia
Evgenij GRABOVSKI	Troitsk Institute for Innovation and Fusion Research (TRINITI), Russia
Alexander KIM	Institute of High Current Electronics SB RAS, Tomsk, Russia
Francis LASSALLE	Centre d'Etudes de Gramat, Gramat, France
Alexander LITVAK	Institute of Applied Physics RAS, Nizhny Novgorod, Russia
Pavel LOGATCHOV	Institute of Nuclear Physics, Novosibirsk, Russia
Efim OKS	Institute of High Current Electronics SB RAS, Tomsk, Russia
Mikhail PETELIN	Institute of Applied Physics RAS, Nizhniy Novgorod, Russia
Nikolai RATAKHIN	Institute of High Current Electronics SB RAS, Tomsk, Russia
Vladislav ROSTOV	Institute of High Current Electronics SB RAS, Tomsk, Russia
Sergey RUKIN	Institute of Electrophysics UB RAS, Ekaterinburg, Russia
Marek SADOWSKI	Soltan Institute for Nuclear Studies, Warsaw, Poland
Victor SELEMIR	All-Russian Research Institute of Experimental Physics, FSUE RFNC – VNIIEF, Sarov, Russia
Edl SCHAMILOGLU	University of New Mexico, Albuquerque, USA
Valentin SMIRNOV	National Research Institute "Kurchatov Institute", Moscow, Russia
Valery SHPAK	Institute of Electrophysics UB RAS, Ekaterinburg, Russia
Victor TARASENKO	Institute of High Current Electronics SB RAS, Tomsk, Russia
Vasily USHAKOV	National Research Tomsk Polytechnic University, Tomsk, Russia
Yuriy USOV	National Research Tomsk Polytechnic University, Institute of Nuclear Physics, Tomsk, Russia
Mikhail YALANDIN	Institute of Electrophysics UB RAS, Ekaterinburg, Russia
Yuriy YUSHKOV	National Research Tomsk Polytechnic University, Tomsk, Russia

Symposium topics

Intense electron and ion beams
Pinches, plasma focus and capillary discharge
High power microwaves
Pulsed power technology
Pulsed power applications
Discharges with runaway electrons
Numerical simulation in high current electronics

Financial support by Russian Foundation for Basic Research (RFBR): № 20-08-22011

REGISTRATION OF ELECTRON AND X-RAY RADIATION SUBNANOSECOND PULSES

S.L.ELYASH[1], T.V.LOYKO[1], A.L.YURIEV[1], A.A.SELEZNEV[1]

[1]Russian Federal Nuclear Center–All-Russian Research Institute of Experimental Physics, Sarov, Russian Federation

To determine time resolution of nanosecond detectors of electron and X-ray pulses, to certify and operability control of measuring lines there was developed in RFNC-VNIIEF a sub-nanosecond accelerator of electrons with a gas-filled shaper [1].

For pulse registration there was applied a broadband registering channel involving a cable communication line (cable RK-50-4-21 ~5 meters long, cable RK-50-2-22 ~ 0.1 meter long) and a splitting capacitor - ceramic chip-capacitor (0.01 μF, 2 kV). There were preliminarily measured transient characteristics of the cable and X-radiation registration channel with the aid of oscilloscope calibrator Fluke 9500 V with various voltage pulses in the form of "a step" the rise time being (25±4) ps and (70±15) ps. The resolution time of cable RK-50-4-21 (length ~ 5 m) constituted ~ 50 ps, while that of the X-radiation registering channel was as long as ~110 ps.

To register the current pulse shape there was used a monitor with a coaxial collector 3 mm in diameter. The resolution of the similar device presented in paper [2] is ~ 22 ps. The signal was sent over cable RK-50-4-21 5 meters long and registered by an oscilloscope (passband – 5 GHz). The typical oscillogram of the electron beam current pulse is available in Fig.1. The duration of the registered electron current pulse at the amplitude half-height lies in the range (240…270) ps.

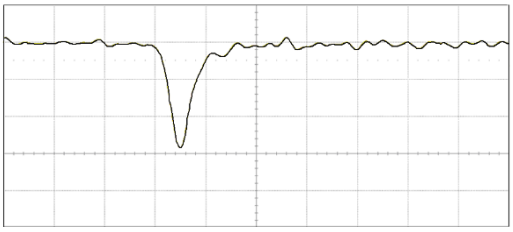

Fig.1. Oscillogram of electron beam current (scan – 0.5 ns per a cell).

The electron beam current was measured with the aid of a current-sensor consisting of a collector in the form of a disc 12 mm in diameter and low-inductance coaxial shunt assembled of high-frequency chip resistors connected in parallel. The value of the electron beam current constituted ~1.5 kA.

The maximal energy of electrons was determined using a method of absorbing filters with the aid of a compact device aimed at prompt measurement of electron energy [3] that was arranged on the output window of the tube. The maximal energy of electrons was as high as ~0.95 MeV. In the mode of X-raying (on the output window of the tube there was located an external target in the form of tantalum foil 50 μm thick and aluminum filter 2 mm thick) there were determined pulse characteristics of X-ray semiconductor detectors SPPD29k and SPPD29-02 [4] that constituted $\tau_{0.5} \approx (320\pm 30)$ ps and $\tau_{0..5} \approx (450\pm30)$ ps correspondingly.

REFERENCES

[1] A.L.Yuriev, S.L.Ehlyash, T.V.Lojko, S.P.Pukhov, D.P.Nikolaev, A.A.Seleznev.// PTEh. 2017, No.6, p.78

[2] Ye.V.Balzovski, D.V.Rybka, V.F. Tarasenko// PTEh.2015, No.5, .P.62.

[3] A.L.Yuriev, S.L.Ehlyash, T.V.Lojko, S.P.Pukhov.// PTEh.2013, No.3, P.87.

[4] A.I.Polyakov. Patent No 213765 RF. Class H01121/02//BI.1998.No3.

PLASMA GRID CATHODE BASED ON ARC DISCHARGE IN A MAGNETIC FIELD FOR GENERATION ELECTRON BEAM OF VARIABLE DIAMETER *

V.N. DEVYATKOV, N.N. KOVAL

Institute of High Current Electronics SB RAS, Tomsk, Russia

The results of the modernization of an electron source with a plasma grid cathode based on a pulsed contracted low-pressure arc discharge burning through a channel with a diameter of 10 mm [1] are presented. The discharge system functions at its partially immersion in an inhomogeneous longitudinal magnetic field with a magnitude of up to (0.01-0.03) T. A feature of the gas-discharge system of plasma cathode is that the discharge current flows around an additional plasma-redistributing electrode of large diameter (70 mm). In the plasma cathode, azimuthally uniform generation of emission plasma was achieved near the emission grid with a diameter of 85 mm. An electron source with presented plasma cathode is capable to generate a pulsed (20–200 μs) electron beam with an electron energy (5–25) keV and a beam current amplitude (50–500) A. A method has been implemented to control the distribution of current density over the beam cross section based on the influence of a magnetic field on the mode of discharge burning in a plasma cathode with an additional electrode redistributing of the emission plasma. It is shown that after transporting a dense low-energy beam to a distance of 350 mm, it is possible to obtain a beam diameter of 20–55 mm controlled by a value of magnetic induction with an inhomogeneous distribution of energy over the beam cross section not more than ± (5–10)%. It is possible to obtain a more compressed (up to a diameter of 10-15 mm) electron beam with some deterioration in the uniformity of the distribution of current density over its cross section. The beam diameter is changed by changing the value of magnetic induction of two solenoids without changing the electrode system of the electron source.

The developed plasma grid cathode and the investigated modes of its operation can be used in electronic sources forming an intense low-energy electron beam, promising for use in the nanostructuring of the surface of materials and products in order to improve their consumer and operational properties.

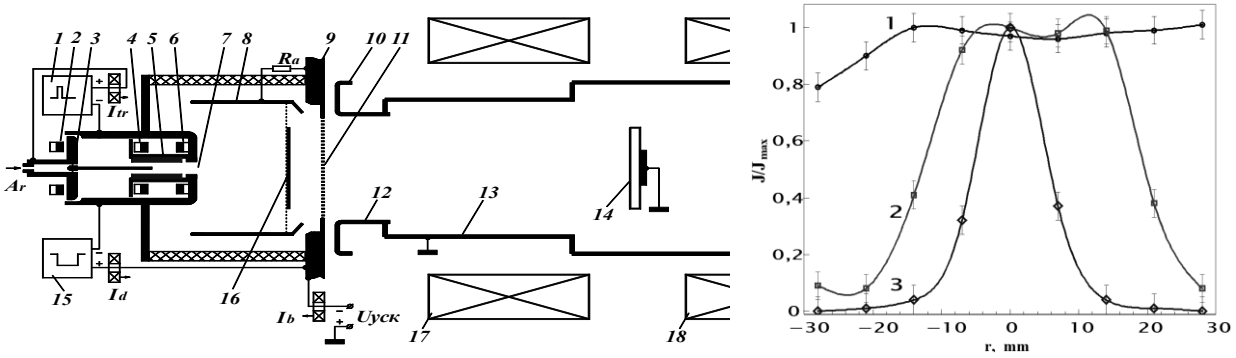

Fig.1. Scheme of the electron source and relative distributions of the energy density J/J_{max} over the cross section of the electron beam in the mode of a homogeneous (1, 2) and maximum compressed (3) beam. *1,15* – discharge power supplies, *2,4,6* – ring magnets, 3 – anode of triggering discharge, 5 – Mg-cathode, *8* – anode insert, *9* – anode electrode, *10* – accelerating electrode, *11* – emission grid, *12,13* – drift tubes, *14* – collector, 16 – additional electrode, *17,18* – solenoids.

REFERENCES

[1] V.N. Devyatkov, N.N. Koval, "Profile formation of emission current of grid plasma cathode in a longitudinal magnetic field", Journal of Physics: Conference Series, 2019. 1393 012040.

* The work was supported by the RFBR (project № 19-08-00248)

LARGE-AREA LOW-ENERGY ELECTRON ACCELERATORS

S.L. KOSOGOROV

NIIEFA JSC, Saint Petersburg, Russia

Large-area low-energy electron accelerators with an energy of 100 - 300 keV and beam extraction to the air or another medium for facilities intended for ionization of powerful gas lasers are applied mainly. The energy complexes based on both pulsed and continuous electro-ionization lasers developed in the USSR has stimulated the development of this class of accelerators. Using of accelerators with axial beam scanning over a large area turned out to be ineffective, since it is necessary to expose simultaneously the entire volume of active medium up to several thousand square centimeter in area, besides, they should have a high average current density of extracted electron beam and a high uniformity of current density over the cross-section

Large-area low-energy electron accelerators are applied

- for preionization in powerful electro-ionization lasers;
- for various industrial and ecological technologies:
  - solidification of polymer coatings on different materials;
  - irradiation of fungous and biological materials to obtain new properties;
  - plasma-chemical processes;
  - gas purification;
  - other applications.

A number of accelerators based on filaments and high-voltage glow discharge with a cold cathode have been developed, manufactured and delivered to customers. Besides, the basis for their calculation and design has been developed for special technological and scientific applications.

- Accelerating voltage 100 – 300 kV
- Beam power in vacuum up 80 kW
- Electron beam area up to 6600 cm^2
- Density of extracted electron beam:
  - pulse-periodic mode up to 10 mA/cm^2
  - continuous mode up to 100 $\mu A/cm^2$
  - nonuniformity of current density distribution over extracted beam cross-section ± 10%

ELECTRON ACCELERATOR BASED ON ION-ELECTRON EMISSION FOR GENERATION OF A WIDE-APERTURE BEAM*

S.YU. DOROSHKEVICH[1], N.N. KOVAL[1], M.S. VOROBYOV[1], S.A. SULAKSHIN[1], A.A. EKAVYAN[2], A.V. CHISTYAKOV[2]
[1] HCEI SB RAS, Academichesky av 2/3., Tomsk, 634055, Russia, E-mail: doroshkevich096@gmail.com, phone:8(382-2)-492-683
[2] LLC "Manolium-processing", Abelmanovskaya str., str. num. 2a, build. 1, Moscow, 109147, Russia

The report reviewed the operating principle, design, and basic parameters of an electron accelerator based on ion-electron emission. Such accelerators have the following advantages: relative design simplicity, lack of heating elements, high durability and stability, moderate requirements for the pump group, control of the beam current without changing the accelerating voltage. Wide-aperture electron accelerators based on ion-electron emission can be used to pump gas lasers, carrying out plasma-chemical processes, radiation technologies, heat treatment of materials, etc.[1-2].

Design of the accelerator (Fig.1) includes two main areas: the area of auxiliary discharge generation to create anode plasma and the area of the main non-self-contained high-voltage glow discharge. The boundary between these areas is set using the anode grid, the configuration of cells in which repeats the configuration of cells in the supporting grid of output foil window. The role of the auxiliary discharge is played by an self-sustained glow discharge, in which two tungsten wires are the anode and walls of vacuum chamber are the cathode. The plasma boundary of the auxiliary discharge is stabilized by the anode grid. Ions extracted from the plasma of auxiliary discharge through cells in the anode grid are accelerated in the accelerating gap and bombard the high-voltage cathode of the main discharge. Some ions are neutralized in the high-voltage gap, and in this case, the cathode is bombarded by neutrals having a wide energy spectrum. As a result of such bombardment, electrons are produced that are also accelerated in the accelerating gap and, passing through the cells of anode and support grids, are output into the ambient atmosphere.

The accelerator allows generating a wide (400 × 650 mm) continuous direct-acting electron beam (not scanning) and outputs it into the ambient atmosphere through an output window covered by a 30-μm thick AMg-2n alloy foil. Beam parameters: electron energy up to 150 keV, beam current up to 50 mA. The main characteristics of such an accelerator, the current-voltage characteristics of auxiliary and main discharges are given.

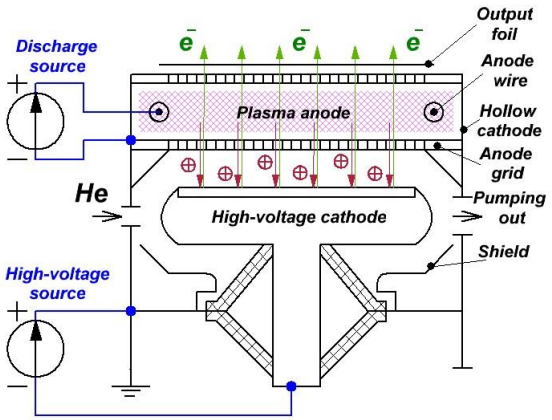

Fig.1. Principle scheme of the electron accelerator based on ion-electron emission.

REFERENCES

[1] Bugaev S P, Kreindel Yu E, Schanin P M 1984 Large section electron beams (Moscow, EAI) 112 pp. (in Russian)

[2] W.M. Clark, G.J. Dunning "A long pulse high-current gun for e-beam sustained eximer lasres", IEEE Journal of quantum electronics, vol. qe-14, no. 2, pp. 126–129, February 1978

* The work was supported by the grant of President of Russian Federation (Projects No MK-123.2019.2).

EVIDENCE OF EXPLOSIVE PROCESSES IN THE PARAMETERS OF A LOW-CURRENT VACUUM ARC*

I.L.MUZYUKIN[1,2]

[1] *Institute of Electrophysics UB RAS, 106 Amundsena Str., Ekaterinburg, 620016, Russia*
[2]*Institute of Physics and Technology Ural Federal University, 19 Mira Str., Ekaterinburg, 620002, Russia*

Complex measurements of several parameters of the low current vacuum arc were conducted. The currents applied in the experiments were close to the threshold values, so only one cathode spot cell burned. The time dependence of discharge current, arc voltage, ion current, and light intensity were stored with nanosecond time resolution. To achieve the time resolution less than 10ns small-sized ion collector was placed near the cathode surface at the distance of 200mkm. It was revealed, that the wavelet spectra of the ion current signal have several local maxima, corresponding to estimated cathode spot lifetime. When discharge current is significantly higher than threshold one the ion current local peaks correspond to arc current fall and cathode spot light flashes.

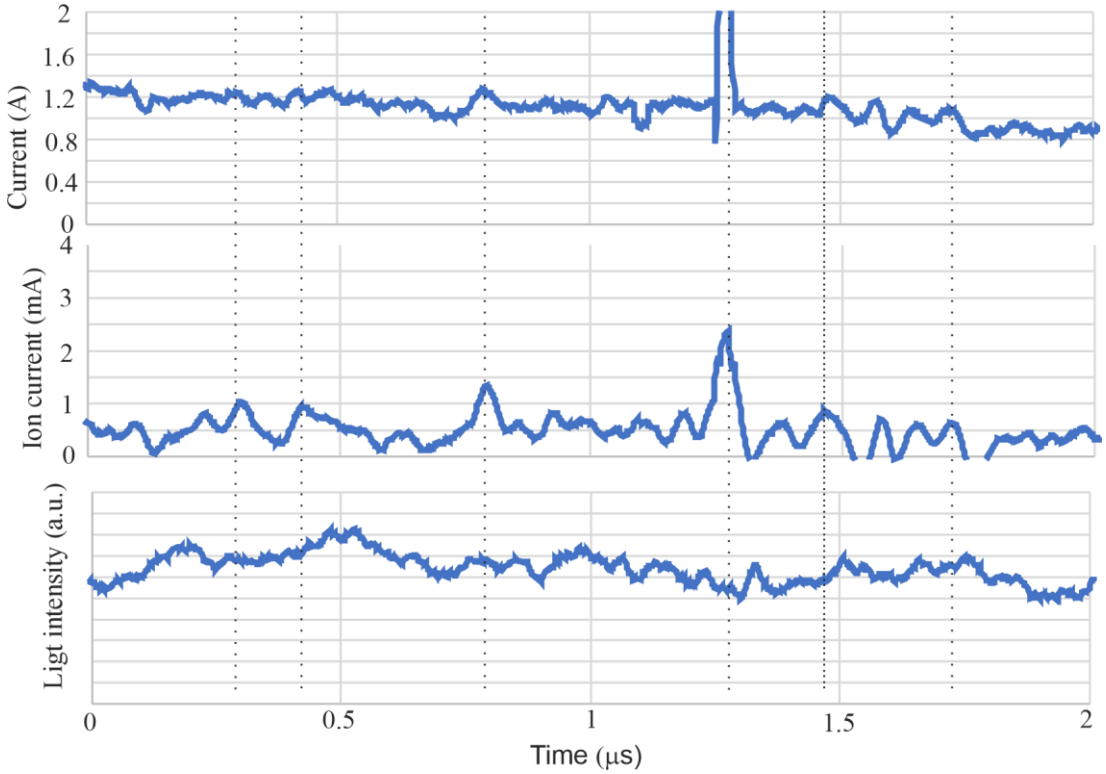

Fig.1. The waveforms fragment of vacuum arc parameters at threshold current. The ion current can be presented as a sequence of local peaks. These peaks correspond to local peaks of discharge current and ones of own glow of plasma.

When the arc current approaches the threshold one the ion current and plasma luminescence become significantly unstable. In this case, ion current can be described as a sequence of short (20-60ns) pulses. These pulses usually correspond to local peaks in arc discharge current. The plasma luminescence also contains short peaks, but it is hard to reveal a strong correlation between these peaks and peaks in discharge and ion currents.

* The work was supported in part by RFBR Grant Nos. 18-08-00547, 19-08-00783, 19-58-53006 .

ION FLOW PARAMETERS OF A HIGH-CURRENT PULSED VACUUM ARC*

I.L. MUZYUKIN[1,2], P.S. MIKHAILOV[1], S.A. CHAIKOVSKY[1], I.V. UIMANOV[1], D.L. SHMELEV[1], YU.A. ZEMSKOV[1]

[1]*Institute of Electrophysics of the Ural Division of the Russian Academy of Sciences, Amundsen 106, Ekaterinburg, Russia*
[2]*Institute of Physics and Technology, Ural Federal University, 21 Mira Str., Ekaterinburg, Russia*

The pulsed vacuum discharge is seriously investigated during a long period of time [1]. It can be a source of multiply charged plasma. The main objective of this paper is to investigate plasma ion flow generated by high-current pulsed vacuum arc, its, angular and temporal parameters.

Spatial distribution

Two types of electrode design were used: «open» and «closed». «Closed» is a kind of plasma gun. It consisted of the cylinder cathode that was inserted into the insulator and pressed against the anode. Anode was made in the shape of a hollow cylinder with an outlet of 2 mm and a length of 5.5 mm. Open electrode design is a usual coaxial one. In both designs, the same materials and sizes were used. The cathode was made of copper and has a round shape with a diameter of 2 mm. The anode-cathode gap was 1 mm. The insulator was made of polyethene. Molybdenum was used as an anode material because of its high melting temperature (2620 °C). To obtain a vacuum arc, a pulsed generator was used. In this experiment, we used pulses with a duration of 12 μs (FWHM) and a current amplitude up to 10.8 kA at a charging voltage up to 10 kV.

In this experiment, ion plasma flow was investigated using four small-sized ion collector analyzers. The ion analyzer externally was a grounded brass cylinder with a diameter of 7 mm and a length of 18 mm. Inside, at a distance of 6 mm from the outlet, was a Faraday cup with a diameter of 2 mm. The entrance aperture was made of copper foil with 9 holes of a diameter 200 μm. The negative potential of -40 V was applied to the Faraday cylinder. This was necessary for sifting out the electrons. The signal from the plasma analyzers was recorded using an oscilloscope and the waves were analyzed. The measurements were taken at different angles and distances between electrodes and detectors. Fig. 1 shows the example of ion flow distribution diagrams.

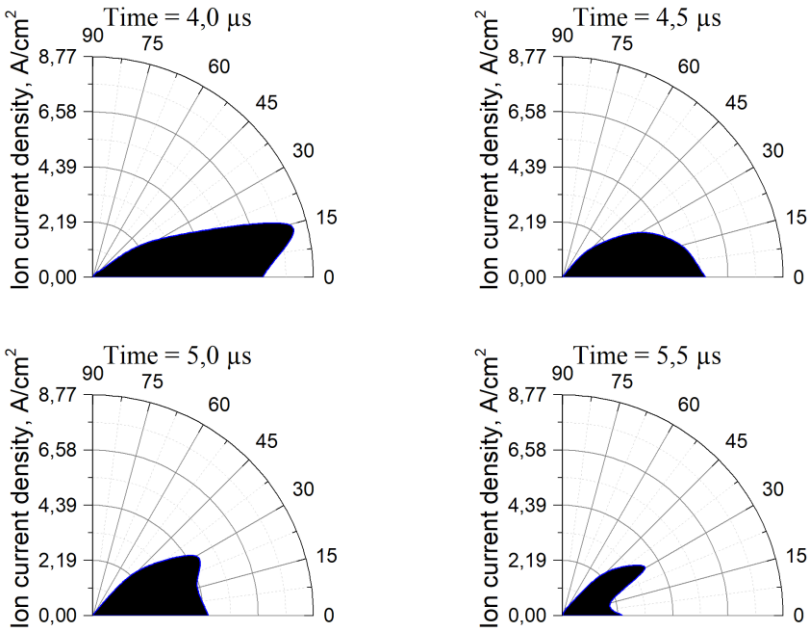

Fig.1. Time and spatial distribution of ion current.

REFERENCES

[1] R.L. Boxman, P.J. Martin, and D.M. Sanders // Handbook of vacuum arc: Science and technology. − 1995.

* This work was supported in part by RFBR Grant Nos. 18-08-00547, 19-08-00783, 19-58-53006.

ANALYSIS OF THE PROBABILITY OF IONIZATION OF ACCELERATED ATOMS DURING PENETRATION IN METAL TARGET *

A. PRIMA, A. PUSHKAREV

Tomsk Polytechnic University, Tomsk, Russia

This report presents an analysis of experimental and theoretical works on the penetration of ions and accelerated atoms in different targets. In [1], it was found that after the penetration of α-particles (5.6 MeV, radon α-decay) of the foil from mica or gold, He^+ ions and neutral helium atoms appear. An additional confirmation of the absence of ionization of accelerated atoms during penetration in a metal target is the results of MD simulation. When the energy of the primary knock-on atom in target is less than 200 keV, only atoms form radiation defects in its cascade, not ions [2].

The processes of elastic collisions, ionization, and charge-exchange of an ion with target atoms are described in the binary collision approximation model, so the processes of changing the charge state of ions and accelerated atoms during penetration in a solid or gaseous target will differ slightly. The first work on charge-exchange of an ion during transportation in gas was carried out by Bohr [3]. It is found that when the ion velocity is less than the electron velocity in the orbit of the hydrogen atom ($2.2 \cdot 10^8$ cm/s); the electron is captured (charge-exchange). The cross-section of the charge-exchange of protons (with an energy of 20 keV/nucl.) by atomic hydrogen is $5 \cdot 10^{-16}$ cm^2, and the cross-section of ionization is $6 \cdot 10^{-17}$ cm^2 [4].

In [5] presents experimental and calculated values of the cross-section of charge-exchange and ionization of heavy ions during penetration in gaseous and solid targets. When an iodine ion with an energy less than 5 MeV passes through gaseous hydrogen and oxygen, the electron capture cross-section is significantly larger than the ionization cross-section. The article [6] provides an overview of experimental data and theoretical methods for calculating the effective cross-sections of charge-exchange and ionization of multicharged ions colliding with neutral atoms in a gas. It is shown that when the ion energy is less than 10 MeV/nucl., charge-exchange processes occur mainly with a decrease in the degree of ionization. When studying radiation processes in a metal target, it was found that the average number of radiation defects in the displacement cascade of one carbon atom with energy 250 keV is 4-5 times greater than the calculated values for SRIM for ion with the same energy [7].

This analysis showed that the probability of ionization of accelerated atoms C or N with energy less 300-500 keV during penetration in the target is insignificant. Irradiation of the target with such atoms is more consistent with neutron irradiation in a nuclear reactor in terms of the spectrum of primary knocked-out atoms, efficiency, and the mechanism of formation of radiation defects [8].

REFERENCES

[1] G. H. Henderson, "Changes in the charge of an α-particle passing through matter," Proceedings of the Royal Society of London, Series A, vol. I02, pp. 496-506, 1923.

[2] W. Cai, J. Li, S. Yip. Molecular Dynamics. In Comprehensive Nuclear Materials, vol. 1. Amsterdam: Elsevier. 2012. pp. 249-265.

[3] Bohr N. The penetration of atomic particles through matter. Medd. Dan. Vid. Selsk 18, 1 (1948).

[4] B. H. Bransden, M.R.C. Mcdowell. Charge exchange and the theory of ion-atom collisions. Clarendon Press, 1992. 474 p.

[5] Hanz-Dieter Betz, "Charge states and charge-changing cross sections of fast heavy ions penetrating through gaseous and solid media," Rev. Mod. Phys. vol. 44, pp. 465-539, 1972.

[6] I.Yu. Tolstikhina, V.P. Shevelko, "Collision processes involving heavy many-electron ions interacting with neutral atoms," Phys. Usp. Vol. 56, no.3, pp. 213–242, 2013.

[7] A. Prima, R. Zyryanova, N. Pereday, V. Medvedsky, "Determination of radiation defects quantity in metals under irradiation by heavy carbon ions," Proceedings of the 24th International Conference on Ion-Surface Interactions. part 1. Moscow, Russia, 2019. pp. 186-189.

[8] A. I. Prima, R. V. Zyryanova, "Comparative analysis of generation of radiation defects in metals when irradiated with ions and accelerated atoms," / / Proceedings of the II International youth "Congress Modern materials and technologies of new generations". Tomsk, Russia, 2019. pp. 46-47.

* Experiments was supported by Russian Foundation for Basic Research, project no. 19-38-90001.

HIGH-FREQUENCY ELECTRON BEAM MODULATION IN AN ELECTRON SOURCE WITH A PLASMA-FILLED OPTICAL SYSTEM*

V.A. GUSHENETS[1], *A.S. BUGAEV*[1], *E.M. OKS*[1,2]

[1]*Institute of High Current Electronics SB RAS, Tomsk, Russia*
[2]*State University of Control Systems and Radioelectronics, Tomsk, Russia*

We have carried out some experiments demonstrating the generation an electron beam with high-frequency modulation of the current in an electron source with a plasma-filled optical system (POS) without the use of a high-frequency power supply. Plasma-filled system is an optical system diode type formed by a plasma cathode with a grid stabilization of the emission boundary and an extended plasma anode with an open moving plasma boundary. POS is characterized by low impedance and high perveance, which allows to reach the required power density in the beam for relatively low accelerating voltages (several tens of kV).

Plasma in the anode area of POS is generated by a plasma-dynamic device built on the geometry of a closed drift plasma accelerator. The plasma cathode consists of a hollow plasma emitter with an arc plasma generator inside. The operating mode of the electron source is pulse-periodic with 10 pulse per second, 100 μs pulse duration and up to 140 A electron emission current. As it was established, the modulation of the beam current in the POS accelerating gap is mainly observed in the accelerating voltage interval 10-20 kV and with an arc discharge current in the plasma emitter above 60 A. High-frequency modulation of the beam current is also observed in the absence of plasma in the anode region of the POS. It was found that the main modulation frequency is about 50 MHz. Very often this modulation of the beam current amplitude reaches values up to 100%.

Based on our experimental results and results given in [1], it can be assumed that the high-frequency modulation of the electron beam current observed in the experiment is caused by plasma electron oscillations within the potential trap, which is created inside the hollow plasma emitter by the positive plasma potential.

REFERENCES

[1] Ya. E. Krasik, A. Dunaevsky, J. Felsteiner, “High-frequency electron beam modulation in a diode with an active plasma cathode,” Appl. Phys. Lett., vol. 86, no. 4, pp. 453-455, July 1998.

* The work was supported by the Russian Foundation for Basic Research under grant No. 19-08-00315.

LOW-PRESSURE PULSED RF DISCHARGE FOR THE FORMATION OF A PLASMA ANODE OF A HIGH-CURRENT ELECTRON GUN

G.E. OZUR, P.P. KIZIRIDI

Institute of High Current Electronics SB RAS, Tomsk, Russia

Inductive RF discharges are widely used for plasma creation in large volumes. As a rule, the stationary systems with average power of about 1 kW are used which provide plasma density of 10^9–10^{11} cm^{-3} at working gas pressures of 5–100 mTorr [1, 2]. In spite of a number of difficulties (coincidence of the impedance of an RF generator and a load, initiation of the discharge at more low pressures), we believe in perspectives of the use of pulsed RF discharge for creation of a plasma anode of a high-current electron gun with an explosive-emission cathode. At that, the plasma density of $(2–3)\times10^{12}$ cm^{-3} at a gas pressure of about 0.5 mTorr should be provided and this is complicated task because of low ionization frequency. There are two main stimulus to use RF discharge for a plasma anode formation: (i) the possibility to provide an enlarged density on the periphery of a plasma anode, that improves the uniformity of a non-relativistic, high-current electron beam formed in the gun [3, 4]; (ii) plasma anode formation does not depend on the condition of the collector surface that is peculiar to the case of traditionally used high-current reflective discharge operating with cathode spots [3, 4].

In the present work, the results of study of charged particles distribution inside the inductor at the power supply frequency of 13.56 MHz and duration up to 8.5 ms are described. Typical distribution of electron density n_e along the inductor axis is given in Fig. 1. Note, that we could not exceed the value of n_e in comparison with the results obtained in [2] in spite of in our case the applied pulsed power exceeded the power (up to 1 kW) suppled the stationary RF in [2] about order of magnitude. We investigated also the glow (integral over pulse) of RF discharge and found it rather uniform and diffused.

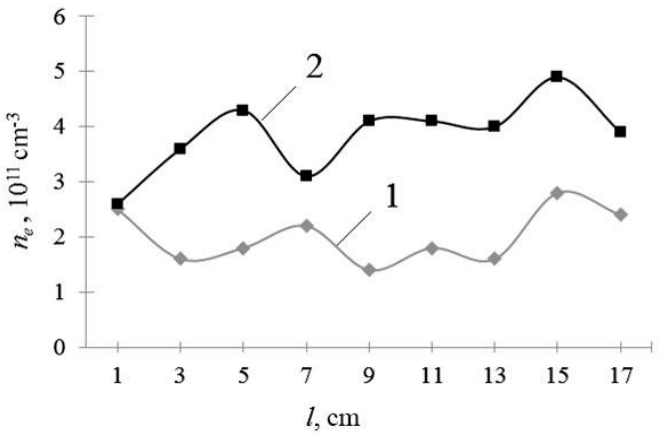

Fig. 1. Plasma density distribution along the inductor axis for different delay times between the start of pulsed guide magnetic field and the start of pulsed RF discharge: 1 – τ_d = 0; 2 – τ_d = 5 ms. Argon pressure is 0.6 mTorr.

Preliminary tests of the electron gun with plasma anode based on pulsed RF discharge have shown unstable operation of this e-gun. We think that it is caused by insufficient plasma density. In future, it may be overcome by the use of more power RF generator and/or increasing energy input into the discharge.

REFERENCES

[1] K.V. Vavilin, A.A. Rukhadze, M.Kh. Ri, V.Yu. Plaxin. “Radio Frequency Inductive Low-Power Plasma Sources for Technological Applications,” Plasma Physics Reports (Russian), vol. 30, No. 8, pp. 739–749, 2004.

[2] E.V. Berlin, V.U. Grigoriev. “Radio Frequency Plasma Generator for Technological Purposes,” Proc. of 10th Int. Conf. on Modification of Materials with Particle Beams and Plasma Flows. Tomsk, Russia, September 19–24, 2010, pp. 88–90.

[3] G.E. Ozur, D.I. Proskurovsky, and K.V. Karlik, “A Wide-Aperture, Low-Energy, High-Current Electron Beam Source with a Plasma Anode Based on a Reflective Discharge,” Instruments and Experimental Techniques, vol. 48, No. 6, pp. 753-760, 2005.

[4] G.E. Ozur and D.I. Proskurovsky, “Generation of Low-Energy High-Current Electron Beams in Plasma-Anode Electron Guns”, Plasma Physics Reports, vol. 44, No. 1, pp. 18–39, 2018.

CHARACTERISTICS OF A PLASMA ANODE BASED ON HYBRID DISCHARGE FOR THE USE IN A HIGH-CURRENT ELECTRON GUN *

P.P. KIZIRIDI, G.E. OZUR

Institute of High Current Electronics SB RAS, Tomsk, Russia

The use of low-energy (up to 30 keV), high current (up to 25 kA) electron beams (LHEBs) is rather effective for the surface treatment and modification of metal products [1, 2] and has good prospects for further development. Typically, LHEB formation is carried out in a high current gun with an explosive emission cathode and plasma anode based on a high-current reflective (Penning) discharge (RD). The operating experience with such guns showed that the electron beam formed in a double layer between the cathode and anode plasmas and being initially uniform in its cross section, transforms during transportation and acquires a pronounced maximum in the near-axis region. Beam uniformity can be improved, for example, by creating a plasma anode with increased plasma density at the periphery of the plasma anode. For this purpose, a hybrid discharge combining a high-current RD with vacuum arcs initiated by spark breakdown across the dielectric surface was used in [3].

This method has given positive results, however, the instability of discharge parameters related, in our opinion, to the insufficient anode voltage (≤ 5 kV) for the reliable operation of all arc sources, was observed. In the work [4], the space structure and temporal dynamics of the hybrid discharge at increased anode voltage (up to 9 kV) has been investigated. The first results on thermal imaging of the energy density distribution of the LHEB formed in such an electron gun were also presented.

In the present work, which is the continuation of the work [4], the results of double probe measurements of the plasma density radial profile in the hybrid discharge are presented. It has been found that plasma density at the periphery of the plasma column (plasma anode) exceeds the density in the central part by 2–3 times (Fig. 1). Such ratio is kept for practically total existing time of the plasma anode. The distributions obtained allow one to choose the modes of an electron gun operation with improved uniformity of the beam.

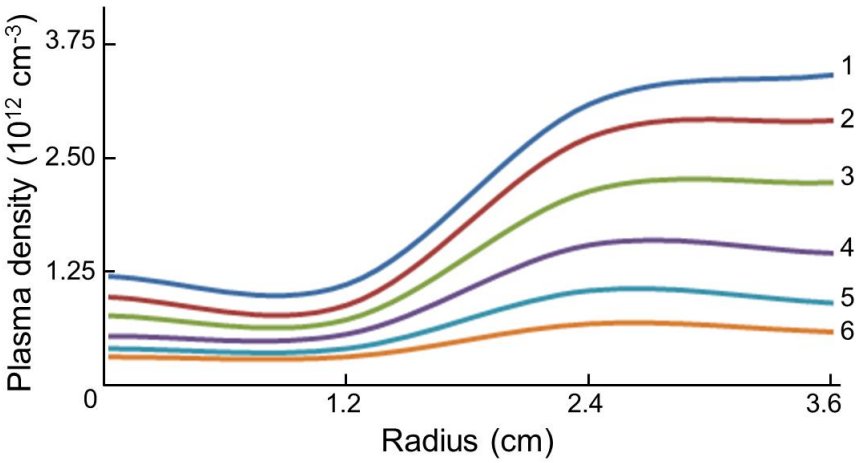

Fig.1. Plasma density radial profile in different time moments after the discharge start: 10 μs (curve 1); 20 μs (2); 30 μs (3); 40 μs (4); 50 μs (5); 60 μs (6). Argon pressure – 0.067 Pa, guide magnetic field – 0.11 T, anode voltage amplitude – 6.7 kV.

REFERENCES

[1] G.E. Ozur, D.I. Proskurovsky, V.P Rotshtein., A.B. Markov, "Production and application of low-energy, high-current electron beams," Laser & Particle Beams, vol. 21, no. 2, pp. 157−174, 2003.

[2] G.E. Ozur, D.I. Proskurovsky, K.V. Karlik, "A wide-aperture, low-energy, high-current electron beam source with a plasma anode based on a reflective discharge," Instruments and Experimental Techniques, vol. 48, no. 6, pp. 753−760, 2005.

[3] P.P. Kiziridi, G.E. Ozur, L.A. Zyulkova, A.V. Batrakov, "Formation of a nonrelativistic, high-current electron beams in a gun with plasma anode based on a combined discharge," Izv. Vyssh. Uchebn. Zaved. Fiz. (Russian Physics Journal), vol. 55, no. 6/2, pp. 42−48, 2012.

[4] P.P. Kiziridi, G.E. Ozur, "Formation of plasma anode in a high-current electron gun with the use of a hybrid discharge," Izv. Vyssh. Uchebn. Zaved. Fiz. (Russian Physics Journal), vol. 62, no. 11, pp. 151−155, 2019.

* The work was supported by the Russian Foundation for Basic Research under grant No. 18-08-00230.

INVERSE SEMIPLANOTRON ION SOURCE

V. DUDNIKOV

Новосибирский государственный университет, ул. Пирогова 2, 630090 Новосибирск, Российская Федерация

The efficient geometrical focusing of negative ions was demonstrated in the SPS with semiplanotrons discharge configuration [1,2,3,4 .] Similar ion source can be used for positive ion production. But more efficient positive ions can be generated in inverse semiplanotron, wich will be described below An ion source “inverse semiplanotron” for intense ribbon ion beams production with breadths from 150 mm to 2100 mm and beyond is proposed. Representative beam currents for argon ions scale up with beam breadth at a rate of 1A per meter at 2 keV and up. A gas discharge is triggered in narrow gap between an anode and a cathode with emission slit in transverse magnetic field like in a semiplanotron surface plasma negative ion source [5]. Plasma drift in crossed ExB fields. Single-slot extraction optics work very well down to 1000 eV with current derated only ~50%. Beam currents vary by species and energy in, so they can be readily inferred from argon currents. In the narrow dimension, the total beam divergence can be as low as +/- 2 degrees at 1 keV. To be enable such versatile scaling, the design eliminates all fields that run in the direction of the beam breadth. The extraction electrodes comprise a single slot three-electrode accel/decel system, avoiding the need for multi-aperture electrode systems that require precisely aligned arrays of a hundred or more circular apertures. The defining slit width is typically 2 mm. The trapping of electrons from the cathode inside the very compact arc discharge chamber is accomplished by means of a combination of electric and magnetic fields. Uniformity of ionization across the full breadth is excellent, and fine adjustment of the source gas distribution is a viable uniformity control method.

REFERENCES

[1] V. Dudnikov, Yu. Belchenko, Preprint, INP 78-95, Novosibirsk, 1978.

[2] V. Dudnikov, Yu. Belchenko, Journal de Physique, v. 40, p. 477, (1979).

[3] V. Dudnikov, and G. Fiksel, Journal de Physique, v. 40, p. 479 (1979).

[4] V. Dudnikov, Proc. Second Symp. Production and Neutralization of Negative Hydrogen Ions and Beams, Brookhaven, 1980 (BNL, Upton, NY, 1980), BNL- 51304, p. 137.

[5] Vadim Dudnikov, "Features of semiplanotron surface plasma sources", Rev. Sci. Instrum. 83, 02A724 (2012).

STRUCTURAL -PHASE STATE OF STAINLES STEEL AFTER HIGH POWER PULSED ION BEAM TREATMENT[1]

M.V. ZHIDKOV[1], *A. E. LIGACHEV*[2], *G. V. POTEMKIN*[3], *G. E. REMNEV*[3]

[1]*Belgorod National Research University, Belgorod, Russia*
[2]*Prokhorov General Physics Institute of the Russian Academy of Sciences, Moscow, Russia*
[3]*Tomsk Polytechnic University, Tomsk, Russia*

The study covers the structural and phase state of 18-10 stainless steel (AISI 321) subsurface layers irradiated by high power pulsed ion beam (HPPIB).

Samples were subjected to powerful ion beams on the TEMP unit [1]. The beam energy was 250 keV, the pulse duration was ~ 100 ns, and the energy density was 3 J/cm^2. The number of pulses varies from 1 to 50. The structure of the subsurface surface was studied by electron backscatter diffraction (EBSD) analysis (SEM Nova Nanosem 450). X-ray diffraction (XRD) analysis was performed, using an ARL X'TRA X-ray diffractometer with CuK_α radiation.

It was shown that surface defects are formed on the surface of the steel after irradiation, namely craters of different shapes and geometries. At the same time, the grain structure and phase composition of the surface layers change (fig.1).

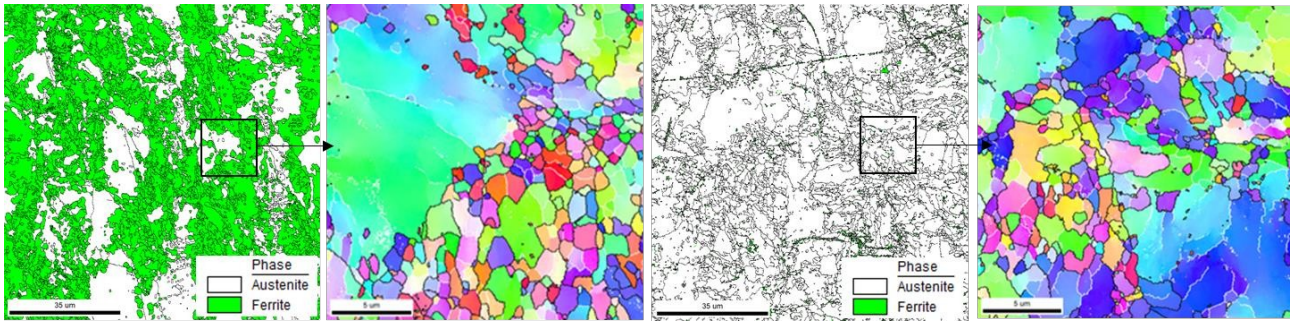

a b c d

Fig.1. Maps of phase distribution (a, c) and crystallographic orientations (b, d) of AISI 321 steel after ion beam treatment: a, b – 10 pulses; c, d – 50 pulses.

It was found that the average grain size increases with increasing number of exposure pulses. The content of a-Fe (ferrite) in the near-surface layers decreases with increasing number of exposure pulses (fig.2)

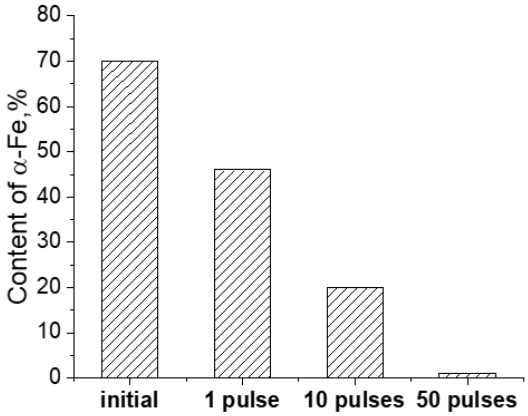

Fig.1. a-Fe content in the AISI 321 steel after ion beam treatment.

REFERENCES

[1] Remnev, G.E. and Shulov, V.A., "Application of high–power ion beams for technology, Laser and ParticleBeams", 1993, vol. 11, pp. 707–731

1 The reported study was funded by RFBR, project number 20-08-00907 (investigations by SEM and EBSD) and program of the RAS 11P Presidium (surface processing of the sample)

MEASUREMENTS OF ELECTRON EMISSION CURRENT DIRECTLY IN APERTURES OF A MULTIAPERTURE DIODE WITH PLASMA CATHODE

I.V. KANDAUROV, V.V. KURKUCHEKOV

Budker Institute of Nuclear Physics of SB RAS, Novosibirsk, Russia

The paper presents an original method for measuring the electron emission current directly in individual apertures of a multiaperture electron optical system (EOS) in a beam source with plasma emitter. The EOS is performed as a diode with flat electrodes in which many circular coaxial openings are drilled forming a hexagonal grid. The diameter of the holes in the extraction electrode (cathode) is 2 mm, in the anode electrode is 4.4 mm, the distance between the centers of the openings is 5 mm. Emission plasma is created by a low-pressure arc discharge with a cold cathode. The emission plasma was created by a low-pressure arc discharge. The arc source with a cold cathode was located on the axis at a distance of 20 cm from the EOS. The discharge occurred in an expanding magnetic field of ~ 0.3 T at the arc source and $7 \cdot 10^{-3}$ T at the EOS. The beam formed in a multiaperture EOS constitutes a set of individual beamlets. When transported in a guiding magnetic field, the radius of beamlet's envelope oscillates due to the presence of a transverse velocity component of the electrons. Thus, placing the target in different cross-sections along the beam propagation axis, it is possible to register both practically homogeneous beam footprints in the oscillation antinodes (where the neighbor envelope boundaries overlap) and discrete beam prints reproducing the initial structure of the EOS openings, in the nodes of oscillation. In our experiments, the imaging two-dimensional X-ray diagnostic [1] was employed to register the beam current density distribution on a plane metal target. The target was placed at 0.8 m downstream from the EOS, the magnitude of the accelerating voltage and the guiding magnetic field were adjusted precisely to obtain the most clear footprint of individual beamlets. The contribution of each beamlet to the total beam current can be found by measuring the integrated intensity of the beamlet image. Experiments with a 241-aperture EOS with an effective diameter of 8.3 cm showed that electron emission takes place in all openings. The current in the outermost apertures was ~ 30% of the current in the central ones. Thus, it was shown that the scheme with a single on-axis arc discharge generator operating in a diverging magnetic field allows the formation of electron beams with a large cross section and good uniformity of the emission current distribution.

.

REFERENCES

[1] I V Kandaurov et al 2017 J. Phys.: Conf. Ser. **830** 012032

GENERATION OF ANODE PLASMA IN THE DRIFT SPACE OF ELECTRON BEAM IN THE PLASMA ELECTRON SOURCE WITH GREED BOUNDARY STABILIZATION*

P.V. MOSKVIN, V.N. DEVYATKOV, I.V. LOPATIN, S.S. KOVALSKY, M.S. VOROBYOV

HCEI SB RAS, 2/3 Akademichesky Avenue, Tomsk, 634055, Russia, pavelmoskvin@mail.ru, +73822491300

Plasma electron sources are used as scientific and technological tools in various fields. Sources with grid stabilization of the cathode plasma boundary have positive aspects, namely, the stability of parameters from pulse to pulse, a wide range of currents, electron energy, pulse durations and a possibility of their independent regulation. These facts make the electron source convenient in the search for technical or scientific-experimental work. In such sources, the anode plasma is usually created by the beam itself, and it is difficult to create short beam current pulses with a duration of several microseconds, especially when the combined operation of several devices requires operation under reduced (10 mPa or less) pressure. The injection of an electron beam into a previously created plasma can expand the ranges of operating parameters of the electron source. For this, the team of authors created the source of additional anode plasma [1]. It was tested together with the SOLO electron source [2, 3], providing a beam current of up to 300 A at acceleration voltage of up to 25 kV and a submillisecond pulse duration, the diameter of emission window was 40 mm.

The discharge system of the anode plasma source is an axisymmetric ion-plasma system with a closed electron drift. It contains a ring anode, with a diameter of 95 mm, a collector anode, cathodes-magnetic conductors and additional cathodes for maintaining of operation in difficult conditions at a reduced working gas pressure and in axial magnetic field up to 50 mT. The device creates a plasma with a concentration of up to 2e-11 cm^{-3} at a discharge current of up to 20 A. The discharge voltage is in the range (320 - 350) V. Discharge current is mainly closed through the collector, which is the anode, and 1-2% of current flows through the annular anode. This part increases slightly with a decrease of axial transporting magnetic field and with decreasing of pressure. At the same time, a beam of accelerated electrons is created in the discharge system, since there is a high accelerating voltage, its current also depends on gas pressure and magnetic field. It is higher at reduced pressure and can reach several amperes, and its radial distribution strongly depends on the accelerating voltage and is substantially inhomogeneous.

Despite the fact that the concentration of beam plasma is an order of magnitude higher than the discharge, its presence allows the plasma cathode to operate at a lower pressure, from 12 mPa without the appearance of high-frequency oscillations, and also makes it possible to initiate the discharge of the plasma cathode at a pressure of up to 7 mPa, even under prolonged conditions continuous work up to 6 hours.

Anode plasma parameters were studied. An increase of working gas pressure from 20 mPa to 60 mPa leads to increase the concentration both of discharge anode plasma and beam anode plasma by 25% and 35%, respectively, at an anode discharge current of 13 A and a plasma cathode current of the same value. In the case of discharge plasma, a decrease of the electron temperature in measurement region from 9 eV to about 6.5 eV was observed, while the measured values for beam plasma increased from 7 eV to almost 14 eV, although there is no such difference at a higher beam current. During the study, it was noted that the operation of the anode plasma generator for 1 ms before electron beam reduces the probability of breakdown of the accelerating gap at a pulse duration of up to 20 us, and the training time of the accelerating gap is reduced.

REFERENCES

[1] *Moskvin, P.V., Devyatkov, V.N., Lopatin, I.V., Vorobyev, M.S. //* Journal of Physics: Conference Series. – 2019. – Vol. 1393. – № 1. P. 012049.

[2] *Akhmadeev, Y.H., Grigoriev, S.V., Koval, N.N., Schanin, P.M. //* Laser and Particle Beams. – 2003. – Vol 21(2). P 249-254.

[3] *Koval, N.N., Grigoryev, S.V., Devyatkov, V.N., Teresov, A.D., Schanin, P.M. //* IEEE transactions on plasma science. – 2009. – Vol 37(10). P 1890-1896.

* The work was supported by the Russian Science Foundation (project No. 20-79-10015).

STUDY OF MAGNETIC INSULATION OF THE PLANAR TYPE ION DIODE*

A.V. STEPANOV[1], *V.A. TARBOKOV*[1], *G.E. REMNEV*[1]

[1]*Tomsk Polytechnic University, Tomsk, Russia*

The self-magnetically insulated ion diode is one of the well-known pulsed sources to produce a high-intensity pulsed ion beam. Given diode type is widely used at experimental researches due to the simplicity and durability of construction [1, 2]. The plasma formation in these diodes is carried out by the voltage prepulse of negative polarity. The electrodes of such diodes usually have a focusing geometry to provide ballistic focusing of ion beam. As a rule the electrode cross section is square with a small fillet radius at the edges. The distribution of electric field intensity on the anode surface is non-uniform [3]. The distortion of the electric field is occurred in the outer anode borders and edges. Since the anode edges has a small fillet radius and the width of anode and cathode is comparable. In the diode with graphite anode the emission centers is located mostly in the outer anode borders and in the region where the electron current closing from the anode to cathode [4].

We have improved the electrodes shape of the self-magnetically insulated ion diode that the distribution electric field intensity on the anode surface is uniform. Also the coils system [5] for creating an external magnetic field in the anode-cathode gap of ion diode was developed. The operation modes of this type ion diode were research. The emitting anode surface and ion beam density distribution were investigated at the ion diode output area. The characteristics of this diode are presented depending on the operation mode.

REFERENCES

[1] T. Yoshikawa, K. Masugata, M. Ito, M. Matsui, K. Yatsui, "Planar-type self-magnetically insulated diode as a new source of intense pulsed light-ion beam," J. Appl. Phys, vol. 56, pp. 3137-3140, 1984.
[2] J.P. Xin, X.P. Zhu, M.K. Lei, "Initial plasma of a magnetically insulated ion diode in bipolar-pulse mode," Phys. Plasmas, vol. 15, 2008.A.V.
[3] A.V. Stepanov, V.I. Shamanin , G.E. Remnev, "Study of plasma formation in a planar type ion diode with self-magnetic isolation," J. Phys. Conf. Ser., vol. 1115, 2018.
[4] A.V. Stepanov , V.I. Shamanin , G.E. Remnev, " The study of operation modes of the self-magnetically insulated ion diode," Review of Scientific Instruments, vol. 90, no. 3, 2019.
[5] A.V. Stepanov, G.E. Remnev, "Influence of the configuration of the magnetic field of an ion diode on the parameters of an ion beam," Instruments and Experimental Techniques, vol. 52, no. 4, pp. 565-568, 2009.

* This work was supported by the Ministry of Education and Science of the Russian Federation no. FSWW-2020-0008

INVESTIGATION OF FACTORS INFLUENCING THE CHARGE-STATE COMPOSITION OF THE CATHODE MATERIAL IONS IN THE PLASMA OF LOW-CURRENT VACUUM ARC*

YU. A. ZEMSKOV, I.V. UIMANOV

Institute of Electrophysics UB RAS, Yekaterinburg, Russia

Decreasing of the average charge of cathode material ions in vacuum arc plasma with the discharge current was observed in the course of several investigations. This suggests that the number of cells in the low current vacuum arc cathode spot influences the charge state of cathode material ions. However, in the investigations mentioned above, other factors could significantly affect the results: substantial variations of the discharge currents during the arc due to capacitor discharge; and plasma generation in the initial stages of vacuum discharge.

The previous investigation was performed to obtain more accurate data about the influence of vacuum arc current on the charge state of cathode material ions [1]. In the course of the investigation, several factors potentially distorting the result were removed. Basic aspects of the work were the usage of a quasi-rectangle current pulse shape, and usage of an electrostatic gate to cut off ions generated in the initial stages of discharge. However, some observations brought into question the necessity of gate usage. And in this work the comparison between data with and without the gate was made.

Another topic in this investigation was the ionization mechanism in the plasma and its dependence on the arc current. On the one hand, possibly the cathode flare plasma density increases with the number of cathode spot cells. On the other hand, possibly the ratio between the metallic and nonmetallic ion fractions in the plasma influences the charge state. The average Cu ion charge with the hydrogen ions fraction in plasma at different values of the arc current was also compared in this work.

To prove the effect of the average charge state variation for other cathode materials the study of the microsecond arc on the CuCr cathode was also carried out.

Copper and Copper-Chromium samples were used as the vacuum arc cathodes in the 3.5 microsecond vacuum arc discharge. Pulse source was an LC-line with a quasi-rectangular pulse shape. Arc current varied from threshold current to 100 A. Charge state distribution and the average charge state of the cathode material ions were measured via the Thomson spectrometer with automated image recording and digital data processing. It was found that the ion charge state distributions were close to the classical data at the hundred-ampere currents, and the average charge state significantly decreased with the arc current decrease. All the ion signals increase with current, and the average charge variation with an increase in the arc current is determined by a remarkable difference between the growth rate of the quantity of single charged ions and the ions with the +2 charge and higher. The quantity of the multiply charged ions increased with the current considerably faster.

The comparison of data obtained with the electrostatic gate and without it showed that the impact of the transient processes corresponding to the gap breakdown stage was not significant. The concentration of hydrogen could affect the ionization of copper cathode ions, especially in the current range lower than 15 - 20 A. However probably it was not a predominant factor. Moreover, the influence of hydrogen possibly was not limited to the region of the cathode spot cell, and could also depend on the plasma density. And besides the hydrogen ions fraction in the plasma, the arc current value itself was a key factor of the charge distribution variation effect. This effect, observed earlier only for copper cathodes, confirmed to be a feature of the plasma generation in low-current vacuum arcs on the CuCr cathodes. Additionally, the measurement results showed, that average charge states of the cathode material component ions can differ from the average charge state in case of the pure Cu and Cr cathodes.

REFERENCES

[1] Yu.A. Zemskov and I.V. Uimanov, " Dependence of the Average Charge State of Copper Ions on the Discharge Current in the Low-current Vacuum Arc Plasma," in Proc. 28th ISDEIV, Greifswald, Germany, 2018, vol. 2, pp. 381-383.

* The work was supported by RFBR Grant Nos. 18-08-00547, 19-08-00783, 19-58-53006.

FEATURES OF ENERGY SPECTRA OF THE CATHODE MATERIAL IONS IN THE LOW CURRENT MICROSECOND VACUUM ARC*

YU. A. ZEMSKOV, I.V. UIMANOV

Institute of Electrophysics UB RAS, Yekaterinburg, Russia

To study the charge composition of ion flows from the plasma of microsecond vacuum arcs, we use a Thomson spectrometer with automatic signal registration and digital data processing. This spectrometer was modified to detect low-intensity signals of ion flows from the plasma of low-current arcs. An amplifier based on microchannel plates is used to amplify the signal, and an electrostatic ion acceleration system at the output of the plasma source is used to ensure stable secondary electron emission at the amplifier input. The voltage in the acceleration unit is 2 - 3 kV. Generally, the energy spectrum of the detected arc discharge ions is rather narrow, its width does not exceed 100 eV, and the signal of these ions occupies a compact region on the particle detector screen. However, a signal of ions with much higher energy was often recorded. Some of these cases were the consequences of resonant charge exchange. For example, a peak appeared in the spectrum of singly charged ions, twice the voltage at the acceleration site, i.e. with the energy characteristic of doubly charged ions. Nevertheless, additional ion signals were recorded. The energy and spectral width of the signal couldn't be explained by resonant charge exchange. These unusual data were accumulated during a series of experiments and generalized.

The main parameters studied for the high-energy ion fraction were: particle energy, energy dependence on the charge, and the moment of generation of high-energy ion flux.

The experiment was carried out in the high vacuum chamber at 10^{-6} Pa. The plasma source consisted of the disk cathode with an 8 mm diameter, wire trigger electrode, and the hollow anode with the ring entrance. The diameter of the anode orifice was 9 mm.

The moment of ion generation was determined in an experiment with an electrostatic gate. The electrostatic gate was installed between the ion acceleration unit and the input collimator aperture of the Thomson spectrometer. When voltage was applied between the gate plates, the ions acquired a tangential velocity component that did not allow them to pass through the aperture of the collimator.

The appearance of a high-energy component in the ion flux from the plasma of microsecond arcs was regular. The contribution of this component to the total ion signal can be quite high.

The use of an electrostatic gate with variable time parameters showed that the generation of these ions apparently occurs at the end of the discharge. An analysis of the energy distributions of ions shows that their acceleration mechanism is of a field type. The ion energy of the cathode material does not exceed several hundred eV per unit charge of the ion. Such ions can be recorded in the hollow anode - electrostatic extractor system even though the arc burning area is located away from the collimator axis.

* The work was supported by RFBR Grant Nos. 18-08-00547, 19-08-00783, 19-58-53006.

APPLICATION OF A PLASMA ANODE IN THE ELECTRON BEAM SOURCE WITH AN EXPLOSIVE EMISSION CATHODE AND ELECTRON BEAM OUTPUT INTO THE ATMOSPHERE *

E.N. ABDULLIN, G.F. BASOV

Institute of High Current Electronics SB RAS, 2/3 Akademichesky Ave., Tomsk 634055, Russia
abdullin@lhfe.hcei.tsc.ru, 8-923-401-9287

The paper presents the results of experiments for obtaining high-power microsecond electron beams of circular and rectangular cross-section in the electron beam source with an explosive emission cathode and plasma anode and output the beam into the atmosphere. The generation of the beam is realized in the presence of an external longitudinal magnetic field. The source of high voltage is the Marx generator with a rectangular form of the voltage pulse at the arbitrary constant resistive load. The electron beams with the electron energy up to 200 keV, current up to 1-1.5 kA, duration of 5 μs, and beam cross-section of 100-200 cm^2 in the electron beam source have been obtained. The rotation of the beam around its axis was registered. The output of a rectangular electron beam with energy of 150-200 J in mode of single pulses was carried out.

* This work was supported by RFBR, Grant No. 16-48-700034 "r-a"

KINETICS OF ELECTRON IN TRANSIENT MODE OF CURRENT SWITCHING IN PLANAR VACUUM DIODE*

V.YU. KOZHEVNIKOV, A.V. KOZYREV

Institute of High Current Electronics SB RAS, Tomsk, Russia

Stationary and non-stationary current flows in planar and geometrically non-uniform vacuum diodes are quite well studied. In stationary case, the current of a planar diode, j_{CL}, is given by the Child-Langmuir expression [1]. However, the most serious limitation of Child's law is that it does not provide a description of transient processes in a diode. Such non-stationary description was obtained later, in [2]. In particular, it was shown that during the transition to stationary current flow, relaxation oscillations of the electron space charge arise. They cause relaxation oscillations of the diode current.

This paper deals with the accurate modeling in terms of fundamental principles of physical kinetics involving the direct numerical solution of kinetic Vlasov equation with Poisson equation for electric field. In order to show the essence of the physical effect under the consideration more clearly, we take the vacuum diode with following parameters: D = 1 см, U_{max} = 2 kV. As parameters of the electron boundary distribution corresponding to the cathode emission characteristics, we set electron number density of $1.5 \cdot 10^{18}$ m^{-3} and temperature of 1 eV. For these values, the emission current is approximately 70 times higher than the Child-Langmuir current ($j_{CL} \sim 2.2$ kA/m^2), which denotes that cathode have an unrestricted emission capability.

In Fig. 1a, a short anode current density pulse is shown corresponding to voltage pulse of 1 ns duration with 0.1 ns front and rear edges. The initial burst of relaxation current is associated with the arrival of an electron beam at the anode. It can be observed that the generation of the current pulse maximum starts when the anode voltage reaches its amplitude value. After producing the current splash, the diode current gradually decreases to zero. The integral energy composition of electron beam, shown in Fig. 1b, is a multimode structure. It is represented by electron energies from zero up to 2.5 keV.

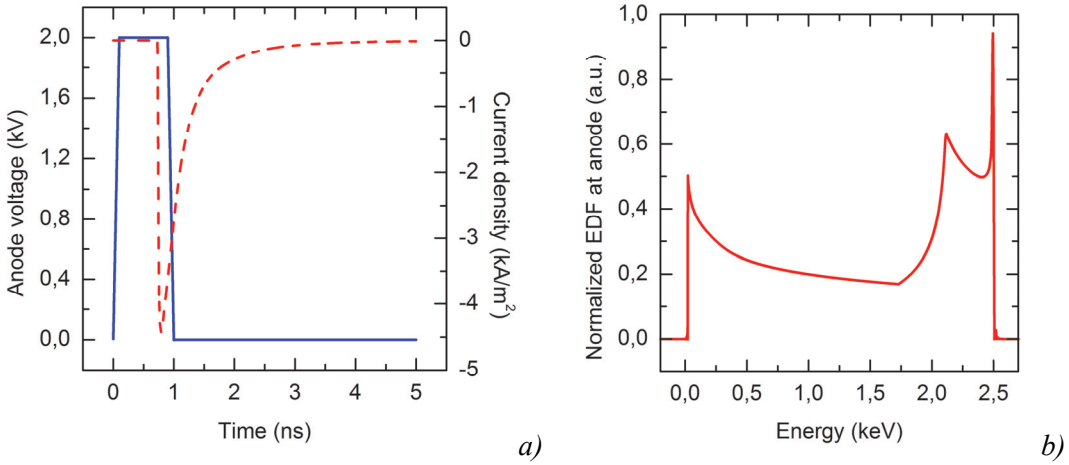

Fig.1. *a*) − Time profiles of the anode voltage (blue solid line) and current density (red dash line) of pulsed nanosecond planar vacuum diode; *b*) − Normalized energy spectrum of the electron beam driven by 1 ns anode voltage pulse.

We show that the origin of abrupt current splash during relaxation oscillations is caused by the "anomalous" component of the electron beam. It was also shown that the appearance of "anomalous" electrons in nanosecond vacuum diodes is caused by the limited duration of the voltage pulse front, but not caused by the presence of cathode plasma, geometrical peculiarities of diode's configuration, etc.

REFERENCES

[1] I. Langmuir, "The Effect of Space Charge and Residual Gases on Thermionic Currents in High Vacuum," *Physical Review*, vol. 2, no. 6, pp. 450–486, 1913.

[2] A. Sh. Airapetov and A. L. Feoktistov, "Current limit in a non-stationary flat diode," *Kratk. Soobshch. Fiz.*, No. 2, 18, 1990.

* The work was supported by the Russian Foundation for Basic Research (RFBR) grant No. 19-08-00286.

ESTIMATION OF THE AL METAL-PUFF DENSITY PROFILE ON THE GENERATOR GIT-12*

R. K. CHERDIZOV, V. A. KOKSHENEV, A. V. SHISHLOV, N. E. KURMAEV, V.I. ORESHKIN, A.G. ROUSSKIKH, A.S. ZHIGALIN

rustam.k.cherdizov@gmail.com
Institute of High Current Electronics, Siberian Branch, Russian Academy of Sciences, Akademichesky Avenue 2/3, 634055, Tomsk, Russia

Experiments with Al metal-puff at a current of 2-3 MA were carried out on the GIT-12 generator (4.7 MA, 1.7 μs) at the IHCE SB RAS in Tomsk. The load unit consists of plasma gun, surrounded by the outer plasma shell. Inner plasma gun electrode with a 4 mm diameter is made of aluminum. The outer plasma shell consisting of hydrogen and carbon ions was formed by 48 plasma guns located at the diameter of 350 mm. The initial density profile of Al metal-puff for various load configurations was estimated using a set of experimental data: current and voltage waveforms, magnetic probes signals, images of optical streak and frame cameras. The radial profile of the initial distribution of Al metal-puff matter can be approximated as the sum of two normal distributions with different dispersions. The main distribution peak is due to aluminum ions from plasma gun electrode. Another distribution curve is due to the contribution of the insulator matter (hydrogen and carbon), because ignition of the vacuum arc occurs on the surface of insulator.

REFERENCES

[1] A. G. Rousskikh, A. S. Zhigalin, and V. I. Oreshkin, "Estimation of the Initial Density Distribution in Plasma–Metal Liners", Technical Physics, vol. 61, no. 5, pp. 676–682, 2016

* The work was supported by Russian Science Foundation Grant # № 19-19-00127.

FIRST MEASUREMENTS OF MAGNETIC FIELDS IN Z-PINCH PLASMAS BY THE ION DEFLECTOMETRY ON THE GIT-12[1]

V. MUNZAR[1], D. KLIR[1], J. CIKHARDT[1], B. CIKHARDTOVA[1], J. KRAVARIK[1], P. KUBES[1], K. REZAC[1], A. V. SHISHLOV[2], V. A. KOKSHENEV[2], R.K. CHERDIZOV[2], N. A. RATAKHIN[2], K. TUREK[3], J. KRASA[4]

[1]Czech Technical University in Prague, Faculty of Electrical Engineering, Czech Republic
[2]Institute of High Current Electronics SB RAS, Tomsk, Russia
[3]Nuclear Physics Institute, Academy of Sciences of Czech Republic, Prague, Czech Republic
[4]Institute of Physics, Academy of Sciences of Czech Republic, Prague, Czech Republic

Ion deflectometry is a novel diagnostic method for measurements of magnetic fields in dense plasmas, where ion deflections measure path-integrated B-fields [1,2]. While capable of measuring the spatial distribution of magnetic fields, this diagnostic method necessitates high energy ion (usually proton) beamsgenerated usually by either a short-pulse high-intensity laser or a fusion reaction. It hinders widespread usage of most of the Z-pinch devices [3,4,5]. However, we have successfully performed ion-deflectometry experiments in deuterium gas-puff MA Z-pinch experiments on the GIT-12. In a unique configuration, we have employed ion beams accelerated during a Z-pinch current disruption [6,7]. Recently, we focus on understanding experimental images (deflectograms) of the deflected ion beams, obtained by pinhole-camera detectors. 3D simulations of B-fields and deflected ion trajectories are used to interpret experimental data and to show the capabilities of this diagnostic method. For the first time, we can study magnetic fields on-axis of the Z-pinch and to estimate a Z-pinch current at a given radius.

REFERENCES

[1] Bott, A. F. A., et al. "Proton imaging of stochastic magnetic fields." Journal of Plasma Physics. 2017.

[2] Palmer, C. A. J., et al. “Field reconstruction from proton radiography of intense laser driven magnetic reconnection,” Physics of Plasmas, 2019.

[3] Manuel, MJ-E., et al. “Mapping return currents in laser-generated Z-pinch plasmas using proton deflectometry.” Applied Physics Letters, 2012.

[4] Mariscal, D., et al. “Measurement of pulsed-power-driven magnetic fields via proton deflectometry.” Applied Physics Letters, 2014.

[5] Munzar, V., et al. "Investigation of Magnetic Fields in Z-Pinches via Multi-MeV Proton Deflectometry." IEEE Transactions on Plasma Science,2018.

[6] Klir, D., et al.: “Ion acceleration mechanism in mega-ampere gas-puff z-pinches,” New Journal of Physics, 2018.

[7] Klir, D., et al. "Acceleration of protons and deuterons up to 35 MeV and generation of 1013 neutrons in a megaampere deuterium gas-puff z-pinch." Plasma Physics and Controlled Fusion, 2018.

1 This research has been supported by the Grant Agency of the Czech Republic (Grant No. 19-02545S), the Ministry of Education, Youth, and Sports of the Czech Republic (Grant No. LTAUSA17084, No. LTT17015, No. 8JPL19014 and CZ.02.1.01/0.0/0.0/16_019/0000778), the CTU (Grant No. SGS19/167/OHK3/3T/13), Naval Research Laboratory Base Program, the Office of Naval Research under Grant #N62929-16-1-2192 and Contract #N68335-18-C-006

RESEARCH OF NEAR ELECTRODE PLASMA AT ELECTROLYTE DISCHARGE

D.L. KIRKO, A.S. SAVJOLOV

National Research Nuclear University MEPhI, Moscow, Russia

Discharges in electrolytes are formed during the passage of electric current 0.1-5 A in a liquid medium and find various technological applications. The best effects are achieved when using these discharges for complex metal surfaces polishing and for water and air purification systems designing [1-3]. At the same time under the influence of electrolyte discharge to titanium electrodes the appearance of surface microstructures: sphere-like formations and a porous surface was detected [4,5].

For experiments cylindrical plexiglass chambers with volume 150-400 cm^3 were used. Electrolytes based on sodium carbonate and sodium hydroxide were applied. For cathodes tungsten and titanium rods with diameter 1-3 mm were used, and for anodes stainless steel and molybdenum plates were used. A rectifier with voltage 0-250 V at pulse repetition rate 50 and 100 Hz was used as a power source. In the experiments the cathode was deposited vertically into the electrolyte and was located at the certain depth relative to the liquid surface. The current pulses are repeated with the frequency of the power source. A separate current pulse is represented as a damped sine wave with period near ~1 ms. At the beginning of each current pulse high-frequency oscillations in the ranges 10–600 kHz and 1–90 MHz are recorded [1,4,5]. The temperature in the discharge region near the cathode was measured by spectral methods using. The discharge radiation contains atomic lines of sodium, hydrogen, oxygen, as well as elements of the cathode material: tungsten and titanium. For diagnostic the method of relative intensities of atomic hydrogen spectral lines H_α, H_β and H_γ was used. The plasma temperature for tungsten and titanium cathodes was in range 2700-3200 K.

The influence of the electrolyte discharge on the electrode material was researched. The area of cathode surface is limited by the ceramic tube and has the value near 1 mm^2. VEGA 3 SEM and Hitachi TM1000 microscopes were used to study the surface of the electrodes. An assumption was made about the possibility of filamentation of the current acting on the surface into micron currents with sizes 1-5 μm. These microcurrents have a specific effect on the surface of the electrodes. In this work we studied the process of spraying the surface of the electrodes used. The subsequent growth of surface micron structures: sphere-like formations, porous surfaces, and fibrous structures was researched. A possible model for the growth of surface microstructures the concept of the current filamentation using is suggested.

REFERENCES

[1] R.R. Kayumov, Al.F. Gaysin, E.E. Son, Az.F. Gaysin, F.M. Gaysin, “Turbulent mixing of plasma and electrolyte in the multi-channel discharge between a droplet and electrolyte,” Physica Scripta, vol. T142, pp. 014038, 2010.

[2] P. Bruggeman, Ch. Leys, “Non-thermal plasmas in and in contact with liquids,” J. Phys. D: Appl. Phys, vol. 42, p. 053001 (28 pp), 2009.

[3] S. Samukawa, M. Hori, S. Rauf et. al., “The 2012 Plasma Roadmap,” J. Phys. D: Appl. Phys., vol. 45, p. 253001 (37 pp), 2012.

[4] D.L. Kirko, “Oscillatory processes in the plasma of the discharge in electrolyte in a magnetic field,” Technical Physics, vol. 60, no. 4, pp. 505–509, 2015.

[5] D.L. Kirko, A.S. Savjolov, “Investigation of plasma properties of discharge in electrolyte surface layer,” J. Phys. Conf. Ser., vol. 941, pp. 012018, 2017.

IMPLODING FOIL LINER EXPERIMENTS ON THE MIG PULSE GENERATOR*

S.A. SOROKIN

Institute of High Current Electronics SB RAS, 2/3 Akademichesky Ave., Tomsk 634055, Russia, s.sorokin@rambler.ru, +7(3822)491617

Implosion of liners (hollow cylindrical shells) by the current of a pulsed generator has been used in research on inertial thermonuclear fusion, generation of soft x-ray pulses and megagauss magnetic fields since the early seventies of the last century. As the original liner, gas puffs, cylindrical foils or cylindrical arrays of wires [1] are used. The liner is accelerated by the magnetic field of the current flowing through it and then stagnates on the axis, forming a column of hot dense plasma. The impedance of the liner motion (dL/dt) can potentially provide a higher energy-transfer efficiency from the generator to the plasma load as compared to the single wire load. For this, it is necessary that the bulk of the liner implosion occur near the maximum current of the generator. With the current rise time τ, the liner velocity before stagnation is about $3r_0/\tau$, i.e., it is determined by the liner initial radius r_0. At $\tau \sim 100$ ns, to reach a velocity of more than 3×10^7 cm/s, it is necessary to choose $r_0 > 1$ cm. The liner implosion process is accompanied by the development of the Relay – Taylor instability, which limits the radial convergence of the liner plasma to ~ 10. An obvious way to increase the density of matter and energy in the pinch formed on the axis is to decrease the initial radius of the liner, which can be realized by reducing the rise time of the current through the liner τ. The mass of the liner accelerated to a given velocity is determined by the energy (maximum current) of the generator. A decrease in τ, and, consequently, r_0 by an order of magnitude (up to ~ 10 ns and 1 mm, respectively) makes it possible to use existing industrial foils with a thickness of several micrometers for the manufacture of liners even at a generator current of about 2 MA.

The paper presents experiments on the implosion of liners of aluminum foil 1.8 and 2.5 μm thick on the 2-MA MIG generator (IHCE SB RAS, Tomsk, Russia). The front of the current through the liner was sharpened to several nanoseconds by preliminary injection of plasma into the liner region [2,3,4]. In the experiment, a column of plasma with a diameter of about 50 μm was observed (a pinhole camera, see Fig. 1), which corresponds to the density of plasma ions several times higher than the density of atoms in solid-state aluminum. Estimates show that the density of internal energy in the pinch plasma exceeds 10^8 J/cm^3.

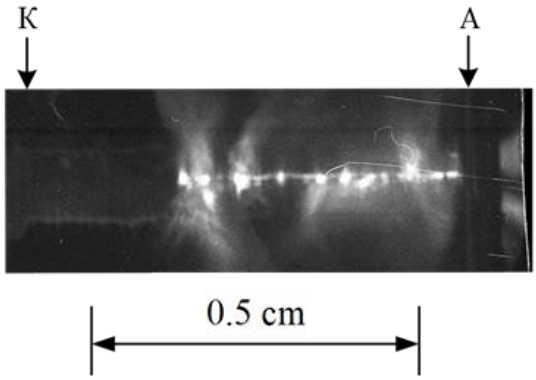

Fig. 1. Side-on soft X-ray image (mylar 2.5 μm + aluminum 0.3 μm filter) for a shot with a 1.0-mm diameter, 5-mm length, 3.6-μm thick aluminum liner. The arrows in the figure indicate the position of the cathode (K) and the anode (A).

References

[1] *Stallings C., Nielsen K., and Schneider R.* //Appl. Phys. Lett. . – 1976. – Vol. 29. – № 7. P. 404–406.
[2] *Sorokin S.A. //* Plasma Physics Reports. – 2017. – Vol. 43. – № 5. P. 542–546.
[3] *Sorokin S.A. //* Physics of Plasmas. – 2018. – Vol. 25. – № 8. P. 082704-1–082704-5.
[4] *Sorokin S.A. //* Physics of Plasmas. – 2019. – Vol. 26. – № 8. P. 082706-1–082706-5.

* This work was supported by the Russian Foundation for Basic Research (grant No. 18-08-00155).

ULTRAFAST WIRE LOADING WITH MULTI-MEGAAMPERE CURRENT*

S.A. SOROKIN

Institute of High Current Electronics SB RAS, 2/3 Akademichesky Ave., Tomsk 634055, Russia, s.sorokin@rambler.ru, +7(3822)491617

In experiments of the early seventies of the last century, high-temperature dense plasma was created by the explosion of fine single wires driven by a terawatt-power pulse generator [1]. Such a plasma is an intense source of soft x-ray radiation. However, with a generator pulse duration of several tens of nanoseconds, the high inductive impedance of the wire (and the destruction of the wire by sausage instability already at the front of the rising current) creates certain problems for the efficient transfer of generator energy to the wire plasma [2]. The paper presents the results of experiments on the ultrafast wire loading with multi-mega-ampere current. Metal wires with radii of 60-100 μm are driven with 2 MA current of the MIG generator. Plasma with density 10^{16}-10^{17} cm^{-3} is preliminarily injected in the area of the wire load using a set of radial plasma guns. The $\boldsymbol{J}\times\boldsymbol{B}$ force sweeps up the injected plasma along the surface of the electrodes and the current switches to the wire in a few nanoseconds [3,4]. Since the rise time of the current through the wire does not exceed the time of development of sausage instability (the radius of the wire divided by the Alfvén velocity in the material of the wire), the wire retains its cylindrical structure by the time the current reaches its maximum value. The fast wire surface explosion [4], the development of sausage instability and the formation of constrictions occur at the maximum current of the generator (see Fig. 1), which, in particular, significantly increases the efficiency of the conversion of the generator energy into the energy of soft x-ray radiation.

For a shot with a 0.1-mm diameter, 11-mm length tungsten wire the total soft X-ray yield (in the quantum energy range of 60-900 eV) was 40 ± 5 kJ. The peak radiation power was 0.7 TW.

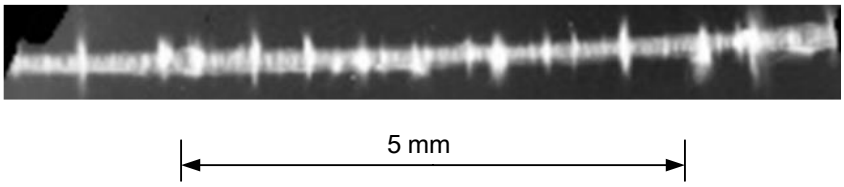

Fig. 1. Time-integrated side-on soft x-ray image (aluminum 1.8 μm filter) for a shot with a 0.1-mm diameter tungsten wire.

REFERENCES

[1] *Mosher D., Stephanakis S.J., Vitkovitsky I.M., Dozier C.M., Levine L.S., and Nagel D.J.* //Appl. Phys. Lett. – 1973. – Vol. 23. – № 8. P. 429–430.

[2] *Stallings C., Nielsen K., and Schneider R.* //Appl. Phys. Lett. . – 1976. – Vol. 29. – № 7. P. 404–406.

[3] *Sorokin S.A. //* Plasma Physics Reports. – 2017. – Vol. 43. – № 5. P. 542–546.

[4] *Sorokin S.A. //* Physics of Plasmas. – 2018. – Vol. 25. – № 8. P. 082704-1–082704-5.

* This work was supported by the Russian Foundation for Basic Research (grant No. 18-08-00155).

NEAR-SURFACE DENSITY DISTRIBUTION IN THE SKIN EXPLOSION OF CYLINDRICAL CONDUCTORS*

I.M. DATSKO, N.A. LABETSKAYA and V.A. VAN'KEVICH

Institute of High Current Electronics, Siberian Branch of the Russian Academy of Sciences
2/3 Akademichesky Ave., Tomsk 634055, Russia

The formation of the near-surface plasma during a skin explosion in a rapidly rising magnetic field was investigated for copper and duralumin cylindrical conductors. The experiment was carried out on the MIG high-current generator at a current of amplitude up to 2.5 MA and rise time 100 ns. The formation of plasma at the conductor surface was detected by the occurrence of visible light which was imaged by a four-frame optical camera with a frame exposure time of 3 ns. In addition, vacuum photodiodes were used to detect the temperature of the surface plasma reaching more than 1 eV in the black body approximation. The internal structure of the surface plasma was observed for an exposure time of 2–3 ns by exposing the plasma to the x radiation with hν > 0.8 keV generated by an X pinch. The shadowgrams obtained were used to evaluate the plasma density and its radial distribution. The X-pinch load was placed immediately in the vacuum chamber of the MIG. It was powered, via a low-inductance flexible transmission line, from a compact high-current pulse generator (XPG-3) located outside the MIG vacuum chamber. The XPG-3 generator produced a current of amplitude up to 200 kA and rise time 150–200 ns that was passed through the X-pinch load. For a duralumin conductor of diameter 3 mm, the visible light emission began at the 80th nanosecond. The temperature of the surface plasma reached more than 1 eV in 90 ns. At the 160th nanosecond, the expanded plasma column, imaged in the visible self-radiation, had a diameter 3.5 mm; its maximum diameter, in view of perturbations, was 3.8 mm. The diameter of its uniform portion, determined from the simultaneously obtained shadowgram, was 3.25 mm. A comparison of the densitogram of the plasma column image with that of the step filter (Fig. 1),showed that the line-of-sight mass per unit length of the column was greater than the mass per unit length of an Al foil of thickness 20 μm. In this case, in the near-surface region within a radius of 1.6–1.7 mm, the mass per unit length corresponded to that of a 10-μm Al foil and decreased rapidly with radius. The strongly perturbed outer boundary absorbed the same amount of probe radiation energy, or had the same mass per unit length, as an aluminum filter of thickness 1–2 μm. The estimated density of the material at the plasma column boundary made 8–12% of the solid-state density.

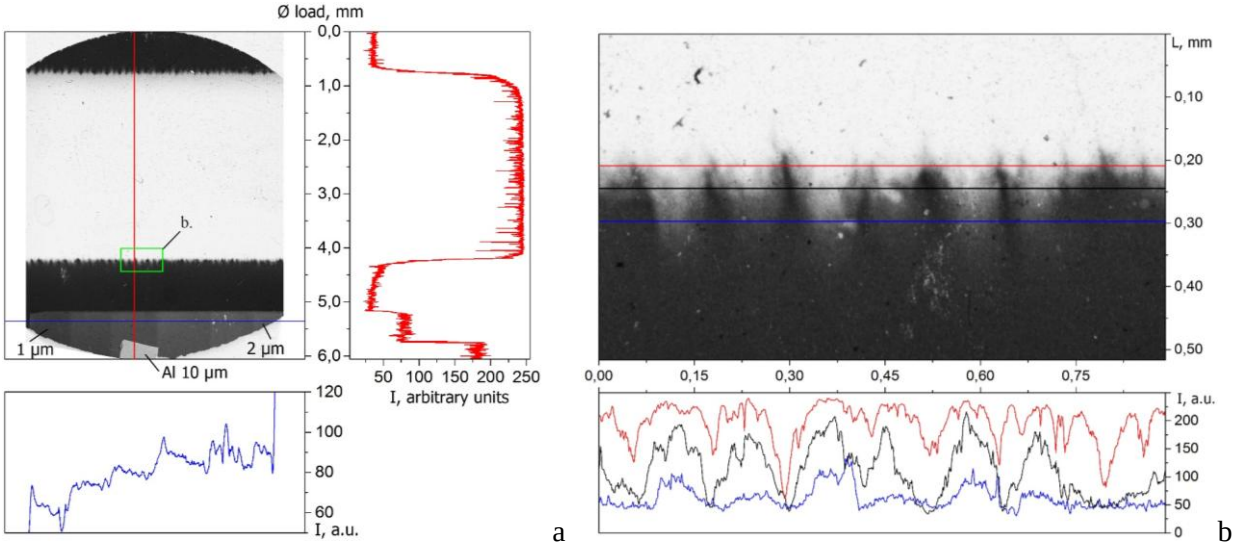

Fig.1. Shadowgram of the plasma column at 220 ns from the beginning of the current and densitograms of its various sections (a) and densitograms of the selected and enlarged section of the surface of the plasma column (b).

* This work was supported by the Russian Foundation for Basic Research (grant No 19-08-00479).

RADIATIVE CHARACTERISTICS OF AL METAL-PUFF Z-PINCHES IN EXPERIMENTS ON THE GIT-12 GENERATOR AT A MICROSECOND IMPLOSION REGIME. *

A.V. SHISHLOV, R.K. CHERDIZOV, F.I. FURSOV, V.A. KOKSHENEV, N.E. KURMAEV, V.I. ORESHKIN,

A.G. ROUSSKIKH, A.S. ZHIGALIN

Institute of High Current Electronics SB RAS, Tomsk, Russia

Study of radiative characteristics of Al metal-puff Z-pinches has been carried out in the experiments on the GIT-12 generator. The generator was operated in a microsecond mode that provides 4.7-MA current with the current rise time of 1.7 μs in a short-circuit load at a charging voltage of 50 kV. A Z-pinch load under investigation consisted of a metal puff surrounded by a plasma shell. The Al metal puff was created on the axis by evaporation of the electrode substance in a vacuum arc discharge. The outer plasma shell was formed at a diameter of 350 mm with the help of 48 plasma guns. Measurements of the radiation power and yield were carried out with a set of x-ray vacuum diodes and photoconducting detectors.

During the experiments, the data on the Al K-shell radiation power and yield were obtained for two different configurations of the Al metal-puff Z-pinches and for a case, when the Al metal puff was used without the outer plasma shell. The experimental data were compared to the theoretical predictions of an expected K-shell yield at a certain current level in order to estimate the efficiency of a new type of K-shell plasma radiation source. Performance of the Al metal-puff Z-pinch with the outer plasma shell as a K-shell plasma radiation sources was also compared with that of the gas-puff-on-wire array and planar wire array loads operating in the microsecond implosion regime. Up to now, the highest Al K-shell radiation power and yield were achieved in our previous experiments with planar wire arrays: 200 GW/cm and 6.5 kJ/cm, respectively. These radiation parameters were reached at the peak implosion current of 3.6 MA. The maximum Al K-shell radiation power and yield observed in the experiments with Al metal-puff Z-pinches with the outer plasma shell were 400 GW/cm and 4.5 kJ/cm, however the peak implosion current was only 2.4 MA. This means that the efficiency of the K-shell plasma radiation source based on the Al metal-puff with the outer plasma shell is significantly higher.

* The work was supported by Russian Science Foundation Project № 19-19-00127.

SELF-MAGNETIC INSULATION IN PLASMA OPENING SWITCHES

S. V. LOGINOV

Institute of High Current Electronics SB RAS, Tomsk, Russia

The paper analyzes the penetration of a magnetic field into the plasma bridge of nanosecond and microsecond opening switches. For switches with a conduction time of ~100 ns, simple formulae are derived to estimate the magnetic field velocity in collisionless and collisional plasmas. It is shown that in both cases this velocity is determined by the magnetic field rise rate to plasma density ratio raised to the 1/2 power. As the conduction time is increased to ~1 μs, the field velocity starts to depend on the plasma aggregation by a magnetic piston. At the same time, irrespective of the conduction time, the electron flow velocity is limited by the radial drift velocity in crossed magnetic and polarization electric fields. Such a limitation suppresses the current channel conductivity with respect to the Spitzer value by a factor equal to the electron magnetization parameter raised to one or another power. On completion of the conduction phase, the rate of rise of the switch resistance is proportional to the electron drift velocity. The peak switch voltage obtained in calculations is compared with its values recorded in experiments on mega-ampere current switching. A procedure is also presented for calculating the switch parameters to obtain the maximum possible voltage in the phase of current cutoff.

ELECTRICAL EXPLOSION OF PLANE COPPER CONDUCTORS IN A SKINNED CURRENT MODE

I.M. DATSKO[1], N.A. LABETSKAYA[1], V.A. VAN'KEVICH[1] AND S.A.CHAIKOVSKY[1,2]

[1]Institute of High Current Electronics, Siberian Branch of the Russian Academy of Sciences, 2/3 Akademichesky Ave., Tomsk 634055, Russia
[2]Institute of Electrophysics, Ural Branch of the Russian Academy of Sciences, 106 Amundsen, Yekaterinburg 620016, Russia

It is well known that in a skin explosion of a hollow or a solid cylindrical conductor, a wave of nonlinear diffusion of the magnetic field propagates toward the conductor axis. It was observed [1] that the time at which large-scale instabilities start developing on the conductor surface is obviously related to the time at which the reflected wave arrives at the surface. The propagation of the nonlinear magnetic diffusion waves that arise in plane conductors electrically exploded in a skinned current mode was investigated experimentally. The magnetic induction values far exceeded those necessary for the plate surface exposed to the magnetic field to explode. The choice of plane conductor loads was motivated by the possibility to observe the plasma formation at the back side of the plate. The experiment was carried out on the MIG high-current generator at a current of amplitude up to 2.5 MA and rise time 100 ns. The formation of plasma at the conductor surface was detected by the occurrence of visible light, which was imaged by a four-frame optical camera with a frame exposure time of 3 ns. It was observed that in the given experimental conditions, a plasma channel formed on the back side of the foil about 75 ns after the onset of current flow [2]. Estimates obtained taking into account the enhancement of the magnetic field at the plate edge showed that it took 70–80 ns for the nonlinear magnetic diffusion wave to propagate from the plate edge to its center. The estimates were in good agreement with the experimental data. This made it possible to connect the formation of the plasma channel with a wave of nonlinear magnetic diffusion converging from the edges to the longitudinal axis of the foil. The channel formation pattern was investigated in relation to the magnetic field strength and the load width.

REFERENCES

[1] I. M. Datsko, S. A. Chaikovsky, N. A. Labetskaya, and V. I. Oreshkin and N.A. Ratakhin, "Dynamics of large-scale instabilities in conductors electrically exploded in strong magnetic fields," Journal of Physics: Conference Series, vol. 552, 2014.

[2] S. A. Chaikovskii, V. I. Oreshkin, N. A. Labetskaya, I. M. Datsko, D. V. Rybka, V. A. Vankevich, N. A. Ratakhin, "Peculiarities of an electrical explosion of flat conductors in the current skinningmode," Russian Physics Journal, vol. 62. no. 7, pp. 1235-1242, 2019.

ON MODELLING THE TRANSPORT LINE WHEN COVERING THE CURRENT-CARRYING SURFACE WITH VARIOUS MATERIALS*

S.I. TKACHENKO [1,2,3], V.V. ALEKSANDROV[2], A.V. BRANITSKII[2], E.V. GRABOVSKII[2], I.N. FROLOV[2], K.V. KHISHCHENKO[1,3], G.M. OLEINIK[2], A.A. SAMOKHIN[2], A.O. SHISHLOV[2]

[1]Moscow Institute of Physics and Technology, ,Dolgoprudny, Moscow Region, Russia
[2]State Research Center of the Russian Federation—Troitsk Institute for Innovation and Fusion Research, Troitsk, Moscow, Russia
[3]Joint Institute for High Temperatures of the Russian Academy of Sciences, Moscow, Russia

When a high-density current pulse flows through a magnetically insulated transmission line (MITL), the gap may be shorted by the explosion products of the current-carrying surface (plasma, electron beams, etc.). This can lead to noticeable current losses, and, consequently, to a smaller contribution of energy to the load under study. To obtain the most extreme parameters in the experiment, it is necessary to study the possibilities of increasing the efficiency of current pulse transportation. The possibility of increasing the efficiency of the transport line when covering the current-carrying surface with various materials was investigated.

Numerical calculations were performed to simulate the processes that occur in a thick-walled tube when a current with a high linear density is passed through it. The profile of current pulse was $I(t) = 0.5I_0(1-\cos(\pi t/\tau))$; $\tau = 180$ ns, with an amplitude of $I_0 = 2.6$ MA. Thus, the amplitude value of the linear current density in these calculations was $I_l = 2.8$ MA/cm. When a submicrosecond current flows with a linear density of more than 1 MA/cm, the metal is significantly heated, up to melting, evaporation, and ionization. A system of one-dimensional MHD equations was solved in the one-temperature approximation. To describe the properties of a real substance, we used wide-range semi-empirical equations of state [1] taking into account phase transformations (melting and evaporation) and the possibility of implementing metastable states, as well as the dependence of transport coefficients (conductivity and heat capacity) on temperature [2–3].

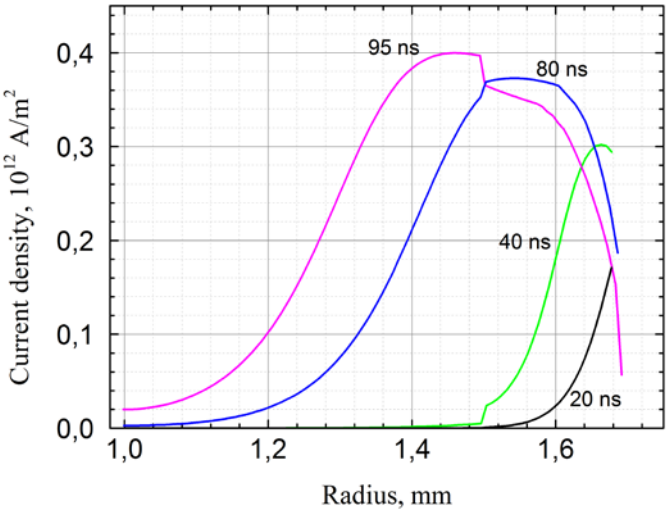

Fig.1. Distribution of current density over stainless steel tube (d =3 mm) covered by lead foil with thickness of 180 μm at different times.

REFERENCES

[1] V.E. Fortov, K.V. Khishchenko, P.R. Levashov, I.V. Lomonosov, “Wide-range multi-phase equations of state for metals”, Nucl. Instr. Meth. Phys. Res. A 415, 604, 1998.

[2] H. Knoepfel, *Pulsed High Magnetic Fields* (North Holland, Amsterdam, 1970).

[3] E.V. Grabovskii, P.R. Levashov, G.M. Oleinik, C.L. Olson, P.V. Sasorov, V.P. Smirnov, S.I. Tkachenko, and K.V. Khishchenko “Formation and Dynamics of Plasma Layers Formed on the Foil Surface under the Action of a High-Current Pulse”Plasma Physics Reports, Vol. 32, No. 9, p. 718, 2006.

* This work was supported by the fundamental research program of the Presidium RAS "New approaches to the creation and study of extreme states of matter."

INTRODUCTION OF AL_2O_3 RODS INTO DBD FOR CO_2 CONVERSION: UNDERSTANDING THE SYNERGISTIC EFFECT OF PLASMA-CATALYSIS

M. ZHU[1], F.F. WU[2], H.MA[2], S.Q. WU[1], C.H. ZHANG[1]

[1] Jiangsu Key Laboratory of New Energy Generation and Power Conversion, Nanjing University of Aeronautics and Astronautics, Nanjing 211106, China
[2] Zhejiang Key Laboratory for Protection Technology of High-Rise Operation, ZheJiang HuaDian Equipment Testing Institute Co.Ltd, Hangzhou 310015, China

Packed bed plasma reactors (PBPRs) are gaining increasing interest for environmental applications, such as dry reforming of methane, CO_2 conversion and hazardous air pollutants, as they improve the product selectivity and enhance conversion efficiency compared to a non-packed reactor. However, the disordered discharge gaps among the packing materials result in complicated electrical and optical characteristics of plasma, leading to the interaction between the plasma and packing materials is not well understood.

In this study, we therefore first introduce the Al_2O_3 rods as the packing material, which apply uniform distributed, by means of 3D printed holder, for keeping the identical plasma characteristics of each rod. And the plasma generation on the surface of rod can be observed in a visualize PBPRs. The effect of the number of rods on the plasma reactivity, optical and electrical characteristics were studied detailed by using CO_2 as the inlet gas and AC supply. Fig. 1 shows the schematic diagram of the experimental setup.

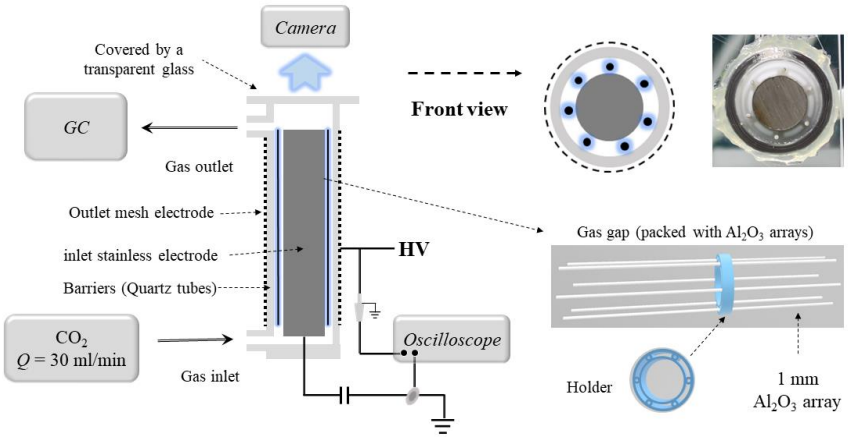

Fig.1. Schematic diagram of the experimental setup.

Fig. 2 shows the discharge pictures of plasma while packing Al_2O_3 rods in the PBPRs and vice-versa. It can be indicated from those pictures that a packing of Al_2O_3 rods is found to shift the discharge behavior from volumetric micro discharges to a combination of surface discharges around the rod and weak micro discharges in the space between the rod and electrode, especially as the number of rods increased to 18.

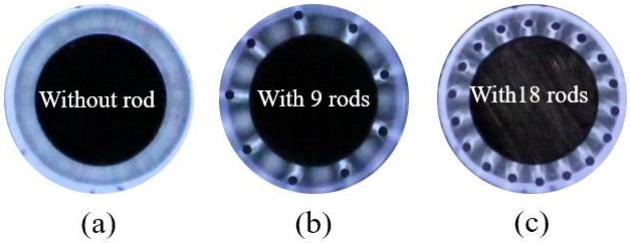

Fig.2. Plasma discharge images (a) without rod, (b) with 9 rods, and (c) with 18 rods, $P_{discharge}$ = 27 W, the camera aperture is 1/30 s.

Furthermore, we also find that discharge electric-characteristic changes considerably when packing the Al_2O_3 rods into PBPRs. As the number of Al_2O_3 rods increased from 6 to 18, the breakdown voltage of plasma decreased from 6.6 kV to 5.3 kV and the injected power of plasma increased slightly when the applied voltage is constant. However, the above changes of discharge behaviors have a weak effect on CO_2 conversion, since the surface of rod without adding any catalytic active component.

LASER BEAM COUPLING WITH A CAPILLARY DISCHARGE PLASMA FOR ELECTRON WAKEFIELD ACCELERATION: SIMULATIONS VS EXPERIMENTS*

G. A. BAGDASAROV, P. V. SASOROV, O. G. OLKHOVSKAYA, V. A. GASILOV

M.V. Keldysh Institute of Applied Mathematics, Miusskaya sq., 4a, Moscow, Russia

Capillary discharges are widely used in many experiments as simple and convenient tool able to generate a “quiet” plasma with reliably controlled parameters. Compact laser-plasma accelerators (LPA) of charged particles are considered as one of the most promising applications of capillary plasmas. Capillary discharge is applied to create plasma waveguide in order to channel an accelerating laser pulse. Such LPAs are able to accelerate electron bunches up to GeV energy level using capillaries ~10-20 centimeters long [1].

The capillary operation parameters principally affects the results of these experiments. The long (several decimetres) and thin (several microns) capillary is needed to achieve maximum acceleration but its fabrication is laborious and unreasonably expensive for the LPA experiments. Also capillary can be damaged by electric current pulse that is used to create plasma waveguide.

Consistent numerical modeling of plasma-dynamics and laser pulse propagation in plasma channel is required to predict results of future LPA experiments with longer capillaries (~10 cm or more). To implement complete start-to-end numerical experiments we developed computer models and numerical techniques incorporated into magnetohydrodynamic (MHD) code MARPLE (KIAM RAS, 2012) [1-4]. Appropriate results of numerical predictions that were done for the BELLA experimental facility (LBLN, USA) are discussed in our presentation.

The computations were carried out using supercomputers K60 and K100 at KIAM RAS.

REFERENCES

[1] G.Bagdasarov et al. Phys. Plasmas 24, 053111 (2017)
[2] G.Bagdasarov et al. Phys. Plasmas 24, 083109 (2017)
[3] G.Bagdasarov et al. Phys. Plasmas 24, 123120 (2017)
[4] A.J. Gonsalves et Al. Phys Rev. Lett. 122, 084801 (2019)

* The work was supported by the Russian Foundation for Basic Research grant 20-31-70015, also by EU Reg.Dev.Fund Ns.CZ.02.1.01/0.0/0.0/15 008/0000162, CZ.02.1.01/0.0/0.0/15_003/0000449 and by the MoEYaS of the Czech Republic No.LQ1606.

DEVELOPMENT OF LARGE-SCALE INSTABILITIES AT FAST-RISING STRONG MAGNETIC FIELDS

N A LABETSKAYA[1], V I ORESHKIN[1], S A CHAIKOVSKY[1,2], I M DATSKO[1], D V RYBKA[1], V A VAN'KEVICH[1]

[1] *Institute of High Current Electronics SB RAS, Tomsk, Russia*
[2] *Institute of Electrophysics UD RAS, Ekaterinburg, Russia*

This work presents experimental results on electrical explosion of metal cylindrical conductors with a diameter of 2 mm at the magnetic field up to 400 T. The experiments were carried out on the MIG high-current generator (current level up to 2.5 MA, current rise time of 100 ns). Plasma jets expanded in radial direction with a velocity of $7 \cdot 10^5$ cm/s have been recorded on the surface of the conductor. One possible cause of formation of such plasma structure is a growth of flut-like instabilities.

FORMATION AND DYNAMICS OF THE CURRENT SHEATH IN THE PLASMA SHELL OF A Z-PINCH IN THE MICROSECOND IMPLOSION REGIME*

R. K. CHERDIZOV, V. A. KOKSHENEV, A. V. SHISHLOV, N. E. KURMAEV, V.I. ORESHKIN, A.G. ROUSSKIKH, A.S. ZHIGALIN

rustam.k.cherdizov@gmail.com
Institute of High Current Electronics, Siberian Branch, Russian Academy of Sciences, Akademichesky Avenue 2/3, 634055, Tomsk, Russia

Experiments with a metal-puff at a current of 2-3 MA were carried out on the GIT-12 generator (4.7 MA, 1.7 μs) at the IHCE SB RAS in Tomsk. The report presents results of a study of the current sheath (CS) formation and dynamics in a Z-pinch shell formed by an arc discharge plasma in fumes of aluminum vaporized from electrodes. The experiments were carried out for two Z-pinch configurations: with the outer plasma shell formed by 48 plasma guns located on a diameter of 350 mm, and without it. To determine the characteristics of the CS, inductive grooves were used to register the derivative of the current at the input of the Z-pinch, an inductive voltage divider was used to register the pulse shape at the input of the load unit, and magnetic probes (B-dot) were used to register the dynamics of the CS during implosion. To record the motion of the shell in the optical range, streak camera and a 4-frame HSFC-Pro camera (exposure time of 3 ns and with an interval between frames of 20 to 60 ns) were used. The B-dots were located inside the holes in the grid covering the end face of the inner cathode electrode, at radii of 2, 3, 6, and 9 cm.

The CS width decreases as it moves toward to the axis from 3-4 cm at a diameter of 18 cm to ~1.5 cm at diameters of 4-6 cm. At the same time, the current density increases from 10 kA/cm^2 to 50 kA/cm^2. In the final stage of implosion, from a diameter of 6.5 cm (from this diameter it is possible to observe implosion by optical diagnostics), visible boundary of the Z-pinch shell, recorded by optical measurements, corresponds to the signals from B-dot at radii of 3 and 2 cm.

Configuration with the outer plasma shell allows increasing the amplitude of the current in the load. Also, at the early stage of implosion, a more compact current sheath is formed. Compact CS allows stabilizing Z-pinch compression from large diameters in the microsecond implosion regime.

The results observed in the experiments can correspond to the structure of a Z-pinch in which there is a 1 cm thick magnetic piston. In front of piston there is a jump in the density of the raked plasma. Intensive processes of ionization and excitation are taking place in this area. When a piston moves at a supersonic speed, a shock wave arises in the plasma. The sharp boundary between the CS and the plasma density front is recorded by optical diagnostics. The foregoing does not contradict the results of numerical modeling and analysis of the structure of the current shell of the Z-pinch in [1].

REFERENCES

[1] V.V. Vikhrev, S.I. Braginsky, "Z-pinch dynamics," Plasma theory issues, vol.10, M., Atomisdat, 1980.

* The work was supported by Russian Science Foundation Grant # № 19-19-00127.

INVESTIGATION OF OSCILLATORY PROCESSES AT PERIPHERAL PLASMA OF VACUUM SPARK

D.L. KIRKO, O.A. BASHUTIN, A.S. SAVJOLOV, P.P. SIDOROV

National Research Nuclear University MEPhI, Moscow, Russia

A low-inductance vacuum spark along with a plasma focus is used to simulate the process of pinching the plasma shell and to research the appearance of plasma dots or micropinches [1-3]. This discharge has intense radiation in the x-ray and ultraviolet spectral ranges. Under the action of a vacuum spark plasma on the surface of the electrodes various types of surface microstructures were registered [4,5].

In the experimental setup a storage capacitor with capacity 10 μF with charging voltage 10–20 kV was used. The discharge system contained an anode with diameter 3-5 mm of a pointed shape and a cylindrical cathode with a hole in the center. For the experiments steel and copper electrodes were used. The pressure in the chamber was maintained in the range 10^{-4}-10^{-5} Torr. The discharge current was 70–150 kA with discharge period 6.0 μs. To turn on the discharge the trigger ignition was used. Near the maximum current on the waveform the feature corresponding to pinching of the discharge is observed. Also plasma points appear at this time. Therefore intense X-ray radiation with quanta energy E>2 keV is registered. At the same time high-frequency electric oscillations in the region 5–95 MHz are formed [4,5].

Using spectral equipment the peripheral plasma of a vacuum spark was diagnosed in the visible and ultraviolet ranges. In the experiments the lines of iron ions, silicon ions and carbon atoms are the most intense. With the help of the hydrogen lines H_α, H_β, and H_γ the plasma temperature for various discharge modes was calculated using the method of relative intensities of spectral lines. The values of the peripheral plasma temperature of the vacuum spark are in the range 8700-9400 K. The measured temperature of the peripheral plasma is much lower than the temperature values existing in the pinch region and in the plasma points. In the time dependences of the intensities of the spectral lines oscillatory processes with frequencies in the kilohertz region are manifested.

The surface of the electrodes was researched by Hitachi TM1000 and VEGA 3 SEM electron microscopes using. The surface near the anode tip contains regions that are most strongly affected by intense electron beams. For this surface in the case of steel electrodes regions a wavy relief containing are registered. Three types of wave-like structures were identified on the wavelength depending: “long” structures with wavelengths 150-200 μm, “middle” structures: 80-120 μm and “short” structures: 20-60 μm. The characteristic height of these waves is in the range 10–50 μm. The arrangement of “middle” waves on the peaks of “long” waves and “short” waves on the peaks of “middle” waves is observed. A similar phenomenon of wavelength decreasing is represented in hydrodynamics in the case of gravitational waves in shallow water (riffles) [6]. In this work the formation of this wave-like surface relief was researched. A possible mechanism of the origin of the wave-like structures is proposed.

REFERENCES

[1] W.A. Cilliers, R.U. Datla, H.R. Griem, “Spectroscopic measurements on vacuum spark plasmas,” Phys. Rev. A, vol. 12**,** no. 4, pp. 1408-1419, 1975.

[2] K.N. Koshelev, N.R. Pereira, “Plasma points and radiative collapse in vacuum spark,” J. Appl. Phys., vol.69, p. 21, 1991.

[3] O.A. Bashutin, A.S. Savjolov, “Suprathermal electrons in a vacuum spark discharge,” Plasma Physics Reports, vol. 42, no. 4, pp. 347–354, 2016.

[4] D.L. Kirko, A.S. Savelov, “Wave processes in the plasma of a low-inductive vacuum spark,” Russian Physics Journal, vol. 57, no. 11, pp.1455-1458, 2015.

[5] D.L. Kirko, A.S. Savjolov, “Investigation of oscillatory phenomena in the near electrode plasma of vacuum spark,” J. Phys. Conf. Ser., 2018. vol. 1115, p. 022010.

[6] B.B. Kadomtsev, “Collective phenomena in plasma”, Moscow, Nauka, 1988.

ON DOUBLE SHELL FORMATION MECHANISM DURING IMPLOSION OF PLASMA PUFF Z-PINCHES*

D.L. SHMELEV[1], A.S. ZHIGALIN[2], S.A CHAIKOVSKY[1], V.I. ORESHKIN[2], A.G. ROUSSKIKH[2]

[1]Institute of Electrophysics, UB, RAS, Ekaterinburg, Russia
[2]Institute of High Current Electronics, SB, RAS, Tomsk, Russia

This work presents the results of experimental and theoretical researches of impact of tailored density profile and application of external axial magnetic field on initial spatial distribution of the plasma density in the plasma metal puff Z-pinch and on its implosion dynamics. It has been discovered that upon implosion of the plasma metal puff Z-pinch some stripes interpreted as the system of two coaxial shells appear on the optical images (Fig. 1,a). With the help of numerical simulation the formation of the plasma liner consisting of a mixture of carbon and bismuth ions and formed by the expansion of the plasma jet of the arc burning on the bismuth electrode has been considered in this work. It has been shown that the lightweight carbon ions facilitate formation of the density distribution smoothly decreasing with the increase in radius, that, in turn, leads to suppression of the Rayleigh–Taylor instability in the current sheath upon further implosion. It has also been demonstrated that availability of the two types of ions in plasma considerably different in mass leads to formation (in the compression phase) of a double shell with externally located heavy ions (Fig. 1,b,c). It has also been shown that the application of the external axial magnetic field leads to reduction in the plasma metal puff Z-pinch initial diameter.

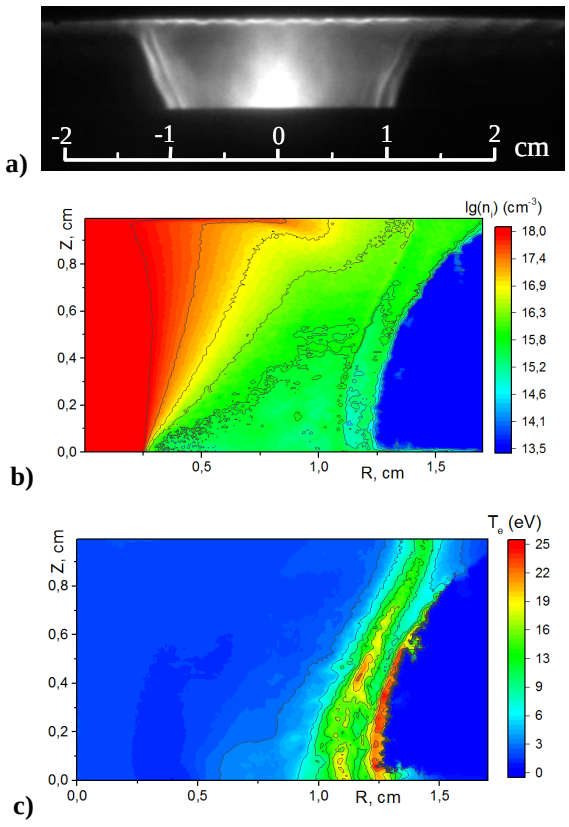

Fig.1. a) Two parallel glowing shells observed during the experiment [1]; b) density of plasma ions (lg(n), n (cm3)); c) electron temperature. Bz0=0, t=230 ns. Two parallel shells can be seen at the external boundary.

REFERENCES

[1] A.G. Rousskikh, A. S. Zhigalin, V. I. Oreshkin, R. B. Baksht, “Measuring the compression velocity of a Z pinch in an axial magnetic field”, Phys. Plasmas, vol. 24, 063519, 2017; doi: 10.1063/1.4986096

* The work was supported by the Russian Foundation for Basic Research (grants No. 18-08-00547; 17-38-50155).

COMPARATIVE ANALYSIS OF THE RAYLEIGH–TAYLOR INSTABILITY SUPPRESSION DURING COMPRESSION OF METALLIC GAS-PUFF Z PINCH AT THE MIG AND GIT-12 FACILITIES.[1]

A. S. ZHIGALIN, A. G. ROUSSKIKH*, V. I. ORESHKIN*,**, A.V. SHISHLOV*, R. K. CHERDIZOV*, V.A. KOKSHENEV*, R. B. BAKSHT**

** Institute of High Current Electronics SB RAS, 2/3 Academichesky ave., Tomsk, 634055, Russia, E-mail: Zhigalin@ovpe2.hcei.tsc.ru*
*** National Research Tomsk Polytechnic University, pr. Lenina 30, Tomsk, 634050 Russia*

We present experiments on compression of metallic gas-puff Z pinches. Experiments were performed on the MIG generator and GIT-12 generator. The MIG generator is a multifunctional generator with current amplitude of 2.5 MA and a current rise time of about 100 ns [1]. The GIT-12 generator is an Arkad'ev-Marx generator. The generator provides the current of 4.7 MA with the current rise time of 1.7 μs in the short-circuit load [2]. Metallic gas-puff was the main element of the load mode on both generators. Metallic gas-puff pinches were formed using plasma guns where plasma production was initiated by a vacuum arc discharge [3]. All of the plasma gun electrodes were made of magnesium or aluminum. The diameter of the central electrode was 4 mm. The pinch length in the experiments on the MIG was 15 mm, and on the GIT-12 was 20 mm. The plasma gun power system is a capacitor battery, consisting of 4 capacitors connected in parallel (Cgun = 20 μF), which were charged to a voltage of 15 to 35 kV.

To visualize the process of metallic gas-puff Z pinch implosion, we performed time-gated imaging of the visible pinch radiation. An HSFC Pro 4-channel, 12-bit intensified charge-coupled device (ICCD) camera was used to take successive images in a single shot. The image analysis had shown that during compression of metallic gas-puff Z pinch, Rayleigh-Taylor instabilities were suppressed. Final pinch compression diameter determined. The optimal (from the point of view of radiation output in magnesium K-lines) formation time of a plasma jet of a vacuum-arc discharge was determined.

.

REFERENCES

[1] *B. A. Kablambaev, A. V. Luchinskii, V. K. Petin, N. A. Ratakhin, S. A. Sorokin, V. F. Fedushchak, S. A. Chaikovskii, and S. V. Shlyakhtun, //* Vopr. At. Nauki Tekhn. - 2001 - Nos. 3–4 - 149.

[2] *A.V.Shishlov, R.B.Baksht, S.A.Chaikovsky, A.V.Fedunin,et al – Laser Physics. – 2006. – V.16, No.1. – Pp.183-193.*

[3] *Baksht R, Oreshkin V, Rousskikh A and Zhigalin A //* Plasma Physics and Controlled Fusion – 2018 -№ **60** - 035015

[1] This work was supported by the Russian Foundation for Basic Research (Grant # 18-08-00728) and by project.

EXPLOSIVE INSTABILITY OF THE SURFACE OF A CONDUCTING FLUID IN AN ELECTRIC FIELD IN CONFINED AXISYMMETRIC GEOMETRY*

O.V. ZUBAREVA[1], N.M. ZUBAREV[1,2]

[1]Institute of Electrophysics, Ural Branch, Russian Academy of Sciences, Yekaterinburg, Russia
[2]Lebedev Physical Institute, Russian Academy of Sciences, Moscow, Russia

It is known that the free surface of a conducting liquid exposed to a sufficiently strong electric field is unstable [1]. For an unbounded free surface, the dynamics of instability development is defined by a nonlinear interaction of three plane waves that form a hexagonal structure [2].

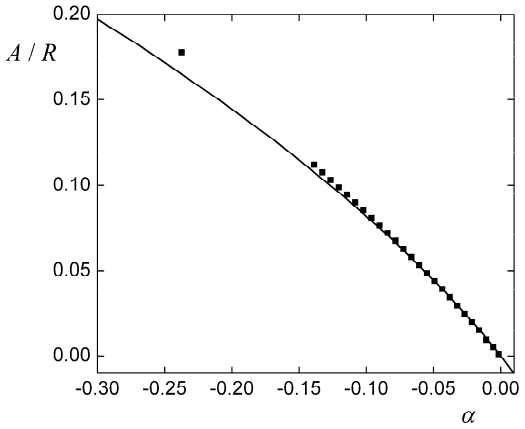

Fig.1. Stationary solutions for the perturbation amplitude. The separate points demonstrate the results of numerical simulations; the solid line corresponds to our analytical results.

In the present work, we consider the case of bounded axisymmetric system geometry: the fluid occupies a domain of radius *R*. We suppose that the fluid is incompressible and inviscid and its (axisymmetric) motion in an applied normal electric field *E* is irrotational. Taking into account the influence of quadratic and cubic nonlinearities, we derive an amplitude equation that describes the evolution of the boundary. In the framework of this equation, we find the conditions for hard excitation of boundary instability, which leads to explosive growth of surface perturbations. In particular, in a subcritical field $E < E_c$ (the instability develops if the electric field exceeds the critical value E_c), such a condition may imply that the surface perturbation amplitude exceeds its stationary value. The amplitude of stationary solutions (the electric and capillary forces are mutually compensated at the boundary for these solutions) can be found analytically using the condition of extremality of the potential energy functional. We arrive at the algebraic equation

$$A\left(56.2\alpha R^2 + 56.8AR + 145.5A^2\right) = 0\,, \qquad (1)$$

where *A* is the surface perturbation amplitude and $\alpha = E^2 / E_c^2 - 1$ is the supercriticality parameter, where E_c is the critical field [1,2]. The nontrivial solution of Eq. (1) is shown in Fig. 1 ($A = 0$ is its trivial solution). The solution branch is directed to the left. This suggests that the high-order nonlinearity plays a destabilizing role. The separate points in Fig. 1 correspond to the results of numerical solution of the problem of finding equilibrium configurations of the free surface of a conducting liquid. As can be seen from the figure, the results of numerical and analytical calculations are in good agreement.

REFERENCES

[1] L. Tonks, "A theory of liquid surface rupture by a uniform electric field," Phys. Rev., vol. 48, no. 6, pp. 562-568, 1935.

[2] N.M. Zubarev, O.V. Zubareva, "Dynamics of the free surface of a conducting liquid in a near-critical electric field," Tech. Phys., vol. 46, no. 7, pp. 806–814, 2001.

*The work was supported by RFBR project No 19-08-00098.

PLASMA FORMATION AT THE INITIAL STAGE OF A SKIN EXPLOSION OF CYLINDRICAL CONDUCTORS *

I.M. DATSKO, N.A. LABETSKAYA and V.A. VAN'KEVICH

Institute of High Current Electronics, Siberian Branch of the Russian Academy of Sciences
2/3 Akademichesky Ave., Tomsk 634055, Russia

Plasma formation at the surface of a conductor is a key issue in terms of the energy deposited in the metal. This process has not been adequately studied for the rise rates of the magnetic field strength characteristic of the magnetically insulated transmission lines of multi-mega-ampere generators. Therefore, this study was aimed at investigating the dynamics of a dense plasma formed at the surface of a metal at a magnetic induction of 2–6 MGs rising with a rate of $(2–5)\cdot10^{13}$ Gs/s. The experiment was carried out on the MIG high-current generator at a current of amplitude up to 2.5 MA and rise time 100 ns. The formation of plasma at the conductor surface was detected by the occurrence of visible light which was imaged by a four-frame optical camera with a frame exposure time of 3 ns. In addition, vacuum photodiodes were used to detect the temperature of the surface plasma reaching more than 1 eV in the black body approximation. The internal structure of the surface plasma was observed for an exposure time of 2–3 ns by exposing the plasma to the x radiation with $h\nu > 0.8$ keV generated by an X pinch. In the experiment, cylindrical conductors of different diameter fabricated of different materials were electrically exploded in magnetic fields at induction rise rates varied from 10^{13} to $5\cdot10^{13}$ Gs/s. It was observed that as the current through a cylindrical conductor increased, bright "spots" appeared on its surface, which were attributed as plasma formation sites, namely, as sources of low-temperature and comparatively low-density plasma. Subsequently, current channels developed in this plasma, as can be seen in Fig. 1.

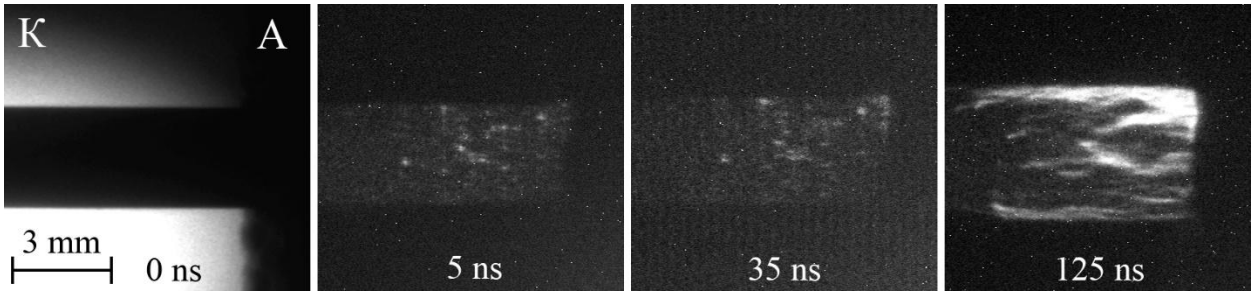

Fig.1. Initial stage of the skin explosion of aluminum conductors of diameter 3 mm.

At magnetic induction rise rates greater than 10^{13} Gs/s, the spots are formed and develop very rapidly. Therefore, to image this process, cameras with a frame exposure time of less than 1 ns are required. In our experimental conditions, for a duralumin conductor of diameter 3 mm we observed that the visible light emission began at the 80th nanosecond. The temperature of the surface plasma reached more than 1 eV in 90 ns. At the 160th nanosecond, the plasma column imaged in the visible self-radiation, with expanded at an average velocity of 10^6 cm/s, had a diameter 3.5 mm; its maximum diameter, in view of perturbations, was 3.8 mm.

* This work was supported by the Russian Foundation for Basic Research (grant No 19-08-00479).

INFLUENCE OF X-PINCH GEOMETRIC PARAMETERS ON THE CHARACTERISTICS OF SOFT X-RAY RADIATION SOURCE*

A.P. ARTYOMOV[1], A.V. FEDUNIN[1], I.M. DATSKO[1], V.A. VANKEVICH[1], D.V. RYBKA[1], V.I. ORESHKIN[1,2], S.A. CHAIKOVSKY[1,3]

[1] Institute of High Current Electronics SB RAS, Tomsk, Russia
[2] National Research Tomsk Polytechnic University, Tomsk, Russia
[3] Institute of Electrophysics, Ural Branch, Russian Academy of Sciences, Ekaterinburg, Russia

The work is devoted to the study of the influence of the wire inclination angle α relative to the X-pinch axis and the load gap size l (fig. 1) on the hot spots number formed into the X-pinch neck and on the x-ray radiation yield. The experiments were performed on the compact pulse power generator XPG-3 (210 kA, 190 ns) [1, 2]. We studied an X-pinch consisting of four molybdenum wires with a diameter of 25 μm. Such configuration of the X-pinch is the most optimal for our pulse power generator in terms of the soft x-ray radiation source characteristics [3, 4]. In the experiment, we studied the X-pinch configurations with the following values of the wire inclination angle α relative to the Z axis: 37°; 40°; 45°; 50° and 56°.

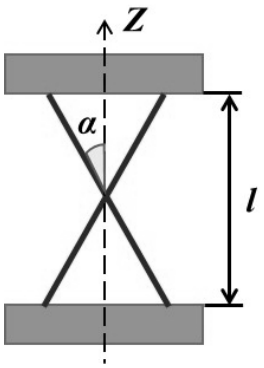

Fig.1. Illustration of the wire inclination angle α relative to the Z axis of the X-pinch, where l is the load gap length.

The diamond radiation detectors DRD (Alameda Applied Sciences Corp.) were used to measure the x-ray pulse power of the X-pinch. To determine the number of the hot spots, we used the technique of obtaining test-object radiographic images [5].

It was shown that the highest X-pinch x-ray yields were observed in the experiments when the wire inclination angle α relative to the Z axis was 40° - 45° (see fig.1). The x-ray pulse yields in this case were 1.1 ± 0.4 J in the spectral range $h\nu = 1.5 – 5$ keV. If the inclination angle α of wires increased or decreased, a sharp drop of the x-ray pulse yield was observed.

The maximum probability of a single hot spot formation was observed when the inclination angle of the wires α = 45°. In this case, a single hot spot formed in 40% of all shots. In other cases, two or three hot spots were formed. Decreasing of the angle α leads to a significant decreasing of probability of appearance of a single hot spot. Increasing of the angle α to 50° and 56° leads to a significant drop in the X-pinch x-ray reproducibility.

The use of a load gap l above 7 mm leads to a rising of the X-pinch inductance and a decreasing of the efficiency of the energy conversion from the primary storage device into x-ray radiation.

REFERENCES

[1] A. G. Rousskikh, A. V. Fedyunin, A. P. Artyomov et al, “Radiograph pr-pzp-m1 based on pz-pinch,” Izv. Vyssh. Uchebn. Zaved. Fiz., vol. 61, no. 9/2, pp. 62-66, 2018.

[2] S. A. Chaikovsky, A. P. Artyomov, N. V. Zharova et al, “Small-size high-current generators for x-ray backlighting, “ Russ. Phys. Jour., vol. 60, no. 8, pp. 1408-1412, December 2017.

[3] A. P. Artyomov, N. A. Labetskaya, A. V. Fedunin, S. A. Chaikovsky, “Size measurement of x-ray source based on X-pinch,” Bull. of Lebedev Phys. Inst., vol. 37, no. 6, pp. 31-34, 2010.

[4] S. A. Pikuz, T. A. Shelkovenko, D. A. Hammer, “X-Pinch. Part II, “ Plasma Phys. Rep., vol. 41, no. 6, pp. 445–491, 2015.

[5] A. P. Artyomov, S. A. Chaikovsky, V. I. Oreshkin, A. V. Fedunin, A. G. Rousskikh, N. A. Ratakhin, “On the size of soft x-ray radiation source based on x-pinch, “ Izv. Vyssh. Uchebn. Zaved. Fiz., vol. 62, no. 12, pp. 33-41.

* The work was supported in part by the Russian Foundation for Basic Research (grant No. 19-08-00479 and No. 18-08-00728).

"ZIPPERING" EFFECT AT ALUMINUM METAL-PUFF LINER IMPLOSIONS ON THE GIT-12 PULSE POWER GENERATOR*

A.G. ROUSSKIKH[1], A.V. SHISHLOV[1,2], V.I. ORESHKIN[1,2], A.S. ZHIGALIN[1], R.K. CHERDIZOV[1], F.I. FURSOV[1], V.A. KOKSHENEV[1], N.E. KURMAEV[1]

[1]Institute of High Current Electronics SB RAS, 2/3 Akademichesky Ave., Tomsk, 634055, Russia
[2]National Research Tomsk Polytechnic University, 30 Lenina Ave., Tomsk, 634050, Russia

The work is devoted to studying a "zippering" effect [1-3] arising in a process of Al metal-puff liner implosions on the pulse power generator GIT-12 (the load current of 4.7 MA with the rate of 3 kA/ns and the current rise time of 1.7 μs). Since a "zippering" effect is a consequence of an initial distribution of a conductive substance of a liner plasma shell, consideration of a liner compression dynamics along its height gives an idea about a initial compression conditions of a plasma shells. An influence of a "zippering" effect on an Al K-shell radiation output power is considered. The relationship between a "zippering" effect and a density gradient of the Al metal-puff liners along its axis for various plasma gun designs is considered.

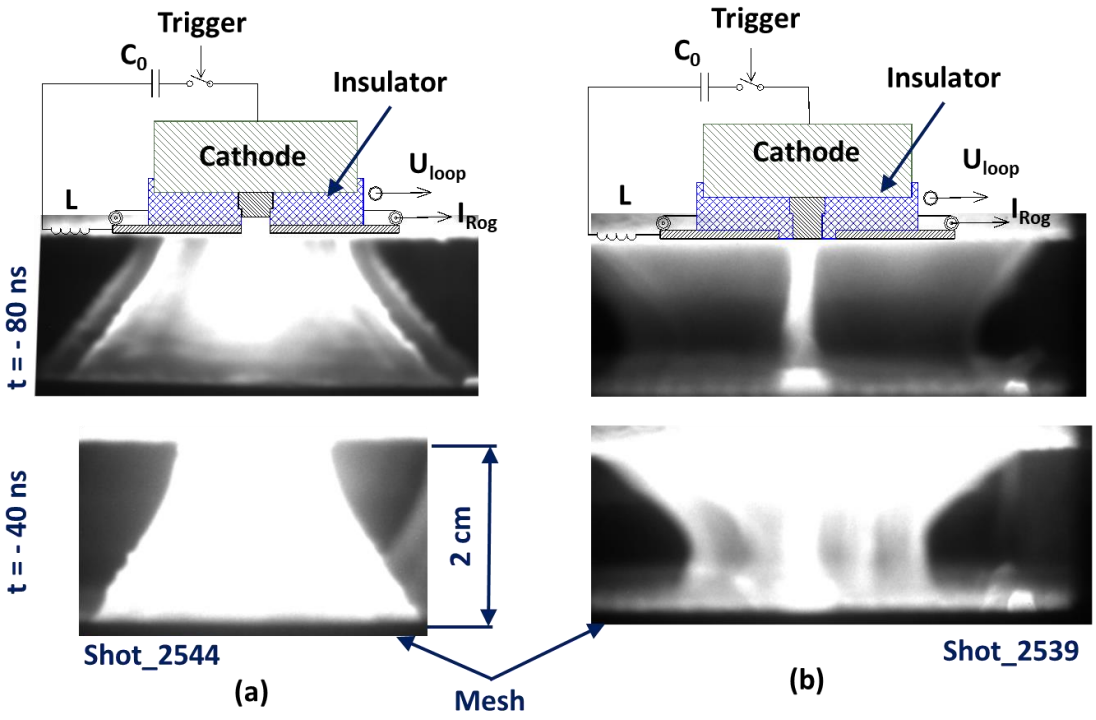

Fig.1. The inclination angle of the plasma shell outer boundary, depending on the plasma gun design.

As shown in Figure 1, an inclination angle of a plasma shell outer boundary varies depending on a plasma gun design. If a plasma jet flows out from a hole in the plasma gun anode (see Fig. 1 (a)), a liner shell with a traditional inclination angle is formed at which a plasma shell expands from cathode to anode. If cathode and anode of a plasma gun are located in the same plane (see Fig. 1 (b)), a liner shell with an inverse inclination angle is formed at which the plasma shell expands from anode to cathode.

REFERENCES

[1] C. Deeney, P. D. LePell, F. L. Cochran, M. C. Coulter, K. G. Whitney, and J. Davis, "Argon gas puff implosion experiments and two-dimensional modeling," Phys. Fluids B 5 (3), March 1993.

[2] T. W. Hussey, M. K. Matzen, N. F. Roderick, "Large-scale-length nonuniformities in gas puff implosions," J.Appl.Phys. 59(8), April 1986.

[3] B. Jones, C. A. Coverdale, D. S. Nielsen, M. C. Jones, C. Deeney, J. D. Serrano, L. B. Nielsen-Weber, C. J. Meyer, J. P. Apruzese, R. W. Clark, and P. L. Coleman, "Multicolor, time-gated, soft x-ray pinhole imaging of wire array and gas puff Z pinches on the Z and Saturn pulsed power generators," Rev. Sci. Instrum. **79**, 10E906, May 2008.

* The work was supported by the Russian Foundation for Basic Research (grants No 18-08-00728).

ELECTRICAL DIAGNOSTICS OF SURFACE DIELECTRIC-BARRIER DISCHARGE WITH COAXIAL CONFIGURATION*

R.A. AZNABAEV,[1,2] *A.M. ASTAFIEV*,[1] *M.E. PINCHUK*,[1] *O.M. STEPANOVA*.[1]

[1]*Institute for Electrophysics and Electric Power of Russian Academy of Sciences (IEE RAS), St.-Petersburg, Russia*
[2]*St.-Petersburg State University, St. Petersburg, Russia*

We studied the surface barrier discharge with a coaxial configuration designed to generate a plasma jet in a helium flow emerging into the ambient air [1]. A technique for determining the extension size of the plasma region based on measuring RMS values of current and applied voltage has been proposed.

The discharge cell is a quartz tube with an inner diameter of 7.5 mm and a wall thickness of 1 mm, inside which we mounted a coaxial electrode system with a total diameter of 4 mm. High voltage is applied to the rod electrode wrapped by fluorine insulation. The ground electrode is made from a piece of copper foil that covers not all of the insulation. Both electrodes are isolated from each other and from the gas by a dielectric layer. The discharge develops along the free surface of the fluorine insulation from the edge of the grounded electrode (Fig. 1, right).

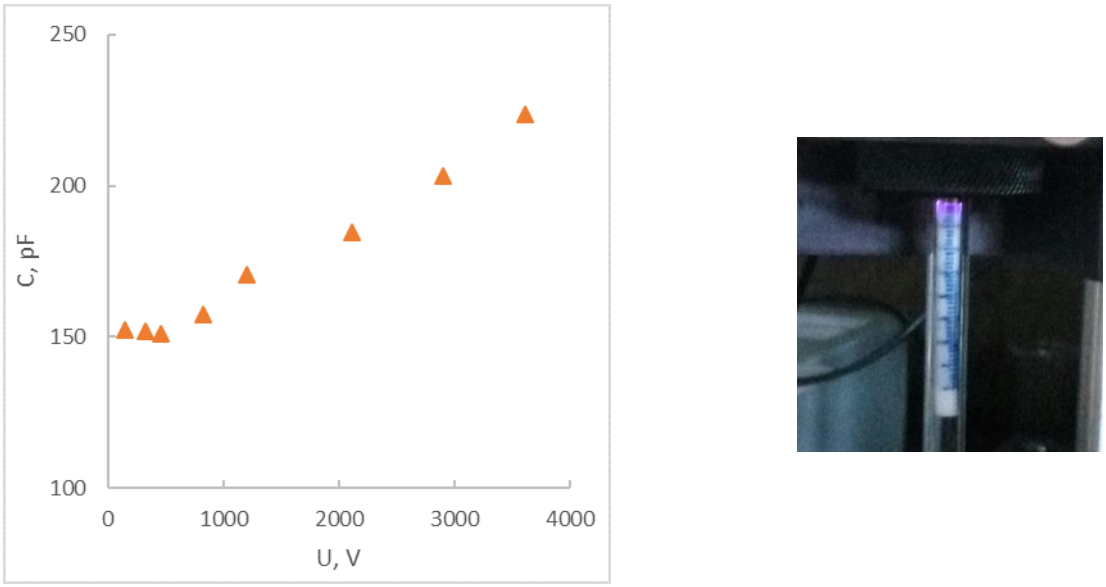

Fig.1. Capacitance of the discharge electrode system vs RMS voltage (left) and photo of the discharge region in helium (right).

With the development of the discharge, the capacity of the discharge region changes in proportion to the discharge region length. The capacitance of the system was calculated from measured currents and voltages (Fig. 1, left). Using photographic images of the discharge region (Fig. 1, right), the specific capacitance of the discharge system was determined depending on the RMS voltages. The obtained values were compared with the calculated capacitance of the given electrode system geometry. We obtained a good agreement. Thus, we can conclude it is possible to determine the size of the discharge region from electrical measurements.

REFERENCES

[1] O. M. Stepanova, O. V. Rybalchenko, M. E. Pinchuk, A. M. Astafiev, O. G. Orlova, V. A. Spodobin, and A. A. Kudryavtsev, “Bactericidal Effect of a Dielectric Barrier Discharge Plasma Jet Generated in Laminar and Preturbulent Helium Flows” Plasma Medicine, vol. 7, n 3, pp.187-200, 2017.

* The work has been supported by the Russian Science Foundation (project 18-79-10048).

OPTICAL DETECTION OF SKIN-ELECTRICAL EXPLOSION COPPER PROFILED CYLINDRICAL CONDUCTORS *

N A LABETSKAYA[1], S A CHAIKOVSKY[1,2], I M DATSKO[1], V I ORESHKIN[1], D V RYBKA[1], V A VAN'KEVICH[1]

[1] *Institute of High Current Electronics SB RAS, Tomsk, Russia*
[2] *Institute of Electrophysics UD RAS, Ekaterinburg, Russia*

This work presents the results of the experiments that were carried out on the high-current generator MIG (the current amplitude up to 2.5 MA, the current rise time of 100 ns) in magnetic fields with the induction of 200 – 800 T. The own glow of conductor surface in the visible range of the spectrum was observed at field strengths of the order of 300-400 T. The formation of plasma jets were registered in experiments with illumination of conductor by external source of radiation. Jets flowed from the edges of steps in the radial direction at a speed up to $2.7 \cdot 10^6$ cm/s, which exceeded several times the speed of surface plasma expansion of steps.

* The work was supported by the Russian Foundation for Basic Research (grants № 19-08-00479)

RESONANCE CHARACTERISTICS IN OVERSIZED SLOW-WAVE STRUCTURE OF A MULTIWAVE CHERENKOV GENERATOR WITH DIFFRACTION REFLECTORS IN SUB-THZ FREQUENCY RANGE

V.A. CHAZOV, M.P. DEICHULY, V.I. KOSHELEV

Institute of High Current Electronics, SB RAS, Tomsk, Russian Federation

Numerical simulations of the electromagnetic resonance characteristics in the complex slow-wave structures (SWS) composed of two periodic sections and a diffraction reflector were carried out. We have investigated the model of oversized SWS (the ratio of the SWS diameter (D) to the radiation wavelength (λ) is much more than one) with diffraction reflectors for searching of electromagnetic fields of hybrid waves [1] and coupled wave resonances [2]. At the same time, we were interested in the SWS options most effective in terms of quality factor and power distributions depending on the diffraction reflector geometries (number of diaphragms, reflector period).

We considered the SWS with the ratio of $D/\lambda \approx 14$ and studied the surface-bulk resonance of TM_{01}-TM_{014} modes and TM_{01} resonance without TM_{014}. To test the main features of the TM_{01}-TM_{014} interaction and to simulate the electromagnetic fields of the coupled wave, the sub-terahertz frequency range (110 -115 GHz) was selected. It is known that the diffraction reflector (Bragg reflector) can provide the power increasing and high electric field intensity in an output section in comparison with structure without reflector [3, 4]. In this work, we study the influence of different diffraction reflectors on the longitudinal resonances in the two-section SWS with different section lengths. We show that the intersection of TM_{01} and TM_{014} resonances leads to the redistribution of the wave mode powers in the marked area (drift tube length is from 0.27 to 0.36 cm) (Fig.1).

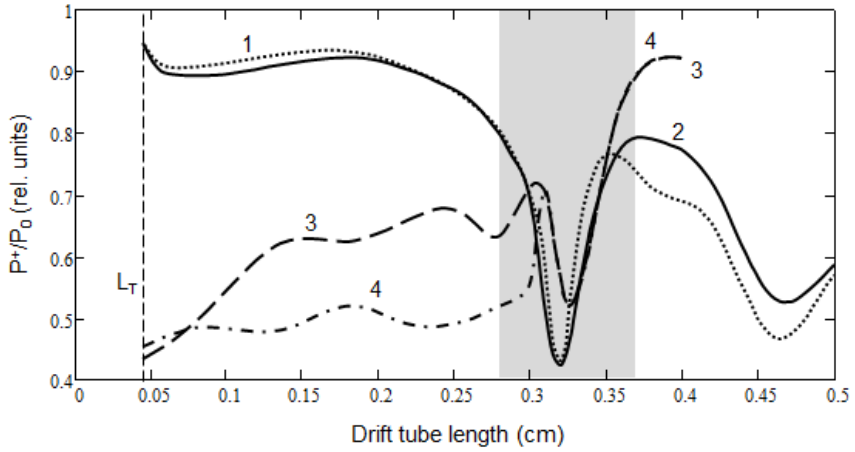

Fig.1. The ratio of the output mode power to the total mode power versus the drift tube length for the SWS composed of two section (20 diaphragms in each section) and 6 reflector diaphragms ((1) –TM_{01} and (3) –TM_{014}), another one SWS – 8 reflector diaphragms ((2) –TM_{01} and (4) –TM_{014}). $L_{drifr\ tube} = L_T$ corresponds to the periodic one-section SWS with 40 diaphragms.

The ratio of the output power to the total one is $P^+/P_0 = 0.5$ for two-section SWS without a diffraction reflector. Numerical simulation of SWS with diffraction reflector have demonstrated the increasing of output power in 1.9 times for TM_{01} as compared with SWS without reflector. Despite the decreasing of P^+/P_0 the surface-bulk resonance of TM_{01} and TM_{014} modes (marked area in Fig.1) provides the transverse synchronization of high-current electron beam and electromagnetic field.

REFERENCES

[1] M.P. Deichuly, V.I. Koshelev, V.A. Chazov, “Bulk resonances of symmetric hybrid waves in overmode biperiodic slow-wave structure,” Rus. Phys. J. , vol. 60, no. 8, pp. 1379–1385, 2017.

[2] V.A. Chazov, M.P. Deichuly, V.I. Koshelev, “Bulk resonances in slow-wave structures with high ratios of diameter to radiation wavelength,” Proc. 20th Int. Conf. on High Current Electronics (ISHCE), Tomsk, Russia, pp. 74–79, 2018.

[3] V.I. Koshelev, M.P. Deichuly, “Reflectors influence on MWCG efficiency and radiation stability,” Proc. 13th Int. Conf. on High Current Electronics (ISHCE), Tomsk, Russia, pp. 296–299, 2004.

[4] J. Gardelle, P. Modin, H.P. Bluem, R.H. Jackson, J.D. Jarvis, A.M. M. Todd, J.T. Donohue, “A Compact THz source: 100/200 GHz operation of a cylindrical Smith–Purcell Free-Electron Laser,” IEEE Transactions on terahertz science and technology, vol. 6, no. 3, pp. 497–502, may 2016.

DIRECTIVITY CHARACTERISTICS OF AN ULTRAWIDEBAND HYBRID OFFSET ANTENNA IN THE 1–4 GHZ FREQUENCY RANGE *

YU. I. BUYANOV, E.V. BALZOVSKY, V.I. KOSHELEV, E.S. NEKRASOV

Institute of High Current Electronics SB RAS, Tomsk, Russia

The paper presents the results of numerical simulation in the 1–4 GHz frequency band of an ultrawideband offset paraboloid antenna, the feed of which is a four-element antenna array (AA). The hybrid antenna is designed for a high-power source of ultrawideband radiation excited by a bipolar pulse of 0.5 ns duration with a central frequency of the spectrum of 2 GHz. The phase centers of the array elements are located around the focus of the paraboloid at a distance equal to transverse dimensions of the combined antenna KA used as the AA elements. Two elements of the AA (elements 2 and 4) are located along the major axis and the other two (elements 1 and 3) are located along the minor axis of the reflector, the aperture of which has the shape of an ellipse (Fig. 1). The patterns of such an antenna at a frequency of 2 GHz are given in [1].

In an offset antenna, the maximum of the feed pattern should be directed to the middle of the reflector. If the feed is an AA, then the normal to its aperture is deviated from the focal axis. As a result, the elements located along the minor axis are shifted away from the focal axis, while the elements located along the major axis are shifted not only to the side but also along the focal axis. Calculations of impedance and patterns of an ultrawideband hybrid antenna with a controlled directivity of the beam were carried out using the 4NEC2 computer code [2]. This code allows simulating the antennas containing conductive surfaces, replacing them with a metal mesh (Fig. 1).

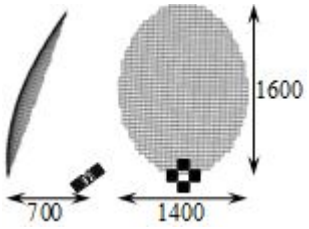

Fig. 1. A wire model of the offset antenna.

For a comparative analysis of the parameters of a hybrid antenna with the parameters of an antenna that uses a single KA with dimensions of 60×65×70 mm as a feed, the pattern and the VSWR in the frequency range of 1-4 GHz were calculated. The gain of a hybrid antenna with an elliptical aperture of 1400×1600 mm and a focal length of 700 mm varies from 16 dB to 30 dB.

Using a four-channel pulse former, one can implement different patterns of the beam, changing the excitation options of the array elements. When the AA elements are alternately excited, the wave beam deviates from the focal axis in the direction which is opposite to the shifting of the element from the focus. Simultaneous excitation of all AA elements forms a wave beam whose direction coincides with the focal axis, and the pattern is close to the pattern of the beam excited by a single KA, as long as the distance between the AA elements does not exceed the wavelength. At high frequencies, where the distance between the elements (12 cm) exceeds the wavelength, the wave beam is divided into four wave beams. This reduces the gain of the hybrid antenna by several dB. Simultaneous excitation of a pair of elements (2 and 4, or 1 and 3) forms wave beams, each of which is split into two wave beams at high frequencies. If elements 2 and 4 have vertical polarization, and elements 1 and 3 have horizontal polarization, then when all four elements are excited, a wave beam with elliptical polarization can be formed.

Thus, in a hybrid antenna, several modes of wave beam formation can be implemented, namely, five positions of the pattern maximum and three types of polarization: vertical, horizontal, and elliptical.

REFERENCES

[1] Yu.I. Buyanov, E.V. Balzovsky, V.I. Koshelev, E.S. Nekrasov, "Radiation characteristics of an offset reflector antenna excited by a combined antenna array," Russ. Phys. J., vol. 62, 2019, pp. 1214–1219.

[2] A. Voor, "NEC based antenna modeler and optimiser [Online]," available: http://www.gsl.net/4nec2/.

* The work was supported by the Russian Foundation for Basic Research under grant No. 20-08-00529.

CREATION OF NON-STATIONARY VOLUME DISCHARGE INSIDE CYLINDRICAL MICROWAVE RESONATOR *

HONGDA LI[1], S.A. SOSNOVSKIY[2], A.A. LUKANIN[3], A.A. TSKHE[4], A.A. TSKHE[5], V.I. SACHKOV[6], M.A. KAZARYAN[7]
[1]School of Equipment Engineering, Ph.D., assistant professor, Shenyang Ligong University, Shenyang, China
[2]Candidate of Physical and Mathematical Science, Senior Researcher, National Research Tomsk State University, Tomsk, Russia
[3]Lead Engineer, Tomsk state university of architecture and building, Tomsk, Russia
[4]Candidate of Technical Science, Tomsk state university of architecture and building, Tomsk, Russia
[5]Doctoral student, National Research Tomsk Polytechnic University, Tomsk, Russia
[6]Doctor of Chemical Sciences, National Research Tomsk State University, Tomsk, Russia
[7]Doctor of Physical and Mathematical Sciences, Lebedev Physical Institute RAS, Moscow, Russia

The need for thermal treatment in various industries has prompted research and development of powerful, non-polluting, inexpensive and low-cost low-temperature plasma source. Microwave induced plasma is another method of producing electrodeless torches, but still it has only been used at relatively low power. The main application has been in chemical analysis and emission monitoring. There have also been some experiments to splitting halogenated organic compounds. We created and operated in the air a highly efficient and powerful plasmatron of atmospheric pressure (Fig.1). Plasma device uses volume cylindrical resonator (2,45 GHz), inside which volume discharge (low-temperature plasma) is formed when supply voltage pulse is applied to magnetron. In the present experiments, a pulse microwave power of 0,6 kW was used. When the discharge was ignited, the power pulse ended, to avoid overheating the medium and resonator. In the experiments, ozone was obtained, which corresponds to an average free electron energy of about 5 eV. The gas flow rate varied from 1 to 30 liters per minute through a 14 mm diameter outlet. The maximum power and volume of gas flow is limited by the currently available hardware components. Significant potential exists to scale up activities. This approach can open up new possibilities for thermal treatment using commercially available and inexpensive magnetrons at 2,45 GHz and 915 MHz frequencies. Capital costs can be less than a dollar per watt for high-power systems (> 75 kW), and there will be no electrodes to wear out. These features can make this technology competitive with traditional plasma arc torch and high-frequency induction plasma.

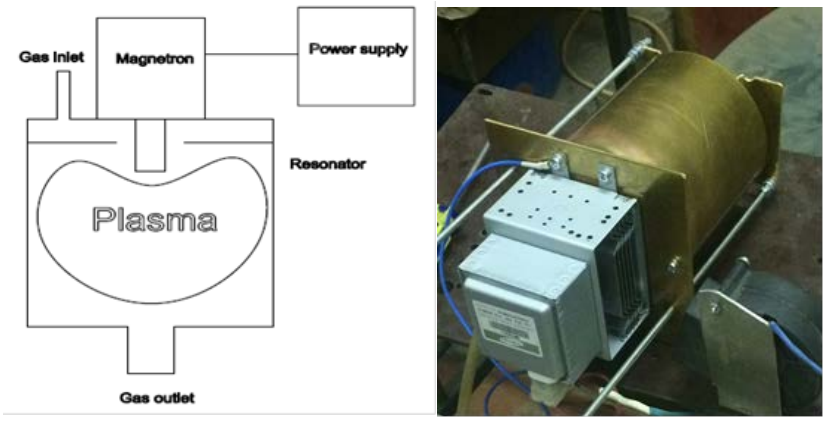

a) b)

Fig.1. Experimental set up microwave plasma torch in air: a) Schematic diagram of experiment system; b) photo of the resonator with magnetron.

The report presents physical and mathematical modeling of the processes of obtained by exposure to a high-voltage microwave pulse discharge and modeling of the physicochemical processes during discharge pulse.

* This research was supported by Ministry of Science and Higher Education of the Russian Federation, project No 0721-2020-0028.

ENERGY EXTRACTION THROUGH MULTICHANNEL INTERFERENCE SWITCH OF MICROWAVE COMPRESSORS*

S.N ARTEMENKO,B.S.IGUMNOV, S.N.NOVIKOV

Tomsk Polytechnic University, Tomsk, Russia

The active microwave compressor comprises a number of cavities [1]. Pulses are formed by releasing the energy in synchronism through the multichannel interference switch of the new design. The switch is a waveguide structure in the form of "embedded" bridges and has the single joint switching gap. Each embedded bridge consists of two waveguide H-tees with the mutual side arm. Increase in the number of cavities and extraction channels, and hence, in power and energy of output pulses occurs in a geometric sequence with the geometric ratio of 2. The switched power, at that, regardless of the number of cavities and channels, is one-fourth as much as the total power of the output channels. This ratio is due to the basic properties of the bridge formed by two H-tees with a mutual side arm. It is shown that S– band compressors of this type can form pulses with a gigawatt power level. The first experimental results oftests of X- band compressor of this type are presented. They comply with the expected characteristics of the compressor.

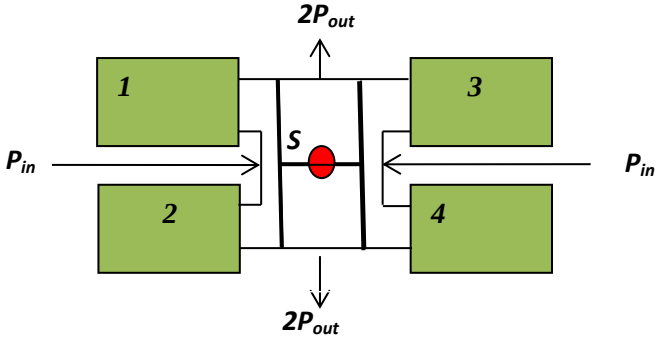

Fig.1. Schematic of the four-cavity compressor. 1,2,3,4 – cavities, S- microwave switch gap, a,b,c,d- embedded bridge.

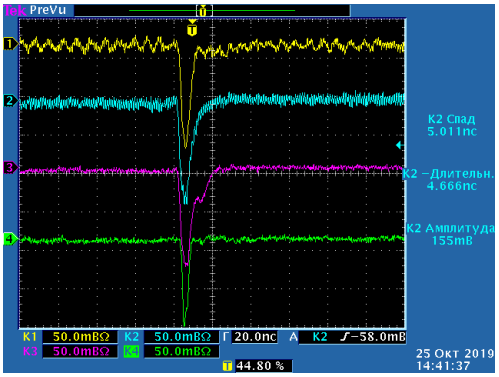

Fig.2. Oscillograms of synchronous energy extraction through the four-channel microwave switch.

REFERENCES

.

[1] S.N.Artemenko, V.S.Igumnov and Yu,G.Yushkov.*"*Multichannel Systems of Resonant Microwave Pulse Compression,"IEEE Transactions onPS, vol.43, no.10, pp.3537-3540, October 2015.

* The work was supported by RFBR. Grant N 08-08-00155-a .

NARROWBAND RADIATION OF PLASMA RELATIVISTIC MICROWAVE EMITTER*

I.E.IVANOV

Prokhorov General Physics Institute of the Russian Academy of Sciences, Moscow, Russia

The operation of a plasma relativistic emitter in the free-running mode is considered. The electron energy of the beam is 0.5 MeV, the beam current is 2.4 kA, and the plasma density in the system is 2 x 10^{12} cm^{-3}.In contrast to [1, 2], the base cavity length is reduced to 0.39 m. This made it possible to obtain rather simple spectra and generation on a small number of longitudinal modes. The experimental spectra of microwave radiation in the range 2 - 4 GHz with duration of up to 300 ns at various values of the plasma density are presented.

A technique is proposed for identifying the parameters of longitudinal microwave modes based on the radiation frequency, the length of cavity L_{base}, and the velocity of electron beam u. The parameters were chosen as variable: the electron velocity of the relativistic beam and the effective cavity length L_{eff}, which should exceed the base length of 0.39 m. An integer number of half-waves *N* must be placed along the length of resonator. The *u* and L_{eff} values were selected that correspond to the smallest deviation of *N* from the integer value, Fig.1.

The following parameters are determined: phase velocity of the wave, effective cavity length Leff, wavelength Lwave and the number of half-waves *N*, which fit the length of the effective cavity, the magnitude of the wave entry into the coaxial output waveguide upon reflection ($L_{eff} - L_{base}$).

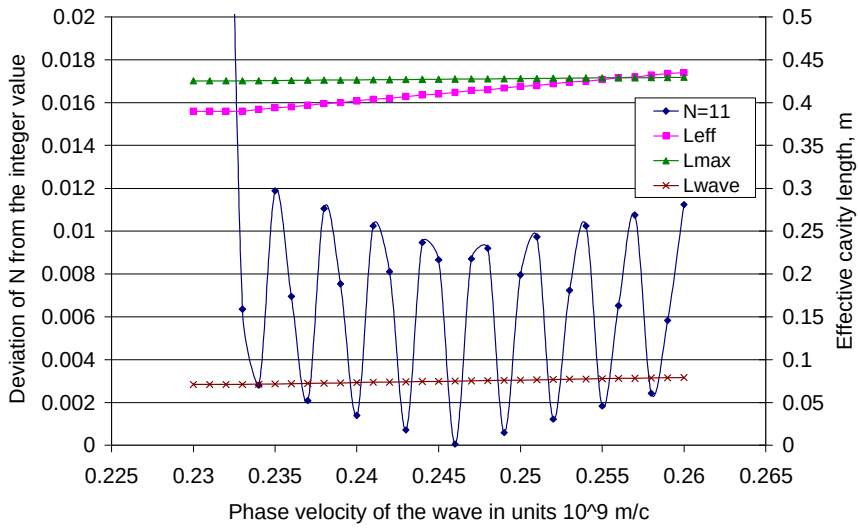

Fig.1. Dependence of the deviation of *N* from the integer value for different phase velocity *u* of the wave in the resonator for a frequency of 3.284 GHz.

The results obtained show that electrons with energies exceeding 0.5 MeV participate in the microwave generation. The decisive factor for generation at a specific wavelength is the speed of the beam electrons, not the plasma density. The plasma density affects the position of the amplification region on the frequency axis, and the specific generation frequency in this region is related to the electrons of the relativistic beam. Since the formation of a relativistic beam is associated with explosive emission of electrons, there is no exact repeatability of the injection of the electron beam into the system; each pulse is individual. This means the fundamental non-repeatability of the generation frequencies from pulse to pulse. Only an approximate binding takes place. To obtain generation at the same frequencies, a calibrated beam is needed.

REFERENCES

[1] I. L. Bogdankevich, I. E. Ivanov, O. T. Loza, et al. "Fine Structure of the Emission Spectra of a Relativistic Cherenkov Plasma Maser". Plasma Physics Reports, 2002, Vol. 28, No. 8, pp. 690–698.

[2] I.E.Ivanov, "Radiation Spectra of the Plasma Relativistic Microwave Oscillator", Plasma Physics Reports , 2019, v. 45, N 7, p. 662-673

* The work was supported by the Russian Science Foundation under grant No. 19-08-00625 A.

TUNING OF POLARIZATION OF A SQUARE 2X2 ARRAY OF HELIX ANTENNAS[1]

YU.A ANDREEV, V.I. KOSHELEV, S.S. SMIRNOV

Institute of High Current Electronics SB RAS, Tomsk, Russia

In the paper, the possibility of smooth tuning of the ellipticity ratio of the radiation of an array of helix antennas is investigated. The array was excited by 1 ns length bipolar voltage pulses. The results of research of a four-element square 2x2 array of helix antennas in a physical experiment are presented. A cylindrical equidistant antenna with an average helix radius r = 48 mm and an inter-turn distance of S = 67 mm was selected as the antenna element. The selected values r and S corresponded to the central frequency f = 1.0 GHz for the axial radiation mode of the helix antenna. The length of the helix was determined by the number of turns N = 6. These helices are equivalent to the array elements presented in [1]. The distance d between the elements in the array was equal to 15, 18 and 21 cm. The design of the studied array is shown in (Fig. 1).

The frequency range of 0.7-1.35 GHz corresponds to the axial radiation mode for a single helix antenna. Studies of the 2x2 array of helix antennas were performed in a wider frequency range: 0.5-2 GHz. The research was performed using the Agilent N5227A vector network analyzer. The matching of the array elements with the feeder at different angles of rotation of the helix around its axis relative to the other array elements was studied. The parameter S21 was also measured between arbitrary array elements at different angles of the helix rotation around its axis relative to the rest of the array elements.

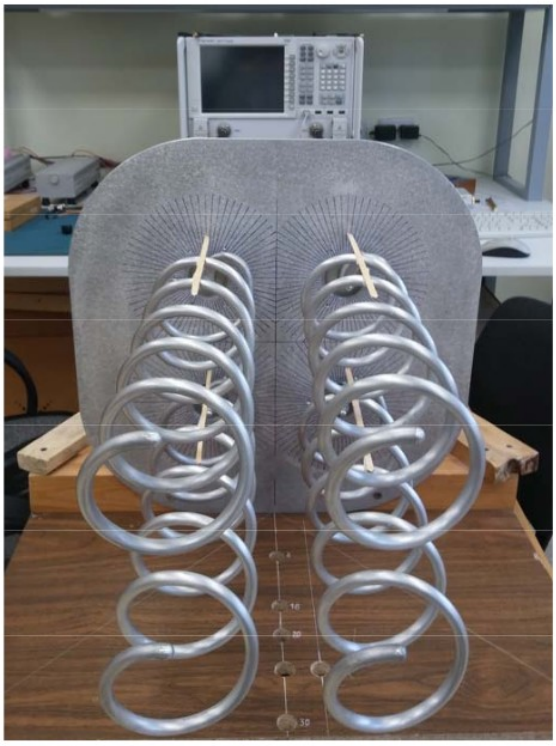

Fig. 1. A square array of helix antennas.

In the radiation mode, ultra-wideband pulses were studied only along the array axis. Finding E y , E x components allows obtaining a hodograph which determines the axial ratio (AR) of the radiated pulse. The dependence of the AR on the rotation of the array elements was studied.

REFERENCES

[1] Yu.A. Andreev, V.I. Koshelev, S.S. Smirnov, "Characteristics of an ultrawidband 8x8 array of cylindrical helical antennas," Proc. 20 th Int.Symposiun on high-current electronics (ISCHE) 2018, pp. 185–189.

1 The work was supported by the Russian Foundation for Basic Research under grant No. 20-08-00529.

HIGH POWER SUB-NANOSECOND MICROWAVE PULSE NON-LINEAR INTERACTION WITH NEUTRAL GAL AND PRELIMINARY FORMED PLASMA[1]

YANG CAO, JOHN LEOPOLD, YURY BLIOKH, GUY SHAFIR, AMONON FISHER, GAD RAANAN, GUY LEIBOVICH, YAKOV E. KRASIK

Physics Faculty, Technion-Israel Institute of Technology, Haifa, 3200003 Israel

We present the first experimental observation of the predicted [1] high-power microwave (9.6 GHz, <500 MW, <0.5 ns) driven plasma wakefield formation in a plasma-filled cylindrical waveguide. The high-power microwave pulse is generated by a super-radiant backward wave oscillator (SR-BWO) driven by an annular electron beam (~280 keV, ~1.5 kA, ~5 ns), produced by a magnetically insulated foilless diode, and guided through a slow-wave structure by a 2.5 T axial magnetic field [2]. Energetic electrons of >20 keV energy were collected in the radial direction outside the waveguide. The appearance of such high energy electrons can be related to the ponderomotive force and the plasma wakefield formation. The transmitted microwave signal shows frequency-modulation and pulse compression, the result of the plasma density modulation appearing in the wake of the propagating microwave pulse. 1D analytical modeling and 3D PIC (Particle-in-Cell) simulations support the experimentally observed frequency modulation of the transmitted microwave pulse and the radial electron accelerations.

REFERENCES

[1] Y. P. Bliokh, J. G. Leopold, G. Shafir, A. Shlapakovski, and Ya. E. Krasik, “Wakefield in a waveguide,” Phys. Plasmas 24, 063112 (2017).

[2] G. Shafir, A. Shlapakovski, M. Siman-Tov, Yu. Bliokh, J. G. Leopold, S. Gleizer, R. Gad, V. V. Rostov, and Ya. E. Krasik, “High power microwave source for a plasma wakefield experiment,” J. Appl. Phys. 121, 033301, (2017).

1 Work supported by a PAZY Government Agency

DYNAMICS OF RADIATION POWER FLOW IN MULTI-WAVE GENERATORS, DEPENDING ON THE DURATION OF THE FRONT OF THE ELECTRON BEAM*

V.N. KORNIENKO, V.A. CHEREPENIN

Kotelnikov IRE RAS, Moscow, Russia

The aim of this work was to search the possible influence of the duration of the front of a relativistic electron beam on the feature of the generation of a multiwave cherenkov generator (MWCG) [1]. The basis for this investigation was the results obtained in the study of the dispersion characteristics of the finite sizes inhomogeneous electrodynamic structure, which was used in the MWCG [2]. Namely, in view of the dense arrangement in space of the "longitudinal wave number - frequency" of the set of admissible eigenmodes, it is possible that the progress of the generating process depends on the spectral width of the exciting pulse formed by the beam front.

The studies were carried out by methods of a computational simulation. It was assumed that the increase of the current at beam front satisfies the linear law. Front durations of 1, 3, and 12 ns were considered. As a controlled quantity, the power flow of electromagnetic radiation in the output section of the device was used. The dependences of the power flow, averaged over the main period of oscillations, on time are shown in Fig. 1.

From the graphs it follows that the alleged relationship exists. The most significant differences in the generation process were observed for a front duration of 1 ns.

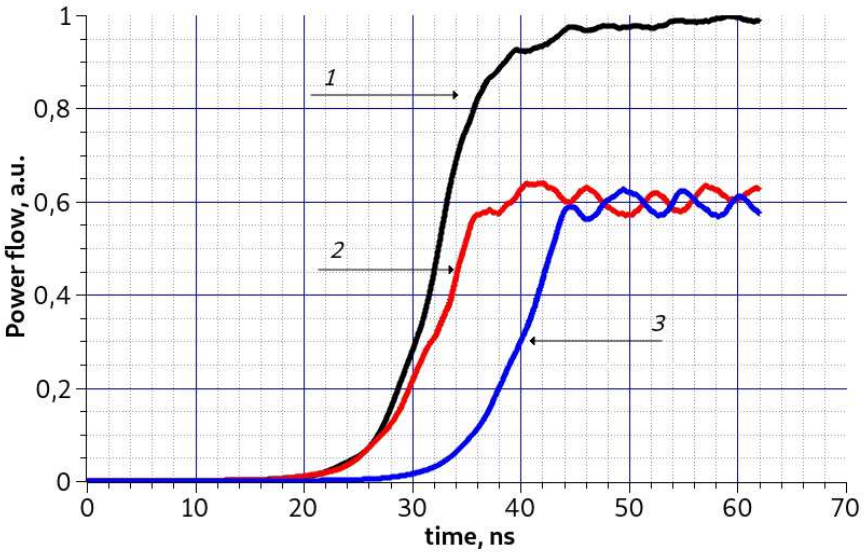

Fig.1. Normalized power flow versus time with a pulse front duration of 1 ns (*1*), 3 ns (*2*) and 12 ns (*3*).

The simulation was performed on the computing resources of the Interagency Supercomputer Center.

REFERENCES

[1] Bugayev S.P., Kanavets V.I., Koshelev V.I., Cherepenin V.A. Relaivistic multiwave SHF-generators. Novosibirsk, Nauka, 1991.

[2] Cherepenin V.A., Kornienko V.N., Investigation of the characteristics of electrodynamic structures of multiwave Cherenkov generators using numerical methods for solving nonstationary problems of electrodynamics, 6th International congress on energy fluxes and radiation effects, Book of Abstracts, Tomsk, Russia, P.91, 2018.

* The work performed as part of the state assignment of the Kotelnikov IRE RAS and partially supported by the RFBR project 19-52-45035-Ind-a

A HETERODYNE CIRCUIT FOR MEASURING THE SPECTRAL CHARACTERISTICS OF KA BAND NANOSECOND HIGH POWER MICROWAVE PULSES

A.I. KLIMOV[1], E.V. EMELYANOV[2], V.YU. KONEV[1], P.V. PRIPUTNEV[1], V.V. ROSTOV[1], R.V. TSYGANKOV[1], A.Y. YUSHCHENKO[2]

[1]Institute of High Current Electronics SB RAS, Tomsk, Russia
[2]JSC "Scientific-Research Institute of Semiconductor Devices", Tomsk, Russia

A circuit have been constructed based on a heterodyne system to measure the spectral characteristics of Ka band high-power nanosecond microwave pulses [1]. The circuit includes a receiving antenna, three input waveguide directional couplers with different coupling coefficients, a variable waveguide attenuator, two coaxial-to-waveguide adapters, a low-loss microwave cable, an additional directional waveguide coupler, as well as a heterodyne system consisting of an electrically controlled electronic attenuator, a mixer and a local oscillator combined in one unit. The input pin-diode attenuator of the system uses a monolithic integrated circuit (MIC) MSM207-02. The MIC MM605 is used as a mixer. The local oscillator was developed based on the MIC HMC506 and two frequency multipliers (MIC's HMC578 and HMC814) with wideband fixed attenuators (MIC's MP503).

The microwave pulse received by the waveguide antenna, attenuated to the acceptable level by one of the input directional couplers, the waveguide attenuator, an additional directional coupler, and also by the cable with coaxial-to-waveguide adapters, is injected into the port of the heterodyne system. Here, the microwave signal is further attenuated by an electronic attenuator. Then the signal is injected into the input port of the mixer. The signal of the local oscillator was injected into the other port of the mixer. The intermediate frequency signal from the mixer output enters the digital oscilloscope for subsequent spectral analysis.

The developed circuit is intended to measure the spectral characteristics of high-power nanosecond microwave pulses in the range of 35.7–37 GHz [2]. The local oscillator frequency was 35.44 GHz. The microwave power at the input port of the heterodyne scheme is to be not more than 50 mW.

This work was funded by the Russian Foundation for Basic Research and the Government of the Tomsk Region of the Russian Federation, grant No. 18-42-700012.

REFERENCES

[1] J. Benford, J.A. Swegle, E. Schamiloglu, High power microwaves. New York–London: Taylor & Francis, 2007, pp. 214–222.

[2] V.V. Rostov, E.M. Totmeninov, R.V. Tsygankov, I.K. Kurkan, O.B. Kovalchuk, A.A. Elchaninov, A.S. Stepchenko, A.V. Gunin, V.Y. Konev, A.Y. Yushchenko, E.V. Emelyanov, "Two-Wave Ka-Band Nanosecond Relativistic Cherenkov Oscillator", IEEE Transactions on Electron Devices, vol. 65, no. 7, pp. 3019–3025, July 2018.

DIRECTIONAL COUPLERS FOR X-BAND HIGH-POWER MICROWAVE OSCILLATORS

A.I. KLIMOV, V.Y. KONEV, E.M. TOTMENINOV, V.V. ROSTOV

Institute of High Current Electronics, Tomsk, Russia

Two directional couplers (for the TM_{01} and TE_{11} modes of a circular waveguide) have been built to use on high-power nanosecond relativistic microwave oscillators [1]. Both couplers operate between 9 and 10 GHz.

Each of the devices consists of a section of circular waveguide connected to a housing in the form of rectangular 23×10 mm waveguide. The waveguides are connected via two holes spaced by $\lambda_g / 4$ where $\lambda_g / 4$ is the wavelength in the main guide. A TM_{01} mode propagating in the circular waveguide has field components E_z, E_r, and H_φ. The component E_z is zero at the waveguide, so the only field components which couple to the rectangular waveguide are E_r and H_φ. These field components leak trough the holes and excite the microwave field in the rectangular waveguide.

In the second coupler, only the field component H_z of the TE_{11} mode couples the waveguides.

The couplers have been tested using the Agilent Technology PNA Network Analyzer N5227A (10 MHz – 67 GHz).

The first coupler was designed to operate with a coupling coefficient of 66.5–69 dB and a directivity of 10–28.5 dB.

The second coupler was designed to operate with a coupling coefficient of about 58 dB and a directivity of 15.8–24.7 dB.

This work was funded by the Russian Foundation for Basic Research and the Government of the Tomsk Region of the Russian Federation, grant No. 18-42-700012.

REFERENCES

[1] J. Benford, J.A. Swegle, E. Schamiloglu, High power microwaves. New York–London: Taylor & Francis, 2007, pp. 214–222.

STUDY OF THE SWITCHING CHARACTERISTICS OF GAAS S-DIODES

S.N. MALTSEV, I.V. ROMANCHENKO, V.Y. KONEV, P.V. PRIPUTNEV, V.V. BARMIN

Institute of high current electronics SB RAS, Tomsk, Russian Federation

This work is devoted to the study of the switching properties of GaAs avalanche S-diodes. The diodes were placed in a special chamber, which is a coaxial waveguide with a gap in the central conductor. Voltage pulses with an amplitude of 600 V and a front equal to 20 ns were applied to the diodes. As a result, it was found that one diode, turned on in the forward direction, sharpes the voltage rise time of 2.5 ns with a response delay of 10 ns. When turned back on, the rise time is reduced to 800 ps with a delay of 12.5 ns. Two diodes connected in series, one of which is turned on in the forward direction and the other in the opposite direction, is triggered with a delay of 15 ns and sharped the voltage rise time by 500 ps. The results obtained show the possibility of using two series-connected GaAs avalanche S-diodes as sharpeners of the front of the modulating pulse in the high voltage mode.

SLOW-WAVE STRUCTURE FOR THE MILLIMETER-BAND BACKWARD-WAVE OSCILLATOR BASED ON THE PSEUDOSPARK-SOURCE ELECTRON GUN*

A.V. STARODUBOV[1,2], A.M. PAVLOV[1], V.V. GALUSHKA[1], R.A. TORGASHOV[1,2], A.G. ROZHNEV[1,2], N.M. RYSKIN[1,2], N. KUMAR[3], VISHANT[3], S. JAIN[3], N. GURJAR[3], K. SINGHAL[3] AND R.K. SHARMA[3]

[1]Saratov State University, Saratov, Russia
[2]Saratov Branch, V.A. Kotel'nikov Institute of Radio Engineering and Electronics RAS, Saratov, Russia
[3]CSIR-Central Electronics Engineering Research Institute, Pilani, Rajasthan, India

Millimeter- and sub millimeter-band sources have attracted significant attention in recent years because of their promising application such as security and counter-terrorism (remote non-destructive monitoring), ultra-high-speed information and communication systems, radio astronomy, spectroscopy, medicine and etc. Nowadays vacuum electron devices still remain the main sources of high power broadband millimeter-wave radiation. Among electron beam sources the pseudospark discharge can be distinguished as a promising pulsed plasma electron beam source with the beam current density up to 10^6 Am^{-2} [1], [2]. The reason is that the pseudospark discharge sourced electron beam has the ability to self-focus due to the unique discharge structure and the formation of ion channel generated by the beam front. Ion channel enables the electron beam to propagate and eliminates the need for a guiding magnetic field [3], [4]. Therefore the development of a compact and high-power vacuum and plasma sources utilizing a pseudospark discharge based hollow cathode electron gun is one of the promising trends.

We have designed the sine-waveguide slow-wave structure (SWS) for the V-band (50-75 GHz) backward-wave oscillator using a pseudospark-sourced sheet electron beam, exploiting the high beam current density of a pseudospark discharge sourced electron beam and the large cross sectional area with reduced space charge effect of the sheet electron beam. The results of the simulation with help of the COMSOL Multiphysics package were obtain. Geometric dimensions of the slow-wave structure were optimized and electrodynamic parameters were simulated. We have considered two cases during numerical simulation: 1) the slow-wave structure is filled with vacuum and 2) the slow-wave structure is filled with plasma. A comparison of the results was carried out. For the fabrication of the slow-wave structure we have used the CNC micro-milling machine [5]. We have verified the dimensions of the fabricated SWS by scanning electron microscopy and optical microscopy studies. Experimental cold-test S-parameters of the fabricated SWS were measured utilizing PNA N5227A vector network analyzer. Also we consider the design and development of the pseudospark discharge based electron gun for a V-band backward-wave oscillator. The backward-wave oscillator is driven with a 30-40 kV, 10-20 A sheet electron beam with 50-100 ns pulse duration. The simulations as per the different beam parameters for the pseudospark-based electron gun has been performed using COMSOL Multiphysics simulation software. The components like hollow cathode, planar anode and multi-gap have been developed. Output power and oscillation frequency are calculated by using 3-D PIC simulation.

Backward-wave oscillator driven by a pseudospark-sourced sheet electron beam can be used in various applications including non-destructive evaluation, spectroscopy and material science, high-data-rate communications, and etc.

REFERENCES

[1] J. Christiansen and C. Schultheiss, "Production of high current particle beams by low pressure spark discharges," *Zeitschrift fur Phys. A Atoms Nucl.*, vol. 290, no. 1, pp. 35–41, Mar. 1979, doi: 10.1007/BF01408477.

[2] H. Yin *et al.*, "Millimeter wave generation from a pseudospark-sourced electron beam," *Phys. Plasmas*, vol. 16, no. 6, 2009, doi: 10.1063/1.3155444.

[3] H. Yin, A. W. Cross, A. D. R. Phelps, D. Zhu, W. He, and K. Ronald, "Propagation and post-acceleration of a pseudospark-sourced electron beam," *J. Appl. Phys.*, vol. 91, no. 8, pp. 5419–5422, 2002, doi: 10.1063/1.1459757.

[4] N. Kumar, R. P. Lamba, A. M. Hossain, U. N. Pal, A. D. R. Phelps, and R. Prakash, "A tapered multi-gap multi-aperture pseudospark-sourced electron gun based X-band slow wave oscillator," *Appl. Phys. Lett.*, vol. 111, no. 21, pp. 1–5, 2017, doi: 10.1063/1.5004227.

[5] A. G. Terentyuk, A. G. Rozhnev, N. M. Ryskin, A. V. Starodubov, V. V. Galushka, and A. M. Pavlov, "Development and Modeling of Folded-Waveguide Slow-Wave Structures for Millimeter-Band Traveling-Wave Tubes," in *2018 43rd International Conference on Infrared, Millimeter, and Terahertz Waves (IRMMW-THz)*, Sep. 2018, pp. 1–1, doi: 10.1109/IRMMW-THz.2018.8510165.

* Work supported by the cooperative grant of Russian Foundation for Basic Research # 19-58-45040 and DST # INT/RUS/RFBR/381.

HIGH-CURRENT LTD SYSTEM FOR MATERIALS RESEARCH*

A.N. GRIGORIEV[1], E.I. KARNAUKHOV[1], I.V. LAVRINOVICH[2], A.D. LENSKIY[2], D.V. MOLCHANOV[2], A.V. PAVLENKO[1], D.V. RYBKA[2], S.A. VAGAYTSEV[2]

[1] Federal State Unitary Enterprise "Russian Federal Nuclear Center - Zababakhin All-Russia Institute of Technical Physics", Snezhinsk, Chelyabinsk Region, Russia
[2] Institute of High Current Electronics SB RAS, Tomsk, Russia

Classical circuits based on a Marx high-voltage generator and a forming line are used, e.g., in multi-module pulsed power facilities such as Z and ZR [1], PTS [2], and GAMMA-16. But such scheme (with one level post-hole convolute) is unsuitable for materials research primarily because the current pulse front duration from their module is limited to $t_{1m} < 200$ ns. That is why such machines cannot provide a flyer impact velocity greater than 8 km/s to a test target at a rated current of 10–15 MA.

For flyer plate impact testing, it is needed to have a current pulse amplitude $I_m \sim 15$ MA and higher at a rise time $t_{1m} \sim 100$ ns (Z, PTS, and GAMMA-16 facilities) or it suffices to have $I_m \sim 8.5$–10.5 MA at $t_{1m} \sim 200$–300 ns.

The use of a linear transformer driver (LTD) generator allows one to eliminate the problem of pulse limitation and to greatly enhance the system efficiency. The energy in an LTD system can be transferred from the primary store to a load without intermediate stores at a pulse rise time of ~200–300 ns determined by the discharge circuit parameters of capacitor-switch assemblies (CSAs).

The paper presents a multi-terawatt LTD system design with an initial energy storage of up to 3 MJ (Fig.1). From a numerical analysis by 0D self-consistent models, the operation of different LTD generator versions is assessed and an optimum one among them is chosen. Also presented is the design of an LTD cavity (Fig.2) based on a new type of bricks—CSAs [4, 5] — which provides a peak power of 7.5 GW at a charge voltage of ±80 kV, CSA inductance of 80 nH, and capacitance of 110 nF.

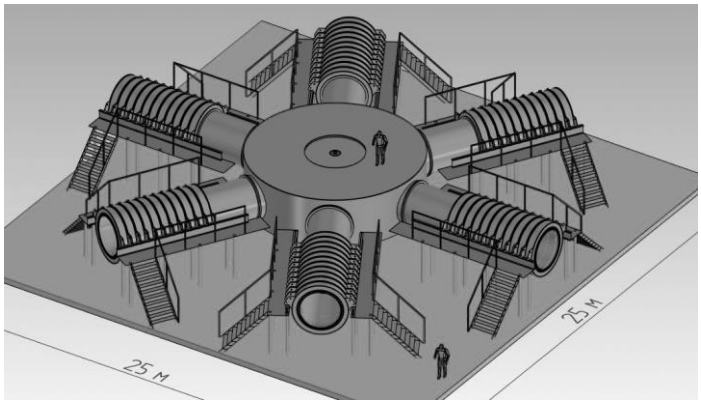

Fig1. Sketch of a general view of the LTD system.

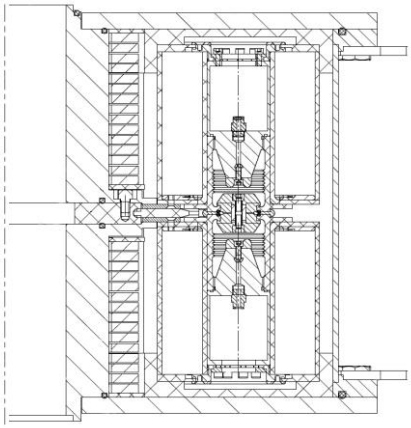

Fig.2 Sketch of LTD cavity and CSA

REFERENCES

[1] D. H. McDaniel, M. G. Mazarakis, D. E. Bliss, J. M., Elizondo, H. C. Harjes, H. C. Ives, D. L. Kitterman, J. E., Maenchen, T. D. Pointon, S. E. Rosenthal, D. L. Smith, K. W. Struve, W. A. Stygar, E. A. Weinbrecht, D. L., Johnson, and J. P. Corley, "The ZR refurbishment, project," in Proc. 5th International Conference on Dense ZPinches, June 23-28, 2002, pp. 23-28.

[2] Deng, W. Xie, S. Feng, M. Wang, H. Li, S. Song, M. Xia,J. Ce, A. He, Q. Tian, Y. Gu, Y. Guan, B. Wei, X. Huang,X. Ren, J. Dan, J. Li, S. Zhou, H. Cai, S. Zhang, K. Wang,Q. Xu, Y. Wang, Z. Zhang, G. Wang, S. Guo, Y. He, Y.Zhou, Z. Zhang, L. Yang, and W. Zou,Matter andRadiation at Extremes1, 48 (2016)

[3] I. Lavrinovich, S. Vagaytsev, A. Erfort, D. Rybka, D. Molchanov, A. Artemov, A. Zhigalin, A. Lensky / New Type Capacitor-Switch Assembly for LTD Technology // 2019 IEEE Pulsed Power & Plasma Science (PPPS), Orlando, FL, USA, 2019, pp. 1-4. DOI: 10.1109/PPPS34859.2019.9009957

[4] D. Molchanov, I. Lavrinovich, A. Artyomov, D. Rybka / New low-inductance capacitor-switch assembly // Journal of Physics: Conference Series. 2018. 1074. 012110.

* The work was supported in part by the Russian Foundation for Basic Research (grant No. 19-48-700017).

A TENS GIGAWATTS REPETITIVE HIGH VOLTAGE PULSE GENERATOR AND ITS APPLICATIONS*

S. LI[1,2], *H. W. YANG*[1,2,*], *Y. W. FAN*[1], *Z. CH. ZHANG*[1,2], *J. M. GAO*[1,2], *T. XUN*[1,2], *D. Q. CHEN*[1,2], *B. L. QIAN*[1]

[1] *College of Advanced Interdisciplinary Studies, National University of Defense Technology, Changsha, China*
[2] *State Key Laboratory of Pulsed Power Laser Technology, Changsha, China*

High voltage pulse generator is crucial for researches on high power microwave and plasma physics. In this paper, a tens gigawatts repetitive rate high voltage pulse generator, which can achieve pulses with ultra-high power level with high repeatability, is investigated numerically and experimentally. Specifically, design considerations of the generator are introduced. Near-field distribution of a spark gap switch is studied numerically and the whole system is analyzed by P-Spice software. An adjustable pulse forming line based on different liquid dielectrics is investigated for widen applications of the generator. Then, the generator was built and experimentally studied in our laboratory. Quasi-square pulses with peak power of 25 GW, peak voltage over 521 kV, peak current of 48 kA, pulse duration of 100 ns, and rise-time of 28 ns were achieved on a dummy load. The repetitive rate was 5 Hz, and peak voltage jitter was approximately 2.7 % in one second. Experimental results show reasonable agreement with numerical studies. Driving by the high voltage pulse generator, microwave pulses with peak power of 4 GW, duration of 50 ns, and repetitive rate of 5 Hz were achieved on series of magnetically insulated transmission line oscillators. Experimental results show reasonable agreement with numerical studies.

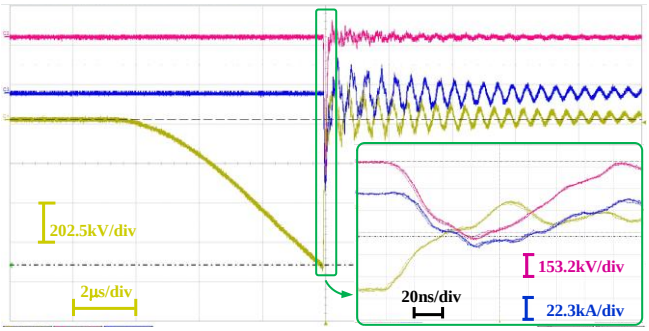

Fig.1. typical repetitive waveforms of the generator

Figures 1 shows the typical repetitive waveform of the generator.

REFERENCES

[1] H. Bluhm, Pulsed Power Systems: Principles and Applications. Springer-Verlag, 2006.

[2] J. Zhang, et al., “Research progresses on Cherenkov and transit-time high-power microwave sources at NUDT,” Matter Radiat. Extremes, 1(3), pp. 163–178, 2016.

[3] W. H. Jiang, K. Yatsui, K. Takayama, et al. (2004). Compact solid-state switched pulsed power and its applications. in Proceedings of the IEEE International Pulsed Power Conference. 92(7), pp: 1180-1196.

[4] E. Schamiloglu, R. J. Barker. Scanning the Special Issue on Pulsed Power: Technology and Applications [J]. Proceedings of the IEEE, 2004(7), pp:1011-1013.

* The authors wish to thank Prof. Jun Zhang, Prof. Juntao He, Prof. Huihuang Zhong, Prof. Jiande Zhang, Prof. Baoliang Qian, Prof. Ting Shu and Prof. Jinliang Liu for their encouragement and valuable suggestions. This work was supported by the National Natural Science Foundation of China under Grant No.51707199 and No.51607183.

GENERATION OF MULTI-GIGAWATT PICOSECOND PULSES BY MAGNETIC COMPRESSION LINES*

E.A. ALICHKIN, M.S. PEDOS, A.V. PONOMAREV, S.N. RUKIN, S.P. TIMOSHENKOV

Institute of Electrophysics UB RAS, 106 Amundsen Str., Yekaterinburg, 620016, Russia

The possibility of creating solid-state picosecond generators with a peak power of tens of GW has been experimentally shown. In the approach, an input pulse of nanosecond duration from a solid-state generator with a semiconductor opening switch (SOS generator) is amplified in peak power and shortened in time by successive stages of gyromagnetic ferrite lines. The essence of the approach is that the lines in each stage operate in a magnetic compression mode (Magnetic Compression Line, MCL), which is realized at close values of the input pulse duration and the period of oscillations generated in the line. In this case, the main part of the input pulse energy is transmitted only to the first peak of the oscillations. In the experiments, we used the SOS generator and a three-stage magnetic compressor based on MCL1–MCL3 lines. Waveforms of power pulses illustrating the process of energy compression are shown in Fig. 1. At the peak power of input pulse of 6 GW (490 kV, 40 Ω) and 7-ns pulse duration generated by the SOS generator, a peak power of 54 GW (1.62 MV, 48 Ω) with 170-ps pulse duration was obtained at the output of the three-stage compressor. Compared with the parameters of the input pulse, the voltage rise rate was increased by ~130 times to 14.8 MV/ns, and the power rise rate was increased by ~350 times to 0.7 TW/ns.

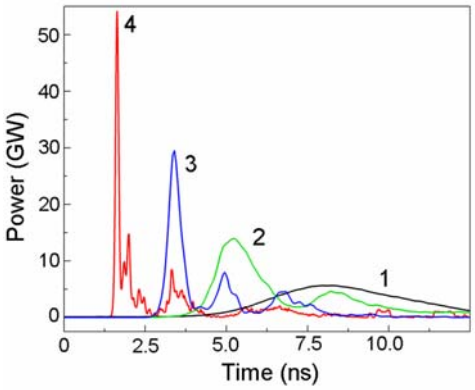

Fig.1. Waveforms illustrating the energy compression process: 1 – input pulse; 2, 3, and 4 – pulses after the first, second and third magnetic compression lines, respectively.

The report will present the design and parameters of the system, as well as the results obtained. The limitations of the approach will be discussed regarding the further reduction in pulse duration and increase in peak power.

* The work was supported by RFBR Grant No. 17-08-00203.

SANDIA-HIGH CURRENT ELECTRONICS INSTITUTE (HCEI) COLLABORATION IN FAST LTD DEVELOPMENT

M. G. MAZARAKIS

Sandia National Laboratories, Albuquerque NM, USA

Following the impressive operational success of the first slow (~1 microsecond) LTD in Gramat, France, that was invented, designed and built by the team at HCEI headed by Boris Kovalchuk [1,2], Dillon McDaniel of Sandia asked the inventors if they could apply this technology for the production of fast ~100 ns pulses. The inventors accepted the challenge, and a number of communications [3] were exchanged between Sandia and HCEI on how the fast LTDs could be used for this research. The first published theoretical analytical study of such fast LTDs was presented in the 1999 Pulsed Power Conference in Monterey, California by M. G. Mazarakis et al., [4]. This paper attracted a lot of interest in the pulsed power community, resulting in a large number of requests for copies. Following that, a strong collaboration started between Sandia and HCEI that culminated in the production of 10 of the largest to-date 1 MA, 1 GW fast LTD cavities which compose now the MYKONOS voltage adders at Sandia. The different stages of the fast LTD development through the years and the up-to-date accomplishments will be presented. Although this technology has mushroomed around the globe, this paper will concentrate solely in the Sandia-HCEI collaboration.

THE COMBINED PLASMA SWITCH WITH INCREASED SUPPLY VOLTAGE AND HIGH PULSE REPEATITION FREQUENCY*

P.A. BOKHAN[1], P.P. GUGIN[1], V.A. KIM, M.A. LAVRUKHIN[1], D.E. ZAKREVSKY[1]

[1]Institute of Semiconductor Physics, Siberian Branch, Russian Academy of Sciences, pr. Akademika Lavrent'eva 13, Novosibirsk, 630090, Russia, gugin@isp.nsc.ru

Investigation of the eptron with an increased supply voltage up to U = 100 kV and a pulse repetition frequency of f = 10 kHz in a train of 10 pulses with He as working gas at a load of 330 Ohm, composed of a set of TVO resistors, is presented. The studies were carried out at a helium pressure of 5.7 and 13 Torr. Eptron is a voltage sharpener consisting of an open-discharge plasma cathode with the generation of counter-propagating electron beams and a special designed capillary structure that complicates the breakdown from the plasma cathode region to the anode. As a result, it is possible to achieve a voltage pulse edge compression degree, which is defined as the ratio of the breakdown delay time to the switching duration, in the range S = 200 - 1000, depending on the conditions, otherwise, it allows one to obtain a voltage edge at various load types less than 1 ns with a breakdown delay of up to 2 μs. The second important feature of the capillary structure is the fast deionization of the channel through ambipolar diffusion after the end of the pulse. This property allows the operation of an eptron at least up to f> 100 kHz at a voltage of up to 30 kV [1]. Earlier, the results of the study of the eptron operation at voltages up to 100 kV at f = 200 Hz were presented [2].

The aim of this work is study of the eptron operating at pulse repetition frequency range of 1 <f <10 kHz and supply voltage 40 <U <100 kV with a new design of the capillary. Figure 1 shows the breakdown delay time as a function of f for various U. A specific feature of the capillary structure used in the work is a rectangular cross section of a 0.2 x 15 mm, as well as a meandric channel of 67 mm long, which excludes direct passing of electrons from the plasma cathode to the anode, which further complicates the discharge. A copper shield with a cathode potential is installed outside the capillary, as in [1]. The sum of all the described modifications leads to the fact that the eptron is low sensitive to f in the entire voltage range, which makes it promising for various applications where high-voltage pulses with a short edge and high pulse repetition frequency are required.

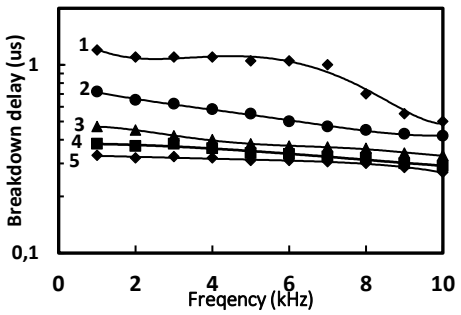

Fig.1. Breakdown delay versus f at U = 40(1), 50(2), 65 (3), 75(4), 82,5(5) kV.

REFERENCES

[1] Bokhan P.A., Gugin P.P, Lavrukhin M.A., Zakrevsky D.E., "Frequency characteristics of a subnanosecond plasma switch," Russian Physics Journal, vol. 62 , no.11, pp. , March, 2020.

[2] Bokhan P.A., Gugin P.P, Kim V.A., Lavrukhin M.A., Zakrevsky D.E. "Switching devices - EPTRON with 100 kV operating voltage and a sub-nanosecond switching times". , J Phys Conf Ser, vol. 1393, no 1, pp. 012038, September 2019.

* The work was supported by Russian Science Foundation, research Project No. 19-19-00069

INVESTIGATION OF THE TEMPERATURE AND RADIATIVE CHARACTERISTICS OF LONG-LIVED PLASMA-VORTEX FORMATIONS BY THE METHOD OF HIGH-SPEED BRIGHTNESS PYROMETRY*

L.Y. VOLODIN, A.S. KAMRUKOV

Bauman Moscow State Technical University, 2-ya Baumanskaya ul., 5, str.1, Moscow, 105005, Russia,
volodinlu@yandex.ru, +7(906)0817253

Multiphase turbulent vortex rings are of scientific and practical interest in the problems of interaction with shock waves [1], flames [2] and increasing the burning rate [3]. Large-scale vortex structures formed during the injection of plasma jets are characterized by high afterglow times exceeding the energy input time, and therefore are considered as effective sources of optical radiation [4]. To understand the physical processes occurring in such structures and construct their mathematical models, it is necessary to know their temperature and radiative characteristics.

Today, most methods of non-contact temperature determination are based on recording the power of thermal radiation. The determination of temperature fields is possible by the methods of single- (brightness), two- and multi-channel pyrometry using digital cameras [5]. These methods can accurately determine the true temperature of fireballs, if the spectral emissivity of the object is known.

In this work, we use the simple method of brightness pyrometry, which allows to determine the fields of spectral brightness and temperature and to analyze the emissive properties using the geometric features of a vortex ring. The technique of high-speed brightness pyrometry using a digital video camera is implemented. The studies show that the brightness temperature of the toroidal vortex formations varies slightly with time in the range 3100 K - 3600 K. A spectral absorption coefficient k_λ were estimated using the analysis of recorded brightness height distribution $B_\lambda(x)$:

$$\frac{B_\lambda(x=R-r)}{B_\lambda(x=0)} = \frac{1-\exp\left[-k_\lambda \cdot l(R-r)\right]}{1-\exp\left[-k_\lambda \cdot l(0)\right]}, \qquad (1)$$

where R – vortex ring radius; r - vortex core radius; l(x) – optical length.

Fig. 1 shows the temperature map of the vortex ring and spectral brightness height distribution. The results allow to conclude that in the recorded spectral range the brightness temperature is close to true.

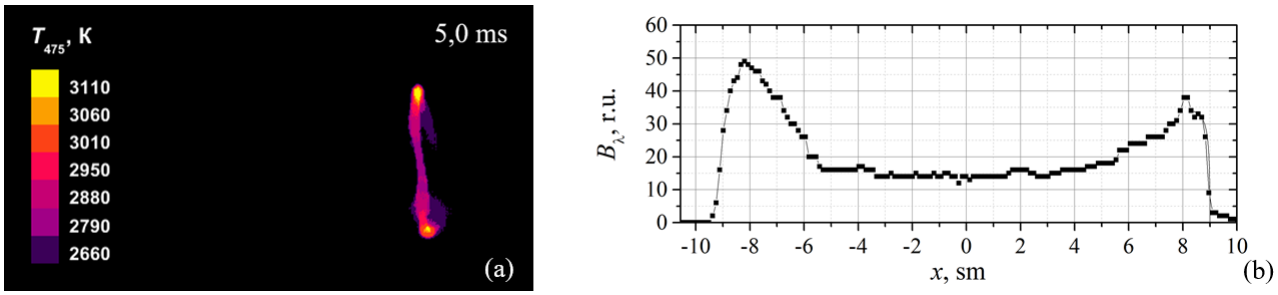

Fig. 1. Radiation characteristics of plasma vortex ring:
(a) spatial temperature map, frame size - 0.75 x 0.4 m.; (b) spectral brightness height distribution

REFERENCES

[1] *A. Lodes. Shock wave interaction with a Toroidal Air Plasma: PhD Thesis - 2013 – 228 p.*
[2] *P.-H. Renard, D. Thévenin, J.C. Rolon et al // Prog. Energy Combust. Sci. – 2000 – V. 26. – No 3. 225–282.*
[3] *S. Ishizuka, T. Yamashita, D. Shimokuri // Proc. Combust. Inst. – 2013 – V. 34. – No 1. 745–753.*
[4] *M.N. Zharnikov, A.S. Kamrukov, I.V. Kozhevnikov et al // Tech. Phys. – 2008 – V. 53. – No 5. 571-578.*
[5] *I.P. Gulyaev, A.V. Dolmatov // Int. J. Heat Mass Tran. – 2018 – V. 116. 1016–1025*

* This work was supported by grant 18-29-21039 from the Russian Foundation for Basic Research

SHARPENING OF THE PULSE FRONT BY A SILICON PULSE SWITCH*

V.V. BARMIN[1], *V.YU. KONEV*[1], *O.B. KOVALCHUK*[1], *I.V. ROMANCHENKO*[1], *S.N. MALTSEV*[1], *S.N. RUKIN*[2]

[1]*Institute of High Current Electronics SB RAS, Tomsk, Russia*
[2]*Institute of Electrophysics UD RAS, Ekaterinburg, Russia*

In this report we investigated the main characteristics of a silicon switch with ultrafast ionization [1] installed in the central electrode break of a coaxial line with a wave resistance of 50 Ohms. The based parameters of the switch were found under experiments on sharpening of the pulse front of subnanosecond duration with amplitude more than 4.2 kV are established.

It was shown that sharpening of the pulse front to hundreds of picoseconds and amplitude more than 4.2 kV could be realized due to the ionization of technological impurities with deep levels [1, 2]. The ionization is caused by the front of the modulating pulse with a high rate of the reverse voltage rise of 8.4 kV/ns. It leads to the formation of an electric field with intensity more than 0.9 MV / cm at the p-n junction [1, 2].

REFERENCES

[1] S.K. Lobutin, E.N. Rukin, B.G. Slovikovsky, S.N. Tsyranov, "Ultrahigh-power picosecond current switching by a silicon sharpener based on successive breakdown of structures," Semiconductors, vol. 44, No. 7, 2010.

[2] A.I. Guisev, M.S. Pedos, S.N. Rukin et al., "On the picosecond switching of a high-density current (60 kA/cm^2) via a Si closing switch based on a superfast ionization front," Semiconductors, vol. 44, No. 8, 2014.

* The work was supported by the Russian Science Foundation under grant No. 18-38-20076.

CURRENT DISTRIBUTION OF A LOW-PRESSURE GLOW DISCHARGE WITH HOLLOW CATHODE AND HOLLOW ANODE OVER THE CATHODE SURFACE*

N.V. LANDL, Y.D. KOROLEV, O.B. FRANTS, G.A. ARGUNOV, V.G. GEYMAN, A.V. BOLOTOV, I.A. SHEMYAKIN

Institute of High Current Electronics SB RAS, Tomsk, Russia

Hollow-cathode low-pressure glow-type discharges are widely used for different applications [1-7]. In particular, such discharges are used for generation of charged particle beams, for surface modification, for generation of extreme ultraviolet radiation, for generation of large volume plasmas and so on. To interpret the regimes of discharge sustainment we had been developed the model, presented in [4, 7, 8, 9]. The main idea of the model is that the main component of discharge current on the cathode surface is an ion current and electrons from the cathode are emitted not only due to the ion bombardment, but also as an external emission current due to photoeffect, field emission and explosive emission.

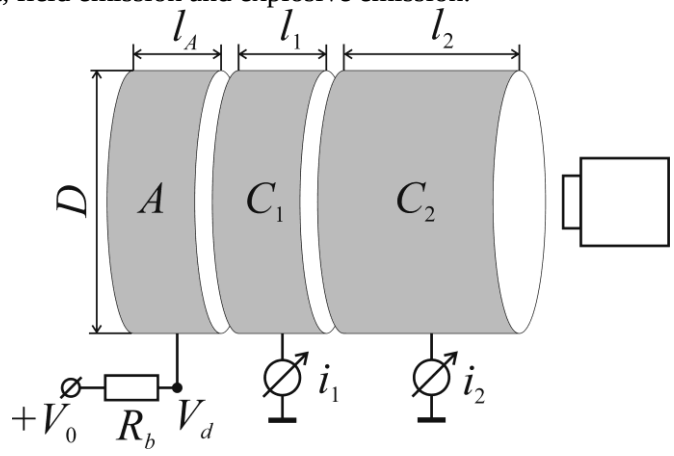

Fig.1. Schematic of the experimental setup. R_b = (50 – 170) kΩ, $V_0 \leq 3$ kV.

In this report, the data on the regimes of the auxiliary glow discharge with a hollow cathode and hollow anode are presented. The schematic of the experimental setup is presented in fig.1. To reveal the discharge current distribution over the cathode surface multi-sectional cathode cavity was used. During the experiments, current-voltage characteristics and images of the discharge for different electrodes dimensions were obtained. A model of the current sustainment of a hollow-cathode discharge was used for estimations of discharge parameters. The results of estimations agree well with the experimental data.

REFERENCES

[1] E. Dewald, K. Frank, D. H. H. Hoffman et.al., “Experimental Analysis of Pseudospark Sourced Electron Beam,” IEEE Trans. Plasma Sci., vol.25, p. 272, 1997

[2] V.N. Devyatkov, Y.F. Ivanov, O.V. Krysina, N.N. Koval et.al., “Equipment and processes of vacuum electron-ion plasma surface engineering,” Vacuum, vol.143, p.464, 2017

[3] Y.D. Korolev and N.N. Koval, "Low-pressure discharges with hollow cathode and hollow anode and their applications," J. Phys. D: Appl. Phys., vol.51, Article Number 323001, 2018.

[4] Y.D. Korolev, K. Frank, “Discharge formation processes and glow-to-arc transition in pseudospark switch,” IEEE Trans. Plasma Sci., vol.27, p.1525, 1999

[5] V.D. Bochkov, V.M. Dyagilev, V.G. Ushich, O.B. Frants, Y.D. Korolev, I.A. Shemyakin, K. Frank, “Sealed-off pseudospark switches for pulsed power applications (current status and prospects),” IEEE Trans. Plasma Sci., vol.29, no.5, pp. 802-808, 2001.

[6] Y.D. Korolev, N.V. Landl, V.G. Geyman, A.V. Bolotov, V.S. Kasyanov, V.O. Nekhoroshev, S.S. Kovalsky, “Nanosecond Triggering for Sealed-Off Cold Cathode Thyratrons With a Trigger Unit Based on an Auxiliary Glow Discharge,” IEEE Trans. Plasma Sci., vol.43, no.8, pp.2349-2353, 2015

[7] Y.D. Korolev, N.V. Landl, V.G. Geyman, O.B. Frants, “Hollow-cathode glow discharge in a trigger unit of pseudospark switch,” Phys. Plasmas., vol.25, no.11, 13510, 2018

[8] Y.D. Korolev, N.V. Landl, V.G. Geyman, O.B. Frants, G.A. Argunov, A.V. Bolotov, “Role of Prebreakdown Currents in a Static Breakdown of a Two-Sectioned Cold-Cathode Thyratron, Russ.Phys.J., vol.62, No.7, pp.1269-1278, 2019

[9] N.V. Landl, Y.D. Korolev, V.G. Geyman, O.B. Frants, G.A. Argunov, A.V. Bolotov, A.V. Akiov, P.A. Bak, “Special Features of Parasitic Current Formation in a Sealed-Off Cold-Cathode Thyratron with Trigger Unit Based On an Auxiliary Glow Discharge” // Rus. Phys. J., vol.62, no.7, pp. 1279-1288, 2019

* This work was funded by RFBR according to the research project № 19-08-00326.

NANOSECOND MICROWAVE PULSE COMPRESSOR

A.A. NIKIFOROV[1], *P.YU. CHUMERIN*[1,2]

[1] *National Research Tomsk Polytechnic University, Tomsk, Russian Federation*
[2] *National Research Tomsk Polytechnic University, Tomsk, Russian Federation*

Radar technologies are one of the promising technologies that provide protection against terrorist threats acts on objects of national importance.

Radar systems are designed to detect air, sea, ground and explosive objects, as well as to determine their distance, speed and geometric parameters.. The radar station operates as follows: a signal is transmitted in the direction of the object of researching, reverberated from objects that impede its distribution, and returned.

The fundamental role of space exploration when using radar stations is played by probing signals. Using of radar probing signals with a wide and ultra-wide frequency band allows us to create new highly informative radar systems that operate in the radio mode of the target. Probing radios pulses of nanosecond duration can increase the range resolution up to tens of centimeters. The signal duration in this case usually varies between 1–10 ns. A significant drawback of such systems is the wide availability of only low-power short-pulse generators due to the complexity of creating high-power pulse generators of about 1 ns duration. This drawback can be overcome with the help of a microwave pulse former, which generates short pulses of high power. This former is a design operating on the basis of the accumulation of the microwave signal from an industrial generator into the storage resonator and the quick output of the microwave signal in the form of a short, increased pulse power.

This paper presents the results of the development, design and study of a nanosecond microwave pulse former for a nonlinear radar. The device contains a microwave generator, a coaxial storage resonator and a semiconductor switch, consisting of a toroidal resonator with P-I-N diodes located inside. This microwave pulse former of nanosecond duration has the parameters: peak power 2 kW, pulse duration at -3 dB level 5 ns, pulse repetition rate 250 Hz, carrier frequency 815 MHz.

REFERENCES

[1] Didenko A.N. High-power microwave pulses of nanosecond duration / A.N. Didenko, Yu.G. Yushkov. - M .: Energoatomizdat, 1984. – P. 112

[2] Artyomenko S.N. Coaxial resonators in microwave pulse compressors / S.N. Artyomenko, S.A. Novikov, Yu.G. Yushkov // News of Tomsk Polytechnic University. – 2009. T. 314. No. 4. – P. 127-131.

[3] Izyumova T.I. Waveguides, coaxial and strip lines / T.I. Izyumova, V.T. Sviridov - Moscow: Energy, 1975. – P. 112

[4] Patent RF No.2532852 MPK: H01R1 / 00 publication date 2014.11.10. Coaxial microwave switch // Patent of Russia No. 2532852 / Chernousov Yu.D., Barnyakov AM, Shebolayev I.V., Levichev A.E.

[5] Dzekhtser G.B. PIN diodes in microwave broadband devices / G.B. Dzehtser, O.S. Orlov. - M .: Soviet Radio, 1970. – P. 200

[6] Grigoryev A.D. Resonators and resonator decelerating microwave systems / A.D. Grigoryev, V.B. Yankevich. - M .: Radio and communication, 1984. – P. 248

[7] Lebedev I.V. Microwave equipment and devices. Edited by Academician N.D. Devyatkov. Textbook for university students in the specialty "Electronic devices", M., "Higher school ", 1970. – P.442

[8] Mironov O.S. High-frequency pulse repetition mode in ultrabroadband radar ranging / O.S. Mironov // News of Russian universities. Radio electronics. 2016.issue 5. – P. 47-51.

[9] Nikiforov A.A. Semiconductor L-band transmitter with radiation pulse compression / A.A. Nikiforov, P.Yu. Chumerin, V.N. Slinko, V.A. Vaulin // Journal of Radio Electronics [electronic journal]. 2018. No. 12. Access mode: http://jre.cplire.ru/jre/dec18/18/text.pdf

[10] Akhtamzyan I.A. Nuclear nonproliferation. Textbook for students of higher educational institutions. In 2 volumes. Volume I. –M .: PIR Center, 2002. – P. 528

[11] Paramuzova O. G. Physical protection of nuclear materials: International Legal Issues // Jurisprudence. – 1998. – No. 2. – P. 191-199..

FORMATION OF BIPOLAR HIGH-VOLTAGE PULSES OF NANOSECOND DURATION IN THE ELECTRIC CIRCUITS WITH A SINGLE SPARK GAP*

A.M. EFREMOV, V.M. ALEXEENKO

Institute of High Current Electronics, Siberian Branch, Russian Academy of Sciences, 2/3 Akademichesky AvenueTomsk 634055, Russia, efremov@oit.hcei.tsc.ru

Traditionally, for the formation of high-voltage bipolar pulses of nanosecond duration pieces of short coaxial lines and cutting and sharpening pressurized spark gaps are used. To obtain stable both in amplitude and in duration bipolar pulses on the load, synchronous operation of spark gaps in the subnanosecond time range is required, which makes it difficult to configure them. This problem is absent in the former circuit with a single spark gap, shown in Fig. 1.*a*. When charging the forming lines FL_1 and FL_2 with the impedance ρ through the decoupling inductance L and the spark gap S triggered, a bipolar a voltage pulse appears at the load R= ρ with a duration equal to double path along the lines and with an amplitude equal to half the charging voltage. The disadvantage of the circuit is that, due to the parasitic capacitance C of supplying the charging voltage to the forming lines, it is impossible to form a second half-wave of the bipolar pulse with a duration of less than 3 ns [1].

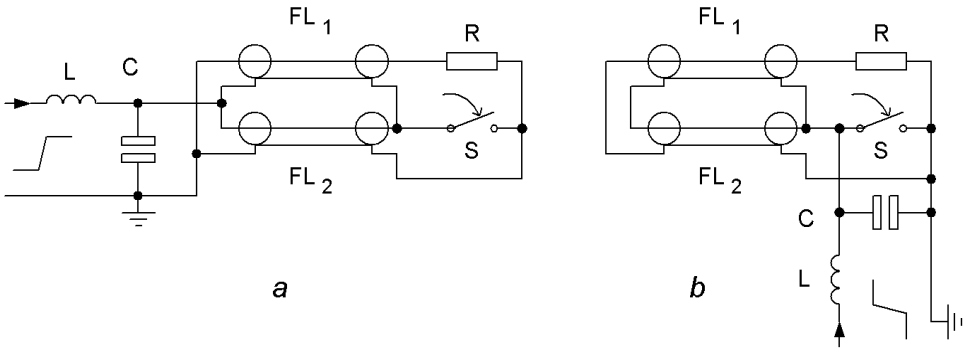

Fig.1. Electric circuits of the bipolar pulse formers with different points of supply of charging voltage to potential conductors of forming lines: a - on the left, b - on the right.

In the case of voltage supply in the immediate vicinity of the spark gap, as shown in Fig. 1*b*, the parasitic capacitance is cut off when the spark gap is triggered and does not affect the formation of a bipolar pulse. Using such a circuit, it was possible to obtain bipolar pulses, shown in Fig. 2, with a duration of up to 1 ns with an amplitude of 60-80 kV at a load of R = 12.5 Ohms at a nitrogen pressure of 65 atm in the spark gap.

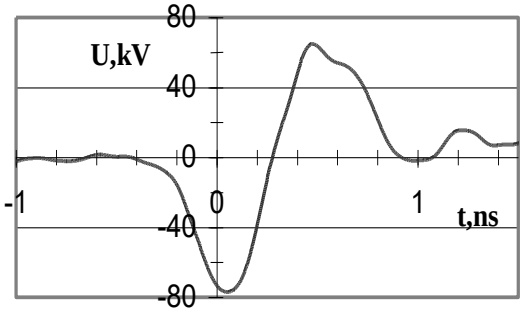

Fig.2. The output bipolar voltage pulse at the load is R = 12.5 Ohms.

REFERENCES

1. A.M. Efremov, Yu. D. Korolev., B.M. Koval'chuk , "Generation of bipolar high-voltage pulses of nanosecond duration in the electric circuits with high-pressure spark gaps," Proc. 16th Int. Symposium on High Current Electronics. Tomsk, pp.308—311, 2010

* The work was supported by Russian Foundation for Basic Research, grant 20-08 -00093 A.

RESEARCH OF SWITCHED POWER BY NITROGEN DIODE SWITCHES IN THE SUBNANOSECOND TIME RANGE[1]

S.N. IVANOV[*], *V.V. LISENKOV*[*,**]

**Institute of Electrophysics, Amundsena Str. 106, Ekaterinburg, 620016, Russia, E-mail: stivan@iep.uran.ru, phone:+7(343)2678776.*
***Ural Federal University, Mira St. 19, Ekaterinburg, 620083, Russia*

The study of the switched power by nitrogen diode switches in the subnanosecond time range depending on the pressure and the degree of the gap overvoltage (the length of the cathode-anode gap) was carried out. The discharge gap was made in the form of a break in the central electrode of a 50-Ohm coaxial gas-filled line. In the experiments, a stainless steel cathode and anode with a tip radius of 1 cm were used. Such a large radius of rounding of the electrodes was chosen to form a uniform electric field in the discharge gap, which facilitated the interpretation of the obtained experimental data. A subnanosecond pulse with amplitude of 100 kV with a front of 250 ps (at the level of 0.1-0.9 in amplitude) was applied to the discharge gap. The gap breakdown occurs at the front of the applied voltage pulse. To measure the voltage pulses, the method of reflectometry was used: the pulse voltages at the output of the pulse generator (PG) and reflected from the tested gas gap were recorded using wide-band capacitive voltage dividers built into the transmitting coaxial line connecting the PG and the discharge gap. Waveforms of the voltage at the gap when it is broken and in the absence of a breakdown (idle mode) were obtained. The method of conducting of such experiments is described in details in [1-4]. We have previously shown [5] that the discharge under these conditions develops with the participation of runaway electrons, which significantly reduce the overvoltage of the discharge gap and the pulse breakdown voltage [1-3].

Two series of experiments were conducted. In the first serie, a fixed-length discharge gap was used, and the nitrogen pressure gradually increased from atmospheric pressure to 40 atm during the experiment. In the second serie of experiments, at a fixed pressure, the length of the gap changed from fractions of a millimeter to values when the gap stopped breaking. Using the method described in [6], the oscillograms of the current flowing through the discharge gap were restored for all experimental points. Important parameters of any switch are coefficient of efficiency and the residual resistance after switching. To determine the coefficient of efficiency, it is necessary to know the pulse energy passed through the spark gap and the energy stored in the line connecting the spark gap and the PG. To determine these values, we used the voltage and current waveforms we obtained. As a result, the coefficient of efficiency dependences on the nitrogen pressure and the degree of the discharge gap overvoltage were obtained.

REFERENCES

[1] S.N. Ivanov, V.V. Lisenkov, “Investigation of the Prebreakdown Stage of the Self-Sustained Subnanosecond Discharge in High Pressure Nitrogen,” Journal of Applied Physics, vol.124, Article Number 103304, 2018.

[2] S.N. Ivanov, V.V. Lisenkov, “Study of the Formation Time of a Self-Sustained Subnanosecond Discharge at High and Ultrahigh Gas Pressures,” Plasma Physics Reports, vol.44, No.3, pp. 369–377, 2018.

[3] S.N. Ivanov and K. A. Sharypov, “Electric Strength of Hydrogen in the Nanosecond Time Range,” Technical Physics, vol.60, No.10, pp. 1478–1482, 2015.

[4] S.N. Ivanov and K. A. Sharypov, “Switching Characteristics of Nitrogen in the Pulsed Mode in a Subnanosecond Time Interval,” Technical Physics Letters, vol.42, No.3, pp. 274–277, 2016.

[5] S.N. Ivanov, “The Transition of Electrons to Continuous Acceleration Mode at Subnanosecond Pulsed Electric Breakdown in High-Pressure Gases,” Journal of Physics D: Applied Physics, vol.46, No.28, Article Number 285201, 2013.

[6] Yu.D. Korolev and N.M. Bykov, “High-Voltage Spark Gap in a Regime of Subnanosecond Switching,” IEEE Transactions on Plasma Science, vol.40, No.10, pp. 2443 – 2448, 2012.

[1] The work was supported by the Russian Science Foundation under grant No. 20-08-00172.

INVESTIGATION OF THE OPTICAL STRENGTH OF MATERIALS IRRADIATED BY HIGH-POWER PULSED LASER RADIATION

O.V. MKRTYCHEV, V.G. SHEMANIN, N.D. SOLODILOVA

Branch of Belgorod V G Shukhov State Technology University, Novorossiisk, Russia

The paper deals with the development of simulation methods. The stochastic nature of the laser-induced destruction of transparent materials under the action of high-power pulsed laser radiation was simulated using the Weibull statistical distribution in order to predict the optical strength dynamics of the irradiated surface.

Composite materials on the basis of ceramics and glasses are widely used, for example, in optoelectronics, nanophotonics [1]. Among the many problems arising in practice, the tasks of interaction of such composite materials under the conditions of irradiation with high-power laser pulses are important [2–4]. Such tasks associated with laser-induced destruction of optical materials require the ability to determine the strength and reliability of the irradiated material and predict the dynamics of reliability over time.

The strength of the irradiated material is an important factor limiting the use of ceramic and other materials in power optics. To solve these problems, materials are often applied with special coatings or special additives are introduced [5].

Theoretical and experimental studies of the optical strength of glass composites were conducted, taking into account the stochastic properties of the breakdown of nano-scale coatings under the action of a single high-power pulsed laser radiation. Coatings were obtained by sol-gel method. As a radiation source, we used a solid-state laser on a yttrium-aluminum garnet doped with neodymium ions (YAG-Nd laser) which generated laser pulses at wavelength of 1.064 μm with duration of 30 ns with energy of up to 0.15 J and with duration of 300 μs with energy of 1.2 J The authors proposed an algorithm for determining the optical strength of the irradiated material by the breakdown stress of the material. It is proposed to determine the breakdown stress by comparing the experimental and simulated dependences of stress, temperature, and reliability of the surface of the irradiated material. Based on the proposed measurement technique, experimental studies were conducted and an algorithm was developed for determining the optical strength of coatings.

REFERENCES

[1] W.Ye.L. Ling, T. Schönherr and Hi. Koizumi, APL,vol.111, Article Number 014101, 2017.

[2] O.V. Mkrtychev 2018 AIP Conf. Proc., vol. 2051, Article Number 020200, 2018.

[3] V.G. Shemanin and O.V. Mkrtychev, Tech. Phys., vol. 63, Article Number 623, 2018.

[4] V.G. Shemanin and O.V. Mkrtychev, JPCS, vol. 653, Article Number 012012, 2015.

[5] S.G. Kazantsev, Atmos. Oceanic Opt., vol. 16, Article Number 390, 2003 (in Russian).

AIR INSULATED LINEAR PULSE TRANSFORMER STAGE*

A.A. ZHERLITSYN, A.M. EFREMOV, V.M. ALEXEENKO, S.S. KONDRATIEV

Institute of High Current Electronics SB RAS, Tomsk, Russia

Linear pulse transformers [1, 2] have several advantages in comparison with the more common Marx generators. Their use allows to reduce the volume of high-voltage isolation and increase the specific energy of a capacitive storage; simplify the control and maintenance of capacitors and switches; avoid the use of transformer oil.

A stage of a linear pulse transformer with air insulation of atmospheric pressure was created and tested. The stage is a transformer with two turns in the primary and one turn in the secondary windings. The primary winding is configured as two parallel-connected inductors. The stage inductor consists of five cores, which are wound up by transformer steel (ET-3425) strip. The capacitive energy storage is switched by a multi-gap multi-channel spark switch to two inductors without the use of high-voltage supply cables. The capacity of the stage energy storage can vary from 250 to 500 nF. The maximum charging voltage of the capacitive storage is 40 kV, the maximum stored energy is ~0.5 kJ. The efficiency of energy transfer from a capacitive storage to a matched load of 3–4 Ohms is about 60 %. The characteristic energy output time is ~1 μs.

At a high-impedance load, the stage allows to generate of voltage pulses with a front of 100 ns and an amplitude close to twice the charging voltage. In the short circuit mode, the stage discharge current is ~20 kA, the time to a maximum of about 400 ns. The test results allow us to recommend a stage for linear pulse transformers for loads with variable resistance with a high resistance state time ≤200 ns.

REFERENCES

[1] V.A. Vizir', A.S. El'chaninov, F.Ya. Zagulov et al., “Powerful pulsed transformer,” Prib. Tekh. Eksp., no. 5, pp. 95-98, 1986.

[2] A.V. Luchinskii, N.A. Ratakhin, V.F. Fedushak, A.N. Shepelev “Powerful pulsed electrophysical transformers from the Institute of High-current Electronics, Siberian Branch of the Russian Academy of Sciences,” Russian Physics Journal, vol.38, no.12, pp .1246-1252, 1995.

* The work was supported by the Russian Foundation for Basic Research under grant No. 19-08-00115.

FEATURE OF THE WORK OF THE MARX GENERATOR WITH SCREENED CASCADES INSTALLED IN A METAL CONDUCTING TANK

V.A. KOKSHENEV

Institute of High Current Electronics SB RAS, Tomsk, Russia

The results of experimental studies and numerical calculations for the operation of a multi-stage Marx generator in a conducting earth tank are presented. A feature of the considered generator designs is the presence of a metal screen in each cascade, forming an increased capacity relative to the walls of the earthen hull. The influence of this structural capacity both on the response speed of the spark gap of the Marx generator and on the shape of the output pulse in the load is considered. It is shown that the defining term in the delay time of the generator relative to the start pulse is the wave propagation time in the line formed by the inductors of the generator cascades and their capacitance on the tank walls, compared to the breakdown delay time of the dischargers.

The possibility of the formation of special-shaped pulses at an active load when the generator is operating in the intermediate inductive storage mode is demonstrated. The conditions for matching the parameters of the generator discharge circuit with the load characteristics are determined. The features of the parallel operation of several sections of such Marx generators when they are arranged in a common earthen tank are considered. It is shown that the variation in the response of the sections depending on their location in the tank, leading to different values of the construction capacities, and possible changes in the characteristics of the dischargers associated with the technology of their manufacture, is significantly less than the duration of the pulse front at the load. Experimental results on the formation of active pulses of voltage pulses with an amplitude of up to 4.5 MV are presented.

SHUNTING Z-PINCH BY LOAD BY PLASMA SWITCH INSTALLED IN A MAGNETICALLY ISOLATED TRANSMISSION LINE

V.A. KOKSHENEV, N.E. KURMAEV

Institute of High Current Electronics SB RAS, Tomsk, Russia

In the Z-pinch experiments, there was a need to protect the load unit with the diagnostics installed in it from severe damage associated with the release of a significant fraction of the energy generator remaining in the elements in this region. The paper considers the possibility of solving this problem by implementing a mode of shunting a load unit (crowbar mode) in a magnetically isolated transmission line (MITL) using a plasma switch. To create a plasma stream, plasma guns (PG) with a high-current discharge in a capillary made of polyethylene with a diameter of 1.5 mm and a length of 5 or 15 mm were used. The current amplitude in the capillary was 9.5 or 18 kA with an oscillation period of ~ 5 μs. To obtain a uniform and dense plasma flow, a plasma duct is used. Figure 1 demonstrates the effect of a metal plasma duct on the propagation of synchronized plasma clots created by a spatially uniform structure from identical sources. It can be seen that at a plasma injection velocity of ~ 9 cm/μs, the plasma duct allows the formation of a uniform plasma flow with a decrease in the angle of the jet opening from 60° to ~ 20°.

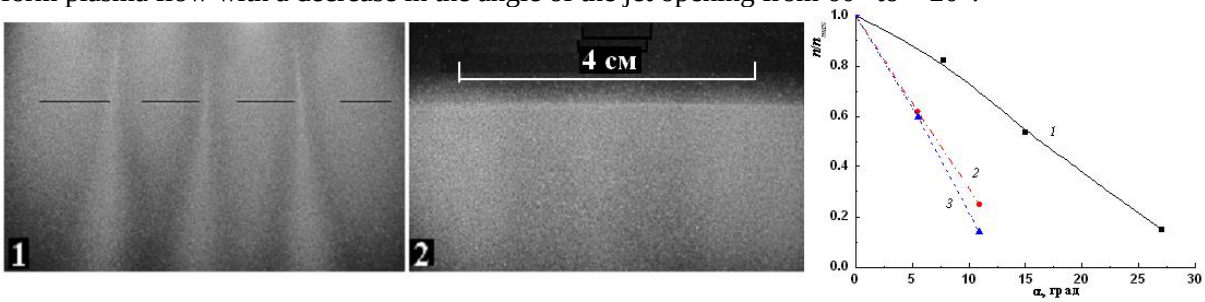

Fig.1. Photograph of a plasma stream created by a capillary-type source with a current of 9.5 kA and a front of ~1.2 μs. Frame 1 - without a plasma duct (the dashed line indicates the location of the end of the plasma duct), frame 2 - with a plasma duct 14 mm wide and 45 mm high. Exposure time frames "Nanogate-2" cameras 10 ns. On the right, the profile of the relative plasma concentration of the capillary type source with a discharge current period of ~ 5 μs: graph 1 – without a plasma duct, current 9.5 kA; 2.3 – with a plasma duct (graph 2 - current in the capillary 9.5 kA, graph 3 – 18 kA).

In Figure 2 presents the results of an experiment on a GIT-12 generator for shunting a load unit with an inductance of 60 nH during the implementation of the crowbar mode in MITL using a plasma switch. The switch was a plasma duct 55 mm long circularly around the outer anode of the MITL external anode with 32 PG evenly installed. The coaxial transmission line had electrode diameters of 500 mm/320 mm. A plasma flow formed on a diameter of 500 mm initially moved in the plasma duct, and then was injected into the interelectrode gap of the line in which the current *Ig(t)* of the GIT-12 generator flowed. The plasma propagation time through the plasma duct was ~ 0.6 μs. In Figure 2 shows the mode with a delay of the current of the *Ig(t)* generator relative to the beginning of the current in the guns *Ipg(t)* by 0.6 μs. At time *tcr*, the plasma flow shorted the interelectrode gap of the MITL. The average velocity of the plasma flow across the magnetic field with an effective intensity of ~ 5.6 kA/cm was ~ 2.5 cm/μs at an initial plasma velocity of ~ 9 cm/μs. For the currents of the generator and the load unit 1.1 MA, the plasma switch made it possible to shunt the load circuit with an inductance of 60 nH from the discharge circuit of the generator for at ≥ 4 μs.

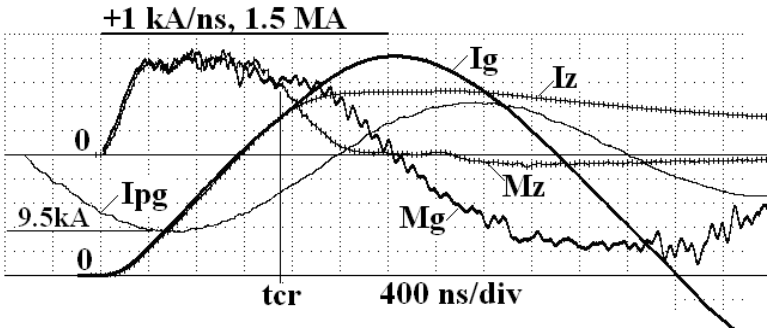

Fig.2. Oscillograms of the currents of the *Ig* generator, load *Iz* and their derivatives *Mg* and *Mz*, as well as current *Ipg* in 1 plasma gun.

ISSUES AND TASKS OF ELECTRO-IMPULSE CLEANING[1]

V V MAKAROV, O P KUZNETSOVA, M YU NIKOLAEV

Omsk State Technical University, Omsk, Russia.
E-mail: makarov@omgtu.ru

Various technologies are used to clean the surfaces from sticking of various substances, to remove these substances. Electro-impulse cleaning systems can be used in construction, engineering, railway transport, heat power engineering and other fields of industrial activity [1,2]. Implementation of such systems to remove various materials from walls and structural elements of the equipment (including icicles and ice from the eaves and roofs of houses) is an effective, low-cost and technological method. The operation of electro-impulse systems is based on eddy-current non-contact interaction of the electromagnetic field of the inductor with electrically conductive surfaces. The resulting intense and high-speed deformation creates instantaneous (10^{-4} - 10^{-5} s) mechanical overloads that break the connection of substances with surfaces without violating the mechanical strength of the surfaces themselves [2]. Functional diagram illustrating the principle of the device operation is shown in Fig.1.

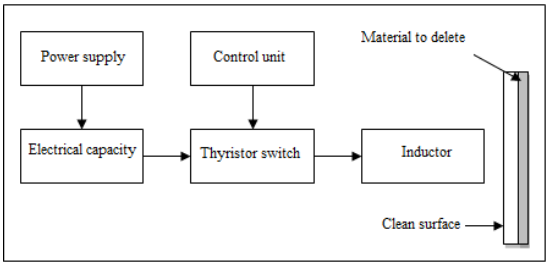

Figure 1. Functional diagram of a pulse cleaning device

The diagram works as follows: the capacitive storage is charged to a high voltage (kilovolts) from the power source, then the thyristor is opened for 10^{-6} s at the control unit command, and the current pulse flows through the inductor, creating eddy currents in the electrically conductive surface. The interaction of eddy currents with the current in the inductor coil creates a pulsed mechanical interaction between the inductor and the electrically conductive surface, which causes elastic deformation of the surface being cleaned [2]. The energy effect in this device is due to the fact that the energy is accumulated for 10^{3} s (up to 10 minutes) in the capacity storage, and is spent for (10^{-4} – 10^{-6} s), the power effect is 10^{6} and more (explosion analog).

The presented circuitry implementations of the electro-impulse cleaning technology of buildings eaves and structures from icicles and ice, and devices developed on its basis, allow cleaning roof eaves without manual labor. However, the use of local electric networks for power supply causes coordination and electrosafety problems. Currently, the issue of electro pulse circuit power supply from a stationary solar battery is being studied.The diagram works as follows: the capacitive storage is charged to a high voltage (kilovolts) from the power source, then the thyristor is opened for 10^{-6} s at the control unit command, and the current pulse flows through the inductor, creating eddy currents in the electrically conductive surface. The interaction of eddy currents with the current in the inductor coil creates a pulsed mechanical interaction between the inductor and the electrically conductive surface, which causes elastic deformation of the surface being cleaned [2]. The energy effect in this device is due to the fact that the energy is accumulated for 10^{3} s (up to 10 minutes) in the capacity storage, and is spent for (10^{-4} – 10^{-6} s), the power effect is 10^{6} and more (explosion analog).

The presented circuitry implementations of the electro-impulse cleaning technology of buildings eaves and structures from icicles and ice, and devices developed on its basis, allow cleaning roof eaves without manual labor. However, the use of local electric networks for power supply causes coordination and electrosafety problems. Currently, the issue of electropulse circuit power supply from a stationary solar battery is being studied.

REFERENCES

[1] XII International Conference Radiation-thermal Effects and Processes in Inorganic Materials; Materials Science and Engineering. 2017. Vol. 168. DOI: 10.1088/1757-899X/168/1/012005

[2] Journal of Physics: Conference Series. 2018. Vol. 1115. DOI: 10.1088/1742-6596/1115/2/022019

1 The submitted work is a partial continuation of the Russian Foundation for Basic research grant 14-08-31109 mol_a "Improving dynamic indicators of the quality of control of the precygonic electric drive" in the part of the frequency regulation system and uses its results.

FAST PUMPING CURRENT IN TWO-CONDUCTOR LINES AND ITS APPLICATION FOR FORMING POWERFUL RECTANGULAR PULSES

V.V. KLADUKHIN[1], S.V. KLADUKHIN[1], S.P. KHRAMTSOV[1]

[1] Institute of Electrophysics of the Ural Division of the Russian Academy of Sciences, Ekaterinburg, Russia

The scheme and the process of fast pumping of a current into a long two-conductor line used as an inductive energy storage are considered. The results of modeling the dynamics of currents and voltages in the line are presented. Relations for currents and voltages are given. A scheme of a rectangular-shaped powerful nanosecond pulse generator based on a coaxial forming line with inductive energy storage and semiconductor switches providing energy output to the load is proposed and investigated.

REFERENCES

[1] B.M. Koval'chuk, G.A. Mesyats, "High-power nano-second pulse generator with a vacuum line and plasma interrupter," Doklady AN SSSR, v. 284, no. 4, pp. 857-859, 1985 (in Russian).

[2] P.V. Vasiliev, S.K. Lyubutin, A.V. Ponomarev, S.N. Rukin, "Operation of a semiconductor opening switch at the pumping time of a microsecond and low current density," Semiconductors, vol. 43, issue 7, pp. 953-956, July 2009.

EFFECT OF ELECTRIC ISOLATION BETWEEN CHANNELS ON THE MULTIGAP SWITCH PARAMETERS*

A.A. ZHERLITSYN, E.V. KUMPYAK, G.V. SMORUDOV

Institute of High Current Electronics SB RAS, Tomsk, Russia

The paper presents the results of a study of the multichannel multigap controlled switch, similar to [1]. Switch operates in air at atmospheric pressure at a voltage up to 100 kV. Such important parameters of the switch as resistance, inductance and dissipated energy are determined by the number of parallel ignited channels. The number of parallel channels and their distribution over consecutive gaps depends on the electrical isolation between the channels. The number of channels in the switch gaps was determined and the switch parameters (inductance, resistance and dissipated energy) were calculated under different operating conditions. Braginskii model [2] (hydrodynamic expansion of a spark channel in approximation of constant conductivity) was used for the simulation.

If there is an electrical isolation between the channels, the number of channels in all the gaps is approximately the same and it is determined by the number of channels initiated in the triggering gap. If there is no electrical isolation, only one channel is mainly ignited in the triggering gap but the number of parallel channels increases as successive breakdown of gaps. It is shown that the switch with electrical isolation between the channels has better characteristics at a high rise rate of a triggering pulse of ~800 kV/μs. The advantage of the switch without isolation between the channels is manifested when using a trigger pulse with a low rise rate. So, for example, the dissipated energy in the switch without electrical isolation between the channels is less than in the switch with electrical isolation at a triggering pulse rise rate of 100–250 kV/μs.

REFERENCES

[1] B.M. Kovalchuk, A.V. Kharlov, E.V. Kumpyak, G.V. Smorudov, A.A. Zherlitsyn, “Capacitor blocks for linear transformer driver stages,” Review of Scientific Instruments, 85, 013501, 2014.

[2] S.I. Braginskii, “Contribution to the theory of development of a spark channel,” Sov. Phys. JETP, vol. 34(7), no. 6, pp. 1068–1074, 1958.

* The work was supported by the Russian Foundation for Basic Research (RFBR) under grant No. 18-08-00159 a.

HIGH-VOLTAGE PULSE SHARPENING USING SPIRAL LINES WITH FERRITE

P.V. PRIPUTNEV, I.V. ROMANCHENKO, V.Y. KONEV, R.K. SOBYANIN, P.V. VYKHODTSEV

Institute of High Current Electronics SB RAS, Tomsk, Russian Federation

For a large number of studies in high-current electronics and high-voltage technology, one of the important tasks is to obtain high-voltage pulses with its rise time of the order of units of nanoseconds or less [1]. Since many of available high-power switches are limited to several ns rise time characteristics, it is quite difficult to form pulses with a subnanosecond rise time on the load. Thus, to solve this problem in experimental installations, it is necessary to use transitional devices that sharpen pumping pulses. Special gas dischargers, solid state devices, as well as transmission lines with non-linear filling, can be used for these purposes [2,3].

This work is aimed at studying the operation of a new scheme for high-voltage pulse sharpening, which is a segment of a spiral line with ferrite core located inside the spiral [4]. The sharpening of the pulse front occurs due to magnetic losses in the ferrite when a high-voltage pulse passes along the line. Several configurations of spiral lines are considered and the main regularities for the formation of the shortest rise time of the pulse are discussed.

REFERENCES

[1] I.V. Romanchenko, V.V. Rostov, V.P. Gubanov, A.S. Stepchenko, A.V. Gunin, I.K. Kurkan, “Repetitive sub-gigawatt RF source based on gyromagnetic nonlinear transmission line”, Rev. Sci. Inst., Vol. 83, 074705, 2012.

[2] G.A. Nesyats, M.I. Yalandin, “High-power picosecond electronics”, Phys.-Uspekhi, vol. 48, no. 3, pp. 211-229, 2005.

[3] J.E. Dolan, H.R. Bolton, A.J. Shapland, “Development of ferrite line pulse sharpeners”, proc. IEEE Int. Pul. Pow. Conf., pp. 795-798, Jun. 1993.

[4] M.R. Ulmaskulov, S.A. Shunailov, K.A. Sharypov, M.I. Yalandin, “Modification of high-voltage pulse waveform by the spiral and core-transformer fierrite-filled lines”, IEEE trans. Plas. Sci., vol. 45, no. 10, pp. 2707-2714, Oct. 2017.

HIGH VOLTAGE CAPACITOR DESIGN OPTIMIZATION*

S.A. VAGAYTSEV, I.V. LAVRINOVICH, A.D. LENSKIY, D.V. MOLCHANOV, D.V. RYBKA

Institute of High Current Electronics SB RAS, Tomsk, Russia

The work presents the research results to improve the design of a low-inductive capacitor which is designed for operation at a charging voltage of 100 kV, to reduce electric field strength on its plate edges and increase the operational life. During the simulation, various edge shape options were considered, as well as possible treating solutions and insulating foils with different dielectric parameters. The displacement distance of adjacent plates was also determined to create a quasi-homogeneous electric field in the internal cavity of the capacitor, in which it is assumed to place a gas switch (fig.1) [1, 2].

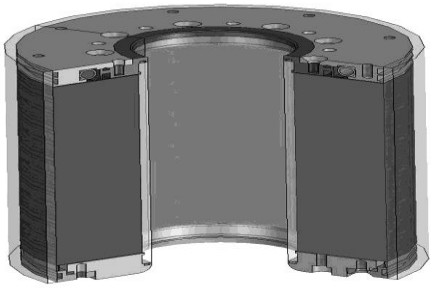

Fig.1. Sketch of capacitor.

As a result, the optimal configuration of the capacitor structure was found to allow winding of high voltage capacitor sections. The results obtained show the possibility of creating a high-voltage capacitor with a total inductance of ~ 25 nH, a capacitance of ~ 160 nF and an outer diameter of ~ 220 mm, which is necessary to create an LTD facility of a multi-terawatt power level with a pulse duration of ~ 100 ns [3].

REFERENCES

[1] I. Lavrinovich, S. Vagaytsev, A. Erfort, D. Rybka, D. Molchanov, A. Artemov, A. Zhigalin, A. Lensky / New Type Capacitor-Switch Assembly for LTD Technology // 2019 IEEE Pulsed Power & Plasma Science (PPPS), Orlando, FL, USA, 2019, pp. 1-4. DOI: 10.1109/PPPS34859.2019.9009957

[2] D. Molchanov, I. Lavrinovich, A. Artyomov, D. Rybka / New low-inductance capacitor-switch assembly // Journal of Physics: Conference Series. 2018. 1074. 012110.

[3] W.A. Stygar, T.J. Awe, J.E. Bailey et al. / Conceptual designs of two petawatt-class pulsed-power accelerators for high-energy-density-physics experiments // Phys. Rev. ST Accel. Beams, 2015. 18. 110401.

* The work was supported by the Russian Foundation for Basic Research (grant No. 19-48-700017).

THE ARCHITECTURE OF 100-NS LTD FACILITY BASED ON A NEW TYPE OF CAPACITOR-SWITCH ASSEMBLIES*

S.A. VAGAYTSEV, I.V. LAVRINOVICH, A.D. LENSKIY, D.V. MOLCHANOV, D.V. RYBKA

Institute of High Current Electronics SB RAS, Tomsk, Russia

The paper presents a technique for calculating the architecture of the LTD facility for high energy density physics applications with a pulse rise time of ~ 100 ns and an initial energy of ~ 50 MJ. The required output parameters in a MagLIF type load were taken from [1]. The design requirements for a new type of capacitor-switch assembly [2, 3], on the basis of which it is possible to develop such type of facility, are determined by the calculation results.

REFERENCES

[1] W.A. Stygar, T.J. Awe, J.E. Bailey et al. / Conceptual designs of two petawatt-class pulsed-power accelerators for high-energy-density-physics experiments // Phys. Rev. ST Accel. Beams, 2015. 18. 110401.

[2] I. Lavrinovich, S. Vagaytsev, A. Erfort, D. Rybka, D. Molchanov, A. Artemov, A. Zhigalin, A. Lensky / New Type Capacitor-Switch Assembly for LTD Technology // 2019 IEEE Pulsed Power & Plasma Science (PPPS), Orlando, FL, USA, 2019, pp. 1-4. DOI: 10.1109/PPPS34859.2019.9009957

[3] D. Molchanov, I. Lavrinovich, A. Artyomov, D. Rybka / New low-inductance capacitor-switch assembly // Journal of Physics: Conference Series. 2018. 1074. 012110.

* The work was supported by the Russian Foundation for Basic Research (grant No. 19-48-700017).

DIAGNOSTIC SYSTEM FOR THE LTD STAGE BASED ON "HCEICSA 160-0.1"

D. MOLCHANOV[1], *I. LAVRINOVICH*[1], *D. RYBKA*[1], *A ZHIGALIN*[1], *A. ARTEMOV*[1], *S. VAGAYTSEV*[1], *A. LENSKIY*[1], *A. ERFORT*[1]

[1] *IHCE SB RAS, Tomsk, Russia*

Currently, this technology is actively developing and attracting an increasing number of research teams from different countries. There are projects of powerful plants for inertial thermonuclear fusion, and less powerful for use in applied fields of knowledge and laboratory research. The basic element of these generators is the LTD stage. Its overall dimensions and output parameters determine the output parameters of the entire LTD module.

This paper presents the test results of a new compact 100nanosecond LTD stage, which is based on a low-inductance capacitor-switch assembly (CSA) «HCEIcsa 160-0.1». The main objective of this study was the development and implementation of a registration system that allows determining the actuation moment of each CSA in LTD stage with high accuracy.This system, supplemented by current and voltage sensors witch was installed in the load and in starting circuits, forms a complete diagnostic system of the LTD stage.It is sufficient to monitor all the main parameters of the stage and to further study the effect of the synchronism of the CSA operation on the parameters of the output pulse of both an individual LTD stage and the entire LTD driver.

PULSE FORMING NETWORKS FOR HIGH VOLTAGE PULSE GENERATORS RATED AT VOLTAGE UP TO 50 KV, CURRENT UP TO 10 KA AND FLATTOP DURATION FROM TENS TO HUNDREDS NANOSECONDS

A.V. AKIMOV[1,2], *P.A. BAK*[1], *M.N. EGORYTCHEV*[1]

[1]*Budker Institute of Nuclear Physics of Siberian Branch Russian Academy of Sciences, Novosibirsk, Russia*
[2]*Novosibirsk State University, Novosibirsk, Russia*

In Budker Institute of Nuclear Physics (BINP) the compact pulse forming networks (PFN) were developed to produce pulses of tens kV, above 10 kA, with flattop of tens and hundreds nanoseconds into a complex resistive-inductive load. PFNs are based on separate wound capacitive sections with a combined paper-film dielectric. Sections are combined and united in a monolithic assembly and filled with a castor oil. Such approach allows to build the compact PFNs with the low stray inductances of the capacitive cells at a quite low price. The paper presents the ways of a PFN's stray inductances reduction, it describes some technological features that help to provide a reliable PFN's assembly for long term use. The test data which demonstrate the pulsed characteristics of the PFNs fired into a matched resistive load and a complex resistive-inductive load are presented. The paper describes the PFN's life test results and the discovered technical disadvantages which could crucially decrease a PFN's life.

A lot of development and debugging were done that resulted in a small scale production of the oil-filled paper-film capacitors and PFNs. At the moment over 500 capacitors and 500 different PFNs are made in BINP. The life tests have shown the PFN's life time is above 10^6 pulses, this is the level that initially was aimed to be achieved. Due to external inductances the PFN's parameters are able to be precisely tuned for the load so the non-uniform PFN's impedance can be provided to produce a flat top for an inductive load. Figure 1 shows a non-uniform PFN rated at 50 kV which is capable of producing into a matched resistive-inductive load the pulses of 25 kV, 10 kA with a flattop of 400 ns and ±1% flatness.

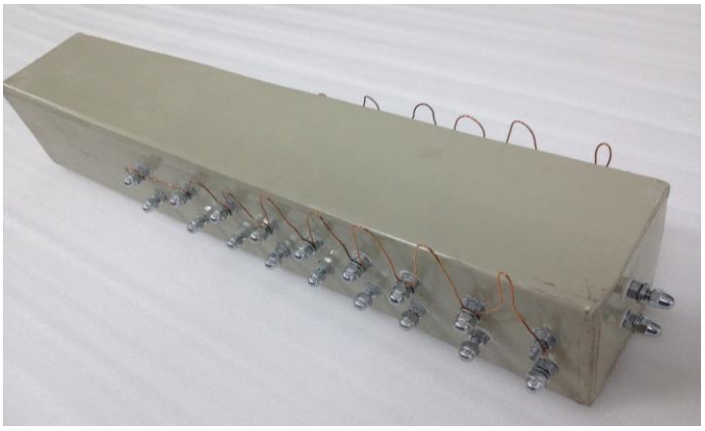

Fig.1. A non-uniform PFN rated at 50 kV, 10 kA, 400 ns flattop. A PFN's length is 700 mm.

REFERENCES

[1] G.S. Kuchinskiy, O.V. Shilin, L.T. Vekhoreva, "Principles of a designing of the power pulse forming networks for producing the nano- and microsecon pulses," Elektrichestvo, no. 9, pp. 16-21, 1997.

OPERATING CHARACTERISTICS OF THE SWITCH BASED ON A CAPILLARY DISCHARGE WITH ADJUSTABLE PREIONIZATION OF CATHODE REGION[1]

P.A. BOKHAN, P.P. GUGIN, M.A. LAVRUKHIN, D.E. ZAKREVSKY

A. V. Rzhanov Institute of Semiconductor Physics SB RAS, Novosibirsk, Russia

The results of studies of a new type of switch [1,2] based on a capillary discharge with a preionization of a cathode region are presented. The cathode region of the switch consists of two flat rectangular SiC cathodes with a total area of 22 cm^2 and two grids remote from the cathodes by a distance of 3 mm each and forming a 6 mm region between each other. A capillary of rectangular cross section with dimensions of 10x0.3 mm and a length of 35 mm is located at the side of cathode region. The inner surface of the capillary has a meander shape with a period of 2 mm, which avoids surface breakdowns along the walls of the capillary. Two copper plates connected to the cathodes of the device are attached to the outer surface of the capillary through an additional insulator. Such a configuration allows to reduce the inductance of the switch and has a great influence on providing a large breakdown development time t_d at high pulse repetition frequency (PRF) [2].

The positive voltage pulses from the generator and following magnetic compression line were applied to the anode of the switch, the cathode of the device was grounded. The charging time of the working capacitance was ~ 200 ns. The load resistance R_L varied from 24.5 to 98 Ohms. Parameters were measured in the burst operation mode at a PRF inside the burst f of 5 to 50 kHz. A positive pulse with an amplitude of up to 8 kV was applied between the grids and cathodes to preionize the cathode region 1 μs before each of the pulses in the burst. Current measurements were carried out using two low-inductance shunts.

The dependences of the switching efficiency η and the time of breakdown development delay t_d in the switch on the energy of the preionization pulse (Fig. 1a), PRF (Fig. 1b), pressure and type of working gas, and the amplitude of the switched voltage U_A are obtained. It is demonstrated that at low PRF the starting losses in the switch significantly depend on the energy of the preionization pulse of the cathode region W_{pre} (Fig. 1a). An increase in the amplitude of the charging voltage U_A leads to an increase in the efficiency of the switch η. For example, with a low load resistance of 24.5 Ohms, the efficiency η increases from 0.45 to 0.54 when voltage rises from 10 to 16 kV in helium. It was shown that in helium for PRF up to 50 kHz, with a switching time of t_{sw} ~ 1.5 ns, the compression ratio of the leading edge of the voltage pulse exceeds $S = t_d / t_{sw} = 300$ at $U_A = 16$ kV.

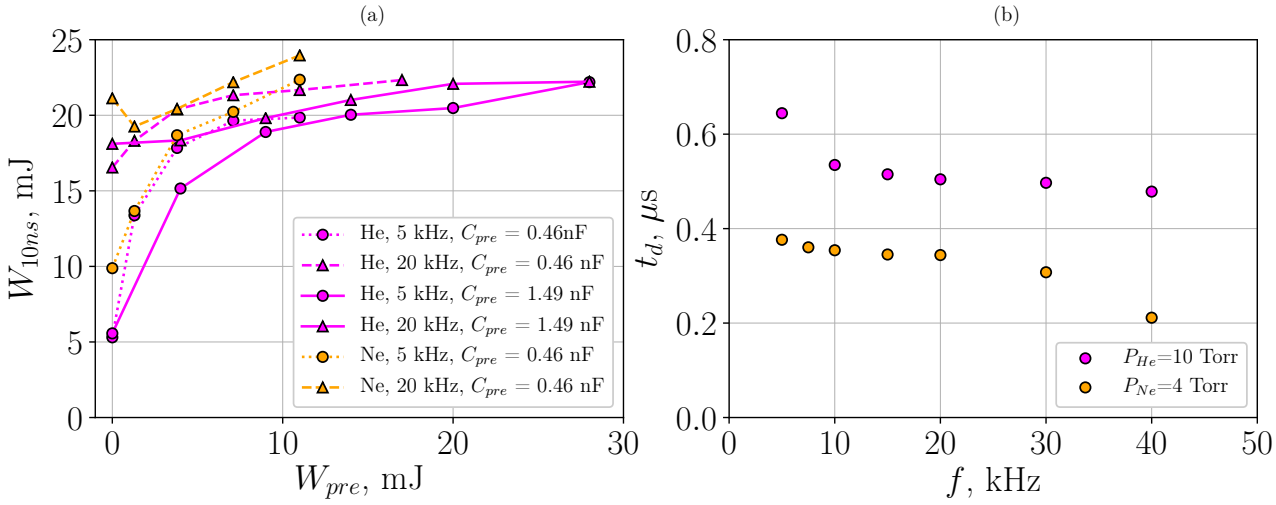

Fig.1. (a) - dependences of the energy dissipated in the load during the first 10 ns W_{10ns} on W_{pre} (U_A =16 kV, R_L=24.5 Ohm), (b) - dependences of the t_d on f (U_A=16 kV, R_L=24.5 Ohm).

REFERENCES

[1] P.A. Bokhan, P.P. Gugin, M.A. Lavrukhin, I.V. Schweigert, A.L. Alexandrov, D.E. Zakrevsky, "A high-voltage subnanosecond sharpener based on a combination of 'open' and capillary discharges", J. Phys. D: Appl. Phys., vol. *51*, p. 364001, 2018.

[2] P.A. Bokhan, P.P. Gugin, D.E. Zakrevsky, M.A. Lavrukhin, "Frequency Characteristics of a Subnanosecond Plasma Switch", Russian Physics Journal, Vol. 62, № 11, p. 2059, 2020.

[1] The work was supported by the Russian Science Foundation under grant No. 19-19-00069.

ELECTRICAL EXPLOSION OF FLAT CONDUCTORS IN MEGAUSS MAGNETIC FIELDS[1]

V. I. ORESHKIN[1], *S.A. CHAIKOVSKY*[2], *N.A. LABETSKAYA*[1], *I.M. DATSKO*[1], *V.A. VANKEVICH*[1]

[1]*Institute of High Current Electronics, SB, RAS, Tomsk, Russia*
[2]*Institute of Electrophysics, UD, RAS, Ekaterinburg, Russia*

On a high-current MIG generator [1] (current amplitude up to 2.5 MA, rise time 100 ns), experiments were conducted on the electric explosion of a copper foil 100 μm thick and 5 mm wide. Using a four-frame optical camera with an exposure time of 3 ns, the intrinsic emission of the external surface of the foil was recorded. Various stages of plasma formation and the development of instabilities were recorded in the images, and it was also shown that by approximately 75 ns from the beginning of the current, a plasma channel forms on the longitudinal axis of the foil. Analytical estimates of the value of the magnetic field gain at the edges of the foil are carried out. Estimates have shown that strengthening the magnetic field can lead to the formation of a shock wave directed from the edge of the foil to its center. The high current density on the axis may be due to a drop in resistivity caused by compression of the substance by the shock wave.

REFERENCES

[1] A. Luchinskii, N. A. Ratakhin, V. Fedushchak, and A. Shepelev, "Multipurpose transformer-type pulse generator", Russ. Phys. J., vol. 40, p. 1178, 1997.

1 The work was supported by Russian Foundation for Basic Research Grants No. 20-21-00036 and 19-08-01004

FORMATION OF THE DISCHARGE OVER SEMICONDUCTOR SURFACE IN TRIGGER UNIT OF COLD-CATHODE THYRATRON*

Y.D. KOROLEV, N.V. LANDL, V.G. GEYMAN, O.B. FRANTS, G.A. ARGUNOV, A.V. BOLOTOV, V.S. KASYANOV

Institute of High Current Electronics SB RAS, Tomsk, Russia

Currently, high-current switching devices based on low-pressure hollow-cathode pulsed discharge (so-called cold-cathode thyratrons) are widely used [1-4]. As in the case of classical thyratrons, a range of operating pressures of the switch corresponds to the left branch of Paschen's curve. Under these conditions, for both self-breakdown of the main gap of the thyratron and for external discharge triggering a considerable pre-breakdown electron current is required [1, 3, 5]. For the case of external triggering, this current is provided due to a special trigger unit that is placed in the main cathode cavity.

One type of the trigger units is based on a discharge over a semiconductor surface [4]. For such trigger units the delay time to breakdown in the thyratron main gap involves the delay time to initiation of the surface discharge, delay time to interception of the surface discharge current to the main cathode cavity and delay time to discharge development in the main gap. Our previous experiments have shown that the main contribution to jitter in delay times to breakdown in the thyratron main gap is provided by jitter in delay times to discharge initiation in the trigger unit and interception of the trigger discharge current to the main cathode cavity [6].

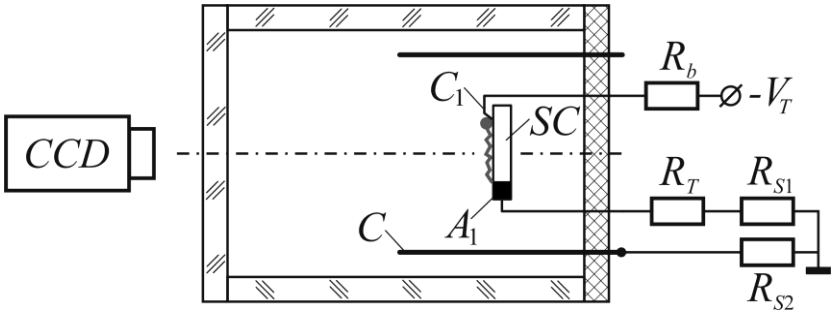

Fig.1. Schematic of the experimental setup. C – cathode cavity, C_1 – cathode of the trigger unit, A_1 – anode of the trigger unit, SC – semiconductor cylinder. R_b = 30 Ω, $R_{S1} = R_{S2}$ = 1 Ом, $R_T \leq 90$ Ω

In this report the results of investigation of the trigger unit based on a discharge over the semiconductor surface are presented. The schematic of experimental setup is shown in figure 1. Trigger unit was placed inside the hollow cathode C and mounted on dielectric flange. Trigger pulse V_T was applied to the multipoint cathode C_1 via a ballast resistor R_b. Due to this voltage the discharge was initiated between cathode C_1 and anode A_1 over the semiconductor surface SC. Surface discharge current and current to the cathode cavity were measured by shunts R_{S1} and R_{S2}. Experiments were carried out with the quarts chamber allowing us optical observation of surface discharge development with high time resolution. Data on surface discharge formation and delay times to current interception to the cathode cavity for different amplitudes of trigger pulse V_T and cathode cavity dimensions were obtained.

REFERENCES

[1] Y.D. Korolev and N.N. Koval, "Low-pressure discharges with hollow cathode and hollow anode and their applications," J. Phys. D: Appl. Phys., vol.51, Article Number 323001, 2018.

[2] K. Bergmann, M. Muller, D. Reichartz, W. Neff and R. Lebert, “Electrode phenomena and lifetime considerations in a radial multichannel pseudospark switch,” IEEE Trans. Plasma Sci., vol.28, pp. 1486-1490, 2000

[3] Y.D. Korolev and K. Frank, “Discharge formation processes and glow-to-arc transition in pseudospark switch,” IEEE Trans. Plasma Sci., vol.27, p.1525, 1999

[4] V.D. Bochkov, V.M. Dyagilev, V.G. Ushich, O.B. Frants, Y.D. Korolev, I.A. Shemyakin, K. Frank, “Sealed-off pseudospark switches for pulsed power applications (current status and prospects),” IEEE Trans. Plasma Sci., vol.29, no.5, pp. 802-808, 2001.

[5] Y.D. Korolev, N.V. Landl, V.G. Geyman, O.B. Frants, G.A. Argunov, A.V. Bolotov, “Role of Prebreakdown Currents in a Static Breakdown of a Two-Sectioned Cold-Cathode Thyratron, Russ.Phys.J., vol.62, No.7, pp.1269-1278, 2019

[6] Y.D. Korolev, N.V. Landl, V.G. Geyman, O.B. Frants, “Hollow-cathode glow discharge in a trigger unit of pseudospark switch,” Phys. Plasmas., vol.25, no.11, 13510, 2018

* This work was funded by RFBR according to the research project № 19-48-700023.

FEATURES OF THE DISCHARGE FORMATION IN THE TRIGGER UNIT BASED ON FLASHOVER*

V.O. NEKHOROSHEV, N.V. LANDL, Y.D. KOROLEV, V.G. GEYMAN, O.B. FRANTS, G.A. ARGUNOV, I.A. SHEMYAKIN

Institute of High Current Electronics SB RAS, Tomsk, Russia

Currently, high-current switching devices based on low-pressure hollow-cathode pulsed discharge (so-called pseudospark switches) are widely used [1-4]. The design and principle of operation of these switches are close to those of a classical hot-cathode hydrogen thyratrons. However, these devices do not have a hot cathode. Therefore, pseudospark switches are often called cold-cathode thyratrons or thyratrons with a grounded grid [3, 4].

As in the case of classical thyratrons, a range of operating pressures of the switch corresponds to the left branch of Paschen's curve. Under these conditions, the electron free path for ionization is much in excess of the electrode separation. For both self-breakdown of the main gap of the thyratron and for external discharge triggering a considerable pre-breakdown electron current is required [1, 3, 5]. For the case of external triggering, this current is provided due to a special trigger unit that is placed in the main cathode cavity. One type of trigger units is based a discharge over a dielectric of semiconductor surface or, in other words, based on a flashover [3, 4].

Any trigger unit is intended for plasma generation of trigger discharge inside the thyratron cathode cavity at a curtain instant of time. When a trigger unit based on discharge formation over the dielectric surface in used, trigger discharge plasma is generated due to the interception of surface discharge current to the main cathode cavity. In this report the results of investigation of the discharge over the dielectric surface with the low value of dielectric permittivity are presented. Schematic of the experimental setup is shown in fig. 1. Experiments were carried out with the demountable quarts chamber. Data on surface discharge development and delay times to current interception to the main cathode cavity are obtained. Surface discharge images with nanosecond time resolution were recorded using CCD camera.

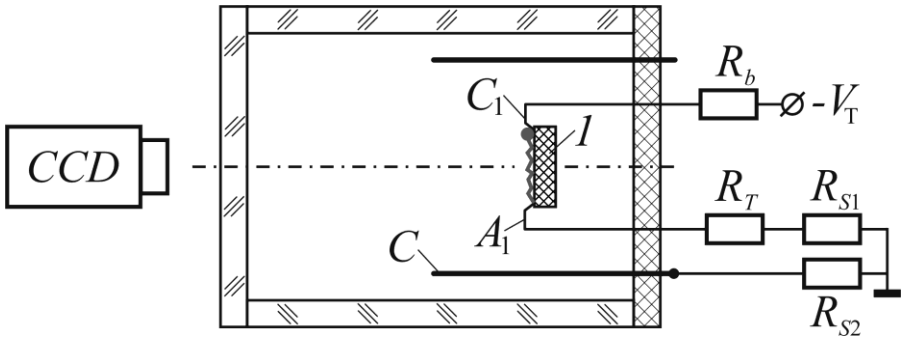

Fig.1. Schematic of the experimental setup. *C* – cathode cavity, C_1 – cathode of the trigger unit, A_1 – anode of the trigger unit, *1* - dielectric. R_b = 30 Ω, $R_{S1} = R_{S2}$ = 1 Ом, $R_T \leq 90$ Ω

REFERENCES

[1] Y.D. Korolev and N.N. Koval, "Low-pressure discharges with hollow cathode and hollow anode and their applications," J. Phys. D: Appl. Phys., vol.51, Article Number 323001, 2018.

[2] K Bergmann, M Muller, D Reichartz, W Neff and R Lebert, “Electrode phenomena and lifetime considerations in a radial multichannel pseudospark switch,” IEEE Trans. Plasma Sci., vol.28, pp. 1486-1490, 2000

[3] Y.D. Korolev, K. Frank, “Discharge formation processes and glow-to-arc transition in pseudospark switch,” IEEE Trans. Plasma Sci., vol.27, p.1525, 1999

[4] V.D. Bochkov, V.M. Dyagilev, V.G. Ushich, O.B. Frants, Y.D. Korolev, I.A. Shemyakin, K. Frank, “Sealed-off pseudospark switches for pulsed power applications (current status and prospects),” IEEE Trans. Plasma Sci., vol.29, no.5, pp. 802-808, 2001.

[5] Y.D. Korolev, N.V. Landl, V.G. Geyman, O.B. Frants, G.A. Argunov, A.V. Bolotov, “Role of Prebreakdown Currents in a Static Breakdown of a Two-Sectioned Cold-Cathode Thyratron, Russ.Phys.J., vol.62, No.7, pp.1269-1278, 2019

* This work was funded by RFBR according to the research project № 19-48-700023.

DISCHARGE CHARACTERISTICS OF DOUBLE-GAP PSEUDOSPARK SWITCH*

WEIDONG DING[1], SAIKANG SHEN[1], JIAQI YAN[1], Y. D. KOROLEV[2], N. V. LANDL[2]

[1]State Key Laboratory of Electrical Insulation and Power Equipment, Xi'an Jiaotong University, Xi'an, China
[2]Institute of High Current Electronics RAS, Tomsk, Russia

Pseudospark switch is a special kind of the pulsed discharge switch, which is triggered from the grounded hollow cathode and operates at the left branch of Paschen's curve [1]. In special cases, the switch allows the nanosecond stability of operation with respect to the trigger pulse. In particular, this is related to the switches with the trigger unit based on the auxiliary glow discharge [2, 3]. On the other hand, the switches with the trigger unit based on the flashover also have the prospects for nanosecond triggering [1]. This paper deals with the investigation and development of the switch, in which the flashover is used in the trigger unit.

The design of the double-gap switch with the intermediate gradient electrode is shown in Fig. 1. The hollow electrodes are made of copper. The thickness of the flat part of the electrodes with the boreholes is 3mm. The trigger unit is installed in the hollow cathode, and the surface discharge in this unit is provided over the $BaTiO_3$ dielectric with high permittivity. The testing results show that such a unit is able to operate with a pulse repetition rate up to 500 Hz.

An example of the discharge waveforms is presented in Fig. 2.

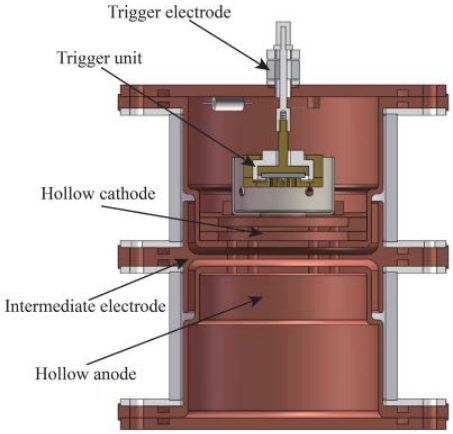

Fig.1. The structure of the double-gap switch.

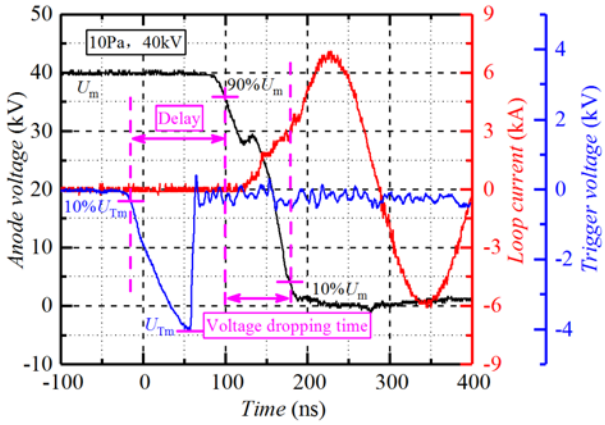

Fig.2. The typical discharge waveforms.

It is seen that the anode voltage for the two-sectioned switch is readily reached to 40 kV. The instant of the sharp voltage drop at the trigger pulse corresponds to the delay time to breakdown in the trigger unit t_1. After that, within a typical time interval of t_2 = 100 ns, the high loop current of the main discharge appears (red trace). Then the total delay time to breakdown in the main gap with respect to beginning of the trigger pulse is $t_d = t_1 + t_2$. The waveforms demonstrate the phenomenon of the current quenching, i.e. certain protraction in the current rise. However, an increase in the gas pressure results in suppression of this phenomenon. Besides, the total delay time decreases with the gas pressure. As a whole, the tests show that the jitter in the switch triggering at a level of 10 ns is achievable.

REFERENCES

[1] Y. D. Korolev, N. N. Koval, "Low-pressure discharges with hollow cathode and hollow anode and their applications," J. Phys. D: Appl. Phys., vol. 51, Article Number 323001, 2018. vol. 2018.

[2] Y. D. Korolev, N. V. Landl, V. G. Geyman, O. B. Frants, and G. A. Argunov, "Hollow-cathode glow discharge in a trigger unit of pseudospark switch," Physics of Plasmas, vol. 25, Article Number 113510, 2018.

[3] Y. D. Korolev, N. V. Landl, V. G. Geyman, G. A. Argunov, O. B. Frants, A. V. Bolotov, "Methods of triggering for the cold-cathode thyratrons with a trigger system based on an auxiliary glow discharge," AIP Advances, vol. 9, no. 8, Article Number 085326, Aug. 2019.

*The work was supported by the National Natural Science Fund of China (Grant No. 51777163) and by the Russian Foundation for Basic Research (Grant # 19-48-700023)

SMALL-SIZED NANOSECOND SOURCE OF POWERFUL WIDE-BAND VUV-UV RADIATION

V.I. BARYSHNIKOV[1], *V.L. PAPERNY*[2]

[1]*Irkutsk State Transport University,*
Irkutsk, 664074, Russia
[2]*Irkutsk State University,*
Irkutsk, 664003, Russia

A powerful VUV-UV volume discharge was observed when a powerful high-voltage subnanosecond pulse (<1 ns) was applied to a matched coaxial low-inductance gas-filled chamber at a xenon pressure of 0.1-3 atm. To form a discharge, a small-sized (length 40 cm, diameter 10 cm) (sub) nanosecond (0.1–5.0 ns) generator with a voltage of 250 kV, a current of 5 kA, and a pulse repetition rate of 0.1–12.5 Hz was used. It was shown that the duration of the radiation pulse in the volume discharge mode does not exceed 1 ns, the radiation power reaches 12 MW, and its spectrum can be approximated by a Planck distribution lying in the wavelength range of λ = 10–400 nm with a maximum at λ = 30 nm.

Evaluation of the parameters of the radiation spectrum by the method of absorbers using aluminum foil with a thickness of 0.5; 1.0 and 1.5 μm confirmed the above spectrum parameters.

MAKING GRADIENT SURFACE CONDUCTIVITY OF STEEL AND STUDY THE EFFECTS UNDER HIGH PULSED MAGNETIC FIELDS*

E.YU. ZAYTSEV, A.V. SPIRIN, S.N. PARANIN, V.I. KRUTIKOV, D.S. KOLEUKH, P.A. RUSSKIKH

Institute of Electrophysics UB of RAS, Yekaterinburg, Russia

The present work is aimed at the development of steel-based materials and approaches for engineering high-field pulsed magnets employed in magnetic pulse welding (MPW) technique. Poor durability of tool coils (inductors) for MPW is the main technical problem which constrains its worldwide application. As known, coil failure occurs at working surface where conductor is subjected to intense thermo-mechanical stresses under the force action of pulsed magnetic field and, especially, Joule heating [1]. To reduce the inductor surface overheating and the thermal stresses, as a consequence, a conductor whose resistivity decreases with depth, monotonically or stepwisely, can be used [1].

The paper focuses mainly on making and study steel conductors with inhomogeneous surface conductivity and its effect on material behavior under generation of high pulsed magnetic fields of tens teslas in amplitude and tens microseconds in duration. Monotonically changing resistivity was realized by pack chromizing several medium-carbon steels (*e.g.*, 30KhGSA), which were treated at 1000°C in Ar for different time and using different chromium load. Some results on chromium distribution with depth are shown on fig. 1a. To achieve a discrete change in resistivity, a powder technology is proposed that involves the use of a base steel powder, *e.g.*, 30KhGSA, and various compositions based on it with chromium addition in different amounts, 3 to 10 wt.%, to form a layered structure by compaction followed by the sintering in vacuum. Let us note, our first results on theoretical analysis of magnetic and thermal effects in such systems were obtained using the model resistivity distributions (*e.g.*, [2]), but a real resistivity distribution across modified layer was unestablished. The assumption that the resistivity over the thickness of steel after chromizing should change in accordance with the distribution of chromium was confirmed by the results obtained on powder samples which showed an effect of chromium addition on steel resistivity (fig. 1b). Here is proposed the approach to investigate the resistivity distribution across diffused layer. It involves the measurement of resistance on steel plate after diffusion chromizing each time after surface layer removal by polishing onto a depth 10–20 μm (fig. 1c).

Finally, testing the obtained samples under high magnetic field generation were performed on the samples after chromizing in the form of small cylindrical single-turn coils, and on the powder samples in the form of thick disks. The obtained results will be discussed in extended paper.

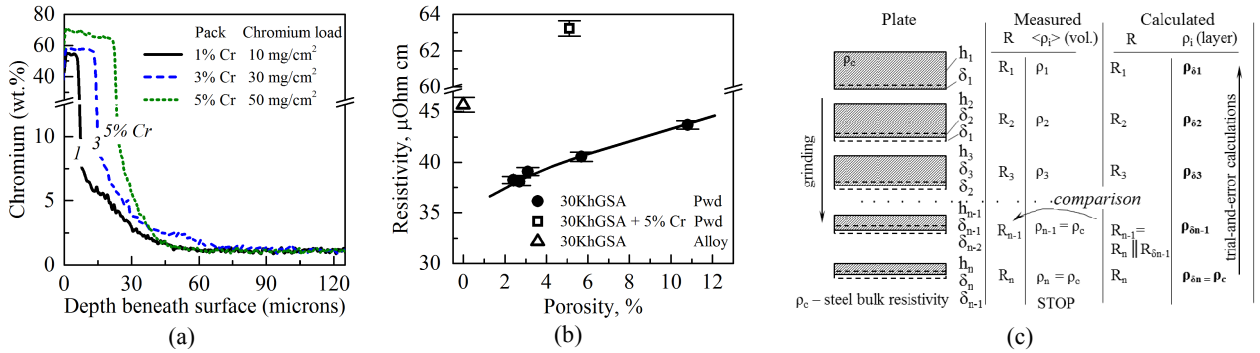

Fig. 1. (a) – chromium profiles at surface layer of 30KhGSA steel after pack chromizing at 1000°C at different chromium content, (b) – an influence of material porosity and chromium addition on resistivity of 30KhGSA steel samples obtained by powder compaction, (c) – schematic diagram of resistivity distribution measurement procedure.

REFERENCES

[1] G.A. Shneerson, M.I. Dolotenko and S.I. Krivosheev, "Strong and Superstrong Pulsed Magnetic Fields Generation, " Walter de Gruyter GmbH, Berlin/Boston, 429 p., 2014.

[2] A.V. Spirin, G.Sh. Boltachev, V.I. Krutikov, S.N. Paranin, P.A. Russkikh, D.S. Koleukh, "Surface Modification of Steel Inductor as an Attempt to Enhance Its Durability in High Pulsed Magnetic Fields," AIP Conf. Proc. Physics, Technologies and Innovation (PTI), 2174, Art.No. 020163, pp. 1-5, 2019. https://doi.org/10.1063/1.5134314.

* The work was partly supported by the RFBR grants No. 19-08-00931 and No. 20-58-00029.

SYNCHRONIZATION OF TWO PULSE VOLTAGE GENERATORS WITH DIFFERENT POLARITY*

E.V. PETRENKO A.S. YUDIN

Tomsk Polytechnic University, Tomsk, Russian Federation

The report is devoted to a method for synchronizing two pulse voltage generators (PVG) for using in electric-discharge materials processing technologies, such as drilling or crushing. Since the implementation of the conditions of electric pulse breakdown and destruction of solids requires a source with certain time and energy parameters [1], capacitive high-voltage pulse generators according to the Arkadyev – Marx scheme [2] are widely used. The synchronization of generators is due to the need to organize the simultaneous effect of voltage pulses of different polarity and microsecond duration on solid dielectric materials, in order to test the idea of improving the energy and resource efficiency of electric-discharge destruction methods.

To achieve this goal, two platform-type generators consisting of five stages were used. Each stage consisted of IK - 100/0.1 type capacitors. Capacitors are charged through inductors. Ball gaps are made of stainless steel and are located in a common dielectric tube. The operating voltage of the PVG was regulated by changing the distance of the interelectrode gaps of the ball gaps at each stage. The charging voltage of each PVG did not exceed 35 kV. From the experiments of idling and short circuit of the generators it was found that the duration of the pulse front is $\tau_f = 0.2 \cdot 10^{-6}$ s., And the wave impedance $Z_w = 12.0$ Ohms. The accuracy of synchronization varies within tens of nanoseconds.

To synchronize the operation of both generators, trigatron-type arresters control circuits were used. To fine tune the synchronous start of two PVGs, the control signal for the triggering pulse generators was supplied via optical channels with the possibility of adjusting the delay within 2 microseconds.

Voltage pulses were recorded using pulse voltage dividers. The voltage signals were recorded using a Tektronix TDS-3032B digital storage oscilloscope. Time and amplitude sweeps made it possible, with sufficient resolution and accuracy, to trace the dependence of voltage on time in the prebreakdown and channel stages.

REFERENCES

[1] Certificate for opening No. A-122 of 04.29.1998 with priority of 12.14.1961. A.A. Vorobyov, G.A., Vorobyov, A.T. Chepikov. Patterns of breakdown of a solid dielectric.

[2] Semkin B.V., Usov A.F., Kurets V.I. Fundamentals of electropulse fracture of materials. St. Petersburg: Science, 1955 - 276p.

* The reported study was funded by RFBR, project number 19-38-90071.

DIFFERENT SENSITIVITY OF NORMAL AND TUMOR CELLS TO PULSED RADIOFREQUENCY EXPOSURE

A.A. EVTINA[1,3], *P.V. PRIPUTNEV*[2], *L.P. ZHARKOVA*[1,2], *M.A. BULDAKOV*[3], *M.A. BOLSHAKOV*[1,2], *I.V. ROMANCHENKO*[2], *V.V. ROSTOV*[2]

[1]*National research Tomsk state university, Tomsk, 634050, Russia*
[2]*Institute of High Current Electronics SB RAS, Tomsk, 634055, Russia*
[3]*Cancer Research Institute, Tomsk National Research Medical Center, RAS, Tomsk, 634009, Russia*

In recent years, a number of biomedical studies has been conducted in both preclinical and clinical settings to determine the safety and effectiveness of microwave radiation on biological objects. For example, many works are devoted to the study of the antitumor effect of non-ionizing radiation. Various mechanisms of destruction of the membrane structures of tumor cells [1], their genetic apparatus [2,3], inhibition of mitochondrial respiratory activity [4] etc have been shown.

In this work, the effect of a pulsed radiofrequency field on the proliferative activity of tumor and normal cells *in vitro* was evaluated. Tumor cells – cervical cancer cells (HeLa) and normal rat fibroblast cells (3T3) were used as cell lines. The cells were exposed to a RF field using a setup based on a nonlinear transmission line [5]. Irradiated cells located in test tubes with a nutrient medium were placed inside a rectangular waveguide connected with the generator. A microwave energy pulse was fed into the waveguide through coaxial to waveguide adapter, which is a UWB pulse with its central frequency close to 1 GHz and duration of about 10 ns. The proliferative activity of cells was assessed using the MTT-test. For a more detailed study of cell growth kinetics, the RTCA intelligence (USA) system of multiparametric analysis of cell cultures in real time was used.

To estimate the level of absorbed power and electric field strength in the irradiated medium containing cells, the dependence of the real and imaginary parts of its permittivity were measured. Using these data, the portion of the microwave pulse power absorbed in the medium with cells and the value of the electric field strength inside were estimated using numerical simulation techniques.

Experiments have shown that the action of a pulsed radiofrequency field leads to inhibition of HeLa tumor cell proliferation by up to 40% relative to the control group. The magnitude of this effect depended on the number of pulses, as well as the duration of exposure. The maximum effect was observed after exposure to 1000+1000 pulses and a pulse repetition rate of 13 Hz. The reaction of normal cells was significantly different. It was shown that exposure to radiofrequency pulses stimulates the proliferation of normal cells by up to 15%, and after 5 days, the value of the studied indicator approached the control group.

The obtained data allow to conclude that the effect of radiofrequency pulses of microwave radiation is relevant to use in studies aimed at antitumor therapy, since non-thermal action does not cause the destruction of neighboring normal tissues surrounding tumor neoplasms [6].

REFERENCES

[1] M. Pompili, G. Francica, “Irreversible electroporation for hepatic tumors,” J Ultrasound, vol. 22, no. 1, pp. 1–3, March 2019.

[2] A.A. Greschner, X. Ropagnol, M. Kort, N. Zuberi, J. Perreault, L. Razzari, M.A. Gauthier, “Room-Temperature and Selective Triggering of Supramolecular DNA Assembly/Disassembly by Nonionizing Radiation,” J. Am. Chem. Soc., vol. 141, pp. 3456−3469, 2019.

[3] G.H. Elgemeie, R.A. Mohamed, “Microwave chemistry: Synthesis of purine and pyrimidine nucleosides using microwave radiation,” Journal of Carbohydrate Chemistry, vol. 38, no. 1, pp. 1–47, 2019.

[4] L.P. Zharkova, I.V. Romanchenko, M.A. Buldakov, P.V. Priputnev, M.A. Bolshakov, V.V. Rostov, “Mitochondrial Membrane Permeability After Nanosecond Electromagnetic Pulsed Exposure”, 20th Int. Symp. on High-Current Electronics, pp. 158–161, 2018.

[5] I.V. Romanchenko, V.V. Rostov, A.V. Gunin, V.Yu. Konev, “Gyromagnetic RF source for interdisciplinary research,” Review of Scientific Instruments, vol. 88, no. 2, 024703, 2017.

[6] T. Lyu, X. Wang, Z. Su, J. Shangguan, C. Sun, M. Figini et al., “Irreversible electroporation in primary and metastatic hepatic malignancies,” Medicine, vol. 96, no. 17, pp. 1–7, 2017.

THE PIG ION SOURCE PULSE MODULATION

N.N. SCHITOV

Dukhov Automatics Research Institute (VNIIA), 22 Suschevskaya Ul., Moscow 127055, Russia, nschitov@mail.ru, phone.: 89160820555

The investigations' onset of pulsed fields influence on Penning ion sources (PIG IS) in pulse or frequency regimes was described in [1]. This modulation was carried out by pulsed fields generated at the storage capacitance discharge through flat spiral antennas [2] being cathodes of a Penning cell in H_2. It turned out that the stable discharge initiation in this configuration was possible only at rather high pressures. The completion of the investigations program implied the fabrication of anodes in solenoid forms both outside (to compare) and inside cell surfaces. Thus the number of possible combinations (mutual fields direction etc) rose up to 9.

However, the fabrication of all PIG IS electrodes from wire (as in [1]) besides poor manufacturability leads to low results reproducibility and high eddy currents. That is why they were made of a metalized ceramics whereas coils fabrication was done by turning lathe cutter (grooves). Cathodes were washers Ø 40 mm with central holes Ø 4 mm and one side coated by magnetron sputtered two-layer Cr/Cu (~0.4 μm) film formerly copper plated (~100 μm). Finally the Al layer (~0.1 μm) was thermally evaporated on this coating just to compare with [1]. In this metal coating the spiral groove was cut by the 0.2 mm cutter with the 1 mm lead of helix so that the total number of turns consisted around 15 that corresponded to the inductivity around 0.8 μH. The anode was made in two ways: the spiral coil was fabricated on the Ø 40 mm ceramic cylinder (30 mm height) inner surface and outer surfaces. In the later case the inner (unbroken) surface was separated from the outer by removing metallization from cylinder flanks and cowling faying surface. The anode coil contained in both cases 25 turns that corresponded to around 18 μH inductivity.

The modified equivalent scheme including spiral anode was composed and analyzed. Total pulse fields generated through store capacitor discharge were calculated. Using these calculations electrons trajectories and correspondingly ionization probabilities were estimated for various fields' directions' combinations. These estimates were compared with the experimental results.

The modulation investigation experimental unit was described in detail in [1]. Bigger than in [1] inductivity values led to the discharge duration rising up that allowed in addition to the other pulse magnetic field configuration to initiate the discharge at smaller residual pressure. The feed circuit optimal parameters as well as the hydrogen pressure range corresponding to effective modulation are presented. The calculated pulsed fields – magnetic as well as curl electric one were used to plasma characteristics estimation according to the method presented in the "plasma module" [2]. These estimates are also presented.

REFERENCES

[1] *N N Schitov 2019* J. Phys.: Conf. Ser. **1393** 012053. doi:10.1088/1742-6596/1393/1/012053

[2] *V.A. Kadetov* Diagnostics and modeling of an inductively coupled radio frequency discharge in hydrogen // Dissertation zur Erlangung des Grades eines Doctors der Fakultät für Physik und Astronomie der Ruhr-Universität Bochum, 2004.

This work was partly supported by Russian Foundation for Basic Research under grant #12-02-13513 – ofi_m_RA.

SMALL PULSED PLASMA THRUSTER BASED ON FLASHOVER DISCHARGE*

I.L. MUZYUKIN[1,2], *P.S. MIKHAILOV*[1]

[1]*Institute of Electrophysics of the Ural Division of the Russian Academy of Sciences, Amundsen 106, Ekaterinburg, Russia,*
[2]*Institute of Physics and Technology, Ural Federal University, 21 Mira Str., Ekaterinburg, Russia*

Currently, the space industry is actively developing, and with it, the demand for different space thrusters is growing [1]. In this work, a prototype of a small size pulsed plasma engine is described and investigated.

The main idea was to make a small electric propulsion system that could be used on CubeSat and other small satellites. It follows that the mass of the propulsion system should not exceed 250g and the power consumption of 5W [2]. The design of the thruster is simple; it consists of a metal cathode and anode and a solid insulator between them as a propellant. Thrust is produced by plasma flow generated by pulsed vacuum flashover discharge. In this prototype, coaxial electrode design with a gap about 0.3 mm was used. As the material for the electrodes, Cu or Al can be used. In addition to the thruster, it was necessary to develop a Power processing unit (PPU) which could generate high voltage impulses with an amplitude of several kV. By changing the frequency of the generator, thrust can be adjusted. With the right pulse parameters, it is possible to achieve a working model with minimal cathode erosion, to ensure high system stability.

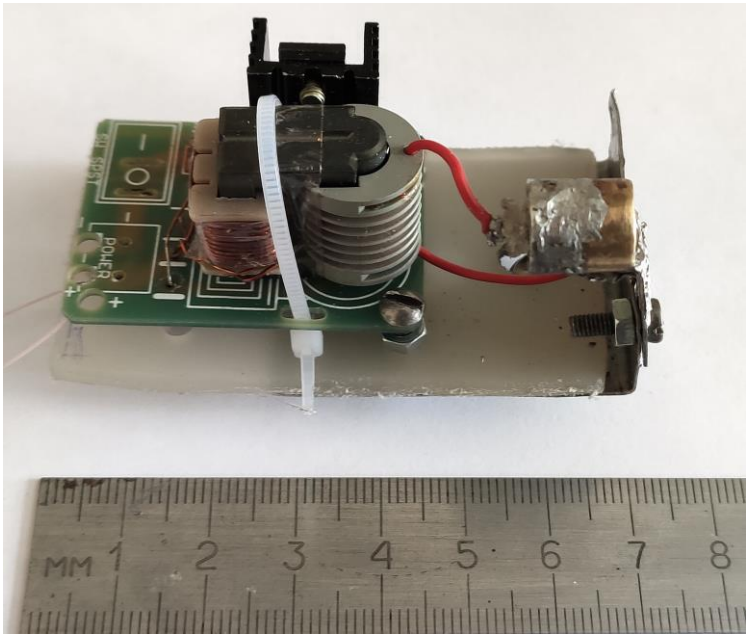

Fig.1. A laboratory prototype of a small size pulsed plasma thruster consists of a coaxial electrode and a blocking oscillator.

Fig. 1 shows a laboratory prototype of a thruster with mass less than 80g. Blocking oscillator was used as a high-voltage pulse generator due to its simplicity. The generator can operate at a frequency of from 7 to 16 kHz with pulse amplitude up to 4.5 kV and a length of 100 − 200 ns. To measure a thrust value, a torsion pendulum was used. With an electricity consumption of 20 W o, a thrust of 200 μH was achieved.

REFERENCES

[1] Levchenko, Igor, et al. "Space micropropulsion systems for Cubesats and small satellites: from proximate targets to furthermost frontiers." Applied Physics Reviews 5.1 011104, 2018; doi:10.1063/1.5007734

[2] CubeSat Design Specification (2014) Rev. 13, The CubeSat program, Cal Poly SLO, February 2014

* This work was supported in part by RFBR Grant Nos. 18-08-00547, 19-08-00783, 19-58-53006.

DOSE DEPTH DISTRIBUTION OF PULSED ELECTRON BEAM WITH WIDE ELECTRON KINETIC ENERGY SPECTRUM FOR POLYETHYLENE TARGET*

M.A. SEREBRENNIKOV[1], A.V. POLOSKOV[1], I.S. EGOROV[1]

[1]Tomsk Polytechnic University, 2a Lenin Avenue 634028, Tomsk, Russia, mas48@tpu.ru, 8(3822)701777 (add. 2577)

Pulsed electron beams are widely used for surface and bulk materials processing [1,2], including commercial irradiation of polymers [3]. The result of a sample irradiation is determined by characteristics of used electron beam, that provides the required distribution of the absorbed dose in the volume of the processed material. This paper presents a study of the depth dose distribution of a pulsed electron beam with a wide kinetic energy spectrum of the ASTRA-M accelerator (up to 350 kV of accelerating voltage, up to 0.6 kA of beam current, 150 ns of beam pulse duration at FWHM) [4] for polyethylene target. The pulsed electron beam was ejected from the vacuum diode through a titanium foil (60 μm) of the diode exit window. Polyethylene film of varying thickness was used as a target. A total absorption calorimeter was used to measure the beam characteristics after it passing through the target. The research was carried out for two modes of accelerator operation, providing different spectra of electron kinetic energies: we used two amplitudes of accelerating voltage pulses of 200 kV and 305 kV. The results are presented in Fig. 1.

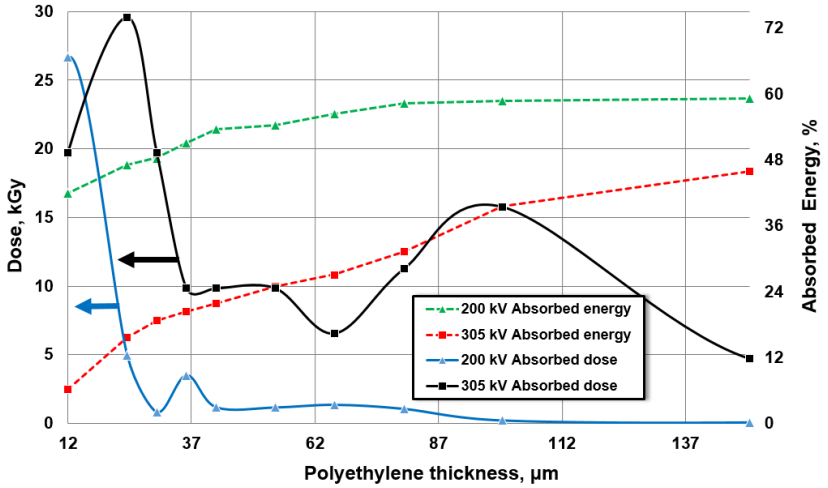

Fig. 1. – Distribution of absorbed dose and electron beam energy in a polyethylene target

Analysis of the measurement results shows that the absorbed dose maximum of the pulsed electron beam in used operation modes concentrates in the layer from 12 to 30 μm of the polyethylene target. The accelerator operating mode of 200 kV provides the maximum absorbed dose at a depth of 12 μm in the measurement range. The second maximum of the absorbed dose curve is present in the 305 kV mode, which indicates a non-monotonic character of the kinetic energy spectrum curve. Thus, the experimental study of dose depth distribution for polyethylene target showed the possibility of using a pulsed electron beam both to create the maximum dose at the surface (200 kV mode) and at the target depth (305 kV mode). The obtained data can also be used for comparative research and monitoring of electron diodes characteristics for accelerator adjusting and testing.

REFERENCES

[1] S. Korenev, Electron beam curing of composites, Vacuum. 62 (2001) 233–236. https://doi.org/10.1016/S0042-207X(00)00421-8.

[2] M. Emami-Meibodi, M.R. Parsaeian, R. Amraei, M. Banaei, F. Anvari, S.M.R. Tahami, B. Vakhshoor, A. Mehdizadeh, N. Fallah Nejad, S.P. Shirmardi, S.J. Mostafavi, S.M.J. Mousavi, An experimental investigation of wastewater treatment using electron beam irradiation, Radiat. Phys. Chem. 125 (2016) 82–87. https://doi.org/10.1016/j.radphyschem.2016.03.011.

[3] R.L. Clough, High-energy radiation and polymers: A review of commercial processes and emerging applications, Nucl. Instruments Methods Phys. Res. Sect. B Beam Interact. with Mater. Atoms. 185 (2001) 8–33. https://doi.org/10.1016/S0168-583X(01)00966-1.

[4] I. Egorov, G. Remnev, A. Poloskov, M. Serebrennikov, Effect of emission current delay on the efficiency of electron beam production, Vacuum. (2017) 1–5. https://doi.org/10.1016/j.vacuum.2017.03.030.

* Preparation of the experiments and analysis of the data were supported by RFBR grant № 20-02-00870.

CHARACTERISTICS OF LASERS ON SELF-TERMINATING TRANSITIONS OF METAL IONS PUMPED BY EPTRON-BASED PULSE GENERATOR[1]

P.A. BOKHAN, P.P. GUGIN, M.A. LAVRUKHIN, D.E. ZAKREVSKY

A. V. Rzhanov Institute of Semiconductor Physics SB RAS, Novosibirsk, Russia

A feature of lasers on self-terminating transitions is an increase in laser efficiency and the optimal pulse repetition frequency (PRF) of radiation, and as a result of the average output power, with a reduction of the voltage pulse edge of pumping generator. In particular, this effect was experimentally demonstrated in [1] for a copper vapor laser when a kivotron with a transition time to the conducting state of ~ 1 ns was applied as a switch. However, the operating mode of the kivotron with a switching time of ~ 1 ns and a compression ratio of more than ~ 50 has a limitation (even in the burst operating mode) of maximum PRF to a value of less than 20 kHz [2], which does not allow reaching the ultimate values of laser characteristics. For lasers based on self- terminating transitions of metal ions, in general, the optimal PRF is greater than in case of atoms. For example, for a mercury vapor laser with λ = 398.4 nm, in [3], by the double pulse method an increase in the laser energy with an increase in PRF to values ~ 200 kHz was demonstrated. Implementation of a pumping generator operating at such a high PRF is possible with the use of a new type of a switch - eptron [4].

In the burst operating mode, the frequency characteristics of a mercury vapor laser were studied up to 200 kHz. The gas discharge tube had an internal diameter of 0.5 cm and a length of 30 cm; an external heater was used to create the required mercury vapor pressure. Typical waveforms of voltage, current and laser pulses are shown in Fig. 1a. Also, characteristics of a laser on self-terminating transition of a barium ion with λ = 614.2 nm was studied up to PRF 50 kHz (Fig. 1b.) Active medium had diameter of 1.5 cm and length of 50 cm. Two electrical circuits were used for pumping: based on magnetic compression with a voltage rise time on laser element of ~ 30 ns; with the use of eptron, which sharpened the edge of the voltage pulse on the tube up to ~ 2 ns. For both lasers, the use of the second circuit contributed to an increase in the optimal laser PRF and pulse energy. It should be also noted that the study of lasers on self-terminating transitions of metal ions pumped by high-voltage pulses with such a short edge was carried out for the first time.

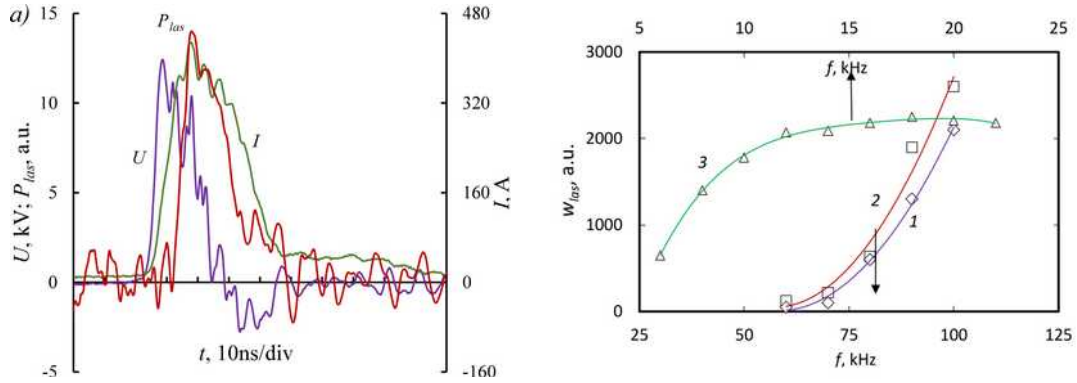

Fig.1. (a) - Voltage *U*, current *I*, and lasing power P_{las} waveforms of *He-HgII* laser, *f* = 100 kHz; (b) - frequency characteristics of *He-HgII* laser for second(1) and third(2) pulses in the burst and of *He-BaII* laser λ=614 nm.

REFERENCES

[1] P.A. Bokhan, P.P. Gugin, D.E. Zakrevskii, M.A. Lavrukhin, "Frequency and energy characteristics of a Cu–Ne laser at different durations of the leading edge of the excitation pulse". Quantum Electronics, vol. 49, № 8, p. 749, 2019.

[2] P.A. Bokhan, P.P. Gugin, M.A. Lavrukhin, I.V. Schweigert, A.L. Alexandrov, D.E. Zakrevsky, "Limit characteristics of switches based on planar open discharge", J. Phys. D: Appl. Phys., vol. *51*, p. 404002, 2018.

[3] S.V. Markova, G.G. Petrash, "Pulsed laser based on a resonance—metastable level transition in mercury ion" Quantum Electronics, vol. 25, № 9, p. 841.

[4] P.A. Bokhan, P.P. Gugin, D.E. Zakrevsky, M.A. Lavrukhin, "Frequency Characteristics of a Subnanosecond Plasma Switch", Russian Physics Journal, Vol. 62, № 11, p. 2059, 2020.

[1] The work was supported by the Russian Science Foundation under grant No. 19-19-00069.

APPLICATION OF REPETITIVELY PULSED X-RAY RADIATION IN EXPERIMENTAL ONCOLOGY

M.A. BULDAKOV[1], A.A. EVTINA[2], M.A. BOLSHAKOV[2,3], O.P. KUTENKOV[3], V.V. ROSTOV[3], N.V. CHERDYNTSEVA[1]

[1]Cancer Research Institute, Tomsk National Research Medical Center, Russian Academy of Sciences, Tomsk, Russia
[2]National Research Tomsk State University, Tomsk, Russia
[3]Institute of High Current Electronics Siberian Branch Russian Academy of Sciences, Tomsk, Russia

Development of new technologies in the field of radiation required new approaches and strategies for their application. Power radiation when one continued pulsed divided to serial pulses with different specific repetition rate could provide more complicated and expressed reaction of the biological objects. Cells and tissues with their biological rhythms and intercellular processes which can be measured in a period of a few nanoseconds are depended on time period of acting factor. In this case tumor cells presents a perspective object for investigation of repetitively pulsed X-ray radiation with nanosecond pulse duration. We used different normal and tumor cell lines in vivo and in vitro to compare efficacy of different pulse repetition rate of X-ray radiation when the total absorbed dose didn't exceed 1 Gy. We observed strong dependent of tumor cell reaction to repetition rate. Using this parameter we can stimulate or inhibit tumor growth up to 90% compare to control group. Irradiation of tumor-bearing mice inhibited growth of primary tumor up to 60% with the total absorbed dose 0,4 Gy. Moreover same experimental conditions allowed to reduce number of metastasis in mouse lung at 70%. That resulted in longer survival of experimental animals compare to control group. Thus we can conclude that pulsed radiation with nanosecond pulse duration has a potential for application in oncology.

COLD CATHODE THYRATRON TRIGGERING METHOD IN A TRIGGER CIRCUIT WITH GROUNDED CATHODE AND GRID*

G.A. ARGUNOV, N.V. LANDL, Y.D. KOROLEV, O.B. FRANTS, V.G. GEYMAN

Institute of High Current Electronics, Tomsk, Russia

The present report presents the results of investigations of a sealed-off cold-cathode thyratron with a novel trigger unit based on an auxiliary glow discharge [1]. The electrodes of the trigger unit designed as hollow cylinders. The thyratron has certain advantages over the thyratron with standard trigger unit [2, 3]. It provides stable trigger discharge formation and requires low voltage for initiating the auxiliary glow discharge.

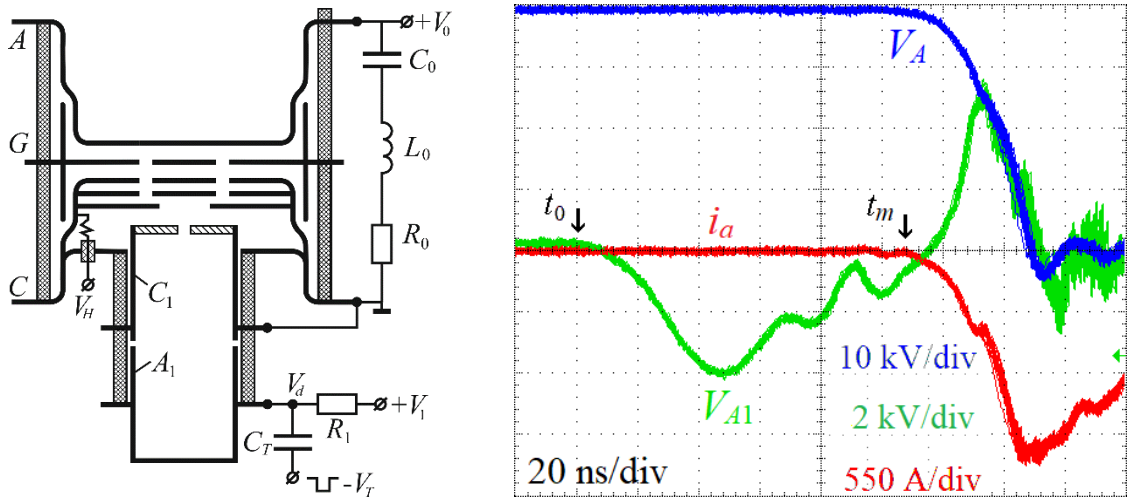

a) *b)*

Fig. 1. The cold-cathode thyratron schematic design along with the experimental circuit – *a)* and the experimental waveforms of the anode current – i_a, anode voltage – V_A and the trigger pulse voltage V_{A1} at the electrode A_1 of 25 pulses superimposed – *b)*. C_0 = 4 nF, L_0 = 1 μH, R_0 = 18 Ω, R_1 = 30 kΩ, R_B = 30 Ω, C_T = 3 nF.

The schematic of thyratron design and electrical circuit for thyratron triggering are presented in Fig. 1, *a*. Feature of the trigger circuit is that cathode of the trigger unit C_1 and the main cathode cavity of the thyratron C (equivalent of the grid of a classic heated-cathode thyratron) are grounded. The electric circuit operates as follows. Initially a high voltage $V_A \approx 40$ kV is applied to the anode A of the thyratron. The auxiliary glow discharge with current of 20 mA is sustained in the trigger unit due to positive voltage V_1 via the resistor R_1. The trigger pulse V_T is applied to the electrode A_1 at the time instant t_0 (Fig. 1, *b*). It caused a high-current trigger discharge ignition in the main cathode cavity followed by the main gap breakdown, occurred at the instant of time t_m.

It is shown that a sufficient fraction of the trigger discharge current intercepts onto the cathode of the cavity C under the action of the trigger pulse. It allows triggering the device with nanosecond stability. The delay time to the thyratron triggering $t_d = t_m - t_0 = 110$ ns. The proposed triggering method allows triggering the thyratron with jitter of ±2 ns. Connecting and grounding the electrodes C and C_1 makes the triggering circuit easier to employ. Moreover, it allows considering further upgrading of the thyratron design, making the cathode of the thyratron C and the cathode of the trigger unit C_1 as a whole.

REFERENCES

[1] Y. D. Korolev, N. V. Landl, V. G. Geyman, O. B. Frants, and G. A. Argunov, "Hollow-cathode glow discharge in a trigger unit of pseudospark switch," Phys. Plasmas, Vol. 25, 113510 (2018).

[2] Y. D. Korolev, N. V. Landl, V. G. Geyman, O. B. Frants, I. A. Shemyakin, V. S. Kasyanov, and A. V. Bolotov, "Study of cold-cathode thyratron triggering stability at high anode voltages", Plasma Physics Reports,Vol. 44, 110 (2018).

[3] Y. D. Korolev, N. V. Landl, V. G. Geyman, O. B. Frants, I. A. Shemyakin, V. O. Nekhoroshev, "Auxiliary Glow Discharge in the Trigger Unit of a Hollow-Cathode Thyratron", Plasma Physics Reports, Vol. 42, No. 8, 799 (2016).

* The work was carried out with the financial support of Russian Science Foundation, grant № 19-19-00123

FORMATION OF GAS CAVITIES AND DEVELOPMENT OF INCOMPLETE BREAKDOWN IN SALINE SOLUTION *

Y.D. KOROLEV[1,2], N.V. LANDL[1], V.S. KASYANOV[1], I.A. SHEMYAKIN[1,2], V.G. GEYMAN[1], A.V. BOLOTOV[1]

[1]Institute of High Current Electronics SB RAS, 2/3 Akademichesky Ave., Tomsk 634055, Russia, kasyanov@lnp.hcei.tsc.ru
[2]National Research Tomsk State University, 36 Lenin Avenue, Tomsk, 634050, Russia

Recently, there has been an interest in pulse discharges in electrolytes, in particular, in saline solutions [1–4]. Interest bases on the use of the discharges in medicine, for example, as so-called plasma scalpels [2] and for the disinfection of liquids [3, 4]. Considerable attention is paid to applications related to the formation of shock waves, to the surface treatment, to solving problems of hydroacoustics [1, 5].

As a rule, the initiation of a breakdown and the appearance of plasma in a conducting liquid is associated with the appearance of gas cavities in it and the ignition of a discharge in them. It is usually assumed that cavities occur as a result of heating and evaporation of a liquid or dissolved gas by conduction currents. The cavities are shaped like micro and macro-bubbles [4, 6, 7], and their characteristic sizes are hundreds of microns and units of millimeters, respectively. In the case of incomplete breakdown the cavities filled with plasma do not close the discharge gap [6]. When the complete breakdown takes place the cavities close the gap, and a high conducting channel occurs in them with a resistance equal to or less than the impedance of the electric circuit [1, 6].

In the electrolyte cavities and plasma in them occur at relatively low voltages applied to the gap. In [6], the concept of threshold critical voltage V_{cr} was introduced as the voltage at which plasma occurs in cavities. This value is hundreds of volts for pulse-periodic discharges of microsecond duration.

Gas cavities and the plasma that occurs in them can have a significant impact on the discharge current. Indeed, if the cavities cover most of the surface of the active electrode and occupy a significant part of the area near it, the electrode is shielded [6, 7]. It is seen that the resistance of the gap increases, and the current falls. In the case of a plasma in the cavities the effect of screening are partially or completely suppressed which leads to an increase in current.

The discharge inside the cavities can be supported in various modes, for example, may be in the form of a glow, spark, incomplete spark discharge and also of a specific type of high-current diffuse discharge [1, 7]. Since the current flow conditions are essentially non-stationary, the interpretation of such discharge phenomena is quite difficult, and many details of the development of cavities and discharges in them have not been clarified yet. The processes of formation of gas cavities in conditions when the voltage applied to the gap is less than V_{cr} were studied in detail in [8]. Now we study the processes of occurrence and disappearance of gas cavities and plasma in them at a voltage close to the threshold and above them, i.e., for the case of incomplete breakdown. Single discharges of micro and millisecond duration were considered with a high initial salt concentration in water and maximum currents up to 200 A.

REFERENCES

[1] P. Bruggeman, C. Leys, “Non-thermal plasmas in and in contact with liquids,” J. Phys. D: Appl. Phys., vol. 42, no. 5, Article Number 053001, March 2009.

[2] L. Schaper, W.G. Graham, K.R. Stalder “Vapour layer formation by electrical discharges through electrically conducting liquids-modelling and experiment,” Plasma Sources Sci. Technol., vol. 20, no. 3, Article Number 034003, June 2011.

[3] S.H.R.Hosseini, K. Mavatari, S.M Nejad, “Two successive shock waves generated by underwater pulse electric discharge for medical application,” IEEE Trans. Plasma Sci., vol. 42, no. 10, pp. 3209–3214, October 2014.

[4] Y.S. Akishev, M.E. Grushin, V.B. Karal'nik, A.E. Monich, M.V., Pan'kin, N.I. Trushkin, V.P. Kholodenko, V.A. Chugunov, N.A. Zhirkova, I.A. Irkhina, E.N. Kobzev, “Generation of a nonequlibrium plasma in heterophase atmospheric-pressure gas-liquid media and demonstration of its sterilization ability,” Plasma Phys. Rep., vol. 32, no. 12, pp. 1052–1061, December 2006.

[5] Y.H.Sun, Y.X. Zhou, M.J. Jin, Q. Liu, P. Yan, “New prototype of underwater sound source based on the pulsed corona discharge,” J. Electrost., vol. 63, no. 6-10, pp. 969–975, June 2005.

[6] R.V. Ivashov, V.G. Geyman, Y.D. Korolev, I.A. Shemyakin, “Influence of non-stationary processes on the formation and development of a discharge in an electrolyte in electrode systems,” Izv. Vyssh. Uchebn. Zaved. Fiz., vol. 50, no. 9. Supplement, pp 368–371, September 2007.

[7] I.A. Shemyakin, Y.D. Korolev, V.S. Kasyanov, V.G. Geyman, A.V. Bolotov, Y. Sun, T. Shao, Y. Gao, “Initial stages of the high-current pulsed discharge in saline solutions,” Izv. Vyssh. Uchebn. Zaved. Fiz., vol. 58, no. 9/2, pp. 268–272, September 2015.

[8] Y.D. Korolev, I.A.Shemyakin, V.S. Kasyanov, V.G. Geyman, A.V. Bolotov, V.O. Nekhoroshev, “Development of discharge in a saline solution at near-threshold voltages,” Plasma Phys. Rep, vol. 44, no. 6, pp. 581–587, June 2018.

* The study is a continuation of the work supported by RFBR project No 16-08-00652.

SUPPRESSION OF VACUUM BREAKDOWN IN HIGH-POWER MICROWAVE TUBES BY ALLOYING THE INNER SURFACES OF LOW-WAVE STRUCTURES[1]

A.V. BATRAKOV, I.K. KURKAN, E.V. NEFEDTSEV, S.A. ONISCHENKO, V.V. ROSTOV, R.V. TSYGANKOV, E.V. YAKOVLEV

Institute of High Current Electronics, Siberian Branch, Russian Academy of Sciences (IHCE SB RAS), Tomsk, Russia

The efficiency of converting the energy of an electron beam into microwave energy can be increased by suppressing vacuum breakdown in slow-wave structures. It was previously shown [1] that surface alloying with titanium of the inner surfaces of low-wave structures made of stainless steel lengthens the microwave pulse, which increases output energy by 30%. We continued this study and performed experiments on copper structures with surface alloying by titanium. Preliminary experiments on pulsed DC voltage have given encouraging results. So, an electric strength of higher than 1 MV/cm was achieved at a voltage of 200 kV for a duration of 100 ns applied to a gap with an electrode area of about 10 cm^2. The results of suppressing vacuum breakdown and lengthening the output radiation pulse will be presented at the symposium.

REFERENCES

[1] A.V. Batrakov, I.K. Kurkan, E.V. Nefedtsev, S.A. Onischenko, V.V. Rostov, R.V. Tsygankov, E.V. Yakovlev, Comparative Study of Breakdown Strength of Vacuum Insulation in Gaps with Electron-Beam Polished Electrodes under Pulsed DC and Microwave Electric Fields, Proc. 28th International Symposium on Discharges and Electrical Insulation in Vacuum (ISDEIV), 2018, pp. 77-80.

1 The work was supported by the Basic Research Program # I10P of the Presidium of the Russian Academy of Sciences, project # 066-2018-0018, and in part by the Russian Foundation for Basic Research (RFBR) under grant # 18-08-00230-a.

RESEARCH AND SUPPRESSION OF SECONDARY ARCING IN POWER EQUIPMENT OPERATING IN VACUUM[1]

A.V. BATRAKOV[1], S.A. POPOV[1], K.V. KARLIK[1], D.A. ZUSA[1], I.A. KURZINA[2], S.B. SUNTSOV[3], D.A. MUTASOV[3]

[1]Institute of High Current Electronics, Siberian Branch, Russian Academy of Sciences (IHCE SB RAS), Tomsk, Russia
[2]National Research Tomsk State University, 634050 Tomsk, Russia
[3]Academician M.F. Reshetnev Information Satellite Systems, Zheleznogorsk, Krasnoyarsk region, Russia

Secondary arcing appears when primary plasma covers non-insulated wires connected to a power supply being power enough to feed the self-sustained arc discharge. Protective dielectric coverings prevent equipment against secondary arcs but defects in covering fail protection measures. It was found previously [1] that the defect size in the covering film plays a significant role in the secondary arcing probability. In the present work, we have analyzed how primary plasma penetrates to bare wires when coverings are thick while defects in coverings are thin, and what are the criteria of dangerous defects in thick coverings. Issues concerning technique for detecting defects in thick covering are also discussed.

REFERENCES

[1] A.V. Batrakov, S.A. Popov, K.V. Karlik, D.A. Zusa, I.A. Kurzina, S.B. Suntsov, A.V. Seloustev, A.A. Hvalko, Suppression of Prebreakdown Emission Activity Inside the On-board Spacecraft Equipment by Local Polymerization in Discharge, Proc. 28th International Symposium on Discharges and Electrical Insulation in Vacuum (ISDEIV), 2018, pp. 777-780.

1 The work was supported by the Russian Foundation for Basic Research (RFBR) under grant # 18-48-700029-p_a.

MEASUREMENT AND CALCULATION OF THE ABSORBED DOSE DURING IRRADIATION OF THE GRAIN BY A PULSE ELECTRON BEAM WITH ENERGY UP TO 160 KEV*

M.S. VOROBYOV, S.YU. DOROSHKEVICH, K.P. ARTYOMOV

HCEI SB RAS, Academichesky av., Tomsk, 634055, Russia, E-mail: vorobyovms@yandex.ru

The paper presents the results of measuring the absorbed dose, performed using dosimetric films on a wide-aperture pulse-periodic electron accelerator "DUET" with a grid plasma cathode based on a low-pressure arc discharge and the output of the generated beam into the ambient atmosphere. The possibility of using this accelerator to irradiate wheat, barley, oats, peas, and corn has been previously shown. In this work, we performed numerical calculations of the distribution of the absorbed dose over the grain depth. Calculations show that the absorbed dose depends on the initial energy of the electron beam (in the range 100–160 keV) and is distributed substantially non-uniformly. The main absorbed dose is concentrated in the outer layer (grain shell), while the absorbed dose in the inner part of the grain was four orders of magnitude lower. The results of numerical calculations are consistent with experimental measurements.

REFERENCES

[1] *[1] S.P. Bugaev, Yu.E. Kreindel, P.M. Shcanin* // Large-Cross-Section Electron Beams. – Moscow, Energoatomizdat, 1984 (in Russian)

[2] *[2] E. Oks* // Plasma Cathode Electron Sources: Physics, Technology, Applications. – WILEY-VCH, 2006, 171 pp

* The work was supported by the Russian Science Foundation (project No. 20-79-10015).

HEALING OF THE SKIN THERMAL DAMAGE BY NANOSECOND REPETITIVE PULSED MICROWAVE RADIATION

A.V. KEREYA[1-3], M.A. BOLSHAKOV[1,3], A.A. GOSTYUKHINA[1,4], K.V. ZAITSEV[4], O.P. KUTENKOV[1], V.V. ROSTOV[1]

[1]Institute of High-Current Electronics SB RAS, Tomsk, Russia
[2]Siberian state medical university, Tomsk, Russia
[3]National research Tomsk state university, Tomsk, Russia
[4]Siberian Federal Scientific Clinical Center (SFSCC) of the Federal Medical and Biological Agency (FMBA), Tomsk

The problem of restoring skin after thermal damaging in humans is an urgent biomedical problem [1]. One of the promising ways to solve this problem is the creation of new recovery methods using high-frequency low-intensity electromagnetic factors. From this point of view, data on the wound healing effect of pulsed radio-frequency radiation [2, 3], as well as nanosecond pulsed electromagnetic radiation (RPMs) are of some interest. RPMs under certain parameters can stimulate the reparative regeneration of a full-layer skin wound in mice [4]. According to some reports, the positive effects of wound healing using extremely high-frequency exposure are explained by a decrease in the intensity of inflammatory processes due to increased microcirculation in the wound site and adjacent tissues [5].

The experiment was performed using 30 mature male rats of the Wistar line (250-280 g). All animals were divided into three groups: control – animals with a burn of the III degree without exposure to electromagnetic radiation; experimental group 1 – animals that, after modeling a III degree burn were exposed to local burn wound effects with exposure to radiation with peak power flux density (pPFD) of 140 W/cm^2, with a pulse repetition rate of 8 Hz; experimental group 2 – animals that, after modeling a III degree burn were exposed to local burn wound effects with exposure to radiation with pPFD of 1500 W/cm^2, with a pulse repetition rate of 8 Hz. Thermal burns were modeled according to the standard method using a metal rod heated to 100 °C (d = 2 cm). The pulsed laboratory generator based on the MI-505 magnetron was used as a source of nanosecond RPMs. Statistical processing of the results was carried out according to standard procedures of mathematical statistics using the capabilities of the program Statistica 8.0 for Windows.

In the irradiated rats of the first group, after 4 times local irradiation of burn wounds with RPMs of intensity of 140 W/cm^2, the wound healing dynamics did not significantly differ in comparison with the control group. There was a statistically significant decrease in the area of the wound relative to the control group after the 19th day of the experiment, with complete healing of all burns by 28 days of the experiment. Moreover, in group of irradiated rats a partial separation of the formed scab was observed at 12 days after the burn. Epithelization of irradiated wounds in rats was noted at 24 days with its completion in all animals on day 28 of the study. In rats of the second experimental group irradiated with nanosecond RPMs with a higher intensity of 1500 W/cm^2, the wound area did not differ from that in the control group from 1 to 14 days of the study. There was a statistically significant decrease in the area of the wound relative to the control group after the 19th day of the experiment, with complete healing of all burns by 30 days of the experiment. On the 19th day after wounding, the formed scab was separated with an accelerated decrease in the area of the wound surface. When comparing the results of wound healing of both irradiated groups, it turned out that exposure with less intensity contributes to a more effective reduction in the area of the wound surface.

Thus, from the obtained results it follows that RPMs with the used parameters accelerates the wound healing processes. In this case, the rate of healing of burn wounds as a result of irradiation of low intensity RPMs is higher compared to high intensity RPMs.

References

[1] A.A. Alekseev, A.E. Bobrovnikov, “Contemporary technologies of local conservative treatment in patients with burns” // Annals of surgery. № 2. pp. 32–38. 2012.

[2] A.B. Gapeyev, “Study of the mechanisms of biological effects of low-intensity extremely high-frequency electromagnetic radiation: progress, problems and prospects” // Biomedical Radioelectronics. № 6. pp. 20-30. 2014.

[3] B. Strauch, C. Herman, R. Dabb et al., “Evidence-based use of pulsed electromagnetic field therapy in clinical plastic surgery” // Aesthet. Surg. J. № 29 (2). pp. 135–143. 2009.

[4] I.R. Knyazeva, M.A. Medvedev, L.P. Zharkova, et al., “The influence of nanosecond microwave pulses on the regeneration processes” // Бюллетень сибирской медицины. Vol. 10. № 6. pp. 109–113. 2011.

[5] K.V. Lushnikov, A.B. Gapeev, Yu.V. Shumilina, et al., “Suppression of cell-mediated immune response and nonspecific inflammation on exposure to extremely high frequency electromagnetic radiation” // Biophysics.Vol. 38, № 5. pp. 918–925. 2003.

LIMITATIONS ON THE DURATION OF THE RADIATION PULSE DISCHARGE F LASER[1]

YU. N. PANCHENKO, A.V. PUCHIKIN, S. A. YAMPOLSKAYA, AND I. N. KONOVALOV

Institute of High Current Electronics SB RAS, 2/3 Akademichesky Ave.,
Tomsk, 634055, Russia, yu.n.panchenko@mail.ru (3822)491891

This article presents the results of numerical and experimental studies of the generation of lasing in the red region of the spectrum of an atomic TEA F laser. It was shown that for the ratio of the components of the gas mixture He/F_2 = 1500/7 mbar, a group of intense spectral lines at 731.1, 739.9, and 755.2 nm corresponding to atomic fluorine transitions corresponding to $3p\ ^2S^0_{1/2} \rightarrow 3s^2P_{3/2}$, $3p\ ^4P^0_{5/2} \rightarrow 3s^4P_{5/2}$, and $3p^4P^0_{5/2} \rightarrow 3s\ ^4P_{3/2}$, respectively. Also in the output radiation there is a spectral line of 634.8 nm, corresponding to the transition $3p^4P^0_{3/2} \rightarrow 3s\ ^4P_{3/2}$.

The population of the upper electronic level 3p of the excited fluorine atom flows through the ion-ion and charge-transfer collisions channels [1, 2]:

$$He^+ + F^- \rightarrow He + F^*;\ He_2^+ + F^- \rightarrow 2He + F^*;\ He^* + F_2 \rightarrow He^* + F^* + F.$$

In our numerical calculations, it was shown that the rates of formation of excited fluorine atoms in ion-ion recombination reactions and collision reactions with excitation transfer were close to each other and amounted to ~ 1.8×10^{21} $cm^{-3}s^{-1}$.

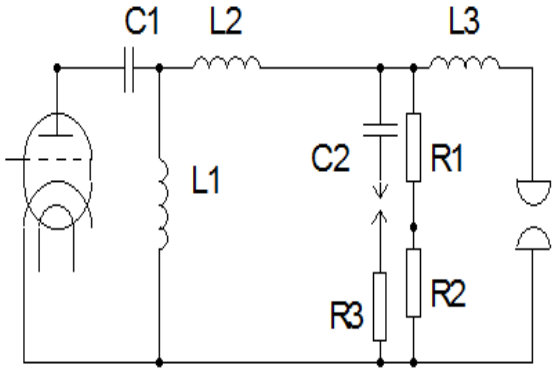

Fig.1. Schematic diagram of excitation circuit. C1= 5.6 nF, C2= 4.4 nF, L1= 0.15 mH, L2 = 200 nH, L3 = 3 nH.

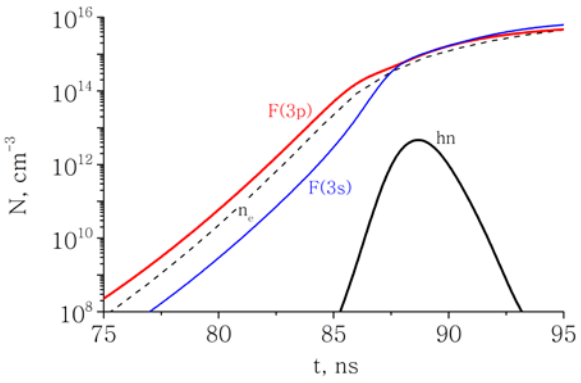

Fig. 2. Time dependences of the concentration of plasma particles: concentrations of excited atoms F*(3p), F*(3s), electrons – ne, radiation – hn.

The experiments were carried out on discharge F_2 laser with a pulse repetition rate of 500 Hz, the electrical pump circuit of the laser is shown in Fig. 1. Preionization of the discharge gap was carried out by UV - radiation that occurs at triggering spark gaps installed in the second loop of the circuit. Storage capacitors C1 and discharge capacitor C2 had the values of 5.6 and 4.4 nF respectively. Thyratron TPI1-10k/20 was used as the HV-switch. The inductance of the first L2 and the second L3 discharge contours were 200 and 4 nH respectively. The length of the electrodes was 250 mm, the electrode gap – 12 mm. Electrodes were of cylindrical shape work surface with the radius of 3 mm.

It was experimentally shown that at a charging voltage of 20 kV, the energy of the output radiation of the F-laser was 0.05 mJ, with pulse duration of 3.5 ns. The results of numerical simulations presented in Fig. 2 show that the limitation of the pulse duration of the induced radiation is due to the population of the lower laser level F*(3s).

REFERENCES

[1] C. B. Collins, F. W. Lee, and J. M. Carroll, “An atomic fluorine laser pumped by charge transfer from He^+_2 at high pressures,” Appl. Phys. Lett., vol. 37, no. 10, pp. 857-859, 1980.

[2] H. Mehravaran, P. Parvin, and D. Dorranian, “Changeover in the molecular and atomic fluorine laser transitions,” Appl. Opt., vol. 49, no. 15, pp. 2741-2748, 2010.

[1] This work was supported by RFBR (projects No. 20-08-00371 A)

POWER SUPPLY FOR POWERFUL GENERATORS WITH HIGH PULSE REPETITION RATE*

A.V. PONOMAREV, S.R. KORZHENEVSKIY, A.A. KOMARSKIY, O.D. KRASNIY, A.S. CHEPUSOV

Institute of Electrophysics UD RAS, Ekaterinburg, Russia

Constant voltage sources in the form of a rectifier and a capacitive filter are most often used for powerful pulse generators. For installations with power consumption of several kilowatts or more, a three-phase rectifier is used with power supply from the industrial network of 3x380 V 50 Hz according to the Larionov circuit. At the output of the device there is constant rectified pulsating voltage with the ripple frequency of 300 Hz, the ripple is about 17% of the voltage maximum. This voltage is acceptable not for all types of installations, therefore, to smooth the ripple at the output of the rectifier, a capacitive filter is added. The more powerful the installation, the greater the filter capacity required. So in the S-5N generator [1] with the average power up to 30 kW a filter with the capacity of 32 mF was used. The filter ensures the stability of the supply voltage only if the operating frequency of the device is less than 300 Hz. In some powerful installations, the output pulse repetition rate can exceed this value many times over. During the pauses between filter charging cycles, the voltage across it decreases in accordance with the frequency and energy of the pulses consumed by the generator. It is not always reasonable, since a small change in the voltage at the input of the generator can lead to a significant change in its output and a change in the operating parameters of the device as a whole. This problem is especially inherent in the devices in the electric circuit of which magnetic switch are used to form short high-voltage pulses [2, 3].

To ensure a stable input voltage, it is proposed adding an auxiliary supply source to the electrical circuit of the installation. This power supply is connected between the rectifier and the filter and provides the filter with stable supply voltage. The main power for the device is provided by a traditional rectifier, and the ripple of the supply voltage is eliminated by a relatively low-power auxiliary power source. Moreover, the filter capacity can be significantly reduced without compromising the stability of the supply voltage. Thus, the weight and dimensions of the capacitive filter are reduced, as well as its cost. In addition, a reduction in the energy content of the filter will positively affect the reliability of the installation in the event of a malfunction.

REFERENCES

[1] S.N. Rukin, G.A. Mesyats, A.V. Ponomarev, B.G. Slovikovsky, S.P. Timoshenkov, A.I. Bushlyakov, “Megavolt repetitive SOS-based generator”, Proc. of 13th IEEE Int. Pulsed Power Conf., Las Vegas, Nevada, USA, V. 2, pp. 1272-1275, 2001.

[2] V.A. Bessonova, P.V. Gavrilov, A.A. Komarskiy, S.R. Korzhenevskiy and A.S. Chepusov., " Reduction of Patient Radiation Dose During Diagnostics with the Digital Pulsed Nanosecond X-ray Systems", Medical Radiology and Radiation Safety, vol.61, № 2, pp. 53 – 57, 2016.

[3] A. Komarskiy, S. Korzhenevskiy, A. Chepusov, O. Krasniy, "The pulsed X-ray radiation source based on a semiconducror opening switch with the focal point diametr of 0.5 mm and its application", Rev. of scientific instruments., vol.90, №9, Article Number 095106, 2019.

* The work was supported by the RFBR under grant No. 19-08-00117a.

METAL CERAMIC CATHODE ASSEMBLY FOR URT SERIES ACCELERATORS

M.E. BALEZIN[1], *S.Ju. SOKOVNIN*[1,2]

[1]*Institute of Electrophysics Ural Division Russian Academy of Sciences, Ekaterinburg, Russia*
[2]*Ural Federal University, Ekaterinburg, Russia*

In many technological applications are required large electron beams along one of the coordinates with a uniform distribution of current density. The cold cathode used for this purpose should also have high stability of performance and durability.

On the URT-1M accelerator [1],were examined the properties of the metal ceramic (MC) cathode [2] in the cathode housing structure similar to the metal dielectric (MD) cathode [3] to directly compare the capabilities of different types of cold cathodes.

Was inverstigated the influence of quantity and relationship of radiating elements (metal ceramic plates) of cathode on parameters of beam and uniformity of distribution of current density with application of previously developed method of measurements on the basis of phosphor and TV chamber.

It was found that compared to the MD cathode in the same geometry, the electron beam current obtained using the MC cathode was 3 times higher. In order to study spatial distribution of plasma emission on cathode plates, was obtained TV image of luminophore illumination for different cases of MC plates arrangement on cathode (from 2 to 8 plates) according to the method [3]. Analysis of TV image frames in the MathCAD program allows to obtain distribution of electron beam current density. Obtained distributions are compared with results of dosimetry by plastic detectors.

Proposed MC cathode can be used for various technological applications, including on accelerators of URT type, for obtaining electron beams in vacuum diodes with low vacuum (~ 0.01Pa) width up to 420 mm, with uniformity of beam current density not worse than 15%, frequency up to 100 Hz and resource before cleaning not less than 40 hours.

REFERENCES

[1] S.Yu. Sokovnin, M.E. Balezin, Repetitive Nanosecond Electron Accelerators type URT-1 for radiation technology, Radiation Physics and Chemistry. V. 144, 2018, pp. 265-270. https://doi.org/10.1016/j.radphyschem.2017.08.023

[2] Yu. A. Kotov, S. Yu. Sokovnin, and M. E. Balezin // Properties of a Metal-Ceramic Cathode / Technical Physics, Vol. 48, No. 4, 2003, pp. 503–507. DOI: 10.1134/1.1568494

[3] S.Yu. Sokovnin, M.E. Balezin // Investigation of Cold Cathode for Nanosecond Electron Accelerators / Vacuum, V. 146, 2017, pp.79-86 https://doi.org/10.1016/j.vacuum.2017.09.014 IF 1.53 Q2

INVESTIGATION OF THE RELATIVE REACTIVITY OF UNSATURATED VOLATILE ORGANIC COMPOUNDS IN AIR UNDER THE ACTION OF PULSED CORONA DISCHARGE PLASMA*

I.E. FILATOV, V.V. UVARIN, D.L. KUZNETSOV

Institute of Electrophysics UD RAS, Yekaterinburg, Russia

Unsaturated volatile organic compounds (VOCs) – compounds that have a double bond (>C=C<) in their structure are an important pollutant of industrial emissions. They are used as monomers in the production of plastics. Halogen-containing unsaturated compounds are used as highly effective solvents and are ozone poisons. The presence of a double bond in molecule provides increased reactivity with respect to the components of low-temperature plasma generated by pulsed discharges. Such VOCs have very different reactivity, which requires careful research of its dependence on the functional structure.

This paper presents studies of air purification from vapors of various unsaturated VOCs using pulsed corona discharge. A special experimental device generating a corona discharge with a duration of 15–40 ns, a voltage of 100–140 kV, and a current of up to 300 A was used as a research tool, described in detail in [1,2]. As a research method, the reaction method based on the use of mixtures of the studied compounds was used, which allows determining the relative reactivity with high accuracy. A number of topical air pollutants – unsaturated compounds were used as test compounds: $CH_2=C(CH_3)COOCH_3$ (MMA), $CH_2=CHCN$ (acrylonitrile), $CH_3C=CHCOH$ (croton aldehyde), $C_6H_5CH=CH_2$ (styrene) and $C_6H_5C(CH_3)=CH_2$ (α-methyl styrene). A number of halogen-containing unsaturated compounds were also studied: $Cl_2C=CH_2$ (DCE), $Cl_2C=CHCl$ (TCE), and $Cl_2C=CCl_2$ (PCE). The components were studied individually and in a mixture at concentrations of 200–1000 ppm in dry air and nitrogen. In the study of air mixtures, the ozone concentration was measured similarly to the method described in [3].

The obtained results showed that the cleaning efficiency for compounds that do not contain chlorine in their composition correlates well with their reactivity with respect to ozone and is in the series: $C_6H_5C(CH_3)=CH_2 > C_6H_5CH=CH_2 > CH_2=C(CH_3)COOCH_3 > CH_3C=CHCOH > CH_2=CHCN$. It can be seen that electron-acceptor groups reduce the reactivity of unsaturated compounds, and donor groups increase it. Measurement of ozone concentration also allows us to assert that ozone is the main product of plasma, leading to the removal of compounds of this series. In nitrogen, the removal efficiency of these compounds is significantly less. Halogen-containing unsaturated compounds, in contrast, are resistant to ozone and are removed more efficiently in nitrogen than in air: $Cl_2CH=CH_2 > Cl_2C=CHCl > Cl_2C=CCl_2$. This suggests various mechanisms for removing these groups of compounds: in the case of halogen-containing compounds, electron adhesion reactions that are blocked by oxygen play a significant role.

The method of competing reactions used in research allows us to evaluate the relative reactivity of several compounds in a single experiment, which significantly increases the productivity of experimental research and allows us to determine the constants necessary for scaling processes from laboratory scales to industrial ones.

The found regularities will be useful for the development of air purification systems in the production of plastics and processes involving halogen-containing solvents.

REFERENCES

[1] I.E. Filatov, V,V. Uvarin and D.L. Kuznetsov, "Estimation of qalitative and quantitative prameters of air cleaning by a pulsed corona discharge using multicomponent standard mixtures,"Technical Physics, vol.63, no.5, pp. 680–688, 2018.

[2] I.E. Filatov, V,V. Uvarin and D.L. Kuznetsov, "Model compound mixtures for studying the main trends of volatile organic compounds conversion in processes of air cleaning by pulsed discharges, " Journal of Physics: Conf. Ser., vol. 1393, No.1, p. 012080, 2019.

[3] I.E. Filatov, V,V. Uvarin and D.L. Kuznetsov, "The use of competitive reactions for studying the process of unsaturated organic vapor removal from air by pusled discharge plasma, " Technical Physics Letter, vol.46, No.1, pp. 94–97, 2020.

* The work was supported by the Russian Foundation for Basic Research, projects No. 20-48-660062 and 20-08-00882.

ABOUT THE ROLE OF OZONE IN AIR PURIFICATION FROM VAPORS OF VOLATILE ORGANIC COMPOUNDS BY PULSED DISCHARGES *

I.E. FILATOV, V.V. UVARIN, D.L. KUZNETSOV

Institute of Electrophysics UD RAS, Yekaterinburg, Russia

Volatile organic compounds (VOCs) are an important component of toxic emissions from industrial plants. One of the promising technologies for air purification from their content is the use of non-equilibrium plasma of pulsed discharges. One of the important components of plasma are atomic oxygen and ozone produced from it. An assessment of the interaction constants of ozone with VOCs at room temperature shows that it reacts at an acceptable rate only with certain classes of compounds. Ozone at room temperature, contrary to common misconceptions, does not oxidize VOCs to H_2O and CO_2. Atomic oxygen reacts with many VOCS at a high rate, however, molecular oxygen, which is in a large excess, intercepts it and deactivates it to form ozone. Measuring the concentration of ozone allows you to assess its role in air purification. Since the process of air purification using non-equilibrium plasma generated by electric discharges is always accompanied by the production of ozone, in some cases it is necessary to remove excess of highly toxic ozone.

We have proposed a method for evaluating the role of ozone in air purification processes. A special experimental device generating a corona discharge with a duration of 15–40 ns, a voltage of 100–140 kV, and a current of up to 300 A was used as a research tool, described in detail in [1,2]. A method of model mixtures based on the phenomenon of competing reactivity. The research tool is a method of competing reactions based on the use of mixtures of tested compounds [3], which uses the measurement of ozone concentration. The results of a study of the effects of discharge on air containing various classes of compounds are shown below and the role of ozone is shown:

1. **Functional compounds with moderate activity:** C_6H_{14} (hexane), C_6H_6 (benzene), $C_6H_5CH_3$ (toluene), CH_3COCH_3 (acetone), $CH_3COOC_2H_5$ (ethyl acetate), $CH_3COOC_4H_9$ (butyl acetate). Discharge treatment is accompanied by ozone production. Much of the atomic oxygen is deactivated by molecular oxygen.
2. **Unsaturated compounds:** $CH_2=C(CH_3)COOCH_3$ (MMA), $CH_2=CHCN$ (acrylonitrile), $CH_3C=CHCOH$ (croton-aldehyde), $C_6H_5CH=CH_2$ (styrene) and $C_6H_5C(CH_3)=CH_2$ (α-methyl styrene). These compounds react effectively with ozone. An excessive amount of ozone is formed after removal of VOCs, similar to [3].
3. **Unsaturated halogen-containing compounds:** $Cl_2C=CH_2$ (DCE), $Cl_2C=CHCl$ (TCE), and $Cl_2C=CCl_2$ (PCE). These compounds are resistant to ozone, and the removal of compounds is accompanied by the formation of ozone. The high efficiency of removing compounds is due to electron adhesion reactions. Molecular oxygen blocks these processes.
4. **Halogen-containing compounds**: CH_2Cl_2, $CHCl_3$, CCl_4, $ClCH_2CH_2Cl$. Similar to point 3, but the removal efficiency of these compounds is low.
5. **Aromatic compounds:** C_6H_6 (benzene), $C_6H_5CH_3$ (toluene), $C_6H_4(CH_3)_2$ (xylene). The removal of compounds is accompanied by ozone production.

The found regularities will be useful in the development of combined air purification technologies and will allow optimizing the stage of ozone destruction combined with catalytic decomposition.

REFERENCES

[1] I.E. Filatov, V,V. Uvarin and D.L. Kuznetsov, "Estimation of qalitative and quantitative prameters of air cleaning by a pulsed corona discharge using multicomponent standard mixtures,"Technical Physics, vol.63, no.5, pp. 680–688, 2018.

[2] I.E. Filatov, V,V. Uvarin and D.L. Kuznetsov, "Model compound mixtures for studying the main trends of volatile organic compounds conversion in processes of air cleaning by pulsed discharges, " Journal of Physics: Conf. Ser., vol. 1393, No.1, p. 012080, 2019.

[3] I.E. Filatov, V,V. Uvarin and D.L. Kuznetsov, "The use of competitive reactions for studying the process of unsaturated organic vapor removal from air by pusled discharge plasma, " Technical Physics Letter, vol.46, No.1, pp. 94–97, 2020.

* The work was supported by the Russian Foundation for Basic Research, projects No. 20-48-660062 and 20-08-00882.

MEASUREMENT OF ELECTRODE VOLTAGE DROP IN A DISCHARGE GAP BY MEANS OF REGRESSION ANALYSIS SOFTWARE PACKAGE*

A.D. MAKSIMOV[1], E.I. AZARKEVICH[1], A.V. BAGAZEEV[1], I.V. BEKETOV[1]

[1] Institute of Electrophysics of the Ural Branch of the Russian Academy of Sciences, Amundsena str., 106, Ekaterinburg, 620016, Russian Federation; a.d.maksimov1415@gmail.com, +7-982-624-4854

The need for further development of the technology for obtaining aerosols and nanopowders by spark discharge, as well as increasing the efficiency of using the energy of the capacitive storage for electrode erosion, requires a more detailed study of the processes in the discharge channel and on electrodes. In particular, it is necessary to measure the electrode voltage drop, which determines the discharge energy release on the electrodes.

For this purpose, in the installation described in [1], simultaneous oscillographic registration of the voltage at the gap and the discharge current derivative was performed. The voltage was measured using a capacitance-resistive voltage divider with a series connection of elements. The current derivative was measured by Rogowski coil, which was loaded on the resistive voltage divider. Signals from the sensors are transmitted via cables to the inputs of the Tektronix TDS1012 digital oscilloscope (USA) with a bandwidth up to 100 MHz. The voltage was measured from two consecutive discharge gaps. One of the electrodes in each gap was of aluminum, the other was of St3 steel.

When processing signals, it is assumed that the voltage at the discharge gap U is the sum of the inductive voltage LdI/dt, the voltage at the resistance of the gap RI, and the electrode voltage drop U_e, which changes it's sign when the current changes its direction:

$$U = L\frac{dI}{dt} + RI + U_e \operatorname{sign}(I), \tag{1}$$

where sign(x) is the argument's sign function.

The problem of model (1) identification, i.e. determining unknown parameters L, R, and U_e, is the same as the problem of linear regression analysis. This problem was solved in Excel using the built-in package "Data analysis". The U and dI/dt values were taken from the waveforms, and the current curve $I(t)$ was calculated using the RLC-circuit model.

Six tests were carried out under the following conditions: the capacitance 0.1 μF; charging voltage 8 kV; the period of discharge current 1.72 μs; interelectrode distance is 2 mm. Average parameter values and their standard deviations are: L = 26.7±1.6 nH; R = 56.5±2.8 mOhm; U_e = 25.3±0.3 V. The resulting determination coefficient R^2 = 0.974 tells about the sufficient adequacy of the model (1). The value found of the electrode drop is approximately the same as the values measured in [2] for copper and titanium electrodes.

The results obtained allow us to calculate the energy released in the gaps during the discharge. Under given conditions, it was 23% of the stored energy.

The regression method proposed in this paper is less time-consuming and more objective than the method used in [2]. It can serve as a useful addition to existing methods for measuring the electrode voltage drop.

REFERENCES

[1] I.V. Beketov, A.V. Bagazeev, E.I. Azarkevich, A.D. Maximov, A.I. Medvedev, A.I. Beketova, “The installation for production of metal and oxide nanopowders by the spark discharge method, and its testing”, Izv. Vyssh. Uchebn. Zaved. Fiz., vol. 61, no. 9/2, pp. 166–170, September 2018.

[2] D.A. Mylnikov, A.A. Efimov, and V.V. Ivanov, “Investigation of the energy balance in the spark discharge generator for nanoparticles synthesis,” J. Phys. Conf. Ser., vol. 830, 2017, p. 012162.

* The work was supported by the grant of Russian Foundation for Basic Research (Project No. 20-48-660044).

EFFECT OF NANOSECOND REPETITIVE PULSED MICROWAVE EXPOSURE ON PROLIFERATION OF BONE MARROW CELLS

[2]A.A. GOSTYUKHINA, [1, 3,4]A.V. KEREYA, [1, 3]M.A. BOLSHAKOV, [2]K.V. ZAITSEV, [1]O.P. KUTENKOV, [1]V.V. ROSTOV

[1]Institute of high current electronics (IHCE) SB RAS, Tomsk, Russia
[2]Siberian Federal Scientific Clinical Center (SFSCC) of the Federal Medical and Biological Agency (FMBA), Seversk, Russia
[3]National Research Tomsk State University (NR TSU), Tomsk, Russia
[4]Siberian State Medical University (SSMU), Tomsk, Russia

At present, cell therapy is actively used in the correction of various pathological conditions. Imported specialized nutrient media are used to regulate cell activity and cell proliferation. Despite their effectiveness, these methods are quite expensive and require long-term use to obtain the necessary number of stem cells. The principal possibility to stimulate cell growth and to increase the rate of stem cell proliferation is the use of various physical factors [1; 2]. Both inhibiting and stimulating effects on stem cell proliferation in cell cultures have been established for different factors of influence. At present, biological effect of nanosecond pulse-periodic microwave radiation (RPM) is being actively studied. It is shown that RPM with nanosecond pulses effectively influences on the functional state of a wide range of cells and tissues [3;4]. In this connection, the aim of this work was to research the proliferative activity of bone marrow mononuclear cells (BMC) of laboratory rats after irradiation of cells with nanosecond pulse-periodic microwave radiation.

To obtain bone marrow cell cultures it is possible to use generally accepted standard method [5]. The viability of BMC after cultivation was 91.5±2%. Then 8 vials with BMC culture have been divided in three groups: the control one - 2 cell cultures that were not exposed to any effects and were located in a CO_2 incubator; the false-irradiated control one - 2 cell cultures that were placed once near the microwave radiation source for 5-8 minutes without switching on the generator; experiment 1 and experiment 2 - 4 cell cultures that were subjected to single exposure of nanosecond microwave pulses with repetition frequencies of 8 and 13 Hz. Each vial of cell culture before the experiment contained $4 \times 10^5 \pm 63 \times 10^3$ BMC. The cells were viewed and counted using the Optika XDS-2SFL microscope (Italy) with 20x magnification.

The laboratory pulse generator on the base of the MI-505 magnetron (Russia) has been used as the source of RPM. The cells have been irradiated once with 4000 RPM pulses (carrier frequency of the generator is 10 GHz, output peak power is 180 kW, pulse duration on the half power level is 100 ns, which provides influence with peak power flow density (pPFD) of 1500 W/cm^2) with pulse repetition rates of 8 and 13 Hz. Exposure duration was 8 and 5 minutes, respectively. The choice of exposure modes was based on the results of previous experiments for stimulation of tissue regeneration [6].

It has been found that used mononuclear cells of rat bone marrow are sensitive to action of nanosecond RPM. The proliferative activity of irradiated cells varied in dependence on the frequency of pulse repetition. Irradiation of cells with pulse repetition rate of 8 Hz in 2 days after exposure has been accompanied by inhibition of their proliferation by 40% relative to the control. Exposure with frequency of 13 Hz, on the contrary, increased the number of cells in the irradiated culture by 30% relative to the control, and by 51% relative to the false-irradiated culture.

The obtained results have showed that it is possible to effectively stimulate proliferation of bone marrow cells *in vitro* by exposure to nanosecond RPM, which requires further research to identify exposure modes that provide the most effective stimulation of stem cell proliferation. This will serve to solve a practical problem, the rapid development of the necessary number of stem cells required for specific need for regenerative medicine.

REFERENCES

[1] S.V. Moskvin, D.Yu. Klyuchnikov, E.V. Antipov, et al., “The influence of continuous low-intensity laser radiation at the red (635 nm) and green (525 nm) wavelengths on the human mesenchymal stem cells in vitro: a review of the literature and original investigations” // Voprosy kurortologii, fizioterapii i lechebnoj fizicheskoj kul'tury. № 2. pp. 32–42. 2016.

[2] M.V. Ulitko, S.Yu. Medvedeva, V.V. Malakhov, “The influence of low-frequency pulsed electric and magnetic signals or their combination on the normal and modified fibroblasts (an experimental study)” // Voprosy kurortologii, fizioterapii i lechebnoj fizicheskoj kul'tury. № 3. pp. 46–52. 2016.

[3] A.V. Kereya, L.P. Zharkova, V.V. Ivanov, et al., “The epididymal adipose tissue of mice after nanosecond pulse-periodic microwave irradiation” // Radiation biology. Radioecology. V. 54. № 6. pp. 606–612. 2014.

[4] I.R. Knyazeva, V.V. Ivanov, L.P. Zharkova, et al., “The effect of the repetitive pulsed microwaves on functional activity of isolated mitochondria of mice liver” // Vestnik Tomskogo gosudarstvennogo universiteta. Biologiya. № 4 (16). pp. 113–123. 2011.

[5] K.V. Zaitsev, S.A. Mezheritskyi, N.P. Stepanenko, et al., “Immunophenotypical characteristics of cellular composition in breast milk” // Cell and Tissue Biology. Vol. 58. № 7. pp. 543–547. 2016.

[6] I.R. Knyazeva, M.A. Medvedev, L.P Zharkova., et al., “The influence of nanosecond microwave pulses on the regeneration processes” // Bulletin of Siberian Medicine. № 6. pp. 109–113. 2011.

INVESTIGATION OF THE EFFECT OF THE DISCHARGE CHANNEL ORIENTATION ON THE DESTRUCTION EFFICIENCY OF ELECTRONIC PRINTED CIRCUIT BOARDS *

A.A. ZHERLITSYN, E.V. KUMPYAK, S.S. KONDRATIEV, V.M. ALEXEENKO

Institute of High Current Electronics SB RAS, Tomsk, Russia

Studies of the electrical destruction of electronic printed circuit boards (PCB) in order to extract metals show encouraging results. The realized degree of metal extraction is not worse than when using the traditional mechanical method of crushing, and in large fractions the degree of metal extraction can be even higher [1, 2]. Also, we can hope to obtain a narrower distribution of the fractional composition of the particles of crushed PCB, which is important for effective separation of metal and dielectric.

The PCB destruction efficiency depends on the prevailing type of deformation. Thus, the tensile, bending, and chipping strength of brittle materials is ~1–10% of the compressive strength. The type of the impact depends from orientation of the discharge channel relative to the PCB plane (across or along), and, according to this, the destruction efficiency depends on this.

Two orientations of the electrode system with a sharply inhomogeneous electric field were studied. The high-voltage pulse-periodic generator with the 8 nF storage capacity was used. The voltage pulse with an amplitude of up to 300 kV and an average rise rate of ~3 kV/ns was generated at the discharge gap in a water-filled chamber. When a gap is breakdown, a discharge current is ~10 kA (a front of about 200 ns) and pulse pressure is over 200 MPa. The pressure at the shock wave front significantly exceeds the tensile, bending, and chipping strength of PCB. The model experiments shown that the along orientation of the discharge channel has a greater destruction efficiency. With this orientation of the discharge channel, the mass loss of the four-layer fiberglass PCB per pulse was ~7 times greater than with the orientation of the discharge channel across the surface. It is also shown that in the case of orientation of the discharge channel along the PCB plane, the efficiency of flakes the layers with copper foil from the base fiberglass layers is higher.

REFERENCES

[1] C.L. Duan, Z.J. Diao, Y.M. Zhao, W. Huang, “Liberation of valuable materials in waste printed circuit boards by high-voltage electrical pulses,” Minerals Engineering., vol. 70, pp. 170–177, 2015.

[2] R. Martino, C. Iseli, S. Gaydardzhiev, M. Streicher-Porte, A. Weh, “Electro dynamic fragmentation of printed wiring boards as a preparation tool for their recycling,” Minerals Engineering, vol. 107, pp. 20–26, 2017.

* The work was supported by the Russian Foundation for Basic Research (RFBR) under grant No. 18-29-24079 mk.

INVESTIGATION OF PLASMA FLOWS FROM VACUUM SURFACE FLASHOVER OF CERAMICS INITIATED BY NANOSECOND 6-KA CURRENT PULSES*

P.A. MOROZOV[1], *R.V. EMLIN*[1], *I.F. PUNANOV*[1], *V.V. LISENKOV*[1],

[1]*Institute of Electrophysics, Yekaterinburg, Russia*

In this work, we study plasma flow from vacuum surface flashover of ceramic materials under pulsed conditions. We used a pulsed generator, which provide pulses of voltage with amplitude of up to 70 kV. Energy stored is ~3 J, maximum current ~6 kA. Duration of current first half-wave is 20 ns. The discharge unit comprises two linear electrodes with a 20 mm gap between them. The samples are $BaTiO_3$, Al_2O_3 and YAG. We used two types of YAG samples: single crystals and sintered transparent ceramics. We measured mass loss, thrust, ion current of the plasma flow, full ionic charge, and the average ion velocity. Using data on mass loss and full ionic charge, we estimate the plasma ionization degree for ceramics as several percent, which is much higher than that for polymers [1]. Also, we carried out calculations of hydrodynamic expansion of ablated materials.

REFERENCES

[1] R.V. Emlin, P.A. Morozov, I.F. Punanov, V.V. Lisenkov and Y.N. Shcherbakov, "High-Power Plasma Flows Generated by Nanosecond Vacuum Surface Flashover of Polymeric Materials at 80 kV," IEEE Tran. Plasma Sci., vol. 47, no. 6, pp. 2838–2846, June 2019.

* The work was supported in part by the Russian Foundation for Basic Research under grant No 18-08-00185.

PRE-SEED WHEAT STIMULATION BY LOW-DOSE NANOSECOND PULSE-REPETITIVE X-RAY RADIATION *

O.P. KUTENKOV[1], T.P. ASTAPHYROVA[2], E.N. SURNINA[2], E.A. SOSNIN[1,2], A.A. BURENINA[2], Y.Y. FADEEVA[2], M.A. BOL'SHAKOV[1,2], V.V. ROSTOV[1]

[1] Institute of High-Current Electronics SB RAS, Tomsk, Russian Federation
[2]National Research Tomsk state university, Tomsk, Russia

Radiation treatment of plant raw materials [1], including pre-sowing seed treatment [2], should play an important role in increasing the level of food safety in Russia. Seed stimulation by physical factors accelerates the course of the first phases of plant ontogenesis, reduces the ripening time and, ultimately, leads to an increase in the yield of cereals and potatoes by 5-20 %. At the same time, the recommended doses for radiation stimulation of crop seeds are 3-40 Gy. Studies have already been conducted on the stimulating effect of X-rays with small doses (0.2 Gy and less) [3], but this studies should be continue.

We consider the use of nanosecond periodic X-ray radiation (IPRR) to be a promising research direction. High efficiency of IPRR was demonstrated earlier [4, 5]. The purpose of current study was to find out the effect of pre-seed wheat stimulation by IPRR in case of small doses on ontogenesis and structure of the wheat crop.

Seeds of soft spring wheat ("Iren" cultivar) were used, the germination rate of which was not less than 95%. Before sowing, the seeds were exposed to pulse-periodic X-ray radiation in doses from 0.02 Gy to 0.4 Gy with different pulse repetition rates. The source of X-ray radiation was a small-sized electron accelerator SINUS-150, produced by IHCE SB RAS.

It is shown that at the end of the vegetative season, the IPRR treatment of seeds had an impact on the crop yield. Increased plant height, number of productive shoots, weight of spike and grain per spike and grain yield exceeded the control by 11%. It is important that IPRR treatment did not affect the quality of wheat grain. The amount of protein in the grain of the studied samples was almost the same and amounted to 12.6-12.8%, grain moisture – 10.2%, vitreous content varied within 37.3-38.4%, and the gluten content from 20.3 to 21.1%.

Obtained results on the pre-seed IPRI stimulation of wheat seeds showed the prospects of such a technological approach. In the future, it will be necessary to identify the optimal treatment modes and expand the range of studied valuable crops in order to identify their species and variety specificity.

REFERENCES

[1] T. V. Chiz, G. V. Koz'min, L. P. Polyakov, T. V. Mel'nikova “Radiation treatment as a technological technique for improving food safety,” Bulletin of the Russian Academy of Natural Sciences, no. 4, pp. 44–49, 2011 (in russian).

[2] E. P. Pimenov, A. N. Pavlov, G. V. Kozmin, E. V. Spirin, N. I. Sanzharova, “A study into the effectiveness of radiation sterilization of vegetable materials using gamma-emitter GUR-120,” Radiation and risk, vol. 22, no. 4, pp. 37–42, 2013.

[3] C. E. Mokobia, O. Anomoharan, “The effect of gamma irradiation on the germination and growth of certain Nigerian agricultural crops,” Journal of Radiological Protection, vol. 25, no. 2, 2005.

[4] M. A. Buldakov, I. A. Klimov, O. P. Kutenkov, N. V. Cherdyntseva, V. V. Rostov, M. A. Bolshakov, “Potential application of nanosecond pulsed X-ray in medicine,” Abstracts of 3-rd Congress on Radiation Physics and Chemistry of Condensed Matter, High Current Electronics and Modification of Material with Particle Beams and Plasma Flows, Tomsk, Russia, pp. 253–254, 2012.

[5] M. A. Buldakov, M. S. Tretyakova, V. B. Ryabov, I. A. Klimov, O. P. Kutenkov, J. Kzhyshkovska, M. A. Bolshakov, V. V. Rostov, N. V. Cherdyntseva, “Macrophage and tumor cell responses to repetitive pulsed X-ray radiation,” Journal of Physics: Conf. Series, vol. 830, 012045, 2017.

* This research was supported by “Tomsk State University competitiveness improvement program” grant (№ 8.1.29.2018).

NEW PULSE GENERATOR BASED ON A LINEAR PULSE TRANSFORMER FOR ELECTROPULSE DRILLING

D. MOLCHANOV[1], *I. LAVRINOVICH*[1], *D. RYBKA*[1], *A. LENSKIY*[1], *N. ZHAROVA*[1]

[1] *IHCE SB RAS, Tomsk, Russia*

Geothermal energy is currently the most progressive renewable energy source. It is safe, practically independent of the external environment, and has practically inexhaustible reserves. The main limiting factor of this technology is the large depth of the underground heat source. The production of ultra-deep wells by traditional mechanical drilling is very expensive and has great technical difficulties. The most promising solution to this problem is electropulse drilling.

However, the creation of the main element of such a rig - a high-voltage generator - is a complex technical problem, which has not yet been solved. This article presents a model of a new drilling generator based on Linear Pulse Transformer circuit. The external diameter of this generator does not exceed the diameter of the well it creates, which suggests that this generator can be created in a downhole design. The design features of a new generator allow us to vary the energy released in the plasma channel in a wide range to achieve optimal drilling efficiency for different types of rocks.

THE SOLID-STATE GENERATOR FOR DIRECT PUMPING OF A CUBR LASER WITH THE ADJUSTABLE PULSE SHAPE*

P.P. GUGIN[1], E.O. DEGTYAREV[1,2], V.A. KIM[1]

[1]Institute of Semiconductor Physics, Siberian Branch, Russian Academy of Sciences, pr. Akademika Lavrent'eva 13, Novosibirsk, 630090, Russia, gugin@isp.nsc.ru
[2]Novosibirsk State Technical University NETI, 20 Prospekt K. Marksa, Novosibirsk, 630073, Russia

Traditionally, pulsed thyratrons and powerful generator vacuum tubes are used for CuBr laser pumping. The advantage of thyratrons is a significantly larger pulsed power at smaller dimensions, while the tubes have a fully controllable mode of operation, which makes it possible to form not only the front edge of the pulse, but also back edge, thereby limiting the input of energy to the discharge at the end of the lasing pulse, which positively affects laser's energy conversion efficiency. Significant disadvantages of vacuum and gas-discharge switch are the presence of powerful heating circuit, low lifetime and the need for high voltage power supply. To eliminate these disadvantages, the adjustable pulse shape generator based on MOSFET is proposed for CuBr-laser direct pumping by a longitudinal discharge. It is a forward converter with step-up transformer. The number and type of transistors is selected based on the requirements of the laser gas-discharge tube for the current amplitude and the necessary current slew rate to form an acceptable leading edge, taking into account the transformation coefficient. The primary winding of the transformer consists of one turn and is distributed around the entire perimeter of the transformer core. The secondary winding consists of several parallel sections to increase the coupling coefficient of the windings with sufficient electrical insulation.

The optimization of topology of transistor driver's current loop and the symmetrical distribution of the control signal with its electromagnetic filtering made it possible to control a large number of transistors synchronously enough to ensure safe current slew rate through each switch at the level of 1,5 – 1,7 A/ns at the both states of transistors: switched on, switched off. To sum up, the generator can provide a front and back edge of impulse at the level of 40 – 60 ns with a pulse duration of less than 200 ns, a current of up to 200 A, a voltage of up to 10 kV, and a frequency of at least 10 kHz with passive cooling. An additional advantage of the generator design is the ability to connect transformer outputs both series and parallel to increase voltage and current, respectively.

* The work was supported by Russian Science Foundation, research Project No. 19-19-00069

ACTION OF SUBNANOSECOND PULSED ELECTRIC FIELD ON U87 CELLS**

A.A. PETROV[1], A.A. MORALEVA[1,2], N.V. ANTIPOVA[1,2,3], R.KH. AMIROV[4], I.S. SAMOYLOV[4], S.YU. SAVINOV[1]

[1]P.N. Lebedev Physical Institute of RAS, Moscow, Russia
[2]Shemyakin-Ovchinnikov Institute of Bioorganic Chemistry RAS, Moscow, Russia
[3]NRU Higher School of Economics, Moscow, Russia
[4]Joint Institute for High Temperatures RAS, Moscow, Russia

The effect of the pulsed electric field of the subnanosecond range on human tumor cells U87 is studied. Studies of the effects of nanosecond electric fields on cells are widely carried out [1-3], but there is no data on the effect of the duration of the pulse rise time on the processes leading to cell death. The use of pulsed electric fields with subnanosecond rise time can effectively affect the internal structures of the cell, since the polarization time of the outer cell membrane is ~ 1 ns. These fields can be used in the development of new methods for the treatment of human tumor diseases.

In this work the U87 cell lines were treated with a pulsed electric field for 1 - 5 minutes with a frequency of 100 Hz, electric field strength in the cell medium of 1 - 2 kV/cm, pulse duration 7 ns and duration of voltage rise of 150 ps (Fig. 1).

To determine the level of cell death, 4 hours after the electric field treatment, the cells were stained with Trypan Blue (0.4%). Dead cells and cells with damaged membranes are stained. For glioblastoma cells survival is over 70%.

In 4 hours after treatment with electric fields, the efficiency of mitochondria was measured using the lipophilic dye Rhodamine 123. For U87 cells, the fluorescence intensity at a length of 570 nm in the treated groups after 4 hours was significantly lower and amounted to ~ 40% of the control, which indicates a decrease in transmembrane potential and a decrease in the efficiency of mitochondrial functioning.

The state of the cells in 4 days after treatment was monitored by detecting changes in metabolic activity using resazurin based alamarBlue ™ Cell Viability Reagent. The decrease in cell viability estimated by resazurin metabolism on day 4 was on the range of 70% of the control.

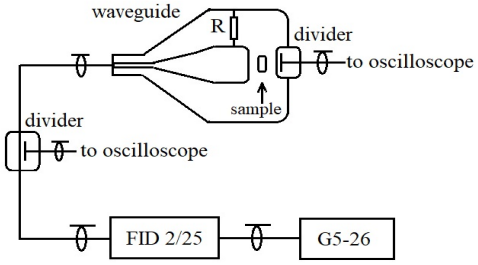

Fig.1. Experimental setup.

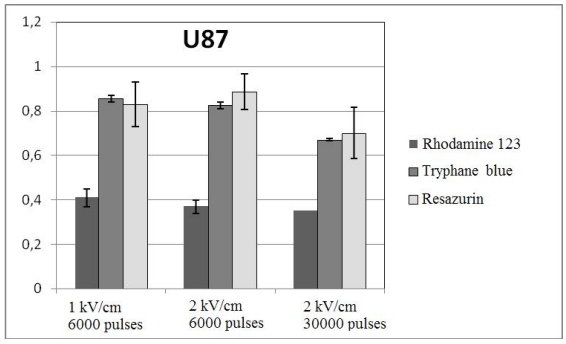

Fig.2. Results of Rhodamine 123, Thypan blue and Resazurin tests.

In the U87 line, 4 hours after field treatment of the cells the rhodamine fluorescence is up to 40% compared with the control, which indicates a pronounced effect of ultrawideband electric field pulses on the mitochondria of the cells. Changes in cell viability of the U87 line after 4 hours and 4 days after treatment show the presence of processes of instant and delayed cell death. Authors would like to thank FID Technology for technical help.

REFERENCES

[1] Soueid, M., Dobbelaar, M.C.F., Bentouati, S. et al. Delivery devices for exposure of biological cells to nanosecond pulsed electric fields // Med Biol Eng Comput doi: 10.1007/s11517-017-1676-0

[2] Tina Batista Napotnik, Matej Reberšek, P. Thomas Vernier, Barbara Mali, Damijan Miklavčič, Effects of high voltage nanosecond electric pulses on eukaryotic cells (in vitro): A systematic review // Bioelectrochemistry 110 (2016) 1–12. doi:10.1016/j.bioelechem.2016.02.011

[3] Karl H. Schoenbach. From the basic science of biological effects of ultrashort electrical pulses to medical therapies // Bio Electro Magnetics. 2018. https://doi.org/10.1002/bem.22117

* The work was supported by the Russian Science Foundation under grant No. 18-79-00312.

FEATURES OF PULSE DISCHARGE FORMATION IN TRIGGER UNITS OF SEALED-OFF COLD CATHODE THYRATRONS*

G.A. ARGUNOV, N.V. LANDL, O.B. FRANTS, Y.D. KOROLEV, V.G. GEYMAN

Institute of High Current Electronics, Tomsk, Russia

The two-sectioned TPI-type cold-cathode thyratron investigated in this work has a trigger unit based on an auxiliary glow discharge (Fig. 1 *a*) [1]. It was demonstrated in our previous works that this device has remarkable triggering characteristics for various trigger circuits [2]. The present paper deals with study of cold-cathode thyratron operating towards a novel trigger circuit with grounded cathode and grid.

It is shown that there are two different regimes of the auxiliary glow discharge. Transition from one regime to another occurs spontaneously. In turn, the initial regime of the auxiliary discharge determine the modes of the trigger discharge formation [3]. This circumstance influences the thyratron triggering stability, causing a vast jitter in delay times to the main gap breakdown.

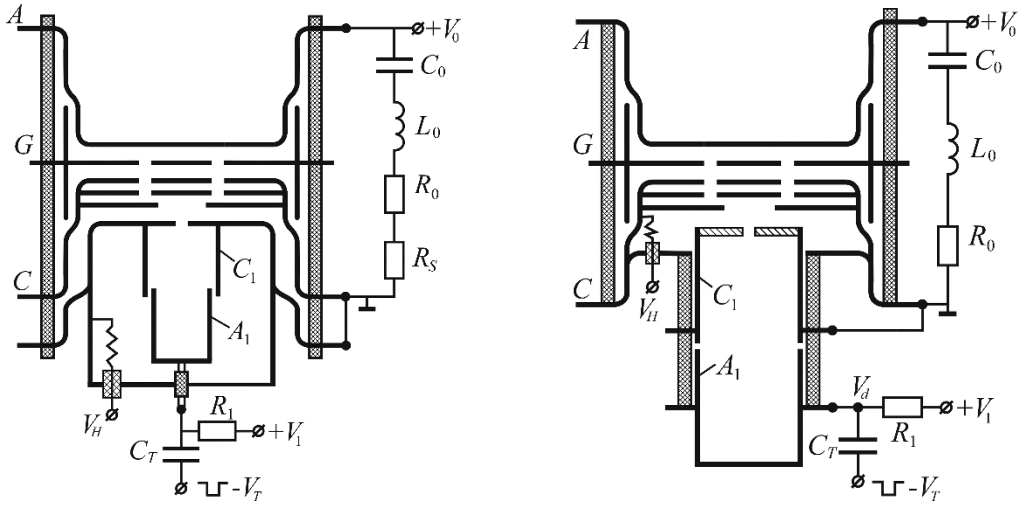

Fig. 1. The TPI1-10k/50 cold-cathode thyratron – *a)* and its upgraded sealed-off prototype – *b)* along with the electric trigger circuit. C_0 = 4 nF, L_0 = 1μH, R_0 = 18 Ω, R_1 = 30 kΩ, R_B = 30 Ω, C_T = 3 nF.

An upgraded cold-cathode thyratron with a new trigger unit was developed (Fig. 1 *b*). The electrodes of the new trigger unit designed as hollow cylinders separated with a ceramic insulator. It is demonstrated that the regime of the auxiliary discharge is stable, as well as formation of the trigger discharge. It determines a high triggering stability of the upgraded thyratron.

REFERENCES

[1] N. V. Landl, Y. D. Korolev, V. G. Geyman, O. B. Frants, G. A. Argunov, and A. V. Bolotov, "Features of the discharge ignition in the trigger unit of the coldcathode thyratron," J. Phys. Conf. Ser. 1115, 022031 (2018).

[2] Y. D. Korolev, N. V. Landl, V. G. Geyman, G. A. Argunov, O. B. Frants, and A. V. Bolotov, "Methods of triggering for the cold-cathode thyratrons with a trigger system based on an auxiliary glow discharge", AIP Advances 9, 085326 (2019).

[3] Y. D. Korolev, N. V. Landl, V. G. Geyman, O. B. Frants, I. A. Shemyakin, V. S. Kasyanov, and A. V. Bolotov, "Study of cold-cathode thyratron triggering stability at high anode voltages", Plasma Physics Reports,Vol. 44, 110 (2018).

* The work was carried out with the financial support of Russian Science Foundation, grant № 19-19-00123

SPECTROSCOPIC STUDY OF PULSE DISCHARGES IN SALINE SOLUTIONS*

I.A. SHEMYAKIN[1,2], *Y.D. KOROLEV*[1,2], *V.E. PROKOPEV*[1], *A.V. BOLOTOV*[1], *V.S. KASYANOV*[1], *V.G. GEYMAN*[1]

[1]*Institute of High Current Electronics SB RAS, 2/3 Akademichesky Ave., Tomsk 634055, Russia, shemyakin@lnp.hcei.tsc.ru*
[2]*National Research Tomsk State University, 36 Lenin Avenue, Tomsk, 634050, Russia*

Discharges in saline solutions are widely used in medicine, surface treatment [1–3]. Recently the development of sample destruction systems and echolocation problems have stimulated interest in discharges in micro and millisecond solutions with amplitudes ranging from hundreds of amperes to kiloamperes [4, 5]. As a rule, the concentration of salt in such solutions is high and is one percent.

Due to the high conductivity of the solution, gas cavities appear near the active electrode at values of the applied voltage significantly lower than the breakdown voltage V_{br} [6–8]. Under certain conditions, these cavities shield the electrode, which leads to an increase in the gap resistance and a limitation of the discharge current.

When the voltage at the discharge gap reaches the threshold critical values of $V_{th} < V_{br}$ a gas-discharge plasma occurs inside the gas cavities at the initial stage. Everyone can consider this as a stage of delay in the development of the breakdown. The appearance of gas-discharge plasma can lead to both growth and suppression of the shielding effect. In the final stage, high-conducting plasma usually bridges the gap [5–8].

The processes of formation and development of gas cavities, as well as discharges in them, are non-stationary. As a rule, these processes occur at different time scales, due to different physical mechanisms that initiate them. Preliminary studies conducted in [5–8] have shown that the forms of discharge occurring at different stages of breakdown may differ significantly and have not been definitively identified to date. This work is devoted to the study of this issue based on the analysis of plasma radiation spectra recorded at different times.

Registration of spectra was carried out using a spectrometer Ocean Optics USB 2000+ and Hamamatsu PMA-12. The behavior of the radiation spectrum over time in different regions of the spectrum was studied using the photoelectronic multiplier FEU-38 and a set of light filters. The time resolution was no worse than 100 ns and the spectral range was $\Delta\lambda$ = 330–850 nm.

REFERENCES

[1] L. Schaper, W.G. Graham, K.R. Stalder “Vapour layer formation by electrical discharges through electrically conducting liquids-modelling and experiment,” Plasma Sources Sci. Technol., vol. 20, no. 3, Article Number 034003, June 2011.

[2] S.H.R.Hosseini, K. Mavatari, S.M Nejad, “Two successive shock waves generated by underwater pulse electric discharge for medical application,” IEEE Trans. Plasma Sci., vol. 42, no. 10, pp. 3209–3214, October 2014/

[3] Y.D. Korolev, G.A. Mesyats, A.M. Yarosh, “Film etching by particles produced by a pulsed bulk discharge in CF4,” High Energy Chem., vol. 21, no. 5, pp. 389–392, September 1987.

[4] P. Bruggeman., C. Leys, “Non-thermal plasmas in and in contact with liquids,” J. Phys. D: Appl. Phys., vol. 42, no. 5, Article Number 053001, March 2009.

[5] Y.H.Sun, Y.X. Zhou, M.J. Jin, Q. Liu, P. Yan, “New prototype of underwater sound source based on the pulsed corona discharge,” J. Electrost., vol. 63, no. 6-10, pp. 969–975, June 2005.

[6] R.V. Ivashov, V.G. Geyman, Y.D. Korolev, I.A. Shemyakin, “Influence of non-stationary processes on the formation and development of a discharge in an electrolyte in electrode systems,” Izv. Vyssh. Uchebn. Zaved. Fiz., vol. 50, no. 9. Supplement, pp 368–371, September 2007.

[7] Y.D. Korolev, I.A. Shemyakin, V.S. Kasyanov, R.V. Ivashov, N.V. Landl, Y. Sun, T. Shao, Y. Gao, “Investigation of the electrical discharge in the saline solutions in a vicinity of the threshold voltages,” Izv. Vyssh. Uchebn. Zaved. Fiz., vol. 57, no. 11/3, pp. 12–16, November 2014.

[8] Y.D. Korolev, I.A. Shemyakin, R.V. Ivashov, V.S. Kasyanov, N.V. Landl, Y.H. Sun, T. Shao, Y. Gao, “Discharge in the saline solutions in a vicinity of the threshold voltages,” J. Physics: Conf. Ser., vol. 552, Article Number UNSP 012005, September 2014.

* The study is a continuation of the work supported by RFBR project No 16-08-00652.

MEASUREMENT OF MOMENTUM AND RECOIL FORCE OF CATHODE PLASMA JET OF VACUUM ARC[1]

S.A. POPOV, E.L. DUBROVSKAYA, A.V. BATRAKOV

Institute of High Current Electronics SB RAS, Tomsk, Russia

To measure the mechanical momentum of a plasma jet, we analyzed the deflection of a shield suspended on long threads in front of the jet (ballistic pendulum method). The method does not require calibration, and allows to measure the impact of a single pulse with a high accuracy~ 0.01 μN•s (in our experiment). Alternatively, the recoil momentum in frequency mode of arc operation was measured with a specially designed analytical dynamometer. The error in measuring force does not exceed 5 μN, i.e. at a frequency of 10 Hz, the corresponding accuracy in the recoil momentum (per single arc pulse) is not worse than 0.5 μN•s and can be improved by increasing the pulse repetition rate.

The dependence of the plasma jet momentum and recoil force on the arc current amplitude was studied in the range of the current up to 400 A. The experiment shows that:
(1) measurements by two methods correlate well with each other;
(2) at a relatively weak arc current (<100 A), the specific force is close to 150 μN/A, which is consistent with the known data [1];
(3) with a further increase in the arc current (>100-150 A), the specific force increases and can significantly exceed the above value. The compression and additional acceleration of the current-carrying plasma jet by its own azimuthal magnetic field as well as the emission of micro-droplets by the cathode are discussed as possible reasons for such an increase.

In addition, the dependence of the shield deflection on the residual pressure in the vacuum chamber is studied and discussed. The experiments performed with two cathode materials are also compared.

The material presented in the paper is of interest both from the point of view of fundamental and methodological issues in the study of a vacuum arc, and from utilitarian point of view, primarily in relation to the creation and testing of vacuum arc based micro-thrusters for small/ultra-small satellites.

REFERENCES

[1] R. Tanberg, "On the Cathode of an Arc Drawn in Vacuum", Phys. Rev. 35, 1080 (1930).

[1] The work was supported by the Russian Science Foundation under grant No 18-19-00270.

VACUUM ARC MICRO-THRUSTER WITH LIQUID METAL CATHODE[1]

S.A. POPOV, E.L. DUBROVSKAYA, A.V. BATRAKOV

Institute of High Current Electronics SB RAS, Tomsk, Russia

Vacuum arc micro-thrusters (micro-VAT) in which the thrust is generated by a cathode plasma jet, are known as promising for ultra-compact satellites, including CubeSat satellites weighing few kilograms (nanosatellites). As a radical solution to the cathode resource problem, we propose using the liquid metal as a consumable cathode material, which flows to the cathode working surface under the action of capillary forces.

In the experiments, we used Wood's alloy with the addition of indium (melting point ~ 50 °C), as well as pure gallium (~40 °C). A simple low-voltage RLC pulser was applied, with which arc ignition was achieved due to Joule heating and evaporation of a portion of the cathode material covering the surface of the ceramic insulator separating the cathode and the anode.

The mechanical impulse of the cathode plasma jet was measured by the pendulum shield method. Alternatively, the recoil momentum was measured with a specially designed analytical dynamometer. The formation of an arc plasma jet and the droplet fraction of cathodic erosion were studied using a high-speed video camera.

Clearly demonstrated that the force of the jet pressure and the recoil force are in good agreement with each other, increasing with increasing amplitude of the discharge current and can significantly exceed 150 μN/A (15 dyne/A), while the energy efficiency exceeds 10 μN/W.

The paper discusses the general issues of the applicability of micro-VAT with liquid-metal cathode: resource, reliability, maintenance of the required temperature regime, as well as specific issues, such as cathode plasma jet formation and acceleration including the application of axial magnetic fields for improving thrust characteristics.

[1] The work was supported by the Russian Science Foundation under grant No 18-19-00270.

STUDY OF SPACE-CHARGE STRUCTURE OF A CATHODE PLASMA JET[1]

E.L. DUBROVSKAYA, S.A. POPOV, A.V. BATRAKOV

Institute of High Current Electronics SB RAS, Tomsk, Russia

It is known that the current-carrying cathode plasma jet of a vacuum arc is contracted by its own azimuthal magnetic field. In present paper this effect was studied by the method of spectrally-selective photorecording. To record radiation of neutral atoms, single- and double charged ions of a cathode material we used high-speed 4-channel HSFC Pro camera in which on three channels narrow-band interference filters were installed. Thus, spatial distribution of different charge particles in the plasma jet was recorded.

As a result, it is clearly shown that with increasing arc current amplitude the nonuniformity of ion distribution in the radial direction increases. That is the predominant concentration of high charge ions is in the axial region of the discharge. The dynamics of these processes is investigated and discussed.

The influence of an external axial magnetic field on the processes of jet contraction and on the additional acceleration of particles under these conditions is also studied and discussed.

[1] The work was supported by the Russian Science Foundation under grant No 18-19-00270.

IGNITION DIFFERENT MODE OF CORONA DISCHARGE IN AIR AT ATMOSPHERIC PRESSURE *

V.F. TARASENKO, E.KH. BAKSHT, V.S. KUZNETSOV, V.A. PANARIN, V.S. SKAKUN, E.A. SOSNIN

Institute of High Current Electronics SB RAS, Tomsk, 634055, Russia
E-mail: VFT@loi.hcei.tsc.ru, phone: +7 (3822) 491-685

A corona discharge in air at atmospheric pressure is intensively studied and applied. The appearance of a corona in the transmission lines of electric energy and other devices results in energy loss. There is a wide spectrum of applications of corona discharge. It is known that various corona discharge regimes, including a stationary corona, are implemented on conductors with a small radius of curvature. At negative voltage polarity on the tip electrode, a nonstationary corona occurs and current pulses (Trichel pulses) are recorded with the repetition rate increasing with the voltage. At positive polarity on the tip electrode, a corona discharge occurs at higher voltages than at negative polarity. Some authors attribute the recorded current pulses to the formation of streamers.

The purpose of this work is to study the ignition of different mode of a corona discharge in the air at atmospheric pressure at low voltages and high electric field strengths, to achieve which a tip with a small radius of curvature was used.

It has been shown, that the ignition of a corona discharge in air at atmospheric pressure in a nonuniform electric field occurs at both polarities owing to the formation of ball streamers. Moreover, a streamer from the positive polarity tip starts at a higher voltage across the gap than from the negative polarity tip. With the same voltage across the gap, the larger average corona discharge currents in the mode of ball streamers are recorded at the negative tip polarity. The increase in the average current of the corona discharge is achieved at the negative tip because the repetition frequency of the individual pulses is much (two or more orders of magnitude) higher than that at the positive tip polarity. The formation of cylindrical streamers from the positive tip, see figure 1, with an increase in the voltage leads to a significant increase in the current pulse amplitudes, and they become higher than current pulse amplitudes from the negative tip for the same voltage.

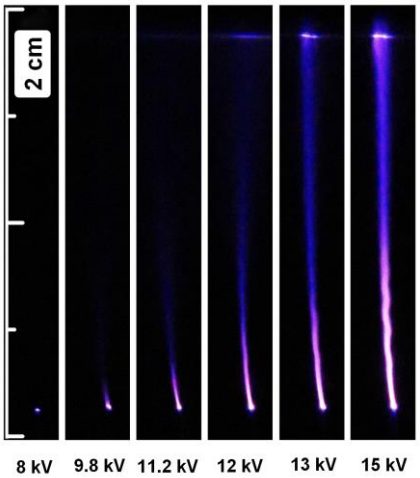

Fig. 1. Modes of corona discharge at different voltages positive polarity on the tip. Configuration "needle - plane", d = 2 cm.

These data are consistent with our results obtained previously [1, 2]. We believe that the ignition of the corona discharge at large corona electrodes with arbitrary shape and polarity begins with the formation of streamers, which start due to the amplification of the electric field on the microheterogeneities of the electrode with a small radius of curvature.

REFERENCES

[1] V. F. Tarasenko, V. S. Kuznetsov, V. A. Panarin, V. S. Skakun, E. A. Sosnin, E. Kh. Baksht, “Role of streamers in the formation of a corona discharge in a highly nonuniform electric field,” JETP Letters, vol. 110, no. 1, pp. 85-89, 2019.

[2] V. S. Kuznetsov, V. F. Tarasenko, E. A. Sosnin, “On Pulsed Modes of the Glowing Corona Region,” Russian Physics Journal, vol. 62, no. 5, pp. 893-899, 2019.

* The work is performed in the framework of the State task for HCEI SB RAS, project #13.1.4.

SUBNANOSECOND ELECTRON ACCELERATOR WITH GAS-FILLED FORMER

S.L.ELYASH[1], T.V.LOYKO[1], A.L.YURIEV[1], S.P.PUKHOV[1], D.P.NIKOLAEV[1], A.F POKOLEV[1], S.M.LASHMANOV[1]

[1]Russian Federal Nuclear Center–All-Russian Research Institute of Experimental Physics, Sarov, Russian Federation

A subnanosecond electron accelerator based on small-sized accelerator ARSA [1] with gas-filled former has been developed, manufactured and studied at RFNC-VNIIEF. The accelerator is meant for generating electron pulses with energy up to 800 keV and half-amplitude duration 0.3 ns.

The procedure of providing ultra-short electron beams is described in [2, 3]. The operation principle of the prototype accelerator is based on charging a short storage line followed by its discharge to a stepped line, along which a high-volt pulse of subnanosecond duration is transmitted onto an accelerating tube generating electrons. A high-volt unit of the 1 MV nanosecond accelerator ARSA is used for charging the former's short storage line.

The former is filled with nitrogen compressed up to pressure 4 MPa (40 atm.), which, in contrast to oil insulation. allows operating the accelerator in frequency mode and the possibly, under severe climatic conditions.

For the gas-filled former, a metal-ceramic accelerating tube, capacitor voltage divisors with nano- and subnanosecond resolution have been developed and manufactured. All the mentioned units are meant for their operation in the hign-pressure gas atmosphere. The accelerating tube is a part of transmitting line with the same wave resistance, that allows eliminating subnanosecond pulse distortions.

Fig. 1 gives an oscillogram of the electron beam current of the subnanosecond accelerator (tube SNIT-1000), obtained using a low-inductance shunt and Le Croy 5 GHz oscilloscope. With regard to the oscilloscope and shunt resolution times the pulse length of electron beam does not exceed $t_{0,5} \approx$ 0.3 ns. The electron beam current amplitude is ~1.5 kA.

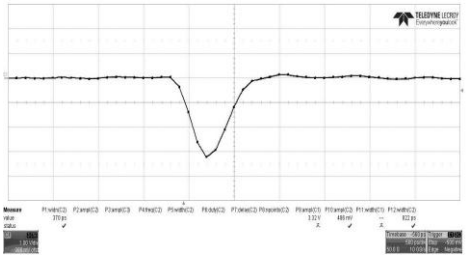

Fig.1. Oscillogram of electron beam current of subnanosecond accelerator with a tube SNIT-1000 (scan – 0.5 ns per a cell).

The subnanosecond accelerator will be used to determine the time resolution of nanosecond pulse detectors of electron and bremsstrahlung radiation, calibration and control of the working capacity of measuring channels, as well as to examine electrophysical characteristics (life time, carrier mobility) of wide-band gap insulators and promising heterogeneous semi-conductor structures.

REFERENCES

[1] Elyash S.L., Aleksandrin A.I., Donskoi E.N., Kalinovskaya N.I. et al. Accelerator APCA – small-sized source of X-ray pulses and electron radiation // Collection of proceedings of Russia nuclear centers. 1996. №5. P. 229-237.

[2] Zheltov K.A. Picosecond high-current accelerators. M.: Energoatomizdat, 1991.

[3] Mesyats G.A., Yalandin M.I. Picosecond high-power electronics // Physical Science Progress. 2005. vol. 175, №3. P.226-246.

ANALYSIS OF THE MINIMUM DURATION OF THE RUNAWAY ELECTRON FLOW IN AN AIR ELECTRODE GAP*

N.M. ZUBAREV[1,2], *G.A. MESYATS*[1,2], *M.I. YALANDIN*[1,2], *A.G. SADYKOVA*[2], *K.A. SHARYPOV*[2], *V.G. SHPAK*[2], *S.A. SHUNAILOV*[2], *M.R. ULMASKULOV*[2], *O.V. ZUBAREVA*[2], *A.V. KOZYREV*[3], *N.S. SEMENIUK*[3]

[1]*Lebedev Physical Institute, Russian Academy of Sciences, Moscow, Russia*
[2]*Institute of Electrophysics, Ural Branch, Russian Academy of Sciences, Yekaterinburg, Russia*
[3]*Institute of High-Current Electronics, Siberian Branch, Russian Academy of Sciences, Tomsk, Russia*

We present and analyze detailed characteristics of the runaway electron flow that occurs in a high-voltage (with the voltage rising at a rate of up to 1.5 MV/ns) air-filled electrode gap with a strongly nonuniform electric field (conical cathode – planar anode). Using a special electron current probe, we have demonstrated that such a flow initiated near the tip of a conical cathode contains a high-energy electron component of duration no more than 10 ps [1]. Analytical and numerical considerations show that the generation/termination of the runaway electron flow is governed by a combination of (i) impact ionization of the gas near the cathode, resulting in multiplication of free electrons and expansion of the cathode plasma layer, and (ii) dynamic processes that switch on/off a critical electric field at the plasma boundary which is high enough for electrons to run away. The characteristic time of generation/termination of a runaway electron flow can be estimated from the ionization rate at a near-critical field. Such an estimation yields 2–3 ps. This time determines the pulse duration of the runaway electron current. It was calculated (using a kinetic model based on Boltzmann's equation with collision integrals) to be ~6 ps, see Fig. 1, which is close to its experimental value.

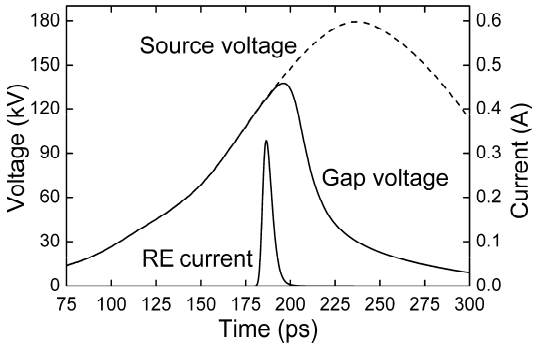

Fig.1. Waveforms of the source and gap (dashed and solid lines, respectively) voltage (in absolute value) and of the runaway electron (RE) current [1].

REFERENCES

[1] G.A. Mesyats, M.I. Yalandin, N.M. Zubarev, A.G. Sadykova, K.A. Sharypov, V.G. Shpak, S.A. Shunailov, M.R. Ulmaskulov, O.V. Zubareva, A.V. Kozyrev, N.S. Semeniuk, "How short is the runaway electron flow in an air electrode gap?" Appl. Phys. Lett., vol. 116, art. no 063501, February 2020.

*The work was supported in part by the RFBR Grants Nos. 19-08-00292 and 20-08-00172. The study was carried out on the equipment of the Collective Use Center at the Institute of Electrophysics, UB, RAS. Also, the authors are grateful to the representative office of Keysight Technologies in Russia for offering the possibility to perform tests using a Keysight DSAZ594A signal analyzer.

THE EFFECT OF GAS PRESSURE ON CUMULATION OF AN ELECTRON BEAM GENERATED IN A HIGH-VOLTAGE NANOSECOND DISCHARGE*

M.I. LOMAEV[1,2], *V.F. TARASENKO*[1], *A.V. DYATLOV*[2]

[1]*Institute of High Current Electronics, Tomsk 634055, Russia*
[2]*National Research Tomsk State University, Tomsk 634050, Russia*

The cumulation of relativistic electron beams with currents of tens-hundreds of kA in vacuum diodes is well-known effect [1-4]. It takes place when the electron beam current exceeds the Alfven current: $I_A = 17 \cdot \beta \cdot \gamma$, where υ – electron beam velocity, and c – velocity of light, $\beta = \upsilon/c$, $\gamma = 1/(1 - \beta^2)^{1/2}$ – relativistic factor. The physical reason of electron beam self-focusing effect in this case was found to be the cumulation by its self-magnetic field [2]. The cumulation of an electron beam at current value up to ~ 1 kA in gas and vacuum diodes was observed as well [5-8]. However, to date there is no satisfactory explanation of the electron beam cumulation effect at beam currents below the value of the Alphen current. Various reasons are indicated in various articles: a repulsion of electrons emitted by the explosive-emission plasma on a cathode [5]; a breakdown on runaway electrons, developing in the cathode-anode gap [8]; compensation of the charge of the electron beam due to the space charge of positive ions arising in the discharge gap during ionization by the runaway electrons of the residual gas [9].

The purpose of this investigation is the study of the effect of pressure on cumulation of an electron beam generated in a high-voltage nanosecond discharge and space-time distribution of electron beam current density at the anode surface near the zone of cumulation (fig. 1) at the current values < 1 kA.

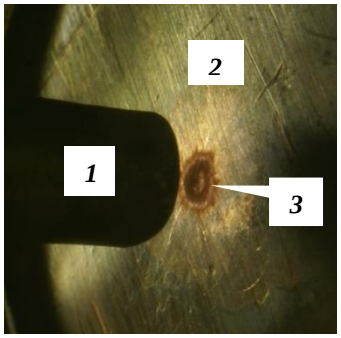

Fig.1. Discharge gap photo: 1 – cathode, 2 – anode made of a 400 μm-thick copper foil, 3 – zone of electron beam cumulation. Interelectrode gap length – 2.7 mm, residual air pressure in the discharge chamber 25 Pa.

REFERENCES

[1] S.A. Goldstein, R.C. Davidson, J.G. Siambis, L. Roswell, "Focused-Flow Model of Relativistic Diodes," Phys. Rev. Lett. Vol. 33, no. 25, pp. 1471–1474, 1974.

[2] E.E. Tarumov, Generation and Focusing of High-Current Relativistic Electron Beams [in Russian], (Ed. L.I. Rudakova), Moscow: Energoatomizdat, 1990.

[3] G.A. Mesyats, Pulsed Power and Electronics, Moscow: Nauka, 2004.

[4] V.I. Baryshnikov, and V.L. Paperny. "Collective "overacceleration" of electrons in a pinched picosecond electron beam," Phys. Plasmas, vol. 25, no. 8, 083106, 2018.

[5] S. Anishchenko, V. Baryshevsky, N. Belous, A. Gurinovich, E. Gurinovich, E. Gurnevich, and P. Molchanov, "Cumulation of High-Current Electron Beams: Theory and Experiment," IEEE Trans. Plasma Sci., vol. 45, no. 10, pp. 2739–2743, 2017.

[6] A.G. Burachenko, V.F. Tarasenko, I.D. Kostyrya, E.Kh. Baksht, "Formation of diffuse jets and runaway electron beams in air, SF_6 and helium at low pressures," Atm. Ocean. Optics, vol. 31, no. 1, pp. 96–100, 2018.

[7] K. I. Almazova, A. N. Belonogov, V. V. Borovkov, E.V. Gorelova, I.V. Morozova, A.A. Tren'kin, and S.Yu. Kharitonov, "Microstructure of a Spark Discharge in Air in a Point–Plane Gap," Tech. Phys., vol. 63, no. 6, 801–805, 2018.

[8] V.I. Oleshko, V.F. Tarasenko, A.G. Burachenko, and V.V. Nguyen, "Filamentation and Self-Focusing of Electron Beams in Vacuum and Gas Diodes," Tech. Phys. Lett, vol. 45, no. 4, pp. 309–313, 2019.

[9] M.I. Lomaev, V.F. Tarasenko, and A.V. Dyatlov, "Cumulation of a high-current electron beam during a nanosecond high-voltage discharge in a low-pressure diode," Russ. Phys. J., vol. 62, no. 6, pp. 996-1000, 2019.

* The work was supported by the Russian Science Foundation (Project No. 18-19-00184).

ELECTROHYDRODYNAMIC FLOW CAUSED BY HIGH-FREQUENCY BARRIER DISCHARGE DISTRIBUTED OVER THE DIELECTRIC SURFACE

V.A. YAMSHCHIKOV, V.YU. KHOMICH

Institute for Electrophysics and Electric Power RAS, 18 Dvortzovaya nab., Saint Petersburg, Russia, E-mail: yamshchikov@ras.ru

In this work we studied the formation of electrohydrodynamic (EHD) flows due to ions extracting from the plasma of a near-surface barrier discharge by an external electric field and a gas flow forming in the direction of ion drift when ions interact with neutral particles. A model for calculating the EHD flow is developed. Using this model, analytical expressions for quantitative estimates of the current-voltage and velocity dependences of the flow were obtained. Also a computer simulation of the EHD flow for a plane-cylindrical electrode module was performed. Electric discharge systems for active control of flows with a high (more than 15 l/s) volumetric gas flow have been developed and investigated. A multi-discharge actuator system (MAS) based on an improved three-electrode circuit with a shielding electrode was developed and investigated. The geometric and physical parameters of the MAS were optimized in order to increase the speed and energy efficiency of the generated flow. Experimental dependences of the spatial profiles of the air flow velocity on the frequency, voltage amplitude, average power supply, and thickness of the dielectric substrate are obtained. The results of the effect of the substrate material for actuators and power modes on the degradation of the outer surface of the MAS are also presented. As a result of the research, a highly efficient MAS was created for controlling the air flow on aerodynamic surfaces with significantly higher power and energy characteristics than world-famous analogues.

INFLUENCE OF INHOMOGENEOUS ELECTRIC FIELD GEOMETRY FACTORS ON RUNAWAY ELECTRONS GENERATION CONDITIONS*

Y.I. MAMONTOV[1], *N.S. SEMENIUK*[2], *N.M. ZUBAREV*[1], *I.V. UIMANOV*[1]

[1]*Institute of Electrophysics UB RAS, Amundsena Str. 106, Ekaterinburg, 620016, Russia*
[2] *Institute of High-Current Electronics SB RAS, Academicheskiy Av. 2/3, Tomsk, 634055, Russia*

The runaway electrons phenomenon is known to be observed in strong electric fields. For example, the commonly accepted value of the critical homogeneous electric field E_{cr} for an air of atmospheric pressure is about 450 kV/cm [1]. Usually, in experiments, such a high electric field strength may be reached either for small discharge gap length about 1 mm or smaller or in vicinity of a discharge gap cathode with a small curvature radius, where an electric field amplification factor is high enough for electrons to transit into a continuous accelerating regime. For the latter case, the condition $E \geq E_{cr}$ may be satisfied only near the cathode, not over a whole discharge gap, but, since braking force acting on electrons from gas particles decreases with an increase of electron energy, electrons may still be continuously accelerated by an electric field. On the other hand, if the electric field amplification factor decreases rapidly enough (that is typical for the cathodes with extremely small curvature radii and high amplification factors), in a weak electric field, even fast electrons may lose their energy in collisions with gas particles, and, thus, they may become thermalized slow plasma electrons.

In this paper, dynamics of runaway electrons was investigated in Nitrogen of 1 atm pressure for various curvature radii of a cathode of the discharge gap of constant length 1 cm. 3D Monte-Carlo technique and pseudo 1D Boltzmann's equation were employed. The dependence of E_{cr} near the cathode from the cathode curvature radius and dynamics of electron energy distribution function were obtained. A comparison of the results obtained with analytical ones [2] was carried out.

REFERENCES

[1] Y.D. Korolev and G.A. Mesyats, Physics of Pulsed Breakdown in Gases. Yekaterinburg: UrB RAS, 1998.

[2] N.M. Zubarev, M.I. Yalandin, G.A. Mesyats, S.A. Barengolts, A.G. Sadykova, K.A. Sharypov, V.G. Shpak, S.A. Shunailov, O.V. Zubareva, "Experimental and theoretical investigations of the conditions for the generation of runaway electrons in a gas diode with a strongly nonuniform electric field," J. Phys. D: Appl. Phys, vol. 51, no. 28, 284003, June 2018.

* The work was supported in part by RFBR Grants Nos. 18-08-00547, 19-08-00783, 19-58-53006, 20-08-00172 and UB RAS Program Project No 18-2-2-16.

FEATURES OF THE DEVELOPMENT OF NEGATIVE AND POSITIVE STREAMERS IN A SHARPLY INHOMOGENEOUS ELECTRIC FIELD*

D.V. BELOPLOTOV, M.I. LOMAEV, D.A. SOROKIN, V.F. TARASENKO

Institute of High Current Electronics SB RAS, Tomsk, Russia

Nanosecond gas discharges in diffuse form are used as sources of low-temperature plasma [1–3]. Various chemically active species are generated in the plasma of such discharges, which can, for example, inactivate microorganisms on the surfaces of various materials, and remove pollutants in gases and liquids. The prospects for the use of nanosecond discharges determine the urgency of studies of both the formation of nanosecond discharges [4–11].

It is known from experiments that a nanosecond discharge in a sharply inhomogeneous electric field is ignited in diffuse form in any atomic and molecular gases and their mixtures (including in air) both with negative and positive polarity. Studies using high-speed imaging methods have shown that a plasma formation with large transverse dimensions develops in the gas-discharge gap [6, 8–11]. Modern theoretical models can describe the formation of such discharge either in air or in a mixture of nitrogen and oxygen [9]. However, in pure gases, this mechanism does not work and it is difficult to simulate the discharge under these conditions.

Breakdown at high overvoltages is also accompanied by the generation of subnanosecond runaway electron beams and X-ray radiation [12, 13]. As shown in [14], runaway electrons (REs) can provide effective preliminary ionization of the gas before the start of the streamer. However, there are no direct experimental data indicating the effect of REs on the formation of a streamer.

This report presents the results of studies of the streamer formation in a sharply inhomogeneous electric field in atmospheric pressure air, nitrogen and other gases at various voltages and polarities. Data on the instantaneous streamer velocity were obtained using the streak camera and a four-channel intensified charge-coupled device (ICCD) camera with simultaneous recording waveforms of the discharge current and voltage.

.

REFERENCES

[1] R. Hippler, H. Kersten, M. Schmidt, and K. H. Schoenbach (eds), Low Temperature Plasma Fundamentals, Technologies, and Techniques, Weinheim, Wiley-VCH Verlag GmbH&Co., 2008.

[2] P. K. Chu and X. Lu (eds), Low Temperature Plasma Technology, Boca Raton, CRC Press, 2014.

[3] I. Adamovich, S. D. Baalrud, A. Bogaerts, P. J. Bruggeman, M. Cappelli, V. Colombo, U. Czarnetzki, U. Ebert, J. G. Eden, P. Favia, D. B. Graves, S. Hamaguchi, G. Hieftje, M. Hori, I. D. Kaganovich, U. Kortshagen, M. J. Kushner, N. J. Mason, S. Mazouffre, S. Mededovic Thagard, H-R. Metelmann, A. Mizuno, E. Moreau, A. B. Murphy, B. A. Niemira, G. S. Oehrlein, Z. Lj. Petrovic, L. C. Pitchford, Y-K. Pu, S. Rauf, O. Sakai, S. Samukawa, S. Starikovskaia, J. Tennyson, K. Terashima, M. M. Turner, M. C. M. van de Sanden, and A. Vardelle, "The 2017 Plasma Roadmap: Low temperature plasma science and technology," J. Phys. D: Appl. Phys. vol. 50, Article Number 323001, 2017.

[4] L.P. Babich, T.V. Loiko, and V.A. Tsukerman, "Highvoltage nanosecond discharge in a dense gas at a high overvoltage with runaway electrons," Sov. Phys. Usp., vol. 33, Article Number 521, 1990.

[5] T. M. P. Briels, E. M. van Veldhuizen, U. Ebert, "Positive streamers in air and nitrogen of varying density: experiments on similarity laws, " J. Phys.D: Appl. Phys., vol. 41, Article Number 234008, 2008.

[6] P. Tardiveau, L. Magne, E. Marode, K. Ouaras, P. Jeanney, and B. Bournonville, "Sub-nanosecond time resolved light emission study for diffuse discharges in air under steep high voltage pulses," Plasma Sources Sci. Technol. vol. 25, Article Number 054005, 2016.

[7] A. Komuro, R. Ono, and T. Oda, "Effects of pulse voltage rise rate on velocity, diameter and radical production of an atmospheric-pressure streamer discharge," Plasma Sources Sci. Technol. vol. 22, Article Number 045002, 2013.

[8] M.I. Lomaev, D.V. Beloplotov, V.F. Tarasenko, and D.A. Sorokin, "The breakdown features of a high-voltage nanosecond discharge initiated with runaway electrons at subnanosecond voltage pulse rise time," IEEE Trans. Diel. Electr. Insul., vol. 22, Article Number 1833, 2015.

[9] N.Y. Babaeva and G.V. Naidis, "Modeling of streamer dynamics in atmospheric-pressure air: influence of rise time of applied voltage pulse on streamer parameters," IEEE Trans. Plasma Sci. vol. 44, Article Number 899, 2016.

[10] D.A. Sorokin, V.F. Tarasenko, D.V. Beloplotov, and M.I. Lomaev, "Features of streamer formation in a sharply non-uniform electric field," J. Appl. Phys., vol. 123, Article Number 143301, 2019.

[11] D.V. Beloplotov, M.I. Lomaev, D.A. Sorokin, and V.F. Tarasenko, "Measurement of the Dynamic Displacement Current as a New Method of Study of the Dynamics of Formation of a Streamer at a Breakdown of Gases at a High Pressure," JETP Letters, vol.107, Article Number 606, 2018.

[12] L.P. Babich, High-Energy Phenomena in Electric Discharges in Dense Gases, Arlington, Futurepast, 2003.

[13] V.F. Tarasenko (ed.), Runaway Electrons Preionized Diffuse Discharges, New York, Nova Science Publisher, 2014.

[14] N.Y. Babaeva G.V. Naidis, D.V. Tereshonok, and E.E. Son, "Modeling of streamer dynamics in atmospheric-pressure air: influence of rise time of applied voltage pulse on streamer parameters," J. Appl. Phys. D: Appl. Phys., vol. 51, Article Number 43, 2018.

* The work was performed in the framework of the State task for HCEI SB RAS, project number 13.1.4.

BURSTS OF FAST ELECTRONS GENERATED IN ATMOSPHERIC PRESSURE DISCHARGES BY APPLICATION OF NANOSECOND VOLTAGE PULSES*

N.YU. BABAEVA[1], *G.V. NAIDIS*[1], *V.F. TARASENKO*[2]

[1]*Joint Institute for High Temperatures RAS, Moscow 125412, Russia*
[2]*Institute of High Current Electronics SB RAS, Tomsk 634055, Russia*

In this work, we discuss the results from two-dimensional computational and experimental studies of nanosecond pulsed discharges in air. We analyze the mechanisms of diffuse discharges formation and demonstrate the role of fast electrons in the atmospheric pressure gas breakdown. The discharge is initiated near the cathode having a small radius of curvature and propagates towards the flat anode as shown in Fig. 1. The electric field near such electrodes is amplified resulting in the formation of fast and runaway electrons which ensure the diffuse discharge formation [1-4]. Fast electrons are periodically emitted from the surface of the cathode during ion or photon bombardment. The pulse is of 2 ns duration, 0.2 ns rise and 0.2 ns fall time with a peak voltage -100 kV.

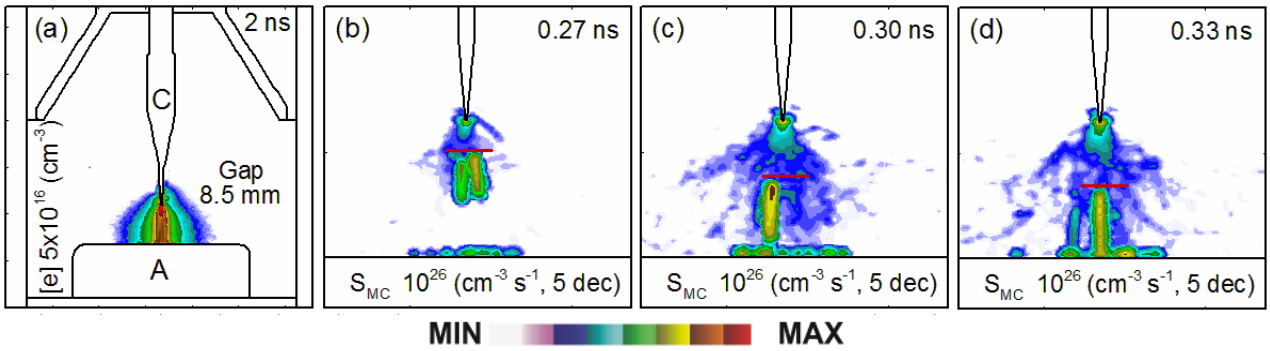

Fig. 1. (a) Geometry of the computational region and the diffuse discharge at the end of the pulse. (b), (c) and (d) Tracks of fast electrons obtained from Monte Carlo simulations. Red lines in each frame indicate the position of the moving streamer front. Fast electron emitted from the cathode are visible in these frames as the blue background. More intense tracks of fast electrons first appear at the front of the streamer after the streamer travels approximately a third of its path.

In our prior studies, we showed that the effect of fast electrons on streamer evolution is similar to that of the photoionization but it is more stochastic by nature. For rather small voltages, we observed one burst of fast electrons. At least two bursts were observed at higher voltages [1, 2]. In this work, we demonstrate that fast electrons can be also produced in the streamer head where the electric field is high enough to further accelerate the electrons and their progenies. The sources of these electrons are shown in Fig. 1(b,c,d) as intensive tracks located below the red lines. These intensive tracks first appear when the streamer crosses approximately 1/3 of the gap. These findings correlate with the results of work [4].

The model, *nonPDPSIM*, used in this paper is a two-dimensional code which is executed on unstructured numerical meshes. In the model, energetic secondary electrons emitted from surfaces are treated by the kinetic Electron Monte Carlo Module. This module integrates the trajectories of the fast electrons. The energies of fast electrons are recorded to compute electron energy distributions (EEDs). From the EEDs, electron impact source functions and sources of secondary electrons are computed.

REFERENCES

[1] N. Yu. Babaeva, Ch. Zhang, J. Qiu, X. Hou, V. F. Tarasenko, Tao Shao, "The role of fast electrons in diffuse discharge formation: Monte Carlo simulation", Plasma Sources Sci. Technol., vol. 26, Article Number 085008, 2017.

[2] N. Yu. Babaeva , G. V. Naidis , D. V. Tereshonok and E. E. Son, "Development of nanosecond discharges in atmospheric pressure air: two competing mechanisms of precursor electrons production", J Phys. D: Appl. Phys., vol. 51, Article Number 434002, 2018.

[3] V. F. Tarasenko, "Runaway electrons in diffuse gas discharges", Plasma Sources Sci. Technol., vol. 29, Article Number 034001, 2020.

[4] D. V. Beloplotov, V. F. Tarasenko, M. I. Lomaev, D. A. Sorokin, "Experimental Determination of the Generation Moment of Runaway Electrons", IEEE Trans.Plasma Sci., vol. 47, 4521 – 4524, 2019.

* The computational work of NB and GN was supported by the Russian Science Foundation under grant No. 20-02-00320. The experimental work was carried out under the state assignment in IHCE (project No. 13.1.4.).

COMPARATIVE CHARACTERISTICS OF THE WORKING MEDIUM OF KIVOTRONS*

P.A. BOKHAN[1], P.P. GUGIN[1], V.A. KIM[1], M.A. LAVRUKHIN[1], D.E. ZAKREVSKY[1,2].

[1] Rzhanov Institute of Semiconductor Physics SB RAS, Novosibirsk, Russia
[2] Novosibirsk State Technical University, Novosibirsk, Russia

A study was made of the switching characteristics of kivotrons - devices based on an “open” discharge with the generation of counterpropagating electron beams. The working media were helium *He*, nitrogen N_2, and oxygen O_2. A study was made of the effective generation of electron beam in the geometry of “open” discharge for these gases at a low working pressure, and it was found that the total emission coefficient $\langle\gamma\rangle$ under the action of fast heavy particles $\langle\gamma\rangle_{He} << \langle\gamma\rangle_{N2} < \langle\gamma\rangle_{O2}$. In the switching mode, the time of the kivotron transition to a highly conducting state $\tau_{s(He)} < \tau_{s(O2)} < \tau_{s(N2)}$, and the discharge development delay time τ_d and, accordingly, the compression ratio $S=\tau_d/\tau_s$ of the pulses are correlated as $\tau_d,S_{(He)} > \tau_d,S_{(O2)} > \tau_d,S_{(N2)}$. Therefore, helium filled kivotrons have much better switching characteristics than N_2 and O_2 filled kivotrons.

The figure shows the dependences of $\tau_s(U)$ for a planar kivotron with a drift space for N_2 (*a*) and for O_2 (*b*). Here, for comparison, the τs value for pure helium in the same cell is given. From these figures it follows that a helium-filled kivotron has much better switching properties than with oxygen: more than 2 times fast switching and more than 3 times a high degree of compression. This advantage of helium is due to the presence of a “dead" phase in the CVC — the incident region — during which the development of the discharge is delayed [1]. It is also seen that an increase in pressure does not lead to a decrease in the switching time in molecular gases, when the main type of emission is emission under the action of heavy particles, in contrast to a discharge in pure helium, where $\tau_s \sim 1/p_{He}$ [2] and photoemission predominates.

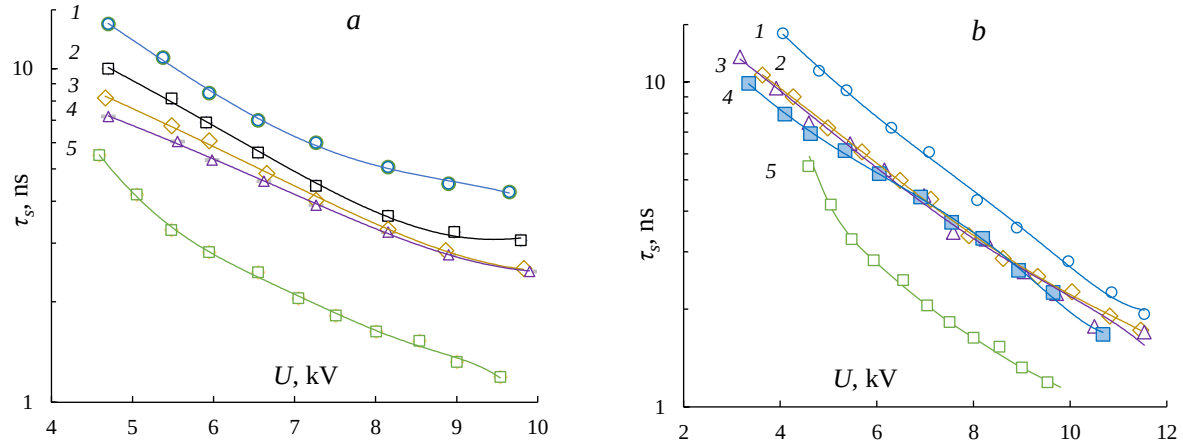

Fig 1 Breakdown time τs versus *U* in N_2 (*a*) and O_2 (*b*)
a p_{N2}=1 (*1*); 1.5 (*2*); 2(*3*) и 2.5 Torr (*4*); p_{He}=14 (*5*)Torr.
b p_{O2}=1 (*1*); 2 (*2*); 2.5 (*3*) и 3 Torr (*4*); p_{He}=14 (*5*)Torr.

Based on the study of the current-voltage characteristics, the mechanisms of electron emission are identified. It is concluded that in helium the main emission mechanism that provides fast switching and a long delay time is photoemission under the influence of resonant photons. In nitrogen and oxygen, emission is dominated by fast molecules and ions.

REFERENCES

[1] P. A. Bokhan, P. P. Gugin, and Dm. E. Zakrevskii, “Specific Features of the *I–V* Characteristics and High-Efficiency Electron-Beam Generation in a Continuous Open Discharge” Technical Physics Letters, V. 44, P. 1092 (2018).

[2] P A Bokhan, PP Gugin, MA Lavrukhin, I V Schweigert, A L Alexandrov and Dm E Zakrevsky “Limit characteristics of switches based on planar open discharge” J. Phys. D: Appl. Phys. V. 51. P.404002 (2018).

* The work was supported by the Russian Science Foundation under grant No. 19-19-00069.

EMISSION OF ELECTRONS FROM COLD CATHODS IN A GAS DISCHARGE AND ITS INFLUENCE ON CURRENT-VOLTAGE CHARACTERISTICS *

P.A. BOKHAN[1], P.P. GUGIN[1], M.A. LAVRUKHIN[1], D.E. ZAKREVSKY[1,2]

[1] Rzhanov Institute of Semiconductor Physics SB RAS, Novosibirsk, Russia
[2] Novosibirsk State Technical University, Novosibirsk, Russia

The mechanisms of electron emission in a gas discharge are still the subject of debate. The author's concept is that emission properties are determined by a modified surface layer of cold cathodes. The modification consists in its saturation with particles of the working gas to a density comparable to the packing density of particles in a liquid working gas. As a result of the modification under the influence of fast heavy particles accelerated in the region of the cathodic potential drop and VUV resonance photons, various emission mechanisms are realized upon discharge in noble gases and molecular gases. In turn, the emission mechanism in light and heavy noble gases also varies.

In helium and neon, fast atoms and ions produce mainly the excitation of embedded atoms. Excited atoms in the Penning process ionize the atoms of the matrix, which leads to the appearance of a fast electron that emits from the cathode (Auger effect). Heavy noble gases with high efficiency produce both excitation with the subsequent Auger effect, and ionization with the release of an electron. For all noble gases, resonant photons absorbed by the surface layer also lead to efficient electron emission. In molecular gases, in particular, in nitrogen and oxygen, the resonance states lie above the dissociation boundary. Therefore, they do not play a noticeable role in a gas discharge.

Differences in the mechanisms of action of noble gases on the surface lead to a qualitative difference in the *I–V* characteristics of the discharge in noble and molecular gases, Fig. 1ab. It can be seen from the figure that in pure helium the current – voltage characteristics at p_{He}<4Torr have a smooth increasing character with an exponent $y\approx3$. In the range p_{He}=6–28 Torr, the character of the *I–V* characteristic changes, showing regions with falling regions. It is characteristic that the absolute value of the current density j at p_{He}=28Torr and *U*=2.4kV is ~ 275 times lower than that calculated for $j=2.5\times10^{-12}p_{He}{}^{x}U^{y}$ [A/cm^2] is the current density, where $x=2$, $y=3$; p_{He}[Torr] - pressure of helium; *U*[V] is the cathodic potential drop [1]. The introduction of molecular impurities completely changes the character of the *I–V* characteristic; in particular, irregularities disappear and the current density sharply increases. The *I–V* characteristics in pure oxygen and nitrogen in the studied range of pressures of ~ 20–200mTorr and voltages from the ignition threshold to *U*=6kV have a smooth increasing character. It is noteworthy that the current in the mixture with helium is 1–2 orders of magnitude higher than in pure molecular gases at the same pressure of the latter.

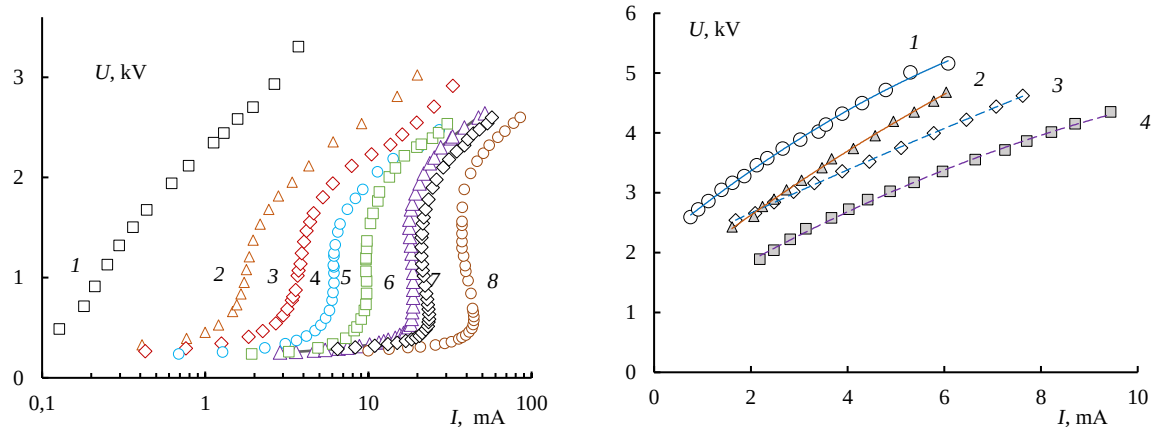

Fig. 1. (*a*) CVCs of continuous (1–8) discharges in *He* at p_{He}=(*1*) 4, (*2*) 6, (*3*) 8, (*4*) 10, (*5*) 12.5, (*6*) 16, (*7*) 20, and (8) 28 Torr; (*b*) CVCs of continuous discharges in O_2 (*1,2*) and N_2 (*3,4*) at p_{O2}=(1) 73 and (2) 110 mTorr and p_{N2}=(3) 73 and (4) 115 mTorr.

1. K. A. Klimenko and Yu. D. Korolev, Sov. Phys. Tech.Phys. V.35, P.1084 (1990).

* The work was supported by the Russian Science Foundation under grant No. 19-19-00069.

INVESTIGATION OF THE CHARACTERISTICS AND MECHANISM OF SUBNANOSECOND SWITCHING OF A NEW TYPE OF PLASMAS SWITCHES – THE KIVOTRON AND EPTRON*

P.A. BOKHAN[1], I.V. SCHWEIGERT[2], D.E. ZAKREVSKY[1]

[1] Rzhanov Institute of Semiconductor Physics SB RAS, Novosibirsk, Russia
[2] Khristianovich Institute of Theoretical and Applied Mechanics, Novosibirsk, Russia

In the report is summarized the study of the characteristics and switching mechanism of two types of switchers based on an open discharge and its combination with a capillary discharge. In the first version of the key - the kivotron, the discharge is carried out under the conditions of generation of counter propagating electron beams *EB* in coaxial or planar geometry with a high electric field strength much stronger than Dreicer criterion for electron runaway $(E/p)>>(E/p)_{cr}$. In this case, when using helium as a working medium, firstly, atoms are effectively excited into the resonance state by fast particles. Secondly, due to the Doppler effect, resonant photons without imprisonment reach the cathode surface, maintaining the discharge current due to photoemission. Thirdly, fast heavy particles modify the cathode surface, thereby significantly (up to an order of magnitude) increasing the photoemission coefficient. The combination of these processes leads to an increase in the switching rate with an increase in the operating voltage U and helium pressure p_{He}. At U>20kV and p_{He}>10Torr, the switching time becomes less than 100ps both in the experiment and according to the simulation. It is preferable to use planar geometry without a drift space as a switching device, in which, on the one hand, the most complete use of *EB* energy is realized in creating a plasma with a high charge density, on the other hand, a small wave impedance of the switch is realized. As a result, currents of tens of kiloamperes are achieved at voltages up to 100kV. In an interpulse period plasma in the discharge gaps fastly recombinates. As a result, switchers can operate up to pulse repetition rate 100kHz.

In the second version of the switcher - the eptron, the kivotron acts as a plasma cathode, ensuring the flow of current during the switching period. Fast switching is carried out due to the discharge in the capillary structure integrated with the kivotron into a single device. The main advantages of a discharge in a capillary are due to different mechanisms of charge death at different plasma densities. At a low density $(10^{10}$-$10^{11})$ cm^{-3}, free passage of electrons to the walls of the capillary occurs, due to which a large delay in the development of the discharge is realized. At a high plasma density, due to Debye screening, a rapid accumulation of charges occurs and fast switching occurs. Under optimal conditions corresponding to the maximum value of the Townsend multiplication coefficient, a switching time of ~ 100ps is achieved.

The comparative characteristics of the kivotron and eptron due to different mechanisms of subnanosecond switching are considered. The kivotron has a much lower inductance, which allows to receive currents of tens of kiloamperes. Eptron operates more efficiently with a small characteristic size of the capillary, preferably a few tens of millimeters square. As a result, plasma recombination in the conductive layer in the eptron in the interpulse interval is much faster than in the kivotron. That allows operating at frequencies above 100kHz and the operating voltage of tens of kilovolts. However, the subnanosecond switching time in the eptron is realized at currents up to ~ 1kA. Together, the kivotron and eptron provide new opportunities for generating pulses with a subnanosecond rise front.

* The work was supported by the Russian Science Foundation under grant No. 19-19-00069.

STREAMER VELOCITY AT THE BREAKDOWN OF AN AIR GAP WITH A SHARPLY INHOMOGENEOUS DISTRIBUTION OF ELECTRIC FIELD STRENGTH*

V.F. TARASENKO[1], G.V. NAIDIS[2], D.V. BELOPLOTOV[1], D.A. SOROKIN[1], M.I. LOMAEV[1], N.YU. BABAEVA[2]

[1]Institute of High Current Electronics SB RAS, Tomsk, Russia
[2]Joint Institute for High Temperatures, Russian Academy of Sciences, Moscow, Russia

In recent years, studies of high-voltage nanosecond discharges in gaps with an inhomogeneous electric field strength distribution filled with atmospheric pressure gases have become extremely topical (see [1] and references there). This type of discharge is ignited and burns in diffuse (volume) form, i.e. a non-equilibrium low-temperature plasma is formed, which is in demand for solving a wide variety of problems in various fields [2]. In this regard, it is important to know the physical processes occurring at the stage of ignition of the discharge. This should be useful from the point of view of choosing the optimal conditions for obtaining a plasma object with the necessary characteristics.

Previously, it was found that, at a point-plane gap discharge in the atmospheric pressure air, a streamer with large transverse dimensions (up to 8 cm) arises near the pointed high-voltage electrode and moves to the grounded plate until the gap being bridged [3, 4]. However, there are few works where the streamer velocity along the gap obtained experimentally and computationally are compared.

The work is deal with results of the experimental, theoretical and computational studies on the velocity of a streamer that occurs at the breakdown stage of a nanosecond discharge in the 8.5-mm-length needle-plane gap filled with atmospheric-pressure air and fed by ±15-kV voltage pulses of nanosecond duration. The influence of the amplitude of the voltage pulse on the parameters of the formed streamers is considered.

It was established that the streamer velocity significantly varies during its motion along the gap (Fig. 1). Under the conditions of this work, the velocity of the negative streamer was higher than that of the positive one. In the calculations, it was shown that this is due to the action of runaway electrons moving from the cathode with a small radius of curvature and preionizing the gas in front of the streamer. The highest streamer velocity is registered near the needle in the region of the high electric field and near the planar electrode. As the streamer moves away from the needle electrode and as the dimensions of the streamer head increase, the velocity of the streamer significantly decreases due to the decrease in the electric field in the gap. As the amplitude of the voltage pulse decreases or/and as its duration decreases, the streamer can stop in the gap, and at low voltages or/and short duration the streamer has no time to form. The increase in the streamer velocity near the planar electrode is caused by a repeated increase in the electric field. As the streamer approaches the planar electrode and under large amplitudes of the voltage pulse, its ball shape is retained, and as the voltage decreases, the streamer's diameter near the planar electrode decreases and the streamer takes the cylindrical shape.

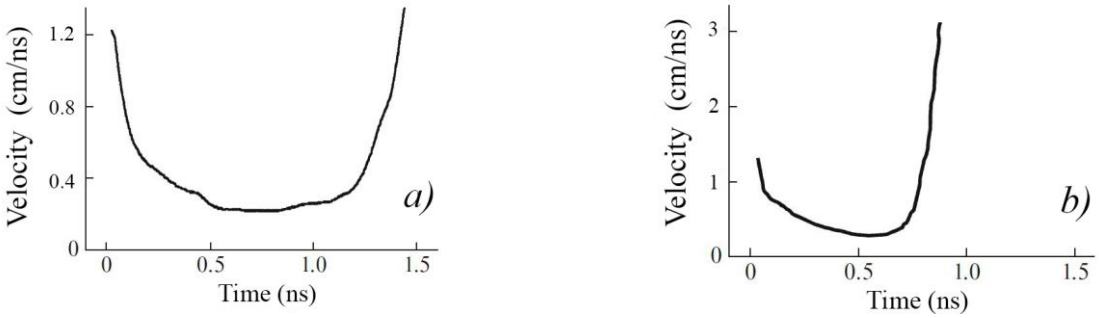

Fig. 1. Streamer velocity at positive (*a*) and negative (*b*) polarities. Air, 100 kPa. Needle-plane gap. Interelectrode distance is 8.5 mm.

REFERENCES

[1] *V.F. Tarasenko (ed.)*. Runaway Electrons Preionized Diffuse Discharges. – Nova Science Publishers, Inc., 2014.

[2] *Paul K. Chu and Xin Pei Lu (eds.)*. Low temperature plasma technology: Methods and applications. – CRC Press, 2013.

[3] *D.V. Beloplotov V.F. Tarasenko, D.A. Sorokin, and M.I. Lomaev*. // JETP Lett. – 2017. – Vol. 106. – Is. 10. – P. 653–658.

[4] *V.F. Tarasenko, G.V. Naidis, D.V. Beloplotov, I.D. Kostyrya, and N.Yu. Babaeva* // Plasma Phys. Rep. – 2018. – Vol. 44. – Is. 8. – P 746–753.

* The work was supported by the Russian Foundation for Basic Research under grants Nos. 18-32-00103 and 17-52-16002.

SPARK DISCHARGE IN ATMOSPHERIC-PRESSURE AIR AND BEAD STRUCTURE OF ITS CHANNEL*

D.V. BELOPLOTOV, V.F. TARASENKO, D.A. SOROKIN, A.G. BURACHENKO, E.KH. BAKSHT

Institute of High Current Electronics SB RAS, Tomsk, Russia

Scientists constantly make attempts to reproduce atmospheric phenomena, in particular electric discharges, in laboratory conditions. One of the most interesting and close to humans is lightning. A huge number of papers are devoted to the study of this phenomenon, which are devoted both to the physics of processes in lightning and to issues of lightning protection. There are several types of lightning, among which there are very rare and studied very poorly, such as bead lightning [1]. Although some researchers even deny the existence of such a lightning, in recent years a number of works have been carried out to study bead lightning in close to natural conditions [2], and the appearance of a bead structure in laboratory spark discharges has also been reported [3–5].

The results of studies on conditions for the formation of the bead structure during spark discharges in a point-to-plane gap (up to 45 mm) filled with atmospheric-pressure air and fed by voltage pulses of both polarities with a rise time from hundreds of nanoseconds to several microseconds and an amplitude of tens-hundreds of kilovolts are presented. The stages of the formation of the spark channel were recorded with a four-channel ICCD camera.

Under these conditions, spark channels consisting of alternating bright and dim regions (bead structure) were observed (Fig. 1). It was observed that the formation of the spark channel begins from the region of the electrode spot, which is characterized by a high concentration of ions and electrons as well as a high temperature. However, it should be noted that after the breakdown, the discharge in the gap with a sharply inhomogeneous distribution of the electric field strength is ignited in diffuse form, and then passes into the spark phase. The channel is formed non-uniform in length. It was established that when limiting the current through the gap, an increase in the rise time and the gap length do not affect the formation of the bead structure. It was found that an increase in the amplitude of the voltage pulse leads to an increase in the length of beads. The appearance of the bead structure is more likely at negative polarity of the pointed electrode.

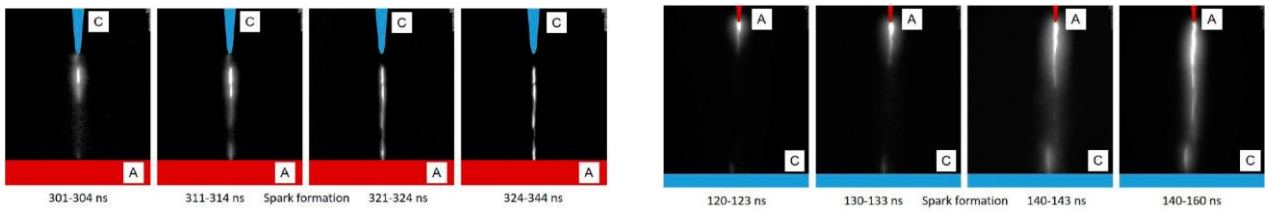

Fig. 1. The process of the spark formation in atmospheric-pressure air recorded with a four-channel ICCD camera. *a*) Negative polarity of a voltage pulse, high-voltage pointed cathode (needle). *b*) Positive polarity of a voltage pulse, high-voltage pointed anode (needle). d = 8.5 mm. U_0 = 18 kV. *3, 4* – bead structure expression.

REFERENCES

[1] *V. Cooray*. An Introduction to Lightning. – Springer Netherlands, 2015.

[2] *G.O. Ludwig, M.M.F. Saba* // Physics of Plasmas. – 2015. – Vol. 12. – Is. 9. – 093509 (15 pp).

[3] *S.P.A.Vayanganie, V. Cooray, M. Rahman, et al.* // Phys. Lett. A. – 2016. – Vol. 380. – Is. 7–8. – P. 816–821.

[4] *D.V. Beloplotov,V.F. Tarasenko* // Phys. Lett. A. – 2019. – Vol. 383. – Is. 4. – P. 351–357.

[5] *D.V. Beloplotov,A.M. Boichenko, V.F. Tarasenko* // Plasma Physics Reports. – 2019. – Vol. 45. – Is. 4. – P 387–396.

* The work was performed in the framework of the State Task for IHCE SB RAS, # 13.1.4.

RESEARCH OF THE RADIATION SPECTRA OF MATERIAL OF ELECTRODES IN A PULSED DISCHARGE IN HELIUM OF ATMOSPHERIC PRESSURE[1]

V.S. KURBANISMAILOV[1], S.A. MAIOROV[2,3], O.A. OMAROV[1], G.B. RAGIMKHANOV[1], D.V. TERESHONOK[3], Z.R. KHALIKOVA[1]

[1]Dagestan State University, str. M. Gadjieva 43a, Makhachkala, 367000, Russia, E-mail: gb-r@mail.ru
[2]A.M. Prokhorov General Physics Institute of the Russian Academy of Sciences, Vavilova Str. 38, Moscow, 119991, Russia
[3]Joint Institute for High Temperatures of the Russian Academy of Sciences, IzhorskayStr.13, Moscow,125412 Russia

The paper presents the results of an experimental study of a pulsed discharge in atmospheric pressure helium. The experimental setup is similar to that described previously in [1,2]. The discharge under study was created between iron electrodes 4 cm in diameter made of stainless steel, spaced d = 1 cm apart. Electrodes with a diameter of 4 cm were used in various shapes and materials: flat and hemispherical (R = 30 cm) aluminum electrodes, flat steel (the cathode is solid, the anode is mesh).

The studied gap was irradiated by a spark discharge through a mesh anode or by the location of a UV source in the same gas - at a distance of 5-7 cm from the axis of the main gap. The UV radiation of the auxiliary discharge, in which an energy of ≈0.3-0.4 J was invested, created an initial electron concentration $n_0 \approx 10^8$ см$^{-3}$in He. The emission spectrum of the near-cathode plasma was recorded by a diffraction grating monochromator (MDPS-3) with a dispersion of 0.2–0.3 nm/mm. To identify the brightest spectral lines excited in the discharge, the panoramic spectrum was recorded using the automated complex MS-3504i monochromator-spectrograph.

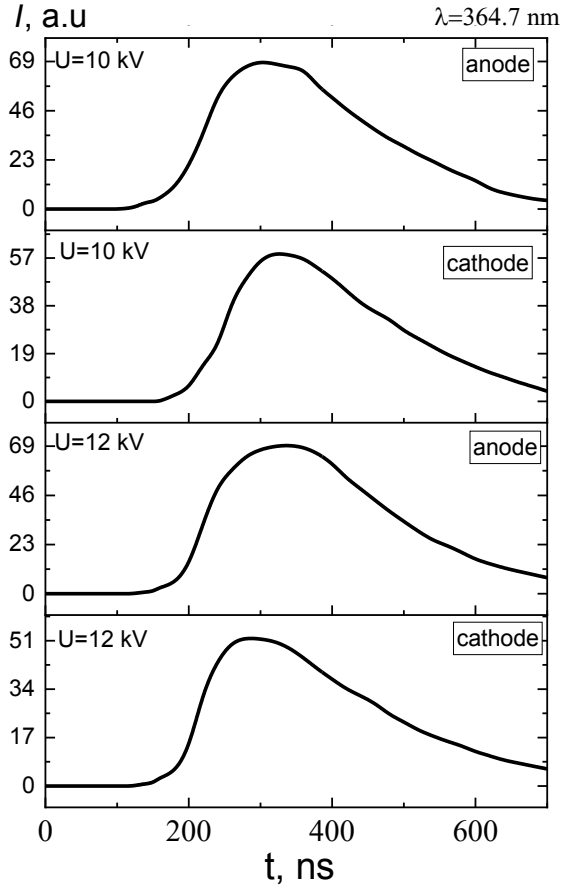

Fig. 1. Typical time dependences of the intensity of the spectral line of Fe from the cathode and anode regions of the charge at fields of 10 and 12 kV.

In this work, we carried out studies to study the patterns of the formation of the optical radiation spectrum of a self-sustained volume discharge in helium at various energy depositions in the discharge (in the mode of uniform combustion, OR with cathode spots and diffuse channels attached to them, a contracted discharge, and SDR). It should be noted that, along with the lines of the gas under investigation (He), the lines of the electrode material (Fe, Al) are also excited in the discharge spectrum. With an increase in the energy input into the discharge, both the relative intensity of the spectral lines increases, and new spectral lines of the gas (He) under study and the material of the electrode material (Fe, Al) are excited in the discharge. The emission lines of metal vapors are recorded both from the surface of the cathode and from the surface of the anode (Fig. 1.). Moreover, the intensity of the lines from the anode weakly depends on the amplitude of the applied field. The results of the study show that the emission spectrum of the lines of the material of the electrodes is also formed at low energy inputs, when the discharge gap is a column of a uniform plasma. This suggests that the vapor line of the electrode material is formed not only during explosive processes at the cathode, but also during emission or erosion of the electrodes. Monte Carlo methods have been used to calculate the ionization-drift characteristics of electrons in helium in the presence of small metal impurities.

References

[1] *Kurbanishmailov V.S., Omarov O.A., Ragimkhanov G.B. et.al. .//*Plasma physics reports. - 2016. - Vol. 42. - № 7. - P. 687-698.

[1]The reported study was funded by RFBR according to the research project № 19-08-00333a.

PULSED DISCHARGE IN ARGON IN AN EXTERNAL MAGNETIC FIELD UNDER THE CONDITIONS OF ATOMIZATION OF THE MATERIAL OF THE ELECTRODE SUBSTANCE[1]

V.S. KURBANISMAILOV[1], S.A. MAIOROV[2,3], O.A. OMAROV[1], P.KH.OMAROVA[1], G.B. RAGIMKHANOV[1], Z.R. KHALIKOVA[1,2]

[1]Dagestan State University, str. M. Gadjieva 43a, Makhachkala, 367000, Russia, E-mail: gb-r@mail.ru
[2]A.M. Prokhorov General Physics Institute of the Russian Academy of Sciences, Vavilova Str. 38, Moscow, 119991, Russia
[3]Joint Institute for High Temperatures of the Russian Academy of Sciences, Izhorskay Str.13, Moscow,125412 Russia

The study of the space-time dynamics of a pulsed discharge formation in atmospheric pressure argon in centimeter inter electrode gaps (with an initial electron concentration in the interval n_0 ~10^7cm^{-3} and insignificant over voltages *W*~ (10-100%) show that during the formation of a discharge, the first recorded luminescence occurs on anode, which propagates to the cathode at a velocity of ≈ 2-5·10^7 cm/s [1]. As the emission front moves toward the cathode, the electron concentration in it increases and reaches values of ~10^{13}-10^{14} cm^{-3}.

At this stage, the discharge current has a value of 1-10 A. The overlapping of the discharge gap by the ionization front leads to the formation of a cathode spot and a spark channel (see Fig. 1, frame 4). The temperature of the cathode flare, estimated from the relative intensity of the spectral lines of argon in 30-40 ns, is 4-5 eV. The temperature of the electrons of the diffuse channel, tied to the cathode spot, is ~ 1-2 eV. After 30-40 ns, the cathode flare begins to stretch over the external field and assumes the shape of an elongated ellipse, and a spark channel sprouts from the cathode spot deep into the gap.

We have carried out investigations of the emission spectra from the near-cathode plasma of the discharge in atmospheric pressure argon. It has been established that with the formation of a cathode spot, the spectrum of the near-cathode plasma is characterized by intense lines of the cathode material *AlII* 396.1 nm, 394.4 nm, 280.1 nm, 281.6 nm with high excitation potentials and an intense continuum in the 260-360 nm range. The lines of aluminum ions are recorded simultaneously with the onset of a sharp current increase and reach a maximum value in 20-30 ns. After 30 ns from the onset of sharp current growth, the Stark half-width of the 480.6 nm argon line is 0.5-0.6 nm, and the line 422.8 nm ≈ 0.5 nm. These half-widths correspond to an electron density of ~ 10^{19} cm^{-3}, and after 20 ns the concentration decreases to a value of 2·10^{18} cm^{-3}.

The effect of a longitudinal magnetic field on the emission spectra of a cathode plasma of a discharge is investigated. It is established that with an increase in the strength of the magnetic field the maximum radiation energy shifted to the short-wave region of the spectrum: at H = 0, λ_{max} = 420 nm, at H = 140 kOe - 400 nm, at H = 200 kOe - 380 nm. Thus, in the magnetic field the intensity of continuous radiation increases, the brightness of the ion lines in the ultraviolet region also increases: *ArII* 280.6 nm, *ArIV* 280.9 nm and lines of the electrode material *Al*-280.1 nm, 281.6 nm.

At the stage of slow channel expansion, i.e. from the moment t = 500 ns, the intensity of continuous radiation decreases, the intensity of ionic lines also decreases, while the brightness of the lines of neutral argon is 394.89 nm, 392.9 nm and aluminum lines *AlI* - 302.9 nm, 308.2 nm; *AlII* - 281.6 nm, 280.1 nm increases. In the longitudinal magnetic field, from the moment t = 700 ns, the emission of *ArI* lines 394.89 nm strongly increases; *ArII* 280.6 nm; *ArIV* 280.9 nm and aluminum 281.6 nm; 280.1 nm; 309.27 nm and 308.216 nm, while the intensity of the lines in the visible range of the spectrum decreases with increasing magnetic field strength.

The electron drift characteristics in argon with aluminum vapor were calculated and analyzed at an electric field strength E / N = 1–100 Td taking into account inelastic collisions. The effect of the percentage of aluminum atoms in argon on the kinetic characteristics was studied, both in the longitudinal and transverse to the electric field magnetic field with H = 0-400 kOe.

REFERENCES

[1] *Kurbanismailov V.S., Omarov O.A., Ragimkhanov G.B.et al. //*Plasma physics reports. - 2016. - Vol. 42. - № 7. - P. 687-698.

[1]This work was supported by the Russian Foundation for Basic Research, project № 19-08-00611a.

CHERENKOV RADIATION AND CATHODOLUMINESCENCE IN DIFFERENT SPECIMENS UNDER THE EXCITATION OF ELECTRON BEAMS *

V.F. TARASENKO, E.KH. BAKSHT, M.V. EROFEEV, V.I. OLESHKO

Institute of High Current Electronics SB RAS, Tomsk, 634055, Russia
E-mail: VFT@loi.hcei.tsc.ru, phone: +7 (3822) 491-685

In recent years, great attention has been paid to the study of the generation and measurements of runaway electrons (RAEs) under different conditions. The largest number of publications are devoted to studies of RAEs in tokamaks; RAEs damage the internal walls of the vacuum vessel and prevent plasma heating. Various sensors and collectors are used for measuring RAEs. In different accelerators, direct measuring of electron beam current parameters is performed using collectors. Collectors with a small receiving area have the highest temporal resolution. Using such collectors, RAE beam current pulses with the duration of up to 20 ps were recorded in an accelerator with a gas diode. In tokamaks, collectors are not used yet. However, Cherenkov-type detectors (CTD) were developed for registration of RAEs. When RAEs pass through the receiving part of CTD, Cherenkov radiation (CR) is generated there. The receiving part is made of diamond and coated with metal films of various thickness to protect the CTD from plasma radiation. CR is recorded with a photomultiplier tube (PMT) situated outside the vacuum chamber. Quartz optic fibers are applied for transmitting CR to the PMT. However, besides CR, cathodoluminescence (CL) may occur in diamonds. In the works known to us, comparisons of the parameters of these types of radiation were not performed. The main objective of this paper is to study the spectral and amplitude-time characteristics of the radiation of diamond specimens grown by different methods, sapphire, MgF_2 and KU-1 quartz, which is transparent up to 160 nm and to find the most suitable specimen. The specimens were excited by nanosecond and subnanosecond electron beams with different electron energies. Figure 1 shows a schematic of the experimental setup used.

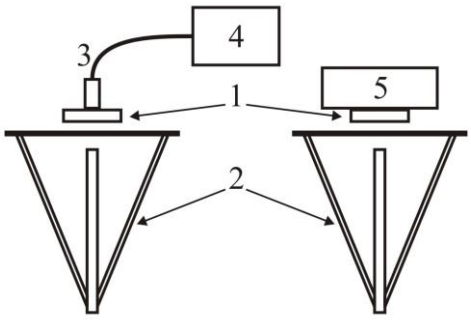

Fig. 1. Experimental setup: 1 – specimen, 2 – gas or vacuum diode, 3 – optical fiber, 4 – spectrometer, 5 – high-speed photodiode.

Data on the spectral and amplitude-time characteristics of the radiation of different specimens of diamonds, sapphire, MgF_2 and KU-1 quartz excited by nanosecond and subnanosecond electron beams were obtained. CR was observed in synthetic diamonds of IIa type, sapphire, MgF_2 and KU-1 quartz using a spectrometer. It was found that in sapphire and KU-1 quartz, the spectral region suitable for recording CR covers a wider spectral range than in diamond. CL in diamonds, sapphire, MgF_2 and KU-1 quartz was observed too. These data are consistent with our results obtained previously [1-5].

REFERENCES

[1] D. A. Sorokin, A. G. Burachenko, D. V. Beloplotov, V. F. Tarasenko, E. Kh. Baksht, E. I. Lipatov, M. I. Lomaev, "Luminescence of crystals excited by a runaway electron beam and by excilamp radiation with a peak wavelength of 222 nm," Journal of Applied Physics, vol. 122, no. 15, pp. 154902, 2017.

[2] V. F. Tarasenko, M. I. Lomaev, E. Kh. Baksht, D. V. Beloplotov, A. G. Burachenko, D. A. Sorokin, E. I. Lipatov, "Spectral and amplitude-time characteristics of crystals excited by a runaway electron beam," Matter and Radiation at Extremes, vol. 4, no. 3, pp. 037401, 2019.

[3] V. F. Tarasenko, V. I. Oleshko, M. V. Erofeev, E. I. Lipatov, D. V. Beloplotov, M. I. Lomaev, A. G. Burachenko, Baksht, E. Kh. "Emission of diamonds, leucosapphire, and KU-1 quartz in the range of 200–800 nm excited by electron beams with a pulse duration of 0.5 and 12 ns," Journal of Applied Physics, vol. 125, no. 24, pp. 244501, 2019.

* Russian Science Foundation supported this work according to the research project No. 18-19-00184.

NANOSECOND ELECTRON ACCELERATOR WITH A DOUBLE FORMING LINE, NON-UNIFORM TRANSMISSION LINE, AND A GAS-FILLED DIODE*

E.KH. BAKSHT, V.F. TARASENKO, S.B. ALEKSEEV, A.G. BURACHENKO, M.I. LOMAEV

Institute of High Current Electronics SB RAS, Tomsk, 634055, Russia

Electron accelerators are used in various fields of science and technology and improved constantly. E-beams are usually formed in vacuum diodes, and thin foil anodes are used in most accelerators to output the e-beam into air and other gases.

The paper presents the design and parameters of a nanosecond electron accelerator based on a gas-filled diode and additional transmission line with variable impedance. E-beam parameters can be controlled by the air pressure in the diode. The e-beam current amplitude of ~700 A with a pulse duration 1.3 ns (FWHM) and the electron energy up to 350 keV were obtained behind the anode foil. At atmospheric air pressure, the beam current amplitude was 1.3 A.

The accelerator was used to irradiate various transparent dielectric samples. Cherenkov radiation was recorded in quartz, sapphire, and synthetic diamond.

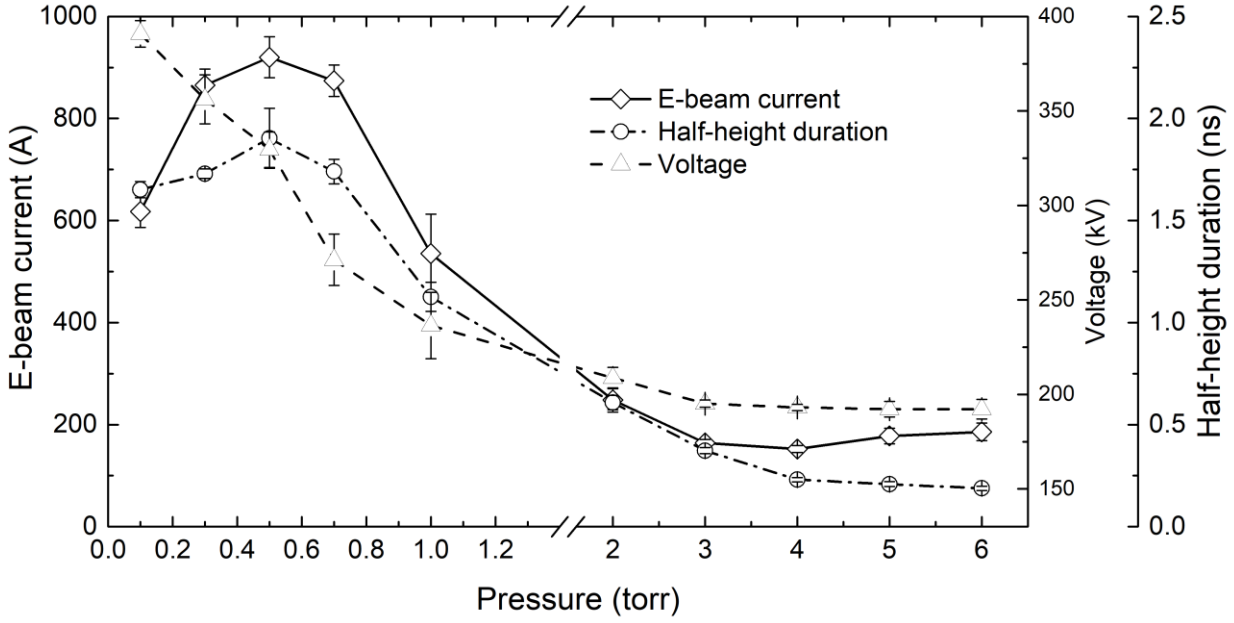

Fig.1. Voltage pulse amplitude versus the diode, the amplitude, and the duration of the beam current behind the anode foil at the air pressure. The interelectrode gap is 11. 5 mm.

* The work was supported by the grant from the Russian Science Foundation, project # 18-19-00184.

CHERENKOV RADIATION IN THE VISIBLE AND UV SPECTRAL REGIONS FROM A QUARTZ PLATE IRRADIATED BY A 6-MEV ELECTRONS*

E.KH. BAKSHT[1], A. V. VUKOLOV[2], M. V. EROFEEV[1], G. A. NAUMENKO[2], A. P. POTYLITSYN[2], V. F. TARASENKO[1], A. G. BURACHENKO[1], AND M. V. SHEVELEV[2]

[1]Institute of High Current Electronics SB RAS, Tomsk, 634055, Russia
[2]National Research Tomsk Polytechnic University, Tomsk, 634050 Russia

Cherenkov radiation and pulsed cathodoluminescence spectra in the ultraviolet, visible, and near infrared regions generated by a 6-MeV electron beam passing through GE-014 and KU-1 quartz plates have been experimentally studied. The Cherenkov radiation spectrum has been recorded in the ultraviolet and visible regions and its change is shown at the variation of the angle between the plane of the plate and the direction of the electron beam. The data on the conditions of recording of the Cherenkov radiation spectra at the excitation of plane-parallel plates of quartz, sapphire, and diamond have been presented. It has been shown that the total internal reflection in the crystals with a high refractive index imposes certain conditions on the geometry of the output of Cherenkov radiation into vacuum at electron energies above 500 keV.

* The work was supported by the grant from the Russian Science Foundation, project # 18-19-00184.

STUDY OF THE DYNAMICS OF SUBNANOSECOND DISCHARGE DEVELOPING IN NITROGEN AT A PRESSURE OF 6 ATMOSPHERES WITH THE PARTICIPATION OF RUNAWAY ELECTRONS[1]

S.N. IVANOV[*], *V.V. LISENKOV*[*,**], *YU.I. MAMONTOV**

**Institute of Electrophysics, Amundsena Str. 106, Ekaterinburg, 620016, Russia, E-mail: stivan@iep.uran.ru, phone:+7(343)2678776.*
***Ural Federal University, Mira St. 19, Ekaterinburg, 620083, Russia*

The dynamics of the development of a subnanosecond discharge in nitrogen at a pressure of 6 atm was studied experimentally and numerically. In this experiment, the anode had a hemispherical shape with a radius of 1 cm. The cathode consisted of a hemispherical base with a radius of 1 cm into which the cylinder with a length of 3 mm and a radius of tip curvature of 1 mm was screwed. The length of the cathode-anode gap was 5 mm. The breakdown occurred at the end of front of voltage pulse with amplitude of 140 kV, which was applied to the discharge gap. The average value of the reduced electric field at the beginning of the breakdown (the upper limit) was 43 V/(cm Torr). In the cathode region, it was 206 V/(cm Torr). That is, the magnitude of the electric field substantially lower than that required by the electron runaway criterion [1-3]. Integral and streak photos of the discharge glow were obtained. It is seen that at the beginning, the gap was bridged by plasma column, which turned into a spark later. The diameter of the spark is approximately 2 mm, which is slightly wider than a typical channel diameter in the streamer breakdown (0.1-1 mm) [4]. The development of the plasma column at the initial stage of discharge formation could be initiated by runaway electrons, which, as shown in [5], can be generated in areas of electric field amplification at pressures up to 40 atm, when the middle electric field in the gap is significantly lower than the required by the runaway criterion [1-3]. As shown in [6], the runaway criterion can realize in area near of micro-tip on a cathode surface at a pressure up to 10 atm. At the same time, the drop in the potential in the region of the amplified field near micro-tip allows the electron to gain energy sufficient to continue of runaway mode in a weak average field, from the point of view of the runaway criterion. Using a 3D model, we performed a numerical simulation of transition into runaway mode of an electron emitted from the top of the micro-tip at the cathode at the initial stage of the discharge development. The Monte Carlo method was used for modeling. As a result, the spatial distribution of the concentration of slow (plasma) electrons in the discharge gap, which occur when the gas is ionized by runaway electrons, was calculated. These electrons are the initiation points for the development of a multi-avalanche discharge. Multiplication of these electrons via ionization leads to the formation of a plasma column at the initial stage of the discharge development. Further development of the spark channel occurs.

REFERENCES

[1] Yu.D. Korolev and G.A. Mesyats, Physics of Pulsed Breakdown in Gases, Yekaterinburg, UrB of RAS, 1991.

[2] L.P. Babich, High-energy Phenomena in Electric Discharges in Dense Gases. Theory, Experiment and Natural Phenomena. ISTC Science and Technology Series. Volume 2, Arlington, Virginia, Futurepast, 2003.

[3] V.F. Tarasenko, D.F. Beloplotov, and M.I. Lomaev, "Dynamics of ionization processes in high-pressure nitrogen, air, and SF6 during a subnanosecond breakdown initiated by runaway electrons," Plasma Physics Reports, vol.41, No.10, pp. 832–846, 2015.

[4] H. Raether, Electron Avalanches and Breakdown in Gases, London, Butterworths, 1964.

[5] S.N. Ivanov, "The Transition of Electrons to Continuous Acceleration Mode at Subnanosecond Pulsed Electric Breakdown in High-Pressure Gases," Journal of Physics D: Applied Physics, vol.46, No.28, Article Number 285201, 2013.

[6] N.M. Zubarev and S.N. Ivanov, "Mechanism of Runaway Electron Generation at Gas Pressures from a Few Atmospheres to Several Tens of Atmospheres," Plasma Physics Reports, vol.44, No.4, pp. 445–452, 2018.

[1] The work was supported by the Russian Science Foundation under grant No. 20-08-00172.

PULSE SOURCE OF ELECTRONS BASED ON THE PYROEFECT*

L. N. ORLIKOV, K. M. MAMBETOWA, S.I ARESTOV, S. M. SHANDAROV

Tomsk State University of Control systems and Radioelectronics, 40 Lenina Prospect, Tomsk, Russia

The conditions of electron flow generation during heating and cooling of a cylindrical lithium niobate crystal with a diameter of 13 mm and a height of 7 mm with a Z-oriented axis of polarization were studied. Studies were conducted at a pressure of 105-1 Pa. Current pulses were observed at temperature points 290, 311, 329, 367, 371, 373, 378, 379, 380 K.

Figure 1 shows the oscillograms of the discharge current when the crystal is heated to 320 K (47 ° C).

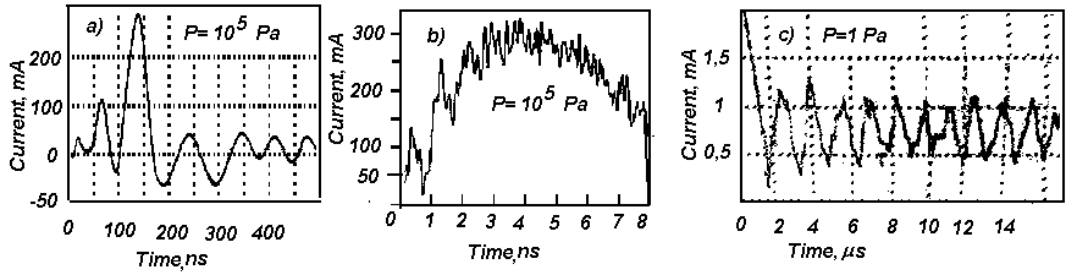

Fig.1. Oscillograms current during heating of the crystal

The discharge mechanism explained based on a barrier discharge with the effect of runaway electrons [1]. The discharge begins to form in the nanosecond range. (Fig. 1 a). The duration of the first half-cycle of the discharge current pulse from the crystal surface is 5–10 ns, with current amplitude of 300–400 mA. (Fig. 1 b). The final stage discharge represented by current fluctuations at frequencies of 50-500 kHz and gas breakdowns along the crystal surface. (Fig. 1 c). The breakdowns explained by the appearance of local regions of electric field strength due to the repolarization of the domains during heating of the crystal.

The preparation of the crystal and the coordination of the indication system made it possible to develop a portable source of electrons on the pyroelectric effect. The source provides a discharge voltage of up to 100 kV at a discharge current of 400 mA nanosecond duration.

REFERENCES

[1] V. F. Tarasenko, I. D. Kostyrya, and D. V. Rybka, “Breakdown in atmospheric pressure air at nanosecond voltage pulses due to runaway electrons,” Opt. Atmosf. Okeana 25 (1), 103–108 (2012)

.

* This work was supported by the State Assignthent of the Ministry of Education the Russian Federation (within the tasks N 3. 8898.2017/8.9) and RFFI (grant 16-29-14046-ofi_m).

FORMATION OF THE SECONDARY RUNAWAY ELECTRON FLOW IN AN ELONGATED ATMOSPHERIC GAP*

N.M. ZUBAREV, A.G. SADYKOVA, K.A. SHARYPOV, V.G. SHPAK, S.A. SHUNAILOV, M.I. YALANDIN

Institute of Electrophysics of UB RAS, Yekaterinburg 620016, Russia

In the experiment described in Ref. [1], where a negative high-voltage pulse with a subnanosecond front was applied to the cathode of an atmospheric pressure elongated air gap with a sharply inhomogeneous electric field (hereinafter "field"), a pronounced burst of fast electron current was observed at the anode with the delay relative to the primary picosecond runaway electron flow (REF1). Similar effects were noted in a number of other experiments (see, e.g., Refs. [2-4]) and in the calculations [5]. In Ref. [2], based on an analysis of the energy of delayed flux in an elongated gap $D \approx 20$ mm, it was established that this flux also represents runaway electrons (REF2). Regarding the nature of REF2, the assumption has been made that REF2 is generated as the result of impact ionization of molecules by particles of REF1 throughout the gap D.

In this communication, the dependence of the REF2 delay on the gap length and on the field strength averaged over the gap is reported and analyzed. The field strength was determined by the amplitude of the voltage pulse applied to the cathode (up to -250 kV in a traveling wave). For a fixed gap distance of 20 mm, it was found that the higher the energy of REF1 (i.e., the electrons emission voltage at the pulse front), the lesser the delay of REF2 with respect to REF1. On the contrary, with an increase in the gap distance at a constant voltage at the cathode, this delay increases. Data on the characteristics of REF2 were also obtained in the mode of the ionization wave (expanding cathode plasma) cutoff by an intermediate floating-potential foil electrode which was partially transparent to REF1. In this case, the generation of REF2 in the gap between the intermediate electrode and the anode occurs in the field with other parameters and dynamics than in the two-electrode system. As a result, the registered delay of REF2 relative to REF1 was reduced in comparison with the two-electrode system. A similar effect of early registration of secondary REF at the anode was observed in the case where it was initiated in the second part of the gap by photoionization of the gas by bremsstrahlung of primary REF from an intermediate non-transparent for electrons electrode made of a tantalum foil.

REFERENCES

[1] A.V. Gurevich, G.A. Mesyats, K.P. Zybin A.G. Reutova, V.G. Shpak, S.A. Shunailov, and M.I. Yalandin, "Laboratory demonstration of runaway electron breakdown of air," Phys. Lett. A, vol. 375, no. 30-31, pp. 2845–2849, July 2011.

[2] A.V. Gurevich, G.A. Mesyats, K.P. Zybin, M.I. Yalandin, A.G. Reutova, V.G. Shpak, and S.A. Shunailov, "Observation of the Avalanche of Runaway Electrons in Air in a Strong Electric Field," Phys. Rev. Lett., vol. 109, no. 8, 085002, August 24, 2012.

[3] G.A. Mesyats, A.G. Sadykova, S.A. Shunailov, V.G. Shpak, and M.I. Yalandin, "Control and Stabilization of Runaway Electron Emission at the Delay Stage of Pulsed Breakdown in an Overvolted Atmospheric Gap," IEEE Trans. Plasma Sci., vol. 41, no. 10, pp. 2863–2870, October 2013.

[4] V.F. Tarasenko, D.A. Sorokin, M.I. Lomaev, "Generation of dual pulses of the runaway electron beam current during the subnanosecond breakdown of atomic and molecular gases," Tech. Phys., vol.61, no.10, pp. 1551-1560, October 2016.

[5] A.V. Kozyrev, E.M. Baranova, V.Y. Kozhevnikov, and N.S. Semenyuk, "Variation of the beam parameters of runaway electrons in a gas discharge under the conditions of nonuniform preliminary ionization," Tech. Phys. Lett., vol. 43, no. 9, pp. 804-807, September 2017.

*The work was supported in part by the RFBR Grants Nos. 20-08-00172 and 19-08-00292. The study was carried out on the equipment of the Collective Use Center at the Institute of Electrophysics, UB, RAS.

THE DYNAMICS OF LOW PRESSURE APOKAMPIC DISCHARGE FORMATION IN ARGON*

V.S. KUZNETSOV, E.K. BAKSHT, V.A. PANARIN, V.S SKAKUN, E.A. SOSNIN, V.F. TARASENKO

Institute of High Current Electronics SB RAS, Tomsk, 634055, Russia
E-mail: ribert_smith_93@mail.ru

The apokampic discharge as a source of plasma plumes is an interesting object for fundamental and applied research. Plasma plumes (so-called apokamps) are positive streamers that propagate from the discharge channel. To obtain data on positive streamers propagation in air and nitrogen at various pressures, optical methods for detecting high-speed processes are used. It is found that in air under various excitation conditions their speed can reach in order of magnitude $10–10^2$ km/s [1-5].

In the present work a new data were obtained on the propagation velocities of the apokamp streamer in argon with air admixture at pressures from 30 to 120 Torr. As preliminary experiments have shown, that in pure Ar the apokamp doesn't form, therefore, admixtures of molecular gases are necessary [6]. To ignite the discharge and record the dynamics of plasma plume formation, the experimental technique and the quartz chamber described in [1-4] were used. Figure 1 shows the dynamics of apokamp discharge plume in the nanosecond time scale. It gives both values the starting velocity of the streamer head and the average for the time of flight in the field of view. The average velocity depends on many conditions (air pressure, amplitude and frequency of voltage pulses).

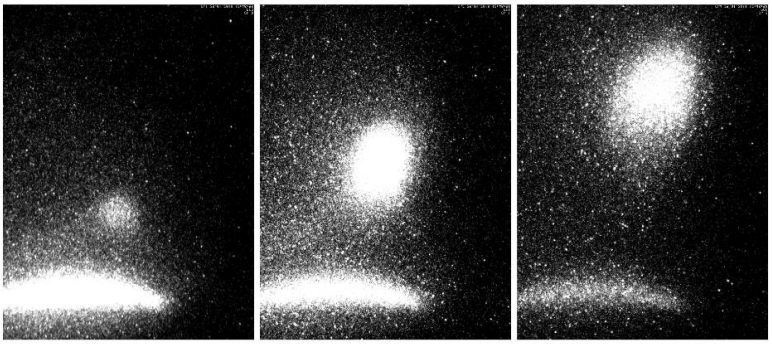

Fig.1. The dynamics of apokampic discharge plume formation in argon at a pressure of 120 Torr and U ~ 3.75 kV. The exposure time of each frame is 20 ns, the pause between them is 40 ns.

Ceteris paribus, a decrease of the discharge frequency initially leads to an increase of average speed of streamer head, and then to its decrease. The measured average velocity values for 120 Torr range between 97 and 195 km/s.

REFERENCES

[1] E.A. Sosnin, V.S. Skakun, V.A. Panarin, D.S. Pechenitsin, V.F. Tarasenko, E.Kh. Baksht, "Phenomenon of Apocamp Discharge," JETF Letters, vol. 103, no. 12, pp. 761–764, June 2016.

[2] E.A. Sosnin, V.A. Panarin, V.S. Skakun, E.Kh. Baksht, V.F. Tarasenko, "Dynamics of apokamp-type atmospheric pressure plasma jets," Eur. Phys. J. D., vol. 71. no 2, p. 25, February 2017.

[3] V.F. Tarasenko, E.A. Sosnin, V.S.Skakun, V.A. Panarin, M.V. Trigub, G.S. Evtushenko, "Dynamics of apokamp-type atmospheric pressure plasma jets initiated in air by a repetitive pulsed discharge," Physics of Plasmas, vol. 24, no. 4, p. 043514, April 2017.

[4] E.A. Sosnin, G.V. Naidis, V.S. Tarasenko, V.S. Skakun, V.A. Panarin, N.A. Babaeva, E.Kh. Baksht, V.S. Kuznetsov, "Apokamps produced by repetitive discharges in air," Physics of Plasmas, vol. 25, no. 8, p. 083513, July 2018.

[5] E.A.Sosnin, E.Kh.Baksht, V.S.Kuznetsov, V.A.Panarin, V.S.Skakun, V.F. Tarasenko, "Laboratory Simulation of Blue Jets with Apokampic Discharge in the Hz Frequency Range," Atmos. Ocean. Opt., vol. 32, no. 6, pp. 710–715, June 2019.

[6] V.S. Kuznetsov, E.A. Sosnin, V.A. Panarin, V.S. Skakun, V.F. Tarasenko, "The Influence of Molecular Gas on the Apokamp Discharge Formation," Optics and Spectroscopy, vol. 125, no. 3, pp. 324–330, October 2018.

* The work is performed in the framework of the grant RFBR according to the research project No. 19-32-90023 and the state assignment of IHCE SB RAS on topic No. 13.1.4.

ATMOSPHERIC PRESSURE CORONA DISCHARGE IN THE NEEDLE-PLANE ELECTRODE SYSTEM: INFLUENCE OF FIELD PEAKING ON ELECTROPHYSICAL PARAMETERS*

V.S. KUZNETSOV, A.O. KOKOVIN, A.V. KOZYREV, V.F. TARASENKO

Institute of High Current Electronics SB RAS, Tomsk, 634055, Russia
E-mail: ribert_smith_93@mail.ru

A corona discharge is observed under conditions of sharply inhomogeneous electric fields [1], in which a high field strength is obtained and its field decreases rapidly with increasing distance from the ionization site, which prevents electric breakdown of the gas-discharge gap. The corona discharge has been studied in most detail in atmospheric pressure air. In particular, it was shown that at a negative polarity at the tip, a corona discharge occurs at lower voltages, compared with a positive one [2]. Despite the large number of publications on corona discharge, the influence of the radius of curvature on the electrophysical parameters has been poorly studied. The work is aimed at determining the initial conditions for the formation of a corona discharge at various radii of curvature of the point electrode in the point-plane configuration.

In the experiments, point electrodes with a curvature radius of 30 and 11 μm and a diameter of 640 and 320 μm, respectively, were used. The discharge was ignited between a point and a plane electrode with a discharge gap of 1–3 cm using a voltage source operating both with negative and positive polarity in the range of 1–20 kV. Depending on the curvature radius of the point electrode and on the interelectrode gap, the voltage at which the corona discharge was ignited could change by more than 1 kV. So, when applying voltage of negative polarity, the minimum starting voltage of the corona discharge was detected in the case of a point electrode with a curvature radius of 11 μm with an interelectrode gap of 1 cm (2.2 kV), and the maximum starting voltage corresponded to an electrode with a radius of 30 μm and an interelectrode gap of 3 cm (3.6 kV).

In addition, theoretical calculations were performed for the configurations used in the experiment. Figure 1 shows the dynamics of the current increase on a point electrode, depending on the curvature radius of the tip.

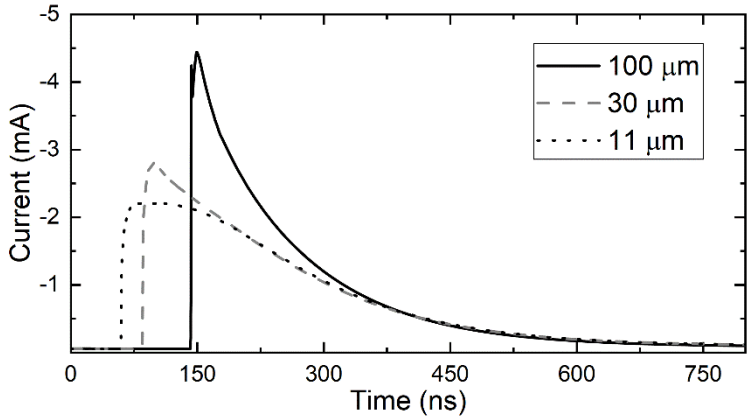

Fig.1. The influence of the curvature radius of the electrode on the current pulse form.

The calculation at an input negative voltage of 3 kV and an interelectrode gap of 2 cm was carried out. It is seen that with a decrease in the electrode tip radius, the current front grows earlier, but the maximum current amplitude decreases, and the pulse itself elongates. Thus, a decrease in the curvature radius of the tip facilitates the ignition of a corona discharge in atmospheric pressure air.

REFERENCES

[1] E. M. Bazelyan and Yu. P. Reiser, Spark discharge. Moscow: MIPT, 1997.

[2] S.B. Afanasyev, D.S. Lavrenyuk, I.N. Petrushenko, Yu.K. Stishkov, “Some features of corona discharge in air,” The Russian Journal of Applied Physics, vol. 78, no. 7, pp. 30–34, August 2008. (in Rusian)

* The studies were carried out within the framework of the grant RFBR according to the research project No. 19-32-90023 and the state assignment of IHCE SB RAS on topic No. 13.1.4.

THE MEASUREMENT OF THE STREAMER PROPAGATION VELOCITY AT HIGH-VOLTAGE NANOSECOND BREAKDOWN IN A SHARPLY NONUNIFORM ELECTRIC FIELD*

M.I. LOMAEV[1,2], *D.V. BELOPLOTOV*[1], *D.A. SOROKIN*[1], *V.F. TARASENKO*[1]

[1]*Institute of High Current Electronics, Tomsk 634055, Russia*
[2]*National Research Tomsk State University, Tomsk 634050, Russia*

Nonequilibrium low-temperature atmospheric-pressure plasma attracts much attention due to its many possible applications in science and technology [1, 2]. As a rule, it is generated by use of some types of an electric discharge in a gas. One of them is a high-voltage nanosecond diffuse discharges in a nonuniform electric field [3-5]. Main feature of this type discharge is a generation of runaway electrons (REs), effecting on a discharge formation. In this case, a large-diameter streamer was shown both experimentally and theoretically to form [6-9]. For a more complete understanding of the development of the streamer and the formation of a discharge at conditions of REs generation, further research is required. In particular, it is necessary to know dynamics of the streamer velocity, influence of REs on the discharge development, relationship between displacement current and ionization processes in a gas gap, as well as the effect of overvoltage on the streamer formation. This report presents the results of measurements of streamer propagation velocity at high-voltage nanosecond breakdown in a sharply nonuniform electric field. When conducting experiments an ultrafast streak-camera *3* and a four-channel ICCD-camera *4* were used (Fig. 1).

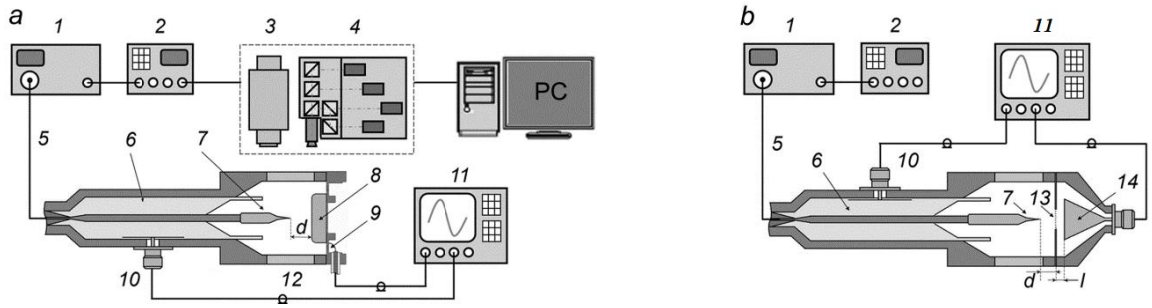

Fig. 1. Experimental setup for measurements of streamer propagation velocity (*a*) and REs and displacement currents (*b*): *1, 2* – high-voltage and timing generators; *3, 4* - Hamamatsu C10910-05 streak camera and HSFC-PRO four-channel ICCD-camera; *5* - high-voltage coaxial cable; *6* - coaxial line; *7, 8* – needle and grounded electrodes; *9* – current shunt; *10* – voltage divider; *11* – oscilloscope; *12* – quartz window; *13* – 2 μm-thick grounded kimfol film; *14* – collector.

The streamer velocity was shown to change during its motion from the needle electrode towards the opposite flat electrode. The data are obtained on the instantaneous streamer velocity. Correlation between the streamer velocity dynamics and the variation of the dynamic displacement current in time was demonstrated. Measuring of the dynamic displacement allowed estimating of the average streamer velocity. Runaway electrons was shown to generate at the start of the streamer at conditions under study.

References

[1] Low Temperature Plasma Technology. Eds. P.K. Chu and X. Lu. Boca Raton: CRC Press, 2014.

[2] Low Temperature Plasma. Fundamentals, Technologies, and Techniques. Eds. R. Hipler, H. Kersten, M. Schmidt, and K. H. Schoenbach, 2nd ed. Weinheim: WILEY-VCH Verlag GmbH&Co. KgaA, 2008.

[3] Yu.D. Korolev and G.A. Mesyats, Physics of Pulsed Breakdown in Gases, URO-PRESS, 1998.

[4] L.P. Babich, High-Energy Phenomena in Electric Discharges in Dense Gases: Theory, Experiment and Natural Phenomena, Arlington: Futurepast, 2003.

[5] Runaway Electrons Preionized Diffuse Discharges. Ed. V.F. Tarasenko, N.Y.: Nova Science Publishers, Inc., 2014.

[6] P. Tardiveau, N. Moreau, S. Bentaleb, C. Postel and S. Pasquiers, "Diffuse mode and diffuse-to-filamentary transition in a high pressure nanosecond scale corona discharge under high voltage," J. Phys. D: Appl. Phys., vol. 42, 175202, 2009.

[7] S. Yatom, V. Vekselman, J.Z. Gleizer, Ya.E. Krasik, "Space- and time-resolved characterization of nanosecond time scale discharge at pressurized gas," J. Appl. Phys., vol. 109, 073312, 2011.

[8] G.V. Naidis, V.F. Tarasenko, N.Y. Babaeva, M.I. Lomaev, "Subnanosecond breakdown in high-pressure gases," Plasma Sources Sci. Technol., vol. 27, 013001, 2018.

[9] D.V. Beloplotov, M.I. Lomaev, D.A. Sorokin, V.F. Tarasenko, "Displacement current during the formation of positive streamers in atmospheric pressure air with a highly inhomogeneous electric field," Phys. Plasmas, vol. 25, 083511, 2018.

* The work has been funded within the terms of reference of the IHCE SB RAS, research line No. 13.1.4.

THE ELECTRIC FIELD GENERATED BY A CRITICAL AVALANCHE OF RUNAWAY ELECTRONS *

E.V. ORESHKIN

Lebedev Physical Institute, RAS, Moscow, Russia

X-ray and gamma-ray bursts observed in a thunderous atmosphere of the earth are usually associated with the generation of runaway electrons (REs) in electric atmospheric fields[1]. It is assumed that in high-altitude discharges that are observed in a thunderstorm atmosphere, the main role is played by runaway electron avalanches initiated by cosmic rays[2]. In this work, using the three-dimensional numerical calculations[3], we studied the laws of development and determined the parameters of critical avalanches in which the field is the electric field created by the space charge is comparable to the external field. It is shown that in air under conditions typical of thunderstorm atmospheric discharges, the number of electrons in a critical avalanche of REs can reach a value of the order of 10^{17} - 10^{18} particles.

REFERENCES

[1] G. K. Parks, B. H. Mauk, R. Spiger, and J. Chin, "X-Ray Enhancements Detected during Thunderstorm and Lightning Activities", Geophysical Research Letters, vol. 8, p. 1176, 1981.

[2] A. Gurevich and K. Zybin, "Runaway breakdown and electric discharges in thunderstorms", Physics-Uspekhi, vol. 44, p. 1119, 2001.

[3] E. Oreshkin, "The critical avalanche of runaway electrons", EPL (Europhysics Letters), vol. 124, Article Number 15001, 2018.

* The work was supported by the Russian Science Foundation under grant No. 19-79-00280.

NANOSECOND DISCHARGE IN A POINT-TO-PLANE GAP FILLED WITH AIR. WHEN IS A SUBNANOSECOND RUNAWAY ELECTRON BEAM GENERATED?*

D.V. BELOPLOTOV, M.I. LOMAEV, D.A. SOROKIN, V.F. TARASENKO

Institute of High Current Electronics SB RAS, Tomsk, Russia

Runaway electrons (REs) can have a significant effect on the formation of nanosecond discharges in inhomogeneous electric fields. Subnanosecond RE beams are generated due to the enhancement of the electric field near the pointed electrode and at the streamer front [1–3]. However, there is no experimental data on the generation of REs with reference to the dynamics of streamer formation. It seems impossible to establish in an experiment where most of the RE beam is generated, but such attempts have been made [4, 5]. Thanks to recent advances in the study of streamers in an inhomogeneous electric field [6], a way has been found to investigate the generation of runaway electrons with reference to the development of a streamer in the gap [7]. It was found that the streamer development is accompanied with a dynamic displacement current (DDC) caused by the redistribution of the electric field in the gap [6]. By measuring DDC, we can accurately determine when a streamer starts and when it reaches the opposite electrode. DDC and RE beam current can be measured together. This makes it possible to determine the moment of generation of REs relative to the appearance of a streamer in the gap [7].

Fig. 1 shows the waveforms of voltage as well as DDC and RE beam current measured with a collector placed downstream the grounded electrode made of a grid. The signal from the collector in Fig. 1a was obtained using the grid and a text-weight paper. The paper absorbs REs and they did not reach the collector. However, the electromagnetic signal (DDC) caused by the appearance and movement of the streamer was recorded. As was shown in our previous studies of positive streamer [6], the rise time of DDC corresponds to the streamer appearance, and the fall of DDC corresponds the moment when streamer reaches the opposite (grounded) electrode. The signal from the collector in Fig. 1b was obtained using only one grid. Both DDC and RE beam current were recorded. It is clearly seen that the pulse of RE beam current is observed during the rise time of DDC. As a result, we can conclude that the REs were generated before the appearance of the streamer in the vicinity of the pointed electrode.

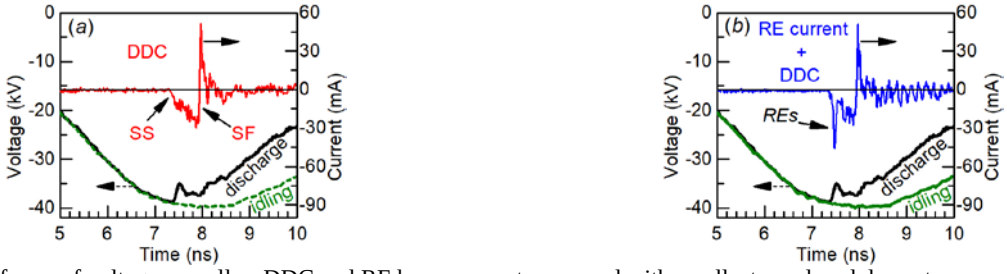

Fig.1. Waveforms of voltage as well as DDC and RE beam current measured with a collectore placed downstream anode made of (a) a grid+paper and (b) only grid. Air at a pressure of 100 kPa. SS – straemer start. SF – streamer finish.

REFERENCES

[1] L.P. Babich, High-Energy Phenomena in Electric Discharges in Dense Gases, Arlington, Futurepast, 2003.

[2] V.F. Tarasenko (ed.), Runaway Electrons Preionized Diffuse Discharges, New York, Nova Science Publisher, 2014.

[3] G.A. Mesyats, M.S. Pedos, S.N. Rukin, V.V. Rostov, I.V. Romanchenko, A.G. Sadykova K.A Sharypov, V.G. Shpak, S.A. Shunailov, M.R. Ul'masculov, and M.I. Yalandin, "Formation of 1.4 MeV runaway electron flows in air using a solid-state generator with 10 MV/ns voltage rise rate," Appl. Phys. Lett., vol.112, Article Number 163501, 2018.

[4] T. Shao, V.F. Tarasenko, C. Zhang, A.G. Burachenko, D.V. Rybka, I.D. Kostyrya, M.I. Lomaev, E.K. Baksht, and P. Yan, "Application of dynamic displacement current for diagnostics of subnanosecond breakdowns in an inhomogeneous electric field," Rev. Sci. Instrum., vol.84, Article Number 053506, 2013.

[5] G.A. Mesyats, A.G. Sadykova, S.A. Shunailov, V.G. Shpak, and M.I. Yalandin, "Control and Stabilization of Runaway Electron Emission at the Delay Stage of Pulsed Breakdown in an Overvolted Atmospheric Gap," IEEE Trans. Plasma Sci., vol.41, Article Number 2863, 2013.

[6] D.V. Beloplotov, M.I. Lomaev, D.A. Sorokin, and V.F. Tarasenko, "Measurement of the Dynamic Displacement Current as a New Method of Study of the Dynamics of Formation of a Streamer at a Breakdown of Gases at a High Pressure," JETP Letters, vol.107, Article Number 606, 2018.

[7] D.V. Beloplotov, V.F. Tarasenko, M.I. Lomaev, and D.A. Sorokin, "Experimental determination of the generation moment of runaway electrons," IEEE Trans. Plasma Sci., vol.47, Article Number 4521, 2019

* The work was supported by RFBR, project number 20-02-00733.

PHYSICAL PECULIARITIES OF CURRENT DEVELOPMENT IN EPTRON*

P.A. BOKHAN[1], P.P. GUGIN[1], M.A. LAVRUKHIN[1], I.V. SCHWEIGERT[2], D.E. ZAKREVSKY[1,3]

[1] *Rzhanov Institute of Semiconductor Physics SB RAS, Novosibirsk, Russia*
[2] *Khristianovich Institute of Theoretical and Applied Mechanics, Novosibirsk, Russia*
[3] *Novosibirsk State Technical University, Novosibirsk, Russia*

Eptron is a gas-discharge device based on a combination of two successively developing discharges, one of which provides the formation of a plasma cathode (such can be discharges with the generation of counterpropagating electron beams), and the other closes the current development circuit (discharge in the capillary. The capillary, on the one hand, complicates the ignition, but, on the other hand, weakly affects the development and combustion of the discharge and provided acceleration of plasma recombination in the inter-pulse period. When a high voltage is applied to the eptron, runaway electrons are generated in the capillary structure, which fly freely from the plasma cathode to the anode of the capillary structure. This makes it possible to use eptrons as a switching device with characteristic parameters: delay times of discharge development with τ_d~1μs, switching time - τ_s<1ns, and pulse compression ratio $S=\tau_d/\tau_s\geq 103$ at an operating voltage of up to U=30kV [1].

In the present work, theoretical and experimental studies of the switching parameters of the eptron were performed, in which a hollow cathode discharge, coaxial and planar open discharges acted as a plasma cathode, and the capillary section was removed from the volume and built in from the outside on one of the sides of the plasma cathode design. A necessary element of the capillary design was the organization of an external grounded shield in order to provide a mechanism for neutralizing surface charges on the inner wall of the capillary due to the bias current and a decrease in the electron concentration inside the channel, which leads to an increase in the delay time for the development of the discharge and ensuring the frequency of functioning of the electron up to 200 kHz. Advancement in large working voltages required a constructive modification of eptrons. Capillary discharge structures were developed and implemented, in which the possibility of generating runaway electrons with an energy sufficient to fly along the entire length of the capillary from the plasma cathode to the anode was limited. The modernization consisted in the displacement of the axes of the rings forming the capillary, so as to prevent the penetration of runaway electrons generated in any ring into the hole in the subsequent ring. As a result, typical discharge parameters turned out to be the following: τ_d~1μs, τ_s~0.5ns at a working helium pressure of p_{He}≈5Torr and U=60kV. Using similarly upgraded slotted capillaries with geometries, the parameters τ_d~0.2μs, τ_s~0.150ns were obtained at a working pressure of up to p_{He}≈30Torr and up to U=70kV (Fig. 1*ab*).

Calculation of the breakdown of a capillary in an eptron gas-discharge device was carried out in a cylindrical formulation using the diffusion-drift approximation with an additional solution of the transport equation for the average electron energy according to the model [2] and confirmed the main parameters of the current development in the eptron.

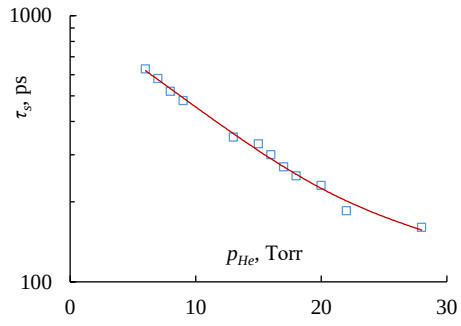

Fig.1*a* Dependence $\tau_s(p_{He})$ at U=65kV

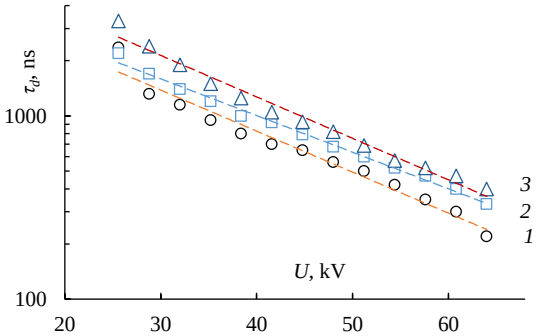

Рис.1*b* Dependence $\tau_d(U)$ at p_{He}=16(*1*); 13(*2*) и 9.5Torr (3)

[1] P A Bokhan, PP Gugin, MA Lavrukhin and DmE Zakrevsky. A high-voltage subnanosecond sharpener based on a combination of 'open' and capillary discharges // *J. Phys. D: Appl. Phys.* V.51, 364001 (2018)

[2] I .V. Schweigert, S.Vagapov, L. Lin and M.Keidar. Enhancement of atmospheric plasma jet–target interaction with an external ring electrode // *J. Phys. D: Appl. Phys.* V.52, 295201 (2019)

* The work was supported by the Russian Science Foundation under grant No. 19-19-00069.

INFLUENCE OF ELEMENTARY PROCESSES ON THE FORM OF APOKAMPIC DISCHARGE*

A.G. SITNIKOV, V.YU. KOZHEVNIKOV, A.V. KOZYREV

Institute of High Current Electronics SB RAS, Tomsk, Russia

The apocampic discharge at atmospheric pressure was first experimentally detected in 2016 [1]. A theoretical model of this type of discharge was proposed in [2]. In the present paper, new calculations based on this model are given at atmospheric pressure in an oxygen medium with varying rates of elementary processes such as dissociation of oxygen molecules by electron impact and electron attachment.

For accelerate the computation, the calculations were carried out in two-dimensional geometry. Blade electrodes with a curvature of 0.1 mm were located at an angle of 120 degrees to each other (Fig. 1). The distance between the electrodes was 8 mm. One electrode was at a floating potential. A trapezoidal pulse with a duration of 2.5 μs and an amplitude of 15 kV was applied to another electrode through a ballast load of 10 kΩ.

The calculation results are presented in Fig. 1 (a) and (b) for the 1 μs time point and (c) for the 0.65 μs time point from the beginning of the voltage pulse. In the case of (a), cross sections of processes were taken from well-known sources [3-5]. In the case of (b), the sticking cross section wos an order of magnitude smaller than the tabular. And in the case of (c), the dissociation by electron impact was not taken into account at all.

It can be seen that in case (b) and (c) the discharge extend faster than in case (a). This is due to the fact that with a decrease in cross sections of both the sticking process and the dissociation process, the concentration of charged particles increases. The absence of the dissociation process leads to a significant change in the shape of the discharge, while a decrease in the influence of the sticking process changes the shape of the discharge slightly.

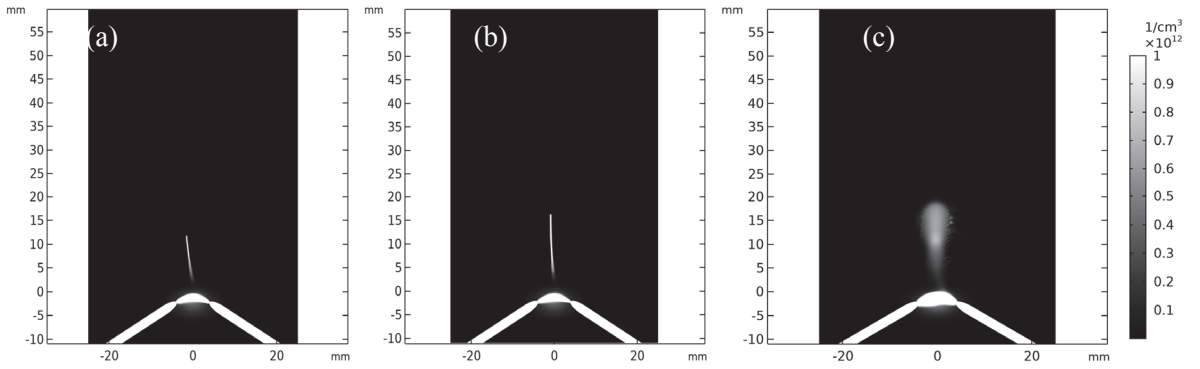

Fig.1. Calculated spatial distribution of the O_2^+ number density (scale in cm^{-3}) for gas discharge at the different rate of elementary processes.

REFERENCES

[1] Sosnin E A, Panarin V A, Skakun V S, Baksh E K and Tarasenko V F "Dynamics of apokamp-type atmospheric pressure plasma jets," EPJ D, vol. 71, no. 2, pp. 25-1-25-6, 2017.

[2] V. Kozhevnikov et al. "Apokamp-type gas discharge phenomenon: Experimental and theoretical backgrounds," EPL, vol. 129, pp. 15002-p1 – 15002-p6, 2020.

[3] Kossyi I. A., Kostinsky A. Yu., Matveyev A. A. and Silakov V. P., "Kinetic scheme of the non-equilibrium discharge in nitrogen-oxygen mixtures," Plasma Sources Sci. Technol., vol. 1 no. 3, 207, 1992.

[4] He J, Zhang Y T, "Modeling study on the generation of reactive oxygen species in atmospheric radio-frequency helium–oxygen discharges," Plasma Process. Polym. vol. 9, 2012.

[5] M. A. Lieberman and A. J. Lichtenberg, Principle of Plasma Discharges and Materials Processing, New York: Wiley, 2005.

* The work was supported by the Russian Foundation for Basic Research (RFBR) grant No. 19-08-00286.

PULSED CATHODOLUMINESCENCE AND CHERENKOV RADIATION IN DIAMOND, SAPPHIRE AND QUARTZ UNDER THE ELECTRON BEAM EXCITATION WITH AN ENERGY UP TO 350 KEV*

A.G. BURACHENKO, V.F. TARASENKO, E.KH. BAKSHT, D.V. BELOPLOTOV, M.I. LOMAEV

Institute of High Current Electronics SB RAS, Tomsk, 634055, Russia

When an electron beam acts on various transparent materials, an emission of a different nature can arise – Cherenkov radiation (CR) and (or) cathodoluminescence (CL). An analysis of such emission makes it possible to obtain information both about the specimen itself and about the parameters of the electron beam. CR is widely used for registration of high-energy particles [1-6]. It is known that CR is easiest to detect in those substances that have a high refractive index and are also transparent in the UV region and have a low CL intensity in this region. Research of the radiation excited in sapphire, quartz KU-1 and synthetic diamond at a wavelength range of 200–800 nm by a pulsed electron beam with an energy of up to 350 keV were conducted. Diamond is often used as a radiator in Cherenkov detectors in Tokamaks, because diamond has high thermal conductivity, radiation resistance and refractive index. The energy of runaway electrons in Tokamak systems can range from tens of kilo- to tens of mega-electron volts [7, 8]. The refraction indices of sapphire and quartz are much lower that diamond but fundamental absorption edge in sapphire and quartz lies in the VUV region (< 200 nm). Moreover, the intensity of pulsed CL in sapphire and quartz in UV range is below its value in diamonds.

It has been shown that CR of specimens of synthetic diamond, sapphire and KU-1 quartz was reliably detected by a standard spectrometer in the spectral region of 200–400 nm and in which there are no intense CL bands.

Moreover registration of CR in the UV region in all specimens is confirmed by measurements of the amplitude-time parameters of the emission using the photodiode and the UV filter. It has been shown that in synthetic diamond, CR is superimposed by pulsed CL, including an intense exciton band with its maximum at 235 nm. Accordingly, when creating Cherenkov detectors, the influence of the exciton band, as well as other CL bands, on an optical signal must be taken into account.

REFERENCES

[1] V.P. Zrelov, Cherenkov radiation in high-energy physics, Washington, DC: ERDA Div. Phys. Res., 1973.

[2] B.M. Bolotovskii, "Vavilov–Cherenkov radiation: its discovery and application," Physics-Uspekhi, vol. 52, no. 11, pp. 1099–1110, November 2009.

[3] V. Ginis, J. Danckaert, I. Veretennicoff, and P. Tassin, "Controlling Cherenkov radiation with transformation-optical metamaterials," Physical review letters, vol. 113, no. 16, pp. 167402(1–5), October 2014.

[4] T. Sumiyoshi, I. Adachi, R. Enomoto, T. Iijima, R. Suda, M. Yokoyama, and H. Yokogawa, "Silica aerogels in high energy physics," J. of non-crystalline solids, vol. 225, pp. 369–374, April 1998.

[5] G.S. Bowers, W. Blaine, X.M. Shao, B. Dingus, D.M. Smith, M. Schneider, F. Martinez-McKinney, M.P. McCarthy, S. BenZvi, L. Nellen, and N. Fraija, "Combining Cherenkov and scintillation detector observations with simulations to deduce the nature of high-energy radiation excesses during thunderstorms," Physical Review D, Vol. 100, no. 4, pp. 043021(1–10), August 2019.

[6] A.P. Potylitsyn, and S.Y. Gogolev, "Vavilov–Cherenkov Radiation in an Inclined Dielectric Plate and Violation of Azimuthal Symmetry, " Physics of Particles and Nuclei Letters, vol. 16, no. 2, pp. 127–132, June 2019.

[7] J. Zebrowski, L. Jakubowski, M. Rabinski, M.J. Sadowski, M.J. Jakubowski, R. Kwiatkowski, K. Malinowski, R. Mirowski, J. Mlynar, O. Ficker, V. Weinzettl, F. Causa, "Studies of runaway electrons via Cherenkov effect in tokamaks," J. Phys. Conf. Ser., vol. 959, 2018.

[8] M.J. Sadowski, "Generation and diagnostics of fast electrons within tokamak plasma," Nukleonika, vol. 56, no. 2, pp. 85–98, 2011.

* Russian Science Foundation supported this work according to the research project No. 18-19-00184.

GENERATION OF RUNAWAY ELECTRONS AND X-RAY AT A MICROSECOND VOLTAGE RISE TIME IN DIFFERENT GASES*

A.G. BURACHENKO, V.F. TARASENKO, E.KH. BAKSHT

Institute of High Current Electronics SB RAS, Tomsk, 634055, Russia

The first papers reporting the registration of x-ray radiation during breakdown of helium [1, 2] and air [3, 4] at atmospheric pressure (100 kPa) were published in the 60s of the last century. In these papers, voltage pulses of a relatively short duration and cathodes with a small radius of curvature were used. The registration of a runaway electron beam (REB) in atmospheric pressure air with an increase in the duration of the voltage rise time to ~ 1 μs was reported in [5-7].

However, the simultaneous studies of the generation of x-ray radiation and REB in most known papers with a microsecond voltage rise time have not been carried out. In addition, the studies were mainly aimed at studying the characteristics of air breakdown at atmospheric pressure.

The purpose of this paper is to investigate the generation of runaway electrons and x-ray radiation at a voltage pulse rise time duration of 1.5 μs and air, nitrogen, argon, and helium pressures from 1 to 100 kPa, as well as to compare the obtained data with known results obtained with a microsecond voltage rise time.

In experiments four cathodes of various designs were used. X-ray radiation was detected by a scintillator and a PMT behind an aluminum foil anode in the total pressure range and in all four gases. In helium, a runaway electron beam at a pressure of 100 kPa was recorded by a collector. In air, nitrogen, and argon, a runaway electron beam had relatively small amplitudes and energies, and was recorded by the collector only at low pressures (<20 kPa). It has been shown that runaway electron generation is significantly affected by the cathode design, while the best results in terms of intensity and stability of the occurrence of x-ray radiation at the anode are achieved using cathodes having two parts, both with a small and a large radius of curvature (fig. 1). In this case, runaway electrons are mainly generated in a diffuse discharge from the electrode surface with a large radius of curvature.

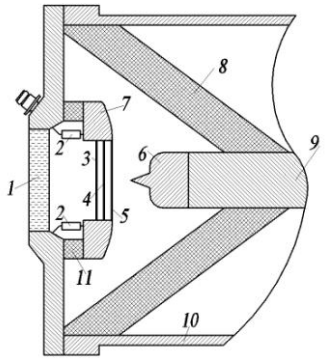

Fig. 1. Design of the discharge chamber. 1 - quartz window, 2 - shunt resistances, 3 - film scintillator, 4 - metal foil, 5 – anode grid, 6 - cathode, 7 - flange for attaching the anode grid and shunt resistances, 8 - discharge chamber insulator, 9 - high-voltage electrode, 10 - the camera body and the external cylinder of the coaxial line, 11 - the shunt insulator.

REFERENCES

[1] S. Frankel, V. Highland, T. Sloan, O. Van Dyck and W. Wales, "Observation of X-rays from spark discharges in spark chamber," Nuclear Instruments and Methods, vol. 44, no. 2, pp. 345–348, October 1966.

[2] R.C. Noggle, E.P. Krider, and J.R. Wayland, "A search for X rays from helium and air discharges at atmospheric pressure," J. Appl. Phys., vol. 39, no. 10, pp. 4746–4778, April 1968.

[3] Yu.L. Stankevich and V.G. Kalinin, "Fast electrons and X-radiation during the initial stages of an impulse spark discharge in air," Doklady Akademii Nauk SSSR, vol. 177, no. 1, pp. 72–73, November 1967.

[4] L.V Tarasova and L.N. Khudyakova, "X rays from pulsed discharges in air," Soviet Physics Technical Physics, vol. 14, p. 1148, February 1970.

[5] T.V. Loiko, "Energetic electron recording at electric-discharges of microsecond duration in the air of atmospheric density," Zhurnal Tekhicheskoi Fiziki, vol. 50, no. 2, pp. 392–393, 1980.

[6] L.P. Babich, T.V. Loiko, "Subnanosecond pulses of runaway electrons generated in atmosphere by high-voltage pulses of microsecond duration," Doklady Physics, vol. 54, no. 11, pp. 479–482, April 2009.

[7] I.D. Kostyrya, V.F. Tarasenko, "Generation of runaway electrons and X-ray emission during breakdown of atmospheric-pressure air by voltage pulses with an ~ 0.5-μs front duration," Plasma Phys. Rep., vol. 41, no. 3, pp. 269–273, March 2015.

* The work was supported by RFBR, project #18-52-53003 and performed in the framework of the State task for HCEI SB RAS, project #13.1.4.

CURRENT IN PLANAR DIODE WITH A MOVING CONDUCTING CHANNEL

V.A. SHKLKYAEV, S.YA.BELOMYTTSEV, A.A. GRISHKOV

Institute of High Current Electronics SB RAS, Tomsk, Russia

In this work, based on the current continuity equation and the Gauss theorem, we analyze the currents when the boundary of the conductive layer moves at a constant speed in the gap bounded by two parallel electrodes.

The nonrelativistic model consider that the conductive layer has a finite resistivity. It leads to the fact that an uncompensated space charge and an electric field arise in the conductive layer. The intensity of this electric field decreases monotonically into the depth of the conductive layer. The length at which the volume charge in the conductive layer decreases to 0 depends on the resistivity of the layer and the velocity of its boundary.

It is shown that at a constant voltage on the electrodes, in the moment of touching the boundary of the conducting layer of the opposite electrode, the current in the system is determined only by Ohm's law and doesn't depend on the speed of the boundary.

NUMERICAL SIMULATION OF THE EFFECT OF AN ELECTRON BEAM ON THE SURFACE OF MATERIALS*

K.T. ASHUROVA, T.V. KOVAL, M.S. VOROBYOV

Institute of High Current Electronics SB RAS, Tomsk, Russia

Electron beam modification of the material's surface is one of the most urgent topics since it allows the formation of protective, hardening and wear-resistant coatings. Furthermore, there is the possibility of obtaining new surface properties by controlling power during irradiation. Studies were conducted on the irradiation of steel A 276 420 by using an electron source SOLO with a grid plasma cathode based on a low-pressure arc discharge. The source makes it possible to generate a beam with a current of 20–300 A, electron energy of 5–25 keV, and a pulse duration of 20–200 μs with an energy density of up to 100 J/cm^2 [1]. The main advantage of using these sources is their ability to control beam parameters over a wide range and independently of each other.

The influence of the dynamics of power density on the material temperature can be shown by considering the solution of the heat equation for a semi-infinite body with a surface source ($-\lambda\partial T/\partial z\big|_{z=0} = q\varphi(t)$) power density$q\varphi(t)$:

$$T(z,t) = [q(a^{1/2}/\lambda]\int_0^t \varphi(t-\xi)\xi^{-1/2}\exp(-z^2/4a\xi)d\xi, \quad (1)$$

It follows from the further solution that the temperature *T(0, t)* depends on the form of function (1) and the thermophysical characteristics of the target, which allows controlling the dynamics of the surface temperature by changing the power density of the electron beam. A numerical solution of the heat equation is carried out taking into account the temperature dependences of the thermophysical coefficients K (T) [3].

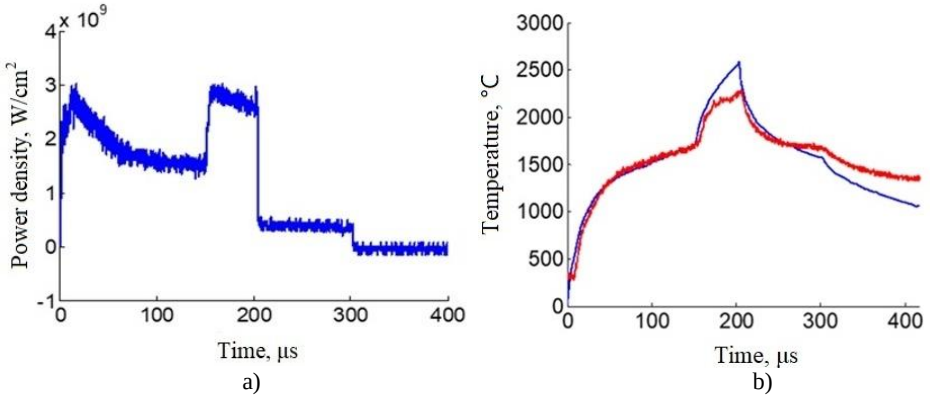

Fig. 1. The time dependence of the power density of the electron beam on the target (a); calculated (blue line) and experimentally measured (red line) target surface temperature.

The difference between the experimental dependence *T(t)* (Fig. 1b) and the calculated one at the maximum temperature is most likely due to the sputtering of the target, which introduces distortions in the measurements. The shelf (200–300 μs) on the temperature curve is associated with crystallization. One of the reasons for the difference between the calculated and experimental cooling rates after 300 μs may be a change in the structure and thermophysical characteristics of the surface layer of the sample under high-energy exposure. Numerical simulation of thermal showed a satisfactory agreement between the calculated values and experimental data, which in the near future will allow more precise selection of technological parameters.

REFERENCES

[1] N.N. Koval, YU.F. Ivanova, Evolyutsiya struktury poverkhnostnogo sloya stali, podvergnutoy elektronno-ionno-plazmennym metodam obrabotki. Tomsk: Izdatel'stvo NTL, 2016.

[2] N.N. Koval, YU.F. Ivanova, Elektronno-ionno-plazmennaya modifikatsiya poverkhnosti tsvetnykh metallov i splavov. Tomsk: Izd-vo NTL, 2016.

[3] T.V. Koval, A.D. Teresov, Chan Mi Kim An, P.V. Moskvin, "Eksperimental'noye i chislennoye issledovaniye impul'snogo vozdeystviya elektronnogo puchka na metallicheskiye misheni," Proc. 6th Int. Conf. on Plazmennaya emissionnaya elektronika. Ulan-Ude, Russia, pp. 76–81, 2018.

* The reported study was funded by RFBR and ROSATOM, project number 20-21-00111.

MODELING OF VACUUM ARC IN ANODE SPOT OR ANODE PLUME MODES WITH CONSIDERATION OF DIFFERENT COMPONENTS

L.J. WANG, Z. YANG, M. LUO, S.L. JIA

State Key Laboratory of Electrical Insulation and Power Equipment, Xi'an Jiaotong University, Xi'an, China

Anode phenomena has been studied experimentally by arc appearance and optical emission spectroscopy (OES) [1-3]. Under the effect of anode evaporation, anode vapor is emitted into the arc column leading to different kinds of anode modes including footpoint mode, anode spot (AS, type 1 and type 2) mode and anode plume (AP) mode. Under different discharge modes, the temporal and spatial distributions of different components have been reported in many works. This paper investigates the arc behaviors with CuCr25 also CuCr50 electrodes considering the anode vapor using 2D magneto-hydro-dynamic model[4][5]. Different kinds of components are considered including ions (Cu and Cr) with different charge numbers, electrons and atoms (Cu and Cr). The effect of the anode sheath is also considered. The density distributions of these components are analyzed and compared with the experiments during anode spot (AS) mode and anode plume (AP) mode. Simulation results show that the anode vapor can enter the arc column forming a cool and poorly conducting region (i. e. neutral atom vapor area, NAVA) under high anode temperature. Atoms and single-charged ions mainly gather near each electrode. The highest double-charged ion density can be seen in front of the NAVA. Triple-charged ion density is negligibly low and reaches its maximum where electron temperature is high. Cr is more likely to be ionized to higher ionization level compared with Cu. Our results agree with experimental measurements of density distributions of different components and plasma temperature. The typical comparisons between simulation and experimental result are shown in Fig.1.

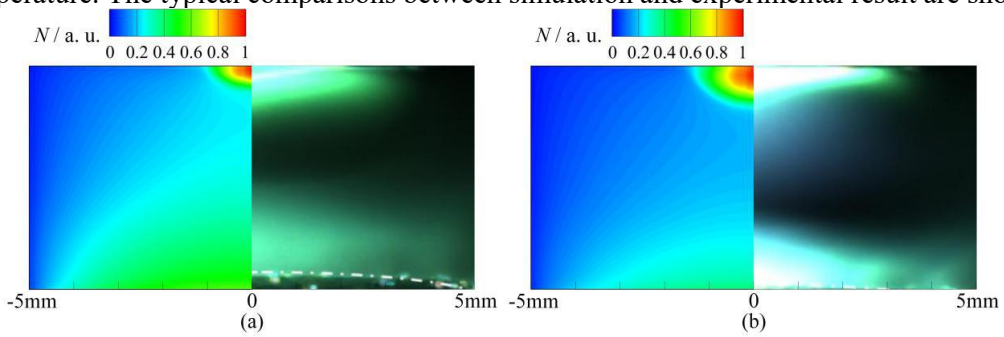

Fig. 1. Comparison of arc appearance during AS mode. (a) Simulation result when T_{anp} = 2250K with experimental appearance at 5.32ms [6], and (b) simulation result when T_{anp} = 2300K with experimental appearance at 5.42ms [6].

Here are some conclusions. Atoms and ions are ionized level by level. Atom density is very high inside the NAVA. Single-charged ion density has two maximum values: one in the NAVA and the other near the cathode. The highest double-charged ion density can be seen in front of NAVA. Triple-charged ions have very low density and gather where electron temperature is high. Compared with Cu, Cr is easier to be ionized to high ionization level. So inside the NAVA, Cu^{1+} density reaches its maximum farther from the anode than Cr^{1+} density. The Cr^{1+} layer is thinner than Cu^{1+} near the cathode, where Cr^{2+} density reaches its maximum. Similarly, Cr^{3+} density can even higher than Cu^{3+} density in front of the NAVA. These distributions of agree with the experimental results. The sign of the anode sheath potential remains negative and the magnitude of it decreases with the increase of anode surface temperature.

REFERENCES

[1] H. Craig Miller, "Anode Modes in Vacuum Arcs: Update", IEEE Trans. Plasma Sci., vol. 45, no. 8, pp. 2366-2374, August 2017.

[2] A. V. Batrakov, S. A. Popov, A. V. Schneider, G. Sandolache, and S. W. Rowe, "Observation of the plasma plume at the anode of high-current vacuum arc", IEEE Trans. Plasma Sci., vol. 39, no. 6, pp. 1291-1295, June 2011.

[3] A. Khakpour, D. Uhrlandt, R. Methling, S. Franke, S. Gortschakow, S. Popov, A. Batrakov, and K. Weltmann, "Impact of different vacuum interrupter properties on high-current anode phenomena", IEEE Trans. Plasma Sci., vol. 44, no. 12, pp. 3337-3345, December 2016.

[4] Lijun Wang, Ze Yang, Jing Jiang, Yuan Wang, Shenli Jia, "Modeling of Vacuum Arc Behavior under Anode Spot and Anode Plume Modes", Applied Physics Letters, vol. 115, pp. 014101, 2019.

[5] Ze Yang, Lijun Wang, Jie Deng, Shenli Jia, "Modeling of vacuum arc plasmas in anode spot or anode plume mode taking into account multiple ion components", Journal of Applied Physics, vol. 126, pp. 193306, 2019.

[6] A. Khakpour, R. Methling, S. Franke, S. Gortschakow, and D. Uhrlandt, "Vapor density and electron density determination during high-current anode phenomena in vacuum arcs", J. Appl. Phys., vol. 124, pp. 243301, 2018.

EXPLOSIVE ELECTRON EMISSION PULSES PLASMA PARAMETERS ESTIMATION FROM MODEL BASED ON TRANSITION OVER CRITICAL STATE*

M.M. TSVENTOUKH[1], D.L. SHMELEV[2], and S.A. BARENGOLTS[3,1]

[1]Lebedev Physical Institute of Russian Academy of Sciences, Moscow, Russia
[2]Institute of Electrophysics of Ural Branch of Russian Academy of Sciences, Ekaterinburg, Russia
[3]Prokhorov General Physics Institute of Russian Academy of Sciences, Moscow, Russia

Pulsed-periodic formation of explosive electron emission (EEE) splashes plays essential role in operation of vacuum arc cathode spot providing both electron emission and current-carrying plasma. Estimation of its parameters is a key question of cathode-spot theory and requires detailed numerical modelling and general phenomenological approach.

A simple throughout model explosive-electron emission pulses in a vacuum arc cathode spot based on transition of the matter over the critical state during the explosion has been recently developed in [1-2]. It predicts set of parameters for plasma of the cathode-spot explosive cells, in particular, average plasma density – of about 10^{20} cm^{-3} and temperature – about eV. The estimated electron drift (current) velocity v_{1e} is about the ion acoustic velocity ~$(T_{cr}/M_i)^{1/2}$. The measured ion velocity v_i ~ 5-20 km/s nearly corresponds to $(T_{cr}/M_i)^{1/2}$ with proportionality coefficient of about 12 for different materials see Table.

The EEE plasma momentum per transferred charge has been estimated as

$$\mu = \frac{T_{cr}}{Zev_{1e}} \approx \frac{\sqrt{M_i T_{cr}}}{Ze}.$$

This formula yields μ of some tens of g cm / (s C), which complies with the measured specific recoil force and the EEE plasma flare momentum estimated as $v_i \times \gamma_i$, the product of the measured ion velocity and erosion rate: v_i ~10 km/s, γ_i ~0.1 mg/C. In addition, it agrees with the liquid-metal fraction momentum that can be estimated as $v_l \times \gamma_{liq}$, where $v_l \sim 10^4$ cm/s and γ_{liq} ~ 1 mg/C. Thus, one may note that

$$v_l \times \gamma_{liq} \approx \mu \approx v_i \times \gamma_i.$$

The average over the EEE-pulse ohmic electric field providing the current transfer through the EEE plasma has been estimated to be about few V/μm. This agrees with known experimental results on the cathode potential fall and its oscillations and EEE-plasma size.

The relationship between the critical parameters of a surface material with a developed micro and nanostructure and the charge state of vacuum arc ions has been determined [3]. It was proposed that reduction of effective critical temperature due to formation of nanostructure being responsible for the ion charge reduction. The developed model is consistent with the latest experimental data from [4]. Whereas the single-metal cathodes exhibit correlation in the plasma velocity and burning voltage with the corresponding critical temperatures the mixed materials demonstrate lower velocity and voltage that may be attributed to the their fine-stricture of surface.

	T_{cr}, K	M_i/M_p	α_i	Z	v_i, cm/s	μ, g cm/s C	$v_i \times (M_i/T_{cr})^{1/2}$
Li	3223	6.9	~0.1	1	2.30E+06	14.5	11.5
Cu	8390	63.55	0.114	2.06	1.32E+06	34.4	12.4
W	21010	183.9	0.05	3.07	1.11E+06	62.1	11.2
Pb	4980	207.2	0.143	1.64	5.80E+05	60.0	12.7

REFERENCES

[1] G.A. Mesyats and M.M. Tsventoukh 2015 *IEEE Trans. Plasma Sci.* **43** 3320
[2] M.M. Tsventoukh 2018 *Physics of Plasmas* **25** 053504
[3] S.A. Barengolts *et al* 2020 *Nucl. Fusion* **60** 044001
[4] Siegfried Zöhrer *et al* 2020 *Plasma Sources Sci. Technol.* **29** 025022

* The work was supported in part by RFBR grant 19-08-01249.

DURABILITY OF INDUCTOR MATERIAL WITH INHOMOGENIOUS RESISTANCE UNDER HIGH PULSE MAGNETIC FIELD GENERATION*

P.A. RUSSKIKH, G.SH. BOLTACHEV, S.N PARANIN

Institute of Electrophysics UB of RAS, Ekaterinburg, Russia

When generating high pulsed magnetic fields with an amplitude of 40-60 T with a half-wave duration of 5-20 microseconds, the working surface of the inductor is subjected to large thermomechanical stresses caused by both Joule heating of the skin layer and Ampere force. As a result of such action, the material of the working surface of inductor is destroyed either by plastic deformation or by the formation of cracks perpendicular to the current direction. One of way to solve this problem is presented in the work [1], in which without considering thermal effects was shown, that in material with decreasing by depth resistance heating significantly reduces due to that the current-carrying layer, and, accordingly, the heating and the force action are at some depth from the working surface of the inductor. This work is aimed simulation and estimation of durability of conductive material with temperature dependant inhomogeneous resistance in high pulsed magnetic fields.

A set of electromagnetic, thermal, elastic and plastic processes occurring in conductive material with some surface layer simulated in single dimension plane geometry based on magnetic diffusion and heat-transfer equations, Hooke's law and yield criterion von Mises. External magnetic field was taken as decreased sinusoid. Evolution of thermomechanical stresses and deformations appearing in material was simulated both during the magnetic pulse and subsequent process of thermomechanical relaxation until complete cooling. Initial resistance was assumed as two parameters function with close to step form. The first parameter is the ratio of surface and bulk resistance ρ^*/ρ_{bulk} and the second one is depth of modified layer x_c. Resistance and tensile strength dependences on temperature were approximated by linear function. Expansion coefficient, specific heat and other parameters were assumed constant for the process and the same through the material. In calculation ρ^*/ρ_{bulk} and x_c were less than 2.5 and 1.6 mm, respectively. The magnetic field value B_{th} that results in growth of residual plastic deformations under action of the same subsequent pulses was assumed as destruction criterion. Simulating and experimental results have a good agreement for steel 30KhGSA with homogeneous resistance under magnetic field with an amplitude B_{th} of 50 T with a half-wave duration of 12 us [2].

Simulation results show that in calculating area for any value of ρ^*/ρ_{bulk} there is an optimal value of surface layer thickness x_c, which increases with growth of ρ^*/ρ_{bulk} but being less than 0.5 mm. The best effect in simulating space was achieved at ρ^*/ρ_{bulk} and x_c equaled 2.5 and 0.45 mm, respectively. In this case B_{th} was enlarged from 50 to 60 T.

REFERENCES

[1] G.A. Shneerson, Fields and transients in equipment superstrong currents, Leningrad: Energoizdat Publ., 1981.

[2] A.V. Spirin, G.Sh. Boltachev, V.I. Krutikov et al, “Surface Modification of Steel Inductor as an Attempt to Enhance Its Durability in High Pulsed Magnetic Fields,” Proc. VI International Young Researchers’ Conference: Physics, Technologies and Innovation, Ekaterinburg, Russia, pp. 198–199, 2019.

* The work was supported by RFBR grant No. 19-08-00931 (P.A. Russkikh, S.N. Paranin) and RSF grant No. 20-19-00364 (G. Sh. Boltachev).

NON-EQUILIBRIUM MODELLING OF DC NITROGEN MICROPLASMAS: FROM GLOW TO ARC DISCHARGE*

A.I. SAIFUTDINOV, A.A. SAIFUTDINOVA, B.A. TIMERKAEV

[1] *Kazan National Research Technical University named after A.N.Tupolev, Kazan, Russia*

Atmospheric pressure direct current discharges are of interest as plasma sources for a number of technological applications, including plasma decontamination and sterilization, biomedical applications, material processing, modification of electromagnetic waves propagation, and plasma aerodynamics.

In this work micro-plasma discharges in nitrogen, at atmospheric pressure, are simulated using a one-dimensional extended fluid model. The model includes charged, exited and neutral species conservation with fairly complete set of chemical reactions, including several processes with the participation of electronically exited nitrogen atoms describing the energy balance and charged particles kinetic processes in the discharge, a self-consistent solution of the electric field, electron and neutral gas temperatures, vibrational relaxation and an external circuit model. In addition, conjugate heat transfer in both the cathode and the anode is considered [1-3].

Special attention is given effects of the conjugate heat transfer on the gas temperature and discharge characteristic predictions, such as the current–voltage characteristics (CVCs). A classical shape for the CVCs [4] of a discharge is obtained, with all observable sections: a glow discharge, an abnormal glow discharge and an arc (Fig.1). Dependences of the electrode surface temperatures on the discharge current density are obtained. For each point of the CVC, all basic parameters of the electrical discharge, including a temperature field in the electrode gap and in the metal electrodes, are obtained.

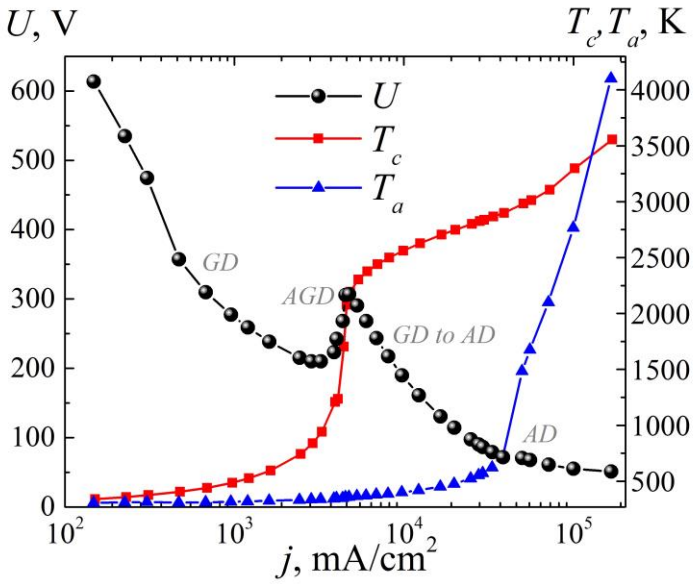

Fig.1. Dependence between the reduction of voltage in the discharge interval, and dependence between the cathode and anode surface temperature, and the current density in the cathode.

REFERENCES

[1] A. I. Saifutdinov, I. I. Fairushin, N. F. Kashapov,"Analysis of various scenarios of the behavior of voltage-current characteristics of direct-current microdischarges at atmospheric pressure", JETP Letters, vol.104, №3, 180–185, 2016.

[2] M.Baeva , D.Loffhagen , M.M.Becker , D.Uhrlandt , Plasma Chem. Plasma Process., 39:4, 949–968, 2019.

[3] S.I. Eliseev, A.A. Kudryavtsev, H. Liu, Z. Ning, D. Yu, A.S. Chirtsov "Transition from glow microdischarge to arc discharge with thermionic cathode in argon at atmospheric pressure", IEEE Trans Plasma Sci Vol.44, Article number 2536, 2016

[4] L.B. Loeb, Fundamental Processes of Electrical Discharges In Gases, New York, 1950.

* The reported research was funded by Russian Foundation for Basic Research, grant № 19-31-90101

NUMERICAL STUDY OF THE KINETICS AND GAS HEATING EFFECTS ON THE FORMATION AND EVOLUTION OF MICROWAVE STREAMERS IN AIR *

A.I. SAIFUTDINOV[1], *E.V. KUSTOVA*[2]

[1] *Kazan National Research Technical University named after A.N.Tupolev, Kazan, Russia*
[2]*Saint-Petersburg State University*

Advances in microwave electronics created possibilities to initiate various types of microwave discharges in a wide range of conditions. The objectives of the present study are: 1) to generalize the model proposed in [1] for the focused microwave discharge in air by taking into account, in a self-consistent way, coupled electrodynamic, gas dynamic, kinetic processes; 2) to apply the developed model for the description of the focused microwave air discharge obtained experimentally using a cylindrical paraboloid in [2]; 3) to perform numerical simulations of such discharges in a wide range of input power (100-250 kW) and gas pressure (23-70 Torr) and analyze the dynamics of plasmoid formation and their number as well as distributions of fluid dynamic variables: molar fractions of charged and excited species, gas temperature, nitrogen vibrational temperature. Moreover, key channels of fast air heating and gas-dynamic parameters in the domain of discharge formation are discussed.

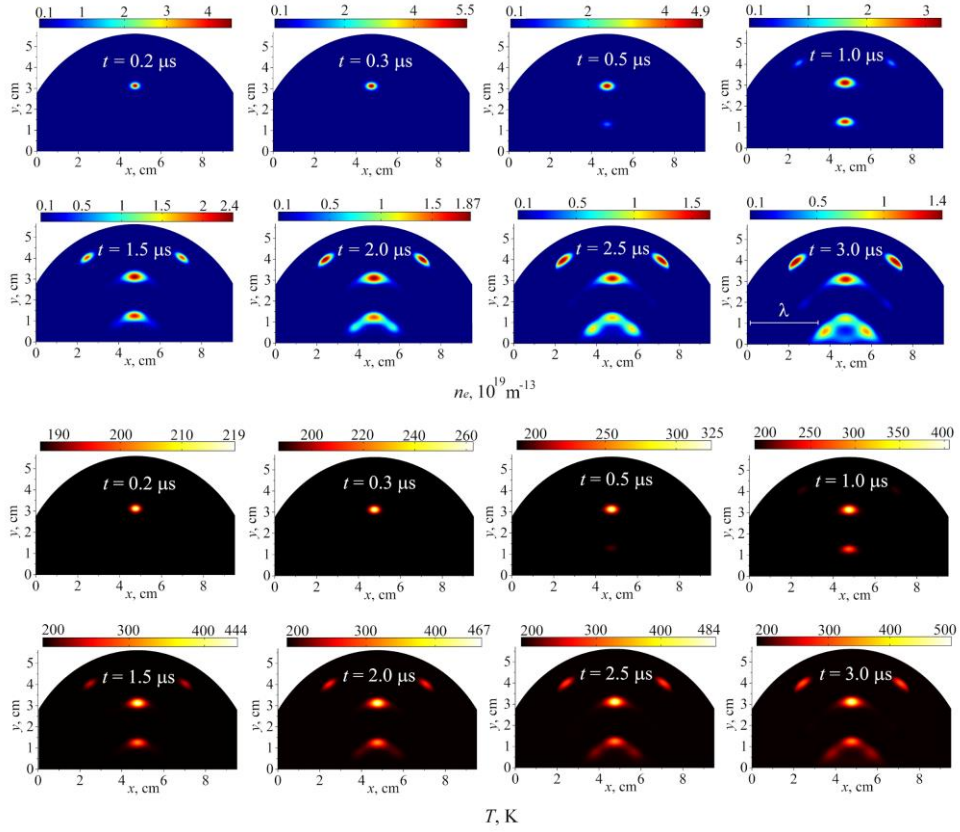

Fig.1. Spatial distributions of electron number density and gas temperature at different times.

REFERENCES

[1] A.I.Saifutdinov, E.V.Kustova, A.G.Karpenko, et al. "Dynamics of Focused Pulsed Microwave Discharge in Air", Plasma Phys. Rep. Vol. 45, 602–609, 2019.

[2] V. A.Lashkov, A. G.Karpenko, R. S.Khoronzhuk, and I. Ch.Mashek, "Effect of Mach number on the efficiency of microwave energy deposition in supersonic Flow", Physics of Plasmas vol.23, Article Number 052305, 2016.

* This study received support from the Russian Foundation for Basic Research, project 18-08-00707 and a grant from the President of the Russian Federation for young scientists MK-272.2019.1

CURRENT-VOLTAGE CHARACTERISTICS OF THE HIGH-FREQUENCY ARC DISCHARGE IN THE AIR.

A.F. KOKORIN

40 let komsomola 32a-41, Yekaterinburg, 620072, RF, a.f.kokorin@urfu.ru, 79089099061

The paper considers the results of a theoretical and experimental study of a high-frequency arc discharge [1] in air at pressures above atmospheric. The model of this type of discharge allowed the calculation of current-voltage characteristics and the energy balance of the high-frequency arc, depending on the geometrical dimensions of the discharge chamber of the plasma torch for different pressures and flow rates of the plasma gas.

The main dependences obtained by theoretical analysis of the high-frequency arc discharge are current-voltage and current-temperature characteristics of the discharge. Due to the used theoretical model, the calculated characteristics are applicable not only to the high-frequency arc, but also to high-voltage low-current arcs of direct current.

The calculated current-voltage characteristics have a falling character. In this case, the degree of inclination changes insignificantly with changes in pressure and gas flow rate, length of the discharge gap, and diameter of the discharge tube.

An important feature of the arc discharge in air is the appearance of overheating instability associated with the non-monotonic dependence of the thermal conductivity of air on temperature. The non-monotonous nature of thermal conductivity is associated with the dissociation of nitrogen and oxygen molecules and has two peaks: in the temperature range (3500-4500) K and (7000-10000) K. The position of the peaks depends on pressure. With its increase, the peaks are shifted toward higher temperatures. As a result of overheating instability, current surges and plasma temperatures appear, and loop-shaped sections appear on the current-voltage characteristics of the arc.

Overheating instability was confirmed by an experimental study of the high-frequency arc discharge. The current jumps were accompanied by a sharp rise in plasma temperature and radiation from the discharge region. The active power of the discharge increased, but the reactive power of the discharge increased especially strongly. This is due to both an increase in current and discharge inductance caused by a decrease in the radius of the conductive zone.

Some of the materials presented in this work were obtained during the implementation of the stages of work on the RFBR project No. 18-38-00598 (manager R. Muftakhetdinova, completed in March 2020).

REFERENCES

[1] *Kokorin // Vestnik UGTU-UPI. – 1976. – Vol.231. – № 2. 326-329.*

ESTIMATION OF THE NEUTRON GENERATION INTENSITY IN THE MAGNETO- INERTIAL PLASMA CONFINEMENT SCHEME*

V.V. KUZENOV, S.V. RYZHKOV, A.V. STAROSTIN

Bauman Moscow State Technical University, 2 Baumanskaya Street, 5, 1, Moscow, 105005, Russia, E-mail: svryzhkov@bmstu.ru, +7(499)263-65-70

The paper presents mathematical modeling of the interaction of a magnetized target with laser radiation [1-15], and the incoming laser radiation flux is divided into two parts - the first along the cylindrical surface, and the second is introduced through the end face of the target. The laser switching circuit works sequentially after a certain period of time. Methods and models for numerical simulation of individual characteristics of the target in external and spontaneous magnetic field under combined (laser plus plasma jet) exposure are developed.

Graphs for target temperature, pressure, density, velocity, and magnetic pressure are plotted for different time after the onset of laser action with intensities 10^{14} W/cm^2, 10^{15} W/cm^2 and 10^{16} W/cm^2. As an example, the temperature distribution along the target radius is shown for neutron flux $3{,}08 \times 10^{14}$ n/cm at time 9.99 ns.

The results of calculating the combined (a system of pulsed jets and laser radiation acting on a target in the end and perpendicular generatrix directions) effects of intense energy flows on a cylindrical target located in an external magnetic field are presented. The parameters of a compressed plasma are demonstrated and the possibility of creating neutron generators based on a combined scheme is shown — the number of neutrons per unit length Nfus $\approx 10^{15}$ n/cm by the time the exposure is completed.

REFERENCES

[1] *Sivkov A.A., Shanenkov I.I., Ivashutenko A.S., Gukov M.I., Li L., Li G., Khan V.* // Russian Physics Journal. – 2019. – V. 62. – P. 1001-1008.
[2] *Kuzenov V.V., Ryzhkov S.V., Starostin A.V.* // Russian Physics Journal. – 2019. – Vol. 62.
[3] *Ryzhkov S.V., Kuzenov V.V.* // ZAMP. – 2019. – Vol. 70. – P. 46.
[4] *Kuzenov V.V., Ryzhkov S.V.* // Laser Physics. – 2019. – Vol. 29. – P. 096001.
[5] *Kuzenov V.V., Ryzhkov S.V.* // Journal of Physics: Conference Series. – 2017. – V. 815. – P. 012024.
[6] *Ryzhkov S.V., Kuzenov V.V.* // International Journal of Heat and Mass Transfer. – 2019. – Vol. 132. – P. 587-592.
[7] *Shanenkov I.I., Sivkov A.A., Ivashutenko A.S., Medvedeva T., Shchetinin I.* // Journal of Alloys and Compounds. – 2019. – V. 774. – P. 637-645.
[8] *Kuzenov V.V., Ryzhkov S.V.* // Physics of Plasmas. – 2019. – Vol. 26. – P. 092704.
[9] *Kuzenov V.V., Ryzhkov S.V.* // Journal of Physics: Conference Series. – 2017. – V. 830. – P. 012124.
[10] *Kuzenov V.V., Ryzhkov S.V., Frolko P.A.* // Journal of Physics: Conference Series. – 2017. – V. 830. – P. 012049.
[11] *Kuzenov V.V., Ryzhkov S.V.* // Mathematical Models and Computer Simulations. – 2018. – Vol. 10. – P. 255-264.
[12] *Kuzenov V.V., Ryzhkov S.V.* // Journal of Enhanced Heat Transfer. – 2018. – V. 25 (2). – P. 181-193.
[13] *Kuzenov V.V., Ryzhkov S.V.* // Physics of Atomic Nuclei. – 2018. – Vol. 81, No. 10. – P. 1460-1464.
[14] *Kuzenov V.V., Ryzhkov S.V., Shumaev V. V* // Applied Physics. – 2014. – No. 3. – P. 22-25.
[15] *Sivkov A., Shanenkova Y., Saigash A., Shanenkov I.* // Surface and Coatings Technology. – 2016. – Vol. 292. – P. 63-67.

* The work was partially supported by the Russian Ministry of Science and Higher Education (Project No. 0705-2020-0044).

MODELLING LINE PROFILES OF THE HELIUM SPECTRA EXCITED BY AN ALTERNATING ELECTRIC FIELD

E.V. KORYUKINA[1], *V.I. KORYUKIN*[2]

[1]*National Research Tomsk state University, Tomsk, Russia*
[2]*Siberian State Medical University, Tomsk, Russia*

In this work, we develop a new theoretical method for calculating the line profiles in atomic emission spectra excited by an alternating electric field. In the framework of the suggested approach based on a numerical solution of the non-stationary Schrödinger equation the spectral line profiles are determined by the three-step procedure. In the first step, the wave functions and the energies of an atom in an alternating electric field are computed by diagonalization of the energy matrix of an atom in the electric field. In the second step, the obtained wave functions and energies are used for calculating the spectroscopic characteristics of atoms such as the positions of the Stark components of spectral lines, the transition probabilities between the Stark states of atoms, and the Stark component intensities. In the third step, these spectroscopic characteristics are used for calculating the total profiles of atomic spectral lines in the electric field.

It should be noted that we calculated the krypton line profiles in alternating electric fields earlier [1]. But, in those computations, the influence of the electric field was taken into account only in calculating the positions and the intensities of spectral lines, in doing so, the Stark profile itself was not calculated. In the present work, we use a new formula for calculating the quadratic Stark-effect constant C_4, where C_4 contains the dependence on the electric field strength and frequency in an explicit form. Using this formula, we compute the profile of each spectral line as a convolution of the Doppler and the Stark profiles. The algorithm of the developed approach is implemented in a special software package StarkD written in FORTRAN and Maple.

In the present work, the helium atom is chosen as the object of study, since exactly this atom has been studied better than other atoms both experimentally and theoretically; therefore, it is the best object to test the adequacy and the efficiency of the developed theoretical approach. First of all, to verify the correctness and the efficiency of our theoretical approach, we calculate the profile of the 2^1P_1-3^1D_2 spectral line of the helium spectrum radiated by the plasma of a current sheet. The results of our calculations completely agree with experimental results [2]. Then, in the framework of our approach, we study the behavior of the helium line profiles depending on the electric field strength and frequency. In addition, we investigate the dependences of the spectral line profiles on the electron density of plasma and the temperature of the helium atoms.

As our calculations have shown, the suggested theoretical approach implemented in the package StarkD is an efficient and reliable instrument for the simulation of the spectral line profiles of atoms in alternating electric fields. This method is free from limitations of perturbation theory and valid for electric fields with the frequency and strength changing in wide ranges. The results obtained allow one to analyze mechanisms of the formation of atomic emission spectra in the electric field and to explain processes taking place in plasma.

Wide potentialities of the developed approach are very useful in solving many practical problems of plasma diagnostics, magnetic reconnection and all branches of physics, where one needs to investigate the influence of alternating electric fields on properties of the object of study. In addition, the software package StarkD can be used for the development of new radiation sources and for searching the optimal operating mode of already existing radiation sources.

REFERENCES

[1] E. V. Koryukina, V. I. Koryukin, “Simulation of line profiles of the krypton spectra emitted by the plasma of current sheets,” Rus. Phys. J., vol. 61, no. 12, pp. 2268–2276, April 2019.

[2] A. G. Frank, V. P. Gavrilenko, N. P. Kyrie, E. Oks, “Spectroscopic study of anomalous electric fields in peripheral regions of a current sheet plasma,” J. Phys., vol. B39, no. 24, pp. 5119–5129, December 2006.

SELFCONSISTENT SIMULATION OF DEVELOPMENT OF ANODE SPOT IN HIGH CURRENT VACUUM ARC*

D.L. SHMELEV[1], I.V. UIMANOV[1], S.A. BARENGOLTS[2], M.M. TSVENTOUKH[3], LIJUN WANG[4]

[1]*Institute of Electrophysics, UB, RAS, Ekaterinburg, Russia*
[2]*Prokhorov General Physics Institute, RAS, Moscow, Russia*
[3]*Lebedev Physical Institute, RAS, Moscow, Russia*
[4]*State Key Laboratory of Electrical Insulation and Power Equipment, Xi'an Jiaotong University, Xi'an, China*

A self-consistent simulation of anode heating by heat fluxes from interelectrode plasma of high-current vacuum arc (HCVA) during the 50 Hz contact opening was carried out. The calculations were done in the framework of hybrid HCVA model [1]. As a result of the simulation, the appearance of an anode plasma spot of type II was obtained [2], which was accompanied by a sharp increase in the voltage drop across the arc and the appearance of a plasma plume similar to the plume observed in the experiment [3]. It is shown that one of the main reasons for the appearance of the anode plasma plume may be the energy flux of linear radiation from the interelectrode plasma to the anode.

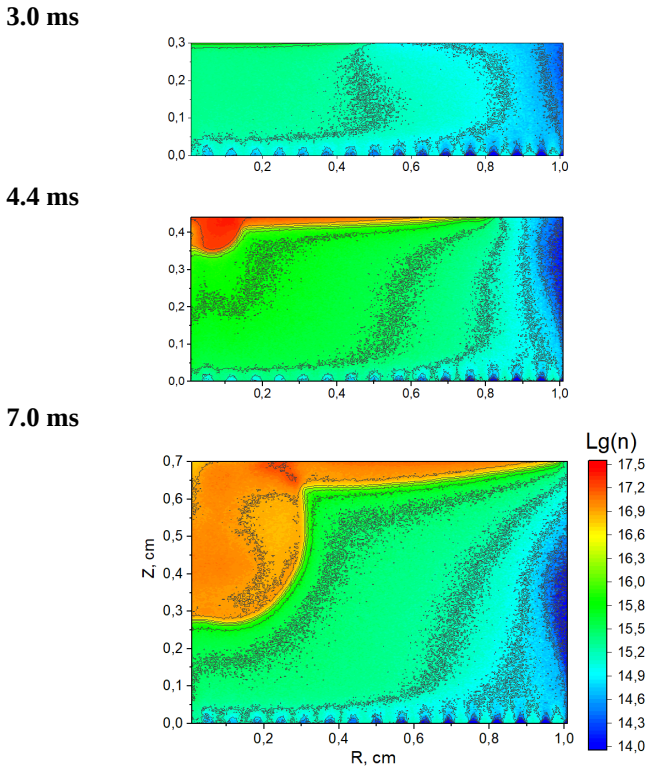

Fig.1. Distributions of total (ions + atoms) plasma density in interelectrode gap at different instants. Anode is at the top.

REFERENCES

[1] D.L. Shmelev, V.I. Oreshkin, I.V. Uimanov, "Hybrid numerical simulation of high-current vacuum arc taking into account secondary plasma generation", IEEE Trans. Plasma Sci., vol. 47, pp. 3478- 3483, 2019.

[2] H.C. Miller, "Anode modes in vacuum arcs: Update", IEEE Trans. Plasma Sci., vol. 45, pp. 2366-2374, 2017.

[3] A.V. Schneider, A.V. Popov, V.F. Lavrinovich, and D.D. Maral, "An investigation of regular patterns of the anode spot glow in a high-current vacuum arc by the method of high-speed photography", Russian Phys. J., vol. 61, pp. 1324-1328, 2018.

* The work was supported by the Russian Foundation for Basic Research (grants No. 18-08-00547, 19-08-00783, 19-58-53006). The work partially supported by National Natural Science Foundation of China (project No: 51911530113).

EVOLUTION OF THE SPECTRAL CHARACTERISTICS OF LASER RADIATION IN A GAS AMPLIFIER OF A THL-100 LASER SYSTEM *

A.G. YASTREMSKII, V.F.LOSEV

Institute of High Current Electronics SB RAS, Tomsk, Russia

The main goal of the work is to study the effect of the frequency shift in the XeF (C-A) amplifier on the spectral characteristics and energy of the output radiation of the THL-100 laser system. We studied the amplification of linearly chirped Gaussian laser beams of full width at half maximum of the intensity (FWHM) 250 ps with input energy of 2 mJ and central wavelength λ_0=475 nm. Time-frequency distributions of input linearly chirped Gaussian pulses W(t,λ) were obtained using the Wigner function of these pulses [1, 2]. The calculated emission spectra at the input to the amplifier and at its output window are consistent with experimental data.

At the amplifier pump energy of E_p= 270 J the calculated maximal density of output radiation spectral intensity was 0.12 10^{12} W cm^{-2} nm^{-1} at the wavelength λ_0 = 481.705 nm and 0.128 10^{12} W cm^{-2} nm^{-1} at λ_0 = 471.50 nm at positive and negative chirps, respectively. The dependences of the spectral energy density S (λ) of the laser radiation at the amplifier output window are obtained for the positive and negative input radiation chirp. It is shown that in the gain saturation mode, these values differ insignificantly and are equal to S(λ)=5.9 mJ cm^{-2} nm^{-1}.

REFERENCES

[1] L.Cohen. Time-Frequency Analysis, Prentice-Hall, PTR. 1995.

[2] L. Praxmeier and K. Wókiewicz. “Time and frequency description of optical pulses”, Laser Physics, vol 15, no 10, pp 1477-1485, 2005.

* The work was supported by Russian Science Foundation under grants No. 18-08-00407, 18-08-00383,.

CALCULATION CHARACTERISTICS OF THE ELECTRON BEAM INJECTED INTO THE PLASMA OF THE OPEN MAGNETIC TRAP GDT *

V.T. ASTRELIN, P.A. BAGRYANSKY, D.I. SKOVORODIN, E.I. SOLDATKINA

Budker Institute of Nuclear Physics SB RAS, Novosibirsk, Russia

Studies on heating and confinement of dense subthermonuclear plasma are conducted at the open magnetic trap (GDT) at the Budker INP SB RAS [1]. The trap is a mirror cell with a large mirror ratio based on gas-dynamic plasma confinement. Recent experiments with plasma generation and electron heating at the cyclotron frequency by microwave radiation and heating of ions by powerful beams of neutral atoms [2] have demonstrated high plasma parameters and the promising methods of heating. Then, the experiments were conducted to introduce a radial electric field into the plasma using a system of ring diaphragms with different potentials installed inside the end expanders. They demonstrated stabilization of azimuthal instabilities and suppression of transverse losses [3].

An experiment is currently being conducted to inject the electron beam into the trap from the expander [4]. We study the possibility of gas ionization by the beam to create plasma in the trap, form a radial electric field in it, and suppress longitudinal energy losses from the plasma.

The plasma flowing out of a magnetic trap can enter the beam source and interfere with its operation, deforming the field structure of the electron-optical system, affecting the beam characteristics and even leading to electrical breakdowns in the source. Therefore, the source is located in the expander in the region of a small magnetic field with a safe energy flux density. In this case, it should form an electron beam with a small angular divergence of electrons, which will pass into the trap through the inlet plug with a large magnetic field. To calculate such a source, it is necessary to carry out a numerical simulation of its operation, taking into account the entering plasma flow.

The electron-optical characteristics of the beam formed in the source are determined by the configuration and potentials of its surfaces. The surface of the plasma entering the source is one of such electrodes. However, shape of plasma surface itself depends on electric field in the source and plasma characteristics. Therefore, an analysis was made of the equilibrium state and boundary conditions on the plasma surface for the conditions of the GDT experiment [5]. The results of the analysis are implemented in computational algorithms.

In the numerical simulation of the source, the angular and spatial characteristics of generated beam are determined. It was shown that the liner installed at the source output absorbs electrons with large angular velocities at the periphery of the beam (~ 20-30% of the beam current), decreasing the number of electrons reflected by the trap. Thus, in the experiment, large beam pulse duration without breakdowns was achieved.

REFERENCES

[1] A.A. Ivanov, V.V. Prikhodko, "Gas dynamic trap: experimental results and future prospects", Phys. Usp., vol.60, pp.509–533 (2017). DOI: 10.3367/UFNe.2016.09.037967

[2] P.A. Bagryansky, A.G. Shalashov, E.D. Gospodchikov et al. "Threefold increase of the bulk electron temperature of plasma discharges in a magnetic mirror device", Phys. Rev. Lett., vol.114, p.205001, 2015. DOI: 10.1103/PhysRevLett.114.205001

[3] A.D. Beklemishev, P.A. Bagryansky, M.S. Chaschin, E.I. Soldatkina, "Vortex confinement of plasmas in symmetric mirror traps", Fus. Sci. Tech., Vol. 57, No 4, PP.351-360, 2010. https://doi.org/10.13182/FST10-A9497

[4] E.I. Soldatkina, V.T. Astrelin, P.A. Bagryansky et al. "Megawatt electron beam for GDT device", Abstracts of the XLVI International Zvenigorod Conference on Plasma Physics and Controlled Fusion, Zvenigorod, March 18 - 22, 2019, p. 96. http://www.fpl.gpi.ru/Zvenigorod/XLVI/Zven_XLVI.html

[5] V.T. Astrelin. Boundary conditions in the source of an electron beam on the surface of the anode plasma with a supersonic ion stream // Russian Physics Journal, 2020, Vol. 63, No 8 (paper in press).

* The work was supported by the Russian Ministry of Science and Higher Education. Theoretical part was supported by RFBR Grant 18-72-10084.

EFFECT OF THE GEOMETRY OF CATHODE MICROPROTRUSIONS ON THE PARAMETERS OF THE EXPLOSIVE EMISSION PROCESSES[1]

E.V . ORESHKIN[1], *S.A. BARENGOLTS*[2], *V. I. ORESHKIN*[3], *K.V. KHISCHENKO*[4], *G.A. MESYATS*[1]

[1]*Lebedev Physical Institute, RAS, Moscow, Russia*
[2]*Prokhorov General Physics Institute, RAS, Moscow, Russia*
[3]*Institute of High Current Electronics, SB, RAS, Tomsk, Russia*
[4]*Joint Institute for High Temperatures, RAS, Moscow, Russia*

Explosive electron emission in a diode is accompanied not only by an increase in diode current and formation of plasma jets, but also by splashing of molten metal from the cathode and formation of microcraters on the cathode surface. These processes are extremely undesirable, in particular, for future fusion devices, in which the initiation of explosive electron emission leads to unipolar arcing at surfaces exposed to the reactor plasma [1, 2]. Explosive emission processes also underlie the radio frequency vacuum breakdowns that may occur at the walls of accelerating structures in linear electron-positron colliders [3–6].

We have investigated the parameters of the microexplosion processes in relation to the cathode microprotrusion geometry for tungsten, as a candidate for the divertor material in future fusion devices, and copper, which will be used for the accelerating structure of the Compact Linear Collider (CLIC) being developed at CERN [7]. In the study presented here, the JULIA magnetohydrodynamic (MHD) code [4, 5] was used. The system of MHD equations that was solved with this code was composed of hydrodynamics equations describing the laws of conservation of mass, momentum, and energy. The semi-empirical wide-range equations of state [8] used in the simulation took into account high-temperature melting and evaporation. To calculate the electrical characteristics of the microprotrusion and its thermal conductivity, tabulated data on the conductivity of copper were used [9].

The microexplosion parameters (the pre-explosion time and the specific current action integral) have been estimated, in view of the explosive electron emission from the cathode, in relation to the (conical and cylindrical) geometry of the microprotrusion and the type (direct-current and high-frequency) voltage across the diode. The parameters of the microcrater formed on a cathode as a result of the electrical explosion of a microprotrusion have been analyzed.

REFERENCES

[1] S. Kajita, S. Takamura, and N. Ohno, “Prompt ignition of a unipolar arc on helium irradiated tungsten,” Nucl. Fusion , vol. 49, p. 032002, 2009.

[2] S. A. Barengolts, G. A. Mesyats, and M. M. Tsventoukh, “The ecton mechanism of unipolar arcing in magnetic confinement fusion devices,” Nucl. Fusion, vol. 50, p. 125004, 2010.

[3] G. A. Mesyats, High Power Microwave Generation and Applications , , Bologna, Italy: SIF, 1992, p. 345.

[4] S. A. Barengolts, V. G. Mesyats, V. I. Oreshkin, E. V. Oreshkin, K. V. Khishchenko, I. V. Uimanov, and M. M. Tsventoukh, “Mechanism of vacuum breakdown in radio-frequency accelerating structures,” Phys. Rev. Accel. Beams, vol. 21, no. 6, June 2018, Art. no. 061004.

[5] S. A. Barengolts, E. V.Oreshkin, V. I. Oreshkin, and K. V. Khishchenko, “Simulation of the Explosion of a Surface Microprotrusion During a Radio Frequency Breakdown,” IEEE Trans. Plasma Sci., vol. 47, no. 8, pp. 3406–3411, Aug. 2019.

[6] S. A. Barengolts, I. V. Uimanov, and D. L. Shmelev, “Prebreakdown Processes in a Metal Surface Microprotrusion Exposed to an RF Electromagnetic Field,” IEEE Trans. Plasma Sci., vol. 47, no. 8, pp. 3400–3405, Aug. 2019.

[7] A. G. Guignard, “A 3 TeV e+ e − Linear Collider Based on CLIC Technology,” CERN, 2000-008, 2000.

[8] V. Fortov, K. Khishchenko, P. Levashov, and I. Lomonosov, "Wide-range multi-phase equations of state for metals," Nuclear Instruments and Methods in Physics Research Section A: Accelerators, Spectrometers, Detectors and Associated Equipment , vol. 415, pp. 604–608, October 1998.

[9] V. I. Oreshkin, R. B. Baksht, A. Y. Labetsky, A. G. Rousskikh, A. V. Shishlov, P. R. Levashov, K. V. Khishchenko, and I. V. Glazyrin, "Study of metal conductivity near the critical point using a microwire electrical explosion in water," Tech. Phys., vol. 49, pp. 843–848, July 2004.

1 The work was supported by Russian Foundation for Basic Research Grants No. 20-08-00378, 20-21-00036 and 19-08-01004.

DYNAMICS OF FOREVACUUM SPARK PLASMA EMITTED ELECTRONS AND INFLUENCE OF RESIDUAL GAS IONIZATION ON A FOREVACUUM SPARK CURRENT*

Y. I. MAMONTOV[1], *I. V. UIMANOV*[1]

[1]*Institute of Electrophysics UB RAS, Amundsena Str. 106, Ekaterinburg, 620016, Russia*

Most of interpretations of vacuum discharge phenomenon suggest the absence of residual gas in a vacuum gap investigated. It is considered that on the spark stage of the vacuum discharge constant rate propagation of explosive emission plasma front from a cathode to an anode of a vacuum diode is observed. At this time, the voltage is applied almost completely between the plasma boundary and the anode. So, the current of electrons field emitted from plasma boundary may be observed in an external circuit. And under such conditions, the only factor determining the current flow (beside power supply capacity and power magnitude of voltage applied) is throughput of a vacuum gap between the cathode spark plasma front and the anode [1,2]. The throughput is determined by the Child-Langmuir law (the law of three second degree). However, there are a lot of technical applications of explosive emission cathodes with the vacuum of low quality. If the diode is operated under pressure about 10^{-1} Pa (forevacuum), there are a lot of residual gas particles in the gap. These particles may be ionized by the emitted electrons. The question is whether positive charge of ionized gas particles is able to influence on the current flow through the diode. In this paper, the 1D-3V spherical symmetric PIC-MCC technique was applied to investigate this question. The propagation of explosive-emission plasma front with constant velocity in the hemi-spherical vacuum diode was considered in terms of simple analytical approach. PIC technique was applied for modeling of charged particles movement between the cathode spark plasma front and the anode and for calculation of the self-consistent electric field taking into account volume charges of electron beam emitted and secondary particles of residual gas ionization origin. Monte-Carlo technique was applied to account for kinetic processes such as excitation and ionization of residual gas particles, elastic scattering of electrons, as well as a recombination process. One was considered that the vacuum spark plasma had a hemi-spherical form with the initial radius 10 μm, the propagation rate was constant $\sim 2 \cdot 10^6$ cm/s [1,2]. The anode of the diode was also considered to be hemispherical of constant radius 10^{-2} m. The voltage between the plasma boundary and the anode was 50 kV. For spark plasma of set temperature, the plasma-emitted electrons current density was calculated taking into account a velocity distribution function of emitted electrons. The electron emission data obtained were compared with the Child-Langmuir law as well. As a result of modeling, volt-ampere characteristics of a vacuum spark in the hemi-spherical diode were calculated for a quazi-rectangular voltage pulse for various residual gas pressures. The ranges of pressure and pulse duration were determined for which sufficient influence of residual gas ionization on the vacuum spark current was observed.

REFERENCES

[1] G.A. Mesyats and D.I. Proskurovsky, Pulsed Electrical Discharge in Vacuum. Berlin: Springer, 1989.

[2] G.A. Mesyats, Cathode Phenomena in a Vacuum Discharge: the Breakdown, the Spark and the Arc. Moscow: Nauka, 2000.

* The work was supported in part by RFBR Grants Nos. 18-08-00547, 19-08-00783, 19-58-53006, 20-08-00172 and UB RAS Program Project No 18-2-2-16.

OPTIMIZATION OF THRUST BASED ON VACUUM ARC BY MEANS OF PULSED MAGNETIC FIELD [*]

E.V. NEFEDTSEV, L.A. ZJULKOVA

Institute of High Current Electronics SB RAS, Tomsk, Russia

Recently there are a lot of designs for spacecraft engines based on electric propulsion. Capabilities of the pulsed arc discharge [1], which has several advantages to create thrust in small and ultra-small spacecraft, have not been fully studied. Important advantages include the possibility of using a condensed working medium (including one with a significant atomic mass), high supersonic plasma flow rates, and an ability to adjust the thrust in the ~ 1–10 μN range with a sufficiently high accuracy by several independent parameters: frequency, duration and power of ignition pulses.

As a rule, disadvantages of the vacuum arc plasma source include erosion of electrodes, which reduces engine lifetime [2]. However, as demonstrated in [3, 4], this problem can be solved by means of a liquid-phase metal propellant automatically fed to the discharge zone through a steel capillary.

The principal disadvantage of the high-current vacuum arc plasma is its wide spray pattern resulting in large momentum losses in radial direction and, consequently, to low propulsion efficiency. This disadvantage can be eliminated by plasma compression by an external magnetic field. Considering the pulsed mode of vacuum-arc plasma generation, it is more appropriate in this case to use the inductive interaction between the plasma and the magnetic field. Such interaction is realized, for example, in pulsed gas-plasma engines [5]. However, taking into account the initially high plasma expansion rate, it is not so much about its inductive acceleration, but rather about correction the angular diagram of its expansion. In addition to search for the optimal spatial configuration of the magnetic field, the problem of optimizing the delay of the magnetic field pulse relative to the arc ignition pulse also is of high importance.

In this paper, based on magnetohydrodynamic plasma model, estimates of configurations and parameters of the magnetic field pulse are given, providing significant changes in the traction force of the vacuum arc plasma source. These estimates may also be applicable to a plasma source based on pulsed overheating of a material by a laser beam.

REFERENCES

[1] M. Keidar, T. Zhuang, A. Shashurin, G. Teel, D. Chiu, J. Lukas, S. Haque, L. Brieda, “Electric propulsion for small satellites”, Plasma Phys. Control. Fusion, 2015, vol. 57, p. 014005 (1-10). DOI:10.1088/0741-3335/57/1/014005.

[2] A.K. Martin “Performance scaling of inductive pulsed plasma thrusters with coil angle and pulse rate”, J. Phys. D: Appl. Phys., 2016, vol. 49, p. 025201 (16 pp.). DOI: 10.1088/0022-3727/49/2/025201.

[3] S.A. Popov, A.N. Panchenko, A.V. Batrakov, F.N. Ljubchenko, V.V. Mataibaev, “Experimental Study of the Laser Ablation Plasma Flow From the Liquid Ga–In Target”, IEEE Trans. Plasma Sci., vol. 39, no. 6, part 1, pp. 1412–1417, June 2011. DOI: 10.1109/TPS.2011.2134872.

[4] S.A. Popov, E.L. Dubrovskaya, A.V. Batrakov, “The concept of a hybrid pulsed plasma thruster for small-size space satellites”, Russian Physics Journal, March 2019, vol. 61, no. 11, pp. 2079-2084 (Translated from Izvestiya Vysshikh Uchebnykh Zavedenii, Fizika, no. 11, pp. 122–126, November 2018). DOI: 10.1007/s11182-019-01640-z.

[5] A.K. Hallock, A.K. Martin, K.A. Polzin, A.C. Kimberlin, R.H. Eskridge, “Single- and Repetitive-Pulse Conical Theta-Pinch Inductive Pulsed Plasma Thruster Performance”, IEEE Trans. on Plasma Sci., 2015, vol. 43, no. 1, pp. 433–443. DOI: 10.1109/TPS.2014.2368835.

[*] This study has been supported by a grant from the Russian Science Foundation (Project No. 18-19-00270).

ELECTRIC EXPLOSION OF LIQUID METAL JETS IN THE CATHODE SPOT OF A VACUUM ARC*

I.V. UIMANOV[1], G.A. MESYATS[1,2]

[1]Institute of Electrophysics, UB RAS, Ekaterinburg, Russia
[2]P. N. Lebedev Physical Institute, RAS, Moscow, Russia

The explosion of the liquid metal jets is considered to be the basic mechanism of the birth of new cathode spot cells [1-4]. According to ecton model, the appearance of new cathode spot cells is due to the interaction of a liquid-metal jet with dense cathode spot plasma [2]. With this important part played by the liquid-metal phase in the self-sustainng of a vacuum discharge, for a long time, a quantitative description of the hydrodynamic processes responsible for the jets and droplets formation was so far confined to estimating or very simplified calculations. The study of thermal processes was also limited only by the static case without taking into account the liquid metal jet dynamics [3, 4].

In this work a two-dimensional axisymmetric model has been developed to describe the formation of a liquid metal jet, the droplet pinch-off and temperature runaway in the droplet-jet neck during melt splashing from the cathode crater in a vacuum arc. The presented model is a further development of the approach [5]. Here, the jet dynamics is modeled taking into account the heating of the droplet-jet neck. Thus, the proposed model in this work is a self-consistent description of hydrodynamic and thermal processes during the formation of a current-carrying liquid metal jet. The development of hydrodynamic and thermal instabilities has been self-consistent simulated in a copper current-carrying liquid metal jet in the "inertial" mode of the melt splashing. In this case, a jet with a longitudinal velocity gradient is formed and the droplet-jet neck becomes unstable due to the action of capillary forces (Rayleigh–Plateau instability). As a result, the neck radius decreases rapidly and the droplet splits off (see Fig. 1). In a current-carrying jet, this process is accompanied by a strong increase in the current density in the neck and its rapid heating due to the Joule effect to a critical temperature at certain values of current from the cathode spot plasma (see Fig. 1). It is shown that the heating process has the nature of a temperature runaway and, accordingly, can lead to its electric explosion. Assuming a constant current density on the jet surface, its minimum "explosion" value was calculated depending on the diameter, velocity and initial temperature of the jet. It is shown that for craters and jets of low-current arcs this density does not exceed 10^7 A/cm^2 and, accordingly, can be provided by the ion current from the plasma of the cathode spot.

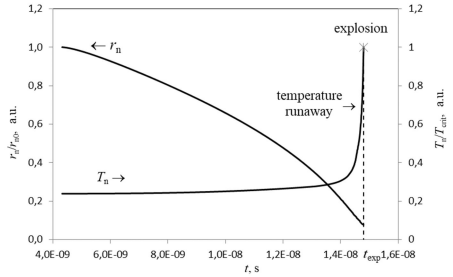

Fig. 1. The droplet-jet neck radius and maximum temperature versus time (the self-consistent modeling of hydrodynamic and thermal instabilities). Calculated parameters: r_{ib} = 0.5 μm, r_1 = 1.5 r_{ib}, t_{off} = 1ns, T_0 = 2000 K, v_{z0} = 250 m/s.

REFERENCES

[1] G. A. Mesyats and D. I. Proskurovsky, Pulsed Electrical Discharge in Vacuum, Berlin: Springer, 1989, pp. 110–114.

[2] G. A. Mesyats, Cathode Phenomena in a Vacuum Discharge: The Breakdown, the Spark and the Arc, Nauka, Moscow, 2000. pp. 167–170.

[3] G. A. Mesyats, JETP Lett., vol. 60, pp. 593–596, April 1994.

[4] E. A. Litvinov, G. A. Mesyats, A. G. Parfenov and A. I. Fedosov, Zh. Tekh. Fiz., vol. 55, p. 2270, May 1985.

[5] I. V. Uimanov and G. A. Mesyats, "Numerical simulation of the liquid-metal jet formation and droplet pinch-off in the cathode spot of a vacuum arc," Journal of Physics: Conference Series, vol. 1393, p. 012034, 2019, doi:10.1088/1742-6596/1393/1/012034.

* This work was supported in part by RFBR Grant Nos. 18-08-00547, 19-08-00783, 19-58-53006.

SIMULATION OF VACUUM ARC WITH HIGH AVERAGE CATHODE CURRENT DENSITY*

I.V. UIMANOV[1], D.L. SHMELEV[1], S.A CHAIKOVSKY[1]

[1]Institute of Electrophysics, UB, RAS, Ekaterinburg, Russia

This work presents the results of theoretical modeling of high current vacuum arc (HCVA) with average cathode current density (arc current divided by the cathode area) in the order of 10^5 A/cm^2. This type of HCVA is used as pumping plasma gun in experiments with plasma puff z-pinches ([1] for example). As it known from these experiments, the mass of plasma liner pumped by such kind of HCVA is much higher than the liner mass estimated via conventional values of the vacuum arc specific erosion [2]. The simplest explanation of this discrepancy is an assumption that the cathode surface, which is not occupied by cathode spots, is heated during the arc burning up to temperature higher than evaporation temperature. After that the cathode surface evaporation can provide the additional erosion. To test this assumption we made a computer simulation of vacuum arc on copper cathode with radius 1 mm, current pulse duration ~ 15 microseconds, and current pulse amplitude ~ 8 kA. During the simulation (which based on hybrid model [3]) of the arc burning we calculated the cathode heating by heat fluxes from the arc plasma and the cathode evaporation. The vaporized substance supplied the arc plasma in parallel with cathode spots. Some preliminary results are shown in Fig.1. It is seen that after 5.5 μs the cathode surface temperature exceeds the evaporation temperature, after which the total erosion increases approximately by factor of four, and the mass of the plasma liner increases approximately by factor of ten. The difference in the rate of increase in liner mass and cathode erosion is explained by a decrease in the average plasma velocity in the gap.

Thus, it was shown that the evaporation of the cathode due to plasma heating can explain the sharp increase in the mass of the plasma liner observed in the experiment.

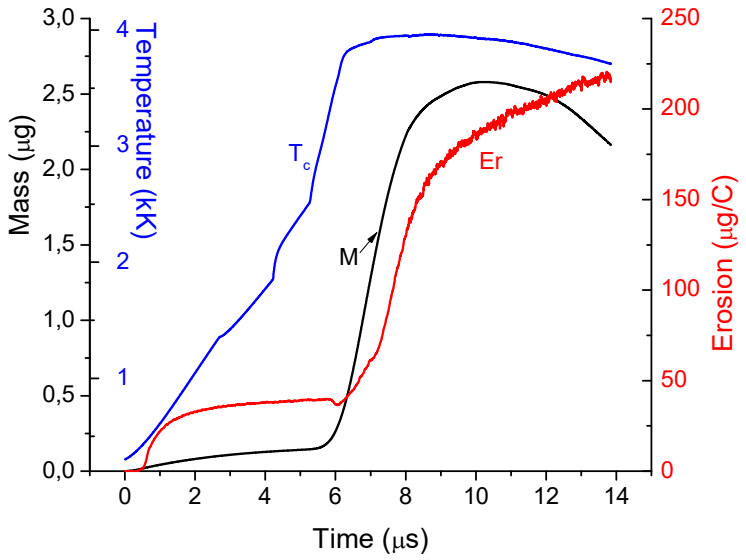

Fig.1. Maximal cathode surface temperature (T_c), total plasma mass in the gap (M), cathode erosion (Er) as functions of time.

REFERENCES

[1] A.G. Rousskikh, A. S. Zhigalin, V. I. Oreshkin, R. B. Baksht, "Measuring the compression velocity of a Z pinch in an axial magnetic field", Phys. Plasmas, vol. 24, 063519, 2017; doi: 10.1063/1.4986096

[2] A. Anders, E.M. Oks, G.Yu. Yushkov, K.P. Savkin, I.G. Brown, A.G. Nikolaev, "Measurements of the total ion flux from vacuum arc cathode spots", IEEE Trans. Plasma Sci., vol. 33, pp. 1532- 1536, 2005.

[3] D.L. Shmelev, V.I. Oreshkin, I.V. Uimanov, "Hybrid numerical simulation of high-current vacuum arc taking into account secondary plasma generation", IEEE Trans. Plasma Sci., vol. 47, pp. 3478- 3483, 2019.

* This work was supported in part by RFBR Grant Nos. 18-08-00547, 19-08-00783, 19-58-53006.

IONIZATION PROCESSES IN THE ARC PLASMA OF W-FUZZ CATHODES*

D. L. SHMELEV[1], M. M. TSVENTOUKH[2], E. M. OKS[3], G. YU. YUSHKOV[3], S. A. BARENGOLTS[4]

[1]*Institute of Electrophysics, UB, RAS, Ekaterinburg, Russia*
[2]*Lebedev Physical Institute, RAS, Moscow, Russia*
[3]*Institute of High Current Electronics, SB, RAS, Tomsk, Russia*
[4]*Prokhorov General Physics Institute, RAS, Moscow, Russia*

Unipolar arcs arising at sites where metal surfaces are in contact with plasma are extremely undesirable for future nuclear fusion devices. For the present, tungsten is the most promising material for plasma facing components of fusion devices. Two factors significantly increase the probability that unipolar arcs will occur in fusion devices. The first one is periodic magnetohydrodynamic instabilities of fusion plasmas, which are known as edge localized modes (ELMs). The ELM activity reveals itself in coarse plasma blobs moving from the center and penetrating far outside the separatrix surface, in contrast to single particles, which settle in the divertor. The second factor is a change in the morphology of a tungsten surface exposed to helium plasma. Helium ions are generated as a by-product of the fusion reaction. A tungsten surface interacting with helium plasma is nanostructured, resulting in the formation of so-called 'fuzz' [1].

Our investigations showed that the formation of a fuzzy layer on the surface of a tungsten cathode decreased the mean charge of tungsten ions in the arc plasma [2]. To numerically simulate the ionization processes in the arc plasma of a W-fuzz cathode, we used the one-dimensional MHD model of a plasma jet described in [3]. The simulation has demonstrated that the presence of an additional component (helium) in the arc plasma actually reduces the mean charge of tungsten ions in the arc plasma (Fig. 1).

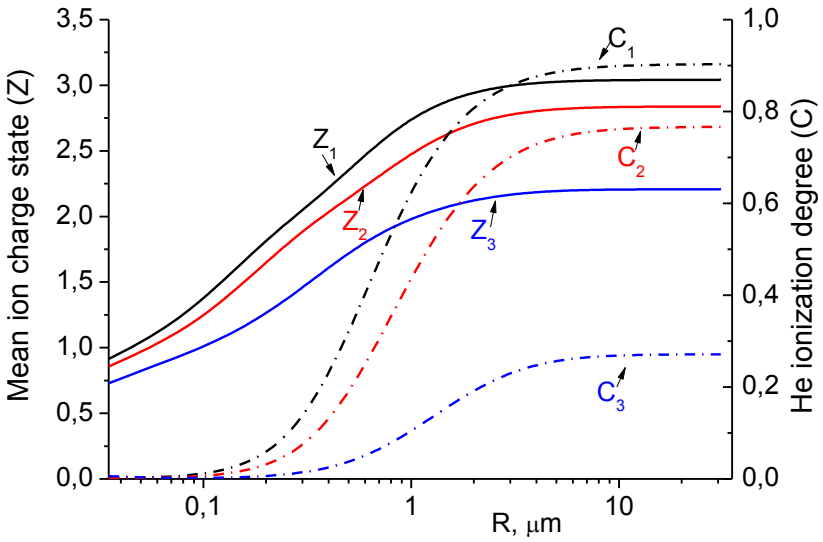

Fig. 1. The mean charge of tungsten ions (Z) and the degree of ionization of helium (C) in relation to the relative content of atomic helium in the cathode: 10% (1), 20% (2), and 30% (3) for a 16-V potential drop across the plasma jet.

REFERENCES

[1] S. Takamura, N. Ohno, D. Nishijima, and S. Kajita "Formation of nanostructured tungsten with arborescent shape due to helium plasma irradiation", Plasma Fusion Research, vol. 1, p. 051, Sept. 2006.

[2] S.A. Barengolts, D. Hwangbo, S. Kajita, N. Ohno, V.P. Frolova, A.G. Nikolaev, E.M. Oks, D.L. Shmelev, M.M. Tsventoukh and G. Yu Yushkov "Dynamics of the changes in the parameters of the arc plasma during the destruction of a helium-induced tungsten fuzz by arc pulses" Nuclear Fusion, vol. 60, no. 4, p. 044001, Feb. 2020.

[3] S.A. Barengolts, V.P. Frolova, A.G. Nikolaev, E.M. Oks, K.P. Savkin, D.L. Shmelev, I .V. Uimanov, and G.Yu. Yushkov "Cathode and plasma phenomena in vacuum-arc sources of hydrogen isotope ions. II. Ionization processes in the arc plasma" Plasma Sourc. Sci. Techn., vol. 29, no. 3, p. 035004, Feb. 2020.

* The work was supported by the Russian Science Foundation (grant No. 18-19-00069).

2-D AND 3-D NUMERICAL SIMULATION OF FERRITE LOADED COAXIAL TRANSMISSION LINES

P.V. PRIPUTNEV[1], *I.V. ROMANCHENKO*[1], *V.P. TARAKANOV*[2,3], *I.V. PEGEL*[1]

[1]*Institute of High Current Electronics SB RAS, Tomsk, Russian Federation*
[2]*Joint Institute for High Temperatures RAS, Moscow, Russian Federation*
[3]*National Research Nuclear University MEPhI, Moscow, Russian Federation*

Coaxial transmission lines filled with saturated ferromagnetic material have been used for a long time for high-voltage pulse sharpening purposes and high-frequency oscillation generation [1, 2]. As the voltage pulse propagates along such a line, its front is first sharpened at a small length, and then this process is changed to microwave oscillation behind the front. This process has been well studied experimentally, while its analytical description is complicated; simplified models provide a qualitative agreement only [3]. Quantitative description of the process requires a joint solution of Maxwell equations and the Landau-Lifshitz [4] equation describing the dynamics of the magnetization vector $\boldsymbol{M}$ of saturated ferromagnetic material:

$$\frac{\partial \boldsymbol{M}}{\partial t} = -\frac{\gamma}{M_s}[\boldsymbol{M} \times \boldsymbol{H}] + \frac{\alpha}{M_s}[\boldsymbol{M} \times \frac{\partial \boldsymbol{M}}{\partial t}], \quad (1)$$

The paper presents the results of numerical simulation of the process of a high-voltage pulse sharpening and excitation of high-frequency oscillations in coaxial line filled with saturated ferrite. The simulation used the electromagnetic code KARAT [5] in axisymmetric (RZ), three-dimensional Cartesian (XYZ) and three-dimensional cylindrical (RΘZ) versions. The simulation results are compared with the previous experiments. The effect of ferromagnetic material properties on the amplitude, duration and frequency of the excited oscillations is analyzed.

REFERENCES

[1] V.V. Rostov, N.M. Bykov, D.N. Bykov, A.I. Klimov, O.B. Kovalchuk, I.V. Romanchenko, “Generation of subgigawatt RF pulses in nonlinear transmission lines”, IEEE Trans. Plasma Sci., vol. 38, no. 10, pp. 2681-2685, Oct 2010.

[2] J.-W.B. Bragg, J.C. Dickens, A.A. Neuber, “Material selection consideration for coaxial, ferrimagnetic-based nonlinear transmission lines”, J. Appl. Phys., vol. 113, no. 6, pp. 064904-1 – 064904-4, Feb. 2013.

[3] J.E. Dolan, “Simulation of shock waves in ferrite-loaded coaxial transmission lines with axial bias”, J. Phys. D: Appl. Phys, vol. 32, no. 15, pp. 1826-1831, Aug. 1999.

[4] T.L. Gilbert, “A phenomenological theory of damping in ferromagnetics materials”, IEEE Trans. On Mag., vol. 40, no. 6, pp. 3443-3449, Nov. 2004.

[5] V. P. Tarakanov, “ Multipurpose electromagnetic code KARAT,” in Mathematical Modeling: Problems and Results (Nauka, Moscow, Russia, 2003), pp. 456–476.

NUMERICAL SIMULATION OF ION BEAM EVOLUTION IN MAGNETIZED PLASMA*

G.I. DUDNIKOVA[1], *M.A BORONINA*[1], *E A.GENRIKH*[1], *V.A. VSHIVKOV*[1]

[1]*Institute of Computational Mathematics and Mathematical Geophysics SB RAS, Novosibirsk, Russia*

The problem of the interaction of high-current ion beam with plasma is investigated on the basis of computer simulation. The two-dimensional axisymmetric hybrid numerical model is based on the MHD approximation for electrons and the particle-in-cell method (PIC) for the ion beam and plasma ion component. The application of the particle-in-cell method for studying non-stationary phenomena in plasma physics and astrophysics [1-2] is limited by the difference in the mass of ions and electrons. We use a different approach, the hybrid MHD-PIC, which reduces computational costs and takes into account the final value of the Larmor radius of ions [3-4]. To solve the Vlasov equations by the PIC method, a transition to Cartesian coordinates and back to cylindrical coordinates is used. As a result of computer simulation, the evolution of the ion beam depending on its energy and current, magnetic field and plasma density is studied. The possibility of forming regions with a low plasma density and a displaced magnetic field is shown.

REFERENCES

[1] C.K. Birdsall, A. B. Langdon. Plasma Physics via Computer Simulation, Bristol: IOP Publishing, 1991.

[2] G. Dudnikova, E. Berendeev, A. Efimova, V. Vshivkov. “Generation of terahertz radiation by electron beam-plasma interaction,” Proc. 20th Int. Conf. on High Current Electronics (ISHCE), Tomsk, Russia, pp. 39–42, 2018.

[3] A.S. Lipatov. The hybrid multiscale simulation technology. An introduction with application to astrophysicaland laboratory plasmas. Berlin, Heidelberg: Springer, 2002.

[4] L. Vshivkova, G. Dudnikova. “Hybrid model of particle acceleration on a shock wave front”, Lecture Notes in Computer Science, vol.10187, LNCS, pp.737-743, 2017.

* The work was supported by the Russian Foundation for Basic Research (project №18-29-21025). Numerical computations were carried out at Siberian Supercomputer Centre of ICMMG SB RAS, Novosibirsk.

NUMERICAL STUDY OF TRANSIENTS IN THE NEGATIVE DC CORONA*

A.A. SAIFUTDINOVA, B.A. TIMERKAEV, D.ZAINUTDINOVA, A.KAMALETDINOVA, A.I. SAIFUTDINOV,

[1] Kazan National Research Technical University named after A.N.Tupolev, Kazan, Russia

The presented work is aimed at conducting numerical experiments to study the characteristics and combustion regimes of the negative corona in argon at atmospheric pressure.

To model the corona discharge, an extended fluid model was used, based on the equations of continuity for the density of charged and excited particles, the equations for the electron energy density, the heat equation for the heavy plasma component (ions, excited and neutral particles), the heat equation for the metal tip cathode, and the equation Poisson for electric potential. A more detailed description of the model can be found in [1,2]. The set of plasma-chemical reactions used to describe the discharge in argon was taken from [1,2].

As a result of a series of numerical experiments, two modes of corona discharge in argon at atmospheric pressure were reproduced: pulsed-periodic and glow. An analysis of the results showed that the observed pulse-periodic regime with its characteristic Trichel pulses [3] is similar to the self-oscillating regime characteristic of the transition from a low-current Townsend discharge to a highly accurate normal glow discharge with classical flat electrodes. This phenomenon, which was previously associated only with corona discharge in electronegative gases, is also inherent in discharges whose working medium is inert gases, in particular argon.

The results demonstrated that with an increase in the power deposited in the discharge, the oscillation frequency increases, and the amplitude decreases. When the threshold current is reached, the corona discharge goes into glow mode. Since the corona discharge is characterized by a high electric field near the tip, considerable heating is observed in this region of the interelectrode gap, even at low currents at atmospheric pressure. In this regard, a falling current-voltage characteristic of the discharge is observed. A further increase in the input power in the discharge will lead to its disruption in the arc discharge.

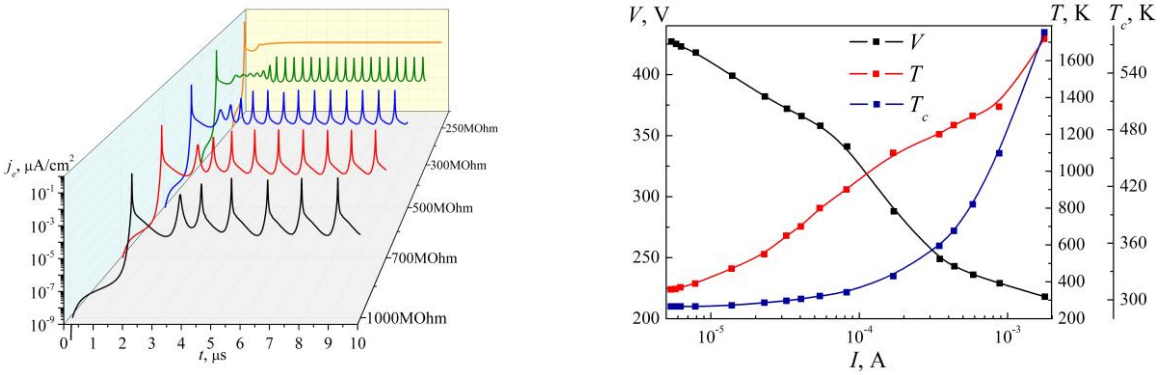

Fig.1. a) Temporal evolution of current density at the tip of the cathode for various values of the input power in the discharge and b)dependence of voltage (CVC), maximum gas temperature and maximum pin temperature in corona discharge on total current.

REFERENCES

[1] A. I. Saifutdinov, I. I. Fairushin, N. F. Kashapov,"Analysis of various scenarios of the behavior of voltage-current characteristics of direct-current microdischarges at atmospheric pressure", JETP Letters, vol.104, №3, 180–185, 2016.

[2] A. I. Saifutdinov,A. A. Saifutdinova, B. A. Timerkaev, "Numerical Study of the Voltage Waveform Effect on the Spatiotemporal Characteristics of a Dielectric Barrier Microdischarge in Argon", Plasma Physics Reports volume 44, pages359–368, 2018.

[3] L.B. Loeb, Fundamental Processes of Electrical Discharges In Gases, New York, 1950.

* The reported research was funded by Russian Foundation for Basic Research, grant № 19-31-90101

15th International Conference on Modification of Materials with Particle Beams and Plasma Flows

Chairman	Nikolai Koval,	Institute of High Current Electronics, Tomsk, Russia
Co-Chairman	Valery Krivobokov,	National Research Tomsk Polytechnic University, Tomsk, Russia
Program Chairman	Alexander Batrakov,	Institute of High Current Electronics, Tomsk, Russia
Program Co-Chairman	Nikolai Koval,	Institute of High Current Electronics, Tomsk, Russia

Program Committee

Georgi YUSHKOV	Institute of High Current Electronics SB RAS, Tomsk, Russia
Valery KRIVOBOKOV	National Research Tomsk Polytechnic University, Tomsk, Russia
Yuri IVANOV	Institute of High Current Electronics SB RAS, Tomsk, Russia
Nikolai KOVAL	Institute of High Current Electronics SB RAS, Tomsk, Russia
Yuriy SHARKEEV	Institute of Strength Physics and Materials Science SB RAS, Tomsk, Russia

International Advisory Committee

Andre ANDERS	Leibniz Institute of Surface Engineering (IOM), Leipzig, Germany
Valiantsin ASTASHYNSKI	State Scientific Institution «A.V. Luikov Heat and Mass Transfer Institute of the National Academy of Sciences of Belarus», Minsk, Belarus
Massimiliano BESTETTI	Politecnico di Milano, Milan, Italy
Ian BROWN	on retired from Lawrence Berkeley National Laboratories, USA
Mihai Cosmin COTRUT	University Politehnica of Bucharest, Bucharest, Romania
Oleg DOLMATOV	National Research Tomsk Polytechnic University, Tomsk, Russia
Viktor DRAGUNOV	National Research University "Moscow Power Engineering Institute", Moscow, Russia
Igor GARKUSHA	National Science Center Kharkov Institute of Physics and Technology, Kharkov, Ukraine
Nikolai GAVRILOV	Institute of Electrophysics UB RAS, Ekaterinburg, Russia
Yuri IVANOV	Institute of High Current Electronics SB RAS, Tomsk, Russia
Kairat KADYRZHANOV	L.N. Gumilyov Eurasian National University, Astana, Kazakhstan
Alexander KOROTAEV	National Research Tomsk State University, Tomsk, Russia
Georgy MLADENOV	Institute of Electronics, Sofia, Bulgaria
Jindrich MUSIL	University of West Bohemia, Plzen, Czech Republic
Efim OKS	State University of Control Systems and Radioelectronics, Tomsk, Russia Institute of High Current Electronics SB RAS, Tomsk, Russia
Kamil RAMAZANOV	Ufa State Aviation Technical University, Ufa, Russia
Timothy RENK	Sandia National Laboratories, Albuquerque, New Mexico, USA
Alexander RYABCHIKOV	National Research Tomsk Polytechnic University, Tomsk, Russia
Alexander SEMENOV	Institute of Physical Material Science SB RAS, Ulan-Ude, Russia
Yuriy SHARKEEV	Institute of Strength Physics and Materials Science SB RAS, Tomsk, Russia
Vyacheslav SHULOV	National Research University «Moscow Aviation Institute», Moscow, Russia
Yang SI-ZE	Institute of Physics, Chinese Academy of Sciences, Beijing, China
Anatoly SMYSLOV	Ufa State Aviation Technical University, Russia
Kensuke UEMURA	ITAC Ltd., Takarazuka, Japan
Vladimir UGLOV	Belarusian State University, Minsk, Belarus
Alexander YALOVETS	South Ural State University, Chelyabinsk, Russia
Georgi YUSHKOV	Institute of High Current Electronics SB RAS, Tomsk, Russia
Vitaly ZALESSKY	Physical-Technical Institute, Minsk, Belarus

Conference topics

Beam and plasma sources
Fundamentals of modification processes
Modification of material properties
Coatings deposition
Nanoscience and nanotechnology

Financial support by Russian Foundation for Basic Research (RFBR): № 20-08-22015

A METHOD OF CONTROLLING A RATE OF AN ENERGY INPUT INTO A TARGET SURFACE USING A SUBMILLISECOND ELECTRON BEAM*

M.S. VOROBYOV, P.V. MOSKVIN, A.D. TERESOV, N.N. KOVAL

HCEI SB RAS, Academichesky av., Tomsk, 634055, Russia, E-mail: vorobyovms@yandex.ru

The paper presents the features of the electron source SOLO with a grid plasma cathode, the operation principle of which is based on the use of a fine-mesh grid that stabilizes the boundary of the emission plasma. The SOLO source allows the generation of wide (up to several cm^2) low-energy (up to 25 keV) intense (hundreds of amperes) submillisecond electron beams and use these beams in vacuum to modify the surface of various inorganic materials (an energy density up to 100 J/cm^2). It was shown that the presence of the grid stabilization allows us to provide an important distinguishing feature of such an electron source, namely, the ability to generate the electron beam with variable power by changing its amplitude during a pulse of submillisecond duration. This unique feature of electrical sources with plasma cathodes allows not only to control the surface temperature of the irradiated sample, but in some cases provides conditions for a more stable operation of the electron source, which allows a greater specific energy to be introduced into the sample surface.

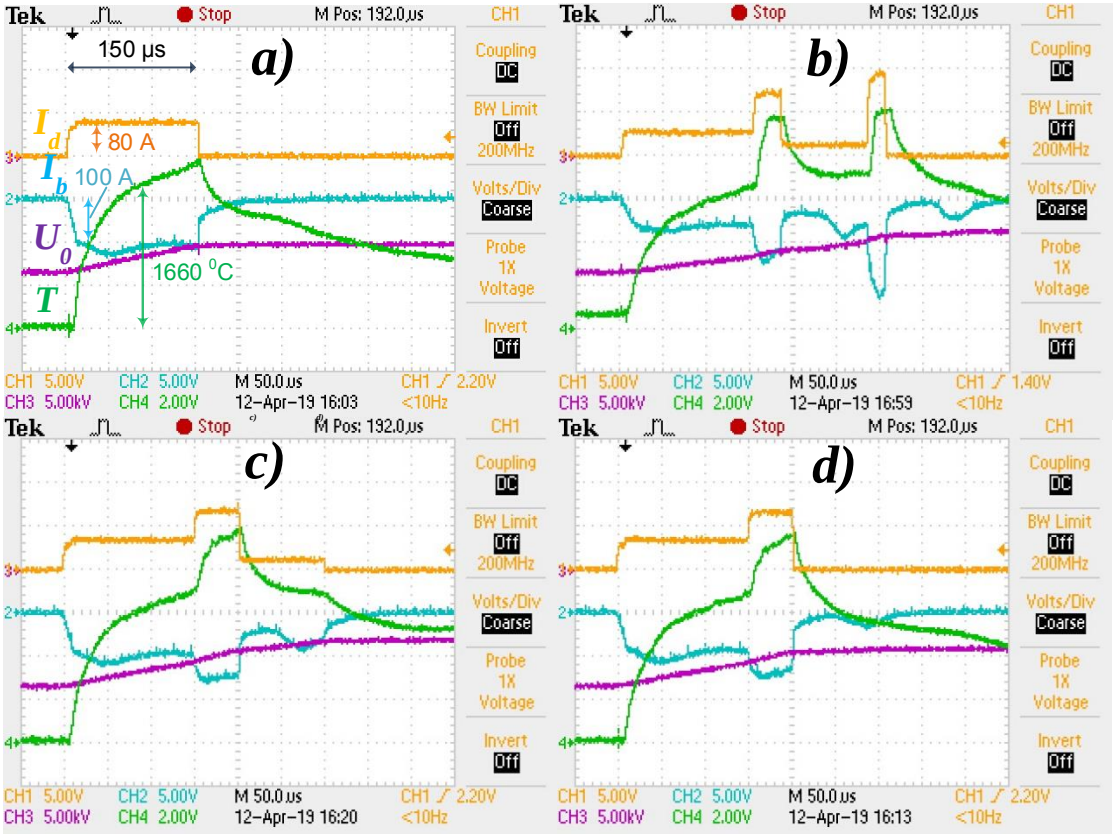

Fig. 1. Oscillograms of discharge current I_d (100 A/div.), beam current I_b (100 A/div.), accelerating voltage U_0 (5 kV/div.) and temperature T of the surface sample (298+199·U, where U has 2 V/div.) for different forms of the beam current.

REFERENCES

[1] *S.P. Bugaev, Yu.E. Kreindel, P.M. Shcanin* // Large-Cross-Section Electron Beams. – Moscow, Energoatomizdat, 1984 (in Russian)

[2] *E. Oks* // Plasma Cathode Electron Sources: Physics, Technology, Applications. – WILEY-VCH, 2006, 171 pp.

* The work was supported by the Russian Science Foundation (project No. 20-79-10015).

TRAJECTORY ANALYSIS OF THE CORPUSCULAR FLOW EXTRACTED FROM A SMALL-SIZED LINEAR ACCELERATOR PLASMA SOURCE

I.A. KANSHIN

Dukhov Automatics Research Institute (VNIIA), 22 Suschevskaya Ul., Moscow 127055, Russia, ilia.kanshin2011@yandex.ru, phone.: 89267930525

When developing small-sized linear accelerators, the design of which includes the Penning ion source and the accelerating system [1, 2], special attention is paid to the device electrical strength. In particular, its decrease is associated with deposition on the accelerating system high-voltage insulator inner surface by products of the ion beam interaction with accelerating system electrodes [3].

In this case, a conductive layer is formed on insulator inner surface. It contributes to the insulator surface breakdown [4], degradation of the vacuum shell and the device failure. To prevent the consequences of the above processes during the development of the small-sized linear accelerator accelerating system, the main attention is paid to the corpuscular flows trajectory analysis, which, as a rule, is based on numerical modeling results. Several approaches are used. One of them is "through" modeling of the product, including an plasma formation processes analysis in the plasma source, and then ion beam extraction from it. The other approach is modeling the beam dynamics without taking into account the plasma source influence, when the ion-emitting surface is the surface of the plasma penetrating into accelerating system from the plasma source - the meniscus [5].

In this paper a different approach is presented, which allows us to simulate the dynamics of corpuscular flows in the accelerating system without using a plasma meniscus and at the same time take into account the influence of a plasma source without resorting to "through" modeling. The ion beam emittance is used as the initial simulation data. Its dependence on the accelerating system geometric parameters is experimentally studied in the process of factor analysis and expressed as a corresponding function of the accelerating system parameters. With this approach it is possible to calculate the beam emittance subsequently and to simulate beam dynamics without conducting a physical experiment.

Figure 1a shows a photo of the ion beam luminous trace in the accelerating system. Figure 1b shows the ion beam trajectories simulation result obtained in the COMSOL Multiphysics 5.3 taking into account the calculated emittance at the plasma source exit aperture. A comparison of the figures allows us to conclude that the results of modeling the beam trajectories in the accelerating system agree with the results obtained in a physical experiment.

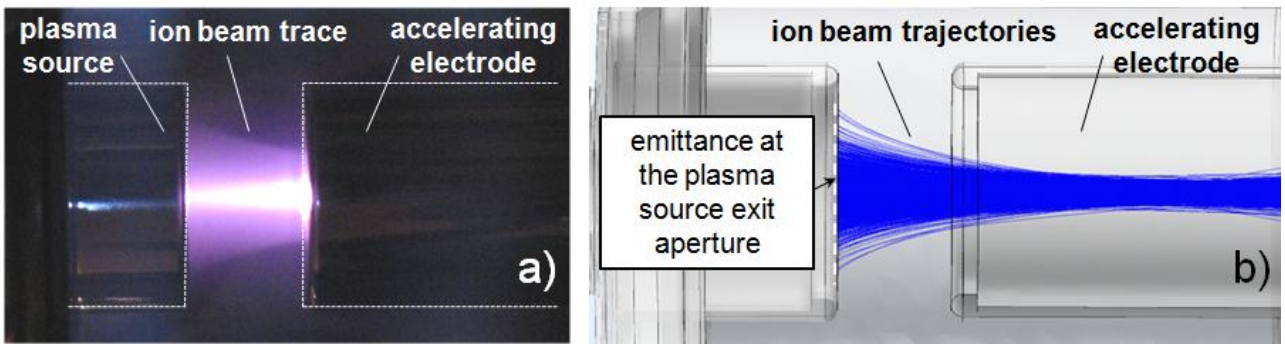

Fig. 1. Photo of the ion beam luminous trace in the accelerating system (a) and the ion beam trajectories simulation result taking into account the calculated emittance at the plasma source exit aperture (b).

These studies were supported by RFFI grant № 12-02-13510-ОФИ_М_РА.

REFERENCES

[1] Rachkov R.S., Presnyakov A.Yu., Yurkov D.I "Investigation of the well's magnetic field influence on the neutron tube of geophysical equipment", Atomic energy, V. 126, №. 6, 2019, pp. 334-337.

[2] N.V. Mamedov, D.E. Prokhorovich, D.I. Yurkov, I.A. Kanshin, A.A. Solodovnikov, D.V. Kolodko, I.A. Sorokin "Measurements of the Ion-Beam Current Distribution over a Target Surface under a High Bias Potential", Instruments and Experimental Techniques, Vol. 61, No. 4, 2018, DOI: 10.1134/S0020441218030223.

[3] Butolin S.L., Chermenskij V.G., Hasaev T.O. "Gas-filled neutron tube", Patent RF, no.2451433.

[4] Grishnyaev E.S."Generator of fast neutrons for the calibration of detectors for weakly interacting particles", 128 p., 2016.

[5] Soliman, B.A., Abdelrahman, M.M., Helal A.G., Abdelsalam F.W. "Simulation of ion beam extraction and focusing system", Chinese Physics C, Vol. 35, No. 1, 2011, pp. 83 – 87., DOI: 10.1088/1674-1137/35/1/017.

THE PLASMA BEAM TESTS OF FUSION REACTOR MATERIALS

A.Z. MINIYAZOV[1], M.K. SKAKOV[1], A.V. GRADOBOEV[2], O.A. STEPANOVA[3], TULENBERGENOV T.R.[1], SOKOLOV I.A.[1]

Institute of Atomic Energy, RSE NNC RK, Kurchatov, Kazakhstan
Tomsk Polytechnic University, Tomsk, Russia
State University named after Shakarim, Semey, Kazakhstan

Studies of plasma interaction with structural materials of ITER are conducted on operating tokamaks and simulation installations (line simulators), which represent the plasma sources with arc or plasma-beam discharge in the longitudinal magnetic field. A simulation test-bench with plasma-beam installation is one of these installations, which allows Kazakhstan conducting researches of candidate and structural materials of fusion facilities. The main aim of this work is obtaining relevant data on interaction between low-temperature plasma and a surface of tungsten for application in fusion reactor.

To test the materials for plasma exposure, we used a simulation stand with a plasma-beam installation (fig. 1) [1, 2], developed at the Institute of Atomic Energy of the National Nuclear Center of the Republic of Kazakhstan (IAE NNC RK). It was developed in support of the developing and operation of the Kazakhstan Materials Science Tokamak (KTM) for testing small-scale samples of materials and equipment of KTM [3]. The plasma-beam installation is universal and allows testing materials under the complex effect of both a plasma flow and a powerful heat load generated by an electron beam. The use of the installation makes it possible to quickly obtain preliminary experimental data on the behavior of materials under the conditions of their interaction with plasma at high heat load, which will allow adjusting the methodology of experimental studies on the KTM.

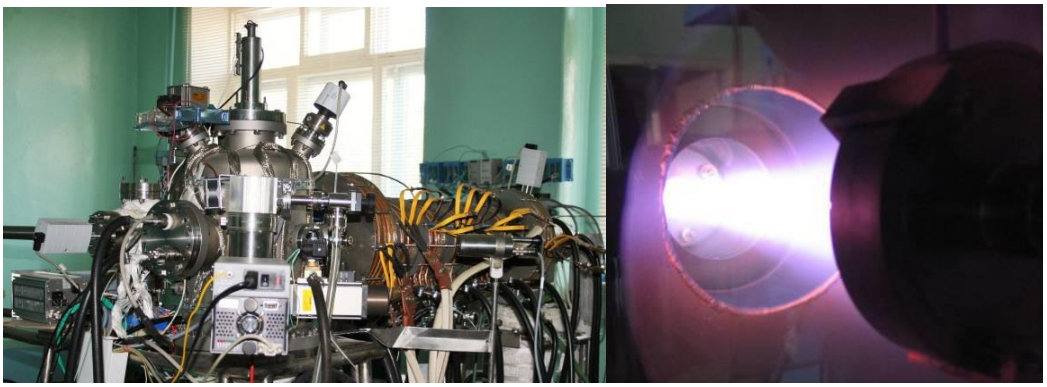

Fig.1. Simulation test-bench with plasma-beam installation and plasma beam mode.

The data on the change of surface layer of fusion candidate materials after low-temperature plasma effect were obtained based on studies and experiments. The glow and plasma-beam discharge of the simulation test-bench was used to achieve the objective. It is determined that after the effect of hydrogen plasma on the tungsten surface, ions etched out pits in the grain body and grain boundaries are revealed as well as the decrease in grain size is observed.

To fully understand the research in the installation, a method of gas evolution from the volume previously irradiated with plasma material in situ will be developed.

REFERENCES

[1] V. Kurnaev, I. Vizgalov, K. Gutorov, T. Tulenbergenov, I. Sokolov, A. Kolodeshnikov, V. Ignashev, V. Zuev, I. Bogomolova, N. Klimov, “Investigation of plasma-surface interaction at plasma beam facilities”. Journal of Nuclear Materials.– Vol. 463.– P. 228-232. – Aug. 2015.

[2] T. Tulenbergenov, M. Skakov, A. Kolodeshnikov, V. Zuev, B. Rakhadilov, I. Sokolov, D. Ganovichev, A. Miniyazov, O. Bukina. “Interaction between nitrogen plasma and tungsten”. Nuclear Materials and Energy. – P. 1-5. – July 2017.

[3] Suchugov D.Yu., Shapovalov G.V., Chektybaev B.Zh., Skakov M.K., Gasilov N.A., Sadykov A.D.et al., “The numerical code TOKSCEN for modelling plasma evolution in tokamaks”. Vol. 55(4), Nuclear Fusion. 2015.

THE EFFECT OF EMISSION PROCESSES ON THE PROPERTIES OF MAGNETRON DISCHARGE WITH INJECTION OF A BEAM OF ACCELERATED IONS*

A.P. SEMENOV, I.A. SEMENOVA, D. B.-D. TSYRENOV, E.O. NIKOLAEV

Institute of Physical Materials Science of SB RAS, Sakhyanovoy 6, Ulan-Ude, 670047, Russia, dmitriyzak@mail.ru, +7(3012)628458

An abnormal glow discharge is used in planar-type magnetron sputtering systems that are widely used for the deposition of multifunctional coatings. The discharge is ignited in crossed electric and magnetic fields, and the magnetic field holds the discharge plasma near the target cathode, which contributes to an increase in the plasma density and, as a consequence, an increase in the ion current to the cathode. The discharge is characterized by [1], firstly, the constant area on the cathode into which the current flows, secondly, an increase in the discharge current with increasing combustion voltage. Typically, the discharge stably ignites and burns stationary in the range of working gas pressures of 0.2-6 Pa. However, at these pressures the relation $l << \lambda$ is not satisfied, the collisionless transfer of knocked out atoms to the substrate.

The condition $l < \lambda$ is satisfied at pressures <0.2 Pa, for which l is relatively large, $\lambda > 10$ cm. However, at low pressures, the ignition voltage is highly dependent on pressure, and the discharge ignites at relatively high voltages >10 kV.

Below are the results of a study of the effect of longitudinal injection of fast ions into a magnetron on the ignition characteristics of an anomalous low-pressure glow discharge, < 0.10 Pa, under conditions of bombardment of the cathode and anodes of a magnetron by an ion beam and the expansion of the magnetron's functionality.

Based on the principle of ion beam injection into a planar magnetron, a gas discharge device has been developed [2, 3]. The design of the experimental gas discharge device is shown schematically in Fig. 1(a).

Ignition of an abnormal glow discharge in a magnetic field and a given gas pressure occurs by applying a rectified voltage between the cathode (target) and the electrically connected annular and central anodes. Fig. 1(b) shows the dependence of the ignition voltage on the ion beam current at an accelerating voltage of 8 kV with increasing discharge current in the ion source. The threshold character of the dependence of the ignition voltage on the ion beam current indicates the existence of a lower limit value of the ignition voltage, in our case ~ 0.42 kV, less than which the discharge does not ignite.

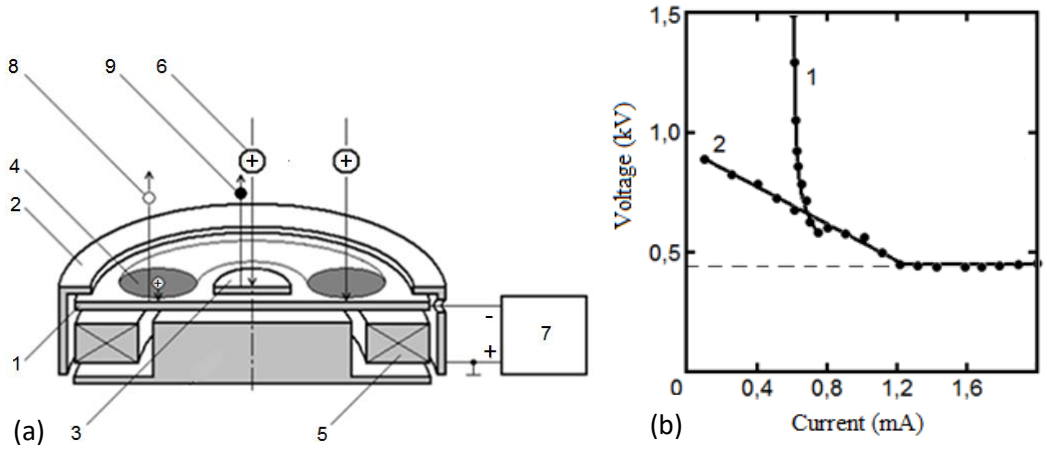

Fig.1. a) Planar type magnetron with injection of a beam of accelerated ions; b) Ignition voltage on the ion beam current: 1 – I = 50 mA; 2 – U = 8 kV.

REFERENCES

[1] Yu. P. Raizer, Gas discharge Physics, M.: Science, 1987.

[2] A. P. Semonov, Siberian physical-technical journal, vol. 6, pp. 68-72, 1993.

[3] A. P. Semonov, I. A. Semonova, PTE, no. 1, pp. 110-114, 2009.

*The work was supported by the Russian Foundation for Basic Research (project 20-08-00207_A) and budget project №0336-2019-0009

EXPERIENCE OF JSC "NIIEFA" IN DEVELOPING PLASMA AND BEAM TECHNOLOGICAL FACILITIES

YU.N. GAVRISH, D.A. KARPOV, S.L. KOSOGOROV, V.P. OVCHINNIKOV, I.YU. RODIN, K.I. TKACHENKO, N.G. TOLSTUN

Joint Stock Company "D.V. Efremov Institute of Electrophysical Apparatus", St. Petersburg, Russia

For many years the JSC "NIIEFA", with its wide experience and necessary competence in developing plasma and beam facilities, has developed and supplied the following high-tech equipment to scientific institutions and industrial enterprises:

- ion-plasma facilities for modification of surface properties of materials and deposition of functional coatings on metal and polymer products and carriers (including the large-size and long-length ones);
- high-current pulse electron accelerators (electron energy up to 500 keV, energy density in pulse up to 500 J/cm^2, beam area on sample/product up to 100 cm^2, pulse length up to 250 μs) for improvement of the surface properties of materials and products (treatment of surface of gas-turbine motor blades, shells of fuel elements, et al.);
- high-voltage electron accelerators (electron energy up to 1 meV, beam power up to 500 kw) with the beam extraction to the atmosphere for accelerated polymerization of materials, radiation treatment of flue gases, waste water cleaning, radiation-chemical conversion of hydrocarbon gases into liquid state, et al.;
- wide-aperture low energy electron accelerators (electron energy up to 100 – 300 keV, beam power up to 80 kW) with the beam extraction to the atmosphere or other medium with cross-sectionan of the electron beam up to 0.7 m^2 for intensification of plasma-chemical processes, solidification of polymer coatings, modification of the biomaterial properties, ionization of the working medium of powerful gas lasers, et al.

The D.V. Efremov Institute has developed and delivered to different enterprises in Russia and abroad more than 60 plasma and beam technological facilities, including those operating in industrial processing lines.

The report presents the main plasma and beam facilities developed by the Institute, their technical characteristics and operational features, discusses the prospects for development of the plasma-beam technologies and their industrial applications.

COMPLEX METHOD OF STRUCTURAL STEEL TREATMENT *

I.V LOPATIN, YU.H AKHMADEEV, YU.F .IVANOV, E.A. PETRIKOVA, M.E. RYGINA

Institute of high current electronics SB RAS, Tomsk, Russia

The work is devoted to the identification and analysis of the regularities of the modification of the elemental and phase composition, defective substructure and mechanical properties of carbon steel subjected to complex processing, combining the saturation of the surface layer of the samples with aluminum atoms (alitization) and subsequent nitriding. The material used for the study was carbon steels AISI 5135 and AISI 1020, which in the initial state have a ferrite-pearlite structure. The complex modification was carried out in a single vacuum space on a TRIO installation with a chamber size of 600×600×600 mm, additionally equipped with a switching block to implement the elion (electron and ion) mode. Alitization was carried out at a temperature of 963 K and a time of 4 hours. Subsequent nitriding of the alitized layer was carried out at a temperature of 803 K for 2 hours. The arc evaporator cathode was made of ASTM 1100 aluminum alloy (98.8% Al). As a result of the performed studies, it was found that the thickness of the modified layer reaches 80 μm. The hardness of steel is maximum on the modificated surface and exceeds the hardness of the initial material by 4 times (steel AISI 1020) and 2.7 times (steel AISI 5135). It is shown that the complex modification of carbon steel is accompanied by the formation of a multiphase state containing iron nitrides of the composition Fe_4N, Fe_3N and aluminum - AlN.

* The work was supported by RFBR and ROSATOM, project number 20-21-00111.

GAS DISCHARGE DEVICE FOR SYNTHESIS OF COMPOSITE COATINGS BASED ON SPRAYING OF PLANAR MAGNETRON ELECTRODES BY ION BEAM*

A.P.SEMENOV, I.A.SEMENOVA, D.B.-D.TSYRENOV, E.O.NIKOLAEV

Institute of Physical Materials Science of SB RAS, Sakhyanovoy 6, Ulan-Ude, 670047, Russia,
semenov@ipms.bscnet.ru, +7(3012)433184

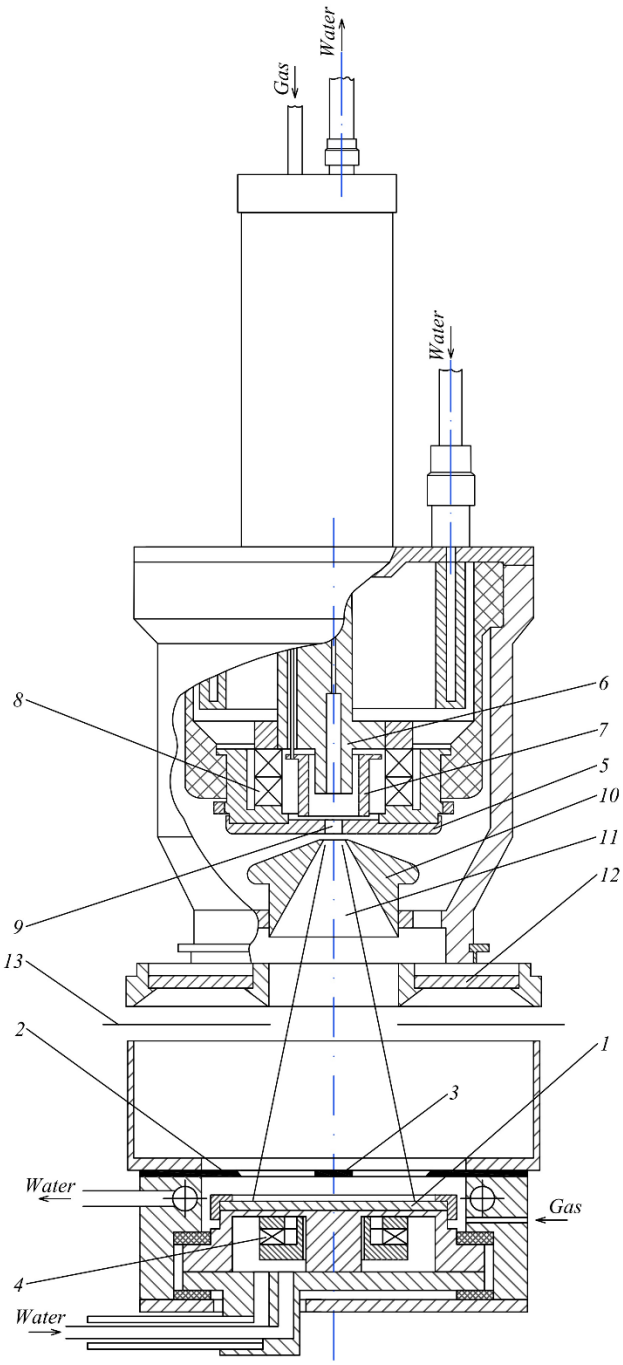

A gas-discharge device based on a planar magnetron and a plasma ion source is considered. The design of the gas discharge device is formed by a planar magnetron and an ion source and is shown schematically in Fig. The magnetron contains a copper cathode 1, a ring anode 2 and a central anode 3. Anode 3 serves as a target. At the periphery of the magnetron, along the axis of the anode 2 at a distance of 0.1 m, a discharge chamber of a plasma ion source is installed on the basis of a hollow cathode reflective discharge. The discharge chamber is formed by an emitter 5, a hollow 6 cathodes and a cylindrical anode 7.

Ions longitudinally injected initiate emission processes, - sputtering of the anode 3 and cathode 1 and ion-electron emission. Perform the functions associated with the ignition of a glow discharge low pressure.

Longitudinal injection of the ion beam into the magnetron and sputtering of the cathode and the central anode of the magnetron by the ion beam affects the ignition of an anomalous low-pressure glow discharge $< 8 \cdot 10^{-2}$ Pa in the magnetron. It has been established that the discharge ignition voltage decreases with increasing ion energy and threshold depends on the ion beam current. The prospect of expanding the functionality of planar magnetrons in growing composite TiN-Cu coatings with a nanocrystalline structure was shown [1-3].

Fig. Planar magnetron with ion beam injection: 1,5,6-cathodes, 2,3,7-anodes, 4,8-magnets, 9-emission channel, 10-accelerating electrode, 11-ion beam, 12-substrates, 13-flap shutter

REFERENCES

[1] Semenov A.P., Tsyrenov D.B.-D., Semenova I.A. // Instruments and Experimental Techniques. 2017. Vol. 60. No. 6. P. 892.
[2] Semenov A.P., Tsyrenov D. B.-D., Semenova I.A. RF Patent 2649355, Izobret., Polezn. Modeli, 2018, No. 10.
[3] Ivanov Yu.F., Koval N.N., Krysina O.V., Baumbach T., Doyle S., Slobodsky T., Timchenko N.A., Galimov R.M., Shmakov A.N. // Surface and Coatings Technology. 2012. V. 207. P. 430.

* The work was supported by the Russian Foundation for Basic Research, project 20-08-00207_a and budget project № 0336-2019-0009

DISTRIBUTED FERROMAGNETIC ENHANCED ICP FOR LARGE-SCALE PLASMA PROCESSING*

M.V. ISUPOV, A.V. FEDOSEEV, N.A. DEMIN, G.I. SUKHININ

Kutateladze Institute of Thermophysics SB RAS, Novosibirsk, Russia

Distributed ferromagnetic enhanced inductively coupled plasma (FMICP) source has been proposed by V. Godyak and C.-W. Chung [1] as an alternative for radio-frequency inductively coupled plasma (RF ICP) sources. It was shown that inductive coupling enhanced with ferrite cores resulted in a great improvement of the power transfer efficiency to the plasma, allowed to operate the FMICP source at a considerably lower frequency than existing RF ICP sources. The low frequency operation resulted in a complete elimination of parasitic capacitive coupling between the coil and plasma. Conclusion was made about the prospects of the distributed FMICP sources as an alternative tool for large-scale plasma processing.

Electrophysical properties of a large-scale (processing chamber diameter up to 560 mm) distributed FMICP have been thoroughly investigated for inert plasma-forming gases (Ar, Xe, Ar/He) in the pressure range of 2–600 mTorr [1–6]. However, addition of halogen containing gases typical for plasma processing would dramatically change the FMICP properties due to a significant change in electron energy balance and reaction rates. To investigate the effects of a strong electronegative gas (Cl_2) addition on a large-scale distributed FMICP, an experimental setup has been created shown below. To analyze parameters of the distributed FMICP in Ar/Cl_2 mixture, a global (volume averaged) model of Ar/Cl_2 discharge [7] was used.

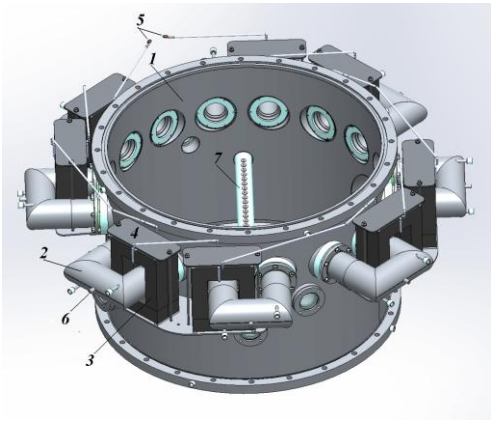

Fig.1. Experimental distributed FMICP source. 1 – Chamber (int. diameter of 700 mm), 2 – U-shaped tubes, 3 – Ferrite cores, 4 – ICP Coils, 5 – Power supply (100 kHz), 6 – Gas inlets, 7 – Flat probes array.

Distributed FMICP electrophysical parameters were measured for various values of plasma forming gas pressure (2−10 Pa) and chlorine content (0−5 vol%), and compared with the results of calculations. Effects of Cl_2 addition on the reaction rates, ionization and energy balances of the distributed FMICP were analyzed using the global model [7]. The features of the large-scale distributed Ar/Cl_2 FMICP were discussed.

REFERENCES

[1] V. Godyak, C.-W. Chung, " Distributed ferromagnetic inductively coupled plasma as an alternative plasma processing tool," Jpn. J. Appl. Phys., vol. 45, no. 10B, pp. 8035–8041, 2006.

[2] K. Lee, Y. Lee, S. Jo, C.-W. Chung, V. Godyak, "Characterization of a side-type ferrite inductively coupled plasma source for large-scale processing," Plasma Sources Sci. Technol., vol. 17, Article Number 015014, 2008.

[3] V. Godyak, "Electrical and plasma parameters of ICP with high coupling efficiency," Plasma Sources Sci. Technol., vol. 20, Article Number 025004, 2011.

[4] J.-Y. Bang, J.-Y. Kim, C.-W. Chung, "Electron energy flux control using dual power in side-type inductively coupled plasma," Phys. Plasmas, vol. 18, Article Number 073507, 2011.

[5] H.J. Kim, H.-J. Hwang, D.H. Kim, J.H. Cho, H.S. Chae, C.-W. Chung, "On uniform plasma generation for the large area plasma processing in intermediate pressures," J. Appl. Phys., vol. 117, Article Number 153302, 2015.

[6] D. Han, H.-C. Lee, J.-Y. Bang, C.-W. Chung, S.Y. Moon, "Measurements of the spatially resolved electron temperature and plasma potential in ferrite-core side type Ar/He inductively-coupled plasmas," Curr. Appl. Phys., vol. 15, pp. 1036–1041, 2015.

[7] E.G. Thorsteinsson, J.T. Gudmundsson, "A global (volume averaged) model of a Cl_2/Ar discharge: I. Continuous power," J. Phys. D: Appl. Phys., vol. 43, Article Number 115201, 2010.

* The work was supported by the Russian Science Foundation under grant No. 18-19-00205.

INCREASING THE OPERATION STABILITY OF AN ELECTRON SOURCE WITH A PLASMA CATHODE DUE TO THE BEAM DEFLECTION BY THE LEADING MAGNETIC FIELD*

V.I. SHIN, M.S. VOROBYOV, P.V. MOSKVIN

Institute of High Current Electronics SB RAS, Tomsk, Russia

Sources of pulsed high-current electron beams are of considerable interest, primarily due to the promise of their use for processing the surface of materials, improving the wear resistance of the cutting tool, increasing the fatigue strength of turbine blades and compressors, increasing the corrosion resistance of metallic materials, increasing the electrical strength of vacuum insulation, etc. [1-3], and need further study and technological improvement.

In any electron source, regardless of the type of cathode is used, when the cathode and target are located on the same axis, the emission electrode is contaminated with the target material as well as ion bombardment of this electrode which is most often accompanied by a decrease in the electric strength of the high-voltage accelerating gap. In this work, it was investigated the operation stability of an electron source with a plasma cathode with a grid (layer) stabilization of the emission plasma boundary and the plasma anode. The increase in the stability of the source's operation was achieved by reducing the reverse gas and ion flows by changing the trajectory of the electron beam, which made it possible to place the electron source and the target in different planes. The deflecting system is a sector tap with a total angle of rotation of 90 degrees, on which solenoids are mounted, creating a leading magnetic field.

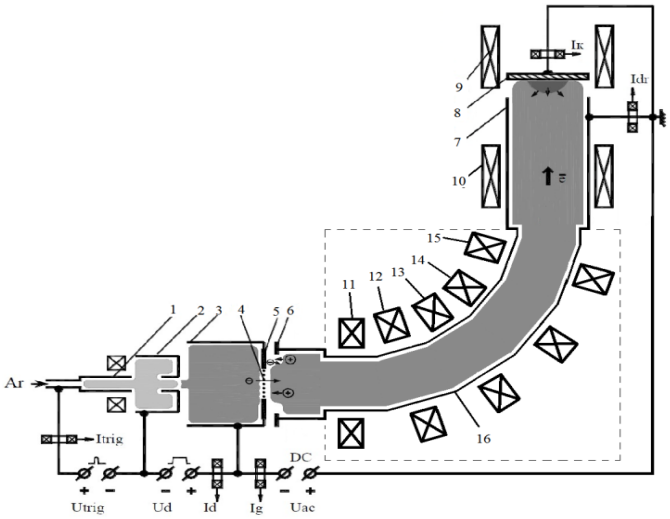

Fig.1. Scheme of the pulsed-beam installation with a plasma cathode, allowing to deflect the electron beam.

It has been experimentally shown that the stability of the electron source when the beam is deflected increases significantly, which allowed us to expand the range of beam parameters and opens up new possibilities for using such an electron source for both scientific and technological purposes.

REFERENCES

[1] D.I. Proskurovsky, V.P. Rotshtein and G.E. Ozur, Proc. of 11th Int. Conf. on High Power Particle Beams (BEAMS-96), pp 259-262, 1996.

[2] D.I. Proskurovsky, Yu.F. Ivanov, V.P. Rotshtein et al., Journal of Vac. Sci. & Techn A16(4), pp 2480-2488, 1998.

[3] V. Engelko, G. Mueller, H. Bluhm, Vacuum 62(2-3), pp 97-103, 2001.

* The work was supported by the grant of President of Russian Federation (Projects No MK-123.2019.2).

EFFECT OF ATMOSPHERIC-PRESSURE PLASMA JET ON NORMAL AND TUMOR CELLS *IN VITRO*

A.A. EVTINA[1,3], *V.O. NEKHOROSHEV*[2], *M.A.BULDAKOV*[3], *N.V. LANDL*[2], *Y.D. KOROLEV*[2]

[1]*National research Tomsk state university, Tomsk, Russia*
[2]*Institute of High Current Electronics SB RAS, Tomsk, Russia*
[3]*Cancer Research Institute, Tomsk National Research Medical Center, RAS, Tomsk, Russia*

Currently, the plasma jets based on atmospheric pressure discharges in a gas flow are of interest both for research and for practical use in biology and medicine. In particular, a number of research have studied the effect of low-temperature plasma jets on brain, skin, breast, and cervical cancer cells [1-5]. It has been shown that in some cases the plasma jet can selectively destroy tumor cells *in vitro*, preserving untransformed cells, and also significantly reduce the size of the tumor *in vivo* [3, 4].

The purpose of this work is investigation the effect of atmospheric-pressure plasma jet on the proliferation of tumor cells – cervical cancer cells (HeLa) and normal rat fibroblast cells (3T3). During the experiment, the cells were placed in Petri dishes with a nutrient medium, then treated with a plasma jet and incubated at 37°C in the atmospheric humidity with 5% of CO_2. The plasma source based on the discharge in the airflow is used for obtaining the plasma jet. The high voltage power supply provides the ignition and sustaining of discharge by applying to the electrodes pulsed voltage with the magnitude up to 15 kV and a pulse duration about of 1 μs at the repetition frequency f in the range from 1.5 kHz to 4.5 kHz. The compressor provides an air mass flowrate of up to 0.05 g/s for transferring of active species from the discharge plasma region to the processed sample. The proliferative activity of cells was estimated by using the MTT-test one day and five days after treatment.

Experiments have shown that plasma jet exposure leads to inhibition of the proliferative activity of HeLa tumor cells. The effect depends on the pulse repetition frequency and the exposure time. Inhibition of cell proliferation is observed when exposed for 120 s at f = 2.5 kHz and reaches a maximum (70%) on the 5th day. The reaction of rat fibroblast cells (3T3) was significantly different. It was shown that plasma jet treatment leads to reduce the proliferation of normal cells by less than 30%, and after 5 days has a stimulating effect up to 25%. This effect may be due to a selective increase of reactive oxygen species in tumor cells that differ from normal cells in their metabolic characteristics [5]. The revealed effect indicate a high potential for using atmospheric-pressure plasma jet in oncological practice.

REFERENCES

[1] C. Weishaupt, S. Emmert, “Connecting basic cold plasma technology to dermato-oncology,” Clinical Plasma Medicine, vol. 10, pp. 16–19, March 2018.

[2] K. D. Weltmann, M. Polak, K. Masur, T. von Woedtke, J. Winter, S. Reuter, “Plasma Processes and Plasma Sources in Medicine,” Contrib. Plasma Phys., vol.52, no. 7, pp. 644–654, 2012.

[3] Y. Sato, S. Yamada, S. Takeda, N. Hattori, K. Nakamura, H. Tanaka et al., “Effect of Plasma-Activated Lactated Ringer’s Solution on Pancreatic Cancer Cells In Vitro and In Vivo,” Annals of Surgical Oncology, vol. 25, no. 1, pp. 299–307, 2017.

[4] M. Keidar, D. Yan, I.I. Beilis, B. Trink, J.H. Sherman, “Plasmas for Treating Cancer: Opportunities for Adaptive and Self-Adaptive Approaches,” Trends in Biotechnology, vol. 36, no. 6, pp. 586–593, 2018.

[5] D. Yan, J.H. Sherman , M.Keidar, “Cold atmospheric plasma, a novel promising anti-cancer treatment modality,” Oncotarget, vol. 8, no. 9, pp. 15977–15995, 2017.

THE FORMATION OF ION ENERGY SPECTRA IN NONLINEAR WAVES*

I.L.MUZYUKIN[1,2]

[1] Institute of Electrophysics UB RAS, 106 Amundsena Str., Ekaterinburg, 620016, Russia
[2]Institute of Physics and Technology Ural Federal University, 19 Mira Str., Ekaterinburg, 620002, Russia

The most probable plasma turbulence type is the ion-acoustic turbulence. The ion-acoustic turbulence has one of the biggest increments. Thus, it is very likely that there is a spectrum of ion-acoustic waves propagating in the vacuum arc plasma. These waves can be the cause of ion acceleration and scattering inside and outside the plasma. It can be assumed that the velocity of disturbances propagation in the plasma may be the velocity of nonlinear ion-acoustic waves.

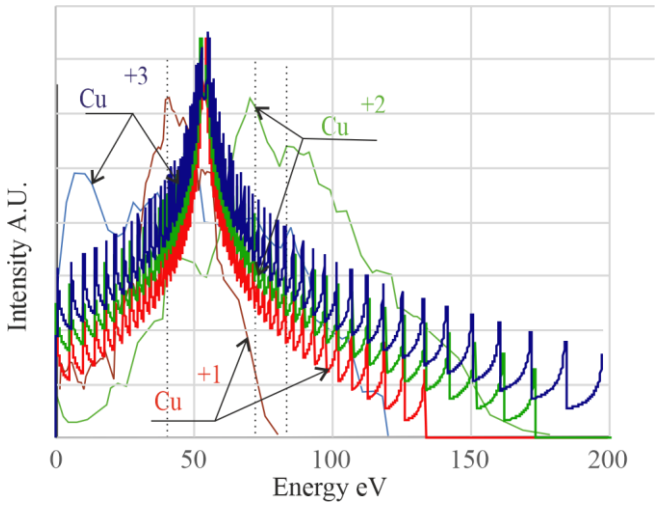

Fig.1. The calculated ion energy distribution for ion-acoustic shock wave/ The potential of the wave is given by(1). The effective electron temperature is 20eV.The average charge is 2. The correspondent ion-acoustic wave velocity, is 12.8 km/s The experimental ion spectra is presented for comparison.

In general, the ion-acoustic waves can be the cause of the formation of vacuum arc ion flow velocities measured by different experimental methods.

According to this approach, the final energy distribution of ions is formed at the energy spectrometer entrance, where plasma ions separated from the electrons. The energy distribution is forming by a set of incoming ion-acoustic waves. The potential dependence of the wave on x coordinate in the wave coordinates is given by the equation:

$$U = U_m \sin(\frac{2\pi}{\lambda} x) e^{(-\gamma x))}, \quad (1)$$

Final energy distribution measured using a long-time energy scanning technique or averaged over a big amount of single measurements is a sum of distributions produced by nonlinear ion-acoustic waves with different velocities and initial amplitudes. According to this approach, the velocity rule is a fundamental rule. But sometimes when charge state composition is dependent on electron temperature there may be the dependence of most probable energy on the ion charge state.

* The work was supported in part by RFBR Grant Nos. 18-08-00547, 19-08-00783, 19-58-53006

HIGH POWER DC ELECTRON ACCELERATORS OF THE ELV-TYPE FOR RESEARCH AND INDUSTRIAL APPLICATION

N.K.KUKSANOV, Y.I. GOLUBENKO, R.A. SALIMOV, S.N. FADEEV, P.I. NEMYTOV, A.I. KORCHAGIN, A.V. LAVRUCHIN, A.V. SEMENOV, V.G. CHEREPKOV, D.A. KOGUT, E.V. DOMAROV, D.S. VOROBIEV, M.G. GOLKOVSKY

Budker Institute of Nuclear Physics SB RAS, Novosibirsk Russia

Electron-beam technologies have been used extensively in radiation treatment of polymer compositions. The use of these technologies enabled to develop the manufacture of a wide range of wires, cables and heatshrinking goods, films, bands, etc. All of them are of high security and reliability during operation as under standard and extreme operating conditions. The powerful industrial electron accelerators are perfect instruments for radiation treatment of polymers. This paper reviews the development and status of the ELV electron accelerators that are intent for industrial application. The ELV electron accelerators are DC machines meant for wide application in various technological processes. They are designed and produced by the Budker Institute of Nuclear Physics of the Siberian Branch of the Russian Academy of Science. The ELV accelerators are the most famous accelerators in the world. Over 180 accelerators have been supplied from 1973 to date. The accelerator life time is several decades and 120 accelerators are still under operation. One of the advantages of ELV is high-efficiency conversion of electrical power to electron beam power (70-80%). Main parameters of the accelerator are energy and beam power. The energy governs the penetration depth i.e. the thickness of treated material, while the level of beam current affects the efficiency of the accelerator (m/min or ton/hour).

The maximum beam power of a regular accelerator is 100 kW and the maximum beam current is 130 mA. The accelerators cover the energy range from 0.3 to 2.5 MeV. The accelerator with energy range of 0.6 - 1.0 MeV was developed for environmental applications.

The ELV accelerators fully meet the requirements of radiation technologies. Designed for the industrial application, the ELV electron accelerators make electron-beam product treatment actually a highly efficient technique to produce high-quality products. We follow the requirements of accelerators market and the requests of electron beam technology users. The ELV accelerator can be equipped with a wide set of additional devices that extend its application and improve the quality of electron beam treatment. Such devices include two-side and 4-side irradiation systems, and ring irradiation and transportation systems for cables, films and grain. Some special devices can be used in order to improve dose uniformity during film and band irradiation. Due to the control system based on PC software, the ELV accelerators can easily be adapted to technological processes. On the request of Leibnitz Research Centre Rossendorf (Germany) [4], we designed the accelerator for use in fast X-ray tomography. The energy and the beam power of this accelerator are 1 MeV and 100 kW respectively. The beam optics allows production of the beam of 1-2 mm in diameter at a distance of 1.5 meter from the focusing lens. Accelerating tube is separated from the high-voltage rectifier and connected to it by a 500 mm gas feeder. Accelerating tube can be inclined at an angle of 30° to the vertical axis.

The ELV accelerators can be equipped with the differential pumping system in order to extract the electron beam into atmosphere [3]. A beam of 70 kW power is extracted through the hole of 1 mm in diameter. A power density of the beam of about 5 MW/cm 2 can be achieved at the exit which allows using the accelerator in other application areas, such as evaporation of various materials, production of nanopowders, surface hardening of metals, welding, melting, and cutting of metals, production of special types of ceramics etc.

The local shielding of the accelerators has been upgraded. The dimensions of shielding depend on the size of extraction window and can be up to 2 meters in length. Typically, a scanning angle of 30 degree is used in the accelerators. The accelerator with energy of less than 1 MeV can be equipped with a local steel shielding weighing about 50 T.

REFERENCES

[1] [1] Kuksanov N.K. et al., 2012, Development of the model range and improve performance accelerator ELV. Problems of Atomic Science and Technology, Issue 3, 15-18.

[2] [2] Kuksanov N.K. et al., 2016, The development of ELV accelerators for the optimization EB processing of polymers. 12th International Conference on Electron Beam Technologies, 13-18 June 2016, Varna, Bulgaria, 2016; Electrotechnica&Electronica, N 6, CEEC, Bulgaria.

[3] [3] Golkovsky M.G. et al, 2016, Corrosion resistance of Ti-Ta-Zr coatings fabricated on VT14 titanium alloy substrates using the electron beam injected into the atmosphere. -. - Electrotechnica&Electronica, N 6, CEEC, Bulgaria.

[4] [4] Hampel U. et al., 2012, Feasibility study for mega-electron-volt electron beam tomography. Review of Scientific Instruments. - Vol. 83.- Issue 9.September 2012.-ArtNumber 093707

PLASMA DEVICES FOR SYNTHESIS AND TREATMENT OF POWDER MATERIALS *

A.S. ANSHAKOV, P.V. DOMAROV, V.A. FALEEV

Kutateladze Institute of Thermophysics SB RAS, Novosibirsk, Russia

Creating an industry of new powder materials requires the implementation of new methods for their preparation and new hardware equipment of modern technological processes. These include the plasma chemical synthesis of powder materials and the modification of powders in a stream of electric arc thermal plasma.

Plasma heating of the feedstock allows you to evaporate almost any material and carry out the necessary chemical reactions in the gas phase and then condense the vapor into a dispersed solid phase. At the same time, plasma technology provides high versatility with respect to the processed materials, the possibility of synthesizing a complex composition and the continuity of the process. The last condition assumes a long service life of electric arc plasmatrons, calculated in hundreds of hours.

A description is given of a plasma generator for spraying and processing powders with an interelectrode insert, and the measured fields of temperatures and plasma flow velocities are presented. It is shown that the constructive solution of the device provides a diffuse distribution of the anode section of the arc with the aim of high repeatability of the technology and electrode life.

A plasma-thermal reactor for the synthesis of silicon carbide nanopowders has been created on the basis of a two-jet plasmatron. The reactor layout is shown in the figure.

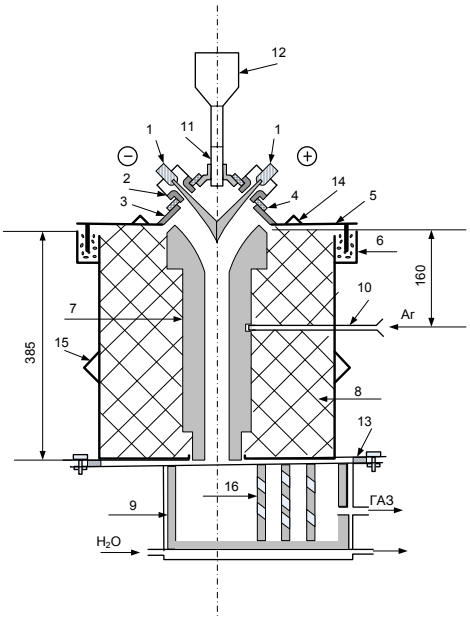

Fig.1. Scheme of a plasma thermal reactor.

The reactor has been based on a two-jet plasmatron 1 with a capacity of 12-23 kW, a plasma-forming gas is argon. The graphite cylinder is located along the axis of the metal casing lined with fireclay brick. The mixture of silicon dioxide and carbon is fed through a dispenser 12. The target product is collected on the fridge plates 16. The highest content of silicon carbide is formed in the temperature range of 1900 K. Using literature data and our own studies, it was shown that in a two-jet reactor, a uniform temperature distribution over its cross section is realized in the reaction zone. The result significantly affects the efficiency of processing the starting material in the reactor.

REFERENCES

[1] V.S. Cherednichenko, A.S. Anshakov, M.G. Kuzmin, Plasma Electrotechnological Installations, Moscow, 2019.

[2] A.S. Anshakov, P. B. Domarov, V.R. Bauer, M.V. Cherednichenko, University News. Physics, vol. 61, Article Number 8-2, 2018

[3] A.C. Anshakov and E.K. Urbakh, et al. Thermophysics and Aeromechanics, Article Number 3, 2017.

* This work was carried out under state contract with IT SB RAS (AAAA-A17-117030910025-7)

SOFT X-RAY RADIATION SOURCES BASED ON HIGH-ENERGY PLASMA FLOW THERMALIZATION WITH GAS AND SOLID-STATE TARGETS*

V.V. GAVRILOV[1], A.M. ZHITLUKHIN[1], D.M. KOCHNEV[1], V.A. KOSTYUSHIN[1,3], I.M. POZNYAK[1], S.A. PIKUZ[2,3], S.N. RYAZANTSEV[2,3], I.YU. SKOBELEV[2,3], D.A. TOPORKOV[1]

[1]*Troitsk Institute for Innovation and Fusion Research, Moscow, Russia*
[2]*Joint Institute for High Temperatures, Russian Academy of Sciences, Moscow, Russia*
[3]*National Research Nuclear University MEPhI, Moscow, Russia*

Experimental results on high-power X-ray generation in the interaction of high-energy plasma flow with gas and solid targets are presented. The hydrogen plasma flows with velocities of $(4\div6)\times10^7$ cm/s, ion density $(2\div4)\times10^{15}$ cm^{-3}, and energy of ≤ 40 kJ were produced by an electrodynamic coaxial plasma accelerator with pulsed gas injection. Supersonic gas jets of nitrogen or neon were used as gas targets. This jet was formed by a flat Laval nozzle. The maximum density in the gas jets reached 10^{17} cm^{-3} with a jet thickness of ≈ 5 cm and a width of ≈ 15 cm. Flat samples of graphite, boron nitride, and tungsten were used as the solid-state targets. The interaction of a powerful hydrogen plasma flow with all used targets took place in a magnetic field with induction up to 2 T.

An extensive set of experimental data was received by varying the density and velocity of the plasma flow and the target parameters. The main efforts were focused on obtaining time-resolved X-ray images of the target plasma and spectral intensity data of the X-ray radiation emitted from the plasma produced by the interaction of a high-power plasma stream with gas or solid-state target. The diagnostic equipment is described, and the experimental results obtained under different operating conditions are discussed. In particular, the dynamics of the plasma flow interaction with the gas jet or solid-state target was recorded as the X-ray images by a four-frame MCP camera through pinholes. Measurements provided with a set of photodiodes covered by different filters showed that soft X-ray (photon energies ≤ 0.4 keV) pulses with a duration of 10÷20 μs were generated in the collision region. Data obtained with the help of the diodes allowed determining the temporal evolution of the plasma electron temperature in each experiment. The transmission grating spectrometer with the gratings of a 500 nm/200 nm period was used for recording emission spectra in the wavelength range of 1÷70 nm with a spatial and temporal resolution. Observed intensities of spectral lines were compared with the results of detailed kinetic calculations performed in a steady-state approximation to determine the plasma electron temperature.

The experimental results on the interaction of the hydrogen plasma flow with gas are compared with ones obtained in the interaction with solid targets. The characteristic features of specific sources of powerful x-ray radiation are analyzed. It was found that in the case of solid-state targets produced from low Z materials (graphite, boron nitride), resonance lines of H- and He-like ions were detected, while only He-and Li-like ions radiation was observed in the short wavelength region of spectra when the plasma flow collided with a nitrogen/neon jet. As for the high Z material, the radiation from the tungsten target plasma, in turn, is characterized by a broadband quasi-continuous emission spectrum in the range of 2-60 nm with a maximum intensity at 5-20 nm. This demonstrates a more effective conversion of plasma flow energy to short wave radiation in hydrogen plasma flow collision with the solid target compared with the gas jet. In experiments with solid-state targets, the thickness of the emitting tungsten layer near the target was about 5 cm, while in the case of graphite and boron nitride, the emitting zone extended to a distance of at least 50 cm. The relative compactness of a radiation source with low Z targets was ensured by applying supersonic gas jets.

* The work was supported by the Russian Foundation for Basic Research (Project No. 18-29-21013).

DEVELOPMENT OF A TWO-DIRECTION WAVE PLASMA SOURCE[1]

A.I. SHUMEIKO, V.D. TELEKH**

**Bauman Moscow State Technical University, 2nd Bauman str., 5, Moscow, 105005*
shumeikoandrei1995@gmail.com, +7 967 0779765

In the last decades, a significant interest has been focused on the electrodeless methods of the plasma generation and acceleration. Such methods are use of wave plasma sources for plasma production and magnetic nozzles of plasma acceleration.

A wave plasma source and a magnetic nozzle, consisting of an applied convergent-divergent axysimmetric magnetic field, constitute the main plasma production and acceleration stages of several advanced plasma source concepts. Illustrative examples in the aerospace field is the Helicon Thruster [1,2]. Also, these sources could be used for plasma flow control in technological applications.

The use of electrodeless methods for plasma production and acceleration in the space are necessary to meet requirements of future space missions and are designed to produce high specific impulse and greater thrust than current electric propulsion systems while having a lifetime much greater than conventional space propulsion systems.

This paper presents the experimental results on the plasma characteristics in the wave plasma source with two magnetic nozzles. This source is the first prototype of a currently designed two-direction wave plasma source with two open ends. The studies were carried out under different parameters (including the types of feed gases, RF-power, etc.). The possibility of effectively creating independent high-density plasma flows using a single bi-directional RF plasma source is demonstrated

REFERENCES

[1] *Shumeiko, A. I., & Telekh, V. D. Probe diagnostics of the plasma plume created by a magnetic nozzle of an inductively coupled plasma source. Journal of Physics: Conference Series. 2019. Vol. 1393, No. 1, p. 012027.*

[2] *Shumeiko, A. I., & Telekh, V. D. Helicon engine in outboard air as a successful solution for maintaining small space vehicle in orbits up to 200 km. AIP Conference Proceedings. 2019. Vol. 2171, No. 1, p. 170019.*

[1] The work was supported by the Russian Foundation for Basic Research under grant No. 18-29-21039 and has been performed at “Beam-M” facility of Bauman Moscow State Technical University

STUDY OF THE DEPENDENCE OF THE DISTRIBUTION OF THE PLASMA PARAMETERS ALONG THE HOLLOW CATHODE FROM THE BASIC PARAMETERS OF THE NON-SELF-SUSTAINED GLOW DISCHARGE*

D.Y. IGNATOV[1], *I.V. LOPATIN*[1], *V.V. DENISOV*[1]

[1] *Institute of High Current Electronics SB RAS, 2/3, Akademichesky ave., Tomsk, 634055, Russia,*
Phone: +7(3822) 492-683, E-mail: danilabay29@ya.ru

The plasma of a non-self-sustained hollow cathode glow discharge is generated using a two-digit system in which the pipeline is the glow discharge cathode and the anode is a water-cooled flat electrode located near the end of the pipeline and through which the working gas is supplied. The opposite end of the pipeline is overlapped by a grid, which, together with the outer surface of the pipeline, is an anode for an auxiliary arc discharge with a combined incandescent and hollow cathode (PINK) [1]. The injection of electrons from the auxiliary discharge plasma is performed through a grid located at the end of the hollow cathode. Electrons flying through the grid ionize the plasma-forming gas. Also, the grid is necessary to stabilize the boundary of the auxiliary plasma at the time of ignition of the discharge. Since the walls of the pipeline are a cathode and form an electrostatic trap, accelerated electrons begin to oscillate in the treated cavity until they lose their energy in inelastic collisions with gas molecules or escape to the anode.

In this system, the main characteristics and combustion conditions of a non-self-sustained glow discharge were investigated. The dependences of the distribution of the ion current density along the hollow cathode on the basic conditions and parameters of the discharge combustion (pressure, voltage, discharge current) are established. The ion current density was measured using 5 collectors installed along the axis of the hollow cathode at an equal distance from each other. The graph (Fig. 1) shows the results of measuring the ion current density using collectors along the hollow cathode at various voltages of a non-self-sustaining glow discharge.

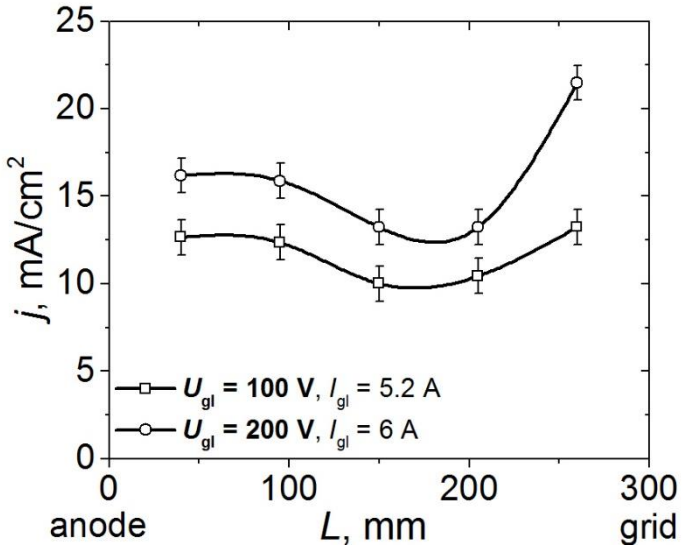

Fig.1. Measurements of the distribution of ion current density along the internal cavity of a hollow cathode.

REFERENCES

[1] D.P. Borisov, N.N. Koval, P.M. Schanin Patent of Russia No. 216707. 1998.

* The work was supported by RFBR according to the research project № 18-38-00836.

NON-SELF-SUSTAINED GLOW DISCHARGE AT CURRENTS UP TO SEVERAL HUNDRED AMPERES WITH ELECTRON INJECTION FROM TWO ELECTRON SOURCES[1]

E.V. OSTROVERKHOV, V.V. DENISOV

Institute of High Current Electronics SB RAS, 2/3 Akademichesky ave., Tomsk, 634055, Russia, e-mail: evgeniy86evgeniy@mail.ru, Tel.+7(3822)491713

For ion-plasma treatment of large-sized products from metals and alloys at low (≈ 1 Pa) pressure, it is necessary to use chambers of the corresponding volume, usually more than 0.1 m^3. A non-self-sustained low-pressure glow discharge with a hollow cathode (usually it is inner walls of the vacuum chamber) [1], allows the generation of a relatively uniform plasma in large vacuum volumes. The main glow discharge is initiated between the hollow cathode and the flat anode. With additional injection of electrons, a glow discharge stably ignites and burns at low voltages, starting from several tens of volts. Electrons can be emitted, for example, from a plasma formed in an auxiliary arc discharge ignited in a gas plasma source with an integrally cold hollow cathode [2]. The anode of the auxiliary arc discharge is an electrode covered by a fine-structure grid (0.4 × 0.4 mm), through which some electrons pass and inject into the plasma of the main glow discharge. For practical use, the most important is to ensure a high uniformity of the distribution of plasma concentration in the volume of the working chamber. In chambers of extended shape or complex geometry the problem of uniformity can be solved by using of several electron sources. The shape and location of the anode of the main glow discharge is also important for reducing heterogeneity. In this paper, we determine the validity of using the principle of superposition of ion current density distributions on a probe from a glow discharge plasma with a current of up to 200 A obtained by using of two electron sources. The study was carried out for hollow cathodes with ratios of diameter to length of 1:1 and 2:1 and volumes of 0.21 m^3 and 0.34 m^3, respectively. The results of the work are useful for carrying out of estimated calculations of the influence of injection processes on the distribution of plasma concentration in the hollow cathode and designing of large-sized systems based on the non-self-sustained low-pressure glow discharge for ion-plasma processing of metal and alloy products.

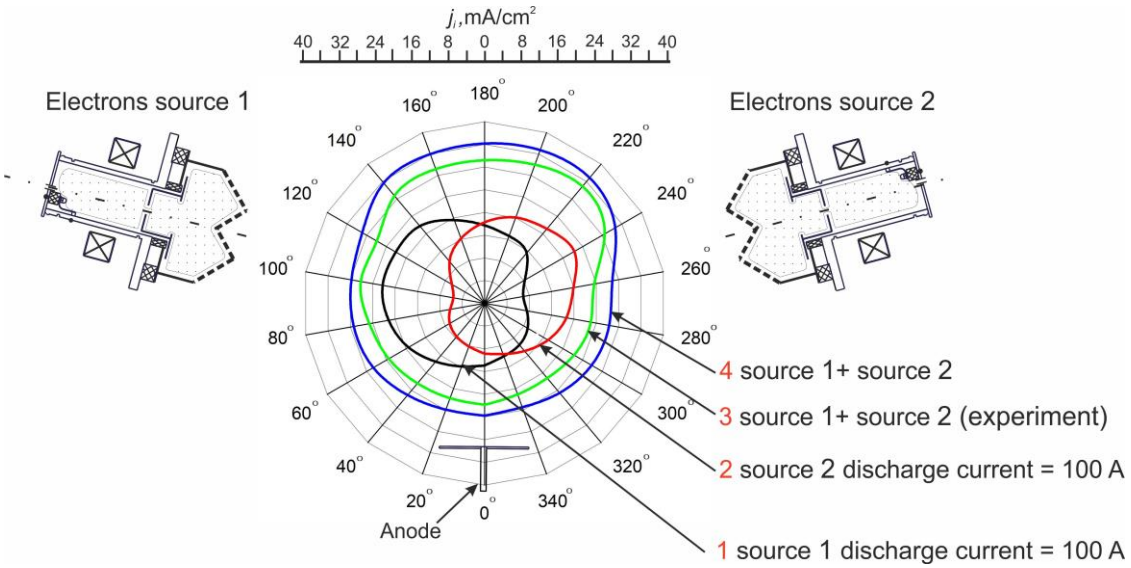

REFERENCES

[1] *V.V. Denisov, Yu.H. Akhmadeev, N.N. Koval, S.S. Kovalsky, I.V. Lopatin, E.V. Ostroverkhov, N.N. Pedin, V.V. Yakovlev, and P.M. Schanin. The source of volume beam-plasma formations based on a high current non-self-sustained glow discharge with a large hollow cathode // Phys. Plasmas. –2019. – V.26. – 123510.*

[2] *V. V. Denisov, Yu. H. Akhmadeev, N. N. Koval and E. V. Ostroverkhov Low-temperature plasma source based on a cold hollow-cathode arc with increased service life // High Temp. Mater. Prosess. – 2016. – V.20(4). – pp.309–316.*

[1] The work was carried out with the financial support of the RFBR grants (№18-38-00836 mol_a and № 19-08-00370 A).

GENERATION AND DIAGNOSTICS OF RE-PULSING GLOW DISCHARGE IN CENTIMETER ORDER AIR GAPS

V. A. GAMALEEV[1], *M. HORI*[1]

[1]*Center for Low-temperature Plasma Science, Nagoya University, Nagoya, Japan.*

Fast development of non-equilibrium atmospheric pressure plasmas in last two decades led to a wide use of plasma technologies in surface modification, gas conversion, medicine and agriculture.[1] Glow discharge looks promising for those applications owing to a wide range of plasma parameters and high efficiency of production of reactive species; however, generation of stable ambient air glow discharge in centimeter order gaps is still challenging.[3] In this work we propose simple method for generation of re-pulsing ambient air glow discharge with predefined parameters in centimeter order gaps.

Re-pulsing glow discharge was generated between two copper rod electrodes by supplying high voltage to the first electrode when the second electrode was electrically grounded. High voltage was supplied a using custom power supply consisting of push-pull generator powered by regulated direct current power supply (DC PSU), high voltage transformer, diode rectifier and reservoir capacitor. Power supply used in the present work allows to generate corona discharge, repeating spark discharges with corona discharge and repulsing glow discharge between two metal electrodes with spacing up to 2 cm, as it shown on the Fig. 1. Type of the discharge depends on the parameters set on the power supply.

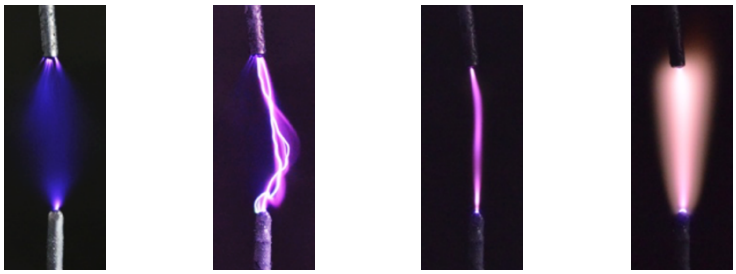

(a) (b) (c) (d)

Fig. 1 Photos of corona (a), spark (b), subnormal glow (c) and normal glow (d) discharges in 2 cm gap.

Re-pulsing glow discharge was ignited as a sequence of spark and glow discharges and sustained in a glow regime after ignition. The discharges were characterized by high speed camera, current and voltage measurements and optical emission spectrometry (OES). Typical structure of the glow discharge consisting of cathode glow, dark faraday space, positive column and anode glow was observed. Transition from subnormal to normal glow mode was confirmed by analysis of current and voltage waveforms. It was found by OES that type of the discharge is having strong effects on the ratio of produced reactive species. It was confirmed that with change of discharge from subnormal to normal glow regime rotational temperature could vary in a wide range (from 1650 to 3500 °K). Developed device allows to ignite glow discharge with predefined parameters which makes possible control of the gas temperature and ratio of reactive species by setting the discharge parameters prior ignition.

In conclusion, re-pulsing glow discharges in centimeter order gaps were successfully generated in atmospheric pressure air as a sequence of spark and glow discharges. Simple setup and wide range of plasma parameters which could be defined prior ignition of the discharge are looking promising for practical use in gas conversion, generation of radicals and surface treatment applications. Results of electrical diagnostics, fast speed camera imaging and OES will be reported.

This research was funded by JSPS KAKENHI Grant Numbers 19H05462, 19H01889, and Plasma-bio consortium project (01221907).

REFERENCES

[1] J. Winter, R. Brandenburg, K. Weltmann, “Atmospheric pressure plasma jets: an overview of devices and new directions“, *Plasma Sources Sci. Technol.*, **24**, 64001 (2015).

[2] D. Staack, B Farouk, A. Gutsol, A. Fridman, “DC normal glow discharges in atmospheric pressure atomic and molecular gases“, Plasma Sources Sci. Technol., 17, 025013 (2008).

PLASMA ELECTRON EMITTER BASED ON LOW PRESSURE NON-SELF-SUSTAINED GLOW DISCHARGE WITH HOLLOW CATHODE[1]

V.V. YAKOVLEV, V.V. DENISOV, N.N. KOVAL, M.V. SAVCHUK

Institute of High Current Electronics SB RAS, 2/3 Akademichesky ave., Tomsk, 634055, Russia, e-mail: vlad000@rambler.ru, Tel.+7(3822)492683

Low pressure gas discharge plasma is widely used as an electron emitter in pulsed electron beam sources. In use to generate intense pulse electron beams with sub-millisecond duration of currents to several hundred Amperes in plasma emitter, the arc discharge is used. Commonly, the arc discharge counteracting leads to high plasma inhomogeneity in the area of the emission grid. This makes it difficult to create plasma emitters with a large (>10 cm) diameter of the emission grid electrode that can stably generate submillisecond electron beams with a current of up to several hundred amperes, with energies of up to several tens of kiloelectronvolts at pressures of about 0.1 PA. In this paper, the modes of pulsed electron beam generation in a system with a plasma emitter were studied. For plasma generation, a pulsed low-pressure non-independent glow discharge with a hollow cathode with a current of up to several hundred amperes and duration of up to 1 mS, was used.

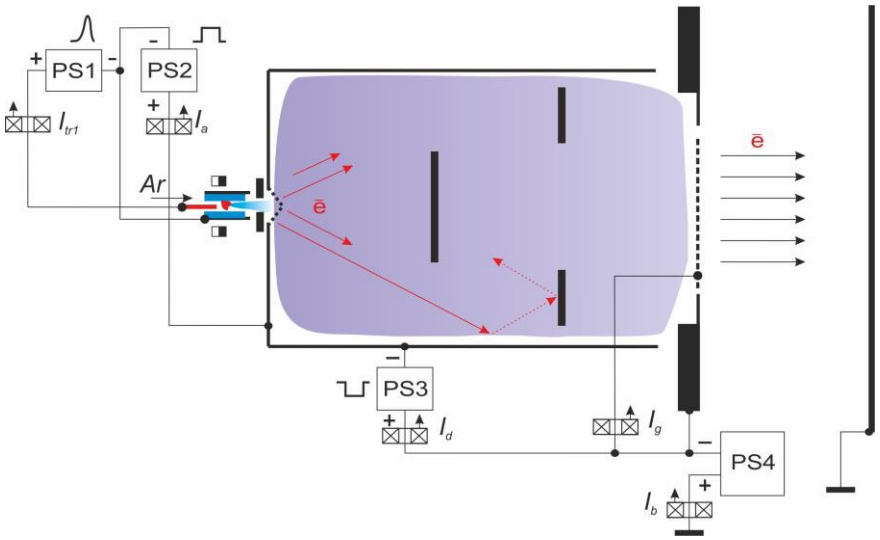

[1] The work was carried out with the financial support of the RFBR grant №18-38-00836.

BEAM-PLASMA FORMATIONS IN A HOLLOW CATHODE OF A NON-SELF-SUSTAINED GLOW DISCHARGE FOR TECHNOLOGICAL APPLICATION [1]

V.V. DENISOV, N.N. KOVAL, YU.A. DENISOVA, E.V. OSTROVERKHOV, S.S. KOVALSKY

Institute of High Current Electronics SB RAS, 2/3 Akademichesky ave., Tomsk, 634055, Russia, e-mail: volodyadenisov@yandex.ru, Tel.+7(3822)492683

The report discusses the features and advantages of using of a low (≈ 1 Pa) pressure non-self-sustained hollow cathode glow discharge [1] for generation of bulk (0.2-0.3 m^3) beam-plasma formations. Beam-plasma formation (BPF) is understood as a plasma medium, for the formation of which it is necessary to have an electrode system that provides self-sustaining of the discharge in a certain range of operating parameters or burning of the discharge with a certain degree of non-independence. Secondly, it is necessary to inject into the discharge system a beam of charged particles, for example, electrons, which are injected into the plasma, significantly changing the characteristics of the discharge, and accordingly the parameters and composition of the plasma, and, in addition, the beam is a source of additional reactions near and on the surface of the processed substrate.

Particular attention is paid to the generation of extended beam-plasma formations in an extended (≈ 1 m long) hollow cylindrical cathode. To increase the uniformity of plasma generation, an extended arc plasma electron emitter based on an arc discharge is used. Successful examples of the implementation of surface hardening technologies for tool steels in the presented type of discharge are considered.

[1] *V.V. Denisov, Yu.H. Akhmadeev, N.N. Koval, S.S. Kovalsky, I.V. Lopatin, E.V. Ostroverkhov, N.N. Pedin, V.V. Yakovlev, and P.M. Schanin. The source of volume beam-plasma formations based on a high current non-self-sustained glow discharge with a large hollow cathode // Phys. Plasmas. –2019. – V.26. – 123510.*

[1] The work was carried out with the financial support of the RFBR grant № 19-08-00370 A.

DYNAMICS OF PLASMA PARAMETERS CHANGING IN A PULSED MODE OF THE NON-SELF-SUSTAINED ARC DISCHARGE [1]

S.S. KOVALSKY, E.V. OSTROVERKHOV, V.V. DENISOV

Institute of High Current Electronics SB RAS, 2/3 Akademichesky ave., Tomsk, 634055, Russia, e-mail: skov@sibmail.com, Tel.+7(3822)492683

Non-self-sustained arc discharge with thermionic and hollow cathodes is currently used in technological processes of surface treatment of materials and products [1]. This type of discharge is also used to generate pulsed electron beams based on plasma electron emitters with grid stabilization of the emission plasma boundary [2].

The article [3] describes the laws of plasma formation in a stationary mode, but of particular interest is the pulsed mode of this type of discharge. Work in pulsed mode can significantly increase the amplitude of the discharge current with an increased value of the burning voltage, as well as pulsed power. At the same time, in order to determine the advantages of using such kind of plasma, it is necessary to study the processes of plasma formation.

In this work, we determined the influence of the conditions of the discharge burning (pressure, type of gas, burning voltage) on the duration of the transition to the stationary state. We studied the dynamics of changes in plasma parameters (electron temperature, plasma concentration, floating potential) during a discharge pulse, including a long (up to several hundred microseconds) rise and fall front. Plasma emission spectra were measured for various types of gas.

REFERENCES

[1] *N.N. Koval, Yu.F. Ivanov, I.V. Lopatin, Yu.H. Akhmadeev, V.V. Shugurov, O.V. Krysina, V.V. Denisov. Generation of low-temperature gas discharge plasma in large vacuum volumes for plasma chemical processes.//Russian Journal of General Chemistry, 2015, V. 85, № 5, pp. 1326-1338.*

[2] *Бугаев С.П., Крейндель Ю.Е., Щанин П.М. Электронные пучки большого сечения. – М.: Энергоатомиздат, 1984. – 112 с.*

[3] *Korolev, Y.D., Koval, N.N. // Journal of Physics D: Applied Physics. – 2018. – V.51 – № 32. – p, 323001.*

[1] The work was carried out with the financial support of the RFBR grants №18-38-00836.

ELECTRICAL DIAGNOSTIC OF ATMOSPHERIC-PRESSURE PLASMA JET

V.O. NEKHOROSHEV[1], Y.D. KOROLEV[1,2], N.V. LANDL[1], O.B. FRANTS[1]

[1]Institute of High Current Electronics SB RAS, Tomsk, Russia
[2]National Research Tomsk State University, Tomsk, Russia

Currently, the atmospheric-pressure plasma systems attract considerable attention. The well-known examples of such systems are plasmatrons, where the ionized gas forms the plasma jet in a special outlet nozzle [1 – 4].

The paper describes the results of the investigations of a plasma jet based on the discharge in a gas flow. The glow-type discharge with contracted plasma column sustains in the plasmatron with coaxial electrodes *1* and *2* shown at the fig. 1. In the experiment the air mass flowrate is variated up to 0.5 g/s and average discharge current was up to 0.15 A. The plasma jet at the exit of the plasmatron nozzle is observed in these conditions. The value of the averaged discharge current was chosen to limit the power dissipated in the plasma region and gas temperature in the jet.

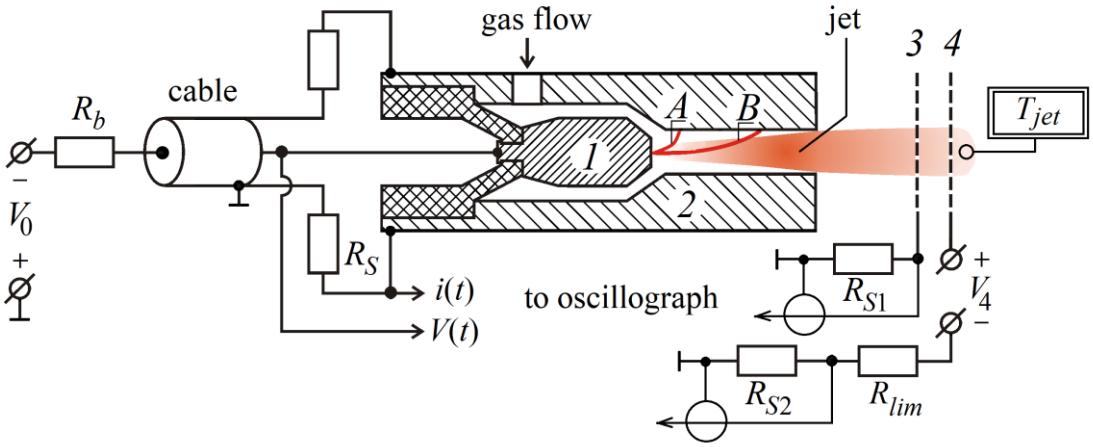

Fig. 1. Simplified circuit of the experimental setup for electrical diagnostic of the plasma jet. *1* – cathode, *2* – anode/nozzle, *3*, *4* – system of diagnostic grid-type electrodes, the gap length d_{34} = 0.5 mm. *A*, *B* – positions of the positive column; $i(t)$ – discharge current, $V(t)$ – discharge burning voltage; $V_0 \leq 5$ kV, R_b = 20 kΩ, R_S = 1 Ω, R_{S1} = 1 kΩ, R_{S2} = 10 kΩ, R_{lim} = 100 kΩ, $V_4 \leq 3$ kV, T_{jet} – thermocouple for measuring the temperature of gas in the jet.

The method for the jet diagnostics based on currents measuring in the system of additional electrodes *3* and *4* located at the plasmatron outlet nozzle has been proposed. The main idea of the investigation is the characterizing of the current sustaining modes in the system of diagnostic electrodes when the bias voltage V_4 is varied.

The experimental data show that the main charged particles is the jet are the electrons that are emitted from a plasma column of the glow discharge and these electrons carry the jet current. The model that describes the formation of electron flow in the jet has been proposed. Typical electron density in the jet estimated with a usage of the model is at a level of 10^9 cm^{-3}.

REFERENCES

[1] J. Winter, R. Brandenburg, K. D. Weltmann, "Atmospheric pressure plasma jets: an overview of devices and new directions," *Plasma Sources Sci. Technol.*, vol. 24, Article Number 064001, December 2015.

[2] Y. D. Korolev, V. O. Nekhoroshev, O. B. Frants, N. V. Landl, A. I. Suslov, V. G. Geyman, "Nonsteady-state processes in a low-current discharge in airflow and formation of a plasma jet," *J. Phys. Communications*, vol. 3, no. 8, Article Number 085002, August 2019.

[3] Y. D. Korolev, O. B. Frants, N. V. Landl, V. G. Geyman, A. I. Suslov, "Parameters of a positive column in a gliding glow discharge in air," *Phys. Plasmas*, vol. 24, Article Number 103526, October 2017.

[4] Y. D. Korolev, V. O. Nekhoroshev, O. B. Frants, N. V. Landl, A. I. Suslov, A. V. Bolotov, "Features of the current sustainment in a low-current discharge in airflow," *Plasma Chem. Plasma Process.*, vol. 39, pp. 1519 – 1532, July 2019.

MECHANISMS FOR SUSTAINING THE POSITIVE COLUMN PLASMA OF LOW-PRESSURE HOLLOW-CATHODE GLOW DISCHARGE WITH LARGE-VOLUME HOLLOW ANODE*

N.V. LANDL, Y.D. KOROLEV, I.V. LOPATIN, S.S. KOVALSKY, V.S. KASYANOV, V.O. NEKHOROSHEV

Institute of High Current Electronics SB RAS, Tomsk, Russia

Hollow-cathode low-pressure glow-type discharges are widely used for different applications [1-5]. In particular, such discharges are used for generation of charged particle beams, for surface modification, for generation of extreme ultraviolet radiation, in high-current switching devices and so on. One of the applications is for generation of large volume plasmas [6, 7].

One of the methods for generation of large-volume plasmas is application of generator "PINK" with a combined thermionic and hollow cathode [3, 6]. Usually, "PINK" is mounted at the body of large-volume camber and chamber wall are, typically, serve as an anode. Despite the presence of thermionic cathode inside the cathode cavity, discharge in such type of installations can be characterized as hollow-cathode glow discharge with an external injection of electrons [8]. Therefore, plasma in hollow anode is a positive column plasma.

In our previous papers, we proposed the model that allows us to explain the mechanisms for sustaining a negative glow plasma in the cathode cavity of a low-pressure glow discharge [4, 8]. The main idea of the model is that the plasma in the cathode cavity represents a potential trap for electrons due to cathode voltage drop between negative glow plasma and cathode surface. The main component of discharge current on the cathode surface is an ion current and electrons from the cathode are emitted not only due to the ion bombardment, but also as an external emission current due to photoeffect, field emission and explosive emission.

Currently, when describing hollow-cathode glow discharges, main attention is payed to the plasma generation inside the cathode cavity. The problem of plasma generation inside the anode cavity is almost out of consideration. We believe that the positive column plasma, like the negative glow plasma, is a potential trap for electrons. The negative anode voltage drop forms this trap [9]. Consequently, the main states of the model of plasma sustaining inside the cathode cavity can be applied to that for the positive column.

In this report the results of investigation of glow discharge with hollow cathode and hot filament inside the cavity, and large-volume hollow anode are resented. Based on the model, estimations of plasma parameters inside the anode cavity were done. Mechanisms for positive column plasma sustaining inside the large-volume anode are proposed. It is shown that the estimations agree well with experimental data.

REFERENCES

[1] E. Dewald, K. Frank, D. H. H. Hoffman et.al., "Experimental Analysis of Pseudospark Sourced Electron Beam," IEEE Trans. Plasma Sci., vol.25, p. 272, 1997

[2] V.N. Devyatkov, Y.F. Ivanov, O.V. Krysina, N.N. Koval et.al., "Equipment and processes of vacuum electron-ion plasma surface engineering," Vacuum, vol.143, p.464, 2017

[3] Y.D. Korolev and N.N. Koval, "Low-pressure discharges with hollow cathode and hollow anode and their applications," J. Phys. D: Appl. Phys., vol.51, Article Number 323001, 2018.

[4] Y.D. Korolev, K. Frank, "Discharge formation processes and glow-to-arc transition in pseudospark switch," IEEE Trans. Plasma Sci., vol.27, p.1525, 1999

[5] V.D. Bochkov, V.M. Dyagilev, V.G. Ushich, O.B. Frants, Y.D. Korolev, I.A. Shemyakin, K. Frank, "Sealed-off pseudospark switches for pulsed power applications (current status and prospects)," IEEE Trans. Plasma Sci., vol.29, no.5, pp. 802-808, 2001.

[6] I.V. Lopatin, Y.H. Akhmadeev, N.N. Koval, "Effect of thermionic cathode heating current self-magnetic field on gaseous plasma generator characteristics", Rev. Sci. Instrum. vol. 86, 103301, 2015

[7] N.N. Koval, Y.F. Ivanov, I.V. Lopatin, Y.H. Akhmadeev, V.V. Shugurov, O.V. Krysina, V.V. Denisov, "Generation of low-temperature gas discharge plasma in large vacuum volumes for plasma chemical processes", Russian Journal of General Chemistry, vol. 85, p. 1326, 2015

[8] N.V. Landl, Y.D. Korolev, V.G. Geyman et al., "The Regimes for Sustaining a Hollow-Cathode Glow Discharge with a Hot Filament Inside the Cavity", Russ Phys J, 2020

[9] Y.D. Korolev, O.B. Frants, N.V. Landl, I.A. Shemyakin, V.G. Geyman, "High-current stages in a low-pressure glow discharge with hollow cathode", IEEE Trans. Plasma Sci. vol. 41, pp. 2087–2096, 2013

* This work was funded by RFBR according to the research project № 19-08-00326.

FEATURES OF MAGNETRON SPUTTERING DURING THE DEPOSITION OF TIN-CU COMPOSITE COATINGS FROM A PLASMA OF LOW-PRESSURE VACUUM-ARC AND MAGNETRON DISCHARGES*

D.B-D. TSYRENOV, A.P. SEMENOV, E.O. NIKOLAEV

Institute of Physical Materials Science SB RAS, Ulan-Ude, Russia,

The paper presents a magnetron sputtering of copper features in jet nitrogen gas or inert argon gas during the deposition process of TiN-Cu composite coatings in a VU-1B vacuum installation.

To determine the optimal process parameters of the sputtering target of the magnetron it is necessary to know the relationship between technological process parameters (speed of the sputtering cathode and growth of the formed coating, uniformity of coating thickness, coating composition, etc.) and physical parameters of the gas discharge in the DSM. To determine the optimal parameters of the sputtering process of magnetron target, it is necessary to know the relationship between technological process parameters (cathode sputtering rate and growth of the formed coating, uniformity of coating thickness, coating composition, etc.) and physical parameters of the gas discharge in the MSS. The physical parameters include external parameters - the geometry of the discharge gap, the pressure of the plasma forming gas, the magnitude and topography of magnetic field, the current and voltage of discharge and also internal parameters - the electrons temperature in the plasma, the electric field distribution, etc. The main parameters of a glow discharge for constructing the corresponding discharge model were determined. Further some results of measurements are given, in particular, it is given the magnetron's discharge current-voltage diagram at different values of argon pressure in the chamber [Fig. 1]. In the range of discharge currents from 0.04 to 4 A, the discharge voltage was 145–550 V. The current – voltage characteristics shift to the region of high operating voltages with a decrease in pressure.

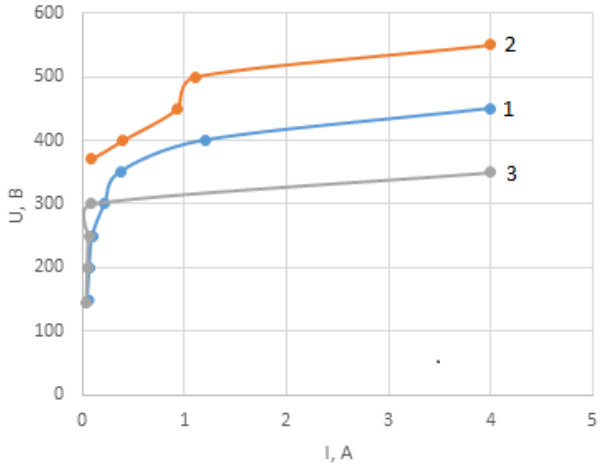

Fig. 1. The current-voltage diagram of magnetron discharge at various values of working gas pressure
1 - P_{Ar} = 0,11 Pa, 2 - P_{Ar} = 0,026 Pa, 3 - P_{Ar} = 0,013 Pa

* The work was supported by the Russian Foundation for Basic Research (project 20-08-00207_A) and budget project №0336-2019-0009

GAS DYNAMIC PROPERTIES OF LOW VOLTAGE PARTIAL DISCHARGES

E.A.YAKOVLEV[1], A.D.MEKHTIYEV[1], V.V YUGAY[1], L.A ZINOVYEV[2], N.B.KALIASKAROV[1]

1.Karaganda technical state university. N.Nazarbaev av.,56, Karaganda, Kazakhstan
2. Karaganda state university, Universitetskaya, 28, Karaganda, Kazakhstan

Experiments were carried out on the apparatus described in [1].

When a low-voltage (300-1000 V) pulsed partial discharge in the presence of 1.5% sodium chloride solution using a digital recording (30 frames / sec) detected spherical luminous entity not associated with the discharge region and the with time existence of about 1/30 s after discharge (Fig. 1)

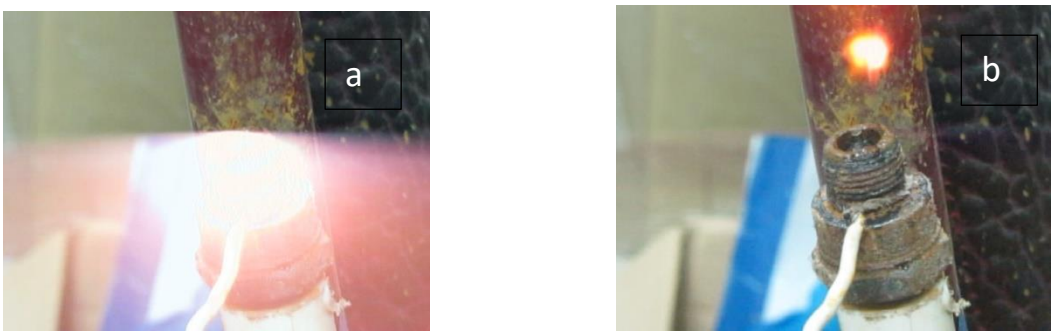

Figure 1. A photograph of a spherical object flying out of a plug spark. Rb=68 Ohm, U=950 V, Δt=1/30 c:
a- discharge radiation, b- a spherical object after discharge

In the course of the experiments, gas pressure values were measured when a discharge occurs. They made 25-30 kPa at Rb=0, U=950 V up to and 250-400 Pa at Rb=68 Ohm, U=950 V.

At work on installations with power supply of the double voltage and quadruple voltage of industrial frequency (fig. 2) moments of discharge with formation of a shock wave (a) and discharge with formation of spherical luminous area (b) are filmed.

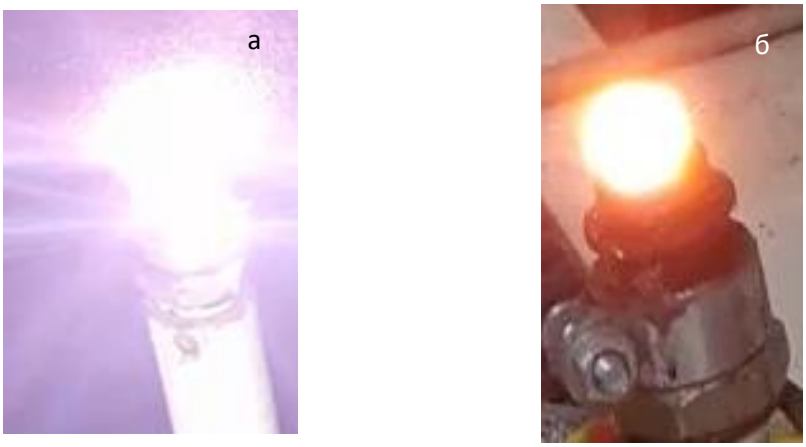

Figure 2: Photographs of objects at different operating modes: a). Rb=0 , U=1200 V, b). Rb=68 Ohm, U=610 V

A shock-wave discharge is formed at high discharge power when the discharge current is not additionally limited. If the discharge power is limited by the ballast resistance, the shock wave is not formed and the discharge area is formed as a bright glowing ball.

REFERENCES

[1] Yakovlev E.A., Mekhtiyev A.D., Yugay V.V., Zinovyev L.A. Research of generators of impulses for electrotechnological installations with solutions of electrolytes. Bulletin of the Karaganda university. Physics series, vol.90, pp.65-70, 2018

PROBE DIAGNOSTICS OF DENSE PLASMA IN HIGH CURRENT MODE OF A RING-SHAPED CLOSED DRIFT PLASMA THRUSTER*

V.A. GUSHENETS[1], *A.S. BUGAEV*[1], *E.M. OKS*[1,2]

[1]*Institute of High Current Electronics SB RAS, Tomsk, Russia*
[2]*State University of Control Systems and Radioelectronics, Tomsk, Russia*

The paper presents experimental data concerning the local plasma parameters: electron temperature, electron density; as well as their spatial distribution in a cylindrical hollow cathode formed by ring-shaped closed drift plasma thruster. This hollow cathode is a lengthy plasma-filled channel and is designed to transport an intense low-energy electron beam to the target. The plasma thruster is based on the geometry of a gridless ion source with an anode layer. For the formation of plasma in the transport channel, the so-called "plasma" high-current operational mode of the thruster discharge system was used. The amplitude of the discharge current in this mode can reach several tens of amperes, with a current pulse duration of not more than 200 μs.

Plasma diagnostics was carried out using the double probe method. The choice of this method is due to two reasons - the presence of a magnetic field, as well as the high plasma potential (several hundred volts) relative to the grounded electrodes. The dual probe method does not require a reference electrode, and the dual probe system can be isolated or have a high floating potential. Plasma probe measurements showed that the spatial distribution of plasma density is inhomogeneous within a certain region adjacent to the axis. The length of this region along the channel axis is close to its radius. Outside this region, the distribution of plasma concentration is quite uniform. The maximum plasma density on the axis is close to 7×10^{12} cm^{-3}, and the electron temperature is in the range of 3.5–5.5 eV.

* The work was supported by the Russian Foundation for Basic Research under grant No. 19-08-00315.

METAL ION SOURCE BASED ON VACUUM MAGNETRON DISCHARGE *

A.V. VIZIR[1], E.M. OKS[1,2], M.V. SHANDRIKOV[1], G.YU. YUSHKOV[1]

[1]Institute of High Current Electronics SB RAS, Tomsk, Russia
[2] Tomsk State University of Control Systems and Radioelectronics, Tomsk, Russia

An ion source based on a vacuum magnetron discharge was designed, fabricated and tested. The magnetron discharge is initiated by a vacuum arc discharge, the cathode of which faces the magnetron target. The discharges operate at a residual pressure of $3 \cdot 10^{-6}$ Torr without working gas feed. The magnetron discharge was powered by HiPIMS (High Power Impulse Magnetron Sputtering) power supply APEL-M-2HIPIMS-1500 [1]. Pulses of vacuum arc (30 μs) and magnetron discharge (up to 300 μs) are applied simultaneously. After ignition by the vacuum arc, the magnetron discharge run on in self-sustained mode. An ion beam was extracted from the discharge plasma by applying positive accelerating voltage of up to 20 kV to the discharge system electrodes. The ion beam composition was analyzed by a time-of-flight (TOF) spectrometer [2]. An example of output oscillogram of the spectrometer for zinc magnetron target is shown on Fig. 1.

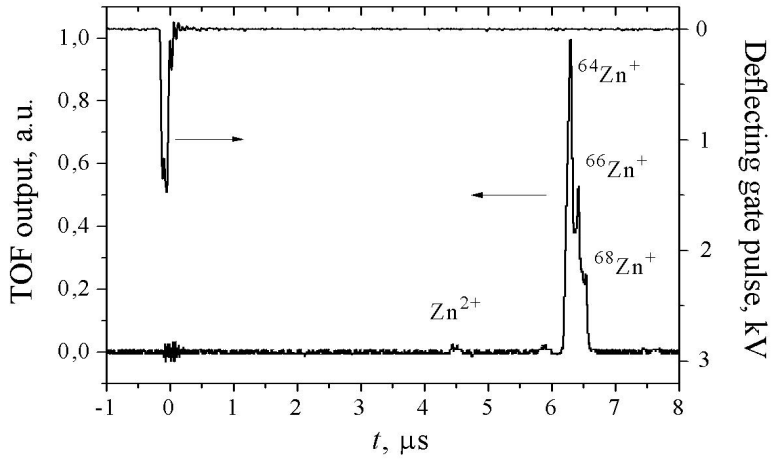

Fig.1. Time-of-flight spectrum of ion beam generated using zinc magnetron target.

As follows from data presented on Fig. 1, the ion beam completely consists of magnetron target material ions.

REFERENCES

[1] http://apelvac.com/

[2] V.I. Gushenets, A.G. Nikolaev, E.M. Oks, L.G. Vintizenko, G.Yu. Yushkov, A. Oztarhan, I.G. Brown, Simple and inexpensive time-of-flight charge-to-mass analyzer for ion beam source characterization, Rev. Sci. Insrum., vol. 77 no. 6, p. 063301, 2006.

* The work was supported by Russian Foundation for Basic research under grant #19-48-700008.

INVESTIGATION OF THE FORMATION OF MICROSECOND INTENSE DEUTERIUM ION BEAMS BASED ON A VACUUM ARC WITH A DEUTERIUM-SATURATED ZIRCONIUM CATHODE*

A.G. NIKOLAEV, V.P. FROLOVA**, E.M. OKS**, G.YU. YUSHKOV**

*Institute of High Current Electronics SB RAS, 2/3 Academichesky Ave., Tomsk, 634055, Russia, Email: nik@opee.hcei.tsc.ru, phone: +7(3822)-491776
**Institute of High Current Electronics SB RAS, 2/3 Academichesky Ave., Tomsk, 634055, Russia, and Tomsk State University of Control Systems and Radioelectronics, 40 Lenin Ave., Tomsk, 634050, Russia*

A vacuum arc discharge with a zirconium cathode saturated with deuterium is used to generate pulsed neutron fluxes in vacuum neutron tubes. The efficiency of such a device is determined by the achieved level of intensity of generation of neutron fluxes in it. The paper presents the results of a study of the processes of formation of deuterium ion beams under operating conditions and with specific arc parameters realized in neutron tubes — an arc current of several hundred amperes and a pulse duration of less than 1 microsecond. A real zirconium cathode saturated with deuterium used in neutron tubes was also used. The cathode was made in the form of a washer 1.8 mm thick with an external diameter of 23 mm. An ion beam extraction and formation system was used based on the MevvaV.Ru ion source [1]. Based on the studies, the optimal parameters of the source of microsecond ion beams based on a vacuum arc were selected, such as the geometry of the discharge system, the parameters of the arc pulse, and the parameters of the ion beam that ensure the maximum current of deuterium ions.

REFERENCES

[1] A.G. Nikolaev, E.M. Oks, K.P. Savkin, G.Yu. Yushkov, and I.G. Brown, "Upgraded vacuum arc ion source for metal ion implantation," Rev. Sci. Instrum., vol. 83, Article Number 02A501, 2012.

* The work was supported by the Russian Science Foundation under grant No. 18-19-00069.

HIGH-CURRENT VACUUM-ARC PLASMA SOURCE FOR PRODUCING SUPERSONIC PLASMA FLOWS IN MAGNETIC FIELDS *

*A.G. NIKOLAEV**, V.P. FROLOVA**, D.A. MANSFELD***, E.M. OKS**, A.V. VODOPYANOV***, G.YU. YUSHKOV**

**Institute of High Current Electronics SB RAS, 2/3 Academichesky Ave., Tomsk, 634055, Russia,*
Email: nik@opee.hcei.tsc.ru, phone: +7(3822)-491776
***Institute of High Current Electronics SB RAS, 2/3 Academichesky Ave., Tomsk, 634055, Russia, and Tomsk State University of Control Systems and Radioelectronics, 40 Lenin Ave., Tomsk, 634050, Russia*
****Institute of Applied Physics of RAS, Nizhny Novgorod, 603950, Russia*

Supersonic plasma flows are used to modify the surface of steels and alloys, to simulate the effects of plasma on the walls of thermonuclear plants, and to laboratory simulation of astrophysical phenomena such as coronal loops on the Sun or planetary magnetospheres. The paper presents a high-current source of a vacuum arc, which creates dense supersonic plasma flows of metal ions, the calculated velocities of which lie in the range of Mach numbers M = 3–6. The source is intended to study the interaction of dense pulsed plasma flows with strong magnetic fields near several tesla at electron cyclotron resonance. A source with a power source allows you to widely vary the plasma density (10^{13}-10^{15} parts/cm^3), the arc current and its pulse duration, as well as generate pulses of the arc current of various shapes. In the experiments described, we used two different forms of pulses of the arc current: a quasi-rectangular pulse with an arc current of 0.2–3.5 kA and a duration of 700 μs and a sinusoidal pulse with an arc current of 1–25 kA and a duration of about 120 μs. The pulse repetition rate was up to 0.1 Hz. The pulse energy of the source was up to 2.5 kJ. The article discusses the design features and parameters of the plasma source, the results of measurements of the plasma flow parameters and the influence of a strong magnetic field.

* The work was supported by the Russian Foundation for Basic Research under Grant # 18-29-21014-mk.

MICROWAVE PLASMATRON BASED ON A WAVEGUIDE BRIDGE.[1]

V.N.TIKHONOV, I.A. IVANOV, A.V.TIKHONOV

Russian Institute of Radiology and Agroecology, Kievskoe shosse, 109th km, Obninsk, Kaluga region, 249032, Russian Federation, E-mail: v.n.tihonov@yandex.ru, phone +7 (484)399-69-36

The paper deals with the development of a new microwave plasma torch design, which has several advantages over the known ones.

A classical microwave plasmatron is a rectangular waveguide on a H_{10} wave and a dielectric discharge tube passing through the middle of its wide wall. Such a plasma torch can be connected via a console or through a passage scheme. In the first case, the waveguide after the discharge tube should be shorted by a movable or fixed short circuit. Herewith, microwave energy is effectively invested in the process of initiating and maintaining the discharge, however, the magnetron must be protected from the reflected wave in the absence of plasma (by circulator). In the second case, the waveguide after the discharge tube is loaded onto a matched load and, thus, provides protection for the magnetron, however, the conditions for initiating the discharge are worsened, and all the microwave energy transmitted through the discharge is lost in the load.

The basis of the presented plasma source is a three-decibel waveguide bridge with communication over a wide wall. Both output arms of the bridge are loaded onto identical short-circuited segments of the waveguides. At a quarter wavelength from the short-circuited ends of these waveguides, in the middle of their wide walls and perpendicular to them, a discharge tube crosses them (Fig. 1) [1].

Fig.1. General view of the bridge-powered plasma torch.

The output arms of the bridge are loaded symmetrically, therefore, the microwave power of the generator reflected from the short circuit in the absence of a discharge (or not absorbed in the discharge) is returned to the untied shoulder of the bridge and, thus, the magnetron is always protected from the reflected wave without the need for an expensive circulator.

As a source of microwave power can be used a budget generator, built on the basis of components for household microwave ovens [2]. The presented device can be used to expand the functionality of a universal microwave complex for obtaining low-temperature plasma at atmospheric pressure [3].

REFERENCES

[1] V.N. Tikhonov, I.A. Ivanov, A.V. Tikhonov "Microwave plasmatron" // Application for the grant of a patent of the Russian Federation for invention No.2019125924 of 08/15/2019.

[2] V.N.Tikhonov, S.N.Aleshin, I.A.Ivanov and A.V.Tikhonov "The low-cost microwave plasma sources for science and industry applications" // Journal of Physics: Conf. Series 927 (2017) 012067 doi:10.1088/1742-6596/927/1/012067.

[3] I.A. Ivanov, V.N. Tikhonov, A.V. Tikhonov "Microwave complex for obtaining low-temperature plasma at atmospheric pressure" // Journal of Physics: Conf. Series 1393 (2019) 012042, doi:10.1088/1742-6596/1393/1/012042.

1 The work was supported by the Russian Science Foundation under grant No. 20-08-00894.

THE LOW-COST MICROWAVE SOURCE OF NON-THERMAL PLASMA[1]

I.A. IVANOV, V.N. TIKHONOV, A.V. TIKHONOV, S.A. GORBATOV

Russian Institute of Radiology and Agroecology, Kievskoe shosse, 109th km, Obninsk, Kaluga region, 249032, Russian Federation, E-mail: v.n.tihonov@yandex.ru, phone +7 (484)399-69-36

The aim of this work is the presentation of a stationary microwave source of atmospheric non-thermal plasma (ANTP), intended for R&D in the development of new technologies, as well as for the modernization of existing technological processes.

As a source of ANTP we propose using special optimised a multi-electrode microwave discharger in argon. This discharger is made on a tip of segment of a hard coaxial line of resonant length, fed from a waveguide-coaxial transition. The coaxial line passes through the waveguide in the middle of its wide side, perpendicular to it. One of the protruding ends of the line is short circuit, the second end is open-circuit. The short-circuited end of the coaxial line has a collet joint configured to change the length of the line, the area of the movable contact on the central conductor is placed in the region of the minimum surface currents of the standing wave. An axial hole was made along the tip of the central conductor at the open-circuit end of the coaxial line and radial cuts of resonance length have been made here (Fig.1).

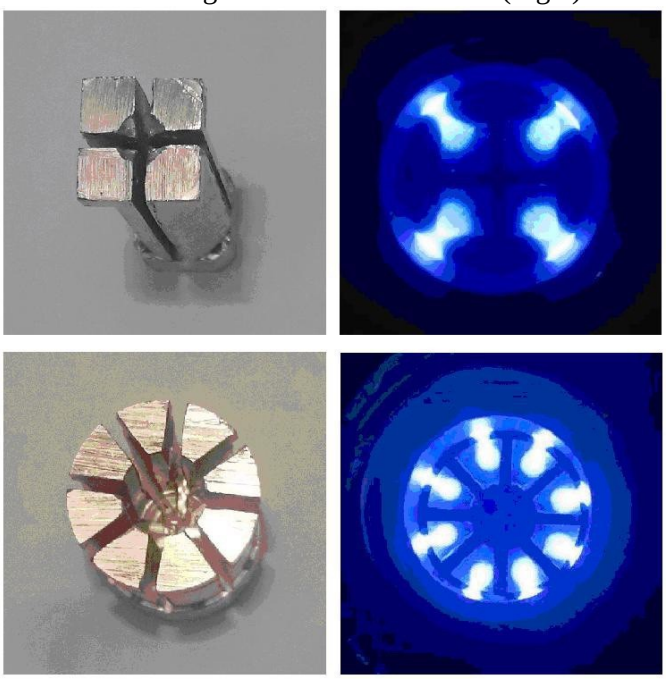

Fig.1. Options for the tip of the central conductor (left), corresponding discharge images in argon (right).

The supply of working gas to the discharge zone can be carried out either, directly into the gap of the coaxial line, or through the central conductor, in this case the central conductor made of a hollow tube. To reduce the temperature of the outgoing gas stream could be provided forced cooling of both, the external and internal tips of the coaxial microwave discharge gaps.

Calculations using The Finite Element Method and subsequent experiments showed that with the optimal ratio of the parameters of the waveguide-coaxial transition, the described device will operate in the traveling wave mode in the supply waveguide. Thus, this device can be used both – independently [1] and as part of a universal, low-cost hardware complex for producing low-temperature and non-thermal microwave plasma [2] - without the need for a clumsy and expensive circulator and a moving short-circuit piston.

REFERENCES

[1] V.N.Tikhonov, S.N.Aleshin, I.A.Ivanov and A.V.Tikhonov "The low-cost microwave plasma sources for science and industry applications" // Journal of Physics: Conf. Series 927 (2017) 012067 doi:10.1088/1742-6596/927/1/012067.

[2] I.A. Ivanov, V.N. Tikhonov, A.V. Tikhonov "Microwave complex for obtaining low-temperature plasma at atmospheric pressure" // Journal of Physics: Conf. Series 1393 (2019) 012042, doi:10.1088/1742-6596/1393/1/012042.

1 The work was supported by the Russian Science Foundation under grant No. 20-08-00894.

PRE-SOWING STIMULATION OF WHEAT WITH UV-B RADIATION OF XeCl-EXCILAMP*

E.A. SOSNIN[1,2], *T.P. ASTAPHYROVA*[2], *A.A. BURENINA*[2], *E.N. SURNINA*[2], *A.N. BUTENKOVA*[2], *Y.Y. FADEEVA*[2], *V.A. PANARIN*[1]

[1]*Institute of High-Current Electronics SB RAS, Tomsk, Russian Federation*
[2]*National Research Tomsk State University, Tomsk, Russian Federation*

In modern plant science are relevant search for ways of seeds dormancy breaking to obtain earlier and good sprouts, laying the basis for increasing the yield, obtaining early and high-quality products. Currently, it has been established that various physical factors, such as plasma, gamma radiation, microwave fields, as well as optical radiation in optimal doses can stimulate seed germination and plant development [1, 2]. In particular, a lot of research is devoted to ultraviolet radiation effect on plants [3].

The UVB spectrum range (290-320 nm) action on plants is rather scantily known. Its share in the solar radiation flux accounts for an average of about 1.5% of the radiant flux on the planet. Taking into account the fact that plants adapt to living conditions in the course of evolution, it can be assumed that the flow of UVB radiation is also used by plants, but at the level of *subdoses* that reach the Earth's surface (that is, not in the same way as visible and infrared radiation is used). In our works [4, 5] it was found that UVB radiation has a stimulating effect on a variety of crops during pre-sowing seed treatment. Independent studies confirm our data (see review [6]).

The aim of current work is to study the growth and development of spring wheat ("Irgina" cultivar) when treated with subdoses of UV-B radiation. For processing, XeCl excilamp radiation was used. The spectrum of this lamp is a narrow band with a maximum at a wavelength of 308 nm, which corresponds well to the UV-B range of the spectrum.

In the course of research, incident dose of seeds were found, under the influence of which wheat sprouts had an increase in such indicators as the length and dry weight of the root, the length of the leaf and the ratio of the root/shoot masses. UV-B irradiation changed the mode of water absorption by seeds compared to non-irradiated seeds.

As plants developed, the nitrogen balance index, calculated as the ratio of chlorophylls to flavonoids, was always higher in the experiment with radiation in plants whose seeds were subjected to pre-sowing treatment with UV-B radiation. This indicates the activation of growth and development processes in plants, as well as the accelerated absorption and assimilation of nitrogen compounds.

The indicators of the structure of the wheat crop (grain yield, the number of grains in the spike, the length and weight of the spike) were determined. They significantly exceeded the control by 10.2 %.

It is important that the processing did not affect the quality of the wheat grain. The amount of protein in the grain of the studied samples was almost the same and amounted to 12.8 %. Such indicators of grain quality as humidity and vitreous content also did not differ significantly from the control.

Based on the obtained data, it is concluded that the use of XeCl-excilamp UVB radiation for pre-sowing stimulation of wheat is promising.

REFERENCES

[1] T. Ohta, M. Shiratani, M. Hori, “Current status and future prospect of agricultural applications using atmospheric-pressure plasma technologies,” Plasma Process. Polym. vol. 15, no. 2, 201700073, 2018.

[2] S. S. Araújo, S. Paparella, D. Dondi, A. Bentivoglio, D. Carbonera, A. Balestrazzi, “Physical Methods for Seed Invigoration: Advantages and Challenges in Seed Technology,” Front. Plant Sci., vol. 7, 646, 2016.

[3] D. Thomas, T. T. Jos, T. Puthur, “UV radiation priming: A means of amplifying the inherent potential for abiotic stress tolerance in crop plants,” Environmental and Experimental Botany, vol. 138, no. 6, pp. 57–66, 2017.

[4] E. A. Sosnin, Y. V. Chudinova, I. A. Victorova, I. I. Volotko, “Application of excilamps in agriculture and animal breeding (review),” Proc. SPIE : XII International Conference on Atomic and Molecular Pulsed Lasers, vol. 9810, 98101K, 2015.

[5] E. A. Sosnin, P. A. Gol'tsova, Y. V. Chudinova, L. V. Lyasheva, V. A. Panarin, I. A. Prok, V. S. Skakun, I. A. Viktorova, T. P. Astaphyrova, “Photoregulation of agricultural plants growth and development by XeCl-excilamp,” Proc. SPIE : XIV International Conference on Pulsed Lasers and Laser Applications, vol. 11322, 1132226, 2019.

[6] M. Schreiner, J. Martínez-Abaigar, J. Glaab, M. Jansen, “UV-B Induced Secondary Plant Metabolites: Potential benefits for plant and human health,” Optik & Photonik, 2014, no. 2, pp. 34–37, 2014.

* This research was supported by “Tomsk State University competitiveness improvement program” grant (№ 8.1.29.2018) and by State Task for HCEI SB RAS, project #13.1.4.

ABOUT SOME FEATURES OF THE VACUUM ARC OPERATION WITH BORON-CONTAINING CATHODES*

A. BUGAEV[1], *V. GUSHENETS*[1], *E. OKS*[1,2]

[1]*Institute of High Current Electronics, Tomsk, Russia*
[2]*State University of Control Systems and Radioelectronics,, Tomsk, Russia*

The report presents the results of an experimental study of a pulsed vacuum arc discharge operation with pure boron and lanthanum hexaboride cathodes. For the experiments reported here, the arc discharge triggering was carried out due to breakdown on a ceramic button installed in the center of the cathode surface. Two pure boron cathodes and one LaB6 cathode were tested. Pure boron cathodes are cast rod with diameter 10 mm and hot pressed target (diameter 1 inch). The cathode of lanthanum hexaboride is a hot pressed rod with small porosity (not more than 1%).

So pure boron is a non-metallic element, but a semiconductor under normal conditions with a very high resistivity (~ 2 Mohm/cm), therefore, for the triggering and the stable discharge operation require the cathode preheating up to temperatures above 600 Celsius. Under these conditions, the cathode resistance drops by more than five orders of magnitude. A strong temperature dependence of the resistance and relatively low thermal conductivity lead to the fact that the cathode spot is localized in one place, it is stationary, unlike the spot on metal cathodes, and increases in size with the discharge current.

Unlike pure boron, lanthanum hexaboride, although it is considered a refractory ceramic material, differs from pure boron in that it has a very low resistivity under normal conditions. Therefore, there is no need to preheat the cathode to initiate an arc discharge. Another difference is that LaB6 has a metallic type of conductivity - its resistivity increases with increasing temperature. This leads to the fact that the behavior of the cathode spot on the surface of the LaB6 cathode is similar to the behavior of the spot on a purely metal cathode. When burning an arc discharge, several cathode spots arise, their number depends on the magnitude of the discharge current, and they move at high speed along the surface of the cathode. This contributes to more uniform cathode wear.

The vacuum arc operation with boride cathodes is accompanied by a large flow of hot droplets - macroparticles. The flow is especially significant when hot pressed target is used as a cathode. And we ascribe to the high porosity (60%) of the material.

* The work was supported by Russian Scientific Foundation # 16-19-10034.

FUNGICIDAL EFFECT OF APOCAMPIC DISCHARGE PLASMA JET ON WHEAT SEEDS INFECTED WITH *ALTERNARIA SP.* AND *BIPOLARIS SOROKINIANA SHOEMAKER*[*]

V.A. PANARIN[1], *S.A. NUZNICH*[2], *E.A. SOSNIN*[1,2], *V.S. SKAKUN*[1], *Y.Y. FADEEVA*[2]

[1]*Institute of High-Current Electronics SB RAS, Tomsk, Russian Federation*
[2]*National Research Tomsk State University, Tomsk, Russian Federation*

In recent years, methods for using atmospheric plasma for microbial inactivation have been actively studied. The effect of atmospheric plasma is mainly regulated by chemically active substances or radicals, such as atomic oxygen, ozone, hydroxyl, and nitric oxide [1–3]. Barrier discharge (DBD) and atmospheric pressure plasma jets (APPJ) were particularly successful here [3, 4]. The first publications appeared on inhibiting the growth of mold and fungi on the surface of food products and plant seeds, as well as on inactivating the toxins released by them [5–8].

In this report, a new approach is developed, according to which pre-sowing treatment of plant seeds is carried out using a relatively new source of atmospheric plasma – the so-called plasma jet of the apokampic discharge in air. This is a pulse discharge that generates a plasma jets – apokamps at the place of discharge channel bend (see more details in [9, 10]).

In the apokamps, active forms of oxygen and nitrogen (as well as the radiation of molecules) are formed in the air of atmospheric pressure, which increases their concentration in the streamer head by orders of magnitude, compared to traditional APPJ based on inert gases [3]. Owing to this, we believe to increase the RONS concentration *in situ*, on the biological target. In our case, this can intensify the processes of inactivation of microscopic mold fungi on the surface of seeds.

We tested our hypothesis by acting by apokamp on wheat seeds («Irgina» cultivar) infected with helminthosporiosis (*Bipolaris sorokiniana Shoemaker*) with a degree of infection of 50% and early blight (*Alternaria sp*.), whose infection rate was 10%. In the first case, the seeds were treated by apokamp plasma for 1 and 10 minutes. It provided a significant reduction in the degree of infection of seeds with helminthosporiosis by 1.7 and 2.3 times. In addition, compared to the control, the treated seeds maintained high rates of germination and germination energy. This is important because plasma exposure is multi-factorial and it is necessary to be sure that these indicators at least will not decrease.

In the case of *Alternaria sp*. the 3-minute apokamp treatment completely decontaminate wheat seeds.

Thus, in our experiments, the fungicidal effect of atmospheric plasma of the apokamp was proved for the first time on the example of abovementioned biological objects.

REFERENCES

[1] N. Hayashi, Y. Yagyu, A. Yonesu, M. Shiratani, “Sterilization characteristics of the surfaces of agricultural products using active oxygen species generated by atmospheric plasma and UV light,” Japanese Journal of Applied Physics, vol. 53, 05FR03, 2014.

[2] E. Stoffels, Y. Sakiyama, D. B. Graves, “Cold Atmospheric Plasma: Charged Species and Their Interactions With Cells and Tissues,” IEEE Transactions on Plasma Science, vol. 36, no. 4, pp. 1441–1457, 2008.

[3] X. Lu, G. V. Naidis, M. Laroussi, S. Reuter, D. B. Graves, K. Ostrikov, “Reactive species in non-equilibrium atmospheric-pressure plasmas: Generation, transport, and biological effects,” Phys. Rep., vol. 630, no. 4, pp. 1–84, 2016.

[4] A. Zahoranová, L. Hoppanová, J. Šimončicová, Z. Tučeková, V. Medvecká, D. Hudecová, B. Kaliňáková, D. Kováčik, M. Černák, “Effect of cold atmospheric pressure plasma on maize seeds: enhancement of seedlings growth and surface microorganisms inactivation,” Plasma Chem. Plasma Process., vol. 38, pp. 969–988, 2018.

[5] S.A. Ouf, A.H. Basher, A.A. Mohamed, “Inhibitory effect of double atmospheric pressure argon cold plasma on spores and mycotoxin production of *Aspergillus niger* contaminating date palm fruits,” J. Sci. Food. Agric., vol. 95, no. 15, pp. 3204–3210, 2015.

[6] L. Kordas, W. Pusz, T. Czapka, R. Kacprzyk, “The effect of lowtemperature plasma on fungus colonization of winter wheat grain and seed quality,” Polish J. Environ. Studies, vol. 24, pp. 433–438, 2015.

[7] N. Hojnik, M. Modic, G. Tavčar-Kalcher, J. Babič, J. L. Walsh, U. Cvelbar, “Mycotoxin Decontamination Efficacy of Atmospheric Pressure Air Plasma,” Toxins, vol. 11, 219, 2019.

[8] M. C. Pina-Perez, D. Martinet, C. Palacios-Gorba, C. Ellertb, M. Beyrer, “Low-energy short-term cold atmospheric plasma: Controlling the inactivation efficacy of bacterial spores in powders,” Food Research International, vol. 130, 108921, 2020.

[9] E. A. Sosnin, V. S. Skakun, V. A. Panarin, D. S. Pechenitsin, V. F. Tarasenko, E. Kh. Baksht, “Phenomenon of Apocamp Discharge,” JETF Letters, vol. 103, no. 12, pp. 761–764, 2016.

[10] V. Y. Kozhevnikov, A. V. Kozyrev, A. O. Kokovin, A. G. Sitnikov, E.A. Sosnin, V. A. Panarin, V. S. Skakun, V. F. Tarasenko, “Apokamp-type gas discharge phenomenon: Experimental and theoretical backgrounds,” EPL, vol. 129, 15002, 2020.

[*] This research was supported by “Tomsk State University competitiveness improvement program” grant (№ 8.1.29.2018) and by State Task for HCEI SB RAS, project #13.1.4.

ON THE ROLE OF SECONDARY ELECTRONS IN THE BEAM PLASMA FORMATION*

V.A. BURDOVITSIN[1], *E.M. OKS*[1, 2], *D.B. ZOLOTUKHIN*[1], *K.I. KARPOV*[1]

[1]*Tomsk State University of Control Systems & Radioelectronics, Tomsk, Russia*
[2]*High Current Institute SB RAS, Tomsk, Russia*

An increase in the efficiency of using the electron beam energy for the formation of a beam plasma can be realized by using a collector under a floating potential [1]. This is due to the contribution of secondary electrons accelerated by the potential difference between the collector and the plasma, since at the electron beam energies from units to tens kiloelectronvolts, the potential of an isolated collector is usually negative, and the plasma potential is close to zero. In the case of a metal collector, the contribution of secondary electrons to plasma formation can be estimated by comparing measurements with an earthed and isolated collector. For a dielectric collector, this approach is not feasible. In this paper, we present an original technique that allows us to separate the secondary plasma from the true-beam plasma for both the metal and dielectric collectors. The essence of the technique is to use a non-zero angle of beam incidence on the collector. The angle of incidence was measured from the normal to the surface of the collector. A photograph of the glow (Fig. 1) gives a clear idea of the essence of the technique. The discovered fact that the column of secondary plasma is always perpendicular to the surface of the collector indicates that this plasma was created by secondary rather than reflected electrons. The spatial separation of the beam and secondary plasmas made it possible to measure the parameters and compare the contributions of the beam and secondary electrons to the plasma formation. The relative contribution of each group of electrons is determined by a number of factors, including the energy of the primary beam, the target material, and the gas pressure. Moreover, the gas pressure manifests itself through the floating potential of the collector, which, in turn, sets the energy of the secondary electrons. Table 1 shows the experimental conditions and parameters of both plasmas. As can be seen, the secondary plasma has a concentration n comparable with the beam plasma and a lower electron temperature T_e.

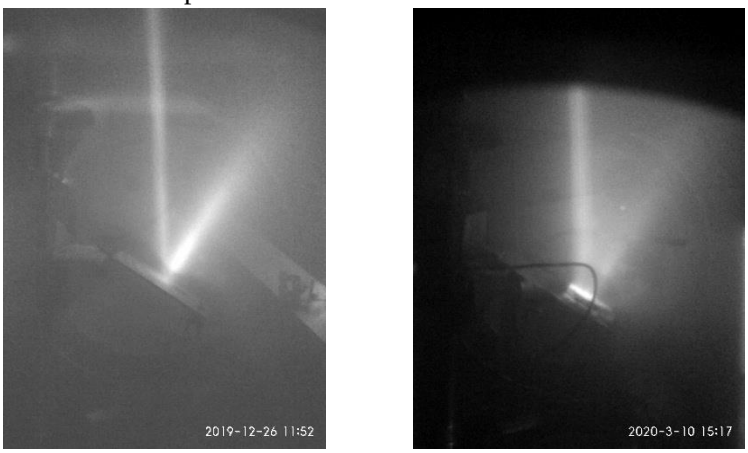

(a) (b)

Fig. 1. The picture of the plasma glow with an oblique incidence of the electron beam on (a) metal (stainless steel) and (b) quartz collector. Gas is argon.

Tab. 1. Parameters of primary and secondary plasmas for a metal target.

Angle of incidence, grad	0	30	30
Probe position	in beam	in beam	in secondary plasma
n, m^{-3}	$7 \cdot 10^{15}$	$4 \cdot 10^{15}$	$5 \cdot 10^{15}$
T_e, eV	2,13	2,59	2,08

REFERENCES

[1] V A Burdovitsin , E M Oks and D B Zolotukhin, “Effect of collector potential on the beam plasma formed by a forevacuum-pressure plasma-cathode electron beam source,” J. Phys. D: Appl. Phys. 51 (2018) 304006 (5pp)

* The work was supported by the Russian Foundation for Basic Research, grant No. 19-08-00170.

OXYGEN DISSOCIATION DEGREE IN ARC WITH HOLLOW ANODE*

P.V. TRETNIKOV[1], *N.V. GAVRILOV*[1], *A.S. KAMENETSKIKH*[1]

[1]*Institute of Electrophysics of the UB of RAS, Yekaterinburg, Russia.*

The degree of dissociation of reactive molecular gas (O_2, N_2) has a significant effect on the interaction of particles in the plasma and on the surface of the deposited coating. It was possible to achieve a high deposition rate (~5 μm/h) of α-Al_2O_3nanocrystalline coatings at a low temperature (~ 600 ^oC) by reactive anode evaporation in a high current discharge with a self-heated hollow cathode[1]. The result was achieved under conditions of a high current density (up to 20 mA/cm2) of ion assistance and a high concentration of atomic oxygen in the discharge plasmagenerated in the electrode system with hollow anode. The imposition of the dense electron flux (up to 100 A) and the oxygen flux in the hollow anode aperture provided a significant increase in the concentration of atomic oxygen in the plasma and an increase in the degree of oxygen dissociation with an increase in the discharge current [2].

The aim of present work was to determine the degree of oxygen dissociation in an arc discharge when oxygen was supplied through the anode cavity. Atomic oxygen concentrations were measured using a catalytic Ni probe [3]. Optical emission actinometry [4] was used as a duplicating method for determining the degree of oxygen dissociation from the spectra of optical emission of Ar-O_2 plasma with a gas flow ratio of 40 and 150 sccm. Measurements were carried out using helium (2 %) as an actinometer. It was found that the degree of O_2 dissociation increases up to ~ 40% with increasing current to the anode to 70 A (Fig. 1).

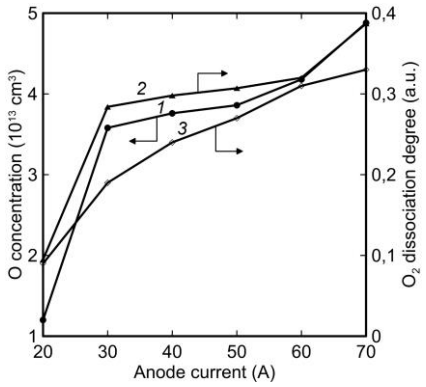

Fig.1. The atomic oxygen concentration (*1*) and O_2 dissociation degree measured by probe (*2*) and actinometrical (*3*) methods as function of anode current.

REFERENCES

[1] N.V. Gavrilov, A.S. Kamenetskikh, P.V. Tretnikov, A.V. Chukin. “Ion assisted deposition of α-Al_2O_3 coatings by anodic evaporation in the arc discharge”. Surf. Coat. Technol., vol. 337, pp. 453-460, 2018.

[2] N.V. Gavrilov, A.S. Kamenetskikh, P.V. Tretnikov, A.V. Chukin. “High-rate low-temperature PVD of thick 10 μm α-alumina coatings”. J. Phys.: Conf. Ser., vol. 1393, p. 012082, 2019.

[3] I. Sorli, R. Rocak. "Determination of atomic oxygen density with a nickel catalytic probe". J. Vac. Sci. Technol. A, vol. 18, p. 338, 2000

[4] D. Pagnon, J. Amorim, J. Nahorny, M. Touzeau, M. Vialle, J. Phys. D Appl. Phys., vol. 28, pp. 1856-1868, 1995.

*The work was supported by RFBR, project number 20-08-00169.

PLASMA BEHAVIOR IN E_XH PULSE DISCHARGE

N.V. MAMEDOV[1,2], *A.S. ROHMANENKOV, S.P. MASLENNIKOV* [2], *A.A. SOLODOVNIKOV*[1], *A.I. SOROKIN*[2,3], *D.V. KOLODKO*[2,3]

[1] *Dukhov Research Institute of Automatics (VNIIA), Sushchevskaya st. 22, Moscow, Russia, 127055, vniia4@vniia.ru*
[2] *National Research Nuclear University MEPhI, Kashirskoe st., 31, Moscow, Russia, 1154092*
[3] *Kotel'nikov Institute of Radio Engineering and Electronics, Fryazino Branch, Russian Academy of Sciences, pl. Vedenskogo 1, Fryazino, Moscow oblast, Russia, 141190*

The *ExH* gas pulse discharge (penning pulse discharge) was studied using three-dimensional Particle-in-cell (PIC) code combined with Monte-Carlo simulated gas kinetics. Plasma behavior (electron and ion density in axial and radial dimensional) depending on magnitude (and configuration) of the magnetic field and pressure (working gas is deuterium) was shown. The obtained results are revealed the existence of different (stable and unstable) discharge modes which realized depending on the physical conditions (see fig 1). A comparison of simulation results with experimental data (discharge current, electron density and temperature) is presented.

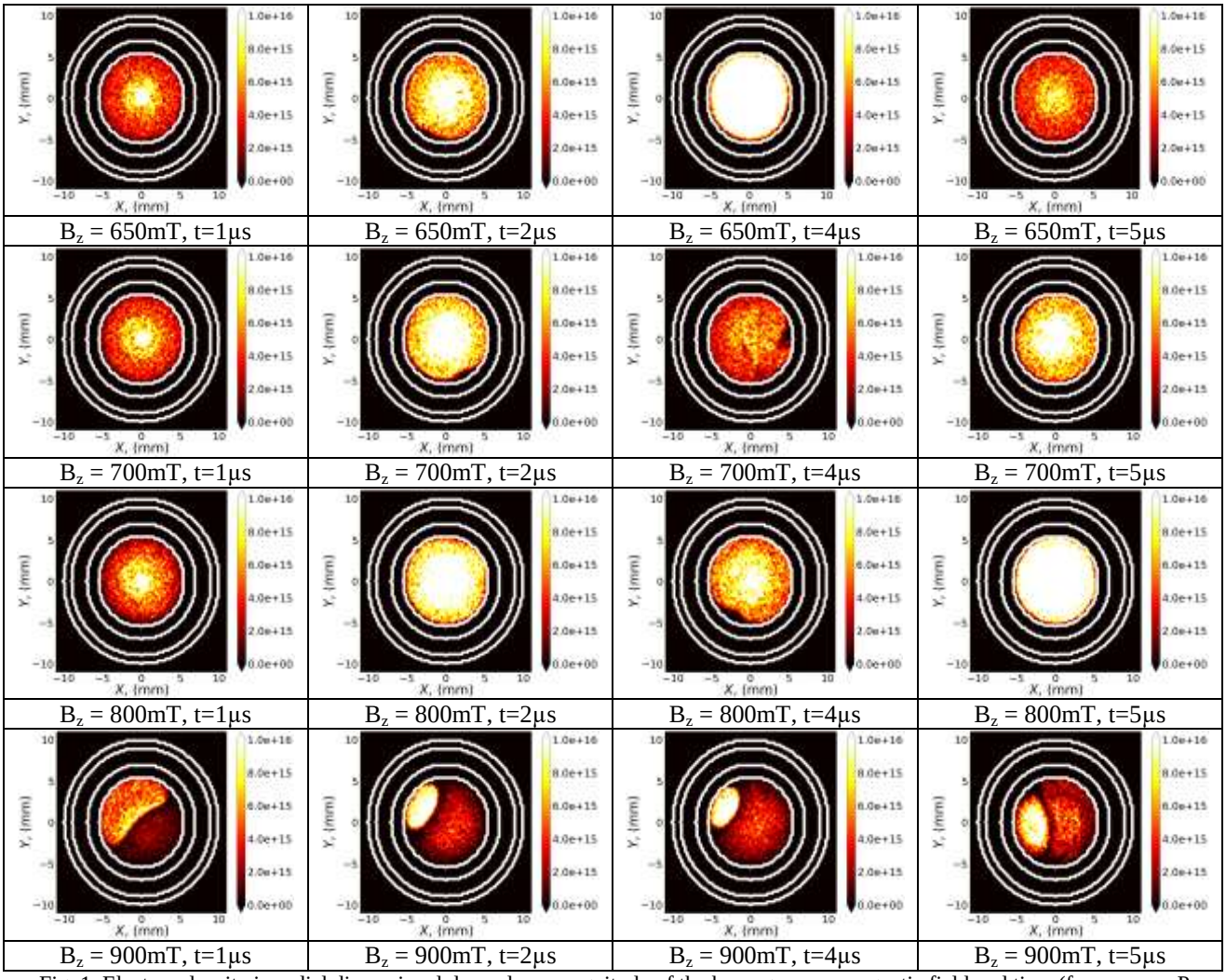

B_z = 650mT, t=1μs	B_z = 650mT, t=2μs	B_z = 650mT, t=4μs	B_z = 650mT, t=5μs
B_z = 700mT, t=1μs	B_z = 700mT, t=2μs	B_z = 700mT, t=4μs	B_z = 700mT, t=5μs
B_z = 800mT, t=1μs	B_z = 800mT, t=2μs	B_z = 800mT, t=4μs	B_z = 800mT, t=5μs
B_z = 900mT, t=1μs	B_z = 900mT, t=2μs	B_z = 900mT, t=4μs	B_z = 900mT, t=5μs

Fig. 1 Electron density in radial dimensional depends on magnitude of the homogeneous magnetic field and time (for pressure P =6mTorr).

This work was supported by RFFI grant № 12-02-13510-ОФИ_М_РА.

A NEW DESIGN OF HIGH–VOLTAGE PULSE GENERATORS FOR IGNITION OF VOLUME DISCHARGES AT SUPER–ATMOSPHERIC PRESSURES IN A PULSE–PERIODICAL REGIME

B. A. KOZLOV[1], D. S. MAKHANKO[2], V. I. SEREDINOV[1], S. A. PYANCHENKOV[1]

[1] Department of Electronic Devices, Ryazan State Radio Engineering University, 390005, Ryazan, Gagarin str. 59/1, Russia, e–mail: kozlov.qe.ryazan@mail.ru

[2]AA "Plasma", 390023, Ryazan, Tsyolkovski str. 24, Russia, e–mail: mds@plasmalabs.ru

High–pressure volume discharges in laser physics are the main method for pumping gas–discharge lasers based on carbon dioxide, nitrogen, and excimer molecules. When volume discharges in dense gases are excited in a pulse–periodical regime pulsed pumping generators must generate voltage pulses of up to 100 kilovolts and more with a rise time of first front of voltage pulse duration in the range of 10–20 nanoseconds and with a volume discharge current duration of 20–40 nanoseconds.

In the single pulse mode (pulse repetition rates 1–10 Hz) these parameters of high–voltage pulses are quite easily implemented in combinations of pulse transformers and spark sharpeners gap working at total pressures up to 100 atmospheres [1, 2]. The use of such sharpeners is excluded at pulse repetition frequencies of more than 50 Hz. In the pulse–periodical mode (pulse repetition frequency 0.1–10 kHz), only pulsed hydrogen thyratrons with their own time of discharge forming in the limit of 30–50 nanoseconds can be used as switches in pumping generators.

To achieve of such high voltage parameters we can use the next types of generators – an inverse LC–generator, a Marx generator and a pulse transformer. The simplest from these types of generators is a pulse transformer in which only one switch is used. However for high–voltage pulse generators based on a pulse transformers when the switches energy are up to 10 J and more the rise time of the voltage pulses can reach 100–200 nanoseconds.

In this regard, there is a need to create compromise variant for pulse pumping generators for use in a pulse–periodical regime, which would ensure the achievement of the necessary values of the high–voltage pulses amplitude with minimum values of the rise time duration.

A diagram of one of these generators is shown in Figure 1. In it a high–voltage pulse from a two–stage Marx generator GM applied to an primary winding of pulse transformer PT.

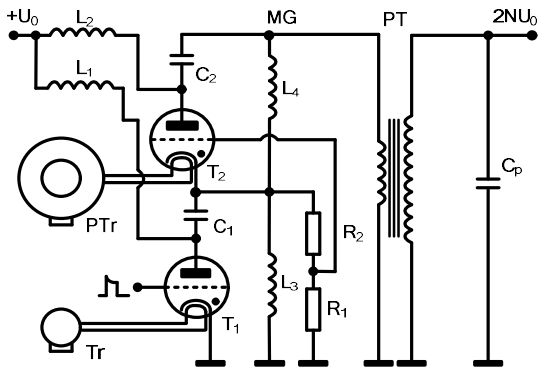

Fig.1. Electrical scheme of pulse generator: T_1, T_2 – thyratrons ТГИ1–1000/25; C_1, C_2 – storage capacitors; C_P – peaking capacitors; $L_1 \div L_4$ – inductances; Tr – heating transformer of thyratron T_1; PTr – "potential" heating transformer of thyratron T_2; MG – Marx generator; PT – pulse transformer; R_1 , R_2 – resistive divider for triggering of second thyratron T_2

An pulse transformer PT with a closed magnetic core made from M – 2000 NN brand ferrites was manufactured with a transformation ratio of N = 5. Ceramic storage capacitors C_1 and C_2 had capacitance values of 10 nF. The sharpening ceramic capacitor capacitance C_P had values from 120 to 160 pF and was discharged directly to the gas–discharge gap.

The created generator ensures the excitation of volume discharges in CO_2–laser mixtures in the active value V = 30×1,5×1 cm^3 with a discharge current durations of τ = 20–30 ns at pulse repetition frequencies up to 2 kHz at total pressures of working mixtures CO_2: N_2: He in the range from 1 up to 5 atmospheres.

REFERENCES

[1] http://plasmalabs.ru/ Spark Gaps (Sharpeners).

[2] B.A. Kozlov, Do Kuang Man, Mai The Nguyen, A.Ya. Payurov, A.B. Yastrebkov, "Super–atmospheric pressure CO_2–lasers with duration of radiation pulses less than 10 nanoseconds and pulse repetition rates up to 20 Hz", Proceedings of SPIE, Vol. 11322, 113220I (2019) DOI: 10.1117/12.2550678

VOLUME DISCHARGES IN CO_2–LASER MIXTURES AT ATMOSPHERIC PRESSURES WITH HIGH ENERGY DENSITY

B.A.KOZLOV[1], MAI THE NGUYEN[1], D.S.MAKHAN'KO[2]

[1] Department of Electronic Devices, Ryazan State Radio Engineering University
390005, Ryazan, Gagarin str. 59/1, Russia
e–mail: kozlov.qe.ryazan@mail.ru
[2]AA "Plasma", 390023, Ryazan, Tsyolkovski str. 24, Russia
e–mail: mds@plasmalabs.ru

The volume discharges plasma is the main pumping method for gas lasers working at atmospheric and super atmospheric pressures. Stable volume discharges with high density of pumping energy forms at intense initial ionization of gas mixture before breakdown gas discharge gap and effective reproduction of electrons in cathode region after breakdown [1–3]. Basic mechanism of electron reproduction in cathode region of discharges at current densities up to $j \le 10^2$ A/cm^2 is ion–electron emission. At $j \ge 10^2$ A/cm^2 auto–electron emission to take part significant fraction in total volume discharge current.

The purpose of this experimental work was to determine the conditions for a substantial increase in the pumping energy density in CO_2 laser mixtures at atmospheric pressure. To achieve of this goal the level of initial ionization of the gas mixture in the main discharge gap was varied and the field emission characteristics of the cathode surfaces were changed as a result of applying carbon soot containing carbon in various nano– and microstructure forms.

An increase in the initial ionization level was achieved as a result of application an effective source of VUV radiation based on a surface discharge (fig.1, a) as well as put in nitrogen oxides (NO and NO_2) and iodine vapor into the working mixture. All these gas impurities have ionization potentials less than 10 eV. During the studies the concentrations of the initial photoelectrons at the stage of preliminary ionization and the current – voltage characteristics of the volume discharge were recorded. The volt–ampere characteristics of volume discharges in CO_2–laser mixtures were studied in the real inter–electrode gap of small–sized TEA–CO_2 laser. Geometrical parameters of discharge gap V = 18x0.8x0.8 cm^3, cathode surface S = 18x0.8 cm^2. In a separate high–vacuum chamber the current – voltage characteristics of autoelectronic currents were studied. The initial ionization level was measured using an ionization chamber IC (fig.1, b) which was installed in the place of the main electrode (cathode) and filled by a working gas mixture.

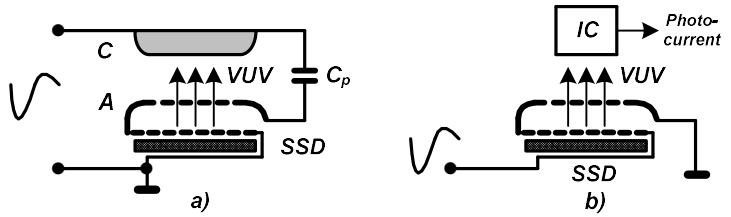

Fig.1. .Electrical scheme of discharge module for initiation by VUV–radiation and forming of volume discharge (a) and method of initial concentration of photoelectrons in main discharge gap measurement (b): SSD–high current sliding spark discharge

The main results of the research are as follows:

- the put–in of nitrogen oxides or iodine vapors into the working mixture ensures a concentration of photoelectrons up to 10^8–10^9 cm^{-3} at the stage of preliminary ionization;
- the presence of carbon soot on the surface of the maim electrodes leads to an increase in the field emission currents by a factor of 2–10;
- the maximum current density of a volume discharge in CO_2 laser mixtures when was used carbon soot on the working surfaces of cathodes reaches 400–600 A.cm^{-2};
- the pumping energy density when was used carbon soot on the working surfaces of cathodes increases from 250–400 mJ.cm^{-3} to 800–1200 mJ.cm^{-3};
- the put in of nitrogen oxides or iodine vapor into the working mixture when carbon soot is deposited on the cathode surface leads to an increase in the energy density up to 2000 mJ.cm^{-3}.

REFERENCES

[1] G.A. Mesyaz, Pulse energetic and electronics. –Moscow. Nauka. 2004.

[2] V.N. Karnushin, R.I. Soloukhin, "Macroscopic and molecular processes in gas lasers". –Atomizdat. Moscow, 1981.

[3] V.V. Osipov, "Pulsed Repetitive TEA–CO_2 Lasers". Proceedings of SPIE. vol. 2916, pp. 32–38, 1995.

INFLUENCE OF AXIAL MAGNETIC FIELD ON MASS-TO-CHARGE COMPOSITION OF HIGH-CURRENT VACUUM ARC PLASMAS WITH Cu-Cr CATHODES*

K.P. SAVKIN[1], *E.M. OKS*[1,2], *G.YU. YUSHKOV*[1], *A.S. BUGAEV*[1], *A.V. VIZIR*[1], *V.I. GUSHENETS*[1], *A.G. NIKOLAEV*[1], *M.V. SHANDRIKOV*[1], *V.P. FROLOVA*[1,2]

[1]*High Current Electronics Institute, Russian Academy of Science, Tomsk 634055, Russia*
[2]*Tomsk State University of Control Systems and Radioelectronics, Tomsk 634050, Russia*

Copper-chromium composites are successfully use as a material for electrodes of high-current vacuum circuit breakers. In its turn, the axial magnetic field increases the uniformity of the distribution of current density over the surface of the anode. The ignition of high-current vacuum arcs leads to the emission of plasma from cathode spots from the surface of these electrodes. The elemental and charge composition of the plasma depends on the fraction of chromium in the cathode material, as well as on the magnetic field in the interelectrode gap. In this work, using the time-of-flight technique, we studied the mass-charge composition of a vacuum arc plasma with cathodes based on a copper-chromium composite at a current density of 1 kA/cm^2 and an axial magnetic field B of 1.2 T, typical of high-current vacuum current interrupters. Without a magnetic field, with an increase the fraction of chromium in the cathode material from 0 to 50 %, the average charge state of chromium ions increases from 1.98 to 2.13, respectively, and copper ions decreases from 2.15 to 1.95. The dependences of the average charge state of the metal ions on the magnetic field are nonmonotonic with a maximum at B=0.8 T. The increase in the average charge state of copper and chromium ions is due to an increase in the arc burning voltage to the level of several tens of volts, with an increase in the magnetic field induction. A subsequent decrease in the average charge of metal ions is associated with an increase in the fraction of hydrogen and carbon ions.

* The work is supported by Russian Science Foundation under the grant # 18-19-00069.

SURFACE MODIFICATION BY BEAMS AND PLASMA FLOWS OF BORON IONS GENERATED BY VACUUM ARC SOURCES *

K.P. SAVKIN[1], *A.S. BUGAEV*[1], *V.I. GUSHENETS*[1], *E.M. OKS*[1,2], *G.YU. YUSHKOV*[1], *A.G. NIKOLAEV*[1], *V.P. FROLOVA*[1,2]

[1]*High Current Electronics Institute, Russian Academy of Science, Tomsk 634055, Russia*
[2]*Tomsk State University of Control Systems and Radioelectronics, Tomsk 634050, Russia*

Boron ions can be used not only for ion implantation of silicon wafers for semiconductor manufacturing but also for ion beam modification or plasma surface deposition of other materials and metal products, e.g., machine parts, tools, etc., to increase their surface properties, and therefore lifetime. The purity of boron ion beams or plasma flows for these purposes is not so critical as for semiconductor technologies and vacuum arc plasma can be used for these purposes. At this work we present experimental results on the generation of pulsed boron ion beams and pulsed plasma flows generated by vacuum arc sources with cathode made from lanthanum hexaboride. The plasma composition of the vacuum arc with the cathode of lanthanum hexaboride was measured using time-of-flight and magnetic mass spectrometers. It was shown that the composition of both the plasma in the plasma arc generator based on the vacuum arc and the ion beam in the vacuum arc ion source corresponds to the atomic composition of the cathode. These boron ion beams and plasma flows were used to surface modification of samples. The results of changes in surface properties of the samples are also presented in this work. The possibilities of using boron ion beams and plasma flows generated by the vacuum arc are discussed.

* The work is supported by Russian Science Foundation under the grant # 16-19-10034.

FORMATION OF HIGH-INTENSITY BEAMS OF LOW AND ULTRA LOW ENERGY IONS USING A TWO-ELECTRODE GRID SYSTEM

A.I. RYABCHIKOV, D.O. SIVIN, A.I. IVANOVA, O.S. KORNEVA, S.V. DEKTYAREV

National Research Tomsk Polytechnic University, Lenin Avenue 30, Tomsk, 634050, Russia
E-mail: bai@tpu.ru, phone (3822) 70-17-77 ext. 2362

Low-energy, high-intensity ion implantation into various materials demonstrates the possibility of formation of extended, ion-doped, layers with thicknesses reaching dozens and hundreds of microns. However, a significant ion sputtering due to ultrahigh-fluences of irradiation (10^{20}–10^{22} ion/cm^2) results in a substantial surface erosion, changes in morphology as well as in properties of ion-modified layers.

The report presents the experimental results of studying the regularities of the formation of ballistic-focused high-intensity ultra-low and low energy ion beams with negative bias potentials with amplitude of (50 - 500) V using a two-grid focusing system of different-potential electrodes providing the acceleration-braking principle under conditions of the ion beam space charge compensation. The influence of preliminary plasma injection into the drift space of the ion beam, gas pressure and the presence of an «electronic shower» on the efficiency of transportation and focusing of a high-intensity titanium ion beam has been studied.

FORMATION OF PULSED LOW-ENERGY ELECTRON BEAM BY A PLASMA-CATHODE ELECTRON SOURCE BASED ON CATHODIC ARC IN THE FOREVACUUM PRESSURE RANGE*

A.V. KAZAKOV[1], *A.V. MEDOVNIK*[1], *E.M. OKS*[1,2]

[1]*Tomsk State University of Control Systems and Radioelectronics, Tomsk, Russia*
[2]*Institute of High Current Electronics, Siberian Branch of the Russian Academy of Sciences, Tomsk, Russia*

Wide application of glasses, ceramics and polymers, requires improvement of current methods and development of new methods of their treatment [1, 2]. In particular, wide range of surface modification methods of glasses, ceramics and polymers are developed [3]. Most glasses, ceramics and polymers do not conduct electric current under normal conditions [1, 2], i.e. are dielectrics, so to treat this material by electron beam at standard gas pressure for electron-beam sources (10^{-3}–10^{-1} Pa) it is required to use additional equipment to compensate negative charge on dielectric surface. Forevacuum plasma-cathode electron sources generating low-energy (up to 20 keV) electron beams in the forevacuum pressure range (3–100 Pa) provide direct treatment of dielectric materials [4, 5]. In particular, pulsed forevacuum plasma-cathode electron sources provide surface modification of dielectric materials [5].

The research of formation of pulsed large-radius low-energy (up to 10 keV) electron beam by a plasma-cathode electron source based on the cathodic arc in the forevacuum pressure range is presented. A hollow anode and a redistributing electrode have been used to generate broad, uniform emission plasma. Increase of the diameter of hollow anode and increase of diameter of emission aperture (window in the plane part of the anode covered by metal mesh) up to inner diameter of hollow anode has provided, as expected, an increase in efficiency of electron extraction from the arc plasma. However, increase of emission aperture has led to decrease maximal operating gas pressure due to intensification of the influence of back-streaming ion flow on the emission (arc) plasma. The use of two emission meshes with different cell sizes has provided generation electron beam with current of up to tens of amperes and pulse duration up to 5 ms at gas pressure of up to 15 Pa (N_2). The maximal operating pressure and optimal efficiency of electron extraction from arc plasma (at low pressure) are provided in case of the first mesh with large cell sizes is mounted inside the hollow anode, and second fine mesh covers the emission window on side, facing the extractor (optimal distance between meshes is about 2 mm). The use of the redistributing electrode and two emission meshes provided an increase in the uniformity of the current density distribution across the electron beam.

REFERENCES

[1] M. A. Spalding, A. Chatterjee, Handbook of Industrial Polyethylene and Technology: Definitive Guide to Manufacturing, Properties, Processing, Applications and Markets, John Wiley & Sons, Hoboken, NJ, USA, 2017.

[2] Handbook of advanced ceramics: materials, applications, processing, and properties, ed.S. Somiya, Academic press, Waltham, MA, USA, 2003.

[3] S. M. Desai, R. P. Singh, “Surface modification of polyethylene” in Long Term Properties of Polyolefins, ed. A.C. Albertsson, Ed. Berlin: Springer, 2004. – pp. 231–294.

[4] V. A. Burdovitsin, A. S. Klimov, A. V. Medovnik, and E. M. Oks, “Electron beam treatment of non-conducting materials by a fore-pump-pressure plasma-cathode electron beam source,” Plasma Sources Sci. Technol., vol. 19, no. 5, pp. 055003, October. 2010.

[5] V. Burdovitsin, A. Kazakov, A. Medovnik, E. Oks, I. Puhova, and A. Smailov, “Processing of polypropylene by low-energy pulsed electron beam from forevacuum plasma source,” Key Eng. Mater., vol. 683, pp. 95–99, February 2016.

* The work was supported by the Russian Foundation for Basic Research (RFBR) under the Grant No. 18-38-20044.

PARAMETERS OF CONSTRICTED ARC FOR THE PULSED FOREVACUUM PLASMA ELECTRON SOURCE*

A.V. KAZAKOV[1], *A.V. MEDOVNIK*[1], *E.M. OKS*[1,2], *N.A. PANCHENKO*[1]

[1]*Tomsk State University of Control Systems and Radioelectronics, Tomsk, Russia*
[2]*Institute of High Current Electronics, Siberian Branch of the Russian Academy of Sciences, Tomsk, Russia*

The characteristics of plasma-cathode electron-beam sources are greatly determined by the parameters of emission plasma, which generated by various types of gas discharges [1, 2]. In pulsed plasma-cathode electron sources the arc discharge with cathode spot is often used to generate emission plasma [1, 2]. Despite the advantages (for example: high discharge current, high plasma density, long pulse duration), the arc discharge with cathode spot has disadvantages caused by operating features of the cathode spots. In particular, the chaotic movement of the cathode spot may significantly affect the emission plasma uniformity, and macroparticles (liquid or solid debris particles) formed at the cathode spots can penetrate the regions of acceleration and propagation of electron beam [3]. In order to reduce the negative influence of operating processes of the cathode spot a constricted arc discharge is used to generate emission plasma in electron souses operating at standard gas pressure 10^{-3}–10^{-1} Pa [4]. Therefore, the features of the constricted arc discharge are rather well studied for the plasma-cathode electron sources operating in pressure range 10^{-3}–10^{-1} Pa. The use of the constricted arc discharge to generate emission plasma in forevacuum pulsed electron sources has not been previously studied. Therefore, the aim of this work is to research the features of the constricted arc discharge operating in the plasma-cathode ("discharge gap") of the pulsed forevacuum source generating large radius electron beam in the pressure range 3–30 Pa.

The research of features of the constricted arc discharge operating in the forevacuum plasma-cathode electron source is presented for various operating gases. In case of using helium the constricted arc discharge does not stable operate in the studied pressure range 3–30 Pa: either there are arc current drops, or arc discharge operates in a cascade mode (i.e. cathode spots appear on a constricting electrode). The use of argon and nitrogen at pressure higher than 5 Pa provide stable operation of the constricted arc discharge, but maximal current of constricted arc is limited by initiation of cathode spot on the constricting electrode. The use of argon provides an almost twofold decrease in the operating voltage of constricted arc discharge, and also provides higher maximal arc currents. An increase in gas pressure leads to a decrease in the arc discharge voltage and provides higher arc current of the constricted arc. The influence of gas pressure on the operation of the constricted arc is caused by ionization processes occurring inside and near the constricting channel. The use of argon provides a lower arc voltage and high current due to argon has a higher ionization cross-section.

REFERENCES

[1] N. N. Koval, E. M. Oks, P. M. Schanin, Y. E. Kreindeland, and N. V. Gavrilov, "Broad beam electron sources with plasma cathodes," Nucl. Instrum. Methods Phys. Res. A, vol. 321, no. 3, pp. 417–428, October 1992.

[2] E. Oks, Plasma Cathode Electron Sources: Physics, Technology, Applications. Berlin, Germany: Wiley, 2006.

[3] A. Anders, Cathodic Arcs: From Fractal Spots to Energetic Condensation. New York, NY, USA: Springer, 2008.

[4] A. F. Zlobina, G.S. Kazmin, N.N. Koval, and B.E. Kreindel, "Plasma parameters in the expander of an electron emitter with a constricted arc discharge," Sov. Phys. Tech. Phys., vol. 25, no. 6, pp. 689–691, June 1980.

* The work was supported by the Russian Foundation for Basic Research (RFBR) under the Grant No. 20-08-00123.

STUDYING THE REGULARITIES OF FORMING HIGH-INTENSITY BEAMS OF METAL IONS OF LOW AND ULTRA-LOW ENERGY

A.I. RYABCHIKOV, D.O. SIVIN, O.S. KORNEVA, A.I. IVANOVA, S.V. DEKTYAREV, A.I. BUNIN

National Research Tomsk Polytechnic University, Lenin Avenue 30, Tomsk, 634050, Russia

Low energy, high intensity ion implantation provides the ability to form ion-doped layers in metals and alloys at depths of tens and hundreds of micrometers [1, 2]. Ultra-high-dose implantation of low-energy ions is accompanied by significant ion sputtering of the irradiated surface. At ion irradiation fluences exceeding 10^{21} ion/cm^2, the thickness of the ion-sputtered layer can exceed 100 micrometers. When sputtering the target surface layer, both matrix material and implanted dopant are sputtered, which leads to a decrease in the efficiency of dopants accumulation and a decrease in the ion-doped layer depth. One of the solutions to the problem of significant ion surface sputtering can be based on high-intensity implantation at ultra-low ion energy, when ion sputtering is minimized and provides only dynamic cleaning of the irradiated surface from contamination with oxides and carbides.

The paper presents the results of studying the laws governing the formation of high-intensity low and ultra-low energy beams of metal ions using plasma of a pulsed and continuous vacuum arc discharge. The features and regularities of the formation of beams with a single-grid extraction system and ballistic focusing of ions in the drift space are studied at bias potentials amplitudes from 50 to 2000 V. The regularities of the electron current suppressing in the accelerating gap during the traditional ion beam formation by a single-grid electrode with an accelerating voltage applied to the plasma generator are described. The influence of grid cell sizes from 100 to 500 μm, preliminary plasma injection into the drift space and the “electron shower” on the transport efficiency and ballistic focusing of high-intensity beams of titanium ions of low and ultra-low energy is studied.

REFERENCES

[1] A.I. Ryabchikov, P.S. Ananin, S.V. Dektyarev, D.O. Sivin, A.E. Shevelev, High intensity metal ion beam generation, Vacuum 143 (2017) 447–453

[2] A.I. Ryabchikov, D.O. Sivin, O.S. Korneva, I.A. Bozhko, A.I. Ivanova, Modification of the microstructure and properties of martensitic steel during ultra-high dose high-intensity implantation of nitrogen ions, Surface and Coatings Technology 388 (2020) 125557

INFLUENCE OF UV RADIATION AND DISCHARGE PLASMA ON FEED WHEAT SEEDS FOR ACCELERATION OF PLANTS*

M.A. SHULEPOV, S.Yu. DOROSHKEVICH, M.S. VOROBYOV, E.I. LIPATOV

[1]*Institute of High Current Electronics SB RAS, Tomsk, Russia*

Food safety is a strategic purpose of any state. In an unstable climate, this problem becomes the most emergency. For Russia, due to its geographical location, food safety has always been and remains a problem. To solve this problem, in the USSR a powerful agrochemical complex was created. But careless, thoughtless use of chemical fertilizers increases the danger of food for human health and its descendants. At the same time, soil fertility sharply decreases. Genetic modification of agricultural plants is also not an option, since we still have a poor idea of the impact of such plants on humans in the long term. Today, the most optimal solution for Russian territories is to build large greenhouse complexes that reduce the impact of the environment on plant growth to almost zero. But the more complex the climate conditions, the more energy are required to maintain the growth and fruiting of greenhouse plants.

A partial solution to the problem is to accelerate the development of plants so that the fruits have time to ripen during the small vegetative period at high latitudes, because in some cases, plants do not have enough for just a few days to ripen in the open ground. Given the above criteria, the most appropriate approach to accelerate plant growth is to expose seeds to UV radiation excilamps and/or plasma radiation of an electric discharge [1]. In the latter case, the electron beam can additionally be affected by the electron beam.

Here are the results of an experiment on the effect of pre-treatment of seeds with UV radiation and electric discharge plasma on the growth of fodder wheat [2,3]. The experiment was further complicated by the fact that inoculation of the radiation-treated excilamps and electric discharge plasma was carried out in unprepared soil. The plot for sowing has been under steam for more than 20 years and, in fact, was virgin soil.

REFERENCES

[1] Gordeev Yu.A., Yuldashev R.Z. Bioactivation of seeds of cultivated plants with ultraviolet and plasma radiation // Bulletin of the St. Petersburg State Agrarian University, 24, p. 343-348, 2011.

[2] Koval, N & Vorobyov, Maxim. (2018). Possible applications of the electron source with a wide-grid plasma cathode and the output beam into the atmosphere. Journal of Physics: Conference Series. 1089. 012011. 10.1088/1742-6596/1089/1/012011.

[3] Sosnin E.A., Tarasenko V.F., Panarin V.A., Chudinova Yu.V., Viktorova I.A., Cheglokov A.E. Device for ultraviolet seed treatment / Patent RU No. 139005. Priority date 11/27/2013, published 03/27/2014, Bull. No 9.

*****The work was supported by the Russian Science Foundation under the grant No. 9.5.2. (IHCE SB RAS)

THE SOURCE OF HIGH-INTENSITY REPETITIVELY PULSED BEAMS OF LOW AND ULTRA-LOW ENERGY METAL IONS

A.I. RYABCHIKOV, S.V. DEKTYAREV, D.O. SIVIN, D.O. VAKHRUSHEV

National Research Tomsk Polytechnic University, Tomsk, Russia

To implement a low-energy high-intensity ion implantation (LEHI^3) method, beams with a current density of 10 – 10^3 mA/cm^2 are required. Given that ultra-high dose implantation is accompanied by significant sputtering of the surface layer of the irradiated target for ion doping of materials, high-intensity sources with low and ultra-low ion energies are required to control ion surface sputtering.

This report describes an ion source based on a vacuum-arc discharge with ballistic ion focusing. A vacuum-arc evaporator of the Raduga-5 installation operating in a pulsed or continuous mode was used as a plasma generator. Repetitively pulsed accelerating voltage with an amplitude of 100 V – 2 kV is applied to the plasma generator. An ion extractor in the form of a fine-grained grid in the shape of a part of a spherical surface is at zero potential and is installed at the output of the arc evaporator anode. The spherical shape of the grid electrode provides ion ballistic focusing. The report presents the study results of the laws of formation, transport efficiency and focusing features of ion beams with a current of tens and hundreds of milliamps per square centimeter depending on the size of the grid cell of 0.1 – 1.8 mm and accelerating voltage. Data are presented on the features and efficiency of the space charge neutralization of low and ultra-low energy ion beams due to the preliminary plasma injection into the space of the beam drift, increase in the pressure of the residual gas in the experimental chamber and under the conditions of an “electron shower” formation.

VISUALIZATION OF PLASMA FORMING SUBSTANCE FLOWS IN A VACUUM DIODE USING CATHODE WITH WATER INJECTION INTO ACCELERATING GAP*

M.A. SEREBRENNIKOV[1], A.V. KLIMKIN[2], M.V. TRIGUB[2], A.V. POLOSKOV[1], I.S. EGOROV[1]

[1]Tomsk Polytechnic University, 2a Lenin Avenue 634028, Tomsk, Russia, mas48@tpu.ru, 8(3822)701777 (add. 2577)
[2]Institute of atmospheric optics SB RAS, Tomsk, Russia

The expansion of commercial applications of pulsed electron beam sources stimulates the development of high-resource electron beam accelerators. Lifetimes of vacuum electron diode as a whole and cathode in particular are often limit a lifetime of the accelerator. The work contains results obtained by experimental installation based on a vacuum diode of the ASTRA-M pulsed electron accelerator [1] using a cathode with water injection into the accelerating gap [2]. Vacuum camera of the accelerator is equipped with visual-optical diagnostics system for detailed study of the processes in the gap. The system allows high-speed visualization of the substance flow, as well as spectral analysis of both its own glow, and using additional probe radiation. Data obtained upon injection of the Rhodamine-6G were used as a test spectra. The influence of the pumping pipe location was evaluated by comparing the data obtained in different projections of measurements (opposite the pumping pipe, at right and acute angles). The study results are necessary for the conditions evaluation of plasma formation in a vacuum electron diode with the injection of water into the accelerating gap.

REFERENCES

[1] I. Egorov, V. Esipov, G. Remnev, M. Kaikanov, E. Lukonin, A. Poloskov, A high-repetition rate pulsed electron accelerator, IEEE Trans. Dielectr. Electr. Insul. 20 (2013) 1334–1339. https://doi.org/10.1109/TDEI.2013.6571453.

[2] I. Egorov, A. Poloskov, M. Serebrennikov, G. Remnev, Experimental demonstration of a single capillary, water-activated cathode for a sub-microsecond electron accelerator, Nucl. Instruments Methods Phys. Res. Sect. A Accel. Spectrometers, Detect. Assoc. Equip. 943 (2019) 162459. https://doi.org/10.1016/j.nima.2019.162459.

* Preparation of the experiments and analysis of the data were supported by RFBR grant № 20-02-00870.

PARAMETERS OF A BEAM PLASMA GENERATED BY AN ELECTRON BEAM WITH A POWER OF UP TO 10 KW IN THE FOREVACUUM PRESSURE RANGE

A.A. ZENIN, I.YU. BAKEEV*, A.S. KLIMOV*, E.M. OKS***

** Tomsk State University of Control Systems and Radioelectronics, Russia, Tomsk, 40 Lenina ave., 634050*
*** Institute of High Current Electronics SB RAS, 2/3 Academichesky Ave., Tomsk, 634055, Russia*

Low energy high current electron beams are widely used in surface and dimensional material processing technologies because electron beam processing can significantly improve the initial parameters of a material, such as roughness, microhardness, and corrosion resistance [1]. Recently developed forevacuum plasma electron sources, which feature the ability to generate electron beams in the pressure range of 1-100 Pa, have reached the level of generated power of more than 5 kW. The ability of such sources to function in medium vacuum conditions opens the possibility of direct processing of non-conducting materials, such as ceramics, polymers, borides, etc. [2-3]. This article describes the features of transporting an electron beam generated by a plasma electron source in the medium vacuum pressure range. The characteristics of the plasma of a beam-plasma discharge that produced during the transport of the powerful electron beam are studied. It is shown that the change in the accelerating voltage and current of the beam leads to a significant change in the concentration of the beam plasma (by 1-2 orders of magnitude) and an increase in the electron temperature to 4-5 eV.

This work was funded by the Russian Federation for Basic Research under Grant No. 19-48-700004.

REFERENCES

[1] Rotshtein *V.P, Proskurovsky D.I, Ozur G.E, Ivanov Y.F, Markov A.B.* // Surface modification and alloying of metallic materials with low-energy high-current electron beams// Surface and coating technology, Vol. 180 Pages: 377-381 MAR 1 2004

[2] *Burdovitsin V.A, Klimov A.S, Oks E.M, // On the possibility of electron-beam processing of dielectrics using a fore-vacuum plasma electron source.// TECHNICAL PHYSICS LETTERS Volume: 35 Issue: 6 Pages: 511-513 Published: JUN 2009.*

[3] Yushkov *Y.G., Tyunkov A.V., Oks E.M., Zolotukhin D.B.* // Electron beam evaporation of boron at forevacuum pressure for plasma-assisted deposition of boron-containing coatings.//Journal of Applied Physics. 2016. Т. 120. № 23. С. 233302.

NUMERICAL MODELLING OF FERROMAGNETIC ENHANCED INDUCTIVELY COUPLED PLASMA DISCHARGE PARAMETERS IN OXYGEN *

N.A. DEMIN, A.V. FEDOSEEV

Kutateladze Institute of Thermophysics SB RAS, Novosibirsk, Russia

The active use of low-temperature plasma in many technological processes, in particular, for ion-plasma etching in microelectronics, stimulates exploratory work on the development of new gas-discharge devices that expand the capabilities of existing ion-plasma technologies and allow to overcome their inherent limitations. Currently, the ferromagnetic enhanced inductively coupled plasma discharge allows to obtain large volumes of dense pure plasma of halogen-containing gases, with a high concentration of ions and chemically active particles, at a low plasma-forming gas pressure [1], and it appears to be a perspective technology for future large etching reactors in microelectronics.

Oxygen discharges are applied in plasma processing for different applications such as ashing of photoresist, removing polymer films and oxidation or deposition of thin film oxides [2]. It is of fundamental importance to determine the densities of neutral species, in particular, the oxygen radicals, and influence of these densities on various plasma and control parameters (i.e. pressure, power, dilution gas ratio, etc). In current work properties of ferromagnetic enhanced inductively coupled plasma discharge in oxygen for large reactor were studied numerically.

To explore the distributions of overall plasma parameters the global model that was developed for rf discharge [3] was used and adopted for current conditions. In the gas discharge plasma, electrons, oxygen and argon molecules, atoms, ions, metastable states of atoms and exited atoms are considered. The time dependent balance equations were solved for each sort K of particles:

$$\frac{dn^{(K)}}{dt} = \sum_i R_{G,i}^{(K)} - \sum_i R_{L,i}^{(K)},$$

where $R_{G,i}^{(K)}$ and $R_{L,i}^{(K)}$ are the rates of generation and loss of particles in i-th process. The reaction set and rate coefficients for all volume reactions and heterogeneous processes in O_2/Ar discharge were taken exactly as reported by Thorsteinsson et al. [4]. It was assumed that electrons have Maxwellian energy distribution functions, and that discharge is electrically quasi-neutral. The ion flux to the walls was calculated in approach of electropositive gas. The electron temperature was determined from the power balance equation. The calculations were made for chamber with R=35cm and L=50cm.

The reactions of creation and destruction of oxygen atoms and negative oxygen ions were investigated. It was found that for the studied type of reactor most of the reactions included in the model influence negligibly and may not be considered in future research. The increase in the fractional dissociation of the oxygen molecules with an increase of argon content was observed. Finally it was revealed that the metastable oxygen atoms and molecules play in important role in the discharge dynamics.

REFERENCES

[1] Godyak V., "Ferromagnetic enhanced inductive plasma sources" J. Phys. D: Appl. Phys., vol.46, Article Number 283001, 2013.

[2] D. A. Carl, D. W. Hess, and M. A. Lieberman, "Oxidation of silicon in an electron cyclotron resonance oxygen plasma: Kinetics, physicochemical, and electrical properties" Journal of Vacuum Science & Technology A., vol.8, Article Number 2924, 1990.

[3] E. G. Thorsteinsson and J. T. Gudmundsson, "A global (volume averaged) model of a chlorine discharge" Plasma Sources Sci. Technol., vol.19, Article Number 015001, 2010.

[4] Yu.D. Korolev and G.A. Mesyats, "Oxygen discharges diluted with argon: dissociation processes" Plasma Sources Sci. Technol., vol. 16, 399–412, 2007.

* The work was carried out under state contract with IT SB RAS.

DESIGN OF A COLD ATMOSPHERIC PLASMA JET GENERATOR*

P.P. GUGIN[1], D.E. ZAKREVSKY[1,2], E.V. MILAKHINA[2]

[1] *A. V. Rzhanov Institute of Semiconductor Physics SB RAS, Novosibirsk, Russia*
[2] *Novosibirsk State Technical University, Novosibirsk, Russia*

The plasma devices generating the streamer type of breakdown in a mixture of noble gases and air have been widely used in medicine [1]. The streamer appears over the positive cycle of the applied voltage and propagates along a gas jet in the surrounding air at atmospheric pressure [2, 3]. Several designs of plasma devices with axial and planar geometries generating a low-temperature plasma jet were developed and studied.

The coaxial device is a dielectric (quartz) channel with a length of 100 mm and an inner diameter of 8 mm a copper electrode with a length of 50 mm and a diameter of 2 mm and a dielectric capillary are inserted in the center. A copper grounded ring with an inner diameter of 18 mm is outside the quartz tube. Similarly, a design was developed to increase the area of impact of the plasma jet with the object, consisting of 7 dielectric coaxial channels. Copper electrodes and dielectric capillaries are placed in the center of the channels. The discharge is formed by internal copper electrodes and an external grounded electrode.

The planar structure is a dielectric case with a gap of ~ 40 mm in length. Quartz plates inserted into the gap form an internal channel of 2 mm. This is how the slot hole (nozzle) is formed. The thickness-adjustable dielectric plates form a capillary gap of 1 mm, which are located at the outlet of the nozzle. The discharge is formed by an internal copper multi-point electrode located along the gap, and an external grounded electrode. Similarly, a multi-gap design with three flat channels was developed.

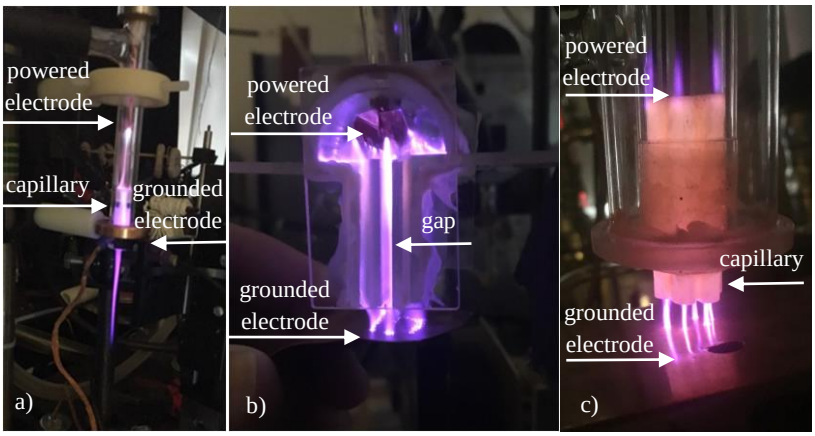

Fig.1. à) The coaxial device; b) The planar device; c) The complex coaxial device.

The gas system supplied working gases He/Ne/Ar with the typical gas flow rate *v* of 1–10 L/min at an excess pressure in the gas main of 1 atm. The power supply provided a sinusoidal voltage with a frequency of 40 kHz, voltage amplitude *U* up to 10 kV.

REFERENCES

[1] S Kalghatgi, D Dobrynin, G Fridman, M Cooper, G Nagaraj, L Peddinghaus, M Balasubramanian, K Barbee, A Brooks, V Vasilets, A Gutsol, A Fridman, G Friedman, “Applications of non thermal atmospheric pressure plasma in medicine” Plasma Assisted Decontamination of Biological and Chemical Agents. Springer, Dordrecht, 2008, pp.173-181.

[2] G. Fridman, G. Friedman, A. Gutsol, A. B. Shekhter, V. N. Vasilets, A. Fridman, "Applied Plasma Medicine” Plasma Processes and Polymers, vol. 5, pp. 503-533, 2015.

[3] I. Schweigert, Dm. Zakrevsky, P. Gugin et al. "Interaction of Cold Atmospheric Argon and Helium Plasma Jets with Bio-Target with Grounded Substrate BeneathGeneration peculiarities of cold atmospheric plasma jet in biomedical applications," Applied Sciences, vol. 9, p.4528, 2019.

* The work was supported by the Russian Science Foundation under grant No. 19-19-00255.

ISOPOTENTIAL MAPPING OF ELECTRON BEAM INDUCED DIELECTRIC CHARGING OF THE PHB NONWOVEN FABRIC STRUCTURES USING ISOPOTENTIAL MAPPING

O.V. GRADOV, M.A. GRADOVA, A.A. OLKHOV, A.L. IORDANSKII

N.N. Semenov Federal Research Center of Chemical Physics, Russian Academy of Sciences, Moscow, Russia

Dielectric (especially polymer material) charging under the electron beam during electron microscopy studies is a well known effect. The charge centroids usually have uneven and relief-specific distribution, characterizing the sample surface and being a source of dielectric and the following structural descriptors of polymer materials. However, as in microelectronics and microsystem engineering, this charge is often considered as an undesirable side-effect, requiring elimination by changing the operation conditions and the measurement mode (which is especially critical in low-voltage electron microscopy - LVEM) or by the metal sputtering on the sample surface, which prevents from obtaining further information about the electrical properties of the sample. Meanwhile, the charge spatial distribution, are very informative, and even more interesting is the dynamics of this distribution. To date there are no dynamical approaches to the analysis of the spatial-temporal charge distribution on the dielectric sample surface within the conventional research methods. It is possible to perform the dielectric charging registration using the level of the cooperative flashover, traveling along the sample under the electron beam in accordance with the sample surface structure / morphology and its chemical composition, which locally determine the charge generation efficiency. The charge propagation speed and delay for different dielectric materials can also be informative descriptors of the sample surface, and hence, a variable in the profiling and dynamic mapping of the charging process. We performed the charge propagation studies [1] on the polyhydroxybutyrate (PHB) nonwoven materials produced by electrospinning for biomedical applications [2,3] using special SEM systems [4-6].

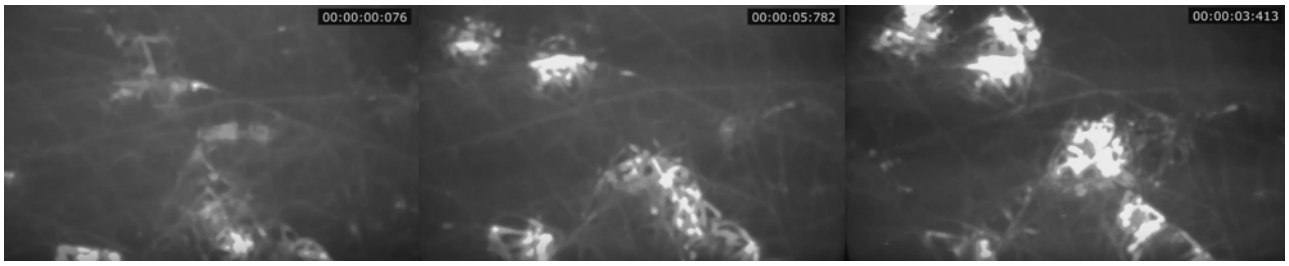

Fig.1. LVEM-assisted imaging of the dielectric charging of the nonwoven electrospun PHB structures.

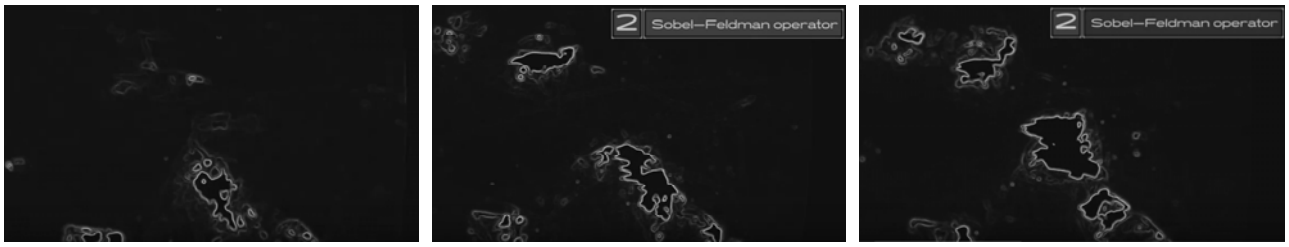

Fig. 2. Isopotential mapping of the dielectric charging of the nonwoven PHB structures using Sobel–Feldman operator (Sobel filter).

REFERENCES

[1] O. Gradov, A. Olkhov, "SEM-assisted (LVEM-assisted) isopotential mapping of the dielectric charging of the nonwoven fabric structures using Sobel–Feldman operator (Sobel filter)", IEEE Dataport, 2018. [Online]. DOI: 10.21227/tjfe-ry55.

[2] V.N. Gorchenev, A.A.Olkhov, O.V. Gradov, M.A. Gradova, P.L. Aleksandrov (2019). [Emergent topological approach for integration of physical properties of solid and soft matter media in porous scaffolds and tissue-engineered constructs: case of PHB and HAp with multi-angle CLSEM visualization]. Genes and Cells, 14(Supplement 1): 69. [in Russian]

[3] O. Gradov, A. Olkhov, M.t Gradova and A. Iordanskii, "Electrophysical properties of polyhydroxybutyrate fibers as materials for regenerative medicine and neuromorphogenesis. Is it possble to use the electrical neutrality concept in the analysis of biocompatibility of PHB with excitable tissues?" Subm. to Conference: KPM-2019, 2019. DOI: 10.13140/RG.2.2.20825.88166

[4] O. V. Gradov and M. A. Gradova, "Methods of electron microscopy of biological and abiogenic structures in artificial gas atmospheres," Surface Engineering and Applied Electrochemistry, vol. 52, no. 1, pp. 117–125, 2016.

[5] O. V. Gradov and M. A. Gradova, "Cryoelectron microscopy as a functional instrument for system biology, structural analysis and experimental manipulations with living cells," Problems of Cryobiology and Cryomedicine, vol. 24, no. 3, pp. 193–210, 2014.

[6] O. V. Gradov, "Multi-angle goniometric computer-assisted lab-on-a-chip reading system stage for vacuum-gas chambers based on analytical scanning electron microscopy platform (goniometric CLEM chambers)," Comput. nanotech, no. 4, pp. 9–16, 2018.

TITANIUM SURFACE IMPLANTATION BY MULTICHARGED BISMUTH IONS*

V.P. FROLOVA[1,2], A.G. NIKOLAEV[1], E.M. OKS[1,2], G.YU. YUSHKOV[1,2]

[1]Institute of High Current Electronics SB RAS, Tomsk, Russia
[2]Tomsk State University of Control Systems and Radioelectronics, Tomsk, Russia

The main advantage of vacuum arc sources is the possibility of generating high current wideaperture ion beams of any conductive solidstate material. Such beams are widely used to solve the problems of surface modification of various structural materials operated under conditions of intense mechanical, temperature and radiation loads, for example, such applications as engine production, aviation and nuclear power. This paper presents studies on the implantation of a titanium surface by a bismuth ion beam. The depth distribution profile of implanted ions, measured by the method of secondary ion mass spectrometry, is shown. For all experiments, the accelerating voltage was 40 kV, the implanted dose on the surface was $1*10^{16}$ ion cm^{-2}. The pressure in the vacuum chamber was $3*10^{-7}$ Torr. Samples for implantation were 15x15 mm rectangular plates of titanium. It was shown that the use of a high-current vacuum arc discharge with a duration of a few microseconds makes it possible to increase the depth of the implanted surface layer due to the higher energy of multicharged ions in the beam.

* This work was supported by RFBR under grant numbers RFBR-17-08-00133 A.

GENERATION OF BEAM-PLASMA FORMATION IN A CYLINDRICAL EXTENDED HOLLOW GRID ANODE [1]

T.V. KOVAL[1], V.V. DENISOV[2], N.N. KOVAL[2], S.S. KOVALSKY[2], E.V. OSTROVERKHOV[2], V.P. TARAKANOV[3]

[1]*National Research Tomsk Polytechnic University, 2/3 Lenin ave., Tomsk, 634050, Russia, e-mail: tvkoval@mail.ru*
[2]*Institute of High Current Electronics SB RAS, Tomsk, Russia*
[3]*Joint Institute for High Temperatures RAS, National Research Nuclear University MEPhI, Moscow, Russia*

Designing of the materials surface with predetermined properties requires the development of scientific and technical fundamentals of beam-plasma technologies, knowing of conditions for the efficient generation of beam-plasma volume formations and developing of methods for controlling their parameters. An experimental bench based on an electric-discharge system [1] created at the HCEI SB RAS and designed to study the processes of generation of beam-plasma formations in a non-self-sustained glow discharge with a hollow cathode (≈ 0.3 m^3) at a low pressure of about 1 Pa, which allows one to determine the relationships between the parameters of the generated beam-plasma formations with the conditions of their impact on the surface and the final surface properties of materials and products. To solve the problem of plasma concentration inhomogeneity in the hollow cathode (the working zone for loading parts and products), electron injection from a cylindrical extended hollow grid emitter located on the axis of the hollow cathode is used.

The experimental and numerical studies of the formation of a beam-plasma formation in a cylindrical extended hollow grid emitter (hollow anode of an arc discharge in crossed electric and magnetic fields [2]) was implemented in this work. It has been shown experimentally that the system for generating of extended beam-plasma formations in a non-self-sustained glow discharge with a plasma electron emitter based on an arc discharge allows one to obtain a longitudinal degree of inhomogeneity of the concentration of the formed plasma over a length of 1 m in a hollow anode at a pressure of 0.15 Pa in an argon atmosphere of about ± 25 %, and in pure nitrogen ± 40%.

A numerical simulation using the large particle method has been carried out to study the influence of combustion parameters of an arc discharge in a hollow anode and the ion flux entering in it, on the uniformity of the generated plasma formation and the density of the electron emission current from the boundaries of the arc plasma. It is shown that the longitudinal heterogeneity of the plasma formation substantially depends on the external source of the plasma and (or) the electrons, on the processes of ionization of the working gas and charge exchange of ions in the anode cavity.

The obtained results make it possible to determine the mechanism for generating a beam-plasma formation, to optimize the dimensions of a hollow extended grid anode, and to control the beam-plasma system as a whole.

REFERENCES

[1] V.V. Denisov, Yu.H. Akhmadeev, N.N. Koval, S.S. Kovalsky, I.V. Lopatin, E.V. Ostroverkhov, N.N. Pedin, V.V. Yakovlev, and P.M. Schanin. The source of volume beam-plasma formations based on a high current non-self-sustained glow discharge with a large hollow cathode // Phys. Plasmas. –2019. – V.26. – 123510.

[2] V. V. Denisov, Yu. H. Akhmadeev, N. N. Koval and E. V. Ostroverkhov Low-temperature plasma source based on a cold hollow-cathode arc with increased service life // High Temp. Mater. Prosess. – 2016. – V.20(4). – pp.309–316.

[1] The work was carried out with the financial support of the RFBR grant №18-38-00836.

TWO MODES OF TRANSPORTATION OF A HIGH CURRENT ION BEAM WITH BALLISTIC FOCUSING [1]

T.V. KOVAL[1], V.P. TARAKANOV[2]

[1]Tomsk Polytechnic University, Tomsk, Russia
[2]Joint Institute for High Temperatures RAS, National Research Nuclear University MEPhI, Moscow, Russia

Ion sources are used to modify the surface layers of various materials and products. Minimization of radiation damage of a treated surface determines the tendency to lower ion beam energy (<1.5 keV). To control the processes of transportation of a metal ion beam of submillisecond duration with ballistic focusing, one should take into account the dynamic process of neutralizing the space charge of the ion beam and the formation of ion-beam plasma [1, 2].

By the PiC simulations [3], the ion beam transportation in equipotential drift spaces with ballistic focusing (spherical and cylindrical) was studied. It is shown that at the energy of injected ions $W < W_c$, (W_c is the critical energy, which depends on the gas concentration and beam current), the collector current passes into a pulsed mode due to dynamic processes of formation of a virtual anode and neutralization of its positive charge by secondary electrons. So, in the hemispherical drift space with a radius of 7.5 cm at a ion beam injected current I_b = 0.3 A and gas concentration $n_g = 5\text{x}10^{12}$ cm^{-3}, the critical energy is W_c = 2 keV, and at $n_g = 2\text{x}10^{13}$ cm^{-3} the energy is W_c = 1 keV. The frequency of oscillations of the beam current at the collector depends on the energy, the geometry of the system, and the gas concentration.

The existence of a periodic collector current mode with a decrease of the beam energy ($W < W_c$) is associated with a decrease in the role of secondary electrons in the process of compensating the space charge of the ion beam, which leads to a sequential alternation of formation processes: a virtual anode with switching the current to the grid electrode and neutralizing the positive space charge slow ions of the beam by electrons arising from ionization of the gas in the chamber and secondary electrons from its boundaries.

Plasma in the ion beam transport region is formed from next components: the beam itself, its slowed-down part, electrons generated during secondary ion-electron emission and ion-electron pairs that arose during ionization of a neutral gas by electrons accelerated in the beam field. An important factor determining the transportation mode of an ion beam is the heating of electrons during the development of instabilities in the resulting plasma. All these processes are taken into account in the PiC simulation presented.

The formation time of the ion-beam plasma and the repetition period of the collector current pulses decrease with increasing energy of the transported ions W and gas concentration.

REFERENCES

[1] A. I. Ryabchikov, A. E. Shevelev, D. O. Sivin, T. V. Koval, and Tran My Kim An, “High intensity, macroparticle-free, aluminum ion beam formation”, J. Appl. Phys., vol. 123, no. 233301, 2018.

[2] T. V. Koval, Tran My Kim An, and V. P. Tarakanov, “Modeling Transport in a System with Ballistic Focusing of a High Intensity Beam of Metal Ions”, ISSN 1062-8738, Bulletin of the Russian Academy of Sciences: Physics, vol. 83, no. 11, pp. 1387–1391, 2019.

[3] V. P. Tarakanov, Mathematical Modeling: Problems and Results (Nauka, Moscow, 2003) [in Russian].

* The work was supported by the RFBR grant № 19-08-00248.

SPATIAL-TEMPORAL DISTRIBUTION OF PARAMETERS IN THE PLASMA LAYER FORMED BY SURFACE EVAPORATION WITH HIGH-BRIGHTNESS WIDEBAND SHORTWAVE RADIATION[1]

A.V. PAVLOV, YU.YU. PROTASOV, V.D. TELEKH, T.S. SHCHEPANUK

Bauman Moscow State Technical University, Educational and Scientific Center of Photon Energy
2nd Bauman str., 5, Moscow, 105005

The report analyzes the spatial-temporal variation in the parameter's distribution (temperature, electron and ion concentrations, etc.) in the plasma layer formed by surface evaporation of flat targets by wideband VUV spectrum range radiation

The processes occurring on the surface and in the near-surface vapor-plasma layer when exposed to VUV radiation on different materials understanding is relevant for the creation and optimization of different plasma energy devices (ablative pulsed plasma accelerators, plasmodynamic sources of ultraviolet and soft X-rays, radiation surface strengthening, photochemical installations, etc.) where information is needed on the distribution of heat fields and energy flows arising from the operation of such devices. This explains the interest in these studies.

Short-wave radiator of non-synchrotron type based on high-current plasma accelerator - magnetic plasma compressor (MPC) of erosion type was used as radiation source. In MPC plasmodynamic heating of electric discharge plasma is carried out as a result of shock-wave thermalization of directed kinetic energy of high-speed flow of dense radiating plasma at its braking in gas medium. The buffer gas simultaneously acts as a filter for the harsh component of the radiating plasma emission spectrum [1, 2]. As a consequence, since the rise times of the light pulses are determined only by the time profile of the hydrodynamic energy flow of the plasma jet in the braking zone, it is possible to significantly differ from the characteristic discharge times in the electrical circuit, which allows to form powerful pulses of VUV radiation with steep leading edge.

Targets in the form of bars with dimensions of 30 mm by 50 mm and thickness of 10 mm were installed with a long side along the discharge at a distance of 45 mm from the MPC axis. Thus, the near-to-discharge end of the target received 2-2.5 times more energy than the far one. This made it possible to register significantly different dynamics of vapor-plasma flow disperse when moving from one edge of the target to the other [3].

For visualization of shock waves (SW) and other expansion zones of vapor-plasma flow in external gas with large concentration gradients, two-exposure laser holographic interferometry with visualization of large optical fields and the Toepler method in the light field mode were used. The second harmonic of a Solar LQ-115 Nd:YAG laser operating in the modulated Q-factor (532 nm; 40 mJ, 7 ns) was used as a probing radiation source [4].

On the schlieren-pictures and interferograms, the zones characteristic of the studied type of radiation effect on materials are recorded: the gas-dynamic evaporation mode is realized (plasma piston mode), there is a shock wave in the gas, the contact boundary between the shock-compressed gas and the vapor plasma. The processing of interferograms, together with the analysis of other data of the experiment, allows to find the distribution of parameters in the plasma layer above the target surface. It has been found that the maximum energy absorption is inside the plasma layer. Possible mechanisms and elementary processes leading to this distribution of parameters are discussed.

REFERENCES

[1] "Radiative Plasmodynamics" vol. 1, ed Yu S Protasov. Moscow: Energoatomizdat, 1991

[2] A.V. Pavlov, Y.Y. Protasov, V.D. Telekh, T.S. Shchepanuk "Experimental research of dynamics and macrostructure of light erosion radiative plasmodynamic discharges," J. Phys.: Conference Series, vol. 830, No 1, Article Number 012062, 2017

[3] A.V. Pavlov, Y.Y. Protasov, V.D. Telekh, T.S. Shchepanuk "Investigation of the dynamics of expansion of the near-surface light erosion plasma formed during the evaporation of a material by broadband high-brightness radiation," J. Phys.: Conf. Ser., vol. 1393 No 1, Article Number 012019, 2019

[4] A.V. Pavlov, Y.Y. Protasov, V.D. Telekh, T.S. Shchepanuk "Laser holographic interferometry of short ultraviolet radiation with high power density interaction with condensed matters," Scientific Visualization, vol. 11, No 3, P. 111-125, 2019

1 The work was supported by the Russian Foundation for Basic Research under grant No. 18-29-21039 and has been performed at "Beam-M" facility of Bauman Moscow State Technical University.

STABILITY OF ZR-BASED METALLIC GLASS STRUCTURE UNDER HIGH-TEMPERATURE PLASMA IMPACT*

N.N. CHERENDA[1,2], V.V. UGLOV[1,2], V.I. SHYMANSKI[1], D.V. ESIPENKO[1], G.E. REMNEV[2], V.M. ASTASHYNSKI[3], A.M. KUZMITSKI[3], A.N. SUCHKOV[4], D.M. BACHURINA[4], X. MEI[5]

[1]*Belarusian State University, Minsk, Belarus*
[2]*National Research Tomsk Polytechnical University, Tomsk, Russia*
[3]*A.V.Lyikov Heat and Mass Transfer Institute of the National Academy of Sciences of Belarus, Minsk, Belarus*
[4]*National Research Nuclear University MEPhI, Moscow, Russia*
[5]*Key Laboratory of Materials Modification by Laser, Ion and Electron Beams, Dalian University of Technology, Dalian, China*

Development of materials with the structure stable under radiation is still a challenging task of modern materials science. Metallic glasses due to their amorphous structure effectively absorb radiation defects formed by ions and neutrons. This type of material can be applied in fusion reactors as mirrors for optical diagnostic devices etc. At the same time metallic glasses preserve it amorphous structure during heating only up to the glass-transition temperature. That is why heating of metallic glass for example during ELM events in fission reactors can result in transformation from amorphous to crystalline state worsening material radiation resistance. Investigation of Zr based metallic glass (11 % Ti, 14 % Ni, 13 % Cu, Zr - balance) structure transformation during compression plasma flows impact was the main aim of this work.

Compression plasma flows were obtained using a gas-discharge magneto-plasma compressor of compact geometry powered with the capacitive storage of 1200 mF. Nitrogen was used as a plasma forming gas. The discharge duration amounted to ~ 100 μs. The heat flux absorbed by the surface layer (registered by calorimetric measurements) varied in the range of 3-35 J/cm^2 per pulse. Energy absorbed by the surface was varied by the change of capacitive storage initial voltage (2-3 kV), distance between sample and cathode (12-20 cm) and the pressure of the plasma forming gas during the discharge (400-1300 Pa). Structure, element and phase composition of the surface layer were characterized by the X-ray diffraction analysis, scanning electron microscopy and energy-dispersive X-ray microanalysis.

The findings showed that increase of the energy absorbed by the surface layer resulted in decomposition of metallic glass amorphous structure. Critical value of energy necessary for transformation beginning was found. α-Zr, α-Ti, Cu and Ni crystalline phases were found in the surface layer after plasma impact. Besides that high-temperature polymorphic phase β-Ti and transition Zr-based ω phase were registered. The dependence of metals crystalline precipitates size and morphology on the energy absorbed by the surface layer was analyzed.

Initial sample of metallic glass and sample treated by compression plasma flows were irradiated by helium ions up to the dose of $2 \cdot 10^{17}$ cm^{-2} to investigate the radiation resistance. The mechanisms and the reasons of the observed effects are discussed.

* The work was supported by the Russian Foundation for Basic Research under grant No. 19-58-53019\19.

EVOLUTION OF THE TARGET STATE AFTER RADIATION TREATMENT

A.P. YALOVETS

South Ural State University (national research university), Chelyabinsk, Russia

Processing of structural materials by intense flows of corpuscular radiation or plasma leads to heating and even melting of the material in the near-surface region. After the end of irradiation, the material cooling phase begins, resulting in the crystallization of the melt and its subsequent deformation, due to the inhomogeneity of the temperature field and its high rate of change (10^5 - 10^7 K/s). The consequence of these processes is the formation of fields of mechanical stresses that can lead to cracking of the treated surface. This work is devoted to the description of the evolution of the state of the target material from the moment of crystallization to complete cooling.

The solution to this problem is possible within the framework of a model of an elastic-plastic medium, the implementation of which in this case is based on the solution of the equations of motion for an elastic medium and the heat equation. The relationship between the stress tensor and the strain tensor is described by Hooke's law, plastic flows are taken into account through the Mises flow condition.

The dimensions of the heated region and the melt depend on the energy flux density and processing time. At a unit power flux density of tens of MW / cm2 and an exposure duration of 1–100 μs, the thickness of the heated region is 10–100 μm, and the melt thickness h is of the order of tens of μm. As a rule, large-area beams of electrons, ions or plasma (more than 10 cm^2) are used to process structural materials, as a result of which the thickness of the area heated during irradiation is hundreds to thousands of times smaller than its radius R. Since h << R, the use of standard numerical methods for solving formulated system of equations becomes impossible.

In this paper, we describe a method for describing dynamic processes during cooling in systems with h << R. This inequality allows us to replace the equation of motion for the transverse velocity component with the equilibrium equation. The small film thickness compared to its transverse dimensions allows us to neglect the radial heat fluxes. The approximations made it possible to develop a method for solving the system formulated above and to trace the evolution of the deformation fields and stresses from the moment of melt crystallization to the complete cooling of the target.

Numerical studies of the formation of stress fields during the cooling of various materials after processing by a plasma beam with energy densities from 10 to 200 J/cm^2 were carried out. It is shown that the cooling of the material causes the formation of tensile stresses, which quickly reach the yield strength. Radial deformations on the free surface are inhomogeneous and create conditions for crack formation at a certain radius. Radial tensile stresses contribute to the growth of the crack deep into the target, which leads to the appearance of a free coaxial surface, which in some cases causes an avalanche of such damage. As a result of these processes, the target surface is divided into a number of ring fragments. Tensile stresses in ring fragments can cause them to crack into separate sectors. As a result, on the target surface, in addition to the ring structures, their individual sectors will be observed, having the form of jets of radial direction. It is this relief of the target surface that was observed in experiments [1, 2].

REFERENCES

[1] *Astashinski V M, Leyvi A Ya, Uglov V V, Cherenda N N, Yalovets A P.* // Journal of Surface Investigation: X-ray, Synchrotron and Neutron Techniques – 2014.– **8** .– P. 519

[2] *Poznyak L.M., Klimov N.S., Podkovyrov V.L., Safronov V.M., Zhitlukhin A.M., Rjvalenko D.V.* // VANT. Ser. Thermonuclear Fusion. – 2012. – V. 4.– P. 23 - 33

INFLUENCE OF THE ARCHED MAGNETIC FIELD ON THE CATHODE EROSION RATE OF THE VACUUM ARC DISCHARGE*

D.V. DUKHOPELNIKOV, D.V. KIRILLOV

Moscow State Technical University n.a. Bauman,
2-nd Baumanskaya str., 5-1, Moscow, 105005, Russia, kirillovdv@bmstu.ru, +7-499-263-60-43

Introduction. Vacuum arc discharge is used in technological units to produce different functional coatings and in the ion sources to produce high intensity pulsed ion beams. The feature of this discharge is the rapidly moving cathode spots which are formed on the cathode surface and are an intensive material source ejecting to an operating volume. This jet consists of plasma (ions and electrons), macroparticles and a small part of neutral atoms [1, 2]. The cathode mass loss rate is characterized as the erosion rate:

$$\gamma = \frac{\Delta m}{I\,t} = \frac{\Delta m_i + \Delta m_n + \Delta m_p}{I\,t}, \quad (1)$$

where Δm – cathode mass decrease over the time t at the discharge current I; $\Delta m_i, \Delta m_n, \Delta m_p$ – cathode mass decrease due to ions, neutral atoms and macroparticles respectively.

It is assumed that the erosion rate depends only on the cathode material and does not depend on the discharge current, magnetic field and other parameters. In the work [3] erosion rate reduction for silicon cathode was noted. In this paper, it was experimentally shown that the erosion rate decreases significantly with the arched magnetic field applied for different materials. This phenomenon should be taken into account in the development and operation of the vacuum arc evaporation units, where the arched magnetic field is used to control the erosion zone location and to reduce the macroparticles mass fraction.

Experiment. The work was carried out using the vacuum arc evaporator in continuous steady operation mode. The magnetic system produces the arched magnetic field of variable configuration on the cathode surface [4, 5]. The erosion rate was measured by direct cathode weighing before and after continuous operation for a number of materials (Si, Ti, Al, Cu) at various values of magnetic field in the range from 0 to 13 mT. It was shown that the decrease of the cathode erosion rate takes place for all the materials considered (Fig. 1).

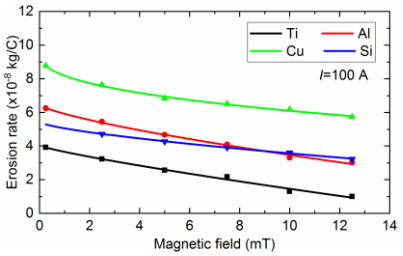

Fig.1. Dependence of the erosion rate on the magnetic field value for different materials.

Discussion. It was shown that the cathode erosion rate decreases by 1.5-4 times depending on the cathode material when the arched magnetic field value increases from 0 to 13 mT. This reduction is maximum for titanium, which is widely used in the wear-resistant coatings technology. It was shown that this effect occurs due to a decrease of the macroparticles and the ions parts in erosion products. The determining factor in this effect is the decrease of macroparticles mass.

REFERENCES

[1] A. Anders, E.M. Oks, G.Yu. Yushkov, "Production of neutrals and their effects on the ion charge states in cathodic vacuum arc plasmas," Journal of Applied Physics, vol. 102, is. 4, No. 043303, 2007. DOI: 10.1063/1.2769789.

[2] D.T. Tuma, C.L. Chen, D.K. Davies, "Erosion products from the cathode spot region of a copper vacuum arc," Journal of Applied Physics, vol. 49, is. 7, p. 3821-3831, 1978. DOI: http://dx.doi.org/10.1063/1.325386.

[3] D.V. Dukhopel'nikov, D.V. Kirillov, "Cathodic Arc Evaporation of Polycrystalline Silicon," Russian Physics Journal, vol. 62, is. 11, p. 2033-2040, 2020. DOI: 10.1007/s11182-020-01941-8.

[4] D.V. Dukhopelnikov, D.V. Kirillov, V.S. Bulychev, "Characteristics of silicon microdroplets in coatings deposited by vacuum arc evaporation", Polymer Science. Series D, vol. 9, is. 2, p. 238-242, 2016. DOI: 10.1134/S1995421216020040.

[5] D.V. Dukhopel'nikov, A.V. Zhukov, D.V. Kirillov, M.K. Marakhtanov, "Structure and features of the motion of a cathode spot on a continuous titanium cathode", Measurement Techniques, vol. 48, is. 10, p. 995-999, 2005. DOI: 10.1007/s11018-006-0010-2.

* This work is the extension of Russian Science Foundation under grant No 12-08-31098 мол_а

OXIDATION RESISTANCE OF TITANIUM AND TUNGSTEN TREATED WITH COMPRESSION PLASMA FLOWS

V.I. SHYMANSKI[1], N.N. CHERENDA[1], V.V UGLOV[1], V.M. ASTASHYNSKI[2], A.M. KUZMITSKI[2]

[1]Belarusian State University, Minsk, Belarus
[2]A.V. Luikov Heat and Mass transfer Institute of National Academy of Science of Belarus, Minsk, Belarus

Improving of oxidation resistance of different materials is important problem that should be solved for their practical application. Indeed, a lot of metals and alloys are exploiting in the conditions of opened air and elevated temperatures. It results in oxygen atoms migration inside the surface layer of the materials, solid solution and oxide phases growth that, in turn, provides the degradation of mechanical and other physical properties. Foe instance, titanium and titanium-based alloys are widely used in turbine plates production. The turbines work at the temperature about 600 ^{o}C. Increase in the working temperature can rise the effectiveness of the turbine but it is restrained by the titanium oxides growth. In the present work it was suggested to increase the oxidation resistance of titanium by means of its surface layer alloying with different metals by compression plasma flows impact.

A lot of previous experiments were carried out with metals on compression plasma flows impact. The results showed the modification of the microstructure and phase composition which improve the mechanical properties.

In the experiments the samples of titanium and tungsten as rectangular were used. The samples were treated with compression plasma flows in the residual nitrogen atmosphere with different absorbed energy density. After the treatment the samples were subjected to air annealing at the temperature 600 ^{o}C at different times. The analysis of the structure and phase composition the annealed samples shown the formation of rutile TiO_2 phase after an hour temperature influence. But, the preliminary deposition of the chromium or molybdenum coating on the titanium surface before the plasma treatment results in formation of solid solutions based on the high-temperature titanium bcc phase. The internal mechanical stresses in the solid solution slowing down the migration of the oxygen atoms and prevent the surface layer from the intensive oxidation.

A set of tungsten samples were also treated with compression plasma flows and annealed at the temperature 500 ^{o}C. The annealing in the air atmosphere results in formation the tungsten oxide WO_3 on the surface. But, the formation the tungsten-based alloys like W-Ti or W-Nb alloys provides the formation of the alloying metals-based oxide phases and decrease in the volume fraction of the tungsten oxide.

THERMOPHYSICAL MODEL OF ELECTRON BEAM BORIDING OF TITANIUM ALLOY VT-1*

A.E. LAPINA, N.N. SMIRNYAGINA

Institute of Physical Materials Science SB RAS, Ulan-Ude, Russia

In work, the stages of construction of thermophysical model of electron-beam boriding of titanium alloy VT-1 are considered.

The use of electron beam as a heating source makes it possible to significantly expand the possibility of modifying the surface of alloys and metals.

When analyzing the thermal effects of highly concentrated energy sources, various assumptions are often introduced that greatly simplify the form of the thermal conductivity equation. As a result, the efficiency of accounting for and describing characteristics inherent in the action of highly concentrated energy sources, such as high process rates, phase transformations, and structural non-uniformity, is reduced [1]. Samples of the shape shown in Figure 1 were selected to simulate electron beam processing. The electron beam is first focused on the surface of the sample, and then converted into a raster with the help of an electron beam control unit and scanned across its diameter.

To define the physical model of the electron-beam processing process is taken: the electron beam exposure power - *P [W]*; part processing speed; processing time; data on the dimensions of the part - *15 x 7 mm* (diameter and height of the sample); the penetration depth of electrons into the sample is $h = 2.1 \cdot 10^{-12} \cdot U^2 / \rho$; the depth of maximum energy release is $h = 0.75 \cdot S$ [2]. Surface processing by electron beam is performed in scanning mode. For frequencies greater than 50 Hz, the effective heat source is distributed and has a constant density q_0.

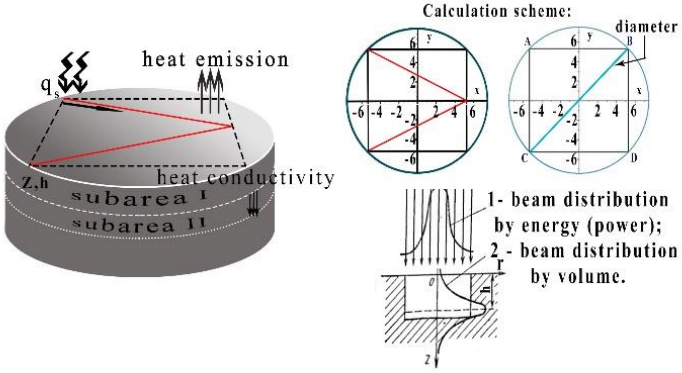

Fig.1. Scheme of energy input to the sample surface.

Thermophysical processes were modeled using the COMSOL Multiphysics software package. Issues of interaction of electron beam with sample (thermal processes in processing zone), peculiarities of interaction of electron beam with titanium alloy of VT-1 are considered, the analysis of thermal processes was carried out.

The distribution of temperature and its rate of change from the action of the electron beam has been investigated [3]. On the basis of numerical calculations of temperature fields, it is revealed that temperature-time conditions of heating and cooling of titanium alloy VT-1 determine character of structural transformations.

REFERENCES

[1] A.E. Lapina, N.N. Smirnyagin, D.E. Dasheev. "Modeling of thermal processes during processing titanium alloy VT-1 by an electron beam in a vacuum," Vestnik of the Buryat State University. Chemistry. Physics., vol. 2–3, p. 55-63, 2018.

[2] Rykalin N.N., Uglov A.A., Zuev I.V. Fundamentals of electron beam processing of materials. M .: Engineering, 1978.-239p.

[3] A.E. Lapina, N.N. Smirnyagin, D.E. Dasheev. "Heat and mass transfer during the formation of boride and carbide layers on steel and titanium alloy VT-1 under the influence of powerful electron beams," Materials of the International conference "Radiatoin Solid State Physics"., p. 50-57, 2017.

* The work was carried out within the framework of the project of fundamental research programs of SB RAS No. 0336-2019-0009.

* The work was supported by RFBR (project No. 15-48-04217, r-Siberia-a).

PLASMA ANISOTROPY AROUND AN INFINITE CHAIN OF DUST PARTICLES*

M.V. SALNIKOV[1], G.I. SUKHININ[1]

[1] Institute of Thermophysics SB RAS, Ave. Lavrentyev, 1, Novosibirsk, 630090, Russia

It is well known that dust particles in etching or deposition plasmas negatively affect the production efficiency, are a cause of sufficient yield loss of a final product and lead to an increase in the time required to maintain equipment in working condition [1]. Dust particles, also referred to as dust grains, being injected into the gas discharge plasma, are charged to large values of negative charge Zd = 10^3 -10^5e. Dust particles and their influence on the material processing - the subject of study of a separate research field. These studies have shown that negatively charged dust particles interact with each other to form ordered structures called dust crystals [2]. The simplest dust grain structure is the dust chain.

In this paper, using a numerical method demonstrated in [3], a self-consistent potential is iteratively calculated using the following formula:

$$U(r,\theta) = -\frac{\tilde{Q}}{r} - \sum_k \frac{\tilde{Q}}{r_{k,2}} - \sum_k \frac{\tilde{Q}}{r_{k,1}} + \int \frac{n(r',\theta')d^3r}{|r-r'|} + \sum_k \int \frac{n(r',\theta')d^3r}{|r_{k,1}-r'|} + \sum_k \int \frac{n(r',\theta')d^3r}{|r_{k,2}-r'|} - \tilde{E}r\cos\theta, \quad (1)$$

$$r_{k,1}{}^2 = (D^2 + r^2 - 2kDz), \quad r_{k,2}{}^2 = (D^2 + r^2 + 2kDz), \quad (2)$$

where D is the interparticle distance, $\tilde{Q}$ is the dimensionless dust particle charge, $\tilde{E}$ is the dimensionless external electrostatic field strength.

As a result of an iterative calculation of formula (1), the dependences of the self-consistent potential on the strength of the external electrostatic field are obtained.

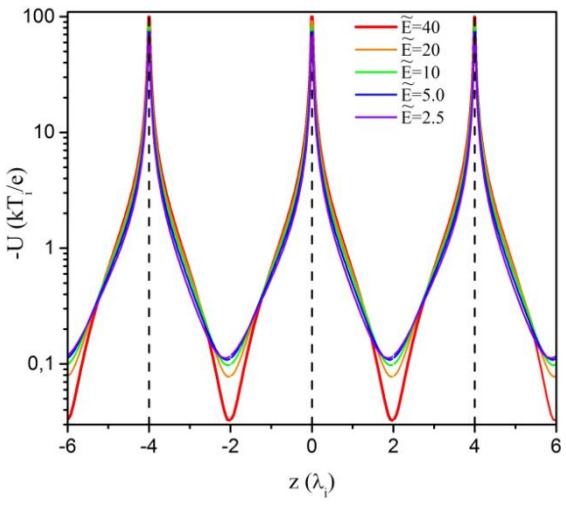

Fig. 1. Potential spatial distribution in the plane of an endless dust particles chain.

The data obtained demonstrate that the anisotropy that manifests itself in the system when an external field arises decreases with increase of the external electrostatic field strength. Also, with increasing strength of the external electrostatic field, the local maximum potential between dust particles grows.

REFERENCES

[1] G S Selwyn, “Optical characterization of particle traps”, Plasma Sources Science and Technology, vol. 3, no. 3, pp. 340-347, January 1994

[2] A. Melzer, T. Trottenberg, and A. Piel, “Experimental determination of the charge on dust particles forming Coulomb lattices”, Phys. Lett. A vol 191, pp. 301-308, 1994.

[3] M V Salnikov, A V Fedoseevand and G I Sukhinin, “Plasma potential around a single-dimensional dust particle chain placed in an external electric field”, Journal of Physics: Conference Series, vol. 1393, pp. 012-022, 2019.

* The work was supported by the by RFBR (Grant No. 17-08-00731).

VELOCITY DISTRIBUTION AROUND AN ISOLATED DUST PARTICLE*

M.V. SALNIKOV[1], G.I. SUKHININ[1]

[1] Institute of Thermophysics SB RAS, Ave. Lavrentyev, 1, Novosibirsk, 630090, Russia

Dust particles could present a significant source of product yield loss in etching or deposition plasmas [1]. Due to this coagulation of dust grains in a gas discharge plasma is generally referred to as a negative effect. In a plasma dust particles are negatively charged Zd = 10^3 -10^5e. Studies of isolated dust particles have shown that in external plasma flow behind a dust particle appears oscillating structure called wake [2]. However these studies, more often than not, does not take into consideration velocity distribution of ions around said dust particle.

In this paper, using a numerical method demonstrated in [3], a self-consistent potential is iteratively calculated using Legendre polynomial expansion by the following formula:

$$U(r,\theta) = -\frac{\tilde{Q}}{r} + \sum_k \frac{1}{2k+1}\left[\frac{1}{r^{k+1}}\int_{r_0}^{r} n_k(r)x^{k+2}dx + r^k\int_{r}^{\infty} n_k(r)x^{1-k}dx\right]P_k(\cos\theta) - \tilde{E}r\cos\theta. \quad (1)$$

$$n_k(r) = \frac{2k+1}{2}\int_0^{\pi} n(r,\theta)P_k(\cos\theta)\sin\theta d\theta, \quad (2)$$

where $n(r,\theta)$ is the spatial space charge distribution, $\tilde{Q}$ is the dimensionless dust particle charge, $\tilde{E}$ is the dimensionless external electrostatic field strength.

Ion trajectories were calculated by Newton equations in selfconsistent potential (1) and the spatial distributions of radial speed u_r were measured. Distribution u_r (with the drift velocity u_d subtracted) calculated for the $\tilde{E}$ =10 and spherical dust particle radius r_0 = 1 μm is presented in figure 1:

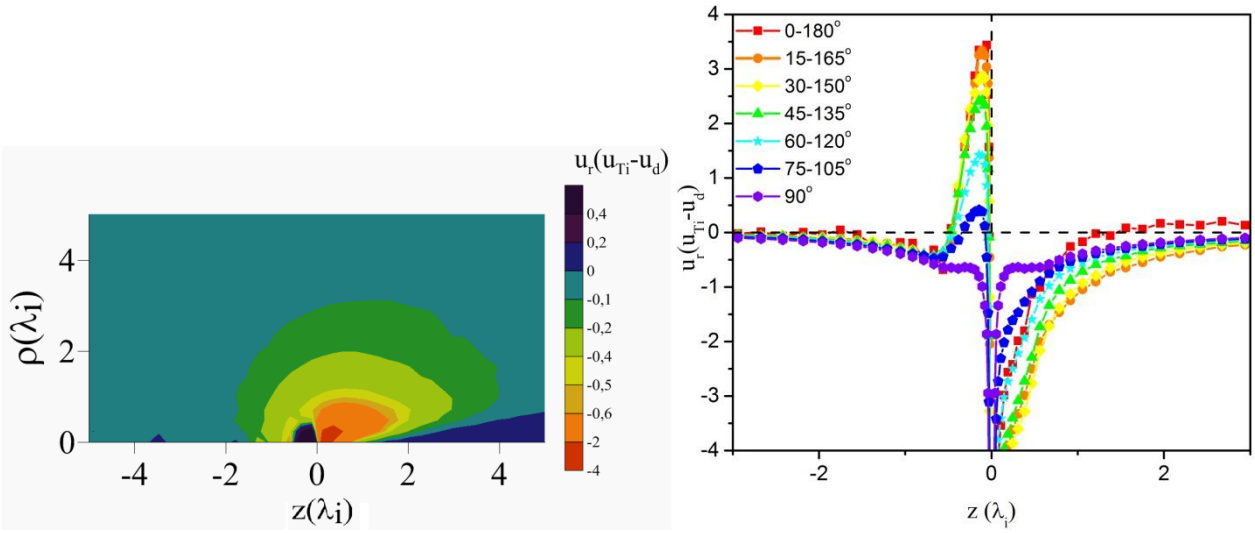

Fig. 1. Radial velosity spatial disrtibition presented as two-dimanetional contour-plot (left) and the selection one-dimentional radail funtcions for the wide array of angles (right).

REFERENCES

[1] G S Selwyn, “Optical characterization of particle traps”, Plasma Sources Science and Technology, vol. 3, no. 3, pp. 340-347, January 1994

[2] P Ludwig, W J Miloch, H Kählert and M Bonitz “On the wake structure in streaming complex plasmas”, New Journal of Physics, vol. 14, no. 5, pp. 053016, May 2012

[3] G I Sukhinin, M V Salnikov, A V Fedoseev and A Rostom, “Plasma Polarization and Wake Formation Behind a Dust Particle in an External Electric Field”, IEEE Transactions on Plasma Science, vol. 46, no. 4, pp. 749-754, April 2018.

* The work was supported by the by RFBR (Grant No. 17-08-00731).

SELF-SUSTAINED MAGNETRON SPUTTERING OF EVAPORATING METAL TARGETS AND ITS INFLUENCE ON THE PROPERTIES OF DEPOSITED COATINGS

G. A. BLEYKHER, V. P. KRIVOBOKOV, D. V. SIDELEV, V. A. GRUDININ, A.S. SHABUNIN, R. V. POPOV

Tomsk Polytechnic University, Tomsk, Russia

The mechanisms and regularities of the discharge functioning during the operation of a magnetron sputtering system (MSS) under low pressure in a vacuum chamber (less than 0.1 Pa) in the self-sustained mode are studied. It was found that the MSS is able to work without the supply of working gas if, in addition to the sputtering, evaporation or sublimation of the target is created, due to which the concentration of atoms near the target surface becomes sufficient to maintain the discharge.On the example of an MSS with molten copper and aluminum targets placed in crucibles, as well as with a hot solid chrome target, the minimum required power values are determined, starting from which it is possible to operate the discharge without letting in the working gas. The power threshold value depends on the target substance, the degree of blackness of the crucible surface (for liquid-phase targets), and the type of power source (medium-frequency, high-current pulsed, etc.). For example, in the case of a copper target in a molybdenum crucible and a medium-frequency power supply, the minimum power density Q_{min} required for stable self-sputtering without the supply of working gas is 19.4 W/cm^2, and in the case of a high-current pulsed power supply is 33 W/cm^2. For an aluminum target in a ceramic crucible and with a medium-frequency power supply, Q_{min} is 50.4 W/cm^2, and for a chrome target is 35.4 W/cm^2. It turned out that thermionic emission is not a necessary factor in maintaining the discharge of a magnetron operating on vapors of the target substance.

It was found that the erosion yield of metal targets during evaporation or sublimation reach several tens of atoms per ion, which is an order of magnitude higher than the sputtering yield. As a result, deposition of coatings under self-sputtering conditions occurs without reducing the deposition rate compared to the cases of working gas participation. In experiments and calculations, it was determined that the deposition rates of copper, aluminum and chrome coatings both in the argon atmosphere and in the mode of full self-sputtering are approximately an order of magnitude higher than the deposition rates that occur during conventional sputtering of cooled targets with similar values of MSS power.

The evolution of the intensity of spectral lines of optical plasma radiation during the transition of a magnetron with an evaporating copper target to the self-sustained mode was studied. The correlation of the intensity of spectral lines of copper atoms and ions with the evolution of evaporation was found. As the evaporation rate increases, argon atoms are displaced from the combustion region of the discharge in front of the target.

The densities of deposited particles and energy fluxes under conditions of intensive target evaporation were studied. It is found that in the considered power range of the MSS due to evaporation (or sublimation in the case of chromium), the flux density of the deposited particles increases by about an order of magnitude. The main source of energy entering the substrate is thermal radiation from the target. The value of the total energy flux is approximately the same both when the target is sputtered in the argon atmosphere and in the self-sustained mode. The possibility of controlling the kinetic component of energy fluxes to the substrate by applying a negative bias potential to it is revealed. The density of the ionic current on the substrate is approximately the same both in the case of deposition with argon injection at a pressure above 0.1 Pa, and in the mode of full self-sputtering at a pressure of 0.01 Pa or lower.

The structural and functional characteristics of coatings were analyzed depending on the type of power source and the atmosphere in the chamber (sputtering with working gas at a pressure of 0.18-0.4 Pa and in full self-sustained mode at a pressure of 0.01 Pa or lower). It was found that under conditions of intensive evaporation (or sublimation), there is no noticeable effect of the self-sputtering factor and the type of power supply on the crystal and growth structure of the studied films. However, there is evidence of improved electrical conductivity for copper coatings, hardness and corrosion resistance of chrome coatings, as well as the reflectivity of aluminum films deposited under conditions of complete self-sputtering at a chamber pressure of 0.01 Pa or lower compared to deposition in an argon atmosphere.

The study was supported by the Russian Foundation for Basic Research (Project No.18-08-00454).

SYNTHESIS CARBON NANOMODIFICATORS IN ARC DISCHARGE PLASMA AND MODIFICATION BUILDING MATERIALS

N.N. SMIRNYAGINA[1], B.O. TSYRENOV[1], L.A. URKHANOVA[2]

[1]Institute of Physical Material Science, 6, Sakhyanovoy st., Ulan-Ude Russia, 670047, E-mail: bulatzsk@gmail.com
[2]East Siberia State University of Technology and Management, 40V, Klyuchevskaya st., Ulan-Ude, Russia,

The report describes the synthesis carbon nanomodifiers in arc discharge plasma at atmospheric pressure and the modification of building materials with carbon nanomodifiers. Carbon nanomodifier (CNM) was obtained in plasma chemical reactor at atmospheric pressure. Helium gas was used as a buffer gas. Carbon nanomodifier contains fullerenes C_{60} and C_{70}, carbon nanotubes. The yield of higher C_{70} fullerenes varies with pressure and compound of composite electrodes. The use of composite electrodes with additives makes it possible to obtain a carbon nanomodifier of various compositions.

The effect of using a carbon nanomodifier depends on the type and composition of the additive when modifying building materials. Carbon nanomodifier changes the properties of mixing water. Modified water affects the hydration process of Portland cement. The degree of cement hydration can be determined in various ways by measuring: the amount of Ca(OH)2 in cement paste; heat during hydration; specific gravity of cement paste; amount of chemically bound water; the amount of unhydrated cement (using X-ray diffraction analysis), as well as indirectly by the strength of the cement stone.[4]

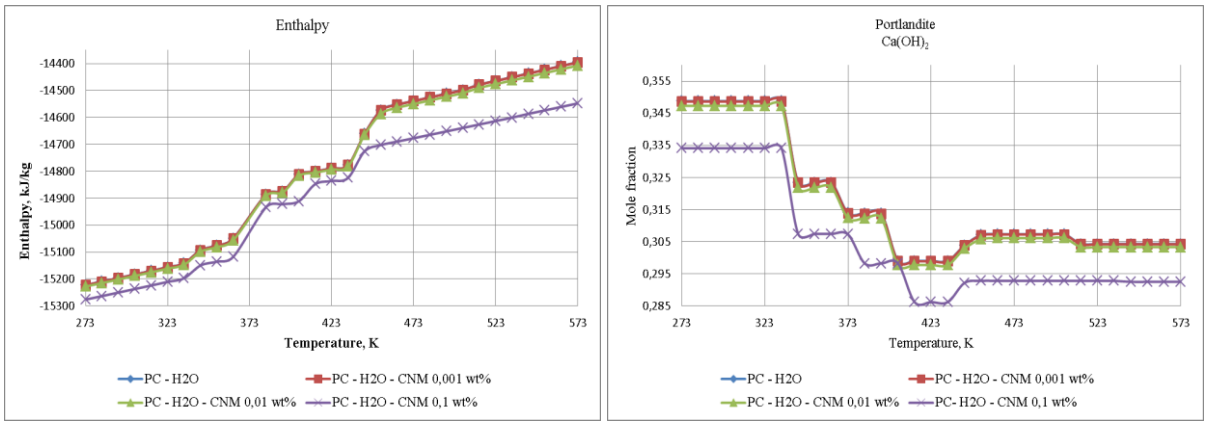

Fig.1. Change enthalpy and Portlandite content in PC –H2O – CNM system.

Thermodynamic modeling of Portland cement hydration was performed in the TERRA program [2]. Thermodynamic calculations made it possible to evaluate the contribution of CNM to the process of Portland cement hydration and the effect of CNM on exothermic reactions in Portland cement - water - CNM system. Experimental study of rheological characteristics was carried out in the work. [1,2]. The change in $Ca(OH)_2$ yield indicates that CNM acts as retarder in the setting of cement paste. CNM increases the induction period with the subsequent set of strength. After the initial hardening period (7 days), the strength of the modified cement stone is formed at an increasing rate and by 28 days of hardening exceeds the strength of the control sample by 35%. [1,2]

REFERENCES

[1] A.P. Semenov, N.N. Smirnyagina, L.A. Urkhanova et al., "Reception carbon nanomodifiers in arc discharge plasma and their application for modifying of building materials" IOP Conference Series: Materials Science and Engineering vol. 168 (1) article number 012059, 2017

[2] Smirnyagina N N, Semenov A P, Tsyrenov B O, Dasheev D E, Khaltarov Z M "Plasma-chemical synthesis of carbon nanotubes and fullerenes to create frost-resistant composite building materials". International Congress on Energy Fluxes and Radiation Effects vol.830 article number 012123, 2017

[3] B.G. Trusov "Program system TERRA for simulation phase and thermal chemical equilibrium". Proc. XIV Intern. Symp. on Chemical Thermodynamics vol. 1, pp. 483-484

[4] Pukharenko Yu V, Ryzhov D I and Staroverov V D 2017 Peculiar properties of structural formation of Cement Composites in the Presence of Fueleroid Type Carbon Nanoparticles Proc. of Moscow State University of Civil Engineering (Moscow: Vestnik MGSU) vol.12, issue 7 pp. 718-723

TEMPERATURE GRADIENTS IN THE TARGETS DURING HIGH-INTENSITY IMPLANTATION IN FORCED COOLING

A.I. RYABCHIKOV, D.O. SIVIN, A.I. IVANOVA, O.S. KORNEVA, G.A. BLEYKHER

National Research Tomsk Polytechnic University, Lenin Avenue 30, Tomsk, 634050, Russia
E-mail: bai@tpu.ru, phone (3822) 70-17-77 ext. 2362

High-intensity ion implantation is a new tool for deep modification of the elemental composition and microstructure of metallic materials. Low-energy ion implantation at ion current densities of tens and hundreds of mA/cm^2 is accompanied by a significant increase in the temperature of the irradiated target. The negative effects of increasing temperature, such as grain growth of the target crystal structure, can be eliminated by post-implantation exposure to the ion-doped layer, for example, a pulsed high-current electron beam. To implement this approach successfully, it is important to determine the parameters and modes of ion irradiation including heat removal conditions by using a massive target holder or forced cooling of the non-irradiated side of the target in which the temperature value in the ion-doped layer will correspond to the conditions of radiation-stimulated diffusion of the implanted element and the temperature in matrix material will not lead to significant grain growth.

The work is devoted to the study of the dynamics of the temperature gradient formation over the depth and on the surface of metal targets during the implantation process of high-intensity ion beams.

The results of numerical simulation of the dynamic and gradient characteristics of temperature fields in metal targets with different thermal conductivity during high-intensity ion implantation are presented. The gradients of temperature fields under the influence of repetitively pulsed ion beams with a current density of 10 – 500 mA/cm^2 at ion energies of 0.2 – 2 keV were studied. The laws of temperature field variation over the target depth are described depending on the target material, its geometric dimensions and heat removal conditions including during forced cooling to the cryogenic temperatures of the back side of the sample. Variants of high-intensity low-energy ion implantation providing optimal temperature field gradients in various materials are discussed.

THERMAL STABILIZATION OF THE LAYERED SYSTEM FE_3ZR-α-FE

A.K. ZHUBAEV, G.Zh. OMARPATSHA, A.Sh. AMANTAYEVA

Aktobe Regional State University, Aktobe, Kazakhstan

A feature of the Fe–Zr binary system [1] is the low mutual solubility of the components and the presence of intermetallic compounds, which is of interest from the standpoint of the possibility of obtaining a thermally stable inhomogeneous layered system.

The study of phase-structure transformations in alpha-Iron with a Zirconium coating during thermal annealing at 900°C was performed.

The substrates for the studies were prepared from a bar of armco iron (99.8% Fe) by rolling on a roll to a thickness of ≈5 μm and subsequent homogenizing annealing at a temperature of 850°C for 2 hours. The deposition of Zirconium on Iron foil substrates was carried out by method of ion-plasma sputtering. Sequential isothermal annealing of two-layer Zr(2 μm)-Fe(5 μm) systems was carried out at a temperature of 900°C up to 20 hours. Samples were studied by Mossbauer spectroscopy (MS) method on ^{57}Fe nuclei were performed. The fitting of the experimental spectra was carried out using the DISTRI program [2] by reconstructing the distribution functions of the hyperfine parameters of the partial spectra.

After annealing at 900°C in the Mössbauer spectra against the background of the lines from α-Fe, a set of additional sextets of the ferromagnetic phase with significantly lower (Hn≈206 kOe) hyperfine fields appears. The dependences of the relative intensities of the partial spectra of α-Fe and intermetallic compounds were constructed (Figure 1). The obtained dependences can be interpreted as dependences of the relative phase content in atomic units of Iron.

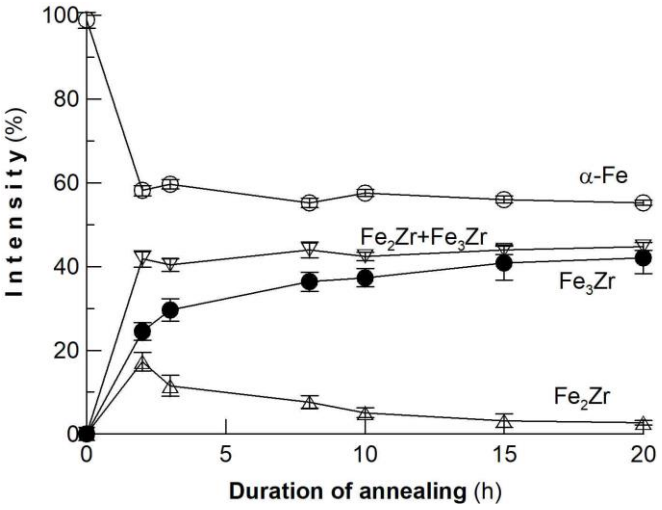

Fig.1. Model spectra of various phases in the system Fe-Zr

The sequence of phase transformations in layered Fe-Zr systems subjected to isothermal annealing is established. The relative content of phases formed in the sample volume at each of the annealing stages was obtained. It is shown that the direction of phase transformations is determined by a change in the local concentration of components in the sample in the process of their mutual diffusion. The possibility of obtaining thermal stabilization of the intermetallic phase Fe3Zr on an armco iron substrate is shown.

REFERENCES

[1] N.P. Lyakishev, Diagrams of the state of double metal systems. Moscow, 1997. (in Russian)
[2] V.S. Rusakov, Mossbauer Spectroscopy of Locally Nonhomogenous Systems, Almaty, INP NNC RK, 2000. (in Russian)

INVESTIGATION OF REGULARITIES OF HIGH-INTENSITY ION IMPLANTATION IN COMBINATION WITH SUBSEQUENT EXPOSURE TO THE SURFACE OF A HIGH- CURRENT ELECTRON BEAM

A.I. RYABCHIKOV[1], S.V. DEKTYAREV[1], O.S. KORNEVA[1], I.V. LOPATIN[2], D.O. SIVIN[1]

[1]National Research Tomsk Polytechnic University, Lenin Avenue 30, Tomsk, 634050, Russia
[2]Institute of High Current Electronics,Siberian Branch, Russian Academy of Sciences, 2/3 Akademichesky Avenue, Tomsk 634055, Russia

Low energy, high intensity ion implantation method opens up unique opportunities for ion-doping of metals and alloys at depths of tens and hundreds of micrometers. Ion implantation at ion current densities of tens and hundreds of mA/cm^2 is carried out at elevated temperatures of the surface layers of the irradiated target. High temperatures can lead to an increase in the grain size of crystalline materials and, as a result, to a degradation of material properties. One of the possible solutions to this problem seems to be a combination of high-intensity implantation of ions with subsequent exposure to the surface of a high-current electron beam.

The paper presents the results of studies of the regularities of changes in the elemental composition and microstructure of titanium alloy during high-intensity implantation of nitrogen, aluminum ions of low and ultra-low energy. The influence of the target temperature regimes on the depth distribution of the implanted dopant and the structure of doped and matrix material is studied. The influence of subsequent modification of the ion-doped layer by the action on the surface of the pulsed high-current electron beams of microsecond duration is studied. The work presents the results of the studying the regularities of changes in the depth distribution of alloying elements, microstructure and phase composition of the modified and matrix layers by optical metallography, x-ray spectral and x-ray structural analysis.

DEPENDENCE OF THE THERMAL RESPONSE IN THIN METAL FILMS ON THE VARIATION OF PARAMETERS OF HIGH-SPEED EXTERNAL INFLUENCE

G.A. VERSHININ, A.A. KULIKOV

Dostoevsky Omsk State University, Omsk, Russia,

The solution of the one - dimensional hyperbolic heat conduction equation, when a sample of finite thickness is affected by a short pulsed laser beam, is presented in work [1]. The temperature gradient was assumed to be related to the heat flow by the Maxwell-Cattaneo equation. The thermophysical characteristics of the medium were assumed to be constant. The heat source was selected in the form

$$Q(x,t) = (Q_0 / (\pi^{1/2} t_p \delta)) \exp(-x/\delta - (t/t_p)^2),$$

where Q_0 is the total energy of the heat source, t_p is the time of action of the heat source, and δ is the depth of heat penetration. In this work we study the nature of the thermal response of the medium at changing of the source parameters t_p, δ and L film thickness.

The analysis of the model temperature fields showed that a sample of smaller thickness reaches full equilibrium faster. Such a behavior may be due to the fact, that the reflection of the heat wave from the sample walls reduces its energy.

The simulation of heat transfer depending on the time of action of the heat source showed that at times t_p, less than the relaxation time of the heat flow τ, the amount of heat energy transferred to the sample per unit of time is so large, that the thermal disturbances caused by it do not have time to spread evenly across the sample. Consequently, a heat wave occurs in the sample. At times comparable to (or greater than) the relaxation time of the heat flow, a smaller amount of thermal energy penetrates the sample per unit of time, so thermal disturbances propagate in the sample without accumulating at its irradiated boundary. As the characteristic time t_p increases, the relaxation time of the system to its equilibrium temperature decreases.

At values of the parameter δ of the order of 10% of the total thickness of the sample, heat transfer occurs in waves, within the framework of a locally non-equilibrium approximation: thermal disturbances occur in a limited area, thereby forming a peak of the heat wave. The greater the absorption depth δ, the faster the thermal energy penetrates into the film, respectively, without forming significant thermal disturbances at the irradiated border of the sample. For example, when the penetration depth is equal to half the thickness of the film, heat transfer occurs by a diffusion mechanism. The relaxation time of the temperature in the sample decreases with the growth of the parameter δ.

REFERENCES

[1] G. A. Vershinin, “The wave mechanism of heat transfer in finite samples irradiated by short pulse lasers”, Izv. Vyssh. Uchebn. Zaved. Fiz., vol. 62, no. 8/2, pp. 77–81, August 2018.

DEPENDENCE OF THE THERMAL RESPONSE OF THIN METAL FILMS ON THE PARAMETERS OF HIGH - SPEED EXTERNAL INFLUENCE*

G.A. VERSHININ, A.A. KULIKOV

Dostoevsky Omsk State University, Omsk, Russia,

The solution of the one - dimensional hyperbolic heat conduction equation, when a sample of finite thickness is affected by a short pulsed laser beam, is presented in work [1]. The temperature gradient was assumed to be related to the heat flow by the Maxwell-Cattaneo equation. The thermophysical characteristics of the medium were assumed to be constant. The heat source was selected in the form

$$Q(x,t) = (Q_0 / (\pi^{1/2} t_p \delta)) \exp(-x/\delta - (t/t_p)^2),$$

where Q_0 is the total energy of the heat source, t_p is the time of action of the heat source, and δ is the depth of heat penetration. In this work we study the nature of the thermal response of the medium at changing of the source parameters t_p, δ and L film thickness.

The analysis of the model temperature fields showed that a sample of smaller thickness reaches full equilibrium faster. Such a behavior may be due to the fact, that the reflection of the heat wave from the sample walls reduces its energy.

The simulation of heat transfer depending on the time of action of the heat source showed that at times t_p, less than the relaxation time of the heat flow τ, the amount of heat energy transferred to the sample per unit of time is so large, that the thermal disturbances caused by it do not have time to spread evenly across the sample. Consequently, a heat wave occurs in the sample. At times comparable to (or greater than) the relaxation time of the heat flow, a smaller amount of thermal energy penetrates the sample per unit of time, so thermal disturbances propagate in the sample without accumulating at its irradiated boundary. As the characteristic time t_p increases, the relaxation time of the system to its equilibrium temperature decreases.

At values of the parameter δ of the order of 10% of the total thickness of the sample, heat transfer occurs in waves, within the framework of a locally non-equilibrium approximation: thermal disturbances occur in a limited area, thereby forming a peak of the heat wave. The greater the absorption depth δ, the faster the thermal energy penetrates into the film, respectively, without forming significant thermal disturbances at the irradiated border of the sample. For example, when the penetration depth is equal to half the thickness of the film, heat transfer occurs by a diffusion mechanism. The relaxation time of the temperature in the sample decreases with the growth of the parameter δ.

REFERENCES

[1] G. A. Vershinin, “The wave mechanism of heat transfer in finite samples irradiated by short pulse lasers”, Izv. Vyssh. Uchebn. Zaved. Fiz., vol. 62, no. 8/2, pp. 77–81, August 2018.

* The presented work is a continuation of the Russian Science Foundation project No. 15-48-04410

MAGNETRON DISCHARGE ON THE LIQUID-METAI TARGET

S.N. YANIN, D.V. KORJENKO

Tomsk polytechnic university, Tomsk, Russia

In our opinion, one of the most perspective technologies of the coating production is the magnetron sputtering from a liquid phase target. It allows to combine advantages of two different technologies as thin film deposition methods as vacuum evaporation and ion sputtering. The films, created by means of the first way are featured by high deposition rate and purity, but have poor adhesive properties. The magnetron sputtering process is more convenient, allows creating of chemical compounds and ensures the more small fractionating during deposition from the multicomponent target. This method can allow enhancing efficiency process of the sputtering and improving of the thin films properties.

It is known that for DC magnetron sputtering system MSS) the sufficient part of input power (up to 80%) is transformed to heat in the target, which should be cooled. This makes realization of sputtering process on liquid phase target not complicated. It is enough to put the target material into the hard-melting and heat-insulated crucible. In this case, the ion bombardment of the target surface raises its temperature until it melts. The sputtering efficiency of the liquid surface in comparison with solid is greater, because the binding energy of atoms located on the surface is smaller. the melt temperature approaches the boiling point. So the plasma energy that absorbed by target and lost through the cooling system can be used for intensification of evaporation process.

At sufficient energy density there is opportunity to transform the magnetron discharge in a regime when evaporated atoms of target are used as a working gas for sputtering process. That allows decreasing the film contamination by residual gases.

For investigation of this process we had created the magnetron system [1]. The drawing is presented in Fig. 1. Target (1) is put into the hard-melting crucible (2), which is heat-insulated from magnetron body by means of ceramic elements (3) and is encircled by pole pieces of central (4) and external (5) magnetic circuit. Magnetic system (6) includes permanent magnets, cooled by flowing water. The ring (7) is made of nonmagnetic material.

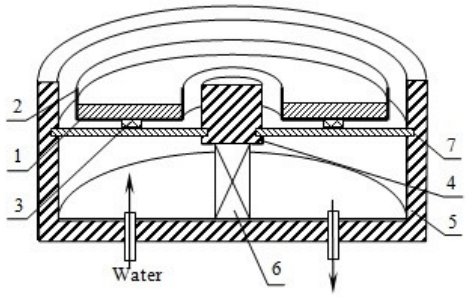

Fig.1. The construction of magnetron diode: 1 – target material; 2 –crucible; 3 – ceramic units; 4 –central magnetic circuit; 5 – magnetron body; 6 – permanent magnets; 7 – nonmagnetic ring

The results of our research confirm the high effectivity of the magnetron sputtering of metal from a liquid phase for thin film technologies. In particular, the significant increasing of deposition rate in comparison with solid target sputtering is observed. There is ability to exclude the impurity atoms of working gas from the deposited film structure. It is shown that sputtering target atoms after ionization in discharge area have substantial contribution in a plasma formation process.

REFERENCES

[1] V.P. Krivobokov, S.N. Yanin, “Influence of Sputter Atoms on Magnetron Discharge”, in: Proc. 9th Int. Conf. on Modification of Materialswith Particle Beams and Plasma Flows, 2008, pp. 23–26.

MAGNESIUM MODIFICATION UNDER HIGH POWER ION BEAM TREATMENT

T.V.PANOVA,,V.S. KOVIVCHAK

Omsk State University, Omsk, Russia

The influence of a high power ion beam (HPIB) on metals and alloys leads to a significant change in the morphology of the irradiated surface, including the formation of craters of various shapes and wave relief. The formation of such a relief may be associated with the generation of surface waves in the melt due to the action of a local pressure impulse caused by the evaporation of the irradiated material.The study of the formation of surface relief is easier to perform on materials that have low melting points and evaporate well when heated. Such material are magnesium, which has a melting point of 923K and a saturated vapor pressure at a temperature of 860.6 K - 10^2 Pa, and at a temperature of 1142 K it is already 10^4 Pa. Magnesium is a good structural and biocompatible material. The creation of a fine-grained structure on the surface of magnesium will improve its workability. A promising way to create a fine-grained structure on a magnesium surface is to irradiate with a HPIB due to intense plastic deformation. The rapid introduction of energy into metals leads to an increase in temperature (up to the boiling point) and the generation of stress fields and shock waves. This causes structural transformations and plastic deformation. The samples were treated with a proton-carbon beam of nanosecond duration (30% H^+ + 70% C^+, E ~ 200 keV, j ~ 150 A/cm^2, τ = 60 nsec) was carried out using the “Temp” accelerator. The study of surface morphology and elemental analysis was performed using a Philips SEM-515 scanning electron microscope with an EDAX. The structural phase state was estimated from X-ray diffraction patterns recorded on a DRON-3M diffractometer. The analysis of the grain structure was carried out using a Neophot-2 optical microscope. Using optical microscopy methods, it was found that upon irradiation of polycrystalline magnesium by HPIB grain sizes are halved by irradiation with a current density of 50 A/cm^2 and 3 times by irradiation with a current density of 150 A/cm^2. When magnesium is irradiated with HPIB, craters and capillary waves are formed on the magnesium surface, as well as deposited particles of evaporated magnesium. This is associated with the recoil momentum of the intensively evaporating magnesium arising from HPIB probably. A single irradiation of magnesium by HPIB with a current density of 50 A/cm^2 leads to the formation of a periodic structure in the form of a wavy relief, the spatial period of which is ~ 9 μm. With an increase of the current density above 100 A/cm^2, especially with repeated irradiation, the ridges of the wave-like structure become more localized, their height and spatial period increase, which reaches 42 μm. An increase in the number of HPIB irradiation pulses with a current density of 150 A/cm^2 from 3 to 5 slightly changes the average value of the spatial period of the wave-like relief, which reaches 46 μm. It was found that the wavy structures that form in neighboring grains of polycrystalline magnesium have a significant misorientation relative to each other, in most cases. This indicates the possible influence of the initial crystallographic orientation of the grain on the crystallization of the melt and the formation of a wavy relief. Possible mechanisms of the observed morphological and structural transformations during the modification of magnesium by a powerful ion beam are discussed.

The reported study was funded by RFBR and Government of the Omsk Region (project № 15-48-04410).

ELEMENTAL AND PHASE COMPOSITIONS OF WC-TiC-Co HARD ALLOY AFTER TREATMENT BY COMPRESSION PLASMA FLOWS

V.V. UGLOV[1], A.K. KULESHOV[1], E.A. KRUTSILINA[1], V.M. ASTASHINSKI[2], A.M. KUZMITSKI[2]

[1]*Belarussian State University, Minsk, Belarus*
[2]*A.V. Luikov Heat and Mass Transfer Institute of the NAS of Belarus*

The influence of compression plasma flows (CPF) on the surface layers of WC-TiC-Co hard alloy (T15K6) allows to modify significantly its elemental and phase compositions. That is mainly due to the presence of plasma-forming gas – nitrogen and CPF thermal action, that causes heating of the surface layers up to the melting temperatures of its individual components and higher [1]. So, according to AES data, as a result of CPF action at accelerating voltage 3.5, 4 and 4,5 kV and nitrogen pressure 3 and 10 Torr formation of thin (~0,2 μm) surface layer enriched by nitrogen. Total nitrogen content in the analyzed layer is in the range of 17-23 at.%. It was also found that surface layer of thickness approximately 0,1 μm is enriched by titanium and cobalt but is depleted in tungsten while irradiating by CPF at accelerating voltage 4,5 kV (Fig.1).

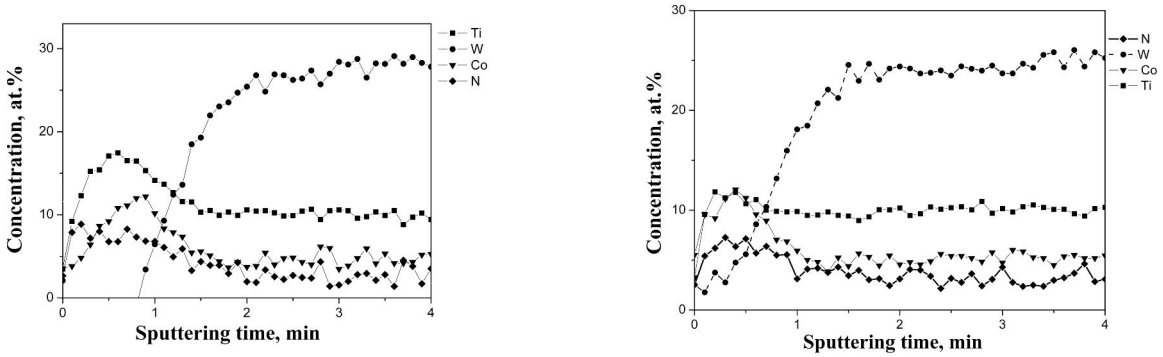

a *b*

Fig.1. Concentration profiles of T15K6 hard alloy after CPF treatment with the following regimes: 4,5 kV, 10 Torr (a) and 4,5 kV, 3 Torr (b)

The separation of elements can be associated with the establishment of diffusion fluxes of hard alloy components (titanium, tungsten, cobalt) to the surface enriched with nitrogen. So, in [2], a model of nitride phases formation as a result of sintered hard alloys nitriding was proposed. According to this model the surface layers of the hard alloy are saturated with nitrogen, i.e. a gradient of nitrogen concentration appears, while the depth of nitrogen diffusion into the bulk of the material is limited by its low solubility in the transport medium — cobalt. Next, the selective diffusion of the hard alloy components to the surface is established. So the surface maximum on the titanium concentration profile is due to its high affinity for nitrogen in comparison with tungsten one. A similar effect was also observed in [3] when studying the structure of the TiC– (Ti, W) C – WC – Ni alloy sintered in a nitrogen atmosphere, depending on its pressure. The enrichment of the surface layer with cobalt can probably be explained if we take into account the enthalpies of mixing the melts of the Co – Ti and Co – W systems. So, in the Co-Ti system this value is -33 kJ/mol, which is significantly less than that for the Co-W system ~ -1-2 kJ/mol. Thus, the mixing of Co and Ti melts is more energetically beneficial. Then, it can be assumed that cobalt diffuses to the surface of the nitrogen-enriched hard alloy after titanium. Investigations by XRD method revealed formation WN, $W_{4.6}N_4$ nitride phases, $(Ti,W)C_xN_y$ carbonitride phase and Co_2Ti intermetallic phase.

REFERENCES

[1] A.K. Kuleshov, A.S. Yakushevich, V.V. Uglov, V.M. Astashinsky, N.N. Koval, Yu.F. Ivanov, E.A. Krutsilina, “Microstructure, heat transfer, and melting of layers of a hard alloy containing Ti and W carbides under conditions of powerful pulsed processing”, University News. Powder metallurgy and functional coatings (Rus. J.), № 1, 2014, p. 55-62.

[2] C.Barbatti, J.Garcia, F.Sket, A.Kostka, A.R.Pyzalla, “Influence of nitridation on surface microstructure and properties of graded cemented carbides with Co and Ni binders”, Surf. and Coat. Technol., vol. 202, p. 5962-5975, 2008.

[3] Y. Kang, S. Kang, “The surface microstructure of TiC –(Ti,W)C – WC – Ni cermets sintered in a nitrogen atmosphere”, Materials Science and Engineering A, vol. 527, p. 7241-7246, 2010.

MULLIT, SYNTHESIZED BY DC ARC PLASMA

V.A. VLASOV[1], A.A. KLOPOTOV[1,2], K.A. BEZUKHOV[1], Yu.A.ABZAEV [1], N.N. GOLOBOKOV, [3]. O.G. VOLOKITIN[1], V.V. SHEHOVZOV [1], V.I. VERESHCHAGIN[4]

[1]Tomsky State University of Architecture and Building, 2 Solyanaya sq. Tomsk, 634003 Russian Federation
[2]National Research Tomsk State University, 36 Lenin Ave,Tomsk, 63405, Russian Federation
[3] Tomsk branch of the Institute of structural Macrokinetics SB RAS, 10/4 Akademicheskiy Prospekt, Tomsk, 634055 Russian Federation
[4]National Research Tomsk Polytechnic University, 30 Lenin Ave,Tomsk, 634050 Russian Federation

Mullite is often part of a range of inorganic materials. At the same time, mullite has a good combination of physicomechanical and chemical properties (high crystal strength, thermal stability, high melting point, corrosion resistance, radio transparency, etc.) The combination of such a set of properties serves as the basis for its use in industry. For the synthesis of mullite, it is necessary to create high temperatures. This is the main obstacle to its synthesis. The use of plasma technologies for mullite synthesis is of interest in this regard. The aim of the work was to develop approaches to the use of high plasma temperature for mullite synthesis.

Silicon-containing "marshalite" quartz powder and aluminum powder were used as starting materials. The proportional composition was selected based on a 50x50 ratio. Chemical composition of the Marshalite is presented in the table 1.

Table 1. The chemical composition of marshallite weight%

Compound	SiO_2	Al_2O_3	TiO_2	Fe_2O_3	Na_2O	K_2O
Concentration	97.5	1.54	0.03	0.01	0.14	0.10

Mechanical mixing of marshalite and aluminium powder was carried out using a liquid reagent. The reagent contains a solution of urea (caramide) 32.5% in demineralized water 67.5%. Then, the prepared solution is sintered in an oven at a temperature of 150 ° C.

Plasma action on the thus prepared briquette was carried out at the original installation with the following power supply characteristics: current in 200 A, voltage in 120 V and power W = 24kW. Nitrogen was used as plasma-forming gas.

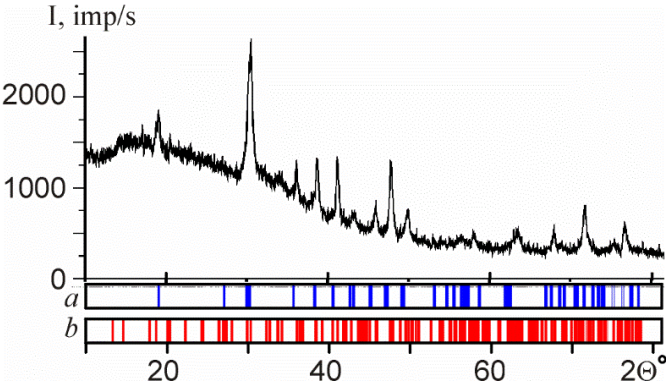

Fig. 1.Diffractogram of a sample synthesized using arc plasma (a) and a bar chart of mullite compounds with orthorhombic syngony: b $Al_{6.9}Si_{1.22}O_{4.85}$; in $Al_5SiO_{9.5}$.

According to the results of calorimetrically installed specific average of Hg plasma jet was established on the cut of the output section of the anode nozzle, which is in the range of values from 2413235739 kJ/kg, which corresponds to the medium-weight temperature T = 6100÷7300 K. The solution was melted within 3 minutes. Upon completion of melting, the solution cooled at room temperature. For further investigation, and to obtain an x-ray, the solution was mechanically crushed and ground into a powder. X-ray phase studies of the synthesized samples showed that the main phase is mullite Al_4SiO_8 with orthorhombic syngony ($D9_{2h}$=*Pbam*). Mullite refers to compounds with variable composition: from $3Al_2O_3 \cdot 2SiO_2$ to $2Al_2O_3 \cdot SiO_2$. An important structural feature of mullite is the non-integer content of oxygen atoms in the elemental cell. This is reflected in the obtained diffractograms from synthesized samples (Fig. 1). On diffractograms, in addition to crystalline phases, the halo related to the X-ray amorphous phase is fixed. This indicates that the process of phase formation of crystal structures is incomplete.

EFFECT OF THE POLYMER NATURE AND THE CATALYTIC ADDITIVE ON THE FORMATION OF CARBON NANOFIBERS ON THE SURFACE OF POLYMERS UNDER THE ACTION OF A HIGH POWER ION BEAM OF NANOSECOND DURATION*

V.S.KOVIVCHAK[1,2]

[1]*Dostoevsky Omsk State University, Omsk, Russia*
[2] *Omsk Scientific Center SB RAS, Omsk, Russia*

A promising material for the mass production of inexpensive flexible elements of mobile electronics devices is nanostructured carbon, which is formed directly on a flexible polymer basis. A high power ion beam of nanosecond duration has great advantages over pulsed laser radiation for this purpose.

In this work, the formation of carbon nanofibers on various polymers containing catalytic additives (organic and inorganic compounds of iron, cobalt, nickel) under irradiation by high power ion beam was investigated.

Irradiation was carried out at the Temp accelerator with an ion beam (30% H^+ + 70% C^+, E ~ 200 keV, j≤150 A / cm^2, τ = 60 nsec). It has been established that chlorinated polyvinyl chloride is the optimal polymer for carbon nanofibers growth, and ferrocene is the optimal catalyst. In this case, carbon nanofibers have a length of up to 10-15 microns and ~ 40% of the nanofibers have a diameter of 70-80 nm (Fig. 1).

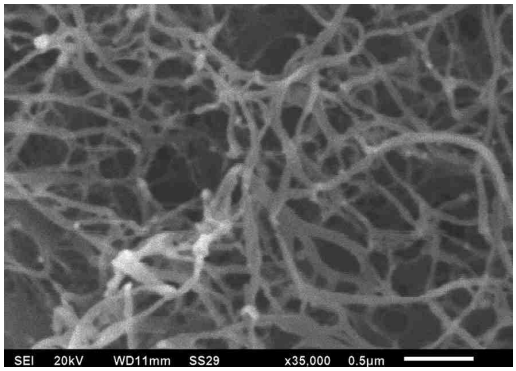

Fig. 1 SEM images of CPVC with an additive of ferrocene after high power ion beam irradiation with j = 100 A/cm^2.

Possible mechanisms for the growth of carbon nanofibers under the action of high power ion beam are discussed.

* The work was supported by RFBR and the government of the Omsk region, grant № 18-43-550009 r_a

POTASSIUM TITANYL PHOSPHATE SPUTTERING FEATURES BY ARGON CLUSTER IONS*

I.V. NIKOLAEV[1,2], *N.G. KOROBEISHCHIKOV*[1], *M.A. ROENKO*[1]

[1] *Department of Applied Physics, Novosibirsk State University, Novosibirsk, Russian Federation*
[2]*Kutateladze Institute of Thermophysics SB RAS, Novosibirsk, Russian Federation*

The paper deals with the surface processing of potassium titanyl phosphate ($KTiOPO_4$, KTP) single crystals by gas cluster ions that have distinctive features in interaction with the target surface in comparison with monomer ion beams. The feature of the cluster ions is that the sputtering process of the target surface at the small energy per atom in the cluster ($E/N_{mean} \leq 20$ eV/atom) leads to a subnanometer level of the surface roughness with a minimum damage of the structure targets [1, 2].

The experiments were performed using a nonsize-selected beam of argon cluster ions, which has high beam intensity and, thus, a sufficient etching rate for technological applications [3]. The description of the experimental setup CLIUS is given of Ref. [4].

To study the surface morphology, we used the atomic force microscope (AFM) Ntegra Prima HD. Figure 1 shows the AFM measurements before and after processing at the same scan sizes (2×2 μm^2) with a resolution of 1024×1024 pixels. The total dose of cluster ions was 1.9×10^{16} cm^{-2}. The surfaces of the KTP samples were preliminarily processed by the method of chemical-mechanical polishing.

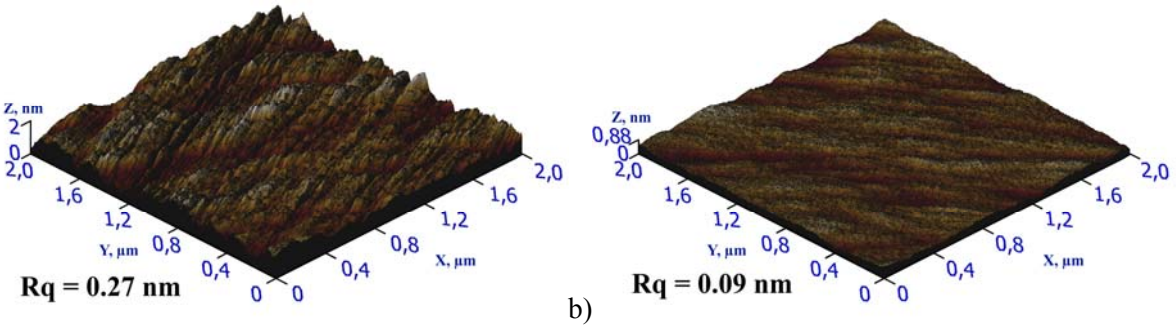

Fig.1. 3D AFM images 2x2 μm before (a) and after (b) surface processing by argon cluster ions.

At the small scales (2×2 μm^2), the greatest decrease in roughness is observed — by a factor of 3, while the etching depth was only 40 nm. We analyze the important (especially, for optical materials) complex characteristic of surface quality is the power spectral density (PSD) function of surface roughness for studying the surface smoothing effect of KTP single crystals by argon cluster ions. It is possible to estimate the light scattering at the optical surfaces using the PSD function [5]. The sputtering yields and etching rates for KTP single crystals in a wide range of energy per atom in the argon cluster (E/N_{mean} = 10–115 eV/atom) have been determined. Low-damaged surface processing leads to an improvement in optical surface quality by minimization of a subsurface damaged layer (SSD), which is undoubtedly one of the most important limiting peculiarities for nonlinear optical materials such as KTP [6, 7].

REFERENCES

[1] I. Yamada, J. Matsuo, N. Toyoda, T. Aoki, and T. Seki, "Progress and applications of cluster ion beam technology," Curr. Opin. Solid State Mater. Sci., vol. 19, pp. 12–18, 2015.

[2] A. E. Ieshkin, K. D. Kushkina, D. S. Kireev, Yu. A. Ermakov, and V. S. Chernysh, "Polishing superhard material surfaces with gas-cluster ion beams," Tech. Phys. Lett., vol. 43, no. 1, pp. 95–97, 2017.

[3] N. G. Korobeishchikov, I. V. Nikolaev, M. A. Roenko, and V. V. Atuchin, "Precise sputtering of silicon dioxide by argon cluster ion beams," Appl. Phys. A, vol. 124, Article Number 833, 2018.

[4] N. G. Korobeishchikov, I. V. Nikolaev, and M. A. Roenko, "Effect of argon cluster ion beam on fused silica surface morphology," Nucl. Instrum. Methods Phys. Res., Sect. B, vol. 438, pp. 1–5, 2019.

[5] A. Duparre, J. Ferre-Borrull, S. Gliech, G. Notni, J. Steinert, and J. M. Bennett, "Surface characterization techniques for determining the root-mean-square roughness and power spectral densities of optical components," Appl. Opt., vol. 41, no. 1, pp. 154–171, 2002.

[6] A. Mamrashev, N. Nikolaev, V. Antsygin, Y. Andreev, G. Lanskii, and A. Meshalkin, "Optical Properties of KTP Crystals and Their Potential for Terahertz Generation," Crystals, vol. 8, no. 8., Article Number 310, 2018.

[7] Y. Wang, Y. Zhao, X. Xie, G. Hu, L. Yang, Z. Xu, and J. Shao, "Laser damage dependence on the size and concentration of precursor defects in KDP crystals: view through differently sized filter pores," Opt. Lett., vol. 41, no. 7, pp. 1534–1537, 2016.

* The work was supported by the Ministry of Education and Science of the Russian Federation under grant No. 11.1402.2017/4.6 and the Russian Foundation for Basic Research under grant No. 17-01-00512.

ABOUT THE EFFECT OF THE DURATION OF ELECTRIC ARC SYNTHESIS ON ITS PRODUCT IN A SYSTEM WITH TUNGSTEN AND CARBON*

A.I.KOKORINA[1], *A.Ya.PAK*[1]

[1]*Tomsk Polytechnic University, Tomsk, Russia*

Tungsten carbide is of interest for various applications (cutting tools, ammunition elements, etc.) due to the favorable combination of physical and mechanical properties (high hardness, low friction coefficient). A group of methods for producing tungsten carbide, based on the generation of plasma, is popular today. One possible known source of plasma is an arc discharge. Method, based on generation of direct current arc under ambient air conditions, is popular in the last years [1]. Today this method is mainly applied for synthesis of carbon nanostructures, for example, carbon nanotubes [2]. The main feature of this approach is the possibility of synthesis of non-oxide materials in atmospheric plasma. It is possible due to the self-shielding effect, which arises as a result of generation of carbon monoxide and carbon dioxide gas stream. These gases protect reaction zone against air oxygen. The possibility of metal carbides and non-metal carbides synthesis discussed by us earlier [3], but individual aspects of the issue of tungsten carbide synthesis have not been investigated in details.

In this work influence of duration of electric arc synthesis at the product in a system with tungsten and carbon was investigated. Typical X-ray diffraction pattern is showed in Figure 1. Two carbon graphite-like phases, initial tungsten and two phases of tungsten carbide WC and W_2C were identified in the product. Possibility of influence at the phase composition of the synthesis product by changing the duration of the arc discharge was established.

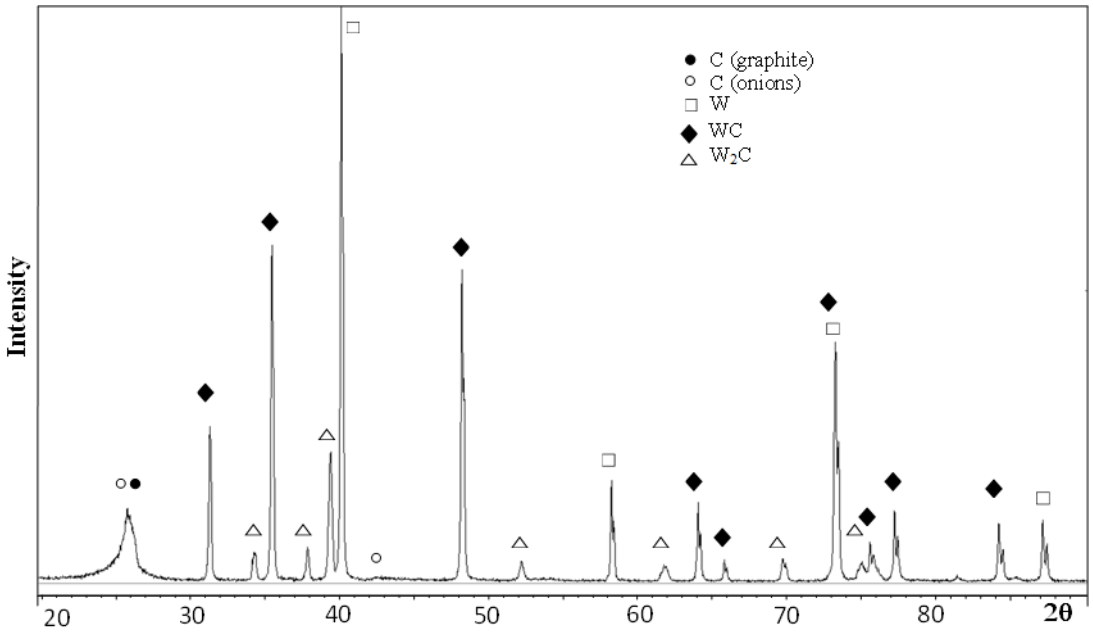

Fig.1. Typical X-ray diffraction pattern of obtained specimens (λ=1.54060 Å).

REFERENCES

[1] Neha Arora. Arc discharge synthesis of carbon nanotubes: Comprehensive review/ Arora Neha, N.N. Sharma // Diamond & Related Materials.-2014.-№50.-pp.135-150.

[2] Jiang Zhao. Arc synthesis of double-walled carbon nanotubes in low pressure air and their superior field emission properties / Zhao Jiang [et al.] // Carbon.-2013.-№58.-pp.92-98.

[3] Pak A.Ya. Boron Carbide Synthesis in Low-Voltage DC Electric Arc Initiated in Open Air/ A.Ya.Pak, G.Ya.Mamontov // Technical Physics Letters.-2018.-№7.-pp.615-617

* The research was funded by the Russian science Foundation project No. 19-79-00086

ELECTRON-BEAM SURFACE MODIFICATION OF LOW-CARBON STEEL*

U.L. MISHIGDORZHIYN[1,2], *N.S. ULAKHANOV*[1], *A.S. MILONOV*[2], *A.P. SEMENOV*[2]

[1]*East Siberia State University of Technology and Management, Ulan-Ude, Russia*
[2] *Institute of Physical Material Science SB RAS, Ulan-Ude, Russia*

Electron-beam processing (EBP) as a method of surface modification is continuously studied and is of high interest due to the perspective of its application [1-4]. It can be used to obtain protective coatings on the surface of steels and alloys in two ways - electron beam alloying (EBA) and combined treatment. The latter process comprises of two stages:

- thermal-chemical surface treatment (TCT) as a first step, where diffusion layers are formed on the surface of base metal during high-temperature exposure in treatment media (B_4C/Al-paste, with the ratio of 5/1) in a muffle furnace [5];
- the second step involves modification of obtained diffusion layers by means of EBP.

Low-carbon steel was used as a bench mark material in this study. The conducted experiments on combined treatment generated the following findings: TCT at 950 °C and 4-hour exposure resulted in predominantly aluminized layer formation with a thickness of 130 μm and simple microstructure (Fig. 1a). The subsequent EBP modification of the layer leads to transformation of its microstructure and enhancement of the layer thickness up to 400 μm (Fig. 1b). In addition, metallographic analysis showed that combined treatment results in coarsening of grain size in the base metal just below the layer.

The same composition of treatment paste was used in EBA process. The layer with the thickness of about 240-260 μm was obtained as a result of alloying (Fig. 1c). The microstructure of the layers after both combined treatment and EBA is similar. However, the first treatment results in formation of light dendrites in the layer and the latter process – dark ones, which indicates phase composition difference. It should be also noted that EBA has the lowest impact on the base metal microstructure.

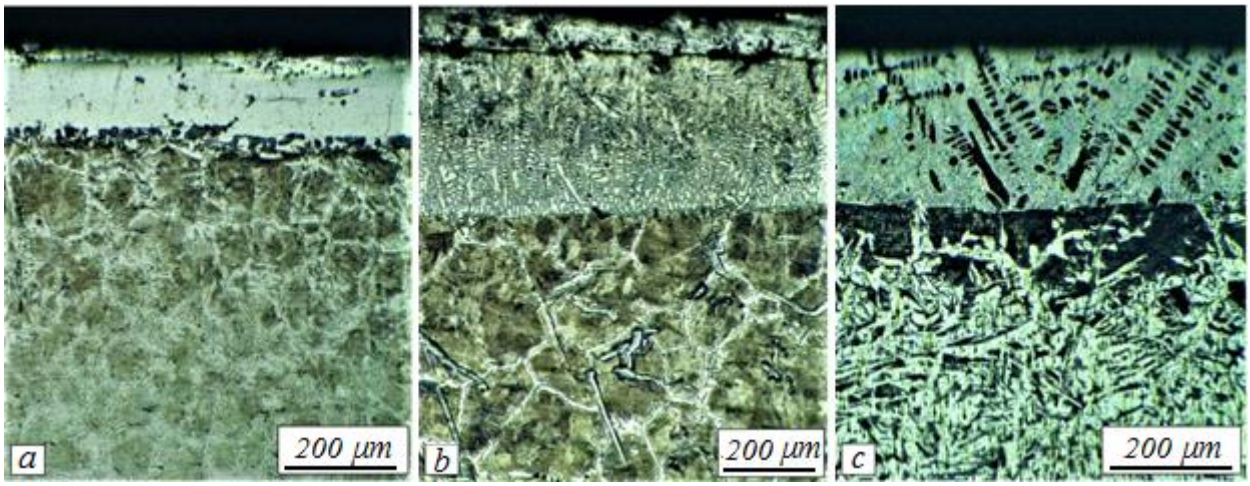

Fig.1. Microstructure of low-carbon steel after: a – TCT (950 °C, 4 hours), b – TCT+EBP (U=20kV, I_{beam}=20mA), c – EBA

References

[1] R. Zenker, Electron Beam Surface Technologies. In: Wang Q.J., Chung YW. (eds) Encyclopedia of Tribology. Boston, MA: Springer, 2013.

[2] I.G. Sizov, N.N. Smirnyagina, A.P. Semenov, "The structure and properties of boride layers obtained as a result of electron-beam chemical-thermal treatment," Met. Sci. Heat Treat., vol. 11, pp. 45-46, 2001.

[3] R. Zenker, "Structure and properties as a result of electron beam surface treatment," Adv. Eng. Mater., vol. 6, no. 7, pp. 581-588, 2004.

[4] U.L. Mishigdorzhiyn, N.S. Ulakhanov, A.S. Milonov, A.P. Semenov, "Modification of the surface of steel 3Kh2V8F by application B-Al-coatings by methods of thermal-chemical treatment and electron-beam processing," IOP Conf. Ser.: Mater. Sci. Eng., vol. 759, 012017, 2020

[5] U. Mishigdorzhiyn, I. Sizov, "The influence of boroaluminizing temperature on microstructure and wear resistance in low-carbon steels," Mater. Perform. Charact., vol. 7, pp. 252–265, 2018.

* The work was supported by the Russian Foundation for Basic Research under grant No. 18-38-00939.

INVESTIGATION OF TRIBOLOGICAL AND STRENGTH PROPERTIES OF STAINLESS STEEL SAMPLES PRODUCED BY AN ADDITIVE METHOD AFTER A PULSE ELECTRON BEAM EXPOSURE*

YU.H. AKHMADEEV[1], A.D. TERESOV[1], E.A. PETRIKOVA[1], O.V. KRYSINA[1], YU.F. IVANOV[1], G.V. SEMENOV[2]

[1]Institute of High Current Electronics SB RAS, Tomsk, Russia
[2]LLC «TETA», Loskutovo, Tomsk, Russia

Modern machining technologies, as a rule, work on the principle of phased removal of material from the workpiece to obtain the desired shape and size (the principle of "subtraction"). Rapidly developing additive manufacturing technologies (AM technologies) are carried out according to the principle of layer-by-layer growing of a product based on its 3D computer model by applying layers of different thicknesses (the principle of “adding”) [1-3]. At this time, 3D printers are most often used to grow metal products. Their principle of operation is based on sintering of a metal powder or wire with laser radiation or an electron beam [1-5]. In the case of using metal powder, the formation of the product occurs in a thin (50-100 μm) layer, where individual particles are sintered by selective heating. When using wire, the layer thickness is characterized by the diameter of the wire used (0.8-3 mm) and the parameters of the energy effect, and the process itself is more reminiscent of layer-by-layer surfacing [1, 2].

A common problem that is typical for all types of AM technologies is the problem of ensuring the proper microstructure of the synthesized material, eliminating porosity. The next disadvantage of AM technology is the anisotropy of the structure and properties of the material, high internal stresses, which is inevitable with the layered principle of creating the product. To solve these problems, the authors proposed a method for finishing the surface of metal products produced by an AM technologies using a pulsed electron beam in vacuum [6].

The aim of this work was to study the tribological and strength properties of samples made of AISI 308LSi stainless steel, created by the method of layer-by-layer electron-beam surfacing of ø 1 mm wire in vacuum after pulsed electron-beam treatment at the SOLO installation [7]. In the process of irradiation, the following parameters were varied: energy density per pulse 15-30 J/cm^2, pulse duration 50-200 μs, number of pulses 3-20.

Tribological investigation of the surface showed an 18% decrease in the wear parameter and a slight decrease in the friction coefficient of the samples after irradiation with a pulsed electron beam in certain modes compared to the initial ones. In tensile tests, the treated samples showed an increase in strength by 10% and plasticity by 6%. Thus, surface treatment of AISI 308LSi stainless steel samples manufactured using AM technologies using a pulsed electron beam in certain modes allowed improving tribological and strength properties compared to the initial material.

REFERENCES

[1] I. Gibson, D. Rosen, B. Stucker, Additive manufacturing technologies: 3D printing, rapid prototyping, and direct digital manufacturing. Moscow: Technosfera, 2016 [in Russian].

[2] I.V. Shishkovsky, Basics of high-resolution additive technologies. St. Petersburg: Piter Publ., 2015 [in Russian].

[3] B. Evans, Practical 3D printers: The science art of 3D printing. New York: Apress, 2012.

[4] V.A. Valetov, Additive technologies: state and prospects. St. Petersburg: ITMO Univ., 2015 [in Russian].

[5] E.M. Sachs, M.J. Cima, P. Williams, D. Brancazio and J. Cornie, “Three dimensional printing: rapid tooling and prototypes directly from a CAD model,” J. Eng. Ind., Vol. 114, №4, pp. 481–488, april 1992.

[6] A.D. Teresov, N.N. Koval, Yu.F. Ivanov, E.A. Petrikova, “Application of a pulsed electron beam for surface polishing of metal products obtained by laser or electron-beam powder sintering,” Izv. Vyssh. Uchebn. Zaved. Fiz., Vol. 59, № 9/2, pp. 264–266, september 2016 [in Russian].

[7] N.N. Koval, Yu.F. Ivanov, “Nanostructuring the surface of metal-ceramic and ceramic materials under pulsed electron-beam treatment,” Izv. Vyssh. Uchebn. Zaved. Fiz., Vol. 51, №5, pp. 60–70, may 2008 [in Russian].

* The reported study was funded by RFBR and Tomsk region according to the research project № 19-48-700021.

EXCHANGE BIAS IN THIN CO-COO FILMS: DEEP SECRETS REVEALED BY POLARIZED NEUTRON REFLECTIVITY

KRISTIAAN TEMST[1], ENRIC MENENDEZ[1], JOOST DEMETER[1], ROLAND STEITZ[2], ANDREW R. WILDES[3], AMIR S. MOHD[4], ALEXANDROS KOUTSIOUMPAS[4], EARL BABCOCK[4], STEFAN MATTAUCH[4], JOSEP NOGUÉS[5], ANDRÉ VANTOMME[1]

[1]Instituut voor Kern- en Stralingsfysica, KU Leuven, Belgium
[2]Helmholtz-Zentrum Berlin für Materialien und Technologie, Berlin, Germany
[3]Institut Laue-Langevin, Grenoble, France
[4]MLZ, Garching, Germany
[5]ICN2 and ICREA, Barcelona, Spain

Exchange bias (EB) is the interfacial coupling between a ferromagnet (FM) and an antiferromagnet (AFM). It induces a unidirectional magnetic anisotropy in the FM upon cooling in a magnetic field. Since its discovery, this phenomenon has been widely studied in bilayers, core-shell clusters, and patterned films. Polarized neutron reflectivity has played an important role in the study of exchange bias, in particular for the identification of the unusual asymmetry in the magnetization reversal mechanism that is present in e.g. Co/CoO and Fe/FeF_2. In order to induce exchange bias we have explored a new approach, namely EB systems produced by oxygen ion implantation into Co thin films [1]. The oxygen implantation leads to the local formation of antiferromagnetic CoO buried within the ferromagnetic Co layer, thus creating multiple internal FM/AFM interfaces. Polarized neutron reflectivity (PNR) allows reconstructing the magnetization depth profile in such an implanted system.

Ferromagnetic Co layers with a thickness of 100 nm were prepared by molecular beam epitaxy. These layers were implanted with oxygen ions using an implantation energy of 60 keV. A strong exchange bias shift is observed once a minimum oxygen fluence has been implanted. We have investigated the correlation between the implantation depth profile and the magnetic depth profile using specular polarized neutron reflectometry and found that the local Co magnetization varies in depth as a result of the Gaussian-like implantation profile. PNR experiments also indicated that the implanted exchange bias system does not have the asymmetric magnetization reversal modes typically observed in Co/CoO bilayers. The implantation profile can however also be altered by combining implantations with different energy, leading to a more uniform implantation depth profile, which is then also reflected in the magnetization reversal mechanism.

REFERENCES

[1] J. Demeter, J. Meersschaut, F. Almeida, S. Brems, C. Van Haesendonck, A. Teichert, R. Steitz, K. Temst and A. Vantomme, Appl. Phys. Lett. 96, 132503 (2010).

[2] J. Demeter, A. Teichert, K. Kiefer, D.Wallacher, H. Ryll, E. Menendez, D. Paramanik, R. Steitz, C. Van Haesendonck, A. Vantomme, and K. Temst, Review of Scientific Intruments **82**, 033902 (2011).

[3] J. Demeter, E. Menendez, K. Temst, and A. Vantomme, Journal of Applied Physics 110 (2011), 123902.

[4] E. Menéndez, J. Demeter, J. Van Eyken, P. Nawrocki, E. Jedryka, M. Wojcik, J.F. Lopez-Barbera, J. Nogués, A. Vantomme, K. Temst, ACS Applied Materials & Interfaces 5, 4320-4327 (2013).

[5] E. Menéndez Dalmau, H. Modarresi, C. Petermann, J. Nogués, N. Domingo, H. Liu, B.J. Kirby, B. Maranville, J.A. Borchers, A. Syed Mohd, Z. Salhi, E. Babcock, S. Mattauch, L. Lagae, C. Van Haesendonck, A. Vantomme, K. Temst, Small 13, 1603465 (2017).

Ti-Ta-Si-Ni METALLIC GLASS SURFACE ALLOY ON TiNi SUBSTRATE: ADDITIVE THIN-FILM ELECTRON-BEAM SYNTHESIS, MICROSTRUCTURAL CHARACTERIZATION AND PROPERTIES*

L.L. MEISNER[1], *V.P. ROTSHTEIN*[3], *A.B. MARKOV*[2], *V.O. SEMIN*[1], *S.N. MEISNER*[1], *E.V. YAKOVLEV*[2], *F.A. D'YACHENKO*[1], *A.A NEIMAN*[1], *E.YU. GUDIMOVA*[1]

[1]*Institute of Strength Physics and Materials Science of Siberian Branch Russian Academy of Sciences, Tomsk, Russia,+7-3822-286989, llm@ispms.tsc.ru ,*
[2]*Institute of High Current Electronics, Siberian Branch, Russian Academy of Sciences, Tomsk, Russia,*
[3]*Tomsk State Pedagogical University, Tomsk, Russia*

An important factor limiting the wide application of magnetron sputtered thin-film metallic glass (TFMG) coatings for improving surface-sensitive properties of structural alloys is the poor adhesion of TFMGs to substrates. This problem can be overcome through the synthesis of MG surface alloys (MGSAs) by additive pulsed electron-beam melting of film/substrate systems of high glass-forming ability.

In this work, this approach is applied to the "film ($Ti_{60}Ta_{30}Si_{10}$, at.%, 100 nm)/substrate (TiNi alloy)" system using a low-energy, high-current electron beam (~2.5 μs, ~15 keV, 1.7 J/cm^2) at 10 synthesis cycles and 10 pulses per cycle. The initial temperature of TiNi substrate was ≤ 473 K to the end of the synthesis.

Using surface AES, SEM/WDS/EDS, XRD and cross-sectional HRTEM/EDS/SAED analyses it has been found that ~1.5 μm thick SA has fully MG structure, in which the top surface Ni-depleted layer of thickness ~200 nm has composition ~$Ti_{44}Ta_{32}Si_{16}Ni_3$. Beneath MGSA, the ~300 nm thick nanocomposite $Ti_{50}Ni_{30\div40}(Ta+Si)_{20\div10}$ sublayer, consisting of amorphous phase and Ti_2Ni nanograins is formed. The nanocomposite sublayer is followed by the transition zone with a B2-phase eutectic columnar structure, which provides the diffusion bonding of MGSA with unmelted TiNi substrate on the depth of ~2 μm.

The monotonic depth dependences of nanohardness, elastic modulus, depth recovery ratio and plasticity, obtained by nanoindentation, indicate the mechanical compatibility of MGSA and underlying sublayers with the TiNi substrate. MGSA possesses simultaneously enhanced elastic modulus and plasticity compared to those of untreated TiNi substrate.

Evaluation of shape memory effect and superelasticity by torsion deformation technique have shown that synthesis of MGSA results in an almost 2-fold increase in the martensitic shear stress compared with that of untreated TiNi samples, which is consistent with a corresponding increase in the elastic modulus. In addition, the stress hysteresis width in the stress-strain loop markedly decreases. The irreversible inelastic strain is ~0.8% at a maximum strain of 6%, and a complete recovery of the residual strain is achieved when sample is heated to 323 K.

Potentiodynamic polarization measurements have shown, that synthesis of Ti-Ta-Si-Ni MGSA with Ni-depleted top surface layer results in the significant enhancement in corrosion resistance of test samples in the Lock-Ringer salt solution.

* The reported study was carried out with the financial support of Russian Science Foundation according to the project No. 18-19-00198 (26.04.2018)

STRUCTURE CHANGES IN METALS DURING THEIR LASER TREATING

A.YU. IVANOV, A.L. SITKEVICH, N.G.VALKO, S.V. VASILIEV

Grodno State University, Osheshko, 22, Grodno, 230023, Belarus, ion_ne@mail.ru, (0152)610098

The interaction of moderate-intensity laser beams with metals has been investigated. The radiation of the GOR-100M ruby laser (λ = 0.694 mm) operating in the free oscillation regime (pulse duration ~1.2 ms) passed through the focusing system and was directed onto the surface of metal sample. Both mono-lens and two-lens systems were used for focusing of laser radiation that avoided to form a diaphragm image on the surface of irradiated samples as a spot with the sharp borders. During the experiments a spot diameter was varied from 1 to 2 mm. This allowed to vary the flux density of laser radiation q from 10^4 to 10^6 W cm^{-2}. The energy of the laser pulses has been varied from 5 to 60 J. Titanium and copper were chosen as objects of study.

By the method of X-ray powder diffraction (XRD) have been determined the structure volumetric changes of irradiated metal samples (continuous polycrystalline) having in equilibrium state the cubic side-centered crystalline grid before and after effect of laser radiation.

During interaction of laser radiation with matter a number of changes in the treated sample can take place: changes of chemical composition of matter, phase transitions, defects of new types appearance, increase of already existing defects concentration, changes of inter-crystalline planes properties. It was obtained that irradiation of copper samples by ruby laser leads to formation structural described by spatial group Fm3m Therefore in the case under investigation two first mechanisms are not able to lead to the changes that can be registered by XRD method. It leads to necessity of elucidation of the influence of laser irradiation on the defects of copper crystal structure. For copper samples irradiated by laser beam with the flux density of radiation q ~ $5\cdot10^5$ W cm^{-2} not only erosion but even splitting of the first maximum of correlation function was observed. It testifies to the transformation of the matter crystalline structure after its laser treating. In the irradiated zone the form of the crystalline elementary cell was changed from the cubic side-centered to the distorted (having a form of parallelepiped, different from the cub). Micro-hardness of metal samples in the irradiated zones considerably (30 % and even more) increased. It is also to be mentioned that after treating of copper sample by laser radiation with the flux density enough for the melting of metal in the irradiated zone (q > 10^6 W cm^{-2}) any changes of X-ray difractograms were not observed and micro-hardness of metal samples in the irradiated zones slightly decreased.

Estimation of the height of the first maxima of correlation functions before and after laser treating of copper samples permitted us to discover that 83 % of crystalline elementary cells were subjected to the transformation from the cubic side-centered to the distorted (having a form of parallelepiped, different from the cub). These data are in good consent with the results of calculations using the methods [1, 2] (~ 80 % of total number of the crystalline elementary cells).

For the titanium samples treated by laser radiation with the flux density of radiation q ~ $5\cdot10^4$ W cm^{-2} splitting of correlation function maxima was not observed. The analysis of the X-ray diffraction patterns of the investigated titanium samples was shown growth of crystalline grid defects concentration in the irradiated zone. Microhardness of titanium samples in the irradiated zones also considerably increased from 277 MPA to 324 MPa. The calculations using the methods [1, 2] show that after treating of titanium sample by laser radiation with the flux density q ~ $5\cdot10^5$ W cm^{-2} number of crystalline elementary cells were subjected to the transformation from the cubic side-centered to the distorted (having a form of parallelepiped, different from the cub) can reach 50 %.

REFERENCES

[1] P.V.Pavlov, A.F.Hohlov. Physics of Solids. – M: Vysshaia Shkola, 2000.
[2] V.I.Zinenko, B.P.Sorokin, P.P.Turchin. Principles of Physics of Solids. – M: Izd-vo fiziko-matematicheskoi literature, 2001.

PLASMONIC PROPERTIES OF COPPER NANOPARTICLES IN MGAL2O4 AT STAGE ANNEALING*

A.N. KIRYAKOV, A.F. ZATSEPIN, A.SH. VAGAPOV

Ural Federal University, Mira st. 21, Yekaterinburg, Russia

Plasmonics and plasmonic technologies are actively developing and attracting great interest in biomedicine, optics, photonics, etc. due to a wide range of effects arising from the interaction of plasmon particles with the environment, for example, increased luminescence of rare-earth ions, increased sensitivity of chemical sensors, enhanced Raman vibrations and so on [1]. Metal nanoparticles of Cu, Ag, Au are actively studied as a material for plasmonic applications due to their low oxidation potential and plasmon resonance in the visible part of the spectrum. Using ion implantation methods, it is possible to obtain plasmonic copper nanoparticles, including in radiation-resistant wide-gap oxides of the $MgAl_2O_4$ type, which is a promising material in optoelectronics and photonics. However, the mechanisms of plasmon nanoparticle formation in this case are not clear. The questions related to the influence of step annealing on the plasmonic properties of such nanoparticles also remain open. In this regard, the aim of this work is to synthesize copper nanoparticles in a $MgAl_2O_4$ matrix and to study the effect of step annealing on the plasmonic properties of such nanoparticles.

Transparent $MgAl_2O_4$ ceramics were used as a matrix for implantation. Implantation was carried out under the following synthesis conditions: Ar atmosphere, acceleration of Cu^{2+} ions was 30 keV, pulsed mode, fluence range from $5x10^{15}$ to $1x10^{17}$ cm^{-2}. The certification of the samples was performed by Raman spectroscopy (Raman), X-ray phase analysis (XRD) and X-ray photoelectron spectroscopy. Step annealing was performed in the temperature range from 100 to 530 °C with a step of 30 °C and a holding time of 10 min followed by quenching. Optical spectroscopy was recorded on a Lambda 35 PerkinElmer fluorometer.

In the original matrix, as a result of special synthesis, an increased concentration of anti-site defects is observed, which means aluminum cations replacing magnesium cations and vice versa. In addition, it was found that O *1s* states are a superposition of octahedral and tetrahedrally coordinated oxygen atoms.

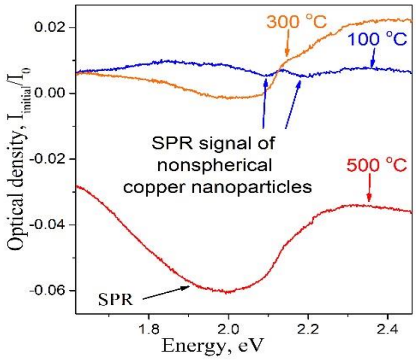

Fig. 1. Optical absorption spectra in the SPR band of ceramics modified by $1x10^{17}cm^{-2}$ after step annealing. Along the Y axis, the ratio of the optical absorption of the implanted ceramic to the optical absorption of the annealed implanted ceramics

As a result of pulsed ion implantation with fluences $F \geq 5x10^{16}$ cm^{-2}, metal non-spherical plasmon nanoparticles are formed in spinel ceramics. The step-by-step annealing of modified ceramics leads to the oxidation of such nanoparticles and, at the same time, to a change in their shape, which affects the nature of the SPR, Fig. 1. Based on the obtained data, the oxidation activation energy was determined, and in addition, a model of the oxidation of nonspherical plasmon nanoparticles was proposed.

REFERENCES

[1] *Maier S. A. Plasmonics: fundamentals and applications. – Springer Science and Business Media, 2007.*

* This work was funded by RFBR and Sverdlovsk region, project number 20-42-660012

COMPARATIVE STUDIES OF THE IRRADIATION EFFECTS OF ZrWN COATING WITH HELIUM AND KRYPTON IONS AT LOW AND HIGH TEMPERATURES*

S.B. KISLITSIN[1], *A.I. POTEKAEV*[2], *A.A. KLOPOTOV*[3], *T.M. ALDABERGENOVA*[1]

[1]*The Institute of Nuclear Physics, Almaty, Kazakhstan*
[2]*National Research Tomsk State University, Tomsk, Russia*
[3]*Tomsk State University of Architecture and Building, Tomsk, Russia*

The investigation results of the effect of low-energy He and Kr ions on the structure and physical-mechanical properties (hardness, corrosion resistance) of ZrWN coatings formed on a steel substrate by magnetron sputtering are presented. The purpose of the research is the synthesis of a coating that can serve as a protective against ionizing radiation. The ZrWN coating is selected from the following considerations. It was previously established [1] high stability of the structure and insignificant degradation the physical-mechanical properties of ZrN and ZrTiN coatings after irradiation with low-energy Xe ions. Tungsten, as is known [2-3], has a number of properties that make it possible to consider it as refractory material for use in nuclear installations. Replacing of Ti with tungsten in the ZrWN coating, according to our ideas, will give more high strength and thermal resistance to the coating.

For ZrWN coating deposition, the sputtering targets Zr (99.96 wt.% purity) and W (99.97 wt.% purity) were used. As a plasma-forming gas, a gas mixture with a nitrogen content of ~ 25% was used. As a result, samples with ZrWN coatings ~ 600 nm thick were obtained.

Irradiation with low-energy He and Kr ions at temperatures <100 °C and 600 °C was carried out on the ECR source channel of the DC-60 heavy ion accelerator (see table 1).

Table 1. Irradiation conditions for samples with ZrWN coatings

Coating	Ion	Ion energy keV	Irradiation temperature	Fluencecm^{-2}	Beam current, μA	Irradiated square, cm^2
ZrWN	$^4He^{2+}$	45	100˚C	10^{16}	25	4
ZrWN	$^4He^{2+}$	45	600˚C	10^{17}	25	3.01
ZrWN	$^{84}Kr^{14+}$	280	100˚C	10^{16}	10	4
ZrWN	$^{84}Kr^{14+}$	280	600˚C	10^{17}	10	3.01

Before and after irradiation, the structure, elemental composition, and physical-mechanical properties of the coatings were studied by X-ray diffraction, scanning electron microscopy, energy dispersive analysis, atomic force microscopy, Rutherford backscattering, hardness and corrosion resistance measurements.

The results of studies of the effects of irradiation with low-energy He and Kr ions at room and 600 °C temperatures on the structure and properties of ZrWN coatings are as follows:

- irradiation of the ZrWN coating with helium ions does not lead to the formation of new phases and does not cause significant changes in the surface structure;
- irradiation with low-energy Kr ions leads to surface sputtering, a decrease in coating thickness and is accompanied by a change in the surface elemental composition due to differences in partial sputtering coefficients;
- mechanical properties (hardness) and corrosion resistance of ZrWN coatings are degraded by irradiation with He and Kr ions. Irradiation at high temperatures leads to a more significant degradation of the properties of the ZrWN coating.

REFERENCES

[1] Uglov V.V, Rusalski D.P., Zlotski S.V., Sevriuk A.V., Abadias G., Kislitsin S.B., Kadyrzhanov K.K., GorlachevI .D.,.Dub S.N. “StabilityofTi-Zr-Ncoatings under Xe-ion irradiation”. Surface&Coatings Technologies. vol. 204. pp.2095 – 2098, 2010.

[2] Neu R.”Tungsten as a Plasma Facing Material in Fusion Devices”. IPP Berichter. vol.. 10, no. 25, 217 p., 2003.

[3] Aldabergenova T.M., Kislitsin S. B., Ganeev G. Z., Wieleba W. Thermal annealing effect on structure and properties of tungsten surface irradiated with high fluence and low energy alpha-particles. Russian Physics Journal, vol. 61, no. 8, 2018.

*This work was carried out as part of the targeted financing program “Kazakhstan Tokamak for Materials Science” of the Ministry of Energy of the Republic of Kazakhstan

FORMATION OF BORON FILM ON SURFACE OF AUSTENITIC STEEL IN SCHEME OF PLASMA-ASSISTED RF-SPUTTERING OF CATHODE FROM BORON*

YU. IVANOV, V. SHUGUROV, A. TERESOV, E. PETRIKOVA, O. TOLKACHEV

Institute of High Current Electronics SB RAS, 2/3, Akademichesky ave., Tomsk, 634055, Russia

The purpose of the present work is to examine the structure and properties of a «boron film / steel» system formed on the surface of specimens of high-chromium austenitic steel in a plasma assisted RF-sputtering of a boron powder cathode.

High-chromium steel of 12Cr18Ni10Ti and 20Cr23Ni18 grade was used as the study material. Formation of boron film on steel surface was performed at the following process parameters: temperature of specimens - 380 °C, duration of process - 1 hour, argon pressure - 0.55 Pa, PINK current I_p = 100 A, bias voltage U_{bs} = 950 V, bias frequency 50 kHz, specimens under floating potential (heating of boron cathode by irradiation from PINK discharge anode). Investigations of elemental and phase composition, state of defective substructure were carried out by scanning and transmission electron microscopy, X-ray diffractometry. Microhardness of modified steel surface also was determined.

As a result of the performed studies, the mode allowing to form boron films on the surface of the high-chromium steel was revealed. The boron film with thickness varies between (400-450) nm is shown to be amorphous. It has been found that when boron films are deposited on the steel surface, a multilayer system is formed, represented, firstly, by a thin (15-20) nm interlayer located at the «film (B) -substrate (steel)» interface and formed by borides of iron and chromium composition of FeB, Fe_2B, CrB_6, secondly, adjacent to interlayer of transition layer of solid solution on the basis of γ-iron, thickness of which reaches 130 nm, divided into sublayers with thickness (60-80) nm, having a nanoscale structure with crystallite dimensions (10-30) nm, and thirdly, thermal diffusion transformation layer of steel with thickness up to 500 nm, containing particles of CrB and Fe_3Ni_3B, which dimensions vary within (2-3) nm (Fig. 1).

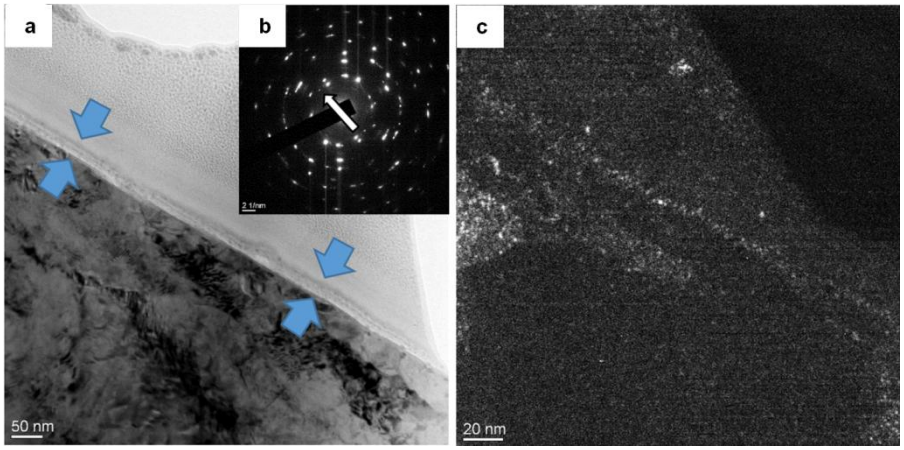

Fig.1. TEM image of the structures of the steel surface layer with deposited boron film.

It has been suggested that the penetration of boron atoms into the surface steel layer at such low temperatures appears to be due to the presence of a highly defecated nanostructured steel interlayer formed, obviously as a result of pre-mechanical grinding and polishing of the specimens. The hardness of the «film (B) / (steel 12Cr18Ni10Ti) substrate» system was found to increase by 2.2 times relative to the initial state and Young 's modulus by 1.8 times. The increase in hardness of the steel surface layer at formation of the «film (B) / (steel) substrate» system is due to the following physical mechanisms based on the results of the analysis of the structure and phase composition of the material. Firstly, strengthening by nano-sized particles of borides by Orovan mechanism, secondly, strengthening by grain boundaries due to action of Hall-Petch mechanism, thirdly, strengthening due to formation of dislocation substructure and fourthly, hard solution strengthening related to doping of crystal lattice of γ-iron by boron atoms.

* The work was supported by RFBR project No. 19-48-700010 and RSF project No.19-19-00183.

COMPRESSION PLASMA FLOWS APPLICATION FOR ZIRCONIUM ALOYS MODIFICATION

V.V. UGLOV[1], N.N. CHERENDA[1], V.I. SHYMANSKI[1], V.M. ASTASHYNSKI[2], A.M. KUZMITSKI[2]

[1]Belarusian State University, Minsk, Belarus
[2]A.V. Luikov Heat and Mass transfer Institute of National Academy of Science of Belarus, Minsk, Belarus

Zirconium-based alloys are widely used as fuel cladding in water cooled nuclear reactors because of their low neutron absorption cross section, excellent mechanical properties, resistance to oxidation and radiation damage. When a loss of coolant accident occurs, the temperature of the zirconium-based elements reaches about 1200 °C, this enhances the surface oxidation rate and zirconium oxide (ZrO_2) growth. This process is accompanied by hydrogen pick-up with the formation of zirconium hydrides and consequent embrittlement. So, slowing down in oxidation process of zirconium is an important problem in practical application of such materials.

In the present work it was suggested to use the compression plasma flows (CPFs) with a high energy density to modify the surface layer of zirconium for improving their oxidation resistance due to structure and phases changes. A pure zirconium was used as a model material allowing to exclude the influence of any impurities and additional phases on the oxidation process.

The samples of pure zirconium were treated with three pulses of compression plasma flows (pulse duration 100 μs, the time between pulses 10 s) in a residual nitrogen atmosphere (pressure 400 Pa) in a magnetoplasma compressor of compact geometry. After the treatment the phase composition and microstructure of the modified layer were investigated. According to the X-ray diffraction results, the zirconium samples save the low-temperature hcp phase, but a thin surface layer of zirconium nitride ZrN is appeared. The oxidation process in an air atmosphere during different times at the temperatures of 500, 700 and 900 ^oC of the treated samples showed the influence of the plasma impact on the structure and phase changes. In the first short time of the oxidation the Zr(O) solid solution with a deformed hcp crystal lattice predominantly forms. The lattice parameters of the Zr(O) solid solution formed in the treated zirconium samples and oxidized at 500 ^oC are lower than the standard values. Meanwhile, the oxidation process at 700 ^oC the plasma treated samples results in the Zr(O) solid solution formation with the higher lattice parameters. The found difference can be a result of the point defect density changes during the thermal heating. Indeed, after the CPF impact the surface layer of zirconium is solidified with a high cooling rate that provides the increased density of point defects. These defects serve as possible positions for the oxygen atoms localization during the oxidation. The defects annealing effect appearing more evidently at 700 ^oC change the structure of the solid solution which transforms from a substitution type to an interstitial one. Further oxidation, at longer time, increases the oxygen concentration and transforms the solid solution to the monoclinic zirconium oxide ZrO_2, and then to mix of tetragonal and orthorhombic oxide phases.

According to theoretical predictions, the alloying of zirconium with certain additional elements, first of all chromium, can prevent hydrogen penetration of these alloys and slowing down the oxide phase formation. For this aim, the coatings of chromium and niobium were deposited on the surface of the zirconium samples before the CPF impact. After the CPF treatment the chromium (or niobium) atoms are dissolved in crystal lattice of zirconium cause the condition of stabilizing the high-temperature cubic phase. It appears at the absorbed energy density providing the at least critical concentration of the metals (several atomic percent). In this case the cubic phase with distorted lattice was produces. The annealing of the samples in the air atmosphere at 350 °C during 7 hours showed the influence of the alloying elements on the rate of oxide phase growth. Indeed, by means of X-ray diffraction was shown that ZrO_2 oxide phase with monoclinic structure starts to form after an hour annealing in the untreated zirconium sample. However, incorporation of chromium as well as niobium atoms prevent the surface layer from the rapid oxidation process. Only after 7 hours of annealing the first diffraction reflexes of the oxide phase were revealed. The improved oxidation resistance of the formed alloys was approved by the results of mass growth after annealing which demonstrated slower rate of the mass in several times. It was shown the highest oxidation resistance was related to the samples with stabilized cubic phase of zirconium. In this case the lattice is deformed by incorporation of additional atoms with different radius and the mechanical stress influence on the diffusion oxygen atoms inside. Oxygen atoms have a tend to increase the lattice parameter of the zirconium matrix, but mechanical stress caused by CPF impact slow down the oxygen penetration inside the sub-surface layer. So, the obtained result showed the possibility to improve oxidation resistance of the zirconium-based alloys by compression plasma flows impact with alloying of the surface with additional metals.

INFLUENCE OF HIGH-CURRENT ELECTRON BEAM IRRADIATION ON THE CHARACTERISTICS OF THE SURFACE LAYER OF TARGET SAMPLES MADE OF COBALT-CHROMIUM ALLOY OBTAINED USING SLM TECHNOLOGIES

O. A. BYTCENKO [1,2] ,I.G. STESHENKO [2] ,E. E. DZHAFAROV[1], A. B. MARKOV[3]

[1] Moscow Aviation Institute (National Research University), Moscow, Russian Federation
[2] - Chernyshev Moscow Machine-Building Enterprise, Moscow, Russian Federation
[3] Tomsk Scientific Center of the Siberian Branch of the Russian Academy of Sciences, Tomsk, Russian Federation

In this paper reviews experimental results on the effect of irradiation with intense pulsed electron beams on the surface layer of target samples obtained by additive manufacturing from cobalt-chromium powder. Investigations of the physical and chemical state of surface layers before and after irradiation were performed using scanning electron microscopy, optical metallography, as well as topographic analysis and microhardness measurement. The study results of the of the influence of irradiation modes on the surface roughness, physical and chemical state of the surface and subsurface layers of samples are presented, as well as a significant reduction in surface layer defects inherent in additive manufacturing.

The presented scientific work is a continuation of the work under the grant of the Russian Foundation for basic research № 14-08-97046 r_povolzhye _a .

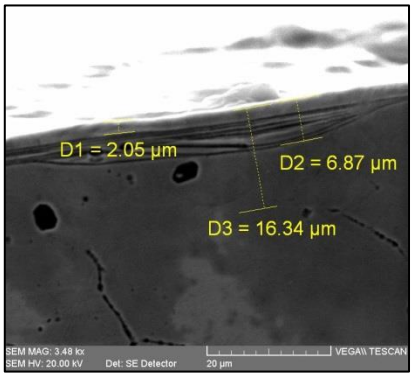

Fig.1. Microstructure of the irradiated target surface layer (SEM)

REFERENCES

[1] Shulov V.A., Engelko V.I., Gromov A.N. Influence of irradiation regimes by high-current pulsed electron beams on the process of crater formation on the surface of nickel alloy targets. Hardening Technologies and Coatings. 2013, 11 (107), 15-19.
[12] Bytsenko O.A., Filonova E.V., Markov A.B. The effect of intense beams on the surface layers of modern heat-resistant alloys with ion-plasma coatings of various compositions. London: Interaction of radiation with solid, 2015, 193-195.
[3] Bytsenko O.A., Filonova E.V., Markov A.B. High-current pulsed electron beams for surface engineering of ion-plasma coatings. News of materials science. Science and Technology, 2017, 2 (26), 9.
[4] Bytsenko O.A., Grigorenko V.B., Lukina E.A. The development of methods of metallophysical research: methodological issues and practical significance. Aviation materials and technologies, 2017, S, 498-515
[5] Bytsenko O.A., Filonova E.V., Markov A.B., Belova N.A. The effect of irradiation with high-current electron beams on the surface layers of modern heat-resistant nickel alloys with ion-plasma coatings of various compositions. Proceedings of VIAM. Electronic Journal, 2016, 6 (42). URL: http://viam-works.ru (17.07.2016). DOI: 10.18577/2307-6046-2016-0-6-10-10.

INFLUENCE OF NITROGEN CONTENT IN THE WORKING GAS MIXTURE ON THE STRUCTURE AND PROPERTIES OF THE NITRIDED SURFACE OF DIE STEELS [1]

YU.A. DENISOVA, A.A. LEONOV, E. V. OSTROVERKHOV, V.V. DENISOV

Institute of High Current Electronics SB RAS, 2/3 Akademichesky ave., Tomsk, 634055, Russia, e-mail: yukolubaeva@mail.ru, Tel.+7(3822)492683

Nitriding is one of the modern technologies that increase wear resistance of the die tool. After the treatment of cold deformation tool made of high-chromium steel, the nitrided layer should consist only of a diffusion zone [1]. The formation on the surface of a continuous layer of a brittle ε-phase and a nitride network at the grain boundaries is undesirable, since the strength of the tool decreases. Nitriding in a plasma of low (~ 1 Pa) pressure discharges allow to independently regulate of the main operating parameters (density of the ion current to the material surface, ion energy, product temperature). The main factors affecting the structure and phase composition of the surface layer formed during nitriding are the temperature and duration of the process, pressure and composition of the working gas mixture. This work is devoted to studying of regularities of the structure and phase composition formation of tool steels (Cr6WV, Cr12MoV) surface layer during ion-plasma nitriding in a low (~1Pa) pressure glow discharge with a hollow cathode [2]. The effect of the nitrogen content in the nitrogen-argon gas mixture on the structure and properties of the nitrided layer was investigated. Nitriding processes were carried out at the same pressure, 1 Pa, for the following nitrogen contents in the working mixture: 100%, 50%, 25%, 10%. The main operating parameters were as follows: glow discharge burning voltage - 165 V, glow discharge current - (18 - 30) A, negative bias voltage to the samples – (-)200 V ÷ (-)600 V, nitriding temperature –520 ºC, nitriding time –3 h.

Investigations of the samples cross section microstructure showed that after nitriding in a mixture with a nitrogen content of 100%, 50%, and 25% in the gas mixture, the surface structure of the Cr6WV and Cr12MoV steels consists of a thin nitride layer and a diffusion sublayer. In a gas mixture with a nitrogen content of 10% (nitrogen partial pressure of about 0.1 Pa), only the diffusion layer is observed, the nitride layer is absent. The nitride layer consists of ε and γ′ phases. By the method of x-ray diffraction analysis, it was shown that by changing of the ratio of nitrogen and argon in the gas mixture, the content of ε and γ′ phases in the nitride layer can be regulated, up to its complete elimination. The smallest surface wear after nitriding is observed for samples processed in a mixture of N_2(10%) + Ar(90%), in which ε-$Fe_{2-3}N$ and γ′-Fe_4N phases are not formed. The thickness of the nitrided layer of the Cr6WV and Cr12MoV die steels in this nitriding regime was about 70 μm at a nitriding temperature of 520 ºC for 3 hours.

REFERENCES

[1] *Lachtin Yu.M., Kogan D.Ya., Shpis G.I.et al. «Theory and technology of nitriding» - M. Metallurgy, 1991 – p.320.*

[2] *V.V. Denisov, Yu.H. Akhmadeev, N.N. Koval, S.S. Kovalsky, I.V. Lopatin, E.V. Ostroverkhov, N.N. Pedin, V.V. Yakovlev, and P.M. Schanin. The source of volume beam-plasma formations based on a high current non-self-sustained glow discharge with a large hollow cathode // Phys. Plasmas. –2019. – V.26. – 123510.*

[1] The work was carried out with the financial support of the RFBR grant № 19-08-00370 A.

FORMATION OF HIGH-STRENGTH NEAR-SURFACE LAYERS IN HYPEREUTECTIC SILUMIN ALLOYS WITH AN ELECTRON-ION-PLASMA TREATMENT*

E. PETRIKOVA, A. TERESOV, YU. IVANOV

Institute of High Current Electronics SB RAS, 2/3, Akademichesky ave., Tomsk, 634055, Russia

The aim of this work is to identify patterns of modification of elemental and phase composition, defective substructure, mechanical and tribological properties of carbon steel subjected to combined treatment in a single vacuum cycle, including high-melting and silicon coating deposition and irradiation with an intense pulsed electron beam to obtain a surface layer with improved strength and tribological properties. The aim of this work is to obtaining fundamental knowledge about the regularities of the formation of the structural-phase state and the physical mechanisms of hardening of the hypereutectic silumin, subjected to electron-ion-plasma treatment. The obtained knowledge will be used in the development of methods for modifying silumin, which is an applied component of the work, oriented to use in the interests of industry.

The material under study was a silumin of a hypereutectic composition with a silicon content (22-24) wt.%. The modification of the structural-phase state and properties of the silumin surface layer has been carried out by two methods: (1) by the thermal method realized by irradiating samples with an intense pulsed electron beam at the SOLO setup (HCEI SB RAS), and (2) by the "surface alloying" which is realized in a single vacuum cycle during the formation of the film / substrate system by arc-sputtering the cathode of Zr-5% Ti-5% Cu composition and its irradiation with an intense pulsed electron beam at the COMPLEX facility (HCEI SB RAS).

Irradiation of the silumin surface and the "film / substrate" system with an intense pulsed electron beam is formed a thin (up to 100 μm) surface layer with a submicron nanosized multi-element multiphase structure due to ultrahigh crystallization rates and subsequent cooling (105-106 K/s). This layer has high mechanical and tribological properties as shown by preliminary studies on silumins of the eutectic composition [Modification of the structure and properties of the eutectic silumin by electron-ion-plasma treatment]. Laskovnev [and others]; Ed. A.P. Laskovneva. - Minsk: Belarus. Navuka, 2013. - 287 p.].

* The work was supported by RFBR project No. 19-52-04009

SURFACE TOPOGRAPHY AND ELEMENTAL COMPOSITION OF CRATERS ON THE SURFACE OF STAINLESS STEEL*

A. E. LIGACHEV,[1] *G. V. POTEMKIN*[2], *M.V. ZHIDKOV*[3], *Y. R. KOLOBOV*[3], *G. E. REMNEV*[2]

[1]*Prokhorov General Physics Institute of the Russian Academy of Sciences, Moscow, Russia*
[2]*Tomsk Polytechnic University, Tomsk, Russia*
[3]*Belgorod National Research University, Belgorod, Russia*

The structure of the crater formed on the surface of 12Cr18Ni10Ti steel (AISI 321) after the impact of high power pulsed ion beam (HPPIB) (C^{n+}, power density 2.8 j/cm^2, current density 70 A/cm^2) was studied by scanning elecron microscopy and energy-dispersive X-ray spectroscopy.

It was shown that craters of different shapes and geometries are formed on the surface of the steel after irradiation. Some craters are elongated, their length 10 times or more may exceed their width (fig.1a and 1b)

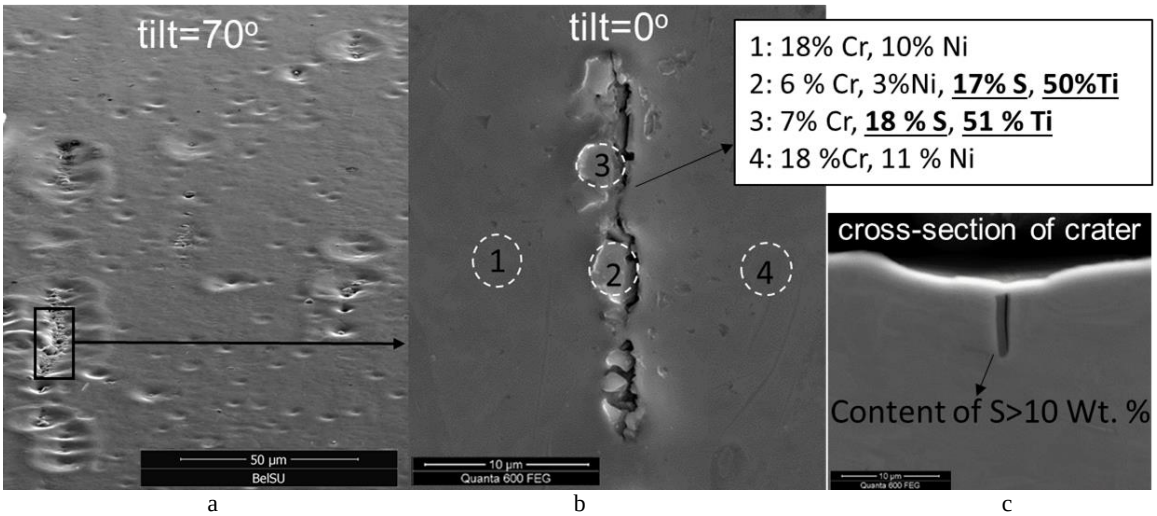

a b c

Fig. 1. Craters on the surface of stainless steel

An increased content of titanium, sulfur, and phosphorus was found in the central region of the craters (Fig. 1b). Manganese and titanium sulfides are possibly present in the initial state of the steel. Perhaps these compounds (Ti_nS, MnS, etc.) are preferred sites for the formation of craters (fig.1c).

* The reported study was funded by RFBR, project number 20-08-00907 (investigations by SEM) and program of the RAS 11P Presidium (sample processing)

MORPHOLOGY OF MAGNESIUM SURFACE AFTER IRRADIATION BY PULSED X-RAY RADIATION*

M.V. ZHIDKOV[1], A.E. LIGACHEV[2], S.A. SOROKIN[3], G.V. POTEMKIN[4], YU.R.KOLOBOV[5]

[1]Belgorod State National Research University, Belgorod, Russia
[2]Prokhorov Institute of General Physics of the Russian Academy of Sciences, Moscow, Russia
[3]Institute of High Current Electronics of Siberia Branch of the Russian Academy of Sciences, Tomsk, Russia
[4]Tomsk Polytechnic University, Tomsk, Russia
[5]Institute of Problems of Chemical Physics of the Russian Academy of Sciences, 1 Academician Semenov prospect, Chernogolovka, Russia

Effect of the pulsed soft X-ray fluxes on the surface topography of magnesium has been investigated. Energy density of the radiation on the specimen surface in a single pulse is ~13 J/cm^2. As a result of melting and subsequent fast solidification, a wavy relief is formed on the surface of magnesium after a single X-ray pulse (fig. 1a).

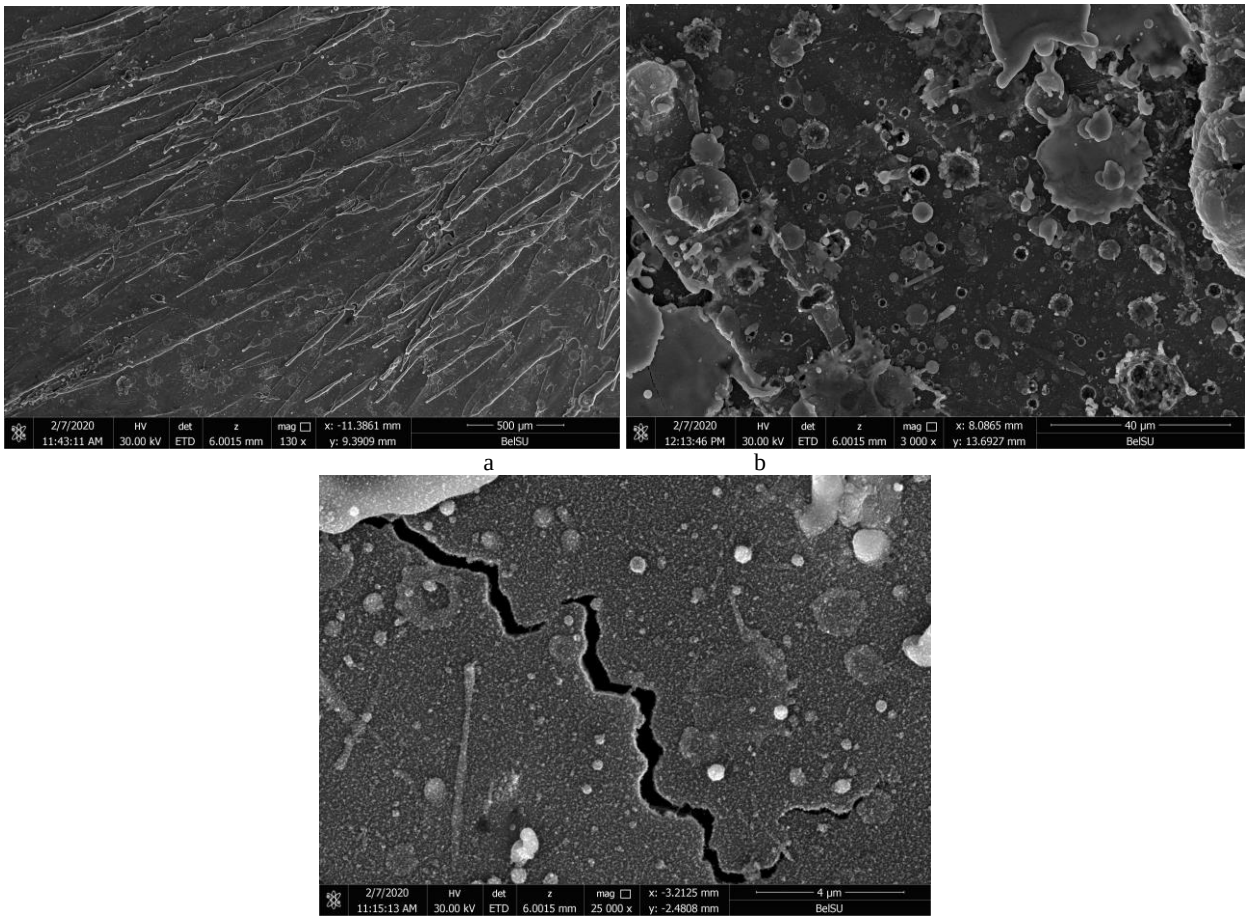

a b

c

Fig.1. Topography of the surface of magnesium after pulsed X-ray radiation

Also of crater-like defects was observed on the irradiated surface (fig.1b). Small cracks are formed on the surface of magnesium due to the high cooling rate of the molten metal after exposure to pulsed X-rays (fig.1c.).

* The reported study was funded by RFBR, project number 20-08-00907 (investigations by SEM) and program of the RAS 11P Presidium (surface processing of the sample)

INFLUENCE OF SIZES OF METAL-CERAMIC COMPOSITES ON THEIR ELECTRON-BEAM SINTERING IN THE FOREVACUUM PRESSURE RANGE[1]

A.S. KLIMOV, I.YU. BAKEEV*, A.A. ZENIN**

** Tomsk State University of Control Systems and Radioelectronics, 40 Lenin ave,. Tomsk, 634050, Russia, E-mail: klimov@main.tusur.ru, phone: 8-905-990-52-41*

Currently, there are various ways to create metal -ceramic materials – such as reactive metal infiltration, reactive metal penetration, hot pressing, spark plasma sintering et. al. Despite the wide variety of methods for producing cermets, new methods are still being sought. One of them may be electron-beam sintering in the forevacuum pressure range. Plasma electron sources are successfully used for sintering ceramics, electron-beam welding of metal-ceramic, creating functional gradient materials and other technologies for processing dielectrics. Previously, we have shown the principal possibility of creating metal-ceramic FGM materials based on aluminum oxide and titanium.

This article is aimed at studying the influence of the thickness of a metal-ceramic composite on the possibility of obtaining a uniformly sintered material. In this work, we use electron-beam irradiation in the range of forevacuum pressures for sintering cermets.

[1] The work was supported by Russian Foundation for Basic Research, grant 18-48-700015.

FORMATION OF PARTICLE FLOWS FROM A BEAM PLASMA GENERATED BY A FOREVACUUM PLASMA ELECTRON SOURCE [1]

A.S. KLIMOV, I.YU. BAKEEV*, A.A. ZENIN**

** Tomsk State University of Control Systems and Radioelectronics, 40 Lenin ave,. Tomsk, 634050, Russia, E-mail: klimov@main.tusur.ru, phone: 8-905-990-52-41*

Plasma material processing technologies are used in microelectronics, automotive, medicine, aerospace, and other high- tech industries. Plasma is used for surface cleaning, selective and anisotropic etching, implantation and deposition of dielectric and semiconductor films. The growing demand for microelectronics devices and increasing requirements for their parameters require a corresponding improvement in their processing technologies. One of the methods for creating dense plasma can be the ionization of a gas when an electron beam passes through it. The parameters of such plasma can be controlled in a wide range by changing the parameters of the electron beam, as well as the type and pressure of the gas medium.

In this paper, the parameters of electron-beam plasma, as well as the parameters of ion and electron flows from it, are studied. The modes of dense beam plasma generation are determined, as well as the dependence between the parameters of the beam and the parameters of the plasma generated by it.

[1] The work was supported by Russian Foundation for Basic Research, grant 18-48-700015.

SURFACE SMOOTHING OF POLYCRYSTALLINE ALN THIN FILMS BY ARGON CLUSTER IONS*

N.G. KOROBEISHCHIKOV[1], I.V. NIKOLAEV[1,2], M.A. ROENKO[1], P.V. GEYDT[3], V.I. STRUNIN[4]

[1]*Department of Applied Physics, Novosibirsk State University, Novosibirsk, Russian Federation*
[2]*Kutateladze Institute of Thermophysics SB RAS, Novosibirsk, Russian Federation*
[3]*Analytical and Technological Research Center, Novosibirsk State University, Novosibirsk, Russian Federation*
[4]*Omsk State University, Omsk, Russian Federation*

Because of the attractive physical characteristics (the highest thermal conductivity, good mechanical strength, corrosion resistance, high breakdown voltage, and the largest piezoelectric coefficients), AlN-based thin films are prospective engineering material for MEMS, optoelectronics, radiophotonics, biosensors, and other applications [1, 2].

Gas cluster ion beams (GCIB) are provided unique properties for surface processing of various materials. Based on the collective nonlinear interaction of multiatomic incident clusters with a solid interface, the precise low-damage etching and smoothing to the subnanometer level surface roughness can be obtained [3].

In this work, the samples of polycrystalline AlN thin film were processed by argon cluster ions. The initial films with a thickness of 1 μm were deposited on a ceramic substrate by RF magnetron sputtering of Al (99.99%) target in an N_2 environment. The samples processing was carried out at the experimental setup CLIUS shortly described in Ref. [4]. The nonsize-selected cluster ion beam at the normal incidence on the surface target was applied. Atomic force microscope NTEGRA Prima HD (NT-MDT) was used to analyze the surface morphology.

Fig.1 shows the AFM images of AlN film surface initial and after cluster ion processing. The pristine surface has a typical microstructure of polycrystalline films (see Fig. 1, a). Earlier it was established that the processing mode with high energy-per-atom E/N=105 eV/atom (kinetic energy of cluster ions E=22 keV, mean cluster size N=210 atom/cluster) leads to the intensive sputtering of the materials [5]. As a result of polycrystalline AlN thin-film processing, the sputtering depth was 105 nm. At AFM scan size of 2×2 μm, the maximum peak-to-valley surface roughness R_t decreases from 170 nm to 69 nm, and the root-mean-square roughness R_q decreases from 29.6 nm to 11.5 nm (see Fig.1, b). At the processing mode with low energy-per-atom E/N=10 eV/atom (kinetic energy of cluster ions E=10 keV, mean cluster size N=1000 atom/cluster), the sputtering yield is a decline by almost two orders compared to high energy mode [5]. Unexpectedly, highly effective smoothing of polycrystalline AlN thin-film surface is obtained. The surface roughness R_t decrease to 38 nm, RMS roughness R_q decrease to 5.2 nm, while the surface sputtering depth is only less than 20 nm (see Fig.1, c).

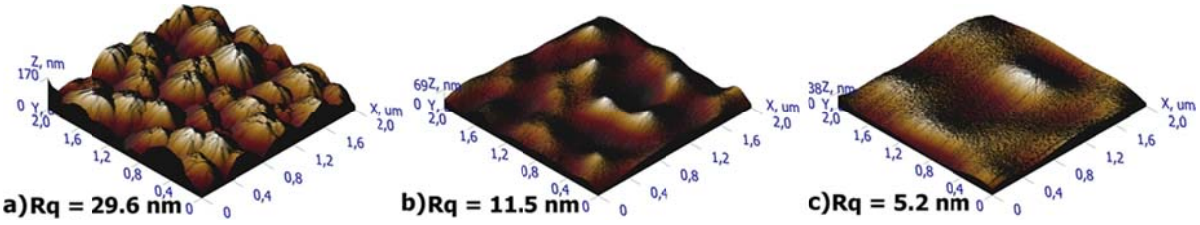

Fig.1. 3D AFM images 2x2 μm of polycrystalline AlN thin-film surface initial (a) and after cluster ion processing (b, c).

REFERENCES

[1] K. Tonisch, V. Cimalla, Ch. Foerster, H. Romanus, O. Ambacher, D. Dontsov, "Piezoelectric properties of polycrystalline AlN thin films for MEMS application", Sensor Actuat. A - Physics, vol. 132, pp. 658-663, 2006.

[2] Y.Q. Fu, J.K. Luo, N.T. Nguyen, e.a., "Advances in piezoelectric thin films for acoustic biosensors, acoustofluidics and lab-on-chip application", Prog. Mater. Sci., vol. 89, pp. 31-91, 2017.

[3] I. Yamada, Materials Processing by Cluster Ion Beams: History, Technology and Applications, London: CRC Press, 2016.

[4] N.G. Korobeishchikov, I.V. Nikolaev, M.A. Roenko, "Effect of argon cluster ion beam on fused silica surface morphology," Nucl. Instrum. Methods Phys. Res., Sect. B, vol. 438, pp. 1–5, 2019.

[5] N.G. Korobeishchikov, I.V. Nikolaev, M.A. Roenko, V.V. Atuchin, "Precise sputtering of silicon dioxide by argon cluster ion beams," Appl. Phys. A, vol. 124, 833, 2018.

* The work was supported by the Ministry of Education and Science of the Russian Federation under grant No. 2019-1085 and the Russian Foundation for Basic Research under grant No. 17-01-00512.

MODIFIED LAYERS IN DIELECTRIC AND SEMICONDUCTOR SUBSTRATES FABRICATED USING DIFFERENT TYPES OF ION IMPLANTERS

V.L. PAPERNY, S.P GORBUNOV, A.V. RYABYKH, A.A. CHERNIKH AND V.I. KRASOV

Irkutsk State University, Irkutsk, 664003, Russia, +7(914)9333884, paperny@math.isu.runnet.ru

Substrates of a Si mono-crystal, as well as of alkali-halide crystals (AHC), were irradiated with metallic ion beams emitted by a MEVVA high-voltage ion implanter and a low-voltage vacuum spark. The SIMS method showed that in both cases a modified layer several tens of nanometers thick containing implanted ions is formed in the substrate. The plasmon resonance bands due to the formation of nanoclusters of the corresponding metal are found in the absorption spectrum of the modified layer in the AHC.

The paper was supported by the Russian Foundation for Basic Research, grant #20-02-00322

EFFECTS OF HIGH-VOLTAGE NANOSECOND PULSES ON PHYSICAL-CHEMICAL AND TECHNOLOGICAL PROPERTIES OF PYRRHOTITE AND PENTLANDITE*

I.Zh. BUNIN, I.A. KHABAROVA

Institute of Comprehensive Exploitation of Mineral Resources of the Russian Academy of Science, IPKON RAN, Moscow, Russia

In order to increase contrast between technological properties of mineral raw material, the various kinds of power influences on minerals, mineral suspensions and water, such as electrochemical, microwave treatment, electropulse, magnetic-pulse processing, the effect by accelerated electrons flow, high-power nanosecond electromagnetic pulses (HPEMP) are used. In recent years, research into the application of microwave irradiation in the comminution and flotation of ores has made great progress. Microwave irradiation promotes the oxidation of sulfide minerals during exposure, and the extent of the oxidation is an important factor in the flotation of microwave-treated sulfides. In this paper we present the main experiment results on the *nonthermal* effect of high-power (high-voltage) nanosecond pulses on the chemical surface composition and physical-chemical and technological (flotation) properties of pyrrhotite and pentlandite. Morphology, dimensions (sizes), elementary composition of new micro- and nanoformations on mineral surface of pentlandite and pyrrhotite have been investigated using up-to-date methods of Scanning Electronic Microscopy, X-ray Spectral Microanalysis (SEM–EDX) and Atomic Force Microscopy (AFM).

The nanosecond pulse generator operates at a frequency of 100 Hz (pulse repetition rate), the output pulse amplitude is ~25 kV, the duration of the leading edge of the pulse corresponds to the arrester's time to flashover and varies from pulse to pulse within 2-5 ns, and the pulse duration is the combined arrester's time to flashover and its extinction time and varies within 4-10 ns. Video pulses of a bipolar shape are generated, pulse energy ~0.1 J, electric field strength in the interelectrode gap $(0.5\text{-}1)\times10^7$ V/m, time range of the pulsed treatment of the mineral samples t_{treat}=10-150 s, i.e. $N_{imp}=(1\text{-}15)\times10^3$ HPEMP.

Using SEM–EDX, chemical analysis of the liquid phase, the stage of sequential oxidation of the surface of pyrrhotite together with the formation of oxides and hydroxides (Fig.1) and divalent and ferric sulfates under HPEMP-irradiation are established; whereas the formation of elemental sulfur on pentlandite observed. This effect provides the contrast of electrochemical, sorption and flotation properties of pyrrhotite and pentlandite.

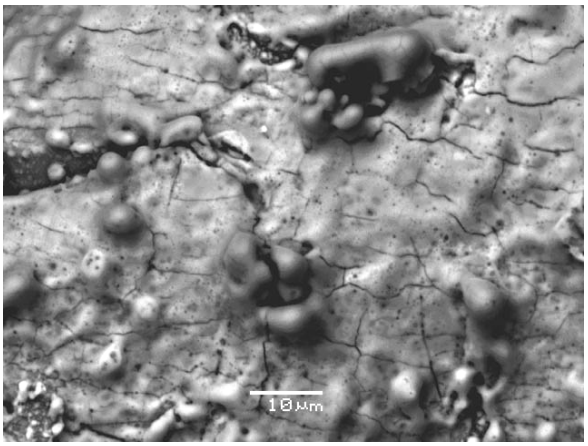

Fig.1. SEM-images of new products (probably iron oxides or hydroxides) on a surface of pyrrhotite as a result of HPEMP treatment.

HPEMP caused a different change in the electrode potential of minerals: an increase in the negative value of the electrode potential of pyrrhotite and an increase in the positive value of the pentlandite potential. The shift of the pentlandite electrode potential to the region of more positive values increased the anionic collector adsorption and the hydrophobization of the mineral surface. The transition of the pyrrhotite potential to the region of negative values prevented the xanthate adsorption and decreased the mineral floatability. For monomineral flotation of pyrrhotite and pentlandite, we established the optimal mode of preliminary electromagnetic pulsed processing of minerals (t_{treat} =10 s, $N_{imp}=10^3$), at which the contrast of their flotation properties increases in the mean on 20%.

* The work was supported by the Russian Foundation for Basic Research under grant No. 15-35-20598 mol-a-ved.

RESEARCH OF HYPEREUTECTIC SILUMIN`S STRUCTURE AND PROPERTIES AFTER MODIFICATION BY ELECTRON BEAM*

M.E. RYGINA[1,2], *E. PETRIKOVA*[2], *A. TERESOV*[2], *M. VOROBYOV*[2]

[1]*National Research Tomsk Polytechnic University, 30, Lenin ave., Tomsk, 634050, Russia*
[2]*Institute of High Current Electronics SB RAS, 2/3, Akademichesky ave., Tomsk, 634055, Russia*

Silumin is the alloy of aluminum and silicon. Used for the manufacture of bearings and pistons. In this work, AK22 alloy is considered, the silicon content of which is (22-24) wt.%. The main disadvantages of this alloy are the presence of primary silicon grains, inclusions of intermetallic compounds and gas pores [1]. The processing of metals and alloys by the electron beam pulse on the "SOLO" (IHCE SB RAS) [2] allows the formation of a submicro-nanocrystalline structure in the surface layer due to high (up to 106 K / s) cooling rates.

The aim of this work is to study the structure and properties of a hypereutectic silumin treated by pulsed electron beam of submillisecond exposure duration.

The research material was hypereutectic silumin (22-24 wt.% Si). After preliminary preparation, the samples were irradiated by the "SOLO" installation. Irradiation parameters: accelerated electron energy 18 keV, electron beam energy density 30 J / cm^2, pulse repetition rate 0.3 s^{-1}, pulse duration of the electron beam 150 μs, number of irradiation pulses 5. The irradiation mode was selected according to thermal calculations [3]. After modification, the samples were subjected to a tensile test (Instron 3369 installation) in accordance with GOST 1497-84.

In the silumin`s surface layer modified structure was formed after irradiation by pulsed electron beam.. It was characterized by the absence of micropores, primary silicon grains, and intermetallic inclusions (Figure 1) . The surface mircohardness was 18,000 MPa, which is more in 2.5 times than the hardness of the untreated sample.

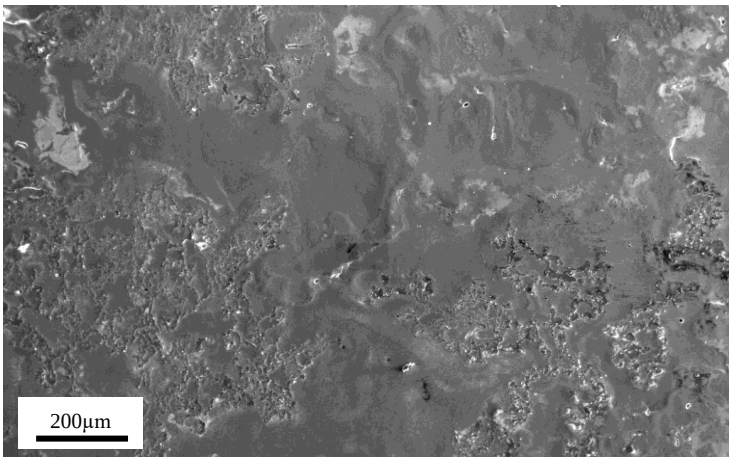

Fig.1. SEM image of the hypereutectic silumin surface (30 J / cm^2, 150 μs, 0,3s^{-1}, 5 imp.)

Tensile tests showed that after modification (30 J / cm^2, 150 μs, 0,3s^{-1}, 5 imp.), the yield strength of silumin increases in 1.5 times compared with the untreated samples.

Thus, irradiation of hypereutectic silumin samples with an intense pulsed electron beam eliminates surface macrodefects, dissolves coarse inclusions of primary silicon and intermetallic compounds, and increases the hardness and yield strength of the material.

REFERENCES

[1] Belov N.A., Savchenko S.V., Hvan A.V. Phase composition and structure of silumins: a reference publication. Moskow: MISIS. - 2007.

[2] N.N. Koval, Yu. F. Ivanov, " Nanostructuring of the surface of ceramic-metal and ceramic materials during pulsed electron-beam processing," Izv. Vyssh. Uchebn. Zaved. Fiz., V. 51, no 5, pp 60-70, 2008.

[3] [3] Yu.F. Ivanov, E.A Petrikova, O.V. Ivanova, I.A..Ikonnikova, A.V.Tkachenko, "Numerical simulation of the temperature field of silumin irradiated by an intense electron beam," Izv. Vyssh. Uchebn. Zaved. Fiz., V. 58, no 4, pp. 46-51, 2015.

*The work was supported by the Russian Science Foundation (project No. 20-79-10015)

MORPHOLOGY SPHERICAL PARTICLES OBTAINED PROCESSING AGGLOMERATES OF SYCATE COMPOSITION IN PLASMA JET*

V.V. SHEKHOVTSOV, O.G. VOLOKITIN

Tomsk State University of Architecture and Building, Salt Sq., 2, Tomsk, 634003, Russia, shehovcov2010@yandex.ru, +79138722777

During the global financial crisis, the guarantee of an intensive economic recovery in Russia is the development of priority industries, including the production of building materials. Analyzing the limitations in traditional technological processes for the production of building materials and composite coatings, one can identify a number of significant shortcomings that do not allow the use of standard methods and raw materials. The ratio of low density and high strength distinguish microspheres as a promising product in the market of building materials. To date, there are many methods and compositions for producing microspheres of various structures (hollow, dense). All methods are reduced to heat treatment of prepared powders of different compositions [1, 2]. Figure 1 presents optical microscopy images of processed agglomerated powders based on the ash residue of a state district power station with a fraction of 90–100 μm at various plasma flow rates of 0.5–1.5 g/s [3-5].

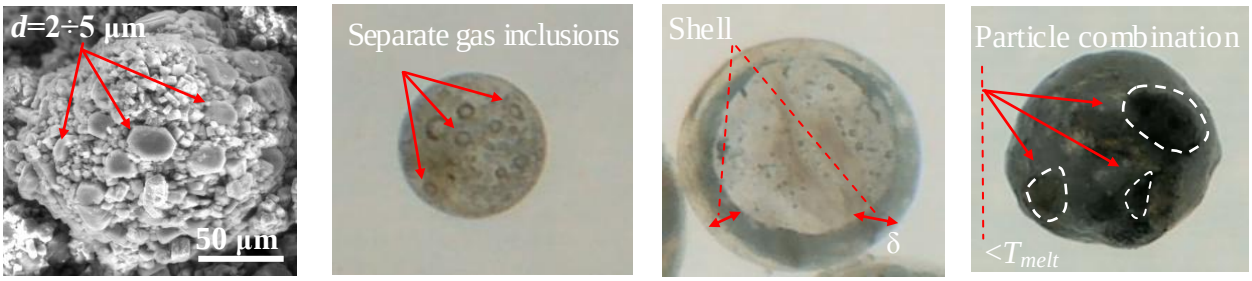

Fig. 1. Optical microscopy images of the treated agglomerated powder based on the ash residue of a state district power station in a plasma jet with a fraction of 90÷ 100 μm: *a* - agglomerated particle; *b* - dense microsphere with individual gas inclusions in the surface layer; *c* - hollow microsphere; *d* - vitrified agglomerate

At a minimum flow rate of 0.5 g/s, particles are overheated, followed by the formation of dense microspheres with individual gas inclusions in the surface layer. At a flow rate of 1.0 g/s, a rational heating mode is carried out, contributing to the formation of a hollow microsphere with a wall thickness of 4 ÷ 5 μm. An increase in flow rate to 1.5 g/s leads to vitrification of the surface of the agglomerate, a thin film ≤ 1 μm is formed, the diameter and density of the particles are under initial conditions. It should be noted that the process of structure formation of the obtained microspheres with a dense and hollow structure at a plasma-forming gas flow rate of 0.5 ÷ 1.0 g / s can be considered completed due to the clarification of the glass melt, during which the homogenized mass is rationally cooled by eliminating the barrier thermal stresses.

As a result of the studies, the technological aspects underlying the creation of an industrial technology for the production of microspheres from agglomerated oxide compounds with melting points from 1900 to 2300 K based on natural and technogenic materials have been established.

REFERENCES

[1] Gulyaev I. Experience in plasma production of hollow ceramic microspheres with required wall thickness. Ceramics International. 2015. V. 41. № 1. P. 101-107.

[2] Arkhipov V.A., Kozlov E.A., Zharova I.K., Titov S.S., Usanina A.S. Evolution of liquid-drop aerosol cloud in the atmosphere. Arabian Journal of Geosciences, 2016. V. 9. № 2. P. P. 114.

[3] Shekhovtsov V.V., Vlasov V.A., Volokitin G.G., Volokitin O.G. The use of low-temperature plasma to obtain ash microspheres. Russian Physics Journal. 2016. V. 59. No. 9-3. P. 305-308.

[4] Vlasov V.A. , et al. Calculation of the melting process of a quartz particle under low-temperature plasma conditions / V.A. Vlasov, O.G. Volokitin, G.G. Volokitin, N.K. Skripnikova, V.V. Shekhovtsov / Journal of Engineering Physics and Thermophysics. 2016. Vol. 89. № 1. P. 152-156.

[5] Vlasov V.A. , et al. Physical processes of SiO_2 spherical particle formation in thermal plasma flow / V.A. Vlasov, V.V. Shekhovtsov, O.G. Volokitin, G.G. Volokitin, N.K. Skripnikova, A.A. Klopotov // Russian Physics Journal. 2018. Vol. 61. No. 4. P. 708-714.

* The reported research was funded by Russian Foundation for Basic Research and the government of the region of the Russian Federation, grant № 18-48-703004

GAS SATURATION OF HOLLOW SUBSTANDARD PARTICLES IN PLASMA JET DUE TO EVAPORATION OF ITS OWN CONDENSED PHASE*

V.V. SHEKHOVTSOV, O.G. VOLOKITIN, N.K. SKRIPNIKOVA, M.A. SEMENOV, V.A. VLASOV

Tomsk State University of Architecture and Building, Salt Sq., 2, Tomsk, 634003, Russia, shehovcov2010@yandex.ru, +79138722777

Considering the processes of gas saturation of hollow substandard particles during active heating in a high-energy environment, it is necessary to distinguish two groups of factors. The first group of factors includes parameters related to the structural features of the initial particles introduced into the stream. Such parameters that make a fundamental contribution include the content of open and closed intergranular pores, their size and the presence of a concentration of fusible components in the composition. The second group of factors is associated with the interaction of the carrier medium with particles (mass transfer). Due to the fact that the main factor of gas saturation, nevertheless, is the structural features of the initial particles, the gas saturation of hollow particles under the influence of evaporation of the condensed phase during heating is estimated. Figure 1 shows the transition of condensed phases to gaseous ones (the software package [1] allows you to set all possible phases for a given composition, which allows an objective assessment of gas saturation) when heating hollow substandard particles. As a model composition, ash and slag waste was used, which is represented by silicon oxide and aluminum oxide (56.25% and 21.84%, respectively).

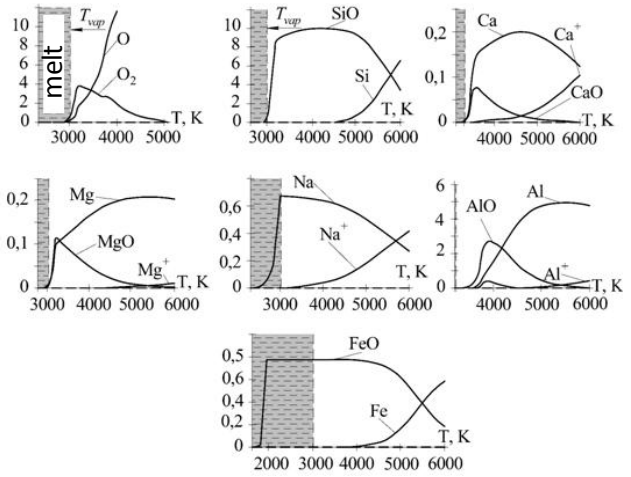

Fig. 1. The formation of gaseous phases during heating of a multicomponent oxide system in a wide temperature range

According to the results of thermodynamic modeling, the dynamics of the formation of gaseous phases during the heating of a multicomponent oxide system in a wide temperature range is established. Due to the fact that relaxation (formation of a stable liquid phase) of agglomerated particles is achieved in the temperature range from 1993 to 2750 K and the mass loss of the condensed phase does not exceed less than 1 wt. % the level of gas saturation due to partial evaporation of the condensed phase is observed at a level of not more than 1 wt. % Considering the region of a stable state of the liquid phase (1993 ÷ 2750 K) based on the oxide system under consideration, the gas saturation of a hollow droplet is achieved due to the incoherent evaporation of minerals represented by the initial Fe_2O_3 and Na_2O oxides. The studied range of heating temperatures showed the presence of atomic and molecular particles capable of contributing to the gas saturation of the hollow microsphere with pores of FeO and Na, but it should be noted that oxides are evaporated both on the surface and in the volume of the hollow particle and in the shell (the difference between the inner and the outer diameter of the drop).

REFERENCES

[1] Belov, G.V. Thermodynamic modeling of chemically reacting systems [Text] / G.V. Belov, B.G. Cowards. Moscow: MSTU named after N.E. Bauman, 2013.– 96 p.

* The reported research was funded by Russian Foundation for Basic Research and the government of the region of the Russian Federation, grant № 18-48-703004

MATHEMATICAL SIMULATION OF THE PROCESS OF CREATING THE SILICA PARTICLES MORPHOLOGY IN PLASMA FLOW

V.A. ARKHIPOV[1], V.D. GOL'DIN[1], V.V. SHEKHOVTSOV[2], N.N. ZOLOTOREV[1]

[1]Tomsk State University, Tomsk, Russia
[2]Tomsk State University of Architecture and Building, Tomsk, Russia

Today the progress in thermal processing of multicomponent powder materials for production of small hollow spheres (with the diameter of tens microns) remains a topical problem because those particles have many applications in different industries [1]. A promising approach for powder treatment is the heating with plasma flow. It has a high energy density and the working temperatures in the range (3000–10000)°C. The plasma technologies are available for production of hollow ceramic microspheres made from zirconium dioxide powder, silicon dioxide and other materials, as well as spray pyrolysis technology for synthesis of metal oxide powders from precursor solutions [1–5].

The presented report is focused on mathematical simulation of the process of plasma-aid production of hollow silica microparticles. The first part of this study deals with dynamics, heating, and melting of primary powder in the plasma flow as a function of diameter and porosity of initial particles. The second part of the research deals with processes of creating the hollow particle morphology in the plasma flow.

In contrast to the known models [1–5], the proposed physical and mathematical model of the formation of hollow microspheres at heating and melting the porous silica particles (precursor) in the flow of low-temperature plasma takes into account the partial encapsulation of the gas during the formation of the shell from the molten metal.

The solid particles of SiO_2 (with air in pores) are fed to the high-temperature zone (plasma flow). We take the following assumptions in the simulation problem:

– gas flow (a turbulent nonisothermal submerged jet) is uniform and steady;

– the temperature and velocity of gas over the plasma jet length are known;

– gas pressure is constant over the jet length and equals the atmospheric pressure: $p_g = p_{atm} = \text{const}$;

– SiO_2 porous particles are almost spherical; we know the diameter D, volumetric porosity P_{po}, initial temperature T_{po}, and the velocity u_{po} of injected particles;

– pores in the particles are filled with air with the parameters corresponding to initial conditions $T_g = 293$ K, $p_g = p_{atm}$;

– volumetric concentration of particles $C_V < 0.02$;

– after the particles enter the high temperature gas flow, they evolve during the four stages. The first stage is particle heating from the initial temperature T_{po} to the melting temperature T_{melt}; meanwhile, all air captured in the pores undergoes thermal expansion and it releases through the open pores. The second stage is the formation of the primary coating. When a porous particle is heated to the melting temperature, a liquid coating of molten particulates is produced. This liquid coating captures a certain amount of air. The remained air coalescences into a single spherical cavity. The third stage is the formation of the final coating. During the fourth stage, liquid coating undergoes amorphous solidification (after the particle exits the high temperature zone).

REFERENCES

[1] I.P. Gulyaev, O.P. Solonenko, "Modeling of the behavior of hollow ZrO_2 particles in plasma jet with regard to their thermal expansion", Thermophysics and Aeromechanics, vol. 20, no. 6, pp. 769–782, 2013.

[2] I.P. Gulyaev, "Peculiarities of production and treatment of hollow particles of zirconium dioxide in plasma flow", Vestnik Yugorskogo Universiteta, vol. 13, no. 2, pp. 10−22, 2009.

[3] V.A. Arkhipov, S.S. Bondarchuk, V.V. Shekhovtsov, O.G. Volokitin, A.S. Anshakov, V.I. Kuzmin, "Simulation of production of hollow silica particles in a plasma flow. Part 1. Dynamics of motion and heating of porous particles", Thermophysics and Aeromechanics, vol. 26, no. 1, 2019.

[4] V.A. Arkhipov, O.G. Volokotin, A.I. Konovalenko, A.S. Usanina, V.V. Shekhovtsov, "Formation of hollow ceramic particles in plasma flow", Proc. 6th Int. Cong. on Energy Fluxes and Radiation Effects (EFRE), Tomsk, Russia, p. 298, 2018.

[5] V.A. Vlasov, O.G. Volokitin, G.G. Volokitin, N.K. Skripnikova, V.V. Shekhovtsov, "Calculation of the melting process of a quartz particle under low-temperature plasma conditions", J. Eng. Phys. Thermophys, vol. 89, no. 1, pp. 152−156, 2016.

POSSIBILITY OF LOW-EROSION CONDITIONING OF LARGE VACUUM GAPS BY BREAKDOWNS USING HIGH-RESISTANCE MATERIALS*

S.A. ONISCHENKO[1], *E.V. NEFEDTSEV*[1]

[1]*Institute of High Current Electronics, Tomsk, Russia*

Breakdown conditioning is one of the traditional methods for removing uncontrolled breakdown provocateurs from the surface of electrodes (particles, dielectric films, inclusions, etc.) and stabilizing the electrical strength of vacuum insulation. The disadvantage of this method is the arising of new breakdown provocateurs, such as craters formed at the site of remote "weak sites" and solidified drops of material scattered on the surface of the electrodes. Therefore, in cases where the surface of the electrodes is preliminary carefully prepared and smoothed, it is necessary to severely limit the current of the conditioning discharge. For large vacuum gaps, it is impossible to exclude deep crater formation by increasing the ballast resistance in the voltage source circuit, since in case of disturbance of the electrical strength all the energy stored in the gap capacitance is released at the site of breakdown initiation.

In our practice, we use pre-treatment of each electrode with a low-energy high-current electron beam (LEHCEB) in the mode of melting and partial evaporation of the surface layer. After this operation (which can be compared with simultaneous conditioning of the entire electrode surface and its polishing), millimeter vacuum gaps have a record high pulsed electrical strength [1], more than 1 MV / cm. However, ideal vacuum gaps should hold-off significantly stronger fields (> 10 MV / cm).

In order to further increase the pulsed electrical strength of the vacuum gaps, in our work, we considered the method of separate conditioning of each of the electrodes in pair with a third electrode, the material of which has a high electrical resistivity. The idea was that when the two electrodes of the future electrode pair (each of which was a cathode) were separately conditioned, the current of the conditioning discharge was limited by the spreading in the high-resistance material of the anode.

In the experiment, stainless steel electrodes pre-treated with LEHCEB were used. During separate conditioning, high-resistance materials having electrical resistivity in the range of 0.5–10^8 Ω/m were used as an anode. The subsequent measurement of the electrical strength of the vacuum gaps was carried out by nanosecond voltage pulses on a separate test stand.

The paper presents the pre-breakdown characteristics of vacuum gaps with a high-resistance anode and analyzes the effectiveness of the electrodes separate conditioning method with respect to improving of vacuum insulation at various levels of conditioning current limitation.

REFERENCES

[1] S.A. Onischenko , A.S. Grenadyorov , K.V. Oskomov , E.V. Nefedtsev and A.V. Batrakov, “Short pulse dielectric strength of vacuum gaps with different electrode materials”, Proc. 27 Int. Symp. on Discharges and Electrical Insulation in Vacuum (ISDEIV), pp.64-67, 2016.

* The work was supported by the Russian Foundation for Basic Research, Project No. 18-08-00230-A.

COMBINED TREATMENT OF ELECTRODES AS A MEANS OF INCREASING THE ELECTRICAL STRENGTH OF VACUUM INSULATION*

S.A. ONISCHENKO[1], *E.V. NEFEDTSEV*[1], *G.E. OZUR*[1]

[1]*Institute of High Current Electronics, Tomsk, Russia*

One of the methods for increasing the electrical strength of vacuum insulation is the preliminary polishing of the electrodes with a low-energy high-current electron beam (LEHCEB) [1]. A specially selected mode allows us to evaporate or dissolve a significant part of the foreign inclusions in the near-surface volume of the electrode, and make the surface itself smooth. Such treatment allows to increase the pulsed electrical strength of millimeter vacuum gaps to values exceeding 1 MV/cm. However, these values remain more than an order of magnitude less than the theoretically achievable limit which due to the onset of intense field emission from a smooth and chemically pure homogeneous metal surface. A probable reason for this limitation is residual dielectric or semiconductor inclusions fixed in the matrix of the substance, creating triple points on which the electric field is concentrated.

Earlier, we pointed out the possibility of selective removal of the initial surface inclusions by separate short-pulse conditioning of stainless steel electrodes under plasma [2]. After finishing treatment the conditioned electrodes by the LEHCEB, the results were contradictory. Despite the fact that the average value of the pulsed electrical strength of the vacuum gaps practically did not change, the spread of this value increased so much that individual vacuum gaps showed record high values close to 2 MV/cm. This indicated the possibility of further work to improve the quality of vacuum insulation. Based on the short-pulse plasma conditioning method developed in [2], in this paper, additional actions were taken to stabilize the pulsed electrical strength of vacuum gaps at relatively high levels close to 2 MV/cm.

REFERENCES

[1] A.Batrakov, D.Nazarov. G.Ozur, S.Popov, D.Proskurovsky, and V.Rotshtein, IEEE Trans. Dielectr. Electr. Insul., V. 4, pp. 857–862, 1997.

[2] E.V. Nefedtsev, S.A. Onischenko, G.E. Ozur, D.I. Proskurovsky, “Improvement of Electrical Insulation in Vacuum by Comprehensive Treatment of Electrodes under Plasma”, Proc. of 28th International Symposium on Discharges and Electrical Insulation in Vacuum (ISDEIV), pp.97-100, 2018.

* The work was supported by the Russian Foundation for Basic Research, Project No. 18-08-00230-A.

NANOSECOND PULSE LASER ABLATION OF THE GLASS COMPOSITES

O.V. MKRTYCHEV[1], *V.E. PRIVALOV*[2], *V.G. SHEMANIN*[1], *N.D. SOLODILOVA*[1]

[1]*Branch of Belgorod V G Shukhov State Technology University, Novorossiisk, Russia*
[2]*Peter the Great Saint-Petersburg Polytechnic University, Saint-Petersburg, Russia*

The laser ablation [1–3] is the basics of the laser materials processing and can be applied to the laser surface modification due to its high energy flux [4, 5]. The major problems of the laser ablation studies is the stochastic character of the ablation destruction process [6]. It is caused by the spatial probable distribution of the absorbing defects and these defects various characteristics. The different values of the laser breakdown threshold can be appear from the probable character of the plasma plume formation and the strong dependence of the destruction threshold values versus the volume size of the laser radiation interaction with the sample area.

This work purpose is the experimental study of the laser ablation threshold energy density of the glass composites of the various structure under the pulse YAG-Nd^{3+} laser radiation action and the laser ablation threshold parameters dependences from these composites optical and physical properties.

The laser ablation destruction threshold energy density values measurements have been fulfilled for the glass composites experimental studies at the laboratory laser ablation station created on the basis of experimental setup in [2, 5]. The YAG-Nd laser generates pulses at the 1064 nm wavelength with time duration of 20 ns and pulse energy up to 80 mJ.

The threshold energy density in nanosecond range versus the light transmittance values dependences for the silicon dioxide samples have been approximated by the second power polynomial expression. The laser destruction threshold energy density F_b value decreases with the samples light transmittance T growth for the silicon dioxide nanofilms in 20 ns laser pulse time duration regime. This fact may be explained by the difference in the oxide films refractive index values that determines the light scattering and absorption in the sample.

In the reference to the previous case the laser destruction threshold energy density F_b value is nearly constant with the samples light transmittance T growth in our experimental error of 12% for the titanium dioxide films in 20 ns laser pulse time duration. These results may be explained by all of these samples refractive index high value of 1.97 that was depends on their chemical composition and structure.

At the same time it can be caused by the various absorbing characteristics of the defects at the film surfaces. The surface nonideality and similar absorbing defects in the films initiate the laser ablation destruction by the thermoelastic mechanism [6, 7]. But the laser ablation destruction results in the craters or cracks on the sample surface. The different geometrical and physical characteristics of the absorbing defects do not allow to describe exactly the origin and the morphological feature of the composites destruction and the breakdown threshold energy density values dependence on the thermophysics characteristics of the composites. These data are the basic for the composites optical resistance estimation.

REFERENCES

[1] A.B. Atkarskaya, O.V. Mkrtychev, V.E. Privalov and V.G. Shemanin, Optical Memory and Neural Networks (Information Optics), vol. 23, no. 4, Article Number 265, 2014.

[2] E.I. Voronina, V.P. Efremov, V.E. Privalov, P.V. Charty and V.G. Shemanin, Tech. Phys., vol. 79, no. 5, Article Number 145, 2009.

[3] E.I. Voronina, V.P. Efremov, V.E. Privalov and V.G. Shemanin, Tech. Phys., vol. 34, no. 23, Article Number 59, 2008.

[4] A.B. Atkarskaya, O.V. Mkrtychev and V.G. Shemanin, Izvestiya VUZov. Physics, vol. 55, no. 8/2, Article Number 238, 2012 (in Russian).

[5] V.P. Efremov, V.E. Privalov, P.V. Skripov, P.V. Charty and V.G. Shemanin, Proc. SPIE, vol. 5447, Article Number 234, 2004.

[6] M.F. Koldunov, A.A. Manenkov and I.L. Pokotilo, Quant. Electron., vol. 25, no. 9, Article Number 833–837, 1998.

[7] S.I. Anisimov and B.S. Lukyanchuk, Phys.-Usp., vol. 172, no. 3, Article Number 301–333, 2002.

ANALYSIS OF THE STRUCTURE AND MICROHARDNESS OF CASTING ALLOYS AL-11SI-2CU AND AL-5SI-1.3CU AFTER ELECTRON-BEAM SURFACE MELTING*

D.V. ZAGULIAEV[1], *YU.F. IVANOV*[2], *A.D. TERESOV*[2], *I.I. CHUMACHKOV*[1], *A.A. LEONOV*[2]

[1]*Siberian State Industrial University, Novokuznetsk, Russia*
[2]*Institute of High Current Electronics SB RAS, Tomsk, Russia*

Currently, internals combustions engines produced most of the mechanical energy. They are the most common power units and are used both in small hand tools and in the aviation industry [1].

During engine operation, its parts experience intense external influences, such as high temperatures of working gases, loads from inertia and friction forces, etc [2]. Because, pistons are manufactured from aluminium and Al-based alloys [3], intense external influences leads to scuff on the piston skirt [4, 5]. A perspective method of aluminium-silicon casting alloy modification is the pulse electron beam processing in the milting regime [6-7].

In this context, the purpose of the research is to electron-beam treatment as a method of surface modification, allowing increase surface hardness of piston alloys Al-11Si-2Cu and Al-5Si-1.3Cu due to structural phase modification.

Casting alloys Al-10Si-2Cu and Al-5Si-1.3Cu was used as the materials under study. Chemical composition of the first alloy (wt%): Al - 84.88, Si - 11.10, Cu - 2.19, Ni - 0.92, Mg - 0.58, Fe - 0.25, Ti - 0.05, Mn - 0.02, Cr - 0.01. Chemical composition of the second alloy (wt%): Al - 90.50, Si - 5.39, Cu - 1.33, Ni - 0.07, Mg - 0.64, Fe - 0.64, Ti - 0.03, Mn - 0.24, Cr - 0.03.

Surface melting was carried out with electron-beam on the help of a SOLO unit [8]. Electron beam parameters were set: energy of accelerated electrons 17 keV, electron beam energy density 10, 30, and 50 J/cm^2, pulse duration 50 and 200 μs.

It has been established that maximum microhardness value (950 MPa) of Al-5Si-1.3Cu alloy surface layer is observed at pulse duration of 50 μm and energy density of electron beam of 50 J/cm^2 that increases the initial material microhardness by 83%. The irradiation results in the complete dissolution of intermetallide and silicon particles in the surface layer. In the volume of grains a structure of high-speed cellular crystallization whose dimensions vary in the limits of 500-800 nm is formed that, in our opinion, is the reason for the increase in the strength properties of the material.

The research has pointed out a thickness of the modified layer in Al-10Si-2Cu alloy to depend directly on a beam energy density, being 1-2 μm at 10 J/cm^2, 25-30 μm at 30 J/cm^2, and 60-90 μm at 50 J/cm^2, and not connected with a pulse time (50 or 200 μs). If irradiated in mode 50 J/cm^2 has been established that a surface layer has a structure of high-speed cellular crystallization with cells in a range from 500 to 650 nm.

A relation between microhardness and beam energy density is non-monotonous for various pulse times, e.g. in comparison to the as cast state microhardness decreases at an energy density of 10 J/cm^2, a further raise of a beam energy density up to 20-50 J/cm^2 increases microhardness, which is maximal (1.16 GPa) for a beam energy density of 40 J/cm^2 and pulse time 200 μs. The study has revealed no dependence of microhardness upon the pulse time of an electron beam.

REFERENCES

[1] A. Alagumalai, “Internal combustion engines: progress and prospects”, Renew. Sustain. Energy. Rev., vol. 38, pp. 561-571, July 2014.

[2] R. S. Benson, N. D. Whitehouse, “Internal combustion engines: a detailed introduction to the thermodynamics of spark and compression ignition engines, their design and development,” New York: Pergamon Press, 1979.

[3] M. Javidani, D. Larouche, “Application of cast Al-Si alloys in internal combustion engine components,” Int. Mater. Rev., vol. 59, no. 3, pp. 132–158, March 2014.

[4] J. B. Heywood, “Internal combustion engine fundamentals,” New York: McGraw-Hill., 1988.

[5] H. N. Gupta, “Fundamentals of internal combustion engines”, New Delhi: Prentice-hall of India, 2006.

[6] Y. Hao, B. Gao, G. F. Tu, H. Cao, S. Z. Hao, C. Dong, “Surface modification of Al-12.6Si alloy by high current pulsed electron beam,” Appl. Surf. Sci., vol. 258, no. 6, pp. 2052–2056, January 2012.

[7] L. Zhao, S. Wang, Y. Jin, Y. Chen, “Microstructural characterization and mechanical performance of Al-Cu-Li alloy electron beam welded joint,” Aerosp. Sci. Technol., vol. 82–83, pp. 61-69, November 2018.

[8] D. V. Zaguliaev, S. V. Konovalov, Yu. F. Ivanov, V. E. Gromov, E. A. Petrikova, “Microstructure and mechanical properties of doped and electron-beam treated surface of hypereutectic Al-11.1%Si alloy,” J. Mater. Res. Technol., vol. 8, no. 5, pp. 3835–3842, October 2019.

* The work was supported by the Russian Science Foundation (RSF) [project № 19-79-10059].

MANAGING THE TEXTURAL PROPERTIES OF CAF_2 NANOPOWDERS*

O.A. ZLYGOSTEVA[1,2], *S. YU. SOKOVNI*[1,2] , *V. G. ILVES*[1]

[1]*Institute of Electrophysics Ural Branch Russian Academy of Sciences, Yekaterinburg, Russia*
[2]*Ural Federal University, Yekaterinburg, Russia*

The application of nanopowders (NPs) depends on their textural properties, such as specific surface area (S_{BET}), nanoparticle size and shape, volume and shape of pores [1]. The ability to control these properties will make it possible to set the optimal parameters of nanomaterials and expand the range of NP's applications.

The alkaline earth metal nanofluorides are the promising materials for the use as catalysts, photonics materials, optical ceramics precursors, and materials for biomedical applications [2]. In this study, the methods of managing textural properties of CaF_2 NPs are investigated. The researched NPs were synthesized by pulsed electron beam evaporation in vacuum using a pulse-periodic accelerator URT-1M [3]. The researched methods include heating and irradiation of NPs with relativistic electrons.

Before irradiation, CaF_2 NPs were annealed in alundum crucibles at a temperature of 200, 400, and 900 °C for 10 min. Then, NPs were irradiated for 15 and 30 minutes. The absorbed doses (AD) on the surface of the samples were 31.5 and 63 MGy, respectively.

The S_{BET}, pore volume and size of the nanopowders were determined by the Brunauer–Emmett–Taylor and Barrett-Joyner-Halenda (BET-BJH) method. A numerical evaluation of the number of pores on the surface area and the number of pores in the total pore volume was performed. The proportion of pore area to the total surface area was calculated as the ratio of the pore surface area to the S_{BET}.

The textural analysis showed that the CaF_2 NPs have mesoporous type.

A significant increase in the S_{BET} of unirradiated CaF_2 NPs was observed after annealing at a temperature of 200 °C, while annealing at 900 °C led to an increase in particle size and loss of mesoporosity.

Irradiation led to a significant increase in the S_{BET} of the NPs and unexpectedly affects the total volume and average pore diameter — these values increased and evened out, especially at 31.5 MGy AD. Notably, a similar increase in the S_{BET} was previously observed during the annealing of BaF_2 NPs. [4].

Generally, the nature of the change in the evaluated properties of CaF_2 NPs is nonlinear. The number of pores of irradiated samples that were not subjected to heating remains virtually stable, which indicates that all processes have occurred with pore-filling.

Thus, it was found that annealing at low temperatures (without loss of mesoporosity) of NPs and irradiation with relativistic electrons can be considered as the methods for managing the textural properties of NPs, and the difference in the effects of these methods is normalization of the textural properties of NPs after irradiation.

REFERENCES

[1] S.W. Shin, I.H. Song, S.H. Um, "Role of Physicochemical Properties in Nanoparticle Toxicity", Nanomaterials (Basel, Switzerland), vol. 5, no. 3, pp. 1351–1365, September 2015.

[2] P.P. Fedorov, A.A. Luginina, S.V. Kuznetsov, V.V. Osiko, "Nanofluorides", Journal of Fluorine Chemistry, vol. 132, no. 12, pp. 1012-1039, December 2011.

[3] S.Y. Sokovnin, M.E. Balezin, "Repetitive nanosecond electron accelerators type URT-1 for radiation technology", Radiation Physics and Chemistry, vol. 144, pp. 265-270, March 2018.

[4] S.Yu. Sokovnin, V.G. Il'ves, S.V. Zayatsa, M.G. Zuev, "Properties of compacts of barium fluoride nanopowder produced by pulsed electron beam evaporation", Ceramics International, vol.45, no. 13, pp. 16591-16599, September 2019.

* The work was partially supported by the Russian Foundation for Basic Research and the Sverdlovsk Region in the framework of the scientific project No. 20-48-660019

FORMATION OF COATINGS BASED ON VANADIUM BORIDES ON DIE STEEL D5 ELECTRON BEAMS IN VACUUM*

A.S. MILONOV, D.E. DASHEEV, N.N. SMIRNYAGINA.

Institute of Physical Materials Science SB RAS, Sakhyanovoy str., Ulan-Ude, 670047, Russia, terwer81@mail.ru, +7 (301-2) 43-31-84.

The work considers the features of surface hardening of die steel D5 under the influence of powerful electron beams due to the formation of layers based on vanadium borides. The experiments used a vacuum electron beam installation "SOLO", created in IHCE SB RAS, which is based on an electron source with a plasma cathode based on a pulsed low-pressure arc discharge with grid stabilization of the cathode plasma boundary.

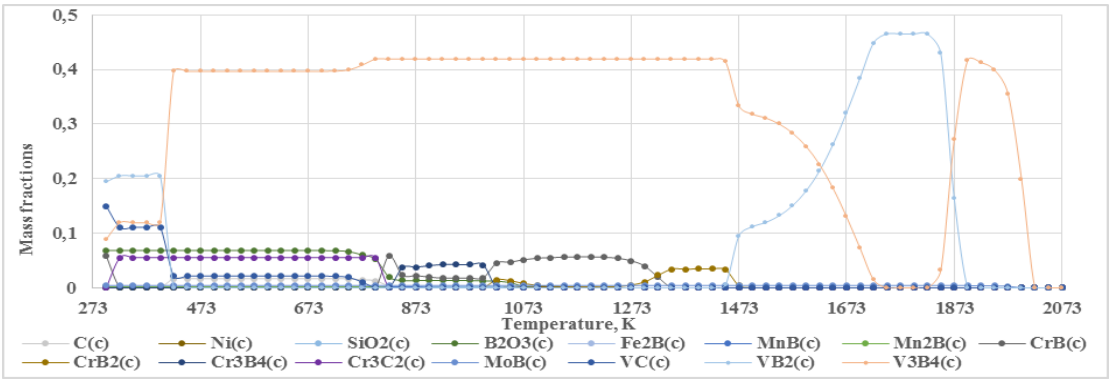

Fig.1. The yield of condensed phases in the synthesis of boride V_3B_4 on D5 steel (C1.5Si0.4Mn0.4Ni0.4Cr12Mo0.5V0.3Fe84+V47.44B13.43C16.78O22.35+B19)

Thermodynamic calculations showed that boride V_3B_4 using the stoichiometric mixture V_2O_3-B-C cannot be obtained due to the formation of iron borides Fe_2B, FeB (interaction with the metal base) and borides of alloying elements (CrB_2, MnB, MoB). The introduction of excess amount of boron made it possible to choose the optimal compositions for the preparation of composite layers with the maximum yield of borides. To do this, vary the concentration of boron in the mixture of 50-50 (C1.5Si0.4Mn0.4Ni0.4Cr12Mo0.5V0.3Fe84+V47.44B13.43C16.78O22.35). We find the consumption of boron for a maximum output of V_3B_4 19 wt% (Fig. 1)

Analysis of the thermodynamic calculations made it possible to determine the optimal conditions for the interaction of the V_2O_3:B:C reaction mixture with the surface of die D5 steel for forming the composite coating to a depth of 5-100 μm.

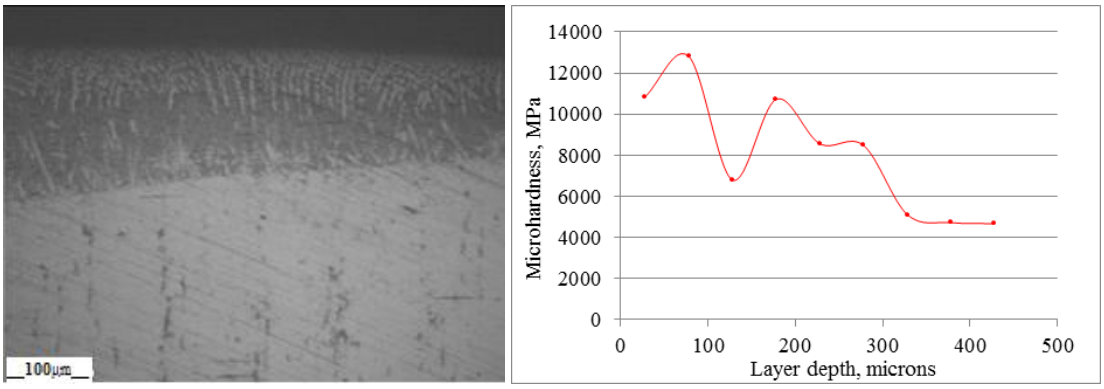

Fig.2. Structure and microhardness of V_3B_4 layers on D5 steel ($P = 10^{-3}$ Pa)

In figure 2 shows the measurement of the microhardness of the vanadium boride layers with a step of 30-50 microns. An uneven distribution of microhardness in thickness was found. Some very rare inclusions have HV≈13000 MPa and are located in the surface zones of the layer.

* The work was supported by the Russian Science Foundation under grant No. 16-48-030875 r-a.

ACTIVE SCREEN PLASMA HYTROGEN FREE PLASMA NITRIDING STEEL*

V.O. OSKIRKO, I.M. GONCHARENKO, A.N. ZAKHAROV, A.P. PAVLOV, S.V. RABOTKIN, A.S. GRENADEROV

Institute of High Current Electronics, 2/3 Akademicheskii Ave., Tomsk, 634055, Russia

The paper presents the results of experiments on active screen plasma nitriding (ASPN) treatment of steel AISI 5140. Previously, the authors of [1] have already shown that nitriding of AISI 5140 steel can be performed in a system with an active screen in an NH_3 environment. In this paper, the formation of a diffusion layer in a similar system was provided without the use of hydrogen. Two nitriding regimes are compared, in which the samples were processed inside the active screen and kept at either cathode potential or at floating potential. After processing for 3 hours at a temperature of 550 ° C, a uniform diffusion layer with a total thickness of approximately 150 μm was formed on the surface of the samples kept at floating potential. On the surface of samples kept at the cathode potential, an increase in hardness was detected only on the area of the outer ring with a width of ~ 1 mm along the edge of the disk. Fig. 1.a shows the distribution of microhardness by the depth at a distance of ~ 0.3-0.4 mm from the edge of the round surface of the samples. The treated sample kept at a floating potential has a higher hardness at a depth of 25-75 microns from the surface. The difference in the uniformity of processing is visible to the eye. On the treated sample, which was kept at the cathode potential (photo in Fig. 1.b.), rings were formed that are characteristic of the technology of standard nitriding in a glow discharge. On the treated sample, which was kept at floating potential, no rings are observed, and the surface in the center and on the edge has the same gray color. The surface hardness does not change from the edge to the center of the sample and amounts to HV~ 800 kgf/mm^2.

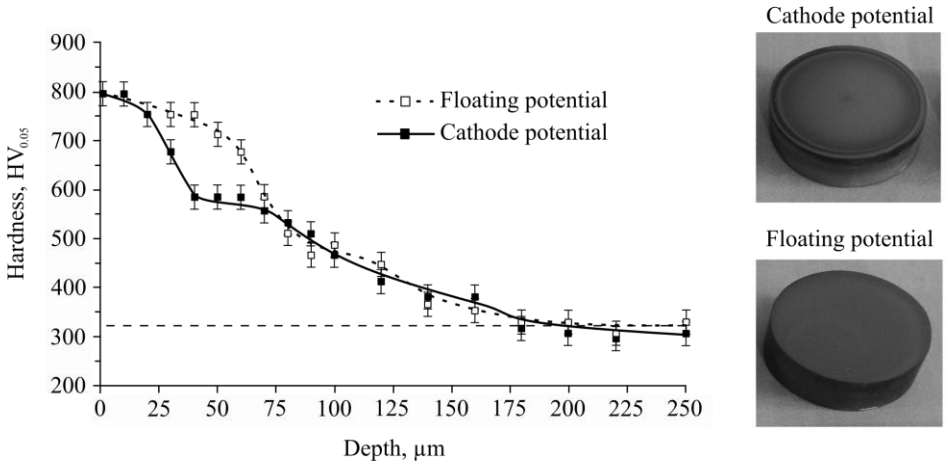

(a) (b)

Fig. 1. The distribution of microhardness by the depth (a), photos (b) of nitrided samples kept at cathodic and floating potential in the ASPN system.

REFERENCES

[1] *L. Wang, Y. Li, X. Wu* // Applied surface science – 2008. – V. 254, pp. 6595-6600.

* The work was funded by Russian Foundation for Basic Research and the government of the Tomsk region of the Russian Federation, grant № 18-42-703005

RESIDUAL STRESSES IN VT6 TITANIUM ALLOY AFTER FEMTOSECOND LASER PROCESSING*

M.V. ZHIDKOV[1], *N. A. SMIRNOV*[2], *J. CHEN*[2], *S. I. KUDRYASHOV*[2]

[1]*Belgorod National Research University, Belgorod, Russia*
[2] *Lebedev Physical Institute, Russian Academy of Sciences, Moscow, Russia*

In our work VT6 (Ti6Al4V) titanium alloy samples were surface treated by femtosecond laser pulses (τ=320 fs, λ=1030 nm). An impulse frequency of 400 kHz and a scanning speed of 100 mm/s were used. Surface topography, elemental composition, and structural-phase state of the surface-modified layers were studied by scanning electron microscopy and X-ray diffraction analysis.

It was found that femtosecond laser processing leads to the formation of laser-induced periodic surface structures (LIPSS) on the surface of VT6 titanium alloy (Fig. 1a). The period of the structures depends on the number of pulses (N) and the energy density (F_0).

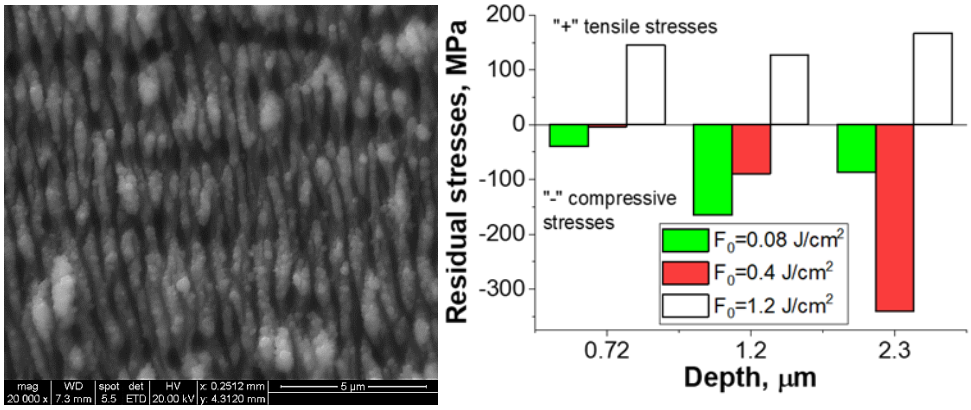

a b

Fig.1. Topography of surface of VT6 titanium alloy samples after fs laser treatment (F_0=0.4 J/cm^2, N=100) (a) and residual stresses distribution in near-surface layers of samples of VT6 alloy after femtosecond laser processing (b)

It is shown that laser processing with energy densities 0.08 and 0.4 J/cm2 leads to the formation of compressive residual stresses in the surface layers (up to 2.3 μm). After processing with 1.2 J/cm2, tensile residual stresses are formed in the surface layers of the VT6 titanium alloy.

* The study was carried out with a grant from the Russian Science Foundation (project No. 19-79-00257)

EFFECTIVENESS OF ELECTRON RADIATION APPLICATION FOR PRESEEP TREATMENT OF SPRING WHEAT

N.N. LOY[1], N.I. SANZHAROVA[1], S.N. GULINA[1], M.S. VOROBYEV[2], O.V. SUSLOVA[1], T.V. CHIZH[1]

+7(903)812-70-33, e-mail: loy.nad@yandex.ru
[1]RIARAE, Obninsk, 249032, Kaluga region, Kiev highway, 109 km, Russia
[2]IHCE SB RAS, Tomsk, 634055, 2/3 Akademichesky Avenue, 2/3, Russia

Ecological farming is looking for new, more effective elements of the fight against pathogenic organisms that provide quality indicators of grain and its environmental safety without the use of pesticides. When growing grain, these methods include presowing irradiation of seeds with ionizing radiation [1].

We have previously shown that pre-sowing irradiation of spring barley seeds of the cultivar Vladimir with a low-energy electron beam in the dose range from 1 to 8 kGy contributed to a decrease in the development of helminthosporiosis on seedlings depending on the dose of radiation and the post-radiation period [1, 2].

Studies on presowing irradiation of spring wheat seeds of the Setora variety on the Duet electronic accelerator in the dose range from 1 to 5 kGy and dose rates of 100 and 500 Gy / imp. Allowed us to establish that the degree of damage to seedlings by *Helmintosporium sativum*, as well as the prevalence of the disease, decreased 2 times at doses of 4 and 5 kGy (post-radiation period of 7 days) and 2-7 times at 3 and 5 kGy (post-radiation period of 14 days) at a dose rate of 100 Gy / imp, and also decreased 2 times at a dose of 5 kGy (post-radiation period of 14 days) at a dose rate of 500 Gy / imp. (Fig. 1).

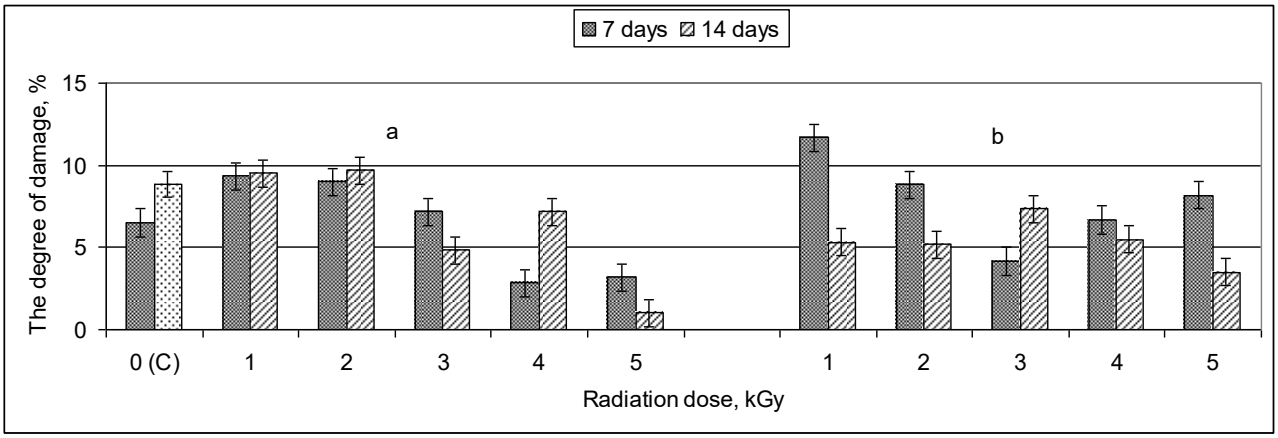

Figure 1. The effect of radiation on the defeat of wheat *Helminthosporium sativum* depending on the post-radiation period and dose rate (a - 100 Gy / imp., b - 500 Gy / imp.)

It was shown that electron irradiation contributed to an increase in laboratory germination of seeds by 3-10% at doses of 3-5 kGy (radiation dose rate of 100 Gy / imp), sprout length - by 17-37% at doses of 1-5 kGy (dose rate of 500 Gy / imp), root lengths - by 13-15% at doses of 2-4 kGy (power 500 g / imp).

Thus, as a result of the studies, it was found that pre-sowing electron irradiation of Setora spring wheat seeds reduces the degree of damage and the prevalence of the disease depending on the radiation dose, dose rate and post-radiation period and causes an increase in laboratory germination, the length of the sprout and root of seedlings.

REFERENCES

[1] *Chizh T.V., Loy N.N., Pavlov A.N., Vorobyev M.S. and Doroshkevich S.Yu*. Low-energy electron beams for protection of graincrops from insect pests and diseases. IOP Conf. Series: Journal of Physics: Conf. Series **1115** (2018) 022025 doi :10.1088/1742-6596/1115/2/022025.

[2] *Loy N.N., Sanzharova N.I., Gulina S.N., Vorobiyov M.S., Koval N.N., Doroshkevich S.Yu., Chizh T.V., Suslova O.V*. Influence of electronic irradiation on the affection of barley by root rot. IOP Conf. Series: Journal of Physics: Conf. Series **1393 (**2019) 012107 doi:10.1088/1742-6596/1393/1/012107

MODIFICATION OF THE SURFACE OF POLYMER ELECTROLYTE MEMBRANE NAFION BY ION BEAM ASSISTED DEPOSITION OF CATALYTIC METALS [1]

V.V. POPLAVSKY, O.G. BOBROVICH, A.V. DOROZHKO

Belarusian State Technological University, Minsk, Belarus, e-mail: vasily.poplav@tut.by

The Nafion membrane, which is a fluoropolymer-copolymer of sulfonated tetrafluoroethylene, has proton conductivity in the wet state and is used as an electrolyte for low-temperature fuel cells. Catalysts are needed for effective operation of fuel cells with polymer membrane electrolyte. Before the inclusion of the electrolyte in membrane electrode assemblies of fuel cells we subjected the membranes to pretreatment to remove surface contaminants, and to ion beam modification. Active layers were prepared by ion beam assisted deposition (IBAD) of platinum and iridium on Nafion® N 115 membrane. Formation of layers in IBAD mode, by means of the deposition of metal and mixing of precipitating layer with the substrate by accelerated (U = 5 kV) ions of the same metal, was carried out. In this process, a neutral fraction of metal vapor and ionized plasma of vacuum pulsed electric arc were used.

Investigation of the composition and morphology of prepared surface layers was carried out by RBS, SEM, EDX and XRF methods. According to EDX, RBS (Fig. 1) and XRF (Fig. 3) atoms of deposited metals, of components of membrane (C, F, S), and oxygen as impurity enter into the composition of layers. At the same time, the surfaces contain deposited metals inclusions with sizes of the order of a micrometer (Fig. 2), which arise from the precipitation of metal droplets from the arc discharge of the ion source.

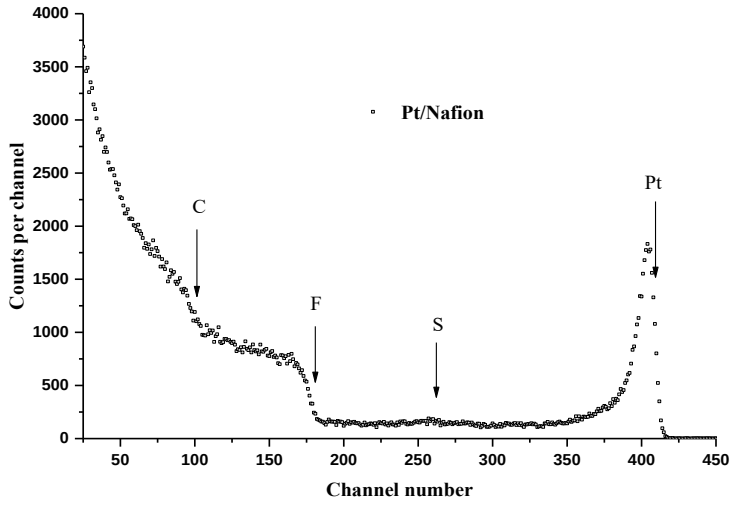

Fig. 1. RBS spectrum of ^{4}He ions from surface of Nafion® N 115 membrane with layer formed by IBAD of Pt

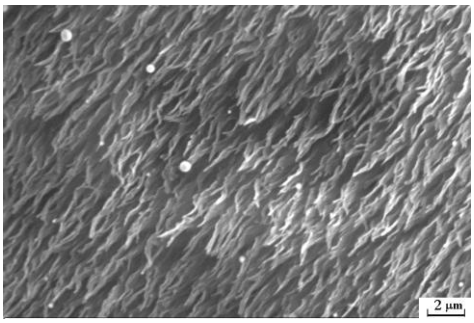

Fig. 2. SEM image of the Nafion® N 115 membrane with layer formed by the IBAD of Pt

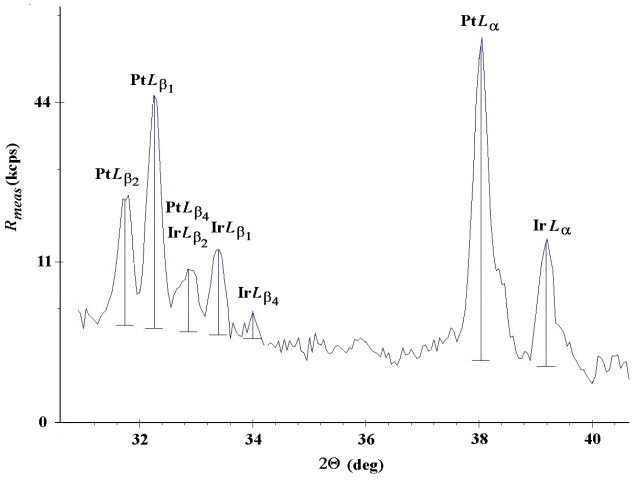

Fig. 3. Fragment of the X-ray fluorescence spectrum of elements in the composition of the layer formed by IBAD of Ir and Pt on Nafion® N 115

The thickness of the prepared layers is ~30 nm; content of each of deposited metal atoms in the layers – ~$n\times10^{15}$ cm^{-2}. In the maximum of distribution located near the surface, the concentration of each of the deposited metals is about atomic percent. In the process of IBAD of metals in the proposed mode, ionic mixing of all components of the layer being formed takes place.

[1] This work was supported by the Republic of Belarus state research program "Physical material science, new materials, and technologies"

HIGH-INTENSITY NITROGEN ION IMPLANTATION IN AISI 5140 ALLOY STEEL UNDER CONDITIONS OF ION SURFACE SPUTTERING COMPENSATION BY THE DEPOSITION OF SPUTTERED ATOMS

A.I. RYABCHIKOV, D.O. SIVIN, O.S. KORNEVA, A.I. IVANOVA, S.V. DEKTYAREV, D.O. VAKHRUSHEV

National Research Tomsk Polytechnic University, Tomsk, Russia

High-intensity implantation of low-energy gas and metal ions in various materials demonstrates the possibility of forming ion-doped layers with thicknesses of tens and hundreds of micrometers [1-3]. However, the modification at very high dose irradiation fluences (10^{20}–10^{22} ion/cm^2) is accompanied by significant erosion of the target which changes the morphology of its surface and affects the parameters of the ion-doped layer. This work is devoted to the studies of implantable nitrogen dopant accumulation dynamics, changes in the dopant depth distribution profile under conditions of ion sputtering suppression of AISI 5140 alloy steel during high-intensity implantation of nitrogen ions with an average energy of 1 to 2 keV. The surface ion sputtering compensation was ensured by the deposition of ion-sputtered atoms from an additional target. To sputter the additional target, a part of a focused nitrogen ion beam was used. The study data of the characteristic features of the sputtered atom stream formation from the target surface using an axially symmetric repetitively pulsed high-frequency nitrogen ion beam with a density of up to several hundred mA/cm^2 are presented. Data on the results of studying the laws of changes in the microstructure, elemental composition and properties of steel modified layers during high-intensity nitrogen ion implantation under conditions of ion sputtering compensation of the irradiated surface by the deposition of sputtered atoms are given.

REFERENCES

[1] A.I. Ryabchikov, A.E. Shevelev, D.O. Sivin, A.I. Ivanova, V.N. Medvedev, “Low energy, high intensity metal ion implantation method for deep dopant containing layer formation,” Surface and Coatings Technology, vol. 355, pp. 123-128, 2018.

[2] A.I. Ryabchikov, D.O. Sivin, P.S. Ananin, A.I. Ivanova, I.V. Lopatin, O.S. Korneva, A. E. Shevelev, “High intensity, low ion energy implantation of nitrogen in AISI 5140 alloy steel,” Surface and Coatings Technology, vol. 355, pp. 129-135, 2018.

[3] A.I. Ryabchikov, A.E. Shevelev, D.O. Sivin, I.A. Bozhko, E.B. Kashkarov, G.A. Bleykher, I.B. Stepanov, A.I. Ivanova, “Ultra high fluence implantation of aluminum ions into CP–Ti,” Journal of Alloys and Compounds, vol. 793, pp. 604-612, 2019.

INTEGRATED MAGNETRON-ARC METHOD FOR CREATING METAL-DIELECTRIC FUNCTIONAL COATINGS

SHUGUROV V.V., KOVAL N.N., IVANOV YU.F.

Institute of High Current Electronics SB RAS, Tomsk, Russia

The results of studies on the production of surface alloys based on silicon and niobium on steel 40x are presented. Layers of silicon and niobium were sequentially deposited, and then mixing was carried out by a pulsed electron beam. The coating method, the method of mixing the surface layer are described, and the mechanical characteristics of the obtained layer are investigated.

RESEARCH OF THERMODYNAMIC PROPERTIES OF WATER ADSORPTION ON N-DOPED CO_3O_4

G.KAPTAGAY[1], *YU.MASTRIKOV*[2], *N.KOILYK*[3], *L.BAIKADAMOVA*[1], *A.UTEBAEVA*[1]

[1] *Kazakh National Women's Teacher Training University, Almaty, Kazakhstan*

[2] *Institute of Solid State Physics, Riga, Latvia*

[3] *RIDLRPS of RK*

Calculations were performed using the DFT method as implemented in the computer code VASP 5.4[1]. Core electrons were substituted with the US potentials with the PAW method [2].

Exchange-correlation described by the PBE functional [3]. The Hubbard correction U-J=3eV [4] was applied to d-electrons of Co tet as well as Co oct atoms [5]. For defects modeling cubic 56-atom supercell model has been used. For Brillouine zone [6] was sampled with the 2x2x2 Monkhorst-Pack scheme.

Plain-waive basis set has the kinetic energy cut-off of 550 eV. Charge redistribution was analysed by the Bader method, as implemented by Henkelmann et al..

Doping by nitrogen was performed by substitution of oxygen atoms. Four concentrations have been tested – 1, 2, 4 and 8 N per 32(O+N) atoms.

The adsorption energy of the water molecule and the intermediate decomposition products of the water molecule on the nitrogen of the doped surface (100) increases within 0.1-0.52 eV compared to the clean surface. Also, when the water molecule is adsorbed over the position of tetrahedral cobalt, the dissociation energy decreases. The change in the adsorption energy on the nitrogen of the doped surface is due to the transfer of the charge density to the cobalt position due to the introduction of nitrogen impurities. Nitrogen is a donor impurity. When replacing the surface oxygen ion with nitrogen on the surface (100) Co_3O_4 , no change in the excess potential is observed when the water molecule is adsorbed over the position. At the same time, when the water molecule is adsorbed over the oxygen in octahedral position, the excess potential decreases by 0.37 V compared to the clean surface. This is due to a decrease in the change in the free energy of Gibbs, due to the transition of the charge state of the cobalt position from 4+ to 3+.

REFERENCES

[1] Kresse G., Furthmüller J. Ab-initio simulation package for quantum modeling // Phys. Rev. B. – 1996. – Vol. 3. No54. – P.11169-5.

[2] Blochl P.E. Projector augmented-wave method// Phys.Rev.B. – 1994. – Vol. 50, – P.17953.

[3] Perdew J.P. Generalized Gradient Approximation Made Simple// Phys.Rev.Lett. – 1996. – Vol. 77, – P.3865-3868.

[4] Dudarev S.L., Botton G.A., Savrasov S.Y., Humphreys C.J., Sutton A.P. Electron-energy-loss spectra and the structural stability of nickel oxide // Phys.Rev.B: Condens. Mater.Phys. − 1998. – Vol. 3. No 57. − P. 1505-1512.

[5] 3eV for Co

[6] Monkhorst H.J., Pack J.D. Special points for Brillouin-zone integrations Phys. Rev. B. – 1976. – Vol.13. – P. 5188-5192.

THE SYNTHESIS OF INTERMETALLIC NI3AL ON TITANIUM ALLOY VT-6 *

N.N. SMIRNYAGINA[1], D.E. DASHEEV[1], A.S. MILONOV[1]

[1]Institute of Physical Materials Science SB RAS, Sakhyanovoy Street, 6, Ulan-Ude, 670047, Russia, dasheevdorzho@gmail.com, 89834264332

The work is aimed at investigating the synthesis of nickel-based intermetallics by electron-beam treatment. ntermetallics are a unique class of materials that retain an ordered structure up to the melting point. Intermetallics have such properties as high strength, which does not decrease with increasing temperature, anomalous yield strength dependence (in particular for Ni_3Al) [1].

One of the main tasks for creating a coating from Ni3Al intermetallic on a titanium alloy is to determine the parameters of the electron beam treatment mode. An electron-beam unit with a continuous axial gun on thermocathodes was used to conduct the experiments.

Power density of the electron beam W = 5.7×10^2 W/mm^2, diameter of the electron beam d=1 mm, processing time 1-2 min. The experiments were carried out at a pressure of 10^{-3} Pa. Reaction daubs of stoichiometric composition NiO-Al_2O_3-C and Ni-Al were applied to the surface of the titanium alloy. Initial components used were NiO and Al_2O_3 oxides and birch carbon, Ni powder derived from carbonyl nickel and aluminum powder. The reaction mixture was used to prepare the daubs by mixing it with BF-6 glue solution in acetone. When the highly concentrated energy flows are exposed on the reaction daub, the SHS process is initiated.

After treatment with an electronic beam of BT-6 titanium alloy samples with reaction daubs applied on them, heterogeneous layers of 50-100 microns thick are formed on the surface (fig.1). The layer has good adhesion and is firmly held on a metal base.

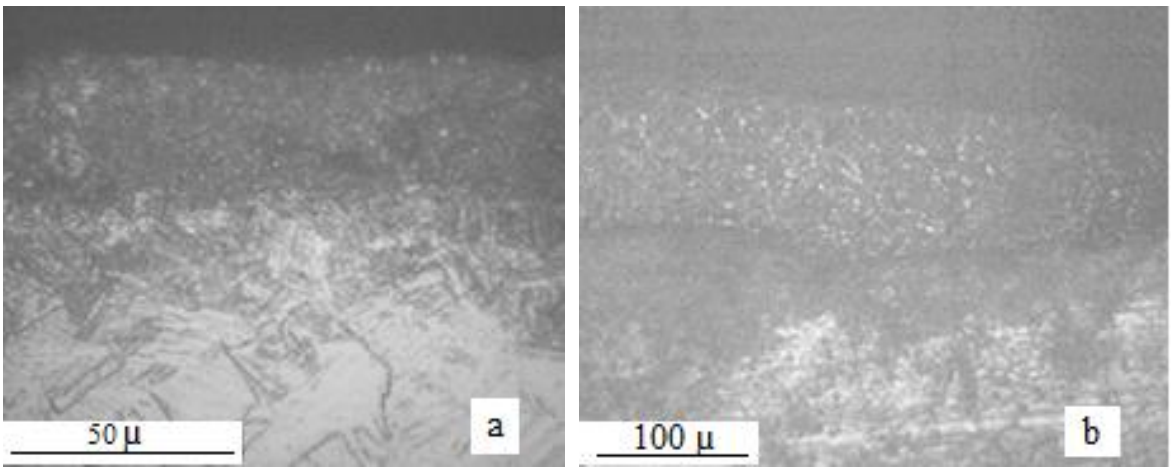

Fig. 1. Microstructure of intermetallic layer Ni-Al on VT-6 titanium alloy: a – Ni-Al powder; b – NiO-Al_2O_3-C.

X-ray phase analysis showed that two polymorphic modifications of Ni_3Al, PDF 00-050-1265 and PDF 00-021-0008, and Ni_5Al_3 PDF 00-040-1157 were synthesized in the formed layers. All investigated samples contain crystalline and amorphous phases in the amount from 68.4 to 82.1%.

Microhardness in intermetallic layer is 3000-3500 MPa.

REFERENCES

[1] B.A. Greenberg, M.A. Ivanov, Ni_3Al and TiAl intermetallics: microstructure, deformation behavior. Ekaterinburg: Ural Branch of RAS, 2002.

* *This work was carried out within the framework of the project of fundamental research program of SB RAS No. 03336-2019-0009.*

* *This work was supported by RFBR grant No. 15-48-04217, r-Siberia_a.*

ADHESION OF STEEL AND COPPER SURFACE TREATED BY RUNAWAY ELECTRON PREIONIZED DIFFUSE DISCHARGE*

M.V. EROFEEV, V.S. RIPENKO, V.F. TARASENKO

Institute of High Current Electronics, Tomsk, Russia

Surface clearing from hydrocarbon contaminations and increasing surface free energy leads to increasing of adhesion properties that can be used for development of reliable interconnections in semiconductors and for high-adhesive coatings. Measurements of adhesion by means of X-cut test (ISO 16276-2:2007) have shown that adhesion of aerosol paint KIM TEC (Germany) on polished and rinsed in ultrasonic bath untreated copper (Fig. 1, a-b) and steel specimens corresponds to 2 points, and increased up to 4 points after treatment by plasma of 40000 runaway electron preionized diffuse discharge pulses (Fig. 1, c-d).

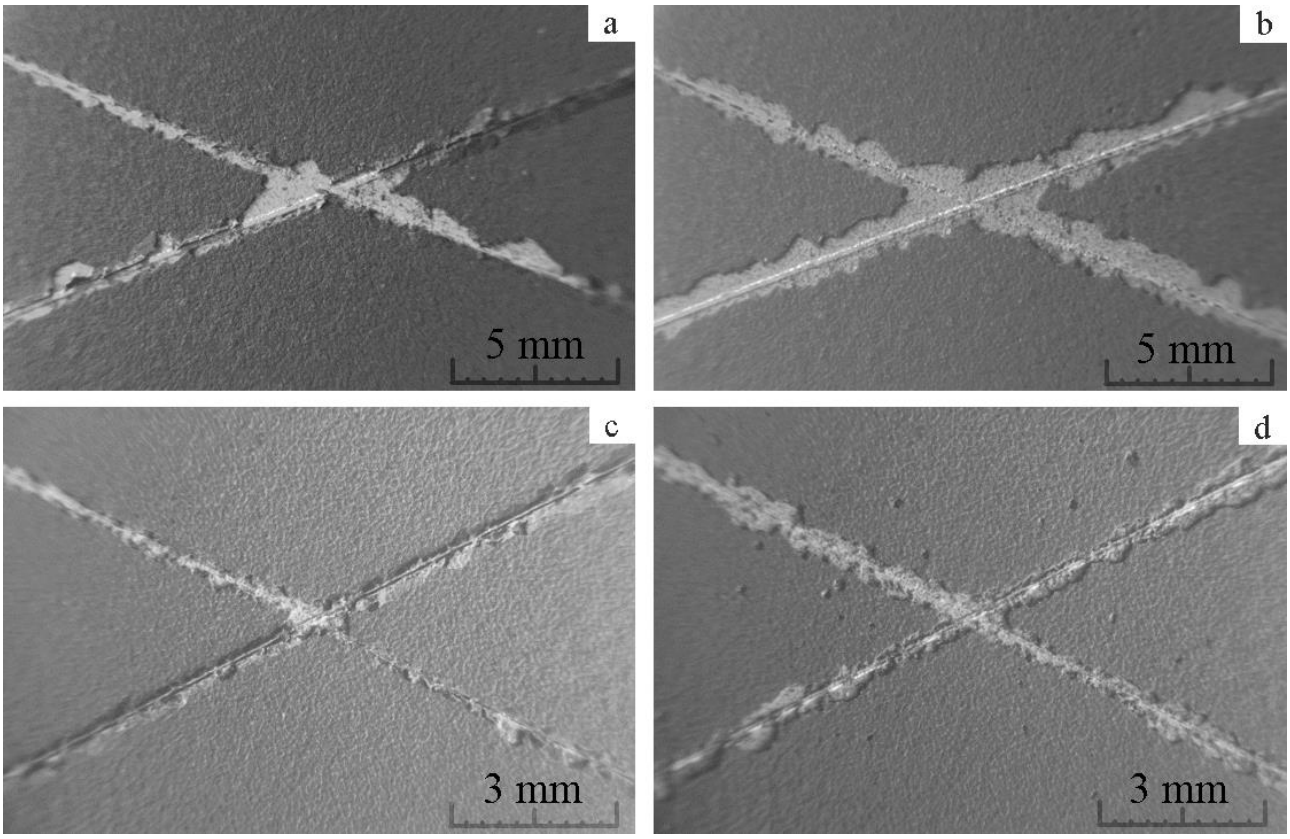

Fig.1. X-cuts in paint on untreated copper specimen before (a) and after (b) tearing off adhesive tape. X-cuts in paint on the treated copper specimen with 40000 REP DD pulses before (c) and after (d) tearing off adhesive tape.

Nanoidentation has shown that nanohardness of the treated specimens decreased up to 20 % for copper and up to 10 % for steel. Nanohardness decreased (opposite to [1]) due to raising of stretching tension with small angles disorientation of fragments in near-surface layer induced by discharge thermal deformation.

REFERENCES

[1] M. Erofeev, V. Ripenko, M. Shulepov, V. Tarasenko, "Surface treatment of metals in the plasma of a nanosecond diffuse discharge at atmospheric pressure," Eur. Phys. J. D, 71: 117, 2017.

* This work has been performed within the framework of the State task for HCEI SB RAS, the project # 9.5.2.

ION BEAM IMPLANTATION AND PROPERTIES OF STAINLESS STEEL *

M.S. DOROFEEVA[1], *T.A. GUBAIDULINA*[2], *T.I. DOROFEEVA*[2], *V.P. SERGEEV*[2]

[1]*Tomsk state University, Tomsk, Russia*
[2] *Institute of Strength Physics and Materials Sciences of the Siberian Branch of the Russian Academy of Science, Tomsk, Russia*

Surface treatment is an effective method to improve the high physico-mecanical properties of construction metal alloy. Typical surface modification techniques include anodic oxidation [1], microplasma oxidation [2], electroplating [3], physical vapor evaporation [4], chemical vapor deposition, and ion implantation [5]. Of these techniques, ion beam implantation is one of the most favorable technologies for stainless steel protection. It is necessary to select such ions and the implantation mode so as not to change the product dimensions (typical for threaded joints) and increase their service life.

The ion implantation was performed step by step. First, an oxygen (O) was implanted. Then, aluminium (Al^+) and boron (B^+) were implanted together. Ions were implanted using IBI with the accelerate voltage of 10-80 kV, and with various implantation fluences (10^{17} - 10^{18} ions/cm^2).

From the SIMS calculations it was determined that an ion energy of 10 keV at fluences of 10^{18} ions/cm^2 would result in the implanted O concentration being contained within the 50nm layer, without significant spill-over into the 200 nm layer. In addition, the composition profile analysis from SIMS taken in depth for ion modified layers. Oxygen is implanted to a depth of not more than 25 nm, aluminum and boron are implanted to a depth of more than 200 nm. The O modulation signal was greater than the Al and B signals, for this case; however, the O signal could reach up to 30 times the Al and B signals in bilayers with 10nm thicker.

The (non-implanted and implanted) were chosen to evaluate corrosion resistance in aggressive medium through long-term corrosion tests in a salt spray chamber. The weight loss of the non-implanted specimen is comparatively high. The weight of the implanted specimen is practically unchanged. This becomes especially relevant for testing times beyond 480 h.

For the electrochemical investigation, the experiments were controlled by potentiostat PI-50-1 complete with compensation two-axis potentiometer N307/1 advanced electrochemical system, using the conventional three-electrode technique. Polarization curves were obtained at room temperature under static conditions (without aeration). The corrosion potentials before and after implantation were 50mV and 150mV, respectively. The latter moved to a more positive position, which indicated that the structural stability of stainless steel in corrosive medium was improved by ion implantation treatment. During a corrosion test, the corrosion current density decreased from 1.26 to 0.708μA/cm2.

Although the present study focused on the O/AlB system, it is expected that other ion implantation layers can be formed similarly. A deeper understanding of the corrosion characteristics of ion modified layers is essential for their development and testing if they are to contribute to the continued reduction of environment impact on the mechanical devices. This work demonstrates how ion implantation can be a powerful tool to further this effort. In the future, a number of strategies will be explored to control the amount of ions required for corrosion resistance of stainless steels to make this material more stable and thus increase the economic benefits of using these alloys.

REFERENCES

[1] Kai An, Chengqiang An, Chuanning Yang, Yongquan Qing, Yan Shang, Changsheng Liu, Effect of Phosphating and Post-sealing on the Corrosion Resistance of Electro - galvanized steel, Int. J. Electrochem. Sci., vol.12, pp. 2102 – 2111, 2017.

[2] V.A. Mamaeva, A.I. Mamaev, T.I. Dorofeeva, Y.Y. Bydnitskaia, Research cyclic voltammetric dependences during microplasma formation of bioceramic coatings on titanium alloys 8th Korea-Russia International Symposium on Science and Technology - Proceedings: KORUS 2004, vol. 3, pp. 133-136, 2004.

[3] Y. Reda, A.M. El-Shamy, Ashraf K. Eessaa, Effect of hydrogen embrittlement on the microstructures of electroplated steel alloy 4130, Ain Shams Engineering Journal, vol. 9, pp. 2973–2982, 2018.

[4] Y.P. Purandare, M.M. Stack, P.Eh. Hovsepian, Velocity effects on erosion-corrosion of CrN/NbN "superlattice" PVD coatings, Surf. Coat. Technol., vol. 201, pp. 361–370, 2006.

[5] C. Zheng, A. Gentils, J. Ribis, V.A. Borodin, L. Delauche, B. Arnal, Nano-size metallic oxide particle synthesis in Fe-Cr alloys by ion implantation, Nuclear Instruments and Methods in Physics Research B, vol. 409, pp. 333–337, 2017.

* The work was performed under the government statement of work for ISPMS Project No. III.23.1.1.

SURFACE AND VOLUME STRUCTURAL CHANGES IN THE AL-ZN-MG-CU ALLOY AS A RESULT OF ARGON ION BEAM IRRADIATION[1]

N.V. GUSHCHINA[1], V.V. OVCHINNIKOV[1], F.F. MAKHIN'KO[1], L.I. KAIGORODOVA[2], D.Y. RASPOSIENKO[2]

[1] *Institute of Electrophysics, UB RAS, Amundsena Str. 106, Yekaterinburg, 620016, Russia, viae05@rambler.ru, (343)267-87-84*
[2] *Institute of Electrophysics, Ural Branch of Russian Academy of Sciences, Amundsena Street 18, Yekaterinburg, 620990, Russia*

This work focuses on the study of structural-phase state of the samples cut from 6-mm-thick pressed V95 alloy (Al-Zn-Mg-Cu) profiles after artificial aging (T=140ºC, 16 h) and subsequent irradiation with 20–40 keV Ar^+ ions.

The samples were irradiated with continuous Ar^+ ion beams in an ILM-1 ion beam implanter equipped with a PULSAR-1M ion source based on a glow discharge with a hollow cold cathode [1]. The samples during irradiation were moved relative to the line-focus beam 100×20 mm^2 at a speed of 2 cm/s. The temperature of a target was continuously controlled with the help of a chromel-alumel thermocouple welded to an identical test sample. We used the following irradiation modes: (1) E = 20 keV, j= 400 μA/cm^2, F = $2\cdot10^{15}$ cm^{-2}; (2) E = 20 keV, j= 400 μA/cm^2, F = $1\cdot10^{16}$ cm^{-2}; and (3) E = 40 keV, j= 500 μA/cm^2; F = $9.4\cdot10^{16}$ cm^{-2}. The maximum temperature to which the samples were heated during irradiation was in the range from 30 to 200°C.

Electron microscopy analysis was carried out by the method of thin foils using a JEM-200 CX transmission electron microscope, at the Electron Microscopy Center of Collaborative Access of the Institute of Metal Physics, UB RAS. The microstructure was examined in two cross-sections parallel to the irradiated surface, directly near the surface and at a distance of ~150 μm from it.

The irradiation effect on the initial subgrain structure is shown to decrease at a distance from the irradiated surface. Near the surface, the elements of the subgrain structure becomes coarser or this structure partly or completely transforms into a coarse-grained one (when the ion fluence is increased), whereas an increase in subgrain sizes are only observed at a distance of 150 μm from the irradiated surface. The irradiation under all used conditions has been found to change the morphology of intermetallics of crystallization origin $Al_6(Fe,Mn)$; namely, the distribution density of lamellar intermetallics decreases, whereas that of equiaxed ones sharply increases. In addition, the irradiation under the above conditions has been found to affect the size, shape, and the distribution density of the strengthening phase particles θ'(θ") (metastable modifications of the stable phase $CuAl_2$) as well as the phases η' and η (modifications of the stable phase $MgZn_2$). Irradiation with 20-keV Ar^+ ions at low fluences of $2\cdot10^{15}$ and $1\cdot10^{16}$ cm^{-2} (the samples are hardly heated) activates phase transformation η' → η. An increase in the volume fraction of the stable η phase suppresses the nucleation and growth of the metastable aluminium–copper θ" (θ') phases through the partial dissolution of copper atoms in the η phase. Irradiation with 40-keV ions at a higher fluence of $9.4\cdot10^{16}$ cm^{-2}, which heats the V95 alloy profiles up to 200°C for a short period of time, on the contrary, reduces the distribution density of the stable η' phase, increases the amount of the metastable η' phase, and increases the θ'-phase particle size. The above-mentioned changes in phase composition are observed both in the surface layer of the samples under study and at a distance of 150 μm from the irradiated surface.

REFERENCES

[1] N.V. Gavrilov, G.A. Mesyats, S.P. Nikulin, G.V. et al., "A new broad beam gas ion source for industrial applications", J. Vac. Sci. Technol., vol. A14, 1050-1055, 1996.

[1] This work was supported in part by RFBR grant № 19-08-00802-a.

X-RAY ANALYSIS OF THE EFFECT OF ACCELERATED 15-KEV Ar^+ IONS ON THE DEFORMED Ni + 13.9 wt. % W ALLOY[1]

N.V. GUSHCHINA[1], F.F. MAKHIN'KO[1], V.V. OVCHINNIKOV[1], V.I. BOBROVSKII[2], V.I. VORONIN[2]

[1]Institute of Electrophysics, UB RAS, Amundsena Str. 106, Yekaterinburg, 620016, Russia, viae05@rambler.ru, (343)267-87-84
[2]Institute of Metal Physics, Ural Branch of Russian Academy of Sciences, St. S. Kovalevskoy 18, Yekaterinburg, 620990, Russia

The work is aimed at studying the effect of Ar^+ ion irradiation on the microstructure of the Ni + 13.9 wt. % W alloy after its cold rolling to a high strain degree (99%). This alloy after deformation and subsequent recrystallization annealing (T = 1000°C, 1 h) acquires a particularly sharp texture and is a promising material for the manufacture of substrates for HTSC cables [1].

Previously, we received data showing that gas ion irradiation of the deformed materials at ion energies of 10-50 keV and ion current densities j = 100-400 μA/cm^2 can be an alternative to thermal annealing [1, 2]. Radiation annealing in aluminum and other alloys occurs at significantly lower temperatures and energy consumption (2-3 times less), and in record time, as compared with isothermal furnace annealing. The depth of the ion influence is not limited to ion penetration range; moreover, it is more than 10^4 times higher [1, 2]. Highly-deformed Ni + 13.9 wt. % W tapes 80 μm thick were chosen as the object of present research.

The samples of the selected alloys were irradiated with continuous Ar^+ ion beams using an ILM-1 ion beam implanter equipped with a PULSAR-1M ion source based on a low-pressure glow discharge with a hollow cold cathode at an Ar^+ ion energy of 15 keV, an ion current density of 100 μA/cm^2, a fluence of $3.1\cdot10^{16}$ (for 50 s) and $4.7\cdot10^{17}$ cm^{-2} (for 12.5 min). In order to estimate the contribution of the purely thermal component and to distinguish it from the radiation-dynamic one, the deformed Ni + 13.9 wt. % W sample was also heated in the furnace at a stationary temperature of 370°C for 12.5 min. It should be noted that during the accumulation of the above mentioned fluences the samples were entered and removed from the beam area. The temperature in this case reached 370°C only in some points (without long exposure).

X-ray structure analysis was performed using a DRON-UM-1 diffractometer and the Rietveld method using FullProf software.

In the initial state after deformation, the material is in a crystalline state with sufficiently large grains fragmented into domains. The reflections were significantly widened due to internal microstress. The (220) plane of most grains was lined up along the rolling plane during deformation. A part of grains with the (200) orientation was observed on the same plane. The lattice parameter of the initial alloy was a = 3.5440 ± 0.0006 Å and the corresponding microstresses was $\Delta d/d\times10^{-4}$ = 30.8 ± 1.2.

After irradiation, the X-ray diffraction patterns were completely similar to the initial X-ray patterns, the lattice parameter remained the same. However, a decrease in the inclination of direct dependencies $\beta(2\Theta)\times cos\Theta$ as a function of $sin\Theta$ indicates a decrease in microstresses in the volume of samples. A sharp drop in the microstress was already observed at a low ion fluence of $3.1\cdot10^{16}$ cm^{-2}: $\Delta d/d\times10^{-4}$ = 21.8 ±0.7. At F = $4.7\cdot10^{17}$ cm^{-2}, $\Delta d/d\times10^{-4}$ = 22.5 ± 2.5 s. Similar processes were observed during the annealing in the furnace at 370°C for 12,5 min. However, the effect was about 2 times less. The texture in the deformed samples was retained after the irradiation and annealing.

It should be noted that changes in the microstress level on the irradiated and unirradiated sides of the 80-μm-thick sample are approximately the same, although the projective range of argon ions with an energy of 15 keV in nickel, according to calculations by the TRIM method, is only 7 nm. This result indicates in favor of the radiation-dynamic nature of the influence of accelerated ion beams on the substance due to the generation of powerful elastic and shock postcascade waves [2].

REFERENCES

[1] V.V. Ovchinnikov, N.V. Gavrilov, N.V. Gushchina, et al., "Radiation annealing of AMg6, 1441 and VD1 aluminum alloys strips using a ribbon source of accelerated ions", Russian metallurgy (Metally), 3, 207-214, 2010.

[2] V.V. Ovchinnikov, "Nanoscale dynamic and long-range effects under cascade-forming irradiation", Surface and Coating Technology, vol. 355, 65-83, 2018.

[3] N.V. Gavrilov, G.A. Mesyats, S.P. Nikulin, G.V. et al., "A new broad beam gas ion source for industrial applications", J. Vac. Sci. Technol., vol. A14, 1050-1055, 1996.

[1] This work was supported by the Russian Scientific Foundation, project No. 19-79-20173.

EXPOSURE OF 15-KEV Ar^+ IONS ON THE STRUCTURE OF ANNEALED ALLOY Ni + 13.9 wt. % W[1]

N.V. GUSHCHINA[1], F.F. MAKHIN'KO[1], V.V. OVCHINNIKOV[1], V.I. BOBROVSKII[2], I.V. GERVASYEVA[2], V.A. MILYUTIN[2]

[1]Institute of Electrophysics, UB RAS, Amundsena Str. 106, Yekaterinburg, 620016, Russia, viae05@rambler.ru, (343)267-87-84
[2] Institute of Electrophysics, Ural Branch of Russian Academy of Sciences, Amundsena Street 18, Yekaterinburg, 620990, Russia

At present, the only way to produce electrical cables based on ceramics with high-temperature superconductivity (HTSC) is to deposit ceramic components on special substrates and to perform subsequent heat treatment. Well-textured, oxidation-resistant tapes made of an Ni–W alloy can be used as such substrates. Such tapes have been fabricated at the Institute of Metal Physics (UB RAS). Tapes with a Ni + 13.9 wt. % W composition are characterized, according to [1], by a particularly sharp cubic texture of a {100}<001> type. This texture in a tape deformed by cold rolling to a very high compression degree (95–98%) is formed by annealing [1].

Superconducting magnet coils with an extremely high magnetic field intensity are considered as possible applications of HTSC cables, the use of which might help to create effective thermonuclear reactors. However, it is important to know the stability of the properties of the considered HTSC cables during the operation of reactors under cascade-forming irradiation conditions.

In view of this to research processes modifying the microstructure of the alloy when exposed to cascading irradiation by accelerated ion fluxes is of interest.

The Ni + 13.9 wt. % W alloy samples 80 μm thick were irradiated after cold working and subsequent recrystallization annealing (T = 1000°C, 1 h) using an ILM-1 implanter with an ion source [2], which generated a continuous Ar^+ ion beam being uniform in its cross section (~100 cm^2). The parameters of the beam included ion energy E = 15 keV, ion current density j = 100 μA/cm^2, and fluence $F = 3 \cdot 10^{16}$ cm^{-2} (irradiation time of 50 s). The samples during irradiation were moved under the ion beam at a speed of 1 cm/s, which ensured the heating temperature below 370°C.

The electron-microscopic examination of the initial and irradiated samples performed on a FEI Quanta 200 scanning electron microscope and the EBSD method showed that ion irradiation under the conditions used did not degrade the quality of the material in terms of its texture. Both in the initial state and after irradiation the samples were in the highly textured state; namely, they exhibited a sharp texture of the {100}<001> type. The fraction of grains with orientation to 5° is 0.87 in initial state and 0.88, after irradiation. The fact that the texture has remained the same after irradiation is an important aspect for the application of this alloy as substrates for superconducting cables.

An interesting result was obtained from the study of grain size distributions. The average grain size was 147 μm after irradiation, whereas it was 195 μm in the initial state.

Further, we are going to irradiate Ni + 13.9 wt. % W alloy samples with high-energy ions at a higher fluence to research their radiation resistance.

REFERENCES

[1] D. P. Rodionov, I. V. Gervas'eva, and Yu. V. Khlebnikova, Textured Nickel-Alloy-Based Substrates, Yekaterinburg, UrB of RAS, 2012.

[2] N.V. Gavrilov, G.A. Mesyats, S.P. Nikulin, G.V. et al., "A new broad beam gas ion source for industrial applications", J. Vac. Sci. Technol., vol. A14, 1996.

[1] This work was supported by the Russian Scientific Foundation, project No. 19-79-20173.

THE USE OF LOW-TEMPERATURE PLASMA FOR PROCESSING REFRACTORIES MODIFIED WITH NANOPARTICLES*

N.K. Skripnikova G.G. Volokitin, V.V. Shehovcov, M.A. Semenovykh

Tomsk State University of Architecture and Building, Tomsk, Russia

Refractory materials find their application in various fields: metallurgical processes, design of furnaces, high-temperature units. Refractories are subjected to high temperature loads. in particular, the surface of the material is exposed to high temperature influences. In this regard, it is worth paying attention to the hardening of this surface.

This paper presents the results of a study on the effect of the introduction of nanomaterials in the compositions of refractory ceramics and its subsequent processing by low-temperature plasma.

The types of refractories studied in this work, namely Met-Silcast and Metpump AZS 20, were made using the following binders: Binder, MI-61 and MI-62 nanotubes. The amount of binder ranged from 10 to 14 wt.%. Refractory samples were made by vibration-assisted molding.

The obtained samples were subjected to physical and mechanical tests, X-ray phase analysis and optical microscopy.

The results of X-ray phase analysis showed that for samples made from a Met-Silcast type refractory and a binder, the amorphous nature of the structure did not change before and after firing. In samples of the Met-Silcast type with a binder containing MI-61 and MI-62 nanotubes, new crystalline phases are not formed. Samples of the Metpump AZS 20 type after firing have a partial change in the crystalline phases, which is associated with the recrystallization of zirconium-containing compounds and the formation of mullite-like phases [1 – 3]. The introduction of nanotubes in this case does not lead to the formation of new crystalline phases.

Microscopic examination was carried out on a Quanta 200 3D scanning electron microscope. The results of the study confirm the results of x-ray phase analysis - Met-Silcast refractories consist mainly of glass phases with a uniform and uniform structure, in places they have small cracks. Metpump AZS 20 samples have a granular structure.

Based on the data obtained, it can be concluded that the use of nanomaterials in refractory compositions does not affect their structure and properties. Further, in order to increase the strength characteristics of the samples, a plasma treatment was carried out. The experiment was carried out as follows: the samples were processed with a low-temperature plasma of an arc plasmatron at temperatures t = 3000 - 5000 ° C, voltage U = 190 V and current I = 340 A, with a plasma arc passing through the surface v = 0.07 m / s. The quality of the visual surface and, accordingly, the heat resistance was evaluated by visual assessment and examination of the samples under a microscope with a magnification of x800. Assessment of the fused surface showed that for all samples there is no cracking. When comparing refractory samples before and after heat treatment, a decrease in porosity is observed, and the remaining pores are fused with glass phase. All studied samples were resistant to thermal shock. At the same time, the surface of the samples of the type of Met-Silcast refractory turned out to be smoother and smoother with respect to the type of Metpump AZS 20 refractory, whose surface is hilly. This tuberosity is in the form of a glass phase. In general, all samples exhibit some nonuniformity of reflow, which can be eliminated by resorting to the selection of technological modes [4].

In the study of physical and mechanical parameters, it was found that the introduction of nanotubes into the composition of refractories does not lead to an improvement in the strength properties of products. Thus, it can be concluded that the use of plasma chemical technologies is advisable.

REFERENCES

[1] Abe J.O., Popoola A.P.I., Popoola O.M. Consolidation of Ti_6Al_4V alloy and refractory nitride nanoparticles by spark plasma sintering method: Microstructure, mechanical, corrosion and oxidation characteristics, Materials science and engineering a-structural materials properties microstructure and processing, No. 774, pp. 138920, 2020

[2] Najmeh L., AmirAbbas N., Nezamoddin M. S. et al A comparison of the effect of nanostructured $MgCr_2O_4$ and $FeCr_2O_4$ additions on the microstructure and mechanical properties of direct-bonded magnesia-chrome refractories, Ceramics International, No. 46, pp. 747-754, 2020.

[3] Avwerosuoghene, M.O. Evaluation of the sinterability, densification behaviour and microhardness of spark plasma sintered multiwall carbon nanotubes reinforced Ti_6A1_4V nanocomposites, Ceramics International, No. 45, pp. 19864-19878, 2019

[4] Gu Q., Zhao F., Liu X. et al Preparation and thermal shock behavior of nanoscale $MgAl_2O_4$ spinel-toughened MgO-based refractory aggregates, vol. 45, No. 9, pp. 12093-12100, June 2019.

*The reported research was funded by Russian Foundation for Basic Research and the government of the region of the Russian Federation, grant № 18-48-703004.

FEATURES OF SYNTHESIS OF CLINK MINERALS UNDER CONDITIONS OF HIGH-CONCENTRATED HEAT FLOWS*

N.K. Skripnikova G.G. Volokitin, V.V. Shehovcov, M.A. Semenovykh

Tomsk State University of Architecture and Building, Tomsk, Russia

The work is devoted to the study of the physicochemical processes of the formation of clinker minerals upon exposure to a crystalline mixture of highly concentrated heat fluxes and their dependence on the technological modes of swimming using traditional and substandard raw materials.

The synthesis of cement clinker was carried out at different thermal exposure times: 75 s, 90 s, 120 s and 140 s. Moreover, a different number of phases characteristic of cement clinker [1].

Cement clinker obtained under conditions of highly concentrated heat fluxes, subjected to a comprehensive physical and chemical study, including x-ray phase analysis using a DRON-3M diffractometer, X-ray spectral - ARL 9900 Oasis Intelli Power, X-ray analyzer, chemical analysis (GOST 5382–91), thermal coefficient analysis (DTA) - DERIVATOGRAPH Q-1500D, structure analysis - POLAM R-312 microscope.

The petrographic analysis of the samples (Fig. 1) obtained under optimal technological conditions showed that the morphology of metastable minerals is characteristic of nonequilibrium clinker formation conditions [2] associated with intensive synthesis of minerals under the influence of highly concentrated heat fluxes on the raw material mixture, sharp heating, and a high temperature gradient during crystallization of the melt. This leads to partial amorphization of the samples and the formation of a nanostructured matrix model of clinker phases, represented by alite grains - needle and lamellar forms, belite - round or dendritic grains.

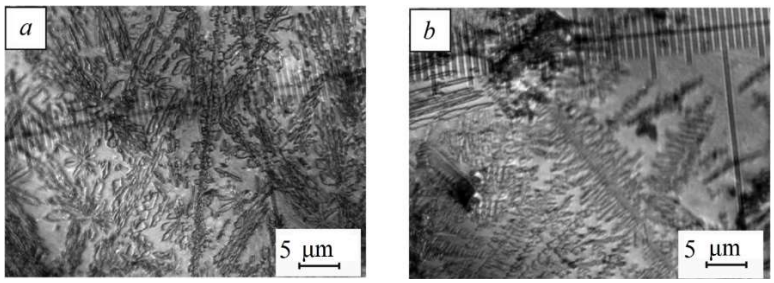

Fig. 1. The structure of the cement clinker (1140 ×) obtained in the NTP based on the mixture: a - TM for 90 s; b - SM for 120 s

The methods of X-ray phase, differential thermal analyzes and petrography have been used to study the physicochemical processes of the formation of the phase composition of cement clinkers synthesized under conditions of highly concentrated heat fluxes based on traditional (TM) and substandard (SM) raw materials. It has been established that the optimal exposure time of low-temperature plasma to NS and TS is 90 and 120 s, respectively. As a result of studying the physicomechanical properties of cements obtained on the basis of fused clinkers using mixtures of TS and NS, it was found that they have activity corresponding to the brands M700 and M500, respectively. High mechanical strength of the samples is ensured by the structural feature of cement clinkers and is associated with the fact that faces that develop more rapidly during crystal growth are less stable during hydration [3]. Along with this, the activity of cement is affected by diffusion averaging of the composition of the sample, regardless of the short duration of exposure to low-temperature plasma and the absence in the structure of the cement clinker of the distinction between alite and belite sections - microvolumes on the surface of the sections. Studies of the physicochemical processes of the formation of the phase composition of cement clinkers are carried out. Under nonequilibrium conditions of low-temperature plasma, modified metastable clinker minerals are formed at the nanoscale: alite (100 nm – 1 μm) × (2–50 μm); whites less than 1 micron.

REFERENCES

[1] Skripnikova N.K., Lutsenko A.V., Sazonova N.A. et al The influence of technological melting conditions in low-temperature plasma on the structure of cement clinker, Vestnik of TSUAB, No 1 (54), pp. 155-162, 2016.

[2] Volokitin G.G. Skripnikova N.K., Volokitin O.G. et al Physico-chemical processes occurring during the plasma-chemical synthesis of silicate melts, Proceedings of universities. Physics, No. 3 / 3, pp. 111-114, January 2014.

[3] Chang L.; Jiang Y.; Wang W. et al, Ultrafine WC-0.5Co-xTaC cemented carbides prepared by spark plasma sintering, International journal of refractory metals & hard materials vol. 84, No. 104994, November 2019.

*The reported research was funded by Russian Foundation for Basic Research and the government of the region of the Russian Federation, grant № 18-48-703004.

APPLICATION OF IMPEDANCE SPECTROSCOPY FOR RESEARCH OF THE MICRO-ARC OXIDATION PROCESS*

P.E. GOLUBKOV, E.A. PECHERSKAYA, G.V. KOZLOV, T.O. ZINCHENKO, O.A. MELNIKOV, J.V. SHEPELEVA[1]

[1]*Penza State University, Penza, Russia*

Currently, the method of impedance spectroscopy [1] - [4] is widely used. It is used both for studying solid dielectric and composite materials, as well as for various electrochemical systems, in particular, for studying charge transfer processes and the corrosion properties of MAO coatings. The method is non-destructive and has a high information content: measuring impedance in a wide frequency range gives maximum information not only about the structure of the sample, but also about the occurrence of physical and chemical processes at the phase interfaces [5].

The study of changes in the structure and properties of the oxide layer formed during the MAO process, depending on the processing time and technological parameters is of great interest. In this case, the method of impedance spectroscopy can be an effective tool for controlling the MAO process and controlling the properties deviations of the formed coatings (thickness and porosity) from the required values in real time.

A galvanic cell with a test sample can be represented as the following equivalent circuit (Fig. 1).

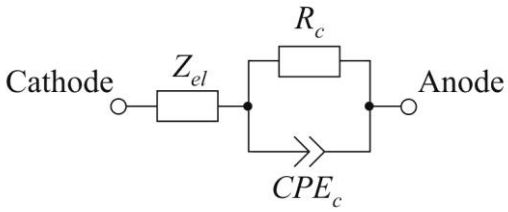

Fig.1. Equivalent electrical model of an MAO galvanic cell.

In Fig. 1 R_c and CPE_c simulate the resistance and capacitance of the coating, respectively; Z_{el} represents the electrolyte impedance, including the active resistance R_{el} of the electrolyte layer between the anode and cathode and the impedance of double electric layers with a C_{dl} capacity. The constant phase element CPE_c was chosen as a model of the coating capacitance, since the sample under study is an imperfect capacitor with leakage through pores.

Based on the given equivalent electrical circuit, the impedance spectra of a sample with an MAO coating were simulated; a regression model of the change in the thickness of the oxide layer depending on the processing time was obtained.

The results can be used both for further theoretical studies of the MAO coatings formation mechanism, and to ensure effective control of the MAO process when creating automated technological equipment [6].

REFERENCES

[1] A. Bordbar-Khiabani, S. Ebrahimi, B. Yarmand, “Highly corrosion protection properties of plasma electrolytic oxidized titanium using rGO nanosheets,” Appl. Surf. Sci., vol. 486, pp. 153–165, 2019.

[2] L. Pezzato, M. Rigon, A. Martucci, K. Brunelli, M. Dabala, “Plasma Electrolytic Oxidation (PEO) as pre-treatment for sol-gel coating on aluminum and magnesium alloys,” Surf. & Coat. Technol., vol. 366, pp. 114–123, 2019.

[3] J. Han, C. Blawert, J. Yang, X. Lu, J. Hu, M. L. Zheludkevich, “Self-cleaning property of AZ31 Mg alloy during plasma electrolytic oxidation process,” Progress in Natural Science: Mater. Int., vol. 29, pp. 94–102, 2019.

[4] A. Heydarian, M. Atapour, A. Hakimizad, K. Raeissi, “The effects of anodic amplitude and waveform of applied voltage on characterization and corrosion performance of the coatings grown by plasma electrolytic oxidation on AZ91 Mg alloy from an aluminate bath,” Surf. & Coat. Technol., vol. 383, pp. 1–12, 125235, 2020.

[5] S. V. Gnedenkov, S. L. Sinebryukhov, “ Impedance spectroscopy in the study of charge transfer processes,” Vestnik DVO RAN, no. 5, pp. 6–16, 2006.

[6] P. E. Golubkov, E. A. Pecherskaya, O. V. Karpanin, Y. V. Shepeleva, T. O. Zinchenko, D. V. Artamonov, “Automation of the micro-arc oxidation process,” IOP Conf. Series: J. of Phys.: Conf. Series, vol. 917, pp. 1–6, 092021, 2017.

* The reported study was funded by RFBR according to the research project № 19-08-00425.

STUDY OF FACTORS INFLUENCING THE CHARACTERISTICS OF MICRO-DISCHARGES IN THE MICRO-ARC OXIDATION PROCESS*

P.E. GOLUBKOV, E.A. PECHERSKAYA, T.O. ZINCHENKO, V.V. ANTIPENKO, D.V. ARTAMONOV, A.V. PECHERSKIY[1]

[1]*Penza State University, Penza, Russia*

As it is known, a specific feature of the micro-arc oxidation process, which leads to the formation of coatings on valve metals and alloys that significantly exceed the properties of traditional anodic oxide films, is the existence of microdischarges on the part surface. Despite the large number of theoretical and experimental works [1] - [3], this phenomenon is still not fully understood, in particular, the question of the influence of the MAO process parameters on the characteristics of microdischarges remains unexplored [4, 5]. This article proposes an approach based on Ishikawa diagrams and graph theory [6], which allows solving this problem.

A model in the form of an oriented graph describing the influence of the MAO process parameters on the microhardness *HV* of coatings is proposed (Fig. 1).

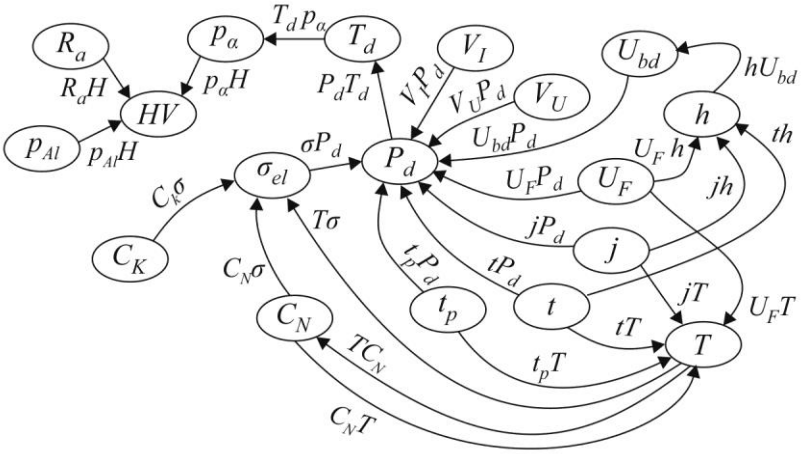

Fig.1. A graph describing the influence of the MAO process parameters on the microhardness of the coating.

The vertices of the directed graph describe the technological parameters of the MAO process (*j* is the current density, *t* is the processing time, etc.), the properties of the coatings (*h* is the thickness, *HV* is the microhardness) and the characteristics of the discharges (P_d is the power of microdischarges, T_d is the temperature of the discharge channel, etc.). The directions of the arcs show the direction of the influence of factors on each other, and the inscriptions on the arcs are parameters that characterize the physical effect.

Based on the directed graph, a mathematical model that describes the influence of the parameters of the MAO process on the characteristics of microdischarges has been developed.

REFERENCES

[1] D. V. Mashtalyar, S. L. Sinebryukhov, I. M. Imshinetskiy, A. S. Gnedenkov, K. V. Nadaraia, A. Yu. Ustinov, S. V. Gnedenkov, “Hard wearproof PEO-coatings formed on Mg alloy using TiN nanoparticles,” Appl. Surf. Sci., vol. 503, pp. 1–12, 144062, 2020.

[2] N. Ao, D. Liu, X. Zhang, G. He, “Microstructural characteristics of PEO coating: Effect of surface nanocrystallization,” J. of Al. and Com., vol. 823, pp. 1–10, 153823, 2020.

[3] W. Tu, Zh. Zhu, X. Zhuang, Y. Cheng, P. Skeldon, “Effect of frequency on black coating formation on AZ31 magnesium alloy by plasma electrolytic oxidation in aluminate-tungstate electrolyte,” Surf. & Coat. Technol., vol. 372, pp. 34–44, 2019.

[4] M. O’Hara, S. C. Troughton, R. Francis, T. W. Clyne, “The incorporation of particles suspended in the electrolyte into plasma electrolytic oxidation coatings on Ti and Al substrates,” Surf. & Coat. Technol., vol. 385, pp. 1–11, 125354, 2020.

[5] T. W. Clyne, S. C. Troughton, “A review of recent work on discharge characteristics during plasma electrolytic oxidation of various metals,” Int. Mater. Reviews, vol. 64, no. 3, pp. 127–162, 2019.

[6] P. E. Golubkov, E. A. Pecherskaya, Y. V. Shepeleva, A. V. Martynov, T. O. Zinchenko, D. V. Artamonov, “Methods of applying the reliability theory for the analysis of micro-arc oxidation process,” IOP Conf. Series: J. of Phys.: Conf. Series, vol. 1124, pp. 1–6, 081014, 2018.

* The reported study was funded by RFBR according to the research project № 19-08-00425.

SIMULATION OF OPTIMAL NITRIDING MODES IN ARC DISCHARGE

R.SH.NAGIMOV[1], E.L.VARDANYAN[1], A.YU.NAZAROV[1], K.N.RAMAZANOV[1]

[1]Ufa State Aviation Technical University, Ufa, Russia

The problem of increasing the durability of metal cutting tools is an important one in modern machine building [1]. One of the most widespread methods to increase physical and mechanical characteristics is ion nitriding [2.3]. Such processing can also serve as an aid for duplex processing, which includes coating application [4-6]. For the best interaction of coating and surface alloying it is necessary to use the most optimal modes.

In order to ensure control over the arc ion nitriding process and reduce the time it takes to predict the process, a model has been developed to determine the optimum modes for use in the duplex process. Bias voltage, arc current, pressure in the chamber were used as input modes. Nitriding depth was calculated as the output parameter because this parameter is the most significant for duplex processing. Nitriding depth dependence on processing time was also obtained. The flexibility of this model allows you to vary the modes, gas composition, metal.

REFERENCES

[1] Borovskiy, G.V.; Grigoriev, S.N.; Maslov, A.R. Modern technologies of the materials processing (in Russian) // MPEI: Mashinostroenie. - – 2015.

[2] T. V. Koval, Le Hu Dung, “Investigation of plasma generation and current transmission of an intense low-energy electron beam,” Izv. Vyssh. Uchebn. Zaved. Fiz., vol. 57, no. 3/2, pp. 118–121, March 2014.

[3] Khusainov Y. G. et al. Low temperature ion nitriding titanium alloy TI-6AL-4V in the coarse grained and ultrafine-grained states //Journal of Physics: Conference Series. – IOP Publishing, 2018. – Т. 1115. – №. 3. – С. 032035.

[4] Vardanyan E. L. et al. Complex modification of the surface of high-speed steel in low-temperature high-density plasma //Journal of Physics: Conference Series. – IOP Publishing, 2019. – Т. 1393. – №. 1. – С. 012145.

[5] Moreno-Bárcenas A. et al. Synergistic effect of plasma nitriding and bias voltage on the adhesion of diamond-like carbon coatings on M2 steel by PECVD // Surface and Coatings Technology. – 2019.

[6] Rousseau A. F. et al. Microstructural and tribological characterisation of a nitriding/TiAlN PVD coating duplex treatment applied to M2 high speed steel tools // Surface and Coatings Technology. – 2015. – Т. 272. – С. 403-408.

SURFACE MODIFICATION OF POLYMER SCAFFOLDS BY REACTIVE MAGNETRON SPUTTERING CONTROLS THE RELEASE OF AN INCORPORATED DRUG*

A.O. FAYT[1], *A.A. VOLOHOVA*[1]

[1] *National Research Tomsk State University, Tomsk, Russia*

The paper is deals with the study of the effect of surface treatment of polymer scaffolds by the method of reactive magnetron sputtering controls the release of an incorporated drug [1]. Drug-loaded polymer scaffolds are treated by magnetron sputtering to change the drug release profile [2]. The object of research is polymer scaffolds obtained by the method of electrospinning from a solution of poly(L-lactide acid) and chloramphenicol as a model drug [3]. Before modification, the obtained scaffolds were loaded into a vacuum chamber with a pressure of 10^{-2} Pa and left for 10 hours to remove residual solvents.

To modify the surface, a magnetron sputtering system was used, in the vacuum chamber of which an extended magnetron was placed horizontally with a target of chemically pure (99.99%) titanium (Ti). Surface modification was carried out under the following technological conditions: working pressure 99.99%, N2 - 0.7 Pa, current 0.2 A, distance between target and sample 40 mm, sprayed target area 240 cm^2, modification time 30 sec.

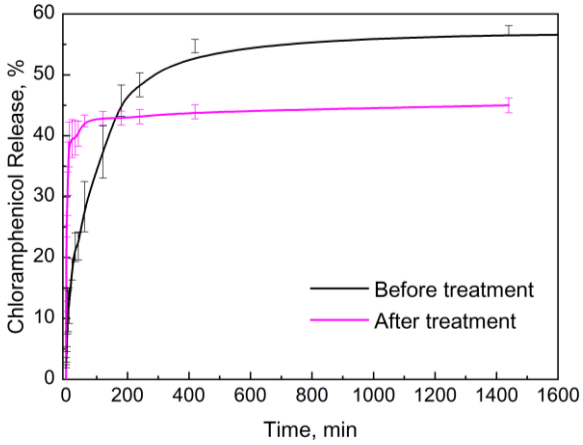

Fig. 1. Drug release from the polymer scaffold before and after magnetron sputtering treatment

It can be seen from the graphs that in the first 500 minutes of drug release from scaffolds that were not subject to change by magnetron sputtering, it is smoother. Modification allows you to increase the amount of drugs released in the first 200 minutes of the substance, however, further release is obviously difficult. Both graphs reach a plateau when the experiment time reaches 1000 minutes, and the maximum values of released substances are 45 and 56% of the mass of the loaded amount.

It was shown that the treatment of the obtained materials with magnetron sputtering does not lead to the destruction of the fibers and a change in their morphology and surface wettability, and the crystallinity of the scaffold material does not change. Magnetron sputtering treatment changes the release profile of chloramphenicol: the rate of reaching the release plateau increases, but the maximum concentration in the solution decreases.

REFERENCES

[1] *Yoshida S. et al. Surface modification of polymers by plasma treatments for the enhancement of biocompatibility and controlled drug release // Surface and Coatings Technology. – 2013. – T. 233. – P. 99–107.*

[2] *Tverdokhlebov S. I., Bolbasov E. N., Shesterikov E. V. Scaffold materials based on fluorocarbon composites modified with RF magnetron sputtering // Osteogenesis/ed. Y. Lin. Rijeka: InTech. – 2012. – P. 83–116.*

[3] *Doxorubicin-loaded electrospun poly(L-lactic acid)/mesoporous silica nanoparticles composite nanofibers for potential postsurgical cancer treatment / Qiu, K. X. [etc.] // J. Mater. Chem. B. – 2013. – №. 1 (36). – P. 4601–4611.*

* This work was supported by supported by the Ministry of Education and Science of the Russian Federation, the Federal Target Program (agreement No. 14.578.21.0031, unique identifier RFMEFI57814X0031).

DEPENDENCE OF THE DIMENSION AND DEFECTS STRUCTURE OF A NANOCRYSTALLINE METAL SURFACE LAYER WHEN TREATED WITH DIFFERENT POWER DENSITIES OF HIGH POWER ION BEAM*

V.A. TARBOKOV, S.K. PAVLOV

Tomsk Polytechnic University, Tomsk, Russia

Coatings deposited by the magnetron method, as a rule, have significant internal stresses. These stresses can have a significant effect on the adhesion strength of the coating-substrate system, especially along the interface. In this regard, preliminary preparation of the coating base is necessary, which will allow the substrate to either successfully resist the forces acting on it from the coating side or serve as an effective "damper" for these stresses. In this case, the nanocrystalline structure of the surface layer that borders the coating can play a positive role in ensuring adhesion strength over a wide range of temperatures and mechanical loads. The use of high-power pulsed ion beams makes it possible to modify the crystal structure of a metal substrate over a wide range, and, depending on the density of the energy deposited, create materials with different sizes of crystal structures.

The report provides a rationale for the HPIB pre-treatment of the substrate to create the necessary level of internal stresses. The mutual influence of the nanocrystalline structure of the coating and the substrate on their ability to mutual relaxation of internal stresses and, as a result, on the adhesion strength is discussed.

* The reported study was funded by RFBR and ROSATOM, project number 20-21-00025

COMPARISON OF THE EFFICIENCY OF SHORT-TIME ANNEALING OF PRODUCTS WITH A HIGH-CURRENT ELECTRON BEAM AND THERMAL ANNEALING FOR SAMPLES TREATED WITH HIGH-POWER ION BEAM

V.A. TARBOKOV, S.K. PAVLOV

Tomsk Polytechnic University, Tomsk, Russia

A treatment with concentrated energy flows (CEF) is accompanied by the creation of a high level of residual internal stresses in the surface layer. This reduces the hardness and elasticity of the material surface and the consequence of this may be the rapid destruction of the CEF treated products. There are several ways to reduce internal stresses, including thermal and radiation annealing. In this work, we performed a comparative study of the effectiveness of these types of processing.

We irradiated a series of carbide alloy samples with a high power ion beam (HPIB) with an energy density in the range of 1÷3 J/cm^2. In this range, the surface of the carbide alloy undergoes various modifications from high-speed hardening to melting and partial ablation. For annealing, we irradiated part of the samples with a high-current electron beam, and the other part was annealed in a furnace in an air atmosphere.

The report presents the results of comparing the mechanical characteristics of the surface of samples after HPIB treatment, thermal annealing, and electron beam annealing using micro- and nanoindentation methods and X-ray diffraction analysis.

RESEARCH OF ALUMINOSILICATE PROPANTS OBTAINED BY PLASMA CHEMICAL TECHNOLOGY*

N.K. Skripnikova G.G. Volokitin, V.V. Shehovcov, M.A. Semenovykh

Tomsk State University of Architecture and Building, Tomsk, Russia

The oil industry is one of the most relevant activities today. Oil production is associated with the destruction of the earth's shell in order to extract useful resources. One of these technologies is hydraulic fracturing. With this method, they resort to the destruction of the earth's crust and the strengthening of the formed inner space by injection of cementing fluid and proppant.

Traditionally, proppants are obtained from raw materials consisting primarily of kaolinites and silica (silicon oxide), the content of which affects the qualitative characteristics of the granules. The main physicochemical parameters for evaluating the suitability of refractory clay raw materials for the production of aluminosilicate proppants are the mineralogical composition. The physicochemical principles of the use of refractory clay raw materials in proppant technology is to create favorable conditions for the formation of the mechanical properties of granular material due to the directional regulation of structure and phase formation processes. Thus, the basic physicochemical principles of the use of refractory clay raw materials in aluminosilicate proppant technology is the creation of favorable conditions for the formation of the mechanical properties of granular material due to the directional regulation of structure formation processes. Cristobalite standing out from the structure of kaolinite, an increase in the content and improvement of the structure of which should also favorably affect the strength of the products. In the case of using additives, phase formation processes will contribute to the creation of mullite by reducing the high temperature viscosity of the resulting silicate melt, which leads to an increase in the density and strength of the products. It was found that the synthesis of mullite is affected not only by the maximum firing temperature, but also by the rate of heating of the mixture [1, 2]. At a high heating rate, the activity of the initial finely dispersed components is preserved to a greater degree, and since components with a defective crystal lattice participate in the reactions, this leads to an acceleration of reactions between solids and to an increase in their solubility in the liquid phase. The use of plasma technologies, which are characterized not only by high temperatures and rates of passage of physicochemical processes, is relevant.

The advantages of using low-temperature plasma as a medium for the production of aluminosilicate proppants include the following: plasma processes do not require multi-stage technological conversions compared to traditional chemical-technological processes, potentially more environmentally friendly, less energy-intensive; low energy efficiency, which follows from the nonequilibrium state of the low-temperature plasma, i.e. it is possible to selectively direct the energy flow to activate the necessary components of a chemically reacting system; the possibility of achieving high temperatures of the gaseous medium and the use of any gaseous atmosphere, high thermal efficiency of plasma sources, a small amount of exhaust gases and small dimensions of the electro-plasma reactor [3].

The use of low-temperature plasma generators in the technology of preparing granular ceramic materials can contribute to the miniaturization of production, ensuring its mobility, expanding the range of substandard inorganic mineral raw materials used. As such raw materials can be used metallurgical waste products, which are characterized by iron content (5-12%) [4]. Under high-temperature action on a multicomponent system, under conditions of nonequilibrium, reactions will occur in the liquid phase with the formation of further complex compounds containing aluminum oxides of silicon and iron. The intensification of the processes of liquid-phase sintering is several times accompanied by an increase in strength due to the formation of an iron-silicate melt with the subsequent formation of solid solutions with mullite.

REFERENCES

[1] Fan J., Bailey T.P., Sun Z., et al Preparation and properties of ultra-low-density proppants for use in hydraulic fracturing, Journal of petroleum science and engineering, No. 163, pp. 100-109, April 2018.

[2] Assem A.I., Nasr-El-Din H.A. Interactions between different acids and bauxitic-based ceramic proppants used in gravel-packed and fractured wells, Journal of petroleum science and engineering, No. 158, pp. 441-453, September 2017.

[3] Vakalova T.V., Reshetova A.A., Revva I.B. Effect of thermochemical activation of clay raw materials on phase formation, microstructure and properties of aluminosilicate proppants, Applied clay science, No. 183, pp. 105335, December 2019.

[4] Usova Z.Yu., Pogrebenkov V.M. Ceramic proppant based on aluminum borate, Refractories and technical ceramics, No. 1-2, pp. 28-32, 2012.

*The reported research was funded by Russian Foundation for Basic Research and the government of the region of the Russian Federation, grant № 18-48-703004.

SINGLE LAYER AND MULTILAYER CHROMIUM NITRIDE COATINGS FOR STRENGTHENING SURFACE OF THE DIE STEELS*

A.A. LEONOV, YU.A. DENISOVA, N.A. PROKOPENKO, V.V. DENISOV

Institute of High Current Electronics SB RAS, Tomsk, Russia

Coatings based on chromium nitride are widely used for strengthening surface of dies, molds and machine parts. These coatings are characterized by high hardness, thermal stability, corrosion resistance and wear resistance. The mechanical properties of the coatings are greatly influenced by their structure and phase composition. The laws of formation of the structure, phase composition of single layer and multilayer coatings based on chromium nitride, formed in gas-metal plasma of low pressure are investigated in the work. The regularities of influence of the gas-metal plasma composition formed in low-pressure discharges and the parameters of the effect on the metal substrate (working pressure, composition of the gas mixture, bias voltage) on the structure, phase composition of the coatings deposited on the Cr6VW, Cr12Mo die steel are established. The regularities of influence of the structure and phase composition of single layer and multilayer coatings based on chromium nitride on hardness, fracture toughness, and tribotechnical characteristics are revealed.

* The work was carried out with the financial support of the RFBR grant № 19-08-00370 A.

ELION METHOD OF NITRIDING OF HIGH-CHROMIUM STAINLESS STEEL: STRUCTURE AND PROPERTIES*

YU. IVANOV, I. LOPATIN, E. PETRIKOVA, YU. DENISOVA, O. TOLKACHEV

Institute of High Current Electronics SB RAS, 2/3, Akademichesky ave., Tomsk, 634055, Russia

The purpose of the present work is to establish and analyze the structure and properties of a high-chromium austenitic steel subjected to elion nitriding in low-pressure gas-discharge plasma.

High-chromium steel of 20Cr23Ni18 grade was used as the object under study. Nitriding was carried out on ELION set-up in low-pressure gas-discharge plasma at specimen temperatures of (450; 550; 600)° C and at nitriding duration of (1; 3; 5) hours. Electron component of plasma is used for efficient heating of specimens. This treatment mode is called as "elion", i.e, that includes the exposure of both the electron and ion components of a non-self-sustained arc discharge plasma with thermionic cathode.

It has been found that the hardness of the surface layer of treated steel is maximum (10.8 GPa) at a specimen temperature of 520 °C at nitriding, regardless of the duration of the nitriding process. The thickness of the hardened layer reaches 50 μm and it is slightly dependent on the specimen temperature during process. It is shown that the minimum value of the wear parameter (maximum wear resistance) is achieved at specimen temperature during nitriding of 520 °C and duration of 3 h. The wear parameter is $0.86 \cdot 10^{-6}$ $mm^3N^{-1}m^{-1}$, it is less by ≈200 times than that for initial steel. It is revealed that the concentration of nitrogen atoms decreases monotonously from ≈10 at. % in the near-surface layer to zero in the layer at the depth of 50 μm. The chain of phase transformations occurring during elion nitriding method of steel at 450 °C was revealed by the X-ray phase analysis methods:

$$\gamma\text{-Fe N (1 h)} \rightarrow (\gamma\text{-Fe} + FeN_{0.085}\ \text{(S-phase)} + CrN) + N\ (3\ h) \rightarrow (\gamma\text{-Fe} + FeN_{0.085}\ \text{(S-phase)} + CrN) + N\ (5\ h) \rightarrow (\gamma\text{-Fe} + Fe_4N + CrN).$$

The structure and phase composition of the nitrided layer of steel were investigated by TEM methods. It has been found that he surface layer with thickness of (1-2) μm contains the grains with nitride-phase inclusions of globular and lamellar shape (Fig. 1, a). At higher distance from the nitriding surface (up to the end of the nitrided layer), the main structure is that of the lamellar type (Fig. 1, b). SAED analysis shows that the globular particles are chromium nitrides of the CrN composition; the structure of lamellar type is formed by the alternating plates of γ-Fe and nitride of iron with Fe_4N composition.

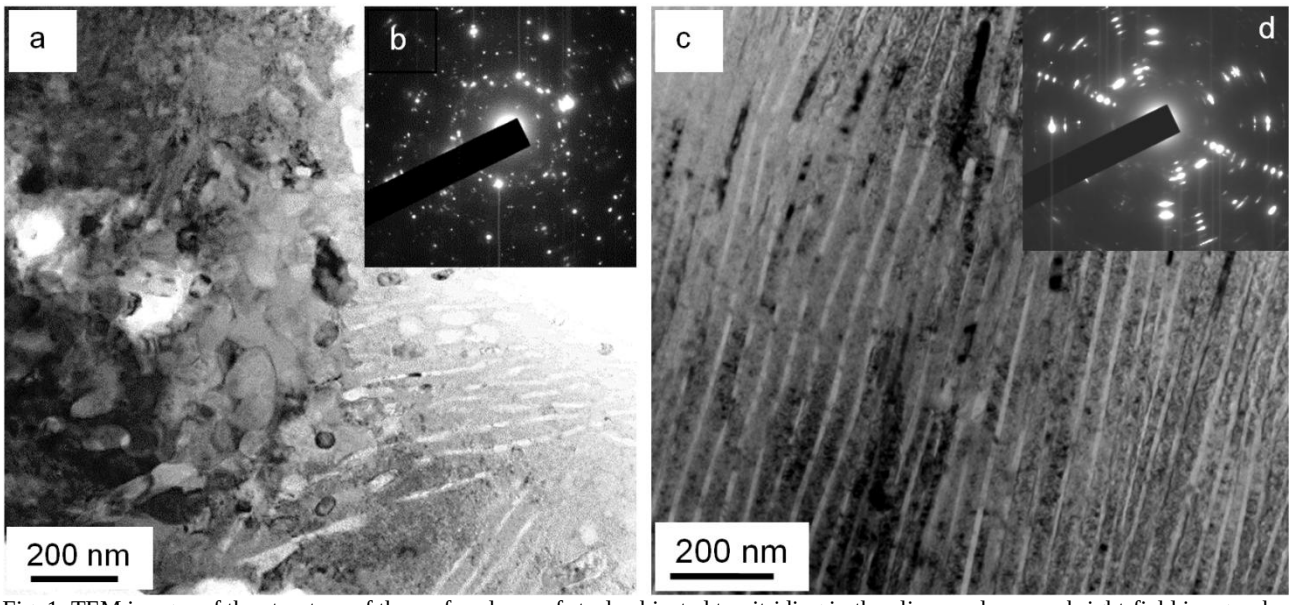

Fig. 1. TEM images of the structure of the surface layer of steel subjected to nitriding in the elion mode; a, c – bright-field images; b, d – microdiffraction patterns.

* The work was supported by RFBR project No. 19-48-700010.

SURFACE MODIFICATION OF PLLA SCAFFOLDS BY REACTIVE MAGNETRON SPUTTERING CONTROLS THE RELEASE OF AN INCORPORATED DRUG*

A.A. VOLOHOVA[1], *S.I. TVERDOKHLEBOV*[2]

[1] *National Research Tomsk State University, Tomsk, Russia*
aar37@tpu.ru
[2] *National Research Tomsk Polytechnic University, Tomsk, Russia*
tverd@tpu.ru

In this paper, the effect of surface treatment of polymer scaffolds by the method of reactive magnetron sputtering on the release of an incorporated drug is studied. Drug-loaded polymer scaffolds were treated by magnetron sputtering in order to change the drug release profile [1]. The objects of research are polymer scaffolds obtained by the method of electrospinning from a poly-L-lactide solution and chloramphenicol as a model drug. Before modification, obtained scaffolds were placed into a vacuum chamber and left for 10 hours to remove residual solvents.

To modify the surface, a magnetron sputtering system was used: the vacuum chamber with a horizontally oriented magnetron [2], a chemically pure (99.99%) titanium (Ti) target. Surface modification was carried out under the following technological conditions: working pressure 99.99% N_2 – 0.7 Pa, current – 0.2 A, distance between target and sample – 40 mm, sprayed target area – 240 cm^2, modification time – 30 sec.

Figure 1 presents data of chloramphenicol release from both treated and untreated scaffolds.

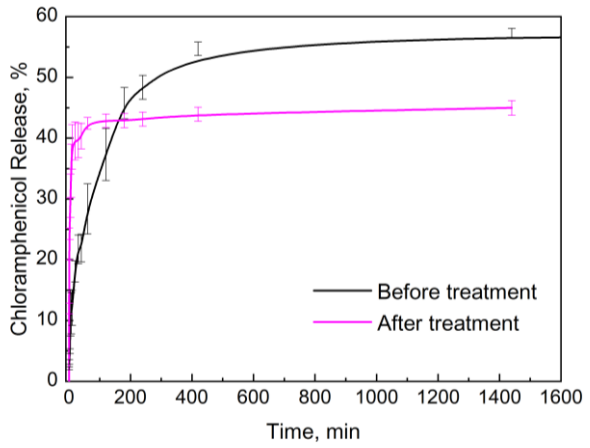

Fig. 1. Drug release from the polymer scaffold before and after magnetron sputtering treatment

Modification allows to increase the amount of released drug in the first 200 min of the experiment, however, further release is obviously hindered. Untreated samples demonstrate a steadier release reaching a plateau only by 500 min of the experiment. Maximum amount of a released drug decreases from 56 wt.% to 43 wt.% average in untreated samples compared to treated ones correspondently.

It was shown that the treatment of the obtained materials with magnetron sputtering does not lead to the destruction of the fibers and a change in their morphology and surface wettability; the crystallinity of the scaffold material does not change. Magnetron sputtering treatment changes the release profile of chloramphenicol from electrospun PLLA scaffolds. Results can be used for designing of new solid dosage forms design with controlled release.

REFERENCES

[1] *Yoshida S. et al. Surface modification of polymers by plasma treatments for the enhancement of biocompatibility and controlled drug release // Surface and Coatings Technology. – 2013. – T. 233. – P. 99–107.*

[2] *Tverdokhlebov S. I., Bolbasov E. N., Shesterikov E. V. Scaffold materials based on fluorocarbon composites modified with RF magnetron sputtering // Osteogenesis/ed. Y. Lin. Rijeka: InTech. – 2012. – P. 83–116.*

* This work was supported by supported by the Ministry of Education and Science of the Russian Federation, the Federal Target Program (agreement No. 14.578.21.0031, unique identifier RFMEFI57814X0031).

HYPEREUTECTIC SILUMIN ALLOYS MODIFICATION BY COMPRESSION PLASMA FLOWS IMPACT FOR IMPROVING MECHANICAL PRPERTIES AND OXIDATION RESISTANCE*

V.I. SHYMANSKI[1], A. JEVDOKIMOVS[1], A.V. BASALAI[3], N.V. BIBIK[1], V.M. ASTASHYNSKI[2]

[1]*Belarusian State University, Minsk, Belarus*
[2]*A.V. Luikov Heat and Mass transfer Institute of National Academy of Science of Belarus, Minsk, Belarus*
[3]*The Physical-Technical Institute of National Academy of Science of Belarus, Minsk, Belarus*

The hypereutectic silumin alloys based on aluminum and silicon with a silicon concentration more than 13 wt.% are considered as new perspective material for aerospace industry, engineering, internal combustion engine production due to low specific weight, low temperature expansion coefficient. The details made of silumin alloy usually work at high temperature in the opened air space. As a rule, the aluminum part of the alloy is more resistant to high-temperature oxidation as a thin layer of aluminum oxide forms very fast on the surface and serves as a barrier layer. Nevertheless, the hypereutectic silumin alloys have a big amount of silicon component which is undergone to oxidation. So, the main purpose of the present work is a hypereutectic silumin surface modification with plasma treatment for improving its oxidation resistance at elevated temperatures.

Two different hypereutectic silumin alloys with a silicon concentrations 44 wt. % and 22 wt. % were used in the experiments. The samples were the plates with a size of 10x10 mm and a thickness of 2 mm. The samples were subjected to compression plasma flows impacts in a magnetoplasma compressor of compact geometry working in the residual gas atmosphere mode. The nitrogen was used as plasma-forming gas. The samples were treated by the compression plasma flows with different absorbed energy densities chosen in the range allowed to melt the surface layer.

Another part of the samples was subjected to a combined treatment including the preliminary metal coating deposition on the surface followed the compression plasma flows impact. Such metals as Cr, Zr and Ni were chosen as coating materials. The thickness of every coating was about 1-2 micrometers. The parameters of the compression plasma flows impact were the same as in the experiments with the uncoated silumin alloys.

The plasma treatment allowed to melt the surface layer with a depth from 20 to 60 micrometers in dependence on the absorbed energy density. Using scanning electron microscopy and optics microscopy it was found decrease in grain size of both primary silicon particles and Al-Si eutectic parts with increase in absorbed energy density of the compression plasma flows. The primary silicon crystals were dispersed down to 300 nm in the result of high cooling rate in the melted layer after its homogenization by means of hydrodynamic mixing. It was found that increase in the absorbed energy density homogenization of the elemental composition in the modifies layer occurs due to increase in life-time of the melted state and more efficiency mixing process.

The compression plasma flows impact of the silumin alloys with the metal coating provides melting of the coating and its mixing with the malted part of the Al-Si ally. After the crystallization the atoms of alloying metals dissolves mainly in the crystal lattice of aluminum particles and form the intermetallics. But, increasing in the absorbed energy density of the compression plasma flows results in falling of the metals concentration lower than the level required for intermetallic compounds forming. In this case only the Al-based solid solutions are formed. The excess in silicon concentration in hypereutectic allows to form the silicides particles which were found in the X-ray diffraction patterns.

The samples of the hypereutectic silumin alloys with the modified surfaces were annealed in a furnace at 350 ^{o}C during different times. The influence of the plasma flows impacts as well as alloying metal presence in the modified layers on the heat resistance of the samples are discussed in the work.

* The work was supported by the grant of the Belarusian Republic Fund for Foundation Research # T19PM-091.

SURFACE TOPOGRAPHY OF SAMPLES OBTAINED USING ADDITIVE TECHNOLOGIES FROM METAL POWDERS AFTER IRRADIATION WITH HIGH-CURRENT ELECTRON BEAMS

O. A. BYTCENKO[1,2], I. G. STESHENKO[2], V. A. PANOV[2], A. B. MARKOV[3], K. M. ERIKOV[1]

[1] Moscow Aviation Institute (National Research University), Moscow, Russian Federation
[2] - Chernyshev Moscow Machine-Building Enterprise, Moscow, Russian Federation
[3] Tomsk Scientific Center of the Siberian Branch of the Russian Academy of Sciences, Tomsk, Russian Federation

This work is devoted to the study of the influence of high-current pulsed electron beams on the surface roughness and topography of metal samples obtained by selective laser melting. It was found that irradiation of samples at various accelerators leads to a marked change in the structure of the surface layer and a decrease in surface roughness in the range from 1.5 to 3.4 times. It is shown that a high-current pulsed electron beam can serve as an effective tool for improving the performance properties of the surface layer of parts obtained using additive technology.

The presented scientific work is a continuation of the work under the grant of the Russian Foundation for basic research № 14-08-97046 r_povolzhye _a .

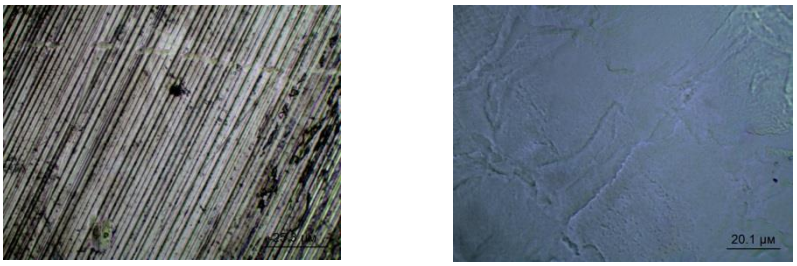

a *b*

Fig.1. Topography of the surface layer of a stainless steel target (OM):
a) before irradiation; b) after irradiation (EB(30;27))

REFERENCES

[1] Shulov V.A., Engelko V.I., Gromov A.N. Influence of irradiation regimes by high-current pulsed electron beams on the process of crater formation on the surface of nickel alloy targets. Hardening Technologies and Coatings. 2013, 11 (107), 15-19.
[12] Bytsenko O.A., Filonova E.V., Markov A.B. The effect of intense beams on the surface layers of modern heat-resistant alloys with ion-plasma coatings of various compositions. London: Interaction of radiation with solid, 2015, 193-195.
[3] Bytsenko O.A., Filonova E.V., Markov A.B. High-current pulsed electron beams for surface engineering of ion-plasma coatings. News of materials science. Science and Technology, 2017, 2 (26), 9.
[4] Bytsenko O.A., Grigorenko V.B., Lukina E.A. The development of methods of metallophysical research: methodological issues and practical significance. Aviation materials and technologies, 2017, S, 498-515
[5] Bytsenko O.A., Filonova E.V., Markov A.B., Belova N.A. The effect of irradiation with high-current electron beams on the surface layers of modern heat-resistant nickel alloys with ion-plasma coatings of various compositions. Proceedings of VIAM. Electronic Journal, 2016, 6 (42). URL: http://viam-works.ru (17.07.2016). DOI: 10.18577/2307-6046-2016-0-6-10-10.

INFLUENCE OF HYDROGEN CONTENT IN WORKING GAS ON GROWTH OF HARDENED LAYER AT ION NITRIDING OF STEELS*

R.S. ESIPOV, YU.G. KHUSAINOV, A.A. NIKOLAEV, K.N. RAMAZANOV

Ufa State Aviation Technical University, Ufa, Russia

At present, for the surface hardening of machine parts, the nitriding method in a glow dis-charge is widely used [1]. It is known [2, 3] that a high chromium content leads to passivation of the steel surface. As a result of this process, nitriding becomes long (20-30 h). Increasing in the growth rate of a hardened layer due to depassivation of the surface of steels is an actual task.

The aim of this work is to study the influence of the hydrogen content on the adsorption-diffusion processes when nitriding steels in a glow discharge plasma.

The experiment consisted in the processing of steels at a different content of hydrogen in a gas environment. Nitriding in a glow discharge was carried out at the ELU-5 installation. The treatment temperature was 550°C at a gas pressure of 150 Pa and an time of 6 hours. The microstructure of the nitrided layer of steels was invesigeted using an optical microscope. The thickness of the hardned layer was estimated by measuring the microhardness in the depth of the samples.

The results of the study showed that the use of hydrogen-containing gas environment for nitriding in a glow discharge plasma is an effective way of intensifying adsorption-diffusion processes. It has been established that an increase in the hydrogen content in the working space of the vacuum chamber from 10 to 30% leads to a change in the thickness of the hardened layer.

Austenitic steel having a low content of chromium have is insignificant effect of surface passivation of the during nitriding. An increase in the content of hydrogen in the gas environ-ment leads to a slight increase in the growth rate of the hardened layer. When processing of martensitic steel, on the contrary, high chromium content leads to passivation of the surface. Therefore, in the case of ion nitriding of high-chromium steels, the use of gas working media containing hydrogen up to 25% is an effective way to increase the adsorption-diffusion processes.

REFERENCES

[1] Yu. M. Lakhtin, Ya. D. Kogan “Nitriding of steel,” Mech. Engin., 256 p. 1976.

[2] P. David “Practical Nitriding and Ferritic Nitrocarburizing,” ASM International, 256 p. 2003.

[3] B. N. Arzamasov “Chemical-thermal treatment of metals in activated gases,” M .: Mech. Engin., 224 p. 1979.

* The study was funded by Russian Foundation for Basic Research, project No. 20-38-70031.

INVESTIGATION OF THE INFLUENCE OF SURFACE PREPARATION METHODS ON NITRIDING OF TITANIUM ALLOYS*

A.A. NIKOLAEV, R.D. AGZAMOV, A.F. TAGIROV, YU.G. KHUSAINOV, R.S. ESIPOV

Ufa State Aviation Technical University, Ufa, Russia

The article is devoted to research of influence of methods of surface preparation on physical-chemical and mechanical properties of nitrated layer of titanium alloys. It is known [1] that the quality of surface preparation before nitriding affects the mechanical and operational properties of the hardened layer. For example, after nitriding corrosion resistance will be higher on parts with lower surface roughness [2]. In this work electrolyte-plasma polishing (EPP) and dry electrochemical polishing (DEP) were used as surface preparation methods. Initial roughness was of the same value and was Ra=0.072 μm. However, in the process of EPP a layer of chemical compounds (phosphates, etc.) was formed on the surface, which had a negative impact on the visual appearance of samples from titanium alloys after low-temperature nitriding. After DEP, the visually nitrified surface has an even golden color over the entire area.

Some samples were ion-cleaned in high-current arc discharge, after such cleaning the defective layer formed after the EPP is removed. Despite the positive result for real parts, such as the compressor blades, cleaning in arc discharge is almost impossible. due to the complex geometry of the blades. At the junction of the pen and shelf of the blade, an area of shading is formed during arc cleaning, so that the defective layer in this place is not removed, and during nitriding will form a characteristic zone.

To assess the effect of surface preparation methods on the hardened layer characteristics, the following results were obtained: microhardness distribution dependencies at depth, microstructure, surface layer chemical composition and surface residual stresses. On the basis of the received results technological recommendations on low-temperature ion nitriding of products from titanium alloys are formed.

REFERENCES

[1] Edrisy, Afsaneh, and Khorameh Farokhzadeh. "Plasma nitriding of titanium alloys." Plasma Science and Technology-Progress in Physical States and Chemical Reactions, 2016.

[2] Mamonov, A. M., Sarychev, S. M., Slezov, et al. "Effect of Vacuum Ion-Plasma Treatment on Surface Layer Structure, Corrosion and Erosion Resistance of Titanium Alloy with Intermetallic a 2-Phase." Metal Science and Heat Treatment vol.60(5-6), Article Number 290-296, 2018.

* The study was funded by Russian Foundation for Basic Research, project No. 20-38-70031.

THE EFFECT OF GRAIN SIZE OF STEEL R6M5 ON THE DIFFUSION RATE AND GROWTH KINETICS OF THE HARDENED LAYER AFTER ION NITRIDING IN A GLOW DISCHARGE*

R.K. VAFIN[1], A.V. ASYLBAEV[1] , E.F. KHAIRETDINOV[1], L.R. SHAIKHUTDINOVA[1], K.N. RAMAZANOV[1]

[1] *Ufa State Aviation Technical University, Ufa, Russia*

Today, due to the continuous improvement of science, engineering and technology, high demands are placed on the materials used for mechanical and operational properties. These requirements contribute to the use of not only expensive materials with the necessary range of properties, but also the structural modification of already used materials by thermal or mechanical treatments. The most promising methods of mechanical and thermal processing methods are intensive plastic deformation and ion nitriding, respectively[1-5].

This work is devoted to studying the effect of grain size and morphology of R6M5 high-speed tool steel on the microstructure and microhardness after ion nitriding in a glow discharge. It has been established that the use of intense plastic deformation of torsion before ion nitriding forms a highly fragmented and disoriented ultrafine-grained structure, which contributes to an increase in the surface microhardness and the thickness of the diffusion layer on high-speed tool steel R6M5.

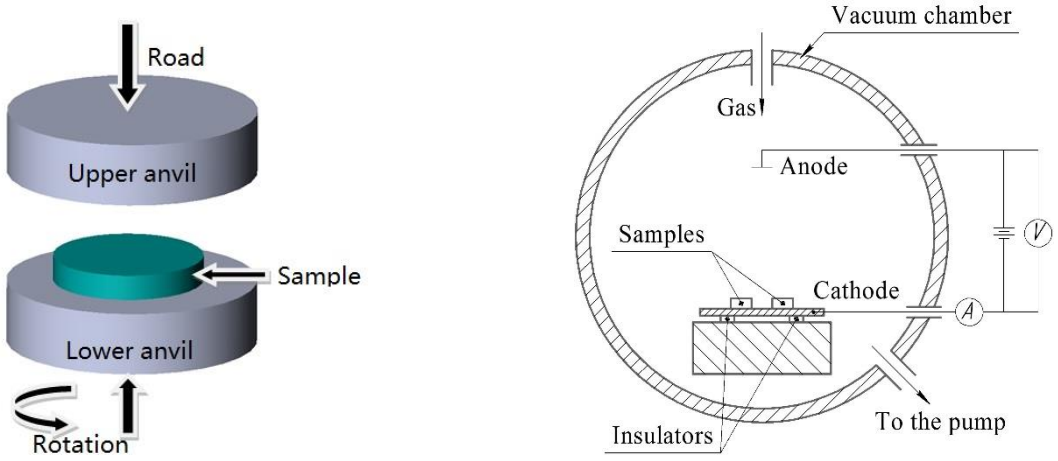

a b

Fig.1. A schematic illustration of the processes: a-severe plastic deformation torsion [1], b-ion nitriding in the glow discharge.

REFERENCES

[1] Zhengjie Lin, Liqiang Wang, Kelvin Wai Kwok Yeung, Jining Qin, "The ultrafine-grained titanium and biomedical titanium alloys processed by severe plastic deformation (SPD)," SOJ Materials Science & Engineering, vol. 1, no. 1, p. 01, November 2013.

[2] Kyun Taek Cho, Kyung Song, Sang Ho Oh, Young-Kook Lee, Won Beom Lee, "Surface hardening of shot peened H13 steel by enhanced nitrogen diffusion," Surface and Coatings Technology, vol. 232, pp. 912–919, October 2013.

[3] Lie Shen, Liang Wang, Yizuo Wang, Chunhua Wang, "Plasma nitriding of AISI 304 austenitic stainless steel with pre-shot peening," Surface and Coatings Technology, vol. 204, no. 20, pp. 3222–3227, July 2010.

[4] Ke Lu, Jian Lu, "Surface nanocrystallization (SNC) of metallic materials-presentation of the concept behind a new approach," J Mater Sci Technol, vol. 15, no. 3, pp. 193–197, March 1999.

[5] Ke Lu, Jian Lu, "Nanostructured surface layer on metallic materials induced by surface mechanical attrition treatment," Materials Science and Engineering: A., vol. 375, pp. 38–45, July 2004.

* The work was supported by the Russian Science Foundation under grant MD-3334.2019.8.

STRUCTURE AND PROPERTIES OF THE STEEL SURFACE LAYER CONTAINING NITRIDES AND SILICIDES OF HIGH-MELTING METALS FORMED BY ELECTRON-ION-PLASMA METHOD*

N. KOVAL, V. DEVYATKOV, V. SHUGUROV, YU. IVANOV, E. PETRIKOVA, A. TERESOV, M. RYGINA, YU. AKHMADEEV

Institute of High Current Electronics SB RAS, 2/3, Akademichesky ave., Tomsk, 634055, Russia

The aim of this work is to identify patterns of modification of elemental and phase composition, defective substructure, mechanical and tribological properties of carbon steel subjected to combined treatment in a single vacuum cycle, including high-melting and silicon coating deposition and irradiation with an intense pulsed electron beam to obtain a surface layer with improved strength and tribological properties.

Steel 5135 ((0.31-0.44) C- (0.17-0.37) Si- (0.5-0.8) Mn-0.3Ni-0.035S-0.035P- (0.8-1.1) Cr-0.3Cu was used as the substrate material, the rest - Fe, wt.%), pre-heat treated to form a ferrite-pearlite structure. The samples were in the form of cylinders 10 mm high and 15 mm in diameter. On the polished surface of steel samples on the COMPLEX installation, developed in the laboratory of plasma emission electronics of the HCEI SB RAS, which is included in the list of unique RF installations (UNIKUUM complex http://ckp-rf.ru/usu/434216/), they were successively applied thin (1 μm) films of silicon and niobium. The deposition of a silicon film was carried out by magnetron, and niobium films by electric arc methods with plasma assisting. Next, the received film / substrate system was irradiated by a pulsed electron beam in the joint melting mode with the surface layer of steel ((20-50) J/cm^2, (100 and 200) μs, (3-30) imp.). Studies of the elemental and phase composition, the state of the defective substructure were carried out by scanning electron microscopy and X-ray diffractometry; microhardness and wear resistance of the modified steel surface were determined.

As a result of the studies, it was found that, regardless of the electron beam pulse duration (100 μs and 200 μs), the maximum hardness of the steel surface is realized when the number of impact pulses is equal to 3. The maximum hardness of the surface layer of modified steel is 9600 MPa (3.3 times exceeding the hardness of steel in the initial state), is achieved with a beam pulse duration of 200 μs, an energy density of 50 J/cm^2 and the number of pulses 3. With a beam pulse duration of 100 μs, the maximum value hardness of the surface layer of modified steel, equal to 6300 MPa, is achieved at an energy density of 30 J/cm^2 and the number of pulses 3.

It is shown that the minimum wear parameter of modified steel, fixed for a beam pulse duration of 200 μs at an electron beam energy density of 50 J/cm^2, is $k = 2.83 * 10^{-6}$ mm^3 / N * m, that is more than 15 times less than the parameter steel wear in the initial (ferrite-pearlite structure) state. When the electron beam pulse duration is 100 μs, the wear parameter reaches the minimum values $k = 0.93 * 10^{-6}$ mm^3 / N * m, that is ≈50 times less than the steel wear parameter in the initial (ferrite-pearlite structure) state. It was found that the wear parameter of the modified steel reaches its minimum values at the same electron beam power density of 0.25 MW / cm^2. Moreover, the shorter the pulse duration of the electron beam, the higher the wear resistance of the modified steel (at 100 μs $k = 0.93 * 10^{-6}$ mm^3 / N * m; at 200 μs $k = 2.83 * 10^{-6}$ mm^3 / N * m).

It was shown that the high strength and tribological properties of steel, revealed by irradiating the film / substrate system with an electron beam (50 J / cm^2, 200 μs, 3 pulses), are caused not only by the high content of the strengthening phase particles (niobium silicides of the composition Nb_5Si_3, $Nb_{3.61}Si_{0.39}$, intermetallic $Nb_{08}Fe_{02}$, niobium oxide NbO_2 and silicon carbide SiC), but also a relatively large thickness of the hardened layer, reaching 30 microns.

* The work was supported by RFBR project No. 19-08-00248.

INVESTIGATION OF STRUCTURE AND MECHANICAL PROPERTIES OF STAINLESS-STEEL SPECIMENS, MADE BY ADDITIVE METHOD, AFTER PULSE ELECTRON BEAM TREATMENT*

A.D. TERESOV[1], *YU.H. AKHMADEEV*[1], *E.A. PETRIKOVA*[1], *O.V. KRYSINA*[1], *YU.F. IVANOV*[1], *G.V. SEMENOV*[2]

[1]*Institute of High Current Electronics SB RAS, Tomsk, Russia*
[2]*LLC «TETA», Loskutovo, Tomsk, Russia*

Modern machining technologies generally operate on the principle of step-by-step removal of material from the workpiece until the necessary shape and size is obtained (the «subtraction» principle). In contrast, the rapidly developing additive manufacturing technologies (AM-technologies) operate on the principle of layer-by-layer growth of the product based on its computer 3D-model by applying layers of different thickness (the principle of «addition») [1-3]. For growing metal products, 3D-printers are currently most commonly used, the principle of which is based on sintering of metal powder or welding of metal wire with laser radiation or electron beam [1-3]. In the case of using a metal powder, the formation of the article takes place in a thin (50-100 μm) layer where the individual particles are sintered by point selective heating. When using the wire, the thickness of the layer is characterized by the diameter of the wire used (0.8-3 mm) and the parameters of energy impact, and the process itself is more similar to layer-by-layer welding [1, 2].

A common problem, to some extent characteristic of all types of AM-technologies, is the problem of ensuring an appropriate microstructure of the synthesized material, eliminating porosity. Another disadvantage of AM-technologies is the anisotropy of the structure and properties of the material, high internal stresses, which is inevitable under the layer-by-layer principle of article creation. In order to solve these problems, the authors have proposed a method of finishing the surface of metal articles, produced using AM-technologies, with a pulsed electron beam in vacuum [4].

The purpose of the present work is to compare the structure and mechanical properties of AISI 308LSi stainless-steel specimens obtained by layer-by-layer electron-beam welding of wire with diameter of 1 mm in vacuum and subjected to subsequent pulse electron-beam treatment at «SOLO» setup [5]. During irradiation the following parameters were varied: energy density in pulse (15-30 J/cm^2), pulse duration (50-200 μs), number of pulses (3-20).

Comparative analysis of the surface structure of the specimens after irradiation in some modes showed the formation of a finer cellular structure in contrast to the original samples. Surface roughness decreased by 2 times, surface microhardness increased by 15%. Thus, the surface treatment of AISI 308LSi stainless-steel specimens, made by AM-technologies, with a pulsed electron beam resulted in a uniform crushed structure having improved mechanical properties in comparison with the initial material.

REFERENCES

[1] I. Gibson, D. Rosen, B. Stucker, Additive manufacturing technologies: 3D printing, rapid prototyping, and direct digital manufacturing. Moscow: Technosfera, 2016 [in Russian].

[2] I.V. Shishkovsky, Basics of high-resolution additive technologies. St. Petersburg: Piter Publ., 2015 [in Russian].

[3] B. Evans, Practical 3D printers: The science art of 3D printing. New York: Apress, 2012.

[4] A.D. Teresov, N.N. Koval, Yu.F. Ivanov, E.A. Petrikova, "Application of a pulsed electron beam for surface polishing of metal products obtained by laser or electron-beam powder sintering," Izv. Vyssh. Uchebn. Zaved. Fiz., Vol. 59, № 9/2, pp. 264–266, september 2016 [in Russian].

[5] N.N. Koval, Yu.F. Ivanov, "Nanostructuring the surface of metal-ceramic and ceramic materials under pulsed electron-beam treatment," Izv. Vyssh. Uchebn. Zaved. Fiz., Vol. 51, №5, pp. 60–70, may 2008 [in Russian].

* The reported study was funded by RFBR and Tomsk region according to the research project № 19-48-700021.

THERMAL STABILITY OF STRUCTURE AND PROPERTIES OF STEEL SURFACE LAYER CONTAINING NITRIDES AND SILICIDES OF REFRACTORY METALS FORMED BY ELECTRON-ION-PLASMA METHODS*

N.N. KOVAL, A.D. TERESOV, E.A. PETRIKOVA, YU.F. IVANOV, V.N. DEVYATKOV, V.V. SHUGUROV, G.E. RYGINA, YU.H AKHMADEEV

Institute of High Current Electronics SB RAS, Tomsk, Russia

The purpose of the present work is to study the thermal stability of the structure, mechanical and tribological properties of carbon steel subjected to combined treatment in a single vacuum cycle, including the deposition of refractory metal and silicon coatings and irradiation with an intense pulsed electron beam to obtain a surface layer with improved strength and tribological properties.

The substrate material used was 5135 steel ((0.31-0.44) C – (0.17-0.37) Si – (0.5-0.8) Mn – 0.3Ni – 0.035S –0.035P – (0.8-1.1)Cr – 0.3Cu, the remainder being Fe, wt%), pre-thermally treated to form a ferrite-pearlite structure. The specimens were in the shape of cylinders with a height of 10 mm and a diameter of 15 mm. Thin (1 μm) silicon and niobium films were sequentially deposited to the polished surface of steel specimens at «COMPLEX» setup developed in the laboratory of plasma emission electronics of HCEI SB RAS, which is included in the list of unique installations of the Russian Federation («UNIKUUM» complex, http://ckp-rf.ru/usu/434216/). Silicon film deposition was carried out by magnetron and niobium film by arc plasma assisted methods. Further, the obtained «film/substrate» system was irradiated with a pulsed electron beam in a co-melting mode with a steel surface layer ((20-50) J/cm^2, (100 and 200) μs, (3-30) pls.). The thermal stability of the structure and properties of the steel was studied on specimens maintained under vacuum ($p = 3.5 \cdot 10^{-2}$ Pa) for 3 hours at 650 °C. Studies of the elemental and phase composition, condition of the defective substructure were performed by scanning electron microscopy and X-ray diffractometry; Microhardness and wear resistance of the modified steel surface were determined.

As a result of the studies carried out, it was found that the stability of the structure and properties of the modified steel layer depends substantially on the modification mode, namely, energy density and pulse duration of the electron beam. System irradiation mode «film (Si (1 μm)+Nb (1 μm))/(5135 steel) substrate» by intensive pulsed electron beam (50 J/cm^2, 200 μs, 3 pls.) was revealed, which allows to form a thermally stable state in the surface layer of steel, the hardness of which after holding for 3 hours at temperature 650 °C exceeds hardness of the initial state of steel by 5 times, wear resistance - by more than 10 times. Note that the hardness of the surface alloy steel layer after heat treatment exceeds the hardness of the modified layer before heat treatment by 1.5 times, however, the wear resistance of the surface alloy steel layer after heat treatment is 1.5 times lower than the wear resistance of the surface alloy steel layer before heat treatment.

By X-ray analysis of 5135 steel specimens subjected to surface alloying by irradiation with an intense pulsed electron beam (50 J/cm^2, 200 μs, 3 pls.) of the «film (Si+Nb)/(40Cr steel) substrate» system and subsequent exposure at 650 °C, 3 hours, a significant change in phase composition during heat treatment was detected. Firstly, isolation of two new phases (Nb_3Si and Nb_6C_5) was detected, and secondly, an increase in the relative amount of the Nb_5Si_3 phase was detected. In total it led to growth of total quantity of the phases strengthening material from 35.7 wt. % (before heat treatment) up to 66.8 wt. % after heat treatment, i.e. by ≈ 2 times that, obviously, was the main reason of additional (by 1.5 times) increasing in hardness of a surface layer of steel. It should be noted that increase in hardness of steel led to decrease in wear resistance in ≈ 1.5 times. The latter may be due to the crumbling of hard inclusions during wear and then their involvement in the destruction of the steel surface layer as an abrasive.

* The work was supported by RFBR project No. 19-08-00248.

EFFECT OF INTENSE PULSED ELECTRON BEAM IRRADIATION ON THE MECHANICAL PROPERTIES OF PRE-EUTECTIC SILUMIN

Ustinov A.M.[1], Ivanov Yu.F.[2], Klopotov A.A.[1,3], Petrikova E.A.[2], TeresovA.D.[2], Abzaev Yu.A.[1], Loskutov O.M.[1], Volokitin O.G.[1]

[1]*Tomsky State University of Architecture and Building, Tomsk, Russia*

[2]*Institute of High Current Electronics SB RAS, 634055, Tomsk, Russia*

[3]*National Research Tomsk State University, Tomsk, Russia*

E-mail: klopotovaa@tsuab.ru

Aluminum-based alloys, including Al-Si (silumins) belong to the class of light materials. Due to its high casting properties and good specific mechanical characteristics, silumins have been used in many branches of modern industry: automotive and aerospace engineering, medicine, construction industry and etc. The flaw of silumins, which limits the scope of application, is the increased brittleness. The purpose of this work is to determine the effect of intense pulsed electron beam irradiation on the mechanical properties of ASTMB179-92A silumin.

Samples of silumin of the ASTMB179-92A brand (Al-10 Si-2 Cu-1 Ni) were used as the research material. Proportional flat samples with a tail section for cantilever attachment were used for testing. Tests of mechanical properties were performed on samples that were not irradiated and irradiated with an intense pulsed electron beam (SOLO installation, ISE SB RAS). Irradiation mode: the pulse duration of the electron beam is 150 microseconds, the number of pulses is 3, the pulse repetition rate is 0.3 s^{-1}, and the energy density of the electron beam is 25 and 35 J/cm^2. Tensile testing of samples was carried out on the INSTRON 3386 test machine. The distribution of deformations in the near-surface layers of the sample under tension was obtained using the VIC-3D optical measurement system

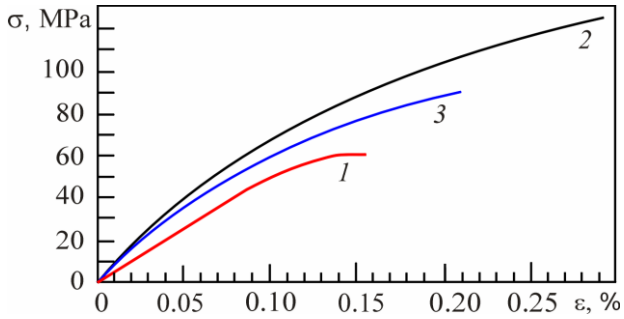

Fig. 1. Diagrams of deformation of silumin samples under tension: 1 – initial state; 2,3 – irradiated with an intense pulsed electron beam with an energy density of 25 J/cm^2 and 35 J/cm^2, respectively

For fig. 1 shows the deformation curves obtained by stretching silumin plates in different states. It is seen that irradiation with an intense pulsed electron beam on the surface of samples leads to a noticeable improvement in the strength properties of silumin. The most significant improvement in the strength properties of silumin is observed when irradiating samples with a beam with an energy density of 25 J/cm^2. These data correlate with the distribution of relative deformations on the surface of a flat plate at the stage preceding the fracture of samples. In local places in the central part of the samples, significant foci of plastic deformation are manifested during stretching, in which the destruction of the samples occurs.

Thus, irradiation of ASTMB179-92A silumin with a pulsed electron beam can increase the strength and plasticity of the material in ≈2 times.

Studies of the silumin destruction surface were carried out. It is shown that the main reason for increasing the mechanical properties of the irradiated material is the formation of a submicrocrystalline structure in the surface layer of high-speed cellular crystallization of aluminum with inclusions of silicon and nanocrystallineintermetallide particles evenly distributed along the cell boundaries.

The work was carried out with the financial support of the RGNF grant (project no. 19-79-10059).

ARGON LOW-TEMPERATURE ATMOSPHERIC PLASMA TREATMENTOF BIOCOMPATIBLE COMPOSITESBASED ON POLYLACTIC ACID AND HYDROXYAPATITE*

O.A. LAPUT[1], *I.V. VASENINA*[3], *M.O. KULIKOV*[1], *A.A.GRUSHEVSKAYA*[1], *K.P. SAVKIN*[2], *I.A. KURZINA*[1]

[1]*National Research Tomsk State University 36 Lenin ave., Tomsk, 634050 Russia,*
olesyalaput@gmail.com, 8-952-899-25-96
[2]*Institute of High Current Electronics SB RAS, 2/3 Akademichesky ave., Tomsk, 634055 Russia*
[3]*P.N. Lebedev Physical Institute, 53, Leninsky Prospect, Moscow, 119333, Russia*

The effect of argon flow low-temperature atmospheric plasma treatment on surface physicochemical properties of biodegradable and biocompatible composites based on polylactic acid with hydroxyapatite (PLA/HA 80/20, 60/40) was investigated. The plasma treatment conditions were following: the amplitude of discharge voltage – 300 V; the amplitude of discharge current – 40 mA; pulse duration – 1 and 5 μs; exposure time – 3 min; frequency – 100 kHz; the electron temperature – 0.3 eV; the plasma concentration –5 × 10^{11}cm^{-3}. Influence of gas-discharge atmospheric plasma on polymer and composite materials is accompanied by their surface property alteration as chemical state and wettability which caused by destruction and new molecular bond formation, surface microrelief modification – smoothing or cratering [1].

It was established that plasma treatment with the pulse duration of 1 μs leads to significant changes in C1s spectra of the PLA/HA 60/40 and PLA/HA 80/20 composites. The content of CH_3-C bonds (1) with a binding energy 285.0 eV is increased and the contents of other typical for the C1s PLA spectrum (-O-CH (2) and O-C=O (3)) bonds are decreased. The proportion of CH_3-C bond (1) increases for PLA/HA 60/40 by 1.8 times and for PLA/HA 80/20 by 1.3 times under the plasma flow pulse duration of 1 μs. The increase in plasma flow pulse duration to 5 μs results in the CH_3-C bond (1) content decrease for both types of composites, but for PLA/HA 80/20 it still exceeds the initial value. In the O1s spectra, the largest changes are observed under the plasma treatment with pulse duration of 5 μs, where the proportion of -C=O bonds (1) decreases by up to 1.6 times and a proportion of -C-O-bonds (2) significantly increases(up to 11 times). Changes of the chemical bond ratios are probably due to parallel processes of bond scission, oxidation and cross-linking of polymer chains in the spectra of C1s and O1s [2].With the increase of the plasma treatment pulse duration, the atomic concentration of oxygen gradually is increased by ~1.4 times and the carbon content is decreased by ~ 3 times for both types of composites. This indicates that oxidative processes in the surface layer of the materials take place. At the same time, the atomic concentrations of calcium and phosphate are increased. The plasma treatment is known to have both radiation and thermal effect on of the material's surface [3]. Therefore, polymer component of the composite material may have been evaporated or melted, while the more heat-resistant particles of hydroxyapatite are surfaced after plasma irradiation.

Wettability of the materials after plasma treatment is significantly improved, as evidenced by a decrease in the contact angle when wetted with water, glycerol and ethylene glycol, and also accompanied by an increase in free surface energy. Surface energy modification can significantly affect the bioavailability and surface cell absorption. Implants may have greater or lesser wettability, ability to adsorb cells that participate in electrochemical processes, and bioresorption characteristics. Thus, it is shown that argon flow low-temperature atmospheric plasma treatment is an effective technique for surface physicochemical property modification of biocompatible composite materials based on polymer and non-organic matrix.

REFERENCES

[1] 1.J. Izdebska-Podsiadły, E. Dorsam // Vacuum. –2017. –145. –278-284.

[2] 2. A.Y. Song, Y.A. Oh, S.H. Roh, J.H. Kim, S.C. Min// Institute of Food Technologists. –2015. –81(1). –86–96.

[3] 3.M. R. Murthy, E. V. Rao // Bulletin of Materials Science. –2002. –25.M.S. Vorobyov, V.F. Tarasenko, E.Kh. Baksht, A.V. Kozyrev, N.N. Koval, S.Yu. Doroshkevich, "Energy spectrum of an electron beam outputted into ambient air on an electron accelerator with a grid plasma cathode," Proc. 20th Int. Conf. on High Current Electronics (ISHCE), Tomsk, Russia, pp. 209–213, 2018.

* Work supported by the Tomsk State University competitiveness improvement program and the Ministry of Science and Higher Education (project number 0721-2020-0037).

ATOMIC SEGREGATION IN CO-DEPOSITED SI-AL COATINGS*

A.A. SERDOBINTSEV[1], *I.O. KOZHEVNIKOV*[1], *A.V. STARODUBOV*[1,2], *N.M. RYSKIN*[1,2], *A.M. PAVLOV*[1], *V.V. GALUSHKA*[1]

[1]*Saratov State University, Saratov, Russia*
[2]*Saratov Branch, V.A. Kotel'nikov Institute of Radio Engineering and Electronics RAS, Saratov, Russia*

Metamaterials (MM) have attracted great interest in many areas of scientific research. Application of MM is very promising in UHF vacuum electronics of mm and sub-THz range [1]. Dielectric substrate with MM coating was used for travelling wave tube with sheet electron beam [2]. It was shown that a 50% improved interaction impedance and a 20% reduced circuit attenuation of SWS can be achieved.

The formation of MM coating is possible when its electrical properties are fully controllable. We used a method of two source magnetron co-sputtering deposition of Si-Al alloys to obtain series of coatings with different chemical composition and thus different resistivity. Control of composition was provided by varying the power of Al magnetron source while power of Si source was constant. Quartz with a thickness of 500 μm was used as a substrate.

Three series of coatings were obtained with various substrate temperatures (373 K, 423 K and 473 K). The resistivity vs. Al composition dependence for each series has sharp decrease at some specific Al percentage (Figure 1). It should be noted that this Al specific percentage is different for various substrate temperatures. The resistivity was measured with four probe method (probes are in line) so it can be considered as surface resistivity.

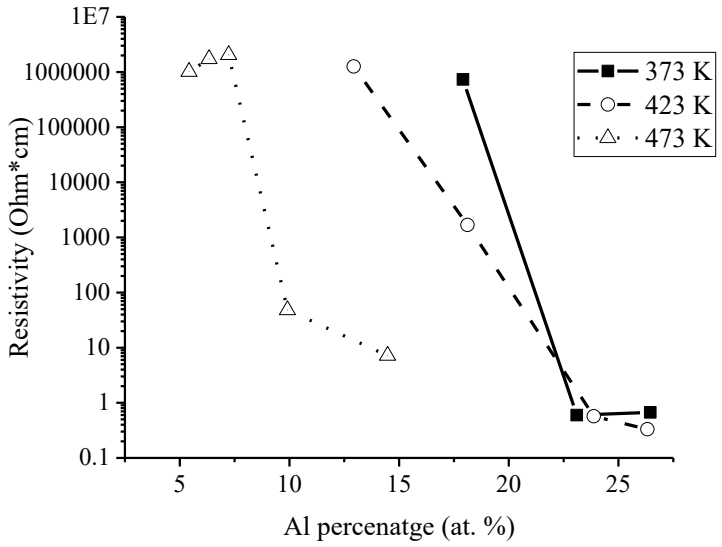

Fig.1. Resistivity vs. Al percentage dependence for series of coatings deposited with various substrate temperatures.

Visual observation of the deposited coatings reveals drastic difference in surface color of the free surface (coating/air) and inner surface (substrate/coating). This phenomenon was found for low resistance coatings only. While inner surface was colored brown the free surface had bright metallic luster. So it can be concluded that there was a segregation of Si and Al atoms in coating during deposition. Si atoms were mainly concentrated at inner surface while Al atoms located at free surface of the coating. Such an explanation was verified with Raman scattering from both coating surfaces. This result is promising for deposition of coatings with controllable concentration profiles.

REFERENCES

[1] G. Shvets, "Plenary Talk: Applications of electromagnetic metamaterials to vacuum electronics devices and advanced accelerators," IEEE International Vacuum Electronics Conference, Monterey, CA, pp. 3-3, 2014.

[2] Bai, N., Shen, M., & Sun, X. Investigation of Microstrip Meander-Line Traveling-Wave Tube Using EBG Ground Plane. IEEE Transactions on Electron Devices, 62(5), 1622–1627, 2015.

* The work was supported by the Russian Foundation for Basic Research under grant No. 20-07-00929.

DEPOSITION OF MULTILAYER COATING OF VARIABLE COMPOSITION BY REACTIVE MAGNETRON SPUTTERING WITH PULSE EXPOSURE OF WORKING MEDIUM BY ELECTRON BEAM*

D.R. EMLIN[1], *A.V. CHUKIN*[2], *N.V. GAVRILOV*[1], *A.S. KAMENETSKIKH*[1], *A.A. ERSHOV*[1]

[1]*Institute of Electrophysics of the UB of RAS, Yekaterinburg, Russia*
[2]*Ural Federal University, Yekaterinburg, Russia*

The structure and phase composition of coatings formed by reactive magnetron sputtering of Ti in the range of reaction gas flow (0-2 sccm) under exposure of N_2-Ar working medium (~ 0.1-0.25 Pa) by the low-energy electron beam (100 eV, 10-25 A) were studied. To increase the degree of dissociation of molecular nitrogen and to reduce the minimal gas flow at which stoichiometric titanium nitride is formed, conditions have been created for the oscillation of injected electrons in the volume of the working chamber [1]. An ion current density was of up to 15 mA/cm^2. Multilayer coatings of variable composition (hexagonal TiN0.3 and cubic TiN titanium nitrides) and hardness (11 and 21 GPa, correspondingly) with an adjustable layer thickness (25-100 nm) were formed using pulse exposure of N_2-Ar working medium by electron beam. A similar approach based on the deposition of multilayer coatings by changing the state of nitrogen in a gas-metal plasma created by separate generators of a metal and gas plasma was previously proposed in [2]. Multilayer coatings of up to 5 μm thick with individual layer number up to 200 were obtained. The results of optical emission spectroscopy of plasma, a study of the structure and composition of coatings by X-ray diffraction, and measurements of the hardness and crack resistance of coatings by indentation are presented.

REFERENCES

[1] A. V. Vizir', E. M. Oks, P. M. Shchanin, G. Yu. Yushkov. "Non-self-sustained hollow-cathode glow discharge for large-aperture ion sources". Technical Physics, vol. 42, pp. 611-614, 1997.

[2] O.V. Krysina, V.V. Shugurov, N.A. Prokopenko. "Synthesis and properties of multilayer and gradient coatings". Proc. of International Science and Technology Conference, "Modern Technologies and Advanced Materials" TPU, Tomsk, Russia, 2017, pp. 182-184, in russian. http://earchive.tpu.ru/handle/11683/43840

* The presented work continues the work supported by the Russian Science Foundation under grant No. 14-08-00249 A

COMPOSITE BIPHASE COATINGS FORMED BY HYBRID TECHNOLOGY FOR BIOMEDICAL APPLICATIONS

A.O. Vorobyev, A.Y. Fedotkin, A.I. Kozelskaya and S.I. Tverdokhlebov

Tomsk Polytechnic University, Tomsk, Russia

This work is dedicated to deposition of composite calcium phosphate (CaP) coatings on the surface of titanium substrates with micro-arc oxidation (MAO) and radio frequency magnetron sputtering (RFMS) modification technologies and to the study of their physicochemical properties. The combination of these methods made it possible to obtain bioactive coatings with a unique set of properties required for personalized implants in order to restore the functions of the musculoskeletal system and bone tissue.

The formed composite coatings consist of two layers: the lower (up to ~ 35 μm thick) is formed using MAO, and the upper (up to ~ 1 μm thick) thin layer is formed by the RFMS method. All the coatings were deposited under the same conditions. A CaO-based electrolyte with the addition of hydroxyapatite (HA) powder was used to form CaP coatings by the MAO. The coatings deposition with the RFMS was carried out by sputtering of powder targets of the following composition: a target from pure HA, a target from pure β-tricalcium phosphate (TCP), a target from Mg-substituted HA (Mg-HA), a target from Mg-substituted TCP (Mg-TCP), a target from Sr-substituted HA (Sr-HA) and a target from Sr-substituted TCP (Sr-TCP).

SEM revealed that the morphology of all CaP coatings formed by a combination of the MAO and the RFMS methods is the same at the macro level and is represented by structural elements of a spheroidal shape (spherulites) with through pores. It was shown with the AFM that, at the micro level, the morphology of the coatings under study is represented by quasi-equiaxed grains of various sizes located on the surface of the initial elements of the MAO coating.

The studied CaP coatings consist of elements of the substrate material: Ti and Al, as well as electrolyte and sputtered targets: Ca, P, O, Sr, and Mg (in the case of Sr and Mg-substituted targets from HA and TCP). Coatings formed by the MAO method are calcium deficient. Deposition of the upper layer with the RFMS leads to an increase in the Ca/P ratio in the coatings under study. An increase in the Ca/P ratio in the coatings under study occurs in the following order: MAO<MAO+Mg-TCP<MAO+TCP<MAO+Sr-TCP<MAO+Mg-HA<MAO+Sr-HA<MAO+HA.

XRD analysis showed that the coatings under study are completely X-ray amorphous, except for coatings formed by the combination of the MAO and RF-sputtering of HA and Sr-HA targets, on the X-ray diffraction patterns of which there are peaks of the crystalline HA phase.

The study of the mechanical properties of the coatings revealed that the value of the elastic modulus of CaP coatings formed by the MAO method is lower than that of composite coatings.

This work was supported by the Tomsk Polytechnic University Competitiveness Enhancement Program project VIU-School of Nuclear Science and Engineering-204/2019 and in part of magnetron sputtering is the continuation of the RFBR project No. 13-08-98052 r_sibir_a.

DEPOSITION OF Gd_2O_3 BY REACTIVE ANODIC EVAPORATION IN ARC WITH SELF-HEATED HOLLOW CATHODE *

A.S. KAMENETSKIKH[1], N.V. GAVRILOV[1], D.R. EMLIN[1], S.V. KRIVOSHAPKO[1], A.V. CHUKIN[2]

[1]Institute of Electrophysics of the UB of RAS, Yekaterinburg, Russia.
[2] Ural Federal University, Yekaterinburg, Russia.

The need for thick (more than 1 μm) gadolinium oxide (Gd_2O_3) coatings grows up currently as their use allows to increase the sensitivity of neutron detectors [1] and improve the characteristics of optical system elements in the UV range of 0.19-16 μm [2]. In the present work, Gd_2O_3 coatings were deposited by evaporation of Gd in a self-heated hollow cathode arc with magnetic focusing of the electron flow onto the anode-crucible in an Ar-O_2 medium at a total pressure of 0.1 Pa. The method [3] allows to control the coating deposition rate over a wide range (0.1–2 μm/h) and to implement the modes that are preferable for deposition both thin and thick coatings.

Optical emission spectra of plasma of arc with evaporating anode contains peaks of neutral Gd^* (368.5 and 452.5 nm) and ionized Gd^+ (405 nm). The intensity of the Gd^* line increases with vapor pressure, the intensity of the Gd^+ line increases sharply with the discharge current. The maximum degree of ionization of metallic vapor reaches 90%.

XRD of Gd_2O_3 coatings showed that the main phase is the cubic oxide, which corresponds peaks (332) $2\theta \sim 39.05$ ° and (440) 47.5 °. A feature of the coatings is the strong texture (440), which is absent in the coating deposited by magnetron sputtering [4] and electron beam evaporation [5].

REFERENCES

[1] G.F. Knoll, Radiation Detection and Measurement, Wiley, 1989.

[2] 7. N.K. Sahoo et al. “Reactive electron beam evaporation of gadolinium oxide optical thin films for ultraviolet and deep ultraviolet laser wavelengths”, Thin Solid Films, vol. 440, pp. 155-168, 2003.

[3] N.V. Gavrilov et al. “Al_2O_3 thin films deposition by reactive evaporation of Al in anodic arc with high levels of metal ionization”. Surf. Coat. Technol., vol. 359, pp. 117-124, 2019.

[4] Y. Li et al. “Effect of the oxygen concentration on the properties of Gd_2O_3 thin films”, J. Crystal Growth, vol. 265, pp. 548-552, 2004.

[5] D.A. Grave et al. “Process–structure–property relations of micron thick Gd_2O_3 films deposited by reactive electron-beam physical vapor deposition (EB-PVD)”, vol. 206, pp. 3094-3103, 2012.

* The work was supported by RFBR, project number 20-08-00169.

POWER SUPPLY FOR SUPERIMPOSED HIGH POWER IMPULSE AND MIDDLE FREQUENCY DUAL MAGNETRON SPUTTERING*

V.O. OSKIRKO, A.N. ZAKHAROV, A.P. PAVLOV, V.A. SEMENOV, A.A. SOLOVYEV

Institute of High Current Electronics, 2/3 Akademicheskii Ave., Tomsk, 634055, Russia

High power impulse magnetron sputtering (HiPIMS) is a promising method of physical vapor deposition (PVD), which allows obtaining high-quality coatings [1]. But this method is characterized by a lower deposition rate [2, 3], relative to traditional DC and medium frequency (MF) magnetron sputtering. Relatively recently, the new superimposition HiPIMS and MF concept, in which the MF pulses are introduced during the off-time of HiPIMS pulses was introduced. Hybrid magnetron sputtering systems using the superimposition concept allow for a high level of ionization of the sputtered particles and the ion current density on the substrate while maintaining the deposition rate at an acceptable level [4–6]. The possibility of realizing the advantages of the superimposition concept depends significantly on the potential of the power supply system. A new power supply for superimposed HIPIMS+MF dual magnetron sputtering was developed in our team and experiments on deposition Al films in different HIPIMS+MF sputtering modes were conducted. Fig. 1,a shows oscillograms of discharge current and voltage pulses at the power supply output in superimposed mode. Experiments have shown that the ratio of HIPIMS power to MF significantly affects such process parameters as deposition rate, ion current density on the substrate and ion-to-atom ratio (Fig. 1,b). The HIPIMS to MF power ratio can therefore be used to control the properties of the sputtered coating.

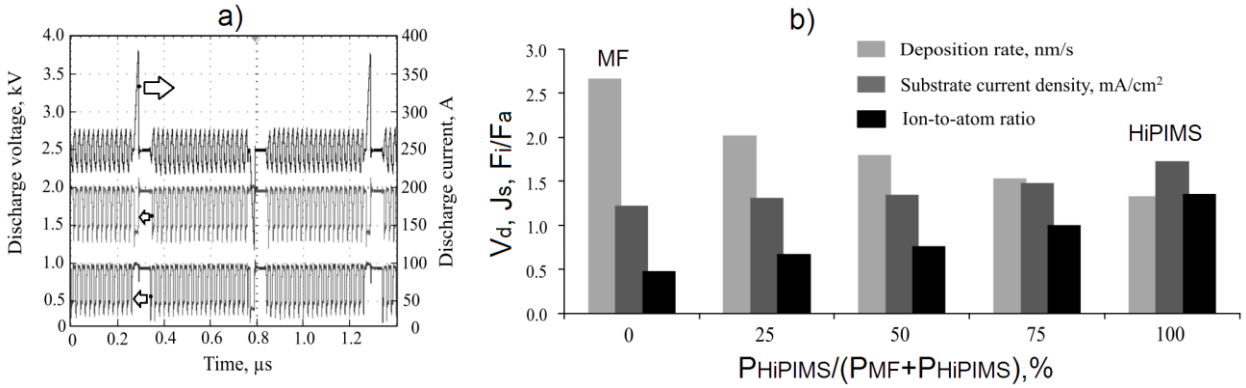

Fig. 1. Oscillograms of discharge current and voltage in HIPIMS+MF hybrid mode of dual magnetron sputtering (a) and dependences of deposition rate (V_d), ion current density on the substrate (J_s) and ion-to-atom ratio (F_i/F_a) from the discharge power ratio of HIPIMS to MF (b).

REFERENCES

[1] *J.T. Gudmundsson et al. //* J. Vac. Sci. Technol. – 2012. – A 30, 030801.
[2] *A. Anders //* J. Vac. Sci. Technol. – 2010. – A 28, pp. 783–790.
[3] *M. Samuelsson et al. //* Surf. Coat. Technol. – 2010. – V. 205, pp. 591–596.
[4] *M. Samuelsson et al. //* J. Vac. Sci. Technol. – 2012. – A 30, 031507.
[5] *V. Sittinger et al. //* The Solid Films. – 2013. – V. 548, 18–26.
[6] *V. Stranak et al. //* Surf. Coat. Technol. – 2012. – 206, pp. 2801–2809.

* The work was funded by Russian Foundation for Basic Research and the government of the Tomsk region of the Russian Federation, grant № 18-42-703005

CALCIUM PHOSPHATE THIN FILMS DEPOSITED AT GLANCING ANGLE BY RADIOFREQUENCY MAGNETRON SPUTTERING UNDER CONSTANT SUBSTRATE ROTATION[1]

K. PROSOLOV[1,2], V. LASTOVKA[1], Yu. SHARKEEV[1,2]

[1] *Institute of Strength Physics and Materials Science of SB RAS, 2/4, pr. Akademicheskii, Tomsk, 634055, Russia, konstprosolov@gmail.com, +7-961-888-58-33*

[2] *National Research Tomsk Polytechnic University,30, Lenin Avenue, Tomsk, 634050, Russia*

Calcium phosphate (CaP) coatings are a widely researched topic that, over the years, resulted in lots of applications in the field of bone regeneration. It is because conventional metallic implants become encapsulated by fibrous tissue, which in turn, not only prolongs the healing time but also leads to implant loosening and, eventually, premature failure of implantation.

A possibility to manipulate nanotopography attracts much attention in recent years. In the field of biomedical engineering, the formation of nanostructures is believed to be an alternative route for improving the osteointegration and osteoinduction properties of the implants' surface. One of the promising approaches for sculpturing thin film morphology is oblique or glancing angle deposition (OAD or GLAD). When the substrate is tilted to an oblique angle, nuclei that condense on it prevent incoming vapor from condensing into the region behind the nuclei, causing the nuclei to develop into columns that tilt towards the vapor source [1]. In the literature, OAD is frequently referred to the case where a coating is deposited on a stationary mounted substrate, while in case of GLAD, substrate rotation under glancing angle is involved.

By employing the variation in deposition parameters such as substrate rotation (ω), angle and rate of deposition, and substrate temperature, different microstructures resulting in unique physical and chemical properties can be achieved.

An emerging method for bioactive coating deposition in the field of PVD is the radiofrequency (RF) magnetron sputtering method [2]. Magnetron sputtering is widely used in the formation of coatings for various applications. There is a significant interest in radiofrequency (RF) magnetron sputtering of bioactive calcium phosphate thin films. This method allows deposition of calcium phosphate-based coatings that are highly adherent to the substrate.

In our work, we show the influence of GLAD at constant substrate rotation on the morphology and structure of thin calcium phosphate films deposited by RF magnetron sputtering method. A coating thickness distribution was significantly improved for the samples under constant substrate rotation compared to the stationary mode for the substrate tilt angle of 80º. The refractive index of the deposited coatings varied from 1.5 to 1.9 for different deposition cases. Surface free energy that was estimated after contact angle measurements was notably increased with an increase in tilt angle. An EDX microanalysis showed homogeneous distribution of elements across the substrate for GLAD with constant substrate rotation. The GLAD of complex calcium phosphate material can lead to the growth of thin films with significantly changed morphological features and can be utilized to create self-organized nanostructures on various types of surfaces [3].

REFERENCES

[1] *A. Barranco et al.* // Progress in Materials Science. – 2016. – 76. – 59-153.
[2] *R.A. Surmenev et al.* // Acta Biomaterialia. – 2014. – 10. – 557–579
[3] *K. A. Prosolov et al.* // Coatings. – 2019. – 9. – 220.

[1] This work was supported by the state program of fundamental research of Russian Academy of Science for 2017–2020, No.III.23.2.5.

THE TECHNOLOGY OF DEPOSITION NEW THERMAL-BARRIER CERAMIC COATINGS BASED ON YTTRIUM ALUMINATE YALO3 BY VACCUM-ARC DEPOSITION *

A. YU. NAZAROV[1], E. L. VARDANYAN[1], K.N. RAMAZANOV[1],

R. SH. NAGIMOV[1], A.A. MASLOV[1]

[1] Ufa State Avioatin Thecnical University, Ufa, 450008, Russia

The aim of this work is solving the problem of finding new ways to increase the efficiency of turbojet engines through the development of new heat-resistant coatings for metal and ceramic composite materials, which are increasingly used in the production of engines of leading engine manufacturers (General Electric, CFM International). Ensuring the operability of the components of the combustion chamber at rising temperatures is a key factor in increasing fuel efficiency and traction characteristics of engines, which has reserves for development.

The urgency of the problem is determined by the need to protect the composites in the combustion chamber and turbine engine from the effects of high-temperature gas flows and fuel combustion products. But in the case of using composites with a ceramic matrix, the priority is the protection against exposure, heat barrier coating properties, which are priority in the application of traditional nickel superalloys, are fading into the background thanks to heat-resistant matrix[1,2,3]

The structure, phase and chemical compositions of developed coatings were investigated. Standard heat resistance tests were carried out for this class of coatings abroad: thermal cyclic tests, thermal aging in the furnace, study of phase transformations during testing, assessment of the rate of degradation and erosion of the coating.

Was study the possibilities of increasing the productivity of the selected technology by using multicomponent cathodes with a given mass ratio of components corresponding to the required stoichiometric composition of the coatings obtained by powder metallurgy, to study the possibility of improving the quality of the deposited ceramics by minimizing the presence of a droplet phase due to the use of plasma filters and screens that create a hollow effect cathode.

The results obtained will allow us to develop new ways of protecting promising and already used composite materials in aggressive high-temperature environments, especially if they are used in turbojet engines, and can be used in the future in the production of new generations of engines.

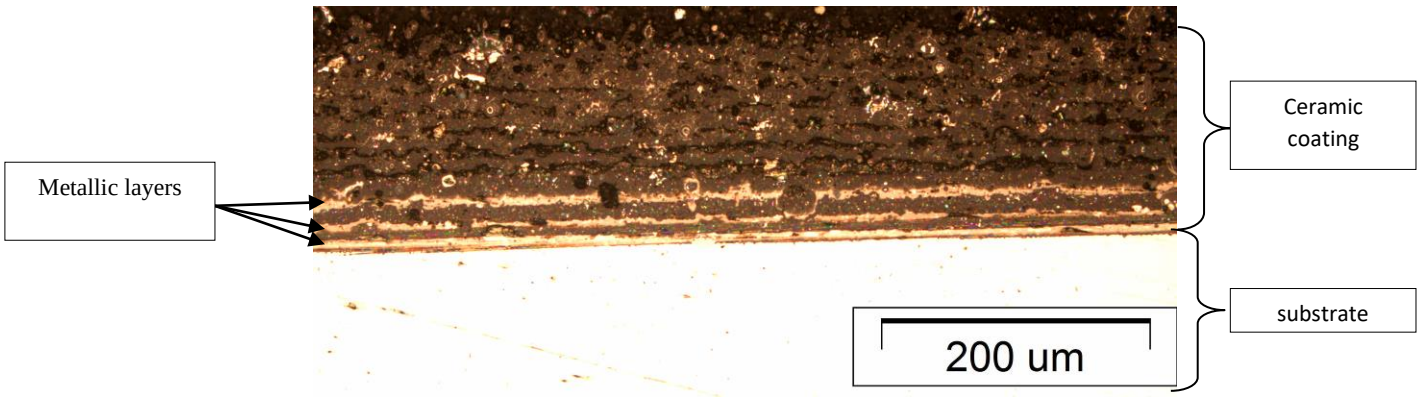

REFERENCES

1. Wei Hao, Qihui Zhang, Chen Xing, Fangwei Guo, Meiyu Yi, Xiaofeng Zhao, Ping Xia. Assessment of the performance of Y2SiO5-YSZ/YSZ double-layered thermal barrier coatings. Journal of the European Ceramic Society.

2. K.N. Lee. Current status of environmental barrier coatings for Si-Based ceramics. Surface and Coatings Technology 133-134 (2000) p.1-7

3. Irene Spitsberg and Jim Steibel. Thermal and Environmental Barrier Coatings for SiC/SiC CMCs in Aircraft Engine Applications. Int. J. Appl. Ceram. Technol., 1 [4] 291-301 (2004)

* The work was partial supported by Russian Foundation for Basic Research, Project No. 20-38-70031

MECHANICAL PROPERTIES AND TRIBOLOGICAL BEHAVIOR OF MULTILAYER INTERMETALLICS TI-AL-N/TI-AL COATINGS DEPOSITED BY VACUUM ARC PLASMA *

E. L. VARDANYAN[1], *K.N. RAMAZANOV*[1], *A. YU. NAZAROV*[1],

R. SH. NAGIMOV[1]

[1] *Ufa State Avioatin Thecnical University, Ufa, 450008, Russia*

Ti-Al-N coatings possess high hardness and good oxidation resistance that provides for their extensive application in the protection of machining tools and engineering components [1-3]. Also wear-resistant coatings deposited by low pressure vacuum arc plasma are widely used to increase life and efficiency of different metal cutting tools. This paper shows the results of a study on the influence of architecture (thickness of layers deposited in environment of argon vs nitrogen) of wear-resistant coatings on physical, mechanical and operational properties of end mills..

At the first stage, the optimal ratio of the thickness of the layer of synthesized in the nitrogen environment was determined in comparison with the layer of formed in the argon environment. After, optimal thickness of layers was determined by deposited coatings with different thickness from 0.1-1mkm. Schematics structure of multilayer intermetallics Ti-Al-N/Ti-Al coatings deposited by vacuum arc plasma presented on fig. 1.

Coatings consisting of alternating Ti-Al-N/ Ti-Al layers of equal thickness demonstrated the best physical and mechanical properties. Durability of coated mills increased as compared to commercial coatings.

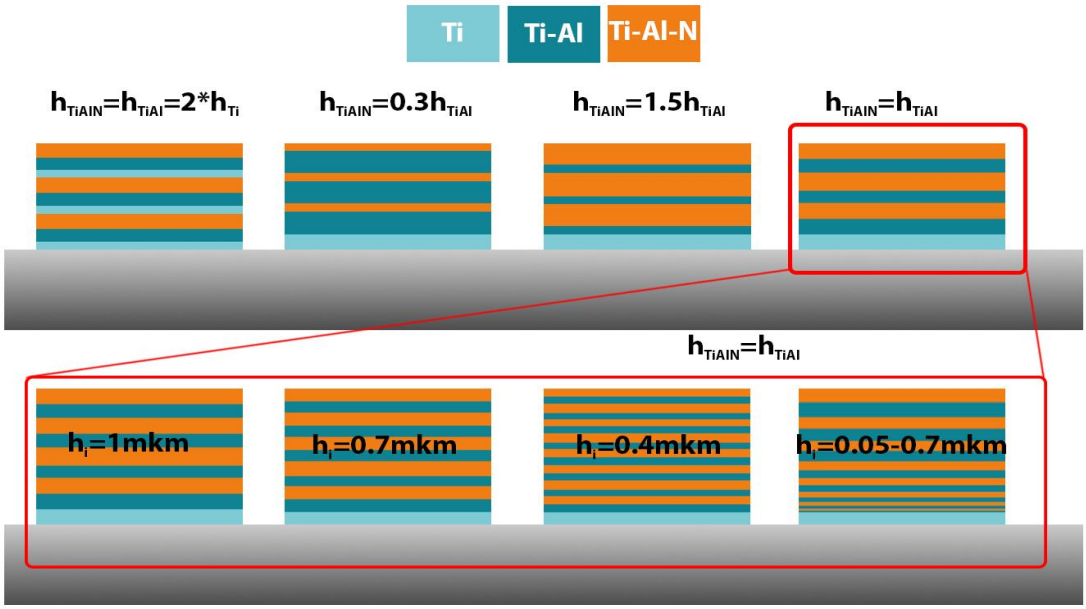

Fig.1. Schematics structure of multilayer intermetallics Ti-Al-N/Ti-Al coatings deposited by vacuum arc plasma.

REFERENCES

[1] A. Shugurov, M. Kazachenok, Surface & Coatings Technology (2018), 10.1016/j.surfcoat.2018.09.001 .

[2] L. Zauner, P. Ertelthaler, T. Wojcik, H. Bolvardi, S. Kolozsvári, P.H. Mayrhofer, H. Riedl, Surface & Coatings Technology (2019), doi: https://doi.org/10.1016/.

[3] O.V. Krysina, V.V. Shugurov, N.A. Prokopenko, E.A. Petrikova, O.S. Tolkachev, Yu.A. Denisova. Russian Physics Journal (2019) DOI 10.1007/s11182-019-01801-0.

* The work was supported by Russian Foundation for Basic Research, Project No. 20-38-70031

PLASMA ASSISTANCE EFFECT ON THE EXAMPLE OF ZrN-BASED COATINGS DEPOSITED BY VACUUM-ARC METHOD AT THE ADDITION OF Al, Ti, Nb*

O.V. KRYSINA, N.A. PROKOPENKO, V.V. SHUGUROV, E.A. PETRIKOVA, O.S. TOLKACHEV

Institute of high current electronics, Tomsk, Russia

The main idea of Al, Ti, Nb addition to ZrN coatings composition is to create the conditions with changeable nitrogen concentration in the wide range of gas discharge parameters. Earlier works showed that we can change the concentration of nitrogen in the nitride coatings as TiN, MoN, TiAlN, and etc. [1, 2] by the varying of the share of nitrogen in the gas-metal plasma with gas-plasma source based on non-self-sustained arc discharge with thermionic and hollow cathodes [3]. Its method is low-inertial, because of the duration of arc current change is about up to tens of milliseconds. The traditional method with change of nitrogen partial pressure is inertial with time of pressure stabilization about 100 ms to 1 s. New low-inertial method allows to deposit the multi-layered metal/nitride coatings with abrupt boundaries of layers with period from tens to hundreds nanometers and gradient nitride coatings with smoothly nitrogen concentration change throughout the thickness. The earlier experiments and literature data [4] showed that the coatings based on ZrN have high ability to form nitride in the nitrogen-containing atmosphere. In addition, the formation of over- or substoichiometric metal nitrides is problematically even at high and low partial pressure of nitrogen, respectively. Therefore, in the present work the Al, Ti and Nb with different concentration were added in the composition of ZrN coatings in order to improve the properties of binary ZrN system coating and to ability of nitrogen concentration variation will appear for this type of coating.

All experiments related to the ternary coating deposition were carried out using the QUINTA ion-plasma setup, designed and manufactured at the Institute of High Current Electronics SB RAS (Tomsk, Russia) [5]. The sources of the metal plasma are the modernized DI100 electric arc evaporator with a 100 mm diameter cathode (Al, Nb) and the DI80 electric arc evaporator with an 80 mm diameter cathode (Zr), and the DP400 electric arc evaporator of extended construction. In dependence of evaporated materials the one of electric arc evaporators was equipped with a magnetic filter to separate metal plasma flow from the droplet phase. As part of a toroid with a rotation angle of 120°, the evaporator is constructed with a non-magnetic material and features water-cooled walls [6]. The source of the gas-discharge plasma is a plasma generator based on a non-self-sustained arc discharge with thermionic and hollow cathodes of an extended design [5]. It was used as device to change share of gas ions in the gas-metal plasma by varying arc current in the wide range.

The coating properties were analyzed using a μVizo-MET-221 metallographic micrograph (LOMO, Russia), scanning electron microscope Philips SEM-515 with EDAX ECON IV microanalyzer (Netherlands), Shimadzu XRD-6000 diffractometer (Japan), PMT-3 microhardness tester (LOMO, Russia), Shimadzu DUH-211 ultramicrotester (Japan), Pin on Disc and Oscillating TRIBOtester tribometer (TRIBOtechnic, France), MNP-1 optical profilometer (TDI SIE SB RAS, Russia), Calotest CAT-S-0000 equipment for measuring thickness of films and coatings (CSEM, Switzerland), and JEOL JEM-2100 F transmission electron diffractive microscope (Japan).

REFERENCES

[1] O.V. Krysina, N.N. Koval, I.V. Lopatin, V.V. Shugurov, S.S. Kovalsky, “Generation of low-temperature plasma by low-pressure arcs for synthesis of nitride coatings,” J. Phys. Conf. Ser., vol. 669, pp. 012032, 2016.

[2] O.V. Krysina, V.V. Shugurov, N.A. Prokopenko, E.A. Petrikova, “Influence of nitrogen concentration on structure, composition and properties of nitride coatings deposited by vacuum arc plasma-assisted method,” J. Phys. Conf. Ser., vol. 1115, pp. 032075, 2018.

[3] L.G. Vintizenko, S.V. Grigoriev, N.N. Koval, V.S. Tolkachev, I.V. Lopatin, P.M. Schanin, “Hollow-cathode low-pressure arc discharges and their application in plasma generators and chargedparticle sources,” Russ. Phys. J., vol. 44, pp. 927-936, 2001.

[4] J. Musil, Š. Kos, M. Jaroš, R. Čerstvý , S. Haviar , S. Zenkin, Z. Čiperová, “Coating of overstoichiometric transition metal nitrides (TMN_x ($x > 1$)) by magnetron sputtering,” Jpn. J. of Appl. Phys., vol. 58, pp. SAAD10 (1- 9), 2018.

[5] V.V. Shugurov, N.N. Koval, O.V. Krysina, N.A. Prokopenko, “QUINTA equipment for ion-plasma modification of materials and products surface and vacuum arc plasma-assisted deposition of coatings,” IOP Conf. Series: Journal of Physics: Conf. Series, vol. 1393, pp. 012131, 2019.

[6] A.I. Dodonov, V.M. Bashkov, “Producing electric arc plasma in a curvilinear plasma guide and substrate coating,” Patent WO/045871, pp. 1-31, 1998.

* The work was supported by the Russian Foundation of Basic Research (project No. 18-48-700016-r_a).

GRADIENT AND MULTI-LAYERED NITRIDE COATINGS DEPOSITED BY VACUUM-ARC METHOD*

O.V. KRYSINA, YU.F. IVANOV, N.A. PROKOPENKO, V.V. SHUGUROV, E.A. PETRIKOVA, O.S. TOLKACHEV

Institute of high current electronics, Tomsk, Russia

The ternary nitride coatings based on the transition metals (e.g., Ti, Zr, and Cr) are of great interest for obtaining structures with various mechanical and tribological properties. For example, there exist coatings of systems, such as Zr–Si–N, Ti–Cr–N, Ti–Al–N, Al–Si–N, and Zr–Nb–N. However, synthesis of the nitride coatings with a stoichiometric composition reduces their adhesive strength to the substrate due to high compressive stresses, which can destroy the coating. Thus, deposition of multi-layered coatings with alternating soft and hard layers [1] is a potential solution. Deposition of a multi-layered TiN/Ti coating was previously demonstrated to lead to an increase in wear resistance and hardness compared to a single-layered TiN coating due to a decrease in the grain size of the formed coating [2]. Another solution includes synthesis of gradient coatings with variable elemental composition throughout the layers. The gradient can be obtained by varying the nitrogen concentration in the deposited coating based on titanium and its nitrides [2]. Furthermore, varying the metal element concentration is possible through the thickness of the synthesized coating [3, 4]. The obtained gradient coatings demonstrate a significant decrease in the internal residual stresses compared to coatings with constant volume composition. Changeable elemental and phase composition through the synthesized layer thickness (transition to gradient coatings) using ion-plasma deposition methods allows for obtaining the required characteristics of protective coatings, such as high hardness, high adhesive strength, and wear and corrosion resistance.

According to literature, the ZrN and (Zr,Nb)N homogeneous coatings offer good protective properties, such as high hardness and adhesion as well as increased wear, corrosion, and radiation resistance, and resistance to high-temperature oxidation. These systems have a high potential to provide scratch-resistant coatings that also satisfy decorative demands [5] as well as the literature accounts of cutting tool applications for these system coatings [6]. Practical applications of gradient and multi-layered (Zr,Nb)N coatings are not entirely defined because the amount of research is not sufficient. Service property investigations for multi-layered gradient (Zr,Nb)N coatings also do not exist.

The present paper focuses on obtaining gradient wear-resistant (Zr,Nb)N coatings using a vacuum-arc method, synthesized by varying ion current densities of plasma source with different construction. They are (1) arc evaporator for obtaining of metal element gradient throughout the thickness and (2) the gas-plasma source based on non-self-sustained arc discharge with thermionic and hollow cathodes for obtainment of nitrogen gradient [7]. The study of structure, phase composition, and mechanical and tribological properties of gradient and multi-layered nitride coatings deposited by vacuum-arc method in detail were carried out and analyzed.

REFERENCES

[1] S. Lin, K. Zhou, M. Dai, E. Lan, Q. Shi, F. Hu, T. Kuang, C. Zhuang, “Structural, mechanical, and sand erosion properties of TiN/Zr/ZrN multilayer coatings,” Vacuum, vol. 122, pp. 179-186, 2015.

[2] X. Cao, W. He, B. Liao, H. Zhou, H. Zhang, C. Tan, Z. Yang, “Sand particle erosion resistance of the multilayer gradient TiN/Ti coatings on Ti6Al4V alloy,” Surf. Coat. Technol., vol. 365, pp. 214–221, 2019.

[3] V.V. Uglov, V.M. Anishchik, S.V. Zlotski, G. Abadias, S.N. Dub, “Stress and mechanical properties of Ti–Cr–N gradient coatings deposited by vacuum arc,” Surf. Coat. Technol., vol. 200, pp. 178 – 181, 2005.

[4] Fei Cai, Ying Gao, Shihong Zhang, Lin Zhang, Qimin Wang, “Gradient architecture of Si containing layer and improved cutting performance of AlCrSiN coated tools,” Wear, vol. 424–425, pp. 193–202, 2019.

[5] H. Klostermann, F. Fietzke, R. Labitzke, T. Modes, O. Zywitzki, “Zr–Nb–N hard coatings deposited by high power pulsed sputtering using different pulse modes,” Surf. Coat. Technol., vol. 204, pp. 1076–1080, 2009.

[6] V.N. Zhitomirsky, “Structure and properties of cathodic vacuum arc deposited NbN and NbN-based multi-component and multi-layer coatings,” Surf. Coat. Technol., vol. 201, pp. 6122–6130, 2007.

[7] V.V. Shugurov, N.N. Koval, O.V. Krysina, N.A. Prokopenko, “QUINTA equipment for ion-plasma modification of materials and products surface and vacuum arc plasma-assisted deposition of coatings,” IOP Conf. Series: Journal of Physics: Conf. Series, vol. 1393, pp. 012131, 2019.

* The work was supported by the Russian Foundation of Basic Research (project No. 18-48-700016-r_a).

THE FORMATION OF MON COATINGS BY VACUUM ARC DEPOSITION IN THE MODE OF PLASMA ASSISTANCE.*

O.V. KRYSINA, N.A. PROKOPENKO, V.V. SHUGUROV, S.S. KOVALSKY

Institute of High Current Electronics SB RAS, Tomsk, Russia

In the current conditions of a difficult economic situation, the need to optimize and improve production processes in various industries is becoming ever more acute. In this regard, studies aimed at improving the strength characteristics of metals and alloys are gaining relevance. One of the advanced methods for increasing the wear resistance of surfaces of parts is the application of heavy-duty coatings having high hardness and low coefficient of friction. Such coatings, for example, include nitrides of transition metals: TiN, CrN, MoN, etc. [1].

There are many methods for the synthesis of such coatings on the surface of products and work parts. But in this work, vacuum-arc plasma-assisted coating is used. This method is characterized by a wide range of synthesized coatings, a high coating rate, and excellent adhesion of the coating to the substrate.

As the studied coating, molybdenum nitride was chosen, because This coating has high hardness, low coefficient of friction, and has chemical inertness to non-ferrous metals. There is also little research on the effect of plasma assisting on the formation of molybdenum nitride coatings.

Thus, the aim of this work is to obtain molybdenum nitride coatings by the vacuum-arc plasma-assisted method. As well as studying the influence of plasma assisted modes on the formation of the resulting coatings.

The work was carried out at the Quinta laboratory installation [2]. The installation is equipped with several plasma generators. To generate metal plasma, the DI-100 plasma generator was used. For preliminary heating and final cleaning of the surfaces of the samples, as well as for plasma assisting during coating, the PINK-P-04M plasma generator was used.

REFERENCES

[1] A.A. Andreev, "Vacuum-Arc Coatings" Kharkov: NSC KIPT Press. – 2010.

[2] V.V. Shugurov, N.N. Koval , O.V. Krysina , N.A. Prokopenko "QUINTA equipment for ion-plasma modification of materials and products surface and vacuum arc plasma-assisted deposition of coatings" Journal of Physics: Conference Series, 2019, V.1393.

* The work was supported by the Russian Science Foundation under grant No. 18-48-700016.

PLASMA-ASSISTED DEPOSITION OF COMPOSITE COATINGS IN BEAM-PLASMA FORMATIONS FORMED IN AN INDEPENDENT GAS DISCHARGE WITH A HOLLOW CATHODE *

N.A. PROKOPENKO[1], *YU.A. DENISOVA*[1], *E.L. VARDANYAN*[2], *A.A. LEONOV*[1], *V.V. DENISOV*[1]

[1] *Institute of High Current Electronics SB RAS, 2/3 Akademichesky ave., Tomsk, 634055, Russia, e-mail: yukolubaeva@mail.ru, Tel.+7(3822)492683*

[2] *Ufa State Aviation Technical University, Ufa, Russia*

Improving the wear resistance of the surface of structural and tool materials is one of the most important tasks in the development of engineering. The creation on the surface of a carbide tool of nitride films up to several micrometers thick increases their service life by several times. One of the main factors affecting the structure and phase composition of coatings deposited on various materials by vacuum-arc or magnetron methods is the magnitude and ratio of the ion flux density and neutral particles J_i / J_a on the surface of the growing film, where J_i is the ion flux density, J_a - the flux density of neutral particles [1]. This ratio can be changed over a wide range by plasma assisted vacuum-arc spraying with a source of additional gas plasma. The use of a gas plasma source generating plasma with a large concentration gradient in the zone of parts placement does not allow maintaining the same value of J_i / J_a in the path of moving the part in the working chamber, which complicates the interpretation of the obtained processing results. A relatively homogeneous plasma medium in the entire volume of the vacuum chamber (hollow cathode) is created by a non-self-contained low-pressure glow discharge with a hollow cathode. The plasma synthesized in a hollow cathode of a glow discharge with external electron injection by the method of its generation can be assigned to beam-plasma formations [2]. In this work, we compared the structure and phase composition of nitride coatings based on Ti and Al, including multilayer coatings obtained by sputtering in a traditional plasma-assisted vacuum-arc spraying system and in a system for generating gas-metal beam-plasma formations formed in non-self-sustaining low pressure hollow cathode discharge.

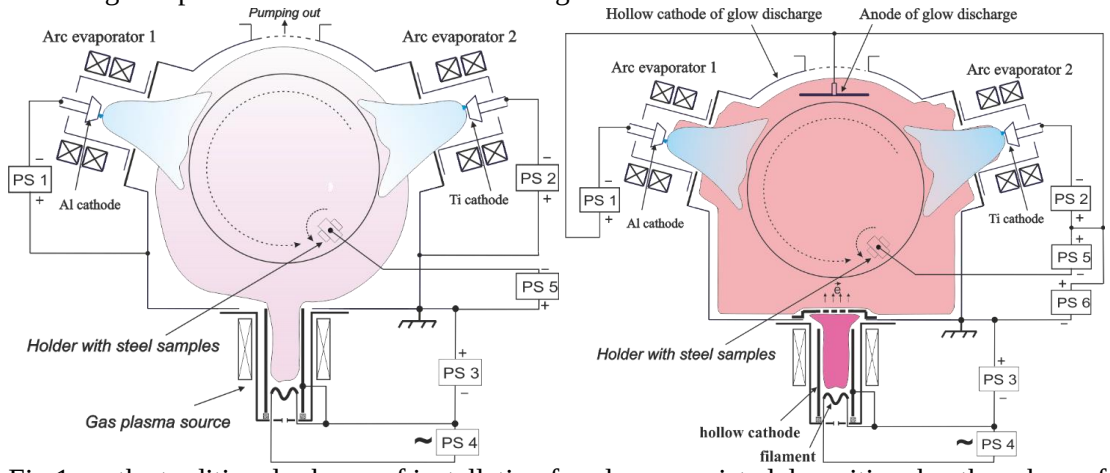

Fig.1 a – the traditional scheme of installation for plasma-assisted deposition, b – the scheme foe plasma-assisted deposition using beam-plasma formation.

REFERENCES

[1] J. Musil, "Hard nanocomposite coatings: Thermal stability, oxidation resistance and toughness" Surface & Coatings Technology, 2012, V.207, p.50–65.

[2] V.V. Denisov, Yu.H. Akhmadeev, N.N. Koval, S.S. Kovalsky, I.V. Lopatin, E.V. Ostroverkhov, N.N. Pedin, V.V. Yakovlev, and P.M. Schanin, "The source of volume beam-plasma formations based on a high current non-self-sustained glow discharge with a large hollow cathode, " Phys. Plasmas, 2019, V.26, Article Number 123510.

* The work was carried out with the financial support of the RFBR grant № 19-08-00370 A.

COMPARISON OF PROPERTIES OF THE CaP COATINGS FORMED BY RF-MAGNETRON SPUTTERING OF THE Mg- AND Sr-SUBSTITUTED β-TRICALCIUM PHOSPHATE AND HYDROXYAPATITE

A.Y. Fedotkin[a], *A.I. Kozelskaya*[a], *N.M. Korotchenko*[b], *A.S. Gigilev*[b], *E.V. Shesterikov*[c,d], *S.I. Tverdokhlebov*[a]

[a]*Tomsk Polytechnic University, Tomsk, Russia*
[b]*Tomsk State University, Tomsk, Russia*
[c]*Institute of Atmospheric Optics V.E. Zuev SB RAS, Tomsk, Russia*
[d]*Tomsk State University of Control Systems and Radioelectronics*

Lack of bioactivity and osteoconductivity of metal implants used for reconstructive surgery is usually overcome by the deposition of various calcium phosphate (CaP) materials. Hydroxyapatite (HA) is the most widely spread material because it is the base substance in the mineral part of human bone. Nowadays the effect of various ionic substitutions into the structure of CaP targets on the deposition rate and properties of coatings formed by their sputtering is actively studied [1]. Ionic substitutions contribute to bone renewal and remodeling.

Mg substitutions adjust bone growth and its metabolic activity influencing osteoblastic/osteoclastic cell activity. Lack of Mg causes osteogenesis disorders and a decrease in mechanical bone strength [2]. Strontium contributes to osteoblast activity and inhibits osteoclasts [3].

Our previous work [4] is dedicated to the effect of Mg and Sr substitutions into the structure β-tricalcium phosphate (TCP) on the properties of coatings formed by RF-magnetron sputtering.

Six various types of powders were used as targets: pure HA, Mg-substituted HA (Mg-HA), Sr-substituted HA (Sr-HA), pure TCP, Mg-substituted TCP (Mg-TCP), Sr-substituted TCP (Sr-TCP). RF-magnetron sputtering of these targets was carried out with the use of universal magnetron sputtering system "Cathode-1M" under the following conditions: target/substrates distance – 40 mm; working pressure – 0.5 Pa; power density for HA-based and TCP-based targets was 5.26 W/cm^2 and 4.8 W/cm^2, respectively; deposition time was 7 hours for the HA-based targets and 21 hours for the TCP-based targets. Grinded and polished Ti (VT6) discs were used as substrates (diameter – 10 mm, thickness – 1 mm). To measure coatings thickness, they were deposited on Si substrates.

It was revealed that all plasma spectra are represented with atomic and molecular ions corresponding to the composition of the targets. Sr significantly increases the deposition rate of TCP-based coatings, while Mg slightly decreases this parameter. These substitutions don't affect the deposition rate of HA-based coatings. This phenomenon can be explained by the difference in crystal lattices of TCP and HA. Ca/P ratio in TCP-based coatings is higher than in respective targets, while HA-based ones are characterized by the opposite trend. The presence of Mg substitutions decreases the Ca/P ratio in TCP-based targets and, especially, coatings. Sr ones, on the contrary, increase this parameter. Both substitutions decrease the Ca/P ratio in HA-based targets and coatings. The presence of ionic substitutions into CaP powder targets shifts their peaks in XRD-spectra. The spectrum of Mg-HA powder is characterized by the presence of peaks corresponding to whitlockite. All coatings formed by sputtering of the targets containing substitutions have a lower crystallinity in comparison with ones formed by the sputtering of non-substituted targets. The preferential orientation of crystals with the plane (002), which is parallel to the substrate surface, is the most pronounced for all the coatings because it is the most energetically beneficial [5].

This work was supported by the Tomsk Polytechnic University Competitiveness Enhancement Program project VIU-School of Nuclear Science and Engineering-204/2019 and in part of magnetron sputtering of HA targets is the continuation of the RFBR project No. 13-08-98052 r_sibir_a.

REFERENCES

[1] J.T.B. Ratnayake, M. Mucalo, G.J. Dias, "Substituted hydroxyapatites for bone regeneration: A review of current trends", J. Biom. Mater. Res. Part B: Ap. Biom., vol. 105, no. 5, pp. 1-15, 2016.

[2] W. Mróz, A. Bombalska, S. Burdyńska, M. Jedyński, A. Prokopiuk, B. Budner, A. Ślósarczyk, A. Zima, E. Menaszek, A. Ścisłowska-Czarnecka, K. Niedzielski, "Structural studies of magnesium doped hydroxyapatite coatings after osteoblast culture", J. Mol. Struct., vol. 977, no. 1-3, pp. 145-152, 2010.

[3] M. Šupová, "Substituted hydroxyapatites for biomedical applications: A review", Ceram. Int., vol. 41, no. 8, pp. 9203–9231, 2015.

[4] A.I. Kozelskaya, S.E. Kulkova, A.Y. Fedotkin, E.N. Bolbasov, Y.M. Zhukov, L. Stipniece, A. V. Bakulin, A.S. Useinov, E. V. Shesterikov, J. Locs, S.I. Tverdokhlebov, "Radio frequency magnetron sputtering of Sr- and Mg-substituted β-tricalcium phosphate: Analysis of the physicochemical properties and deposition rate of coatings", Appl. Surf. Sci., vol. 509, pp. 144763, 2020.

[5] M.R.T. Filgueiras, D. Mkhonto, N.H. de Leeuw, "Computer simulations of the adsorption of citric acid at hydroxyapatite surfaces", J. Cryst. Growth. vol. 294, no. 1, pp. 60-68, 2006.

EVALUATION OF THE PROPERTIES OF A-C:H:SiO_X COATING DEPOSITED ON 316L STAINLESS STEEL*

A.S. GRENADYOROV, A.A. SOLOVYEV, K.V. OSKOMOV

Institute of High Current Electronics SB RAS, Tomsk, Russia

Today, the use of implants and medical products to support the vital functions of the human body is highly relevant. Most of these products are made of stainless steel, which has better mechanical properties compared to other materials. But austenitic stainless steel such as SS316L is prone to corrosion when implanted in a human body. Since body fluids are an aggressive medium, they can induce the release of metallic ions such as chromium and nickel. It may promote allergy, inflammation, hypersensitivity reaction and tissue irritation [1]. One of the ways to solve this problem is to modify the implant and medical devices surface by means of coating deposition [1, 2].

Amorphous carbon (a-C and a-C:H) is often used as a material of barrier, wear and corrosion-resistant coatings [3-6]. It is known that adding Si or SiO_x to these coatings improves a number of their characteristics [7, 8]. Carbon coatings containing in their composition SiO_x phase in literature are called SiO_x-doped DLC, diamond-like nanocomposite (DLN), or a-C:H:SiO_x.

The method of plasma-assisted chemical vapor deposition was used to obtain a-C:H:SiO_x coatings in this work. Film formation was carried out by decomposition of liquid precursor (polyphenylmethylsiloxane) vapors in plasma of non-self-sustained arc discharge with a hot cathode. The elemental content of silicon and carbon in the film was determined by the deposition conditions [9, 10]. Previous research results have shown that the deposition of such coatings on unalloyed titanium and Ti-6Al-4V, silicon and glass can improve the mechanical and tribological properties of the surface of these materials.

The work is dedicated to the study of the properties of a-C:H:SiO_x coating on 316L stainless steel. Mechanical properties of coating, in particular hardness and adhesion, have been investigated. Surface morphology has been studied using atomic force and optical microscopy, while the structure and elemental composition have been analyzed using infrared Fourier and energy dispersion spectroscopy methods.

REFERENCES

[1] Bociaga D, Komorowski P, Sobczyk-Guzenda A et al / Surface properties and biological behaviour of Si-DLC coatings fabricated by a multi-target DC–RF magnetron sputtering method for medical applications // Diamond & Related Materials. – 2016. – V. 67. – P. 41-50.

[2] R. Hauert, K. Thorwarth, G. Thorwarth / An overview on diamond-like carbon coatings in medical applications Surface & Coatings Technology. – 2013. – V. 233. – P. 119-130.

[3] Fabio Ferreira, Asim Aijaz, Tomas Kubart et al / Hard and dense diamond like carbon coatings deposited by deep oscillations magnetron sputtering // Surface and Coatings Technology. – 2018. – V. 336. – P. 92-98.

[4] Ankit K., Ashish Varade, Niranjan Reddy K. et al / Synthesis of high hardness IR optical coating using diamond-like carbon by PECVD at room temperature // Diamond and Related Materials. – 2017. – V. 78. – P. 39-43.

[5] Feng Wen, Jiaqi Liu, Jianlu Xue / The Studies of Diamond-Like Carbon Films as Biomaterials: Review // Colloid and Surface Science. – 2017. – V. 2. – P. 81-95.

[6] Lopes F.S., Oliveira J.R., Milani J. / Biomineralized diamond-like carbon films incorporating titanium dioxide nanoparticles improved bioactivity properties and reduced biofilm formation // Materials Science and Engineering C. – 2017. – V. 81. – P. 373-379.

[7] Barve S.A., Chopade S.S., Kar R., Chand N., Deo M.N., Biswas A., Patel N.N., Rao G.M., Patil D.S., Sinha S. / SiOx containing diamond like carbon coatings: Effect of substrate bi-as during deposition // Diamond & Related Materials. – 2017. – V. 71. – P. 63-72.

[8] Bociaga D, Sobczyk-Guzenda A, Komorowski P, Balcerzak J, Jastrzebski K, Przybyszewska K, Kaczmarek A. / Surface Characteristics and Biological Evaluation of Si-DLC Coatings Fabricated Using Magnetron Sputtering Method on Ti6Al7Nb Substrate // Nanomaterials. – 2019. – V. 9. – P. 812.

[9] Grenadyorov A.S., Solovyev A.A., Oskomov K.V., Rabotkin S.V., Elgin Yu.I., Sypchenko V.S., Ivanova N.M. / Effect of substrate bias and substrate/plasma generator distance on properties of a-C:H:SiO_x films synthesized by plasma-assisted chemical vapor deposition // Thin solid films. – 2019. – V. 669. – P. 253-261.

[10] Grenadyorov A.S., Solovyev A.A., Oskomov K.V., Sypchenko V.S. / Influence of deposition conditions on mechanical properties of a-C:H:SiO_x films prepared by plasma-assisted chemical vapor deposition method // Surface and Coatings Technology. – 2018. – V. 349. – P. 547-555.

* The work was supported by the grant of the President of the Russian Federation MK-1234.2020.8 and is a continuation of the work on RFBR grant № 14-08-31164.

MOLYBDENUM-COPPER ALLOYS AS A BASE MATERIAL FOR MICROFABRICATION PLANAR SLOW-WAVE STRUCTURES OF MILLIMETER-BAND VACUUM ELECTRON DEVICES*

A.A. SERDOBINTSEV[1], *R.A. TORGASHOV*[1,2], *V.V. GALUSHKA*[1], *I.O. KOZHEVNIKOV*[1], *A.M. PAVLOV*[1], *A.V. STARODUBOV*[1,2], *N.M. RYSKIN*[1,2]

[1]*Saratov State University, Saratov, Russia*
[2]*Saratov Branch, V.A. Kotel'nikov Institute of Radio Engineering and Electronics RAS, Saratov, Russia*

The design and development of millimeter and submillimeter-band (THz-band) vacuum electronic devices put forward special requirements to the properties of structural materials that are used to microfabricate such base electronic components as slow-wave structures (SWS), different types of power couplers, elements of energy input/output and etc. The fundamental significance in this area has such properties of materials as low value of the thermal coefficient of linear expansion, high electrical and heat conductivity, and etc [1]. This has required the creation of special composite materials with laminated, fiber or dispersed structure, based on different combinations of metals, alloys, and compounds. Among the most common are copper-based composite materials with a dispersed phase of such refractory metals as molybdenum, tungsten, etc. [1]. Such materials are obtained in fixed compositions and under special production processes [1-2]. This material should have, at least, the following properties: high heat conductivity, high electrical conductivity, a rather narrow interval of thermal coefficient of linear expansion, good shape retention, solder acceptance (braze solders on copper, gold and silver). One of the promising composite materials for vacuum microelectronic devices is molybdenum-copper alloys. This composite combines the high thermal and electrical conductivity of copper and the low thermal expansion of molybdenum. Such properties of structural material are very important to microfabrication planar SWS [3] for millimeter and submillimeter-band (THz-band) vacuum electronic devices with sheet electron beam (traveling-wave tubes, backward-wave oscillators). The design of such devices assumes that the sheet electron beam propagates above the planar SWS and the distance between the sheet electron beam and a planar SWS is about one or a few hundred microns [4]. Therefore it is very important to prevent the SWS from thermal processes caused by surface currents. Even a little deformation of the planar SWS geometry can lead to the process of separation of SWS from the dielectric substrate and to the intersection with the sheet electron beam.

The purpose of this work is to study the properties of the thin alloyed conductive layer on the dielectric substrate made from copper and molybdenum using two source magnetron co-sputtering deposition. The composition of the alloy material can be controlled by varying the power of the magnetron sources, the pressure of the working gas pressure and the substrate temperature. The verification of the alloy material composition was carried out by energy-dispersive X-ray spectroscopy and by the method of secondary ion mass spectrometry. The morphology studies of surfaces of the composite thin layers were carried out with the help of scanning electron microscopy. We are going to apply our original technological approach [3] to the microfabrication of several samples of SWS based on the different composition of copper and molybdenum and compare their electrodynamics parameters (return loss and transmission loss) with the SWS made only from oxygen-free copper. The results of the mentioned above studies will be presented at the conference.

REFERENCES

[1] S. Gorbatyuk, A. Pashkov and N. Chichenev, "Improved Copper-Molybdenum Composite Material Production Technology" Materials Today: Proceedings, vol. 11, 31-35, 2019

[2] V. Kukhar, V. Artyukh, O. Serdvik, E. Balalaeva, "The shape of the curve of the temperature distribution gradient along the length of the preform under differentiated heating to buckling profiling", Methodical Engineering, vol. 165, 1693-1704, 2016

[3] A. V. Starodubov, et al., "A novel microfabrication technology of planar microstrip slow-wave structures for millimeter-band traveling-wave tubes," 2018 IEEE International Vacuum Electronics Conference (IVEC), Monterey, CA, 2018, pp. 333-334

[4] N. M. Ryskin, et al., "Planar Microstrip Slow-Wave Structure for Low-Voltage V-band Traveling-Wave Tube with a Sheet Electron Beam," IEEE Electron Device Letters, Vol. 39, No. 5, 757-760, 2018

* The work was supported by the Russian Foundation for Basic Research under grant № 20-57-12001.

MANUFACTURING AND CHARACTERIZATION OF TANTALUM MICROPLASMA COATINGS FOR BIOMEDICAL APPLICATION[1]

D.L. ALONTSEVA[1], A.L. KRASAVIN[1], A.R. KHOZHANOV[1], S. S. GERT[1]

[1]D.Serikbayev East Kazakhstan State Technical University, Ust-Kamenogorsk, Kazakhstan

Currently, there has been growing interest in the use of biocompatible tantalum (Ta) metal, as well as alloys based on it as materials for medical implants [1-3]. Due to its high chemical stability and hardness, Ta is very promising as an orthopedic biomaterial. Ta biocompatibility is achieved due to the formation of a corrosion-resistant relatively thick (approximately 5 μm) surface oxide layer [3]. However, Ta and its alloys are expensive to manufacture, therefore, they are currently in demand for the production of implants mainly in special circumstances when patients experience problems such as allergies or, more precisely, hypersensitivity to metal [3]. Taking into account the fact that surface characteristics are important for the interaction between the implant and human body [1, 2], we propose using the technology of microplasma spraying (MPS) of coatings from biocompatible materials to modify any implant base material. The coating material may be metallic, such as Ta, Ti, Zr, or non-metallic, such as hydroxyapatite (HA). Thermal spraying methods, which include MPS, are widely used in applications related to the metalworking industry, but for the biomedical field this is an innovative subject with the capabilities that are currently being studied [1, 4]. Coatings for orthopedic or dental implants should be porous; the recommended range of pore sizes from 20 microns to more than 100 microns [1], so that bone tissue and blood vessels can grow through them.

The aim of this work was MPS of Ta wire onto Ti medical implants to obtain the hard coatings of a specified thickness and porosity.

MPS of Ta coatings has been applied with the use of microplasmatron MPN-004 (manufactured by E.O. Paton Electric Welding Institute, Ukraine) maintained on the industrial robot-manipulator Kawasaki RS-010LA (Kawasaki Robotics, Japan). New software has been developed to solve the problem of providing the desired trajectory of the robot arm [5]. To manufacture the medical implants the CTX 510 ecoline CNC turning and milling machine and DMU 50 CNC milling machine (DMG MORI AG, Germany) have been used. High purity tantalum wire 0.3 mm in diameter was applied to Grade 5 ELI titanium alloy substrates. The study of coatings microstructures has been carried out with the use of the metallographic microscope Olympus BX-51 (Japan) and the scanning electron microscope JSM-6390LV (JEOL, Japan). The scanning electron microscopy images of coatings cross-sections have been processed using ImageJ software to evaluate the porosity of the coatings. The Vickers microhardness test was carried out using the DuraScan-20 microhardness meter (EMCO TEST, Austria) in depth from the surface of the coating.

The main results of this work are the following:

1) Robotic microplasma spraying of Ta-wire onto implants of elbow joints made of Ti alloy was performed using new software for the robot arm, and the possibility of forming Ta coatings with a specified thickness and porosity was demonstrated; 2) The parameters of MPS for obtaining Ta coatings with a thickness of up to 500 μm and with a pore size of 20 to 200 μm were established; 3) It was found that the microhardness of the microplasma Ta coating is on average 2 times higher than that of the Ti alloy substrate.

The research results are of significance for a wide range of researchers developing thermal spray technologies for biocompatible coatings manufacturing.

REFERENCES

[1] Cizek J., Matejicek J., “Medicine Meets Thermal Spray Technology: A Review of Patents ”, J. Therm. Spray Tech., vol. 27, no. 8, pp, 1251–1279, 2018. https://doi.org/10.1007/s11666-018-0798-8

[2] Saini, M., Singh, Y., Arora, P., Arora, V., Jain, K ., “Implant biomaterials: A comprehensive review”, World journal of clinical cases, vol. 3, no. 1, pp. 52–57, 2015. doi:10.12998/wjcc.v3.i1.52

[3] Hallab N. J., Jacobs J.J., Orthopedic Applications, in Biomaterials Science (Third Edition), Seattle: Academic Press, 2013. https://doi.org/10.1016/C2009-0-02433-7

[4] Alontseva D., Krasavin A., Abilev M., Zhilkashinova A. “Microplasma Deposition of Biocompatible Coatings Using an Intelligent Robotic System for Plasma Processing”, Acta Physica Polonica A. vol. 136, no.2, pp. 310-313, 2019. doi: 10.12693/APhysPolA.136.310

[5] Alontseva, D., Krasavin, A., Nurekenov, D., Ospanov O., Kusaiyn-Murat, A., Zhanuzakov, Y. “Software development for a new robotic technology of microplasma spraying of powder coatings”, Przegląd Elektrotechniczny, vol. 94, no. 7, pp. 26-29, 2018. doi:10.15199/48.2018.07.06

[1] This work was supported by the Science Committee of the Ministry of Education and Science of the Republic of Kazakhstan for the project AP05130525 “The intelligent robotic system for plasma processing and cutting of large-size products of complex shape”.

ROBOTIC MICROPLASMA SPRAYING AND CHARACTERIZATION OF ZIRCONIUM COATINGS*

A.R. KHOZHANOV[1], *D.L. ALONTSEVA*[1]

[1]*D.Serikbayev East Kazakhstan State Technical University, Ust-Kamenogorsk, Kazakhstan,*

Nowadays, the most promising materials for the manufacture of medical implants are zirconium, niobium and tantalum along with widely used titanium and its alloys [1, 2]. Various surface treatment methods are used to increase the medical implants biocompatibility, including coatings made of biocompatible materials applied by plasma spraying [2, 3]. Fotovvati et al. [3] compared the results of obtaining biocompatible coatings by cold and thermal spraying in favor of thermal spraying. However, despite the advantages and relative economic efficiency of the thermal plasma spraying method, its use for the manufacture of medical implants has not yet become so widespread. This is mainly due to the high heating temperatures of the bulk as a result of the thermal spraying process. Microplasma spraying (MPS) allows avoiding the problem of overheating, because MPS has very little thermal effect on the substrate. The use of robotic MPS can be considered promising for the precision coating of patient-specific implants. Studies [4, 5] proved that it was possible to obtain coatings from biocompatible materials with the desired level of porosity and satisfactory adhesion to the substrate by microplasma spraying. Robotic MPS of coatings from biocompatible titanium and hydroxyapatite materials onto titanium implants was implemented [4, 5]. The goal of this work was to consider the advantages and challenges of using robotic MPS for applying zirconium coatings to medical implants.

Microplasma spraying of the coatings from zirconium wires has been applied on microplasma processing areas based on the industrial robot Kawasaki RS-010LA (Kawasaki Robotics, Japan) at D.Serikbayev East Kazakhstan State Technical University with the use of microplasmatron MPN-004 manufactured by E.O. Paton Electric Welding Institute (Ukraine). New software has been developed to solve the problem of providing the desired trajectory of the robot-manipulator with a microplasmatron maintained on. The scanning electron microscopy (SEM) and metallographic analysis have been used to study the coatings structure. The influence of the main parameters of the microplasma spraying on coatings structure has been studied. The study has been carried out with the use of the metallographic microscope Olympus BX-51 (Japan) and the scanning electron microscope JSM-6390LV (JEOL, Japan) with energy dispersive analysis by INCA ENERGY (Oxford Instruments, UK). The scanning electron microscopy images of coatings cross-sections have been processed using ImageJ computer program to evaluate the porosity of the coatings.

The main results of this work are the following:

1) It has been established that the main parameters controlling the size of the sprayed particles and the porosity of the coatings are the electric arc current and the plasma gas flow rate. The parameters of microplasma deposition of zirconium wire for the formation of porous coatings with rough surface have been established; 2) Technological guidelines and software have been developed enabling to implement robot-aided microplasma spraying of coatings from zirconium on medical implants.

The results of the research are of significance for a wide range of researchers developing the plasma spray technologies of biocompatible coatings manufacturing.

REFERENCES

[1] Saini, M., Singh, Y., Arora, P., Arora, V., Jain, K ., “Implant biomaterials: A comprehensive review”, World journal of clinical cases, vol. 3, no. 1, pp. 52–57, 2015. doi:10.12998/wjcc.v3.i1.52

[2] Cizek J., Matejicek J., “A Review of Patents”, J. Therm. Spray Tech., vol. 27, no. 8, pp, 1251–1279, 2018. https://doi.org/10.1007/s11666-018-0798-8

[3] Fotovvati B., Namdari N., Dehghanghadikolaei A., “On Coating Techniques for Surface Protection: A Review”, J. Manuf. Mater. Process, vol.3. no.1, pp. 1-22, 2019. doi:10.3390/jmmp3010028

[4] Alontseva D.L, A.V., Russakova A.V., Prokhorenkova N.V. “Development of Robotic Microplasma Spraying Technology for Applying Biocompatible Coatings on Medical Implants”, Russian Physics Journal, Vol.61, No 8/2, pp.163-167, August 2018.

[5] Alontseva D., Ghassemieh E., Voinarovych S., Kyslytsia O., Polovetskyi Y., Prokhorenkova N., Kadyroldina A. “Manufacturing and Characterization of Robot Assisted Microplasma Multilayer Coating of Titanium Implants”, Johnson Matthey Technol. Rev., vol.64, no.2, April 2020. In print.

* This work was supported by the Science Committee of the Ministry of Education and Science of the Republic of Kazakhstan for the project AP05130525 “The intelligent robotic system for plasma processing and cutting of large-size products of complex shape”.

EFFECTS OF DUTY CYCLE AND FREQUENCY ON THE ION CURRENT DENSITY ON SUBSTRATE AND ION/ATOM RATIO IN MAGNETRON SPUTTERING OF ALUMINUM*

V.O. OSKIRKO, A.N. ZAKHAROV, A.P. PAVLOV, V.A. SEMENOV, A.A. SOLOVYEV

Institute of High Current Electronics, 2/3 Akademicheskii Ave., Tomsk, 634055, Russia

Ion bombardment of the substrate during magnetron sputtering is an effective tool for controlling the structure and properties of the deposited coating. To increase the density of the ion current on the substrate, magnetrons with an unbalanced magnetic field can be used [1] or additional sources of ionization [2]. Also, an increase in the ion current density on the substrate can be achieved by changing the temporal parameters of the pulses, such as frequency and duty cycle [3]. Modern impulse power supplies allow a wide range of pulse parameters to be regulated, while maintaining a fairly high level of average output power. This paper presents the results of a study of the influence of the frequency and duty cycle of pulses on the density of the ion current on the substrate, the deposition rate of Al, the ion/atom ratio, and the energy flux density to the substrate located under the floating or negative bias potential. The average discharge power in all experiments was 1 kW. It was shown that the ion current and ion / atom ratio increase with decreasing duty cycle (see Fig. 1 and Fig. 2). For each duty cicle value, there is an optimal pulse frequency at which the ion current on the substrate is maximum. In Fig. 2 the dependence of the ion/atom ratio on the duty cycle of the pulses at the maximum values of the ion current density is given. Adjusting the parameters of the pulses allows increasing the ion current density by a factor of more than 2.5 compared to the direct current sputtering mode. The ion / atom ratio increases by a factor of 10 due to a decrease in the deposition rate in the pulsed mode (from 0.28 to 2.73).

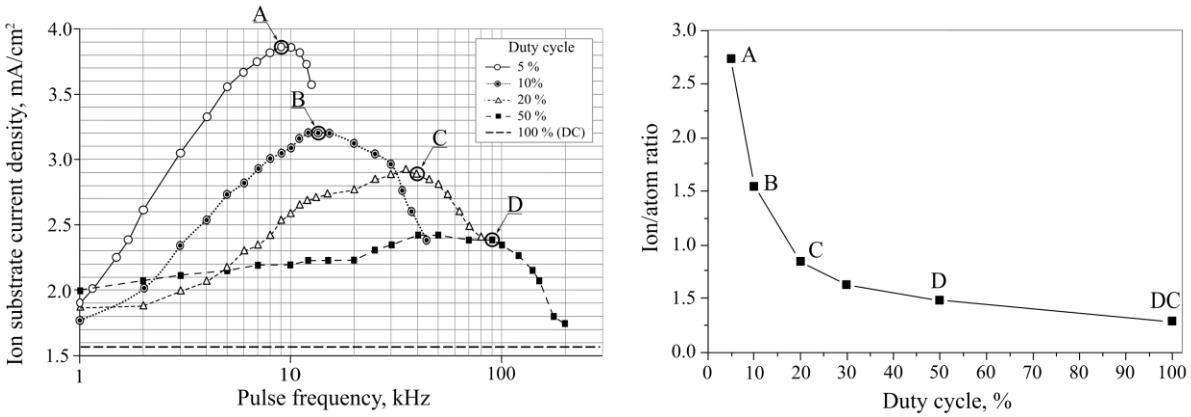

Fig. 1. a) Dependence of the ion substrate current density on the duty cycle and pulse frequency; b) Dependence of the ion / atom ratio on the duty cycle

REFERENCES

[1] *E. Ribeiro et al.* // Surf. Coat. Technol. – 2002. – V. 151-152, pp. 515-520.
[2] *Ch. S. Kim et al.* // Jpn. J. Appl. Phys. – 2005. – V. 44. – № 9A, pp. 6519-6521.
[3] *E. Haye et al.* // Surf. Coat. Technol. – 2018. – V. 350. – pp. 84-94.

* The work was funded by Russian Foundation for Basic Research and the government of the Tomsk region of the Russian Federation, grant № 18-42-703005

APPLICATION OF CERAMIC COATING ON METAL BY METHOD ELECTRON BEAM EVAPORATION IN VACUUM*

I.Y. BAKEEV, Y.A. BURACHEVSKY

Tomsk State University of Control Systems and Radioelectronics, Russia

The creation of electrical insulating coatings on conductive metal surfaces capable of functioning reliably at higher temperatures than polymer coatings is relevant, but at the same time quite challenging.

Currently, there are a large number of methods for applying electrical insulating coatings [1]. One of such methods is the method of electron beam evaporation of a ceramic target in vacuum, which allows creating a durable, with good adhesion, ceramic coating with high mechanical, electrical strength, heat resistance and relatively high values of relative dielectric constant and low dielectric loss tangent [2] . As an electron source, a continuous-flow plasma source of electrons was used, operating in the pressure range provided by pumping only by a fore-vacuum mechanical pump [3].

Ceramic coatings of Al2O3 and ZrO2 + 8% Y2O5 were applied to polished metal surfaces made of stainless steel, copper, and titanium. As a result, a ceramic coating 3–16 μm thick was formed on the metal surface. Its deposition rate was ~ 150 nm / min. The coatings were solid, having a block structure, containing micro cracks, but having high electric strength (50 - 300 kV / mm).

REFERENCES

[1] L. Pawlovski, The Science and Engineering of Thermal Spray Coating, Chichester, John Wiley & Sons, Ltd, 2008.

[2] I.Yu. Bakeev, Yu.A. Burachevsky and Yu.G. Yushkov, "Creating ceramic electrically insulating coating on metal surface," J.of Phys.Conf. Ser., vol.1393, 2019.

[3] V.A. Burdovitsin, A.S. Klimov, A.V. Medovnik, E.M. Oks and Y.G. Yushkov, Forevacuum plasma electron sources, Tomsk University Publishing House, 2014.

* The work was supported by the Russian Foundation for Basic Research (RFBR) project No. 18-08-00539.

BORON COATINGS DEPOSITED BY USING NON-SELF-SUSTAINED ARC DISCHARGE WITH A HEATED AND HOLLOW CATHODE AND A HOT ANODE

SHUGUROV V.V.[1], *IVANOV YU.F.*

Institute of High Current Electronics SB RAS, Tomsk, Russia

The results of the development and research of a boron coating system based on a non-self-sustained arc discharge with a heated and hollow cathode and a hot anode are presented. The discharge anode is made in the form of a graphite crucible filled with amorphous boron powder of grade “A”. When the discharge is turned on, the current initially closes on the surface of graphite and heats the crucible. As it warms up, the conductivity of boron powder increases and the current discharge switches to it, thereby increasing its temperature, which leads to intense evaporation of boron and allows coatings to be obtained on samples and parts. Current-voltage characteristics of the discharge and the dependence of the deposition rate on operating conditions were studied.

MODIFICATION OF METAL SURFACE WITH ORGANIC COMPOUNDS UNDER THE ACTION OF A NANOSECOND ELECTRON BEAM*

M.A. SHULEPOV[1], *YU.V. SAVINYKH*[2], *V.V. ORLOVSKII*[1], *V.A. PANARIN*[1]

[1]*Institute of High Current Electronics SB RAS, Tomsk, Russia*
[2]*Institute of Petroleum Chemistry SB RAS, Tomsk, Russia*

The paper deals with a development of methods for changing the surface properties of metals under the action of an electron beam on organic liquids in the near-surface metal layer. On the one hand, these changes result in an increase in the hardness, corrosion and wear resistance of the surface of materials and a decrease in the coefficient of friction, on the other hand. As a result, the dynamic strength of products increases.

Metacrylic acid having an active carboxyl group and a double bond was used as metal surface modifier. Other reagents were silicone fluids such as tetraethoxysilane (TES) and hexamethyldisiloxane (HMDS).

It is expected that the treatment of the metal surface with these reagents results in the increase in thermal stability and adhesion and improvement of water and dirt-repellent properties due to decrease in the surface tension of films. Copper, brass, and Al-Be foil were selected as the subjects of study.

The pulsed high-current electron accelerator 'Nora' was used as a source of an electron beam for treatment of hydrocarbons [1]. Its parameters were as follows: kinetic electron energy 90 keV, beam current density 65 A/cm^2, beam energy 0.2 J per pulse, pulse width of the current 60 ns (full width at half maximum), and pulse repetition rate 4 imp./s. The electron beam was ejected into the processing zone of the accelerator through outlet window closed by the Al-Be foil. The foil thickness was 45 μm. The metal plate with an organic component deposited on its surface was a sample under study. It was exposed to the irradiation in a stainless steel cuvette with an internal diameter 40 mm and a depth 15 mm. Samples were irradiated using a standard dose 248 kGy under the same conditions.

An analysis of the IR spectra after irradiation of the metal surface with an electron beam in the presence of methacrylic acid showed the disappearance of the double bond band (absorption band 1636 cm^{-1}) and a sharp decrease in the absorption band of the carboxyl OH group (2987 cm^{-1}). This suggests the polymerization of methacrylic acid on the surface of all the metals studied and the interaction of the carboxyl group with the metal surface. The impact of the electron beam on TES and HMDS on the surface of metals leads to the chemical fixation of silanol groups on these surfaces. This is evidenced by the absorption bands (1178 and 1080 cm^{-1}) of the silanol groups.

REFERENCES

[1] Gubanov V.P., Korovin S.D., Orlovskii V.M., Stepchenko A.S., Tarasenko V.F., Kuvshinov V.A., Savinykh Yu.V. Instruments and Experimental Techniques. 1998. T. 41. № 3. C. 368-369.

*****The work was supported by the Russian Science Foundation under the grant No. 9.5.2. (IHCE SB RAS) and by Ministry of Science and Higher Education of the Russian Federation (Project No. V.46.2.3.). (IPC SB RAS)

DEPOSITION OF WSi_2 FILMS BY DC MAGNETRON SPUTTERING AT ULTRA LOW OPERATING PRESSURE [*]

M.V. SHANDRIKOV[1], I.D. ARTAMONOV[1], A.S. BUGAEV[1], A.V. VIZIR[1], E.M. OKS[1,2]

[1] Institute of High Current Electronics SB RAS, Tomsk, Russia
[2] Tomsk State University of Control Systems and Radioelectronics, Tomsk, Russia

The results of WSi_2 films deposition by planar magnetron sputtering at ultra-low operating pressure (up to 6×10^{-4} Torr) are presented. The composite WSi_2 target had a diameter of 125 mm. The operating current of the magnetron was 1 A in DC mode. The dependences of film homogeneity on a 100 mm diameter substrate and substrate temperature on the distance to the magnetron were measured. The spatial distribution of the ion current density was presented. The effect of the working pressure on the roughness and electrical conductivity of WSi_2 films were shown.

[*] The work was supported by Russian Foundation for Basic research under grant # 19-48-700003 p_a.

SYNTHESIS OF LAYERED COATINGS FROM SOLID SOLUTIONS OF NIOBIUM, ZIRCONIUM AND TITANIUM CARBIDES ON HARD ALLOY TOOL USING VACUUM ARC DEPOSITION

A.K. KULESHOV, V.V. UGLOV, D.P. RUSALSKY

Belarusian State University, Nezavisimosti ave., 4, Minsk, 220030, Belarus

Promising coatings for increasing the wear resistance of carbide wood-cutting tools are layered coatings of refractory high-hardness carbide compounds. Layered carbide coatings were formed on a carbide tool as a result of ion exposure by niobium cathode-arc source with energy of 1 keV and subsequent cathodic arc-vacuum deposition (CAVD) of coatings using simultaneous plasma flows of Nb and Zr, Nb and Ti in a methane atmosphere. The samples of the hard alloy on which the coatings were applied were industrial knives of a woodworking tool. The surface temperature of hard alloy samples during ion bombardment with niobium reached 1000–1300 ° C. XRD, GXRD, SEM, EDX methods were used to study hardness, adhesion, wear, microstructure, phase and element composition over the cross section of hard alloy samples with formed coatings.

The thickness of the (Nb,W)C layer with a variable content of metals and carbon formed in the process of niobium ion bombardment is 0,5 – 0,6 μm. The upper coating layer up to 3 μm thick deposited using Nb and Zr cathode-arc sources consists of a (Nb,Zr)C solid solution with a relative concentration of Nb and Zr as 2 to 1. A transition layer is also formed between the described layers with a thickness of 0,8 μm in which the ratio of the concentrations of Nb and Zr metals is 7 to 1. A similar structure of layered carbide coatings and the formation of a (Nb,Ti)C solid solution were also found using Nb and Ti cathode-arc sources.

The hardness of the synthesized layered carbide coatings from (Nb,Zr)C and (Nb,Ti)C solid solutions is 50-60 GPa, which exceeds the hardness CAVD single-layer ZrC, NbC, TiC coatings - 25-40 GPa. Layered coatings with upper layers of (Nb,Zr)C and (Nb,Ti)C solid solutions have a critical cracking load of at least 140 N, which significantly exceeds the adhesion resistance to cracking of single-layer ZrC, NbC, TiC coatings - 80 N.

STUDY OF COATINGS BASED ON CUBIC TUNGSTEN CARBIDE OBTAINED BY PLASMA DYNAMIC METHOD *

A. NASSYRBAYEV[1], *D.S. NIKITIN*[1], *I.I.SHANENKOV*[1,2]

[1]*National research Tomsk Polytechnic University Lenin Avenue 30, Tomsk, 634050, Russia,*
arn1@tpu.ru, +7(913) 810-40-99
[2]*College of Communication Engineering, Jilin University, Changchun, China*

Much attention is paid to high-performance structural and functional materials in industry. The technologies for creating protective and hardening coatings are widespread due to the ability to increase the wear resistance, hardness, Young's modulus and the corrosion resistance of industrial products. Tungsten carbide is a promising material for creating coatings based on it due to the presence of high mechanical characteristics [1]. The most common phases of tungsten carbide are the hexagonal phases WC and W_2C. In addition, according to the phase diagram, there is a metastable phase of cubic tungsten carbide WC1-x in the W-C system [2]. The phase of cubic tungsten carbide has a high electro- and photocatalytic activity [3].

The possibility of obtaining a coating of cubic tungsten carbide by the plasma dynamic method using a coaxial magnetoplasma accelerator with graphite electrodes (CMPA) [4] is presented in this work. During the coating process, the necessary conditions for the synthesis of WC_{1-x} are achieved, consisting in high crystallization of particles (> 10^7-10^8 K/s) [5].

A series of experiments were carried out on various substrate materials: copper, brass, steel. The CMPA was powered from a capacitive energy storage device with a capacitor bank capacity of C = 6 mF and a charging voltage of U = 3 kV. The experiments were carried out at normal temperature and pressure in a reactor-chamber filled with argon. The obtained coatings were studied by X-ray diffractometry (XRD) and scanning electron microscopy (SEM).

The XRD-analysis showed that in the entire series of experiments coatings were obtained, consisting mainly of the WC_{1-x} phase. The SEM images determined the size of the coating, which amounted to at least 15 μm.

The result of this work are the coatings of cubic tungsten carbide on various types of substrates obtained by the plasma dynamic method. Also, in this work was determined the effect of the substrate material on the resulting coatings. The coating with the highest phase content of cubic tungsten carbide (> 90 %) was obtained using a copper substrate

REFERENCES

[1] Cardarelli F. // Materials handbook. – London etc. : Springer, 2000.
[2] Kurlov A. S., Gusev A. I. // Russian Chemical Reviews. – 2006. – Volume 75 (7). – p. 617.
[3] Kim J. et al. // Journal of Power Sources. – 2009. – Volume 193 (2). – pp. 441-446.
[4] Pak A. et al. // International Journal of Refractory Metals and Hard Materials. – 2015. – Volume 48. – pp. 51-55.
[5] Zhang F. G., Zhu X. P., Lei M. K. // Surface and Coatings Technology. – 2012. – Volume 206 (19-20). – pp. 4146-4155.

* This work was supported by the Russian Scientific Foundation (grant No.19-13-00120).

X-RAY STEP FILTER PREPARED BY MAGNETRON SPUTTERING*

V.A. SEMENOV, S.V. RABOTKIN, I.M. DATSKO, A.A. SOLOVYEV

Institute of High Current Electronics SB RAS, Tomsk, Russia

Dense X-pinch plasma is a source of soft X-rays with a duration of 1–3 ns. This radiation is used to study the internal structure of the plasma obtained from an electrical conductor explosion. In this case, to assess the density of the substance in the plasma column and its radial distribution, step filters of X-ray radiation made from the same metal as the exploding conductor are used [1]. The step filter is placed in front of the photo film during investigations.

The task of this work was to show the possibility of forming a multilayer metal structure of the X-ray filter on a light-melting polymer substrate. For this purpose, it was necessary to deposit metal layers of a certain thickness on a thin 6 μm thick polypropylene (PP) film by the method of magnetron sputtering. As a result of the experiments, the optimal magnetron discharge power and distance from the sputtered target to the substrate are determined, at which the polymer film is not destroyed by heat. Preliminarily, a continuous 400 nm thick Al layer was formed on the PP film to protect the photo film from plasma radiation in the visible range. Then 6 layers of Al or Cu with thicknesses of 500, 1000, 1500, 2000, 2500, 3000 nm and 1000, 1200, 1400, 1600, 1800, 2000 nm, respectively were deposited through masks (Figure 1).

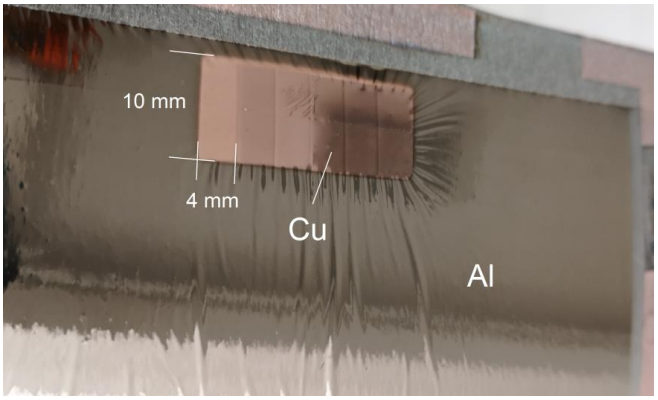

Fig.1. Photo of X-ray step filter on polypropylene film.

The uniformity of the thickness of formed layers is investigated. The continuity of metal layers was controlled by means of optical and electronic microscopy. Transmission of filters was tested by X-pinch radiation in the range of $h\nu > 0.8$ keV, created with a compact pulsed high-current generator XPG-3 (200 kA, 150 ns), which was designed and constructed at the Institute of High Current Electronics.

REFERENCES

[1] I.M. Datsko, N.A. Labetskaya, D.V. Rybka, V.A. Vankevich, V.V. Shugurov, "Delay in plasma generation on the surface of copper and duralumin conductors coated with dielectrics," J. Phys. Conf. Ser., vol. 1393, pp. 012005, 2019.

* The work was supported by RFBR grant No. 19-08-00479

ELECTRON-BEAM DEPOSITION OF MAGNETO-DIELECTRIC COATINGS IN MEDIUM VACUUM*

YU.G. YUSHKOV[1], *E.M. OKS*[1,2], *A.V. TYUNKOV*[1], *D.B. ZOLOTUKHIN*[1]

[1]*Tomsk State University of Control Systems and Radioelectronics, Tomsk, Russia*
[2]*Institute of High Current Electronics SB RAS, Tomsk, Russia*

Materials combining dielectric and magnetic coatings are very attractive to use in such fields of industry as RF electronics, and aerospace industry for the manufacturing of radio-absorbing coatings [1]. The emerging trend towards miniaturization of the various devices such as unmanned aerial vehicles requires deposition of thin and light-weight magnetic films that combine magnetic and dielectric properties.

In this work we propose an advanced approach to formation of such thin magneto-dielectric coatings – by the use of a fore-vacuum plasma-cathode electron source [2]. Using the electron-beam evaporation of dielectric (alumina ceramics) [3] and magnetic targets in medium vacuum (several Pa), we create dense multi-component plasma, which provides the flux of the particles of target materials, allowing to deposit a magneto-dielectric coatings on a metallic substrate with very high deposition rate (approximately microns per minute) and high degree of coating uniformity.

We report the most updated results on the regimes of the electron-beam evaporation of ceramic and magnetic targets, discuss the mass-to-charge composition of the beam plasma at the different stages of the target evaporation, and demonstrate the preliminary results of the mageto-dielectric coatings deposit onto metallic substrate.

REFERENCES

[1] E.P. Elsukov, S.F. Lomaeva, A.S. Shuravin, A.L. Ulyanov, A.A. Chulkina, D.V. Surnin, K.N. Rozanov, A.V. Osipov, D.A. Petrov, S.N. Starostenko, "Influence of shape and chemical and phase compositions of iron-containing particles on microwave performance of composites with an insulating matrix", Technical Physics. The Russian Journal of Applied Physics, vol.54, 569-574, 2009.

[2] V.A. Burdovitsin, E.M. Oks, "Fore-vacuum plasma-cathode electron sources", Laser and Particle Beams, vol.26, 619-635, 2008.

[3] E.M. Oks, A.V. Tyunkov, Yu.G. Yushkov, D.B. Zolotukhin, "Ceramic coating deposition by electron beam evaporation", Ceramic International, vol.325, 1-6, 2017.

* The work on deposition of magnetic coatings was supported by RFBR grant №20-08-00370_A. Research on deposition of dielectric (ceramic) coatings was supported by the Grant of the President of the Russian Federation (№.МК-154.2020.8).

PROPERTIES OF THERMO-CONDUCTIVE CERAMIC-BASED COATINGS DEPOSITED USING FORE-VACUUM PLASMA-CATHODE ELECTRON SOURCE*

YU.G. YUSHKOV[1], *E.M. OKS*[1,2], *A.V. TYUNKOV*[1], *D.B. ZOLOTUKHIN*[1]

[1]*Tomsk State University of Control Systems and Radioelectronics, Tomsk, Russia*
[2]*Institute of High Current Electronics SB RAS, Tomsk, Russia*

At the present moment, polymers are usually used as protective, sealing and functional coatings in microelectronic devices. Polymers properties can be enhanced by including the fibers of aluminum nitride into their structure. Such inclusions lead to a thermal conductivity increase of up to 1 W/m·K [1]. Our analysis allowed us to conclude that the optimal combination of dielectric and heat-conducting properties can be achieved with aluminum nitride or aluminum oxynitride-coatings. Another important issue is the choice of method for the deposition of coatings.

For these purposes, we propose to apply a fore-vacuum plasma electron source that have been developed in our lab. This device allows forming electron beams in the previously inaccessible (so-called fore-vacuum) pressure range of 1-100 Pa. Under such a high pressure, the beam-produced plasma neutralizes the charge of the electron beam accumulated on the dielectric target, and also provides active neutral and ionized nitrogen species, which, in turn, bind free atoms of aluminum [2]. Therefore, the goal of this work was to create the scientific basis of electron-beam and plasma method for deposition of heat-conducting ceramic coatings for various purposes in microelectronics.

In this work, we will present our experimental results on the deposition of heat-conducting ceramic-based coatings on various substrates. The composition of the obtained coatings and their thermo-physical properties has been studied.

REFERENCES

[1] R. Prasher, "Thermal Interface Materials: Historical Perspective, Status, and Future Directions," Proc. IEEE, vol.94, 1571-1586, 2006.

[2] E.M. Oks, A.V. Tyunkov, Yu.G. Yushkov, D.B. Zolotukhin, "Ceramic coating deposition by electron beam evaporation," Ceramic International, vol.325, 1-6, 2017.

* The work was supported by the Russian Foundation for Basic Research (RFBR) under grant No. 18-29-11011 mk.

COMPARATIVE STUDY OF THE CONDITIONS FOR SICN-COATINGS DEPOSITION IN A ELECTRON BEAM GENERATED PLASMA AND IN A DISCHARGE WITH A SELF-HEATED HOLLOW CATHODE *

A.I. MEN'SHAKOV[1,2]

[1] *Institute of Electrophysics UB RAS, 106 Amundsen St., Yekaterinburg, 620016, Russia,*
e-mail: aim@iep.uran.ru, phone (343)2678829
[2]*Ural Federal University named after the first President of Russia B.N.Yeltsin, 19 Mira str., Yekaterinburg, 620002, Russia*

The composition of the hollow cathode arc discharge plasma and low-energy electron beam plasma in a gas medium containing hexamethyldisilazane (HMDS) vapors was studied and it was shown that the decomposition degree of HMDS molecules in a beam plasma is higher than in an arc discharge with a self-heated hollow cathode (figure 2). It is shown that the decomposition degree of the precursor molecules increases with the ion current density and nonmonotonically depends on the electron beam energy. It is shown that the use of low-energy electron beam allows you to change the temperature of the samples in the range of 150-600°C by electron heating without a significant change in the composition of the plasma and without the use of additional heaters. SiCN-based coatings with a hardness of up to 16-18 GPA with a deposition rate of ~1 μm/h at a temperature of 600°C were obtained. The composition of SiCN coatings was studied by IR spectroscopy, and it was shown that in the IR spectra of coatings obtained in a beam plasma, in contrast to deposition in an arc discharge [1], even in the low-temperature regime, the absorption peaks of the bonds of the initial HMDS molecules are rather low, including hydrogen-containing ones (figure 1), which reduce the hardness of the coatings, which may also indicate a more intense decomposition of the precursor in the beam plasma.

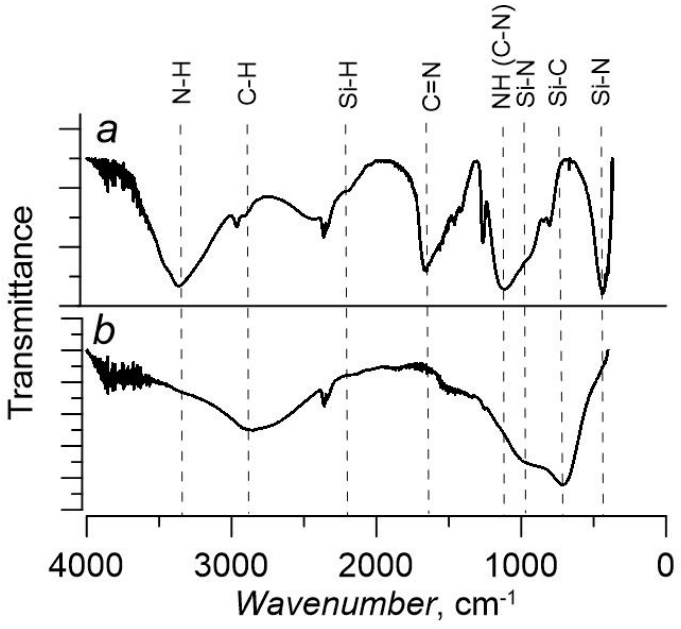

Fig. 1. IR spectra of coatings obtained in a discharge plasma with SHHC (a) and in an electron beam plasma (b). $P_{N2+HMDS}$=1 mTorr, Q_{HMDS}=3 g/h, T=250°C.

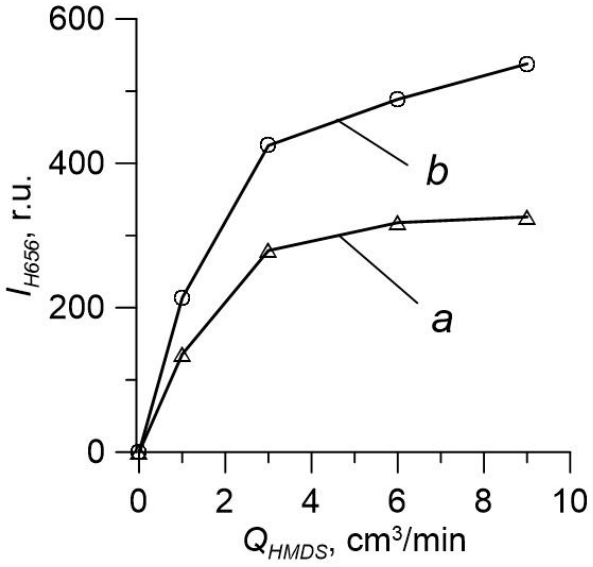

Fig. 2. Dependences of the H* line intensity (656.3 nm) on the HMDS flux in the discharge plasma with SNPC (a) and in the beam plasma (b), j_i=1 mA/cm^2.

[1] *Men'shakov A.I. et. al. //* Journal of Physics: Conference Series. – 2018. – V. 1134. – № 012039.

DEPOSITION OF ALUMINUM OXIDES FROM A VACUUM-ARC DISCHARGE PLASMA *

A. YU. NAZAROV[1], E. L. VARDANYAN[1], K.N. RAMAZANOV[1],

R. SH. NAGIMOV[1], A.A. MASLOV[1]

[1] Ufa State Avioatin Thecnical University, Ufa, 450008, Russia

In modern engineering there is a problem of rapid wear associated with the difficult operating conditions of parts. Surface layers, ranging in thickness from a few nanometers to several micrometers, often have a stronger effect on the overall properties of the product than the rest of the volume. The surface of the product is the part through which it interacts with the environment. In some cases, surface properties take precedence over the product as a whole.

Currently, coatings based on aluminum compounds are widely used [1]. Coatings (Al, TiN, AlCrN) have been developed with an AlN content of more than 50%, which allows working at higher cutting speeds [2]. It is known that oxide coatings (Al2O3, SiO2, TiO2, ZrO2, B2O3, HfO2, CeO2) have a number of properties that are not inherent in metallic and other types of coatings - low thermal conductivity and electrical conductivity. Most oxides have a high melting point, hardness and wear resistance, are most versatile in operating conditions and can be used as corrosion-resistant, heat-resistant, heat-insulating, electrical insulating and wear-resistant. Basically, aluminum oxides is applied by CVD. Due to the fact that the CVD coating temperature is over than 1000 ° C, metastable modifications of Al2O3 are obtained here because the transition temperature of θ-Al2O3 to a less porous and harder modification of α-Al2O3 is 1200 ° C [3].

The aim of this work is to study the physicomechanical properties of a ceramic coating of aluminum oxide obtained by the PVD method.

In the work, a ceramic coating of aluminum oxide was applied to samples of stainless steel 12x18n10t. The effect of the displacement potential on the microhardness, adhesive strength, growth rate, and phase composition of the coating was investigated. The research results expand knowledge of the physicomechanical properties of ceramic coatings of aluminum oxide deposited by their vacuum-arc discharge plasma.

REFERENCES

[1] Loktev D., Yamashkin E. The main types of wear-resistant coatings / D. Loktev, E. Yamashkin // Nanoindustry - 2007. - No. 5. - P. 24.

[2] Maksimov M. Wear-resistant coatings as an engine of an innovative process in tool materials technology and modern metal processing / M. Maksimov // “NanoWeek” - 2010. - No. 106. - April 13 - 19.

[3] Chaly V.P. Metal hydroxides / V.P. Chaly - Kiev .: Naukova Dumka, 1972. - 160 p.

* The work was partial supported by Russian Foundation for Basic Research, Project No. 20-38-70031

THE EFFECT OF THE SUBSTRATE SPATIAL ORIENTATION ON THE PROPERTIES OF AMORPHOUS CARBON COATINGS DEPOSITED FROM PULSE PLASMA FLOWS

S.Y. CHEPKASOV[1], *A.S. ZOLKIN*[1], *D.G. PILIPTSOU*[2], *M.N. KHOMYAKOV*[3], *E.A. MAKSIMOVSKII*[1,4]

[1]*Novosibirsk State University, Novosibirsk, Russia*
[2]*Francisk Skorina Gomel State University, Gomel, Republic of Belarus*
[3]*Institute of Laser Physics SB RAS, Novosibirsk, Russia*
[4]*Institute of Inorganic Chemistry SB RAS, Novosibirsk, Russia*

Coatings based on tetrahedral amorphous carbon (ta-C) are characterized by a complex of unique structural, mechanical and optical properties. This determines their use as wear-resistant coatings in automotive industry, medicine and other fields [1]. It is known [2] that the structure, morphology and properties of carbon coatings depend not only on the energy of ions, but also on the direction of the deposited particles flow. The presence of a macroparticle component of the plasma flow, as a rule, reduces the operational properties of the coatings due to the formation of a surface gradient of mechanical properties, the formation of a macroparticle/carbon matrix interface with a pronounced changing in properties, which reduces the optical properties. Reduction of the macroparticle component of the flow is achieved when using arc sources of direct current by separation of the plasma flow [2], or by switching to a pulsed mode of generating the plasma flow [3]. In order to achieve equal thickness of the coatings during the substrate deposition, as a rule, they are rotated relative to the propagation direction of the incident plasma flow. With a different direction of the plasma flow to the substrate plane, there are features of coatings deposition and growth, determined by the substrate position, the dependence of the deposition rate on its orientation, the flow incidence angle, the energy of the incident particles, the absorption probability of the macroparticle component to the surface, and other factors. Therefore, it is important to establish the relationship of the spatial orientation of the substrate, in which the influence of the macroparticle component on the properties of the coatings is minimal. This will determine the possibility of forming coatings with isotropic properties and expand the range of their applications as coatings of optical elements.

This paper aimed at studying the influence of the substrate position relative to the propagation direction of the pulsed carbon plasma flow on the structure, morphology, mechanical and optical properties of ta-C coatings. Research methods: Raman spectroscopy (T64000), scanning electron microscopy (JSM-6700F), atomic force microscopy (Solver P47-PRO), nanoindentation (Nanoscan-3D), ellipsometry (LEF-72).

The coatings were deposited on silicon substrates at room temperature, an initial discharge voltage of 300 V, a pulse frequency of 5 Hz and a pulse number of 1000. The distance between the cathode of the substrate was 300 mm. The synthesis was carried out at different incidence angles of the carbon ions flow on the substrate, determined from the axis of the flow direction and from normal to the substrate surface, and corresponded to 0°, 15°, 45° and 75°. Using Raman spectroscopy, it was found that a change in the structure of the coating occurs with an increase in the deposition angle. The size of the Csp^2 clusters, as well as their number and ordering, change. Nanohardness and Young's modulus at different incidence angles varied in the ranges from 16.5 to 28 GPa and from 170 to 227 GPa, respectively. The results of studying the coatings surface morphology using SEM and AFM showed the formation of a smoother surface, characterized by a decrease in the number of microdroplets and a decrease in the surface roughness R_{MS} from 19.2 to 0.88 nm with an increase in the deposition angle. The ellipsometry results for ta-C coatings show that with an increase in the angle, the thickness decreases from 90.8 to 27 nm and the refractive index from 2.68 to 2.2, which is typical for the coatings deposition on the inclined substrate [4]. The structure, morphology, and optical and mechanical properties of ta-C coatings have been found to depend on the incidence angle of carbon ions.

REFERENCES

[1] J. Vetter, “60 years of DLC coatings: Historical highlights and technical review of cathodic arc processes to synthesize various DLC types, and their evolution for industrial applications,” Surf. Coat. Technol., vol.257, pp.213-240, 2014.

[2] F.X. Liu, K.L. Yao, Z.L. Liu, "Substrate tilting effect on structure of tetrahedral amorphous carbon films by Raman spectroscopy,” Surf. Coat. Technol., vol.201, pp.7235-7240, 2007.

[3] A.Ya. Kolpakov, A.I. Poplavsky, M.E. Galkina, S.S. Manokhin, and J.V. Gerus, “The local crystallization in nanoscale diamond-like carbon films during annealing,” Appl. Phys. Lett., vol.105, pp.233110, 2014.

[4] W. Trottier-Lapointe, O. Zabeida, T. Schmitt, and L. Martinu, “Ultralow refractive index optical films with enhanced mechanical performance obtained by hybrid glancing angle deposition,” Applied Optics, vol.55, no.31, pp.8796-8805, 2016.

OPTOELECTRONIC PROPERTIES OF 2D-CARBON FILMS VIA PLASMA-ENHANCED CHEMICAL VAPOR DEPOSITION WITH SUBSEQUENT HEAT TREATMENT*

A.R. PROKOPEV[1], *E.P. NEUSTROEV*[1]
[1]*North-Eastern Federal University, Yakutsk, Russian Federation, aisenprokopiev@mail.ru*

Two-dimensional carbon films due to their high value of their electro- and thermal conductivity, good mobility of carriers, unique optical characteristics are promised to be in application in such areas as micro- and nanoelectronics, optoelectronic devices. [1]

To synthesize a two-dimensional carbon structure with a high proportion of sp^2-hybridized regions, we used a two-step consistent technique of acquisition of 2D-carbon films [2,3]: a deposition of carbon-containing films by the plasma method, followed by heat treatment at temperatures from 600° to 800°C. The methods of electron and atomic force microscopy and Raman spectroscopy were used to study the properties of the obtained film, the temperature dependences of the I-V characteristics and charge carrier mobility were measured by the Hall effect method. Fig. 1a shows the dependence of a current strength in a film as a function of illumination (in the dark and under illumination). Figure 1b shows the dependence of a mobility of charge carriers in comparison with reduced graphene oxide (RGO). The report will discuss a results.

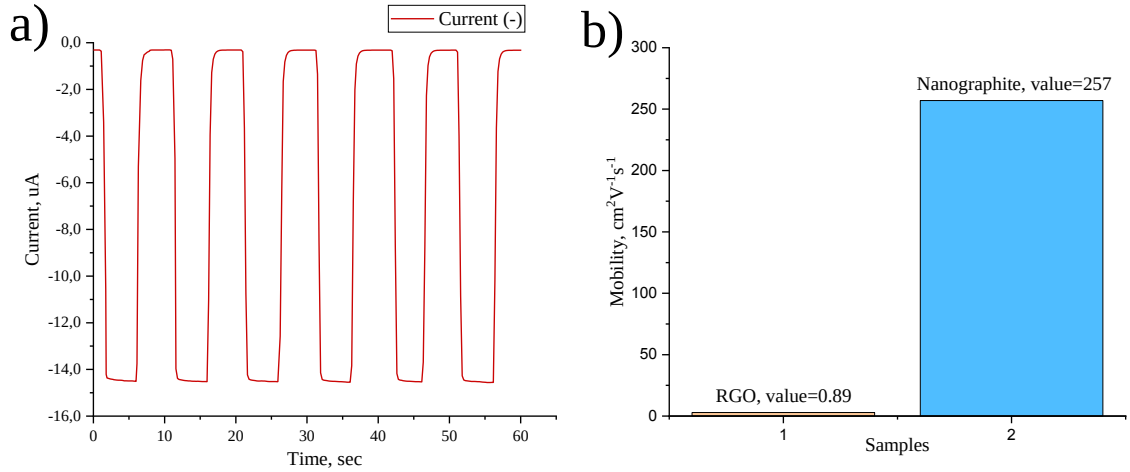

Fig. 1: a) change in the current value on the sample (SiO_2 substrate) under periodic exposure to illumination; b) value of the mobility of charge carriers of the sample compared with reduced graphene oxide.

REFERENCES

1. *Von Keudell A., Möller W.* - A combined plasma-surface model for the deposition of C:H films from a methane plasma. //Journal of applied physics. – 1994. – Т. 75. – №. 12. – С. 7718-7727.
2. *E. P. Neustroev, V. I. Popov, A. R. Prokopiev, Z. Y. Davydova, and S. O. Semenov.* - Formation of nanographite flakes on SiO_2 substrate by plasma deposition of carbon and subsequent annealing. //AIP Conference Proceedings 2179, 020019 (2019).
3. *E. P. Neustroev, A. R. Prokopiev, V. B. Timofeev, V. I. Popov, I. I. Kurkina, Z. Y. Davydova, A. A. Alekseev and S. O. Semenov.* - Impact of plasma treatment in CH_4/N_2 on the properties of reduced graphene oxide. //IOP Conference Series: Materials Science and Engineering, Volume 693, Number 1, 2019.

* The reported study was funded by Ministry of Science and Higher Education of the Russian Federation (project FSRG-2017-0017) and RFBR project number 19-32-90133.

NANODISPERSED CARBON BLACK PRODUCTION BY PYROLYSIS OF HYDROCARBONS

L.V. GERASIMOVA[1,2], *D.I. SUBBOTIN*[1,2], *N.A. CHARYKOV*[1]

[1]*Saint-Petersburg State Institute of Technology (Technical University), Saint-Petersburg, Russia*
[2]*Institute for Electrophysics and Electric Power of the Russian Academy of Sciences (IEE RAS), Saint-Petersburg, Russia*

Soot is a polydisperse substance which is used in the rubber industry as it has ability to increase the mechanical strength of the material [1]. Also it was determined that the larger the specific surface area of soot particles is, the greater is the increasing effect. Today there are three main methods of producing soot: furnace, channel and thermal. Recently, special attention has been given to electric arc methods [2, 3]. The report examines the electric arc pyrolysis of hydrocarbons using o-xylene as an example.

Hydrocarbon pyrolysis was made using a high-voltage AC plasma torch of own production. It consists of three electric arc channels and three graphite electrodes [4]. The synthesis was conducted for 3 minutes at a temperature about 4000 K. In a gas discharge chamber argon (protective gas) was supplied to the electrode zone with a total mass flow rate of G_{Ar} = 3 g/s, and argon was supplied to the arc burning zone with a flow rate of 0.5 g/s. The produced carbon black was collected in a water-cooled refrigerator. As a result of pyrolysis of o-xylene, two carbon black samples were obtained. The method of dynamic scattering was used to obtain information on particle sizes, presented in Figure 1. It is possible to observe fractions in sample 2: with a maximum of about 150 nm and 500 nm. The largest particles reach almost 2 mcm. This is probably due to different mechanisms of formation of these particles. Smaller soot is formed during the pyrolysis of o-xylene, and larger soot is formed during erosion of graphite electrodes.

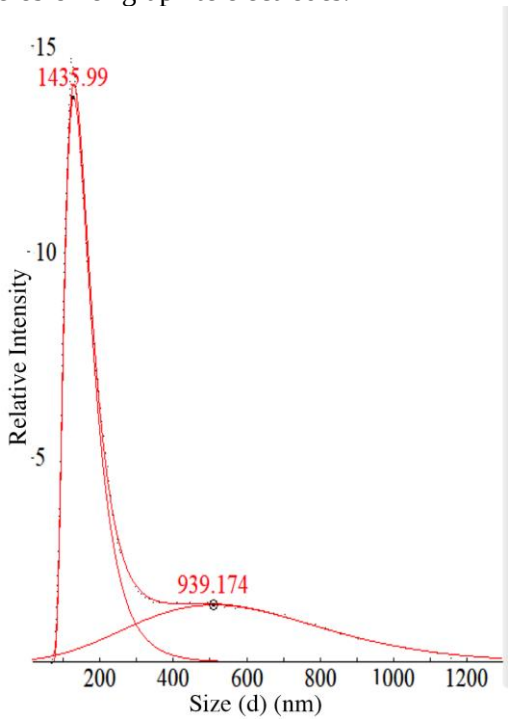

Fig.1 – The diagram of particle size distribution.

REFERENCES

[1] T. Zielinski, J. Kijenski, ―Plasma carbon black—the new active additive for plastics,‖ Composites Part A: Applied Science and Manufacturing, vol. 36, no. 4, pp. 467-471, April 2005.

[2] M. Gautier, V. Rohani, L. Fulcheri, ―Direct decarbonization of methane by thermal plasma for the production of hydrogen and high value-added carbon black,‖ International Journal of Hydrogen Energy, vol. 42, no. 47, pp. 28140-28156, November 2017.

[3] D.L. Sun, F. Wang, R.Y. Hong, C.R. Xie, ―Preparation of carbon black via arc discharge plasma enhanced by thermal pyrolysis,‖ Diamond and Related Materials, vol. 61, pp. 21-31, January 2016.

[4] S.D. Popov, D.I. Subbotin, V.E. Popov, A.V. Surov, V.V. Lizander, N.A. Charykov, Gh.A. Nakonechny, E.O. Serba, N.V. Obraztsov, ―Obtaining nano-disperse soot from orthoxylene by the high-voltage AC plasma torch,‖ Journal of Physics: Conference Series, vol. 1393, p. 012116, November 2019.

The work was supported by Russian Foundation for Basic Research (RFBR) (Projects Nos. 18-33-20238 A)

PRODUCING AND PROPERTIES OF COMPOSITES BASED ON SILVER-COATED ALUMINA BY RADIATION-CHEMICAL METHOD[1]

M.A. KISELEVA[1], *S.YU. SOKOVNIN*[1,2], *M.E. BALEZIN*[1]

[1]*Ural Federal University, Yekaterinburg, Russia*
[2]*Institute of Electrophysics UB RAS, Yekaterinburg, Russia*

To solve the problem of disinfecting household waste and waste water for reuse are applied photocatalytic processes using nanoparticles (HF) catalysts. A promising photocatalytic material [1] is alumina coated with a layer of nanosized silver [2].

Production of silver-coated alumina was carried out on the basis of radiation-chemical technology on nanosecond electron accelerator УРТ-0,5 [3]. The solution consisted of 69 g sorbitol (hexatomic alcohol), 100 ml distilled water, 0.6 g AgNO3 and 0.7 g Al2O3. After irradiation, the suspension was divided into 2 parts depending on the precipitation time: 15 hours - Al2O3Ag15 and 4 days - Al2O3Ag96. According to the results of microscopic and EDX-analyses it was determined that for nanopowder (NP) Al2O3Ag15 size was 50 nm, and quantity of silver coating was 2-3%; for Al2O3Ag96 size was 80 nm, and coating quantity was 16% - 40% [4].

Antibacterial properties of NP were investigated in two ways: cell counting with the help of Goryaev's chamber and disco-diffusion method [5]. Wine yeast was used for the first method. The studies were carried out at concentrations of 100 μg/cm2 and 200 μg/cm2. Compositional HPs showed strong antibacterial properties at both concentrations (41-60%) compared to Al2O3 and Ag by a separate action on yeast, and the large composite (Al2O3Ag96) showed a larger biological effect in relation to the relatively fine NP (Al2O3Ag15).

The evaluation of antibacterial properties by the disco-diffusion method was carried out by E. coli and S. aureus. The results of the study showed that Al2O3 appeared no bactericidal effect against the bacteria under study, and Ag and Al2O3Ag96 appeared a weak antibacterial effect.

To research the photocatalytic properties was used an aqueous solution of methyl violet as a dirt simulator. Each dish was irradiated 4 times for 5 minutes with ultraviolet radiation, and after each irradiation, the optical density was measured on an Ecros PE-5400UF spectrophotometer. At the concentration of 100 μg/ml, all powders exhibited photoprotective properties and at the concentration of 480 μg/ml photocatalytic properties and the solution with the composite at both concentrations had the highest photodegradation rate (2.42).

The resulting data about silver-coated alumina can be used to further investigate the NP in the direction of photocatalytic water disinfection techniques.

REFERENCES

[1] V.Ya. Kofman, “New oxidative technologies for water and wastewater treatment,” Water supply and sanitation, no. 10, pp. 68–78, October 2013.

[2] J.Tanori, D. Vargas et al. “Metallic and bimetallic nanoparticles supported on mesoporous materials: photocatalytic and degradation properties,” in Abstract book of the BIT’s 8th Annual World Congress of Nano Science & Technology-2018, (Postdam, 2018), p. 112.

[3] M.E. Balezin, V.V. Bazarnyiy, E.A. Karbovnichaya, S.Yu. Sokovnin “Using nanosecond electron beam to produce silver nanopowders,” Russian nanotechnologies, vol. 6, no. 9-10, pp. 42- 46, December 2011.

[4] M.A. Kiseleva, S.Yu. Sokovnin, M.E. Balezin, “Obtaining and studying properties of composite nanopowders Al2O3+Ag,” Physical and chemical aspects of the study of clusters, nanostructures and nanomaterials, no. 11, pp. 161-168, December 2019.

[5] Determination of the microorganisms sensitivity to antibacterial preparations: Methodological instructions.—M.: State Sanitary and Epidemiological Surveillance Agency of the Ministry of Health Russian Federation, 2004.—91 p.

[1] The work was supported by the financial support of RFBR and Sverdlovsk region within the framework of scientific project № 20-48-660019 r _ a

paragraphs, single line spacing.

FORMATION OF NANOCRYSTALS BASED ON ZINC SELEN COMPAUNDS USING TRACK TECHNOLOGY*

A.DAULETBEKOVA[1], A. AKYLBEKOVA[1], Z. BAIMUKHANOV[1], A. USSEINOV[1], SH. GINIYATOVA[1], A. KOZLOVSKYI[2], L. VLSUKOVA[3], A.I. POPOV[4]

[1]*L.N. Gumilyov Eurasian National University, Nur-Sultan, Kazakhstan*
[2]*Institute of Nuclear Physics, Nur-Sultan, Kazakhstan*
[3]*Belarus State University, Minsk, Belarus*
[4]*Institute of Solid State Physics, Riga, Latvia*

Ion track technology are a powerful tool for producing new nanomaterials. The most striking use of the technology is related to the creation polymer nuclear membranes. In recent years in addition to polymer materials a-SiO_2/Si structures used as ion track templates. Using this type of templates, the different structures such as nanoclasters, nanocrystals were obtained.

In our work the a-SiO_2/Si (p – and n- type) structures with an oxide layer thickness of 700 nm were irradiated with 200 MeV Xe ions to a fluence 10^8 ions/cm^2 at DC-60 cyclotron (Nur-Sultan). Chemical etching of irradiated SiO_2/Si samples was carried out in a 4% aqueous solution of HF with the addition of palladium (m(Pd)=0.025 g) at 18°± 1°C.. Before and after etching of the tracks, ultrasonic cleaning (6.SB25-12DTS) of the sample surface in isopropanol was carried out for 15 minutes. After processing, the samples were washed in deionized water (18.2 MOhm).

Chemical deposition (CD) were carried out in the following solutions: ,4 g/l $ZnCl_2$ + 0.2 g/l SeO_2. (for 1 hour at 293K) and $ZnSO_4$ - 7.2 g/l, SeO_2 - 0.2 g/l (for 15, 20 and 25 min, at 293 K). The analysis of nanopores after etching and after filling was carried out using scanning electron microscope (Hitachi TM3030, JSM 7500F). X-ray diffraction analysis (D8 ADVANCE ECO X-ray diffractometer) showed formation $ZnSe_2O_5$ nanocrystals in the a-SiO_2/Si (p – and n- type) templates with an orthorhombic crystal structure after CD in the first type and $ZnSeO_3$ nanocrystals with orthorhombic crystal structure and spatial symmetry group Pnma(62) after CD in the second type of solution.

* The work was supported by grant AP05134367 of MES the Republic of Kazakhstan

THE USE OF PLASMA-SOLUTION SYSTEMS FOR PRODUCING METAL AND METAL OXIDE NANOPARTICLES WITH BACTERICIDAL AND PHOTOCATALYTIC ACTIVITY*

N.A.SIROTKIN, V.A. TITOV, A.V. KHLYUSTOVA

G. A. Krestov Institute of Solution Chemistry of RAS, Ivanovo, Russia

The study of discharges in liquids and in contact with them is one of the priority areas in accordance with the Roadmap for the development of work on plasma physics and its applications [1]. Interest in gas discharges in contact with liquids is due to two groups of factors. Firstly, this is connected with the prospects of practical application, among which are the destruction of organic contaminants in water and its disinfection, the modification of polymeric materials, coating, the formation of micro- and nanostructures, as well as the quantitative spectral analysis of solutions for the content of metal ions. Secondly, interest in plasma-solution systems is due to the fact that the plasma-solution system is nonequilibrium, a feature of which can be considered a close relationship between the processes of formation of active particles in the liquid phase and in plasma.The use of plasma discharges in contact with liquids for the synthesis of metal nanoparticles and their oxides has been considered in a number of review papers [2, 3]. Currently, plasma-solution methods have been used to obtain nanoparticles of certain metals and their oxides, primarily nanoparticles of silver, gold and other noble metals. However, a number of problems, including obtaining nanoparticles of a given size, preventing agglomeration and oxidation of the resulting particles, immobilizing nanoparticles on polymeric materials, remain unresolved and require further research.

The main scientific aim of our work was to establish the regularities of the formation of metal and oxide nanoparticles during gas-discharge treatment of electrolyte solutions with various methods of exciting the discharge and to search for ways to immobilize nanoparticles on polymeric materials. The energy-efficient and simple method have been developed for the production of metals oxide nanoparticles (molybdenum, tungsten, silver, copper, titanium, etc.) which consists of the use of atmospheric pressure glow discharge with a liquid anode and metal cathode and low-current contact underwater discharge with metal electrodes (Figure 1). Varying the discharge parameters (current, interelectrode distance) allows one to obtain nanoparticles of specified sizes. In addition, the use of plasma-solution systems makes it possible to combine the process of plasma-chemical activation of the surface of polymers of various structures placed in a solution with the formation of metal and oxide nanoparticles in order to obtain composite materials [4]. We have obtained nanoparticles of metals and oxides with proven photocatalytic [5, 6] and bactericidal properties [7].

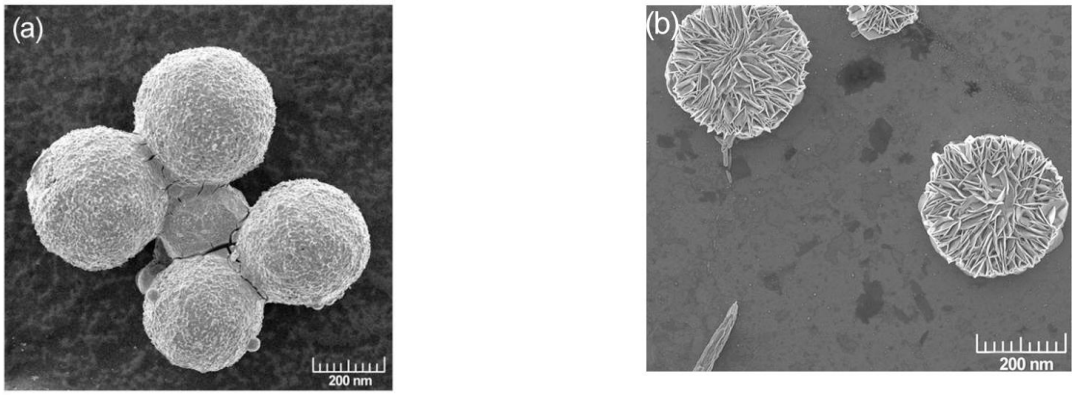

Fig. 1. SEM images of molybdenium oxide nanoparticles obtained after glow discharge (a) and underwater plasma (b).

REFERENCES

[1] P. J. Bruggeman, M. J. Kushner, B. R. Locke, et al., Plasma Sources Sci. Technol., vol. 25., Article Number 053002, 2016.

[2] G. Saito, T. Akiyama, J. Nanomat., vol. 2015. Article Number 123696, 2015.

[3] Q. Chen, J. Li, Y. Li, J. Phys. D: Appl. Phys., vol. 48. Article Number 424005, 2015.

[4] A.V. Khlyustova, N.A. Sirotkin, N.E. Kochkina, et al., Plasma Chem. Plasma Proc., vol. 39, Article Number 311, 2019.

[5] A.V. Khlyustova, N.A. Sirotkin, A.S. Krayev, et al., Plasma Sci. Tech., vol. 21, Article Number 025505, 2019.

[6] N.A. Sirotkin, A.V. Khlyustova, V.A. Titov, et.al., Plasma Chem. Plasma Proc., DOI: 10.1007/s11090-019-10048-z, 2019

[7] V.A. Titov, N.A. Sirotkin, D.I. Nikitin, et. al., Journal of Physics: Conf. Series. vol. 1328, Article Number 012085, 2019.

* The work was supported by the Russian Science Foundation under grant No. 19-73-00022.

COMPARISON OF DIFFERENT TYPES OF NANOPARTICLE SYNTHESIS FOR USE AS A PHOTOCATALYST*

A.V.MYSHKINA, BAZHUKOVA I.N., BAKSHEEV E.O., PUSTOVAROV V.A.

Ural Federal University, Yekaterinburg, Russia

Cerium dioxide nanoparticles can be used as a photocatalytic reagent because of the possibility of the Ce3 + - Ce4 + transition. [1] The activity of cerium dioxide nanoparticles depends on many factors, such as the size and shape of the particles, their non-stoichiometry. [2] These characteristics probably depend on the method of producing nanoparticles. Conditionally distinguish between chemical and physical methods. Chemical methods make it possible to obtain particles with a smaller particle size and more homogeneous, while physical particles are less uniform, but probably have a higher degree of non-stoichiometry due to extreme synthesis conditions. In order to reduce defects in the samples, it is possible to additionally act on nanoparticles, for example, anneal or irradiate with ionizing radiation. To identify the most active photocatalyst, all of these factors must be taken into account. The aim of this work is to evaluate the photocatalytic activity of cerium dioxide nanoparticles.

For comparison, cerium dioxide nanoparticles obtained by the physical method (electron beam evaporation in an inert gas atmosphere) and by the chemical method (coprecipitation method with the introduction of a maltodextrin stabilizer during synthesis), as well as a sample obtained by annealing a chemical powder in vacuum at a temperature of 600 º C, were studied.

A stabilized suspension of cerium dioxide was added in a solution of dye MV with a final concentration of 400 μg / ml, and then irradiated with a DRSH 250-3 UV-lamp with a power of 250 W for 20 minutes. During solution irradiation, the optical density of the sample was measured every 5 minutes using a PE-5400UF spectrophotometer. The measurements were carried out in quartz cuvettes with an optical path length of 1 cm at a wavelength of λ = 595 nm, which corresponds to the maximum of the absorption spectrum of the MV solution.

The non-stoichiometry of cerium dioxide nanoparticles was evaluated by obtaining luminescence spectra upon excitation in the region of 250 nm.

In this work, it was shown that annealed nanoparticles obtained by the chemical method have higher activity, probably due to less non-stoichiometry, smaller particle size, and higher specific surface area, which is critical for photocatalysts.

Presumably, such photocatalytic activity is associated with the ability to transfer electrons and holes. [3] Therefore, in order to select the most active photocatalysts, it is necessary to study in detail the structure of the obtained nanoparticles, as well as to trace possible modification paths, for example, annealing in different media at different temperatures, in order to improve the stoichiometry of the samples.

REFERENCES

[1] H. Balavi Samaneh Samadanian et al. Powder Technology 249:549-555 (2013)

[2] S. Rajeshkumar and Poonam Naik. Biotechnol Rep (Amst). 17:1–5 (2018)

[3] M.E. Khan, M.M. Khan, M.H. Cho. Scientific reports 5928:17 (2017)

* The work was supported by the Russian Science Foundation under grant No. 19-32-90124.

CHEMICAL AND PHASE COMPOSITION OF NICKEL NANOPOWDERS PRODUCED BY SPARK DISCHARGE METHOD*

I.V. BEKETOV[1], *A.D. MAKSIMOV*[1], *A.I. MEDVEDEV*[1], *A.M. MURZAKAEV*[1], *A.V. BAGAZEEV*[1]

[1] *Institute of Electrophysics of the Ural Branch of the Russian Academy of Sciences, Amundsena str., 106, Ekaterinburg, 620016, Russian Federation; a.d.maksimov1415@gmail.com, +7-982-624-4854*

The preliminary experiments on the production of nanopowders of metallic nickel by spark discharge method are described. The apparatus for producing powders is described in [1]. It contains a discharge chamber (reactor) with two discharge gaps, a pneumatic path with a total volume of 5 l; capacitive energy storage, charger, powder collection devices. Gas is pumped by a compressor with a nominal flow rate of 50 l/min.

The main obstacle to obtaining ultrafine metal powders is their high oxidation ability. Therefore, one of the aims of the experiment was to develop a method for purifying the chamber's atmosphere from oxygen. Cleaning was carried out using granules from a titanium sponge located in a specific place in the pneumatic path and heated to 800 °C. The oxygen content in the working gas was monitored using an electrochemical oxygen partial pressure sensor.

Nickel having a low oxidation ability was selected as the material of the electrodes. Nitrogen served as the working gas, since no compounds with nitrogen were found in the nickel powders obtained previously by the electric explosion method. After gas purification, the sensor indicated an almost complete absence of oxygen in it.

A series of experiments was carried out on the production of nickel powder under conditions: storage energy 3–11 J; discharge repetition rate 50–70 Hz; discharge current period 1.7 μs; running time about 1.5 hours. Several product samples were obtained, each weighing about 50 mg. Samples were analyzed using XRD, TEM, and EDX.

According to the XRD, all samples contain metallic nickel (9–19% wt., coherent scattering region (CSR) size 15–28 nm, lattice period 0.353 nm), as well as an unidentified phase (X-phase) (81–91% wt.). An example of a diffraction pattern is shown in Fig. 1.

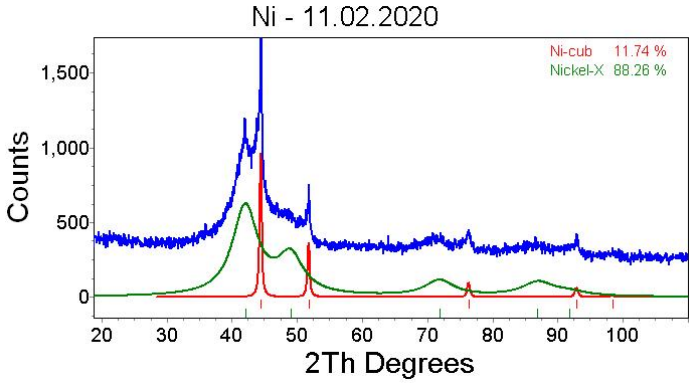

Fig.1. XRD pattern of a fine fraction of nickel powder with the presence of the X-phase.

The X-phase is almost amorphous (CSR 1.5–2.2 nm, peaks are blurred). It is isostructural to nickel, but has a longer lattice period (0.36–0.38 nm). It has been hypothesized that there is the process of diffusion of residual oxygen into the nickel lattice, but no oxide formation occurs. A more detailed study is planned; work is underway to identify the X-phase by TEM and EDX.

REFERENCES

[1] I.V. Beketov, A.V. Bagazeev, E.I. Azarkevich, A.D. Maximov, A.I. Medvedev, A.I. Beketova, "The installation for production of metal and oxide nanopowders by the spark discharge method, and its testing", Izv. Vyssh. Uchebn. Zaved. Fiz., vol. 61, no. 9/2, pp. 166–170, September 2018.

* The work was supported by the grant of Russian Foundation for Basic Research (Project No. 20-48-660044).

SYNTHESIS OF NANOSTRUCTURES BY COMPOSITE ELECTRODES ARC SPRAYING*

S.Z. SAKHAPOV[1]

[1]*Institute of Thermophysics SB RAS, Novosibirsk, Russian Federation*

Sputtering of graphite and composite electrodes in an arc discharge is effectively used for the synthesis of carbon nanostructures [1-2] and nanoparticles in a carbon matrix [3-4]. Main advantages of arc spraying: chemical purity of synthesized materials in a discharge in an inert gas atmosphere; the possibility of modifying materials in a chemically active atmosphere; size control of nanostructures by selecting discharge parameters; simplicity of the process. The sputtering products of composite electrodes in an electric arc are nanoparticles surrounded by carbon, which prevents the coagulation of nanoparticles without stopping the access of gas or liquid to the particle, which allows the use of such composites as highly-efficient catalysts.

The experimental setup (Fig. 1) was a cylindrical vacuum chamber that was previously pumped out and then filled with helium. An arc discharge was ignited between two electrodes that were on the axis of symmetry of the chamber. A negative voltage was applied through a high-current metal-ceramic sealed input to a movable graphite electrode (1), which was a cylinder with a diameter of 2 cm. A grounded stationary composite electrode (2) was attached to the camera body. The replaceable composite anode is a graphite rod with a diameter of 0.8 cm and a length of 8. The arc discharge was ignited and supported by a constant current source, allowing experiments at a current of about 100 A. As the anode was sprayed, the bellows transmission unit allowed the cathode to be moved to maintain a constant voltage across the discharge gap.

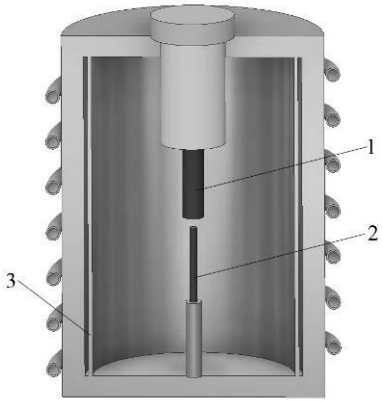

Fig.1. Experimental setup (1 – graphite movable cathode; 2 – composite anode; 3 – cooled removable screen)

In the process of burning the discharge, atomic atomization of the anode and the formation of a fan stream flowing from the interelectrode gap to the chamber walls occur. In the process of approaching the chamber walls, the vapor of materials was cooled and condensed, as a result of which larger agglomerates appeared, which were deposited on a cooled removable stainless steel screen (3) covering the surface of the chamber walls. After electric arc spraying, the synthesized material was collected from a removable screen and annealed in an air atmosphere. The kinetics of the formation of nanomaterials during condensation in an arc discharge is highly dependent on conditions such as grade and pressure of the buffer gas, electrical characteristics of the discharge, and geometry of the chamber. Typical materials for electric arc spraying are metal or carbide nanoparticles encapsulated in carbon with varying degrees of crystallization.

REFERENCES

[1] W. Kratschmer, L.D. Lamb, K. Fostiropoulos, D.R. Hoffman // *Nature. – 1990. – Vol. 3347 – P. 354-358.*

[2] J.H.J. Scott, S.A. Majetich // *Phys. Rew. B. – 1995. – Vol. 52 – P. 12564-12571.*

[3] D.V. Smovzh, S.Z. Sakhapov, A.V. Zaikovskii, S.A. Novopashin // *Ceram. Int. – 2015. – Vol. 41 – P. 8814-8819.*

[4] D.V. Smovzh, S.Z. Sakhapov, A.V. Zaikovskii, S.A. Chernova, S.A. Novopashin // *Ceram. Int. – 2019. – Vol. 45 – P. 7338-7343.*

* The work was supported by the Russian Science Foundation, Project No. 18-19-00213.

PHOTOCATALYTIC ACTIVITY OF THE COMPOSITE TRACK-ETCHED MEMBRANES FOR DECOMPOSITION OF THE ORGANIC DYES*

A.A. MASHENTSEVA[1,2], *M.V.ZDOROVETS*[1,2], *A.T. ZHUMAZHANOVA*[1], *A.N. ZHUMABEKOVA*[2], *S.R. RAKISHEVA*[2], *L.SH. ALTYNBAYEVA*[2], *A.V.RUSSAKOVA*[3]

[1] *The Institute of Nuclear Physics of the Republic of Kazakhstan, Almaty, Kazakhstan*
[2]*L.N. Gumilyov Eurasian National University, Nur-Sultan, Kazakhstan*
[3]*D.Serikbayev East Kazakhstan State Technical University, Ust-Kamenogorsk, Kazakhstan*

The development of highly efficient catalytic systems for the decomposition of such a class of pollutants as organic dyes is a very actual in the development of the processing industry. In the last decade, a lot of researches were focused on the development of nanomaterials as photocatalysts.

In this study, the employment of composite track-etched membranes based on polyethylene terephthalate and electroless deposited silver microtubes (MTs) for the decomposition of the toxic phenothiazine cationic dye methylene blue in presence of visible and UV-light was studied. In order to determine optimal silver plating conditions a series experiments was carried out with the different plating time and using data from SEM as well as manometric method an optimal plating time was selected. Electroless deposition for 5 hours in polymer template with the pores size of 430±15 nm was applied to produce composites with Ag MTs with wall thickness inner diameter of 63.0 and 319 nm respectively. The structure and composition of the composite membranes were elucidated by scanning electron microscopy, energy dispersive analysis, and X-ray diffraction technique. Under visible light irradiation (500 W Halogen lamp) Ag/PET composite displayed high photocatalytic efficiency. The effect of various parameters such as initial dye concentration (Fig. 1a), sample exposure time was studied and rate constant k was elucidated (Fig.1b).

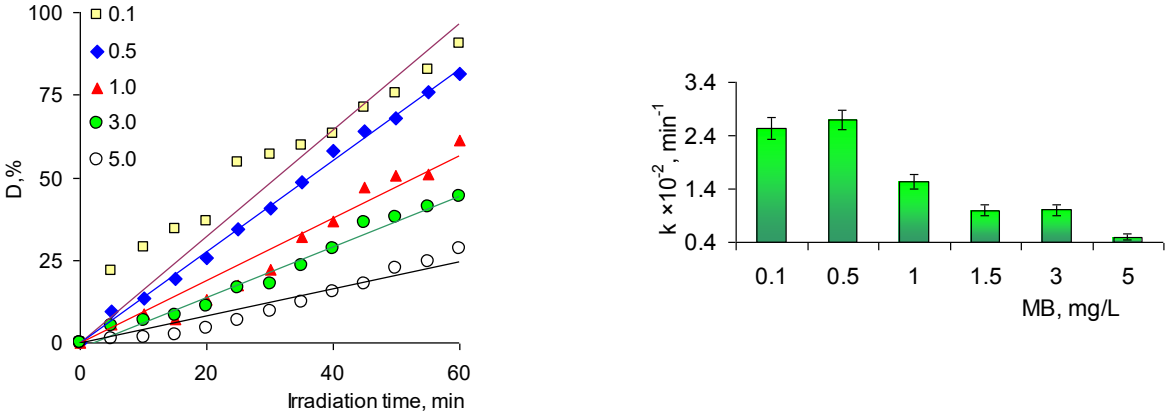

Fig.1. –Decolorization of various concentrations of MB in the presence of Ag/PET composite (a) and the changes of k_{app} values for different MB concentration (b)

The properties of the catalysts were also studied in the temperature range of 17–58 °C. The MB degradation kinetics were somewhat accelerated by increasing temperature and activation energy Ea was calculated to be 27.1 kJ/mol. Reusability of catalyst was also explored for 6 consecutive runs without any activation and regeneration procedures. It was demonstrated a high degradation efficiency over 90% over 6 consecutive uses.

* This work was supported by IAEA coordination research project “F22070”.

TRACK TEMPLATE SYNTHESIS AND INVESTIGATION 0F NANOCRYSTALS BASED ON CADMIUM COMPOUNDS*

A.T. AKILBEKOV[1], R. BALAKHAYEVA[1], Z. BAIMUKHANOV[1], SH. GINIYATOVA[1], A. KOZLOVSKYI[12], L. VLASUKOVA[3], A.I. POPOV[4] A. DAULETBEKOVA

[1]*L.N. Gumilyov Eurasian National University, Nur-Sultan, Kazakhstan*
[2]*Institute of Nuclear Physics, Nur-Sultan, Kazakhstan*
[3]*Belarus State University, Minsk, Belarus*
[4]*Institute of Solid State Physics, Riga, Latvia*

The creation of new technologies for the fabrication of widely known materials is an interesting task. Track technologies allow you to do this using various materials to form a track template from polymers to silicon [1-4].

The a-SiO_2/Si-n structures, with an oxide layer thickness of 700, were normally irradiated with 200 MeV Xe ions, up to a fluence of 10^8 ion/cm^2. Samples for experiments were cut with sizes of 5x5 mm and 20x20 mm. The next stage was the etching of samples in a 4% aqueous HF solution; the etchant included m(Pd)=0.025 g, etching temperature 18˚±1°C, then ultrasonic cleaning of the surface, washing in distilled water, and drying.

Chemical deposition in the n-type template using a sulfate solution was carried out for 1 hour at 298 K and 343K. The solution was prepared as follows: 1M $CdSO_4$ + 1mM TeO_2. $CdSO_4$ was dissolved in water, TeO_2 in a minimum amount of concentrated sulfuric acid, the two solutions were combined, and the pH was adjusted to 2. Also chemical deposition in the solution 0,1 M $CdCl_2$ x 2.5 H_2O + 0,1 M SeO_2 carried out during 30, 40, 50 min at temperature 303K, 308K, and 313K. Electrochemical deposition using sulphate and chloride solutions was performed in the constant voltage mode on the electrodes - 1.5 V for 5 and 10 minutes. Electrochemical deposition was carried out using two systems of solutions:1)1M $CdSO_4$ + 1mM TeO_2. $CdSO_4$ dissolved in water, TeO_2 – in the minimum amount of concentrated sulfuric acid. Combining the two solutions and brought the pH to a value of 2. 2) 1M $CdCl_2$ + 1mM TeO_2. $CdCl_2$. The surface analysis of the samples was carried out after etching and chemical deposition using SEM JSM 7500F. To identify the phases and study the crystal structure, BrukerAXSDIFFRAC.EVAv.4.2 software and ICDD PDF-2 international database was used. X-ray diffraction analysis of samples obtained by chemical deposition showed the creation of CdTe, CdSe and CdO nanocrystals. The study of the current-voltage characteristic of the samples made it possible to estimate the number of grain boundaries, and the height of the grain boundary barrier. Also the photoluminescence of samples was investigated.

REFERENCES

[1] A. Dauletbekova, L. Vlasukova, Z. Baimukhanov, A. Akilbekov, K. Kozlovskyi, S. Giniyatova S, A. Seitbayev, A. Usseinov, A. Akylbekova. Physica Status Solidi (B) Basic Research. 256 (5), 1800408 (2019

[2] Sh. Giniyatova, A. Dauletbekova, Z. Baimukhanov, L. Vlasukova, A. Akilbekov, A. Usseinov, A. Kozlovskiy, A. Akylbekova, A. Seitbayev, Zh. Karipbayev. Radiation Measurements. 125, 5, pp2-56 ,2019

[3] D.K. Ivanou, E.A. Streltsov, A.K. Fedotov, A.V. Mazanik, D. Fink, A. Petrov. Thin Solid Films. 490, pp154-160, 2005.

[4] T.N. Koltunowicz, P. Zhukowski, J.A. Fedotova, V.G. Bayev, E.A. Streltsov and L.V. Baran. Acta Physica Polonica A. 123 (5), 929-931, 2013.

* The work was supported by grant AP05134367 of MES the Republic of Kazakhstan

CHANGE OF THE GRAIN STRUCTURE IN THE ZR-Y-O LAYER IN THE ZR-Y-O / SI AL-N COATING AT HIGHT TEMPERATURE IN THE «IN-SITU» MODE[1]

A.P. PODANEV[1], *M.V. FEDORISCHEVA* [1,2], *M.P. KALASHNIKOV* [1,2], *I.A. BOZHKO*[1,2], *V.P. SERGEEV*[1,2]

[1]*Institute of Strength Physics and Materials Science SB RAS, Tomsk, Russia*

[2]*National Research Tomsk Polytechnic University, Tomsk, Russia*

Zirconium-based ceramics holds the leading place among the fire-resistant constructional materials as it retains the high mechanical properties up to 0.8–0.9 of the melting temperature of 3173 K. That is why ZrO_2 coatings are mainly used as the thermal barrier coatings in hot turbine sections and other engine units.

A special attention is paid to the reversible martensitic transformations in metal alloys (the so-called transformational conversion due to the practical use potential in many fields of science, technology, medicine and industry. These alloys belong to the group of the so-called “smart” functional materials, as they allow controlling their behavior [1–3].

The paper deals with the study of the thin structure and phase composition of a multilayer coating based on Si-Al-N/Zr-Y-O with the X-ray diffraction analysis and an electron microscopy. They are used to trace the thermoelastic phase transition in Si-Al-N/Zr-YO coating in ZrO_2 layer accompanied by a change in the grain structure, intergranular and interphase boundaries, the structure and phase composition with the X-ray diffraction under loading.

The coatings deposition was carried out in KVANT-03MI unit equipped with a mosaic zirconium-yttrium target magnetron. The magnetron was powered from a pulse source at a frequency of 50 kHz. The samples were placed in the chamber on the rotating table. The sample temperature during the deposition was 573K. The temperature was measured with a chromel-alumel thermocouple.

It was shown by X-ray that annealing at a temperature of 900°C leads to an insignificant decrease in the monoclinic phase, a change in the predominant direction. The degree of tetragonality of the crystal lattice does not change, the size of the coherent scattering blocks decreases.

It has been established by TEM that the coatings on the basis of Zr-Y-O produced by the magnetron sputtering methods have a nanograin column structure where the columns are spread through the entire coating thickness. At heating the layer in the TEM column in the “in-situ” mode one can observe a) martensitic transition of the tetragonal phase to the monoclinic one in temperature interval of 400-500°C, b) the grain size decreases compared with the initial grain size in the coating, c) the modification of the grain boundaries, i.e. their total length increases, the form of the grains changes, in initial column grains there are cross boundaries, which suggest the fragmentation of grains.

REFERENCES

[1] A. Petra Langjahr, Rainer Oberacker, and Michael J. Hoffmann,”Long Term Behaviour and Application Limits of plasma-spray zirconia thermal barrier coatings” J. Am. Ceram. Soc., vol.84, 1301–308, 2001.

[2] T. T. Arif and R.S. Qin, “A Phase-Field Model for the Formation of Martensite and Bainite,” AMR, vol. 922, 31–36, 2014

[3] Y. Tamarin, Protective Coatings for Turbine Blades USA (ASM International, 2002). pp. 3-300.

[4] V.P. Sergeev, V.P. Yanovsky, Yu.N. Paraev, et. al., “Installation of ion-magnetron sputtering of nanocrystalline coatings (QUANT)”, Physical Mesomechanics, 7, 333-336, 2004.

[5] Yu. F. Ivanov, V. Kozlov, FMM, “Electron microscopic analysis of polycrystalline materials» vol. 7, 206-208, 1991.

[6] G.Ya. Akimov, “Evolution of the phase composition and physicomechanical properties of ZrO_2 + 4 mol. % Y_2O_3 ”, Solid State Physics, vol. 46, 2, 250 – 253, 2004.

1 The work was performed under the government statement of work for ISPMS Project No. III.23.1.1 and the presented work is a continuation of the RFBR project No. 16-48-700198.

SYNTHESIS OF NANODIAMONDS FROM FUEL OIL PROCESSING PRODUCTS USING AN ARC DISCHARGE*

A.A. SAIFUTDINOVA, B.A. TIMERKAEV, A.I. SAIFUTDINOV

[1] *Kazan National Research Technical University named after A.N.Tupolev, Kazan, Russia*

The synthesis temperature of many nanostructures is much lower than the evaporation temperature of the material, from the vapors of which the synthesis of these nanostructures is carried out. For the successful implementation of the synthesis of nanostructures, it is necessary to study the distribution of temperature fields in various working areas of the plasma chemical reactor, namely, directly in the arc, on the surfaces of the electrodes and on the periphery, including the substrate, and determine the areas for the predominant growth of various nanostructures. This is due to the fact that each type of nanostructure has its own synthesis temperature. Moreover, the traditional method of synthesis of carbon nanotubes involves the evaporation of graphite at a temperature of about 4000 K and their deposition on the cathode. It is clear that the cathode temperature should not be higher than the decay temperature of carbon nanostructures, which is approximately 1800 K. In this situation, the plasma-chemical synthesis of nanostructures on the electrodes of the arc discharge has significant limitations. Various types of catalysts are often used to intensify the production of nanostructures [1].

In this work, we conducted a two-stage experiment on the synthesis of micro diamonds from fuel oil. At the first stage of the experiment, the synthesis of carbon nanostructures was carried out by initiating an arc discharge in fuel oil. When a discharge is ignited in the bulk of a hydrocarbon feed, the discharge burns in vapor of gaseous hydrocarbons. Due to the high temperature of the arc, pressure is created in the thickness of the fuel oil, which is able to maintain the plasma region inside the hydrocarbon feedstock. The edges of this area are in contact with fuel oil. In gas-discharge plasma, electrons in a collision with molecules break carbon bonds, creating atomic carbon, hydrogen and light hydrocarbons. Under the influence of an electric field, atomic carbon is ionized and moves to the electrodes.

At the second stage, the synthesized nanostructures were used as the anode of a low-current arc discharge in an inert gas medium for the direct synthesis of micro diamonds. As a result, carbon atoms will evaporate from the surface of the synthesized carbon neoplasms on the anode. This is due to the fact that the chemical bonds of carbon atoms on the surface of these formations are weaker, therefore, the conversion of these formations into atomic carbon occurs at lower temperatures.

As a result of a series of experimental studies using the proposed method, nanodiamonds with sizes from 50 to 100 nm were synthesized, studied using a Carl Zeiss Auriga Crossbeam electron microscope and X-ray diffraction analysis. The practical appearance of all nanodiamonds is the same. They have clear edges and are more like faceted diamonds. Some of them have a pyramidal shape.

REFERENCES

[1] Timerkaev B.A., Kaleeva A.A., Timerkaeva D.B., Saifutdinov A.I., 390-395. "GERMANIUM CATALYST FOR PLASMA-CHEMICAL SYNTHESIS OF DIAMONDS", High Energy Chemistry, Vol. 53, Number 5, pages 390-395, 2019

* This study received support from the Russian Foundation for Basic Research, project № 18-43-160005 and government of RT.

19th International Conference on Radiation Physics and Chemistry of Condensed Matter

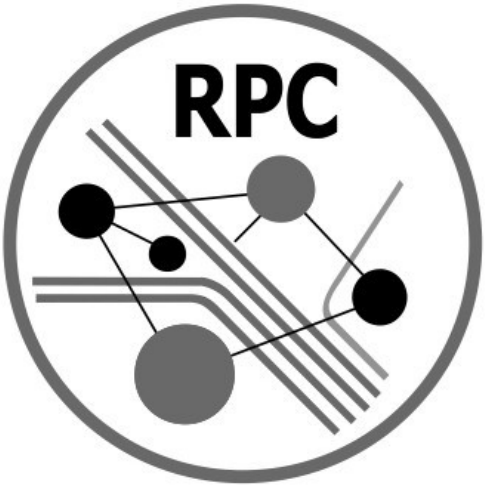

Chairman	Alexey Yakovlev,	National Research Tomsk Polytechnic University, Tomsk, Russia
Co-Chairman	Elena Polisadova,	National Research Tomsk Polytechnic University, Tomsk, Russia
Program Chairman	Elena Polisadova,	National Research Tomsk Polytechnic University, Tomsk, Russia
Program Co-Chairman	Aleksandr Pushkarev,	National Research Tomsk Polytechnic University, Tomsk, Russia

Program Committee

Viktor LISITSYN	National Research Tomsk Polytechnic University, Tomsk, Russia
Evgenij MARTYNOVITCH	Institute of Laser Physics of the Siberian Branch of the RAS, Irkutsk, Russia
Vadim KRIGER	Kemerovo State University, Kemerovo, Russia
Ilya WEINSTEIN	Ural Federal University, NANOTECH Center, Ekaterinburg, Russia
Aleksandr NEPOMNYASHCHIKH	A.P. Vinogradov Institute of Geochemistry of the Siberian Branch of the RAS, Irkutsk, Russia
Maxim ZDOROVETS	Institute of Nuclear Physics, National Nuclear Center of the Republic of Kazakhstan, Almaty, Kazakhstan

International Advisory Committee

Albert ASHRYATOV	Ogarev Mordovia State University, Saransk, Russia
Boris ADUEV	Institute of Coal-chemistry and Material Science of the Siberian Branch of the RAS, Kemerovo, Russia
Habibula ABDULLIN	Al Farabi Kazakh National University, National Nanotechnology Laboratory of Open Type, Almaty, Kazakhstan
Abdirash AKILBEKOV	L.N. Gumilyov Eurasian National University, Astana, Kazakhstan
Gennady BONDARENKO	National Research University Higher School of Economics, Moscow, Russia
Flyura DJURABEKOVA	Helsingin Yliopisto, Helsinki, Finland
Gilles DAMAMME	CEA Gramat, Gramat, France
Boris GRINEV	Institute for Scintillation Materials of NAS of Ukraine, Kharkov, Ukraine
Boris KALIN	National Research Nuclear University MEPhI, Moscow, Russia
Mustafa KIDIBAEV	Kyrgyz National Academy of Sciences, Bishkek, Kyrgyzstan
Evgenij KOTOMIN	Max Planck Institute for Solid State Research, Stuttgart, Germany
Anatoly KUPCHISHIN	Abai Kazakh National Pedagogical University, Almaty, Kazakhstan
Aleksandr LUSHCHIK	Institute of Physics, University of Tartu, Tartu, Estonia
Sergey NIKIFOROV	Ural Federal University, Ekaterinburg, Russia
Hosam OTHMAN	Minufiya University, Department of Physics, Shebin el Kom, Egypt
Anatoli POPOV	Institute of Solid State Physics, University of Latvia, Riga, Latvia
Stanislav SHANDAROV	National Research Tomsk Polytechnic University, Tomsk, Russia
Boris SHULGIN	Ural Federal University, Ekaterinburg, Russia
Han TAO	Research Institute for New Materials Technology, Chongqing University of Arts and Sciences, Chongqing, China
Yurij ZAKHAROV	Kemerovo State University, Kemerovo, Russia
Vladimir ZARKO	Voevodsky Institute of Chemical Kinetics and Combustion, Novosibirsk, Russia
Maxim ZDOROVETS	Institute of Nuclear Physics, National Nuclear Center of the Republic of Kazakhstan, Almaty, Kazakhstan

Conference topics

Luminescence: processes, luminescence centers, scintillators and luminophores, application
Non-linear physicochemical processes under severe energetic impact: breakdown, facture, explosion, etc.
Physical principles of radiation and photonic technologies
Radiation defects: structure, formation, properties
Methods, instruments and equipment for physicochemical studies

RESEARCH OF LUMINESCENT PROPERTIES OF THE BaBr2-BaI2 SYSTEM*

A.I. RUSAKOV[1], A.A. SHALAEV[1], R.Y. SHENDRIK[1], A.S. MYASNIKOVA[1], A.K. SUBANAKOV[2]

[1] Vinogradov Institute of Geochemistry SB RAS, Irkutsk, Russia
[2] Baikal Institute of Nature Management SB RAS, Ulan-Ude, Russia

BaBrI crystals activated by Eu^{2+} ions are of great interest due to the high light yield (of the order of 90,000 photons / MeV) and the relatively fast decay time of the afterglow. Earlier, we studied the luminescent properties of BaBrI: Eu2 + single crystals [1, 2, 3], grown in a stoichiometric 1: 1 $BaBr_2$ / BaI_2 ratio.

To study the $BaBr_2$-BaI_2 system, solid solutions of various compositions were obtained with a step of 10 mol. % from $BaBr_2$ to BaI_2. Using the method of differential scanning calorimetry, the melting and crystallization temperatures of these solid solutions were obtained. Based on the obtained solidus and liquidus points, a phase diagram was constructed for the $BaBr_2$-BaI_2 system (Fig. 1).

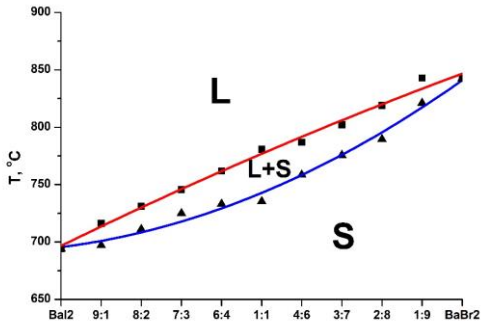

Fig. 1. Phase diagram of the $BaBr_2$-BaI_2 system. Lines of liquidus (red) and solidus (blue). *L* is the region of the liquid phase, *S* is the region of the solid phase, *L+S* is the region of stability of the two-phase association.

The phase diagram is a classic view of a substitutional solid solution system. To confirm that the diagram shows a continuous series of substitutional solid solutions, an X-ray phase analysis will be carried out.

In the work on the structure and luminescent properties of the $BaBr_2$-BaI_2 system [4], it is reported that the most striking samples are BaBrI:Eu and $BaBr_{1.7}I_{0.3}$: Eu. The authors hypothesize that this is due to a more efficient transfer from excitons to Eu^{2+} activator ions in structures rich in Br. To clarify this assumption, we will analyze the luminescent properties of single crystals with different stoichiometry: $BaBr_{1.9}I_{0.1}$, $BaBr_{1.7}I_{0.3}$, $BaBr_{0.3}I_{1.7}$ and $BaBr_{0.1}I_{1.9}$.

REFERENCES

[1] A. Rusakov, A. Shalaev, R. Shendrik, A. Myasnikova, A. Subanakov, “Growth and spectroscopy of BaBrI crystals activated by Eu2+ ions,” AIP Conference Proceedings, vol. 2069, 2019.

[2] A. Shalaev, R. Shendrik, A. Myasnikova, A. Bogdanov, A. Rusakov, A. Vasilkovskyi, “Luminescence of BaBrI and SrBrI single crystals doped with Eu2+,” Optical Materials, vol. 79, pp. 84-89, 2018.

[3] R. Shendrik, A. Shalaev, A. Myasnikova, A. Bogdanov, E. Kaneva, A. Rusakov, A. Vasilkovskyi, “Optical and structural properties of Eu2+ doped BaBrI and BaClI crystals,” Journal of Luminescence, vol. 192, pp. 653–660, 2017.

[4] G. Gundiah, G. Bizarri, S. M. Hanrahan, M. J. Weber, “Structure and scintillation of Eu2+ -activated solid solutions in the BaBr2–BaI2 system,” IEEE Transactions on Nuclear Science, No. 6, vol. 58, December 2011.

* This work was supported by a grant from the Russian Science Foundation, RSF project 18-72-10085.

STUDY OF FAST INTERCONFIGURATIONAL 5*d*-4*f* TRANSITIONS IN $KLuP_2O_7$ DOPED WITH Pr^{3+} IONS UNDER DIFFERENT TYPES OF EXCITATION*

S.A. KISELEV[1], *V.A. PUSTOVAROV*[1]

[1]*Institute of Physics and Technology, Ural Federal University, Ekaterinburg, Russian Federation*
Corresponding author: e-mail sviat-kiselev@yandex.ru, phone number +79221296380

Inorganic scintillator materials with high light output and fast nanosecond luminescence decay kinetics are widely required in modern technologies such as nuclear physics, security, chemistry, space physics, medical imaging, etc. Wide-gap compounds as complex silicates, phosphates, binary rare earth halides doped with Pr^{3+} ions, are used as fast scintillators [1]. Our studies of novel scintillating materials based on complex phosphates are devoted, in particular, to $KLuP_2O_7$ with fast 5*d*→4*f* emission of Pr^{3+} impurity ions.

Powder crystalline materials $KLuP_2O_7$:Pr^{3+} (1%) have been synthesized by a solid state reaction. Preparation was controlled with Raman spectroscopy, the final product was attested with X-ray powder diffraction analysis.

Experimental results for this paper were obtained applying different techniques. Measurements of photoluminescence (PL), PL excitation, X-ray (XRL) and pulse cathode (PCL) excited time-resolved luminescence, their decay kinetics and thermally stimulated luminescence (TSL) were performed.

XRL spectra (Fig. 1, right side), as well as spectra of PL and PCL, exhibit broad UV-emission bands corresponding the parity-allowed interconfiguration radiation transitions from the lowest excited $4f^15d^1$-state of the Pr^{3+} ion to the ^3H_J and ^3F_J multiplets of the main $4f^2$-electronic configuration. These transitions, as was investigated in kinetics measurements, have decay time ~17 ns, what fully correlates with typical decay time of interconfiguration transitions in Pr^{3+} ions [2]. Besides that, intraconfigurational $4f^2 – 4f^2$ transitions (set of lines in visible region) and Stocks defect-related luminescence were observed and studied.

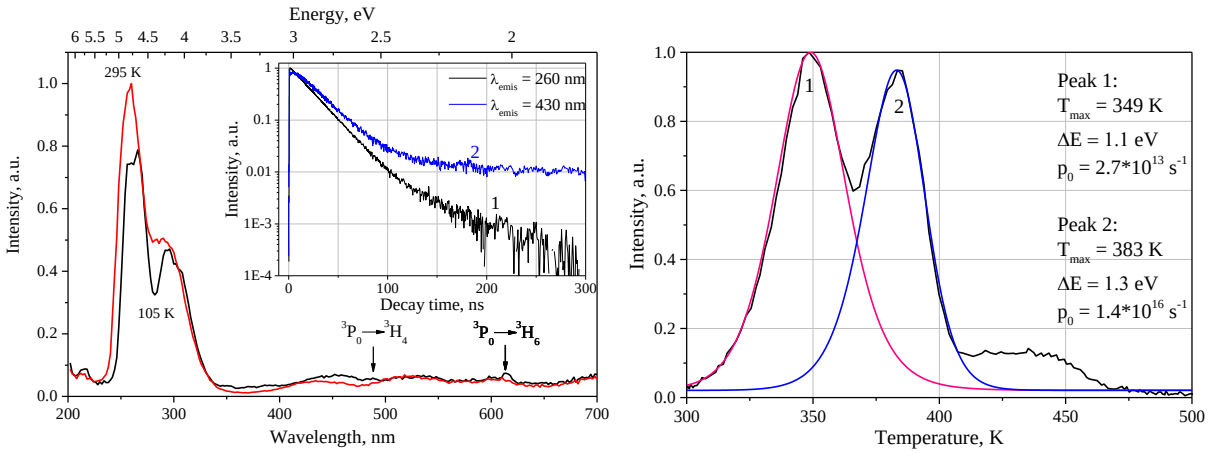

Fig. 1. Left: XRL spectra of $KLuP_2O_7$:Pr^{3+} measured at T = 295 and 105 K. Insert shows PCL decay kinetics measured on 260 (1) and 430 (2) nm emission bands at room temperature. Right: TSL glow at 265 nm emission band with two approximation curves

The features of XRL and TSL (fig. 1, left side) spectra indicate an efficient transport of energy from the impurity center to the defects. This fact limits the recombination luminescence output of the Pr^{3+} impurity center, creating a competing charge carrier capture channel. Delayed recombination emission processes are considered to be connected with retrapping of electrons and/or holes by host defects. Two peaks in TSL spectrum indicate the presence of several trapping centers with different activation energy (values of activation energy and frequency factor are presented in the graph).

REFERENCES

[1] *M. Trevisani, K.V. Ivanovskikh, F. Piccinelli, M. Bettinelli* // Journal of Luminescence. – 2014. – Volume 152. – pp. 2-6.
[2] *A.M. Srivastava* // Journal of Luminescence. – 2016. – Volume 169. – pp. 445-449.

* This work was partially supported by the Ministry of Education and Science of the Russian Federation (through the basic part of the government mandate, project No. 3.8302.2017/8.9), Act 211 Government of the Russian Federation (contract № 02.A03.21.0006). The X-ray excited experiments using SR-radiation were performed at the shared research center SSTRC on the basis of theVEPP-2000 complex at BINP SB RAS, using equipment supported by project RFMEFI62119X0022. Authors thank Prof. Marco Bettinelli (University of Verona, Italy) and Dr. K. Ivanovskikh (UrFU) for helpful discussions.

PHOTOLUMINESCENCE THEORETICAL DESCRIPTION OF NANOCOMPOSITE MATERIAL BASED ON PMMA

NATALIA S. DYURYAGINA, ALEXANDR P. YALOVETS*

South-Ural State University, Chelyabinsk, Russia

**e-mail: nsdiuriagina@susu.ru*

Interest in photoluminescence research of nanocomposite materials based on polymers, such as polymethylmethacrylate (PMMA), due to their common use in the development of various optoelectronic devices [1-5]. Semiconductor nanoparticles, such as CdS are usually used as inclusions due to due to their ability to emit in a wide range of wavelengths depending on their size. Literature rewire showed that the CdS nanoparticle introduction into PMMA not only increases the photoluminescence intensity and absorption coefficient [1-5], but also makes the resulting materials more resistance to radiation [6-8], that allows the use of optoelectronic devices under increased radiation. Change the electrophysical properties of nanocomposite materials is related to the additional localized centers in the bandgap, the energy spectrum of which determined by the size, shape and concentration of nanoparticles.

At the moment there are a lot of numbers of experimental works devoted to the study of the nanocomposite material photoluminescence [1-5], but the theoretical model to describe the experimentally observed phenomena is absent. Thus, the research of processes, which defined optical properties of nanocomposite material and development of an appropriate theoretical model are relevant tasks.

Theoretical model based on Rose-Fowler (RF) model, that describes all the processes, which define electrophysical properties of materials, in the best way [6-8], including such processes as the charge carriers recombination and generation due to the ionization of matrix material and inclusions, the charge carrier remove and capture by localized states. Also, the theoretical model considers radiation transport through the matter and the temperature effects.

In this work, we investigate photoluminescence and absorption spectra unirradiated of the pure PMMA and PMMA with CdS inclusions in size from 2 to 10 nm and concentration up to 10 vol. %, as well as materials after the irradiation with different power and pulse duration using RF model.

REFERENCES

[1] H.M. Zidan, M. Abu-Elnader, “Structural and optical properties of pure PMMA and metal chloride-doped PMMA films” , Physics B, vol. 355, pp. 308–317, Novemver 2005

[2] P.K. Khanna, N. Singh, “Light emitting CdS qantum dots in PMMA: Synthesis and optical studies”, Journal of Luminescence, vol. 127, pp. 474–482, February 2007

[3] A.M. Magerramov, M.A. Ranazanov, F.V. Gadzhieva // INORGANIC MATERIALS: APPLIED RESEARCH – 2008. – 1, P. 71–74. (in rus)

[4] V.A. Svetlichnii, A.A. Biriukov, I.N. Lapin, T.I. Izaak, “ Fetures of fluorewscecne of the CdS nanoparticle/organic dyes, PMMA nanocomposites”, Russian Physics Journal, no. 11/3, pp. 69–72, 2010

[5] R. Kaur, K.S. Samra, “Electrical and mechanical behavior of polymethyl methacrylate/cadmium sulphide composites”, Physica B: Condensed Matter, vol. 538, pp. 29–34, March 2018

[6] N.S. Dyuryagina, A.P. Yalovets, “Using Rouse-Fowler model to describe radiation-induced electrical conductivity of nanocomposite materials”, J. Phys.: Conf. Ser, vol. 830, no.1, pp. 12130–12136, May 2017.

[7] N.S. Dyuryagina, A.P. Yalovets, “Radiation-indued electrical conductivity of nanocomposite materials” // J. Technical Physics, vol. 63, no. 6, pp. 838-847, June 2018.

[8] N.S. Dyuryagina, A.P. Yalovets “Thermoluminescence of Irradiated Nanocomposite Material Based on Aluminum Oxide”, J. Phys.: Conf. Ser., vol. 1115, no. 5, pp. 052022–30, November 2018.

THE GLOW DISCHARGE APPLICATION FOR FORMATION OF A THIN LUMINESCENT LAYER IN WIDE GAP CRYSTALS*

A.A. TYUTRIN, D.S. GLAZUNOV, A.L. RAKEVICH, E.F. MARTYNOVICH

Irkutsk Branch of the Institute of Laser Physics SB RAS,130a Lermontova street, Irkutsk, 664033, Russia, tyutrin.aleks@gmail.com

The development of methods of the luminescent layer formation based on color centers in crystals and films is relevant in numerous practical applications [1,2]. However, in many cases the process is laborious and special equipment is required. Therefore, researchers are trying to simplify it.

The complex investigation of use of glow discharge as a tool for formation of radiation luminescent defects has been carried out. In this work, we continue the study begun in [3,4].

The purpose of the study was to investigate an application of a glow discharge for formation of a luminescent layer in wide gap crystals. It was necessary to measure the optical spectra in different zones of discharge, to determine the VUV-UV radiation dependence on pressure, voltage and distance between electrodes, diameters of tubes; to identify the types of the formed color centers; to study the spectral-kinetic characteristics of their luminescence; to detect the glow discharge zones in which defect formation was most effective.

Scanning confocal fluorescence microscope MicroTime 200 with picosecond time resolution with a spatially-selective time-correlated single photon counting was used to determine spectral-kinetic characteristics of photoluminescence of irradiated samples. Photoluminescence spectra measured under excitation by picosecond lasers were recorded by the spectrometer Ocean Optics 65000.

It is shown that the color centers are mainly formed by photon-induced mechanism, namely, defect formation under the action of VUV radiation. The obtained results give a picture of the distribution of VUV radiation with a wavelength shorter than 130 nm. The VUV radiation intensity distribution has maximum values in the near-electrode regions of the discharge in the wide range of pressures and voltages. The stratified positive column of glow discharge is also a region of intense VUV radiation at high voltage.

There are two types of luminescent centers formed in LiF crystal during irradiation in a glow discharge, namely, F_3^+ - and F_2- color centers with luminescence band maxima at 540 and 680 nm and decay time constants of 7.1 and 17.9 ns.

REFERENCES

[1] M. Leoncinia, M.V. Vincenti, F. Bonfigli, S. Libera, E. Nichelatti, M. Piccinini, A. Ampollini, L. Picardi, C. Ronsivalle, A. Mancini, A. Rufoloni, R. M. Montereali, "Optical investigation of radiation-induced color centers in lithium fluoride thin films for low-energy proton-beam detectors," Optical materials, vol. 88, pp. 580-585, 2019 .

[2] P. Di Lazzaro, S. Bollanti, F. Flora, L. Mezi, D. Murra, A. Torre, F. Bonfigli, R.M. Montereali, "Invisible marking system by extreme ultraviolet radiation: The new frontier for anti-counterfeiting tags," JINST., vol. 11, 2016.

[3] A. A. Tyutrin, A.L. Rakevich, D.S. Glazunov, E. F. Martynovich, "Formation of a Thin Luminescent Layer in LiF Crystals under Glow Discharge Radiation," Technical Physics Letters, vol. 44, pp. 659-662, 2018.

[4] A. A. Tyutrin, A.L. Rakevich, D.S. Glazunov, E. F. Martynovich, "The axial VUV radiation intensity distribution of a glow discharge and its application for creation luminescence centers in crystalline media," AIP Conf. Proc., vol. 2069, pp. 020003, 2019.

* This work was supported by the project II.10.1. of Programs FNI of State Russian Academies № 0307-2016-0004 and RFBR № 17-52-44015 Mong_a.

TUNABLE SPECTRUM OF YAG TRANSPARENT LUMINESCENCE CERAMICS FOR LASER LIGHTING *

Y. CAO[1], *T. HAN*[1,2], *S. CAO*[1], *Y. ZHONG*[1,2], *W.Q. FAN*[1]

[1] *Chongqing University of Arts and Sciences, Chongqing, P. R. China*
[2] *National Research Tomsk Polytechnic University, Tomsk, Russia*

With the rapid development of ceramic preparation technology, the transparent ceramics have been widely used in industrial, medical and defense fields. In this paper, $Y_{2.94}Al_{5-x}O_{12}:Ce_{0.06}$, Mn_x (YAG) transparent ceramics with a red light-emitting component are successfully prepared by the solid-state reaction vacuum sintering method. X-ray diffraction analysis, scanning electron microscope and electron pulse spectrometer were used to characterize the phase, microstructure and thermal properties of ceramic samples. The transfer energy from Ce^{3+} to Mn^{2+} ions in YAG ceramic produces the effective red light emission and improves the light-emitting properties. These results provide the promising application in the field of laser lighting.

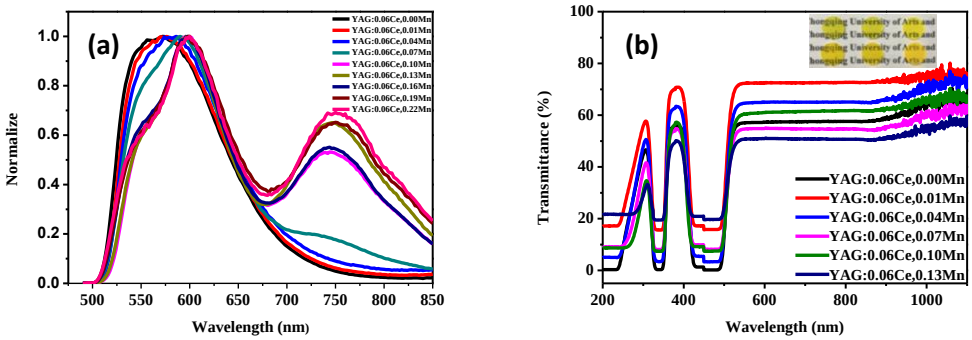

Fig.1. Photoluminescence spectra (a) and UV-Vis spectra (b) of $Y_{2.94}Al_{5-x}O_{12}:Ce_{0.06}$, Mn_x (x=0-0.13) ceramics. The inset is the picture of ceramics under natural light.

REFERENCES

[1] Y. Sun, X. Qin, G. Zhou, H. Zhang, X. Peng, S. Wang, "Gelcasting and reactive sintering of sheet-like YAG transparent ceramics," J. Alloy. Comp., vol. 652, pp. 250–253, 2015.

[2] P. Samuel, G.A. Kumar, T. Yanagitani, H. Yagi, K.I. Ueda, S.M. Babu, "Efficient energy transfer between Ce^{3+}/Cr^{3+} and Nd^{3+} ions in transparent Nd/Ce/Cr:YAG ceramics," Opt. Mater., vol. 34, pp. 303–307, 2011.

[3] T.C. Lang, T. Han, C. Zhao, S. Fang, L. Zhao, V.I. Korepanov, A.N. Yakovlev, "Luminescence properties of color tunable new garnet structure $(Lu_{1-x}Mn_x)_3Al_2(Al_{1-x}Si_x)_3O_{12}$: Ce^{3+} solid solution phosphors," J. Lumin., vol. 207, pp. 98–104, 2019.

[4] T.C. Lang,T. Han, C. Zhao, S.X. Cao, S.Q. Fang, S. Li, L. Zhao, V.I. Korepanov, A.N. Yakovlev, "Color-tunablephotoluminescence and energy transfer of $(Tb_{1-x}Mn_x)_3Al_2(Al_{1-x}Si_x)_3O_{12}:Ce^{3+}$ solid solutions for white light emitting diodes," RSC Adv., vol. 8, pp. 36056-36062, 2018.

* The work was supported by the Basic and Frontier Research Program of Chongqing Municipality (cstc2018jcyjAX0339, cstc2017jcyjBX0051), the Science and Technology Research Program of Chongqing Municipal Education Commission (KJZD-M201901301), Natural Science Foundation of Chongqing (cstc2019jcyj-msxm2493).

RESEARCH OF THE COMBINED INFLUENCE OF NITRO-CONTAINING EXPLOSIVES AND ALIPHATIC AMINES ON THE LUMINESCENCE OF CHEMOSENSORS

I.E. SHCHAPOV, A.A. BARANOVA, K.O. KHOKHLOV

Ural Federal University, Ekaterinburg, Russia

Today, there is an acute problem of controlling the concentration of nitrogen compounds. Compounds containing nitro or amino groups are widely used in industry, in the production of explosives, dyes, etc. It is also known that nitroaromatic compounds harm the environment and human health due to their high toxicity and explosiveness [1]. A number of aliphatic amines can cause serious illness and are considered carcinogens.

The article is devoted to the research of the joint effect of nitroaromatic explosives and aliphatic amines on the change in the luminescence intensity of certain chemosensors.

This study was conducted using a sniffer that detects nitrogen compounds due to the quenching of luminescence. It was developed at the Department of Experimental Physics, UrFU [2]. As a sensor element of the device, fluorescent chemosensor substances synthesized by the IOS Ural Branch of the Russian Academy of Sciences were used [1,3]. Fluorescence-based sensing methods attract huge attention due to their simplicity, high sensitivity and fast response time [4].

Previously, it was established that the luminescence intensity increased upon contact of chemosensors with household chemicals, solvents, etc [5]. Upon contact of the sensors with a number of aliphatic amines, an increase in the luminescence intensity was also noted [1]. However, the fact of a decrease in the luminescence intensity was established upon contact of the chemosensor with nitroaromatic compounds.

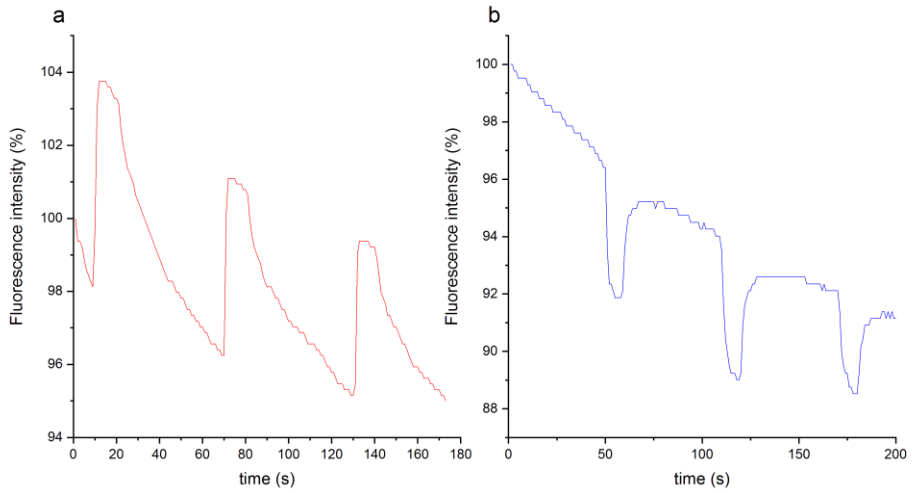

Fig.1. Change of fluorescent intensity cycles for the sensor on the basis of compound **7a** in device «Zaslon-M» with exposure to saturated allylamine (*a*) and DNT (*b*) vapors [1].

The main objective of this research was to check the response of the detector to combination of saturated vapors of volatile toxic substances of various groups: nitroaromatic compounds and aliphatic amines. The article describes the interaction of several combinations on several different sensors. Based on the results obtained, conclusions can be drawn about the possibility of mutual masking of two dangerous groups of compounds. The mechanisms of quenching of fluorophores and the mechanism of luminescence ignition are described. An attempt was also made to explain the joint influence of the two mechanisms using the example of DNT and allylamine.

REFERENCES

[1] E.V. Verbitskiy, A.A. Baranova, K.O. Khokhlov et al., "Synthesis and characterization of linear 1,4-diazine-triphenylamine-based selective chemosensors for recognition of nitroaromatic compounds and aliphatic amines", Dyes and Pigments, vol.178, Article Number 108344, 2020.

[2] K.O. Khokhlov, A.A. Baranova et al., "Device for mobile detection of explosives and drugs", patent RF, no. 159783, 2016.

[3] G.V. Zyryanov, I.S. Kovalev et al., "Sensor element for photoluminescent or optical vapor detector", patent RF, no. 148668, 2014.

[4] Website of the portable detector of nitro-explosives "Zaslon-M", http://escs-zaslon.ru/.

[5] I.E. Shchapov, A.A. Baranova, K.O. Khokhlov et al., "Research of effects of different substances on detection of nitro-containing explosive substances by the method of chemoluminescent", Med.-Ecol. Inf. Techn.-2019, 2019.

TWO MECHANISMS OF THERMOLUMINESCNCE IN LITHIUM MAGNESIUM PHOSPHATE*

M.O. KALINKIN[1], D.A. AKULOV[2], D.G. KELLERMAN[1], R.M. ABASHEV[2,3], A.I. SURDO[2,3]

[1] Institute of Solid State Chemistry, Ural Branch Russian Academy of Sciences, Ekaterinburg, Russia
[2] Ural Federal University, Ekaterinburg, Russia
[3] Institute of Metal Physics, Ural Branch Russian Academy of Sciences, Ekaterinburg, Russia

Lithium-magnesium phosphate with an olivine type structure is transparent over a wide range of wavelengths, chemically and thermally stable, therefore, it is a promising matrix for materials intended for optical dosimetry A few years ago, it was proposed to use $LiMgPO_4$ activated by terbium for OSL and TSL ionizing radiation dosimeters [1-2].

In this work, the study of photoluminescence, thermoluminescence, X-ray luminescence, UV-VIS spectra for Nd, Sm, Gd, Tb, Dy, Ho, Er, Tm doped lithium magnesium phosphate was carried out. Thermoluminescence of pure $LiMgPO_4$ was studied in detail. It has been suggested that oxygen vacancies serve as traps during irradiation. In accordance with the specific features of the crystal structure of $LiMgPO_4$ they can be located at three crystallographically nonequivalent oxygen positions and can be either neutral or once or twice ionized. The positions of the peaks on the glow curve obtained for $LiMgPO_4$ were compared with energies of defects determined earlier by the first-principle calculations [3].

It has been established that two different mechanisms are possible for doped lithium-magnesium phosphate. In the first case, emission bands specific for the RE dopant are observed in the TL or RL spectra. They correspond to intra-4f-shell transitions in RE, such a mechanism is characteristic of samarium, gadolinium, terbium, dysprosium, and thulium ions. In the second case, first observed, the rare-earth element sensitizes the matrix and enhances its thermoluminescence and X-ray luminescence. In this case, there is no spectrum of the RE. We found such a mechanism for neodymium, erbium, and holmium ions. The RL spectra for pure and doped (Tb, Er) $LiMgPO_4$ are shown in Fig. 1.

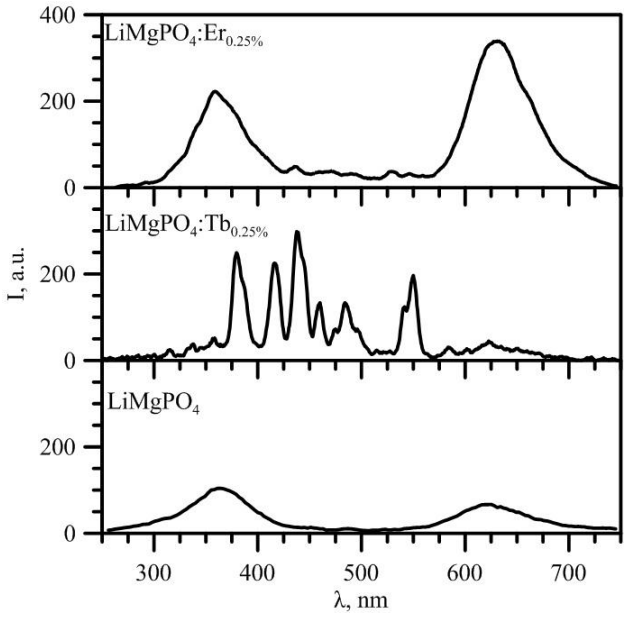

Fig. 1. RL spectra for pristine and doped $LiMgPO_4$

This mechanism allows the creation of dosimetric materials with good properties. Thus, the thermoluminescent properties of $LiMgPO_4$: Er are comparable with those of a commercially available anion defective alpha-Al_2O_3, and even surpass them in the case of optically stimulated luminescence.

REFERENCES

[1] *N.S. Bajaj, C.B.Palan, K. A. Koparkar , M. S. Kulkarni, S. K. Omanwar // J. Lumines. - 2016. - 175. - 9-15.*
[2] *W. Gieszczyk, D. Kulig(Wrobel), P. Bilski, B. Marczewska, M. Klosowski // Radiation Measurements. 2017. - 106. - 100 - 106.*
[3] *N.I. Medvedeva, D.G. Kellerman, M.O. Kalinkin // Mat. Res. Express. - 2019. – 6 (10). - 106304.*

* This work was supported by Russian Foundation for Basic Research, Grant No. 18-08-00093 A

THERMALLY AND OPTICALLY STIMULATED LUMINESCENCE OF NEW COMPOSITE Al_2O_3-BeO CERAMICS AFTER HIGH-DOSE IRRADIATION*

S.V. NIKIFOROV, A.D. BORBOLIN, D.V. ANANCHENKO, A.S. VOKHMINTSEV, I.A. WEINSTEIN

Ural Federal University, 19 Mira street, Ekaterinburg, Russian Federation, 620002

High-dose ionizing radiations (0.01-100 kGy) are widely used in various fields of science and technology. Nanostructured phosphors based, in particular, on simple and complex oxides are promising materials for use in high-dose dosimetry due to their high radiation resistance [1]. The aim of this work is to synthesize ultrafine composite ceramics based on Al_2O_3-BeO and study their luminescent and dosimetric properties.

We have developed a new method for producing Al_2O_3-BeO ceramics which involve high-temperature treatment (1400-1500 °C, 4 hours) of Al_2O_3 pellets (obtained from nanopowders) in vacuum with the presence of carbon (graphite) in crucibles made from beryllium oxide. It was found by X-ray diffraction that the presence of carbon causes the appearance of BeO phase with a high concentration (about 30%) due to solid-phase reactions during the synthesis of ceramics. In addition, the presence of carbon in the synthesis caused the formation of oxygen vacancies in the ceramics, which was confirmed by pulsed cathodoluminescence measurements. The advantage of the synthesis method is that it completely excludes dealing with beryllia powders which are highly toxic.

Thermoluminescence (TL) of the synthesized ceramics exposed to high-dose irradiation contained three peaks at 360 (A), 520 (B) and 720 K (C). TL peak at 520 K is considered as a dosimetric peak. TL spectrum of this peak contains luminescent band at 2.4 eV, which is related to relaxation of the F_2 aggregate centers in Al_2O_3 lattice [2]. Also, a new unknown emission band at 4.1 eV was observed. The detailed study of the influence of the synthesis temperature in the range from 1200 to 1500 °C on TL curves transformation and its spectral composition allowed to determine the complex structure of the luminescent band at 4.1 eV. This band contains luminescence of the F^+-centers in aluminum oxide lattice and complex defects of vacancy or vacancy-impurity nature.

The TL output of the peak at 520 K did not depend on the heating rate, which may indicate the absence of thermal quenching of luminescence in the composite ceramics under study, in contrast to Al_2O_3 and BeO [3,4]. It was found that the traps responsible for peaks A and B, in contrast to the deep trap C, are subject to optical bleaching during stimulation at a wavelength of 470 nm. The same traps cause the appearance of optically stimulated luminescence (OSL). The optical excitation also causes the change in the shape and shift of the TL maximum of peak B in the high-temperature region. This result, along with the analysis of the TL kinetics by the Tm-Tstop method, shows the presence of the energy distribution of the traps responsible for the dosimetric TL peak.

It was found that the range of linearity of the TL dose response after gamma-irradiation is from 0.01 to 1.0 kGy. After irradiation with a pulsed electron beam (130 keV), linear behavior of OSL dose response was observed from 3 to 30 kGy. The TL fading of the obtained ceramics was about 50% for 5 days of storage in the dark. At the same time, it did not exceed 5% for the first 6 hours, which is quite acceptable for the high-dose dosimetry used in radiation technologies.

REFERENCES

[1] V.S. Kortov, “Nanophosphors and outlooks for their use in ionizing radiation detection”, Rad. Meas., v.45, pp. 512-515, 2010.

[2] B.D. Evans, G.J. Pogatshnik, Y. Chen, “Optical properties of lattice defects in α-Al_2O_3”, Nucl. Instrum. Methods Phys. Res. B, v.91, pp.258-262, 1994.

[3] M.S. Akselrod, N. Agersnap Larsen, V. Whitley, S.W.S. McKeever, “Thermal quenching of F-center luminescence in Al_2O_3:C”, J. Appl. Phys. vol. 84, no. 6, pp. 3364-3373, 1998.

[4] S.V. Gorbunov, V.Yu. Ivanov, A.V. Kruzhalov, et al., “Luminescence excitation of colour centers in berillium oxide”, Nucl. Instrum. Methods Phys. Res. A, v. 261, pp. 148-149, 1987.

* The work was supported by Minobrnauki research project.

LUMINESENCE ANALYSIS OF PHOTODEGRADATION OF CRYSTAL VIOLET EXPOSED TO PULSED POWER BEAMS*

E.N. BOCHARNIKOVA[1], *O.N. TCHAIKOVSKAYA*[1] , *N.G. DMITRIEVA*[1], *J. GOMEZ* [2], *M. GOMEZ* [2], *M. DOLOREZ* [2]

[1]*National Research Tomsk State University, Tomsk, Russia*
[2]*Universidad de Murcia, Campus de Espinardo, Murcia, Spain*

The staining dye Crystal Violet is used for human-medical cell diagnosis and serves the purpose of the bacteriological investigation of sample material of human origin [1]. It is a dry staining dye that is used to prepare a staining solution, that when used together with other in vitro diagnostic products makes target structures in bacteriological specimen materials (e. g. Gram-positive or Gram-negative bacteria, by fixing, where necessary embedding, staining with the above Crystal Violet solution, counterstaining, mounting) evaluable for diagnostic purposes. But Crystal Violet should be regarded as biohazardous substances at high concentration. The structural formula of Crystal Violet is shown in Fig. 1.

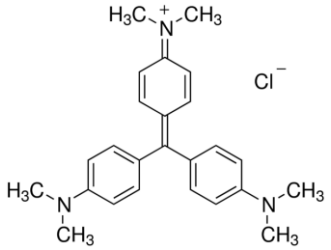

Fig.1. The structural formula of a Crystal Violet molecule

In the order to establish the best operational conditions for the continuous photoreactor, discontinuous photodegradation studies were carried out for Crystal Violet with excilamps in water. In order to establish the mechanism and kinetics of the photocomposition, the advanced oxidation processes (AOPs) were provided [2]. The study was carried out both in the absence and in the presence hydrogen peroxide dose. Initial dye concentration effects were examined. The reaction between •OH and many organic contaminants occurs rapidly; however, this reaction by itself does not directly result in the mineralization of these contaminants but produces organic oxidation by-products, which can further react with •OH. Ideally, AOPs systems are designed to completely mineralize the organic contaminants of concern to CO_2 and H_2O, but this may require more energy and greater chemical dosages and, ultimately, may prove to be cost prohibitive in certain applications. In progress this study experimental setup, analysis, modeling and simulation of continuous photodegradation processes of industrial effluents where organic pollutant, mainly the dye is present. Effluents contain high levels of environmental contaminants, strong color, suspended solids, surfactants and some heavy metals. The aim of the work is to study the spectral and luminescent properties of photoactivated Cristal Violet (CV) when exposed to UV excilamps in solutions. Spectral-luminescent properties were obtained on a SM2203 spectrophotofluorimeter (Solar). A KrCl (222 nm) and a XeBr (283 nm) excilamps were used as sources of UV irradiation. The control exposure time was: 0, 5, 10, 20, 30, 40 and 60 min. The ratio of H_2O_2: Crystal Violet in the aqueous solution was as follows: 0: 1, 1: 1, 2: 1, 3: 1, 4: 1 and 5: 1.

UV radiation can destroy organic contaminants, including Crystal Violet, through direct and indirect photolysis. An analysis of the rate constant of the CV decrease in water under the action of KrCl and XeBr radiation to excilamps indicates that under the influence of excilamp radiation the efficiency of CV degradation without additives in water is only 2%. The addition of hydrogen peroxide (1:1) reduces CV in solutions and the conversion is 93%. The HPLC data of the irradiated solutions for 60 min showed that in addition to CV, the products of its phototransformation are also contained in the solution.

REFERENCES

[1] T. Gessner, U. Mayer, “Triarylmethane and Diarylmethane Dyes,” Ullmann's Encyclopedia of Industrial Chemistry, 6th Edition, 2002.

[2] E.M. Sokolov, L.E. Sheinkman, D.V. Dergunov, “Economical model of cost estimation in mine water treatment using Advanced Oxidation Processes,” Bulletin of the Southern Scientific Center of the Russian Academy of Sciences, vol. 9, no. 2, pp. 23–31, 2013.

*This work was supported in part by the Ministry of Education and Science of the Russian Federation within the framework of State Assignment.

ENERGY TRANSFER IN LISRPO$_4$ DOPED WITH PR^{3+} AND CO-DOPED WITH DY^{3+}, SM^{3+}*

E.S. TROFIMOVA[1], V.A. PUSTOVAROV[1], S.I. OMELKOV[2], I. ROMET[2], M. BETTINELLI[3]

[1]Institute of Physics and Technology, Ural Federal University, Ekaterinburg, Russia
[2] Institute of Physics, University of Tartu, Tartu, Estonia
[3]Laboratory of Luminescent Materials, Department of Biotechnology, University of Verona and INSTM, UdR Verona, Verona, Italy

The report studies fast interconfigurational d-f luminescence and energy transfer in $LiSrPO_4$ doped with Pr^{3+} and co-doped with Dy^{3+} or Sm^{3+} under photoexcitation in UV, VUV range and under cathode-beam excitation. The crystalline micropowder samples of $LiSrPO_4$:Pr^{3+}/Dy^{3+} and $LiSrPO_4$:Pr^{3+}/Sm^{3+} were prepared via solid state reaction method. XRD analysis confirmed the phase purity of all samples. $LiSrPO_4$ doped with Pr^{3+} was previously investigated in [1], the study found a potential of using the material as a fast scintillator.

Various spectroscopic techniques were used. Pulsed cathodoluminescence (PCL) studies were performed in University of Tartu, Estonia, using a Radan-330A pulse electron gun (E = 120 keV, pulse FWHM = 200 ps, rate 5 Hz) as an excitation source. The PCL spectra were measured in "fast" (0-32 ns) and "full" (0-2 ms) time gates, and were recorded using a cooled CCD camera. PCL decay kinetics were registered with a photomultiplier tube. Emission and excitation spectra under UV-VUV excitation were measured in the same laboratory, using a 150-W deuterium discharge lamp Hamamatsu L1835 and a McPherson 234/302 monochromator. Grating monochromator Andor SR 303i-B equipped with H8259-01 photon counting head was used to select the emission.

PCL spectra measured for both samples at room temperature and at T = 5 K are presented in Figure 1 (left panel for $LiSrPO_4$:Pr/Dy, right panel for $LiSrPO_4$:Pr/Sm). The spectra show intense UV emission in the region of 225-300 nm, corresponding to 5d-4f transitions in Pr^{3+}, and a set of narrow lines, arising from 4f-4f radiative transitions in Pr^{3+} and in co-dopant ions in visible and NIR range. While 5f-4f emission transitions are rather fast ($\tau \sim 15$ ns at T = 295 K), the contribution of this emission to a spectrum is much lower, compared with slower 4f-4f emission.

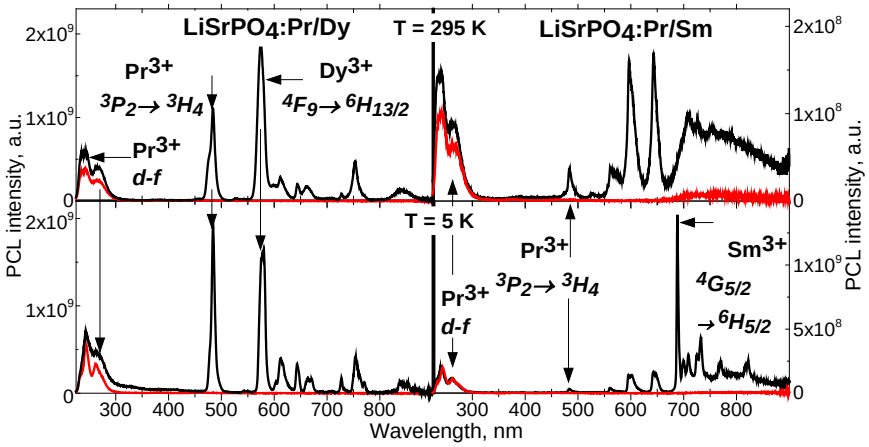

Fig.1. Time-resolved PCL spectra of $LiSrPO_4$:Pr^{3+} co-doped with Dy^{3+} (left panels), Sm^{3+} (right panels) at T = 295 K (top) and 5 K (bottom). Spectra were measured in "full" (0-2 ms, black line) and "fast" (0-32 ns, red line) time gates.

Both samples demonstrate weak temperature dependence of Pr^{3+} 5d-4f emission yield in temperature range 5-295 K. Photoluminescence spectra are influenced by defect emission, being more prominent at low temperatures. The differences and similarities in energy transfer in the objects are discussed in details. In general, the material showed potential for scintillator application, but further investigations of the material in single crystal form are required.

REFERENCES

[1] V.A. Pustovarov, K.V. Ivanovskikh, Y.E. Khatchenko et al., "Energy conversion in LiSrPO4 doped with Pr3+ ions", Radiation Measurements, vol. 123, pp. 39–43, 2019.

* The work was supported by European Regional Development Fund. The authors gratefully acknowledge the financial support of the Estonian Research Council (project PUT PRG111).

STUDY OF PULSED CATHODOLUMINESCENCE OF CALCIUM, BARIUM, LITHIUM AND MAGNESIUM FLUORIDES*

M.V. EROFEEV[1], *E.KH. BAKSHT*[1], *V.I. OLESHKO*[2], *V.F. TARASENKO*[1]

[1]*Institute of High Current Electronics SB RAS, Tomsk, Russia*
[2]*National Research Tomsk Polytechnic University, Tomsk, Russia*

Optical systems based on the Cherenkov radiation [1, 2] are one of the perspective devices for runaway electron beam detection in tokamaks. Usually the reception part of such detectors is made of diamonds, which radiation transferred to the photoelectron multiplayer via fiber.

In this work studies of spectral and kinetic characteristics of CaF_2, BaF_2-Ce, LiF, LiF-W and MgF_2 crystals' glow excited by electron beam with energy of 350 keV have been carried out. It was shown, that cathodoluminescence spectrum of CaF_2 and BaF_2-Ce consists of high-intensity exciton bands irradiated in UV-region, which radiation time exceeds duration of the electron beam current. Radiation of the LiF and LiF-W crystals also have exciton bands in the UV-region, but their transmittance decreased during the pulse of excitation due to accumulation of radiation defects. It was found, that MgF_2 has the lowest intensity of cathodoluminescence (Fig. 1, a) that is allow one to highlight Cherenkov radiation, duration of which corresponds to the electron beam current duration in the wavelength region of 240–400 nm (Fig. 1, b).

It can be also seen, that during the second pulse of the electron bean current I_{eb} (curve *1*) with energy less than energy threshold for Cherenkov radiation (~200 keV), the crystal radiation is absent.

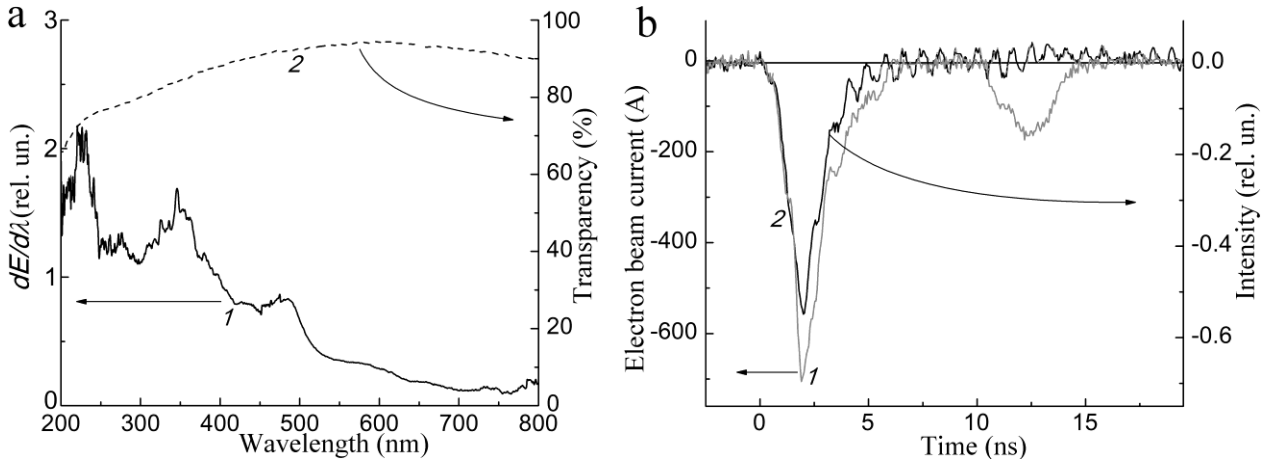

Fig.1. (*a*) – MgF_2 radiation spectra (*1*) excited by electron beam and optical transparency (*2*) of the crystal. (*b*) – electron beam current waveform (*1*) and radiation pulse (*2*) registered by Photek PD025 photodetector.

Therefore, it is possible to use MgF_2 crystals as a Cherenkov detectors of runaway electron beams due to the spectral characteristics and their high radiative resistance. Other crystals studied in this work have intense exciton bands or their transmittance in the UV-region is low that impedes registration of Cherenkov radiation.

REFERENCES

[1] L. Jakubowski, M. J. Sadowski, J. Zebrowski, M. Rabinsky, K. Malinowski, R. Mirowski, Ph. Lotte, L. Gunn, J.-Y. Pascal, G. Colledany, V. Basiuk, M. Goniche, M. Lipa, "Cherenkov-type diamond detectors for measurements of fast electrons in the TORE-SUPRA tokamak," Rev. Sci. Instrum., vol. 81, p. 013504, 2010.

[2] L. Jakubowski, M. J. Sadowski, J. Zebrowski, M. Rabinsky, M. J. Jakubowski, K. Malinowski, R. Mirowski, Ph. Lotte, M. Goniche, L. Gunn, G. Colledani, J.-Y. Pascal, V. Basiuk, "Note: Measurements of fast electrons in the TORE-SUPRA tokamak by means of modified Cherenkov-type diamond detector," Rev. Sci. Instrum., vol. 84, p. 016107, 2013.

* This study has been performed within the framework of a project of the Russian Science Foundation Project No. 18-19-00184.

CREATION AND DESTRUCTION OF COLLOID-LIKE CENTERS IN CORUNDUM USING THERMO AND THERMO-OPTICAL TREATMENT*

A.I. SURDO[1,2], R.M. ABASHEV[1,2], I.I. MILMAN[1,2]

[1]Institute of Metal Physics UB RAS, Ekaterinburg, Russia
[2]Department of Experimental Physics, Ural Federal University, Ekaterinburg, Russia

It was shown in [1] that the thermo-optical treatment (TOT) of anion-deficient corundum (α-$Al_2O_{3-\delta}$) crystals with F center concentration of C_F=10^{17} cm^{-3} at a temperature T_{TOT}=1120 K, photon energy of $h\nu_{TOT}$=3.6-4.8 eV and supplied optical energy density of 10 J/cm^2 ≤ W_{TOT} ≤ 20 J/cm^2 effectively turns simple anion-vacancy F type centers into complex divacancy and interstitial centers of F_2 and Al_i types (Figure 1, curves 1-2). Where such conditions are not met, the efficiency of complex center production reduces. The objective of the study was therefore to investigate the TOT effect systematically over a broad range of W_{TOT}, T_{TOT} and C_F with reference to the luminescent and optical properties of α-$Al_2O_{3-\delta}$ crystals.

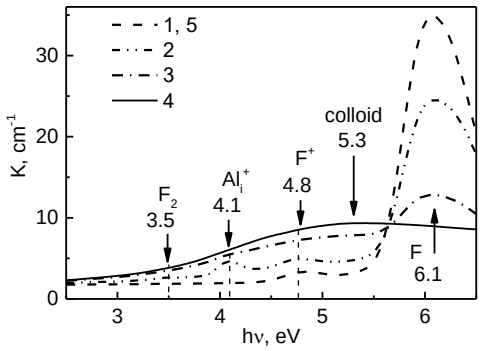

Fig.1. Optical absorption spectra of an α-$Al_2O_{3-\delta}$ sample before (1) and after TOT at T_{TOT}=1120 K under varying W_{TOT}: 15 J/cm^2 (2), 45 J/cm^2 (3), 150 J/cm^2 (4) and subsequent annealing at 1370 K (5).

If we increase W_{TOT} from 30 to 180 J/cm^2 at T_{TOT}=1120 K, centers of not only F type but also F_2 and Al_i types start to disappear (Figure 1, curves 3-4). The OA spectra then show a wide structureless band with a peak at $h\nu_m$=5.3 eV and *FWHM*=1.0 eV, whose intensity increases with W_{TOT}. At the same time, we can observe a decrease in the intensity of photoluminescence (PL) from F, Al_i and F_2 centers as well as in the thermal luminescence (TL) yield in the main peak at 450 K and in the response of optically simulated luminescence (OSL). For W_{TOT}=150 J/cm^2, the above values decrease more than 700 times compared with those in the original samples. For establishing the nature of the defects responsible for the wide OA band, we studied in detail the temperature dependence of its *FWHM(T)* and $h\nu_m(T)$ peak position and the polarization relationships. It has been established that $h\nu_m$ and FWHM do not change in the temperature range of 300-700 K. Nor have we discovered differences in the absorption intensity depending on the crystal's optical axis relative to the plane of polarization of the incident light. Additionally we have studied the efficiency of center transformation under TOT depending on T_{TOT}. It was found that growth in the T_{TOT} and W_{TOT} decreased the value of $h\nu_m$ but insignificantly.

According to [2], all these data together may point to the formation of colloid-like centers in TOT-treated α-$Al_2O_{3-\delta}$ crystals under these parameters similar to those forming in alkali-haloid crystals (AHC) under TOT. Moreover, in contrast to AHC, the annealing of TOT-treated α-$Al_2O_{3-\delta}$ crystals in air at 1300-1400 K restores their original defect structure and optical absorption (Figure 1, curve 5) and luminescent properties. Thus, the concentration and PL response of F centers become similar to such before TOT. At the same time, the OSL yield and the TL yield in the main peak at 450 K recover to the original values.

REFERENCES

[1] A.I. Surdo, R.M. Abashev, I.I. Milman, V.Yu. Ivanov, "Non-radiation creation of complex centers in wide-gap oxide crystals," Radiat. Meas., vol. 123, pp. 74–77, April 2019.

[2] K.K. Schwartz, Yu.A. Ekmanis, Dielectric materials: Radiation processes and radiation resistance. Riga: Zinatne, 1989.

* The research was carried out within the state assignment of Ministry of Science and Higher Education of the Russian Federation (theme "Expertise" No. AAAA-A19-119062590007-2), supported in part by RFBR (project No. 20-48-660045).

FORMATION OF TERMOLUMINESCENCE DOSE RESPONSE NONLINEARITY IN CLUSTER MODEL WITH DEEP HOLE TRAPS

A.S. MEREZHNIKOV[1], *S.V. NIKIFOROV*[1]

[1] *Ural Federal University, Yekaterinburg, Russia*

It is known that the competition processes associated with the presence of deep traps in phosphors can cause nonlinearity of the thermoluminescence (TL) dose dependence. In particular, a sublinear TL dose dependence is observed in the presence of deep hole traps [1]. The mechanisms of the formation of sublinear dose response were previously studied in terms of TL models with uniformly distributed defects only. It is known that models with cluster defects are used for describing TL kinetics in polycrystalline and nanostructured phosphors, as well as phosphors irradiated with high doses [2]. In such models, transitions between different localized levels in the cluster are taken into account along with delocalized transitions. Models with deep hole traps in the cluster have not been investigated earlier. It should be expected that the presence of these traps can cause the appearance of new features of TL dose dependences.

The aim of this work was to simulate TL dose response in a system with clusters which contain TL-active electron and deep hole traps.

The model included uniformly distributed luminescence centers and cluster defects, which contained deep hole traps along with TL-active traps. Calculations were performed with the Monte Carlo method sequentially for irradiation, relaxation, and heating stages to obtain TL dose dependences.

The effect of the model parameters, in particular, the heating rate (b) and the intracluster recombination coefficient (C), on the features of TL dose response was studied (fig. 1). As can be seen from the figure, at relatively low doses TL yield increases linearly. An extended sublinearity region is observed at high doses. In the high-dose range the manifestation of the sublinearity effect decreases and integrated TL increases with growth of heating rate. Also in this case TL dose dependence tends to one observed in the absence of intracluster competition (C = 0).

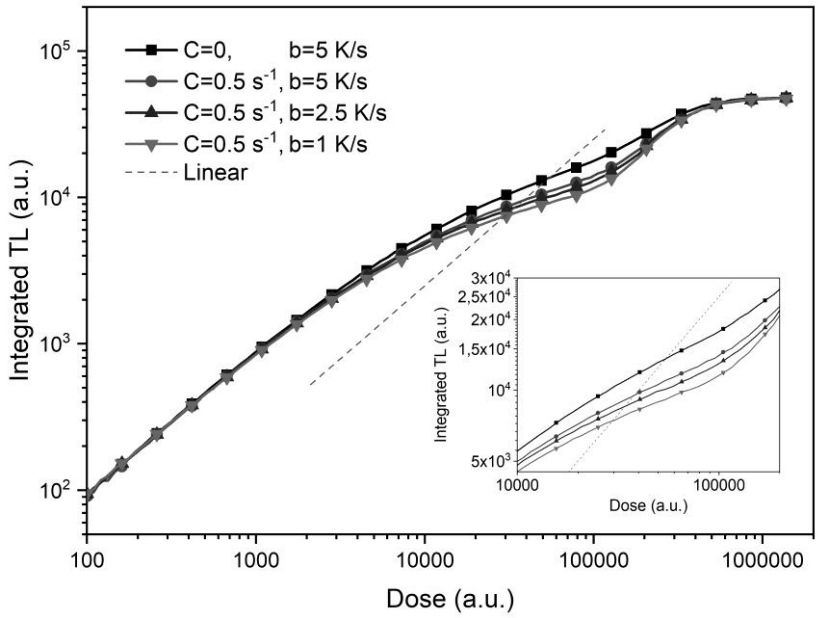

Fig.1. TL dose dependences calculated for various values of the intracluster recombination coefficient C and heating rate b. Dashed line corresponds to a linear dependence.

REFERENCES

[1] S.V. Nikiforov, A.S. Merezhnikov, V. Pagonis, Radiat. Meas., vol. 105, pp. 54-61, 2017.

[2] A. Mandowski, J. Swiatek, Radiat. Meas., vol. 29, pp. 415-419, 1998.

DOPANT EFFECT ON LUMINESCENT AND DOSIMETRIC PROPERTIES OF MAGNESIUM OXIDE CERAMICS*

S.V. ZVONAREV[1], *N.O. SMIRNOV*[1], *K.YU. CHESNOKOV*[2]

[1]*Ural Federal University, Ekaterinburg, Russia*
[2]*Institute of Solid State Chemistry, Ural Branch, Russian Academy of Sciences, Ekaterinburg, Russia*

Mg oxide has a lot of applications, in particular, it can be used as a detector in dosimetry and as a laser in optics [1]. Structures based on magnesium oxide doped with chromium or rare-earth elements are of particular interest since in this case there is a significant change in their luminescent properties [2]. Dosimetric properties determined with the luminescent methods, such as optically stimulated (OSL) and thermoluminescence (TL), can also change in such structures. In this regard, the aim of this paper is to investigate influence of chromium, lanthanum and yttrium impurities on luminescence and dosimetric properties of MgO ceramics.

The ceramics were obtained during sintering in air and under vacuum magnesium oxide compacts at a temperature 1000-1400 ^{0}C for 1 hour. Doping of the compacts before sintering was carried out by the method of impregnation in a solution of a chromium, yttrium and lanthanum nitrate with a concentration varying from 0.01 wt.% to the maximum possible at room temperature. Initial compacts were prepared by the method of cold static pressing of Mg oxide commercial powder. The compacts are disks with a base diameter of 10±0.05 and a height of 1.1±0.05 mm. Thermal tempering of the compacts was carried out after pressing at a temperature of 450 ^{0}C for 2 hours to increase the strength of the obtained compacts. The samples characterization was held by XRD and XRF analyzes methods.

The assessment of the optical properties was conducted by the pulsed cathodo- (PCL) and thermoluminescence (TL) methods. The PCL was measured in the spectral region (350-770) nm by 'Klavi' spectrometer at excitation of an electron beam with the pulse duration of 2 ns, the average energy of electron was 130±10 keV, at a current density of 60 A/cm^2. The TL was measured on an experimental unit during linear heating from 300 to 770 K and at a heating speed of 2 K/s. The ^{90}Y/^{90}Sr β-source with the dose rate of 52 mGy/min and an pulsed electron beam (1,5 kGy per a pulse) were used to irradiate the samples before the TL measurements.

High temperature synthesis contributes to the formation of the luminescence in pure MgO ceramics. Thus, the TL peak with its maximum at 155 K is recorded at a sintering temperature of 1200 ^{0}C. Temperature increase up to 1400 ^{0}C results in a new more intensive TL peak with its maximum at 115 K. Chromium doping of ceramics sintered at 1200 ^{0}C leads to the increase in luminescent peak intensity at 115 K and a new TL peak formation at 360 K. Moreover, the intensity of the peak mentioned increases along with the increase in the Cr content. Luminescence quenching for ceramics with a high Cr content is observed with increasing annealing temperature. The effect of rare-earth metals impurities (lanthanum and yttrium) on the change in luminescent and dosimetric properties of Mg oxide ceramics has also been studied. Synthesis parameters and quantitative concentrations of dopants have been determined at which the highest sensitivity to the ionizing radiation is observed.

REFERENCES

[1] Y. Uenaka, T. Uchino, "Photoexcitation, trapping, and recombination processes of the F-type centers in lasing MgO microcrystals," Phys. Rev. B, vol. 83, 2011.

[2] S.P. Feofilov, A.B. Kulinkin, A.K. Kaveev, N.S. Sokolov, S.M. Suturin, "Fluorescence spectroscopy of Cr^{3+} ions in MgO nanofilms on Al_2O_3 and GaN substrates," Opt. Mater., vol. 83, 2018.

* The work was supported by RFBR according to the research project No 18-33-00085.

LUMINESCENCE IN YAG:CE PHOSPHORS UPON EXCITATION IN THE REGION OF 4 – 6.5 EV[1]

V. M. LISITSYN[1] , V.A. VAGANOV[1] , Z.T. KARIPBAYEV[1, 2] , JU YANGYANG[1] , M. KEMERE[3] , A.T. TULEGENOVA[4]

[1]National Research Tomsk Polytechnic University, Tomsk, 634050, Russia
[2]L.N. Gumilyov Eurasian National University, Nur-Sultan, 010008 Kazakhstan
[3] Institute of Solid State Physics, University of Latvia, Kengaraga 8, Riga LV-1063, Latvia
[4]Al-Farabi Kazakh National University, Almaty, 050040, Republic of Kazakhstan

Phosphors based on YAG:Ce are effective converters of the excitation energy into visible radiation. This luminescence in YAG:Ce phosphors is effectively excited by optical radiation at 340 and 460 nm. The excitation energy is transferred to the luminescence centers, which causes luminescence at 560 nm. It is assumed that absorption and luminescence are due to transition of 4f ($^2F_{5/2}$) to 5d ($^2D_{5/5}$), 5d ($^2D_{3/5}$) and that of 5d ($^2D_{3/5}$) to 4f ($^2F_{5/2}$), 4f ($^2F_{7/2}$) in cerium ions [1]. This effect is widely used in LEDs when converting the blue radiation of an InGaN-based chip to visible one. Luminescence in YAG:Ce phosphors, ceramics at 560 nm is also excited in exposure to ionizing radiation. Therefore, YAG:Ce materials are promising for use as scintillators [2]. Note that the band gap in the YAG crystal is 6.43 eV [3]. It is assumed that the excitation by optical radiation with higher energy than band gap (6.5 eV) causes to generate the electronic excitations in the matrix and transfer their energy to the luminescent centers. Luminescence in YAG:Ce materials also arises upon excitation by optical radiation in the range of 200 – 300 nm. This effect is promising for visualization of UV radiation fluxes. The process of energy transfer to emission centers under this type of excitation has been studied insufficiently.

This paper addresses the study of the dependence of spectral-kinetic characteristics of YAG:Ce phosphors on the radiation wavelength in the range of 4–6.5 eV.

The study employed industrial YAG:Ce phosphors of two series SDL and YAG (SDL - NPO Platan, Russia; YAG - GrandLux, China) with known structural and luminescent properties.

Radiation of pulsed lasers, which generate pulses of 2 ns duration at 193 – 450 nm, and a 250 keV pulsed electron accelerator were used to excite luminescence and to analyze spectral-kinetic characteristics.

Excitation by UV radiation was found to cause luminescence at ≈ 550 nm, and UV luminescence in the range of 300 – 450 nm. It was shown that UV luminescence characteristics and at ≈ 550 nm are different. Therefore, the emission centers responsible for this luminescence differ as well. It is believed that the luminescence in the UV region is associated with intrinsic lattice defects [4].

The luminescence characteristics of phosphors are compared under excitation in different optical ranges and electron fluxes.

It is concluded that emission centers are excited by the energy from electronic excitations generated in nanodefects, where structural elements are luminescence centers, and transferred to these centers.

REFERENCES

[1] P. Dorenbos, “5d-level energies of Ce3 + and the crystalline environment”. IV. Aluminates and "simple" oxides, J. Lumin., vol. 99, pp. 283-299, 2002.

[2] Zhiguo Xia and Andries Meijerink, “Ce3 + -Doped garnet phosphors: composition modification, luminescence properties and applications”, Chem. Soc. Rev., vol. 46, no. 275, 2017.

[3] Y. Xinbo, L. Hongjun, B. Qunyu, S. Liangbi, X. Jun, “Growth of large-sized Y3Al5O12:Ce (Ce: YAG) scintillation crystal by the temperature gradient technique (TGT)”, J. Cry. Grow vol. 311, pp. 3692–3696, 2009.

[4] Yu. Zorenko, T. Voznyak, V. Gorbenko, E. Zych, S. Nizankovski, A. Dan'ko, V. Puzikov, “Luminescence properties of Y3Al5O12:Ce nanoceramics”, J. Lumin., vol. 131, pp. 17–21, 2011.

1* The work was carried out within the framework of the grant AP08052050 of the Ministry of Education and Science of the Republic of Kazakhstan and in continuation of project No 18-43-703014 r_mol_a, supported by Russian Foundation for Basic Research.

EFFECT OF ULTRASONIC TREATMENT ON THE LUMINESCENT PROPERTIES OF CONVENTIONALLY SINTERED YAG: CE^{3+} CERAMICS

D. VALIEV, O. KHASANOV, E. DVILIS, S. STEPANOV, V. PAYGIN

National Research Tomsk Polytechnic University, Lenin Avenue 30, 634050 Tomsk, Russia

Optical properties of ceramic materials depend on the grain size, the size of residual pores, and the presence of defects [1-3]. In order to obtain ceramic materials with desired optical properties, a careful selection of the powder processing and sintering methods should be made. Among numerous manufacturing methods of high-quality ceramics, a promising method is dry compaction of nanopowders by uniaxial static pressing assisted by non-cavitation intense ultrasound followed by conventional sintering. Ultrasonic treatment (UT) during uniaxial dry pressing decreases the forces of internal (inter-particle) and external (near-wall) friction, enables uniform and efficient packing of micrometer- and nano-sized powders such that no binder addition is necessary [4]. In order to achieve the required treatment effect, the amplitude of the ultrasonic vibrations should be optimized.

In this work, we investigated the effect of (UT) on luminescent properties of YAG ceramics doped with Ce^{3+} ions. The powder was pressed uniaxially in an automatic press IP-500 AVTO ZIPO (Russia). Pressing of the powder was carried out in a specially designed die - an acoustic wave guide. During pressing, intense ultrasound was applied to the sample. The power of ultrasound was 400 kW. The pressed compacts had a diameter of 8 mm and a thickness of 1 mm. Sintering was conducted in air in a LHT 02/18 Nabertherm furnace (Germany).

A complex characterization of the crystalline and defect structure of the ceramic by XRD, SEM were carried out. Excitation and luminescence spectra were studied.

The integrated photoluminescence spectra and decay kinetics were investigated with the pulsed optical spectrometer based on a SRS NL100 Nitrogen Laser and a light-emitting diode as excitation source (output power 4 mW, $\lambda_{em.}$=447 nm). The photoluminescence spectra were recorded with a fiber spectrometer AvaSpec-3648 in the spectral range of λ= 300–800 nm. The luminescence decay kinetics was recorded with a photomultiplier tube Hamamatsu H10720-20 using a monochromator MDR-204 and a digital oscilloscope DPO3034 Tektronix (300 MHz) with a time resolution of 2 ns. All measurements were carried out at room temperature. The luminescence spectra were corrected to the spectral sensitivity of the optical path. The nature of luminescent centers and mechanisms of luminescence are discussed.

The reported research was funded by Russian Foundation for Basic Research and the government of the Tomsk region of the Russian Federation, grant № 18-43-703014 r_mol_a.

REFERENCES

[1] C. L. Hardin et al., Optical Materials Express 3 (2013) 893–903.
[2] L. Lei et al., Ceramics International 38 (2012) 23–28.
[3] A. Krell et al., Optical Materials 31 (2009) 1144–1150.
[4] O. L. Khasanov et al., Advances in Applied Ceramics 107 (2008) 135-141.

SPECTROSCOPY OF Bi^{3+} - DOPED LANTHANIDE NIOBATES

A. KISSABEKOVA[1,2], M. BARAN[3], A. KRASNIKOV[1], A. LUSHCHIK[1], V. TSIUMRA[4,5], L. VASYLECHKO[6], S. ZAZUBOVICH[1], YA. ZHYDACHEVSKYY[4,6]

[1]Institute of Physics, University of Tartu, Tartu, Estonia
[2]L.N. Gumilyov Eurasian National University, Nur-Sultan, Kazakhstan
[3]Institute of Electronic Materials Technology, Warsaw, Poland
[4]Institute of Physics, Polish AS, Warsaw, Poland
[5]Ivan Franko National University of Lviv, Lviv, Ukraine
[6]Lviv Polytechnic National University, Bandera 12, 79013 Lviv, Ukraine
asssssemgul@gmail.com

Bi^{3+}-doped complex oxides, where a Bi^{3+}-doped ion substitutes for a trivalent rare-earth ion, became the subject of an extensive research due to their possible applications as scintillator and phosphor materials. The materials co-doped with Bi^{3+} and trivalent rare-earth ions (Dy^{3+}, Er^{3+}, Yb^{3+}, Eu^{3+}, Sm^{3+}, Ho^{3+}, Nd^{3+}) were found to be potentially applicable as spectral converters for solar cells and solid state light sources of new generation, so called white light-emitting diodes, owing to the presence of absorption bands in the ultraviolet (UV) spectral region and intense broad visible Bi^{3+}-related emission bands.

In Bi^{3+}-doped compounds, two types of emission bands with strongly different characteristics exist. The UV emission, usually ascribed to the electronic transitions from the triplet excited state of a Bi^{3+} ion, has a relatively small Stokes shift and FWHM and the ms-decay time at 4.2 K, which remains constant up to 40-110 K indicating a large energy distance D between the emitting and metastable levels of the triplet excited state of Bi^{3+}. The visible (VIS) emission is characterized by the large Stokes shift and FWHM and the temperature dependence of the decay time indicating a very small D value. Despite a huge number of publications, the origin of the VIS emission is still under discussion. This emission was ascribed to the metal-to-metal charge transfer, single Bi^{3+} ions, Bi^{3+} dimers, trapped or localized excitons, etc. Therefore, the detailed spectroscopic study and comparison of various Bi^{3+}-doped compounds is necessary in order to understand the reasons of different origin of the Bi^{3+}-related luminescence centers in different materials.

In this work, Bi^{3+}-doped niobates are considered. The positions of their emission and excitation bands reported in different papers as well as the interpretation of the experimental results are different. So far, the low-temperature luminescence decay kinetics, which could allow to determine the origin, structure, and parameters of the corresponding excited states, is not studied. Therefore, we have carried out a detailed and systematic investigation of the Bi^{3+}-related luminescence in $YNbO_4$:Bi, $LuNbO_4$:Bi, and $GdNbO_4$:Bi with different Bi^{3+} contents by the methods of the steady-state and time-resolved luminescence spectroscopy at 4.2-500 K. For comparison, the luminescence characteristics of the undoped niobates were studied as well.

In the emission spectra of the Bi^{3+}-doped niobates, two visible Bi^{3+}-related emission bands are observed (see Table). The analysis of the temperature dependences of emission decay time allows us to prove their exciton-like origin. The higher-energy VIS emission tentatively arises from an exciton localized around a single Bi^{3+} ion. The intensity of the lower-energy VIS emission superlinearly depends on the Bi^{3+} content. This allows us to ascribe this emission to the radiative decay of an exciton localized around a dimer {Bi^{3+} - Bi^{3+}} center. No UV emission arising at the radiative decay of the triplet excited state of a Bi^{3+} ion, is found. This fact as well as the exciton-like origin of the Bi^{3+}-related VIS emission indicate that the triplet relaxed excited level of Bi^{3+} is located inside the conduction band of the host.

Table. Peak position of the emission (E_{em}) and excitation (E_{exc}) bands, full width at half maximum (FWHM) and the Stokes shift (S) of the emission bands obtained at 4.2 K for the investigated Bi^{3+}-doped lanthanide niobates. Temperature (T_q) at which the emission intensity decreases twice, the activation energy of luminescence thermal quenching (E_q), luminescence decay time (□) at 4.2 K, and energy distance (D) between the emitting and metastable minima of the triplet localized exciton state.

Sample	E_{exc}, eV	E_{em}, eV	FWHM,eV	S, eV	T_q, K	E_q, meV	τ, μs	D, meV
$YNbO_4$:Bi	4.09	2.53	0.53	1.56	250	0.22	33	0.78
	4.06	2.41	0.55	1.65	-	-	46	0.77
$LuNbO_4$:Bi	4.06	2.41	0.55	1.65	200	0.09	34	0.76
	3.97	2.27	0.54	1.7	-	-	40	0.74
$GdNbO_4$:Bi	4.11	2.64	0.57	1.47	310	0.21	~4	~0.2
	4.05	2.56	0.60	1.49	-	-	~5	-

OPTICAL PROPERTIES OF ALUMINA CERAMIC DOPED WITH YTTRIUM*

V.Y. CHURKIN[1], *V.A. PANKOV*[1], *S.V. ZVONAREV*[1], *E.I. FROLOV*[1,2], *A.D. YULIN*[2]

[1] *Ural Federal University, Yekaterinburg, Russia*
[2] *Samara State Technical University, Samara, Russia*

Initial oxide matrixes for phosphors change their optical properties during doping which makes it possible to use them as materials for optical devices and systems. Yttrium and aluminum oxides have their specific defective centers associated with both oxide vacancies and nonstructural defects (Y_{Al}) [1, 2]. Thus, the aim of the work is to study luminescent properties of alumina ceramics doped with yttrium impurities by methods of pulsed cathode (PCL) and thermo (TL) luminescence.

The compacts of 100 mg were formed from high impurity (99.7%) commercial alumina powder by the cold static pressing method at pressure of 125 MPa. To form doped ceramics the compacts were impregnated in the yttrium (III) nitrate hexahydrate pure ($Y(NO_3)_3 \cdot 6H_2O$) solution for 0.5 hour. The nitrate content in the solution was varied for obtaining the samples with yttrium concentration of 1 and 15.9 wt.%. The compacts were sintered in a high-temperature vacuum electric furnace SNVE 9/18 for 1 hour at a varying temperature from 1000 to 1400 ºC. The samples attestation was carried out by methods of X-ray phase and X-ray fluorescence analysis.

The evaluation of optical properties of the samples under study by the PCL method was carried out with "KLAVI" spectrometer within the range of 350-750 nm during irradiation by an electron beam of 130 keV. TL of the samples was investigated on the experimental unit during linear heating from 300 to 720 K and a heating rate of 2 K/s after irradiation by the impulse electron beam (15 kGy).

PCL spectra of pure alumina ceramics have luminescence bands with their maxima at 400 and 693 nm, which correspond to the luminescence of the alumina F-center and Cr impurity center respectively. Doping of the initial matrix with the yttrium impurity leads to appearance of new narrow luminescence bands, characteristic of europium luminescence [3] the presence of which in low concentrations in samples was confirmed during their attestation.

TL curves of pure alumina ceramic after irradiation by the pulsed electron beam have two distinct peaks at 460 and 630 K and their intensity increases along with the temperature growth. Adding yttrium impurity leads to quenching of the peak at 630 K and appearance of two new ones at 365 and 555 K. An increase in yttrium concentration from 1 to 15.9 wt.% results in the increase of TL intensity of these peaks. Thus, with yttrium concentration of 15.9 wt.% for Al_2O_3:Y ceramics annealed at a temperature of 1400 ºC the peak intensity at 460 K increases 5 times compared with pure ceramic obtained under the same synthesis conditions.

REFERENCES

[1] A. Ciric, S. Stojadinovic, "Structural and photoluminescence properties of Y_2O_3 and Y_2O_3:Ln^{3+} (Ln = Eu, Er, Ho) films synthesized by plasma electrolytic oxidation of yttrium substrate," Journal of Luminescence., vol. 217, 2020.

[2] T. Zorenko, V. Gorbenko, A. Petrosyan, W. Gieszczyk, P. Bilski, Yu. Zorenko, "Intrinsic and defect-related luminescence of $YAlO_3$ and $LuAlO_3$ single crystals and films," Optical Materials., vol. 86, pp. 376—381, December 2018.

[3] G.A. Gusev, K.N. Orekhova, V.A. Kravets, A.I. Isakov, A.N. Trofimov, M.V. Zamoryanskaya, "Kinetic properties of YAG: Eu^{3+} emission upon electron beam excitation," Journal of Luminescence., vol. 222, 2020.

* The reported study was funded by RFBR according to the research project No 18-33-00085.

STUDYING THE OPPORTUNITY OF USING POLYAROMATIC HYDROCARBONS IN OIL

U.J. Yolchuyeva, S.A. Suleymanova, A.Sh. Aliyeva, B.J. Tapdıgova

Institute of Petrochemical Processes, Azerbaijan NAS, Baku, Azerbaijan

u.jeyhunzade@gmail.com

Chemiluminescence methods and electronic absorption spectra were used to study the photo- and thermal oxidation of groups I-IV of aromatic hydrocarbons in the Balakhani oil of Azerbaijan. It was shown that the latter oxidations occur as a result of the detachment of hydrogen from the α-carbohydrate atom of the alkyl chain of aromatic hydrocarbons (AC) dissolved by molecular oxygen, which leads to the formation of RO_2 radicals, the recombination of which is accompanied by chemiluminescence. When comparing thermochemiluminescence and photothermochemiluminescence (TXL and FTLC) of petroleum products with aromatic hydrocarbon groups of Balakhany oil, significant differences were found in the number of maximums and in the mechanisms of their oxidation stage. To solve this problem, the characteristic features of the components that are associated with the possibility of their use as photosensitizers for the decomposition of organic compounds, reversible light energy accumulators, photo and thermal oxidation inhibitors, light stabilizers, photochromic materials, phosphors for various purposes, etc., have a large value.

As a result of the experiments, it was determined that bare aromatic hydrocarbons, especially in the case of alkenes, significantly depend on the number of benzene rings. These characteristics are less dependent on the composition and structure in the case of substituted hydrocarbons. However, substituents are of great importance for changing the shades of the color of luminescence. Most of the phosphors obtained on the basis of I-IV AC of Balakhan oil groups have mainly luminescence of blue, turquoise and yellow. However, like many other oil phosphors, they undergo thermal and photooxidative transformations, which lead to a decrease in the intensity of their luminescence.

A feature of the thermal oxidation of these groups is that the binding energy of the C-H α-carbon atom of the substituent in them decreases with an increase in the number of aromatic nuclei. In contrast to thermal oxidation, a feature of photoradiated AC is that as the degree of condensation of aromatic nuclei increases, the energy of their triplet state decreases, which leads to a weakening of the efficiency of energy transfer to alkyl chains and the degree of photooxidation of the system. These features are reflected in the nature of their chemiluminescence, which is one of the most sensitive methods for studying their oxidation.

It was proved that based on chemiluminescence of groups III and IV of the Balakhani oil with bright photoluminescence and with large raw material resources, it is possible to create wireless and fuel-free “cold” light sources.

DOUBLE-BAND EMITTING LUAG CERAMICS FOR LASER LIGHTING *

J.Y. YANG[1], *S. CAO*[1], *Y. ZHONG*[1,2], *W.Q. FAN*[1], *T. HAN*[1,2]

[1] *Chongqing University of Arts and Sciences, Chongqing, P. R. China*
[2]*National Research Tomsk Polytechnic University, Tomsk, Russia*

Laser lighting has the obvious advantages of high luminous efficiency, strong directivity and good monochromaticity in the automotive headlights, backlights, projectors and other fields. However, compared to LED, the excitation energy density of laser diode is much higher. If the heat cannot be dissipated in time, the temperature will rise rapidly, and the luminous efficiency, stability and service life will be greatly reduced. The luminescence ceramic is a promising alternative to improve the heat conduction for laser lighting. In this work, the double-band ceramics were synthesized by codoping Ce^{3+} and Mn^{4+} in LuAG. With increasing the content of Mn^{4+} ions, the band centered at 505 nm that is contributed to 5d-4f transition of Ce^{3+} has a spectral broadening and the band peaking at 590 nm arises and enhances that is ascribed to $^4T_1 \rightarrow {}^6A_1$ transition of Mn^{2+}.

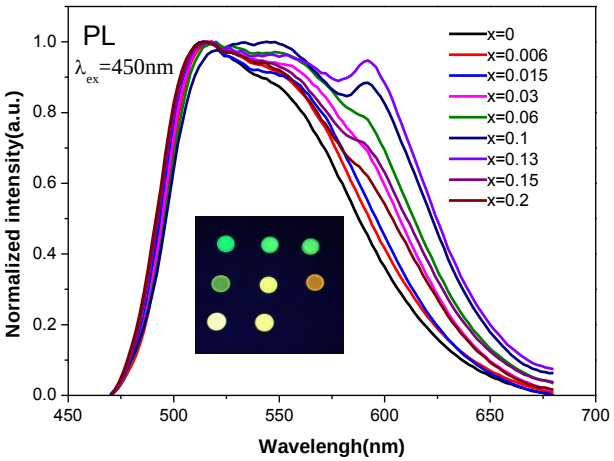

Fig.1. Photoluminescence spectra of LuAG:Ce^{3+}, xMn^{2+} (x=0-0.2) ceramics. The inset is the picture of ceramics under UV light.

REFERENCES

[1] M.R. Krames, O.B. Shchekin, R. Mueller-Mach, G.O. Mueller, L. Zhou, G. Harbers, M.G. Craford, "Status and future of high-power light-emitting diodes for solid-state lighting, " J. Disp. Technol., vol. 3, pp. 160–175, 2007.

[2] J.J.W. Jr, J.Y. Tsao, D.S. Sizov, "Comparison between blue lasers and light-emitting diodes for future solid-state lighting," Laser Photonics Rev., vol. 7, pp. 963–993, 2013.

[3] N. Trivellin, M. Yushchenko, M. Buffolo, C.D. Santi, M. Meneghini, G. Meneghesso, E. Zanoni, "Laser-based lighting: experimental analysis and perspectives, " Materials, vol. 10, pp. 1166, 2017.

[4] T.C. Lang, T. Han, C. Zhao, S. Fang, L. Zhao, V.I. Korepanov, A.N. Yakovlev, "Luminescence properties of color tunable new garnet structure $(Lu_{1-x}Mn_x)_3Al_2(Al_{1-x}Si_x)_3O_{12}$: Ce^{3+} solid solution phosphors," J. Lumin., vol. 207, pp. 98–104, 2019.

[5] T.C. Lang,T. Han, C. Zhao, S.X. Cao, S.Q. Fang, S. Li, L. Zhao, V.I. Korepanov, A.N. Yakovlev, "Color-tunablephotoluminescence and energy transfer of $(Tb_{1-x}Mn_x)_3Al_2(Al_{1-x}Si_x)_3O_{12}$:$Ce^{3+}$ solid solutions for white light emitting diodes," RSC Adv., vol. 8, pp. 36056-36062, 2018.

* The work was supported by the Basic and Frontier Research Program of Chongqing Municipality (cstc2018jcyjAX0339, cstc2017jcyjBX0051), the Science and Technology Research Program of Chongqing Municipal Education Commission (KJZD-M201901301), Natural Science Foundation of Chongqing (cstc2019jcyj-msxm2493).

LUMINESCENT PROPERTIES OF NATURAL SUBSTANCES IN SOLUTIONS UNDER LOW-DOSE RADIATION EXPOSURE

O.N. TCHIKOVSKAYA[1], A.S. SACHKOVA[2], E.N. BOCHARNIKOVA[1], A.A. SOLOKHA[1]

[1]Tomsk Sate University, Tomsk, Russia
[2]Tomsk Polytechnic University, Tomsk, Russia

Promising biologically active agents of natural origin are humic substances (or natural organic materials). These compounds are widely distributed in natural waters and soils, and have a wide range of chemical and physical properties. Their structure includes a large number of diverse functional groups, which determines their complex-forming, surface-active and redox properties, as well as contributes to their biological activity and possess detoxifying properties. Using humic substances, it is possible to reduce the toxicity of an important class of toxicants - radionuclides. Technogenic pollution by radioactive elements is a consequence of the extraction and processing of radioactive materials, the operation of nuclear power stations, the placement of radioactive waste, accidents at nuclear enterprises, etc. In most cases, technogenic radioactive contamination is caused by isotopes of uranium, thorium, etc., as well as tritium, which is one of the most common decay products of radioisotopes used in the nuclear industry. As a rule, enterprises control discharges, conduct wastewater treatment, reducing the content of radionuclides to an acceptable limit. Moreover, even residual radioactivity can lead to disruption of the physiological functions of aquatic microorganisms, which are the initial link in the food chain for all organisms. The influence of biologically active nanostructures is able to correct the state of aquatic microorganisms [1-5].

The aim of the work is to study the spectral and luminescent properties of photoactivated and mechanically activated humic acids (HA) when exposed to UV excilamps in solutions of radionuclides (tritium and thorium -232). Humic acids “Aldrich” were extracted in 0.1 N solution of NaOH with subsequent deposition in 10% solution of HCl to pH 2. The deposit was filtered, washed in distilled water to pH 7, and dried in a vacuum case to a constant mass. Humic acids were prepared from upper peat with a 5% degree of decomposition. To modify the HA structure and to change the content of acidic ionogenic groups, the peat was finally to mechanoactivation (MA) in an AGO-2S planetary activator mill in the following regimes: HA2 - MA without reagent and HA3 - MA in the presence of 5% NaOH (analytically pure). The rotational frequency of the crushing cylinder was 1820 rpm, and the centrifugal acceleration was 600 m/s^2. Grinding bodies were steel balls 8–10 mm in diameter. The mass of the balls loaded into one crushing cylinder was 0.2–0.5 kg, the sample weight was 15–20 g, and the milling time was 2 min. Spectral-luminescent properties were obtained on a SM2203 spectrophotofluorimeter (Solar) in thorium nitrate solutions. Detection of the detoxifying effect of humic acids in model solutions of emitting radionuclides (thorium-232) was studied under conditions of low-dose radiation exposure. In the work, the dependences of the toxic effect of tritium on luminescent bacteria were estimated. The effectiveness of detoxification with humic acids in solutions of various radionuclides (thorium - 232 and tritium) has been established.

REFERENCES

[1] A. S. Tarasova, E. S. Kovel, G. N. Churilov, D. I. Stom, N. S. Kudryasheva, “Biological activity of carbonic nano-structures - comparison via enzymatic bioassay”, Journal of Soils and Sediments, vol. 19, no. 6, pp. 2689–2696, 2019.

[2] N.S. Kudryasheva, A.S. Tarasova, “Pollutant toxicity and detoxification by humic substances: mechanisms and quantitative assessment via luminescent biomonitoring”, Environmental Science and Pollution Research, vol. 22, no. 1, pp. 155–167, 2015.

[3] A. S. Tarasova, D. I. Stom, N.S. Kudryasheva, “Antioxidant Activity of Humic Substances via Bioluminescent Monitoring in vitro”, Environmental Monitoring and Assessment, vol. 187, no. 3. pp. 8–14, 2015.

[4] O. N. Tchaikovskaya, L. V. Nechaev, N. V. Yudina, E.V. Mal’tseva, “Quenching of fluorescence of phenolic compounds and modified humic acids by cadmium ions”, Luminescence (Wiley InterScience), vol. 31, pp. 1098–1102, 2016.

[5] L. V. Nechaev, O. N. Tchaikovskaya, “Investigations of the effect of humic acides on phototransformation of naphthalene illuminated by visible and UV light”, Russian Physics Journal,– Vol. 58, no. 12, pp. 1771–1774, 2016.

A DETECTION SYSTEM WITH LOW SAMPLING DISTORTION FOR APPLICATION IN OPTICAL ARRAY SENSING IN GAS PHASE*

R.D. CHUVASHOV[1], *K.O. KHOKHLOV*[1], *E.V. VERBITSKIY*[1,2], *A.A. BARANOVA*[1]

[1]*Ural Federal University, Ekaterinburg, Russia*
[2]*Postovsky Institute of Organic Synthesis, Ural Branch of the Russian Academy of Sciences, Ekaterinburg, Russia*

Fluorescent detection of hazardous substances holds much promise in the development of low cost, easy in operation, sensitive, and selective sensing systems [1-3]. In the last decades, significant progress was achieved in the development of fluorescent materials for detection of explosives and contaminants. Out of all fluorescence parameters to measure, the simplest and cheapest implementation is for intensity attenuation requiring only fluorophore, UV excitation source, fluorescence detector, and a vapor sampling system driving analyte molecules in contact with a fluorophore. Use of sensor arrays and pattern recognition allows increasing selectivity, broadening the spectra of detectable analytes, and identifying detected analytes [4,5].

Employed fluorescent materials and vapor sampling system will define the ability of the sensor system to detect analyte vapors. With poor design of vapor sampling part, sticky analyte molecules with low vapor pressure such as molecules of explosives will fail to produce signal on fluorophores due to the adsorption on high energy surfaces or dilution in device's internal volumes [6].

In this work, we address vapor sampling issues by presenting a prototype of the device for gas phase sensing employing array of fluorophore materials. The device consists of a brass cylinder with end caps with internal volume of about 40 mL. To decrease amount of the analyte molecules adsorbing at internal parts, heating elements are applied to the cylinder. Sensor element for the device is prepared by dropping fluorophore solutions onto a non-woven material patterned by UV-sensitive solder photoresist. The sensor element is inserted in the cylinder's cross-section perpendicularly to the airflow and thermally isolated via plastic cartridge. The membrane pump generates through airflow of up to 2 L/min and is positioned at the end of the airway at the cylinder end cap. Excitation source, camera and air inlet hole are positioned by another end of the cylinder. The fluorescence is excited by a LED (370 nm) and registered by web camera microcontroller board (ESP32-CAM with OV2640 camera) supported by UV-stopping light filter (405 nm cutoff) to suppress background UV illumination. Additional background suppression is provided by reading data only in red channel, sensors for which have sensitivity cutoff at 500 nm. Microcontroller transmits video stream via Wi-Fi. Intensity is quantified based on video stream from camera at fixed camera settings.

The device works as follow. Heating elements keep temperature of internal surfaces at an elevated level. Low internal volume and upkeep of temperature regime reduce the influence of vapor sampling system on measurements. Fluorophores remain the coolest object in the airway due to thermal isolation and cooling by the airflow, which helps to guide analytes to fluorophores. The camera registers fluorescence intensities of materials on the video stream, which is transmitted to the computer and converted to fluorescence intensity features via image processing script to be used in pattern recognition script.

The developed system allows conducting fluorescence attenuation measurements with an array of fluorophores with low distortion of measurements from vapor sampling part. The overall price for the device is below 50 USD. Besides, it will be possible to utilize colorimetric sensory materials by exchanging excitation source to the white light source. The device can be used as a system for testing and application of optical sensor materials to the tasks of detection and identification of analytes in the gas phase.

REFERENCES

[1] X. Sun, Y. Wang, Y. Lei, "Fluorescence based explosive detection: from mechanisms to sensory materials," Chem. Sov. Rev., vol.44, pp.8019-8061, 2015.

[2] Z. Li, J.R. Askim, K.S. Suslick, "The Optoelectronic Nose: Colorimetric and Fluorometric Sensor Arrays," Chem. Rev., vol.119, pp.231−292, 2019.

[3] A. Zhang, D. Fu, J. Sun, Y. Xuan, H. Ma, "A Multi-channel System for Qualitative Explosive and Drug Detection," Sensing and Imaging, vol.19, Article Number 30, 2018.

[4] K.L. Diehl, E.V. Anslyn, "Array sensing using optical methods for detection of chemical and biological hazards," Chem. Soc. Rev., vol.42, pp.8596-8611, 2013.

[5] J.W. Grate, R.G. Ewing, D.A. Atkinson, "Vapor-generation methods for explosives-detection research," Trends in analytical chemistry, vol.41, pp.1-14, 2012.

[6] J.R. Askim [et al.], "An optoelectronic nose for identif. of expl.," Chem. Sci., vol.7, pp.199-206, 2016.

* The authors thank I.I. Milman and Shulgin B.V. for helpful discussions.

LUMINESCENCE OF ALKALI-EARTH HALIDE CRYSTALS DOPED WITH RARE-EARTH IONS UNDER SYNCHROTRON RADIATION EXCITATIONS *

A. SHALAEV [1], R. SHENDRIK [1], V. PANKRATOV [2] A. RUSAKOV [1], A. MYASNIKOVA [1]

[1]Vinogradov Institute of Geochemistry SB RAS, Irkutsk, Russia
[2]Institute of Solid State Physics, University of Latvia, Riga, Latvia

Alkaline-earth halide crystals doped with rare-earth ions are effective scintillation materials [1]. Their relatively small band gap (4–6 eV) contributes to the efficient formation of electron-hole pairs on each absorbed photon of ionizing radiation. Therefore, alkaline-earth halides have a high light output and good energy resolution. The most effective activators are divalent europium, trivalent cerium and praseodymium with 5d–4f emission in the ultraviolet and visible spectral regions (350-600 nm) [2]. Divalent samarium was never considered to be a scintillation activator candidate, but recent studies show it's possible positive perspectives [3].

BaBrI single crystals were grown from the melt by the vertical Bridgman technique in an evacuated sealed quartz ampoule. The compounds of alkaline earth halides are hygroscopic. Therefore, much attention is paid to drying raw materials before crystal growth. The SmI_2 or $EuBr_3$ was introduced as an activator directly into the mixture before the drying in the concentration range from 0.01% to 5%. The low gradient and slow cooling process prevents cracking and stress accumulations in the crystal. More details of the crystal growth process of alkali earth-halide systems will be discussed in the report.

Luminescence excitation spectra of the obtained single crystals doped with rare-ears ions are studied using synchrotron radiation excitations from the MAX IV 1.5 GeV storage ring (Lund, Sweden). The energy of the edge and the formation of core cation exciton as well as the energy threshold of the multiplications of electronic excitations is found. It was clearly established the energy transfer from intrinsic luminescence centers to Sm^{2+} and Eu^{2+} ions. It was confirmed that energy transfer from self-trapped exciton (STE) to Eu^{2+} ion takes place. On the other hand, the energy transfer to Sm^{2+} occurs via some intrinsic center distinguished from STE. Some peculiarities of the excitation spectra in VUV range of Eu^{2+} emission are explained in terms of multiplication of electronic excitations or excitations of cation exciton.

REFERENCES

[1] M. Nikl and A. Yoshikawa "Recent R&D Trends in Inorganic Single-Crystal Scintillator Materials for Radiation Detection", Adv. Opt. Mater., vol. 3, no. 4, pp. 463-481, 2015

[2] P. Dorenbos, "Locating lanthanide impurity levels in the forbidden band of host crystals", J. Lumin., Vol. 108, no. 1/4, pp. 301-305, 2004

[3] W. Wolszczak, K.W. Krämer, P. Dorenbos, "$CsBa_2I_5:Eu^{2+},Sm^{2+}$—The First High-Energy Resolution Black Scintillator for γ-Ray Spectroscopy", Phys. Status Solidi RRL, Vol. 13 No. 9, pp.1900158, 2019

* This work was supported by the Russian Science Foundation, project no. 18-72-10085 (spectroscopy, optical properties of the obtained crystals and analysis of the results). Crystal growth were performed as part of State Task no. 0350-2016-0024. The data reported in this paper were obtained on the equipment of the Central of Collective Use "Isotope-geochemical studies" of the Institute of Geochemistry, Siberian Branch, Russian Academy of Sciences.

TRANSFER OF ELECTRON FLUX ENERGY TO CERAMICS FORMED IN RADIATION SYNTHESIS

D.A. MUSSAKHANOV[1], V.M. LISITSYN[1], ZH.T. KARIPBAYEV[2], M.G. GOLKOVSKII[3]

[1]National Research Tomsk Polytechnic University, 30 Lenin Ave., Tomsk, 634050, Russia
[2]L. N. Gumilyov Eurasian National University, 2 Satpayev Str., Nur-sultan, 010008, Kazakhstan
[3]Institute of Nuclear Physics SB RAS, 11 Academician Lavrentiev Ave., Novosibirsk, 630090, Russia

It is shown in [1,2] that luminescent ceramics based on MgF_2:W and YAG:Ce with high concentrations of dopants can be synthesized in the field of high-energy 1,4 MeV electron fluxes. Synthesis is carried out using a batch of stoichiometric composition over a period of about 1 s. Spectral-kinetic characteristics of the resulting MgF_2:W based ceramics are similar to those known for LiF:W. Spectral-kinetic characteristics YAG:Ce based ceramics are similar to those of ceramics manufactured by other synthesis techniques. Synthesis in the radiation field seems promising and has a number of advantages over currently used methods.

The analysis of the processes occurring during synthesis in the radiation field shows the need to consider ionization effects during phase transformations of metal oxides into multicomponent yttrium-aluminum phase. The paper presents the results obtained in the study of the radiation energy transfer to the batch and ceramics formed. First of all, energy losses in the batch during electron propagation were calculated using Casino v2.51 software. The energy loss calculation results are shown in the figure.

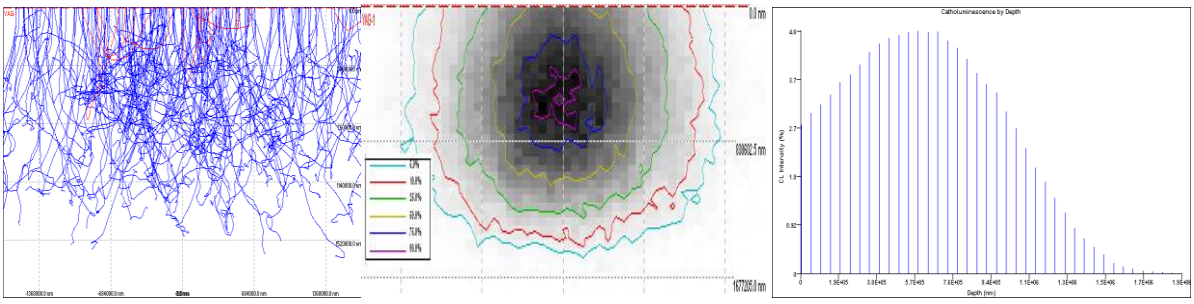

Figure 1. Distribution of energy losses of the electron flux in YAG

In general, the morphology of ceramics formation corresponds to the distribution of the energy loss density of the electron flux. The absorbed energy of the radiation flux is transferred to the material for ionization and heating of the batch. The obtained results suggest that ionization processes in the radiation field are an essential factor to attain high efficiency of the synthesis of MgF_2 and YAG:Ce based ceramics. In the radiation field, reactions in a solid, between particles of different composition are accelerated. High-energy radiation fluxes cause partial radiolysis of the initial micro-, nanoparticles, and transfer of mass between particles.

REFERENCES

[1] V.M. Lisitsyn, M.G. Golkovskii, L.A. Lisitsyna, A.K. Dauletbekova, D.A. Musakhanov, V.A.Vaganov, A.T. Tulegenova, and Zh.T. Karipbayev, "MgF_2-based luminescing ceramics," Russian Physics Journal, vol. 61, no. 10, pp. 1909-1913, 2019.

[2] V. M. Lisitsyn, M. G. Golkovsky, D. A. Musakhanov, A. T. Tulegenova, Kh. A. Abdullin and M. B. Aitzhanov, "YAG based phosphors, synthesized in a field of radiation," IOP Conf. Series: Journal of Physics: Conf. Series, vol. 1115, no. 5, pp. 052007, November 2018.

FEATURE OF THERMOLUMINESCENCE OF ANION-DEFECTIVE α-Al_2O_3 CRYSTALS AT LOW TEMPERATURES*

A.I. BOYARINTSEV[1,2], *I.I. MILMAN* [1, 2], , *R.M. ABASHEV* [1, 2], *A.I. SURDO* [1, 2]

[1]*M.N. Mikheev Institute of Metal Physics of UB RAS, Yekaterinburg, Russia*
[2]*Ural Federal University, Yekaterinburg, Russia*

The thermoluminescent properties of anion-defective crystal (α-$Al_2O_{3-δ}$) in the range from room temperature to 800 °C are studied well enough. Recently, the interest has arisen in the study of low-temperature thermoluminescence (TL) below room temperature [1,2].

TL dosimeters based on α-$Al_2O_{3-δ}$ crystal (TLD-500K, α-Al_2O_3:C) are used for environmental dosimetry. The ambient temperature drops below -20 °C in the winter season or in the northern regions. At such temperatures in the crystal, thermally unstable at room temperature shallow traps become available for filling by charge carriers. Under the influence of ionizing radiation, charge carriers can be captured not only on the main dosimetric trap, but also on slallow traps. This can lead to a decrease in the intensity of the main dosimetric peak at 170 °C, and as a result to a distortion of real dosimetric information.

Therefore, the aim of this work was to create a facility and study the TL properties of α-$Al_2O_{3-δ}$ crystals upon irradiation in the temperature range from -40 °C and upon further heating to 400 °C. The crystals were cooled using Peltier elements; the same elements were used to linearly heat the samples to room temperature. High temperature heating was provided by a standard TL reader.

The experimental technique is based on comparing the intensities of dosimetric peaks obtained by irradiating the samples with the same dose at room temperature and -30 °C.

A preliminary evaluation of the experimental data shows decrease in the intensity of the dosimetric TL peak by at least 15% at the irradiation temperature of -30 °C, as shown in Figure 1. In the future, it is supposed to study the spectral characteristics of TL in the low-temperature region and the kinetics of the processes and dependence of optical transfer of charge carriers from the main dosimetric trap to shallow traps at low temperatures.

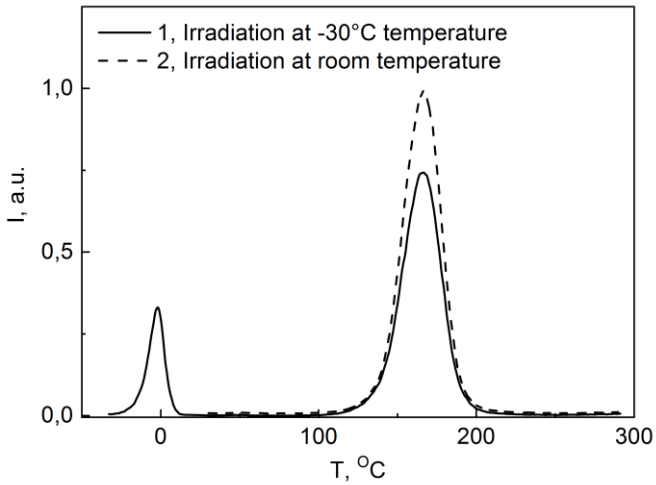

Fig.1. Comparison of the intensities of dosimetric peaks obtained by irradiating samples with the same dose at -30 °C (1) and room temperature (2)

REFERENCES

[1] I. I. Mil'man, E.V. Moiseykin, S.V. Nikiforov, S.V. Solov'ev, I.G. Revkov, E.N. Litovchenko, "The role of deep traps in luminescence of anion-defective α-Al_2O_3:C crystals," Physics of the Solid State, vol. 50, no. 11 pp. 2076-2080, November 2008.

[2] A. Soni, D.R. Mishra, S.S. Gaur, "Development of cryostat integrated TL/OSL reader for its application in radiation dosimetry," Nuclear Inst. and Methods in Physics Research, A., vol. 935, pp. 191-197, April 2019.

[3] D.R.Mishra, M.S. Kulkarni, "Luminescence properties of α-Al_2O_3:C crystal with intense low temperature TL peak," Radiation Measurements, vol. 42, pp. 170–176, 2007.

* The research was carried out within the state assignment of Ministry of Science and Higher Education of the Russian Federation (theme "Expertise" No. AAAA-A19-119062590007-2), supported in part by RFBR (project No. 20-48-660045).

SYNTHESIS OF YAG:CE CERAMICS IN RADIATION FIELD FROM BATCH OF DIFFERENT BULK DENSITY

A.V. ERMOLAEV[1], V.M. LISITSYN[2], D.A. MUSSAKHANOV[3], E.F. POLYSADOVA[4]

[1] National Research Tomsk Polytechnic University, 30 Lenin Ave., Tomsk, 634050, Russia
[2]National Research Tomsk Polytechnic University, 30 Lenin Ave., Tomsk, 634050, Russia
[3]L. N. Gumilyov Eurasian National University, 2 Satpayev Str., Nur-sultan, 010008, Kazakhstan
[4]National Research Tomsk Polytechnic University, 30 Lenin Ave., Tomsk, 634050, Russia

Synthesis of ceramics, metal oxide based phosphors, is a complicated task due to high melting point of the components. It is shown in [1, 2] that high-temperature materials can be synthesized from the batch exposed to direct action of high-energy electron fluxes. MgF_2:W and YAG:Ce were used to show that properties of ceramics formed in the radiation field are similar to those of ceramics manufactured by conventional methods through high temperature solid-state reactions. It is found that during synthesis in the radiation field, the ions of the dopant and modifiers enter ceramics and provide it with properties necessary for luminescence.

The studies allow the conclusion that ionization processes play a significant role in formation of ceramics in the radiation field. It is assumed that under high degree of ionization, radiolysis products, electronic excitations stimulate solid-state reactions, formation of new phases.

The paper presents the results of studies of the dependence of the efficiency of YAG:Ce ceramic synthesis in the field of high-energy electron flux on the bulk density of the initial batch. For the study, the prepared batch was of the composition: Al_2O_3 (43%) + Y_2O_3 (55%) + Ce_2O_3 (2%) with a bulk density of 1.15 g/cm^3. Part of the batch was mixed with alcohol, and the slurry was poured into crucibles. After drying, the batch shrank to a bulk density of 2.1 g/cm^3. In a similar way, a batch was prepared from powdered ceramics synthesized in a radiation field. The bulk density of the batch attained 2.6 g/cm^3.

After that, ceramics from the prepared batches was exposed to electron flux with power of 18 – 23 kW/cm^2. The morphology and luminescent properties of the manufactured ceramics were compared to evaluate synthesis efficiency.

The study results show that preliminary compaction of the batch affects formation of ceramics. The findings are discussed in terms of the effect of the degree of ionization on synthesis processes.

REFERENCES

[1] V.M.Lisitsyn, M.G.Golkovskii, L.A.Lisitsyna, A.K.Dauletbekova, D.A.Musakhanov, V.A.Vaganov, A.T.Tulegenova, and Zh.T.Karipbayev MgF2-BASED LUMINESCING CERAMICS. Russian Physics Journal, Vol. 61, No. 10, 1909-1913, 2019 (Russian Original No. 10, October, 2018) DOI 10.1007/s11182-019-01617-y

[2] V M Lisitsyn, M G Golkovsky, D A Musakhanov, A T Tulegenova, Kh A Abdullin and M B Aitzhanov YAG based phosphors, synthesized in a field of radiation. IOP Conf. Series: Journal of Physics: Conf. Series 1115 (2018) 052007 doi :10.1088/1742-6596/1115/5/052007

INHOMOGENEITY OF THE YAG:CE CERAMICS SYNTHESIZED BY ELECTRON BEAM ASSISTED.

G.K. ALPYSSOVA[1], D.A. MUSSAKHANOV[2], Zh.T. KARIPBAYEV[1,2], V. SHENARSHEEV[2], T.V. GRECHKINA[2], A. KUKENOVA[1]

Eurasian National University named after L.N. Gumilyova, Nur-Sultan, Kazakhstan
Tomsk Polytechnic University, Tomsk, Russia

The luminescent properties of YAG: Ce phosphors strongly depend on the technological modes of their synthesis. In [1], it was shown that the characteristics of the luminescence properties of ceramic samples crushed into powder synthesized from a mixture of the same composition are somewhat different. Provisions band maxima may vary by 4-5 nm, band-width of 0.439 to 0.470. The most probable reason for the difference may be a difference in conditions in which there is formation of ceramic when exposed to the electron flow. This has led to pay attention to the study of the dependence of the spectral and kinetic characteristics of the luminescence on irradiation conditions.

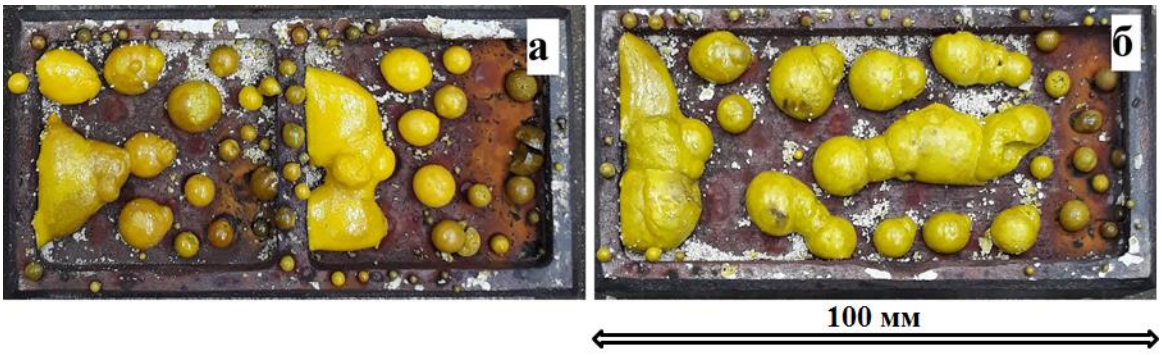

Fig. 1. Photo of a crucible with synthesized YAG: Ce ceramics.

In the synthesis of YAG: Ce ceramics in one crucible up to 10-15 samples are formed. The power of the electron flow does not change. But during the processing of the charge in the crucible, equal to 36 s, the conditions under which the charge is in the crucible can change. The electron beam scans the surface of the crucible at a speed of 1 cm / s across the crucible. Passing a strip 1 cm wide, then it is shifted along the crucible to the width of the strip, etc. Thus, at the beginning, the charge layer is irradiated in a cold crucible, and by the end of the scan, it is already in a heated crucible. It can be expected that the conditions for the formation of ceramics can change when scanning the beam within the crucible in one experiment. In this work, we study the luminescent properties of samples synthesized in a single crucible ceramic. Spectra were measured, the luminescence decay kinetics with respect to energy yield, brightness. Measurements of each value were performed 10 times. Carried out the statistical processing of the results. The analysis of the obtained research results is carried out.

REFERENCES

[1] G Alpyssova, D Mussakhanov, Zh Karipbayev, T Grechkina, Shiming Zheng and A Kukenova. “Luminescence spectra of YAG:Ce phosphors synthesized in a field of radiation”, IOP Conf. Series: Materials Science and Engineering 754, p. 012014, 2019. (2020).

SPECIFICS OF ANNIHILATION OF ELECTRONIC EXCITATIONS IN A NACL CRYSTAL WITH DECREASING LATTICE SYMMETRY

K. SHUNKEYEV[1], A. LUSHCHIK[2], Z. UBAEV[1], L.MYASNIKOVA[1]

[1]Zhubanov Aktobe Regional State University, Aktobe, Kazakhstan
[2]Institute of Physics, University of Tartu, Tartu, Estonia

The spectra of tunnel luminescence (TL) and the spectra of thermostimulated luminescence (TSL) under elastic deformation at 95 K of the natural NaCl crystal were studied using X-ray excitation methods. A rigid X-ray excitation (120 kV, 3 mA) capable of penetrating the entire thickness of the crystal was specially selected, which is necessary for the study of the luminescent characteristics of the studied samples. The maximum scanning speed (50 nm/s) allows you to register the entire spectrum of the TSL of the NaCl crystal with a minimum change in the temperature (0.9 K) of the crystal.

The spectra of creating radiation defects of a natural NaCl crystal under the influence of uniaxial elastic and plastic deformation, as well as local deformation by cations (Li) and anions (Br, I) homologues were studied using the methods of VUF radiation.

Experimental results show that tunnel luminescence with a maximum at 3.8 eV is registered in a pre-elastic deformed NaCl crystal under X-ray excitation. They are interpreted by a tunnel recharge between the main states F' and V_k -centers, which is not typical for VUF excitation. Tunnel luminescence is extinguished to 150 K. In the crystal NaCl in the temperature range 100-130 K range was TSL with a maximum of 2.7 eV; in the range of 165-170 K with a maximum at 3.4 eV, in the area of 200 K – with a maximum of 3.9 eV.

Experiments on VUF excitation show that the luminescence bands at 3.8 eV and 4.0 eV are effectively excited by photons with energy of 7.29 eV and 7.95 eV, respectively. In the spectrum of creating TSL peaks at 250 K, V_k - centers with a maximum at 170 K are effectively created. In this case, the maximum value is reached at 9.0 eV as the excitation energy increases. Low-temperature peaks of TSL responsible for tunnel luminescence (95-130 K) do not appear during VUF excitation.

REFERENCES

[1] A. Elango,S. Sagimbaeva, E. Sarmukhanov, T. Savikhina and K. Shunkeev, “Effect of uniaxial stress on luminescence of X- and VUV-irradiated NaCl and NaBr crystals,” Radiation Measurements, vol. 33(5), 2001, P. 823-827.

A DETECTION SYSTEM WITH LOW SAMPLING DISTORTION FOR APPLICATION IN OPTICAL ARRAY SENSING IN GAS PHASE*

R.D. CHUVASHOV[1], *K.O. KHOKHLOV*[1], *E.V. VERBITSKIY*[1,2], *A.A. BARANOVA*[1]

[1]*Ural Federal University, Ekaterinburg, Russia*
[2]*Postovsky Institute of Organic Synthesis, Ural Branch of the Russian Academy of Sciences, Ekaterinburg, Russia*

Fluorescent detection of hazardous substances holds much promise in the development of low cost, easy in operation, sensitive, and selective sensing systems [1-3]. In the last decades, significant progress was achieved in the development of fluorescent materials for detection of explosives and contaminants. Out of all fluorescence parameters to measure, the simplest and cheapest implementation is for intensity attenuation requiring only fluorophore, UV excitation source, fluorescence detector, and a vapor sampling system driving analyte molecules in contact with a fluorophore. Use of sensor arrays and pattern recognition allows increasing selectivity, broadening the spectra of detectable analytes, and identifying detected analytes [4,5].

Employed fluorescent materials and vapor sampling system will define the ability of the sensor system to detect analyte vapors. With poor design of vapor sampling part, sticky analyte molecules with low vapor pressure such as molecules of explosives will fail to produce signal on fluorophores due to the adsorption on high energy surfaces or dilution in device's internal volumes [6].

In this work, we address vapor sampling issues by presenting a prototype of the device for gas phase sensing employing array of fluorophore materials. The device consists of a brass cylinder with end caps with internal volume of about 40 mL. To decrease amount of the analyte molecules adsorbing at internal parts, heating elements are applied to the cylinder. Sensor element for the device is prepared by dropping fluorophore solutions onto a non-woven material patterned by UV-sensitive solder photoresist. The sensor element is inserted in the cylinder's cross-section perpendicularly to the airflow and thermally isolated via plastic cartridge. The membrane pump generates through airflow of up to 2 L/min and is positioned at the end of the airway at the cylinder end cap. Excitation source, camera and air inlet hole are positioned by another end of the cylinder. The fluorescence is excited by a LED (370 nm) and registered by web camera microcontroller board (ESP32-CAM with OV2640 camera) supported by UV-stopping light filter (405 nm cutoff) to suppress background UV illumination. Additional background suppression is provided by reading data only in red channel, sensors for which have sensitivity cutoff at 500 nm. Microcontroller transmits video stream via Wi-Fi. Intensity is quantified based on video stream from camera at fixed camera settings.

The device works as follow. Heating elements keep temperature of internal surfaces at an elevated level. Low internal volume and upkeep of temperature regime reduce the influence of vapor sampling system on measurements. Fluorophores remain the coolest object in the airway due to thermal isolation and cooling by the airflow, which helps to guide analytes to fluorophores. The camera registers fluorescence intensities of materials on the video stream, which is transmitted to the computer and converted to fluorescence intensity features via image processing script to be used in pattern recognition script.

The developed system allows conducting fluorescence attenuation measurements with an array of fluorophores with low distortion of measurements from vapor sampling part. The overall price for the device is below 50 USD. Besides, it will be possible to utilize colorimetric sensory materials by exchanging excitation source to the white light source. The device can be used as a system for testing and application of optical sensor materials to the tasks of detection and identification of analytes in the gas phase.

REFERENCES

[1] X. Sun, Y. Wang, Y. Lei, "Fluorescence based explosive detection: from mechanisms to sensory materials," Chem. Sov. Rev., vol.44, pp.8019-8061, 2015.

[2] Z. Li, J.R. Askim, K.S. Suslick, "The Optoelectronic Nose: Colorimetric and Fluorometric Sensor Arrays," Chem. Rev., vol.119, pp.231−292, 2019.

[3] A. Zhang, D. Fu, J. Sun, Y. Xuan, H. Ma, "A Multi-channel System for Qualitative Explosive and Drug Detection," Sensing and Imaging, vol.19, Article Number 30, 2018.

[4] K.L. Diehl, E.V. Anslyn, "Array sensing using optical methods for detection of chemical and biological hazards," Chem. Soc. Rev., vol.42, pp.8596-8611, 2013.

[5] J.W. Grate, R.G. Ewing, D.A. Atkinson, "Vapor-generation methods for explosives-detection research," Trends in analytical chemistry, vol.41, pp.1-14, 2012.

[6] J.R. Askim [et al.], "An optoelectronic nose for identif. of expl.," Chem. Sci., vol.7, pp.199-206, 2016.

* The authors thank I.I. Milman and Shulgin B.V. for helpful discussions.

PHASE ABERRATIONS IN DIODE PUMPED LASER AMPLIFIER*

V.A. PETROV[1,2], *G.V. KUPTSOV*[1,2,3], *V.V. PETROV*[1,2,3], *A.V. LAPTEV*[1], *A.O. KONOVALOVA*[1,2]

[1]*Institute of Laser Physics SB RAS, Novosibirsk, Russia*
[2]*Novosibirsk State Technical University, Novosibirsk, Russia*
[3]*Novosibirsk State University, Novosibirsk, Russia*

At the Institute of Laser Physics SB RAS a laser system with both high average and peak power is being developed [1]. To increase the pulse energy at the output of the system, a cryogenic laser amplifier with high power diode pumping is used.

In laser amplifiers with a high average power of radiation, a significant heating of the active elements occurs in the pump region, which leads to a decrease in the laser characteristics of the medium and phase distortions in the amplified radiation [2,3]. To optimize the parameters of the cryogenic amplifier, the dynamics of the formation of phase distortions arising in the active elements of the cryogenic amplifier was analyzed. The analysis was carried out on the basis of a joint numerical solution of the system of balance equations, radiation transfer equations, as well as the non-stationary heat equation [4]. The model features include simultaneous consideration of the thermophysical and laser characteristics of the amplifying medium, which gives a correct description of the process during high-power diode pumping, in presence of strong longitudinal temperature gradient in the absorption saturation mode, and also in saturated amplification mode accounting evolution of the spatial-temporal profile of the amplified radiation.

Based on the results of numerical modeling of the gain dependencies and wavefront phase aberrations on the radius of the pump radiation profile, the possibility of a significant reduction by 50% -80% of the effect of electronic and thermal lenses on the amplified radiation with a small decrease in the gain (less than 20%) by choosing the optimal radius profile of pump radiation at a given pulse repetition rate was shown.

Within the model, the usage of media with a nonlinear distribution of active ions as active elements was analyzed. The results show that a more uniform temperature distribution, as well as a decrease in its average and maximum values occur [5]. Polynomial and exponential profiles of the distribution of active ions were chosen for modelling. With a parabolic concentration distribution profile that varies along the pump axis, the maximum temperature decreases by ~ 60 K (25%) as compared to the constant profile of the concentration of active ion distribution, and the temperature gradient decreases by more than two times. A decrease in the temperature gradient leads to a decrease in phase distortion by ~ 50%.

The results can be used to increase the efficiency of laser amplifiers and reduce the influence of thermal effects on the quality of the spatial radiation profile when creating laser systems with high average power.

REFERENCES

[1] V.V. Petrov, G.V. Kuptsov, V.A. Petrov, A.V. Laptev, A.V. Kirpichnikov, E.V. Pestryakov, "Optimisation of a multi-disk cryogenic amplifier for a high-intensity, high-repetition-rate laser system", QUANTUM ELECTRON, vol. 48, pp. 358-362, 2018.

[2] I. Tamer., S. Keppler, M. Hornung, J. Koerner, J. Hein, M.C. Kaluza, "Spatio-Temporal Characterization of Pump Induced Wavefront Aberrations in Yb Doped Materials", Laser Photonics Rev, 1700211, 2017.

[3] G.V. Kuptsov, V.A. Petrov, V.V. Petrov, A.V. Laptev, A.V. Kirpichnikov, E.V. Pestryakov, "Study of the temperature effect on the laser amplification process", Proceedings of SPIE.- .- Vol. 11322.- P. 113220V

[4] V.A. Petrov, G.V. Kuptsov, V.V. Petrov, A.V. Laptev, M.P. Spichak, "Thermal field model in diode-pumped laser amplifier", Pulsed Lasers and Laser Applications–"AMPL-2019". Abstracts of XIV International Conference,-Tomsk:STT, P. 77, 2019.

[5] Petrov V.A., Kuptsov G.V., Petrov V.V., Kirpichnikov A.V., Laptev A.V., Spichak M.P., Korel I.I., Pestryakov E.V. Modeling of thermal field in active elements with non-uniform concentration distribution of dopant ions // AIP Conference Proceedings.- 2019.- V. 2125.- P. 030060

*The reported study is funded in parts by RAS Presidium Program 'Extreme Light Fields and Their Interaction with Matter', by Ministry of Science and Higher Education of the Russian Federation, by RFBR, project 20-02-00529, RFBR and Novosibirsk Oblast according to the research project 19-42-543007.

ION IRRADIATI ON INDUCED DAMAGE IN GGG SINGLE CRYSTALS*

A. DAULETBEKOVA[1], *K. KUMARBEKOV*[1], *ZH. KARIPBAYEV*[1], *A. AKILBEKOV*[1], *M. ZDOROVETS*[1,2,3], *D. SUGAK*[4,5], *S. UBIZSKII*[4], *A.I. POPOV*[6,7]

[1]*L. N. Gumilyov Eurasian National University, Nur-Sultan, Kazakhstan*
[2]*Institute of Nuclear Physics, Nur-Sultan, Kazakhstan*
[3]*Ural Federal University, Yekaterinburg, Russia*
[4]*Lviv Polytechnic National University, Lviv, Ukraine*
[5]*Scientific Research Company "Electron-Carat", Lviv, Ukraine*
[6]*Institute of Solid State Physics, University of Latvia, Riga, Latvia*
[7]*Institute of Physics, University of Tartu, Tartu, Latvia*

The single crystals $Gd_3Ga_5O_{12}$ or GGG are widely used and studied as solid-state laser materials, and magneto-optical storage materials, as well as, when doped with suitable ions they are used as efficient phosphors and scintillators [1-3].

In this work, we report on the optical properties of GGG single crystals irradiated with Kr^{+15} ions with energy 1,75 MeV/u, up to fluences $1x10^{13}$, $5x10^{13}$, and $1x10^{14}$ ion/cm^2 at cyclotron DC-60 (Nur-Sultan). Czochralski-grown in slightly oxidizing atmosphere GGG crystals were prepared in the form of polished plates with (111) orientation and 0.48 mm thickness. The absorption spectra were recorded using Agilent Cary 7000 spectrophotometer in spectral range 200-1100 nm. In the absorption spectra of unirradiated and both irradiated GGG crystals, Gd^{3+} absorption bands due to $^8S_{7/2}\rightarrow{}^6D_J$ transitions of Gd^{3+} ions bands were observed. irradiation with swift heavy ions led to creation of color centers, most probably, as F^+ centers (300nm).

The photoluminescence was registered using CCD-cell Andor iSTAR DH734-18F-A3 connected with Andor Technology SR-303i-B spectrometer. The luminescence was excited by pulsed solid-state laser Ekspla NT342 / 3UV with pulse duration 4 ns, λ=228 nm. Thermostimulated luminescence spectra were measured using Harshaw TLD 3500 at rate 2K/s. irradiation with Kr ions leads to a shift in the absorption edge from 220 to 270 nm, which is almost independent of the doses applied. Almost dose-independent complex TSL peak at 500 – 530 K was observed in the TSL glow curves of GGG crystals irradiated with $1x10^{13}$, $5x10^{13}$ fluences. However, this peak sharply increases at fluence of 10^{14} ions/cm^2 with peak shift of up to 500K. Dose-dependent behavior of a wide emission in the region 650-800 nm in photoluminescence spectra was also observed.

REFERENCES

[1] B.J. Dinerman, Opt. Lett., vol.19, pp.1143-1145, 1994
[2] Q.C. Liu, X.M. Zhou, S.N. Luo, et al., J. Appl. Phys., vol.121, 145901, 2077
[3] A. Zabiliūtė, S. Butkutė, A. Žukauskas, P. Vitta, A. Kareiva, Appl. Opt., vol. 53, pp. 907-914, 2014

* The work was supported by MES RK

HIGH ENERGY IONOLUMINESCENCE OF LITHIUM FLUORIDE AND ALUMINUM OXIDE SINGLE CRYSTALS*

A.AKILBEKOV[1], *A. SEITBAYEV*[1], *V. SKURATOV*[2,3,4], *YU. TETERIN*[2], *A. DAULETBEKOVA*[1], *M. ZDOROVETS*[1,5,6]

[1]*L. N. Gumilyov Eurasian National University, Nur-Sultan, Kazakhstan*
[2]*Flerov Laboratory of Nuclear Reactions, Joint Institute for Nuclear Research, Dubna, Russia*
[3]*National Research Nuclear University MEPhI, Moscow, Russia*
[4]*Dubna State University, Dubna, Moscow Region, Russia*
[5]*Institute of Nuclear Physics, Nur-Sultan, Kazakhstan*
[6]*Ural Federal University, Yekaterinburg, Russia*

Spectral content and intensity of optical emission generated by energetic ions (ionoluminescence, IL) are strongly dependent on structural changes and this may be used for real-time characterization of irradiating materials. Usually, these are time-integrated measurements when the evolution of the IL spectra affected by accumulated radiation damage and associated mechanical stresses are studied. Much less works are devoted to time-resolved IL measurements, especially to those in which the luminescence decay is registered after single ion impact. Temporal resolution of single ion technique, not limited by beam pulse duration, may reach picoseconds that enabled to reveal new interesting features in dynamics of dense electronic excitations in vicinity of swift ion trajectory, as demonstrated by K.Kimura et al. and M. Koshimizu et al., (for, example [1-3]). These experiments [1-3] have been done using intact crystals, since the single ion excitation assumes a minimal damage production rate thus excluding possible effects of newly formed radiation defects on properties of time-resolved luminescence. Aim of this work is to compare the luminescence decay registered in the intact and pre-damaged Al_2O_3 and LiF crystals under swift heavy ion and photo- picosecond laser pulse excitation.

REFERENCES

[1] Kazuie Kimura, Sumit Sharma, Anatoli Popov, Nucl. Instr. Meth. Bm vol. 191, pp. 48–53, 2002
[2] Kazuie Kimura, Nucl. Instr. Meth. B, vol. 212, pp. 123–134, 2013.
[3] M. Koshimizu et al., Nucl. Instr. Meth. B, vol. 365 pp. 540–543, 2015

* The work was supported by grant AP05134257 of MES the Republic of Kazakhstan

TIME-RESOLVED LUMINESCENCE SPECTROSCOPY OF YAG AND YAG:Ce^{3+} PHOSPHORS UNDER UV-EXITATION*

E.F. POLISADOVA[1], T. HAN[2], V.A. VAGANOV[1], C. ZHANG[2], D.T. VALIEV[1], V.I. OLESHKO[1], A.G. BURACHENKO[3]

[1]*National Research Tomsk Polytechnic University, Tomsk, Russia*
[2]*Chongqing University of Arts and Sciences, Chongqing, China*
[3]*Institute of High Current Electronics, SB RAS, Tomsk, Russia*

Yttrium aluminum garnet $Y_3Al_5O_{12}$ (YAG) is widely used as hosts for doping with different rare-earth ions for use in different applications like laser crystals, fast scintillators, dosimeters for ionizing radiation etc. YAG doped with Ce^{3+} ions (YAG:Ce^{3+}) phosphors are used as luminescent converters in white light-emitting diodes (w-LEDs) [1]. Optical properties of YAG in the different forms (single crystals, films, nanocrystals, and ceramics) are widely studied [1-4].

The phosphor powders of YAG doped with Ce^{3+} concentration 0,02-0,1 mol% were synthesized by solid state reaction method with the addition of BaF_2. A pulsed nitrogen laser (λ = 337.1 nm, 7 ns FWHM) and a UV pulsed KrCl excilamp (λ = 222 nm, 150 ps FWHM) were used to excite luminescence. The luminescence decay kinetics were recorded by an FEU-84-6 photomultiplier tube using an MDR-3 monochromator and a TDS5052 digital oscilloscope (Tektronix). The integrated luminescence spectra were recorded using an AvaSpec-2048 spectrometer, integration time 2 ms.

Optical, structural and morphological properties of YAG powders were studied. The effect of cerium ions on the luminescent characteristics at various types of photoexcitation by UV emission was investigated. The shift in the position of the maximum band of luminescence occurs upon a change in the excitation conditions (quantum energy, duration of the excitation pulse). It was shown that the emission band in the region 450–650 nm consists of two elementary bands with maxima of 2.19 and 2.38 eV (fig.1).

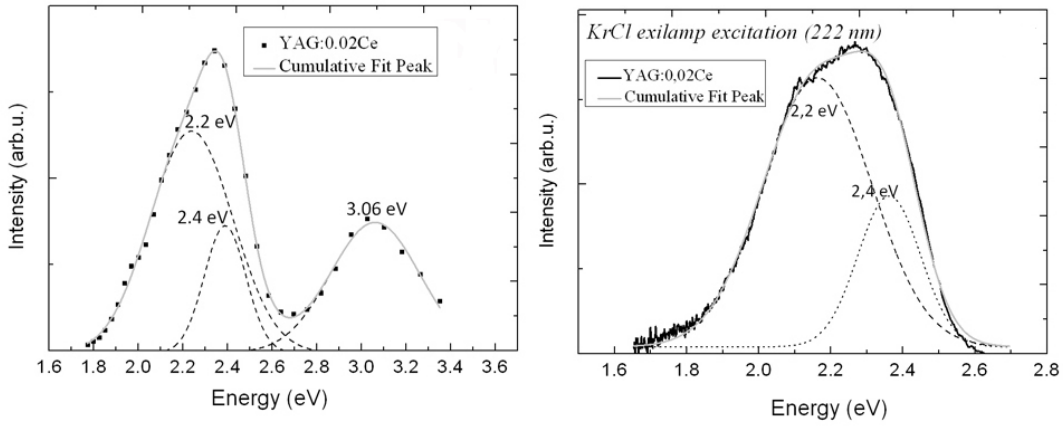

Fig.1. Time-resolved (left) and integrated (right) luminescence spectra for YAG:0.02Ce powder.

Increasing concentration different types of hole centers when introduced Ce^{3+} ions in YAG matrix was showed in the absorption spectra. It is assumed that the intrinsic defects created in YAG phosphors during the synthesis process in form complex defects can becombined with the cerium ion. It possibly these clusters play an important role of the luminescent centers in YAG phosphors.

REFERENCES

[1] S. Ye, F. Xiao, Y.X. Pan, Y.Y. Ma, Q.Y. Zhang “Phosphors in phosphor-converted white light-emitting diodes: Recent advances in materials, techniques and properties”, Mater. Sci. and Engin.:R, vol.71, pp.1–34, December 2010.

[2] J. Krzywinski, A. Andrejczuk, R.M. Bionta, T.Burian, J. Chalupskỳ, M. Jurek, M. Kirm, V. Nagirnyi, R. Sobierajski, K. Tiedtke, S. Vielhauer, L. Juha "Saturation of a Ce: Y3Al5O12 scintillator response to ultra-short pulses of extreme ultraviolet soft X-ray and X-ray laser radiation" Optical Materials Express, Vol. 7, no 3, pp 665-675, March 2017.

[3] E. Polisadova, D. Valiev, V. Vaganov, V. Oleshko, T.Han, C.Zhang, A.Burachenko “Time-resolved cathodoluminescence spectroscopy of YAG and YAG:Ce3+ phosphors”, Optical Materials, vol. 96, no 109289, October 2019.

[4] V. Lisitsyn, L. Lisitsyna, A. Tulegenova, Y. Ju, E. Polisadova, E. Lipatov, V. Vaganov "Nanodefects in YAG:Ce-based phosphor microcrystals" Crystals, vol.9, no 476, September 2019.

* The work was carried out in continuation of project No 18-43-703014 r_mol_a, supported by Russian Foundation for Basic Research

TEMPERATURE QUENCHING OF LUMINESCENCE OF YAG:Ce,BaF_2 AND YAG:Ce,Tb CERAMICS[1]

S.A. STEPANOV, D.T. VALIEV, V.D. PAYGIN, V.A. VAGANOV

National Research Tomsk Polytechnic University, Tomsk, Russia

Ceramics are of great interest for present photonic devices. These optical materials occupy an intermediate position between crystal materials and glass, and combine the best properties of crystals such as a high mechanical and thermal durability and glassy materials (the possibility of pressing, molding, and forming elements of different geometry). One of the last directions in technologies of converting emission in construction of white LED are luminescent ceramics application [1, 2].

Using luminescent ceramics as an emission converter makes it possible to rank LEDs by color temperature with a high precision. This is achieved by more precise proportioning of phosphors. Another advantage of ceramic materials is to produce LEDs with high color homogeneity, a thermal durability, and an elevated temporal stable.

Yttrium-aluminum garnet doped with trivalent cerium ions (YAG: Ce^{3+}) is often used as an inorganic phosphor in the manufacture of lighting and photonic devices. The maximum of emission spectrum of YAG: Ce^{3+} phosphors are in the visible spectral region from 530 to 560 nm. This is due to radiation transitions between 5d and 4f energy levels of Ce^{3+} ions [3].

$Y_3Al_5O_{12}$ phosphor powders doped with Ce^{3+} were synthesized by solid state reaction method with the addition of BaF_2 or Tb_4O_7. Ceramic samples were sintered from obtained YAG:Ce,BaF_2 or YAG:Ce,Tb phosphor powder. The powder was pressed uniaxially in an automatic press IP-500 AVTO ZIPO (Russia).

Integrated emission spectra were acquired on an AvaSpec-3648 optical fiber spectrometer (200–1100 nm spectral range, 2.1 nm spectral resolution, 1s integration time). An LED chip was used as excitation source for photoluminescence spectra measurements: (λ = 447 nm, 20 nm FWHM, 16 $mW \cdot cm^{-2}$ irradiance,). To study the characteristics of photoluminescence and degradation processes at elevated temperatures, ceramic samples were heated to the temperatures of complete temperature quenching of photoluminescence by directly measuring luminescence during heating.

Was shown these ceramics can be operated up to temperatures of about 500 ° C. After cooling, all ceramics returned to their original glow intensity - no temperature degradation of properties was observed in the range of operating temperatures.

REFERENCES

[1] Yi-C. Chen, Y.-T. Nien,“Microstructure and photoluminescence properties of laser sintered YAG:Ce phosphor ceramics”, J. of the European Ceramic Society, vol. 37, pp. 223–227, 2017.

[2] K. Bodiˇsová, R. Klement, D. Galusek, V. Pouchl´y, D. Drdlík, K. Maca,“Luminescent rare-earth-doped transparent alumina ceramics”, J. of the European Ceramic Society, vol. 36, pp. 2975–2980, 2016.

[3] Z. Xia and A. Meijerink,“Ce3+-doped garnet phosphors: composition modification, luminescence properties, and applications”, Chem. Society Rev., vol. 46, pp. 1 – 27, 2016.

1* The work was supported by Russian Foundation for Basic Research and the government of the Tomsk region of the Russian Federation, grant № 18-43-703014

PHOTOCHEMICAL AND PHOTOPHYSICAL PROPERTIES OF NOVEL DIPYRROMETHENE COMPLEXES WITH ZINC

PROKOPENKO ALEKSANDR[1], KUZNETSOVA RIMMA[1], AKSENOVA IULIIA[1], BEREZIN MIKHAIL[2]

[1] Tomsk State University, Tomsk, Russia
[2]G.A. Krestov Institute of Solution Chemistry of the RAS, Ivanovo, Russia
E-mail: alexpr898@gmail.com

Study of dipyrromethene complexes with different structure is one of the most successfully developing areas of modern chemistry. The demand for using a variety of optical devices in modern technology makes it necessary to explore the photonics of new organic luminophores such as coordination complexes of dipyrromethene with p- and d-elements depending on their structure, intermolecular interactions, temperature, etc. In this work was researched dipyrromethene compounds, which can form stable complexes with ions of d-elements. The main advantage complexes of Zn(II) with dipyrromethenes is easy to "self-assembly" in the "soft" conditions on complexing ions in solutions and in biological systems, as well as high sensitivity spectral-luminescence characteristics to changes in the structure of the chromophore and the nature of the solvent. Systematic observation of photochemical and photophysical properties and establishment of their connection with structural features of the complexes are required for successful usage of dipyrromethene complexes and creation of various hi-tech optical devices which are based on them. Therefore, the purpose of the work is to study the spectral-luminescent, sensory properties and stability of different complexes of dipyrromethenes with zinc, the optimal combination of which will indicate the direction of the most effective use of these dyes.

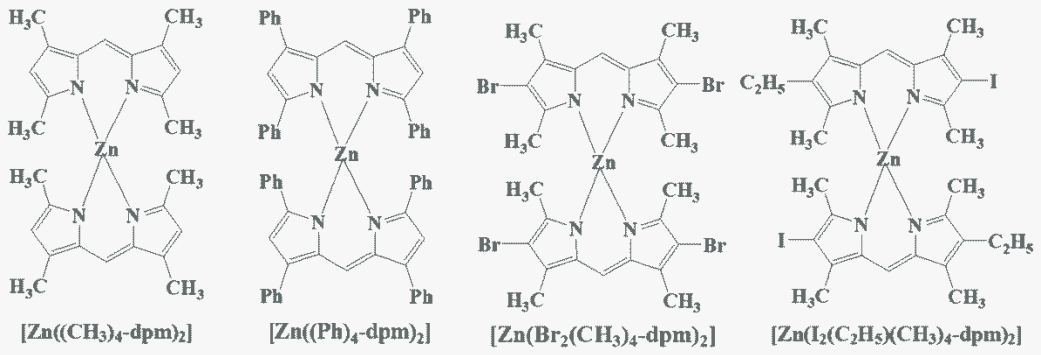

Fig.1. Structural formulas and denotation of investigated compounds

These dipyrromethene complexes with zinc were synthesized in Institute of Solutions Chemistry of the RAS. For this compounds were investigated spectral-luminescent properties in different solvents. It was found that zinc dipyrromethene complexes don't have effective fluorescence but have long-lived emission due to increased nonradiative intersystem processes in the excited state. Introduction of heavy atoms into the dipyrromethene core enhances intersystem crossing, which leads to a long-lived emission. For such complexes, we obtained characteristics of the spectra of long-lived emission of frozen ethanol solutions. For solid samples based on zinc complexes was found dependency of the long-lived emission intensity of the oxygen concentration in gas flow. The presence of line segment indicates the possibility of the use of these complexes as a basis for creation of optical sensors for oxygen determination. For successful application of such complexes need to know something of their behaviors in different solvents, including when acids and alkalides are present, since the stabilities of fluorophores in acidic/alkaline media are closely related to their applicabilities. The complexes stabilities in the ground and excited states are estimated by spectrophotometric titration of ethanol solutions of compounds using water–ethanol solutions of hydrochloric acid. The results obtained in this work can be used as the basis for the design of optical devices.

The work was supported by Russian Foundation for Basic Research (Project No. 18-33-00284-mol_a) and Project FSWM-2020-0033 of Russian Ministry of Science and Education.

LUMINESCENT PROPERTIES OF SINGLE DOPED RE IONS YAG CERAMICS PRODUCED BY CONVENTIONAL SINTERING IN AIR ATMOSPHERE

D. VALIEV, O. KHASANOV, E. DVILIS, S. STEPANOV, V. PAYGIN, A.ILCHUK

National Research Tomsk Polytechnic University, Tomsk, Russia
E-mail: dtdamirka@gmail.com

Currently, LED are the most efficient light sources [1, 2]. UV or “blue” radiation is converted by the phosphor into radiation of the visible light. The magnitude of the physical limit of the light efficiency of white LEDs by half is determined by the conversion of radiation from the phosphor into visible light. Therefore, improving the efficiency of the phosphor - energy converter in the visible radiation is one of the main directions of development of light sources, energy and resource efficiency, creating a comfortable light environment, use in engineering, technology.

Inorganic phosphors used by most manufacturers are modified type of yttrium-aluminum garnet doped with trivalent cerium ($YAG:Ce^{3+}$). The luminescence spectrum of such phosphors is characterized by a maximum wavelength in the range of 530–560 nm [2]. However, the low color rendering index (Ra) (usually below 80) and the high correlated color temperature CCT> 4000 K (cold white light) due to the lack of the red component in the emission spectrum limit the scope of this phosphor [3].

Therefore to solve the existing problem, in particular, (to improve the color and energy characteristics), the approach of replacement of Y3+ ions with other rare earth ions (RE ions) or co-doped with other RE ions can be applied [4].

In this work we demonstrated the possibility of synthesis luminescent YAG ceramics doped with RE ions (Dy^{3+}, Tb^{3+}, Eu^{3+}) obtained by cold uniaxial static pressing followed by sintering in air. A complex characterization such as optical, luminescent and mechanical properties, microstructure and dynamics of linear shrinkage are investigated.

The reported research was funded by Russian Foundation for Basic Research and the government of the Tomsk region of the Russian Federation, grant № 18-43-703014 r_mol_a.

[1] D. Chitnis, N. Thejo Kalyani, H. Swart, S. Dhoble, Renew. Sustain. Energy Rev. 64 (2016) 727-748.
[2] Z. Xia, A. Meijerink Chem. Soc. Rev., 46 (2016) 1-27
[3] V. Bachmann, C. Ronda, A. Meijerink, Chem. Mater. 21 (2009) 2077–2084.
[4] V. P. Dotsenko et al., J. Alloys Compd. 550 159–163 (2013).

UV WATER DISINFECTION DEVICE

T.S. MIKHALCHENKO, A.O. SHARDINA, L.SH. YULDASHOVA, V.S. SOLDATKIN[1]

[1]Tomsk State University of Control Systems and Radioelectronics, Tomsk, 634050, Lenin Ave 40.
E-mail: soldatkinvs@main.tusur.ru, +7 (3822) 701-513

Ultraviolet (UV) radiation sources for disinfection began to be used as early as the 30s of the 20th century. Radiation with wavelengths in the range of 215 - 310 nm has antibacterial properties. Currently, UV radiation is used to disinfect air, water, etc. Currently, industry uses radiation sources based on gas discharge lamps to disinfect UV. Modern advances in semiconductor technology allow the use of UV diodes for disinfection. UV diodes have several advantages compared to discharge lamps: energy efficiency, mechanical strength and high service life. The disadvantage of UV diodes today is the high cost [1].

The device for UV disinfection of water for a volume of one cubic centimeter was calculated taking into account the requirements [2, 3]. The calculation results are given for the selection of the UV diode are shown in table 1.

Table 1.

Wavelength nm	265	270	275	280	285	290	295	300	305	310
Radiation flux, W	0,09	0,093	0,1	0,12	0,17	0,28	0,61	3,06	15,29	91,74

According to the data from table 1, UV diodes were also selected for economic calculations, the photograph is shown in Fig. 1.

Fig. 1. Photograph of a UV diode (wavelength 275 nm)

A mock device for UV water disinfection was manufactured and biological studies were conducted. Using a Levenhuk microscope (magnification range from 40 to 2000 times) with an increase of 400 times, the number of microorganisms was calculated: 20 ± 3 bacilli, 100 ± 10 trematodes. The research process was repeated three times. The results of studies of the effect of the device for UV water disinfection on microorganisms in water samples are shown in Fig. 2.

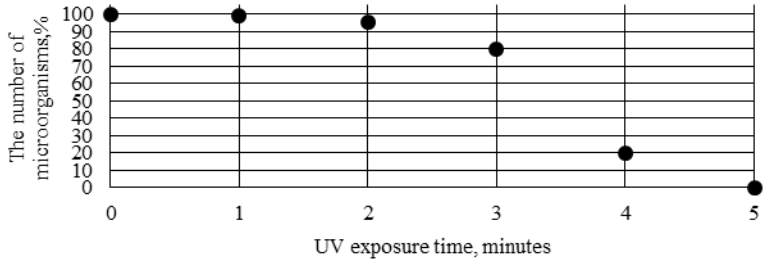

Fig. 2. The dependence of the percentage of microorganisms in 1 cm2 of water sample when irradiated with a device for UV water disinfection, depending on the exposure time

From Fig. 2 shows that the maximum effect on microorganisms occurs after 3 minutes of exposure.

Conclusions:

The device for UV water disinfection was calculated. Based on the calculation results, UV diodes were selected. A mock device for UV disinfection of water was made and biological studies were conducted. As a result of studies, it was found that the maximum effect on the microorganisms of the device for UV water disinfection is observed after 3 minutes of exposure, and 100% disinfection occurs after 5 minutes of exposure.

REFERENCES

[1] Mikhalchenko T.S., Shardina A.O., Yuldashova L.Sh., Soldatkin V.S. The effect of ultraviolet radiation on microorganisms in the aquatic environment // Electronic means and control systems: materials of reports of the XV International scientific and practical conference (November 20–22, 2019): at 2 a.m. - Part 2. - Tomsk: V-Spectrum, 2019. - S. 24-26.

[2] R 3.5.1904-04 The use of ultraviolet bactericidal radiation to disinfect indoor air.

[3] MU 2.1.4.719-98 Sanitary supervision of the use of ultraviolet radiation in the technology of drinking water treatment.

PYROLYSIS OF LIGNITE UNDER THE LASER RADIATION EXPOSURE

KRAFT Y.V.[1], NURMUKHAMETOV D.R.[1], ADUEV B.P.[1], ISMAGILOV Z.R.[1,2]

[1]Institute of Coal Chemistry and Material Science at Federal Research Center of Coal and Coal chemistry SB RAS, 18 Sovetsky ave., Kemerovo, Russia, 650000

[2]Boreskov Institute of Catalysis SB RAS, 5 Lavrentiev ave., Novosibirsk, Russia, 630090

Coal is one of the most common types of fossil fuels. A limitation of the wider use of coal as a fuel is the negative impact of its combustion products on the environment. A large number of works are aimed at converting coal into pure gaseous or liquid fuel. One way to produce gaseous or liquid fuels is by pyrolysis of coal.

It is possible to carry out pyrolysis of coal in various ways, for example, by heating particles of coal with plasma, exposure to a direct current arc, or exposure to radiation from a pulsed xenon lamp. In this work, we investigated the possibility of carrying out laser pyrolysis of coal.

The study of thermal decomposition of Kaichak lignite (Kuznetsk coal basin, Russian Federation) under the pulsed laser radiation exposure in the energy density range from 1.15 to 1.95 J/cm^2 was performed. The results of proximate and ultimate analysis of coal are as follows: moisture content W^a = 11.1%, ash content A^d = 9.5%, content of volatile matter V^{daf} = 51.4%, carbon content C^{daf} = 61.4%, hydrogen content H^{daf} = 5%. For the preparation of samples, coal particles with a size of ≤ 100 μm were used. Then, using the mould pressing method, samples of coal were obtained in the form of tablets. As a source of laser radiation, a YAG:Nd^{3+} laser operating in the free-running mode at a wavelength of λ = 1064 nm was used. The experiment was carried out in an argon medium. The following pyrolysis gases were recorded by mass spectrometry method: H_2, CH_4, H_2O, CO, CO_2. It is shown that in the studied range of the laser radiation energy density, the H_2 concentration in the composition of the gaseous pyrolysis products increases with increasing exposure energy, and the CO_2 concentration, on the contrary, decreases. The values of concentration of CO and CH_4 in this range are close to constants. At the increase in energy density in an impulse in the range of 1.15-1.95 J/cm^2, the yield of combustible components increases and reaches $1.3 \cdot 10^3$ cm^3/g under the exposure with an energy density in an impulse of 1.95 J/cm^2. The sum of combustible components in the mixture of end products of pyrolysis under the exposure with an energy density in an impulse of 1.95 J/cm^2 reaches 93%.

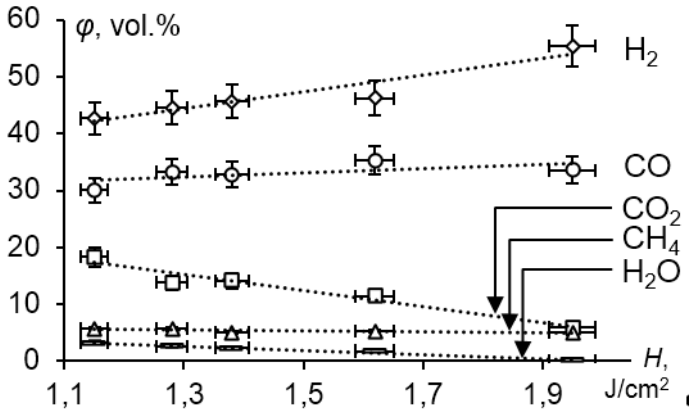

Fig. 1. Dependence of composition of gas mixture on the energy density of laser radiation

Considering the rather high yield of combustible components recorded in this work and the possibility of using widespread dpss-lasers, one can note the promising technology of coal laser pyrolysis.

SIMILARITY AND DIFFERENCES OF REGULARITIES OF LASER INITATION OF COMPOSITES BASED ON PETN AND RDX WITH METALL NANOPARTICLES[1]

N.V. GAZENAUR, A.V. KALENSKII*, A.A. ZVEKOV **, M.V. ANAN'EVA*, B.P. ADUEV **, E.V. GALKINA *, D.R. NURMUKHAMETOV***

**Kemerovo State University,6 Krasnaya st., Kemerovo, 650000, Russia, kriger@kemsu.ru, +7(3842)580591 **Federal Research Center of Coal and Coal Chemistry,18 Sovetsky av., Kemerovo, 650000, Russia*

Nowadays development of new materials selectively sensitive to pulse laser irradiation is relevant. In particular, explosive composite materials with a low laser initiation threshold are of interest and find practical application [1, 2]. The addition of ultrafine metal particles to Pentaerythritol tetranitrate (PETN) and hexogen (RDX) was proved to be promising in this direction. In [1, 2] the threshold of laser initiation of pressed pillet of PETN and RDX sensitized with aluminum nanoparticles (relative to secondary explosives tablets without inclusions of aluminum nanoparticles) was reduced in tens times. The purpose of this work is to compare the explosive and optical characteristics of composites based on PETN and RDX - aluminum nanoparticles. The main differences of explosive decomposition of pressed pillets of composites PETN and RDX – aluminum nanoparticles arise from the peculiarities of their optical characteristics associated with different results of their pressing. Developed method of pressing [3] of pillets of PETN allows to obtain optically transparent samples, that are weakly scattering and absorbing light in the absence of metal nanoparticles. RDX power might be pressed much worse than PETN, and in pressed tablets based on it, one can expect strong light scattering.

Using integrating sphere dependences of transmission coefficients and the sum of the transmission and absorption coefficients of light with a wavelength of the second harmonic of a neodymium laser (532 nm) in pressed tablets PETN and RDX - aluminum nanoparticles (average radius of 50 nm) on the thickness of the sample and the mass fraction of nanoparticles was experimentally studied. Mathematical modeling of absorbing and scattering processes in these systems in terms of Mie's theory and radiative transport equation was made. It was shown that distribution of absorbed energy over the sample depth approximately obeys the Beer–Lambert law. It was shown that the light mainly absorbed by the metal inclusions: the effective absorption rate of the studied pressed tablets depends linearly on the mass concentration of aluminum nanoparticles and at a value of 0.2% reaches a value of more than 200 cm^-1. To describe the experimental values of optical characteristics of pressed pillets PETN – aluminum nanoparticles it is sufficient to use the model of nanoparticles with metal core – dielectric oxide shell, which is in optical contact with the PETN matrix. The model of pressed pillet RDX – aluminum nanoparticles must also take into account residual porosity of matrix: scattering on unfilled pores, scattering and absorption on nanoparticles in the pore. This fact causes the significant changes in the optimal radius of nanoparticles, where the maximum value of the absorption efficiency factor and the minimum critical energy density of initiation are observed. For pressed tablets of PETN-aluminum nanoparticles, these parameters are significantly (more than 25%) less than for RDX-aluminum nanoparticles. The results are necessary to optimize the composition of the cap of optical detonator based on secondary explosive.

The work was carried out with the financial support of the RFBR grant number 19-33-90261.

REFERENCES

[1] *A.V. Kalenskii, A.A. Zvekov, M.V. Anan'eva, A.P. Nikitin, B.P. Aduev //* Combustion, Explosion, and Shock Waves. 2017. 53(1). pp 82–92.

[2] *B.P. Aduev, D.R. Nurmukhametov, A.A. Zvekov, A.V. Kalenskii, I.Y. Liskov.* // Quantum Electronics. 2019. 49(2), pp. 141-143.

[3] *B.P. Aduev, D.R. Nurmukhametov, R.I. Furega, I.Y. Liskov. //* Russian Physics Journal. 2015.58(8). pp. 1093-1097.

[1] This work was supported by RFBR (№18-03-00421_a, №19-33-90261) and was conducted within the framework of the budget project # AAAAA17-117041910150-2 for the Institute of Coal Chemistry and Chemical Material Science of FRC CCC SB RAS (supervised by B.P. Aduev).

INFLUENCE OF LASER PULSE DURATION ON FILAMENTATION PROCESS IN LiF

A.V. KUZNETSOV, V.P. DRESVYANSKIY

Irkutsk branch of Institute of laser physics SB RAS, Irkutsk, Russia

The effect of the duration of femtosecond laser pulses on the processes accompanying laser filamentation in lithium secondary has been theoretically studied. The numerical model takes into account self-focusing, nonlinear ionization (multiphoton, tunneling, avalanche) and the interaction of light with plasma. Electron-hole pairs turn into stable radiation defects (color centers). Thus, the model allows us to predict the dependence of the efficiency of defect formation on the pulse duration.

This work was supported by project SB RAS II.10.1.2 and by RFBR project № 17-52-44015 Mong_a.

MORPHOLOGY OF DESTRUCTIONS OF SOLID BODIES UNDER IRRADIATION BY A HIGH-CURRENT ELECTRON BEAM IN FILAMENTED AND SELF-FOCUSED MODE*

V.I. OLESHKO[1,2], *V.F. TARASENKO*[1,2], *A.N. YAKOVLEV*[1], *V.V. NGUYEN*[1]

[1] *National Research Tomsk Polytechnic University, Tomsk, Russia*
[2] *Institute of High Current Electronics SB RAS, Tomsk, Russia*

The study of physicochemical processes developing in condensed matter when irradiated with pulsed electron beams is of interest for various scientific and applied areas - radiation solid state physics, space materials science, high energy density physics and explosion physics [1-4]. The energy density of the electron beams H in this case varies in the range (1 – 10) J/cm^3. As for the effect of a self-focused high-current electron beam (HCEB) with an energy density of $H \approx (10^3 – 10^4)$ J/cm^3 on solids of various classes, such studies have practically not been conducted before. The stimulus for conducting such studies is the general scientific interest in two problems - the need to study the behavior of solids at high energy densities and to obtain new data on the physical nature of such phenomena as filamentation and self-focusing of a HCEB in vacuum diodes with an explosion-emission cathode.

The aim of this work is to study the morphology of the damage generated in metals and polymers when irradiated with a HCEB in the mode of filamentation and self-focusing in a vacuum diode of a pulsed high-current electron accelerator with a GIN-600 generator. The maximum electron energy in the beam spectrum reached 400 keV, the current pulse duration of a HCEB at half maximum $\tau_{1/2}$ varied from 2 to 12 ns. The vacuum diode was formed by a tubular cathode and a flat anode, the role of which was played by aluminum foil, 10 μm thick. In the experiments, tubular cylindrical cathodes with diameters of 3 – 8 mm were used. The phenomena of filamentation and self-focusing of a HCEB were studied by the morphology of volumetric damage in irradiated targets ("autographs" of the electron beam) using optical microscopy with a spatial resolution of ~ 1 μm. The most interesting results were obtained in the study of the morphology of fractures formed by a self-focused electron beam in polymethyl methacrylate (PMMA). It was found that upon PMMA irradiation with an electron beam in the interaction region of a filamented electron beam with an irradiated target at a depth of 40 - 80 μm, micro-fractures of a round and more complex shape are formed, the diameters of which vary from 1 to 50 μm (fig. 1).

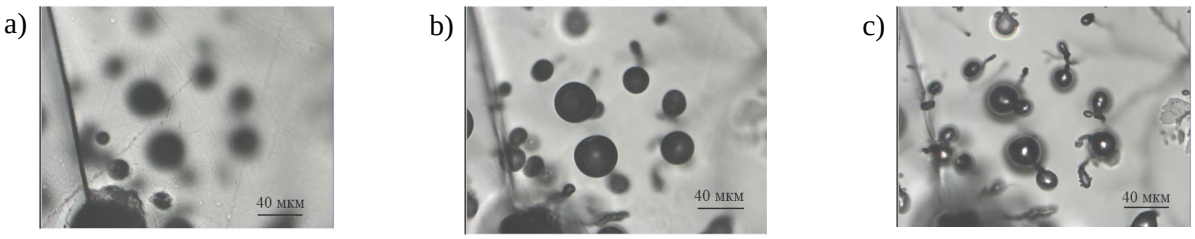

Fig. 1. Microphotographs of the damage generated in the interaction zone of the filamented electron beam with PMMA: a — irradiated surface; b, c - damage recorded at various depths from the irradiated surface: b - 40 μm; c –75 μm

The figures are connected by electric breakdown channels. It is assumed that this type of destruction is formed as a result of irradiation of the polymer with high density electron microbeams, which are formed in the vacuum diode of a pulsed high-current electron accelerator.

FERENCES

[1] D.I. Weissburd, High Energy Solid State Electronics, Novosibirsk: Nauka, 1982.

[2] A.I. Akishin, Space Materials Science, Moscow: SINP MSU, 2007.

[3] Tarumov E.E. Obtaining and focusing of high-current relativistic electron beams in diodes, Moscow: Energoatomizdat, 1990.

[4] V.I. Oleshko, V.F. Tarasenko, A.G. Burachenko, V.V. Nguyen, “Filamentation and Self-Focusing of Electron Beams in Vacuum and Gas Diodes”, Technical Physics Letters, vol. 45, no. 4, pp. 309 - 313, April 2019.

* This work was supported by the Russian Science Foundation (project no. 18-19-00184) and partly by the Competitiveness Enhancement Program of Tomsk Polytechnic University.

LOW-THRESHOLD OPTICAL BREAKDOWN OF COMPACTED SAMPLES FROM ENERGETIC AND INERT MATERIALS[1]

V.I. OLESHKO, V.P. TSIPILEV, A.N. YAKOVLEV, N.A. ALEKSEEV

National Research Tomsk Polytechnic University, Tomsk, Russia

The investigation of processes accompanying the localization of laser radiation energy in porous dielectrics is of interest in various scientific and applied directions: research of the properties of laser-induced microplasma generated in the surface region of the absorbing medium after ablation, methods for obtaining diverse nanoparticles, high-energy-density physics and explosion physics [1–4].

Current treatise presents the measurements of threshold, spectral, kinetic and dynamic characteristics of surface laser plasma (SLP) generated after excitation of compacted powders of energetic and inert dielectrics (pentaerythritol tetranitrate, ammonium perchlorate, TiO 2 , sugar) with or without admixture of aluminium and carbon, and compacted aluminium powders with different particles size (ALEX, ASD-1). The specimens were pellets compacted at ~10^8Pa with a thickness of 1–2 mm and diameter of 3–6 mm. The excitation source was a Q-switched YAG Nd-laser working at the base frequency (λ = 1064 nm) with a half-amplitude duration of ~14 ns. The pulse energy density (H) was varied in the range from 0.02 to 20 J/cm^2 using calibrated filters. The luminosity kinetics of the SLP was recorded by a N5773-04 photo-module (300–850 nm) and DPO 3034 oscilloscope. The luminosity spectra were measured using an AcaSpec-2048 fiber-optical spectrometer. The spatial distribution of the SLP along the irradiated surface and towards the laser beam was photographed by an EOS 600D DSLR in a single excitation pulse through an MBS-10 microscope.

It was elucidated that on the surface of the studied dielectrics (with and without introduced impurities), SLP forms which amplitude, spatial, spectral, kinetic and dynamic characteristics depend on the type of the sample, pressure and laser radiation energy density. The intensity of SLP luminosity after excitation of specimens with aluminium in air at atmospheric pressure is considerably higher then after excitation in vacuum. Concurrently, total SLP emission spectrum contains atomic lines of aluminium, sodium and luminance of AlO molecules in blue-green spectral range (450–550 nm). It was established that the thresholds of SLP formation on compacted aluminium samples depend on their particle size. For example, for the particles with dimensions of ~150 nm, the threshold laser radiation energy density H ~ 0.04 J/cm^2, while for ~10-nm particles, H ~ 1.5 J/cm^2. Close values of SLP formation threshold were identified for composites with nano- and micro-dispersed aluminium powders. Multi-pulse irradiation of the samples with aluminium at H < 0.8 J/cm^2 decreases the luminance intensity of the SLP up to its total disappearance, which is evidently connected with the formation on the irradiated surface of Al_2O_3 film that prevents evaporation of aluminium.

The work has studied the effect of laser radiation energy density on the expansion velocity of aluminium plasma forming after evaporation of compacted ALEX powders in vacuum. It was shown that alteration of H in a range of 2.4–10 J/cm^2, the expansion velocity of the laser plume increases from 30 to 100 km/s.

REFERENCES

[1] V.V.Osipov, V.V. Lisenkov, V.V. Platonov and E.V. Tikhonov, "Processes of interaction of laser radiation with porous transpar ent materials during their ablation," Quantum electronics, vol.48, no. 3, 2018.

[2] V.P. Veiko , S.A. Volkov, R.A. Zakoldaev and etc., "Laser-induced microplasma as a tool for microstructuring transparent media," Quantum electronics, vol.47, no. 9, 2017.

[3] S.I. Anisimov, V.V. Zhakhovsky, N.A. Inogamov, K.P. Migdal, Yu.V. Petrov & V.A. Khokhlov, "High-Energy-Density Physics and Laser Technologies," J. Exp. Theor. Phys., vol. 129, 2019.

[4] B.P. Aduev, D.R. Nurmukhametov, G.M. Belokurov, A.A. Zvekov & N.V. Nelyubina, "Laser Initiation of PETN with Inclusions of Aluminum Nanoparticles under Static Pressure," Combust Explos Shock Waves, vol. 55, 2019.

1 This work was supported by a grant from the Tomsk Polytechnic University Competitiveness Improvement Program.

A KINETIC MODEL OF COAL LASER PYROLYSIS*

A.A. ZVEKOV[1], *A.V. KALENSKII*[2], *B.P. ADUEV*[1], *D.R. NURMUKHAMETOV*[1]

[1]*Federal Research Center of Coal and Coal Chemistry SB RAS, Kemerovo, Russia*
[2]*Kemerovo State University, Kemerovo, Russia*

The application of powerful laser facilities for the coal ignition research is reasonable for the widening of the range of the pyrolysis and ignition conditions. These conditions could be considered as the model ones of the powdered coal ignition in the swirl-type furnace [1]. The ignition in such extreme conditions makes it possible to change the set of limiting stages comparing to the conditions of the slow heating as it was observed in the case of explosion initiation of heavy metal azides with heating and laser pulses. Thus, the formulation of detailed chemical reaction model operating with minimum of variable parameters is essential for understanding the nature of ignition and pyrolysis of fossil fuels stimulated by powerful laser pulses. The aim of the present work is to develop the kinetic model of coal pyrolysis in the conditions of laser impact having microsecond pulse duration and to analyze it.

The pyrolysis of coal is a complex physical and chemical process that includes dissociation of organic structures in coal, secondary reactions of intermediate product, and transport processes.

The heterogeneous reactions of the coal-ash interaction are hindered in the conditions of the intensive laser impact due to short duration of the process. For that reason, we neglected the chemical reactions controlled by the ionic mechanisms on the present step of the study. The model of thermal processes initiated in coal in inert atmosphere should take into account the main groups of reactions:

- Destruction of the organic part of the coal concerned on radical dissociation followed by a chain of β-scission stages;
- Recombination of radicals;
- Other reactions of intermediates;
- Growth of the high-mass polyaromatic islands with formation of the carbonized residue.

The parameters of the lignite from Tisul' coal-field were used in the modelling. The laser heating stimulates the chain of endothermic reactions linked with aliphatic part of the coal dissociation. The maximum temperature of the coal particles increases slightly with the increasing in the laser pulse energy density. The increasing shows slow sublinear character due to strong endothermicity of the decomposition. The calculated temperatures are lower than observed experimentally because the model neglected the temperature distribution inside the coal particle.

A few mechanisms of the aromatic islands growth were discussed. The intermolecular and intramolecular Dielse-Alder reactions provide the most intensive growth of the aromatic constituent. The intramolecular Dielse-Alder reaction's contribution becomes higher when the energy density of the laser pulse increases.

The yields of the gaseous products were calculated. The molecular hydrogen dominates in the gaseous products' composition, which is a feature of the suggested model in the typical pulse energy density range due to the chain character of the aliphatic constituent destruction. It is worth mentioning that hydrogen yield in both experimental data and calculations are much higher than in the case of coking. The typical percentage of hydrogen in the coking gas is 55-60% by volume, while in the case of laser pyrolysis it is about 90%.

The results of the calculations were compared with the experimental data obtained with spectral pyrometry and mass-spectrometry methods. The correlation of the theory and experimental data is satisfactory.

REFERENCES

[1] K.V. Slyusarskiy, S.A. Jankovskiy, A.G. Korotkikh, I.V. Sorokin, "Coal Char Oxidation Kinetics in Air Medium," AIP Conference Proceedings 2017. 020014.

* The work was supported by Russian Foundation for Basic Research (grant 20-43-420012).

SPECTRAL-KINETIC CHARACTERISTICS OF THE GLOW OF RDX-FE COMPOSITES DURING EXPLOSIVE DECOMPOSITION INITIATED BY NEODYMIUM LASER PULSES[1]

ADUEV B.P., NURMUKHAMETOV D.R., NELYUBINA N.V., LISKOV I.YU.

Institute of Coal Chemistry and Material Science at Federal Research Center of Coal and Coal chemistry SB RAS, 18 Sovetsky ave., Kemerovo, Russia, 650000

A prospective direction of the special explosive materials' development for optical detonators initiated by laser pulses is utilization of the secondary explosive pentaerythritol tetranitrate (PETN) containing the ultrafine metal particles. It was shown that the absorption of laser radiation occurs by metal inclusions (Al, Fe, Ni) in the cases of both YAG: Nd^{3+} laser in the Q-switched mode and stationary light sources. In this case of initiation with laser pulse the explosive decomposition threshold of composites PETN-Me is reduced by a factor of ten relative to PETN without inclusions. It is of practical interest to develop similar composites using other explosives. In this work, we studied the spectral and kinetic characteristics of the glow arising in the process of RDX-Fe composite explosive decomposition under the impact of laser pulses (λ=1064 nm, τ_i=14 ns). The inclusions had a narrow particle size distribution with a maximum of d=75 nm. The explosive decomposition threshold at an optimum inclusion concentration of 0.4% by mass was H_{cr}=1.2 J/cm^2. The aim of this work was to measure the time dependent spectrum of the glow in real time during the explosion of samples using a streak-camera. The time dependence of the glow intensity at the wavelength 560 nm is shown in fig. 1. The first pronounce maximum of glow intensity appears during the laser pulse (shown in the inset in fig. 1), the typical time of its decay is ~60 ns. The glow of the explosion products is recorded in the microsecond time range. The glow in the time range of the first intensity maximum has a luminescent nature. The maximum of the spectral intensity of the glow is observed in the visible range. The blue-shift of the maximum position up to $\lambda\approx$420 nm is fixed with an increase in the energy density of laser pulses H. The analysis of the experimental and published data allows us to relate the luminescence observed at various H levels to NO_2 radicals excited to various degrees. The emission spectra of the explosion products are of thermal nature. The glow spectrum at 1 μs after exposure to a laser pulse plotted in the Wien coordinates represents a straight line. The slope gave us the temperature of the explosion products estimated as T=3500 K.

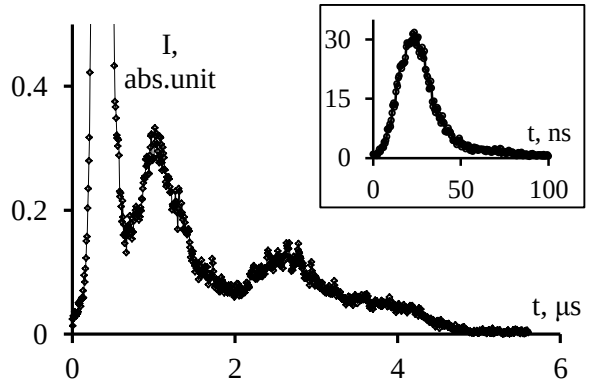

Figure 1. Dependence of the luminescence intensity on time at a wavelength of λ=560 nm during the explosion of an RDX-Fe sample, H = 2 J/cm^2. Inset: luminescence intensity immediately after exposure to a laser pulse (first maximum).

REFERENCES

[1] Aduev, B. P. Effect of Variations in the Gas-Dynamic Unloading on the Laser Initiation of the PETN–Aluminum Composite / B. P. Aduev, D. R. Nurmukhametov, A. A. Zvekov, I. Y. Liskov, G. M. Belokurov, N. V. Nelyubina // Technical Physics. – 2019. – Т. 64 – № 2. – С. 143–147.

[2] Aduev, B. P. Spectrokinetic characteristics of light emission at the early stages of the laser-initiated explosive decomposition of PETN-based composites containing metal nanoparticle inclusions / B. P. Aduev, D. R. Nurmukhametov, G. M. Belokurov, N. V. Nelyubina, A. V. Kalenskii, N. L. Aluker // Russian Journal of Physical Chemistry B. – 2017. – Т. 11 – № 3. – С. 460–465.

[3] Aduev, B. P. Laser initiation of PETN–iron nanoparticle composites / B. P. Aduev, D. R. Nurmukhametov, A. A. Zvekov, A. P. Nikitin, R. Y. Kovalev // Russian Journal of Physical Chemistry B. – 2016. – Т. 10 – № 4. – С. 615–620.

[1] The research was carried out with the financial support of the Russian Foundation for Basic Research (project 18-03-00421 A)

.

A NUMERICAL SIMULATION OF ELECTRICAL BREAKDOWN IN DYNAMIC MODE OF CRYSTALS AMMONIUM PERCHLORATE*

A. V. KHANEFT[1,2]

[1]*Kemerovo State University, Kemerovo, Russia*
[2]*National Research Tomsk Polytechnic University, Tomsk, Russia*

A numerical simulation of the electrical breakdown in dynamic mode of single crystals of ammonium perchlorate has been carried out. The system of differential equations was solved, which describes the processes in the equivalent circuit of the pulse voltage generator together with the kinetic equation of impact electron multiplication and the heat balance equation. The dependences of the electric strength of ammonium perchlorate in dynamic mode on the interelectrode distance (Fig. 1) and the duration of the leading edge of a high voltage pulse (Fig. 2) were calculated. Obtained numerical simulation results are in good agreement with the known experimental data of electrical breakdown of ammonium perchlorate in the dynamic mode.

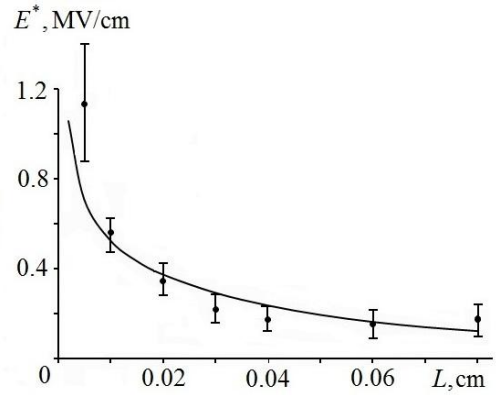

Fig. 1. The dependence of the electric strength of ammonium perchlorate on the interelectrode distance L at $\tau = 1.5$ μs : points – experiment [1], line – calculation.

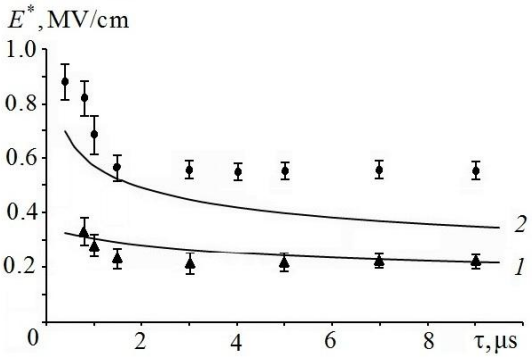

Fig. 2. The dependence of the electric strength of ammonium perchlorate as a function of duration of the front edge of the voltage pulse at L = 0.03 (1) and 0.01 cm (2): ▲, ● – experiment [2]; line – calculation.

REFERENCES

[1] Khaneft I. G., and Khaneft A. V. The effect of interelectrode distance on the electrical breakdown of single crystals of ammonium perchlorate. Tech. Phys. Vol. 40. No. 6, pp. 631–633, 1995.

[2] Khaneft I. G., and Khaneft A. V. Effect of the Duration of the Front Edge of the Voltage Pulse on the Electric Breakdown of Ammonium Perchlorate. Tech. Phys. Vol. 45. No. 4, pp. 423–426, 2000.

* This work was supported by the Russian Science Foundation [grant number 18-13-00031].

NEW PERSPECTIVES OF PHOTOCHEMICAL PROCESSES FOR LASER IGNITION OF ENERGETIC MATERIALS[1]

ANTON S. ZVEREV[1], ANATOLY Y. MITROFANOV[2], ROMAN TSYSHEVSKY[3], NATALYA N. ILYAKOVA[2], SERGEY V. LUZGAREV[2], MAIJA M. KUKLJA[3]

[1]Institute of Coal Chemistry and Material Science SB RAS, Kemerovo, Russia
[2]Institute of Basic Sciences, Kemerovo State University, Kemerovo, Russia
[3]Department of Materials Science and Engineering, University of Maryland, College Park, USA

Laser initiation of high energy density materials provides exciting new opportunities in fundamental science and applied technology for various applications, especially those relevant to improving safety of producing and using high explosive materials and devices. The development of energetic materials (EM) resistant to shock and heat but sensitive to laser radiation is a main goal of this research. The most common way to increase the sensitivity of the energetic material to laser radiation is the introduction of opaque particles, which are heated or exploded (ablated) under the laser radiation. However, with this approach, the final initiating stimulus is still impact or heating. Thereby effectiveness of this technique decreases with decreasing of an energetic material sensitivity.

We propose and discuss approaches of the energetic materials sensitization to laser radiation by introducing photocatalytic additives. The interaction of the additive with the energetic material under the laser radiation dramatically decreases the potential barriers of the explosion reaction initial stages. We investigated the initiation of chemistry theoretically and experimentally by means of DFT calculations, UV-VIS-NIR spectroscopy and laser initiation tests. Two types of photocatalysts were probed.

The first type is a quinones widely used for photopolymerization. The driver of the EM decomposition is a reaction of hydrogen transfer from the EM molecule to the n-π photoexcited quinone. We discovered that quinone added to Pentaerythritoltetranitrate triggers an unusual decomposition pathway, which would require much higher energy in pristine PETN. The hydrogen abstraction is followed by an immediate loss of the NO 2 group. The exothermic reaction proceeds with the energy release of 1.63 eV, which is sufficient to induce thermal decomposition of neighbor PETN molecules in its ground state via the conventional cleavage of the O-NO 2 bond.

The second type of photocatalysts is wide-gap metal oxides. Basis of photocatalytic process is a charge transfer at the interface between the metal oxide and energetic material leading to the formation of the metastable energetic ion. The exothermic decomposition reaction of a metastable intermediate drives an explosive initiation, similarly to the mechanism described above.

Optical absorption spectra and laser initiation thresholds of PETN-MgO and PETN-ZnO composites were determined. The interactions between the oxide surface and EM molecules lead to a charge transfer on the interface, which is indicated by the presence of new bands in the composite absorption spectrum that cannot be explained by the absorption of individual components. The optical transitions of composites are in good agreement with the energy gaps calculated by quantum chemical methods.

The laser initiation thresholds of all the composites are noticeably lower than the pure PETN initiation threshold under the same conditions. This research demonstrated how the laser excitation can be effectively used for photoinitiation of explosive decomposition and how control (or tuning) over the initiation of explosive decomposition can be gained.

1 The reported study was funded by RFBR, project number 19-33-60013.

MARKS ON SINGLE-CRYSTAL COPPER CATHODES AFTER SHORT-PULSE VOLTAGE IMPACT ON VACUUM GAPS [*]

E.V. NEFEDTSEV, S.A. ONISCHENKO

Institute of High Current Electronics SB RAS, Tomsk, Russia

At present, a new view is being forming on the problem of vacuum breakdown initiation, which is, the factor of electrical strength limitation of vacuum gaps should be sought not only on the surface, but also inside surface layer of electrode material. Recent theories indicate that the initiators of the vacuum breakdown may be defects of crystal structure of electrode material, most likely the dislocations [1]-[3]. In works [4]-[6] we obtained some experimental confirmations, that plastic phenomena play a certain role in vacuum breakdown initiation. However, at the moment there are no direct experimental evidences that dislocation phenomena or dislocations themselves may be among initiators or driving factors of vacuum breakdown.

In present work, the objects of experimental research were vacuum gaps with electrochemically polished particularly pure single-crystal copper cathodes. Vacuum gaps were exposed to short (20 ns) voltage pulses of high (200 kV) and low (25 kV) voltage amplitudes. The main goal was to study a spatial correlation of micro-explosion erosion sites caused by vacuum spark with positions of dislocation outcrops that existed before the spark on cathode surface. Also we tried to reveal pre-spark morphological changes on the crystal surface under the influence of short voltage pulse with limited current load.

The results indicate that plastic phenomena occurring inside the electrode material with the participation of linear defects of crystal structure play a significant role in the development of vacuum breakdown if there are no other distinct breakdown provokers on the cathode surface (particles, inclusions, protrusions).

REFERENCES

[1] K. Nordlund and F. Djurabekova, "Defect model for the dependence of breakdown rate on external electric fields," Phys. Rev. Accel. Beams, vol. 15, pp. 071002 (1-7), 2012.

[2] E. Z. Engelberg, A. B. Yashar, Y. Ashkenazy, M. Assaf, and I. Popov. "Theory of electric field breakdown nucleation due to mobile dislocations," Phys. Rev. Accel. Beams, vol..22, pp. 083501-(1-16), 2019.

[3] A. Saressalo, A. Kyritsakis , F. Djurabekova, I. Profatilova , J. Pasz-kiewicz , S. Calatroni , and W. Wuensch.,"Classification of vacuum arc breakdowns in a pulsed dc system,"– Phys. Rev. Accel. Beams, vol. 23, pp. 023101 (1–11), 2020.

[4] E. V. Nefedtsev, S. A. Onischenko, and A. V. Batrakov, "Peculiarities of the short-pulse dielectric strength of vacuum insulation", Russian Physics Journal., vol. 60, no. 8, pp. 1437-1448, 2017.

[5] S. A. Onischenko, E. V. Nefedtsev, and D. I. Proskurovsky, "Magnetic field effect on the pulsed breakdown strength of vacuum gaps," Proc. 27 Intern. Symp. on Discharges and Electrical Insulation in Vacuum, ISDEIV-2016, – Suzhou, China, vol. 1, pp. 13-16, 2016.

[6] S. A. Onischenko, E. V. Nefyodtsev, A. V. Batrakov, and D. I. Proskurovsky, "Erosion traces on a single-crystal Si cathode in an undeveloped nanosecond vacuum breakdown", Proc. 26 Intern. Symp. on Discharges and Electrical Insulation in Vacuum, ISDEIV-2014, Mumbai, India, 2014, vol. 1, pp. 5 – 8.

[*] The work was supported by the Russian Foundation for Basic Research, Project No. 18-08-00230-A. SEM-images were obtained using the equipment of the Tomsk Regional Center for Collective Use of Scientific Equipment.

INVESTIGATION OF THE REINFORCED COMPOSITES DESTRUCTION UNDER PULSED IMPACT OF HIGH-CURRENT ELECTRON BEAM.

B.A. DEMIDOV[1], E.D. KAZAKOV[1], YU.G. KALININ[1], D.I. KRUTIKOV[1], A.A. KURILO[1], M.YU. ORLOV[1], D.N. SADOVNICHII[2], M.G. STRIZHAKOV[1], A.YU. SHASHKOV[1], K.YU. SHEREMETYEV[2]

[1]National Research Center "Kurchatov Institute", Moscow, Russian Federation
[2]The Federal center for dual-use technologies "Soyuz", Dzerzhinsky, Moscow region, Russian Federation
[3]National Research University "Moscow Power Engineering Institute", Moscow, Russian Federation

The active development of materials science leads to the emergence of new polymer and composite materials that are in demand in the space and aircraft industry. However, the features its destruction are often poorly understood. This is especially true for powerful volumetric pulsed impact. At the same time, mathematical modeling of the propagation of shock waves in materials with a complex structure is extremely difficult and requires verification. It was shown in [1-3] that the reaction of materials in this case can significantly differ from the stationary and surface cases.

This paper presents the results of a study of the destruction of a number of polymer and composite materials under high-power pulsed impact using a high-current electron beam. The features of the destruction of composite materials reinforced with carbon nanoparticles are considered. Carbon has a significant effect on the conductivity of the material, and therefore such experiments expand the understanding of the mechanisms of the action of an electron beam on dielectric targets and the effect of charge transferred by electrons on these mechanisms.

The study of plasma dynamics was carried out using laser shadowgraphy. A pulsed laser with a wavelength of 1079 nm with an active element from a single crystal of yttrium orthoaluminate with neodymium was used as a probe radiation source. The laser worked in the mode of intracavity second harmonic generation with radiation output only at a wavelength of 540 nm. The pulse energy was 90 mJ, the duration was ≈ 300 μs, the divergence did not exceed 5 mrad. Such a regime made it possible to obtain a "smooth" in time pulse of free generation, and laser radiation could be considered constant for a long period of time, including the process under study. Registration of a one-dimensional shadow image was performed using an electron-optical streak-camera. Typical plasma dynamics shadow image is presented in fig.1.

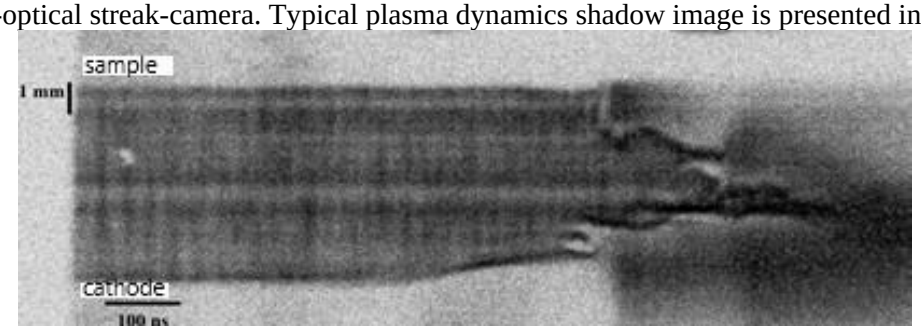

Fig. 1. One-dimensional shadow image of plasma expansion in vacuum diode gap.

A comparative study was conducted for composite and polymeric materials on the dynamics of the expansion of a substance from a sample surface upon irradiation with a high-current electron beam at the Calamary facility at currents of 30 kA and pulse durations of up to 150 ns.

To study the features of structural changes in composite materials, a JSM-6490 scanning electron microscope (Japan) was used.

The experiments at the Calamary facility were supported by the RFBR grant 18-02-00555-a.

REFERENCES

[1] *Demidov B.A., Ivkin M.V., Petrov V.A., et. al. Journal of Surface Investigation: X-Ray, Synchrotron and Neutron Techniques. 2008. - V. 2. - № 4. - P. 631-636..*

[2] *Demidov B.A., Kalinin Yu.G., Kazakov E.D. et. al. Journal of Physics: Conference Series (см. в книгах). - 2015. Vol.653.- № 1. P. 012009.*

[3] *Milekhin Yu.*M., Sadovnichii D.N., Sheremetyev K.Yu. et al. Doklady Chemistry. – 2019 – Vol. 487. – Part 1. – P.184-186.

HYFROGEN GAS DESORPTION FROM TITANIUM MODIFIED WITH SEQUENTIAL DUAL $^{4}He^{+}$ AND $^{1}H_{2}^{+}$ ION IMPLANTATION

S.M.DUVANOV, S.N.DANILCHENKO, V.D.CHIVANOV, V.I.VOZNYI

Institute of Applied Physics of NAS Ukraine, Sumy, Ukraine

The paper presents the results of an experimental study of the kinetics of gas desorption from modified surface and bulk layers of technically pure VT1-0 grade titanium using Thermally Programmed Gas Desorption with Mass Spectrometry (TPD MS). The surface layers were modified using a setup with a Penning ion source, which allows sequential implantation of $^{4}He^{+}$ and $^{1}H_{2}^{+}$ ions under the same vacuum conditions and at close to indoor integral temperature values of the substrates. The implantation energy of helium and hydrogen ions was 8 and 7.5 keV, respectively, at a fluence of ~10^{17} ions/cm^{2}. The dependences of the ion current of desorbed H_2 molecules from Ti samples vs the heating temperature in vacuum on a double logarithmic scale showed: 1) a shift in the start of low-temperature desorption (SLTD) of hydrogen to the low temperature range from samples modified with ion implantation by 300°C compared with the case of electrolytically saturated (ELS) samples with hydrogen; 2) the high-temperature desorption peak at ~900°C is in good agreement with that during hydrogen desorption from ELS and control samples; 3) there was a difference in the shift of SLTD of hydrogen from samples modified only with hydrogen implantation and hybrid ion treatment. Using SRIM2008 programs, the ion ranges and vacancies depth distribution were estimated after ion implantation with individual and dual ion bombardment regimes. The obtained TPD MS hydrogen curves are in good agreement with the literature data and with the phase diagram (PD) of the Ti-H system. Meanwhile, in order to elucidate the details of the TPD MS curves in the case of electrolytic processing of samples, a PD feature of the ternary Ti-H-O system is required. Complementary experiments are also required for non-destructive analysis of the elemental and phase composition of the surface layers of the samples, as well as calculations for estimating the activation energies and reaction orders underlying the observed processes. The applicability of the application of ion-beam processing of samples on this type of equipment for conducting correct imitation experiments of reactor materials in accordance with the recommendations of the ASTM standard is discussed.

THERMAL BREAKDOWN OF THE INSULATOR WITH A STATIONARY MeV $^4He^+$ MICROBEAM

S.M. DUVANOV

Institute of Applied Physics NAS Ukraine, Sumy, Ukraine

A thermal breakdown (TBD) of the "thin-film-nanocomposite-based-on-a-polycrystalline-corundum (PCC)/substrate-from-a-PCC" system (ThF_nc-Al_2O_3/Al_2O_3 system) was observed during its irradiation with a stationary, 3 micron diameter $^4He^+$ ion microprobe (MP) at current of ~300 pA in a scanning mode. The studied system was a gradient electrically conductive composite nanostructured thin film (ECThF) created on a surface of the PCC matrix (α-Al_2O_3) [1]. ECThF was obtained by hybrid ion beam treatment of substrates using MEVVA implantation of 50 ... 150 keV $Ti^{+,++,+++}$ ions with and without subsequent irradiation with a swift, multiply charged 90 MeV Kr ions (SHII irradiation and/or annealing) . For high-current irradiation of the ThF_nc- Al_2O_3/Al_2O_3–system, stationary focused MPs of $^4He^+$ and $^1H^+$ ions with an energy of ~1 MeV were used. All types of particle beam irradiation were performed at room temperature of the substrates. The optical microscopy technique was applied to study the morphology of surfaces in the irradiation zones by MP's impacts and outside them. On the surface of the samples in the areas of its MP $^4He^+$ bombardment, melted, colored regions with a diameter of ~1 mm were found with macro- and microscopic details related to typical ionic crystal's TBDs created with pulsed high-current electron beams. A difference was also found in the effect of irradiation on a surface of the samples subjected to and without SHII irradiation. Moreover, ceteris paribus, TBD effect was absent in the case of its irradiation with $^1H^+$ MP. Using the SRIM2008 code, projective ranges, ionization losses, and a depth distribution of the vacancies under bombardment with MeV ion microbeams of the α-Al_2O_3 matrix were simulated. Further detailed study is required of the 3D distribution of the elemental and phase composition of the melted regions, as well as an estimation of the local stationary temperature values at the MP bombardment zone of the targets. The reason for the differences in the effect of MPs of different types of ions on the studied system, the applicability of MPs of $^4He^+$ MeV ions as a non-destructive analytical technique, as well as possible applications of the observed effect, and as well as those already realized in practice as, for example, in [2,3] are discussed.

REFERENCES

[1] S.M. Duvanov, A.G. Balogh, "Two-stage diffusion and nanoparticle formation in heavily implanted polycrystalline Al_2O_3", Nuclear Instruments and Methods in Physics Research Section B: Beam Interactions with Materials and Atoms, vol.171, 475-480, 2000.

[2] V.I. Gushenets, A.G. Nikolaev, E.M. Oks, K.P. Savkin, G.Y. Yushkov, I.G. Brown, "High-energy metal ion implantation for reduction of surface resistivity of alumina ceramic", Review of Scientific Instruments, vol. 83(2), 02B908, 2012.

[3] M. Zhu, F. Song, F. Li, X. Jin, X. Wang, L. Wang, "Surface insulating properties of titanium implanted alumina ceramics by plasma immersion ion implantation", Nuclear Instruments and Methods in Physics Research Section B: Beam Interactions with Materials and Atoms, vol.407, 155–159, 2017.

CHAIN REACTION OF AZIDE HEAVY METALS EXPLOSIVE DECOMPOSITION IN CONSTANT ELECTRIC FIELD

V.G. KRIGER, A.V. KALENSKII, P.G.ZHURAVLEV, M.V.ANANYEVA, R. A. KAEPKULOV

Kemerovo State University
Krasnaya 6, Kemerovo, 650043, e-mail: kriger@kemsu.ru

Decomposition and explosion of azide heavy metals in contact electric field are observed in relatively weak fields. In system *Ag-AgN₃-Ag* (the interelectrode distance is 0.1 cm) decomposition begins at $U \sim 100V$, at $U \geq 150V$ crystal explodes in 2-5 min [1]. The authors supposed that the main reason of abnormally high sensitivity of initiating explosives (in particular, heavy metal azides) to stationary external influences (heating, irradiation, electric field) is the development of a branched chain reaction in the crystal. In [2] authors analyze a model of a branched solid-phase chain reaction, there the active particles are not only excitations of the electronic subsystem, but also intrinsic defects of the crystal lattice.

During the monopolar injection of holes into the sample, the localization of two azide radicals on the cationic vacancy leads to the formation of the N_6 complex, the decay of which is the main stage of energy release, leading to the development of the chain $N_6 \rightarrow 3N_2^*$. Relaxation of the excited nitrogen molecule leads to the formation of either an electron-hole pair or a pair of Frenkel defects in the neutral charge state [3]. The stages of chain interruption are the recombination reactions of electron-hole pairs and pairs of Frenkel defects.

The model was analyzed, the energy position of the defect levels in the band gap of AgN_3 was determined, and the speed constants of the electron - hole transition stages were calculated. The energies of formation and migration of defects are determined using the barometric dependences of ion conductivity in the terms of the Zener theory. Calculations and comparison with the experiment of current-voltage characteristics and the decomposition speed of AgN_3 in an electric field were made. Critical conditions for the initiation of AgN_3 explosion decomposition during monopolar injection of the main charge carriers are determined.

REFERENCES

1. Zakharov V.Yu., V.I. Krasheninin Slow decomposition of silver and lead azides. – Tomsk: Publishing house of scientific and technical literature. – 2006.-p. 16.
2. V.G. Kriger, A.V. Kalenskii, V.V. Velk Self-imperfection model of azide heavy metals decomposition. // Izvestiya vysshikh uchebnykh zavedenii. Fizika. – 2000. –V.43. – No 11. – pp. 118–123.
3. V.G. Kriger, A.V. Kalenskii, and A.A. Zvekov Relaxation of Electronically Excited Products of Solid State Reactions in the Crystal Lattice // Khimicheskaya Fizika – 2012. – Vol. 31. – No.1. – pp. 18–22.

REGULARITIES OF EXPLOSION DECOMPOSITION PRODUCTS EXPANSION AND THE NATURE OF EXPLOSION OF HEAVY METAL AZIDES

V.G. KRIGER, A.V. KALENSKII, P.G.ZHURAVLEV, M.V.ANANYEVA, R. A. KAEPKULOV

Kemerovo State University
Krasnaya 6, Kemerovo, 650043, e-mail: kriger@kemsu.ru

Measuring the rate of expansion of explosion products is an important step in determining nature of the explosion. A number of works are devoted to this topic [1]. The authors measured the speed of the leading edge of the blast wave. Measured values are in the range 2-5 km/s, but the nature and their distribution over the propagation speeds were not determined.

The authors [1] supposed that the products of azide heavy metals explosion are dense low-temperature plasma, whose radiation spectrum is continuous, and can be characterized by a single temperature value. In this case, the product spread rates should be distributed by Maxwell's low. Thus, the thermal nature of the explosion is actually postulated. In [2] high-speed mass spectrometry methods were used to determine the rates of product expansion (N_2, N_3, N_6, Pb, O_2, CO_2, etc.) of a thermal explosion of a mixture of lead stifnate and azide. The explosion was initiated by a hot spiral.

The aim of this work is to analyze the results [2] and determine the parameters of the distribution of products by the speed of expansion in the explosion wave. The separation rates of products vary from 2 to 6 km/s. The maximum separation rates of the main products (N_2, N_3, N_6, Pb) are $\approx 3.6 \pm 0.2$ km/s. The experimental distribution of molecules by speed shows that neither the distribution of individual molecules nor their aggregate corresponds to the Maxwell distribution. The explosion products are not low-temperature plasma, and cannot be characterized by a single temperature value. The speed distribution of individual particles obeys the Gauss distribution. At the same time, the dispersion of the product distribution by speeds normalized for the maximum speed is equal to 0.206 ± 0.013, which is about 2 times less than the corresponding values for Maxwell distributions.

Thus the nature of the explosion of heavy azides is not thermal even when the process is thermally initiated.

REFERENCES

1. Korepanov V.I., Lisitsyn V.M., Oleshko V.I., Tsipilev V.P. // Combustion, Explosion, and Shock Waves. – 2006. – V. 42 (1). – pp. 94-106.
2. Trinks H., Schilf N. //Gasdyn., Detonation and explosion tech. New-York. – 1981. – N9.– pp. 242 – 252.

SPECTRAL-KINETIC CHARACTERISTICS GLOW OF FAT COAL AT DIFFERENT STAGES OF LASER IGNITION*

ADUEV B.P., NURMUKHAMETOV D.R., KRAFT Y.V., BELOKUROV G.M.

Institute of Coal Chemistry and Material Science at Federal Research Center of Coal and Coal chemistry SB RAS, 18 Sovetsky ave., Kemerovo, Russia, 650000

In our previous work [1], ignition of fossil fuels with particle sizes <63 μm of various degrees of coalification by neodymium laser pulses in the free-running mode (1064 nm, 120 μs) was studied. Three stages of ignition having a threshold character are distinguished. The first stage involves the heating of the surface of the sample and the ignition of microprotrusions on coal particles during the action of a laser pulse. The second stage is associated with the release and ignition of volatile substances. The third - with the ignition of a non-volatile residue. Ignition thresholds H_{cr} for fat coal at different stages, respectively: $H_{cr}^{(1)}$ = 0.47 J/cm^2, $H_{cr}^{(2)}$ = 1.1 J/cm^2, $H_{cr}^{(3)}$ = 5.5 J/cm^2.

In this work, we studied the spectral-kinetic characteristics of the glow of fat coal (grade "Zh") at all stages of ignition in real time. The main elements of the recording system include a polychromator and a streak-camera, which scans the emission spectra over time. We studied samples with a bulk density of 0.6 g/cm^3.

It was shown that the emission spectrum of the sample surface has a thermal character and is approximated by the Planck formula at a temperature of 3500 K.

The kinetics of the flame glow at a distance of 2 mm from the surface of the sample when exposed to laser radiation with an energy density of 2 J/cm^2 is shown in Fig. 1. Measurement of the spectrum at the first maximum ~ 0.5 ms after the start of the laser pulse made it possible to relate the observed glow to excited water molecules. In a narrow time range, 0.7 ms from the beginning of the laser pulse, it is possible to observe a more complex spectrum of volatile substances. As in [1], a glow of the CO flame and excited water and hydrogen molecules is observed in this spectrum. At a time of 0.9 ms, a thermal spectrum with a temperature of 2500 K.

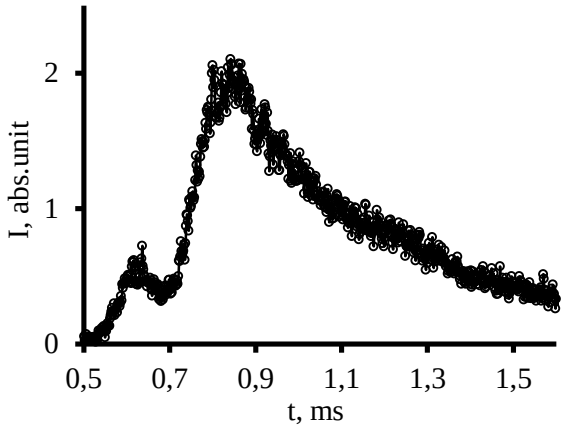

Fig. 1. Oscillogram of the glow of volatile substances of fat coal under the influence of laser radiation with an energy density of 2 J/cm^2.

In the third stage of laser ignition, when exposed to an energy density of 8 J/cm^2, a vertical flame is observed associated with the ignition of the main non-volatile residue. The spectrum of the glow of the flame after 30 ms from the beginning of the laser flame at a distance of 10 mm from the surface of the sample is thermal in nature and is due to the emitted hot carbon particles at a temperature of 1800 K.

REFERENCES

1 B. P. Aduev, D. R. Nurmukhametov, Y. V. Kraft, and Z. R. Ismagilov, “Ignition of Different Metamorphic Grade Coals by Free-Running Laser Pulses,” *Opt. Spectrosc.*, vol. 128, no. 3, pp. 429–435, 2020.

* The research was carried out with the financial support of the Russian Foundation for Basic Research (project 20-43-420019 r_a) and in the framework of the program of fundamental researches of the Institute of Coal Chemistry and Material Science (project V.49.1.5., AAAA-A17-117041910150-2)

MICROWAVE-INDUCED SELF-ORGANIZATION OF MINERAL LIOPHYLIC COLLOIDS

O.V.GRADOV[1], *M.A. GRADOVA*[1]

[1]*N.N. Semenov Federal Research Center of Chemical Physics, Russian Academy of Sciences, Moscow, Russia*

In this report we consider a multifactor nature of the self-organization processes of soft matter dissipative microstructures from the iron-containing colloidal precursors with different particle size under microwave irradiation. The resulting structures' morphology determined by the dehydration-aggregation processes under the microwave field, as well as their phase state, chemical composition and the degree of crystallinity, were shown to be dependent on the irradiation time, the microwave power and the particle size of the initial colloidal precursor. The latter included sols of iron(II,III)hexacyanoferrate(II,III) also known as Prussian blue [1,2], saturated ferric chloride solutions [3-5], FeOOH sols obtained from $FeCl_3$ and Na_2CO_3 solutions [6-9]. Interesting erosion and reticulation effects were observed on the surface of the irradiated area of Prussian blue [2]. Microwave-induced self-organization of membraneous structures with different morphology in hydrolized $FeCl_3$ colloidal systems was registered at the microwave power of 200 W. The local microwave treatment conditions and the precursor layer thickness determined the type of emerging structures in the above experiments. Membraneous structure self-organization in saturated $FeCl_3$ solutions under microwave treatment occurred due to dehydration and hydrolytic polycondensation of ferric oxohydroxides at 450 W [3,4]. A gentle 1 min microwave treatment of the colloidal precursor resulted in a variety of soft matter structures' formation, while the longer exposure led to either amorphous or partially crystallized mineral patterns. Microwave-induced self-organization in iron(III)-containing colloids under high irradiation power (800 W) was strongly dependent on the layer thickness of the precursor (saturated ferric chloride solution) and resulted in less diversity of membraneous structure morphologies because of the too fast water evaporation preventing hydrolytic polycondensation and favoring simple crystallization of the mineral phases [5]. Microwave-induced self-organization of ferric hydroxide colloids obtained from ferric chloride and sodium carbonate solutions resulted in the crystallization of different mineral phases, including the excess sodium carbonate, with the crystal morphology depending on the microwave irradiation power and irradiation time [6-9]. Some of the structures obtained were shown to contain such mineral phases as acageneite (β-FeOOH), ferrihydrite, goethite (α-FeOOH), hematite, lepidocrocite (γ-FeOOH), maghemite, etc.

REFERENCES

[1] O. V. Gradov and M. A. Gradova, "Microwave-induced self-organization in mineral systems. I. Prussian blue (2.45 GHz; 450 W; 3 min)," in Pangaea [Dataset], Microwave-induced self-organization in mineral systems, Alfred Wegener Institute - Helmholtz Center for Polar and Marine Research - CMES, University of Bremen, 2019. DOI: 10.1594/PANGAEA.897646

[2] O. V. Gradov and M. A. Gradova, "Microwave-induced self-organization in mineral systems. II. Prussian blue (conentrated sol; 2.45 GHz | 450 W | 2 min). Erosion and reticulation," in Pangaea [Dataset], Microwave-induced self-organization in mineral systems, Alfred Wegener Institute - Helmholtz Center for Polar and Marine Research - CMES, University of Bremen, 2019. DOI: 10.1594/PANGAEA.897647

[3] O. V. Gradov and M. A. Gradova, "Microwave-induced self-organization in mineral systems. III. $FeCl_3$ colloid (200 W, 2.45 GHz, 1 min)," in Pangaea [Dataset], Microwave-induced self-organization in mineral systems, Alfred Wegener Institute - Helmholtz Center for Polar and Marine Research - CMES, 2019. DOI: 10.1594/PANGAEA.897648

[4] O. V. Gradov and M. A. Gradova, "Microwave-induced self-organization in mineral systems. IV. $FeCl_3$ colloid (450 W, 2.45 GHz)," in Pangaea [Dataset], Microwave-induced self-organization in mineral systems, Alfred Wegener Institute - Helmholtz Center for Polar and Marine Research - CMES, University of Bremen, 2019. DOI: 10.1594/PANGAEA.897649

[5] Gradov, O. V. and Gradova, M. A. (2019). Microwave-induced self-organization in mineral systems. V. $FeCl_3$ colloid (800 W, 2.45 GHz, 30 sec.). In Pangaea [Dataset], Microwave-induced self-organization in mineral systems. Alfred Wegener Institute - Helmholtz Center for Polar and Marine Research - Center for Marine Environmental Sciences, University of Bremen. DOI: 10.1594/PANGAEA.897651

[6] O. V. Gradov and M. A. Gradova, "Microwave-induced self-organization in mineral systems. VI. Saturated FeOOH sol obtained from $FeCl_3$ and Na_2Co_3 solutions (2.45 GHz; 200W; 1 min)," in Pangaea [Dataset], Microwave-induced self-organization in mineral systems, Alfred Wegener Institute - Helmholtz Center for Polar and Marine Research - CMES, University of Bremen, 2019. DOI: 10.1594/PANGAEA.897652

[7] O. V. Gradov and M. A. Gradova, "Microwave-induced self-organization in mineral systems. VII. Diluted FeOOH sol obtained from $FeCl_3$ and Na_2Co_3 solutions (2.45 GHz; 200W; 1 min)," in Pangaea [Dataset], Microwave-induced self-organization in mineral systems, Alfred Wegener Institute - Helmholtz Center for Polar and Marine Research - CMES, University of Bremen, 2019. DOI: 10.1594/PANGAEA.897653

[8] O. V. Gradov and M. A. Gradova, "Microwave-induced self-organization in mineral systems. VIII. Diluted FeOOH sol obtained from $FeCl_3$ and Na_2Co_3 solutions (2.45 GHz; 300W; 1 min)," in Pangaea [Dataset], Microwave-induced self-organization in mineral systems, Alfred Wegener Institute - Helmholtz Center for Polar and Marine Research - CMES, University of Bremen, 2019. DOI: 10.1594/PANGAEA.897654

[9] O. V. Gradov and M. A. Gradova, "Microwave-induced self-organization in mineral systems. IX. Diluted FeOOH sol obtained from $FeCl_3$ and Na_2Co_3 solutions (2.45 GHz; 450W; 1 min; check experiment)," in Pangaea [Dataset], Microwave-induced self-organization in mineral systems, Wegener Institute - Helmholtz Center for Polar and Marine Research - CMES, University of Bremen, 2019. DOI: 10.1594/PANGAEA.897650

PYROLYSIS OF DEMINERALIZED LIGNITE UNDER THE LASER RADIATION EXPOSURE

KRAFT Y.V.[1], NURMUKHAMETOV D.R.[1], ADUEV B.P.[1], ISMAGILOV Z.R.[1,2]

[1]Institute of Coal Chemistry and Material Science at Federal Research Center of Coal and Coal chemistry SB RAS, 18 Sovetsky ave., Kemerovo, Russia, 650000

[2]Boreskov Institute of Catalysis SB RAS, 5 Lavrentiev ave., Novosibirsk, Russia, 630090

Coal gasification allows solving the complex problem of rational use of coal, especially lignite. It was shown in [1] that additives of alkali and alkaline earth metal compounds introduced into coal have a catalytic effect on the pyrolysis process. In this regard, the lignite of the Kaychakskoye field is of particular interest for gasification, since its ash contains a high content of CaO (23.1%). In this work, we investigated the possibility of carrying out laser pyrolysis of demineralized coal.

The study of thermal decomposition of Kaichak lignite (Kuznetsk coal basin, Russian Federation) under the pulsed laser radiation exposure in the energy density range from 1.15 to 1.95 J/cm^2 was performed. Coal demineralization was carried out by acid decomposition in concentrated nitric acid, followed by filtration and washing the residue to a neutral pH. The results of proximate analysis of coal are as follows: moisture content W^a = 8.3%, ash content A^d = 1.1%, content of volatile matter V^{daf} = 46.6%. For the preparation of samples, coal particles with a size of ≤ 100 μm were used. By mould pressing method, coal samples in the form of tablets were obtained. As a source of laser radiation, a YAG:Nd^{3+} laser operating in the free-running mode at a wavelength of λ = 1064 nm was used. The experiment was carried out in an argon medium. The following pyrolysis gases were recorded by mass spectrometry method: H_2, CH_4, H_2O, CO, CO_2. In the studied range of laser radiation energy density, the concentration of carbon monoxide and hydrogen in the composition of gaseous pyrolysis products increases with increasing energy density in a pulse, and the concentration of carbon dioxide and water vapor, on the contrary, decreases. The methane concentration values are close to constant. At the increase in energy density in an impulse in the range of 1.15-1.95 J/cm^2, the yield of combustible components increases and reaches $0.3 \cdot 10^3$ cm^3/g under the exposure with an energy density in an impulse of 1.95 J/cm^2. The sum of combustible components in the mixture of end products of pyrolysis under the exposure with an energy density in an impulse of 1.95 J/cm^2 reaches 65%.

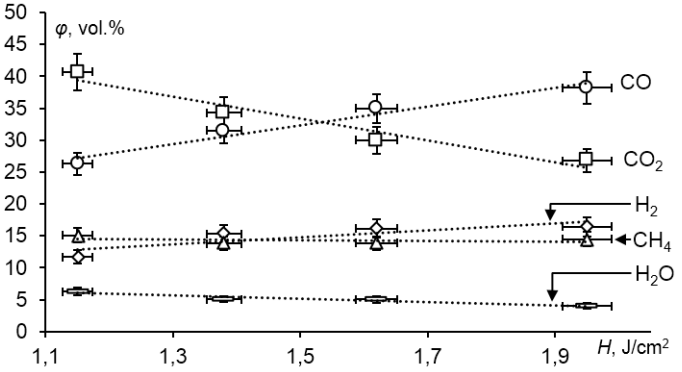

Fig. 1. Dependence of composition of gas mixture on the energy density of laser radiation

Previously, a study was conducted of laser pyrolysis of non-demineralized Kaychak lignite. The yield of combustible components from non-demineralized coal is much higher than from demineralized coal, therefore, it can be concluded that the mineral mass of Kaychak lignite affects the reactivity of its organic mass.

Considering the obtained results, it is possible to note the prospect of using low-metamorphosed high-ash coals for laser pyrolysis.

REFERENCES

[1] Li, S. // Fuel. – 1995. – Vol. 74. – No. 3. – pp. 456-458.

PHOTO-ACOUSTIC AND EXPLOSIVE CHARACTERISTICS OF THE RDX-NI COMPOSITES UNDER THE PULSE LASER IMPACT[1]

ADUEV B.P., NURMUKHAMETOV D.R., NELYUBINA N.V., LISKOV I.YU.

Institute of Coal Chemistry and Material Science at Federal Research Center of Coal and Coal chemistry SB RAS, 18 Sovetsky ave., Kemerovo, Russia, 650000

The work is devoted to research into laser (1064 nm, 14 ns) initiation of RDX-Ni nanoparticles' composites' explosion. The light absorption was studied using photoacoustic approach. The measured linear absorption coefficient k_{eff} is proportional to the weight fraction of Ni nanoparticles in the composites. It corresponds to the absorption of radiation by Ni particles in the scattering medium. The dependence of amplitude of a signal of a piezodetector on the concentration of Ni inclusions has nonmonotonic character. The optimal concentration is n_{opt} = 0.3 mass% when amplitude is maximum. The thresholds of explosive decomposition have nonmonotonic character when laser initiates RDX-Ni composite depending on the concentration of inclusions. The minimal threshold H_{cr}=0.2 J/cm^2 is observed if the concentration n_{opt}=0.3% by mass when the amplitude of pressure is maximum. The regularities described above are explained by the transition from the mode of instant (adiabatic) excitement to quasi stationary with the absorption of pulse laser radiation when the expansion of a layer begins during the pulse where the energy absorption takes place. To initiate the explosion of composite material, it requires to perform the following conditions: (1) the absorption of radiation by Ni particles at necessary concentration and initiation in their region of exothermic reaction with the heat and gases emissions; (2) the increase of pressure in the irradiated layer and the formation of a shockwave when gas-dynamic distressing is being blocked.

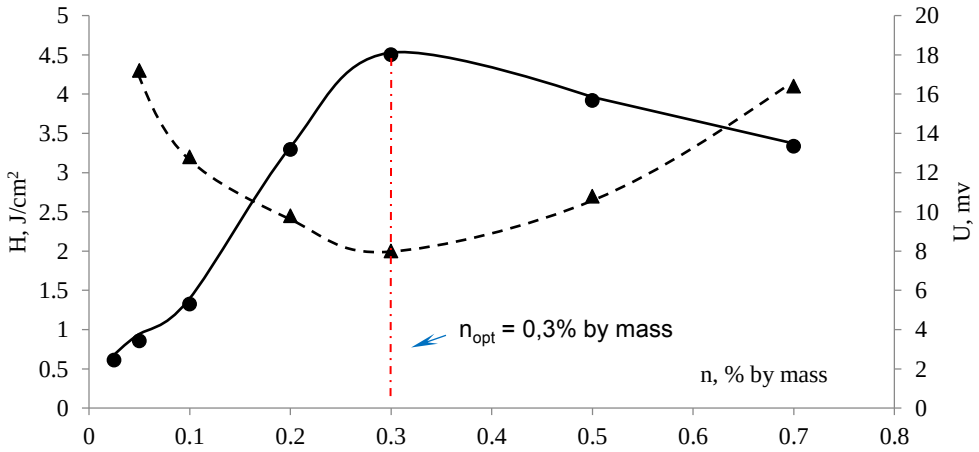

Figure 1. Left: The experimental dependence of the RDX-Ni composites' initiation critical energy density of the laser pulse on the weight fraction of Ni nanoparticles. Right: The amplitude of the photoacoustic response of RDX-Ni pressed composites vs. weight fraction of Ni nanoparticles.

[1] The research was carried out with the financial support of the Russian Foundation for Basic Research (project 18-03-00421 A)

.

THE EFFECT OF ALUMINIUM AND MOLYBDENUM FILM THICKNESS ON IGNITION OF ORGANIC EXPLOSIVES WITH A LASER PULSE*

A. V. KHANEFT[1,2], *S. A. RYBIN*[1]

[1]*Kemerovo State University, Kemerovo, Russia*
[2]*National Research Tomsk Polytechnic University, Tomsk, Russia*

The results of numerical ignition simulation of pentaerythritol tetranitrate (PETN), cyclotrimethylene trinitramine (RDX), cyclotetramethylene tetranitramine (HMX) and 1,3,5 - triamino - 2,4,6 – trinitrobenzene (TATB) by aluminium (Al) and molybdenum (Mo) films heated by nanosecond laser pulses in a three-layer system: glass - metal – explosive material (EM) are presented. Influence of metal film thickness on the time of EM ignition delay is considered. A non-linear dependence of time of delay of ignition of EM from on thickness of a metal film is shown (Fig.). The greatest critical thicknesses of Al and Mo metallic films in which ignition of EM is still possible are determined (Tabl.).

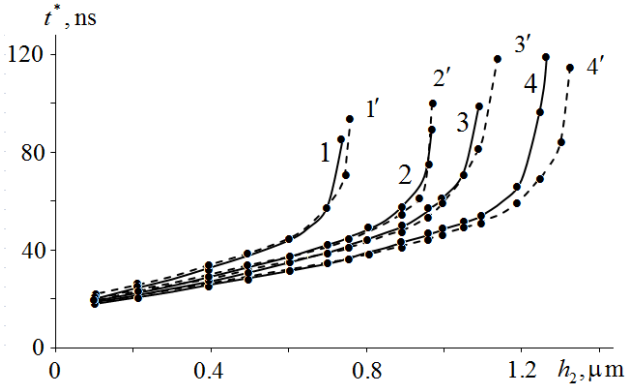

Figure. Dependence of the EM ignition delay time on Mo and Al film thickness: TATB (1, 1'), HMX (2, 2'), RDX (3, 3') and PETN (4, 4').

Table. Dependence of EM ignition delay time t^*, temperature ΔT_s and heat flux density q_s on of critical metal film thickness h_2^*.

	EM	TATB	HMX	RDX	PETN
Al	h_2^*, μm	0.76	0.985	1.125	1.325
	t^*, ns	94.1	97.0	105.0	112.1
	ΔT_s, K	800.0	643.0	626.0	522.0
	q_s, 10^9 W/m^2	1.77	1.06	0.624	0.747
Mo	h_2^*, μm	0.75	0.985	1.1	1.275
	t^*, ns	87.6	92.1	101.9	119.7
	ΔT_s, K	801.0	650.0	621.0	532.0
	q_s, 10^9 W/m^2	1.8	1.18	0.58	0.896

It has been found that the greater the thickness of the metal film and the thermal stability of the EM, the greater the heat reserve is needed in the metal film to ignite the EM. The calculations show that the delay time of the ignition of an EM by laser pulse in a three-layer system increases in the sequence of PETN, RDX, HMX and TATB.

* This work was supported by the Russian Science Foundation [grant number 18-13-00031].

PHYSICO-MATHEMATICAL MODELING AND EXPERIMENTAL STUDY OF CRACKS IN CONCRETE OBTAINED BY EXPOSURE TO A PULSED HIGH VOLTAGE DISCHARGE*

LONG CHE[1], XIAOHUI GU[1], HONGDA LI[2], S.A. SOSNOVSKIY[3], A.A. LUKANIN[4], V.I. SACHKOV[5], M.A. KAZARYAN[6]

[1]*School of Mechanical Engineering, Nanjing University of Sci. & Tech, Nanjing, China*
[2]*School of Equipment Engineering, Ph.D., assistant professor, Shenyang Ligong University, Shenyang, China*
[3]*Candidate of Physical and Mathematical Science, Senior Researcher, National Research Tomsk State University, Tomsk, Russia*
[4]*Lead Engineer, Tomsk state university of architecture and building, Tomsk, Russia*
[5] *Doctor of Chemical Sciences, National Research Tomsk State University, Tomsk, Russia*
[6] *Doctor of Physical and Mathematical Sciences, Lebedev Physical Institute RAS, Moscow, Russia*

Concrete is the most widely used material in civil construction facilities, defense engineering, and etc. The technology of concrete broken by high voltage pulse discharge uses the mechanical effects of shock wave, jet or plasma channel produced by pulse discharge to break concrete. Due to the process of concrete broken by high voltage pulse discharge is complex and there are many factors affecting its breakage effect, the mechanism of concrete broken by high voltage pulse discharge is not clear. Experiments were conducted using a high-voltage pulse discharge that destroys concrete, and the measurement of concrete crack depth on three factors, such as applied voltage, number of pulses, and discharge electrodes, was carried out at three levels. The effects of these three factors on the crack depth loss of concrete were studied by using range analysis and significance analysis test data. The results show that the effects of these three factors on the crack depth of concrete are applied voltage, pulse number and discharge electrodes gap in order from large to small. By changing the value of applied voltage and value of pulse number, the crack depth of concrete can be increased. When the applied voltage is 300kV and the pulse number is 5, the crack depth loss of concrete can be broken by high voltage pulse discharge that is the largest. The schematic diagram of the experimental system is shown in Fig. 1.a). The experimental system composed of high voltage power supply, capacitors, discharge switches, breakdown chamber, discharge electrodes, water, concrete target and oscilloscope (Tektronix). The maximum output voltage of the high voltage pulse discharge generator system is up to 300kV, and the maximum energy output of a single electric pulse is 100J. The schematic diagram of the experimental system for crack depth detection of concrete is shown in Fig. 1.b) The experimental system made up two parts: crack depth detector of concrete and concrete target. The crack depth detector is composed of detector host, plane transducer, signal connecting line, digital display screen and crack sounder scale, etc.

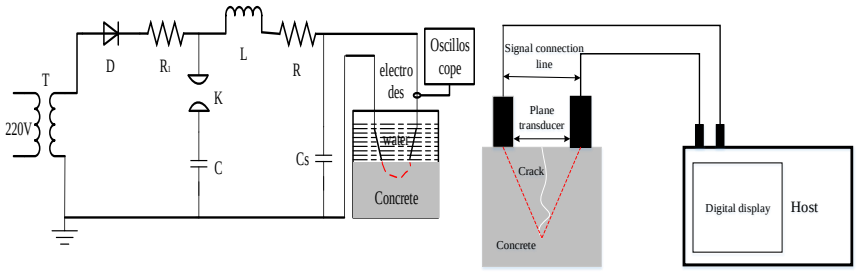

a) b)

Fig. 1.a) Schematic diagram of experiment system for high voltage pulse discharge crushing concrete; b) experiment system of crack depth detection of concrete

The report presents physical and mathematical modeling of the processes of cracking in concrete obtained by exposure to a high-voltage pulse discharge and modeling of the physicochemical processes occurring in the discharge zone. Experimental results are also presented.

* This research was funded by [National Natural Science Foundation of China] grant number [51207096] and [the Jiangsu Scientific Research Innovation Project] grant number [KYCX18_0468]. This work was supported by the National Natural Science Foundation Project (51207096) and the Jiangsu Scientific Research Innovation Project (KYCX18_0468). This research was supported by Ministry of Science and Higher Education of the Russian Federation, project No 0721-2020-0028.

EROSION OF THE LOW-VOLTAGE ELECTRODE OF AN ELECTRIC DISCHARGE REACTOR*

G. G. VOLOKITIN, S. A. GLOTOV, S. V. MELENTYEV, A. A. ALEKSEEV

Tomsk state University of architecture and civil engineering, Tomsk, Russian Federation

If we consider the structural scheme of an electric discharge installation, then its main element is an electric discharge reactor, in which the final useful work is performed. It can carry out various technological processes - dispersion of materials, disinfection of various liquids, synthesis and dissolution of materials, etc.

In this paper, the erosion of the low-voltage electrode of the reactor, the medium of which is represented by tap water, used most often in electric discharge technologies, is investigated. Structurally, the high-voltage electrode Assembly is designed in such a way that it is possible to extract it from the reactor. This technical solution allows you to evaluate the erosion of the electrode in a direct way - by measuring the loss of its mass by weighing.

A review of literature sources allowed us to establish the mechanism of electric erosion of the electrode. It was found that the mechanism of electrode erosion differs depending on the medium represented in the reactor. It is established that the electrode erosion has the maximum value if the medium is a solid. This difference can reach two orders of magnitude [1-3], which eliminates the error of the experiment.

In this paper, the erosion of the electrode is studied depending on: the grade of steel used; the interelectrode distance; the energy in the pulse; and the design features of the low-voltage electrode

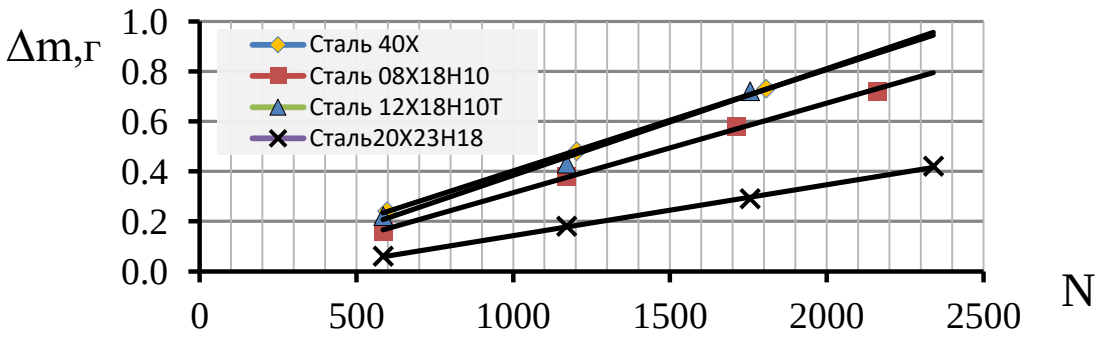

Fig.1 Dependence of the electrode mass loss Δm for different steels depending on the number of pulses n

Assembly. In addition, it shows the change in size (diameter, depth) of the erosion hole depending on the number of electric discharge pulses. The effective radius of a low-voltage electrode is determined experimentally depending on the electrical capacity of the pulse current generator. In Fig.1 shows how the weight loss of the electrode changes depending on the steels used. Both low-alloy and high-alloy steels are used for the electrodes.

The most erosion-resistant steel is the heat-resistant steel of the 20khn23h18 brand. Its erosion resistance can be higher by 2 times than, for example, steel 12X18N10T, which is probably due to the large difference in the operating temperature of these materials.

LITERATURE USED

[1] V. I. Kurets, A. F. Usov, V. A. Zukerman. Electro-pulse disintegration of materials. Apatity: Kolsk.science.center, 2002.

[2] Stepanyan, V. P.. Intensification of the process of extraction of biologically active compounds from plant raw materials by electric pulse discharges: autoref.disu...Cand.Techn.sciences'. - Tambov, 2000.- 16C.

[3] Pat.105290 Russian Federation ipcb C11B-1/10. Installation of electric pulse extraction/ N. S. Nuzhnenko. - No. 2011105497/13; declared.16.02.2011; publ.10.06.2011, Bulletin No. 24.

* The reported research was funded by Russian Foundation for Basic Research and the government of the region of the Russian Federation, grant № 18-48-703004

MONTE CARLO SIMULATIONS OF LIGHT SCATTERING IN ENERGETIC MATERIALS[1]

E.V. FORAT, V.P. TSIPILEV, A.N. YAKOVLEV

Tomsk Polytechnic University, Tomsk, Russia

A problem of understanding light distribution in energetic materials become essential due to a lack of interpretation of several effects regarding laser ignition. It was found that sensitivity of powder-like energetic materials depends on a crystals size [1, 2]. Also a difference in light stability was observed for high density laser exposure of inert materials of different crystals size [3].

From the light scattering physics, it is known that light scattering rate depends on a size of crystals and also multiple scattering process leads to an increase of space distribution value of light in media [4,5]. That position provides a basis for further investigations of dependences between a laser energy density thresholds and light distribution in diffuse scattering media [6].

The purpose of this paper is to create an understanding of dependences from previously collected data regarding laser ignition of powder mixture of ammonium perchlorate and nano-size aluminum [7, 8[1]]. Ammonium perchlorate is a typical scattering crystal medium.

A theoretical explanation of light distribution in a scattering medium has its complex difficulties. The most advanced and reliable method is Monte-Carlo simulation algorithm. An approach based of convolution algorithm suggested by V.P. Tsipilev et al. [9] allows to save significant amount of computation power at the first place. Convolution method has a few disadvantages and can be used only for rough estimations.

In the present work Monte-Carlo light distribution simulation for scattering media was conducted. The approach differs from convolution algorithm in a way of forming initial light beam. A constant concentration of photons was formed on a medium surface for whole light beam. Photons were placed randomly inside a circle of a light spot. A superposition of all photon's fates makes a full picture of light scattering inside a media and also in infinite distance from a center of the beam. Such an approach requires a significant amount computation power but it allows to increase reliability and accuracy of results.

Simulations were conducted for different laser beam diameters, different concentrations of absorbing impurities and crystal sizes. The results allowed create the full picture of light scattering and estimate the energy densities at different depth in a material.

REFERENCES

[1] A.V. Kalenskiy, V.G. Kriger, V.P. Tsipilev, M.V. Ananeva, "Dependence of initiation energy threshold of silver azide monocrystal from exposure zone diameter" (in Russian), Polzunovsky vestnik, vol 2, no. 1, pp. 75-77, 2006

[2] E. I. Aleksandrov, V. P. Tsipilev, "The size effect in laser detonation initiation in pressed lead azide. The effect of the surface energy distribution on the critical flow", Combust., Expl., Shock Waves, vol. 19(1), pp. 74-75, 1983

[3] V. V. E. Osipov, V. V. Lisenkov, V. V. Platonov, E. V. Tikhonov, "Processes of interaction of laser radiation with porous transparent materials during their ablation", Quantum Electronics, vol. 48(3), pp. 235, 2018

[4] A.G.C. Farnell, "Relationships Between Sensitometric and Optical Properties of Photographic Emulsion Layers with Particular Reference to the Wave-Length Variation of Sensitivity", The Journal of Photographic Science, vol. 7(4), pp. 83-92, 1959

[5] A.P. Ivanov, "Optics of scattering media.", 1969

[6] E. I. Aleksandrov, V. P. Tsipilev, "Dimensional effect in the initiation of compressed lead azide by single-pulse laser radiation", Combustion, Explosion and Shock Waves, vol. 17(5), pp. 550-553, 1981

[7] V.V. Medvedev, V.P. Tsipilev, E.V. Forat, "Effect of Ammonium Perchlorate and Aluminum Composition Density on Characteristics of Laser Ignition", Propellants, Explosives, Pyrotechnics, vol. 43(2), pp. 122-125, 2018

[8] V.V. Medvedev, V.P. Tsipilev, E.V. Forat, A. N. Yakovlev, "The effect of aluminum particles dispersity on characteristics of ammonium perchlorate—aluminum composition laser ignition.", Journal of Physics: Conference Series, vol. 830, no. 1, pp. 146, 2017

[9] E. I. Aleksandrov, V. P. Tsipilev, "Characteristics of the optical regime in the volume of a semiinfinite layer of diffusely scattering medium under illumination by a directed beam with finite aperture", Soviet Physics Journal, vol. 31(10), pp. 789-794, 1988

1 The work was supported by Russian foundation for Basic Research Grant 15-03-05385.

PROPERTIES OF SURFACE-IRRADIATED MEAT AND FEED[1]

R.A. VAZIROV[1,2], *S.Y. SOKOVNIN*[1,2,3], *M.E. BALEZIN*[3]

[1]*Ural State Agrarian University Yekaterinburg, Russia*
[2]*Ural Federal University, Yekaterinburg, Russia*
[3]*Institute of Electrophysics UD RAS, Yekaterinburg, Russia*

Most microbiological contamination of food and agricultural products is found on the surface or in a shallow layer. Therefore, the selection of the optimum surface treatment profile of the product is sufficient to increase shelf life and achieve the required level of biosafety.

A novel and promising method of radiation treatment and disinfection is the use of a low-energy electron beam to treat the surface layer of a product. At the same time, complete irradiation of the product is avoided, where this is not necessary, and the effect of irradiation on the product is minimized. The use of low-energy radiation also reduces the cost of the accelerator.

In order to assess the possibility of using low-energy electron beams in radiation surface disinfection, studies were carried out on semi-finished meat products, feed and premix poultry farms to put a barrier against infection and contamination of poultry with food toxicoinfections. Irradiation of products was performed on URT-1 accelerator [1] from both sides by means of turning over. The absorbed dose on the surface was measured using film dosimeters SO PD (F) R-5/50 [2]. Based on calculations and experimental results, is selected the energy of low-energy electron beam to create optimum energy release profile during irradiation.

Table 1 - Bacterial contamination of feed after treatment by low-energy electron beam

Bulk feed		Premixes of industrial production	
Dose, kGy	CFU/g	Dose, kGy	CFU/g
0	$63\ 10^4$	0	$13\ 10^4$
1.6	$8.8\ 10^3$	1.7	$4.8\ 10^3$
5.5	7.1	9.4	$3.3\ 10^3$
13.1	0.0	12.1	0.0
23.1	0.1	26.3	0.0

Table 2 - Bacterial contamination of chicken meat products after treatment by low-energy electron beam

Dose, kGy	Fillets in product packing	Liver in product packing	Hearts in product packing
	10^5, CFU/g		
0	more 10	more 10	7.7
6	6.8	-	-
8	4.4	-	7.7
11	4.3	0.37	-
18	0.85	-	6.8
22	0.072	0.0	0.97
35	0.0021	-	0.22
86	0.0	0.0	-

Microbiological studies of the product after radiation treatment show a decrease in bacteria contamination (Tables 1 and 2). Reduction of total number of microorganisms has dose-dependent effect. In the treatment of feed and premix, the number of colonies formed decreased by 6 orders at a dose of 12 kGy. In the treatment of chicken meat and by-products, a dose-dependent effect was also observed, but the decrease in contamination depended on the type of product. Summing up all of the above, we can conclude that it is promising to use URT accelerators for surface disinfection of food and agricultural products due to the possibility of obtaining the required distribution of absorbed dose in depth, high biological efficiency of low-energy electron beam and acceptable cost of accelerator.

REFERENCES

[1] Sokovnin S.Yu. Nanosecond electron accelerators for radiation technologies/ S.Yu.Sokovnin. – Yekaterinburg: Ural State Agriculture University, 2017. – 348 p. ISBN: 978-5-7691-2494-5

[2] Certificate RU.C.01.999.A No 4715

1 The study was carried out with partial financial support of RFBR and Sverdlovsk region within the framework of scientific project No 20-48-660019

KINETICS OF PYROELECTRIC GENERATION OF PULSE ELECTRON FLOWS BY LITHIUM NIOBATE CRYSTALS*

K.M. MAMBETOVA[1], *L.N. ORLIKOV*[1], *S.I. ARESTOV*[1], *S.M. SHANDAROV*[1], *N.I. BURIMOV*[1], *B.I. AVDOCHENKO*[1], *A.A. ELCHANINOV*[2]

[1]*Tomsk State University of Control Systems and Radioelectronics, Tomsk, Russia*
[2]*Institute of High Current Electronics SB RAS, Tomsk, Russia*

Usually, kinetics of pyroelectric generation of electron flows using to produce high energy x-rays on the base of lithium niobate (LN) crystals placed between two electrodes is studied with temporal resolution about 1 s [1, 2]. We have studied the pyroelectric generator of electron flows with coaxial geometry by using an oscilloscope with the sample rate of 20 GS/s.

The 13 mm diameter and 7 mm height LN crystal whose +Z face was centered on the bottom of an electrically grounded copper cylindrical cup has been used. The gap d between the –Z face of LN crystal and the copper cylindrical collector represented a central conductor of 50 Ω coaxial line was adjusted from 0.5 to 5.0 mm. This collector was loaded on a resistor with R_l = 2.2 Ω connected through a load-matching network with the 50 Ω input of digital oscilloscope TDS-6404. The bottom surface of the cup is heated by the resistive heater from 25 to 80 °C followed by natural cooling to room temperature by removing power from one. All experiments were performed at atmospheric pressure.

We observed on the oscilloscope under certain temperatures the voltage pulses with negative and positive polarities on the heating and cooling cycles correspondingly. In the former case the heating of LN crystal leads to generation of electron flow from collector to the –Z crystal face, and vice versa if LN crystal is cooled. Figure 1 shows the typical time dependences of appropriate discharge current calculated from experimental data for the gap d = 0.5 mm.

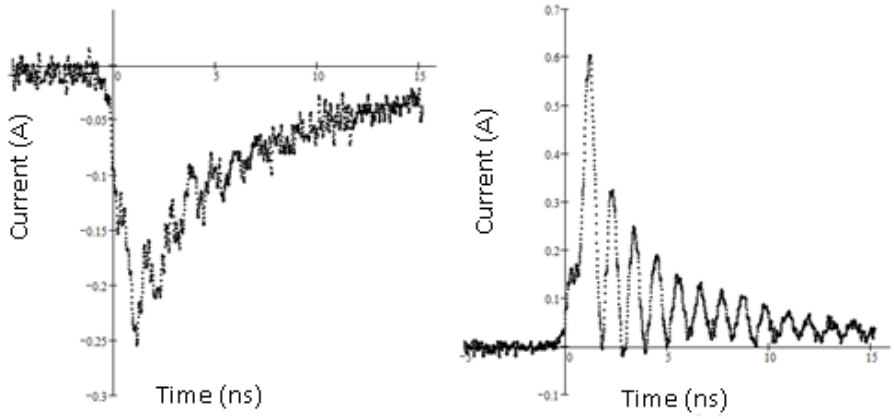

a b

Fig.1. Pyroelectric electron emission current evolution with time from –Z face of LN crystal at the gap of 0.5 mm at heating (a) and cooling (b) processes.

In summary, we have observed, what we believe to be the first time, the pulse electron flows with a nanosecond duration, a subnanosecond rising edge, and a current density reached the magnitudes more than 300 mA/cm^2 by using a coaxial geometry of pyroelectric generator on the base of Z-cut lithium niobate crystal having cylindrical shape with diameter of 13 mm and thickness of 7 mm.

REFERENCES

[1] M.J. Jonson, J. Linczer, D.B. Go, “Thermally induced atmospheric pressure gas discharges using pyroelectric crystaks,” Plasma Sources Sci. Technol., vol. 23, 065018, 2014.

[2] R. Ghaderi, F.A. Davani, “Dynamics of pyroelectric accelerators,” Appl. Phys. Lett., vol. 106, 042906, 2015.

* This work was supported by the Ministry of Higher Education and Science of the Russian Federation for 2020-2022 (State Task No FEWM–2020–0038) and by the RFBR (Grant 16-29-14046-ofi_m).

LASER SCANNING CONFOCAL LUMINESCENT POLARIZATION MICROSCOPY OF SINGLE RADIATION DEFECTS*

V.P. DRESVYANSKIY, S.A. ZILOV, A. RAKEVICH, E.F. MARTYNOVICH

Irkutsk Branch of Institute of Laser Physics SB RAS , 130 a Lermontov st., Irkutsk, 664033, Russia, E-mail: nadvp@list.ru

Color centers in various crystals are used in wide range of applications: gamma-ray detectors, track detectors of charged particles and mixed fields of nuclear radiation, optical carriers of visual and digital information, laser media and passive laser gates, thin film memory fluorescent screens for visualization and digitization of x-ray microimages. The development of new principles for spectroscopic differentiation of radiation defects that complement traditional spectral-kinetic methods and the use of new spectroscopic characteristics is relevant. This is particularly emphasized by the practical significance of radiation defects, including color centers, as model quantum systems in various fundamental studies that can be artificially created in condensed media under action of hard radiation or laser radiation.

The aim of our research is to study the possibilities of spectroscopic differentiation of distinct types of luminescent defects created by radiation in condensed media, on basis of the comparison of generalized numerical characteristics of quantum photoluminescence intensity trajectories, which are measured by confocal scanning luminescence microscopy on single defects in the mode of spatially selective time-correlated counting of single photons.

The possibility of implementing of the laser confocal scanning luminescent spectroscopy method for single radiation defects based on the characteristics of their photoluminescent trajectories and its effectiveness have been experimentally confirmed. Dynamic models of F_2 and F_3^+ centers in lithium fluoride crystals were created. We introduced an additional equation describing the reorientation of color center, based on the mathematical apparatus for the fluorescence of single molecules, in particular the equations for on- and off-intervals for a molecule with a triplet level. The calculated quantum trajectories of single F_2 and F_3^+ color centers are in good agreement with the experimental data.

By example of studying single color centers induced in the volume of a cubic crystal, it is shown that the registered polarized quantum trajectories contain information about the structure, nature, dynamics of the quantum system and its local environment. A new method of laser scanning confocal luminescence microscopy of single quantum systems located in a crystal matrix is proposed. This method is based on the analysis of the ratio of the intensities of polarized quantum trajectories (time dependences of the number of photons with vertical and horizontal polarizations registered in duration of fixed registration time). The mathematical apparatus and algorithms for analysis of polarized quantum trajectories are developed, and tables of patterns quantum trajectories are formed for all possible types of single color centers (quantum systems) in a cubic crystal.

* The work was supported by Project № 0307-2016-0004 of the program of fundamental scientific research of the State Academies of Sciences for 2013-2020, section II.10.1, and by project № 17-52-44015 Mong_a of Russian Foundation for Basic Research and Mongolian Ministry of Education, Culture, Science and Sports.

NONLINEAR PROPERTIES CRYSTALLINE Er:BaY_2F_8 MEDIUM AT FEMTOSECOND LASER AND ELECTRON-BEAM PUMPING

V.I. BARYSHNIKOV[1-2], O.V. GOREVA[1], O.L. NIKONOVICH[1]

[1]Irkutsk State Transport University, Irkutsk, Russia
[2]Irkutsk Filial of Laser Physics Institute at SB RAS, Irkutsk, Russia

The crystallographic structure and nonlinear susceptibility of Er: BaY_2F_8 crystal were studied with a four-photon pumping by femtosecond 2ω:Ti:Sp laser (390 nm, 86 MHz, 50 fs) and a high-current electron-beam pumping (250 keV; 1.0 kA / cm^2; 1 ns).

During the impact interaction of pulses of high-power nanosecond electron-beam pumping at crystal Er:BaY_2F_8, an acoustic pulse is formed and propagated. The Thompson cube of F^- ions, inside which the Er^{3+} ion is, experiences an additional deformation upon passage of a hypersonic pulse and short-lived electric disturbance fields are induced in the vicinity of Er^{3+} ions. As a result, during the electron-beam pumping of Er:BaY_2F_8, the nonlinear susceptibility increases and, accordingly, the efficiency of nonlinear self-frequency conversion of Er^{3+} laser lines increases [1].

It was found that when Er:BaY_2F_8 crystals are pumped by nanosecond electron beams and femtosecond laser pulses ($4h\nu > E_g$), efficient generation of Er^{3+} stimulated emission lines occurs. Based on the experimental results, it was shown that, in femtosecond four-photon laser ionization of crystalline BaY_2F_8 substance, the high efficiency of electron-hole excitation of Er^{3+} in Er:BaY_2F_8 crystals, as well as when exposed to an electron beam, is determined by the degree of difference between the electronic systems of *s-, p-, d-* subgroups of the outer shell cations of its intrinsic substance and activator.

During femtosecond laser excitation of Er:BaY_2F_8 crystal by the mechanism of four-photon ionization of crystalline matter at a duration of 50 fs near a Gaussian focal waist, the volume intensity corresponds to ~ 10 TW/cm^{-3}. At that the concentration of induced band electrons and holes in a filament with a diameter of 10 μm reaches 10^{21} cm^{-3} and corresponds to the volume density of band charge carriers induced by a high-current nanosecond electron beam (1 kA/cm^2, 250 keV, 1 ns).

At four-photon pumping Er:BaY_2F_8 crystal by pulses of femtosecond 2ω:Ti:Sp laser (390 nm, 80 MHz, 50 fs), a femtosecond nonlinear frequency self-summation mode of Er^{3+} stimulated emission lines was achieved in the semiconfocal cavity. In this case, the lines of femtosecond laser pulses are formed in the UV and visible spectral range: 315, 320, 378, 382, 407, 414, 449, 456 nm. This is due to the fact that the duration of the laser excitation pulse (t_{pump}), not exceeding the relaxation time (t_r) of band electrons ($t_r = 10^{-11}$ *s* >> $t_{pump} = 5 \cdot 10^{-14}$ *s*), during four-photon ionization, provides additional polarization. Therefore, the nonlinear susceptibility increases significantly due to a decrease in the probability and even exclusion of the relaxation process of band electrons.

This work was supported by the Russian Foundation for Basic Research (grant № 20-02-00322).

References

[1] V.I. Baryshnikov, V.V. Krivorotova, A.V. Bolondz, "Generation and nonlinear self-conversion of laser line frequencies in Er: BaY2F8 crystals under dense electron and IR diode pumping", Izv. Vyssh. Uchebn. Zaved. Fiz., vol. 54, no. 2/2, pp. 51–57, 2013.

ELECTRON BEAM STIMULATION IN KTP CRYSTALS OF NANOSECOND GENERATION OF THE SECOND HARMONIC OF CW LASER RADIATION

V.I. BARYSHNIKOV[1-2], O.V. GOREVA[1], O.L. NIKONOVICH[1], Y.A. GRIGORYEVA[1]

[1]*Irkutsk State Transport University, Irkutsk, Russia*
[2]*Irkutsk Filial of Laser Physics Institute at SB RAS, Irkutsk, Russia*

A cardinal increase in the power density of electron-beam, optical, and concomitant acoustic radiation sources ensures a high rate of ionization and excitation of the substance, at which intense shock action is transmitted over a time interval from fractions of a nanosecond and in a coherent mode an effective migration of a significant density of hot electrons and holes occurs. Studies of the physics of the interaction of intense pulsed radiation with matter allow us to deepen the fundamental foundations of high-energy solid state electronics and, on this basis, successfully develop new systems of effective optoelectronic diagnostics in science and technology.

In the framework of this research methodology, a single-pulse luminescent spectrometer with nanosecond resolution and tight synchronization with a high-current nanosecond electron accelerator has been developed. The developed software provides a wide range of functionality with the integrated and separate use of these experimental facilities. Using this experimental methodology, the fundamental features of low-inertia luminescence under dense electronic excitation of a substance are studied. New research approaches and excitation mechanisms of doped luminescent media are proposed.

In the experiments, a semiconductor CW laser with a wavelength of 532 nm was used – the second harmonic of a neodymium laser with a 1,0 W diode laser pump. This small-sized system works as follows. A diode infrared laser with a wavelength of 808 nm through a focusing lens pumps the working medium of the laser, which uses a yttrium-vanadium crystal (NdYV) doped with a high concentration of neodymium, which generates an infrared laser beam with a wavelength of 1064 nm. This radiation is transmitted to a nonlinear KTP crystal, which is placed at an angle of phase matching in a vacuum cryostat of a high-current nanosecond electron accelerator. This crystal generates the second harmonic radiation of a neodymium laser with a wavelength of 532 nm.

From the point of view of the electronic structure of KTP-potassium titanium phosphate ($KTiOPO_4$), the main contribution to the formation of the states of the valence-band ceiling is made by hybridized 2p and 2p like states of oxygen. Thus, the electron density distribution in the valence band is formed mainly $2pO^{2-}$ determines the nonlinear susceptibility of organic crystals. Really wide-band (350-900 nm) non-inertial (<1 ns) stable cathodoluminescence (WCL) 78-600 K, excited by high-power electron beams, was detected in a $KTiOPO_4$ crystal and studied as in Al_2O_3, $Y_3Al_5O_{12}$, MgO, $CaCO_3$, SiO_2, H_2O et al. [1]. WCL is due to electronic transitions between the expanding subband valence band formed by the 2p O^{2-} state. Upon impact, displacements of O^{2-} ions in the vicinity of their valence shell are induced by short life time disturbing fields. The degree of deformation of the $2pO^{2-}$ band is determined by the electric intensity (E) of the disturbing fields with a short life time. E depends on the electron energy (W_e) in the beam.

Upon electron-beam irradiation (250 keV; 0.25 kA/cm^2; 10 ns) of the $KTiOPO_4$ crystal the pulse second harmonic generation of 1 ns duration is achieved. During the shock interaction of pulses of powerful nanosecond electron beam pumping, an acoustic pulse is formed and propagated on $KTiOPO_4$ crystal. When a hypersonic pulse passes, the crystal lattice undergoes deformation, and short-lived electric disturbance fields are induced near the O^{2-} ions. As a result, upon electron-beam irradiation on $KTiOPO_4$, the nonlinear susceptibility increases and, accordingly, the second-harmonic generation efficiency increases.

This work was supported by the Russian Foundation for Basic Research (grant № 20-02-00322).

REFERENCES

[1] V.I. Baryshnikov, T.A. Kolesnikova, S.V. Dorohov, ”Excitation of luminescence of oxide inorganic materials by powerful electron beams”, Inorganic materials, vol. 34, no.8, pp. 1–3,1998.

LUMINESCENCE OF SINGLE COLOR CENTERS IN LIF CRYSTALS GROWN IN A REDUCING ATMOSPHERE[1]

R. A. TAZIEV[1,2], *E. F. MARTYNOVICH*[1,2], *V. P. DRESVYANSKY*[1], *A. L. RAKEVICH*[1]

[1]*Irkutsk branch of the institute of laser physics SB RAS, Irkutsk, Russia,*
[2]*ISU, Irkutsk, Russia.*

Lithium fluoride crystals grown in a reducing atmosphere, unlike crystals grown in air, do not contain oxygen centers responsible for blue luminescence (λ_{max} = 419 nm), excited by UV radiation in the region of 200-250 nm.

Irradiation with ionizing radiation leads to the creation of new color centers in such crystals that luminesce in the band with a maximum at 800 nm. Earlier, we discovered these color centers [1]. In this paper, we continue the study of the characteristics of these centers.

The luminescence of single centers with a band of λ_{max} = 800 nm and a decay time constant at room temperature of 28 ns has a flickering character. Flicker due to transitions of centers to the triplet state. The average lifetime in the triplet state is 21 ± 13 s.

With an increase in the irradiation dose, the band intensity λ max = 800 nm quickly saturates, while the luminescence of intrinsic color centers, such as F_2, F_3^+, continues to increase. This indicates the impurity character of the color centers responsible for the observed luminescence band with a maximum of λ_{max} = 800 nm.

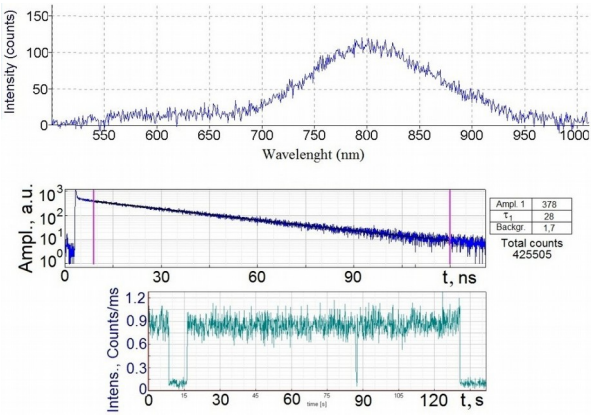

Fig.1. Luminescence spectrum and kinetics of a LiF crystal grown in a reducing atmosphere irradiated with a small dose of ionizing radiation (excitation - 532 nm). Below is the trajectory of the luminescence intensity of a single color center. The kinetics and trajectory in this figure refer to centers with a maximum of the optical absorption band of 800 nm.

It is noted that in the obtained luminescence spectrum, along with the λ_{max} = 800 nm band, a small contribution from the band corresponding to the luminescence of F_2 color centers is visible on the left. The luminescence of such single centers has already been studied previously [2]. In our experiments, these centers were also recorded. The obtained value of their damping time constant 16-18 ns, according to works [2-4], corresponds to F_2 color centers.

From the measured trajectories of the luminescence intensity of single centers, we can determine such characteristics that cannot be determined on ensembles, for example, the decay times of individual single centers or the lifetime of triplet states if there are no radiative transitions from them, which is often realized in practice.

REFERENCES

[1] E.F. Martynovich, R.A. Taziev, V.P. Dresvyansky, A.L. Rakevich. Materials of the Anniversary International Youth Conference on Luminescence and Laser Physics dedicated to the 50th anniversary of the First Summer Luminescence School in Irkutsk. - Irkutsk: Publishing house of the ISU, pp. 95-96, 2019.

[2] V.P. Dresvyansky, S.V. Boychenko, S.A. Zilov, A.L. Rakevich, A.P. Voitovich, E.F. Martynovich. Proceedings of the RAS. The series is physical. vol. 80, no. 1, pp. 97-100, 2016.

[3] Shiran N., Belsky A., Gektin A. et al. Rad. Meas., vol. 56, pp. 23-26, 2013.

[4] Kurobori T., Kanasaki T., Imai Y. et al. J. Phys. C: Solid State Phys., vol. 21, L397-L402, 1988.

1 This work was carried out in the framework of the Program of fundamental scientific research of state academies of sciences for 2013-2020, section II.10.1, project No. 0307-2016-0004, as well as with financialsupport from the Russian Foundation for Basic Research and the Ministry of Culture, Education, Science and Sports of Mongolia, project No. 17-52-44015 Mong_a.

ABOUT ALTERNATIVE APPROACH TO REALIZATION OF NUCLEAR FUSION

V.K. EGOROV[1], *E.V. EGOROV*[1,2,3]

[1] *IMT RAS, Charnogolovka, Moscow district, Russia 142432*
[2] *Financial university under the government of the Russian Federation, Moscow, Russia*
[3] *IRE RAS, Fryazino, Moscow district, Russia*

The main intricate and energy outlaying problem for realization of nuclear fusion reactions is the Coulomb barrier overcoming, which hinders to the direct nuclear interaction. In thermonuclear apparatus of civilian or military designation the barrier overcoming is effected by increasing of ions kinetic energy is ionized ensemble. Owing to the moving ions chaotic directivity the probability increase of ions direct collision in high temperature plasma is realized by pressure magnification in the experimental chamber. This approach competence to the nuclear fusion reactions realization is beyond questions [1,2]. A.D. Sakharov and Ya.B. Zheldovich pointed on the principle possibility of alternative approach to the nuclear fusion reaction realization without high temperature application [3]. The idea of cold nuclear fusion was implemented by I.S. Filimonenko [4]. Some his experimental materials are not published, today. But the cold nuclear fusion or nuclear transmutation phenomenon is beyond questions, today [5]. At the same time, the magnitude of cold nuclear fusion effect registered in experiments is smaller as the expects one on some hundreds thousands times. Low efficiency of the reactions yield is connected with its process mechanisms understanding absence. The work proposes a new direction for the cold nuclear fusion mechanism search on base of the radiation fluxes waveguide-resonance propagation phenomenon consequence and the wave-corpuscle dualism principle. The phenomenon was discovered in process of X-ray characteristic radiation fluxes propagation peculiarities investigation through planar extended slit clearances [6]. Our experimental studies showed that the planar extended slit clearance transports X-ray characteristic radiation fluxes without attenuation when its width is smaller as the radiation coherence length half ($L/2=\lambda_0^2/2\Delta\lambda$). This fact was interpreted as the new phenomenon discovery: the waveguide-resonance propagation of radiation fluxes or the radiation superfluidity. The phenomenon is characterized by appearing of the uniform interference field of radiation standing waves. Devices functioned in frame of the phenomenon were called as planar X-ray waveguide-resonators (PXWR). Study of there devices properties showed that independent radiation fluxes can interact in some conditions in result of mutual influence of uniform interference fields of radiation standing waves excited by these fluxes. Owing to the wave corpuscle dualism principle the radiation standing wave uniform interference field can be excited by particles beams with zero rest mass, too. This hypothesis found own experimental confirmation in investigations of low energy neutrons fluxes propagation peculiarities [7]. Analogical interference fields of radiation standing waves can be formed for atomic and molecular fluxes of hydrogen deuterium, tritium and helium-3 [8]. After the uniform interference fields preparations it will be need to find conditions for there fields interaction and formation atomic and molecular fluxes with different nuclear binding energy. The suggesting approach allows to evade the Coulomb barrier but its realization is not simple arrangement. It is expected that the interference field interaction will demonstrate the resonance disposition.

REFERENCES

[1] L.A. Arcimovich. Controlled thermonuclear reaction. Moscow: PhysMatLit. 1961. 467 p. (In Russian).
[2] K. Miyamoto. Fundaments of plasma physics and controlled fusion. Tokyo: Tokyo University. 2001. 415 p.
[3] Ya.B. Zheldovich, S.S. Fershtein, UFN, V3, 1961, P. 593-623.
[4] I.C. Filimonenko, Priority certificate #717239/38 from 27.07.1962.
[5] E. Storm. The science of low energy nuclear reactors. New Jersey: World Scientific. 2007. 312 p.
[6] V.K. Egorov, E.V. Egorov. Planar X-ray waveguide-resonators. Saarbrucken: Lambert Acad. Press. 2017. 788 p. (In Russian).
[7] V.L. Aksenov, V.K. Ignatovich, Yu.V. Nikitenko, Cryst. Rep., v51(51), 2006, P. 734-753.
[8] I. Esterman, R. Frisch, O. Stern, J. Zs.F.Phys., v73, 1931, P. 348-371 (On German).

KINETIC MODELLING OF THE LONG PULSE MODE IN METAL VAPOR ACTIVE MEDIA[1]

S.N. TORGAEV[1,2,3], *A.E. KULAGIN*[1,2], *M.V. TRIGUB*[1,2]

[1]*Tomsk Polytechnic University, Tomsk, Russia*
[2]*V.E. Zuev Institute of Atmospheric Optics SB RAS, Tomsk, Russia*
[3]*Tomsk State University, Tomsk, Russia*

Metal vapor active media operating in the long pulse mode are used in the tasks of the visual and optical control of remote objects [1]. The kinetic modeling was performed to obtain the spatio-temporal amplifying characteristics of the copper bromide active medium operating in the long-pulse mode. A detailed description of the kinetic model is given in [2-4]. The experimental data presented in [5] were selected as input parameters for the simulation.

The simulation was carried out for the radiation pulse repetition rate of 3, 10, and 15 kHz. As in the experiment (for 3 and 15 kHz), the energy stored in the capacitor per unit of frequency remained the same in the model. This was achieved by changing the capacity of the storage capacitor in the pump circuit. The simulation parameters of the copper bromide active medium are given in Table 1.

Table 1. The simulation parameters

	GDT 1	GDT 2	GDT 3
Pulse repetition rate, kHz	3	10	15
The buffer gas pressure (Ne), torr	30	30	30
GDT wall temperature, ^{0}C	650	650	650
Active zone diameter, cm	5	5	5
Active zone length, cm	90	90	90
Capacity of the storage capacitor, nF	3.4	1.1	0.75

In Fig. 1, amplified spontaneous emission (ASE) pulses obtained by modelling of active media for different frequencies are shown.

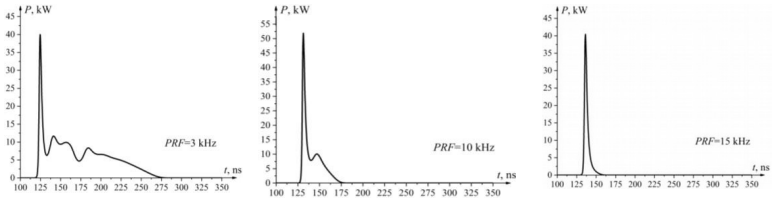

Fig.1. Time dependencies of the volume averaged ASE power: a – GDT 1, b – GDT 2, c – GDT 3 (Table 1).

For the constant energy input into discharge, there is a significant increase in the duration of ASE pulses with a decrease of the pulse repetition rate that is consistent with the experiment [5]. Fig. 2 shows the radial dependences of the gain of the active medium at different time points, which correspond to the times in Fig. 1.

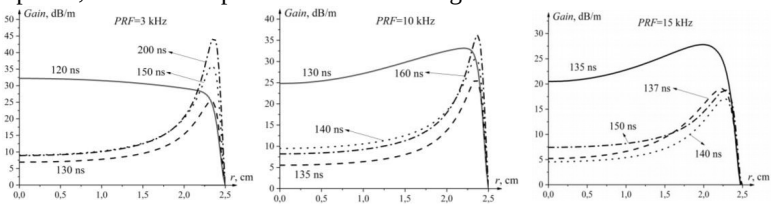

Fig.2. Radial dependences of the gain of the active medium: a – GDT 1, b – GDT 2, c – GDT 3 (Table 1).

It can be seen from Fig. 2 that the relatively uniform spatio-temporal gain profile is observed only at the beginning of the ASE pulse. Then the gain in the GDT center decreases quite quickly. Thus, the use of such active medium, operating in the long-pulse mode, in the visual-optical control of remote objects has anumber of limitations. In particular, the spatio-temporal gain profile is highly nonuniform for almost the entire duration of the population inversion.

REFERENCES

[1] Evtushenko G.S., Torgaev S.N., Trigub M.V., Shiyanov D.V., Evtushenko T.G., Beloplotov D.V., Lomaev M.I., Sorokin D.A., Tarasenko V.F., Methods and Instruments for Visual and Optical Diagnostics of Objects and Fast Processes, New York: NOVA Science Publishers, 2018 - 250 p. ISBN: 978-1-53613-568-5, ISSN: 2473-3679.

[2] Torgaev S.N., Kulagin A.E., Evtushenko G.S., “Kinetic modeling of amplifying characteristics of copper vapor active media for a wide range of input radiation power”, Optics Communications, vol. 460, pp. 1-6., April 2020. DOI: 10.1016/j.optcom.2019.125136

[3] Torgaev S.N., Kulagin A.E., Evtushenko T.G., Evtushenko G.S., “Kinetic modeling of spatio-temporal evolution of the gain in copper vapor active media”, Optics Communications, vol. 440, pp. 146-149, June 2019. DOI: 10.1016/j.optcom.2019.01.061

[4] Kulagin A.E., Torgaev S.N., Evtushenko G.S., Trigub M.V., “Kinetics of the Active Medium of a Copper Vapor Brightness Amplifier”, Russian Physics Journal, vol. 60, no. 11, pp. 1987-1992, March 2018. DOI: 10.1007/s11182-018-1312-y

[5] Trigub M.V., Vlasov V.V., Torgaev S.N., Evtushenko G.S., “An image-brightness amplifier based on copper bromide vapor for operation at increased superradiance pulse duration”, Technical Physics Letters, vol. 43, no. 9, pp. 828-830, October 2017. DOI:10.1134/S1063785017090280

1 The study was financially supported by the Russian Science Foundation, Project No 19-79-10096.

SPATIAL DISTRIBUTION OF THE STORED LIGHT SUM OF FEMTOSECOND LASER RADIATION IN LiF:Mg,Ti*

V.P. DRESVYANSKIY[1], S.V. MURZIN[1], Y.A. SUKHANOVA[1], N.S. BOBINA[2], S. ENKHBAT[3], E.F. MARTYNOVICH[1]

[1]Irkutsk Branch of Institute of Laser Physics SB RAS, 664033, Irkutsk, Lermontova str., 130a, Russia, e-mail: nadvp@listl.ru
[2]A.P. Vinogradov Institute of Geochemistry SB RAS, 664033, Irkutsk, Russia
[3]Institute of Physics and Technology, Mongolian Academy of Science, Ulaan-Baator, Mongolia

The aim of our work was investigation of the mechanism of light sum storage in LiF:Mg,Ti crystals under action of intense femtosecond radiation of a titanium-sapphire laser in the near- IR region of ~800 nm, as well as study of the photoluminescence of irradiated samples in comparison with the results of studies of thermally stimulated luminescence (TSL) of the same crystals irradiated by beta radiation and other types of radiation. The object of our research was dosimetric LiF: Mg (100 ppm), Ti (10 ppm) monocrystals widely used in gamma-dosimetry.

The experimental setup for irradiating of LiF:Mg,Ti crystals with femtosecond laser pulses included a titanium-sapphire laser generating pulses of 50 fs duration with an energy of about 6 mJ and a repetition rate of 10 Hz. A specialized installation was used to carry out TSL studies in the temperature range from 295 K to 673 K with a constant heating rate of 1 Ks^{-1}. After measuring the thermal emission curves of the crystal irradiated with femtosecond radiation, we conducted additional TSL studies of the same sample irradiated with β-radiation from the ^{90}Sr-^{90}It isotope source with a dose rate of 0.6 Gy/min. The sample was irradiated by beta particles for 30 seconds.

The results of thermoluminescence studies show that in case of femtosecond irradiation, the peaks caused by annealing of F_2 and F_3^+ color centers are observed in the thermal illumination curve along with the main dosimetric peak of TSL with a maximum of 485 K. High-temperature peaks after femtosecond laser irradiation were recorded more effectively than after x-ray and β-irradiation. It is known from the literature that high-temperature peaks in TL detectors based on LiF:Mg,Ti are more effectively induced in heavy particle tracks, where the excitation density is significantly higher than in case of x-ray or beta irradiation. The excitation density of the crystal under action of laser radiation is about 10^7 times higher than under the action of x-ray radiation. Also, it is about 10^4 times higher than excitation density provided by the beta radiation source used in our research.

Axial dependence of the energy accumulated by the crystal under the action of single femtosecond laser pulses or series of pulses has a "ragged", non-monotonic character. Microscopic study showed that this effect is determined by the fact that the energy accumulation occurs in the areas of self-focusing filaments of laser radiation, which are small in size and their number is small at the initial stage of irradiation. With an increase in the number of laser pulses, the length of the spurs induced by filaments in the crystal as well as their diameters increase, and the axial dependence of the accumulated energy is smoothed. When the number of laser irradiation pulses increases, the value of the light sum of thermostimulated luminescence emitted by irradiated crystals first increases superlinearly then reaches a maximum and then decreases. The effect of saturation of the stored light sum is caused by the fact that the concentration, aggregation degree and nomenclature of color centers are greater in the central axial part of the spurs than in the peripheral part.

* The work was supported by Project № 0307-2016-0004 of the program of fundamental scientific research of the State Academies of Sciences for 2013-2020, section II.10.1, and by project № 17-52-44015 Mong_a of Russian Foundation for Basic Research and Mongolian Ministry of Education, Culture, Science and Sports.

SYNTHESIS AND OPTICAL PROPERTIES OF LITHIUM NANOPARTICLES IN WIDE-GAP DIELECTRICS*

V.P. DRESVYANSKY[1], *V.L. PAPERNY*[2], *S. ENKHBAT*[3], *E.F. MARTYNOVICH*[1,2]

[1]*Irkutsk branch of the Institute of Laser Physics SB RAS, 664033, Irkutsk, Russia*
[2]*Irkutsk State University, 664003, Irkutsk, Russia*
[3]*Institute of Physics and Technology, Mongolian Academy of Science, Ulaan-Baator, Mongolia*

Recently, there has been a fairly large number of publications devoted to the study of composite materials based on optically transparent dielectrics containing nanosized metal particles. These materials are promising from the point of view of their use in optoelectronics, nanophotonics, nonlinear optics.

This paper presents the results of studies of the optical properties of lithium metal nanoparticles synthesized by ion implantation in alkali-halide crystal matrices. The implantation of Li^+ ions was carried out by a high-current pulsed installation of the MEVVA type (ion energy 50 keV, beam current density 5 mA/cm^2, pulse duration 200 μs, number of pulses 1, 10, 10^2, 10^3). It has been shown that it is possible to obtain crystals containing metal nanoparticles as a result of heat treatment, pre-stained with various types of ionizing radiation, and also as a result of coagulation processes during irradiation of crystals with intense laser femtosecond pulses in the self-focusing and filamentation mode. As research methods, a combination of spectroscopic techniques was used, including laser scanning confocal microscopy with picosecond resolution time and thermoluminescent spectroscopy. When studying the mechanisms of coagulation and the formation of metal nanoparticles during thermal annealing in lithium fluoride crystals, the research results were compared with the data obtained by ion implantation of this type of crystal with Li^+ ions.

It has been shown that the efficiency of coagulation processes depends on the excitation density in the process of radiation coloring of crystals and temperature. The first circumstance causes the formation of a high concentration of complex F_3^-, F_3^+, F_3, F_4 aggregate centers in the anion subsystem, which in turn contributes to the creation of a large number of stable hole X_3^- centers. The effective formation of X_3^- centers in laser defect formation is indicated by high-temperature peaks recorded in the thermal emission curves. In the literature, the process of forming X_3^- centers is treated ambiguously. Most studies support the mechanism associated with the pairwise association of H - centers near bivacancies ($v_a v_c$).

* This work was supported by the Fundamental Scientific Research Program of the State Academies of Sciences for 2013-2020, section II.10.1, project No. 0307-2016-0004, as well as the Russian Foundation for Basic Research and the Ministry of Education, Culture, Science and Sports of Mongolia, project Nos. 17-52-44015 Mong_a and 20-02-00322.

BISMUD-CONTAINING SUPERCODUCTORS WITH A HIGH CONTENT OF CALCIUM AND COPPER, OBTAINED FROMN THE MELT USING THE LIGHT FLUX

D.E. USKENBAYEV, A. S. NOGAI

Kazakh Agro Technical University S. Seifullina, Nur-Sultan. Kazakhstan

At present, stable high-temperature superconducting compounds with a critical transition temperature to the superconducting state (Tc) exceeding the threshold of 100 K have been installed in three types of oxide compounds: mercury-containing, thallium-containing, and bismuth-containing. All these superconducting compounds have a homologous series: $HgBa_2Ca_{n-1}Cu_nO_{2+2n+\delta}$, $Tl_2Ba_2Ca_{n-1}Cu_nO_{4+2n}$ и $Bi_2Sr_2Ca_{n-1}Cu_nO_{4+2n}$ (n=1,2,3,..), and it was found that with an increase in the content of Ca and Cu TC rises. But, for all three systems under normal synthesis conditions, the maximum critical temperatures were established at n = 3 – T_c = 164 K, T_c = 127 K and T c = 110 K, respectively. Model calculations suggest that an increase in the content of Ca and Cu can lead to a further increase in T_c. In work [1], it was reported that superconducting phases in a bismuth-containing system are noticeably higher than T_c = 110 K, but they were metastable.

The authors of [2], when studying the $Bi_{1,7}Pb_{0,3}Sr_2Ca_{n-1}Cu_nO_y$ compositions (n = 4, 5, 6, 7), used the laser ablation method, which allowed them to stabilize compounds with unit cell parameters: c = 3.66 nm; 4.31 nm; 4.94 nm; 5.60 nm and 6.25 nm, which correspond to phases with n = 4 (2234), 5 (2245), 6 (2256), 7 (2267), 8 (2278). However, in this case, in all samples, the superconductivity effect was not detected above the liquid helium temperature of 4.2 K.

This paper presents the results of a study on the preparation of HTSC phases with a high content of Ca and Cu (n > 3) in a bismuth-containing system of starting materials, consisting of glass-crystalline and amorphous phases obtained from a melt using a concentrated light flux from an electric arc lamp. The spectral composition of the light flux consists of an intense continuous ultraviolet, visible and near infrared regions of the spectrum. The synthesis was carried out according to traditional ceramic technology with intermediate grindings. The samples were in the form of tablets with a diameter of 15 mm and a thickness of 2 mm made by pressing from powders. Heat treatment was carried out in the temperature range of 835–848 ° C for 60–120 h, depending on the composition. The results of x-ray phase analysis showed that compositions with n = 4 - 11 consist mainly of the superconducting phase $Bi_{1,7}Pb_{0,3}Sr_2Ca_2Cu_3O_y$ (2223). But at the same time, with an increase in the content of Ca and Cu, reflections appear on the diffractograms that are not related to phase 2223 or other superconducting phases 2201 or 2212. Perhaps they can be attributed to phases based on the CaO-CuO system. At higher contents of Ca and Cu, reflections of SP phases are not observed. The study of critical characteristics shows that in compositions n = 4–7 a clear effect of the superconducting phase is observed T_c = 107 K, characteristic of phase 2223. In addition, traces of superconducting phases are also observed above T_c = 107 K.

REFERENCES

1. Gorobchenko V.D., Irodova A.V., Zharnikov M.V., Lavrova O.A., Laskova G.V., Pilyagin G.V. Superconductivity and phase composition of Bi - Sr - Ca - Cu - O oxides with a high content of Ca and Cu // SFKhT. 1989, T. 2, No. 7, S. 55-59.

2. Yoshiba K., Sasakura H., Tsukuic S., Mizokawab Y., New Bi-cuprate thin films of $Bi_2(La, Ca)_2Ca_{n-1}Cu_nO_z$ (n = 3, 4, 5, 6 and 7) prepared by the laser ablation metod. Phys. C. Supercond. 1999, V. 322, Iss. 1-2, P. 25-30.

FORMATION OF THE SCATTERING PHASE FUNCTION IN THE INTERACTION OF ULTRASHORT LASER PULSES WITH A DROP IN A NONLINEAR MODE*

BABUSHKIN P.A.[1,2], BULYGIN A.D.[1,2], KUCHINSKAYA O.I.[1,2], MININA O.V. [1,2], PETROV A.V. [1]

[1] V.E. Zuev Institute of Atmospheric Optics SB RAS, Tomsk, Russia
[2] National Research Tomsk State University, Tomsk, Russia

The propagation of ultrashort laser pulses in the atmosphere is accompanied by nonlinear effects. The most low-threshold of them is the effect of cubic nonlinearity manifesting in aerosol. This effect should lead to the transformation of the scattering phase function formed in a liquid droplet aerosol. To study this effect, numerical and experimental studies on droplets of various sizes and geometries were carried out. As expected, the cubic nonlinearity inclusion should lead to an increase in the effect of backward scattering. However, as our preliminary experiments show, this does not always happen. Fig. 1 shows the results of experimental studies on the scattering of femtosecond laser pulses from a drop.

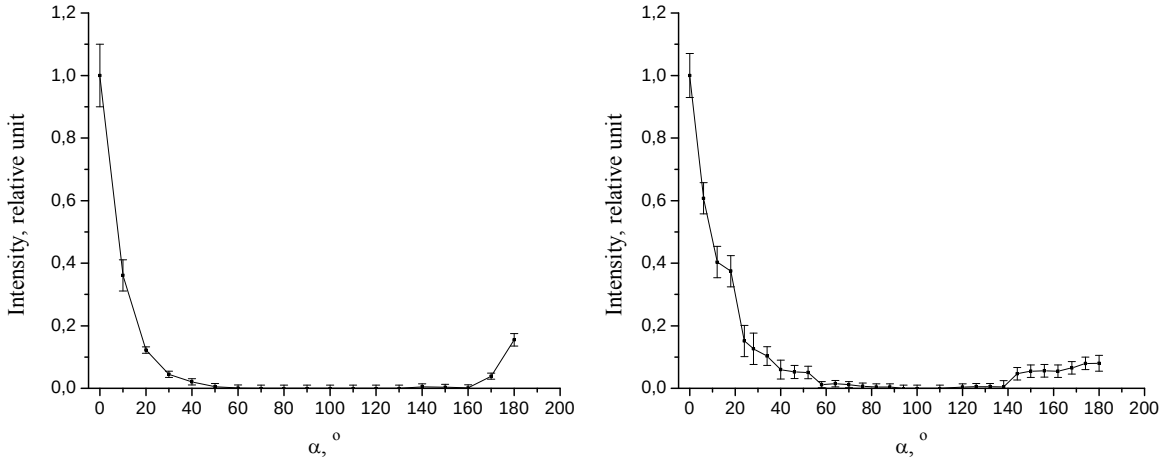

Fig.1. The distribution of the amplitude of the scattering signal as a function of the angle relatively to the drop (the drop diameter d = 1.6 mm) at pulse energy of 0.16 mJ (a) and 0.4 mJ (b)

As can be seen from the fig. 1, contrary to the expectations, the scattering phase function decreases with the manifestation of nonlinear effects in the backward direction. This effect requires further theoretical and experimental research.

* The work was supported by the Russian Foundation for Basic Research under grant No. 19-42-703015.

THE MECHANISM OF DEFECT FORMATION IN DIELECTRIC CRYSTALS UNDER THE INFLUENCE OF INTENSE FEMTOSECOND LASER RADIATION[1]

V.P. DRESVYANSKIY[1], *A.V. KUZNETSOV*[1], *S. ENKHBAT*[2], *E.F. MARTYNOVICH*[1]

[1]*Irkutsk branch of the Institute of Laser Physics SB RAS, 664033, Irkutsk, Russia*
[2]*Institute of Physics and Technology, Mongolian Academy of Science, Ulaan-Baator, Mongolia*

The subject of the study is the formation of luminescent point defects in alkali-halide crystals under the action of femtosecond laser pulses of high intensity. The aim of the work is to construct a physical model of the processes of aggregation and nucleation of defects formed by the interaction of intense femtosecond laser radiation with crystals.

In contrast to the uniform distribution of defects characteristic of crystals irradiated with γ-radiation or x-ray, the distribution of color centers and other stable defects in crystals irradiated with femtosecond laser pulses is spatially inhomogeneous. This is caused by the self-focusing and multiple filamentation of laser radiation and the formation of centers only in the field of light filaments in the form of spatially isolated spurs (traces) consisting of the centers of color induced by these filaments.

On the basis of experimental and literary data, a physical model of the processes of interaction of intense femtosecond laser radiation with wide-band crystals on the example of lithium fluoride was formed. It includes self-focusing and multiple filamentation of laser radiation on the inhomogeneities of light and matter, internal photoionization in the field of filaments, photo- and recombination excitation of the excitons, their decay into the Frenkel pairs, the partial recharge of the components of these pairs in the field of electron-hole plasma, the migration of mobile components of neutral and ionized Frenkel defects (interstitial atoms and ions of fluorine and anion vacancies) with their characteristic thermoactivation parameters of diffusion, association of anion vacancies with F-centers with formation of mobile F_2^+ centers, the hopping migration of the latter, their transformation in the process of migration into stable F_2 and F_3^+ centers and recharge with the formation of F_2, F_3^+ and F_3 centers in case of prolonged irradiation, their association with anion vacancies and F_2^+ centers resulting in the formation of larger aggregates up to the deposition of colloidal metal nanoparticles, the recombination of interstitial atoms and ions with electron color centers with partial restoration of lattice sites and the association of interstitial atoms and ions into unstable V_F, V_t and stable V_3 centers of hole-interstitial type.

1 This work was supported by the Fundamental Scientific Research Program of the State Academies of Sciences for 2013-2020, section II.10.1, project No. 0307-2016-0004, as well as the Russian Foundation for Basic Research and the Ministry of Education, Culture, Science and Sports of Mongolia, project No. 17-52-44015 Mong_a.

UVC EXCILAMPS AS SOURCES OF VIRUCIDAL AND BACTERICIDAL RADIATION *

E.A. SOSNIN[1,2], O.S. ZDANOVA[3]

[1]Institute of High-Current Electronics SB RAS, Tomsk, Russian Federation
[2]National Research Tomsk State University, Tomsk, Russian Federation
[3]Pirogov Russian National Research Medical University, Moscow, Russian Federation

The most common UV radiation sources used to inactivate microorganisms today are low-pressure mercury lamps. Advances in plasma and gas discharge physics have allowed the development of alternative sources of ultraviolet radiation – excilamps. These sources emit due to decay of excimer and exciplex molecules [1–4].

The report provides a brief overview of the results of studies of ultraviolet inactivation of bacteria, living cells and viruses using excilamps, which were conducted from 2002 to 2020 by us and some other scientific teams. The description of excilamp models used in these studies and developed in the Institute of High Current Electronics SB RAS is given.

The scientific evidence accumulated to date shows that short-wave excilamps based on KrCl*, KrBr* and XeBr* molecules are an alternative to low-pressure mercury lamps in their optical parameters. These sources of optical radiation provide a bactericidal effect, while KrCl- and KrBr-excilamp radiation has a virucidal effect. The latter is very relevant due to the consequences of the spread of human coronaviruses in recent years.

It is concluded that the use of excilamps can be the basis for creating advanced inactivation technologies.

REFERENCES

[1] T. Oppenländer, E. Sosnin, “Mercury-free Vacuum-(VUV) and UV Excilamps: Lamps of the Future?”, IUVA News, vol.7, no. 4, pp. 14–18, 2005.

[2] E. A.Sosnin, T. Oppenländer, V. F. Tarasenko, “Applications of Capacitive and Barrier Discharge Excilamps in Photoscience,” Journal Photochemistry and Photobiology C: Reviews, vol. 7, no. 4, pp. 145–163, 2006.

[3] E. A. Sosnin, V. F. Tarasenko, M. I. Lomaev, *UV and VUV excilamps*. Saarbrücken, Deutschland / Germany: LAP LAMBERT Academic Publishing, 2012, 318 p.

[4] E. A. Sosnin, S. M. Avdeev, V. F. Tarasenko, V. S. Skakun, D. V. Schitz, “KrCl Barrier-Discharge Excilamps: Energy Characteristics and Applications (Review),” Instruments and Experimental Techniques, vol. 58, no. 3, pp. 309–318, 2015.

[5] E. A. Sosnin, L. V. Lavrent’eva, M. R. Yusupov, Y. V. Masterova, V. F. Tarasenko, “Inactivation of Escherichia coli using capacitive discharge excilamps,” Proc. 2nd Int. Workshop on Biological Effects of Electromagnetic Fields, Rhodes, Greece (October 7-11), pp. 953–957, 2002.

[6] D. Welch, M. Buonanno, V. Grilj, I. Shuryak., C. Crickmore, A. W. Bigelow, G. Randers-Pehrson, G. W. Johnson, D. J. Brenner, “Far-UVC light: A new tool to control the spread of airborne-mediated microbial diseases,” Sci. Rep., vol. 8, 2752, 2018.

* The review was partially supported by RFBR project № 19-32-90023 and by State Task for HCEI SB RAS, project #13.1.4.

EFFECT OF IRRADIATION WITH LOW-ENERGY ALPHA PARTICLES ON THE STRUCTURAL-PHASE STATE OF COATINGS OF TRIPLE NITRIDE SYSTEMS BASED ON TITANIUM AND NIOBIUM STEEL

A.A. KLOPOTOV[1,2], *A.I. POTEKAEV*[2], *S.B. KISLITSIN*[3], *Yu.A. KAKUSHKIN*[1], *V.V. KULAGINA*[4]

[1]*Tomsk State University of Architecture and Building, Tomsk, Russia*
[2]*National Research Tomsk State University, Tomsk, Russia*
[3]*The Institute of Nuclear Physics, Almaty, Kazakhstan*
[4] *Siberian State Medical University, Tomsk, Russia*

Interest in the structure of triple nitride systems based on transition metals of the 4th, 5th and 6th groups of metals based on titanium and niobium is mainly due to the following points. First, this type of nitrides are technologically important materials that are widely used as functional coatings. Secondly, coatings based on these nitrides are promising for protecting the base material from radiation, heat and other influences. This is confirmed in the works devoted to the study of the effect of alpha-particle irradiation on TiZrN, TiCrN, TiMoN and TiNbN coatings on a steel substrate [1-3]. In [1], coatings were obtained on the surface of a $Cr_{18}Ni_{10}Ti$ steel substrate by vacuum-arc condensation with ion bombardment. Then the influence of irradiation of the surface $(Ti,Cr)N_{1-X}$ coating on carbon steel with low-energy ions ${}_4He^{+1}$ (20 Kev) and ${}_4He^{+2}$ (40 Kev) to a fluence of 1.0×10^{17} ion/cm^2. Important results were obtained. Note some. It was found that irradiation with α-particles does not significantly change the coating structure and leads to the formation of particles of disordered non-stoichiometric nitrides $(Ti,Cr)N_{1-X}$. It was also shown that irradiation with low-energy argon ions leads to sputtering of the coating surface and this prevents the accumulation of implanted argon in the coating and substrate.

This paper presents the results of the analysis of the search for general regularity of structural-phase states and the structure of triple diagrams of nitride systems based on transition metals of the 4th, 5th and 6th groups of metals with titanium and niobium in order to select the most promising ones for their use as protective coatings on structural reactor materials.

In the considered triple nitride systems Ti-Me-N and Nb-Me-N (Me=V, Cr, Zr, Mo, Hf, Ta, W), the third element nitrogen differs significantly in chemical properties from the metals forming this compound. Nitrogen with transition metals can form compounds with an ordered structure. These compounds are formed from solid solutions and can create phases of variable composition. A large variety of phases and various polymorphic transformations is also observed in nitrogen compounds with transition elements. This is due to the different nature of the chemical bond in these compounds: typically, the metal bond that exists in solid solutions of metals with nitrogen, in separate phases and compounds begins to pass into covalent and ionic, with a gradual transition from one compound to another. The manifestation of intermediate types of bonds (combination of metal with covalent, covalent with ionic) was also found.

The nitrides TiN and VN, TiN and CrN, TiN and NbN, NbN and ZrN, NbN and HfN are completely mutually soluble and form continuous solid solutions. The presented nitrides have a cubic B1 structure (NaCl type). The regions of homogeneity of triple compounds ($(Ti,V)N_{1-X}$, $(Ti,Cr)N_{1-X}$, $(Ti,Nb)N_{1-X}$, $(Nb,Zr)N_{1-X}$, $(Nb,Hf)N_{1-X}$ are wide. In systems, the regions of homogeneity of compounds $(Ti,Zr)N_{1-X}$, $(Ti,Ta)N_{1-X}$, $(Nb,Mo)N_{1-X}$, $(Nb,Ta)N_{1-X}$ occupy restricted areas.

TiN_X compounds belong to the class of disordered non-stoichiometric nitrides with a wide area of homogeneity [4]. In the TiN_X compound, Ti atoms form a metal FCC sublattice, in the octahedral internodes of which there may be n embedding atoms or vacancies. The preservation of the type of crystal structure of a non-stoichiometric disordered compound when the concentration of structural vacancies changes causes the presence of a homogeneity region. In this case, the narrow area of CrN nitride homogeneity means that the appearance of structural vacancies leads to a change in the type of crystal structure.

REFERENCES

1 Potekaev A.I., Kislitsyn S.B., Uglov V. V., Klopotov A.A. and et. al. Condensed-state physics Radiation stability of triple coatings based on transition-metal nitrides under irradiation by alpha particles and argon ions. Russian Physics Journal. 2016. V. 59, No.1. P.99-108
2 Kislitsin S., Ivanov I., Zdorovets M., Larionov A. Radiation Effects in TiNbN Coatings Induced by Impact of Low-Energy Helium, Krypton and Xenon Ions. Acta Physica Polonica, A. 2019, Vol. 136, 356-360.
3. Kislitsin S.B., Potekaev A.I., Uglov V.V., Klopotov A.A. and et. al. Steel surface TiCrN, TiMoN coatings structural phase state change features after low-energy alpha particles irradiation. International Conference on Modern Technologies for Non-Destructive Testing IOP Publishing IOP Conf. Series: Materials Science and Engineering. 2017. V.289. 012010
3. Gusev A. I., Rempel A.A. Non-stoichometry, disorder and order in solids. Ekaterinburg: UB RAS. 2001. 580 P.

DEVELOPMENT OF SEMICONDUCTOR PUMPING SOURCES FOR A BISTATIC LASER MONITOR

VASNEV N.A., TRIGUB M.V

V.E. Zuev Institute of Atmospheric Optics SB RAS, Tomsk, Russia

The optical quantum amplifiers are used for amplification of electromagnetic waves by means of stimulated emission radiation. In particular the input signal of the quantum amplifier can be optical image formed by superradiance or stimulated emission. In this case the brightness of resulting image increases even under the high background lighting. The effect is the basis of the laser monitor, which is used for non-destructive testing of high-speed processes like as processing of micro-objects, surface modification for improving their characteristics, obtaining new nanomaterials and welding [1].

The laser monitor can be consist of two active elements on self-terminating transitions: illumination source and brightness amplifier. Such a system is called the bistatic laser monitor and unlike a monostatic laser monitor it provides a long imaging distance (no less 15.5 m) and field of view order of a few cm [2]. The output radiance power depends on time shift between the population inversion production of each active element (Fig.1 a). The high-voltage modulator based on thyratron TGI1 100/8 provides the synchronization of both active elements with jitter 7 ns [2].

The development of pump sources based on transistors with high switching characteristics (tr =1·109 ns, f =1·103 Hz) and low jitter (1·10-9 s) is of great interest. The modern semiconductor switches can increase the efficiency (η) of the a laser active medium pumping with lower mass and size parameters. Besides two semiconductor pump sources can be synchronize with higher precision.

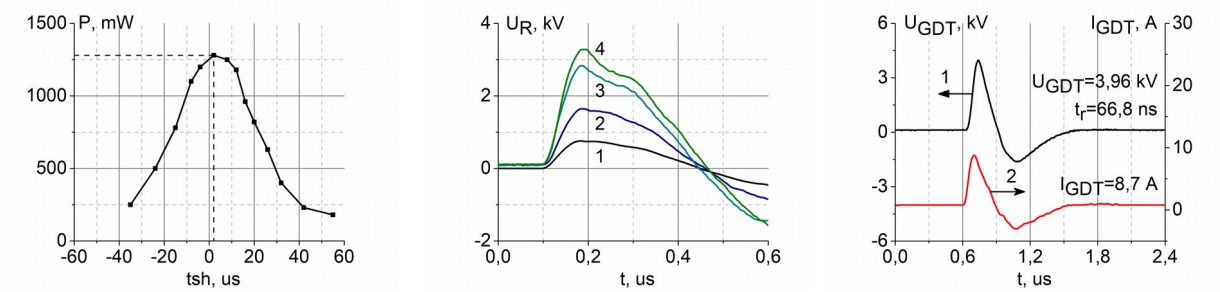

a) b) c)

Fig.1. a) Dependence of output power on time shift; b) voltage pulses at an active load (150 Ohm, 60 W) with simultaneous switching of one (1), two (2), three (3) and four (4) commutation cells based on IRG4PH50UD transistors; c) GDT voltage (U) and current (I) with simultaneous switching of four commutation cells.

IRG4PH50UD, IPAW60R280 and SPW17N80C3 transistors were used as switches. The best result was obtained with IRG4PH50UD. Four commutation cells based on four IRG4PH50UD transistors and four capacitors 2,2 nF 1,6 kV were design. Initially each cell commutated to its own active load (30 kOhm, 60 W) – the amplitude (730 V) and rise time (48 ns) of voltage pulses were identical. Then the load was changed (150 Ohm, 60 W) and the number of switching cells increased one at a time.

Fig.1 b shows that increase a number commutation cells leads to rise of amplitude of voltage pulses, in particular the simultaneous commutation of four cells generate voltage pulse with an amplitude of 3.28 kV and rise time of 55 ns. The commutation on GDT with active zone length of 24 cm and diameter of 4 cm allowed breakdown of the interelectrode gap. The amplitude of excitation pulses reached 4 kV, GDT current was 8.7 A, rise time was 66 ns.

It is required to determine the optimal number of cells to pump the active elements of the bistatic laser monitor and find the precision of their synchronous pumping.

REFERENCES

[1] G.S. Evtushenko, “Methods and Instruments for Visual and Optical Diagnostics of Objects and Fast Processes”, Nova Science Publishers Inc, 184 p, 2018.

[2] N.A. Vasnev, M.V. Trigub, G.S.Evtushenko, “Features of Operation of a Brightness Amplifier on Copper Bromide Vapors in the Bistatic Scheme of a Laser Monitor,” Atmospheric and Oceanic Optics, vol. 32, no. 4, pp. 483-489, March 2019.

The work was supported by RFBR, project no 19-38-90042.

WANDERING QUANTUM DOTS (WQDS) IN THE STRUCTURE OF DISORDERED CONDENSED MATTER*

G.A. MELNIKOV, N.M. IGNATENKO, V.V. SUCHILKIN, P.A. KRASNYKH

Southwest State University (SWSU), Kursk, Russia

The article shows that in the framework of the cluster model of disordered condensed media in the structure of clusters with the most probable number of particles, it is possible to form quantum dots, which are potential pits with a wall height determined by the parameters of the effective interaction potential between the nearest particles in the cluster. As a result of spontaneous cluster decay, the quantum dot disappears and appears in the structure of the newly formed cluster, thus the quantum dot "wanders" in the structure of disordered condensed media.

In the processes of protonation of cluster systems, closed proton currents may appear in their structure, which create magnetic fields in the first coordination sphere and contribute to the formation of a dimer as the core of the cluster system [1–4].

For reasons of symmetry and the assumption of the quasicrystalline structure of the cluster in its structure forms a size-quantum region in the form of a toroid as a conductor of proton current, which creates a magnetic field of the order of 1T.

The additional energy received by an atom in a magnetic field is spent on the energy of dimer formation from nearby atoms. This energy is 2–4^{o}K and is the starting value for enabling the formation of stable dimers of these atoms [5]. The quasicrystalline model based on the "golden" section assumes the formation of quantum-dimensional regions (quantum dots) in the structure of the first coordination sphere of the cluster. When a cluster collapses, the quantum dot passes into the structure of the newly formed cluster, in this sense, the quantum dot migrates (wanders) in cluster systems.

It is also shown that the formation of toroidal potential traps is possible in cluster structures [6].

REFERENCES

[1] G.A. Melnikov, "Heat of melting of small clusters in the model of potential with effective depth of potential pit," Solid state Physics, vol. 60, no. 5, pp. 989–992, 2018.

[2] G.A. Melnikov, N.M. Ignatenko, V.G. Melnikov, E.N. Cherkasov, O.A. Manzhos, "Structure of Small Clusters and IR Spectrum Condensed Matters," Journal of Nano- and Electronic Physics, vol. 7, no. 4, pp. 04087(3pp), 2015.

[3] G.A. Melnikov, N.M. Ignatenko, A.S. Gromkov, "Quantum dots in structure of quasicrystalline systems," Journal of Physics: Conference Series, vol. 1347, pp. 012031(6pp), 2019.

[4] G.A. Melnikov, "Clusters Fidonacci in the structure of condensed medium," Izv. vuz. Fiz., vol. 9/2, pp. 207–210, 2018.

[5] Yu.A. Neruchev, M.F. Bolotnikov, A.K. Radchenko, "Isochoric heat capacity and cluster structure of a simple liquid," High temperature Thermophysics, vol. 56, no. 5. pp. 699–703, 2018.

[6] V. Paul, "Electromagnetic traps for charged and neutral particles. Nobel Lecture in Physics – 1989," Usp. Fiz., vol. 160, no. 12, pp. 109–127, 1990.

* The presented work is a continuation of the RFBR project No. 16-08-01203.

COMBINATION SCATTER OF LIGHT IN LIQUIDS, TAKING INTO ACCOUNT CLUSTERIZATION PROCESSES IN THEIR STRUCTURE*

G.A. MELNIKOV, N.M. IGNATENKO, O.A. MANZHOS, A.S. GROMKOV

Southwest State University (SWSU), Kursk, Russia

The article is devoted to the study of the possibilities of taking into account the processes of formation of cluster systems in the structure of liquids and the influence of these processes on combination scatter of light [1–3]. Within the framework of the classical theory of the Raman effect, a relation is obtained for Stokes and anti-Stokes light scatters, taking into account the influence of clusters on scattered frequencies, and it is shown that scattered frequencies are proportional to the square root of the number of particles in the cluster [4–8]. The calculated frequencies of the Raman spectrum are compared according to the proposed model and experimental data in the frequency range 20–300 cm^{-1}, which showed the adequacy of the proposed model.

The inclusion of clusterization processes in the structure of organic liquids within the framework of the classical theory of combination scatter of light leads to the fact that the experimentally observed frequencies in the Raman spectrum are proportional to the square root of the number of particles in the most stable clusters. The appearance of spectral bands in the Raman spectra (30–350 cm^{-1}) is due to librational vibrations of dimeric formations of various configurations in the cluster structure [4–8].

The number of particles in the clusters can be any, however, according to the Zeckendorf theorem, any integer can be represented as the sum of numbers from the Fibonacci series, and the adjacent numbers from this series are never used and the set of Fibonacci numbers is the only one [4–8, 9].

From a wide variety of clusters in the structure of liquids, a special class of clusters called Fibonacci clusters can be distinguished, which differ in a number of features of composition and internal structure. The sequential formation or collapse of a cluster with the number of particles from the Fibonacci series occurs according to the rule when a newly appeared cluster has the number of particles from the same series of Fibonacci numbers, and the ratio of the number of particles in two successively formed clusters, equal to the "golden section", is preserved.

REFERENCES

[1] C.V. Raman, K.S. Krishnan, "The Optical Analogue of the Compton Effect," Nature, vol. 121, p. 711, 1928.

[2] G.S. Landsberg, L.I. Mandelstam, "A new phenomenon in light scattering," Journal of the Russian Physico-Chemical Society, part physical, vol. 60, no. 4, p. 355, 1928.

[3] G. Plachek, Rayleigh scattering and Raman effect, Kharkov: State. scientific tech. publishing house of Ukraine, 1935.

[4] G.A. Melnikov, V.N. Verveyko, Yu.F. Melikhov, M.V. Verveyko, A.V. Polyansky, "Heat capacity and elastic characteristics of monatomic and organic liquids taking into account the formation of clusters," Thermophysics of high temperatures, vol. 50, no. 2, pp. 233–239, 2012.

[5] G.A. Melnikov, N.M. Ignatenko, A.V. Polyansky, "The polarizability of molecules within the cluster model of matter," Izv. Kursk. gos. univer., no. 4(33), pp. 17–24, 2010.

[6] G.A. Melnikov, "Heat of melting of small clusters in the model of potential with effective depth of potential pit," Solid state Physics, vol. 60, no. 5, pp. 989–992, 2018.

[7] G.A. Melnikov, N.M. Ignatenko, V.G. Melnikov, E.N. Cherkasov, O.A. Manzhos, "Structure of Small Clusters and IR Spectrum Condensed Matters," Journal of Nano- and Electronic Physics, vol. 7, no. 4, pp. 04087(3pp), 2015.

[8] G.A. Melnikov, N.M. Ignatenko, V.M. Paukov, V.V., Suchilkin, "Modeling of dimeric formations in the structure of benzene clusters, " Physical and mathematical modeling of systems. Materials of the XIX International seminar, pp. 145–149, 2018.

[9] J.E. Bertie, C.D. Keefe, "Infrared intensities of liquids XXIV: optical constants of liquid benzene-h6 at 25 C extended to 11.5 cm^{-1} and molar polarizabilities and integrated intensities of benzene-h6 between 6200 and 11.5 cm^{-1}," Journal of Molecular Structure, vol. 695–696, pp. 39–57, 2004.

* The presented work is a generalization of the results of work on the RFBR project No. 16-08-01203.

MOLECULAR DYNAMICS SIMULATION OF IRRADIATION DAMAGE IN DISORDERED ALLOYS WITH ORDERED PRECIPITATION*

SHIJUN ZHAO[1]

[1]*Department of Mechanical Engineering, City University of Hong Kong, Hong Kong, China*

Chemically disordered concentrated solid–solution alloys, including high-entropy alloys (HEAs), have demonstrated good mechanical properties and promising irradiation resistance depending on their compositions. Recently, it has been shown that introduction of ordered precipitates into the HEA matrix can further improve their mechanical performance significantly [1,2], thanks to the formation of $L1_2$ phase that affects dislocation movement during deformation. Here we employ molecular dynamics simulations to study how these ordered phases can influence the evolution of irradiation damage during accumulated cascade conditions. We studied two systems, i.e. L12 Ni-Fe and Ni-Al ordered phases within pure Ni. Different sizes of the $L1_2$ phase are considered. As shown in Fig.1, it is found that dislocations tend to form in the Ni matrix in the Ni_3Al strengthened system, whereas dislocations are found in the interface between Ni_3Fe and Ni. These results indicate that Ni_3Al can suppress defect evolution, since no or less defects are found inside this phase. On the other hand, the ordered Ni_3Fe phase creates interface in the system, at which defects are likely to grow. Our results can be understood by the different defect properties in the matrix and the $L1_2$ phase [3,4]. These results show that the size and density of the ordered phase affect the irradiation damage states of the alloy systems.

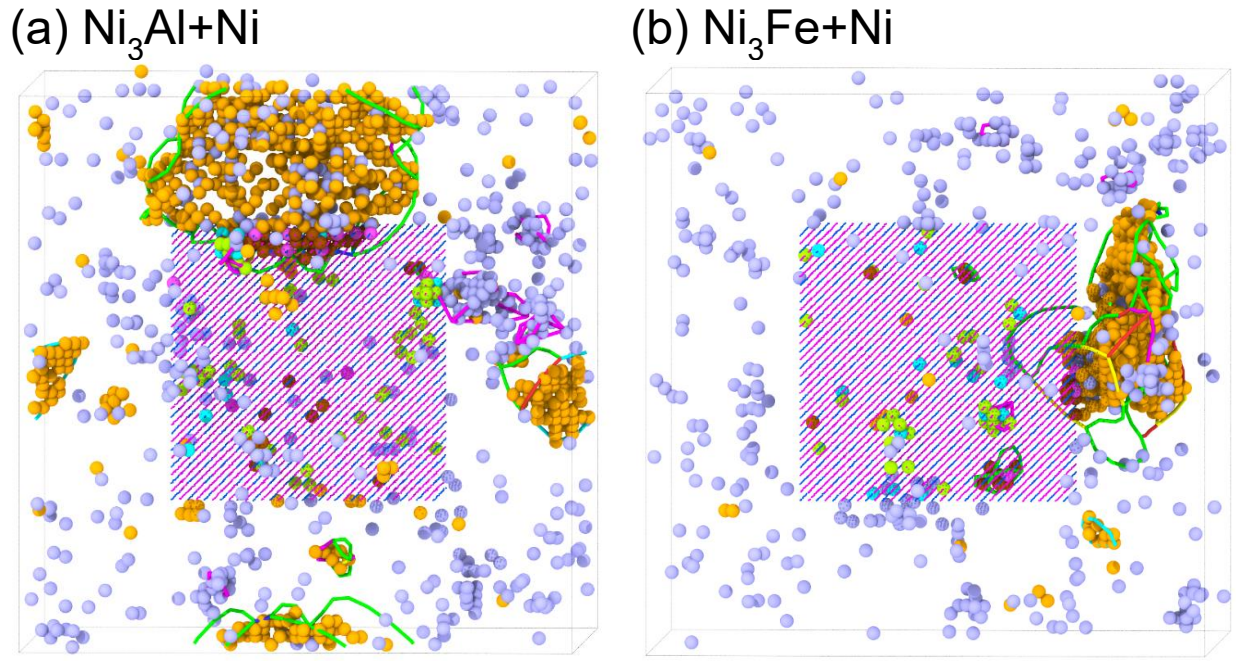

Fig.1. Defect configuration caused by accumulated cascade in (a) Ni_3Al+Ni and (b) Ni_3Fe+Ni system. Yellow balls represent interstitials whereas cyan balls for vacancies.

REFERENCES

[1] T. Yang, Y.L. Zhao, Y. Tong, Z.B. Jiao, J. Wei, J.X. Cai, X.D. Han, D. Chen, A. Hu, J.J. Kai, K. Lu, Y. Liu, C.T. Liu, Multicomponent intermetallic nanoparticles and superb mechanical behaviors of complex alloys, Science (80-.). 362 (2018) 933–937.

[2] Y.J. Liang, L. Wang, Y. Wen, B. Cheng, Q. Wu, T. Cao, Q. Xiao, Y. Xue, G. Sha, Y. Wang, Y. Ren, X. Li, L. Wang, F. Wang, H. Cai, High-content ductile coherent nanoprecipitates achieve ultrastrong high-entropy alloys, Nat. Commun. 9 (2018).

[3] C. Suna, E. Martíneza, J.A. Aguiar, A. Caroa, J.A. Valdeza, K. Baldwina, Y. Xua, B.P. Uberuagaa, O. Anderoglua, S.A. Maloya, Thermally induced interdiffusion and precipitation in a Ni/Ni3Al system, Mater. Res. Lett. 3 (2015) 169–175.

[4] Lee, Tongsik, Alfredo Caro, and Michael J. Demkowicz. "Atomistic modeling of radiation-induced disordering and dissolution at a Ni/Ni 3 Al interface." Journal of Materials Research 30, no. 9 (2015): 1456-1463

* The work was supported by City University of Hong Kong with program number 9610425.

FORMATION OF RADIATION DEFECTS IN A METAL TARGET BY A BEAM OF ACCELERATED ATOMS *

A. PUSHKAREV[1,2], A. PRIMA[1], X.P. ZHU[2], C.C. ZHANG[2], Y. LI[1], M.K. LEI[2]

[1]*Tomsk Polytechnic University, Tomsk, Russia*
[2]*Surface Engineering Laboratory, School of Materials Science and Engineering, Dalian University of Technology, Dalian, China*

Results of irradiation of samples with a pulsed beam of carbon atoms with an energy of 250-300 keV and an energy density at focus of 3-10 J/cm^2 are presented. A beam of fast atoms is formed by charge-exchange of ions C^+ generated by the accelerator TEMP-6 (250-300 kV, pulse duration 150 ns) [1]. Our studies have shown that the dependence of the number of radiation defects in the target on the absorbed energy of the beam of fast atoms is described by a linear function $N_d=K_d \cdot E_{sum}$. Then, the average number of radiation defects in the displacement cascade can be calculated by the ratio:

$$n_d = K_d \cdot E_{atom},$$

where E_{atom} is the average energy of a fast atom in the beam.

The average energy of fast atoms in the beam formed by the TEMP-6 accelerator was calculated based on the beam energy density [2] and ion current density [3] in the focus for the mode without charge-exchange of ions. The SRIM simulation [4] showed that the number of radiation defects in the cascade of C^+ ions is 4−5 times lower than the experimental values.

A comparative analysis of the effect of ion beams and accelerated atoms on a metal target is performed. Fig. 1 shows the efficiency of energy transfer during penetration of various ions in an iron target. The probability of ion and PKA collision normalized, the integral over PKA energies (>10 eV) is equal to one.

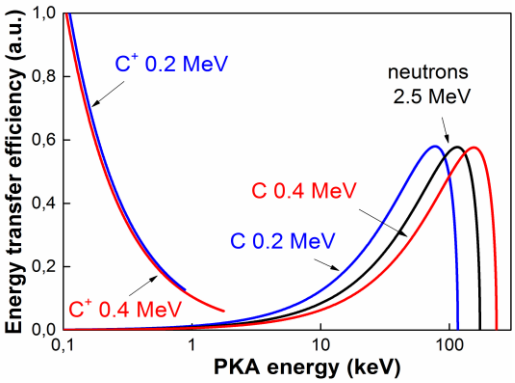

Fig. 1. Dependence of the efficiency of kinetic energy transfer of fast particle from PKA energy during penetration in an iron target

It was found that irradiation of the target with accelerated atoms is more consistent with neutron irradiation in a nuclear reactor in spectrum of primary knocked-out atoms, efficiency, and the mechanism of formation of radiation defects. The PKA energy after irradiation iron target with fast atoms (energy 0.2 – 0.4 MeV), and neutrons (1-3 MeV), differ slightly and exceeds 10 keV. The PKA energy after irradiation with ions with energy 0.2 – 0.4 MeV is less than 0.1 keV. At irradiation iron target with fast atoms the scattering angle of fast atoms and PKA is 100-120°, what corresponds to the mode of neutron irradiation. It is shown that when accelerated atoms (generated by the TEMP-6 accelerator) are absorbed in the target, the probability of their ionization is insignificant.

REFERENCES

[1] X.P. Zhu, L. Ding, Q. Zhang, Yu. Isakova, Y. Bondarenko, A.I. Pushkarev, M.K. Lei, “Generation and transportation of high-intensity pulsed ion beam in varying background pressures,” Laser and particle beams, vol. 35, no. 4, pp. 587-596, 2017.

[2] Y.I. Isakova, A.I. Pushkarev. “Visualization and analysis of pulsed ion beam energy density profile with infrared imaging,” Infrared Physics & Technology, vol. 89, pp. 140–146, 2018.

[3] A.I. Pushkarev, Y.I. Isakova, A.I. Prima. “High-intensity pulsed ion beam composition and the energy spectrum measurements using the time-of-flight method,” Laser and Particle beams, vol. 36, no. 2, pp. 210-218, 2018.

[4] J.F. Ziegler, J.P. Biersack, U. Littmark. The stopping and range of ions in solids. New York: Pergamon, 1985. 372 p.

* Experiments on the accelerator TEMP-6 was supported by the National Science Foundation of China under Grants Nos. 51371043, 51621064. Analysis of experimental data was supported by Russian Foundation for Basic Research, project no. 19-38-90001.

EFFECT OF HIGH ENERGY ION BEAM INDUCED MODIFICATION AND CHARACTERIZATION OF ZINC OXIDE THIN FILMS GROWN BY ATOMIC LAYER DEPOSITION

VISHNU CHAUHAN[1], *NIKHIL KORATKAR*[2], *RAJESH KUMAR*[1,*]

[1]*University School of Basic and Applied Sciences, Guru Gobind Singh Indraprastha University New Delhi-110078, India;*
[2]*Rensselaer Polytechnic Institute 110 8th Street, Troy, New York 12180, USA*
[*]*Email: kumarrrpi@gmail.com*

The generation of defects and modifications in properties of the oxide materials leads to have curiosity under swift heavy ion beam irradiation. The modifications induced in different properties of ZnO thin films deposited by thermal- atomic layer deposition technique on Si/glass substrates were analyzed as a function of high energy ion beam irradiation (120 MeV Ti 9+) on pristine and irradiated thin films with different fluence 5E11, 1E12, 5E12 and 1E13 ions/cm 2 . The role of high energy irradiation on structural, optical, surface topographical and chemical properties were investigated by XRD, PL, AFM, XPS and FTIR techniques. Photoluminescence (PL) emission spectra of virgin and irradiated samples were investigated under excitation wavelength of 325 nm and 370 nm using PL spectroscopy. The change in intensity and PL band position is ascribed to the effect of high energy ion irradiation [1]. Variation in structural parameters (crystallite size, stress and strain) of pristine and irradiated ZnO samples were determined using X-ray Diffraction (XRD) [2]. The Atomic force microscope (AFM) analysis showed the change in grain size and surface roughness of the pristine and irradiated samples. Further, the complete statistical roughness information of ZnO thin films were determined by power spectral density (PSD). The survey spectra of ZnO thin films obtained from X-ray photoelectron spectroscopy (XPS) determine the binding energy of Zn 3d, Zn 3p and Zn 3s at 10 eV, 101 eV and 153 eV respectively. Further, the change in peak intensity of Zn 2p and O 1s region is caused by electronic excitation induced defects under 120 MeV ion irradiation. Fourier-transform infrared spectroscopy (FTIR) spectra recorded in the range of 1000-3000 cm -1 to investigate the vibrational properties of pristine and irradiated samples. The present work shed light on the influence of ion irradiation on development of new diverse materials and possible implications of ZnO thin films in the radiation environment. The detailed results will be discussed during the presentation.

REFERENCES

[1] [1] Vishnu Chauhan, R. Gupta, V. Kumar, J. Ram, F. Singh, M. Prasad, S. Kumar, S. Ojha, P.A. Alvi, R. Mehra, R. Kumar, High energy (150 MeV) Fe 11+ ion beam induced modifications of physico- chemical and photoluminescence properties of high-k dielectric nanocrystalline zirconium oxide thin films, Ceram. Int. 45, 18887–18898, 2019.

[2] [2] Vishnu Chauhan, R. Kumar, Phase transformation and modifications in high-k ZrO 2 nanocrystalline thin films by low energy Kr 5+ ion beam irradiation, Mater. Chem. Phys. 240, 122127. 2020.

STUDY OF THE DEPENDENCE OF THE DEFORMATION OF THIN FILMS OF POLYTETRAFLUOROETHYLENE ON THE DOSE OF ELECTRON IRRADIATION IN UNIAXIAL STRETCHING

N.A. VORONOVA[1], A.I. KUPCHISHIN[1,2], M.N. NIYAZOV[1], B.G. TAIPOVA[1], B.A. TRONIN[1]

[1]Kazakh National Pedagogical University named after Abay, Almaty, Kazakhstan
[2]Kazakh National University named after al-Farabi, Almaty, Kazakhstan

Polytetrafluoroethylene (PTFE), as known, is a fluorine-based monomer that belongs to the fluorocarbon family. It has the chemical formula C_2F_4, which is similar to ethylene or ethene (C_2H_4 or $H_2C – CH_2$). PTFE is the simplest perfluorinated alkane. In industry, it is mainly used to produce polymers such as Teflon. Often it is called ftoroplast or ftoroplast-4 (F-4) [1, 2].

For example, to modify the polymer surface, the effects of mussel polymer coating (PDA) and the further introduction of functional groups were considered in [3]. The works devoted to the study, modification and application of fluoroplastic are diverse. For example, in [4], using PTFE, scientists carried out repairs on the human tendon, where a polymer with satisfactory mechanical properties acted as a suture for the restoration of human tissues. In [5], a study was made of the deformation and mechanical failure of single fluoroplastic chains using molecular dynamics (MD). During compression and twisting, the coefficient of friction of the polymer depends on the direction [6, 7].

This work is devoted to the study of the dependence of the deformation characteristics of polytetrafluoroethylene films on the dose of electron irradiation under uniaxial tension along the vertical axis.

As the studied material, a polytetrafluoroethylene film with a thickness of 40 and 100 μm was chosen. Film samples were cut using a special device. The length of the test material was 7 cm, the working part was 5 cm (2 cm of the polymer sample was fixed in the clamps), and the width was 0.5 cm. This film was subjected to uniaxial tension. Electron irradiation was carried out on an ELU-6 linear accelerator with an energy of 2 MeV. The dose rate was 60 Gy/s. Films for irradiation were installed at a distance of 300 mm from the exit window of the accelerator. The beam current was 0.16 $\mu A/cm^2$. The material temperature during research was maintained equal to 23 ^0C. The obtained samples were irradiated with various doses of 1, 3, 5, 7 and 10 kGy. Some of them were used as control samples. Tensile tests were carried out on a universal explosive machine model RU-50, with a stroke speed of 100 mm/min. For data processing and calculation, an interface with Science Cube sensors was used. The strain collection rate was 2.5 $mm*s^{-1}$.

As a result of studies of the dependence of deformation and return strain on the radiation dose, it was found that the deformation of a sample with a thickness of 100 μm is more than 2 times greater than that of a film 40 μm thick, which can be explained by the influence of the size of the polymer macromolecules.

Electron irradiation in the dose range of 0 – 10 kGy leads to a deterioration in the elasticity of polytetrafluoroethylene under deformations close – to fracture. For this reason, the return strain of the fluoroplastic for two thicknesses decreases.

The elongation of the material after irradiation, regardless of thickness, increases by more than 100%. The reason for this effect is the unwinding of spiral-shaped macromolecules due to weakening of bonds due to defects.

REFERENCES

[1] V.A. Ivchenko, “Atomic structure of cascades of atomic displacements in metals and alloys after different types of radiation,” IOP Conf. Series: Materials Science and Engineering, vol. 110, Article Number 012003, 2016.

[2] A.I. Kupchishin, B.G. Taipova, A.A. Kupchishin, N.A. Voronova, V.I. Kirdyashkin, T.V. Fursa, “Catastrophic models of materials destruction, ” IOP Conf. Series: Material Science and Engineering, vol. 110, Article Number 012037, 2016.

[3] A.P. Surzhikov, O.V. Galtseva, E.A. Vasendina, V.A. Vlasov, E.V. Nikolaev, “Processing line for industrial radiation-thermal synthesis of doped lithium ferrite powders,” IOP Conf. Series: Materials Science and Engineering, vol. 110, Article Number 012002, 2016.

[4] V. N. Zabaev, Application of accelerators in science and industry: textbook, Tomsk: TPU publishing House, 2008.

[5] G.H. Vineyard, Radiation Damage in Solids, Billington, London, 1962.

[6] E. Polykandriotis, F. Besrour, A. Arkudas, F. Ruppe, K. Zetzmann, L. Braeuer, R.E. Horch, “Flexor tendon repair with a polytetrafluoroethylene (PTFE) suture material,” Springer Verlag, vol. 173, pp. 46–51, 2019.

[7] B. Ahmed, S.K. Raghuvanshi, A.K. Srivastava, “Optical and structural study of aromatic polymers irradiated by gamma radiation,” Indian J. Pure Appl. Phys., vol. 50, pp. 892–898, 2012.[i]

[i] The work was performed according to the grant of the Ministry of Education and Science of the Republic of Kazakhstan No. AP05132186.

MONITORING RADIATION PROCESSING OF FOOD PRODUCTS[1]

R.A. VAZIROV[1,2], S.Y. SOKOVNIN[1,2,3], A. N. TSMOKALYUK[1], E. N. AGDANTSEVA[1], M.E.BALEZIN[3]

[1]Ural State Agrarian University Yekaterinburg, Russia
[2]Ural Federal University, Yekaterinburg, Russia
[3]Institute of Electrophysics UD RAS, Yekaterinburg, Russia

According to IAEA requirements, radiation-treated food products should be marked with the symbol "Radura-logo," but in the absence of appropriate marking from unscrupulous suppliers, it is difficult to determine if the product was radiated. At the same time the product itself can be an indicator of radiation treatment - radicals formed in the material of the product are preserved for a long time and can be registered by means of EPR. Thus, the correct preparation and measurement of the EPR spectrum will make it possible to check whether the products have been treated with ionizing radiation. The second important problem of food radiation is control of permitted level of absorbed doses. Exceeding the permissible dose value can lead to a significant decrease in nutritional value, organoleptic and physical-chemical properties. At the same time in different countries there are restrictions on the upper limit of the absorbed dose, for irradiation of food products. EPR spectrometry can be used for dosimetry after irradiation for up to two months.

Determination of application of radiation treatment on chicken eggs by means of EPR spectrometry of shell has high reliability, as registration of EPR spectrum of chicken eggs is possible even at absorbed doses from 1 Gy. [1] Radiation-induced EPR signal manifests itself in egg shell when exposed to gamma radiation ^{60}Co [2] by electron beam 10 MeV [3]. This method is also suitable for monitoring radiation surface disinfection [4].

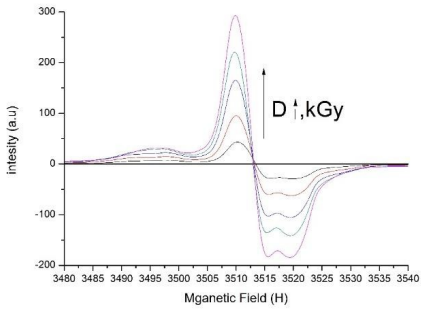

Fig. 1 - Radiation-induced EPR signal after radiation treatment of table chicken eggs.

As the subject of the study were used food chicken eggs from a store don't treated by radiation. Irradiation of samples was carried out in IEF URO RAS on electron accelerator URT-0.5 [3]. Dosimetry was performed using film dosimeters of CO PD (F) P-5/50 with certification error of not more than ± 7%, at P = 0.95 (N 1735:2011 in the MSO Register). The shell of irradiated eggs was powdered by mechanical grinding in a mortar and placed inside a standard (ER221TUB/4) quartz ampoule. Measurements of EPR spectra were performed on EPR spectrometer ELEXSYSE500 one day after treatment. Irradiation and measurements of EPR signals were carried out at room temperature. Operating frequency of spectrometer is 9, 88Ghz, radiation power 2mW, modulation amplitude 6Gs, range of change of magnetic field 150Gs. The results were processed in the OriginPro8 software package.

The results obtained (Figure 1) make it possible to conclude that EPR spectrometry can be used to control the irradiation of chicken eggs, as well as to control the level of absorbed dose. Three molecular ions are observed on the spectra: CO_3^{3-}, CO_3^{2-} and CO^{3-}. [5]. The intensity and area under the peaks are both positive and negative proportional to the value of the absorbed dose.

The prospect of using the investigated EPR method of shell dosimetry can be demanded for radiation treatment control at manufacturers enterprises. This significantly reduces the cost of dosimetry. The second important feature using of the food product as an ionizing radiation detector is the elimination of the methodological error of the detector installation and the avoidance of indirect radiation detection methods.

The study was carried out with partial financial support of RFBR and Sverdlovsk region within the framework of scientific project No. 20-48-660019.

REFERENCES

[1] K. Nakagawa, "Effects of low-dose X-ray irradiation of eggshells on radical production," FreeRadicalResearch, vol. 48, no 6, pp. 679–683, 2014.
[2] N. D.Yordanov, B.Mladenova,"EPR studieson gamma-irradiated food stuffs containing hard tissues," BullChemTechnolMacedonia, vol. 19, pp. 171-176, 2000..
[3] C.Corredor, J. Diaz, J.M.Diaz, H. A. Farach, C.P.Poole,"ESR experiments with egg shells of chickens," Applied Magnetic Resonance, vol. 9, no. 3, pp. 309-317, 1995.
[4] R.A.Vazirov, S.Y. Sokovnin,M.E. Balezin,A.S. Krivonogova, I.M.Donnik, "Surface Disinfection Of Chicken Eggs By Nanosecond Electron Beam," Research Journal of Pharmaceutical, Biological and Chemical Sciences, vol. 9, no. 5, pp. 1846-1854, 2018.
[5] Z. M.DaCosta,W. M. Pontuschka,V. Ludwig,J. M. Giehl, C. R.DaCosta, E. L. Duarte, "A study based on ESR, XRD and SEM of signal induced by gamma irradiation in eggshell," RadiationMeasurements, vol. 42, no. 6-7, pp. 1233–1236, 2007

1 The work was supported by RFBR and Sverdlovsk region within the framework of scientific project No. 20-48-660019

FEATURES OF THE IONIZING RADIATION IMPACT ON THE METAL-HYDROGEN SYSTEM

I.P. CHERNOV[1], *L.A. SVYATKIN*[1], *V.M. SILKIN*[1,2], *YU.I. TYURIN*[1]

[1]*Tomsk Polytechnic University, Tomsk, Russia*
[2]*Donostia International Physics Center, San Sebastián, Spain*

The results of a comprehensive study of the effects of accelerated electrons, X-rays and the electromagnetic field on the metal-hydrogen (M-H) system were discussed. Palladium, nickel, zirconium and titanium, which are widely used as structural materials for energy-storage systems and in aerospace and nuclear industries, were chosen as metals for research. These structural materials are exposed to hydrogen embrittlement and radiation during an operation. It is known that hydrogen is released from metals in atomic and ionic forms under the influence of ionizing radiation, and a gigantic increase in the mobility of hydrogen is observed [1]. Experimental results indicate that hydrogen isotopes, occupying regular positions in the metal lattice, form their own hydrogen subsystem. The energy introduced in the process of radiation exposure is accumulated by the hydrogen subsystem, as a result of which the hydrogen atoms acquire energy that is much higher compared to the matrix atoms. It was shown that the non-equilibrium state of the hydrogen subsystem in metal lattice creates favorable conditions for vibrational-translational exchange, non-equilibrium redistribution and release of hydrogen from a solid during irradiation. Therefore, even in metals with fast electron subsystem relaxation time (10^{-13}–10^{-14} s), the presence of light hydrogen isotopes creates conditions for energy storage.

The experimental studies of the stimulation hydrogen isotopes yield from metals at equilibrium and non-equilibrium heating of the samples using an external coaxial furnace, Joule's heat of electric current, accelerated electrons and weak electromagnetic fields were carried out in a high-vacuum installation [2] with oil-free pumping by turbomolecular and spiral pumps. The study of thermally stimulated gas release carried out using external linear heating of samples by coaxial furnace. It was obtained that the temperature position of the maximum hydrogen and deuterium release rates at comparable heating rates of Ni and Pd samples decrease in the following order: heating the samples by external electric furnace in metal cell → in quartz cell → by Joule's heat (displacement reached of ΔT = 100–200 °C), but for heating by the accelerated electrons beam one has $\Delta T \approx 350$ °C. In the case of Ti and Zr samples the temperature position of the maximum hydrogen and deuterium release rates practically does not change when the samples are heated in a metal cell, in a quartz cell and by AC passing through the samples (ΔT = 5–10 °C). However, this position significantly ($\Delta T \approx 365$ °C) shifts to low temperatures when heated by accelerated electrons beam. It was shown, that the hydrogen isotope effect is relatively weak.

The unique accumulating properties of hydrogen in metals are evidenced by the release of hydrogen from metals at a temperature much lower than with thermal heating under local radiation exposure. Collective electron states (plasmons) are excited in the M–H system, as a result of which electric fields are induced, mainly localizing in the hydrogen vicinity [3]. The reaction of the electronic and atomic subsystems to radiation is theoretically investigated. The all calculations were performed within the framework of the density functional formalism using the method of optimized norm-conserving Vanderbilt pseudopotential [4], implemented in the ABINIT software package. It was obtained that a local displacement of hydrogen atoms causes a displacement of hydrogen atoms in the first and subsequent coordinate spheres of the metal lattice. In particular, the force acting on a hydrogen atom initially displaced (and seeking to return this atom to it regular position) is comparable in magnitude with the forces acting on hydrogen atoms in neighbor interstitial sites of Pd and Ni lattice. In the case of Ti and Zr lattice these forces are much less than the force acting on a hydrogen atom initially displaced.

REFERENCES

[1] Yu.I. Tyurin, V.S. Sypchenko, N.N. Nikitenkov, Hongru Zhang, I.P. Chernov, "Comparative study of the hydrogen isotopes yield from Ti, Zr, Ni, Pd, Pt during thermal, electric current and radiation heating," Int. J. Hydrogen Energ., vol. 44, pp. 20223-20238, 2019.

[2] N.N. Nikitenkov, A.M. Hashhash, I.A. Shulepov, V.D. Khoruzhii, Y.I. Tyurin, I.P. Chernov, "A plant for studying radiation and thermal desorption of gases from inorganic materials," Instrum. Exp. Tech., vol. 52, no. 6, pp. 865–870, 2009.

[3] V.M. Silkin, I.P. Chernov, P.M. Echenique, Yu.M. Koroteev, E.V. Chulkov, "Influence of hydrogen absorption on low-energy electronic collective excitations in palladium," Phys. Rev. B, vol. 76, pp. 245105(1-9), 2007.

[4] D.R. Hamann, "Optimized norm-conserving Vanderbilt pseudopotentials," Phys. Rev. B, vol. 88, no. 8, pp. 085117(1-10), 2013.

HIGH TEMPERATURE CONVERSION OF COLOR CENTERS IN CRYSTALS OF LITHIUM FLUORIDE*

V.P. DRESVYANSKIY[1], S.V. MURZIN[1], S.ENKHBAT[2], E.F. MARTYNOVICH1[1]

[1]Irkutsk Branch of Institute of Laser Physics SB RAS, 130 a Lermontov st., Irkutsk, 664033, Russia, E-mail: nadvp@list.ru
[2]Institute of Physics and Technology, Mongolian Academy of Science

This paper presents the results of color centers photothermal conversion in lithium fluoride crystals irradiated with gamma radiation. The temperature dependence of the luminescence intensity of some types of color centers was studied during annealing with a constant heating rate of 0.5 °C/s, with constant photoexcitation of luminescence by a CW laser (λ_{ex} = 405 nm). The data obtained show that with increasing temperature, F_2 and F_3^+ – color centers decay. Moreover, the rate of decrease in the concentration of different centers is different. F_3^+ – centers are destroyed much faster and as the temperature reaches 300 °C, they are destroyed almost completely. Annealing of F_2 – color centers is happen more slowly and proceeds up to 450 °C. In the high temperature 430-490 °C range, an increase in the band with a maximum at 510 nm is observed in the photoluminescence spectra, which is due to the formation of new color centers. The nature of these centers hasn't been identified yet. We studied the spectral-kinetic characteristics of these centers and suggested that they are complexes of impurity defects and color centers decay products.

It is shown that the action of laser radiation during annealing on gamma-irradiated crystals of lithium fluoride accelerates the conversion of F_2 and F_3^+ centers. This is explained by the fact that, in addition to thermally activated processes in the ground state, activation processes occur in the excited states of centers populated by laser irradiation.

* This work was supported by the Fundamental Scientific Research Program of the State Academies of Sciences for 2013-2020, section II.10.1, project No. 0307-2016-0004, as well as with financial support from the Russian Foundation for Basic Research and the Ministry of Education, Culture, Science and Sports of Mongolia, project No. 17-52-44015 Mong_a

INFLUENCE OF LONG-TERM OPERATION ON THE RESISTANCE OF LEDS TO IRRADIATION BY GAMMA-QUANTA

A.V. GRADOBOEV, V.V. SEDNEV, A.V. SIMONOVA, F.F. ZHAMALDINOV

National Research Tomsk Polytechnic University, 30, Lenin Avenue, Tomsk, 634050, Russia,

According to operating conditions, semiconductor devices made of various device structures can be subjected to the combined and complex action of long-term operation factors and the action of various types of ionizing radiation [1-3]. Nowadays, there are some works on the effect of ionizing radiation on the reliability of light-emitting diodes (LEDs) [4,5]. An analysis of the known literature data showed that there are practically no research works on the influence of long-term operation factors on the resistance of semiconductor devices to the subsequent exposure to ionizing radiation.

The purpose of this work is to research the influence of long-term operation factors on the resistance of LEDs to the effects of ^{60}Co gamma-quanta. The objects of research in the work were used industrial infrared wavelength range LEDs made on the basis of AlGaAs double heterostructures.

For research two batches of LEDs were formed consisting of 20 devises for each batch. The LED-1 batch was not exposed to the preliminary action of long-term operation factors before exposure to gamma-quanta. In turn, the LED-2 batch was subjected to preliminary action of long-term operation factors. Modeling of long-term operation was carried out by using a special certified equipment to research the reliability of LEDs. Irradiation by gamma-quanta was carried out on a stationary gamma installation based on the ^{60}Co isotope in a passive power mode, i.e. without imposing internal and external electric fields.

It has been established that the preliminary action of operational factors leads to a noticeable increase in the resistance of LEDs to irradiation with gamma-quanta. However, at the same time, relaxation processes are detected, in which the decrease in the emissive power is accompanied by its partial recovery, followed by a decrease with the repetition of this process with a further increase in the radiation dose. These relaxation processes may be due to the interaction of radiation defects with defects created as a result of the action of operational factors. In the future, it is necessary to research in more detail the lighting and electrophysical characteristics of LEDs under the combined action of operational factors and gamma-quanta irradiation.

REFERENCES

[1] Claeys C., Simoen E. “Radiation effects in advanced semiconductor materials and devices”. Springer Science & Business Media, 2013. – vol. 57.

[2] Johnston A. H. “Radiation effects in light-emitting and laser diodes”, IEEE Transactions on Nuclear Science, vol 50, no. 3, pp 689-703, March 2003.

[3] Chang M. H. et al. “Light emitting diodes reliability review”. Microelectronics Reliability. vol. 52, no. 5, pp 762-782, May 2012.

[4] Gradoboev A., Simonova A., Orlova K. “ Influence of irradiation by ^{60}Co gamma-quanta on reliability of IR-LEDs based upon AlGaAs heterostructures”, Physica Status Solidi (C) Current Topics in Solid State Physics (2016) 13(10-12) 895-902.

[5] Gradoboev A., Orlova K., Asanov I. “The fast neutron irradiation influence on the AlGaAs IR-LEDs reliability”, Microelectronics Reliability, 2015, vol. 65, pp 55-59.

INFLUENCE OF ELECTRIC FIELD ON RELAXATION PROCESSES UNDER THE COMBINED ACTION OF OPERATIONAL FACTORS AND GAMMA QUANTUM ON LEDS

A.V. GRADOBOEV, V.V. SEDNEV, A.V. SIMONOVA

National Research Tomsk Polytechnic University, 30, Lenin Avenue, Tomsk, 634050, Russia,

According to operating conditions semiconductor devices made of various structures can be exposed to the combined and complex action of long-term operation factors and the action of various types of ionizing radiation [1-3]. Nowadays, it has been shown that the electric field can make a significant contribution to the radiation resistance of semiconductor devices [4,5]. In addition, it was established [6] that under the combined action of operational factors and gamma-ray irradiation of light-emitting diodes (LEDs), relaxation processes are observed. Moreover, the decrease in the radiation power is accompanied by its partial recovery with subsequent decrease with the repetition of this process with a further increase in the radiation dose.

The purpose of this work is to research the influence of the built-in electric field on relaxation processes in LEDs during postirradiation with gamma rays. Previously, diabetes was exposed to factors of long-term operation. As the objects of study in the work, we used industrial LEDs of the IR wavelength range made on the basis of AlGaAs double heterostructures.

It has been established that the built-in electric field of the p-n junction of LEDs increases their resistance to gamma rays under the combined (sequential) action of operational factors and gamma rays.

REFERENCES

[1] Claeys C., Simoen E. “Radiation effects in advanced semiconductor materials and devices”, Springer Science & Business Media, 2013. – vol. 57.

[2] Johnston A.H. “Radiation effects in light-emitting and laser diodes”, IEEE Transactions on Nuclear Science, vol 50, no. 3, pp 689-703, March 2003.

[3] Chang M. H. et al. “Light emitting diodes reliability review”, Microelectronics Reliability, vol. 52, no. 5, pp 762-782, May 2012.

[4] Brudny V.N., Peshev V.V., Surzhikov A.P. “Radiation defect formation in electric fields: gallium arsenide, indium phosphide”, Novosibirsk, Nauka, 2001, 136 p.

[5] Gradoboev A.V., Sednev V.V. “Effects of p-n junction built-in electric field on ir-led resistance under gamma rays irradiation”, Applied Mechanics and Materials, Vol 770 (2015), pp 522-525.

[6] Gradoboev A.V, Sednev V.V., Simonova A.V., Zhamaldinov F.F. “Influence of long-term operation on the resistance of LEDs to irradiation by gamma-quanta”, EFRE2020.

CHANGES OF W-I CHARACTERISTIC SHAPE OF LEDS DURING THEIR OPERATION

A.V. GRADOBOEV, V.V. SEDNEV, A.V. SIMONOVA, A.A. ASTRAKHANTSEVA

National Research Tomsk Polytechnic University, 30, Lenin Avenue, Tomsk, 634050, Russia,

Light-emitting diodes (LEDs) operate under the conditions of ionizing irradiation. The purpose of this work is to research the influence of preliminary irradiation by fast neutrons on changing watt-ampere characteristic of the LEDs during operation. The objects of the research were LEDs based upon double AlGaAs heterostructures. Long-term operation conditions were simulated by accelerated step-by-step tests.

Analysis of the watt-ampere characteristic shape provides an opportunity to mark several distinctive areas that are defined by electron injection level in active region of the LED. The marked areas can be characterized by corresponded threshold currents. The threshold currents go up when step number rise accompanied with increase of ohmic contact resistance during step-by-step tests and under irradiation by fast neutrons.

Preliminary irradiation by fast neutrons leads to a shift in the threshold currents depending on fluence of fast neutrons. Preliminary irradiation by fast neutrons with fluence in the field of radiation-stimulated reconstruction of the initial defect structure makes it possible to increase the resistance of ohmic contacts during operation and, therefore, to increase their reliability. Preliminary irradiation by fast neutrons in the field of impact of only radiation defects leads to the accelerated increase of resistance of ohmic contacts during operation, which decreases their reliability.

Preliminary irradiation by fast neutrons can be used in the manufacturing technology of the LEDs with the purpose of the reliability increase.

REFERENCES

[1] Stanley, A.G. Comparison of Light Emitting Diodes in a Space Radiation Environment / A.G. Stanley // IEEE Trans. Nucl. Sci. 1970 – Vol. 17. – № 6. – P. 239–244.

[2] Johnston, A. H. Radiation damage of electronic and optoelectronic devices in space / A.H. Johnston. – 2000. – P. 56-59.

[3] Ukolov D. S. et al. Radiation Hardness Evaluation of LEDs Based on InGaN, GaN and AlInGaP Heterostructures //2019 IEEE 31st International Conference on Microelectronics (MIEL). – IEEE, 2019. – С. 197-200.

RADIATION-INDUCED DEFECTS AND LUMINESCENT PROPERTIES OF ALUMINUM OXIDE SINGLE CRYSTALS

D.V. ANANCHENKO[1], S.V. NIKIFOROV[1], G.R. RAMAZANOVA[1]

[1]Ural Federal University, Ekaterinburg, Russia

The α-Al_2O_3 single crystals are widely used in electronic technology (radiation-resistant substrates of microcircuits) and luminescent dosimetry (TLD-500K detectors). It is known that high-dose irradiation (> 10 Gy) produces radiation defects and changes the charge state of defects existed in α-Al_2O_3, which affects dielectric and luminescent properties of crystals [1]. However, at the moment, the relationship between luminescent properties and paramagnetic defects, as well as defects formed under pulsed ion irradiation, are insufficiently studied. The presented work is concerned with the study of radiation-induced defects formed in α-Al_2O_3 single crystals under high-dose irradiation.

Two types of samples were investigated: 1) stoichiometric α-Al_2O_3 single crystals grown by the Kyropoulos method (Ti and Cr impurities <0.5 ppm); 2) anion-deficient α-Al_2O_3 single crystals grown under reducing conditions (Stepanov's method) with F-center concentration of 10^{17} $см^{-3}$ [2]. The radiation-induced defects were created by the following radiation sources: 1) β-irradiation $^{90}Sr/^{90}Y$, 2) RADAN-EXPERT pulsed electron accelerator (130 keV, τ = 2 ns, 60 A/cm^2); 3) a pulsed ion accelerator TEMP (~ 80% C^+ and ~ 20% H^+, 300 keV, τ = 100 ns). Identification and study of the properties of radiation-induced defects were carried out by the methods of optical, luminescent and ESR spectroscopy.

It was found that high-dose irradiation and thermo-optical treatment (UV irradiation with a xenon lamp at 573 K) of anion-deficient α-Al_2O_3 lead to the formation of paramagnetic centers with g = 2.008 in the crystals. The ESR intensity increase linearly with irradiation dose. It is accompanied by a growth of optical absorption (OA) and photoluminescence (PL) in the bands associated with F_2-type aggregate centers, which is consistent with [1]. The radiation-induced paramagnetic centers have high thermal stability (up to 820-973 K). The intensity of the ESR decreases after heating at mentioned temperatures, it is accompanied by a reduction of OA and PL of F_2-type aggregate centers, as well as a growth in the PL and OA of single F and F^+-centers. The foregoing suggests a relationship between the radiation-induced paramagnetic centers and F_2-type aggregate or more complex defects.

The irradiation of stoichiometric α-Al_2O_3 with high-power pulsed ion beams (C^+/H^+ ions) with subthreshold energy of defect creation causes the formation of single F and F^+-centers, as well as F_2-type aggregate centers. The dependence of PL of the F-type defects on the energy density of the ion beam (0.5 - 2 J/cm^2) is nonmonotonic. The reason for this may be the simultaneous generation and thermal annealing of radiation defects due to the intense heating of the crystals during irradiation. PL spectrum of the crystals irradiated with ions contains a new luminescence band at 2.85 eV, probably associated with the formation of vacancy – impurity complexes. The thermal stability of radiation-induced F-type defects formed under pulsed ion beam irradiation is comparable with the known data for neutron-irradiated α-Al_2O_3 crystals [3]. Theoretical analysis of the PL annealing kinetics was performed in terms of the diffusion-controlled bimolecular recombination of Frenkel defects in irradiated oxides [4]. It showed that a probable mechanism of annealing of F^+-centers created by a pulsed ion beams is recombination with mobile interstitial oxygen O_i.

REFERENCES

[1] V. S. Kortov, S. V. Zvonarev, V. A. Pustovarov, A. I. Slesarev, "Features of thermoluminescence in anion-defective alumina single crystals after highdose irradiation", Rad. Meas., vol. 61. – pp. 74-77, 2014.

[2] M. S. Akselrod, V. S. Kortov, D. J. Kravetsky, V. I. Gotlib, "Highly sensitive thermoluminescent anion-defective alpha-Al_2O_3: C single crystal detectors", Rad. Prot. Dos., vol. 32, no. 1, pp. 15-20, 1990.

[3] A. I. Popov, A. Lushchik, E. Shablonin, E. Vasil'chenko, E. A. Kotomin, A. M Moskina, V. N. Kuzovkov, "Comparison of the F-type center thermal annealing in heavy-ion and neutron irradiated Al_2O_3 single crystals", ", Nucl. Instrum. Methods Phys. Res. B, vol. 433, pp. 93-97, 2018.

[4] A. I. Popov, E. A. Kotomin, J. Maier, "Basic properties of the F-type centers in halides, oxides and perovskites", Nucl. Instrum. Methods Phys. Res. B, vol. 268, no. 19, pp. 3084-3089, 2010.

CHANGES IN THE STRUCTURE OF IRRADIATED STEEL 0.12C18Cr10NiTi CAUSED BY PLASTIC DEFORMATION AT DIFFERENT TEMPERATURES*

V.V. FIRSOVA, L.A. DIKOVA, A.S. DIKOV, S.B. KISLITSIN

Institute of Nuclear Physics, Almaty, Kazakhstan

The influence of temperature on change the mechanical properties of austenitic steel 0.12C18Cr10NiTi was investigated. This is important for long "dry" storage of spent fuel assemblies of fast breeder reactor BN-350. For this, uniaxial tension mechanical tests have been performed at temperatures of 24, 350 and 450 °C. The samples for tests were prepared from the ducts of spent fuel assemblies [1]. It was established the decreases of elongation of irradiated steel with increase the temperature tests (fig. 1).

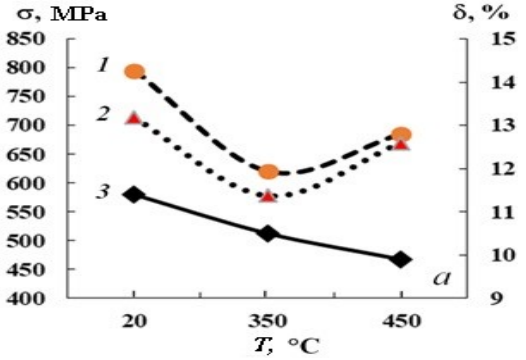

Fig. 1 – The dependence of the change in the mechanical characteristics of steel from the test temperature [2], 1 - ultimate strength, 2 - yield strength, 3 - relative elongation

The microstructural studies revealed grinding of austenitic grain and carbide inclusions at increasing test temperature. Fractography studies of the fracture surface showed a change in the concentration and size of discontinuities in the form of micropores at increasing test temperature. Based on the data obtained, it was concluded that a decrease in the relative elongation of steel with increasing temperature is caused by increase in the number of obstacles for sliding dislocations providing plastic deformation.

REFERENCES

[1] K.K. Kadyrzhanov, S.B. Kislitsin, O.P. Maksimkin, O.G. Romanenko, T.E. Turkebaev "Degradation in Mechanical Properties of Stainless steel 12Cr18Ni10Ti and 08X16H4M3 – Materials for Hexagonal Ducts of Spent Fuel Assemblies from the BN-350 Fast Neutron Nuclear Reactor," Proceedings of NATO Workshop "Safety Related Issues of Spent Nuclear Fuel Storage," NATO Sciences Series, pp.329-349, 2007.

[2] A.S. Dikov, I.I. Chernov, S.B. Kislitsin, "Influence of the Test Temperature on the Creep Rate of 0.12C18Cr10NiTi Structural Steel Irradiated in the BN-350 Reactor," Inorganic Materials: Applied Research, vol. 9, no. 3, pp. 357–360, 2018.

* The work was performed in the framework of BR05236400 project of Ministry of Education and Science of the Republic of Kazakhstan

MECHANISMS OF Fe-10Ni-20Cr NANOCRYSTALLINE ALLOYS RADIATION RESISTANCE FROM MOLECULAR DYNAMICS SIMULATIONS*

A.V. KORCHUGANOV, D.S. KRYZHEVICH, K.P. ZOLNIKOV

Institute of Strength Physics and Materials Science SB RAS, Tomsk, Russia

Metallic nanocrystalline materials with a high density of interfaces are one of the most promising candidates for the role of structural materials for nuclear energy [1-4]. Their promise is primarily due to high radiation resistance. The most important problem for such materials is to study the possibilities of stabilizing their structure at high temperatures and irradiation. In addition to doping, this can be achieved by forming certain types of interfaces that are most resistant to these influences. Introducing the grain boundaries of various types in the microstructure [5], including twin boundaries [6], is one of the most effective ways to increase material radiation resistance. In the area of such interfaces, partial or complete annihilation of structural defects generated by irradiation occurs. To study the radiation resistance mechanisms of nanocrystalline alloys, knowledge of the features of the interaction of grain boundaries with defects formed by atomic displacement cascades is of vital importance. Due to the small spatial and temporal scales of the processes at the micro level, as well as extreme external conditions, one of the most effective approaches for studying the evolution of the atomic structure during irradiation is computer simulation using the molecular dynamics method. This method allows obtaining complete information about the dynamics of structural rearrangements, since it explicitly takes into account the atomic structure of the material.

In this work, the object of research was the model fcc alloy Fe-10Ni-20Cr (at.%), the content of Ni and Cr in which is close to the values for austenitic stainless steels widely used as structural materials in nuclear power plants. Molecular dynamics simulations were performed in the LAMMPS software package [7]. The interatomic interaction was described using the many-body potential [8], constructed in the framework of the embedded atom method.

The interaction of atomic displacement cascades with energies up to 20 keV with various symmetric tilt grain boundaries and general grain boundaries was studied. The number and type of surviving radiation defects in Fe-10Ni-20Cr bicrystals with different grain boundaries were determined for different cascade energies and irradiation doses. The features of the migration of grain boundaries of various types during the formation of atomic displacement cascades in bicrystals were studied. Characteristic structural rearrangements initiated by irradiation that lead to grain growth have been identified. Based on the analysis of the simulation results, the features of the internal structure and mechanisms that provide high radiation resistance and stability of the initial structure of the Fe-10Ni-20Cr nanocrystalline alloy under various irradiation conditions have been revealed.

REFERENCES

[1] X. Zhang, K. Hattar, Y. Chen et al., "Radiation damage in nanostructured materials," Prog. Mater. Sci., vol. 96, P. 217–321, 2018

[2] J. Li, H. Wang and X. Zhang, "A review on the radiation response of nanoporous metallic materials," JOM, vol. 70, P. 2753–2764, 2018

[3] K.Y. Yu, C. Fan, Y. Chen et al., "Recent studies on the microstructural response of nanotwinned metals to in situ heavy ion irradiation," JOM., vol. 72, P. 160-169, 2020

[4] W. Han, M.J. Demkowicz, N.A. Mara et al., "Design of radiation tolerant materials via interface engineering," Adv. Mater., vol. 25, P. 6975–6979, 2013

[5] C. Sun, S. Zheng, C. C. Wei et al., "Superior radiation-resistant nanoengineered austenitic 304L stainless steel for applications in extreme radiation environments," Sci. Rep., vol. 5 Article Number 7801, 2015

[6] G. Meric de Bellefon, M. Robertson, T.R. Allen et al., "Radiation-resistant nanotwinned austenitic stainless steel," Scr. Mater., vol. 159, P. 123–127, 2019

[7] S. Plimpton, "Fast parallel algorithms for short-range molecular dynamics," J. Comput. Phys., vol. 117, P. 1–19, 1995

[8] L.K. Béland, A. Tamm, S. Mu et al., "Accurate classical short-range forces for the study of collision cascades in Fe–Ni–Cr," Comput. Phys. Commun., vol. 219, P. 11–19, 2017

* The work was supported by the Russian Science Foundation (Project No. 20-19-00466).

ON THE IMITATION ASSESSMENT OF THE RADIATION RESISTANCE OF MATERIALS[1]

V.V. OVCHINNIKOV[1]

[1]*Institute of Electrophysics, UB RAS, Amundsena Str. 106, Yekaterinburg, 620016, Russia, viae05@rambler.ru, (343)267-87-84*

Materials for the internals of modern fast neutron reactors must withstand a radiation load of up to 80–100 dpa or more, without experiencing adverse changes in properties. This requires the development of new classes of materials with increased radiation resistance.

In-situ reactor testing of promising materials, taking into account storing operations in order to eliminate induced activity, take at least 5−7 years. This does not allow you to quickly adjust the composition, as well as processing technology of the proposed compositions.

The terms of non-activating simulation experiments using ion beams fit in 1 year with a full cycle of analytical studies. Moreover, given the lack of induced activity of the samples, it is possible to conduct a wide range of studies not available when working with active materials.

Currently, on the one hand, a generally optimistic view has been formed on the possibility of simulating the irradiation of materials with reactor neutrons using beams of accelerated ions. On the other hand, an exhaustive justification for the legitimacy of such an imitation is still missing.

It is most important to maximally fully analyze in theory and in practice the factors that determine the similarities and differences between these two types of exposure. After that, it is necessary to try to ensure the maximum degree of similarity of the processes under consideration.

This primarily concerns the conditions determining the maximum similarity of cascade formation processes (under reactor and ion irradiation) at the collisional stage and the stage of intracascade diffusion. It is necessary to take into account the type of introduced ions, their energy, charge, mass, fluence (dpa and the effective value of dpa), and the rate of fluence gathering. The issues related to the geometric and energy parameters of cascades (and the presence of so-called "dense cascades"[2] in their composition) generated by primary knocked on atoms or accelerated ions during in-situ reactor and simulation testing are important. This applies, in particular, to giant local temperatures (3000–6000 K) and thermal pressures (5–40 GPa) in the thermalized nanoscale regions of passage of dense cascades of atomic displacements

The question of the ratio (similarity) of the integrated (average macroscopic) temperature of the targets in field and simulation experiments should be theoretically and practically resolved. It is also necessary to take into account the effects of emission and propagation in irradiated media of nanoscale post-cascade powerful elastic and shock waves of compression, the pressure at the front of which can exceed not only the real, but also the theoretical yield strength of materials. The role of this factor was practically not taken into account by classical radiation physics. In metastable media, such waves can propagate theoretically over unlimited distances, initiating structural and phase transformations at their front [1][3]. This applies equally to reactor and simulation experiments.

The work is devoted to the review and analysis of these issues in order to outline their circle, as well as to attract the maximum number of researchers to their solution.

REFERENCES

[1] *V.V. Ovchinnikov //* Surf. & Coat. Techn. – 2018. – V. 355. – P. 65-83.

[1] This work was supported by the Russian Scientific Foundation, project No. 19-79-20173.

[2] Compact regions, all of whose atoms participate in collisions.

[3] Analogies are examples of explosive crystallization of supercooled liquid and the decomposition of supersaturated solid solutions upon impact or shaking.

SPATIAL DISTRIBUTION OF THE LUMINESCENCE INTENSITY AND CENTER CONCENTRATIONS CREATED BY COHERENT PAIRS OF FEMTOSECOND LASER PULSES*

N.L. LAZAREVA[1,2], *E.F.MARTYNOVICH*[1,2]

[1]*Irkutsk Branch of the Institute of Laser Physics, SB RAS, Irkutsk, Russia*
[1]*Irkutsk State University, Irkutsk, Russia*

Currently, new methods are being developed to study the interaction of intense laser radiation with matter, based on the use of highly non-linear volumetric fluorescent photographic materials [1-5]. These media make it possible to experimentally visualize, record, digitize, memorize, and study the three-dimensional spatial picture of the highly nonlinear interaction of light and matter. This can be done in the mode of action on the medium of both single femto- and attosecond laser pulses, and their series. A set of such materials with varying degrees of non-linearity of their photosensitivity allows one to obtain a number of such spatial distributions, restore the configuration of light fields from them in the process of highly nonlinear interaction, and study the mechanisms of such interaction.

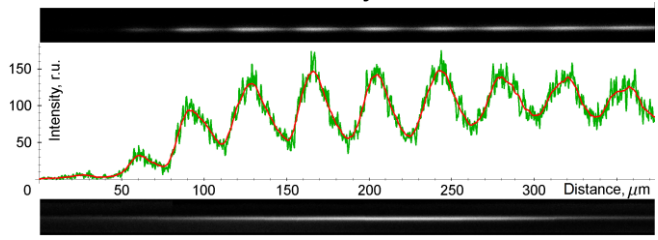

Fig.1. Photoluminescence of color centers in traces induced by filaments in the same experiment at different crystal depths (above and below). In the middle is a scan of the longitudinal distribution of the PL intensity in the upper trace

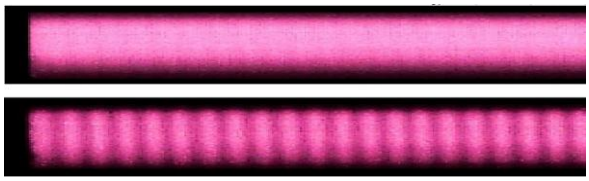

Fig.2. Photoluminescence of a crystal with a uniformly distributed concentration of color centers in the excitation channels with a uniform longitudinal distribution of the excitation intensity

In developing such methods, problems arise of studying the influence of inhomogeneities of exciting optical fields, as well as the concentrations of luminescence centers, on the picture of the spatial distribution of the intensity of the recorded luminescence. It is important to note that direct proportionality between the concentration of centers and the intensity of their photoluminescence, even with linear excitation, is realized only in rare cases. The experimental results shown in FIG. 1 and FIG. 2, demonstrate an example of such a situation. Here are traces of color centers visualized in photoluminescent radiation created in MgF_2 crystals by components of a coherent pair of femtosecond pulses propagating in the sample at different speeds (left). The longitudinal distributions of the luminescence intensity of color centers in Al_2O_3 crystals excited by pairs of continuous coherent waves propagating at different speeds are shown on the right.

The purpose of this work was to test methods for studying the interaction of intense laser radiation with matter, based on the use of highly non-linear volumetric luminescent photographic materials.

REFERENCES

[1] Martynovich E.F., Dresvyansky V.P., Rakevich A.L., Lazareva N.L., Arsentieva M.A., Tyutrin A.A., Bukhtsoozh O., Enkhbat S., Kostryukov P.V., Perminov B.E., Konyashchenko A.V. Creating of luminescent defects in crystalline media by a scanning laser beam. Appl. Phys. Lett. V.114. pp. 121901-1 – 121901-4, 2019.

[2] Чекалин С.В., Компанец В.О. Метод лазерной колорации в экспериментах по филаментации одиночных импульсов и образованию световых пуль в однородных прозрачных диэлектриках. Оптика и спектроскопия, Т. 127, № 7, С. 94-100, 2019.

[3] Martynovich E.F., Dresvyansky V.P., Lazareva N.L., Mikhailova S.V., Konyashchenko A.V., Kostryukov P.V., Perminov B.E., Bagayev S.N. The memorizing luminescent crystalline materials based on color centers for investigating highly nonlinear interaction of light and matter and for other applications. Advanced Photonics 2017, OSA, paper NoW2C.6.

[4] E.F. Martynovich, A.V. Kuznetsov, A.V. Kirpichnikov, E.V.Pestryakov, S.N.Bagayev. Formation of luminescent emitters by intense laser radiation in transparent media. Quantum Electronics V. 43, № 5, pp. 463-466, 2013

[5] E. F. Martynovich, D. S. Glazunov, A. V. Kuznetsov, E. V. Pestriakov, A. V. Kirpichnikov, and S. N. Bagayev, "3D Fluorescent Imaging with Highly Nonlinear Photosensitive Materials," in Advanced Photonics, OSA Technical Digest (Optical Society of America, 2011), paper SWD6.

* The work was supported by Grants of RFBR 19-32-90275 and by the Program of fundamental scientific research of the state academies of sciences for 2013–2020, section II.10.1 Project No. 0307-2016-0004.

DEFECT PROCESSES AND FORMATION OF WIGNER ENTHALPY IN BORON CARBIDE UNDER NEUTRON IRRADIATION

M.N. MIRZAYEV[1,2], KH.F. MAMMADOV[2], D.M. MIRZAYEVA[1], V.A. SUKRATOV[1], E. DEMIR[1,3], E. POPOV[1,4,5]*

[1] *Joint Institute for Nuclear Research, Dubna, Moscow distr., 141980, Russia*
[2] *Institute of Radiation Problems, Azerbaijan National Academy of Sciences, Baku, AZ1143 Azerbaijan*
[3] *Yeditepe University, Physics Department, Istanbul, 34755, Turkey*
[4] *Institute for Nuclear Research and Nuclear Energy, Bulgarian Academy of Sciences, Sofia 1784, Bulgaria*
[5] *Georgi Nadjakov Institute of Solid State Physics, Bulgarian Academy of Sciences, Sofia, 1784, Bulgaria*
[*] *matlab@jinr.ru*

Due to the good thermal conductivity, thermal resistance and a high melting point of boron carbide compounds, recent studies have shown that these compounds have become an important subject [1-3]. They also play an important role in nuclear applications involving neutron absorbing materials and the structure of neutron detectors [4-8]. In the present abstract, boron carbide samples were irradiated neutrons ($E \geq 1$ MeV) for different neutron flux up to 10^{15} $n \cdot cm^{-2} \cdot s^{-1}$ at room temperature at the IBR-2 M pulsed reactor in Joint Institute for Nuclear Research, Dubna, Russia. Thermal kinetic dynamics and parameters of boron carbide samples changed with a different mechanism. Boron carbide samples have shown exothermic effects and oxidation reactions at the $100 \leq T \leq 1200$ K temperature range in the DSC analysis. The heat flow rate, specific heat capacity, thermodynamic function and degree of oxidation of boron carbide samples are more complex. The unirradiation and irradiation of the thermodynamics kinetics of samples at the low-temperature changes with a differential mechanism.

REFERENCES

[1] M.N. Mirzayev, R.N.Mehdiyeva, R.G.Garibov, N.A.Ismayilova, S.H. Jabarov, Influence of gamma irradiation on the surface morphology, XRD and thermophysical properties of silicide hexoboride, Modern Physics Letters B, Vol. 32, No. 14, 1850151, 2018. DOI: 10.1142/S0217984918501518

[2] Matlab N. Mirzayev, Simultaneous measurements of heat flow rate and thermal properties of nano boron trioxide under neutron irradiation at the low and high temperature, Vacuum. (2019) 109162. doi:10.1016/j.vacuum.2019.109162.

[3] Matlab N. Mirzayev, Oxidation kinetics of boron carbide ceramic under high gamma irradiation dose in the high temperature, Ceramics International, 2019, https://doi.org/10.1016/j.ceramint.2019.09.273

[4] M.N. Mirzayev, Kh.F. Mammadov, V.A. Skuratov, E. Demir, S.H. Jabarov, N.A. Ismayilova, S. Biira, B. Abdurakhimov, E. Popov, Oxidation kinetics and thermophysical properties of gamma irradiated silicon hexaboride, Journal of Alloys and Compounds, Volume 801, 2019, Pages 151-157, https://doi.org/10.1016/j.jallcom.2019.06.135

[5] Matlab Mirzayev, Ertugrul Demir, Khagani Mammadov, Ravan Mehdiyeva, Sakin Jabarov, A. Beril Tugrul, Saphina Biira, Nguyen Tiep, Thabsile Thabethe, Thermodynamics kinetics of boron carbideunder gamma irradiation dose, International Journal of Modern Physics B, Vol. 33, No. 9 (2019) 1950073, DOI: 10.1142/S02179792195007356.

[6] M.N. Mirzayev, R.N. Mehdiyeva, S.Z. Melikova, S.H. Jabarov, T.T. Thabethe, S. Biira, M.A. Kurbanov, N.V. Tiep, Formation of Color Centers and Concentration of Defects in Boron Carbide Irradiated at Low Gamma Radiation Doses, Journal of the Korean Physical Society, Vol. 74, No. 4, 2019, pp. 363-367, DOI: 10.3938/jkps.74.363

[7] Ertuğrul Demir, Matlab N. Mirzayev, A. Beril Tugrul, Yury M. Gledenov, Vitali A. Turchenko, Ozan Yılmaz, Bülent Büyük and M. Lütfi Öveçoğlu, Investigations on surface morphologies, microstructure and thermal properties of tungsten-based composites, Modern Physics Letters B 33(19):1950216, 2019, DOI: 10.1142/S0217984919502166

ACCUMULATION AND ANNEALING OF RADIATION DONOR DEFECTS IN ARSENIC–IMPLANTED $Hg_{0.7}Cd_{0.3}Te$ FILMS*

A.V. VOITSEKHOVSKII[1], I.I. IZHNIN[1,2], K.D. MYNBAEV[3], J. MORGIEL[4], Z. SWIATEK[4], A.G. KOROTAEV[1], O.I. FITSYCH[5], O.YU. BONCHYK[6], H.V. SAVYTSKYY[6], V.S. VARAVIN[7], S.A. DVORETSKY[1,7], N.N. MIKHAILOV[7], M.V. YAKUSHEV[7]

[1]National Research Tomsk State University, Tomsk, Russia
[2]Scientific Research Company "ELECTRON-CARAT", Lviv, Ukraine
[3]Ioffe Institute, St.–Petersburg, Russia
[4]Institute of Metallurgy and Material Science PAN, Krakow, Poland
[5]P. Sagaydachny Army Academy, Lviv, Ukraine
[6]Ya.S. Pidstryhach Institute for Applied Problems of Mechanics and Mathematics NASU, Lviv, Ukraine
[7]A.V. Rzhanov Institute of Semiconductor Physics of SB RAS, Novosibirsk, Russia

The most common method of the fabrication of a p^+–layer in n–type $Hg_{1-x}Cd_xTe$ (MCT) with the aim of the development of 'p^+–n'-type photodiodes is ion implantation of arsenic followed by a two-stage activation annealing. The latter treatment is used for the annealing of radiation-induced defects and for the electrical activation of implanted ions. Fabrication of the photodiodes with ultimate parameters requires the knowledge of the processes of accumulation and annealing of the radiation-induced defects. Studies of these processes were performed earlier on MCT films with the composition of the active layer x_a~0.22, which serve as a basis for the fabrication of LWIR photodiodes. In this work, we report on the results of similar studies performed on MCT films with x_a~0.30, which are suitable for the development of MWIR devices.

The studies were performed on films with p– (due to the presence of mercury vacancies, acceptors in MCT) and n–type conductivity of the photodiode 'base'. The films were grown by Molecular Beam Epitaxy on GaAs and Si substrates and their active layers were covered with graded-gap surface layers (GSL). Implantation was performed with arsenic ions with energy 190 and 350 keV and fluences ranging from 10^{12} to 10^{15} cm^{-2}. The electrical characterization of the implanted films was performed by studying the magnetic field B dependences of the Hall coefficient $R_H(B)$ and conductivity $\sigma(B)$ at the temperature T=77 K. The data obtained in these studies were processed with the discrete mobility spectrum analysis, which allowed for obtaining the information on the set of carriers and their parameters, such as concentration, mobility and partial conductivity. Other methods of characterization included optical reflectivity studies in the VIS wavelength region and transmission electron microscopy; these were used for the study of radiation-induced damage, types of extended structural defects formed as a result of the implantation, and of their behavior under annealing.

It was found that implantation with the energy 190 keV and fluences 10^{12}–10^{15} cm^{-2} in the films with p–type base resulted in the formation of either an 'n^+–p' or a 'n^+–n–p' structure. The exact type of the structure was defined by the concentration of residual donors, which were responsible for the formation of the n–layer. Implantation with ion energy 350 keV lead to the formation of n^+–p structures for all the fluences used. In similar MCT structures with x_a~0.22, arsenic implantation with ion energy 190 keV and fluences 10^{12}–10^{15} cm^{-2} always resulted in the formation of 'n^+–n–p' structures.

It was found that the main structural defects in radiation-damaged layers were dislocation loops of various sizes. The dominating contribution to conductivity (~80% of the total conductivity) in the implanted films was due to electrons with low mobility (2500 – 4000 $cm^2/(V \cdot s)$ belonging to the n^+–layer formed as a result of implantation. These electrons originate in donor centers formed when the loops captured atoms of interstitial mercury. In films with x_a~0.3 we observed rather weak dependences of layered concentration and partial conductivity of the low-mobility electrons on the ion fluence. These values reached the saturation points at the fluence of 10^{13} cm^{-2}. In MCT films with x_a~0.22, the saturation was not observed at fluences as high as 10^{15} cm^{-2}; this difference resulted from lower internal electric field induced by GSL in the films with x_a~0.3.

The activation annealing of films with x_a~0.3 resulted in full annihilation of the loops (in contrast to films with x_a~0.22, where after the annealing the loops transformed into single dislocations), and, as a consequence, in the disappearance of the low-mobility electrons. Also, in nominally un-doped structures with x_a~0.3 with n–type base we did not observe the recovery of the electrical parameters of the base after the second stage of the activation annealing, which means that fabrication of photodiodes on the basis of this material requires a donor doping of the base.

*The work was supported by the Russian Science Foundation (Grant No. 19-12-00135).

PECULIARITIES OF THE EXTERNAL PHOTOELECTRIC EFFECT IN NARROW-BAND SEMICONDUCTORS CAUSED BY SOFT X-RAY RADIATION

V.G. SREDIN[1], *A.V. VOITSEKHOVSKII* [2], *A.P.MELEKHOV* [3], *R.S.RAMAKOTI* [3],

1. Peter the Great Military Academy of Strategic Rocket Forces, 8 Karbysheva Str., Balashikha, 143900 Russia

2.National Research Tomsk State University, 36 Lenin Ave., 634050 Tomsk, Russia

3.National Research Nuclear University MEPhI, 31 Kashirskoe shosse,115409 Moscow, Russia

When studying the effect of soft x-ray irradiation (SXrayI) of a laser plasma on single crystals and epitaxial layers of $Cd_xHg_{1-x}Te$ solid solutions, the appearance of time-stable point defects in the surface region of the material was discovered [1]. It is assumed that their generation is caused by relaxation of electronic excitations, as well as by the influence of a pulsed electric field arising in the material as a result of an external photoelectric effect, which leads to intense emission of electrons from the surface region [2]. In accordance with the proposed model, SXrayI excites the electrons of the inner shells of the ions, additionally ionizing them, and the field induced by the external photoelectric effect contributes to the exit of the excited ions from the equilibrium position in the crystal lattice with the formation of point defects. To test this hypothesis, we undertook studies of the external photoelectric effect under the influence of SXrayI laser plasma on $Cd_xHg_{1-x}Te$ with the composition x~0.2, InSb and brass (CuZn). The parameters of SXrayI laser source are described in [1]. The measurements were performed at 300K. The measurement results are presented in Fig. 1.

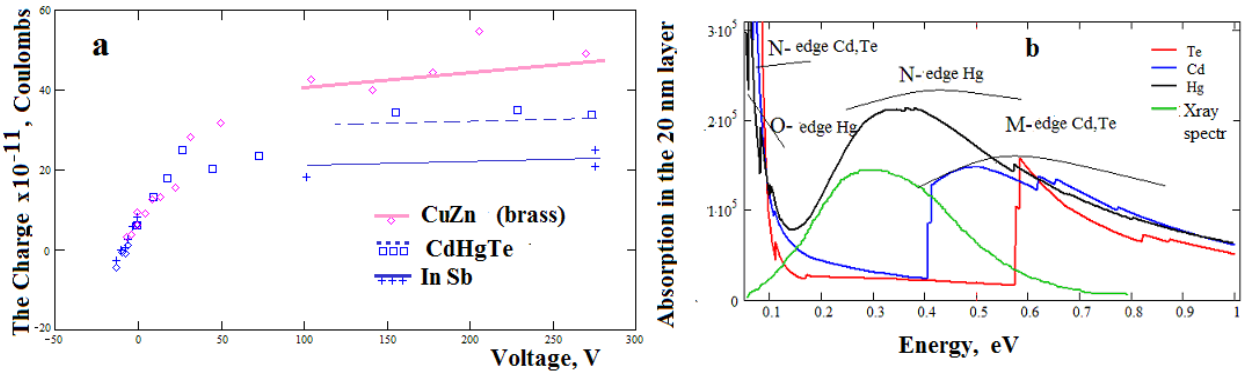

Fig.1. a-dependence of the emitted charge value on the applied voltage ; b- absorption spectra of some elements and the SXrayI spectrum of the laser-plasma source

The maximum yield of photoelectrons in our experiments is $Ne \approx 1.3 \cdot 10^8$ for InSb and $Ne \approx 2 \cdot 10^8$ for $Cd_{0.2}Hg_{0.8}Te$ at a buoyant voltage $U = -273V$ (Fig. 1a).As can be seen from the figure, the emission intensity is higher for materials with higher concentration of free charge carriers, which indicates the interaction of SXrayI with valence electrons. It follows from Fig. 1b that the SXrayI of the source used excites N levels of the Hg ion almost resonantly.

As follows from Fig. 1a, the photoelectric effect is also observed for the locking directions of the external field, which is apparently associated with a large value of the energy of the excitation quantum, which gives the photoelectron an energy enough to overcome the inhibitory field.

REFERENCES

[1] V.G. Sredin, O.B. Ananin, I.D.Burlakov,A.E.Mirofyanchenko,A.P. Melekhov, I.K Novikov, "Influence of soft X-ray on thesurface properties of Cd $_x$Hg $_{1-x}$Te solid solutions," Applied Physics (in russian), no.6, pp.17-20, december 2013 .

[2] V.G Sredin, A.V. Voitsekhovskii, O.B. Anan'in A.P. Melehov, , S.N.Nesmelov S.M.Dzyadukh. "Formation of surface defects in n-Cd*x*Hg1-*x*Te by soft X-ray radiation of laser plasma " Applied Physics (in russian), no.4,pp 54-60,august 2018.

[3] http://henke.lbl.gov/optical_constants/filter2.html

CONNECTION OF THE CASCADE-PROBABILITY(CP) METHOD WITH THE BOLTSMAN EQUATION AND ITS APPLICATION TO THE PROBLEMS OF DEFECT GENERATION IN MATERIALS IRRADIATED BY ELECTRONS

A.I. KUPCHISIN[1,2]

[1]*Kazakh National Pedagogical University named after Abay, Almaty, Kazakhstan*
[2]*Kazakh National University named after al-Farabi, Almaty, Kazakhstan*

In the interaction of charged particles with the substance it occurs sufficiently large number of processes: the ionization and excitation of atoms, the generation of defects, the creation of secondary particles, etc. In electron irradiation with an energy of < 8 MeV, most of the energy is spent on the so-called ionization processes (about 99 %) and only ~ 1 % goes to the generation of primary knocked out atoms, which are the founders of atomic-atom cascades, the formation of Frenkel pairs, vacancy clusters, and clusters of interstitial atoms [1 - 4]. Earlier, in [3], a connection was made between the cascade probability method (CP) and the Boltzmann equation for the case of passage of uncharged particles through matter. However, these issues were not considered for electrons. In this work, we obtain an inegro-differential equation for the electron flux with allowance for their energy loss due to ionization and excitation with the generation of primary knocked out atoms.

$$\frac{dF(E,h)}{dh} = -F(E,h)*\sigma_0\left(1-\frac{1}{a(E_0-kh)}\right)+\int_E^{E_m} F(E',h)\omega(E',E)*\sigma_0\left(1-\frac{1}{a(E_0-kh)}\right)dE', \quad (1)$$

where dF(E, h)/dh is the change in the number of cascade particles at a depth h; the first term on the right side is a decrease in the number of particles as a result of interactions; $\sigma_0\left(1-\frac{1}{a(E_0-kh)}\right)$ – approximated range for the interaction of electrons with materials with the formation of PKA; ω(E′, E) is the normalized differential energy spectrum of secondary particles in an elementary act; E_m – maximum energy of the primary particles.

The second term on the right side represents the generation of secondary particles in the range of depths h, h ÷ dh of all primary particles, whose energy is above E.

The method of Laplace transform is the integral equation is reduced to further solved by the method of successive approximations.

$$F(E,h) = \sum_{i=0}^{n} M_i(E)\frac{1}{\mathrm{n}!\lambda_0^{\mathrm{n}}}\left(\frac{E_0}{E_0-kh}\right)^{\mathrm{i}}\exp\left(-\frac{h}{\lambda_0}\right)*\left[h-\frac{\ln\left(\frac{E_0}{E_0-kh}\right)}{ak}\right],$$

where k is the energy loss coefficient, E_0 is the energy of the primary particles, and *a* is the approximation coefficient, $M_i(E)$ is the collision [4].

It was found that the solution includes the CP function taking into account the energy loss, which we found earlier [3]. This function has a sufficiently large set of physical properties, in particular, depending on the depth and number of particle interactions.

REFERENCES

[1] M. Makhavikou, F. Komarov, I. Parkhomenko, L. Vlasukova, O. Milchanin, J. Zuk, E. Wendler, I. Romanov, O. Korolik, A. Togambayeva, "Structure and optical properties of SiO_2 films with ZnSe nanocrystals formed by ion implantation," Surface Coatings Technology, pp. 596–600, 2018.

[2] M. Trant, M. Fischer, K. Thorwarth, S. Gauter, J. Patscheider, H.J. Hug Tunable ion flux density and its impact on AlN thin films deposited in a confocal DC magnetron sputtering system," Surface and Coatings Technology, vol. 348, pp. 159–167, 2018.

[3] A.A. Kupchishin, A.I. Kupchishin, T.A. Shmygaleva, Computer simulation of radiation-physical problems, Almaty: Kazakh University, 2007.

[4] N.A. Voronova, V.I. Kirdyashkin, A. I. Kupchishin, A. A. Kupchishin, "On the connection of the generalized cascade-probability function with the Boltzmann equation," IOP Conf. Series: Material Science and Engineering, vol. 289, Article Number 012030, 2018.[i]

[i] The work was performed according to the grant of the Ministry of Education and Science of the Republic of Kazakhstan No. AR05132061.

ACCUMULATION AND THERMAL ANNEALING OF RADIATION DEFECTS IN MgO SINGLE CRYSTALS IRRADIATED WITH SWIFT Xe IONS*

G. BAUBEKOVA[1,2], *A. AKILBEKOV*[2], *E. FELDBACH*[1], *E. SHABLONIN*[1], *E. VASIL'CHENKO*[1], *M. ZDOROVETS*[2], *A. LUSHCHIK*[1],

[1]*Institute of Physics, University of Tartu, W. Ostwald Str. 1, 50411 Tartu, Estonis*
[2]*L.N. Gumilyov Eurasian National University, Munaitpassov Str. 5, 0100008 Nur-Sultan*

Magnesium oxide possesses fascinating mechanical and physicochemical properties (high melting point, wide energy gap, high tolerance to irradiation, etc.) and is used for various applications in science and technology. MgO in the form of single crystals, polycrystalline transparent (optical) ceramics or nanoparticles are utilized as protective coating in plasma display panels, hosts for tunable lasers, materials for substrates, catalysis, nuclear waste disposal, fuel cells, refractory isolators, and are even considered as promising diagnostics/window materials in further fusion devices. For numerous nuclear applications, an extremely high resistance against heavy irradiation (predominantly by fast neutrons) or prolonged stay in harsh environment with low swelling, ability to maintain mechanical and electric integrity, acceptable plasticity, low accumulation efficiency of structural defects is of particular importance.

Highly pure MgO single crystals (grown by a variation of arc fusion technique in Tartu, the main impurity – up to 3 ppm of Fe ions) were irradiated with 0.23 GeV ^{132}Xe ions (ion range about 14 μm) at fluences of $\Phi = 5\times10^{11}$–3.3×10^{14} ions/cm^2 at the DC-60 cyclotron in Nur-Sultan. The spectra of optical absorption were measured in a spectral region of 1.5-6.5 eV using a high-absorbance spectrometer JASCO V-660 with a double monochromator, which significantly suppresses scattered light. The spectra were measured at room temperature (RT) just after a sample irradiation or after its additional stepwise preheating to certain temperatures T_i (up to 1200 K, kept 5 min at each T_i) in inert argon atmosphere inside a quartz reactor of a furnace. Cathodoluminescence (CL) spectra were measured at the sample excitation by an electron beam of 10 keV energy and 0.1 μA current, the setup was equipped with a close cycle helium cryostat (5-400 K). Photoluminescence measurements were performed using synchrotron radiation at the FinEstBeAMS beamline of MAX IV Lab (Lund, Sweden).

The spectra of radiation-induced optical absorption (RIOA, difference of the sample spectra after and before irradiation) measured at RT in the region of 1.5-6.5 eV comprise of two bands peaked at 5.03 and 4.92 eV and related to the F and F^+ centers (an oxygen vacancy with two/one trapped electrons), respectively; a band at 3.48 eV is ascribed to so-called F_2 centers (two spatially close F); Fe impurities are responsible for the bands at 4.26 and 5.74 eV; and a complex band with the maximum at ~2.16-eV. In order to separate overlapping absorption bands around 2.16-eV, the decomposition into three Gaussians was performed. Similar to the case of the F and F^+ centers [1], the accumulation of the defects connected with Gaussians at 2.16 eV (the main one), 2.02 and 2.40 eV ongoing with the fluence rise up to 3.3×10^{14} Xe/cm without saturation marks, thus confirming radiation-induced nature of these defects. In addition, the decrease of the defects ascribed to the 2.16-eV component at a crystal heating to 700 K occurs similarly to that of single F and F^+ and is determined by mobile oxygen interstitials. In our opinion, the 2.16-eV band is related to high-order aggregates of anion vacancies (but not to the F_2 centers). The increase in the concentration of two other defects (components at 2.02 and 2.4 eV) in the temperature range above 700 K may be connected with the so-called P-defects (aggregation between an F^+ center and a cation vacancy, eV_OV_{Mg}, see [2]).

In general, the accumulation of the F-type defects with irradiation dose could be also checked via the changes in CL spectra. The peculiarities/limitations of the use of the CL bands, related to the F and F^+ centers in Xe-irradiated MgO crystals, as the measure of defect concentration with respected to the above-mentioned accumulation curves measured via the RIOA bands are thoroughly analyzed. The CL emission bands ascribed to the F and F^+ centers are also compared with the spectra of intracenter photoluminescence.

REFERENCES

[1] G. Baubekova, A. Akilbekov, E. Feldbach, et al., "Accumulation of radiation defects and modification of micromechanical properties under MgO crystal irradiation with swift ^{132}Xe ions," Nucl. Instrum. Meth. B 463, 50-54 (2020).

[2] B. Henderson and J.E. Wertz, Defects in the alkaline Earth oxides. London: Taylor&Francis LTD, 1977.

* The work was supported out within the framework of the EUROfusion Consortium and has received funding from the Euratom research and training programme 2014-2018 and 2019-2020 under grant agreement No 633053. The views and opinions expressed herein do not necessarily reflect those of the European Commission. In addition, the research leading to these results has received funding from the Estonian Research Council grant (PUT PRG619); A.A. appreciates support via the project GF AP05134257 of Ministry of Education and Science of the Republic of Kazakhstan.

THE EFFECT OF IMPURITY ATOMS OF LIGHT ELEMENTS ON THE STRUCTURE AND ELECTRONIC PROPERTIES OF SILICON CLUSTERS

M.YU. TASHMETOV, A.B. NORMURODOV, N.T. SULAYMONOV, SH. MAKHKAMOV, F.T. UMAROVA

Institute of nuclear physics AS RUz, Tashkent, Uzbekistan

Silicon nanomaterials, like crystalline silicon, can contain various defects that affecting both its electronic properties and structural parameters of the nanocrystal. Atoms of light elements (hydrogen, oxygen, carbon) are concomitant impurities in silicon and have high chemical activity in the formation of structural defect states. The presence of these elements even in low concentrations can significantly affect the stability of the properties of crystals under thermal, radiation, mechanical and other types of external influences.

At present, it is generally recognized that oxygen has a significant effect on radiation defect formation and the effect of carbon and hydrogen on the generation of structural defects has not been studied enough and is controversial. A theoretical study of the behavior of typical defects, such as carbon, oxygen, and hydrogen in nanosilicon, makes it possible to predict the changes in the properties of materials, to develop methods to increase the stability of electronic devices based on them under critical conditions of external influences. The wide application use of ion implantation for the production of doped low-dimensional films requires determination of the light elements role in the formation of nanocrystals.

The aim of this work is to determine the role of embedded hydrogen atoms in silicon cluster and its interaction with an impurity atom containing carbon in nanocrystals. As models of nanoparticles, we chose nanoscale clusters Si_{29}, $Si_{29}H_{24}$, $Si_{29}H_{36}$ with a dimerized surface and saturation of surface silicon atoms with hydrogen atoms in the amount of 24 and 36 atoms. These carbon-containing clusters are atomically centered and the symmetry of the central atom is tetrahedral.

We calculated the structural and energy parameters of the formed clusters and obtained computer model of carbon and hydrogen impurities in silicon nanoclusters Si_{29}, $Si_{29}H_{24}$, and $Si_{29}H_{36}$, based on the combination of molecular dynamics and non-conventional tight binding method [1]. Theoretical calculations showed that the interstitial carbon forms bridging bond with two silicon atoms and is located in hexagonal position in center of the cluster. In this carbon is most strongly bound to silicon cluster in pure Si_{29}. Excess negatively charged state of carbon leads to hardening of the nanocluster bond. It has been established that the most energetic favorable state of carbon in silicon clusters is interstitial state. A single impurity carbon atom gives small levels in the forbidden gap of nanosilicon. Intruding of one hydrogen atom into the region of interstitial carbon leads to the formation of defective C-H-Si complex. The structural and energy state of the C atom in the defective C-H-Si complex depends not only on the number of H atoms, but also on the change in the electronic configuration of silicon atoms involved in the formation of this complex. It was revealed that carbon-containing clusters containing one hydrogen atom are more stable silicon nanoclusters to external influences.

REFERENCES

[1] Z.M. Khakimov, P.L. Tereshchuk, N.T. Sulaymonov, F.T. Umarova, M.T. Swihart. Non-conventional tight-binding method for calculation of total energy and spectroscopic energies of atomic clusters. Transferable parameters for silicon. //Phys. Rev. B 2005. V. 72, P.115335.

RADIATION-STIMULATED PROCESSES AT THE BORDER OF SECTION P-N - TRANSITION OF SILICON DIFFUSION STRUCTURES

M.Yu. TASHMETOV, Sh. MAKHKAMOV, A.R. SATTIEV, M.N. ERDONOV, H.M. KHOLMEDOV *, R.P. SAIDOV

Institute of Nuclear Physics, Academy of Sciences of the Republic of Uzbekistan, Tashkent,
**Tashkent Al-Khwarizmi University of Information Technologies, Tashkent, Uzbekistan.*

It is known that for the production of high-voltage silicon rectifier and power diodes, p-n junctions are obtained by the thermal diffusion method. Usually, as a diffused impurity, depending on the initial type of silicon, mainly Al, B, and P are used. By controlling the temperature and diffusion time of these impurities, it is possible to obtain p^+ and n^+ layers with different depths of the p-n junction and to control electrical parameters (U_{rev}, I_{st} and τ_{rec}) of manufactured devices. In practice, it is widely used to control the value of the time to restore the inverse resistance of diodes by introducing p-n in the base region – the transition of generation-recombination radiation defects creating deep energy levels in the band gap, while maintaining the value of I_{st}. However, the data on the possibility of using radiation technology to control the value of the reverse breakdown voltage of diffusion diodes diverge significantly.

In this work, we consider a radiation-technological method for controlling the values of U_{rev} of the breakdown voltage of silicon diffusion diodes and propose a mechanism for a radiation-stimulated process occurring at the boundary of the p-n junction in layered structures. In n-Si, the diffusion p-n junction was created by diffusion of Al at T = 1150-1200 °C for 17-20 hours. The depth of the p-n junction was ≈90 μm. The concentration of the admixture (Al) in the p^+ layer was $3 \cdot 10^{19}$ cm^{-3}. The direct and reverse branches of the current – voltage (I – V) characteristics of the diodes were measured before and after irradiation with 6 MeV electrons in the fluence range 10^{16}–$5 \cdot 10^{17}$ cm^{-2}. The average beam density was 0,08 μA/cm^{-2}. The temperature of the sample during irradiation did not exceed 80 °C.

Measurement of the I – V characteristics showed that, in fabricated silicon diffusion diodes with a depth of p-n – junction of 80 μm, after irradiation with electrons with a fluence of 10^{16} cm^{-2}, a shift in the value of the U_{rev} breakdown voltage is observed toward high applied voltages and reaches saturation at fluences of $5 \cdot 10^{17}$ cm^{-2}. In this case, the increase in U_{rev} of breakdown voltage after radiation treatment was 390 V (before irradiation $U_{rev} \approx 310$ V), and the value of τ_{rec} decreased to values (80-90) ns, there were no significant changes in the values of I_{st}. Annealing at T ≈ 450 °C of the irradiated samples led to a shift of U_{rev} to values of 420 V and an increase in τ_{rec} to values (180-200) ns, and I_{st} to complete reduction to the value of unirradiated samples.

In order to reveal the mechanism of the observed effect of a significant bias U_{rev} of the breakdown voltage in the high-voltage region, the solution of the equation of two flow models of radiation-induced impurity diffusion is considered. The essence of which is as follows. When high-energy electrons are irradiated with silicon p-n structures, the proportion of interstitial atoms increases, some of which are involved in the displacement of Al from the nodes of the crystal lattice of the matrix due to the Watkins reaction. The displaced Al migrating through the internodes before meeting with the vacancies and determine the depth of the p-n junction. Calculations showed that under the indicated irradiation regimes, the displacement of the p^+ layer boundary is 2-3 μm in the base region, which does not correspond to an increase in U_{rev} breakdown voltage to the high voltage region by (25-30)%. The observed effect can be explained with the process of radiation-stimulated diffusion of Al impurity, which leads to equalization of the inhomogeneous distribution of Al impurity in the p-n junction adjacent to the interface due to suppression of fluctuations in Al concentration.

The experimental effect detected, stimulated by radiation of diffusion of Al, confirms the obtained microscopic images of the change in the profile of the interface between p-n structures, using a modernized infrared microscope. Thus, it was found that the radiation-stimulated diffusion of impurities can be controlled by the value of the reverse breakdown voltage of silicon diffusion diodes by equalizing by irradiation the inhomogeneity of the diffusant distribution at the p-n junction boundary.

MECHANISMS FORMATION OF ELECTRON-HOLE TRAP CENTERS IN ALKALI METAL SULPHATES

T.T. ALIBAY[1], T.N. NURAKHMETOV[1], Zh.M. SALIKHODZHA[1], R. F. ALMUKHAMETOV[2], A.M. ZHUNUSBEKOV[1], A.ZH. KAINARBAY[1], D.H. DAURENBEKOV[1], B.M. SADYKOVA[1], K. B. ZHANGYLYSSOV[1], B.N.YUSSUPBEKOVA[1]

[1]L.N. Gumilyov Eurasian national university, Nur-Sultan, Kazakhstan, +7 707 684 69 34, temirulanalibay@gmail.com
[2]Bashkir State University,Ufa, Russia

Activated alkali metal sulfates are promisingly used as dosimeters, phosphors.

Their sensitivity to external electromagnetic effects is associated with the formation of induced defects in them - electron-hole trap centers. The formation of electron-hole trap centers is detected by measuring radio-, thermo-, and photostimulated recombination luminescence and phosphorescence. Irradiated alkali metal sulfates, two types of recombination radiation appear:

-short-wavelength emission at 3.64 ÷ 4.3 eV arising from the recombination of electrons with localized holes SO_4^- nonequivalently located in the lattice;

-long-wavelength emission at 3.0-3.1 eV, 2.6-2.7 eV, 2.2-2.4 eV associated with the formation of electron-hole trap centers.

These recombination radiations occur in almost all alkali metal sulfates in the indicated spectral ranges. It is assumed that the formation of trap centers is associated with electronic transitions on the anionic complexes SO_4^{2-}. With an increase in the irradiation time, the short-wavelength recombination radiation of 3.64 ÷ 4.3 eV does not increase in intensity, and the intensity of long-wavelength emissions of 3.0-3.1 eV, 2.6-2.7 eV, 2.2-2.4 eV increases. In a number of alkali metal sulfates, Na_2SO_4, Li_2SO_4 and $LiKSO_4$ with long-term irradiation, only long-wavelength emission will prevail. After the cessation of external exposure, phosphorescence appears. The spectral composition of the main peak of TSL coincides with the spectrum of photoluminescence and phosphorescence in the spectral range where x-ray luminescence and photoluminescence were registered.

Studies have shown that in a number of sulfates, the recombination radiation band on the trap centers at 3.0-3.1 eV is detected in the spectral region of the creation of electron-hole pairs. The calculations of the authors of [1] showed that in sulfates the upper part of the valence band consists of three subbands located from the bottom of the conduction band in the energy range 5.5–6 eV, 7–8 eV, and 9–12 eV. By measuring the excitation spectrum of the main emission bands at 3.0–3.1 eV, we have shown that it is in these spectral ranges that photons create electron-hole trap centers.

In pure sulfates, the created trap centers proceeds in this way: electrons are trapped by anionic complexes by the reaction $SO_4^{2-} + e^- \rightarrow SO_4^{3-}$, and the hole is autolocated in the form SO_4^-. In crystals, trap centers $SO_4^{3-} - SO_4^-$ - with impurities are created, the efficiency of creating trap centers is an order of magnitude greater than in pure crystals. The impurity Me^+ traps electrons by the reaction $Me^+ + e^- \rightarrow Me^0$, and the hole autolocalizes near the impurity $Me^+SO_4^-$.

It has been experimentally shown that the electron-hole trap centers $M^0 - SO_4^- Me^+$ are created at photon energies, where free electron-hole pairs are created that arise when electrons transition from three subbands of the valence band to the conduction band. An excitation spectrum of recombination radiation of 3.0-3.1 eV was detected at the trap centers. The mechanisms of the formation of impurity electron-hole trapping centers in a number of sulfates activated by various ions are discussed.

REFERENCES

[1] Shchepanskyi, P.A., Stadnyk V.Y., Rudysh, Rudysh M.Ya., Brezvin R.S., Andrievskii B.V., Optics and spectroscopy, vol. 125(3), pp. 353-357, 2018.

MODIFICATION OF YELLOW BAND EMISSION OF GALLIUM NITRIDE DUE TO ELECTRON IRRADIATION*

R.A. REDKO[1,2], *G.V. MILENIN*[1], *S.M. REDKO*[1]

[1]*V. Lashkaryov Institute of Semiconductor Physics of the National Academy of Sciences of Ukraine, Kyiv, Ukraine*
[2]*State University of Telecommunications, Kyiv, Ukraine*

Three samples of wurtzite *n*-type MOCVD-grown GaN/Al_2O_3 have been irradiated with electron fluence of energy 4 MeV with doses: $4\cdot10^{14}$ electrons/cm^2 (sample A) and $4\cdot10^{15}$ electrons/cm^2 (sample B and C) to obtain equivalent doses 10^7 rad (~10^5 Gr), $2.5\cdot10^7$ rad (~$2.5\cdot10^5$ Gr) and 10^8 rad (~10^6 Gr), respectively. Photoluminescent (PL) measurements have been carried out with 315 nm excitation at room temperature. In radiative recombination spectra two bands take place: near-band-edge (NBE) emission at 3.43 eV and so-called broad yellow band (YB) at 2.2 eV. According to literature data these bands are related to the band-to-band transitions and to donor-acceptor pair- type transitions [1], respectively. The feature of yellow band is observed complicate composition, which was explained as interference effects on the boundary of the sample. After irradiation for all three samples no changes in average energy position of YB (~2.2 eV) were detected, so any sufficient changes in mechanism of yellow emission has not expected.

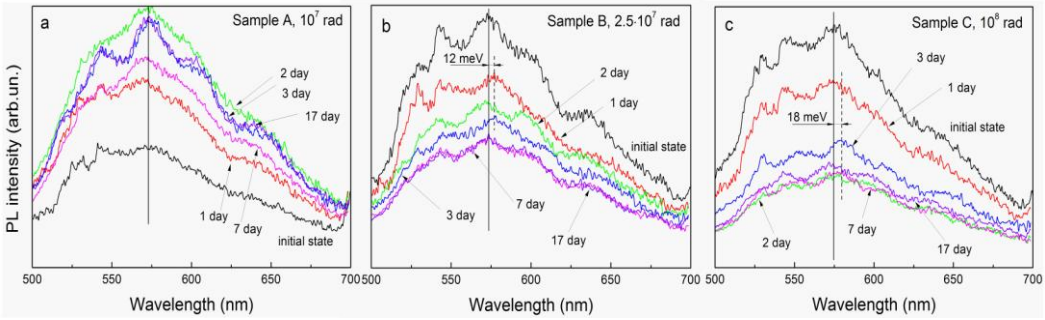

Fig.1. The evolution of YB during 17 days after electron irradiation.

But changes in fine structure of this band were detected on 2-3 day after electron irradiation (Fig. 1). Moreover, for samples B and C we have one type of these changes while for sample A – the others ones. In in case of sample A very weak "maximums" were observed before irradiation. But on the third day after treatment a clear interference frigs were appeared. In cases samples B and C interference was present in initial states but the shift in its energy position on 2-3 day after treatment one can observe (12 meV for sample B and 18 meV for C one). Remarkable is that after 7 day positions of these "maximums" were returned to the initial ones and any significant changes were not detected for sample B as well as for sample C (curves, which correspond 7 and 17 day are almost the same). For neighboring extrema at wavelengths λ_{m_1} and λ_{m_2} the effective thickness of GaN layer is calculated by using expression:

$$d = \frac{\lambda_{m_1}\lambda_{m_2}}{2\left(\lambda_{m_1}n_2 - \lambda_{m_2}n_1\right)}. \qquad (1)$$

By analyzing the maxima, which are marked on Fig. 6, and neglecting the dispersion of the refractive index in this spectral region (from λ_{m_1} to λ_{m_2}), we obtained *d* values for $n \approx 2.4$ using Eq. (1). The decreases of the effective thicknesses of samples B and C on 2-3 day after electron radiation treatment were obtained (from 2.54 to 2.36 μm and from 2.67 to 2.59 μm, respectively). But after 7 days we have the returning to the initial parameters. No shift of interference features of yellow curves for samples B and C were observed after 7 day, so one can think that transformation of effective thicknesses of GaN due to electron radiation treatment was occurred during up to one week term. For establish long-term mechanism of observed transformation in detail further researches are required.

REFERENCES

[1] M. Matys, B. Adamowicz. "Mechanism of yellow luminescence in GaN at room temperature", J. Appl. Phys., vol. 121, 2017.

* The authors are grateful to Profs. V.B. Neymash and V.Y. Povarchuk for electron radiation carried out.

DFT INVESTIGATION OF THE RADIATION SENSITIVITY OF SOLID CHOLINE CHLORIDE, BROMIDE, AND IODIDE*

Y.N. ZHURAVLEV, K.A.GORDIENKO

Kemerovo State University, Kemerovo, Russia

Organic choline halides $[(CH_3)_3NCH_2CH_2OH]^+X^-$ (X=Cl, Br, I) are important biological objects and play an important role in the functioning of the nervous system [1]. The crystal structure of choline chloride, bromide, and iodide was studied in [2,3], and the Infrared spectra (IR) in [4], since they turned out to be important factors in determining their radiation resistance. ChCl, ChBr are radiation-sensitive compounds, while ChI is radiation normal. Radiation decomposition is observed only in the solid phase and at ambient temperature. The present work is devoted to the answer to the question of whether the large differences in the radiation sensitivity of choline are related to their crystallographic differences or more complex molecular mechanisms.

In the framework of the density functional theory (DFT), the structural, electronic, and vibrational properties of choline were calculated using the gradient PBE functional with the D3(BJ) empirical dispersion correction for intermolecular interactions and the basis of localized atomic orbitals of the CRYSTAL17 code [5].

For ChCl, the unit cell parameters were determined for the symmetry group $P2_12_12_1$, ChBr - $P2_1nm$, ChI - $P2_1$. The chlorine atom in ChCl is surrounded by 12 hydrogen atoms with the shortest O–H•••Cl distance of 2.156 Å. The remaining hydrogen atoms belong to methyl CH_3 (8) and methylene CH_2 (3) groups. In ChI, the shortest O–H•••I distance is significantly greater than 2.486 Å and the order of the hydrogen atoms surrounding iodine changes. The average C-H_3 distance for methyl groups in ChCl is 1.099 Å, C4-H_2 1.098 Å, C5-H_2 1.106 Å. The O–H distance in the series of Chl, Br, I cholines decreases: 0.993, 0.992, 0.990 Å.

The effective charge of the chlorine atom calculated by the Mulliken scheme is -0.82 |*e*|, bromine -0.76 |*e*|, iodine -0.85 |*e*|. In the OH hydroxyl group, the oxygen atom is negatively charged -0.52 |*e*|, and the hydrogen atom is positively +0.33 |*e*|. Thus, the bond between the cation of the choline Ch^+ and the anion X^- is provided by a weak electrostatic interaction. The strength of the chemical bonding of atoms can be judged by the population of the overlap *P* of their electron shells. Despite the distances, the population of $P_{I\text{-}H(O)}$= 0.059 *e* is greater than $P_{Cl\text{-}H(O)}$=0.046 *e*. Thus, the dissociation of choline into ions upon energy exposure will be more effective in chloride than in iodide.

In chloride (iodide), the overlap populations $P_{C4\text{-}H}$=0.36 *e*, $P_{C5\text{-}H}$=0.37 *e* do not differ from methyl groups. The C5 atom interacts with oxygen from the hydroxyl group of OH, so that $P_{O\text{-}C5}$=0.25 *e* (0.26 *e*). Thus, in ChCl, the two methylene groups of CH_2 are strongly bonded to each other and to OH. The overlap population of the N–C4 bond is approximately the same, but in ChCl the C5–C4 bond is much stronger (0.34 *e* versus 0.24 *e* in ChI), which means the possibility of the formation of the intermediate radical CH_2CH_2OH recorded in [4]. This may be followed by a cleavage of the OH bond, which in ChCl is less strong than in ChI, and CH_3CHO+H is formed. The first is the final product, and the addition of hydrogen to (Ch) leads to the appearance of the second final product $(CH_3)_3NHCl$.

In the IR spectra of ChCl, ChI, the most intense peaks are at 3340, 3367 cm^{-1} and they relate to O–H stretching vibrations. The C-OH stretching vibrations will correspond to maxima at 1092, 1080 cm^{-1} and 620, 323 cm^{-1} will be referred to as OH strain bands, i.e. directly to the O-H•••Cl(I) bond. This correlates with the data of [4], where it was shown that the molecular motions in choline iodide are significantly different from chloride and bromide.

REFERENCES

[1] R. Velazquez, E. Ferreira, S. Knowles, C. Fux, A. Rodin, W. Winslow, S. Oddo. “Lifelong choline supplementation ameliorates Alzheimer’s disease pathology and associated cognitive deficits by attenuating microglia activation”, Aging Cell. Article Number 13037, August 2019.

[2] M.E. Senko and D.H. Templeton. “Unite cell of Cholin Halides and structure of Choline Chloride”, Acta Cryst.. vol. 13, pp. 281-285, 1960.

[3] D. Wemmer, V. Petrouleas, N. Panaglotopoulos, S. E. Flllppakls. “High-Resolution Solid-state Nuclear Magnetic Resonance and X-ray Structure Study of Choline Chloride, Bromide, and Iodide”, *J. Phys.* Chem. vol. 87, pp. 999-1003, October 1983.

[4] A. Nath, R. Agarwal, and R. M. Lemmon. “Further studies on the solid-state chemistry of irradiated choline chloride”, J. Chem. Phys. vol. 61, pp. 1542-1547, April 1974.

[5] R. Dovesi, A.Erba, R.Orlando, C.M. Zicovich-Wilson, B.Civalleri, L. Maschio, M.Rérat, S.Casassa, J.Baima, S.Salustro, B. Kirtman “Quantum-mechanical condensed matter simulations with CRYSTAL”, WIREs Comput Mol Sci. Article Number 1360, January 2018.

* The work was supported by the Russian Science Foundation under grant No. 18-29-19169.

FUEL CYCLE ANALYSIS OF THE MINIATURE NEUTRON SOURCE REACTOR: GHARR-1 AFTER CORE CONVERSION USING STOCHASTIC METHOD

A. SAMIRU , V. SERGEY

National Research Tomsk Polytechnic University, Tomsk, Russia

This study is based on a recommendation by Integrated Safety Assessment for Research Reactors (INSARR) mission and other dissertations to study the fuel cycle of the reactor core for the Low Enriched Uranium (LEU) fuel. Conversion from one fuel type to another requires a complete reevaluation of the safety analysis. Changes to the reactivity worth, shutdown margin, power density and material properties must be taken into account, and appropriate modifications made. The focus on this article is to study the neutronics analysis including radiation damage assessment on the clad. The GHARR-1 research reactor operates at maximum power of 30 kW in order to attain the flux of 1.0E+12 n/cm 2 .s as the nominal flux of the HEU core. The core excess reactivity of 4 mK, 348 fuel pins would be proven to be appropriate for the GHARR-1 LEU core. K eff Calculations were made to ascertain the fuel campaigning of the GHARR-1 core using LEU-UO 2 with U235-12.5%, U238- 87.05%, U234- 0.2%, U236- 0.25%, with cycle length 2.5 years, for over 57 years at the 17 kW power level. Finally, damage assessment in the TRIM code established Zircaloy-4 clad material as the best among some know steels. It recorded few replacement collisions of 147 with recoiling energy of 0.09 with only point defects and not major defects like void over a duration of the reactor life. The analytical calculations of the radiation damage on Zircaloy-4 using both the Kinchin-Pease and Norgett-Robinson Torrens models was determined as 0.00019 and 0.00015 displacement per atom (dpa) respectively for only 30 minutes of operation. From the calculations and simulations, it is safe to conclude that the GHARR-1 LEU core is safe and more secured in comparison to the largely outlined design basis accidents identified in the Safety Analysis Report.

RECOMBINATION RADIATION IN $BaSO_4$

K.B. ZHANGYLYSSOV[1], T.N. NURAKHMETOV[1], Zh.M. SALIKHODZHA[1], A.M. ZHUNUSBEKOV[1], A.ZH. KAINARBAY[1], D.H. DAURENBEKOV[1], B.M. SADYKOVA[1], B.N. YUSSUPBEKOVA[1], T.T. ALIBAY[1], D.A. TOLEKOV[1]

[1]L. N. Gumilyov Eurasian national university, Nur-Sultan, Kazakhstan, +7 702 783 33 15, Keleshek92@yandex.ru

The $BaSO_4$ crystals with impurities $Eu^{2+}$and $Eu^{3+}$are used as thermoluminescent dosimeters. In irradiated $BaSO_4$ crystals with an impurity, electron-hole trap centers arise upon electron trap by the reaction $Me^{2+} + e^- \rightarrow Me^+$, where Me^{2+} is a two-valence metal. The hole arising together with the electron is localized in the form SO_4^-. In pure $BaSO_4$, $CaSO_4$ crystals, electron-hole trap centers arise upon trap of electrons by anionic complexes by the reaction $SO_4^{2-} + e^- \rightarrow SO_4^{3-}$. The hole is self-trapped in the form of SO_4^-- formed electron-hole trap centers $Me^+ - SO_4^-$ and $SO_4^{3-} - SO_4^-$, they are stable up to 480-440K.

The dosimetric peak of thermally stimulated luminescence (TSL) in commercial dosimeters in $CaSO_4 - Dy$ is at 510-540 K. It is assumed that in $CaSO_4 - Dy$ formed electron-hole trap centers that become mobile at 510-540 K, localized on anionic and cationic vacancies.

The mechanisms for creating anionic and cationic vacancies in sulfates of alkaline earth metals have not been studied. There are separate works in which anionic and cationic vacancies are created during charge compensation with the introduction of isovalent impurities. In the $BaSO_4 - Eu$ crystal with impurities Cl^-, P^-, a high-temperature and dosimetric TSL peak at 490-500 K were detected in the $BaSO_4$ crystal by EPR, F and F^+ centers that are stable above 500-600 K [1]. The mechanism of formation of anionic vacancies (oxygen) on the basis of which F and F^+ centers are formed is not discussed in the literature. We study intrinsic recombination radiation in $BaSO_4$ powder. When excited by photons with energy of 6.0-6.2 eV, short-wavelength emission bands arise at 3.7-3.8 eV and long-wavelength bands at 3.0-3.1 eV

At energies of the exciting photon of 7.3–7.75 eV at 15 K, a wide emission band appears at 3.7–4.3 eV. High-energy photons with an energy of 10.3-12 eV excite wide emission bands in the spectral range of 3.7-5.0 eV, 3.0-3.1 eV and 2.4-2.7 eV at 15 K. Short-wavelength intrinsic emission bands at 3.7–5 eV is excited by photon energy of 5.5–6.2 eV, 7.3–7.75 eV, 9–10.3 eV at 15 K. It is assumed that short-wavelength wide emission bands at 3.7-5.0 eV arise during the recombination of electrons with nonequivalent located holes. Long-wavelength emission of 3.0-3.1 eV and 2.4-2.7 eV is effectively formed at photon energies where electron-hole pairs are created. It is assumed that the electron-hole trap centers are created upon electron trap by the anionic complexes SO_4^{2-} and the localization of the hole in the form SO_4^-. Trap centers can be formed upon dissociation of the excited anionic complex SO_4^{2-} by the reaction $SO_4^{2-*} \rightarrow SO_3^- v_a^+ e^- + O^0$ or $SO_3^- v_a^+ + O^-$.

In this case, electronic F^+ centers and hole O_3^- trap centers are created. Excitation spectra of recombination radiation of 3.0-3.1 eV were detected at 3.8-3.9 eV and 4.4-4.5 eV in the transparency region of the matrix. In alkaline-earth metal sulfates with impurities, the electron-hole trap centers correspond to the recombination radiation in the the long-wavelength of 3.0-3.1 eV. The mechanisms of the formation of the dosimetric peak of TSL in $BaSO_4$ with impurities will be discussed.

REFERENCES

[1] M.Krystek, “ESR Measurements from X-Ray Irradiated $BaSO_4$ Single Crystals , “Phys.stat.sol.”., vol. 57 ,, pp. 171 ,1980 .

MOLECULAR COMPLEXES WITH HYDROGEN BOND IN SODIUM, POTASSIUM AND MAGNESIUM FLUORIDES WITH IMPURITY OF HYDROXYL IONS*

L.I. BRYUKVINA

Irkutsk Branch of Institute of Laser Physics, Siberian Branch, Russian Academy of Sciences, Irkutsk, Russia

Identical molecular complexes with a hydrogen bond (H-bond) were found in NaF:OH, KF:OH crystals and in MgF2:OH crystalline ceramics, which manifest themselves in the same range in the IR vibrational spectra.

We investigated γ-irradiated and unirradiated crystals. Despite this, general patterns were revealed in the behavior of the IR spectra of hydrogen bonds. In particular, the band in the region of ~ 2200 cm^{-1} is present in γ-irradiated LiF and NaF crystals with an impurity of hydroxyl [1-6] and in unirradiated KF:OH crystals.

The transmittance spectra in the IR region of the unirradiated KF:OH crystal are shown in Fig. 1.

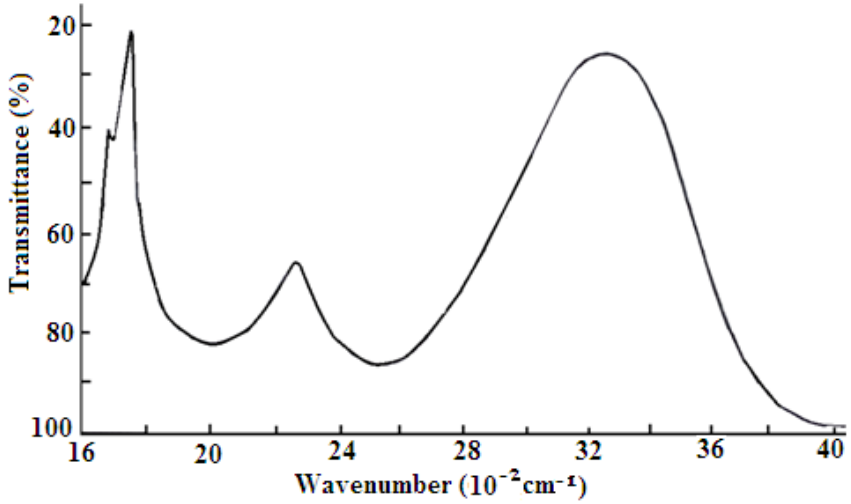

Fig.1. IR transmittance spectrum of a KF:OH crystal.

The spectrum shows a wide band in the region of 2900–3600 cm^{-1}, corresponding to stretching vibrations of water, and bands in the region of deformation vibrations of water at ν=1700–1750 cm^{-1}. The spectrum also has a wide absorption band at ν_{max} = 2260 cm^{-1}, which, apparently, as in the case of fluoride matrices LiF, NaF, and MgF_2, corresponds to the O–H–F hydrogen bond.

Obviously, H-bond includes an F^- ion. This ion can be in the configurations proposed in [7]. Thus, the presence of the OH ... F_i^0 hydrogen bond in radiation-treated LiF:OH crystals need additional analysis.

REFERENCES

[1] L. I. Bryukvina, "Transformation of Radiation-Induced Molecular Point Defects and Color Centers in LiF Crystals under influence of light", Physics of the Solid State, vol. 61, no. 10, pp. 1808 – 1814, October 2019.

[2] L. I. Bryukvina, N. A. Ivanov, D. S. Glazunov, "Stabilization of U_1-centers and laser color centers in LiF:OH crystals", AIP conference proceedings, vol. 2069, is. 1, Article Number 020008, January 2019.

[3] S. A. Nebogin, N. A. Ivanov, L. I. Bryukvina, N. V. Shipitsin, A. E. Rzhechitskii, V. L. Papernyi, "Photoluminescence of magnesium-associated color centers in LiF crystals implanted with magnesium ions", PNFA, vol. 29, pp. 36-41, May 2018.

[4] S. A. Nebogin, L. I. Bryukvina, N. A. Ivanov et. al, "Formation of Color Centers and Molecular Complexes with a Weak Hydrogen Bond in Lithium Fluoride Crystals Depending on the Form of OH-Inclusion", Russian Journal of Physical Chemistry B, vol. 12, no. 2, pp. 1–8, May 2018.

[5] Lyubov Bryukvina, Nikolay Ivanov, Sergey Nebogin, "Relationships between lithium and sodium nanoparticles and color centers formation in LiF and NaF crystals with hydroxide and magnesium ions impurities", J. Phys. Chem. Solids, vol. 120, pp. 133-139, September 2018.

[6] N. A. Ivanov, L. I. Bryukvina, D. S. Glazunov, "Phonon interaction with OH complexes and products of their radiative decomposition in LiF crystals", IOP Conf. Series: Journal of Physics: Conf. Series (6th International Congress "Energy Fluxes and Radiation Effects"), vol. 1115, is. 5, Article Number 052031, 2018.

[7] . Lyubov I. Bryukvina, Nikolay A. Ivanov, "Fermi resonance of molecular complexes with strong hydrogen bond in irradiated LiF:OH crystals", J of fluorine chemistry, vol. 192 Part A, pp. 124–130, December 2016.

* This work was supported by the Program of Fundamental Research Works of State Academies of Sciences for 2013–2021, II.10.1, project no. 0307-2016-0004.

ACCUMULATION OF HELIUM AND HYDROGEN IN AUSTENITIC STEEL DURING HIGH-TEMPERATURE NEUTRON IRRADIATION IN THE ATMOSPHERE OF THESE GASES *

A.O. AKAEV, A.S. DIKOV, S.B. KISLITSIN, A.S. LARIONOV, V.V. FIRSOVA, I.V. KHROMUSHIN

The Institute of Nuclear Physics, Almaty, Kazakhstan

It is known that helium and hydrogen accumulating in steels adversely affect their physical and mechanical properties [1]. One of the key issues here is embrittlement and plasticity reducing of structural materials. To identify the role of helium and hydrogen, were made studies of the accumulation of helium and hydrogen in stainless steel 12Kh18N10T during high-temperature neutron irradiation in a medium of hydrogen and helium.

For this, steel ampoules with wall thicknesses of ~ 2 mm were made, one of which was filled with helium with a pressure at room temperature of 0.3 from atmospheric, and the second was filled with hydrogen with the same gas pressure. Neutron irradiation was carried out in the WWR-K reactor channel to a fluence of 9×10^{19} n/cm^2, with a neutron flux density (E > 0.1 MeV) of 7.6×10^{12} n/s·cm^2. The gas pressure during irradiation did not exceed 50 MPa, the irradiation temperature was 1033 K. The accumulation of helium and hydrogen in steel after irradiation was determined by thermal desorption spectroscopy (TDS) in the temperature range 300–1273 K with a heating rate of 0.7 K/sec. The results of helium and hydrogen evolution are shown in Figure 1.

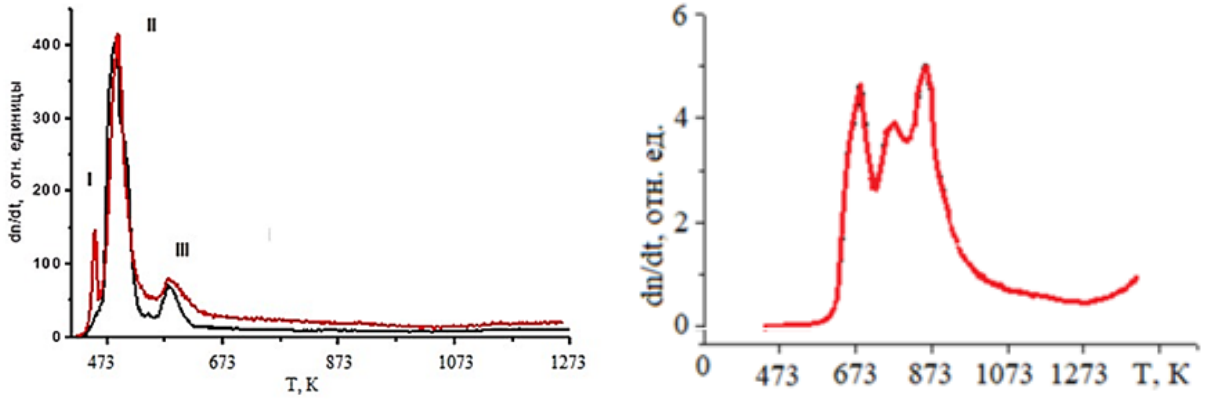

Fig. 1. Thermal desorption spectra of helium (a) and hydrogen (b)

In addition to experiments on gas evolution from steel irradiated in an atmosphere of helium and hydrogen, the structure was studied and the mechanical characteristics determined.

Based on the analysis of the obtained experimental data, the differences in the forms of hydrogen and helium accumulation in steel under neutron irradiation and their effect on the mechanical properties of steel are discussed.

REFERENCES

[1] I.M. Nekluydov, G.D. Tolstolutskay, “Helium and hydrogen in structural materials”. Voprocy atomnoi hauki i techniki. Seria physica radiatsionnyh povrezhdenii i radiatsionnoe materialovedenie, no 3(83), pp. 3-14, 2003 (in Russian).

*This work was carried out as part of the targeted financing program “Development of integrated scientific research in the field of nuclear and radiation physics based on Kazakhstan accelerator complexes” of the Ministry of Energy of the Republic of Kazakhstan

MECHANISMS OF RADIATION DEFECT FORMATION IN THE KI CRYSTAL IN THE DEFORMATION FIELD

K. SHUNKEYEV[1], *L.MYASNIKOVA*[1], *A. MARATOVA*[1], *K. BIZHANOVA*[2]

[1]*Zhubanov Aktobe Regional State University, Aktobe, Kazakhstan*
[2]*Yessenov University, Aktau, Kazakhstan*

Currently, one of the most urgent problems is the study of the mechanisms of radiation defects formation to ensure transparency of optical materials under the influence of radiation, temperature and stress of various types of deformation.

For this purpose, the mechanisms of formation of halogen centers (V_2, V_3, V_{4A}) when the lattice symmetry is lowered by the light cation field (Na), plastic and elastic deformation in a single crystal KI are studied.

Figure 1 shows the absorption spectra of KI crystals under X ray irradiation (RUP-120, W, 5 mA, 120 kV) in isodose mode during 3 hours at 90 K (curved line 1), pre- doped with Na ions (100 pmm) (curved line 2), subjected to plastic deformation (2 %) at room temperature (curved line 3) and elastic deformation (0.8-1.0%) at 90 K (curved line 4).

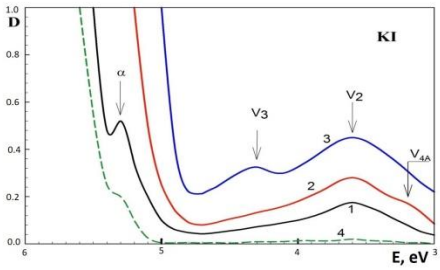

Fig.1. The absorption spectrum of crystals upon irradiation with X-rays in the isodose regime for 3 hours at 90 K.

1 – KI before deformation; 2 – KI-Na before deformation; 3 – KI after plastic deformation at 300 K (2 %);

4 – KI at low temperature (90 K) elastic deformation at 1.0%.

Well known structures of radiation defects (α, V_2, V_3, V_{4A}) in the KI crystal were used as a probe to determine their efficiency after the above-mentioned effects. Experimental results show that absorption bands due to α-centers with a maximum of 5.2 eV are registered in the initial (standard) KI crystal (curved line 1). Here V_2-centers (I_3^-) with a maximum of 3.6 eV and V_3-centers $([I_2]_2)_{aca}$ with a maximum of 4.3 eV, identify the formation of single anion vacancies (α-centers), di- and quartet vacancies (V_2, V_3-centers), respectively.

Local deformation (curved line 2) by a light Na cation (100 ppm) increases the concentration of the above–mentioned centers, and V_{4A}-centers appear, that characterize the creation of halogen formations in the sodium field.

Plastic deformation (2 %) at 300 K of the KI crystal (curved line 3), it significantly increases the concentrations of $V_2=(I_3^-)^0_{aca}$ and $V_3=([I_2]_2)_{aca}$-centers, which are formed when two interstitial halogen atoms interact in the di- and quartet-vacancy fields respectively.

Elastic deformation (0.8-1.0 %) carried out in the cryostat at 90 K (curve line 4) leads to discoloration of the KI crystal from radiation defects, which is important for preserving the transparency of materials when exposed to radiation.

Thus, a decrease in the lattice symmetry by light cations and plastic deformation of the KI crystal leads to an increase in radiation defect formation, elastic deformation leads to a decrease in radiation defect formation, and consequently to an increase in luminescence.

REFERENCES

[1] E. Vasilchenko, E.Sarmukhanov, K. Shunkeev and A. Elango, "Electronic excitations localized in KBr and KI crystals near vacancy defects of different sizes,"Physica Status Solidi (B), vol. 174(1), 1992, p. 155-163.

[2] K.. Shunkeev, E. Sarmukhanov, A. Barmina and L. Myasnikova, "Effect of uniaxial strain on the structure of self-localized excitons in alkali halide crystals," J. Applied Spectroscopy, vol. 74(1), 2007, p. 74-80.

THE EFFECT OF IONIZING RADIATION ON INTERATOMIC INTERACTION IN METALS

S.N. YANIN

Tomsk polytechnic university, Tomsk, Russia

Exposure to intense fluxes of ionizing radiation on metal targets causes various physical phenomena, such as changing the interatomic interaction potentials. It is known that intensive radiation generates ionized atoms within the track of a fast charged particle as well as near the solid surface. The potentials of interactions between these atoms and surrounding particles change considerably.

It is known that intensive radiation generates ionized atoms within the track of a fast charged particle as well as near the solid surface. The potentials of interactions between these atoms and surrounding particles change considerably. The knowledge of corresponding potentials of interatomic interaction is necessary for studying the behavior of partially or entirely ionized substance.

Therefore, aluminum was taken as an example studying the interatomic potentials in metal containing ionized states. Calculations were based on the method of pseudopotentials using Heine-Abarenkov-Animalu model potentials with parameters which were determined from spectroscopic terms of free ions following the method of quantum defect [1, 2].

Ionization leads to the strong decrease in the depth of the first minimum of the potential function corresponding to the distance area between the nearest neighbors for three- or four-charged ions. Moreover, for the pair of particles with four charges the first minimum disappears absolutely. Atoms fall to the repulsion branch of interaction potential. As a result, the crystal lattice changes to the state of nonequilibrium [3].

The equations state for metal were provided on the basis of the pseudopotential method when part of the ionic cores further ionized. The isotherms were obtained for different degrees of the atoms ionization on the example of aluminium. Fig. 1 shows the aluminum isoterms at the 0 K temperature for the different grades of ionization. So the 10% ionization results in the 15 kbar internal pressure appearance.

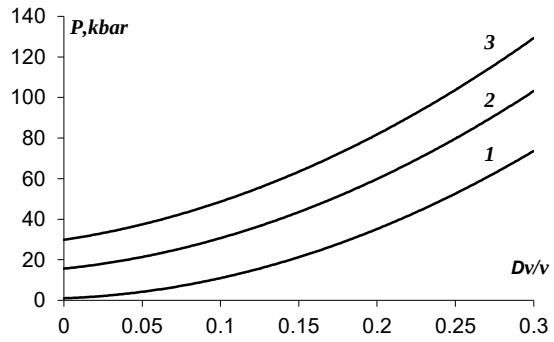

Fig.1. Aluminum isotherms for 0 K temperature: 1 – par, 2 – 10% of ionized atoms; 3 – 20% of ionized atoms

On the basis of pseudopotential approach, the behavior of interatomic interaction potentials under conditions of electronic subsystem excitation has been analyzed. It was discovered that thermal smearing of Fermi surface does not cause any essential change of interatomic interaction forces. At the same time local growth of conduction electron concentration causes “softening” of crystalline lattice when configuration with smaller interatomic distance becomes the equilibrium one. The potentials of interatomic interaction have been calculated for this case [4].

REFERENCES

[1] V. Heine, J.V. Abarencov, “A new Method for Electronic Structure for Metals”, Phil. Mag., vol. 9, pp. 451–465, 1964.

[2] A.O. Animaly, “Electronic Structure of Transition Metals. 1. Quantum Defects and Model Potential”, Phys. Rev., vol. B 8, pp. 3542-3554, 1973.

[3] V.P. Krivobokov, S.N. Yanin, ”Matter States Equation under Strong Radiation”, Eurasian Physical Technical Journal, vol. 2, No 2(4), pp. 39-46, 2005.

[4] S.N. Yanin, “The calculation method of interaction between metal atoms under influence of the radiation”, IOP Conference Series: Materials Science and Engineering, vol. 81, 2015.

FEATURES OF RADIATION-INDUCED DEFECT ACCUMULATION IN Fe-10Ni-20Cr SINGLE CRYSTALS WITH INCREASING RADIATION DOSE *

A.V. KORCHUGANOV, D.S. KRYZHEVICH, K.P. ZOLNIKOV

Institute of Strength Physics and Materials Science SB RAS, Tomsk, Russia

Modern austenitic stainless steels used in nuclear power plants have a number of problems, the main of which are high-temperature radiation embrittlement and radiation swelling [1,2]. To solve these problems, it is necessary to study the features of the formation, recombination, and accumulation of radiation-induced defects. Note that radiation damage defects nucleate at the atomic level due to the generation of atomic displacement cascades and their further evolution determines the response of the material to irradiation [3-5].

In this work, the mechanisms of radiation damage evolution of the model fcc Fe-10Ni-20Cr alloy single crystals were studied in the framework of computer simulation by the molecular dynamics method. The interatomic interaction was described by the many-body potential [6] developed in the framework of the embedded atom method. In order to study the behavior of the material at increasing irradiation dose, atomic displacement cascades with kinetic energies from 5 to 20 keV were successively generated in the simulated sample.

The basic characteristics of atomic displacement cascades with different energies have been calculated: the duration of cascade development stages, the maximum number of displaced atoms, and the volume of the radiation-damaged region. The features of changes in the number of survived point defects, the distribution of their clusters in size and space, including dislocation loops, stacking fault tetrahedra, etc., with increasing radiation dose were studied. The deformation behavior and mechanical characteristics of samples irradiated to various doses under uniaxial deformation and shear were investigated. On the basis of the results obtained, regularities of the change in the mechanical properties and the accumulation of radiation damage with an increase in the radiation dose were determined for the studied alloy.

REFERENCES

[1] K. Fukuya, "Current understanding of radiation-induced degradation in light water reactor structural materials," J. Nucl. Sci. Technol., vol. 50, P. 213–254, 2013

[2] F.A Garner, M.B Toloczko and B.H Sencer, "Comparison of swelling and irradiation creep behavior of fcc-austenitic and bcc-ferritic/martensitic alloys at high neutron exposure" J. Nucl. Mater., vol. 276, P.123–142, 2000

[3] K. Nordlund, S.J. Zinkle, A.E. Sand et al., "Primary radiation damage: A review of current understanding and models," J. Nucl. Mater., vol. 512, P. 450–479, 2018

[4] K.P. Zolnikov, A.V. Korchuganov, D.S. Kryzhevich et al., "Formation of point defect clusters in metals with grain boundaries under irradiation," Phys. Mesomech., vol. 22, P. 355–364, 2019

[5] A.V. Korchuganov, V.M. Chernov, K.P. Zolnikov et al., "MD simulation of primary radiation damage in metals with internal structure," Inorg. Mater. Appl. Res., vol. 7. P. 648–657, 2016

[6] L.K. Béland, A. Tamm, S. Mu et al., "Accurate classical short-range forces for the study of collision cascades in Fe–Ni–Cr," Comput. Phys. Commun., vol. 219, P. 11–19, 2017

* The work was supported by the Russian Science Foundation (Project No. 20-19-00466).

MODELLING OF F-CENTERS IN BERYLLIUM OXIDE NANOTUBES USING CONVOLUTIONAL NEURAL NETWORK

M.A. BOTOV, A.Y. KUZNETSOV, A.B. SOBOLEV

Ural Federal University, Yekaterinburg, Russia

The paper is devoted to computer simulation of intrinsic color centers (namely F-centers) in beryllia nanotubes by means of convolutional neural network (CNN). Developing of neural-network model for calculating of the total energy and electronic structure of complex atomic systems have a goal to decrease the modeling computational cost. We use this approach to predict energies and band structure obtained using ab initio methods. Accuracy of CNN solution and classical quantum chemical solution appeared to be comparable.

The dataset was generated using hybrid functional B3LYP with 30% of exact exchange. We consider single-walled zigzag BeO nanotubes. The (n,0) family was generated in the range from n = 8 (tube radius 3.4 Å) to 64 (tube radius 27.1 Å), with and without defects. Calculations were performed in CRYSTAL program package. Modeling was carried out in periodic boundary conditions.

REFERENCES

[1] K.Ryczko, K.Mills, I.Luchak, C.Homenick, I.Tamblyn, "Convolutional neural networks for atomistic systems", Comp.Mat.Sci. vol.149, 134-142, 2018.

[2] J.Baima, A.Erba, M.Rerat, R.Orlando, R.Dovesi "Beryllium oxide nanotubes and their connection to the flat monolayer", Phys.Chem.C, vol.117 12864-12872, 2013.

[3] J.Bekler, M.Parrinello, "Generalized neural-network representation of high-dimentional potential-energy surfaces", Phys.Rev.Lett., vol.98 146401, 2007.

[4] Dovesi R, Sounders V R, Roetti C, et al. 2013 CRYSTAL09 User's Manual (University of Tourino)

REACTOR STRENGTHENING OF TITANIUM NICKELIDE MODIFIED WITH HIGH- ENERGY CRYPTON IONS[1]

E.A. ZHAKONBAEV, V.P. POLTAVTSEVA, D.A. SATPAYEV, S.B. KISLITSIN, A.S. LARIONOV

Institute of Nuclear Physics of the Republic of Kazakhstan, Almaty, the Republic of Kazakhstan

Alloys, based on titanium nickelide with the shape memory effect, are used in various devices operating under the conditions of hazardous radiation exposure. There are real perspectives for application of such alloys in nuclear power facilities. However, the available literature data on the studies of the structure and properties of titanium nickelide indicate its very high sensitivity to neutron irradiation due to a change in the temperature kinetics of martensitic transformations, a decrease or suppression of the shape memory effect, and formation of amorphous regions or amorphization. It is assumed that the created titanium nickelide based alloys with the nanocoating hardened by irradiation with heavy ions of inert gases of MeV energy [1,2] will be radiation-resistant in relation to the effects of neutron irradiation.

The results of measurements of microhardness and electrical resistivity are provided for titanium nickelide irradiated by neutrons to the fluence of $2.3 \cdot 10^{16}$ and $1.5 \cdot 10^{15}$ n/m^2 respectively for fast and thermal neutrons at $\geq 60^0$C before and after modification. Modification of titanium nickelide was carried out in the martensitic-austenitic state with Kr^{15+} ions of 147 MeV energy at the temperatures of 100 and 250^0C.

According to the Vickers'microhardness measurements, depending on the indenter penetration depth at the loads of 0.098±4.9 N, carried out by the microhardness meter PMT-3M, it was established, firstly, that hardening of titanium nickelide is observed, regardless of the state, to the greatest extent (by 1.2-1.4 times) in the non-modified condition. Secondly, the temperature of the modification does not significantly affect the degree of hardening, whereas after the modification at 250^0C there was a slight softening of titanium nickelide. It should be noted that the obtained data of electrical resistivity measurements correlate well with hardening of titanium nickelide under the influence of neutron irradiation. It follows that the growth of resistvity of titanium nickelide, irradiated with neutrons, is mainly defined by formation of hardened radiation-introduced nano-defects [2]. However, there are still outstanding issues about the role of neutron fluence in hardening of titanium nickelide and keeping of the shape memory effect.

REFERENCES

[1] 1. V.P.Poltavtseva, S.A. Ghyngazov, D.A.Satpayev. The influence of high-energy krypton ion implantation temperature on structure and properties of Ni-Ti allow // Russion Physics Journal. – 2019. – Vol. 61, N. 11. – P. 212-218.

[2] 2. S.Ghyngazov, V. Poltavtseva, A. Larionov, D. Satpayev. Features of changes in the structure and properties of titanium nickelide irradiated with MeV xenon ions // Nuclear Inst. and Methods in Physics Research B. – 2020. – Vol. 464. – P. 23-27.

1 The work was performed as part of the grant financing project of the Ministry of Education of the Republic of Kazakhstan AP08052572

RADIATION DAMAGE OF BAFBR CRYSTALS IRRADIATED WITH KRYPTON IONS*

SH. GINIYATOVA[1], *D. KENBAYEV*[1], *E.F. POLISADOVA*[2], *ZH. KARIPBAYEV*[1], *A. AKILBEKOV*[1], *M. ZDOROVETS*[3,4], *A.I. POPOV*[4], *A. DAULETBEKOVA*[1]

[1]*L.N. Gumilyov Eurasian National University, Nur-Sultan, Kazakhstan*
[2]*Tomsk Polytechnic University, Tomsk, Russia*
[3]*Institute of Nuclear Physics, Nur-Sultan, Kazakhstan*
[4]*Ural Federal University, Yekaterinburg, Russia*
[5]*Institute of Solid State Physics, University of Latvia, Riga, Latvia*

Among the many materials used as detectors, we can distinguish crystals of MeFX class (Me - Sr, Ba, X - Cl, Br, I). In BaFBr crystal, the image created by ionizing as well as nuclear radiation remains stable in the dark for a long time at room temperature. The effect is successfully used to create imaging screens (imaging plate - IP). Memory screens were originally designed for X-ray radiation. BaFBr has several advantages over conventional X-ray films, such as high sensitivity, wide dynamic range, and high spatial resolution [1].

Our work considers defects in the BaFBr crystal created under the irradiation by 147 MeV Kr ions up to fluences: 10^{10} cm-^{2}, 10^{11} cm-^{2}, 10^{12} cm-^{2}, and 10^{13} cm^{-2}. Range, electronic and nuclear energy losses of Kr ion in BaFBr crystal were calculated using code SRIM 2013 [2]. Calculations have shown that electronic energy loss dominates and R=17,87 μm.

Absorption spectra were measured by spectrophotometer SPECORD UV-VIS (200-1000) nm. We did not observe any changes in the absorption spectrum of the crystal irradiated to the fluence 10^{10} cm^{-2} except for the increase of the optical density of the crystal. Starting with fluence of 1×10^{11} cm-^{2}, additional absorption bands with maximums at 240 and 485 nm appear in the spectrum. The intensity of these bands increases with the growth of the fluence.

REFERENCES

[1] Amemiya, Y.,Miyahara, J. Imaging plate illuminatesmany fields. // Nature. Vol. 336. 1988. P. 89-90.

[2] SRIM code 2013 based on Ziegler J.F., Biersak J.P., Littmark U. The Stopping and Range of Ions in Solid. // New York: Pergamon Press, 1985.

* The work was supported by MES of RK

INFLUENCE OF X-RAY IRRADIATION ON STRENGTH CHARACTERISTICS OF SPECIAL PURPOSE ELASTOMERS

N. VALKO[1], *A. KASPEROVICH*[2]

[1] *Yanka Kupala State University of Grodno, Belarus*
[2] *Belarusian State Technological University, Minsk, Belarus*

The work presents experimental studies of the X-ray effect on strength characteristics (tensile strength and tensile elongation at break) of special purpose elastomers and shows modern tendencies in modification of special purpose rubbers with ionizing radiation. The subscribed problem is very actual since remarkable increasing of machinery building operation intensity dictates new requirements to use rubbers.

The special purpose elastomers vulcanized at 70, 80 and 90 degree have been irradiated with X-rays (MoKα 0.7 nm). The X-ray irradiation has been carried out in the range from 0 min to 60 min.

The analysis of experimental data leads to conclude that X-ray irradiation of rubbers did not make basic strength properties worse but improve it. Dependences between strength characteristics, vulcanization and irradiation modes have been found. Particularly the X-Ray irradiation of rubbers promotes to increase the tensile strength more than 10 %. Unmistakably for a 90 % of vulcanizated rubber the tensile strength is equal 23,5 MPa. Almost the same value of the tensile strength (23,6 MPa) has been obtained for a 70 % vulcanizated rubber but it has been irradiated with X-rays. It is known, that tensile strength is indicative of the strength derived from factors such as fiber strength, fiber length, and bonding. In this way irradiation of not completely vulcanized rubbers with the X-rays results appearing additional oriented polymer crosslinking molecules due to interact of polymer radicals and to formation of branched crosslinked structures. The fact of improving rubber properties in the X-rays considerably expands the market for special purpose rubber as well as the areas of rubbers application because a natural rubber is the starting material for introduction of chemistries that introduce damping, abrasion resistance and higher modulus through copolymerization and interacting functional groups.

With help of obtained experimental data the influence of the X-ray irradiation (exposure dose rate of X-rays) and degree of rubber vulcanization on the basic strength properties data have been studied by the method of a full factorial experiment. The core of the plan has been chosen as two-level full factorial experiment. Two factors (a vulcanization degree and an exposure dose rate of the X-ray radiation) influencing on strength characteristics have been considered. A tensile strength and an elongation at break have been considered as responses. All possible combinations of factors have been implemented according to plan. It should be noted that according to the compiled experimental design matrices samples have been obtained under the corresponding vulcanization and irradiation modes.

The developed statistical model allows determining adequately optimal irradiation and vulcanization modes for obtaining rubbers with desired properties.

REFERENCES

[1] A.V. Kasperovich, V.V. Bobrova, N.G.Valko. Modification of thermophysical and operational properties of elastomeric compositions " Modern innovations in the field of science, technology and the integration of knowledge," Materials of the Int. Scientific-practical Conf. dedicated to the 60th anniversary of the Rudny Industrial Institute, Rudny, pp. 115-122, 2019

[2] Zakheim, A.Yu. Introduction in modeling of chemical-technological processes. M .: Chemistry 288 p, 1982.

[3] Montgomery, D.K. Experiment Planning and Data Analysis: Per. with English / D.K. Montgomery : L.: Shipbuilding, 384 p, 1980 Semenov, S.A. Planning an experiment in chemistry and chemical technology / S.A. Semenov. - M.: CPI MITT, 93 p. 2001.

[1]The work was supported by RFBR 18-08-00728

STRUCTURE AND PROPERTIES OF PAINT COATINGS IRRADIATED BY ULTRAVIOLET RAYS

N. VALKO[1], A. HLOBA[2], A. KASPEROVICH[2]

[1] Yanka Kupala State University of Grodno, Belarus
[2] Belarusian State Technological University, Minsk, Belarus

The paper presents experimental research of the UV-radiation effect on the structure formation, phase composition and physical-mechanical properties (hardness, adhesion, impact strength, moisture absorption, etc.) of paint coatings formed from two-component epoxy enamel EP-773. The coatings have been modified with active fillers as hollow glass microspheres (Q-cel 5070) and have been irradiated with UV –rays (207 nm).

A relevance of the work associated with the need of improving a technology for coatings producing and development protective layers with required performance characteristics [1-3].

By the method of scanning electron microscopy it was found that adding of microspheres leads to decrease in a number of microcracks and it's extending in a volume of paint coatings. It is shown that a hardness of the paint coatings increases with adding microspheres while maintaining a high level of adhesion and an impact strength. It has been established that hollow glass microspheres improve the hiding power of the paint coatings, thereby contributing to save paintwork material and to increase its service period due decreasing in the amount of corrosion products on its surface.

It is obtained that effect of the UV radiation on surface of paint coatings formed from two-component epoxy enamel EP-773 and modified with active fillers as hollow glass microspheres (Q-cel 5070) has a positive effect. It leads to increase of polymerization speed due to increase of diffusion processes and due the successive addition of free-radical building blocks.

The experimental date indicate that irradiation with UV rays (wavelength 207 nm) on the surface of paint coatings deposited from two-component epoxy enamel EP-773 with glass microspheres (Q-cel 5070) leads formatting uniformly, dense and non-porous paint coatings [4]. Moreover, it is established the increase in corrosion protection and microhardness as a result of structure modification under radiation effect.

REFERENCES

[1] D. P. Volkov, L. A. Kuliev, M. V. Uspenskaya, A. V. Tokarev. Investigation of the thermal conductivity of polymer composite materials // Izv. Universities. Instrument making. V. 52, No. 1. pp.75–77, 2009

[2] A coating filled with hollow microspheres that prevents icing of the surfaces of various products: Pat. 2349618 RF, IPC C 09 D 5/02 C 09 K 3/18 / V.S. Belyaev; - No. 2006144125/04; declared 12/13/2006; publ. 03/20/2009 // - V.S. Belyaev, P.9, 2009

[3] Composition for the manufacture of low-density material for protecting devices from mechanical stress: Pat. 2574241 of the Russian Federation, IPC C 08 J 9/32, C 09 K 3/00 / M.S. Chervyakov, S.A. Fedotov; - No. 2014125291/05; declared 06/23/2014; publ. 02/10/2016 // Federal State Unitary Enterprise "All-Russian Scientific Research Institute of Automation named after N.L. Spirit ", P.7, 2014

[4] N.G. Valko, S.Yu. Rayunchus, A.I. Globa, A.V. Kasperovich. The effect of UV radiation on the hardness of paint coatings "Petrochemistry – 2019", Materials of the II Int. Scientific, Technical and Investment Forum on Chemical Technologies and Oil and Gas Processing, Minsk, BSTU, pp. 146-149, 2019.

FORMATION OF PERIODICAL COLOR CENTER STRUCTURE IN LITHIUM FLUORIDE BY SINGLE-CYCLE MID IR FEMTOSECOND LIGHT BULLET[1]

A.E. DORMIDONOV[1], V.O. KOMPANETS[1], S.V. CHEKALIN[1], V.P. KANDIDOV[2,1]

[1]Institute of Spectroscopy RAS, Moscow, Troitsk, 108840 Russia
[2]Moscow Lomonosov State University, Physics Department, Moscow, 119991 Russia

We present the results of experimental and numerical studies of color centers (CCs) formation in LiF after a propagation of Mid-IR (2500 – 4000 nm) femtosecond laser pulse. At these wavelengths the pulse group velocity dispersion in LiF is anomalous, and extremely compressed wave packet — the so called light bullet (LB) can be formed [1,2]. The LB's the peak intensity achieves the value more than 10^{14} W/cm^2, its diameter is about 10 μm, and the duration becomes near one oscillation cycle of the light field. The very high light field energy localization in LB leads to the medium ionization and formation of CCs. LiF has been selected in our experiments because of much more bright CC luminescence intensity in comparison with other alkali halide crystals that allowed us to observe a photoinduced transformation produced by a single laser pulse. The mechanisms which led to coloration may be explained by the non-linear excitation of electrons to the conduction band via different processes such as avalanche ionization, tunnelling ionization, and multiphoton absorption and also by a direct multiphoton excitation of excitonic band, which is possible only for Mid-IR exciting pulses. The CCs in LiF are F_2 and F_3^+ with luminescence bands centered near 650 and 550 nm, respectively. Excitation of both CCs types occurs under the blue light illumination.

The photos of luminescence intensity pattern of CCs formed in LiF after propagation of 3500-nm LB are shown in the top of Fig. 1. The experimentally registered LB starts after the pulse has passed about 7 mm in LiF. The full length of the CCs structure is about 1 mm. It can be seen that CCs have a strictly periodic structure with a length of separate sections about 30 μm, which increases with a LB's wavelength decreasing [3,4]. These oscillations of CC density are caused by the periodic change of the LB light field intensity due to the difference between phase and group velocities of light — the so called 'breathing' of the LB [3,4]. The numerically calculated distribution of electron density in the plasma channel $N_e(x,y)$ is shown in the bottom of Fig. 1. The blue curve in Fig. 1 corresponds to the on-axis electron density profile $N_e(x=0)$, while the pink curve — to the maximal on-axis intensity of the light field of the LB (up to $2\cdot10^{14}$ W/cm^2). The peak value of electron density $N_e(x,y)$ is about 10^{19} cm^{-3}, while concentration of CCs is not higher than 10^{18} cm^{-3}.

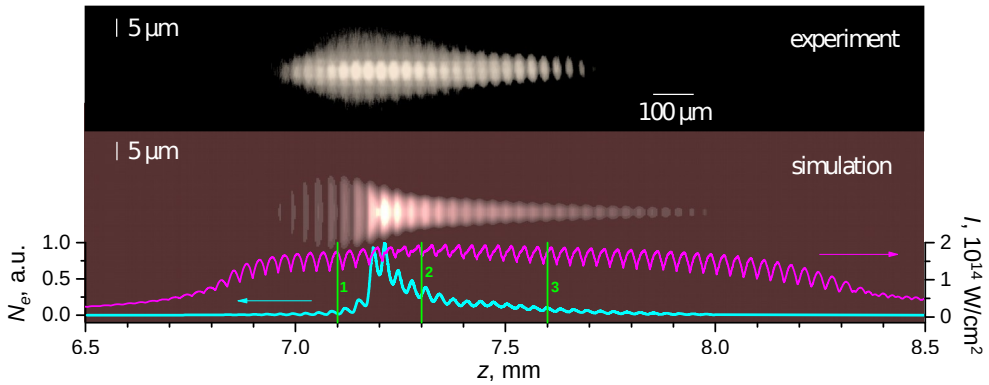

Fig. 1. Luminescence intensity pattern of CCs formed in LiF after propagation of 3500-nm LB: experiment (top) and numerical simulation (bottom). Blue curve — on-axis electron density, pink curve — on-axis LB peak intensity.

REFERENCES

[1] Y. Silberberg, "Collapse of optical pulses," Opt. Lett., vol. 15, p. 1282, 1990.

[2] S.V. Chekalin, V.O. Kompanets, A.E. Dormidonov, V.P. Kandidov, "The light bullet dynamics in uniform dielectrics," Physics – Uspekhi, vol. 62, p. 282, 2019.

[3] A.V. Kuznetsov, V.O. Kompanets, A.E. Dormidonov, S.V. Chekalin, S.A. Shlenov, V.P. Kandidov, "Periodic colour-centre structure formed under filamentation of mid-IR femtosecond laser radiation in a LiF crystal," Quantum Electron., vol. 46, p. 379, 2016.

[4] S.V. Chekalin, V.O. Kompanets, A.V. Kuznetsov, A.E. Dormidonov, V.P. Kandidov, "Regular 'breathing' of a near-single-cycle light bullet in mid-IR filament," Laser Phys. Lett., vol. 13, no 6, p. 065401, 2016.

1 The work was supported by the Russian Foundation for Basic Research under grant No. 14-22-02025-ofi_m and Russian Science Foundation under grant No 18-12-00422.

MICRO HOT-SPOT MODEL OF INITIATION OF COMPOSITES BASED ON THE EXPLOSIVES AND INCLUSIONS OF NANOPARTICLESA WITH SHELL-CORE STRUCTURE[1]

*E.V. GALKINA *, A.V. KALENSKII*, A.A. ZVEKOV **, M.V. ANAN'EVA*, B.P. ADUEV **, V.V. GALKINA **

**Kemerovo State University,6 Krasnaya st., Kemerovo, 650000, Russia, kriger@kemsu.ru, +7(3842)580591*
***Federal Research Center of Coal and Coal Chemistry,18 Sovetsky av., Kemerovo, 650000, Russia*

Remote sensing methods of explosive decomposition initiation is a perspective method to use instead of electric initiation methods. They allow to improve safety of using of explosives, reduce environmental risks and minimize probability of technological disasters. Compositions with selective sensitivity to laser pulse, based on secondary explosives and light absorbing nanoparticles, are being developed. Earlier it was shown [1] that critical energy density of initiation of pentaerythritol tetranitrate (PETN) – metal nanoparticles reduces by more than a hundred times comparing to the pure PETN initiated by neodymium laser pulse. Experimentally found a significant (more than 10-fold) increase in the threshold initiation energy density of composites PETN-aluminum, if the thickness of the oxide shell of metal nanoparticles increases [2], also the influence of residual porosity of pressed hexogen tablets (RDX) on its threshold initiation energy density. The aim of this work is to formulate a micro hot-spot model of the thermal explosion of secondary explosives with additives of metal nanoparticles with a core – shell structure, taking into account the optical and thermophysical properties of the dielectric shell, and to test the model on practically important composites PETN and RDX-aluminum nanoparticles.

The model includes processes of light absorption by nanoparticles with a structure metal core – transparent shell or a metal nanoparticle in pore, conductive heat transfer in the nanoparticle and adjacent matrix, heat release due to chemical decomposition of PETN or RDX with the possible initiation of an explosive decomposition reaction when the critical energy density is exceeded.

The effect of oxide shell or pore on the optical properties of aluminum nanoparticles was calculated in terms of Aden-Kerker and Mie's theory for the spherical particle. Modeling methods and particularities of calculation of the optical properties of spherical particles with the structure of the dielectric shell were discussed in [3]. A new concept is introduced-the absorption efficiency factor of the metal core of a nanoparticle with a non-absorbing shell. It is shown that dielectric shell (including pore) increases citical energy density and complicates the transition of the reaction to a self-accelerating mode. The results were analyzed and compared with the experiment. The study showed not only a qualitative but also a quantitative description of the existing experimental dependencies for initiating explosive decomposition of pressed PETN tablets- metal nanoparticles with shell-core structure. The results of the work are necessary for optimizing the composition of the optical detonator capsule.

REFERENCES

[1] *A.V. Kalenskii, A.A. Zvekov, M.V. Anan'eva ,A.P. Nikitin, B.P. Aduev //* Combustion, Explosion, and Shock Waves. – 2017. - Volume 53. – No. 1. pp 82–92.

[2] *B.P. Aduev, D.R. Nurmukhametov, A.A. Zvekov, N.V. Nelyubina //* Combustion, Explosion, and Shock Waves. – 2014. - Volume 50. – No. 5. pp 578–581.

[3] . Zvekov A.A., Anan'eva M.V., Kalenskii A.V., Aduev B.P., Galkina E.V. /Journal of Applied Spectroscopy. 2019, 86(3), pp. 470-478.

[1] This work was supported by RFBR (№18-03-00421_a, №19-33-90261) and was conducted within the framework of the budget project # AAAA-A17-117041910150-2 for the Institute of Coal Chemistry and Chemical Material Science of FRC CCC SB RAS (supervised by B.P. Aduev).

INDIVIDUALIZED PERSONNEL TRAINING MODE OF EMERGING ENGINEERING FROM THE PERSPECTIVE OF MULTIPLE INTELLIGENCE THEORY*

Z.P. SUN

Chongqing University of Arts and Sciences, Chongqing, The People's Republic of China

Under the background of new economy, new technologies, new formats, new industries and new models represented by big data, cloud computing, internet of things, artificial intelligence and virtual reality have brought new demands to talent. Therefore, accelerating the construction of new engineering is the inevitable choice for universities to implement the national major development strategy. How to deal with the relationship between general training and individual development, single combat and resource integration, overall planning and classified implementation is the practical dilemma of emerging engineering talents training. The introduction of the theory of multiple intelligences brings new views of students, teaching and management to the training of emerging engineering talents. Combined with the theory of multiple intelligences, the main paths of "Qualified +" personalized talents training in emerging engineering include the modes of excellence, innovation and entrepreneurship, compound and specialty. In order to truly implement the "Qualified +" personalized talents training of new engineering, we must innovate the realization mechanism from cross-border cross integration, individualized development, organizational management, cross-border training of teachers, fund management and other aspects.

REFERENCES

[1] R. Chen, R. Zhao, J. Guo, H.H., Hu, “Exploration of project-based new energy courses group teaching mode under the background of emerging engineering education,” University Education, vol. 3, pp. 49-51, 2020.

[2] Q.Q., Zhao, C.F. Wang, “Exploration and practice of training mode of new energy automobile talents under the background of new engineering,” Heilongjiang Science, vol. 10, no. 23, pp. 30-31, 2019.

[3] C.B. Yan, J.Z. Yang, Y. Liang, “Cultivation of engineering consciousness and craftsman spirit under construction of emerging engineering education: a case study of civil engineering majors, ” Journal of Beijing University of Aeronautics and Astronatutics, vol. 32, no. 6, pp. 152-160, 2019.

* The work was supported by Chongqing University of Arts and Sciences.

A PORTABLE RADIOMETRIC SYSTEM FOR EVALUATING LACRIMAL DRAINAGE*

S.V. PANKIN[1], *A.I. SURDO*[1,2], *V.V. PANKIN*[1], *A.V. ZELENIN*[3]

[1]*Ural Federal University, Yekaterinburg, Russia*
[2]*M.N. Mikheev Institute of Metal Physics of the Ural Branch of the Russian Academy of Sciences, Yekaterinburg, Russia*
[3]*Regional Children's Clinical Hospital, Yekaterinburg, Russia*

A portable radiometric system (PRS) was developed at UrFU as a medical diagnostic device for dynamical scintigraphy [1]. The paper considers advantages and disadvantages of the using of PRS for dacryoscintigraphy to study the function of the tear ducts.

Dacryoscintigraphy is usually realized with a gamma camera. The main disadvantage of gamma camera is a lack of sensitivity in contrast to organ probes for dynamical scintigraphy. The developed PRS consists of small gamma-ray detectors that can be attached to the patient's body. The main advantage of such a system is that it allows to carry out synchronized scintigraphy examination in several points of wide area. In contrast with gamma camera, detectors of PRS can be positioned in arbitrary manner and located in different planes to each other.

The aim of this work is development of a lacrimal drainage model to make some tests of developed portable device. This study includes several components: individual selection of collimating system parameters, considering anatomical features of patients; choosing of optimal position of each detector relative to the patient's body; calculating of minimal volume of radiopharmaceutical for one examination. It is necessary due to make radiation hitting from the nearby tissues lower.

Methods of data processing [2] for evaluating of the lacrimal drainage were discussed. In addition, individual parameters of collimators for each detector of the PRS were selected. Analyze of the possibility of reducing the amount of injected radiopharmaceutical was made to reduce the radiation dose on the lens of the eye without loss of diagnostically important information component. A phantom study was conducted in parallel with gamma-camera for competitive analysis of this systems.

REFERENCES

[1] *S. V. Pankin et. al // Radiat. Meas. – 2019. – 121. Pages 10–12.*
[2] *J. M. Malbouisson et. al // ACTA OPHTHALMOLOGICA SCANDINAVICA. – 1997. – 75. Pages 290-294.*

* The research was carried out within the state assignment of Ministry of Science and Higher Education of the Russian Federation (theme "Expertise" No. AAAA-A19-119062590007-2), supported in part by RFBR (project No. 20-48-660045).

INVESTIGATION OF THE ELECTRONIC STRUCTURE OF ATOMS IN MODIFIED METAL ALLOYS IN ANALYSIS OF THE ELASTIC AND DISCRETE SCATTERED ELECTRON SPECTRA

I.A. SHULEPOV[2], A. LOMYGIN[1], L.B. BOTAEVA[1,3], R.S. LAPTEV[1], E.B. KASHKAROV[1], M.S. SYRTANOV[1]

[1]National Research Tomsk Polytechnic University, Tomsk, Russian Federation
[2]Institute of Strength Physics and Materials Science, Siberian Branch of the Russian Academy of Sciences, Tomsk, Russian Federation
[3]Tomsk State University of Control Systems and Radio Electronics, Tomsk, Russian Federation

With any modification processes, whether implantation of high-energy ions, heat treatment, deformation, alloying or other, the electronic states are changed. This is because the atoms change their arrangement in the crystalline structure, the chemical environment of the atoms changes, the crystal structure is deformed, compared with the initial state [1, 2].

In this work, we solved the problem of revealing the relation between the deformation and, as a consequence, the movement of atoms in the crystal lattice, with a change in the shape of the spectra of elastically and discretely scattered electrons, as well as the dependence on the angle of exit of these electrons from the surface of the Ti-6Al-4V alloy.

The studies were carried out at two energies of elastically scattered electrons - 720 eV and 820 eV. We used samples of Ti-6Al-4V alloy of the initial and longitudinally helical rolling at 10000 ° C.

The experiments were carried out on a modernized Auger spectrometer 09 IOS 10, which is equipped with an energy analyzer such as a cylindrical mirror.

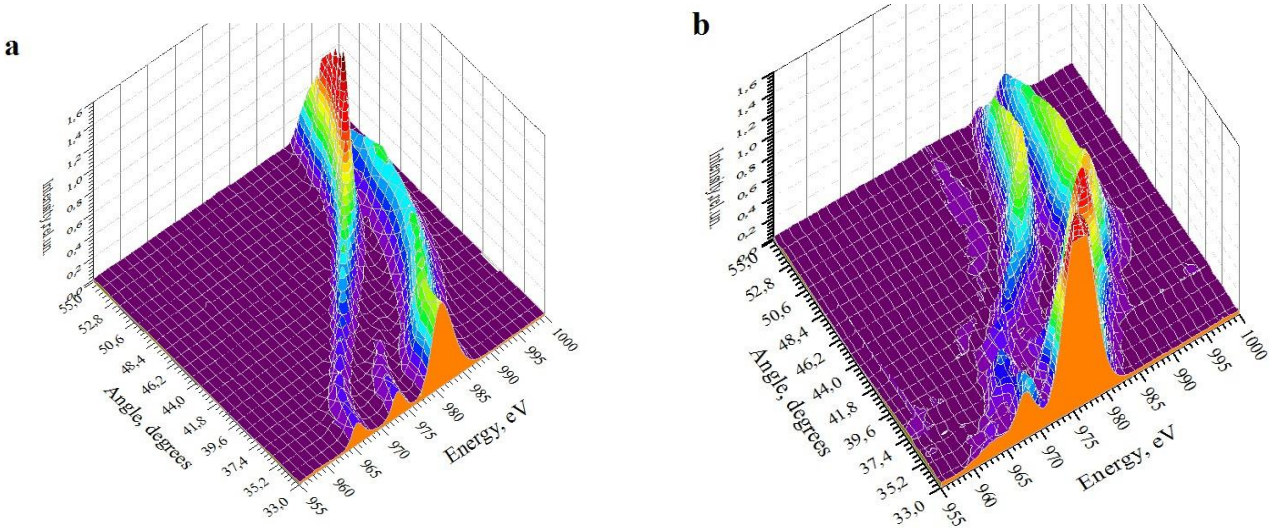

Fig.1. Spectra of elastically and discretely scattered electrons depending on the angle of exit of the Ti-6Al-4V alloy surface: a — initial state, b-subjected to longitudinal helical rolling at 1000 °C. Primary electron energy is 980 eV.

As can be seen from Fig. 1, the spectra of elastically and discretely scattered electrons from the samples in the initial state and deformed are different. This is due to different scattering energies of primary electrons on bulk and surface plasmons. This can be explained by a rearrangement of atoms in the crystal lattice and a change in the energy levels of the electron shells. Due to deformation, the dependences of the intensities of elastically and discretely scattered electrons on the angle of exit from the surface of a solid also change.

REFERENCES

[1] V. E. Panin, I. A. Shulepov, L. S. Derevyagina, S. V. Panin, A. I. Gordienko, I. V. Vlasov, “Creating nanoscale mesoscopic structural states for the formation of martensitic phases in low alloy steel with the aim obtaining high low-temperature toughness”, Fiz. mesomech., vol. 22., No. 6, pp. 5-13, December 2019.

[2] V. E. Panin, I. A. Shulepov, A. V. Panin, O. B. Perevalova, I. V. Vlasov, “The influence of nanoscale mesoscopic structural states associated with the curvature of the crystal lattice on the mechanical behavior of the Ti-6Al-4V titanium alloy”, Fiz. mesomech., vol. 22., No. 6, pp. 14-23, December 2019.

PLASMA FORMATION DURING PULSEPERIODICAL LASER TREATING OF METALS

A.YU. IVANOV, S.V. VASILIEV

Grodno State University, Osheshko, 22, Grodno, 230023, Belarus, ion_ne@mail.ru, (0152)610098

The radiation of the GOR-100M ruby laser (λ = 0.694 mm) operating in the free oscillation regime (pulse duration ~1.2 mc) passed through the focusing system and was directed onto the surface of metal sample. Both mono-lens and two-lens systems were used for focusing of laser radiation. This avoided to form an image of a diaphragm on the surface of irradiated sample as a spot with the sharp borders. During the experiments a spot diameter was varied from 1 to 2 mm. This permitted to vary the flux density of laser radiation q from 10^4 to 10^6 W cm^{-2}. From the front face of the glass wedge a part (4 %) of laser radiation was directed into the IMO-2N energy meter, whose entrance window was located in the focal plane of the lens. The energy of the laser pulses varied from 5 to 60 J. The FEK-14 coaxial photodetector, the signal from which was coupled to the S8-13 oscilloscope, was used to record the temporal shape of the laser pulse. To study the spatial and temporal evolution of the laser plasma torch in the course of laser radiation action on the sample, we used the method of high-speed holographic motion-picture recording. The sample was placed in one of the arms of a Mach – Zehnder interferometer, which was illuminated with the radiation of the second ruby laser operating in the free oscillation regime. The pulse duration of the radiation amounted to 400 mc. The transverse mode selection in the probing laser was accomplished using the aperture, placed in the cavity, and the longitudinal mode selection was provided by the Fabry – Perot cavity standard used as the output mirror.

The probing radiation after the collimator was a parallel light beam with the diameter up to 3 cm, which allowed observation of the steam-plasma cloud development. The interferometer was attached to the SFR-1M high-speed recording camera, in which the plane of the film was conjugate with the meridian section of the laser beam, acting on the sample, by means of the objective.

The high-speed camera operated in the time magnifier regime. The described setup allowed recording of time-resolved holograms of the focused image of the laser plasma torch. Separate holographic frames provided temporal resolution no worse than 0.8 μc (the single frame exposure time) and the spatial resolution in the object field ~ 50 μm. The diffraction efficiency of the holograms allowed one to reconstruct and record interference and shadow pictures of the studied process under the stationary conditions.

The experimental data show that electron density in the plasma formation on the border of irradiated spot and in the centre are different. This effect is connected with different conditions of energy dissipation from the plasma connected with lateral unloading. Lateral unloading has the surface character, and intensive energy dissipation takes place nearly only on the border of the laser beam.

Under different regimes of laser treating of metal difference in electron density maxima position was observed also. For mono-pulse regime of metal treating maximum of electron density was disposed in the centre of irradiated spot. For two-pulse regime a plasma plume had two maxima of electron density disposed symmetrically relative to the centre of irradiated zone. This effect can be connected with the refraction of laser radiation in already existing plasma plume, which leads to defocusing of laser beam after generation of the second pulse.

During two-pulse treating of matter the turbulences of plasma torch were more pronounced. This effect cat be connected with action of the second laser pulse onto the already thrown out of melted bath metal droplets.

High-speed photo-reamers show that each laser pulse brings separate contribution in plasma plume formation near irradiated surface. It is considerable that plasma plumes created by the second and following laser pulses had several plasma fronts supported by laser radiation and propagated along a laser beam in both directions. The shock waves reflecting from the surface of plasma and air connection and from the surface of the irradiated target are well distinct on the plasma photographs. During multi-pulse laser treating of metals formation of quasi-stationary plasma-dynamical structure was also observed.

DEVELOPMENT OF A MIRROR ENERGY ANALYZER OF CHARGED PARTICLES BEAMS BASED ON A MODIFIED ELECTROSTATIC FIELD

ZH.T. KAMBAROVA[1], *A.O. SAULEBEKOV*[2]

[1]*Buketov Karaganda State University, Karaganda, Kazakhstan*
[2]*Lomonosov Moscow State University, Kazakhstan branch, Nur-Sultan, Kazakhstan*

The work is devoted to numerical modeling of the electron-optical scheme of a mirror energy analyzer based on a modified electrostatic field. A modified version of a plane mirror energy analyzer is proposed, the field of which is non-uniform, falling according to the hyperbolic law. The potential of an electrostatic non-uniform field is described by the following expression

$$U = \frac{U_0}{d} y\left(1 - Az\right) \tag{1}$$

where A is dimensionless parameter, at A=0 field (1) is uniform (case of a plane mirror), d is distance between the electrodes.

Theoretical study of the electron-optical properties of an energy-analyzing system based on a non-uniform field at A=0.01 has been previously carried out by authors [1]. Results are obtained by using an approximate-analytical method for calculation the trajectories of charged particles. The optimal version of the analyzer scheme based on a non-uniform field has a higher resolution than a plane mirror.

In the work modeling of electron-optical scheme of a mirror energy analyzer based on a modified electrostatic field was carried out by using numerical method. The "Focus" numerical program for modeling axial-symmetrical corpuscular-optical systems was used for calculations [2]. Varying the value of A dimensionless parameter, the optimal scheme of the energy analyzer with the best focusing properties at the value of parameter A = 0.05 is found. The analyzer consists of two electrodes, one of the electrodes is plane plate *1* with zero potential, the other electrode *2* has a hyperbolic profile and potential U_0 (Fig. 1). The lower plane plate 1 has entrance and exit slits for motion of charged particles beam. According to the scheme, secondary electrons *5* excited from the investigation sample *3*, located near the lower plate, enter into the mirror field at a certain angle α to the plane plate. Under the action of a non-uniform field, the electron beam returns to the lower electrode, having passed the exit slit, is focused into a point image, then it is registered by the detector *4*. All sizes are expressed in relative units.

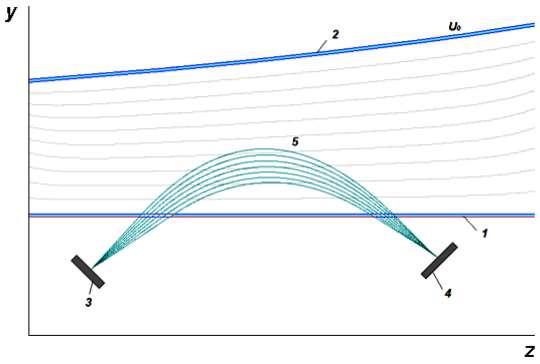

Fig.1. Trajectories of charged particles in an energy analyzer scheme based on a modified field at parameter A = 0.05: 1 is a plane plate, 2 is an deflecting electrode, 3 is an investigation sample with a point source; 4 - detector, 5 - secondary electrons

This scheme provides efficient transportation of the electron beams in the range of emission angles 30 ± 6^0 and second order angular focusing regime. Corpuscular-optical parameters of the proposed energy-analyzing system and the instrumental function of the device are calculated. Results of numerical modeling are in good agreement with calculations data of approximate-analytical method.

REFERENCES

[1] A.O. Saulebekov, D. Vénos, Zh.T. Kambarova, D.A. Saulebekova, K.I. Vassilyeva., Kh.B. Seidualy, "Development of energy analyzer of charged particles based on the basis non-uniform electrostatic field, " Eurasian phys. tech. j., vol.16, no. 1 (31), pp.24-29, June 2019.

[2] A. Trubitsyn, E. Grachev, V. Gurov, I. Bochkov, V. Bochkov, "CAE "FOCUS" for modelling and simulating electron optics systems: Development and application," Proceedings of SPIE., vol. 10250, pp. 0V-1 – 0V-7, 2017.

ANALYZER OF CHARGED PARTICLES BASED ON THE ELECTROSTATIC QUADRUPOLE-CYLINDRICAL FIELD IN THE «AXIS-RING» FOCUSING REGIME

ZH.T. KAMBAROVA[1], A.O. SAULEBEKOV[2]

[1]Buketov Karaganda State University, Karaganda, Kazakhstan
[2]Lomonosov Moscow State University, Kazakhstan branch, Nur-Sultan, Kazakhstan

The work is devoted to calculation the focusing properties of an axial-symmetrical mirror energy analyzer of charged particles based on the electrostatic quadrupole-cylindrical field (QCF) and the search for new angular focusing regimes. The potential of QCF in the coordinate system *r,z* is

$$U_q(r,z) = U_0(\mu + z)\ln r \tag{1}$$

where μ is a coefficient, specifying the weight contribution of the cylindrical field. The field (1) at μ=1 coincides with the well-known Wannberg field [1]. The potential of the Wannberg field is

$$U = \frac{V}{\ln\frac{r_1}{r_o}}(1+Az)\ln\frac{r}{r_o} \tag{2}$$

where *A* is a small dimensionless parameter.

The electron-optical characteristics of some scheme of QCF energy analyzer at *A* = - 0.01 have been previously numerically studied by the authors. “Ring-ring” and “ring-axis” second order angular focusing regimes were found [2, 3].

The investigated QCF is formed in the space between two axial-symmetrical coaxial electrodes. The inner electrode *1* has a cylindrical shape (radius r_0) and is under the Earth’s potential, the outer electrode *2* with deflecting U_0 potential is has a curved profile $r = r_0 \exp\left[\frac{\ln(r_1/r_0)}{1+Az}\right]$. Fig.1 shows the particle trajectories in the electron-optical scheme of the analyzer. The source of primary electrons is an integrated electron gun *7* whose axis coincides with the symmetry axis of the analyzer. According to the scheme, secondary electrons excited from the investigated sample *3* by primary radiation *6*, through the entrance slit in the inner cylinder *1*, enter the analyzer field and then deflect to the cylinder axis *z* and focus ring image. Electrons passing through the exit diaphragm *4* are detected by the detector *5*. All sizes are expressed in relative units.

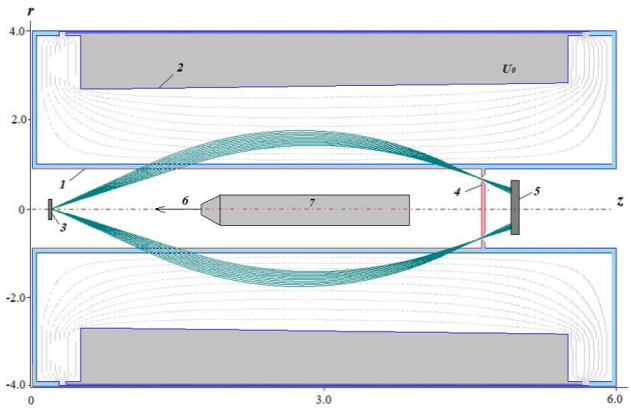

Fig.1. Scheme of a longitudinal section of an QCF energy analyzer (axis-ring focusing regime): 1 is cylindrical electrode, 2 is outer electrode, 3 is sample with a point source of particles, 4 is exit diaphragm, 5 is detector, 6 is primary electrons, 7 is electron gun

Modeling of the electron-optical scheme showed the possibility of achieving “axis-ring” second order focusing of particles. Results of calculation the focusing properties of QCF analyzer are obtained.

REFERENCES

[1] B. Wannberg, "An electrostatic mirror spectrometer with coaxial electrodes for multi-detector operation," Nucl. Instrum. Methods, vol.107, pp. 549-556, 1973.

[2] Zh.T. Kambarova, A.O. Saulebekov, "Calculation and modeling of the motion of charged particles in the quadrupole-cylindrical field," Eurasian phys. tech. j., vol.15, no. 1 (29), pp.55-60, June 2018.

[3] A.O. Saulebekov, A.A Trubitsyn, Zh.T. Kambarova, D.A. Saulebekova, "Electrostatic energy analyzer of charged particles on the basis of quadrupole-cylindrical field in the «ring-axis» focus regime, Eurasian phys. tech. j., vol.15, no. 2 (30), pp.35-39, December 2018.

A NEW MODELS OF BARRIER DISCHERGE EXCILAMPS FOR LIQUID-PENETRANT INSPECTION*

V.A. PANARIN[1], *S.M. AVDEEV*[1], *E.A. SOSNIN*[1,2], *A.N. KALINICHENKO*[3], *D.S. PESHENITSYN*[1], *V.S. SKAKUN*[1], *V.F. TARASENKO*[1]

[1]*High Current Electronics Institute SB RAS, Tomsk, Russian Federation*
[2]*National Research Tomsk State University, Tomsk, Russian Federation*
[3]*National Research Tomsk Polytechnic University, Tomsk, Russian Federation*

Devices based on barrier discharge plasma, including barrier discharge excilamps, have been widely used in science and technology [1–5].

As we have shown in [6], excilamps on the XeCl* molecule can be used in the task of detecting surface defects using the luminescent liquid-penetrant inspection method (LLPI). In case of LLPI, surface defects are detected by brightly glowing indicator traces formed on the developing coating (developing agent) in the locations of discontinuities. This method differs from the color one that the inspection is performed under darkening conditions and requires ultraviolet irradiation, so it is more sensitive, since the visual luminescence of the display is detected better than the color contrast.

Experimentally [6], differences were found in the implementation of the method when using different irradiators (excilamps, mercury UV lamps and UV LEDs). It was shown, that the XeCl-excilamp has the same characteristics as other sources of UV radiation.

In this report, we present the results of testing two new barrier discharge excilamps for the liquid-penetrant inspection tasks.

The first excilamp (BD_EE model) is a bulb with a flat exit window (22 mm diameter). The lamp is connected to the power supply by a cable up to 1.5 m long. The lamp emits radiation with a maximum wavelength of 308 nm, a half-width band of 1.8 nm, and radiant exitance of up to 70 mW/cm^2. The excilamp design provides uniform exposure in the plane of the output window and a high service life of the gas medium. This excilamp is convenient for various sizes irradiating samples and for rapid exposure of various surfaces, which is necessary for LLPI.

The second excilamp (BD_P_A model) is similar to the one we used earlier and described in [5, 6], but it is made with an autonomous power source, which allows it to be used in the field conditions, for example, for operational analysis of pipeline surfaces and industrial metalware.

When exposure the controlled surface with the test excilamps, the luminescence of the indicator traces is clearly distinguishable, the contours are smooth and clear. It is revealed that one of the advantages of the excilamps in comparison with mercury UV lamps and UV LEDs is the convenience of photofixing due to the lack of background illumination. Thus, the proposed barrier discharge lamps are promising for use in luminescent control due to their combination of properties.

REFERENCES

[1] H. Esrom, U. Kogelschatz, “Modification of surfaces with new excimer UV Sources,” Thin Solid Films, vol. 218, pp. 231–246, 1992.

[2] M. I. Lomaev, V. S. Skakun, E. A. Sosnin, V. F. Tarasenko, D. V. Shitts, M. V. Erofeev, “Excilamps: efficient sources of spontaneous UV and VUV radiation,” Phys. Usp., vol. 46, pp. 193–209, 2003.

[3] U. Kogelschatz, “Dielectric barrier discharges: Their history, Discharge physics and industrial applications,” Plasma Chemistry and Plasma Processing, vol. 23, pp. 1–46, 2003.

[4] E. A. Sosnin, T. Oppenländer, V. F. Tarasenko, “Applications of Capacitive and Barrier Discharge Excilamps in Photoscience,” J. Photochem. Photobiol. C: Reviews, vol. 7, pp. 145–163, 2006.

[5] E. A. Sosnin, V. F. Tarasenko, “ Excimer lamp as a perspective photonic instrument,” Photonics, no. 1, pp. 60–69, 2015.

[6] A. Kalinichenko, E. Sosnin, S. Avdeev, N. Kalinichenko, I. Lobanova, “Fluorescent Penetrant Testing by Means of Excilamps,” Modern Problems in Materials Processing, Manufacturing, Testing and Quality Assurance, vol. 942, pp. 131–140, 2019.

* The work was supported by State Task for HCEI SB RAS, project #13.1.4.

MODELLING OF PHASE COMPOSITION OF ZR-FE LAYERED SYSTEM SUBJECTED TO THERMAL ANNEALING

A.K. ZHUBAEV, G.Zh. OMARPATSHA, A.Sh. AMANTAYEVA

Aktobe Regional State University, Aktobe, Kazakhstan

The phase diagram of the Fe–Zr binary system was taken as an object of study. The methods of processing and analysis of Mössbauer data implemented in the form of the MSTools software package [1] were applied in our work. Currently, the MSTools complex consists of ten programs designed to process and analyze both experimental Mössbauer spectra and their parameters. To achieve the goal of the work, we used a model decoding of Mössbauer spectra using a priori information about the object of study (SPECTR) and a comparison of the experimental spectra with the spectra of standard samples (PHASAN).

Using the SPECTR program, spectra of iron nuclei were created at various positions of the crystal lattice of phases present in the phase diagram of the Fe-Zr system. Then, taking into account the population of various positions, the Mössbauer spectra of Fe_3Zr and Fe_2Zr intermetallic compounds were simulated using the PHASAN program and reference spectra of various phases of the Fe-Zr binary system were obtained (Figure 1).

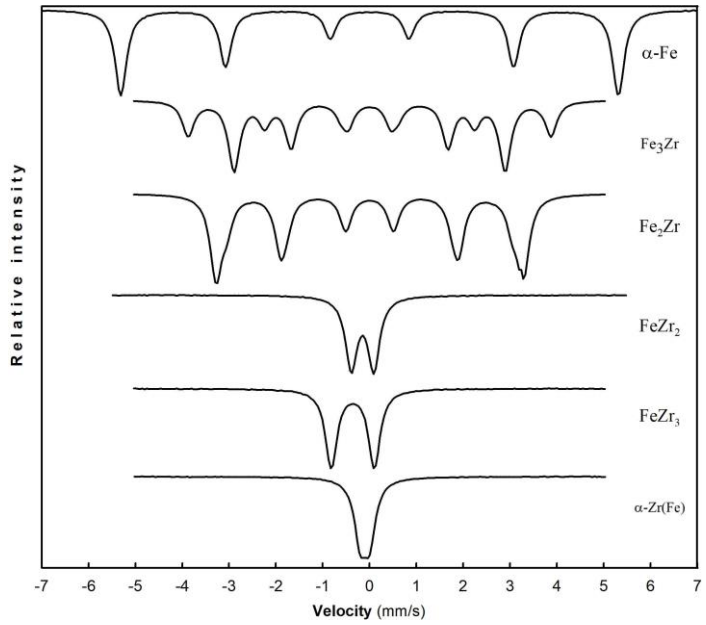

Fig.1. Model spectra of various phases in the system Fe-Zr

Using the phase diagram of the Fe-Zr binary system and the “lever rule”, the relative contributions of intermetallic compounds and α-Fe(Zr) were determined at the calculated zirconium concentration (5%at. and 10%at.). Applying the obtained standard spectra of intermetalides and a solid solution of Zirconium in Iron, the spectra of layered systems Fe-5%Zr and Fe-10%Zr were simulated using the PHASAN program. Comparison with the experimental Mössbauer spectra of the Zr(2μm)-Fe(10μm) layered system subjected to isochronous thermal annealing at various temperatures showed a good correlation.

REFERENCES

[1] V.S. Rusakov, Mossbauer Spectroscopy of Locally Nonhomogenous Systems, Almaty, INP NNC RK, 2000. (in Russian)

A MONTE CARLO STUDY OF NUCLEAR ENERGY LOSS IN SIO_2, LIF AND KAPTON AMORPHOUS TARGETS

J. EL ASRI[1], O. EL BOUNAGUI[2,], N. TAHIRI[3], H. ERRAMLI[4] AND A. CHETAINE[1]

[1] Nuclear reactor and nuclear security, Faculty of Sciences, Mohammed V University in Rabat, Morocco
[2] EPHE-SM, Faculty of Sciences, Mohammed V University in Rabat, Morocco
[3] LaMCScI, Faculty of Sciences, Mohammed V University in Rabat, Morocco
[4] Faculty of Sciences Semlalia, University Cadi Ayyad, Marrakech, Morocco

In this paper, we study the nuclear energy loss in amorphous targets (SiO_2, LiF and Kapton) for different incident charged particles at energy E > 0.1keV, by using Monte Carlo simulations. The nuclear stopping power and range are investigated. However, the nuclear stopping power and their maximum increases with increasing the atomic number of charged particles. The dependence of the mean projected ranges with energy is presented. The range of ions in amorphous targets is evaluated. To complete this study, all results are compared with existing codes data (SRIM, PSTAR and ASTAR).

Keywords: Nuclear energy loss; Amorphous targets; Monte Carlo simulations; Charged particles; Range of ions.

* Corresponding Auther : elbounagui@gmail.com

STUDY OF THE EFFECT OF SOIL TYPE ON RADON FLUX DENSITY*

K.O.STAVITSKAYA[1], N.K.RYZHAKOVA[1], F.I.LOZHNIKOV[2]

[1]Tomsk Polytechnic University, Tomsk, Russia
[2]Tomsk State University, Tomsk, Russia

Radiation and environmental studies of building sites, including an assessment of radon hazard, are carried out before the construction of buildings. In Russia, the radon hazard criterion is the radon flux density (RFD) measured on the earth's surface. A territory is considered radon hazard if 20% or more of the radon flux density measurements exceed a critical value of 80 $mBq \cdot m^{-2} \cdot s^{-1}$ [1]. Unfortunately, this approach does not allow to obtain reliable assessment of radon risks in building plots. It is known that the amount of radon emanating from the surface depends on the type of soil and its physical properties. Usually, loosening soil layers are located on the earth's surface. However, the main source of radon and its decay products is dense soils lying in the basement of buildings at depths of 1 m ... 5 m [2, 3]. The physical properties of such soils significantly differ from the soil properties located on the earth's surface. The scientific literature contains data of the radon flux density from the surface for only some types of loams, clays, and sands. The purpose of this research is to study exhalation of radon from the surface of soil various types, characteristic of building foundation.

Radon flux density was measured in the spring and summer periods of 2018 year at the experimental sites of Tomsk and Gorny Altai using the Alfarad Plus measuring complex. The radon flux density was measured on the terrace of the Tom River, in Tomsk. Types of loesslike loams, clays, shales, were investigated in Tomsk. Measurements of the radon flux density in Gorny Altai were carried out in the Maima river valley, in the Katun river valley, Gorno-Altaysk and Kyzyl-Ozek on sand and gravel deposits, rocky limestone, andesite-basalt porphyrite and quartzites.

The article shows that, depending on the type of soil, the values of the radon flux density vary in a rather wide range of 40 $mBq \cdot m^{-2} \cdot s^{-1}$ ... 810 $mBq \cdot m^{-2} \cdot s^{-1}$. The largest amount of radon emanates from the surface of magmatic rock, and the smallest - from the surface of shale and loam. The revealed dependence of the average RFD values on the type of soil can be used in the development of a new method for assessing the radon hazard of building territories.

REFERENCES

[1] Basic sanitary rules for ensuring radiation safety (OSPORB - 99), SP 2.6.1.799-99, Ministry of Health of the Russian Federation, 2000.

[2] N.K.Ryzhakova, K.O.Stavitskaya., A.A.Udalov "Issues in assessment of potential radon hazard at building sites", Radiatsionnaya Gygiena = Radiation Hygiene. vol.11, no.2, pp. 37-44, 2018 (In Russ.)

[3] N.K.Ryzhakova, K.O.Shilova, "A method for assessing the radon hazard of building sites", Pat. No. 2656131 of 05/31/2018 Bull. No. 16.

* Acknowledgments: The reported study was funded by RFBR, project number 19-35-90044.

INVESTIGATION OF THE INFLUENCE OF SET PARAMETERS ON THE ACCURACY WITH MODELING THE BAND STRUCTURE OF KBR AND KCL CRYSTALS

L. MYASNIKOVA, M. OSPANOV

Zhubanov Aktobe Regional State University, Aktobe, Kazakhstan

The paper presents the results of computer modeling of the band structure of KBr and KCl in various spatial groups, at a temperature of 0 K. To reduce the computational time, pseudopotentials were used, which took into account only the electrons involved in the binding. All computation in this paper were performed using spin polarization on magnetic ions with high spin ferromagnetic initialization. Modeling of the characteristics is implemented in the Burai 1.3 program, as well as a site that allows you to generate CIF files materialsproject.org. It was found that the use of pseudopotentials reduced the number of electrons, as well as reduced the required cutoff energy, which had a rescheduling value in the calculations based on plane waves.

Below are the simulation results of crystals using an example.

Compound	Band gap, eV		Experimental band gap, eV	Run Type
	P m_3m	F m_3m		
KBr	3.971	4.451	7.8	GGA
KCl	4.759	5.139	8.5	

Thus, in this paper, the results of computer simulation of the band structure for different input parameters of the cell are presented, which strongly affect the calculation results. These calculations are fundamental for further research. Despite a wide variety of quantum-chemical methods, not one at present, letting you quantitatively describe the electronic system, and the accuracy depends on the choice of a package that has its pros and cons. The results obtained are fundamental and can be useful in the study of nanocrystals.

REFERENCES

[1] L. Myasnikova, A. Istlyaup, D. Sergeyev, N. Zhanturina, K. Shunkeyev and A. Popov, “Computer simulations of the band structure and density of states of the linear chairs of NaCl ions,” Latvian Journal of Physics and Technical Sciences, vol. 4, 2019, P. 49-56.

[2] A. Jain, G. Hautier, C. Moore, S.P. Ong, C. Fischer, T. Mueller, K.A. Persson and G. Ceder, “High-Throughput Infrastructure for Density Functional Theory Calculations,” Computational Materials Science, vol. 50, 2011, P. 2295-2310.

[3] A. Jain, G. Hautier, S.P. Ong, C. Moore, C. Fischer, K.A. Persson and G. Ceder, “Formation Enthalpies by Mixing GGA and GGA + U calculations,” Physical Review B, vol. 50, 2011, P. 115-121.

[4] R. Godby, M. Schluter and L.J. Sham, “Self-energy operators and exchange-correlation potentials in semiconductors,” Physical Review B, vol. 37, 1988, P. 229-235.

[5] C. R. Gopikrishnan, D. Jose and A. Datta, “Electronic structure, lattice energies and Born exponents for alkali halides from first principles,” AIP Advances, vol. 2, Article Number 012131, 2012.

USING RADON MEASUREMENTS RESULTS AT TWO SMALL DEPTHS IN LOCAL RADON RISK ASSESSMENTS*

N.K.RYZHAKOVA[1],K.O.STAVITSKAYA[1],P.I.LOZHNIKOV[2]

[1]Tomsk Polytechnic University, Tomsk, Russia
[2]Tomsk State University, Tomsk, Russia

An important condition for protecting public health is radiation safety associated with natural sources of radiation. These sources primarily include the radioactive gas radon. Radon is emitted from soils lying in the building base and therefore poses a serious threat to the health of the population living on the lower floors. In this regard, in the design and construction of buildings, radon risks are assessed at building sites. In Europe the volumetric activity of radon (VA) in soil air is measured at depths of 0.8 m ... 1 m [1]. The measurement results at such depths are considered constant, depth-independent VA_∞ values established as a result of equilibrium between the processes of radon formation (radium decay) and its decrease (diffusion). However, the thickness of the loose soil layer, in which radon flows emerging to the surface are formed, reaches 2m ... 3m. In addition, measurements are carried out at points located at distances of several meters from each other. For relatively large areas of development, carrying out such measurements is time- consuming, and for loose soils, measurements give an underestimated result. Obtaining a reliable value of VA_∞ and reducing measurement costs can be achieved by using the diffusion model of radon transfer in homogeneous porous soils and the results of measuring VA at two depths that differ by a factor of 2 [2]:

$$VA_\infty = \frac{VA_1}{2 - (\frac{VA_2}{VA_1})}, \quad (1)$$

where VA_1, VA_2 are the volumetric activity of radon in soil air at depths h and 2·h, respectively.

The research demonstrates the measurement results of VA_1 (0.4 m) and VA_2 (0.8 m), carried out by means of RRA-03 measuring complex, in dense loams at a depth of 1.5m at the building base. The obtained VA results were used to calculate the VA_∞ values. The research shows that the VA_∞ values of homogeneous soils are described by the normal distribution and are agreement with the results of measuring VA in loams at depths of 8 m and 12 m.

REFERENCES

[1] J. Kemski , A. Siehl , R. Stegemann , M. Valdivia-Manchego , "Mapping the geogenic radon potential in Germany", The Science of the Total Environment ,vol. 272,pp.217-230, 2001.

[2] N.K., Ryzhakova, "Criteria of radon risk of territories and methods for their determination", Applied Radiation and Isotopes, vol. 91, pp. 161-164, 2014.

[3] N.K. Ryzhakova, "A new method for estimating the coefficients of diffusion and emanation of radon in the soil", Journal of Environmental Radioactivity, vol.135, pp.63-66, 2014.

* Acknowledgments: The reported study was funded by RFBR, project number 19-35-90044.

PORTABLE MEDICAL RADIOMETRIC SYSTEM

SEVASTIANOV M.S.[1], *KHOKHLOV K.O.*[1] , *PANKIN V.V.* [1] , *MIRONOV A.A.* [1].

[1] *Ural Federal University, Yekaterinburg, Russia*

The creation of new radiopharmaceuticals and the rapid development of radiodiagnostic equipment radically changed the position of radionuclide diagnostics (RND) in clinical medicine, and opened up wide opportunities for obtaining information about biochemical and physiological processes and morphological changes in human organs and systems. Today, leading manufacturers of medical equipment are releasing to the world market equipment used in radionuclide diagnostics, which is practically not produced in the CIS countries, so this is almost 100% imported products. Their significant dimensions and layout provide for use only as stationary diagnostic tools. They are characterized by significant starting cost, complexity and high cost of maintenance during the life cycle. All these features can be considered as constraining factors for the spread of high-tech and informative RND techniques. Taking into account the achievements of industry and new hardware solutions for recording ionizing radiation, the task of developing a portable medical radiometric system devoid of the shortcomings of imported diagnostic equipment becomes urgent [1,2,3].

As a result of the work, a structural block diagram and a circuit diagram of a detecting device, a block for counting and processing information were designed. The counting system is based on 16 independent counting channels and a serial peripheral interface. The microprocessor system consists of a microcontroller and an external memory chip to store the results of radioactivity intensity on time. The simulation of the circuit, tracing the printed circuit board in an integrated computer-aided design of electronic devices. The installation of radio elements on the designed boards with a performance check was completed. A series of experiments with a source of gamma rays.

REFERENCES

[1] Koksharov V.A., Kortov S.V., Bazhukov S.I. “Ural cluster of nuclear medicine”, Medicine target projects, No. 12, 2013.

[2] Pankin S.V., Sarychev M.N., “Portable radiometric system for radionuclide diagnostics”, ANRI, No. 2. p.40-47. 2018.

[3] Bazukov S.I., Kopelyan E.I., Sedunova I.N., “Conception of Nuclear Medicine Center in Ural Federal University”, Collection of reports of the X Issyk-Kul International Conference on Radiation Physics SCORPH-2013, .p. 174-179. 2013.

METHOD FOR STUDYING PHASE TRANSFORMATIONS ON THE SURFACE OF A TANTALUM FOIL IN THE PROCESS OF HEATING BY ELECTRIC CURRENT *

A.V. DOLMATOV, I.V. MILYUKOVA, P.YU. GULYAEV

Ugra State University, Khanty-Mansiysk, Russian Federation
adolmatov@bk.ru

The work is devoted to the creation of a non-contact method for assessing the spectral blackness of a material based on the spectral-brightness pyrometry approach [1]. The theoretical dependence of the spectral blackness of the material ε_s on the actual value ε is obtained:

$$\varepsilon_s = \varepsilon \cdot \exp\left[\lambda_0 \cdot \left(\frac{d(\ln\varepsilon)}{d\lambda}\right)_{\lambda_0}\right], \quad (1)$$

where λ_0 is the given wavelength. The formula showed that in the spectral region, where the degree of blackness of the material does not depend on the wavelength, the value of the estimate coincides with the actual value.

The developed method was implemented by the authors in a thermal imaging system with spatial and temporal resolution of 20 μm and 10 μs, respectively [2-4]. The ability of the method to detect phase transitions on the surface of thin films and measure the characteristic temperature is investigated. The paper presents the results of an experiment with samples of tantalum foil. They were heated by electric current in an argon medium in order to: cause diffusion of impurity atoms O, C, N onto the surface of the sample, promote the formation of solid solutions and chemical compounds there, and reveal the behavior of the spectral degree of blackness of tantalum-based systems during phase changes (Fig. 1).

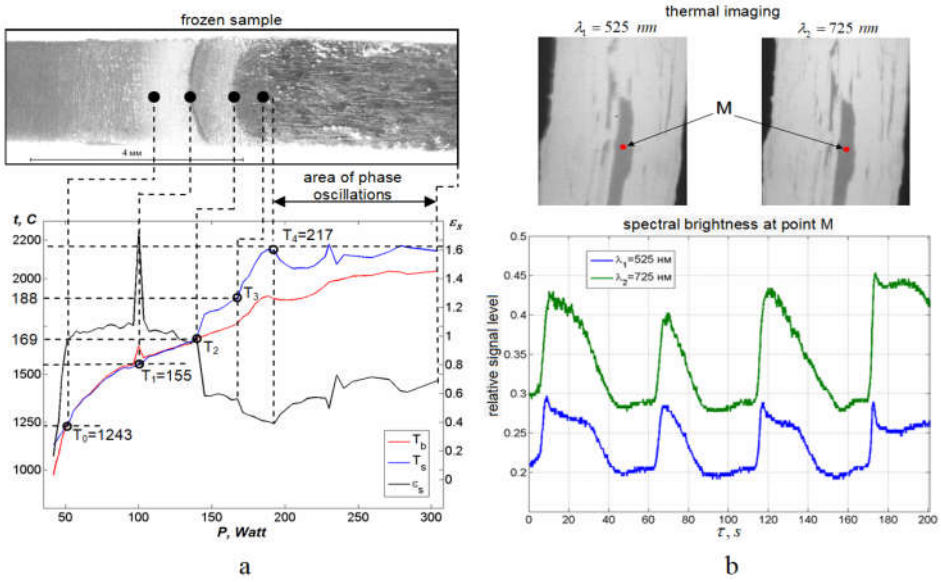

Fig. 1. The results of the study of tantalum samples: a - determination of the temperature of phase transitions; b - confirmation of the hypothesis of oscillations of the state of aggregation

The structural states on the foil surface were identified using microelement and X-ray phase analysis of frozen samples, and Ta-O and Ta-C phase diagrams were used to interpret the observed phenomena.

REFERENCES

[1] *Gulyaev I.P., Dolmatov A.V. // International Journal of Heat and Mass Transfer. – 2018. – V. 116. – P. 1016-1025.*
[2] *Dolmatov, A.V., Milyukova, I.V., Gulyaev, P.Y. // Journal of Physics: Conference Series. – 2019. – V. 1281. – 012010.*
[3] *Dolmatov, A.V., Gulyaev, P.Y. // Journal of Physics: Conference Series. – 2019. – V.1333. – 062006.*
[4] *Gulyaev I.P., Dolmatov A.V. // Journal of Physics: Conference Series. – 2018. – V.1115. – 032072.*

* This work was supported by RFBR (projects: 18-08-01475 и 18-08-01152).

MEASUREMENT OF TRACE ELEMENTS IN A CHEMICAL COMPOSITION OF ITER CONCRETE SAMPLES BY GAMMA SPECTROMETRY AFTER NEUTRON IRRADIATION

Y.A. POPOV, B.S. MEDETBEKOV, I.V. PROZOROVA, M.I. KUKUSHKIN, V.V. BAKLANOV

Institute of Atomic Energy NNC RK, Kurchatov, Kazakstan

The paper is devoted to determination of the concentration of trace elements in ITER concrete samples using neutron irradiation and gamma-spectrometry method [1-6].

The ITER nuclear buildings include Tokamak complex building which contributes to the nuclear safety of the ITER facility and hence is termed as safety related building. Correct assessment of concrete activation is one of the key points for accurate assessment of dose rate maps after shutdown and decommissioning of the reactor.

The assessment of detailed chemical composition of concrete is based on standard X-ray Diffractometry and Inductively Coupled Plasma (ICP-AES). These methods allow to measure basic elements and impurities. However, to measure some important trace elements required for neutronic analysis, standard methods are not enough for accurate measurements. This creates uncertainties in assessment of concrete activation.

The proposed method of chemical composition measurement of concrete is based on gamma ray spectrometry data analysis resulted after neutron irradiation of concrete samples. This method allows measuring chemical composition and some impurities or trace elements, with an emphasis on those isotopes, which can affect the dose formation after reactor shutdown, with higher accuracy comparing with standard methods.

Two reactor experiments for concrete samples irradiation were prepared and implemented.

Gamma-ray spectrometry of samples prepared from concrete cores “normal” and “heavy” after exposure for 1 day and from 5 to 10 days was carried out. Gamma-ray spectrometry of samples will be continued for exposure from 25 to 30 days. Processing of the results of gamma-ray spectrometry is carried out.

Gamma-spectrometry measurements of samples prepared from concrete kerns “normal” and “heavy” have been carried out after irradiation in the IVG.1M research reactor at thermal neutron fluence of $5.3 \cdot 10^{16}$ n/cm^2, with different aging of samples from one day to one month. Gamma-spectrometry results of determination have been processed. Concentration of main and traces elements have been calculated.

Results of element content determination of upper and bottom parts of block “normal” coincide with accuracy up to determination error.

Content of elements of upper and bottom part of block “heavy”, in a general, is the same, excepting differences in some elements as U, Zr, Fe in the whole block.

In the concrete of both marks – “normal” and “heavy”, content of elements was determined that can mainly contribute into radiation situation in premises during ITER operation and decommission.

REFERENCES

[1] The k0-Consistent IRI Gamma-ray Catalogue for INAA / Menno Blaauw. - Delft: Interfaculty Reactor Institute.

[2] F. De Corte, A.Simonits, k0-Measurements and related nuclear data compilation for (n, ?) reactor neutron activation analysis. J. Radioanal. Nucl. Chem., Vol. 133 (1989) P. 43.

[3] Frontasyeva M. Epithermal Neutron Activation Analysis at IBR-2 reactor of the Frank Laboratory of Neutron Physics at the Joint Institute for Nuclear Research (Dubna)// Physics of Atomic Nuclei, 2008, том 71, № 10, с. 1–11

[4] R. Jacimovic. Comparison of relative INAA and k 0-INAA using soil and sediment reference materials. J Radioanal. Nucl. Chem. - 2014. - Vol. 300. - p. 663-672

[5] C.L.Dunford and R.R.Kinsey, NuDat System for Access to Nuclear Data, IAEA-NDS-205 (BNL-NCS-65687), IAEA, Vienna, Austria, 1998. Information extracted from the NuDat data base, version of 06-Sep-2001, using the PC version of the program NuDat.

[6] Practical aspects of operating a neutron activation analysis laboratory. IAEA-TECDOC-564. 1990 г.

DEPOSITION OF OPTICALLY TRANSPARENT COPPER FILMS ON DIELECTRIC SUBSTRATES USING THE PLASMA FOCUS INSTALLATION *

B.N. KOLOKOLTSEV[1], B. YA. NIKULIN[2], G. G. BONDARENKO[3], I.V. BOROVITSKAYA[1], P. V. SILIN[2], B. F. DEGTYAREV[4]

[1]*A.A. Baikov Institute of Metallurgy and Materials Science of RAS, Moscow, Russia*
[2]*P.N. Lebedev Physical Institute of RAS, Moscow, Russia*
[3] *National Research University Higher School of Economics, Moscow 101000, Russia*
[4]*Moscow technical University of communications and Informatics, Moscow, Russia*

Plasma focus (PF) installations are sources of high-intensity pulsed plasma /1/. A feature of PF installation is the release of an intense jet of metal vapor ("metal" plasma) from the installation's anode at the moment of convergence of the current-plasma sheath /2, 3/. Using this phenomenon, thin optically transparent copper films on dielectric substrates (silicate glasses) were obtained on a PF installation with a Mather configuration of the anode (PF-4, FIAN) /4/. For the deposition of thin homogeneous films, a special device was made that allowed to exclude large drops of Cu. The films were deposited in the atmosphere of the working gas Ar at a pressure of ~1 Torr. Analysis of the size of the Cu droplet fraction on the surface of glass plates have been made in an optical microscope with a digital prefix – Leica DM ILM. This analysis showed that it had maximum dimensions distribution in the area < 0.3μm (Fig.1*a*). Cu films had a fairly high adhesion to the glass substrate, which was associated with the formation of a transition layer due to the penetration of Cu particles under the glass surface. The transmission spectra of films on glass substrates were measured on spectrophotometer SF-4 in the wavelength range of 0.3-1.0 μ at a temperature of 300 K (Fig.1*b*). The change in the transmission coefficient of Cu films in the middle and at the edge of the glass plates (1.0x35x35 mm) was ~ 10%. With use of a small number of plasma pulses (less than 10-15 pulses), Cu films were obtained as dielectric ones. With an increase in the number of plasma pulses (more than 30 pulses), the films became electrically conductive. When films of "metallic" plasma are deposited, liquid metal droplets are arranged on the surface of glass plates in a stochastic manner. Cu films were not continuous, so the transmission spectrum was mainly determined by the diffuse scattering of light quanta on metal particles of the order of wavelength.

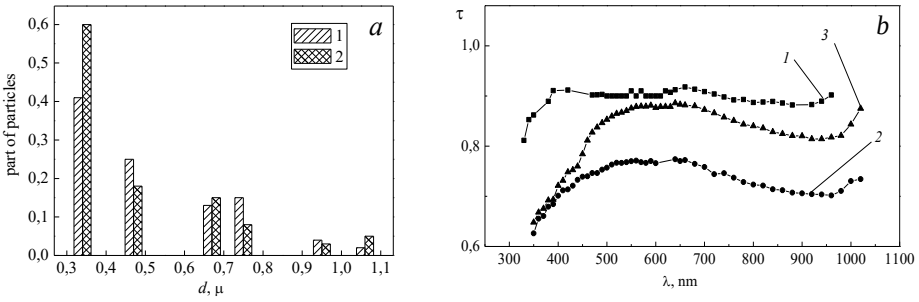

Fig.1. *a* - Histograms of Cu particles distributions in size: *1* - on the edge of the film; *2* - closer to the center; *b* - transmittance spectrum of Cu films on a glass substrate: *1* - the initial sample; *2* - point closer to the center; *3* - point closer to the edge film.

REFERENCES

[1] D.P. Petrov, N.V. Filippov, T.I. Filippova, V.A. Khrabrov, “Plasma Physics and Problems of Controlled Thermonuclear Reactions”. Ed. An USSR, 1958, vol. 4, p. 170-181.

[2] Y.T. Synapsin, “To the question of the mechanism of evaporation of the surface of the Central electrode in the plasma focus”. Proc. XXX Zvenigorod Int. Conference on Plasma Physics and CTR, February 24-28, 2003.

[3] S.N. Polukhin, A.E. Gurey, V. Ya. Nikulin et al., “Studing How Plasma Jets are Generated in a Plasma Focus”. Plasma Physics Reports, 2020, vol.46, №.2, pp. 127-137.

[4] V.D. Ivanov, V.A. Kochetov, M.P. Moiseeva et al., “Experimental Studies on Plasma Focus” Plasma Physics and Controlled Nuclear Fusion, IAEA, Vienna, 1981, p. 161-176.

* This work was supported by the Russian Science Foundation, project no. 16-12-10351.

APPLICATION OF ARTIFICIAL NEURAL NETWORKS FOR DETERMINING THE TEMPERATURE AND PARTIAL PRESSURES OF THE COMPONENTS OF HIGH-TEMPERATURE GASEOUS MEDIA*

D.E. KASHIRSKII

National Research Tomsk State University, Tomsk, Russia

The paper deals with the development of methods for solving the inverse problem of gaseous media optics [1, 2] by determining the parameters of high-temperature gaseous media from its spectral characteristics. It is proposed to use artificial neural networks (ANN) to determine the temperature and partial pressures of water vapor, carbon dioxide, carbon oxide and nitrogen oxide from its transmittances.

For solving the problem under consideration a feed-forward neural network was used [3]. The number of inputs forming the input layer of the ANN corresponded to the number of the used spectral centers. The desired parameters (temperature and partial pressure of gases) were obtained at output neurons of the ANN. Software implementation of the ANN was implemented in the Python language using the open neural network library Keras. The TensorFlow library was as a backend.

For training the ANN, the Adam optimization algorithm was used. The values of the transmittance were used as input data for training the ANN, and the values of the gas temperature and partial pressures at which they were calculated were output data.

Calculating the transmittances was carried out in wide ranges of temperature and partial pressures for the spectral centers that are informative for detecting the considered gases by formula

$$\tau_{\nu_0}(\rho, T) = \frac{1}{\Delta\nu}\int_{\Delta\nu} e^{-k_\nu(P,T)\rho l}\, d\nu ,$$

where $\Delta\nu$ – spectral resolution, k_ν – absorption spectral coefficient, ρ – partial pressure, P – total pressure, T – temperature, l – optical path length.

Absorption spectral coefficient k_ν was calculated by line-by-line method [4] using Voigt contour of the absorption spectral line. Absorption spectral line parameters of gases were taken from high-temperature database HITEMP2010 [5].

The analysis of the errors of the obtained models depending on the number of used spectral centers and the size of the training sample was carried out, which showed a tendency to decrease the magnitude of errors with the growth of these parameters.

REFERENCES

[1] Z. Bacsik, J. Mink, G. Keresztury, “FTIR Spectroscopy of the Atmosphere Part 2. Applications,” Applied Spectroscopy Reviews, vol. 40, pp. 327-390, 2005.

[2] M. Masiol, R.M. Harrison, “Aircraft engine exhaust emissions and other airport-related contributions to ambient air pollution : A review” Atmospheric Environment, vol. 95, pp. 409-455, 2014.

[3] S. Haykin, Neural networks and learning machines, New York: Prentice Hall, 2009.

[4] O.K. Voitsekhovskaya, D.E. Kashirskii, O.V. Egorov, O.V. Shefer, “Modeling absorption spectra for detection of the combustion products of jet engines by laser remote sensing,” Applied Optics, vol. 55, no. 14, pp. 3814-3823, 2016.

[5] L.S. Rothman, I.E. Gordon, R.J. Barber, H. Dothe, R.R. Gamache, A. Goldman, V.I. Perevalov, S.A. Tashkun, J. Tennyson, J., “HITEMP, the High-Temperature Molecular Spectroscopic Database,” Quant. Spectrosc. Radiat. Transfer., vol. 111, pp. 2139-2150, 2010.

* This research was supported by the Grant of the President of the Russian Federation (SP-3875.2018.5).

PICOSECOND DIODE PUMPED ND:YAG LASER FOR INITIATION LOCALIZED ENERGETIC PROCESSES IN NON-LABORATORY APPLICATIONS*

A.D.SAVVIN[1], *A.E.DORMIDONOV*[1], *V.PMITROKHIN*[1], *A.A.SIROTKIN*[2]

[1]*All-Russia Research Institute of Automatics (VNIIA), Moscow, Russia*
[2]*General Physics Institute RAS, Moscow, Russia*

A picosecond diode pumped Nd:YAG laser with active mode locking is presented for the problems of initiating and studying the dynamics of localized energy processes, such as explosive detonation, electric discharge, optical breakdown, evaporation of metal films with plasma formation. The laser master oscillator is made according to a simple linear two-mirror circuit 600-mm long (4.4 ns repetition period). The use of negative feedback [1] allows one to generate a single spectrally limited pulse closed in the cavity with high quality spatial distribution (close to Gaussian). The giant pulse after the opening of the Q-switch electro-optical shutter is a train of 7-10 (half-maximum envelope) picosecond pulses with a peak energy of about 1 mJ. The pulse duration from 150 to 600 ps is set by a simple change in power on the acousto-optical modulator. At the same time, at any repetition frequency from 0 to 10 Hz, the output time does not change, whose stability and predictability is better than 100 ps in the pump interval of about 200 μs. Connecting a short-circuited segment of a coaxial cable of appropriate length to the tee of the pulse extractor allows to select 1, 2 or 3 pulses from the train with a contrast of at least 100 [2]. Diode pumped amplification cascade less than 200 mm in length makes it possible to obtain energy of 100 mJ in a single-pass modular design, which is structurally a cylinder. The control unit contains drivers of pump diodes, temperature regulators, a high-voltage signal generator for pulse extraction, a reference temperature-stabilized crystal oscillator with a block of digital delays and fine phase adjustment and has a volume of about 5 liters. The laser design is adapted for carrying, rapid deployment and measurements in the temperature range from +10 up to +30 ˚C outside the optical laboratory. Laser radiation can be converted into the second and third harmonics and used to pump a parametric generator, for example, for the generation of infrared radiation at a wavelength of 2 μm or terahertz radiation [3].

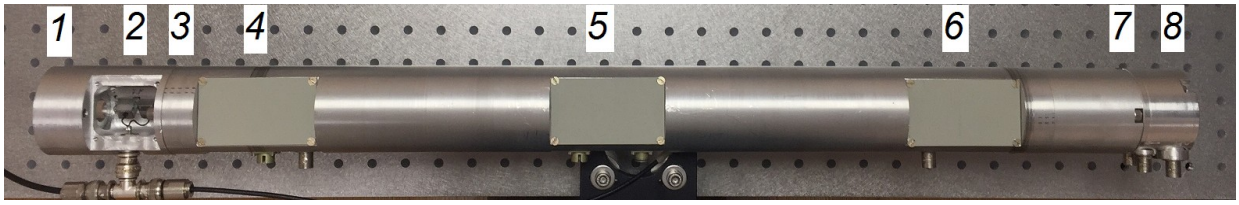

Fig.1. Picosecond laser: 1 — polarizer; 2 — electro-optical modulator EOM.KO1 («Crystal T») of pulse extractor; 3 —output mirror; 4 — acousto-optic modulator; 5 — diode pumped Nd:YAG active element; 6 — electro-optical Q-switch; 7 — HR mirror; 8 — feedback and Q-switch control unit

REFERENCES

[1] I.M. Bayanov, V.M. Gordienko, M.G. Zvereva, S.A. Magnitskiy, A.P. Tarasevitch, “Highly stable picosecond YAG:Nd^{3+} laser with a negative feedback”, Kvantovaya Elektronika, vol. 16, no 8, pp. 1545–1547, August 1989 [Sov J Quantum Electron, vol. 19, no. 8, pp. 994–996, August 1989].

[2] A.D. Savvin, V.P. Mitrokhin, A.E. Dormidonov, V.M. Stepanov, “Nanosecond kilovolt level pulse shaper based on parallel coupled MOSFETs and a transmission line transformer to control picosecond laser light”, Technologies of electromagnetic compatibility, vol. 71, no. 4, pp. 62-71, 2019.

[3] A.A. Sirotkin, S.V. Garnov, A.I. Zagumennyi, Yu.D. Zavartsev, S.A. Kutovoi, V.I. Vlasov, I.A. Shcherbakov, “Diode-pumped two-frequency lasers based on c-cut vanadate crystals”, Kvantovaya Elektronika, vol. 39, no 9, pp. 802–806, September 2009.

* The work was carried out in continuation of projects 05-02-17330-a and 07-02-12109-ofi supported by Russian Foundation for Basic Research

AUTOMATION OF MEASURING PARAMETERS OF SINGLE PHOTON DETECTORS AT A MODULAR RESEARCH QUANTUM KEY DISTRIBUTION SETUP[1]

D.E. Kashirskii, M.S. Mazhitova

National Research Tomsk State University, Tomsk, Russia

In various scientific and industrial fields, problems are solved in which it is necessary to register single photons. For this, single photon detectors (SPD) are used, which is based on various physical principles [1]. One of the rapidly developing areas that can ensure the safe transfer of information is quantum communication. In quantum key distribution setups, SPD based on avalanche photodiodes are mainly used [2-4]. To determine the optimal operating mode of the SPD, it is necessary to measure its parameters.

The paper considers the issue of developing software for automated measurement of SPD parameters based on avalanche photodiodes operating in the asynchronous photon detection mode on a modular research setup for quantum key distribution produced by QRate [5]. Setup is controlled from a personal computer using the NI PCIe 7841R board and software written in LabVIEW. This approach makes it possible to build various optoelectronic circuits and provides a relatively quick and easy development of software that implements the logic of their work.

The experiment for measuring the SPD parameters is as follows. A thermostabilized semiconductor laser operating in a pulsed mode with a pulse repetition rate in the range from 0.5 kHz to 15 kHz generates radiation with a wavelength of 1550 nm. The radiation attenuated by means of constant and variable attenuators falls on the detector. Within a given time, SPD responses are fixed, and statistics are accumulated over a time equal to the pulse repetition period. Using the obtained time distribution of SPD responses, the time and number of SPD responses at the moment of arrival of pulses, the time of occurrence, and the number of afterpulses are determined. The following SPD parameters are calculated: photon detection probability, afterpulses probability, and dead time.

The software can be divided into three parts. The first part is a user interface that provides a task for the laser pulse repetition rate, attenuation coefficients of constant and variable attenuators, the number of measurements, the duration of one measurement, confidence probability, the path to the file on the hard disk to save the measurement results. The second part is the firmware for the Virtex-5 LX30 FPGA located on the NI PCIe 7841R board and is responsible for controlling the operation of the laser and processing the signals received from the SPD. The third part is the statistical processing of the collected measurement data, which includes determining the average value of the measured quantity, the absolute and relative measurement errors.

Using the developed software, the dependences of the SPD parameters on the pulse repetition rate, the degree of attenuation of laser radiation, the duration of one measurement, and the value of the confidence interval are analyzed.

References

[1] M.D. Eisaman, J. Fan, A. Migdall, S.V. Polyakov, “Invited Review Article: Single-photon sources and detectors,” Review of Scientific Instruments, vol. 82, p. 071101, 2011.

[2] J. Zhang, M.A. Itzler, H. Zbinden, J.-W. Pan, “Advances in InGaAs/InP single-photon detector systems for quantum communication,” Light: Science & Applications, vol. 4, p. e286, 2015.

[3] X. Meng, S. Xie, X. Zhou, N. Calandri, M. Sanzaro, A. Tosi, C.H. Tan, J.S. Ng, “InGaAs/InAlAs single photon avalanchediode for 1550 nm photons,” Royal Society Open Science, vol. 3, p. 150584, 2016.

[4] D. Chitnis, S. Collins, “A SPAD-based photon detecting system for optical communications,” Journal of Lightwave Technology, vol. 32, no. 10, pp. 2028-2034, 2014.

[5] Rodimin V.E., Kiktenko E.O., Usova V.V., Ponomarev M.Y., Kazieva T.V., Miller A.V., Sokolov A.S., Kanapin A.A., Losev A.V., Trushechkin A.S., Anufriev M.N., Pozhar N.O., Kurochkin V.L., Kurochkin Y.V., Fedorov A.K., Modular quantum key distribution setup for research and development applications // Journal of Russian Laser Research., vol. 40, no 3, pp. 221-229, 2019 .

[1] This research was supported by Ministry of Science and Higher Education of the Russian Federation within the framework of the State Assignment № 0721-2020-0048, the Tomsk State University Competitiveness Improvement Programme and the project № 14-02-31132 of Russian Foundation for Basic Research.

ASPECTS OF THE USE OF MULTILAYER CARBON NANOTUBES IN THE CREATION OF COMPOSITES FOR PROTECTION AGAINST ELECTROMAGNETIC RADIATION[1]

A. V., SHCHEGOLKOV[1], A. V., SHCHEGOLKOV[1], F. F. KOMAROV[2], O. V. MILCHANIN[2], I. D. PARFIMOVICH[2], B.S. TRUFANOV[3], V.D. KHMYROV[3], V.B. KUDENKO[3], A. S., SEMENOV[4]

[1] *TSTU, Tambov, Russia*

[2] *Research Institution "Institute of Applied Physical Problems named after A.N. Sevchenko, Belarusian State University, Minsk, Belarus*

[3] *Michurinsky GAU, Michurinsk, Russia*

[4] *RUDN University, Miklukho-Maklaya Str. 6, Moscow, 17198, Russian Federation*

The creation of materials absorbing electromagnetic radiation is an urgent task [1-3]. The paper presents the results of studies of elastomers modified by multilayer carbon nanotubes (MWCNTs). An elastomer – polydimethylsiloxane was used as a polymer base; MWCNTs synthesized on Co – Mo / Al_2O_3 – MgO and Fe – Co / $2.1Al_2O_3$ catalysts were used as fillers.

In the course of research, a structural analysis of the sizes of MWCNTs particles was carried out, as a result of which it was found that MWCNTs synthesized on a Co-Mo / Al_2O_3-MgO catalyst have an outer diameter of about 25-35 nm and an inner diameter of 10-15 nm, and MWCNTs on Fe-Co / $2.1Al_2O_3$ have an outer diameter of 5-15 nm and an inner diameter of 5-7nm. Studies of the interaction of electromagnetic radiation (EMR) with manufactured samples based on MWCNTs synthesized on Co-Mo / Al_2O_3-MgO and Fe-Co / $2.1Al_2O_3$ catalysts showed that samples made with MWCNTs on an Fe-Co / $2.1Al_2O_3$ catalyst exhibit broadband attenuation (up to 20%) of incident radiation.

Figures 1a and b show the results of studies of the processes of interaction of electromagnetic radiation with composite materials based on polydimethylsiloxane (KCNT) with various additions of mass. % MWNT-2. Samples of composite materials with MWNT-2 demonstrate large reflectance values in comparison with the starting polymer (Fig. 1).

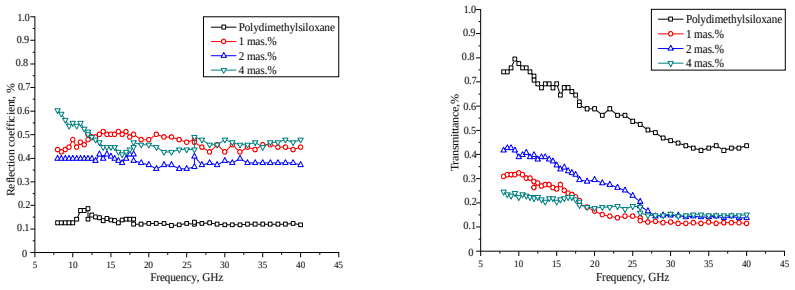

a) b)

Fig.1. The frequency dependence of the reflection coefficients of EMR from composite materials with MWCNTs -1 and MWCNTs -2: a – reflection coefficient of EMR , samples KCNT-2.1 ... 2.4, b – transmission coefficient of electromagnetic radiation, samples KCNT-2.1 ... 2.4..

The studied parameter varies from 40% to 50% for samples with additive concentrations of 1 and 2 wt. %. A sample with an additive concentration of 4 wt.% Shows a decrease in the reflection coefficient from 60% to 40% in the frequency range 8 - 18 GHz. In the range from 18 to 40 GHz, a constant value is observed for this sample near 45%.

REFERENCES

[1] Y. Huang, Y. Feng, T. Jiang. Optics Express. 15(18). 11133–11141 (2007)

[2] B.-Z. Yong, T.-J. Cui Progress In Electromagnetics Research B. 27.151–163 (2011)

[3] T.Liu, P.H. Zhou, J.L. Xie, L.J. Deng. J. Appl. Phys. 110. 033918. (2011)

1 The reported study was funded by RFBR within the framework of Research Project no. 18-53-00032 BEL−A.

4th International Conference on New Materials and High Technologies

Chairman	Alexey Markov,	Tomsk Scientific Center SB RAS, Tomsk, Russia
Co-Chairman	Yuri Maksimov,	Tomsk Scientific Center SB RAS, Tomsk, Russia
Program Chairman	Alexey Markov,	Tomsk Scientific Center SB RAS, Tomsk, Russia
Program Co-Chairman	Yuri Maksimov,	Tomsk Scientific Center SB RAS, Tomsk, Russia

Program Committee

Sergey ZELEPUGIN	Tomsk Scientific Center SB RAS, Tomsk, Russia
Alexander KIRDYASHKIN	Tomsk Scientific Center SB RAS, Tomsk, Russia
Yuri MAKSIMOV	Tomsk Scientific Center SB RAS, Tomsk, Russia

International Advisory Committee

Mikhail ALYMOV	Merzhanov Institute of Structural Macrokinetics and Materials Science RAS, Chernogolovka, Moscow Region, Russia
Alexander BARDENSHTEIN	Danish Technological Institute, Taastrup, Danish
Massimiliano BESTETTI	Politecnico di Milano, Milan, Italy
Fengchun JIANG	Harbin Engineering University, Harbin, P.R. China
Alexander KIRDYASHKIN	Tomsk Scientific Center SB RAS, Tomsk, Russia
Irina KURZINA	National Research Tomsk Polytechnic University, Tomsk, Russia
Nikolay LYAKHOV	Institute of Solid State Chemistry and Mechanochemistry SB RAS, Novosibirsk, Russia
Zulkhair MANSUROV	Institute of Combustion Problems, Almaty, Kazakhstan
Sergei MINAEV	Far Eastern Federal University, Vladivostok, Russia
Nahum TRAVITZKY	Friedrich-Alexander-Universität Erlangen-Nürnberg, Erlangen, Germany
Zbigniew WERNER	National Center for Nuclear Research, Otwock, Poland
Sergey ZELEPUGIN	Tomsk Scientific Center SB RAS, Tomsk, Russia

Conference topics

Non isothermal methods for materials synthesis
Combustion waves: theory and experiment
Functional materials and coatings
Carbon materials in electronics and photonics

Financial support by Russian Foundation for Basic Research (RFBR): № 20-03-22004

SYNTHESIS OF MAX-PHASE-BASED COMPOSITES IN THE Ti-Al-C SYSTEM AND STUDY OF THEIR STRUCTURE AND PROPERTIES[1]

AFANASYEV N.I., LEPAKOVA O.K., SHULPEKOV A.M.
Tomsk Scientific Center of the Siberian Branch of the Russian Academy of Sciences 10/4, Akademicheskii Pr., 634055, Tomsk, Russia

The most studied MAX phases in the Ti-Al-C system [1-2] are Ti_2AlC (211) and Ti_3AlC_2 (312) [1]. In the work [2], another phase was discovered, $Ti_5Al_2C_3$ (523), which belongs to the higher-order MAX - phases.

The goal of this work was to obtain $Ti_5Al_2C_3$-based samples by the SHS method and optimize the structure and properties of MAX-phase-based materials in the Ti-Al-C systems.

Analysis of X-ray diffraction patterns showed that the Ti_2AlC and Ti_3AlC_2 phases are formed during the SHS process. The $Ti_5Al_2C_3$ phase was not found in the synthesis products. To obtain high order phases, the SHS samples were additionally annealed.

Figure 1 shows the X-ray diffraction patterns of a stoichiometric SHS product (Ti: Al: C = 5: 2: 3) before annealing (a) and after annealing (b) at T = 1350 °C for 3 hours.

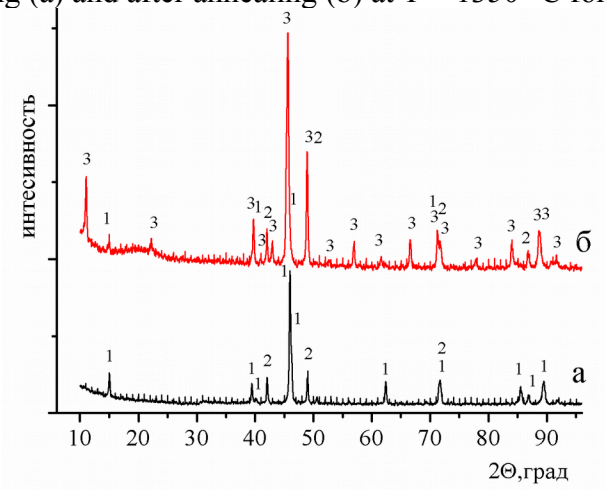

Figure 1 – X-ray diffraction patterns of SHS products for the composition Ti: Al: C = 5: 2: 3 before annealing (a); after annealing (b) at T = 1350 °C for 3 hours
1 – Ti_2AlC, 2-TiC, 3 – Ti_3AlC_2

The analysis of the X-ray diffraction patterns shows that the main phase in the product Ti_3AlC_2 after isothermal treatment is the MAX-phase; weaker reflections belonging to Ti_2AlC and TiC are also identified. At the same time, the energy dispersive analysis demonstrates that after annealing the product contains the grains whose composition corresponds to the $Ti_5Al_2C_3$ phase.

References:

1. Barsoum M.W. The $M_{N+1}AX_N$ phases: a new class of solids; thermodynamically stable nanolaminates // Prog.Solid State Chem. 2000. 28. 201-281.
2. Wilhelmsson O., Palmquist J.P., Lewin E., et al. Deposition and characterization of ternary thin films within the Ti-Al-C system by DC magnetron sputtering // J. Cryst. Growth. 2006. 291. 290-300.

[1] This work was supported by the Russian Foundation for Basic Research (project No. 19-03-00081)

MATHEMATICAL MODELING OF MECHANOCHEMICAL SYNTHESIS OF PRECURSOR PARTICLES*

O.V. LAPSHIN, A.I. RYABKOVA

Tomsk Scientific Center SB RAS, 10/4 Akademicheskii Pr., Tomsk, 634021, Russia, ovlap@mail.ru, +7 (3822)492294

Building the scientific foundation for the development of materials with specified physical and chemical properties for specific operating conditions is a fundamental problem of modern materials science. This problem lies in the development of model concepts about the ways of the formation of structural-phase material states that are responsible for a certain set of physical and chemical properties. One of the ways for solving the problem is the mechanochemical method of activation of solid-phase reactions, which has now found wide practical application [1, 2].

The mechanochemical synthesis of inorganic substances is usually conducted in a high-energy mill. Powders of various substances and elements are usually used as starting components. Mechanochemical synthesis results in not only a significant dispersion of reagents and an increase in their contact area, but also in the creation of a new highly defective structure characterized by an increased amount of excess energy in them. In addition to increasing the excess energy and the activity of the processed system, the passivation of the material can occur due to further processes (deactivation, relaxation, decrease in the activity, contamination by the substance milled from the walls of the mill and grinding bodies, etc.).

Intense mechanical treatment of a powder mixture is an effective way to obtain precursors (particles) including the initial components of the mixture and chemical transformation products, which can be used for the manufacture of nanocomposites and hardening coatings [3, 4].

A mathematical model is a very convenient tool to analyze the mechanochemical synthesis of precursors. To model mechanosynthesis, the model uses a macroscopic approach [5], which assumes an averaged description of the process in the entire mechanoreactor in which a mixture of reagents is subjected to intense mechanical stress.

A macroscopic mathematical model of the mechanochemical synthesis of precursors has been constructed in this work. The model comprises the equations of heat balance of the mechanoreactor, the dynamics of excess energy in condensed matter, grinding, changes in the interfacial reaction surface, and the kinetics of chemical conversions. The effect of physical and chemical parameters of the mixture components and the conditions of mechanical activation on the main characteristics of the synthesis is studied: temperature, chemical conversion depth, particle size of precursors, and their phase composition. Relations are obtained which determine the probability of agglomerating the components of the precursors. The main process control parameters are revealed. The synthesis of precursors is shown to be most effectively controlled by the following parameters, which are varied in a practical experiment: the amount of inert diluent, mill power, activation time, and ambient temperature. The dynamics of synthesis is numerically investigated.

References

1. *Rogachev A.S.* Problems and prospects for the development of mechanochemistry // Russ. Chem. Rev. 2019. V. 88. No. 9. P. 875 - 900.
2. *Boldyrev V.V.* Research in mechanochemistry of solid substances // Journal RFBR. 2004. No. 3 (37). P. 38 - 59.
3. Mechanocomposites are precursors for creating materials with new properties. Ed. by O.I. Lomovsky. Novosibirsk: SB RAS, 2010. 424 p.
4. *Khina B.B., Formanek B.* On the Physicochemical Mechanism of the Influence of Preliminary Mechanical Activation on Self-Propagating High-Temperature Synthesis// Solid State Phenomena. 2008. Vol. 138. pp. 159-164.
5. *Smolyakov V.K., Lapshin O.V.* Macroscopic kinetics of mechanochemical synthesis. Tomsk: IAO SB RAS, 2011.192 pp.

* This work was supported by RFBR (Project No. 19-03-00081-a).

PREPARATION OF CERAMIC NITRIDE-CARBIDE COMPOSITION AlN-SiC BY SHS METHOD USING HALIDE SALT AND SODIUM AZIDE*

A.P. AMOSOV[1], Yu.V. TITOVA[1], D.A. MAIDAN[1], K.S. SMETANIN[2]

[1]Samara State Technical University, Samara, Russia
[2] Vyksa Metallurgical Plant, Vyksa, Nizhegorogskii region, Russia

Micro-and nanopowders AlN and SiC are very promising for creating new composite materials AlN-SiC, giving them a set of unique properties, such as high strength, thermal stability, and chemical resistance [1]. There are several different methods for obtaining the AlN-SiC composition: mechanical mixing of commercially available SiC and AlN powders, thermal reduction of synthetic silicon dioxide and aluminum oxide, mixing Si_3N_4 and Al_4C powders to form a solid solution of $Si_3Al_4N_4C_3$, hot pressing of a mixture of SiC and AlN powders [2]. Much attention is drawn to the use of a simple energy-saving method of self-propagating high-temperature synthesis (SHS) in various ways of organizing the combustion process of a powder mixture: $Si_3N_4+4Al+3C=3SiC+4AlN$ under an electric field or on microwave heating, $Si_3N_4+8Al+3C$ in air, Al+Si+C in low-pressure nitrogen gas, 2.3 Al+SiC in high-pressure nitrogen gas [3]. Each of these options has its own advantages and disadvantages. In this paper, we investigate the use of another variant that is azide SHS, in which the nitriding reagent is not nitrogen gas, but sodium azide (NaN_3) powder, as well as halide salts [4]. The process of azide SHS provides great opportunities for regulating the dispersion and structure of synthesized ceramic powders, bringing them to the nanoscale level. A successful experience have been accumulated in using the azide SHS process to produce nanopowders of nitride compositions TiN-BN, AlN-BN, Si_3N_4-TiN [5].

The compositions of initial reagent mixtures for obtaining single-phase powders AlN and SiC using the SHS azide technology are known [4]. On this basis, the following chemical reaction equations are used for the synthesis of the AlN-SiC composition:

$$Si + 20Al + 6NaN_3 + (NH_4)_2SiF_6 + 2C = 2SiC + 20AlN + 6NaF + 4H_2, \quad (1)$$

$$4Si + 20Al + 6NaN_3 + (NH_4)_2SiF_6 + 5C = 5SiC + 20AlN + 6NaF + 4H_2, \quad (2)$$

$$6Si + 20Al + 6NaN_3 + (NH_4)_2SiF_6 + 7C = 7SiC + 20AlN + 6NaF + 4H_2, \quad (3)$$

$$8Si + 20Al + 6NaN_3 + (NH_4)_2SiF_6 + 9C = 9SiC + 20AlN + 6NaF + 4H_2, \quad (4)$$

$$10Si + 20Al + 6NaN_3 + (NH_4)_2SiF_6 + 11C = 11SiC + 20AlN + 6NaF + 4H_2, \quad (5)$$

The results of thermodynamic calculations of these reactions are presented, according to which, adiabatic temperatures are sufficient for the combustion regime, and the condensed reaction products are the target phases of AlN and SiC with an admixture of a water-soluble side salt NaF. The experimental study showed that in combustion of mixtures (1)-(5) it is possible to synthesize the target composition AlN-SiC in the form of equiaxed particles of size from 100 to 600 nm, but the condensed reaction products, along with AlN, SiC and an impurity of NaF, easily removed by water washing, also includes a water-insoluble impurity of cryolite Na_3AlF_6 in noticeable quantities from 7.7 to 15.5 wt.%. The washed product of azide SHS of this composition can be used for liquid-phase hybrid reinforcement of aluminum-matrix composites with ultrafine AlN and SiC powders, in which the impurity of cryolite plays a positive role of flux and is not included in the final composition of the composite, without contaminating it [6].

REFERENCES

[1] P. Gao, C. Jia, W. Cao, Wang C.,Liang D., Xu G.-I., "Dielectric properties of spark plasma sintered AlN/SiC composite ceramics", Int. J. Miner., Metallur., Mater., vol. 21, no. 6, pp. 589-594, 2014.

[2] W.-Ch.J. Wei, R.-R. Lee" Pressureless sintering of AIN-SiC composites", J. Mater. Sci., vol. 26, pp. 2930-2936, 1991.

[3] I.P. Borovinskaya, T.G. Akopdzhanyan, E.A. Chemagina, and N.V. Sachkova, "Solid solution $(AlN)_x(SiC)_{1-x}$ (x=0.7) by SHS under high pressure of nitrogen gas", Int. J. Self-Prop. High-Temp. Synth., vol. 27, no. 1, pp. 33-36, 2018.

[4] G.V. Bichurov, "Halides in SHS azide technology of nitrides obtaining", in "Nitride Ceramics: Combustion synthesis, properties, and applications", Eds. A.A. Gromov, L.N. Chukhlomina, Weinheim: Wiley-VCH Verlag GmbH & Co. KGaA, pp. 229-263, 2015.

[5] A.P. Amosov, G.V. Bichurov, L.A. Kondrat'eva, and I.A. Kerson, "Nitride nanopowders by azide SHS technology", Int. J. Self-Prop. High-Temp. Synth., vol. 26, no. 1, pp. 11-21, 2017.

[6] Y.V. Titova, A.V. Sholomova, A.A. Kuzina et al.,"Azide SHS of aluminum nitride nanopowder and its application for obtaining Al-Cu-AlN cast nanocomposite", IOP Conf. Series: Mater. Sci. Eng., vol. 156, Article Number 012037, 2016.

* The reported study was funded by RFBR, project number 20-08-00298.

PRODUCING TiC-Al CERMET BY COMBUSTION SYNTHESIS OF TiC POROUS SKELETON WITH SPONTANEOUS INFILTRATION BY ALUMINUM MELT*

A.P. AMOSOV, E.I. LATUKHIN, E.R. UMEROV, E.A. AMOSOV

Samara State Technical University, Samara, Russia

The ceramic-metal composite materials (cermets) possess unique properties, first of all, high hardness and heat resistance, and are of great interest for the application in metallurgy, mechanical engineering, aircraft and rocket science, nuclear energy [1, 2]. However, existing technologies for their production are energy-intensive and are implemented with the use of sophisticated expensive equipment, and the achieved level of properties is not always sufficient for the application of cermets. The use of a simple energy-efficient process of combustion synthesis or self-propagating high-temperature synthesis (SHS) for producing ceramic skeletons with increased strength followed by impregnation with molten metals can become the basis of a new technology for economically viable production of cermets and contribute to the creation of new materials for modern technics. The experience has been gained in obtaining the skeleton cermets with the simultaneous use of the SHS process for synthesizing a ceramic skeleton and melting a metal for infiltration (impregnation) of the synthesized skeleton [3, 4]. But at the same time, due to the heat of SHS reaction, a small amount of metal can be melted, which limits the size of the synthesized cermet. In addition, for complete impregnation and production of non-porous cermet, the application of excess pressure is required, which greatly complicates the process. In the present work, we study a new simple method for producing TiC-Al cermet based on the application of the SHS process of TiC porous skeleton followed by spontaneous infiltration with an aluminum melt prepared previously by heating from an external source, which makes it possible to use a melt mass sufficient to completely impregnate the ceramic skeleton without application of the excess pressure [5].

The results of theoretical estimates of both the temperature of the synthesized TiC porous skeleton necessary for spontaneous infiltration by an aluminum melt due to the phenomenon of thermosmosis, and the depth of spontaneous infiltration are presented.

In an experimental study, a stoichiometric mixture of powders of titanium Ti and graphite C was pressed into briquettes with a diameter of 23 mm and a height of 10-12 mm and burned using various melt infiltration schemes: in a sand backfill in contact with a molten aluminum with a temperature of 900 °C and vertical or horizontal directions of infiltration, also when the hot TiC skeleton is immersed in the molten bath, and when the hot skeleton is poured with aluminum melt. Full melt impregnation of vertically arranged briquettes with a height of 48 mm and horizontally arranged briquettes with a length of 130 mm was obtained via unidirectional mode of combustion and infiltration, and an infiltration depth of 60-70 mm of horizontal briquettes in the case of counter directional mode. The density, structure, phase composition, and mechanical properties of the obtained samples of TiC-Al cermet were studied.

REFERENCES

[1] Cermets, Ed. by J.R. Tinklepaugh and W.B. Crandall, New York: Reinhold Publ. Co, 1960.

[2] J. Binner, H. Chang, R. Higginson, “Processing of ceramic-metal interpenetrating composites”, J. Europ. Ceram. Soc., vol. 29, pp. 837-842, 2009.

[3] A.P. Amosov, A.F. Fedotov, E.I. Latukhin, V.A. Novikov, “TiC–Al Interpenetrating composites by SHS pressing”, Int. J. Self-Prop. High-Temp. Synth., vol. 24, no. 4, pp. 187-191, 2015.

[4] A.P. Amosov, E.I. Latukhin, A.M. Ryabov, E.R. Umerov, V.A. Novikov, “Application of SHS process for fabrication of copper-titanium silicon carbide composite (Cu-Ti_3SiC_2)”, IOP Conf. Series: J. of Physics, vol. 1115, Article Number 042003, 2018.

[5] A.P. Amosov, E.I. Latukhin, E.R. Umerov, “A method of producing ceramic-metal composite materials”, Appl. for invention No. 2019139339 of the Russian Federation, Priority dated 11.21.2019.

* The reported study was funded by RFBR, project number 20-08-00435.

COMPUTER SIMULATION OF RESIDUAL STRESSES IN MODERN CONCRETE MIXES *

A.O. TOVPINETS, V.N. LEITSIN, M.A. DMITRIEVA

Immanuel Kant Baltic Federal University, Kaliningrad, Russia

The active use in the construction of modern concrete mixtures requires a detailed study of concrete, as a complex material whose properties are directly related to its structure. One of the important features of the stress state of concrete during hardening is the occurrence of local residual stresses in them, which determine the deformation and strength characteristics of the material [1, 2, 3].

To study residual thermal stresses in multicomponent concrete mixtures, an approach to computer modeling of materials was developed taking into account the hierarchy of rheological processes in powder bodies and the modification of hierarchically organized structures [4]. The approach of physical mesomechanics is used in presented investigation. It combining the ideology and tools of solid state physics and micromechanics of media with structure [5]. A series of computational experiments was conducted to determine the residual thermal stresses in the matrix of concrete model samples.

As a result of computational experiments, it was shown that during hardening of a mixed compact of concrete due to anisotropy of the elastic moduli and linear expansion coefficients of its components, the residual stresses at the micro level can reach a significant value. This can lead to hardening or softening of the material of the finished structure in certain conditions. The control of the values and behavior of the residual stresses is possible by optimizing the concentration composition of the components of the initial concrete mixture.

REFERENCES

[1] Novel A.M. Properties of concrete (translated from English) M., Stroyizdat, 1972, p. 341.

[2] Mechanics of frakture. Vol. 5» Stress analysis of noth problems. Edited by G.C. Sih-Noordhoff Int. Piblishing ALPHEN AAN PENTRITN, the Netherlands, 1978.

[3] Thielen G., Hintzen W. Investigation of Concrete Behavior Under Restraint with a Temperature-stress Test Machine. Proceding of the International RILEM Symposium. Munich, 1994, no. 25, pp. 142—152.

[4] Vladimir N. Leytsin, Mariya A. Dmitrieva, Alexandr O. Tovpinets, Ivan V. Ivonin, and Sergey V. Ponomarev Determining Factors in the Formation of Low-Temperature Ceramics Structure // AIP Conference Proceedings 1783, 020132, 2016.

[5] Vladimir N. Leitsin, Maria A. Dmitrieva, Tatiana V. Kolmakova Governing Factors of Physical and Chemical Behavior of Reactive Powder Materials // Powder Metallurgy Research Trends / Editors Lotte J. Smit and Julia H.Van Dijk. Nova Science Publishers, Inc. NY, 2008.

* The work was supported by the Russian Foundation for Basic Research under grant No. 19-48-390001.

MECHANICAL PROPERTIES OF WELD JOINTS OF HIGH-STRENGTH STEEL UNDER DYNAMIC LOADING*

V.V. SKRIPNYAK, A.A. KOZULIN, A.V. BEVZ, E.G. SKRIPNYAK, V.A. SKRIPNYAK

National Research Tomsk State University, Tomsk, Russia

The article presents a computational model for predicting the mechanical behavior of welded joints of metal alloys under dynamic loads, taking into account the change in the properties of the steel in the welding zone.

Advanced high-strength steels (AHSS) are second-generation steels that are characterized not only by high strength, but also by very high ductility. This class of steels used in line pipes or sheet form for automotive structures. The microstructures of AHSS were initially multiphase, with ferrite as the dominant phase. The grades of AHSS developed more recently are fully martensitic or austenitic.

The structural integrity assessment of welded structures or components was estimated using by the experimental data on existing residual stress field and macrostructure of welded zone within the steel. The computational model uses the theoretical basis of continuum damage mechanics [1].

The deformation of the samples, the nucleation and growth of cracks under tension, with a strain rate varying from 0.1 to 1000 s^{-1}, were simulated.

The material structure in the weld zone is specified taking into account data on the phase and grain structure [2-4]. The model takes into account the difference in grain size between the grains in the weld area and the base metal.

The computer simulations were performed with the use of LS DYNA (ANSYS WB 15.2, ANSYS, Inc., Canonsburg, PA, USA) software. The calculations were carried out using the finite-difference scheme of second order accuracy.

The strains to fracture of the weld zones of AHSS steel showed significantly larger scatter range than those of ferritic steel.

The fracture of welded joins at high strain rates depends on relationships between critical plastic strains and stress triaxiality for the individual weld zones. It was shown that the mechanical fields in the inner layers of welded joints significantly differ from those observed on the surface of volume specimen.

The strength of the welded joints strong depends on the level of residual stress and plastic strain localization in the inner layers of the joints.

Areas were determined in which the localized plastic strains in welded joints took place, and which indicated the places of crack formation.

The results of numerical modeling confirm that the model proposed in the work allows predicting the strength and mechanical behavior of welded joints of steel structures in a wide range of deformation rates taking into account data on residual stress, phase and grain structure in a weld region.

REFERENCES

[1] N.V.Skripnyak, E.G. Skripnyak, V.A. Skripnyak, V.V. Skripnyak, I.K. Vaganova, "Failure mechanisms of light alloys with a bimodal grain size distribution". In Proceedings of the 11th World Congress on Computational Mechanics, WCCM 2014, 5th European Conference on Computational Mechanics, ECCM 2014 and 6th European Conference on Computational Fluid Dynamics, 20–25 July 2014, Barcelona, Spain.

[2] A. Sudheer, S. Jos, "Analysis of seam weld strength and micro structural properties of welded dual phase steel tubes". IJEAT, vol. 6, pp. 172-176, 2017.

[3] V.A. Skripnyak, N.V. Skripnyak, E.G. Skripnyak, V.V. Skripnyak, "Influence of grain size distribution on the mechanical behavior of light alloys in wide range of strain rates". AIP Conf. Proc. vol. 1793, Article 110001, 2017.

[4] I. Dzioba, T. Pala, "Influence of LWE on Strength of Welded Joints of HSS S960—Experimental and Numerical Analysis". Materials, vol.13, Article 747, 2020.

* The work was supported by the Russian Science Foundation under grant No. 16-19-10264.

PENTAMODE METAMATERIALS UNDER DYNAMIC LOADING *

V.A. SKRIPNYAK, M.O. CHIRKOV, E.G. SKRIPNYAK, V.V. SKRIPNYAK

National Research Tomsk State University, Tomsk, Russia

Metamaterials currently are of interest for a wide variety of applications including damping systems. This work aimed to evaluate dissipative effect of pentamode metamaterials subjected to dynamic loading. The results of numerical modelling of the mechanical behavior of pentamode metamaterials from alpha titanium alloys were received and compared with available experimental data. The model of inelastic deformation and ductile damage criterion were used to describe the ductility of the framework of metamaterials in a wide range of strain rates, temperature and stress triaxiality [1, 2]. A method is presented for predicting energy dissipation during inelastic deformation of metamaterials at high strain rates. The numerical simulation of the mechanical response of a pentamode metamaterial from the Ti-5Al-2.5Sn titanium alloy was carried out during dynamic compression at 100 m/s.

The evolution of the framework structure is the cause of different values of the dissipated work and coefficient of energy dissipation. Fig. 1 shows calculated values of the specific mechanical energy W over time (curves 1 and 3) and the specific internal energy W_{int} (curves 2 and 4) over time.

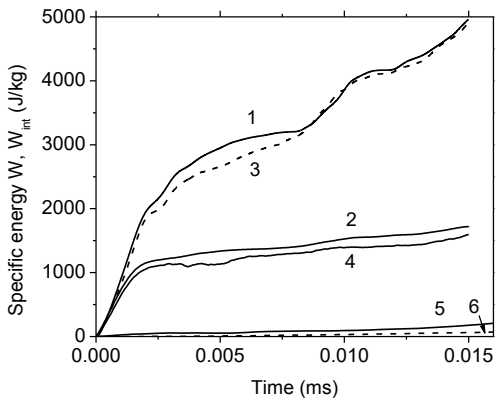

Fig.1. Specific internal energy of deformed framework elements under compression at the velocity of 100 m/s. Curves 1, 2 correspond to W (t), and curves 3,4 correspond to W_{int} (t)), respectively.

Curves 5 and 6 indicate the change in W and W_{int} during high-speed deformation of the bulk titanium alloy Ti-5Al-2.5 Sn at a strain rate of 100 s^{-1}. Calculated normalized Young modulus $\langle E \rangle / E_s$ and value of the normalized effective yield stress σ_y/σ_{ys} agree with experimental data obtained by Hedayati and coworkers [3]. A methodology to analyze the energy dissipation due to inelastic deformation of structured materials at high strain rates was presented for metamaterials. The values of the energy dissipation coefficient were determined for uniaxial compression of the pentamode metamaterial with the relative mass density of 3.145% at strain rates of ~20.8 10^3 s^{-1} and initial temperatures of 300 K and 900 K. The values of the energy dissipation coefficient during uniaxial dynamic compression of the pentamode metamaterial are 1.5 times higher than for the bulk alloy counterpart. The energy dissipation coefficient under uniaxial compression decreases by a factor of 1.5 - 2 with an increase in the initial temperature from 300 K to 900 K.

It was shown that the values of the energy dissipation coefficient during uniaxial dynamic compression of the pentamode metamaterial are 1.5 times higher than for the bulk alloy counterpart.

REFERENCES

[1] V.V. Skripnyak, A.A. Kozulyn, V.A. Skripnyak, "The influence of stress triaxiality on ductility of α titanium alloy in a wide range of strain rates", Mater. Phys. Mech. Vol. 42, 415-422, 2019.

[2] V.V. Skripnyak, V.A. Skripnyak, E.G. Skripnyak, "Ductility of titanium alloys in a wide range of strain rates". Paper presented at 6th International Conference Integrity-Reliability-Failure Lisbon/Portugal 22-26 July 2018. Editors J.F. Silva Gomes and S.A. Meguid Publ. INEGI/FEUP (2018); Paper REF: 7127 (2018)

[3] R. Hedayati, A. M. Leeflang, and A. A. Zadpoor, "Additively manufactured metallic pentamode meta-materials," Appl. Phys. Lett. Vol.110, Article Number 091905, 2017.

* The work was supported by the Russian Science Foundation under grant No. 16-19-10264.

MODEL OF THE STRENGTH PROCESSES OF MECHANICALLY ACTIVATED CONCRETE MIXTURES *

M.A. DMITRIEVA, V.N. LEITSIN, A.V. SHARANOVA

Immanuel Kant Baltic Federal University, Kaliningrad, Russia

The approach of determining the macrokinetics parameters for the concrete setting through the kinetic characteristics of curing at different temperatures is discussed. Mechanical activation provides an increase in the strength of concrete in the initial time of hardening, reducing the setting time and a more complete use of cement binding properties [1–3]. The activation nature of the concrete hydration processes has been experimentally confirmed and the macrokinetics parameters required for computer simulation of concrete setting taking into account the mechanical activation of initial components has been determined. Computer simulation of concrete early stages hardening processes allows to obtain a prediction of the structure and properties of concrete.

In model the thermomechanical state and phase composition of the hardening concrete are considered simultaneously at macro and microscopic levels. The formation of the structure of composite materials is based on cement is associated with the formation of synthetic calcium hydrosilicates. The structure of the initial compact reflects the heterogeneity of the initial powder mixture and pores in separate layers and interlayer interfaces, the polyfractionality of the components and their conglomerates. At each modeling step in each microlayer, the effective characteristics of the material are used. These characteristics are determined by the macroscopic structure of the initial representative volume of concrete mixture, by the distribution of the initial components and pores in it, by the heterogeneity of the concentrations of the phase and fractional composition of the components [4].

An approach is proposed for estimating the macrokinetic parameters of the cement hydration process based on the results of mechanical tests of determining the kinetics of the curing of concrete samples at different temperatures. The results allow us to use a model of coupled processes in reacting media [4] for computer simulation of the setting of a concrete mixture.

REFERENCES

[1] A.V. Andreeva, O.N. Burenina, and M. E. Savvinova, Mater. Sci. Forum 945, 3–8, 2018.

[2] L.M. Sulimenko and Yu. R. Krivoborodov, Russ. J. Appl. Chem. 73(5), 757–759, 2000.

[3] K. Sobolev, Z. Lin, Y. Cao, H. Sun, I. Flores-Vivian, T. Rushing, T. Cummins, and W. J. Weiss, Cement Concret. Compos. 71, 53–62, 2016.

[4] V.N. Leitsin, M.A. Dmitrieva, and T.V. Kolmakova, “Governing Factors of Physical and Chemical Behavior of Reactive Powder Materials”, in Powder Metallurgy Research Trends, edited by L. J. Smit and J. H. VanDijk, Nova Science Publishers, Inc. NY, 2008.

* The work was supported by the Russian Foundation for Basic Research under grant No. 19-48-390001.

COMPARISON OF FINITE ELEMENTS AND MESHLESS METHODS FOR MODELING OF SOLID PHASE CHEMICAL REACIONS UNDER EXPLOSIVE LOADING*

R.O. CHEREPANOV[1], *S.A.ZELEPUGIN*[1], *O.V. IVANOVA*[1]

[1] *Tomsk Scientific Center of Siberian Branch of RAS, 10/4 Akademicheskiy av., 634055, Tomsk, Russia*

Perspectivity of solid-phase reactions under explosive loading [1] consists in that such mode of course of reaction allows to provide non-equilibrium modes of reaction at high pressures and temperatures. This makes it possible to obtain materials with unique properties and structure. However, the extreme conditions of such reactions and the short time of the process require careful mathematical simulation of the corresponding processes in order to control and predict the reaction results.

To solve a wide range of problems in the mechanics of continuous media, the finite element method has been the main numerical method for a long time [2,3]. However, meshfree methods, in particular the smoothed particle hydrodynamics [4-7], have been gaining popularity in recent years.

This paper compares the results of modeling a solid-phase chemical reaction in detonation mode obtained by the finite element method [1] with different variants of the smooth particle method.

At modelling of shock-wave loading the deformation of a design grid leading to instability of the solution is a disadvantage of the finite element method. In this case a computationally complex reconstruction of the design grid is required.

The advantage of the meshfree methods is that they do not use computational meshes. Their disadvantages include lower approximation accuracy.

The results obtained by SPH, CSPM, xSPH and variational SPH are considered.

The phenomenological model of a zero order chemical reaction is used [8], the mechanical properties of the reaction mixture and reaction products are described in the framework of the theory of multi-component mixtures [9]. The results of calculations by netless methods are compared with the results of modeling by finite element method and with some experimental data.

REFERENCES

[1] O. Ivanova, S. Zelepugin, A. Yunoshev, V. Silvestrov. "A Multicomponent Medium Model for Reacting Porous Mixtures under Shock Wave Loading" , J. of En. Mat., 28 (1), pp. 303-317, 2010.

[2] Timon Rabczuk, Jeong-Hoon Song, Xiaoying Zhuang, Cosmin Anitescu, "Chapter Three: Extended finite element method", Extended Finite Element and Meshfree Methods, Academic Press, pp. 29-151, 2020.

[3] Dimitrios G. Pavlou, Essentials of the Finite Element Method, Academic Press, 2015

[4] A. Lucy. "A numerical approach to the testing of fusion hypothesis". Astronomical Journal, 82, pp.1013 -1024, 1977

[5] M.B. Liu, G.R. Liu "Restoring particle consistency in smoothed particle hydrodynamics", Applied Numerical Mathematics, 56(1), pp. 19-36, January 2006.

[6] Shaofan Li, Wing Kam Liu, Meshfree Particle Methods, Springer Science & Business Media, 2007, 502pp.

[7] Jing Tang Xing, "Chapter 12 - Mixed finite element—smoothed particle methods for nonlinear fluid–solid interactions" Fluid-Solid Interaction Dynamics, pp. 487-575, Academic Press, 2019

[8] S.A. Zelepugin, A.Yu. Dolgoborodov, O.V. Ivanova, A.S. Zelepugin. Shock Wave Synthesis inSolid Mixtures: Monograph. Tomsk: Institute of Atmospheric Optics SB RAS, 2012, p. 230

[9] R.I. Nigmatulin. Dynamics of multiphase media. 1. New York: Hemisphere. 507 p. 1991

* The work was supported by the Russian Foundation for Basic Research (Project No. № 19-08-01152 a).

NUMERICAL MODELING OF EROSION OF SURFACE OF 3D-PRINTED METAL PARTS UNDER MICROMETEROIDS IMPACT*

R.O. CHEREPANOV[1], *S.A.ZELEPUGIN*[1]

[1] *Tomsk Scientific Center of Siberian Branch of RAS, 10/4 Akademicheskiy av., 634055, Tomsk, Russia*

Prediction of erosion rates is important for spacecraft life cycle planning and mission planning. The main mechanism causing erosion of the surfaces of space technology is exposure to micrometeorites. Due to the development of additive manufacturing of space technology elements in general, and 3D printing of metal parts in particular, it is necessary to develop models of material behavior under the influence of such meteoroids, taking into account the peculiarities of additive manufacturing. Characteristic features [1] of the thermal cycle of metal additive manufacturing are: (1) fast heating due to high energy density of beam source; (2) fast crystallization with high cooling rate due to the small volume of the melt pool; and (3) melt-back, including simultaneous melting of the top layer of powder and remelting of the underlying previously crystallized layers. Residual stress caused by the unique thermal cycle in AM of metal parts, and high residual stress gradients cause deformation of the parts, which dramatically impairs the functionality and properties of the final parts [2,3].

In this paper a numerical model of impact loading of material produced by the method of electron-beam fusion of powders is proposed. The model is based on the smoothed particle hydrodinamics method [4,5]. Special attention is paid to heterogeneity of distribution of mechanical properties of the material at the microlevel. It is known that the selective fusion of metallic powders produces an inhomogeneous residual stresses. At the same time multiple areas with increased microhardness (quenched areas) are formed. Two models of spatial distribution of such areas are considered in this paper: a probabilistic approach [6] and a pattern according to scanning strategy. The probabilistic model uses probabilistic law proposed in [6] and Perlin noise [7]. The influence of track width, degree of hardness variation and parameters of probabilistic distributions on mass histograms of fragments after impact and parameters of resulting craters is considered. Comparison results with impact experiments at speeds up to 3 km/s are given.

REFERENCES

[1] C. Li, Z.Y. Liu, X.Y. Fang, Y.B. Guo, "Residual Stress in Metal Additive Manufacturing", Procedia CIRP, 71, pp. 348-353, 2018.

[2] E. Uhlmann, R. Kersting, T. B. Klein, M. F. Cruz, A. V. Borille, "Additive manufacturing of titanium alloy for aircraft components". Procedia CIRP, 35, pp. 55–60, 2015

[3] L.E. Murr, E.V. Esquivel, S.A. Quinones, S.M. Gaytan, M.I. Lopez, F. Medina, D.H. Hernandez, E. Martinez, J.L. Martinez, S.W. Stafford, D.K. Brown, T. Hoppe, W. Meyers, U. Lindhe, R.B. Wicker, "Microstructures and mechanical properties of electron beam-rapid manufactured Ti–6Al–4V biomedical prototypes compared to wrought Ti–6Al–4V", Mater. Charact., 60, pp. 96–105, 2009

[4] A. Khayyer, H. Gotoh, H. Falahaty, Y. Shimizu, "An enhanced isph–sph coupled method for simulation of incompressible fluid–elastic structure interactions", Comput. Phys. Commun., 232, pp. 139-164, 2018

[5] R.A. Gigold, J.J. Monaghan "Smoothed particle hyrodynamics: theory and application to non spherical star", Mon. Not. R. Astron. Soc., 181 (3), pp. 375-389, 1977

[6] A. V. Gerasimov, S. V. Pashkov, "Numerical simulation of high-velocity projectile interactions with groups of spaced rods and plates", Procedia Engineering, 204, pp. 284-291, 2017

[7] Cheng WC., Lin WC., Huang YJ. Controllable and Real-Time Reproducible Perlin Noise. In: Christie M., Li TY. (eds) Smart Graphics. SG 2014. Lecture Notes in Computer Science, vol 8698. Springer, Cham

* The work was supported by the Russian Foundation for Basic Research (Project No. № 19-08-01152 a).

CdTe nanosheets colloidal synthesis

A.S.AKHMETOVA, A.ZH. KAINARBAY, T.N.NURAKHMETOV

L.N. Gumilyov Eurasian National University, Nur-Sultan, Kazakhstan,
aizhan.s.akhmetova@yandex,kz, +77058642678

Two-dimensional (2D) semiconductors exhibit unique electronic and optical properties arising from the atomic-scale thickness and two-dimensional electronic structure.

CdTe, with its low band gap (Eg = 1.44 eV), is a very interesting material for photovoltaic and photodetection applications.

In addition to the widely used spherical quantum dots and nanocrystals in the form of tetrapods, several recent studies have synthesized semiconductor colloidal quasi-two-dimensional nanostructures-CdTe nanosheets with a transverse size of several atomic layers and a characteristic longitudinal size of 30-200 nm [1].

In this paper we report a detailed study of the synthesis of colloidal CdTe nanosheets.

CdTe nanosheets were obtained using a method similar to that described in [1, 2].

We show that CdTe nanosheets can be extended laterally to obtain nanosheets with lateral dimensions in the micrometer range. We present the study of the reaction conditions for the formation of CdTe nanosheets and for their lateral extension. The reaction products are analyzed with optical and photoluminescent spectroscopy, thermal activation spectroscopy (in the temperature range 260 to 300°C).

Thus, in this paper, quasi-two-dimensional nanostructures that are single-component CdTe nanosheets are synthesized and studied.

Based on the results of studies of luminescence of CdTe nanosheets, it is planned to produce a prototype of the solar cell.

REFERENCES

[1] *Pedetti, S.; Nadal, B.; Lhuillier, E.; Mahler, B.; Bouet, C.; Abecassis, B.; Xu, X.; Dubertret, B. – Optimized Synthesis of CdTe Nanoplatelets and Photoresponse of CdTe Nanoplatelets Films //* Chem. Mater. 2013, 25, 2455−2462.

[2] *Roman B. Vasiliev, Elizabeth P. Lazareva, Daria A. Karlova, Alexey V. Garshev, Yuanzhao Yao, Takashi Kuroda, Alexander M. Gaskov, and Kazuaki Sakoda. – Spontaneous Folding of CdTe Nanosheets Induced by Ligand Exchange //* Chem. Mater.. – 2018. – 30. – 1710-1717.

USING THE WAVELET TRANSFORM FOR MECHANICAL ACTIVATION AND THERMAL EXPLOSION OF A TI – NI MIXTURE

O.A. SHKODA

Tomsk Scientific Center SB RAS, Tomsk, Russia

Experimental results of mechanical activation (MA) of a powder mixture of titanium and nickel, and subsequent self-propagating high -temperature synthesis (SHS) in the mode of thermal explosion with the formation of synthesized products are considered in the paper.

Analyses of graphs of various dependencies, diagrams constructed from experimental data at MA and when studying various temperature characteristics of a thermal explosion are carried out. The self-consistent system under study is suitable for microfractal calculations [1, 2], since it meets the conditions: the system has a limit value of the MA time at which this system exists and remains holistic. All existing processes in the system are subject to two main processes of opposite nature, relaxation and tension processes. They always work together, simultaneously, helping the system achieve its goal. For fig.1 shows the frequency diagram of the fraction size after grinding in a planetary mill.

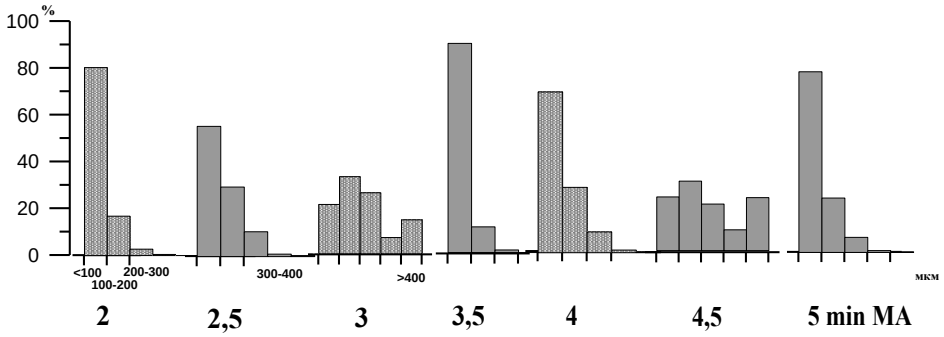

Fig.1 Histogram of the distribution by size of fractions at different MA times .

It shows experimental data from 2 to 5 min. MA. Periodic bursts of the brittle fraction and changes in the values of other fractions are visible. A value of 5 min. MA is not the limit value. The maximum value is 7 min. which was found from data cloud analysis and graphical phase portraits [3, 4]. The histogram is clearly divided into self- similar zones. It was found that the role of resonant effects (bursts) is played by the amount of the most fragile fraction in this self- similar diagram. Such high-profile self- similarity is observed for the other factions.

Comparison with the Bernoulli diagram allowed us to calculate the parameter through which the Euclidean dimension is transformed into a fractal one. Using it, you can calculate the location of the main events located on the x-axis. This is how the updated MA time values were obtained, in which the main events occur, i.e. extreme values are observed. We also obtained refined values of the limits of the system operation, using combinatorics we refined and determined the maximum limit value, it = 6, 75 min. MA. Thus, the identified inheritance of the behavior of each subsystem to the subsequent process steps to obtain the synthesized product, found the time MA receive major system events, found an updated limit values of the system, identified the times of MA optimal for obtaining the target compositions of the particular phase.

Acknowledgements: The blessed memory of Raskolenko Larisa G. whose ideas are the basis of this work.

REFERENCES

[1] Oxagoev A.A. Procedures with sharpening in self-organize processes of high-intensity treatment of metal systems. Applied synergetic, fractals and computer structures simulation. ed.by Oksogoev A.A. Tomsk State university,2002

[2] R.I. Zainetdinov. Applied synergetic, fractals and computer structures simulation. ed.by Oksogoev A.A. Tomsk State university,2002.

[3] O.A. Shkoda, L,G. Raskolenko «Study of changes of coherent scattering domains at mechanical activation with use holistic approach», Journal «Problems of open systems evolution » , Almaty, 2008, issue 10, v. 2

[4] O.A. Shkoda, L,G. Raskolenko “Using of holistic approach for study of influence of preliminary mechanical activation on parameters of thermal explosion in dispersed Ti-Ni system» Journal « Problems of open systems evolution » , Almaty, 2008, issue 10, v. 2

This work was carried out within the RFBR grant 14-03-00666A

STUDY OF THE MICROSTRUCTURE OF SYNTHESIZED LAMINATES*

O.K. LEPAKOVA[1], *O.A. SHKODA*[1], *A.S. ZELEPUGIN*[1,2], *S.A. ZELEPUGIN*[1,2]

[1]*Tomsk Scientific Center SB RAS, Tomsk, Russia*
[2]*National Research Tomsk State University, Tomsk, Russia*

Advanced structural and multifunctional materials include metal-intermetallic laminates (MIL) [1], which have useful properties and characteristics, such as high temperature resistance, high oxidation resistance, good creep resistance and others, making them attractive for use in many industry fields. The study of diffusion processes, the formation of intermetallic layers, and the study of the microstructure of synthesized composites play an important role to obtain such materials.

This work is devoted to microstructural studies of metal - intermetallic laminates Ti-Al_3Ti obtained by several methods [2, 3].

Titanium (VT1-0) and aluminum (8011) foils with a thickness of 0.3 and 0.15 mm, titanium (0.5 and 0.6 mm) and aluminum (1 mm) plates (the same grades), titanium powders, and aluminum (ASD-4) were used in the experiments. A titanium–titanium tri-aluminide laminate composite was obtained in a thermal explosion mode by the method of reaction sintering, reaction pressing, explosion welding with further sintering. The synthesized samples were studied by X-ray diffraction (DRON-2, CuK radiation), metallography (Axiovert 200M), and X-ray spectrometry (CAMECA).

The studies showed that the most suitable structure of a laminate is formed using the explosion welding of titanium and aluminum plates with further reaction sintering in a muffle furnace. Fig. 1a shows a microstructure of the laminate composite after explosion welding. Fig. 1b demonstrates narrow titanium layers and wide intermetallic layers (Al_3Ti) obtained after reaction sintering. All intermetallic layers in the central part contain darker regions which are a two-phase material with an increased porosity.

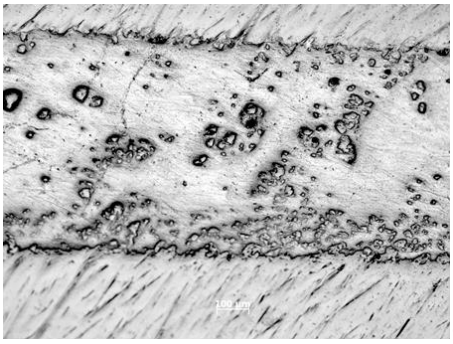
a

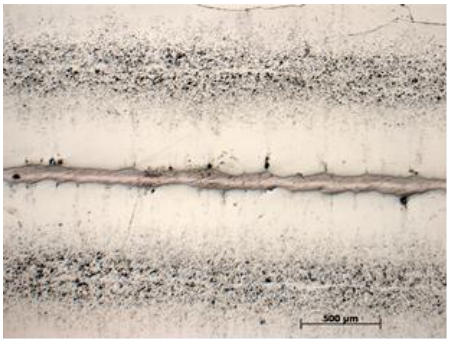

b

Fig. 1. Microstructure of the laminate composite after explosion welding (a) and reaction sintering at T = 700ºC for 6 hours (b).

Thus, four approaches to the obtaining of Ti-Al_3Ti metal-intermetallic laminates were implemented. The structure and composition of the samples were studied by X-ray diffraction, X-ray metallography and X-ray spectrometry. The conducted studies can be used to obtain laminate composites with a required layer thickness.

REFERENCES

[1] *Vecchio K S //* JOM. - 2005. - Vol. 57(3). - P. 25-31.
[2] *Zelepugin S.A., Mali V.I., Zelepugin A.S., Ilina E.V. //* Shock Compression of Condensed Matter. USA: American Institute of Physics. - 2012. - Vol. 1426. - P. 1101-1104.
[3] *Zelepugin S.A., Shkoda O.A., Lepakova O.K., Zelepugin A.S. Kasatsky N.G. //* Journal of Physics: Conference Series. - 2018. - Vol. 1115(4). - 042019.

* The reported study was funded by RFBR, project number 19-08-01152.

RESIDUAL ENERGY MEASUREMENT AT PICOSECOND LASER IMPACT ON METALS*

E.Y. LOKTIONOV[1], E.S. SHARABOROVA[1], D.S. SITNIKOV[2]

[1]Bauman Moscow State Technical University, Moscow, Russia
[2]Joint Institute for High Temperatures of the Russian Academy of Sciences, Moscow, Russia

Residual energy or thermal coupling coefficient shows what fraction of laser pulse energy is spent for target heating. High residual energy rates lead to low impact efficiency and sometimes to unwanted effects like phase transitions and chemical reactions. Experimental works on its measurement at nano- and femtosecond laser impact are not numerous but still can be found, while picosecond range is poorly studied. The latter is interesting since thermal coupling effects are close to ultrashort impact, while lasers efficiency, complexity, and price are closer to nanosecond devices. Existing numerical simulation results appear to be underestimated die to lack of available experimental data. Residual energy is usually evaluated using target temperature measurement, containing methodical errors, for pulse trains particularly, since actual absorbed energy fraction is unknown, temperature field across the target is complicated, and for pyrometry – exact emissivity is not known. To overcome this, we have used calorimeter to evaluate heat flux through a target at focused and non-focused irradiation. Such approach, to our mind, reduces errors.

Data obtained for Aluminium at 1064 nm, 71 ps, 15 Hz irradiation are of high novelty and is significant for proper thermal coupling modelling and adequate transition from lab modelling to real-world systems using pulse-periodic picosecond impact. The results evidence big need for experimental data on realistic laser technology impact regimes for adequate modeling, residual energy, and efficiency evaluation. Thermal coupling coefficient depends not on target material and pulse length, but on the whole set of impact conditions.

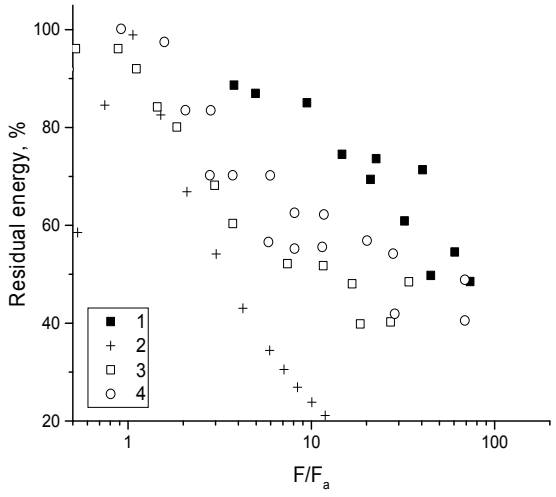

Fig.1. Residual energy data normalized by absorptivity A of Al target as a function of laser fluence F normalized by ablation threshold F_a: 1 – our data, F_a=4 J/cm^2; 2 – calculated for 1064 nm, 100 ps single pulse, A=0.20, F_a=0.7 J/cm^2 [1]; 3 – for 1064 nm, 55 ns single pulse, A=0.25, F_a=2.7 J/cm^2 [2]; 4- for 800 nm, 60 fs single pulse, A=0.37, F_a=0.058 J/cm^2 [2].

REFERENCES

[1] C. R. Phipps, M. Boustie, J. M. Chevalier, S. Baton, E. Brambrink, L. Berthe, M. Schneider, L. Videau, S. A. E. Boyer, S. Scharring, "Laser impulse coupling measurements at 400 fs and 80 ps using the LULI facility at 1057 nm wavelength," J. Appl. Phys., vol. 122, p. 193103, 2017.

[2] A. Y. Vorobyev, V. M. Kuzmichev, N. G. Kokody, P. Kohns, J. Dai, C. Guo, "Residual thermal effects in Al following single ns- and fs-laser pulse ablation," Appl. Phys. A, vol. 82, pp. 357-362, 2006.

* The work was supported by the Russian Foundation for Basic Research (RFBR) according to the research project No. 18-38-20032; experimental data were obtained using "Beam-M" research facility (BMSTU). Aluminium samples were provided by S.A.E. Boyer. Authors are grateful to C.R. Phipps for his comments and help with experiments.

PHOTOGRAPHIC RESEARCH OF THIN METAL FILM ELECTRIC EXPLOSION EXPANSION INTO A FREE SPACE*

A.S. SKRYABIN[1], A.V. PAVLOV[1], V.D. TELEKH[1], A.M. KARTOVA[1]

[1]Department of Power Engineering, Bauman Moscow State Technical University, Baumanskaya 2-ya 5/1, Moscow, 105005, Russia

The paper presents the results of thin metal film electric explosion [1] dynamics and explosion products expansion in the mode of slow energy input into a free space. Electric explosion of thin metal films [2] nowadays found application for determination different materials thermophysical properties under the extreme conditions [3]. However, the main goal of those investigations is to find out the values of different material properties excluding studying the process of explosion.

Applied in experimental studies films (Cu, Ti) were received by the method of magnetron sputtering on quartz glass (20x50 mm), their thickness was 40 nm, electrical resistance – 100…130 Ohm. A power circuit [4] included a pulsed capacitor $C_0 = 0.6$ μF charged up to 8…30 J (U_0=5.0÷8.0 kV) through an electrical ballast R_b=10 kΩ. The circuit commutation was fulfilled with a quick-acting thyratron module. The studies were performed in inert argon atmosphere with the pressure of ≈ 1 bar.

Current $I(t)$ and voltage $U(t)$ waveforms (fig. a) were registered by current monitor and voltage dividers. Maximum value of the current reached I_{max}=1,1 – 1,5 kA, time of the process τ=50…70 μs.

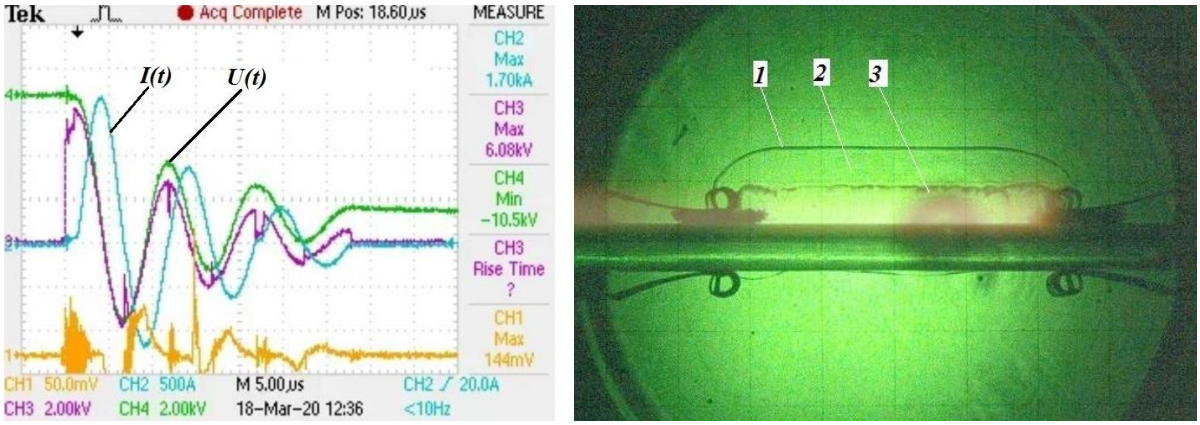

a b

Current $I(t)$ and voltage $U(t)$ waveforms (a) and Schlieren picture of Ti film explosion (b)

Two methods of optical diagnostics were used for the explosion process visualization: method of direct photography with a high – speed camera and method of shadow photography (schlieren scheme in light field mode). The laser beam was produced by the Nd-YAG laser with λ_2 = 532 nm and τ = 10 ns. Setting a fixed delay for laser operation allowed to receive data abot the explosion process in difeerent moments of time: from 5 μs to 70 μs.

Typical schlieren picture of Ti film explosion is shown on fig. 1b. There were visualized areas of a generated shock wave front (1), a shock compressed gas area (2) and an extended high temperature explosion products (3).

REFERENCES

[1] A.L. Surkaev, M.M. Kumysh, V.I. Usachjov, “Technique of research of electric explosion of the cylindrical conductor and ring foil” News of Volga University, 621.3.018.2:537.528.

[2] Surkaev A L 2015 Technical Physics 85(7) pp 37-44

[3] A.I. Savvatimsky et al, “Investigation of high temperature properties of zirconium nitride by the pulse current heating” High temperature termophysics, vol. 53, no. 3, pp. 478–480, 2015.

[4] A.S. Skryabin, A.V. Pavlov, A.M. Kartova, V.D. Telekh, M.M. Serov, A.E. Sytchev “Experimental study of slow electrical explosion of thin titanium wires” Journal of Physics: Conference Series 1250 012018, 2018

* The work was supported by the Russian Foundation for Basic Research under grant No. 18-29-21039 and has been performed at “Beam-M” facility of Bauman Moscow State Technical University

FEATURES OF THE SYNTHESIS OF TICAL (FE2O3 / TIO2) METAL MATRIX COMPOSITES UNDER NONEQUILIBRIUM CONDITIONS *

A.G. KNYAZEVA[1,2], E.N. KOROSTELEVA[1,2], I.O. NIKOLAEV[2]

[1]Institute of Strength Physics and Materials Science, Siberian Branch of the Russian Academy of Sciences, Tomsk, Russia
[2]Tomsk Polytechnic University, Tomsk, Russia

In recent years, materials containing MAX phases or MXenes have been of considerable interest. MAX-phases due to the combination of properties of metals and ceramics may be used in a wide range of applications - from medicine to engineering. MAX-phases are used as an additional phase in composites, but there are attempts to produce three-dimensional objects consisting entirely of MAX phases. Currently the coatings based on MAX-phases are successfully synthesized, or the blanks of simple form are obtained by classical powder metallurgy techniques.

The main problem at the stage of producing products of complex shape containing MAX phases is the low knowledge of the thermodynamics for such materials under various conditions. The study of the production methods and properties of two-dimensional materials called MXene, consisting of carbides, nitrides or carbonitrides of transition metals, is currently the main direction of scientific research in many universities and research institutes.

In the present work, the synthesis of composites in the Ti-C-Al, Ti-Al-C-Fe_2O_3 and Ti-Al-C-TiO_2 systems, which is accompanied by the formation of MAX phases and intermetallic compounds with different properties, is studied theoretically and experimentally.

An attempt was made to determine under what conditions (and for which the compositions of the starting powder compositions) composite powders with fundamentally different properties are formed, caused by not only the inclusion properties, but also the matrix structure. Including, the result of the synthesis is a metal matrix composite or ceramic composite depending on the composition of the initial powders. Using metallothermal reactions to obtain composites with oxide inclusions (the system Ti-Al-C-Fe_2O_3 and Ti-Al-C-TiO_2) results in appearance of the non-equilibrium phases that not predicted from preliminary thermodynamic evaluation. Additional research of the reasons and conditions of their formation made it possible to establish a reduced transformation scheme and formulate a model for composites synthesis under sintering.

* The work was supported by Russian Science Foundation, Grant Number 17-19-01425.

NITRIDING OF MECHANICALLY PRE-ACTIVATED FERROCHROMALUMINIUM IN THE COMBUSTION MODE*

A.A. REGER[1,2], K.A. BOLGARU[1], A.A. AKULINKIN[1]

[1]TSC SB RAS, Tomsk, Russia
[2] National Research Tomsk Polytechnic University, Tomsk, Russia

At present, nitrides are of particular interest due to their unique physical and chemical properties. The cost of production of nitrides can be significantly reduced if ferroalloys will be used as precursors, which are relatively cheap high-tonnage materials [1]. In our opinion, the most promising method for producing nitrides is the method of filtration self-propagating high-temperature synthesis (SHS) [2]. One of the ways to control the combustion conditions of powders is the mechanical activation of a reaction mixture [3,4].

In this work, the effect of mechanical activation on nitriding of a complex ferroalloy (ferrochromaluminium) was studied.

Ferrochromaluminium (FCA) represented by the phases such as AlFe, Cr and $AlFeCr_2$ was chosen as the starting material. According to the chemical analysis, the ferroalloy contained 6.4% aluminum, 32.6% iron and 61.0% chromium.

The phase composition was determined on a Shimadzu XRD6000 diffractometer (Japan). The content of nitrogen and oxygen was determined on a LECO-ONH836 (United States) analyzer at the Tomsk Regional Center for Collective Use, TSC SB RAS. The starting powders were mechanically activated in an APF-5 planetary mill with a centrifugal force of 60 g.

In the work, the effect of mechanical pre-activation on the nitriding parameters of ferrochromaluminum was studied varying the diameter of the sample (Fig. 1) and the nitrogen pressure (Fig. 2). The use of mechanically processed starting powder in SHS reactions expands the limits for the initiation of combustion reactions from P = 0.02 MPa and D = 20 mm, as well as increases the amount of absorbed nitrogen in products up to 13.6% and the combustion rate.

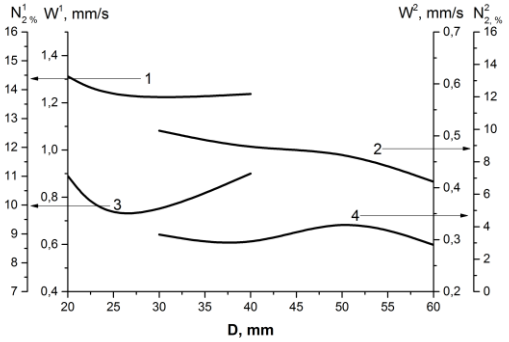

Figure 1. Nitrogen content (N^1-activated powder (1),N^2- unactivated powder (2)) and combustion rate (W^1-activated powder (3), W^2-unactivated powder (4)) as a function of the diameter of the FCA samples.

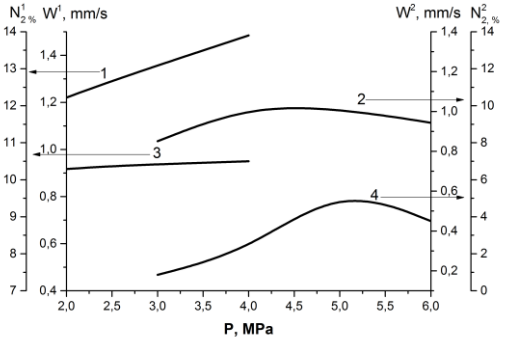

Figure 2. Nitrogen content (N^1-activated powder (1),N^2- unactivated powder (2)) and combustion rate (W^1-activated powder (3), W^2-unactivated powder (4)) as a function of the nitrogen pressure.

REFERENCES

[1] A.V. Baranovsky, G.A. Pribytkov, A.A. Korzhov, M.G. Krinisyn, V.V. Khomyakov, G.O. Dankovtsev, "Mechanical activation of SHS synthesis in powder mixtures of ferrotitane and carban," National research Tomsk Polytechnik university, 2019.

[2] K.A. Bolgaru, A.A. Reger, L.N. Skvortsova, "Nitriding of ferrochromium-aluminum during combustion and evaluation of the photocatalytic activity of obtainedcomposites, " IOPConf. Series: Materials Science and Engineering, 511, 2019.

[3] O.V. L`vov, N.G. Kasatsky, N.I. Radishevskaya, "Influence of mechanical activation on phase composition and structure of SHS spinel pigments," Tomsk State University Journal pf Chemistry, 1, pp. 26-32, 2015.

[4] A.Yu. Potanin, P.A. Loginov, E.A. Levashov, Yu.S. Pogoshev, E.I. Patsera, N.A. Kochetov, "Effect of Mechanical Activation on Ti_3AlC_2 Max Phase Formation under Self-Propagation High-Temperature Synthesis, " Eurasian Chemico-Technological Journal, 17, pp. 233-242, 2015.

* The work was supported by RFBR (project № 18-33-00387 mol_a).

3D MATHEMATICAL MODEL OF "CHEMICAL FURNACE"*

V.G. PROKOF'EV[1,2]

[1]*Tomsk Scientific Center, Russia*
[2]*Tomsk State University, Russia*

The method of forming powder materials in the form of a layer package allows synthesizing material for a low exothermic or even endothermic mixture in the "chemical furnace" [1, 2]. Three-dimensional modeling of gasless combustion of a three-layer sample was carried out. We considered a sample in the form of a combination of thermally conjugated flat layers consisting of two mixtures of different chemical activity — the model of a "chemical furnace" [2, 3]. Numerical simulation was previously performed of unsteady modes of gasless combustion in rectangular rods prepared from a mixture of two powdered reagents with an admixture of low-melting inert metal powder [4]. Gasless combustion of a flat three-layer package of rectangular cross section was considered. The parameters and composition of the outer layers are the same, and the inner layer has a homogeneous structure. Unsteady spin combustion regimes were studied in detail with a change in the layer thickness and sample size (fig. 1). Critical combustion conditions are established depending on the ratio of the volumes of mixtures in the sample or the content of reaction products. The time, burning rate and combustion regimes of the layer composition are determined depending on the volumetric content of the mixtures, the thickness and number of layers.

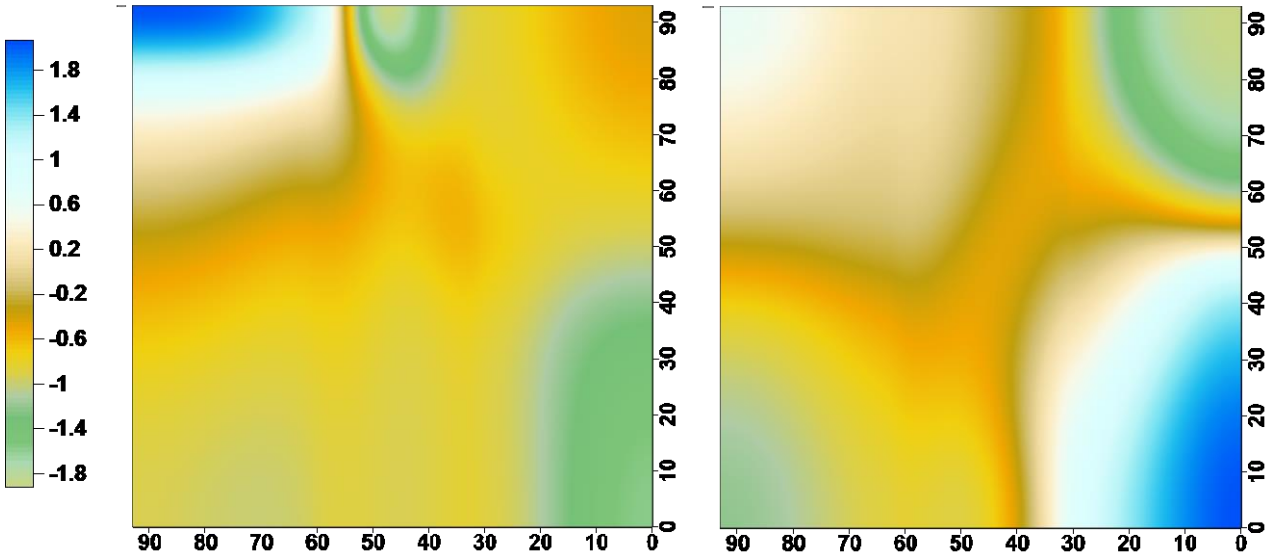

Fig.1. Spin combustion regime (temperature fields)

REFERENCES

[1] A.G. Merzhanov, "Thermally coupled processes of self-propagating high-temperature synthesis", Dokl. Phys. Chem. Vol. 434, pp. 159–162, 2010.

[2] A.V. Linde, I.A. Studenikin, A.A. Kondakov and V.V. Grachev, "Thermally coupled SHS processes in layered (Fe 2 O 3 + 2Al)/(Ti + Al)/(Fe 2 O 3 + 2Al) structures: An experimental study", Combust. Flame, vol. 208, pp. 364-368, 2019.

[3] V.G. Prokofiev and V.K. Smolyakov, "Gasless Combustion of a System of Thermally Coupled Layers", Combust., Expl., Shock Waves, vol. 52, no. 1, pp. 62-66, 2016.

[4] [1] V.G. Prokofiev and V.K. Smolyakov, "Gasless Combustion in Two_Layer Structures: A Theoretical Model", Int. J. Self-Propag. High-Temp. Synth., vol. 22, no. 1, pp. 5-10, 2013.

[5] V.G. Prokof'ev, "Unsteady Combustion Modes in Rectangular Rods", Int. J. Self-Propag. High-Temp. Synth., vol. 28, no. 3, pp. 155-158, 2019.

* The work was supported by the Russian Foundation for Basic Research (project no. 19-03-00081).

FEATURES OF FILTRATION GAS COMBUSTION INSIDE A POROUS CYLINDRICAL PIPE WITH AXIAL GAS FLOW*

E.P. DATS, S.S. MINAEV, A.A. PONOMAREVA

Institute of Applied mathematics FEB RAS, Vladivostok, Russia

The filtration gas combustion in a porous tube with injection of a combustible mixture through the end surface of a porous cylindrical tube is theoretically studied. This scheme of filtration gas combustion can be used to create chemical reactors for non-contact heating of various materials to high temperatures. The samples under treatment can be placed inside a porous tube, the side surface of which is covered with quartz shells transparent for infrared radiation emitted by porous carcass. The outer surface of porous reactor is heat insulated. Radiation from the surface of the porous solid phase allows heating materials under treatment to high temperatures. The simulation of the filtration gas combustion was carried out in the framework of the two-temperature thermal-diffusion model [1–3]:

$$\rho_g c_g \left(\frac{\partial T_g}{\partial t} + u_z \frac{\partial T_g}{\partial z} \right) = \lambda_g \left(\frac{1}{r}\frac{\partial T_g}{\partial r} + \frac{\partial^2 T_g}{\partial r^2} + \frac{\partial^2 T_g}{\partial z^2} \right) + Q \cdot A \cdot Y \cdot \exp\left(-\frac{E}{T_g R} \right) - \frac{2Nu}{d_p^2}(T_g - T_s)$$

$$\rho_s c_s \frac{\partial T_s}{\partial t} = \lambda_s \left(\frac{1}{r}\frac{\partial T_s}{\partial r} + \frac{\partial^2 T_s}{\partial r^2} + \frac{\partial^2 T_s}{\partial z^2} \right) + \frac{2Nu}{d_s^2}(T_g - T_s) \qquad (1)$$

$$\frac{\partial Y}{\partial t} + u_z \frac{\partial Y}{\partial z} = D \left(\frac{1}{r}\frac{\partial Y}{\partial r} + \frac{\partial^2 Y}{\partial r^2} + \frac{\partial^2 Y}{\partial z^2} \right) - A \cdot Y \cdot \exp\left(-\frac{E}{T_g R} \right)$$

The problem has following boundary conditions:

at the inlet ($z = 0$) and outlet ($z = h$) end of the pipe:

$$T_g(r,0) = T_0, \qquad \frac{\partial T_s(r,0)}{\partial z} = 0, \qquad Y(r,0) = Y_0, \qquad \frac{\partial T_g(r,h)}{\partial z} = \frac{\partial T_s(r,h)}{\partial z} = \frac{\partial Y(r,h)}{\partial z} = 0, \qquad (2)$$

at the inner ($r = a$) and outer ($r = b$) surface of the pipe:

$$\lambda_s \frac{\partial T_s(a,z)}{\partial r} = \sigma_{sb}(\Theta^4 - T_s^4), \qquad \frac{\partial T_g(a,z)}{\partial r} = \frac{\partial Y(a,z)}{\partial r} = 0, \qquad \frac{\partial T_g(b,z)}{\partial r} = \frac{\partial T_s(b,z)}{\partial r} = \frac{\partial Y(b,z)}{\partial r} = 0, \quad (3)$$

Where Θ – the parameter, which sets the level of radiation heat flux from the inner surface of the pipe.

Simulation was performed by using of the finite element method. The result of the calculations is a sequence of stationary solutions of the system (1-3). Numerical modeling allowed to evaluate the range of gas flow rates at which a stable combustion regime was observed, to find the temperature distribution in the gas and the porous body, and to evaluate the radiation fluxes inside the reactor. The influence of heat loss and the geometric characteristics of the reactor on the flame stabilization was studied.

REFERENCES

[1] J. Howell J., Hall M., and Ellzey J, “Combustion of hydrocarbon fuels within porous inert media” , Progress in Energy and Combustion Science, vol .22, pp. 121-145, 1996.

[2] L. Kennedy, A.Fridman and A. Saveliev, “Superadiabatic combustion in porous media: Wave propagation, instabilities, new type of chemical reactor”, International Journal of Fluid Mechanics Research, vol .22, pp. 1-26, 1996.

[3] E. P. Dats, S.S. Minaev and A.I. Kirdyashkin, Filtration combustion inside a porous cylindrical pipe with axial gas flow, Journal of Physics: Conf. Series, vol. 1404, pp. 012056, 2019.

* The present study was financially supported by RFBR (project № 20-38-70119).

INVESTIGATION OF THE KINETICS OF THE SHS PROCESS, INITIATED USING ELECTRON-BEAM TECHNOLOGY*

S.V. FEDOROV, M.P. KOZOCHKIN, T.H. MAUNG

Moscow State Technical University "STANKIN", Moscow, 127994, Russia

This paper presents experiments on the hardening of the aluminum alloy surface by intermetallic phases of the NiAl system. The aluminum plate was coated with a thickness of about 0.2 μm of heat-resistant nickel alloy $NiCr_{20}TiAl$. After, the plate with a metal coating applied to it was exposed to a series of pulses of a wide-aperture low-energy high-current electron beam with duration of about 5 μs in the installation "RITM-SP". As a result, the SHS process is started between the metal film and the aluminum base, which lasts several tens of milliseconds.

However, the control of the surface electron-beam alloying process of significantly complicates the instability of the electron beam pulse parameters and the process of its interaction with the processed material, which leads to some random changes in quality indicators that occur spontaneously, regardless of the control system. In this situation it is convenient to use vibroacoustic analysis to track the process.

To register the vibroacoustic signal generated during the technological process, the substrate was connected to the accelerometer using a waveguide in the form of a copper wire with a cross section of 2.5 mm^2. The use of a wire waveguide made it possible to have the recording equipment at a distance from sources of electromagnetic interference.

Experiments have shown that the components in the frequency range up to 40 kHz stand out against the background of noise. Low-frequency components up to 1 kHz were excluded from consideration. The recorded vibroacoustic signal was subjected to time and frequency analysis. Effective (mean square) values of the amplitude of these signals filtered in different frequency ranges were taken as parameters of the vibroacoustic signal reflecting the kinetics of the process.

It is observed that the amplitude of the vibroacoustic signal for the case of a coated sample increases significantly, starting from the third-fourth pulse. Analysis of optical images confirmed that the formation of intermetallic phases on the surface of the aluminum plate under irradiation by the first pulse, as a rule, does not occur. The film is partly evaporated and partly mixed. With further irradiation, in place of these crystals appear intermetallic phase inclusions up to several microns in size.

It is seen that in the presence of an alloying coating in the processes of changing the structure of the sample surface, short discrete pulses prevail, giving a contribution to energy at higher frequencies, which is in good agreement with [1,2]. The growth of high-frequency energy in the spectrum of the vibroacoustic signal is accompanied by an increase in the content of the intermetallic phase.

In order to effectively control the results of irradiation of various materials in an automated mode, a deterministic algorithm for processing vibroacoustic information has been developed that allows us to evaluate the quality of the results obtained in real time, despite a fairly limited set of diagnostic parameters, whose digital values nevertheless allow us to control the quality of the process and make a decision about its repetition or changing the initial parameters.

REFERENCES

[1] P. Gulyaev, Temperature hysteresis in the unstable combustion mode of SHS: experiment with high-speed micro-pyrometry, *IOP Conf. Series: Journal of Physics: Conf. Series 1115* (2018) 042026 doi:10.1088/1742-6596/1115/4/042026.

[2] R.M. Gabbasov, A.I. Kirdyashkin, V.G. Salamatov, Acoustic emission during combustion of Ni-Al composites, *IOP Conf. Series: Journal of Physics: Conf. Series 1115* (2018) 042025 doi:10.1088/1742-6596/1115/4/042025.

* This work was carried out with the financial support from the Russian Foundation for Basic Research (scientific project No. 19-08-00899).

COMBUSTION OF A PRE-MIXED METHANE-AIR MIXTURE IN A CO-AXIAL COUNTER FLOW REACTOR

V.A. KOSYAKOV[1,2], *R.V. FURSENKO*[2], *V.V. GUBERNOV*[3]

[1]*Novosibirsk State Technical University, Novosibirsk, Russia*
[2]*Khristianovich Institute of Theoretical and Applied Mechanics SB RAS, Novosibirsk, Russia*
[3]*P.N. Lebedev Physical Institute RAS, Moscow, Russia*

Environmental issues come to the fore for today's society stimulating development of eco-friendly technologies. Thus, fundamental studies of combustion regimes and extinction limits in perspective systems for low-calorific fuels burning are of great importance.

In this work, the combustion of premixed methane-air mixtures in co-axial counter flow reactor is studied. Reactor consists of inner and outer tubes nested into each other as shown in Fig.1. A fuel-lean methane-air mixture with equivalence ratio φ_{out} varied from 0.4 to 0.8 is fed into the outer tube. In the inner tube either pure methane ($\varphi_{in}=\infty$) or a rich methane-air mixture with φ_{in}=1.5, 2.5 and 3.5 is supplied. Numerical simulations were performed by means of OpenFOAM software. In the course of numerical simulations mixture flow rates and equivalence ratios in the inner and outer tubes were varied.

It was found that depends on problem parameters various combustion regimes characterized by the number, shape and relative position of the flame fronts can be realized. In the case of pure methane flow in the inner tube the two-layered flame structure is observed. In this case shown in Fig.1 the lean premixed cup-like flame and small diffusion flame near the outlet of the inner tube are stabilized. Results of numerical simulations allowed us to conclude that high-temperature zone appearing due to the diffusion combustion play stabilizing role for cup-like flame and causes expansion of extinction limits. In the case of rich methane-air mixture supply in the inner tube the three-layered flame structure consisting of lean premixed flame, diffusion flame and rich premixed flame is observed. Effect of mixtures equivalence ratio and flow rates on flame structure and shape are discussed. Results of numerical simulations are compared with experimental data. Example of such comparison is shown in Fig.1. It was shown that applied simplified model allow to reproduce main features of combustion in the examined system and provides a clear physical interpretation of experimental findings.

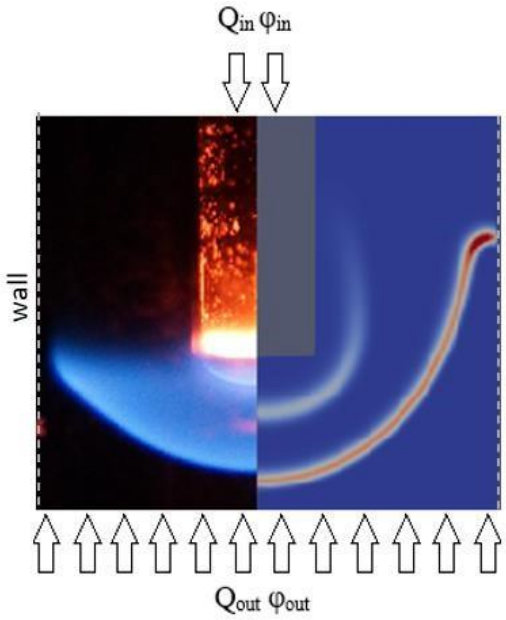

Figure 1. Experimental photo and numerical result on heat release demonstrating cup-like flame and diffusion flame typical for twolayered flame structure (Q_{in}=0.005 l/min, $\varphi_{in}=\infty$, Q_{out}=5.9 l/min, φ_{out}=0.7)

Keywords

Fuel-lean mixtures combustion, premixed flames, diffusion flame, counterflow reactor, CFD.

Thanks for the grant РФФИ № 17-53-12018 ННИО_а.

PORE-SCALE NUMERICAL SIMULATION OF THE COMBUSTION WAVE PROPAGATION: LOCAL PHENOMENA*

I.A. YAKOVLEV

Tomsk Scientific Center SB RAS, Tomsk, Russia

The study is devoted to a theoretical analysis of a combustion wave propagation in an irregular inert packed bed of spheres during the combustion of lean and reach methane-air mixtures under the low-velocity regime. Experimental works reported that the combustion wave propagates thought the media at the macroscale with constant velocity order of 10^{-4} m/s [1]. Hence at the pore scale, the local unsteady effects such as fluctuations of the flame front take place [2]. Experimental measurements of this phenomena are complicated due to limited optical access and tortuous interstitial paths. Because of that, the method of numerical simulation when the geometry of porous matrix and interstitial flow are simulated explicitly at pore scale can be a promising way to consider local instabilities in detail.

3D model of packed bed was generated using the discrete element method and contained 10^3 particles. The model describes directly interfacial thermal interaction by solving Navier–Stokes equations in the void region and energy transport equation in the solid region with coupled heat transfer condition on the interface. The model includes a detailed chemical kinetics model and solid-to-solid radiation.

Fig. 1a demonstrates the temperature distribution at the central longitudinal section of the model for three different moments. The wave propagates upstream with averaged velocity of 0.032 mm/s that correlates with experimental data in [3]. It can be noticed that in the preheating and hear release regions the temperature distribution reflects the local irregular structure of the packed bed.

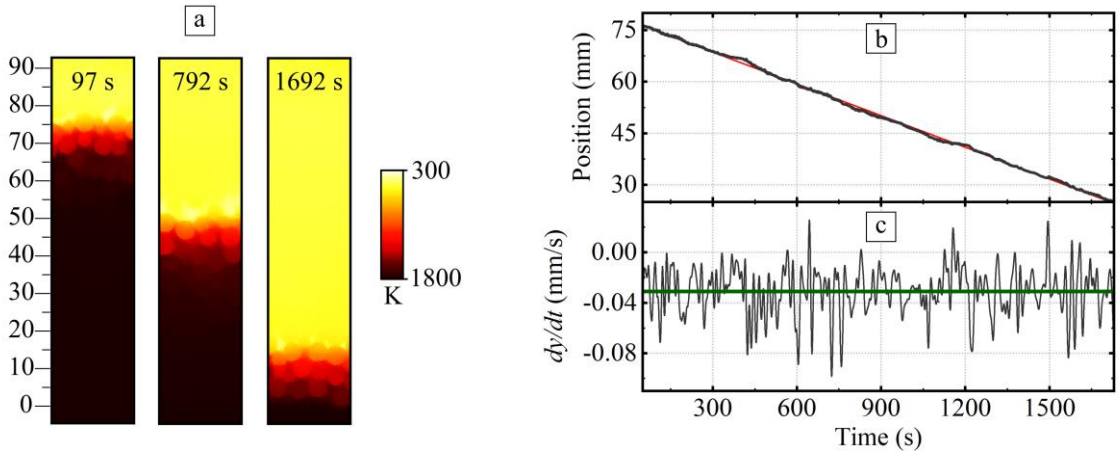

Fig.1. Contours of the temperature distribution (a), averaged flame front position (b) and axial coordinate derivative (c)

The evolution of the averaged position of the flame front calculated as coordinate of maximum CH_4 mole fraction gradient is shown in Fig. 1b. The evolution can be approximated by linear function fairly well that indicates the quasi-stationary regime of propagation. For estimation of local fluctuation of the flame front, the temporal derivative of the flame front position was made (see Fig. 1c). The local velocity of the combustion wave propagation varies significantly up to zero. During propagation different fragments of the flame front propagates asynchronously to each other with anchoring in narrow channels of the porous media. At the macroscopic scale, the process is quasi-steady whereas at the pore-scale the unsteady effects take place.

REFERENCES

[1] V.S. Babkin, "Filtrational combustion of gases. Present state of affairs and prospects," Pure Appl. Chem., vol. 65, no. 2, pp. 335–344, 1993.

[2] G.A. Fateev, O.S. Rabinovich, M.A. Silenkov, "Oscillatory combustion of a gas mixture blown through a porous medium or a narrow tube," Symp. (Int.) Combust., vol. 27, no. 2, pp. 3147–3153, 1998.

[3] C. Zheng, L. Cheng., A. Saveliev et al. "Gas and solid phase temperature measurements of porous media combustion," Proc. Combust. Inst., vol. 33, no. 2, pp. 3301–3308, 2011.

* The work was supported by the Grant of President of Russian Federation No. 075-15-2020-456.

INVESTIGATION OF COMBUSTION WAVE PROPAGATION IN THE SOLID LAYERED MATERIALS[1]

T.P. MIROSHNICHENKO, V.V. GUBERNOV

P.N. Lebedev Physical Institute of the RAS, Moscow, Russia

Combustion waves in layered solid fuel samples is usually investigated due to its significance for applied technology of the production of advanced materials, Self-propagating High temperature Synthesis (SHS) [1] and in relation with the concept of chemical furnace [2, 3]. In this work we consider the model describing propagation of a combustion wave in a system of two layers of different solid energetic materials under conditions of thermal contact between them through a common surface. This system is directly relevant to chemical furnace regime of SHS when one of the reactants serves as a heat source (donor layer) for the other reacting material (acceptor layer) and facilitates the chemical reaction in the latter.

We undertook a detailed parametric study to find out which parameters affect the process of reaction wave propagation in this system based on the reaction sheet model and direct numerical simulations in one spatial dimension. It is shown that depending on the parameters of the problem a leading wave is formed in one of the layers. Propagation of the leading front creates the conditions for preheating of the secondary wave traveling behind it in the different layer and this can lead to the significantly superadiabatic temperature of combustion in the material in which the secondary front propagates. This flame structure is demonstrated in Fig. 1.

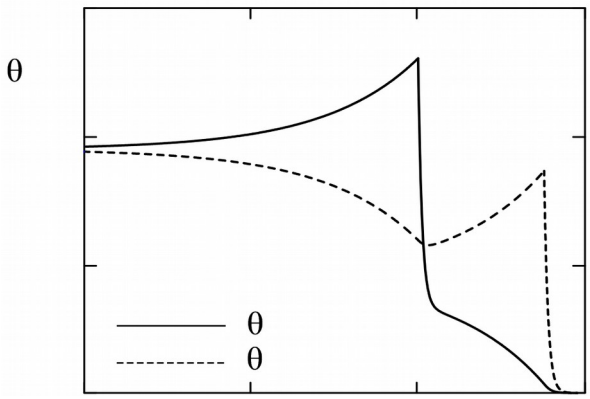

Fig.1. Distribution the temperature in donor (θ_1) and acceptor (θ_2) layers in co-moving coordinate frame.

The results of our work show which regimes of combustion wave propagation exist in the layered solid fuel systems and how they depend on the choice of thermophysical and chemical parameters of the reacting materials composing the layered structure as well as on geometrical properties of the latter. In particular, the results of stability analysis indicate the occurrence of nontrivial exchange of stability of combustion waves propagating in different layers.

REFERENCES

[1] E. Levashov, A. Mukasyan, A. Rogachev, and D. Shtansky, “Self-propagating high-temperature synthesis of advanced materials and coatings,” Int. Mater. Rev., vol. 62, no. 4, pp. 203–239, 2017. doi:10.1080/09506608.2016.1243291.

[2] A. Merzhanov, “Thermally coupled processes of self-propagating high-temperature synthesis,” in Dokl. Phys. Chem., vol. 434, pp. 159–162, Springer, 2010. doi:10.1134/S0012501610100015.

[3] A. Merzhanov, “Thermally coupled shs reactions,” Int. J. Self Propag. High Temp. Synth., vol. 20, pp. 61–63, Mar 2011. doi:10.3103/S1061386211010109.

1 This work was supported financially by the Ministry of Science and Higher Education of the Russian Federation (project No 075-15-2019-1878).

NUMERICAL STUDY OF THE SINTERING PROCESS OF LOW-CALORIFIC SOLID FUEL SUPPORTED BY FILTRATIONAL COMBUSTION WAVE*

E.V. SERESHCHENKO[1,2], *R.V. FURSENKO*[1,2], *S.S. MINAEV*[2]

[1]*Khristianovich Institute of Theoretical and Applied Mechanics SB RAS, Novosibirsk, Russia*
[2]*Institute of Applied Mathematics FEB RAS, Vladivostok, Russia*

The paper presents the results of a numerical study of the dynamic behavior of a chemical reaction in a low-calorific solid material thermally coupled with a filtration gas combustion wave. The system under consideration is represented by a cylindrical solid fuel surrounded by a coaxial porous tube through which a gaseous air-fuel mixture flowed. This system has been studied in terms of promising ways to control the combustion of low-calorific solid fuels. This problem is relevant for the use of solid fuels in rocket engines [1] and the production of new advanced materials [2-3]. The main problems in this case is that the heat released during combustion is not enough to maintain a self-propagating chemical reaction wave, as well as the presence of pulsating diffusive-thermal instability [4-6].

Numerical studies were carried out in the framework of one-dimensional model, which had previously proved itself in studies of a similar type problems [4, 6]. Within the framework of the proposed model, the influence of the chemical properties of the solid material and the gas velocity on the dynamic behavior of thermally coupled combustion waves was numerically investigated. It was shown that, depending on the problem parameters, various combustion modes are realized. So, for the case when the filtrational combustion wave propagates downstream, the burning velocity of solid energetic material increases significantly and creates difficulties in organizing stable combustion in the considered system. For the case when the combustion wave propagates upstream, the combustion waves in the gas and solid phases propagate together in a strong thermal coupling, and thus the burning rate of the solid material can be controlled by the flow rate of the gas mixture. Numerical results shown that thermal interaction extends the extinction limits of solid phase flame and can stabilize oscillations caused by diffusion-thermal pulsating instability. The results obtained indicate that the proposed system can be used for sintering of low-calorie solid fuels.

REFERENCES

[1] V.F. Komarov, V.A. Shandakov, “Solid Fuels Their Properties and Applications”, Combust. Explos. Shock Waves, vol.35, no. 2, pp. 139-143, 1999.

[2] E.A. Levashov, A.S. Mukasyan, A.S. Rogachev, D.V. Shtansky, “Self-propagating high-temperature synthesis of advanced materials and coatings”, Int. Mater. Rev., vol 62, no. 4, pp. 203-239, 2017.

[3] G.P. Shveikin, N.V. Lukin, L.B. Khoroshavin, “Sialons - Promising Refractory and Ceramic Materials”, Refract. and Indust. Ceram., vol. 44, no. 1, pp. 52-58, 2003.

[4] B.J. Matkowsky, G.I. Sivashinsky, “Propagation of a pulsating reaction front in solid fuel combustion”, SIAM J. Appl. Math., vol. 35, no. 3, pp. 465-478, 1978.

[5] A.S. Mukasyan, A.S. Rogachev, A. Varma, “Mechanisms of pulsating combustion during synthesis of advanced materials”, AIChE Journal, vol. 45, no. 12, pp. 2580-2585, 1999.

[6] A.P. Aldushin, A. Bayliss, B.J. Matkowsky, “Dynamics in layer models of solid flame propagation”, Physica D, vol. 143, no. 1-4, pp. 109-137, 2000.

* This work was supported financially by the Ministry of Science and Higher Education of the Russian Federation (project №075-15-2019-1878)

FEATURES OF LASER IGNITION OF HEM CONTAINING MIXTURES OF AL AND B*

A.G. KOROTKIKH[1], *I.V. SOROKIN*[1]

[1] *Tomsk Polytechnic University, Tomsk, Russia*
[2] *Tomsk State University, Tomsk, Russia*

The use of metal powder as a fuel in high-energy materials (HEMs) for the propulsion is the most energy efficient method allows to increase of HEMs combustion and ignition characteristics [1-3] and specific impulse [3]. In this study, we investigated the HEMs samples based on a mechanical mixture of powders such as aluminium with different dispersions and amorphous boron to determine the ignitability and ignition delay time as a function of the heat flux density.

We used three HEM samples to determine the ignition characteristics. The first HEM sample contained 64.6 wt.% ammonium perchlorate, 19.7 wt.% energetic binder and 15.7 wt.% amorphous boron as a metal fuel. In the other HEM samples, boron was partially substituted by aluminium powders with particle size 0.18 μm (Alex) or 10.8 μm (ASD-4).

The ignition process was studied via the setup for radiant heating based on a CO_2 laser with 10.6 μm wavelength and 200 W powers. The ignition delay times of HEM compositions t_{ign} were measured in the range of the heat flux density q = 60–220 W/cm^2.

Figure 1 shows the dependence of the ignition delay time for the HEM samples on the mean radiative heat flux density. A partial replacement of boron with aluminum Alex leads to a decrease in the ignition delay time of the HEM sample by 1.03–1.56 times in the range of heat flux density of 90–200 W/cm^2. The use of aluminum powder ASD-4 makes it possible to increase the ignition delay time of the HEM sample by 1.20–1.28 times in comparison with the boron-based composition.

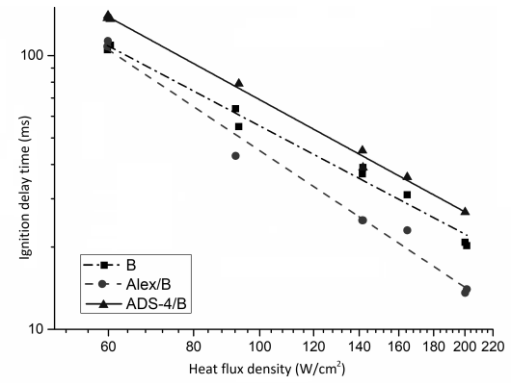

Fig.1. The ignition delay time of the HEM samples vs. the heat flux density.

The difference of the ignition delay time for the HEM samples heated by a radiant flux depends on the oxidation rate and the heat released from the chemical reaction for the metal fuels under study. Aluminum microparticles are difficult to ignite and react slowly [4] unlike nanosized aluminum powder [5]. Therefore, the ignition delay time for compositions with Alex/B takes smaller values than compositions with ASD-4/B.

REFERENCES

[1] A.G. Korotkikh, O.G. Glotov, V.A. Arkhipov, V.E. Zarko, A.B. Kiskin, "Effect of iron and boron ultrafine powders on combustion of aluminized solid propellants," Combust. Flame, vol. 178, pp. 195–204, 2017.

[2] Sh.L. Huseynov and S.G. Fedorov, Nanopowders of aluminum, boron, aluminum borides and silicon in high-energy materials, Moscow: Torus Press, 2015.

[3] A.G. Korotkikh, V.A. Arkhipov, O.G. Glotov, I.V Sorokin, "Effect of ultrafine powders of metals on the combustion characteristics," Chem. Phys. Mesoscopy, vol. 18, no. 2, pp. 173-179, 2018.

[4] W.Q. Pang, F.Q. Zhao, L.T. DeLuca, C. Kappenstein, H.X. Xu, X.Z. Fan, "Effects of nano-sized Al on the combustion performance of fuel rich solid rocket propellants," Eurasian Chem. Technol. J., vol. 18, no. 3. pp. 197-206, 2016.

[5] D. Sandaram, V. Young, V. E. Zarko, "Combustion of aluminum nanoparticles (review)," Combust. Explo. Shock+, vol. 51, no. 2, pp. 37-63, 2015.

* The work was supported by RFBR, project number 19-33-90015.

LASER INITIATION OF HEM CONTAINING METAL BORIDES*

A.G. KOROTKIKH[1], I.V. SOROKIN[1], E.A. SELIKHOVA[1], V.A. ARKHIPOV[2]

[1] Tomsk Polytechnic University, Tomsk, Russia
[2] Tomsk State University, Tomsk, Russia

Boron and its compounds are among the most promising metal fuel components to be used in solid propellants for solid fuel rocket engine and ramjet engine. The specific energy released during its oxidation is one of highest values per unit mass or volume [1]. However, its application is significantly complicated by the fact that the inert oxide layer is formed on the boron particle surface during storage and combustion. This layer prevents the access of oxidizer [2] and increases the ignition delay time and burning time for particles [3, 4]. Promising direction of solving the problem for increasing the efficiency of metallic fuels in high-energy materials is the complete or partial replacement of aluminum by energy-intensive boron-containing components.

This paper presents the results of an experimental study of the high-energy material (HEM) samples based on ammonium perchlorate, ammonium nitrate, and an energetic combustible binder, containing powders of aluminium (based composition), amorphous boron and aluminum borides (AlB_2 and AlB_{12}).

Thermal analysis of HEM samples was carried out using of the simultaneous thermal analyzer NETZSCH STA 449 F3 Jupiter under argon at the heating rate of 10 °C/min. The ignition process was studied via the setup for radiant heating based on a CO_2-laser with 10.6 μm wavelength and 200 W powers.

It was established that the oxidation of amorphous boron powder begins at lower temperature of 560-800 ℃ with a high heat release value compared with aluminium powders (over 800 ℃) and aluminum borides (over 870 ℃). The decomposition onset temperature of HEM containing these powders does not change in argon and amounts to ~ 120–400 ° C, which is determined by the temperature of intensive decomposition of the combustible-binder and oxidizer.

Fig. 1 shows the dependences of the ignition delay time for the HEM samples on the radiation heat flux density. A complete replacement of aluminum with amorphous boron powder results in a decrease in the ignition delay time of the HEM sample by 2.2–2.8 times in the range of heat flux density of 90–200 W/cm^2. The use of aluminum diboride powder makes it possible to reduce the ignition delay time of the HEM sample by 1.7–2.2 times in comparison with the Al-based composition.

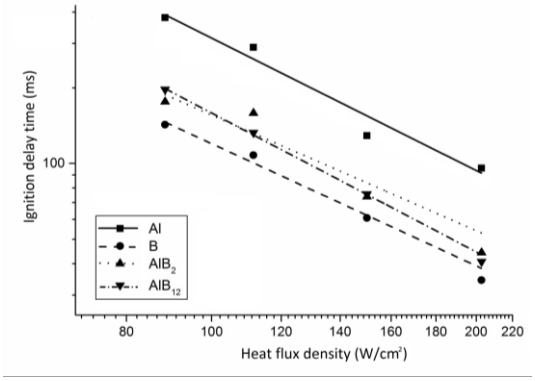

Fig.1. The ignition delay time of the HEM samples vs. the heat flux density.

REFERENCES

[1] D. Sandaram, V. Young, V. E. Zarko, "Combustion of aluminum nanoparticles (review)," Combust. Explo. Shock+, vol. 51, no. 2, pp. 37-63, 2015.

[2] V. Ao, Tsz.-Kh. Chzhou, Tsz.-Ch. Lyu, V.-Tsz. Yan, Yu. Van, Kh.-R. Li, "Kinetic model of single boron particle ignition based upon both oxygen and $(BO)_N$ diffusion mechanism," Combust. Explo. Shock+, vol. 50, no. 3, pp. 21-31, 2014.

[3] K.-L. Chintersingh, M. Schoenitz, E.L. Dreizin, "Oxidation kinetics and combustion of boron particles with modified surface," Combust. Flame, vol. 173, pp. 288-295, 2016.

[4] G. Young, K. Sullivan, M.R. Zachariah, K. Yu, "Combustion characteristics of boron nanoparticles," Combust. Flame, vol. 156, pp. 322-333, 2009.

* The work was supported by RFBR, project number 20-03-00588.

STABILITY LIMIT, RADIATION EFFICIENCY AND CO/NO_X EMISSION OF RADIANT BURNERS: STATE-OF-THE-ART*

A.S. MAZNOY[1]

[1]*Tomsk Scientific Center SB RAS, Tomsk, Russia*

Gas-fired radiant burners are widely used for heating industrial premises, as well as for drying and thermal processing of materials. In the last decade, the use of radiant burners has been increasing for: (i) domestic heating devices such as water boilers or gas kitchen stoves, (ii) thermoelectric (TE)- and thermophotovoltaic (TPV)-based power generators, (iii) appliances for clean burning of low-calorific gases, bio-gases, bio-syngases. Over recent years, the new design of radiant burner was proposed by a collaborative team from Tomsk Scientific Center SB RAS, Far Eastern Federal University and Khristianovich Institute of Theoretical and Applied Mechanics SB RAS [1–4]. The new burner is operated in the internal combustion mode, when the combustion reactions is aerodynamically stabilized in the cavity of annular cylindrical burner made from intermetallic alloy with advanced high-temperature properties.

The most important characteristics of radiant burners are stability limits, radiation efficiency, CO and NO_X emission, as well as fuel-interchangeability potential. In order to evaluate the prospects of the new burner a comprehensive literature survey was performed. As a result of the review, the operational mode of any radiant burner can be represented by a diagram in the coordinates «*firing rate* [kW/m^2]»-«*equivalence ratio*» (Fig.1). The A-B-D-F-G-A domain is of interest, in which the burner works in the stable radiant combustion mode and the emission of CO and NOx meets a regional eco standard. The eco-radiant mode is limited by: the lift-off limit on the left, thermal limit (AC isotherm) at the top, either increased CO/NOx emission or flash back limit on the right, and increased CO emission at the bottom. The design of the burner significantly affects the flash-back limit and CO/NO_X emission. The material used determines the maximum temperature for the long-term operation, i.e. thermal limit of the burner. However, the lift-off limit seems to be a universal characteristic for all types of radiant burners and is determined by the ratio of the fresh mixture flow rate to the laminar burning velocity. As for the requirements defined by environmental standards, the area of the eco-radiant mode expands when burning hydrogen-rich fuels or synthesis-gas blends and decreases when burning biogas. There is no the best burner over all operational parameters. Some burner' designs provide lower emissions, but radiation efficiency is decreased and stable range parameters are narrowed. The new burner design is the best in terms of stability range and radiation efficiency, but CO/NO_X emission is increased. Oral presentation will discuss all observations in detail.

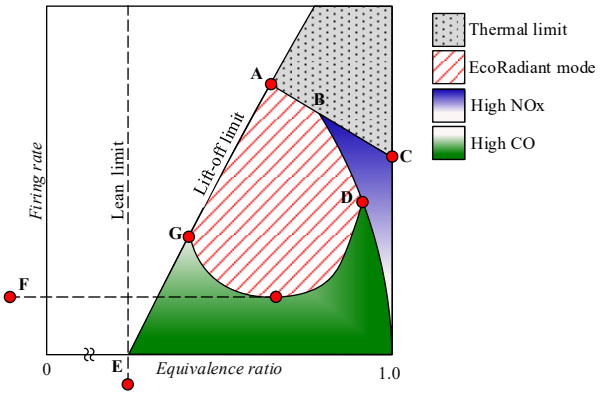

Fig.1. Diagram of combustion modes of radiant burners.

REFERENCES

[1] R. Fursenko, A. Maznoy, E. Odintsov, A. Kirdyashkin, S. Minaev, K. Sudarshan, "Temperature and radiative characteristics of cylindrical porous Ni–Al burners," Int. J. Heat. Mass. Transf., vol. 98, pp. 277–284, 2016.

[2] A. Maznoy, A. Kirdyashkin, S. Minaev, A. Markov, N. Pichugin, E.Yakovlev, "A study on the effects of porous structure on the environmental and radiative characteristics of cylindrical Ni-Al burners," Energy, vol. 160, pp. 399-409, 2018.

[3] A. Maznoy, A. Kirdyashkin, V. Kitler, N. Pichugin, V. Salamatov, K. Tcoi, "Self-propagating high-temperature synthesis of macroporous B2+$L1_2$ Ni-Al intermetallics used in cylindrical radiant burners," J. Alloys Compd., vol.792, pp. 561-573, 2019.

[4] R. Fursenko and A. Maznoy, "A simple model with detailed chemistry for estimation of NOx and CO emission of porous burners," Combust. Theory Model, 2019.

* The work was supported by Russian Foundation for Basic Research (grant № 20-38-70119)

RICH PREMIXED HYDROGEN/AIR OSCILLATORY FLAMES: DETAILED MODELLING AND MODEL REDUCTION*

VIATCHESLAV BYKOV[1], *SUDHI SHASHIDHARAN*[1], *ETELE BERSZANY*[1], *VLADIMIR GUBERNOV*[2], *ULRICH MAAS*[1]

[1]*Karlsruhe Institute of Technology, Institute of Technical Thermodynamics, Engelbert-Arnold-Strasse 4, Geb.10.91, 76131 Karlsruhe, Germany*

[2]*I.E. Tamm Theory Department, P.N. Lebedev Physical Institute of Russian Academy of Sciences, 53 Leninskii prosp., Moscow 119991, Russian Federation*

The appearance of different dissipative structures emerging as a result of oscillatory diffusive-thermal instabilities are observed in experiments for various fuel-air mixtures mostly with Lewis numbers greater than one (see e.g., [1]), which include pulsating axial, radial, drumhead modes, spirals, target, mixed mode and chaotic pulsations. Theoretical study and quantitative modelling of such complex spatio-temporal regimes with the detailed reaction and diffusion mechanisms is a challenging task [2]. We have recently shown [3] that even for a one-dimensional model characteristics of pulsating regimes predicted by using different reaction mechanisms are sensitive to the choice of mechanism and may differ significantly especially for elevated pressures. This makes the phenomenon as extremely important which can be considered for further development and validation of detailed and reduced reaction models. The latter can be efficiently applied for numerical computational studies. Therefore, one dimensional models to describe the onset of pulsating instabilities and influence of detailed kinetic models are in the focus of the current study.

Mechanism	Ref.	Comment	symbol/Fig. 1
O'Conaire	[4]	no change needed	+
ELTE	[4]	OH(*hv*) is eliminated	*
Keromnes	[4]	C-.., OH(*hv*) removed	◇
San Diego	[4]	no change needed	△
Warnatz	[4]	no change needed	□
GRI	[4]	C-.. are eliminated	○

Table 1: Considered mechanisms with references and information regarding the implementation for the considered combustion regime.

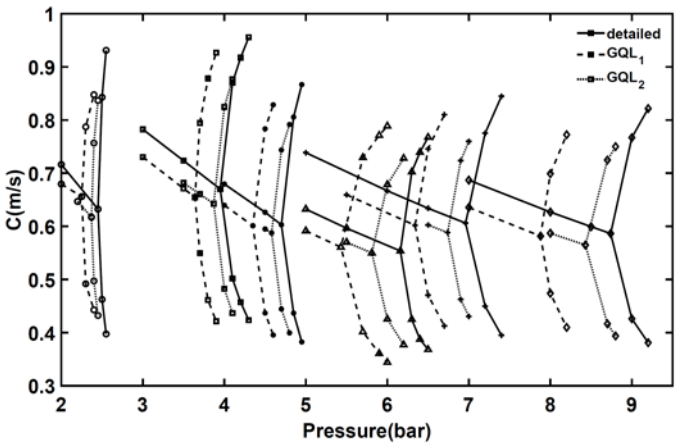

Fig.1. Bifurcation diagram [3] of H_2 / O_2 / N_2 combustion system in the pressure and flame velocity C plane with all detailed and reduced models for the onset of flame pulsations. Symbols correspond to different mechanisms and are provided in Tab. 1.

Figure 1 illustrates and summarizes the main results, where different detailed (Tab. 1) and reduced (e.g. 4D Global Quasi-Linearization (GQL) reduced chemistry, see e.g., [4] for GQL_1 and GQL_2) are considered to address onset of pulsations in the rich hydrogen/air flames. The figure shows how a number of well-established and validated hydrogen combustion mechanisms performs to reproduce the onset (bifurcation) of oscillations. Although the flame velocity is reproduced relatively good, the scatter for the critical pressure of about 7 bar is observed and reported. However, the accuracy of the GQL reduced models, which is much less than the differences between detailed mechanisms, signifies that the GQL reduced chemistry is capable of accurately predicting near limit behavior in rich hydrogen/air systems in a wide range of system parameters.

REFERENCES

[1] E. W. Christiansen, C. K. Law, C. J. Sung, Steady and pulsating propagation and extinction of rich Hydrogen/Air Flames at elevated pressures, Combustion and Flame 124 (2001) 35-49.

[2] G. Goyal, U. Maas, J. Warnatz, Simulation of the Behavior of rich hydrogen-air flames near the flammability limit, Combust. Sci. and Tech. 105 (1995) 183-193.

[3] A. Korsakova, V. Gubernov, A. Kolobov, V. Bykov, U. Maas, Stability of rich laminar hydrogen-air flames in a model with de-tailed transport and kinetic mechanisms, Combustion and Flame 163 (2016) 478-486.

[4] V. Bykov, C. Yu, V. Goldshtein, U. Maas, Model reduction and mechanism comparison of hydrogen/oxygen auto-ignition, Proceedings of the Combustion Institute 37 (2019) 781-787.

* The work was supported by the DFG-RFBR grant number 17-53-12018 (RFBR) / BY 94/2-1 (DFG).

COMBUSTION OF MULTICOMPONENT MATERIALS AS A WAY OF ENERGY PRODUCTION AND MATERIALS UTILIZATION*

K. LARIONOV[1], K. SLYUSARSKY[1], A. GROMOV[2]

[1]National Research Tomsk Polytechnic University, Tomsk, Russia
[2] National University of Science and Technology MISIS, Moscow, Russia

With the stable growth of large cities in various countries of the world, there is an intensive increase in the volume of municipal solid waste (MSW). According to [1], in 2016, the global value of solid waste production was about 2 billion tons, of which 11% is utilized by direct combustion. According to IEA [2], in 2016 the share of generated electric energy using solid waste was 0.43% (in energy units - 108,407 GW·h). At the same time, over the past 25 years, there has been an almost continuous increase in the consumption of solid waste as the main type of fuel used for the production of electrical energy. Taking into account the data [1], 33% of the total mass of MSW are non-food waste, which can also be used as fuel RDF and SRF [3] for the production of electrical energy [4].

Nowadays, thermal conversion of MSW is one of the most effective methods of disposal with a relatively low environmental impact [5]. The most common problems of this process are the heterogeneity of the fuel composition and its technical characteristics [6], affecting the ignition temperature, stability of the combustion mode, completeness of combustion, the concentration of the formed gas-phase products [7] and the kinetics of process in general [8].

This paper presents a comparison of the results of an experimental study of the conditions and characteristics of oxidation, ignition and combustion of solid non-food waste in a thermogravimetric analyzer and a combustion chamber, the heating conditions in which are similar to real fuel-burning equipment.

Oxidation was studied by means of thermogravimetry in the temperature range 25-1000 °C at 10 °C/min heating rate in oxidizing environment. Kinetic characteristics were calculated by the Coats-Redfern method. The ignition and sequential combustion of non-food solid waste pellets was studied in experimental incinerator at temperature range of 600-800 °C using high-speed video imaging.

Sawdust and skin sample had the lowest value of the initial temperature of intense oxidation (250 and 255 °C, respectively). The shortest time of the complete oxidation process (T_f=18.5 min) was obtained for a textile sample, which is usually associated with high reactivity. The maximum ignition delay times were obtained for fabric and rubber samples (11.3 and 12.8 s), the maximum flaming combustion times – for rubber and plastic (37 and 41 s), the maximum complete combustion times – for leather and rubber (200-285 s). The time of ignition, combustion and complete burnout of samples decreased with increasing temperature of the environment up to 800 °C. A phenomenological assessment of the correlation between parameters of the oxidation in thermal analyzer and ignition in the furnace was made. The determination coefficient values of such dependences were quite low (0.40-0.65) allowing only rude evaluation. The best correlations were obtained for burnout characteristics dependences on properties of chemical reactions which could were defined by means of thermogravimetry.

REFERENCES

[1] *Kaza S., Yao L., Bhada-Tata P., Van Woerden F.// What a Waste 2.0: A Global Snapshot of Solid Waste Management to 2050.* - The World Bank. Washington. 2018.
[2] Key World Energy Statistics, 2017. International Energy Agency. https://www.iea.org/statistics/ (accessed 23 march 2020).
[3] *Białowiec A., Pulka J., Stępień P., Manczarski P., Gołaszewski J. //* Waste Manage. – 2017. – 70. – 91-100.
[4] *Yang H.T., Xie J., He F., Mei S., Fang D.* // J. Chem. Eng. Jpn. – 2016. – 49 (11). – 967-972.
[5] *Sakawi Z. //* J. Appl. Sci. Environ. Sanit. – 2011. – 6 (1). – 29-38.
[6] *Zhou H., Meng A., Long Y., Li Q., Zhang Y. //* J. Air Waste Manag. Assoc. – 2014. – 64 (5). – 597-616.
[7] *Cheng H., Hu Y. //* Bioresour. Technol. – 2010. – 101 (11). – 3816-3824.
[8] *Nzioka A.M., Kim M.G., Hwang H.U., Kim Y.J. //* Waste and Biomass Valorization. – 2019. – 10 (6). – 1679-1691.

* This work was supported by grant from the President of the Russian Federation (grant №. NSh-2513.2020.8).

NUMERICAL SIMULATION OF COMBUSTION PROCESS IN ROTARY RANGE EXTENDER WITH HYDROGEN DIRECT MULTIPLE INJECTION*

S.D. ZAMBALOV[1]

[1]Tomsk Scientific Center SB RAS, Tomsk, Russian federation

The range extender is used for recharge batteries of electric vehicles in order to increase driving range. The range extender typically uses a combination of an internal combustion engine and an electric generator. In this study the rotary engine was studied because this type of engines has valuable advantages: low weight and dimensions, large specific power and excellent engine balance [1]. The choice of the fuel type is crucial for the range extender due to the world emission concern. Application of the hydrogen as an energy carrier can provide near-zero emissions of carbon and reduced emission of nitrogen oxides (NOx) [2]. The multiple direct injection of hydrogen was investigated [3]. Three types of injection with different injection pressure, duration, timings and quantity of injections were analyzed.

The alternative method for the quantitative analysis of the process parameters was proposed. Instead of the volumetric region where the averaged values can be calculated we created a probe surface offset from the flame front at the distance of *s* as it is shown in Fig. 1a. The probe surface was split into two sub-surfaces from leading (L) and trailing (T) spark plugs. The flame offset distance *s* was defined with using Göttgens et al. [4] correlation for the preheat zone thickness in hydrogen flames.

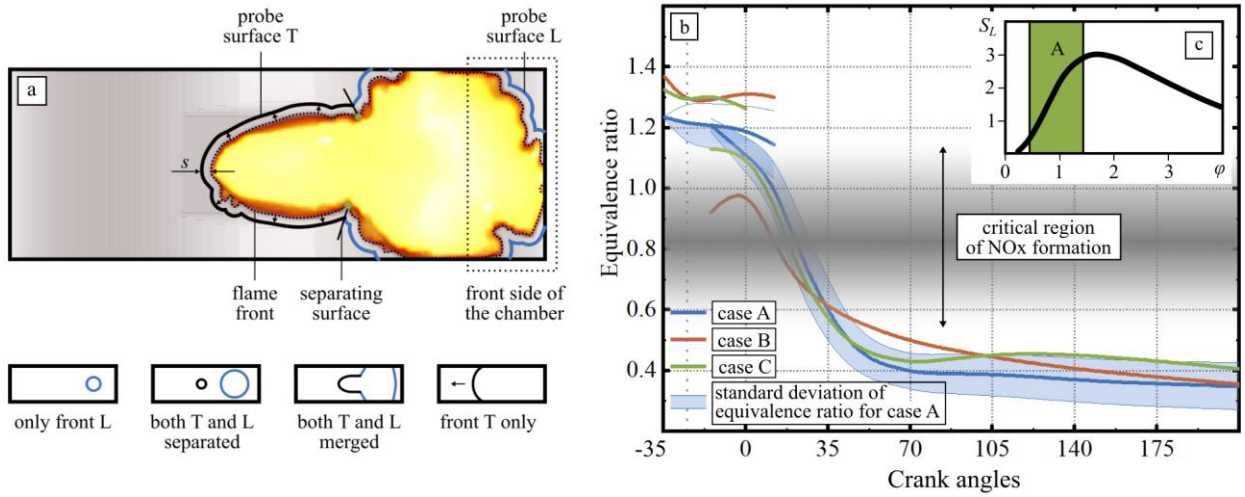

Fig.1. Method of flow parameters estimation ahead of the flame front and equivalence ratio evolution.

The evolution of the averaged equivalence ratio (φ) near the L and T flame fronts during is shown in Fig. 1b. The hydrogen concentration near the L and T is different. The dependency of the laminar flame speed S_L to the φ is shown in Fig. 1c. The range of the maximum φ variation is shown with the region A. In this region the dependency can be approximated fairly well by a linear and the relation between S_L and φ. The flame fronts initiated by the L and T are characterized by significantly different parameters which is conditioned not only by different locations and ignition timing delay but also by local hydrogen distribution. The considered injection system provides a rich mixture composition near the LSP and a stoichiometric to lean composition near the TSP. The direct multiple injection strategy allows using higher integral equivalence ratio up to 0.8 that results in larger power density in combination with low NOx emission.

REFERENCES

[1] В. С. Бениович, Г.Д. Апазиди, А.М. Бойко, Ротопоршневые двигатели, Москва: Машиностроение, 1968

[2] F. Amrouche, P. Ericson, J. Park, S. Varnhagen, “An experimental investigation of hydrogen-enriched gasoline in a Wankel rotary engine”, International journal of hydrogen energy, vol. 39, pp. 8525–34, 2014.

[3] B.D. Gowda, T. Enchekki, “Complex injection strategies for hydrogen-fuelled HCCI engines”, Fuel, vol. 97, pp. 418-427, 2012.

[4] J. Göttgens, F. Mauss, N. Peters, “Analytic approximations of burning velocities and flame thickness of lean hydrogen, methane, ethylene, ethane, acetylene and propane flames”, International symposium on combustion, vol. 24, pp. 129-135, 1992.

* The work was supported by RFBR 20-38-70119

FILTRATION COMBUSTION OF NATURAL GAS FOR FORMING DENSE REFRACTORY CERAMICS*

A.I. KIRDYASHKIN[1], R.M. GABBASOV[1], V.D. KITLER[1], A.S. MAZNOY[1], R.V. FURSENKO[2]

[1]*Tomsk Scientific Center SB RAS, Tomsk, Russia*
[2]*Khristianovich Institute of Theoretical and Applied Mechanics SB RAS, Novosibirsk, Russia*

Progress in modern engineering is largely determined by the use of dense functional ceramics based on oxides (Al_2O_3, MgO), nitrides (Si_3N_4, AlN), oxynitrides (alones, sialons), carbides (SiC, TiC) and a number of other refractory inorganic compounds. Due to the combination of extreme strength characteristics, heat and corrosion resistance, these materials are widely used for chemical, energy, and aerospace equipment, and also as protective shields, cutting tools, etc. At present the calcination of powders in electric furnaces at temperatures above 1900K is often used to obtain dense ceramic materials with a melting point above 2300K. This process is accompanied by significant costs for electricity and sophisticated equipment, which leads to an increased cost of final products.

An efficient high-temperature heat treatment of materials uses heat from filtration combustion of gases (FCG). The term "FCG" means the wave exothermic transformation of gases during their filtration in porous condensed media. Compared with open gas flames, FCG waves are distinguished by the high power density (due to the increased rate of fuel combustion), the ability to concentrate thermal energy (due to the presence of a condensed medium), and the ability to achieve super-adiabatic combustion temperatures (due to heat recuperation).

A reactor, thermocouple and spectrometric temperature measurement methods were used to study the dynamics of heating of solids during the combustion of a fuel blend (natural gas (92 vol% CH4) + air (21÷35 vol% O_2)) covered with spherical granules ZrO_2 (with a diameter of ϕ = 5.8 mm and ϕ = 2mm). Varying the composition of the fuel blend (φ = 0.40÷3.00) and the specific thermal combustion power (w = 24÷300 W/cm^2) have been found to make it possible to control the propagation velocity of combustion from U_c = - 0.18 mm/s (minus sign is combustion against the filtration flux) up to U_c = + 0.12 mm/s (plus sign is combustion along the flux) and the maximum heating temperature of materials in the range Tsm = 1230÷2210K. The Tsm values were shown to substantially depend on the U_c value, the filtration rate of the mixture and were largely determined by the enthalpy effects of the condensed medium. The filtration combustion rate limits and the optimal heating conditions were determined for the ceramic structures with a characteristic size D >> ϕ.

Powder briquettes were covered with granules to conduct test sintering and synthesis of refractory substances. According to the data obtained, the heat treatment of briquettes in the wave and behind the FCG wave at Tsm = 1900÷2200 K for 0.3÷1.0 hours provides sintering of Al_2O_3 and MgO samples (porosity reduction from 50% to 10%) and almost complete conversion a powder mixture of Si + 30wt.% C into a composite SiC-Si_2N_2O.

* This work was partially supported by the Russian Foundation for Basic Research (project no. 18-48-700037) and performed as a part of the state task for the Tomsk Scientific Center (project no.0365-2019-0004).

CAPILLARY PROCESSES DURING THE FORMATION OF POROUS NI-AL MATERIALS IN THE SHS MODE[1]

V.D. KITLER, A.I. KIRDYASHKIN

[1]*Tomsk Scientific Center SB RAS, Tomsk Russia*

Ni-Al intermetallic alloys are characterized by the combination of such unique properties as heat resistance, strength, ductility and a number of other important physical and chemical properties. They are widely used in mechanically stressed elements of aerospace, heat-energy and chemical equipment operating in corrosive high-temperature media. Porous materials based on such alloys are very promising for chemically resistant filters, high-temperature heat exchangers and infrared emitters of gas burners. Practical application of the latter is often restricted by the complexity of preparing NI-AL materials with the necessary combination of phase composition and pore morphology.

The most efficient method for obtaining porous intermetallic compounds is self-propagating high-temperature synthesis (SHS). SHS provides an autothermal reaction for the synthesis of compounds and sintering of materials in a special powder reaction mixture in a one stage. A peculiarity of SHS is a strong dependence of the process dynamics on the effects of capillary redistribution of melting components in a reaction mixture: melt spreading over the surface of solid particles, Marangoni convection. These effects have not yet been fully studied in detail.

The goal of this work is to experimentally study the combined effect of the initial structure of a mixture and capillary processes on the reaction dynamics and the product formation during the SHS of Ni-Al materials. The initial structure of the reaction mixture was varied by changing its porosity (P = 10÷60%), the concentration of Al (CAl = 13÷ 0 wt.%), the diameter of Ni, Al particles (d Ni = 10÷100 μm, d Al = 10÷1000 μm) and the form of Al (particles, plates). The reaction conversions were recorded with high-speed video at the macro-and micro-levels of the reaction mixture, and were controlled by thermocouple measurements, hardening operation, and the physical and chemical analysis of the products.

The main results:

- The active conversion of the mixture was shown to take place in the SHS wave when Al starts melting. Two qualitatively different SHS modes were found, which depended on the particle size ratio of the components. Mode 1: d Al >> d Ni . The reaction mixture is a system of large Al particles surrounded by porous layers of small Ni particles. At the macroscopic level, conversions are divided into two consecutive stages. Fast dissolution of Ni particles in the Al melt, primary capillary spreading of the liquid solution through the Ni layer and an exothermic heterogeneous reaction simultaneously take place at the first stage (t≈1÷3 ms). Dissolution occurs with the participation of Marangoni convection, which stimulates the transport of a part of the Ni layer from the Ni-AL contact boundary to the melt. At the second stage, a relatively slow (t≈100÷200 ms) capillary redistribution of the liquid solution over the Ni layer and the system overreaction are observed. The stepwise temperature SHS-wave profile, which corresponds to the microscopic stages of the system transformation, is recorded at the macroscopic level. By varying porosity, the maximum SHS propagation velocity is observed for the conditions when the initial volume of pores and aluminum is equal. The pores of the synthesized Ni-Al materials are mainly isolated: the shape of large pores follows the contours of initial Al particles, and the size of small pores is equal to the diameter of initial Ni particles. Mode 2: d Al ≈ d Ni . The reaction mixture is a relatively homogeneous mixture of Ni and Al particles. At the microscopic level, there is a one-stage process of spreading liquid Al particles over the Ni surface (t≈1ms) followed by the heterogeneous reaction. A monotonic temperature profile of the SHS wave is recorded at the macroscopic level, and the wave propagation velocity monotonically increases with decreasing porosity. In the region of Π > 20%, open porosity of the final product is observed.

- The SHS of the laminate material was conducted in the form of soldered plates from a dense Ni-Al alloy (C Al = 16 wt.%, the plate thickness was 1.5 mm), separated by open voids. The synthesis was conducted in a system of alternating layers of dense Al and porous powder layers of Ni. The self-sustaining reaction process consisted of consecutive stages of Al melting followed by melt spreading over Ni layers and an exothermic reaction. The material obtained can be used as highly permeable heat-resistant heat exchangers and infrared emitters.

1 This work was partially supported by the Russian Foundation for Basic Research (project no. 18-48-700037) and performed as a part of the state task for the Tomsk Scientific Center (project no.0365-2019-0004).

COUPLING MODEL OF THE COMBUSTION SYNTHESIS OF COMPOSITE WITH REINFORCING INCLUSIONS[1]

ANNA KNYAZEVA

[1]*Istitute of Strength Physics and Materials Science SB RAS, Tomsk, Russia*

The stress-strain state plays a important role in the synthesis of new materials. The phenomenon of a change inthe rate and staging of phase formation with a change in the stress-strain state is known and is used to control the process. However, the features of phase formation during the synthesis of composites in different states are poorly studied. In this paper, for the first time, a coupled mathematical model is formulated (taking into account the interrelation between the processes of different physical nature - thermal, chemical and mechanical), taking into account the staged nature of the transformation for systems of the type Al + Cr2O3 + Ti; Al + Fe2O3 + Ni for conditions of plane stress and plane strain state. The first situation is realized during the synthesis of a composite in a layer on a thin substrate, which takes heat from the reaction zone. The second situation can be realized during the reaction in a mixture of reagents in the gap between inert materials that prevent deformation in the direction perpendicular to the direction of reaction propagation of the front. In the framework of the thermodynamics of irreversible processes, relations for the chemical affinity of the main reactions are established, taking into account the presence of stress-strain state. For some limiting cases, a traveling wave type solution is constructed using the method of joint asymptotic expansions. The stability of the reaction front to thermomechanical disturbances was studied taking into account heat losses.

1 This work was supported by the Russian Foundation for Basic Research, grant No. 20-03-00303

EXPERIMENTAL OBSERVATION OF THE INSTABILITY MODE IN THE COMBUSTION WAVE BY THE DIFFERENTIAL CHRONOSCOPY METHOD *

P.Y. GULYAEV[1], *A.A. GRIGORYEVSKAYA*[2], *V.I. JORDAN*[2]

[1]*Yugra State University, Khanty-Mansiysk, Russian Federation*
[2]*Altai State University, Barnaul, Russian Federation*

The aim of this study is to report on the observation of the spin instability mode during the propagation of a combustion wave in a mixture of Ni and Al powders. The paper presents the results of temperature and velocity measurements during the propagation of a SHS combustion wave [1], obtained using a special television micropyrometer (1200 x 800 pixels) with high spatial (5.85 μm / pixel) and resolution time (1 ms / frame) [2]. High accuracy of temperature measurement was ensured by using the new spectral-light pyrometry method (Patent RUS 2616937) from 800 to 2000 ºC, with an error of less than 1% [3].

For processing the experimental video data, the differential chronoscopy method (DCS-map) was used [4], which allows to select the image of the combustion front in the form of a continuous line with nodal points where the spin instability of the combustion wave is observed. An example of a DCS-map is shown in Figure 1.

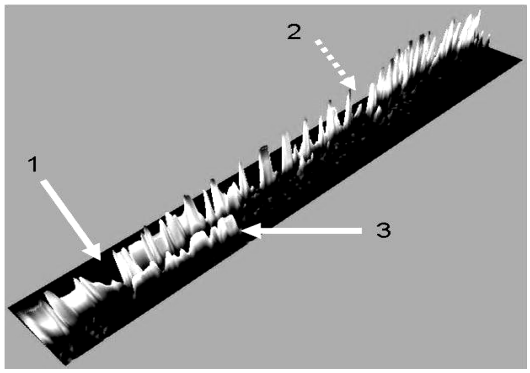

Fig.1. DCS-map of spin instability: 1- node of “strong” instability; 2 - node "weak" instability; 3 - a branch of a part of the combustion front in the direction of the opposite spin.

The appearance of nodal points of spin instability is a sign of a transition from a thermal instability mode to a diffusion instability mode of a combustion wave, which is explained by the phenomenon of thermal hysteresis of the combustion wave velocity from the synthesis temperature [4].

REFERENCES

[1] D.A. Garkol', P.Ju. Guljaev, V.V. Evstigneev, A.B. Mukhachev, “A new high-speed brightness pyrometry method to investigate self-propagating high-temperature synthesis,” Combustion, Explosion, and Shock Waves, vol. 30, no. 1, pp. 72–76, January 1994.

[2] M.P. Boronenko, A.E. Seregin, K.G. Poluhina, P.Y. Gulyaev, “Increasing the noise immunity of optical-electronic systems based on video cameras with an optical converter,” Journal of Physics: Conference Series, vol. 643, no.1, pp. 012028, 2015.

[3] A.V. Dolmatov A.V., I.P. Gulyaev, V.I. Iordan, “Control of dispersed-phase temperature in plasma flows by the spectral-brightness pyrometry method,” IOP Conference Series: Materials Science and Engineering, vol. 110, pp. 012058, 2016.

[4] K. Borodina, S. Sorokina, N. Blinova, M. Boronenko, P. Gulyaev, “Thermal analysis of reaction producing KxTiO2,” Journal of Thermal Analysis and Calorimetry, vol. 131, no. 1, pp. 561–566, 2018.

[5] P. Gulyaev, “Temperature hysteresis in the unstable combustion mode of SHS: Experiment with high-speed micro-pyrometry,” Journal of Physics: Conference Series, vol. 1115, no.4, pp. 042026, 2018.

* The work was supported by RFBR according to the research projects No. 18-08-01475, 18-41-220004.

CONNECTION OF THE COMBUSTION PROCESS OF SHS SYSTEM "TI-CO-N" WITH THE STATE DIAGRAM

O.A. SHKODA

Tomsk Scientific Center SB RAS, Tomsk, Russia

Self-propagating high-temperature synthesis (SHS) of the Ti–Co–N system was investigated in the work and the relationship of combustion parameters with the state diagram was found. The zone of chemical reactions for combustion is a solid-liquid melt, which receives nitrogen gas corresponding to the"L-S" melt of the state diagram. All the obtained parameters of the combustion system under different initial conditions characterize the behavior of the high-temperature chemically active solid-liquid environment [1-3]. The work goal is to analyze the variation of different initial parameters, to clarify the mechanism of phase formation during the reaction, the relationship of the phase composition of the combustion product with the type of intermediate unstable nitrides [4] formed in the combustion wave and the diagram of the system state.

SHS of samples (diameter 20 mm, weight 16 g.) of bulk density and pressed samples was carried out in a constant pressure reactor. The relative density varied from 0.22 to 0.38. The initial composition changed in the ratio: Co/Ti % weight. within 5/50 values. The final products were studied using RFA analysis. Changes in the concentration of the environment, the rate of nitrogen flow, and the rate of combustion of samples were obtained by changing the initial parameters (initial concentration of substances, initial density of samples, diameter, height of samples, etc.)

When the powder of one metal is heated to a temperature above solidus, a pure melt is formed, which prevents the penetration of nitrogen to the reaction zone. The vortex motion that delivers nitrogen gas to the reaction zone is formed in a multi- density medium at high temperatures. Regardless of the start composition, dispersity of powders, the density of the sample, the values of the combustion parameters as completeness of conversion (η), the maximum temperature of combustion, the amount of stoichiometric absorbed of nitrogen, obtained in the experiment lie in the region between the lines of solidus and liquidus, i.e. in the area of solid-liquid suspension, or are define by the area. The values for the fullness of the transformation filled a space that completely coincided with the space bounded by the liquidus and solidus lines. This means that the SHS processes take place only within the solid-liquid melt "L-S". Each trajectory corresponds to the same size of solid particles in the "L-S" melt, as spaced at the same distance from the liquidus line, as shown in figure 1.

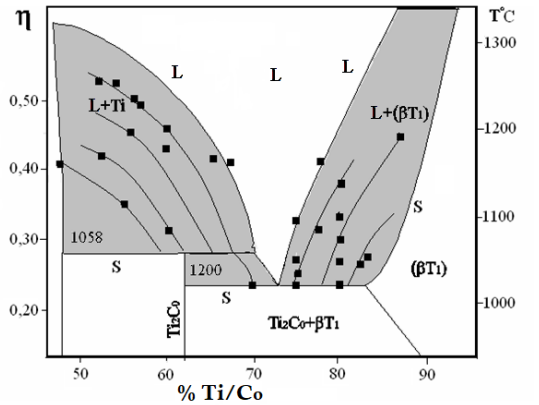

Fig.1. Диаграмма плавкости системы «Ti-Co», совмещенная с «облаком» экспериментальных данных

Acknowledgements: The blessed memory of Raskolenko Larisa G. whose ideas are the basis of this work. Peleneva S. P. for assistance in the experiments.

REFERENCES

[1] Биниология, симметрология и синергетика в естественных науках/ Папин Ю.С., Дмитриев А.Н. , Пономарев Е.А. и др.//Труды IV междунар. конф. – Тюмень:ТюмГНГУ. – 2004.-С.52 – 59.

[2] Расколенко Л.Г. Отображение состояний n – мерной химически активной среды «металл – металл - азот» в двумерных пространствах// Труды IV междунар. конф. – Тюмень:ТюмГНГУ. – 2004.-С.52 – 56.

[3] Круглова Н.В., Расколенко Л.Г., Максимов Ю.М. Самораспространяющийся высокотемпературный ситенз трехкомпонентных систем на основе титана и металлов III, VI, VIII групп с азотом. – Известия вузов. Цветная металлургия, 2002, № 2, с. 55-59.

[4] Расколенко Л.Г., Герульский А.Ю. Интерметаллидные соединения WAl4, WAl3, W3Al7, WAl2 в продуктах горения СВС системы «Al-W-N». Неорганические материалы. 2008, № 1, стр. 1-10.

This work was carried out within the RFBR grant 14-03-00666A

ESTIMATION OF TIME PARAMETERS OF COAL PARTICLE COMBUSTION IN AIR FLOW UNDER THERMAL RADIATION

A.A. PONOMAREVA[1,2], *K.A. TCOI*[2]

[1]*Institute of Applied Mathematics FAB RAS, Vladivostok, Russia*
[2]*Far Eastern Federal University, Vladivostok, Russia*

Although renewable energy sources are becoming increasingly important for future energy systems, coal combustion is still the dominant source for power generation in some regions. Nowadays it is necessary to perform the modernization of outdated power plants in order to decrease the emissions of various hazardous trace elements and to implement a new effective coal combustion technology. For such modernizations, novel construction approaches and new materials for burners are often used. The study of effective combustion of fossil fuels is important for finding optimal regimes for burning coal particles in various domestic and industrial boilers and power plants.

In this work, thermal decomposition and time parameters of a coal dust combustion were studied. The numerical investigations were performed using standard formulas and some simple models like the shrinking core model and etc.. Experiments were carried out using a laboratory-made setup described in [1]. In the laboratory-made setup the thermal radiation used for coal particles decomposition and ignition was emitted by porous burner during propane/butane combustion. The porous cylindrical Ni-Al alloy burner prepared by self-propagating high-temperature synthesis was used as external heater [2]. Such type of heater was chosen because of its high radiative and heat flux density [3].

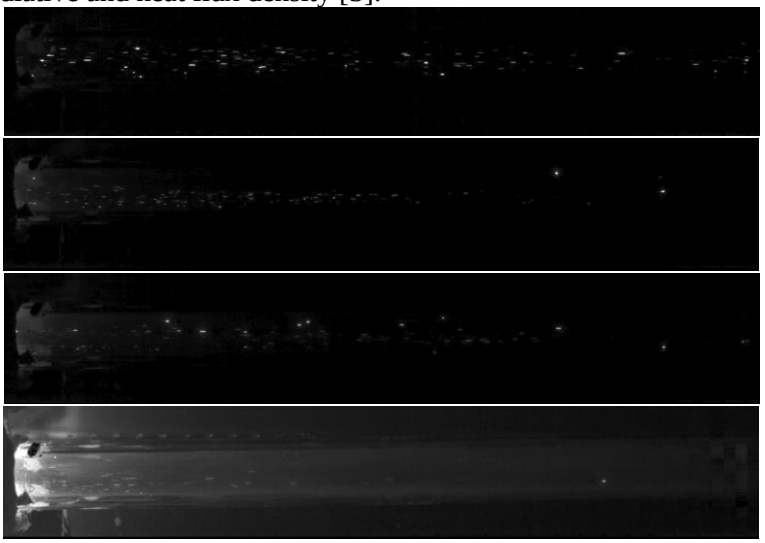

Fig.1. Images of ignited coal particles recorded by the high-speed camera in the outlet of porous burner in dependence of the calculated heat release of the internal surface of the burner: a – 395 kW/m^2, b – 448 kW/m^2, c –475 kW/m^2, d – 1052 kW/m^2.

Of particular interest is the prediction of char properties, such as composition, surface areas, and morphology, since these impacts on char combustion. This information is also important for the gasification systems development [4]. The processes of devolatilization, char formation, and heterogeneous oxidation depend on temperatures and a heating-up rate. In this work we carried out the numerical calculations of burnout times and heating-up times of particles before ignition. All calculations were based on experimental parameters and results.

This work was supported financially by the Ministry of Science and Higher Education of the Russian Federation (project №075-15-2019-1878).

REFERENCES

[1] A.A. Ponomareva, K.A. Tcoi, S.N. Mokrin, .K.A. Shtym, "A laboratory setup based on porous burner for coal particles combustion investigation", J. Phys.: Conf. Ser. 1369, 012041, 2019.

[2] Patent RU 2640305 – S.S. Minaev, A.N. Gushchin, K.A. Tcoi, D.A. Gushchin, A.I. Kirdyashkin, K.A. Shtym, A.S. Maznoi, D.A. Filippov, 2017.

[3] R. Fursenko, A. Maznoy, E. Odintsov, A. Kirdyashkin, S. Minaev and K. Sudarshan, "Temperature and radiative characteristics of cylindrical porous Ni–Al burners", Int. J. Heat and Mass Transfer, vol. 98, pp. 277–284, 2016.

[4] A.V. Lesnykh, K.A. Shtym, S.V. Golovaty, "Conditions of effective use of gas generators in the industrial energy of the Primorsky region", Vologodskie chteniya, vol. 80, pp. 179-181, 2012.

EXPERIMENTAL DETERMINATION OF THE OPTIMAL FOCUSING ZONES FOR LASER IGNITION OF BUTANE-AIR COMBUSTIBLE MIXTURES*

Y. V. ANISHCHANKA[1], *E. Y. LOKTIONOV*[1]

[1] *Bauman Moscow State Technical University, Moscow, 105005, Russia, stcpe@bmstu.ru, +79037869566*

Laser ignition is widely discussed and investigated subject today. Recently, in this area of research significant progress has been made. Though laser spark plugs already have practical application, nevertheless the main aspects of ignition of fuel mixtures by means of the laser, for example, the most advantageous position of focus in combustion chamber not fully explored. There are two modes of focusing of laser beam in combustion chamber: focusing in air in the volume of the chamber and focusing on the ablator. Fuel ignition at the first mode of focusing requires high power consumption, increasing the cost and the sizes of laser spark plug, at the second mode of focusing of energy of laser pulse for ignition of fuel it is required 10 times less, however the resource of the ablator is obstacle for realization of this method in practice. Therefore it is necessary to investigate the optimal zone for focusing of laser radiation in which it is possible to realize low energy-intensive ignition and at the same time without destroying the ablator.

In the work results of experiments on ignition fuel mixture (butane based) compositions with various equivalence ratios ($\varphi \sim 0.4$-1.1) and pressures ($p \sim 1$–3 bars) depending on the position of the focus ($l \sim 0$-12 mm) in combustion chamber concerning the ablator are presented. The change in the minimum energy of the laser pulse required foe ignition the fuel mixtures is fixed and also with use shliren's method dynamics development of burning core and propagation of shock wave at laser ignition (1064 nm, 12 ns) was investigated. It was revealed that the optimum zone of focusing of laser radiation where energy of laser pulse accepts the minimum values, was not on the ablator, and in some removal from it.

The received results are of interest to use of laser ignition in the practical purposes.

* The work was supported by the Russian Foundation for Basic Research (RFBR) grant No.18-38-20032.

FABRICATION OF BIOSENSING COATINGS WITH TAILORED FUNCTIONALITY BY USING ATMOSPHERIC-PRESSURE PLASMA POLYMERIZATION

E. MAKHNEVA[1], L. BARILLAS[1], Z. FARKA[2], M. PASTUCHA[2], P. SKLADAL[2], K.-D. WELTMANN[1], K. FRICKE[1]

[1]Leibniz Institute for Plasma science and Technology (INP), Greifswald, Germany
[2]Central European Institute of Technology (CEITEC), Brno, Czech Republic

Various types of biosensors are convenient tools for fast, economic and user friendly analysis of complex biological samples. For stable biomodification of the sensing surfaces, a thin functional layer is required to provide a sufficiently high surface reactivity towards the adopted bioreceptor as well as good stability in the presence of sample matrix.

We report on a novel method for the preparation of thin reactive plasma-polymerized (pp) films, using atmospheric pressure plasmas, for biosensing applications. Our original approach for generating pp films is a versatile, fast and eco-friendly procedure. Three different types of pp films were developed and characterized. Chemical composition, morphology and stability in water of the obtained plasma polymerized films were carefully scrutinized. The pp films provided unique functionality and excellent level of adhesion to the substrates. Furthermore, after an initial thickness loss during washing, which is based on non-polymerized oligomers, prolonged immersion in water (up to 120 h) did not indicate any significant thickness losses or deterioration of the sensing properties.

SPR immunosensors were successfully developed using cost-efficient model pair of AL01 antibody and HSA antigen. The pp films provided an excellent platform for the efficient immobilization of antibody molecules and the obtained immunosensors showed selective and high response towards the analyte, excellent regenerability and level of stability. A limit of detection of 50 ng/mL of HSA was achieved for all of the developed immunosensors. The developed immunosensors provided a linear response in the range of 50 ng/mL to 20 µg/mL concentrations of HSA. Hence, pp film–based immunosensors exhibited performances similar to widely used SAM– or CMD–based immunosensors but with enhanced level of stability and regenerability.

SELF-PROPAGATING HIGH-TEMPERATURE SYNTHESIS OF Si_3N_4-SiC USING FERROSILICIUM AND SHUNGITE*

O.G. Kryukova[1], A.N. Avramchik[1]

[1]Tomsk Scientific Center SB RAS, Tomsk, Russia

A new approach to the synthesis of silicon nitride powders by nitriding multicomponent reaction mixtures containing industrial iron-containing (ferrosilicon) and natural oxide materials (zircon, ilmenite) by the SHS method was developed at the Tomsk Scientific Center of SB RAS [1, 2]. The main advantage of the SHS method is minimal energy costs, since the synthesis is supported by the energy of chemical reactions. The method for obtaining composite powders is based on the silicon nitride reaction during the interaction of Si with nitrogen, which provides the main heat release during the propagation of the combustion reaction wave. This work is a continuation of our studies and is aimed at obtaining the Si_3N_4-SiC composition during the SHS- nitriding of ferrosilicon with the addition of natural oxide materials (schungite).

To estimate the maximum combustion temperature and the equilibrium composition of the products, a thermodynamic calculation of the synthesis of silicon nitride composites during the interaction of ferrosilicon with schungite additives in nitrogen was performed. The TERRA software package was used for calculations [3]. Calculations showed that with an increase in the amount of shungite, regardless of the nitrogen pressure, a slight decrease in the combustion temperature was observed; at adiabatic temperature, silicon nitride was in equilibrium with the dissociation products such as silicon and nitrogen. The composition of the reaction products is represented by the components as follows: Si_3N_4, SiC, Si, SiO_2, Fe, Fe_3C. In addition, SiO is formed, which is in the gas phase.

The mechanisms of the combustion of ferrosilicon in the presence of a natural material (schungite) was revealed for the synthesis of the Si_3N_4–SiC composition. It was shown that the addition of shungite (1–30 wt.%) to the starting "ferrosilicon – schungite" mixture led to a decrease in the nitriding degree of ferrosilicon. This is due to a decrease in the proportion of nitride-forming element in the starting mixture. An increase in the nitrogen pressure from 1.5 to 6 MPa led to an increase in the nitriding degree due to the increased supply of nitrogen to the reaction zone. The minimum sample diameter at which the combustion process takes place was 30 mm.

SHS nitriding of ferrosilicon with the addition of shungite was conducted in the surface combustion mode, as evidenced by the heterogeneous structure of the combustion product. The external layer of the burned samples is the unburned starting material in the form of a "crust". The thickness of the external layer of the sample decreases with an increase in the addition of 20-30% schungite. The macrostructure of the samples is homogeneous, has a light gray color with a greenish tint. It should be noted that an increase in the nitrogen pressure contributes to the decrease in the layer of the unburned starting material (i.e., the "crust" becomes thinner throughout the height of the sample). The phase composition of the synthesis products with the addition of schungite up to 15% both in the central part and in the external layers of the sample is represented by the phases as follows: β-Si_3N_4, SiC, Si_2N_2O, $FeSi_2$, FeSi и α-Fe. The presence of the initial alloy component such as the $FeSi_2$ phase in the combustion products indicates the incompleteness of the nitride formation process. The addition of shungite in an amount of 20% or more results in the formation of the phases as follows: β-Si_3N_4, SiC, Si_2N_2O, FeSi и α-Fe. Thus, it was shown that SHS nitriding of ferrosilicon powders with schungite additives makes it possible to obtain a Si_3N_4-SiC composition of different purity depending on the pressure N_2 and the composition of the starting mixture.

References

1. Chukhlomina L.N., Maksimov Yu.M., Vereshchagin V.I. Self-propagating high-temperature synthesis of composite nitride-containing ceramics. - Novosibirsk: Nauka, 2012.
2. Chukhlomina L.N., Vitushkina O.G., Avramchik A.N. Interaction of ferrosilicon with nitrogen in the presence of zircon and ilmenite concentrates during the SHS process // Russian Journal of Non-Ferrous Metals. - 2011, No. 3. - Pp. 28-32.
3. Trusov B.G. Computer simulation of phase and chemical equilibria, Inzh. Vestn.- 2012, No. 8. - Pp. 1–7. - URL: http://engbul.bmstu.ru/doc/483186.html.

* This work was supported by RFBR (Project No. 16-03-00635 a).

COMBUSTION SYNTHESIS IN MECHANOACTIVATED FeTi+C POWDER MIXTURES*

A.V. BARANOVKSKIY[1, 2], G.A. PRIBYTKOV[1], V.V. KORZHOVA[1], M.G. KRINITCYN[1, 2]

[1]Institute of Strength Physics and Materials Science, Akademicheskii pr., 2/4, Tomsk, 634055, Russia.
[2]National Research Tomsk Polytechnic University, Lenin pr.,30, Tomsk, 634050, Russia.

Metal-matrix composites (MMC) “titanium carbide - iron binder” are widely used as materials of wear resistant coatings and cutting tools because of their relatively lower cost and high mechanical properties [1, 2]. Self-propagating high temperature synthesis (SHS) seems to be highly productive and economical method to obtain MMCs from titanium, carbon and iron powder mixtures [3]. However, the incompleteness of TiC chemical reaction in SHS products and subsequent decrease of mechanical properties is observed. Combustion synthesis negates chemical reaction incompleteness due to prolonged heating, but the TiC grain coarsing can take place. Grain growth can be slowed down by increased inert additive content. But excess inert binder content can completely inhibit wave propagation in SHS and combustion process in furnace method. The mechanical activation (MA) of powder mixtures can extend the inert binder concentration limits for SHS wave mode and initiate combustion [4].

The MA of FeTi35C5 and carbon black powder mixtures were held. It was shown, that depending on processing time the coherent scattering regions (CSR), lattice micro distortions and specific surface area are affected. The combustion synthesis in MA FeTi+C powder mixtures were carried out in cylindrical air-tight reactor with Ar media, placed into preheated to 800°C oven. The temperature were measured by the thermocouples inside the titanium cylindrical cup filled with reaction powder mixture and on the outer reactor surface.

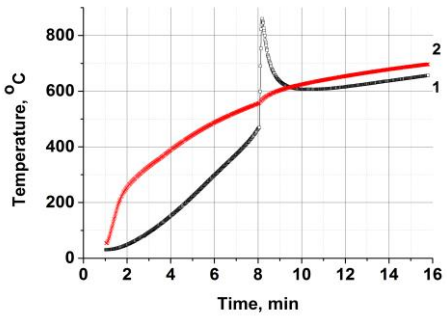

a

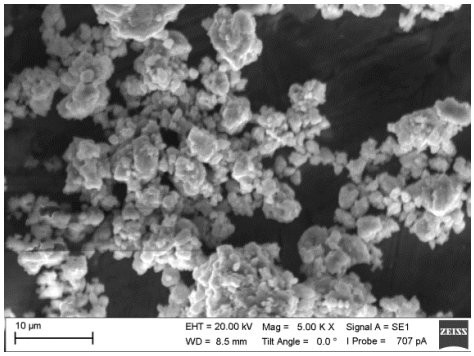

b

Fig.1. Temperature measurement results (a) in thermal explosion mode: 1 – powder mixture; 2 – furnace; (b) loose conglomerates in crushed MASHS product (88 g, 20 : 1, τ = 10 min).

According to XRD results there are next phases appear: TiC the - main phase, α-Fe solid solution and minimum of unreacted ferrotitanium. Comparing to SHS products XRD results [5] it was concluded, that MA and subsequent combustion synthesis negates the TiC reaction incompleteness and combustion synthesis appear to provide MMC with submicron TiC grains in Fe-based binder.

REFERENCES

[1] Borisova A.L., Borisov Y.S. Self-propagating high-temperature synthesis for the deposition of thermal-sprayed coatings, Powder Metall. Met. Ceram., 2008, Vol. 47, № 1–2, P. 80–94.

[2] Wang Z. et al. Fabrication and properties of the TiC reinforced high-strength steel matrix composite, Int. J. Refract. Met. Hard Mater. Elsevier Ltd, 2016, Vol. 58, P. 14–21.

[3] Levashov E.A. et al. Self-propagating high-temperature synthesis of advanced materials and coatings , Int. Mater. Rev., 2017, Vol. 62, № 4, P. 203–239.

[4] A. V. Baranovskiy, G. A. Pribytkov, M. G. Krinitcyn et al., Extending the SHS combustion concentration limits in Ti + C + Fe powder mixtures by preliminary mechanical activation, Materials Today: Proceedings, https:,doi.org/10.1016/j.matpr.2019.12.176. – 2020.

[5] G.A. Prbytkov, A.V. Baranovskiy, V.V Korzhova et. al., Mechanoactivated SHS in Ferrotitanium–Carbon Black Powder Mixtures , Int. J. of SHS – 2020.

*This work was carried out in the framework of Program for basic research in state academies of sciences (line of research III.23) and financially supported by the Russian Foundation for Basic research (project no. 18-32-00330).

OXYGEN CONCENTRATION INFLUENCE ON THE PHASE CONTENT OF THE PLASMA DYNAMIC SYNTHESIS PRODUCT IN Ti-O SYSTEM

A.A. SIVKOV[1,2], YU.N. VYMPINA[3], YU.L. SHANENKOVA[1,2], A.S. IVASHUTENKO[2], I.A. RAHMATULLIN[2]

[1]Jilin University, Changchun, People's Republic of China
[2]National Research Tomsk Polytechnic University, Lenin Avenue 30, Tomsk, 634050, Russian Federation
[3]National Research Tomsk Polytechnic University, Lenin Avenue 30, Tomsk, 634050, Russian Federation, xyulyashax@mail.ru, +79293727270

Titanium dioxide TiO_2 has gained tremendous attention as a non-conventional material for application in photocatalysis due to a wide range of properties, such as high catalytic activity, chemical stability, non-toxicity and low cost [1,2]. Among the known structural modifications of TiO_2, anatase is more preferred due to the low recombination rate of electron-hole pairs [3]. However, obtaining pure anatase is a rather time consuming task, and TiO_2 synthesis products are a mixture of various crystalline phases frequently. Some papers indicate that a mixture of anatase and rutile has increased photocatalytic activity in comparison with pure anatase [4].

Nowadays various synthesis methods are used to create the TiO_2 nanocrystalline material. There are the sol-gel method, the solvothermal method, chemical vapor deposition, etc. [5]. However, none of these methods is universal in terms of time and energy costs. Earlier in papers [6], the possibility of obtaining dispersed titanium dioxide by means of plasma dynamic synthesis method was shown. The advantages of method are simplicity, one-step and synthesis time of less than 1 ms. One of the important parameters of the plasma dynamic synthesis system for obtaining TiO_2 is the ratio of the components in the gas mixture (O_2+Ar), which directly affects the final product characteristics. Therefore, in this paper, the effect of the oxygen concentration in the gas mixture (O_2+Ar) on the phase composition of the product is investigated.

A series of experiments was conducted to study the effect of oxygen concentration; the change in the oxygen content in the gas mixture with argon was carried out in the range from 5% to 80%, respectively. According to the results of X-ray diffractometry, only two crystalline modifications of TiO_2 — anatase and rutile — were identified in the powder material. It was found that the rutile phase is dominant (~ 80%) at the lowest oxygen concentration. It is due to the fact that argon is a denser gas in comparison with oxygen. Thereby, argon interferes with the movement of the plasma flow and, as a result, the quasi-stationary mode duration increases, which is accompanied by the formation of large particles with a rutile structure. However, after an increase in the oxygen concentration, anatase content monotonously increases. At the level of O_2 concentration ~30–40%, the anatase and rutile contents in the powder material are stabilized – their phase contents are 78% and 22%, respectively.

The possibility of regulating the phase composition of the TiO_2 powder material synthesized by the plasma dynamic method by changing the oxygen concentration in the gas mixture (O_2+Ar) is shown. It was found that the maximum anatase content in the final product at the level of 78% is stabilized at O_2 concentration ~ 30–40%.

REFERENCES

[1] *Chung I. et al. // Nature. – 2012. – Vol. 485. – № 7399. – pp. 486-489.*
[2] *Yu H. et al. // Chemical Engineering Journal. – 2019. – Vol. 375. – № 7399. – pp. 1-9.*
[3] *Tao T. et al. // Ceramics International. – 2019. – Vol. 45. – № 17. – pp. 23216-23224.*
[4] *Cheng-Long Yu. et al. // Material Letters. – 2019. – Vol. 246. – № 4. – pp. 133-136.*
[5] *Chen X., Mao S.S. // Chemical Reviews. – 2007. – Vol. 107. – № 7. – pp. 2891-2959.*
[6] *Sivkov A.A. et. al. // Technical Physics Letters. – 2017. – Vol. 43. – № 1. – pp. 16-19*

EFFICIENCY OF USING TITANIUM BORIDE AS A NEUTRON-ABSORBING COATIN[1]

S.O. AKAYEV, D. DYUSSAMBAYEV, S.B. KISLITSIN, A.S. LARIONOV

[1]*Institute of Nuclear Physics of the Republic of Kazakhstan, Almaty, The Republic of Kazakhstan*

Safe storage of spent nuclear fuel (SNF) is actual now day problem of nuclear energetic. Today, nuclear power generates more than 10% of the world's electricity. The volume of accumulated SNF is more than 310 thousand tons. It makes necessity to undertake measures to increase the level of security during SNF storage and manipulations with them. One of the important factors that pose a radiation hazard during long-term storage and handling of spent nuclear fuel is the regeneration of part of the “unburned” fuel when irradiated with thermalized neutrons. To reduce neutron flux, SNF storage containers are manufactured using neutron-absorbing materials. For that purposes both volume and surface alloying metal of container walls with absorbing materials are used. The wide distribution when using protective coatings is amorphous boron carbide [2]. The boron content in such coatings does not exceed 9 - 15%.

In our work, we will focus on neutron-absorbing coatings of titanium boride deposited by magnetron sputtering. The technique developed at the Institute of Nuclear Physics of the Republic of Kazakhstan [3], allows obtaining a high concentration of boron in the coating on metallic substrates. Using developed technique allowed us to form titanium boride coating on a stainless austenitic steel substrate - the main structural material of SNF storage containers. Obtained coating is characterized as a mixture of two phases: the hexagonal phase Ti2B5 and the orthorhombic phase TiB12. The first is a matrix, the second is presented as an interstitial phase, i.e. particles of TiB12 with diameter of ~ 0.5 microns uniformly distributed in the matrix. The matrix has a grain structure with a grain size of ~ 10 nm. The total boron content is ~ 80 at. %, that is 4 times higher than the concentration of boron in coatings obtained by plasma spraying of B4C powder.

Modeling using the MCU-REA code with a library of nuclear constants DLC / MCUDAT-2.1 showed a higher efficiency of reducing the thermal neutron flux by a titanium boride coating in compare to existing analogues [4]. Currently, research aimed the experimental confirmation of the effectiveness of titanium boride coatings are conducted. The critical facility reactor of INP RK and the radioisotopic (Pu-Be) source are used as neutron generators.

REFERENCES

[1] N. S. Cebakovskaya, S. S. Utkin, I. V. Kapyrin, N. V. Medyancev, A. V. SHamina, edited by I. I. Linge and YU. D. Polyakova. Review of foreign practices for SNF and RW, Moscow: Komtekhprint, 2015.

[2] J. S. Choi, C. K. Lee, B. L. Anderson, M. Sutton, B. B. Ebbinghaus. Applications of Neutron-Absorbing Structural-Amorphous Metal (SAM) Coatings for Criticality Safety Controls of Used Fuel Storage, Transportation, and Disposal. ICNC 2015 Charlotte, NC, United States September 13-17, 2015.

[3] Larionov A.S., Suslov E.E., Dikov A.S. The method of applying a neutron absorbing coating of titanium boride // Patent Application RK - Utility Model. – 10/18/2019. – entrance. No. 2019 – 44317, bar code – 2105319. – 9 p.

[4] Larionov A.S., Chekushina L.V., E.E. Suslov «Development and Investigation of High-Strength Neutron-Absorbing Composite Coatings Based on Borides of Metals» // Materials Science Forum. – 2019. – Vol. 945. – P. 660-664.

1 The work was performed as part of the grant financing project of the Ministry of Education of the Republic of Kazakhstan AP05134758

*ELEMENTAL COMPOSITION AND MICROSTRUCTURE OF ULTRASOUND-ASSISTED MICRO-ARC CALCIUM PHOSPHATE COATINGS

E.A. KAZANTSEVA[1,2], *E.G. KOMAROVA*[1], *YU.P. SHARKEEV*[1]

[1]*Institute of Strength Physics and Materials Science SB RAS, 2/4 Academicheskii pr., Tomsk, 634055, Russian Federation, e-mail: kati10_95@mail.ru, phone: +7 (3822) 286-809*
[2]*National Research Tomsk State University, 36 Lenina pr., Tomsk, 634050, Russian Federation*

The aim of this work was to study the elemental composition and microstructure of the calcium phosphate (CaP) coatings deposited by the ultrasound-assisted micro-arc oxidation (MAO) method. The synthesis of the CaP coatings on titanium samples was carried out by the MAO method under the conditions described previously [1,2]. There were three types of the coatings depending on the conditions of external ultrasound (US): 1) MAO coating (control regime without US); 2) MAO/US coating (US-assisted MAO regime, P_{US} = 100 W, υ_{US} = 35 kHz); 3) MAO/PUS coating (pulsed US-assisted MAO regime, P_{US} = 35 W, υ_{US} = 35 kHz).

The SEM data show that the surface morphology of all types of coatings is represented by the spheroidal structural elements (sphere) with inner pores and pores between the spheres (Fig. 1a). The EDX microanalysis reveals the following elements in the all types of the CaP coatings: oxygen, phosphorus, calcium, and titanium (Fig. 1b). It was found that the application of the US field during the MAO process intensified the diffusion in the electrolyte and activated the crystallization of molten compounds. As a result, the Ca, P, and Ti contents are larger in the US-assisted MAO coatings than in MAO coatings (Fig.1b).

The cross-sectional SEM-images show that the all types of the coatings are characterized by the hierarchic porous structure with the numerous branched porous channels (Fig. 1c). As can be seen from the EDX scan line, the Ti amount decreases, the P and Ca amounts increase, and the O amount almost does not change throughout the coating thickness of the all types of the coatings.

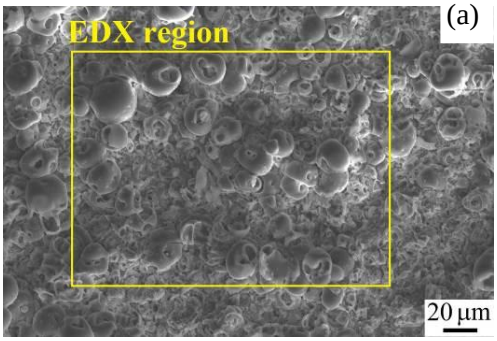

(b)

Element, at.%	MAO	MAO/ US	MAO/ PUS
O Kα	69.7	52.6	51.7
P Kα	14.9	22.8	23.2
Ca Kα	4.4	7.7	7.8
Ti Kα	11.0	16.9	17.3
Ca/P	0.3	0.3	0.3

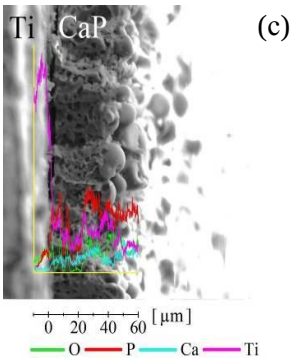

Fig. 1. SEM image of surface (a), quantitative elemental composition (b) and the EDX scan line of the elements through the thickness of the CaP coatings

The TEM studies showed the amorphous-nanocrystalline microstructure in the all types of the CaP coatings. The SAD patterns include the both point reflections from different crystalline phases and diffuse halos from amorphous phase. Indication of SAD patterns showed the presence of the following phases in the MAO coatings: $CaHPO_4$, β-$Ca_2P_2O_7$, and TiO_2 (anatase). In the US-assisted MAO coatings, the additional to previous phases the α-$Ca_2P_2O_7$ phase is detected. This high-temperature phase is formed at the temperature above 1170 °C [2]. Such significant increase of the electrolyte temperature occurrs in the local electrical breakdown areas under the action of US vibrations. TEM data indicating the amorphous-nanocrystalline state in the MAO and MAO-assisted coatings are in agreement with the XRD results described in ref. [2].

REFERENCES

[1] E.A. Kazantseva, E.G. Komarova, Yu.P. Sharkeev "Structural and morphological features of the ultrasound-assisted micro-arc oxidation coatings" AIP Conf. Proc., vol. 2167, p. 020156(4), 2019.

[2] E.G. Komarova, E.A. Kazantseva, M.B. Sedelnikova, Yu.P. Sharkeev "Influence of ultrasonic field during micro-arc oxidation on the structure and properties of calcium phosphate coatings" IOP J. Phys. Conf. Ser., vol. 1393, p. 012098(6), 2019.

* This work was supported by the Fundamental Research Program of the State Academies of Sciences for 2013-2020, direction of research III.23.2.

A NEW METHOD FOR THE SYNTHESIS OF COATINGS OF HA-GELATIN ON TITANIUM*

O.A. GOLOVANOVA

Department of Inorganic Chemistry Omsk F. M. Dostoevsky State University, Russian Federation

The disadvantage of all the above methods is insufficient adhesion of the coatings to the metal substrate. Strong chemical bonding between the coating and the substrate can be formed through fusion temperatures 1073–1273 K, which results in a hard diffusion layer.

An alternative method is formation of biomimetic coatings on metals and their alloys. In this case, the implant–bone bonding develops through the biomimetic formation of an active carbonate-hydroxyapatite (HA) layer on the material surface. This layer is formed as a result of the transition of calcium ions from the implant material into the fluid which composition is similar, as an example, to that of the simulated body fluid (SBF). Biomimetic apatite coatings may be formed on an inert material stable to dissolution, polymer as an example. This method has been successfully used for coating various polymeric materials, including the surface of fibers or fabrics. In this research, we aimed to produce a biomimetic gelatin-calcium-phosphate coating on the VT1-0 titanium alloy and to determine its composition and physicochemical properties.

Synthesis of the coatings on the plates for the HA system was performed in the presence of 1%, 2% and 3% gelatin. A hydroxyapatite suspension was prepared with the addition of gelatin, and then the titanium substrate samples were immerged in the suspension. The pH was 7.4, which corresponds to the physiological pH value. A VT1-0 grade titanium alloy was used for the study. This material has high tensile strength; it is highly biocompatible, non-toxic and corrosion resistant. Its characteristics are similar to the mechanical properties of the bone tissue. The surface of the samples was polished and etched; the etchant composition was HNO_3, NaF (1:1).

As can be seen from the figure, the HA crystals formed in the presence of gelatin are of large sizes. The XRD results showed that the samples synthesized in the simulated body fluid under varying concentration of gelatin are single-phase and represent hydroxyapatite.

During formation of the coatings based on the synthesized composites (Fig. 1), dendritic crystals are seen to start growing on the plate edge.

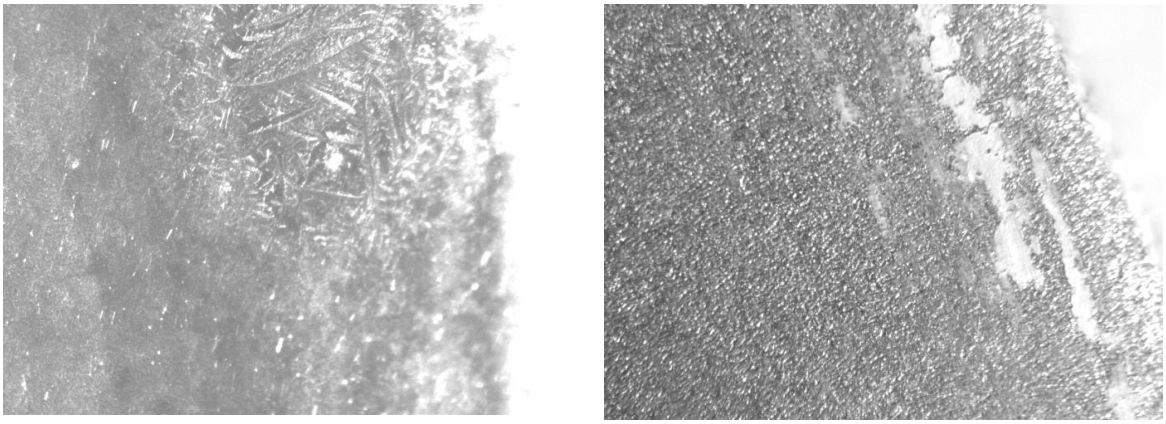

a. b.

Fig. 1. Surface morphology of the hydroxyapatite crystals grown on the VT1 titanium alloy surface in the presence of gelatin after 3 day soaking in the solution: etched surface (a), polished surface (b) (100x magnification).

The crystallization rate was found to depend on the technique used for treating the implant surface. More rapid growth of crystals was observed in the microsections of the polished samples, whereas on the etched samples, dendritic growth occurred in bulk defects caused by etching. Enhanced HA-gelatin deposition on the titanium substrate surface is found to occur on etched samples. It is revealed that exposure of titanium substrates to PIB with j=100 A/cm^2 makes possible further growth of HA crystals and regeneration of the metal implant surface.

* The presented work is a synthesis of the results of the RFBR project № 15-29-04839 ofi_m

THE EFFECT OF NICKEL ALLOYING ON PHASE FORMATION IN CERMETS BASED ON THE Mo-Fe-B-C SYSTEM

T.N. VERSHININA[1], *M.B. IVANOV*[2]

[1] *Joint Institute for Nuclear Research, Dubna, Russian Federation*
[2]*S7 R&D Center, Moscow, Russian Federation*

The development of technologies in the field of cutting processing is directly dependent on the development of new tool materials with higher physical and mechanical properties. Cermets based on Mo-Fe-B and Mo-Ni-B systems are one of the promising and not yet widely used materials. The solid phases in them are the borides Mo_2FeB_2 and Mo_2NiB_2, and the metal matrix acts as a binder. These materials, according to a few published data [1-3], have an excellent combination of mechanical properties, wear resistance and corrosion resistance. And since the composition of these cermets does not include expensive tungsten, their development also has economic feasibility.

The purpose of this investigation is to determine the effect of Ni addition on the microstructure, phase composition and mechanical properties of Mo_2FeB_2-Fe hard alloys doped with carbon.

As can be seen from Fig. 1, the alloying of cermets of the Mo-Fe-B-C system with nickel leads to significant changes in their phase composition. The tetragonal boride Mo_2FeB_2 acts as a solid phase in a material containing 10 wt. % Ni. Also, due to the presence of carbon, M_6C type carbide is precipitated with an estimated composition of $(Ni,Si)_3Mo_3C$. The latter is formed due to the presence of silicon, which is included in the initial powder components as an impurity. The amount of the binder phase is very small and therefor a high hardness and low fracture toughness of the sintered material are observed. An increase of nickel concentration to 15 wt.% result in the precipitation of κ-phase $Mo_{10}Ni_3C_3B$ in the cermet. Its formation leads to a significant decrease in the volume fraction of M_6C carbide and increase of the amount of binder phase on the base of FCC-(Fe, Ni). When 20 wt.% Ni is added to the composition the formation of the orthorhombic boride Mo_2NiB_2 and the complete replacement of the carbide by the κ-phase are detected.

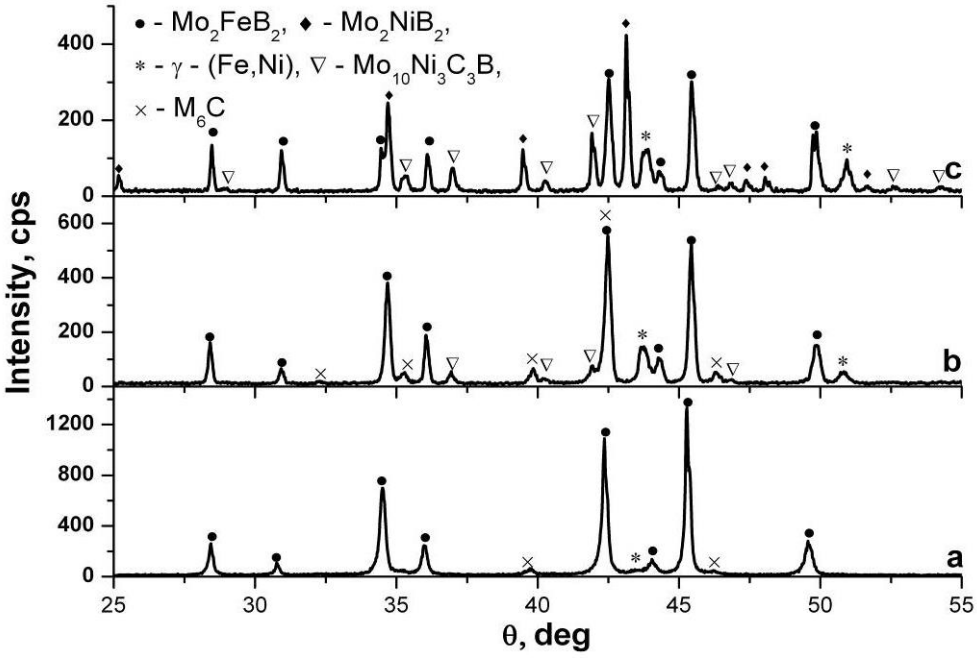

Fig.1. XRD patterns of cermets: a – 10 wt.% Ni, b – 15 wt.% Ni, c – 20 wt.% Ni.

REFERENCES

[1] T. Ide, T.Ando "Reaction Sintering of an Fe-6 Wt Pct B-48 Wt Pct Mo Alloy in the Presence of Liquid Phases", Metall. Mater. Trans. A., vol. 20, pp.17–24, August 1989

[2] Nishiyama K., Keino M., Furuyama Y. et. al. "Internal friction of boride cermets at elevated temperatures", J. Alloys Compd., Vol.355, pp. 97-102, June 2003.

[3] M.B. Ivanov, T.N. Vershinina, V.V. Ivanisenko "The effect of composition and microstructure on hardness and toughness of Mo_2FeB_2 based cermets", Mat. Sc. & Eng. A, vol. 763, 138117, August 2019.

THE REFINEMENT OF β-Fe_6Ga_5 CRYSTAL STRUCTURE*

T.N. VERSHININA[1], I.A. BOBRIKOV[1], S.V. SUMNIKOV[1], A.O. BOEV[2], A.M. BALAGUROV[1],

A.K. MOHAMED[3], I.S. GOLOVIN[3]

[1] *Joint Institute for Nuclear Research, Dubna, Russian Federation*
[2]*Belgorod National Research University, Belgorod, Russian Federation*
[3]*NationalUniversity of Science and Technology "MISIS", Moscow, Russian Federation*

Magnetostrictive materials, such as Fe-Ga alloys, are a type of functional materials, the main feature of which is the interaction of magnetic and mechanical energy when an external magnetic field or stress is applied. Ferromagnetic alloys based on the Fe-Ga binary system have highest saturation magnetostriction among iron-based alloys [1]. These alloys are used for the manufacture of pressure sensors and sonars due to a good combination of functional and mechanical properties.

Low-temperature diffusion-controlled phase transformations in alloys of the Fe-Ga system proceed slowly. This helps to maintain at room temperature nonequilibrium high-temperature phases, which were formed during crystallization from the melt. The structure of the Fe-45at.%Ga alloy quenched from the melt is β-Fe_6Ga_5. This phase exists in a narrow temperature range of 770–800°C according to the equilibrium diagram of Fe-Ga [2]. The crystal structure of the β-Fe_6Ga_5 has been refined using the R-3m space group in [3] were it was called as ζ_2-GaFe.

In our studies, neutron and X-Ray diffraction patterns were measured for several samples of the Fe-45Ga alloy in different states. Dependently on heat treatment the structure changed from single to multiphase state. In the paperthe refinements of crystal structure for all studied samples will be presented as well as density functional theory calculations. In Fig. 1 a preliminary result of the Rietveld refinement is shown, where good agreement between experimental and calculated values is seen.

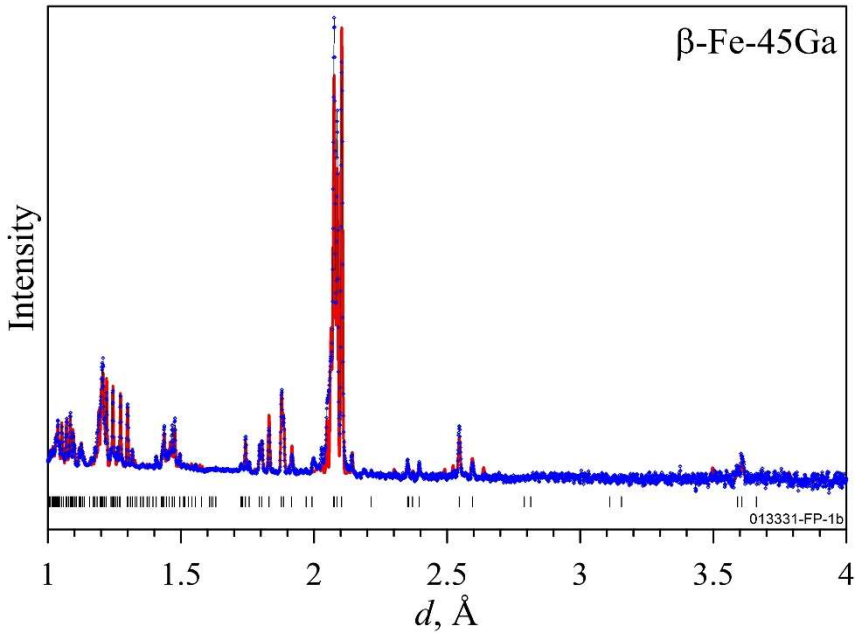

Fig.1. Neutron diffraction pattern for as cast Fe-45Ga alloy measured at room temperature and processed by the Rietveld method. Experimental points and calculated line are shown. The vertical bars indicate calculated peak positions of the β-Fe_6Ga_5.

REFERENCES

[1] A.E. Clark, J.B. Restorff, M. Wun-Fogle, T.A. Lograsso, D.L. Schlagel "Magnetostrictive properties of body-centered cubic Fe-Ga and Fe-Ga-Al alloys" IEEE Trans. Magn. Vol.36, P.3238-3240, October 2000.

[2] H. Okamoto, "The Fe-Ga (Iron-Gallium) system" Bulletin of Alloy Phase Diagrams, Vol. 11(6), P. 576–581, December 1990.

[3] O. Gourdon, S.L. Bud'ko, D.Williams, G.J. Miller, "Crystallographic, Electronic, and Magnetic Studies of ζ_2-GaM (M = Cr, Mn or Fe): Trends in Itinerant Magnetism" Inorganic Chemistry, Vol. 43(10), P. 3210–3218, December 2004.

*The reported study was funded by RFBR, project number 18-02-00325_a

MeSiBCN (Me: Ti, Cr, Al, Mo, Zr, Ta) NANOFILMS WITH HIGH WEAR-, OXIDATION- AND CORROSION RESISTANCE PRODUCED IN VACUUM USING SHS-CATHODES*

PH.V. KIRYUKHANTSEV-KORNEEV, E.A. LEVASHOV

National University of Science and Technology "MISIS", Moscow, Russia

The metal carbide, nitride, and boride coatings are the materials of choice for a wide variety of protective applications, especially for cutting/forming tools, automobile and aircraft mechanical components. These coatings demonstrate relatively low friction coefficient, high hardness (H), wear-, oxidation-, and corrosion- resistance. The oxidation resistance (OR) and thermal stability (TS) of coatings can be farther improved by Si or Al alloying. In this work we present a thorough study of nanocomposite and amorphous MeSiBCN (Me: Ti, Cr, Al, Mo, Zr, Ta) coatings deposited by direct current or pulsed magnetron sputtering, pulsed cathodic arc evaporation (P-CAE), IIAMS and HIPIMS of multiphase electrodes obtained using self-propagating high-temperature synthesis (SHS).

The simple boride, carbide, and silicide targets as well as multicomponent TiSiB, TiAlSiB, TiCrB, TiSiC, TiCrSiC, TiAlSiCN, MoSiB, MoAlSiB, MoHfZrSiB, ZrSiB, ZrAlSiB, ZrMoSiB, TaZrSiB, TaSiCN, TaSiBN, and CrAlSiB SHS-electrodes were sputtered in Ar, Ar-N_2, and Ar-C_2H_4 gas mixtures. The metal and non-metal model materials (alumina, silicon) were used as the substrates. To evaluate the OR and anti-diffusion properties the coatings were annealed in air or in vacuum at T=500-1700°C. The structure of as-deposited and annealed coatings was studied by XRD, SEM, HR-TEM, XPS, GDOES, FTIR, and Raman. The samples were characterized using nanoindentation, impact-, RT/HT tribo- and scratch-testing.

The results obtained show that TiSiBN coatings demonstrated H~30 GPa, good long-time OR at 900^0C, but exhibited a poor resistance to the metal atoms diffusion from the metal substrates. TiAlSiBN had extremely low crystallite size <3 nm and good OR at 1100^0C. CrAlSiBN, MoSiBN, and ZrSiBN showed hardness 30-40 GPa, and good OR in range 1200-1400^0C. CrAlSiBN revealed the best wear resistance in terms of cyclic impact loadings and in sliding conditions at room temperature. On the other hand MoSiBN showed the low wear rate and low friction coefficient at T≥500^0C due to formation of MoO_3 which play role of solid lubricant. Moreover MoSiBN successfully resisted to the diffusion of metal atoms from the substrate up to 1000^0C. Nitrogen-free ZrSiB, MoAlSiB, and MoSiB with high Si content exhibited record OR up to 1500, 1600, and 1700^0C, respectively. $TaSi_2$-based coatings demonstrated medium OR with maximal T=1100-1500°C and posses self-lubricant properties in temperature range of 100-500^0C. TiCrBN have H=35 GPa stable in range 20-1000^0C, good OR at 1000^0C, relative low friction coefficient ~0.4, and minimal wear rate ~$1.8x10^{-7}$ mm^3/(Nm). TiAlCN coatings have the best combination of H~35 GPa and friction coefficient <0.25. TiAlCN remains stable up to 1200^0C. TiAlSiCN coatings exhibit H=37-42 GPa up to 1300^0C. Even after annealing at 1500^0C TiAlSiCN demonstrates acceptable H=20 GPa, and crystallite size <50 nm. For CrAlCN the H=25 GPa, high OR and diffusion-barrier properties up to 1000^0C were achieved. Best corrosion resistance in acid and alkaline environments were obtained for nitrogen-contained TiCrBN, TiAlCN, TiAlSiCN, and TiCrSiCN coatings.

The developed coatings are found to prolong the lifetime of WC-Co instruments by 2-7 times compared with the Ti(C)N coatings and to increase the work temperature of base materials onto 200-500^0C. Combination of relatively high H, remarkable TS, and OR resistance makes new materials promising candidates for protective coatings to be used in high-temperature tribological applications.

REFERENCES

[1] E.A. Levashov et al**. International Materials Reviews** 62 (2017) 203-239

[2] Ph.V. Kiryukhantsev-Korneev et al. **Corrosion Science** 123 (2017) 319–327

[3] Ph.V. Kiryukhantsev-Korneev et al. **Appl. Surf. Sci.** 314 (2014) 104-111

[4] Ph.V. Kiryukhantsev-Korneev et al. **Ceramics International** 46 (2020) 1775-1783

[5] Ph.V. Kiryukhantsev-Korneev et al. **Surf. Coat. Technol.** 201 (2007) 6143

* The work was supported by the Russian Science Foundation (project No. 19-19-00117).

PLASMA ASSISTED MAGNETRION DEPOSITION OF DLC COATING*

I.V LOPATIN, D.YU IGNATOV, YU.H AKHMADEEV, S.S KOVALSKIY

Institute of high current electronics SB RAS, Tomsk, Russia

The results of experiments on DLC coatings producing using a deposition system including an unbalanced magnetron with a graphite target and a PINK gas plasma generator, based on a non-self-sustained arc discharge with a thermionic cathode are presented. Investigations with a single-grid energy analyzer showed that ions arriving at the substrate have an energy higher than with conventional magnetron sputtering. This become possible thanks to the original electrode and magnetic systems, as well as the electrodes connection scheme of plasma generators. It was shown that the use of such plasma-physical system allows to deposit a DLC coating.

* The reported study was funded by RFBR and Tomsk region according to the research project № 19-41-000001

STUDY OF THE TINI-BASED POWDER ALLOY SURFACE BY NON-DESTRUCTIVE TESTING METHODS *

S.G. ANIKEEV, N.V. ARTYUKHOVA, V.N. KHODORENKO, O. MAMAZAKIROV, M.N. VOLOCHAEV, A.N. MONOGENOV, E.V. YAKOVLEV.

Tomsk State University, Tomsk, Russia
Tomsk Scientific Center SB RAS, Tomsk, Russia

As a rule, in order to gain access to the developed internal structure of the porous material, it is necessary to carry out preliminary cross breaking of the porous sample. Stress fields and cracks can distort the surface structure of the pore walls, and due to the volumetric developed structure of the porous material not always research can be undertook. To solve this problem, the task was set of obtaining two-dimensional porous samples with a similar structure to the porous body of the TiNi-based alloy. For this purpose, hydride-calcium TiNi-based powder was placed on TiNi-based monolithic plates and sintering was carried out under similar conditions to obtain porous TiNi-based alloys. Due to this, it became possible to create an identical structure of the porous body obtained by diffusion sintering. This approach is effective in studying the surface morphology of a material using scanning, transmission, atomic force microscopy, and profilometry without preliminary sample preparation procedures that could potentially distort the results of the study. The objective of this work is to develop a TiNi-based powder alloy obtaining method for the use of non-destructive methods of studying the state of the surface of a material.

Samples were obtained by a single diffusion sintering method at a temperature in the range of 1240–1260 ° C and a sintering time of 15 min. The powder was placed on the plate and evenly distributed on its surface in such a way as to prevent the appearance of layer discontinuity. The thickness of the powder layer was about 300–350 μm, which corresponds to the size of 1–2 particles of TiNi-based powder. The macro- and microstructure of the obtained samples was studied by scanning electron microscopy using a Quanta 200 3D system with electron and focused ion beams with an integrated EDAX ECON IV energy dispersive spectrometer. X-ray diffraction studies were conducted on a Shimadzu XRD 6000 X-ray diffractometer. Building of the three-dimensional surface reconstruction and determination of roughness parameters were performed using an interference microscope of the MNP-1 profilometer using the software of the same name.

Leading of the used sintering mode to the homogenization of the TiNi-based powder alloy was established. X-ray diffraction analysis confirmed the presence of the austenitic phase TiNi (B2), Ti_3Ni_4, Ti_2Ni and Ti_4Ni_2 (O, N, C) in the composition of the obtained TiNi-based powder alloy. The obtained result is explained by the structure of the initial powder materials, which contain a TiNi intermetallic compound in a two-phase state – B2 (austenite) and B19’ (martensite), and phases enriched with titanium Ti_2Ni, as well as traces of nickel-enriched phases — $TiNi_3$ and metastable phases Ti_3Ni_4.

On the surface of the material obtained by diffusion sintering, an amorphous layer of titanium oxide TiO_2 is formed in the rutile modification with a thickness of about 40-60 nm. In the structure of the surface layer the globular shape of particles that form the surface layer with a thickness of 20–30 nm can be distinguished; the structure of the substance in this layer does not differ from the main layer. It is known that during the formation of the oxide layer, it is possible to delaminate and separate into sublayers with different structures. Due to the presence of surface layers of titanium oxide, the corrosion properties of a material TiNi-based increase and when interacting with tissue media in the human body, the surface layer of TiO_2 promotes the adhesion of proteins and osteogenic cells.

Many individual TiNi-based powder adhered to the surface of the monolithic plate particles constitute the structure of the obtained sample. Variation of the temperature-time modes of diffusion sintering can make it possible to obtain a material with an increased roughness index R_a when a TiNi-based powder alloy is used. A high value of the latter can positively affect the adhesive properties of the implant material, which has a developed surface.

* The work was supported by the Russian Science Foundation under grant No. 19-79-10045.

EXPERIMENTAL STUDY OF LASER TREATMENT OF Ti_3AlC_2 MAX PHASE*

M.G. KRINITCYN [1,2], M.P. RAGULINA [1], A.V. BARANOVSKIY [1,2], I.A. FIRSINA [2]

[1]Tomsk Polytechnic University, Tomsk, Russia, 634050
[2]Institute of Strength Physics and Material Science SB RAS, Tomsk, Russia, 634055

Ternary carbides and nitrides, called MAX phases, form a new class of materials that has very specific properties, combining the properties of both metals and ceramics [1]. Some of the most promising MAX phases are formed in the Ti-Al-C system. The materials of this system can be used as materials with high strength and deformation resistance, including cyclic loadings [2]. The chemical etching of aluminum in MAX phases forms the so-called MXenes, which, due to their nanolaminate structure, can be used for storing electric energy or hydrogen [3, 4].

Bulk samples from the powder of the MAX phase Ti_3AlC_2 were obtained by selective laser sintering (SLS). A comprehensive structural-phase study was carried out using optical and electron microscopy techniques, as well as XRD and EDX analysis. This study allowed to describe the elemental and phase composition, as well as the morphology of both the initial powders and bulk SLS samples. Modes of selective laser sintering are established at which the maximum presence of the MAX phase in the samples after SLS is observed.

It was found that at a laser power of 60 W and a scanning speed of at least 100 mm/s, the maximum appearance of the MAX phase in the samples after SLS is observed.

The laser scanning speed affects the sintering of the powder between the tracks and between the layers, so it must be varied simultaneously with the distance between the tracks and the thickness of the bulk powder layer.

In the center of the laser beam, the maximum destruction of the MAX phase with the formation of titanium carbide is observed (Fig. 1). The highest recorded content of the MAX phase of Ti_3AlC_2 in the sintered layer is 95%.

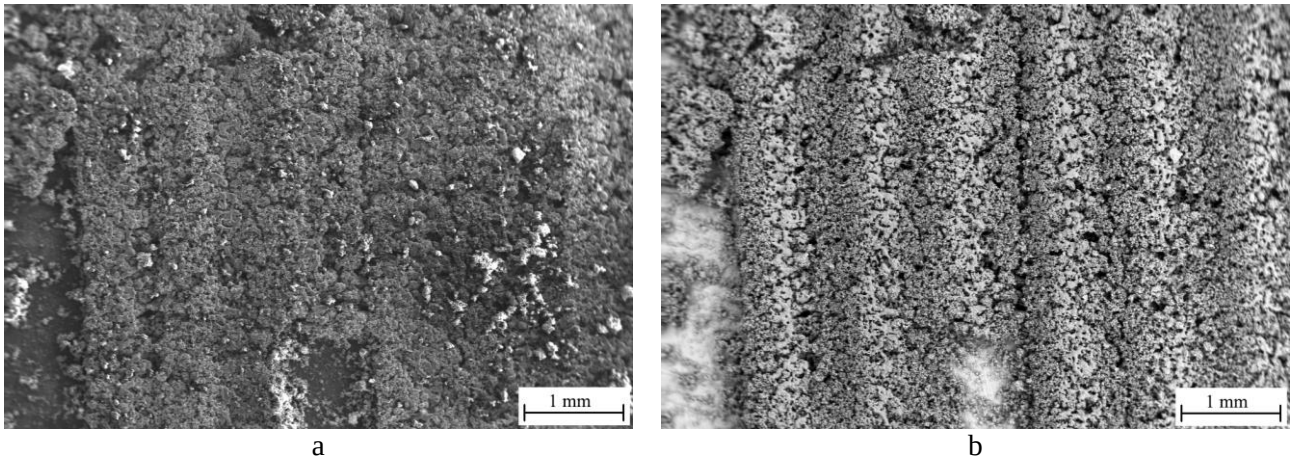

a b

Fig.1. Surface of Ti_3AlC_2 powder after laser treatment at 60 W using SE (a) and BSD (b) detectors.

REFERENCES

[1] Wang X. H., Zhou Y. C. “Layered machinable and electrically conductive Ti2AlC and Ti3AlC2 ceramics: a review” J. Mat. Sc. & Tech, Vol. 26, no. 5, pp. 385-416, 2010.

[2] Barsoum M. W., Radovic M. “Elastic and mechanical properties of the MAX phases” Ann. Rev. Mat. Res., Vol. 41, pp. 195-227, 2011.

[3] Tang Q., Zhou Z., Shen P. “Are MXenes promising anode materials for Li ion batteries? Computational studies on electronic properties and Li storage capability of Ti3C2 and Ti3C2X2 (X= F, OH) monolayer” J. Am. Chem. Soc., Vol. 134, no. 40, pp. 16909-16916, 2012.

[4] Shein I. R., Ivanovskii A. L. “Graphene-like titanium carbides and nitrides Tin+ 1Cn, Tin+ 1Nn (n= 1, 2, and 3) from de-intercalated MAX phases: First-principles probing of their structural, electronic properties and relative stability” Comp. Mat. Sc., Vol. 65, pp. 104-114, 2012.

* The reported study was funded by RFBR and Tomsk region according to the research project № 19-48-703011.

STRUCTURE OF "METAL / TI_3ALC_2" COMPOSITES OBTAINED BY SELECTIVE LASER SINTERING*

M.G. KRINITCYN [1,2], O.M. KASHNIKOVA [1], M.P. RAGULINA [1], I.O. NIKOLAEV [1]

[1]Tomsk Polytechnic University, Tomsk, Russia, 634050
[2]Institute of Strength Physics and Material Science SB RAS, Tomsk, Russia, 634055

MAX phases are ternary compounds having a specific structure and combining the properties of metal and ceramics [1]. Like metals, these compounds show high thermal and electrical conductivity, as well as a relatively high resistance to thermal shock. Moreover, like ceramics, they have a high modulus of elasticity, low thermal coefficient of expansion, and high heat resistance.

The combination of metal and ceramic properties makes the MAX phase attractive for use in composites. Composites containing MAX phases of Ti-Al-C systems in combination with other materials are known from the literature. The main components are TiC [2] and intermetallics of the Ti-Al system [3]. There are also composites with metals (copper [4], silver [5], etc.), nickel alloys [6], silicon carbide [7], aluminum oxide [8], and others.

The paper presents a study of the preparation of composite materials with a metal matrix and Ti_3AlC_2 particles (Fig. 1) from powder mixtures of various compositions. The bulk products were obtained from these mixtures using the selective laser sintering technology at powers providing dense samples, but not allowing significant destruction of the MAX phase. Investigations are made of the structure and phase composition of the obtained samples using optical and electron microscopy, as well as XRD and EDX analysis.

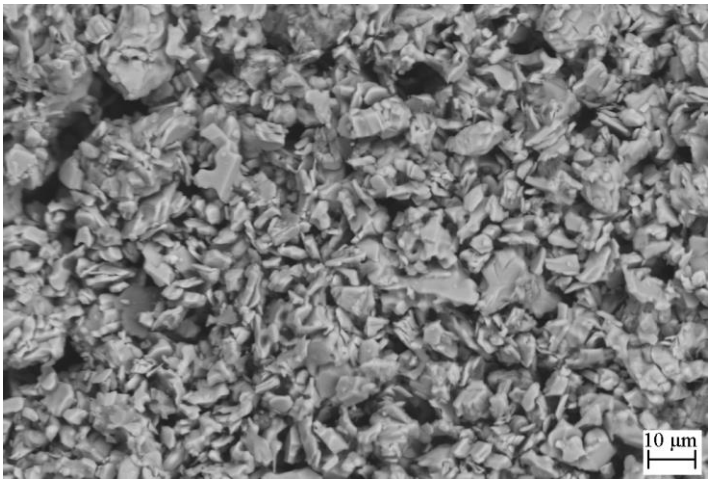

Fig.1. The morphology of Ti_3AlC_2 powder.

REFERENCES

[1] Wang X. H., Zhou Y. C. "Layered machinable and electrically conductive Ti2AlC and Ti3AlC2 ceramics: a review" J. Mat. Sc. & Tech., vol. 26, no. 5, pp. 385-416, 2010.

[2] Ruan M. et al. "Microstructure and Mechanical Properties of TiC/Ti 3 AlC 2 In-situ Composites Prepared by Hot Pressing Method" Mat. Sc. Forum, Vol. 816, pp. 200-214, 2015.

[3] Akhlaghi M. et al. "Spark plasma sintering of TiAl–Ti3AlC2 composite" Ceram. Int., vol. 44, no. 17, pp. 21759-21764, 2018.

[4] Huang X. et al. "Physical, mechanical, and ablation properties of Cu–Ti3AlC2 composites with various Ti3AlC2 contents" Mat. Sc. & Tech., vol. 34, no. 6, pp. 757-762, 2018.

[5] Liu M. et al. "Ag/Ti3AlC2 composites with high hardness, high strength and high conductivity" Mat. Letters., vol. 213, pp. 269-273, 2018.

[6] Hu W. et al. "Preparation and mechanical properties of TiC x-Ni 3 (Al, Ti)/Ni composites synthesized from Ni alloy and Ti 3 AlC 2 powders" Mat. Sc. & Eng.: A, vol. 697, pp. 48-54, 2017.

[7] Guo S. et al. "SiC (SCS-6) fiber-reinforced Ti3AlC2 matrix composites: Interfacial characterization and mechanical behavior" J. Eur. Ceram. Soc., vol. 35, no. 5, pp. 1375-1384, 2015.

[8] Zhou W. et al. "In situ synthesis, mechanical and cyclic oxidation properties of Ti3AlC2/Al2O3 composites" Adv. In Appl. Ceram., vol. 117, no. 6, pp. 340-346, 2018.

* The reported study was funded by RFBR and Tomsk region according to the research project № 19-48-703011.

PLASMA-ASSITED DEPOSITION OF DIELECTRIC COATINGS FOR ELECTRICAL INSULATION*

D.A. ZUZA[1], *V.O. NEKHOROSHEV*[1], *I.A KURZINA*[2], *A.V. BATRAKOV*[1]

[1] *Institute of High Current Electronics SB RAS, Tomsk, Russia*
[2] *National Research Tomsk State University, Tomsk, Russia*

Currently, plasma polymerization of films is a rapidly developing field of plasma technology [1–4]. One of the possible applications of this method is the deposition of protective dielectric coatings on defects in the electrical insulation of a spacecraft [1, 3]. As dielectric coatings in exploitation process are subjected to temperature extremes, solar radiation, etc., special attention should be paid to the operational properties of the resulting coatings [2, 3].

In this paper, we consider the methods of plasma polymerization using the low-pressure and atmospheric-pressure discharge in argon as a plasma source. The aim of investigation is obtaining a polymer layer with both high electrical strength and good mechanical properties. In our experiments we have used a flowing type plasma chemical reactor operates with argon mass flowrate up to 0.03 g/s and the monomer mass flowrate up to 1 mg/s. The vapors of organic (Methyl methacrylate, Paracyclophane) or organosilicon (Hexamethyldisiloxane) compounds have been generated in special constructed vaporizer at temperature range from 120 ºC to 180 ºC. The monomer vapor flow is transferred via the discharge plasma region and subsequently is deposited on an aluminum, copper or glass substrate. The discharge power was adjusted to limit the temperature in the substrate area at level less than 120 ºC.

To study the stability of the obtained films, thermal cycling from -70 ºC to 120 ºC experiments was carried out. Experiments to estimation the electric strength of coatings have also been done. It was found that the operational properties of the deposited films strongly depends on the parameters of the deposition process, such as carrier-gas flowrate, precursor concentration and the discharge power. Based on the investigation results a basically principals of construction for novel system for eliminating defects in dielectric coatings using plasma-assisted deposition has been proposed.

REFERENCES

[1]. A.V. Batrakov, S.A. Popov, K.V. Karlik et al., "Suppression of Prebreakdown Emission Activity Inside the On-board Spacecraft Equipment by Local Polymerization in Discharge," Proc. 28th Int. Symposium on Discharges and Electrical Insulation in Vacuum (ISDEIV), Vol. 2, Greifswald, Germany, pp. 777-780, 2018.

[2]. X.-Y. Zhao, M.-Z. Wang, J.-Q. Ji et al., "Structural Analysis and Dielectric Property of Novel Conjugated Polycyanurates," Polym. Eng. Sci., Vol. 54, no 4, pp. 812-817, 2014.

[3]. A. Michelmore, J.D. Whittle1, J.W. Bradley, R.D. Short, "Where physics meets chemistry: Thin film deposition from reactive plasmas," Front. Chem. Sci. Eng., Vol. 10, no 4, pp. 441-458, 2016.

[4]. S. Bhatt, J. Pulpytel, F. Arefi-Khonsari, "Low and atmospheric plasma polymerisation of nanocoatings for bio-applications," Surf. Innov., Vol. 3, no SI2, pp. 63-83, 2015.

* The work was supported by the Russian Foundation for Basic Research under grant No. 18-48-700029-p_a.

CORRECTION OF THE DISTRIBUTION PROFILES OF THE INTENSITIES OF ELEMENTS CONSIDERING THE UNEVEN DISPERSION OF THE GLOW-DISCHARGE OPTICAL EMISSION SPECTROMETER FOR MULTILAYER COATINGS ANALYSIS

I.A. SHULEPOV[2], A. LOMYGIN[1], R.S. LAPTEV[1], E.B. KASHKAROV[1], M.S. SYRTANOV[1]

[1]National Research Tomsk Polytechnic University, Tomsk, Russian Federation
[2]Institute of Strength Physics and Materials Science, Siberian Branch of the Russian Academy of Sciences, Tomsk, Russian Federation

Thin films and coatings are used in various fields of technology, from microelectronics and optics to protective coatings from multiple influences. Optimization of the deposition processes and determination of coating destruction mechanisms are based on studies of the microstructure and chemical composition using electron microscopy, X-ray diffraction analysis and photoelectron spectroscopy [1]. However, in this case, in addition to technical problems associated with the deposition of a large number of layers, methodological problems also arise in-depth profiling due to physical and instrumental artefacts that accompany ion sputtering of ultrathin and thin multilayer coatings [2]. Thin-film analysis by depth profiling methods is based on surface erosion as a result of bombardment by particles with different energies, and the substance is continuously removed depending on the bombardment time. One of these methods is GD-OES [3].

This work aimed to model the dependence of the distribution profiles of the intensities of the elements, taking into account the non-uniformity of spraying.

The multilayer CrN/ZrN coating was deposited by magnetron sputtering onto a stainless steel substrate. The total thickness of the resulting coating was 17-18 microns. To analyse the chemical composition of the coatings and the distribution of the layers, a GD-Profiler 2 glow discharge spectrometer was used. When adjusting the profiles of the distribution of intensities of the luminescence of the elements, an exponential dependence was used. Auger spectroscopy was used to analyze the coatings quantitatively.

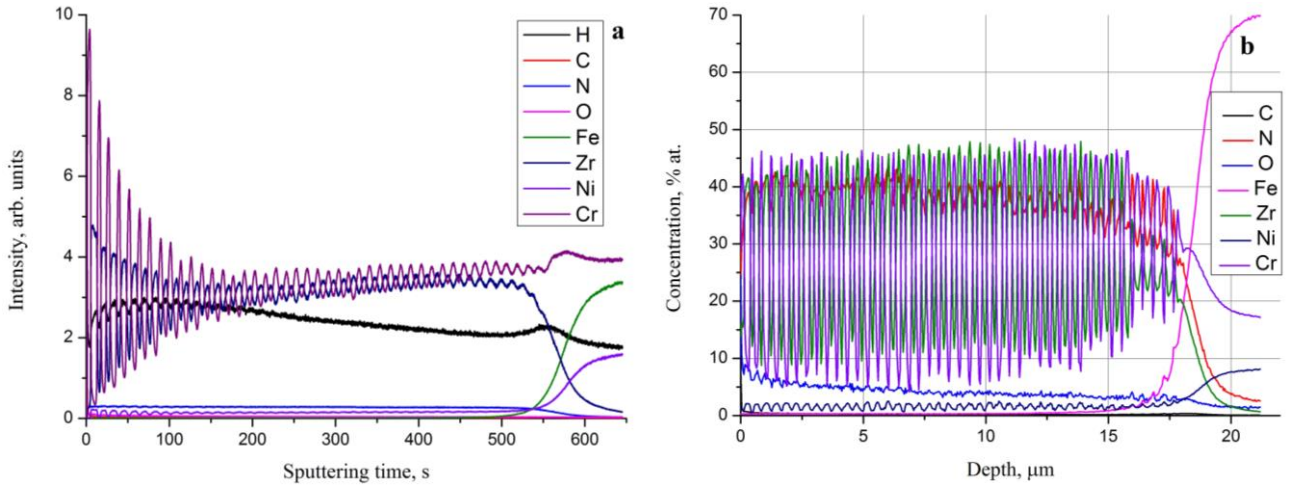

Fig.1. Distribution profiles of elements: a - initial profile, b - distribution profile corrected and recalculated to atomic concentrations.

As a result of this work, the possibility of eliminating from physical and instrumental artefacts was shown, the initial spectrum was corrected after taking into account the spraying unevenness. The luminescence intensities of the elements in atomic concentrations were also recounted to understand the quantitative chemical composition of the resulting CrN/ZrN coating.

REFERENCES

[1] Y. Y. Chang, C. P. Chang, D. Y. Wang, S. M. Yang, W. Wu, “High temperature oxidation resistance of CrAlSiN coatings synthesized by a cathodic arc deposition process”, Journal of Alloys and Compounds, vol. 461, no. 1-2, pp. 336-341, August 2008.

[2] A. B. Tolstoguzov, “Multilayer thin-film coatings based on chromium nitride and aluminum nitride: Comparative depth profiling by secondary ion mass spectrometry and glow-discharge optical emission spectrometry”, Journal of Analytical Chemistry, vol. 65, no. 13, pp. 1370-1376, December 2010.

[3] M. Nekhin, A. Kuznetsov, P. Shapon, “Glow discharge spectrometer PROFILER-2 is a powerful analytical tool for layer-by-layer analysis of materials”, Analytics, no. 4, pp. 34-43, May 2012.

THE OCT APPLICATION IN OPTIC GRADIENT COATING OPTIMIZATION

N.N. SCHITOV

Dukhov Automatics Research Institute (VNIIA), 22 Suschevskaya Ul., Moscow 127055, Russia,
nschitov@mail.ru, phone.: 89160820555

The possibilities of multilayered gradient optic coatings (with smooth refractive index variation inside every layer) to produce the photonics effective gadgets – mirrors, filters and in the wide sense optic metamaterials were investigated in [1]. However, conventionally such gadgets were fabricated as multilayer coatings on a glass substrate with the constant refractive index value inside every layer. Moreover, in [2] the optimality of piecewise constant control parameter (refractive index) variation law at such gadgets designing is proved using the optimal control theory (OCT). The question arises: are the advantages of gradient structures the consequences of unjust or incomplete OCT problem statement or the OCT cannot give smooth functions as solutions, for optic coatings at least?

One has to make a reservation consisting in the fact that conventional multilayer interference filters and mirrors have layers' thickness around the wavelength in the layer materials. Whereas in [1] the periodic gradient structures with periods significantly smaller than the light wavelengths passing through them are considered: "Like schemes in microwave domains including elements with dimensions smaller than working wavelengths the nanostructures with subwave dimensions were elaborated to work in the optic range".

It is clear that smooth solutions of the OCT problem may occur only if the control variables enter nonlinearly in the optimal Hamiltonian or the state equations contain the control variables derivatives that move the problem out of the classic OCT. The general field's wave equations containing dielectric and magnetic permittivity's gradients correspond just to the last case but in the equation considered in [1] this gradient is absent. If the coating material is nonmagnetic so that μ=Const, but $\varepsilon = \varepsilon(z) \neq$Const, in the general wave equation for the electric field in the plane wave approximation the dielectric permittivity gradient is really absent. But for the magnetic field the vector product of this gradient and the field's curl is not zero in the general case and particularly for the plane wave when $\mathbf{H}=\mathbf{H}(z,t)$. The equation for the Fourier transform upon time of the magnetic field *y*-component both for TE and TM modes in the case of normal incidence contains the $\varepsilon(z)$ logarithm's gradient (a "hatch" means differentiation):

$$H'' - \frac{\varepsilon(z)'}{\varepsilon(z)} H' + \varepsilon(z)\frac{\omega^2}{c^2} H = 0$$

The OCT problem statement on this equation solutions class is considered. At that unlike the classic statement used in [2] the control variable *is not the dielectric permittivity but its gradient*, whereas itself is defined *as the state variable*. As far as this new control variable is all the same linear within the optimal Hamiltonian the solution $\varepsilon'(z)$ is piecewise constant coordinate's function so that $\varepsilon(z)$ represents the "saw" or periodic trapeze due to the Pontryagin's maximum principle. It means that one has to introduce another auxiliary state variable which derivative – the dielectric permittivity's second derivative – will be the control variable. Now the optimal piecewise constant solution for this control variable will represent the parabola set for "*genuine control*" that is the refractive index as in [1]. Generally, choosing as the control variable the corresponding derivative of the "*genuine*" one can obtain functions of any smoothness degree. However, the presented in this report solutions of primal problems for smooth and piecewise constant refractive index variation laws prove for a while yet the advantages of latter's for spectrum filtration except for apodizing filters. The question about the artificially made dispersion will be considered elsewhere.

REFERENCES

[1] *Shkatula S.V., Volpian O.D., Shvartsburg A.B., Obod Yu.A.* Artificial dispersion of all-dielectric gradient nanostructures: frequency-selective interfaces and tunneling assisted broadband antireflection coatings // Photonics Russia, 2016, **60**, No6, pp. 108-127 (in Russ.) DOI: 10.22184/1993-7296.2016.60.6.108.127.

[2] *Schitov N.N.* The optimal control theory application in the vacuum coating like "interference filter" elaboration // 7-th All Russia scientific and technical conference "Rapid solidification materials and coating". M.: «MATI» - K.E. Tsiolkowski RSTU, 2008. – pp. 120-127 (in Russ.).

ON THE PROBLEM OF FORMATION OF DEFECT-FREE PRODUCTS FROM NICKEL-BASED SUPERALLOY OBTAINED BY ELECTRON BEAM ADDITIVE MANUFACTURING*

D.A. GURIANOV[1], *S.V. FORTUNA*[1], *S.Y. NIKONOV* [1], *K.N. KALASHNIVOV*[1], *V.R. UTYAGANOVA*[1]

[1]*Institute of Strength Physics and Materials Science SB RAS, Tomsk, Russia*

Formation of products from nickel-based superalloys by additive manufacturing is an important and urgent tusk [1]. Nowadays for obtaining products with directional or single-crystalline structure substrates from the same material as the additive product itself are used [2]. With the purpose of reduction of expenses on technological process, as a substrate it is possible to apply cheaper material with isomorphic structure. As it is known [3], different approaches in additive manufacturing are characterized by different propensities to defect formation. The most widespread defects in the products obtained by the methods of additive manufacturing processes are the loss of fusible alloying elements, the formation of porosity and non-smelting, cracks and stratification. The last type of defects is most relevant for 3D printing of products on substrates made of a material with chemical composition different from product material. In this work by the wire-feed electron beam additive manufacturing (EBAM) defect-free product in the form of a wall from nickel-based superalloy ZhS6U were obtained on a steel substrate. In earlier works, the authors obtained similar products, but they contained defects in the form of cracks [4]. It should be noted that the EBAM process is characterized by such technological printing parameters as accelerating voltage (***U***, kV), beam current (***I***, mA) and printing velocity (***V***, mm/min) [5]. These parameters can be linked via the heat input:

$$E = \frac{60 \cdot U \cdot I}{1000 \cdot V}. \quad (1)$$

During the work three walls (products marked "1", "2" and "3") were obtained from ZhS6U superalloy on SS304 austenitic steel substrates with different heat input values of 0.37, 0.40 and 2.07 kJ/mm. The first two walls (obtained at lower heat input values) contained cracks, the third wall was defect-free. Since products from superalloys need to be obtained with directional structure, it makes sense to estimate the primary dendrite arm spacing (λ_1, μm - the main structural characteristic in directional solidification). In products with the lowest heat input at the substrate boundary, λ_1^{bottom} = 9.6 μm, and near the product upper surface, λ_1^{top} = 30.5 μm. In case of the largest heat input, λ_1^{bottom} = 7.6 μm and λ_1^{top} = 40 - 50 μm. On this basis, it is possible to calculate the values of temperature gradients at the substrate and the product surface, using the dependence:

$$\lambda_1 = A \cdot (G \cdot R)^{-n}, \quad (2)$$

where *A* is the coefficient proportional to the solidification interval; *n* is the dimensionless coefficient; *G* is the temperature gradient, °C/cm; *R* is the solidification rate, mm/s. Estimates made taking into account ratio (2) showed that for products "1" and "2" the value of temperature gradient changes from substrate to top in the range from 1493.87 to 9.8 °C/cm. And for article "3" the temperature gradient ranges from 3663.61 to 1.47 °C/cm. Thus, this paper shows that an increase in heat input reduces crack formation, but there is an enlargement of dendritic structure elements. This effect is undesirable for products with directional structure and further research is required to find a compromise solution.

REFERENCES

[1] A. V. Zavodov, N. V. Petrushin, D. V. Zaitsev, “Microstructure and phase composition of ZHS32 superalloy after selective laser melting, vacuum heat treatment and hot isostatic pressing,” Letters on materials, vol. 7 (2), pp. 111-116, 2017.

[2] Yao-Jian Liang, Jia Li, An Li, Xiao-Tong Pang, Hua-Ming Wang, “Solidification path of single-crystal nickel-base superalloys with minor carbon additions under laser rapid directional solidification conditions,” Scripta Materialia 127 (2017) 58–62.

[3] T. DebRoy, H.L. Wei, J.S. Zuback, et. al., “Additive manufacturing of metallic components – Process, structure and properties,” Progress in Materials Science 92 (2018) 112–224.

[4] D. A. Gurianov, S. V. Fortuna, and K. S. Osipovich, “Defects formation features of nickel-based superalloy product obtained by wire-feed electron beam additive manufacturing,” AIP Conference Proceedings 2167, 020125 (2019).

[5] S. Yu. Tarasov, A. V. Filippov, N. L. Savchenko, et. al., “Effect of heat input on phase content, crystalline lattice parameter, and residual strain in wire-feed electron beam additive manufactured 304 stainless steel,” Int J Adv Manuf Technol, volume 99, pages2353–2363(2018)

* The work was performed according to the Government research assignment for ISPMS SB RAS, project No. III.23.2.11. The reported study was funded by RFBR, project number 19-38-90072.

MICROSTRUCTURE FEATURES OF AN ADDITTIVELY FORMED NICKEL-BASED SUPERALLOY ON AN ISOSTRUCTURAL SUBSTRATE [i,ii]

S.V. FORTUNA[1], *D.A. GURIANOV*[1], *S.Yu. NIKONOV*[1], *K.V. IVANOV*[1], *E.S. KHOROSHKO*[1]

[1]*Institute of Strength Physics and Materials Science SB RAS, Tomsk, Russia*

In modern industry, the formation of products with single-crystalline or directional structures (for example, the fan blades of gas turbine engines from nickel superalloys) is carried out by directional solidification with a liquid-metal cooler. In this approach, the mold box with the crystallizing product is moved from the heating zone to the cooling zone, which is a molten easily fusible metal (e.g. aluminum). Such a process takes place at relatively low solidification rates (5mm/min), but the probability remains that undesirable radial components of the temperature gradient will be appear, leading to distortion of the growth direction of the structural elements. From this point of view, the application of additive manufacturing is a promising approach. In spite of the fact that in additive manufacturing the transition region from columnar structures to equiaxial structures (CET) is always formed [1], this region is melted at subsequent deposition of a new layer. Thus, in additive manufacturing products, equiaxial structures are observed only near the surface. Based on the above, the actual task is to identify structural features of products from nickel-based superalloys obtained by additive manufacturing.

At present, there are already works [2-4] devoted to this problem. A common approach among various authors is the use of a substrate made of the same material as the additive formed product. And the substrate, as a rule, already has a directed or single-crystalline structure. Due to the high cost of this approach, the use of substrates from more accessible materials is of interest. It is obvious that the use of a substrate made of a foreign material will lead to the appearance of a transition zone from the substrate to the formed product. This transition zone can have chemical and crystallographic effects on the material structure of the formed article. In addition, the appearance of undesirable phases in the substrate material may lead to distortion of the structural elements growth direction.

In order to assess the impact of the substrate on the formed product in this work by the method of wire-feed electron-beam additive manufacturing was obtained several walls of superalloy ZhS6u on a substrate of austenitic SS321 steel sheet.

According to the results of the research it was found that the border with the substrate is characterized by the thinnest dendritic structure, which indicates significant values of the temperature gradient. As the product grows, dendrites enlargement is observed, due to temperature gradient decrease. At the same time, directed solidification is realized with some inclination relative to the direction of additive growth. From the authors' point of view, the appearance of the slope is explained by the bending of the solidification front and one-way direction of 3-D printing. In turn, the bending of the molten pool boundaries is the result of two components of heat dissipation: into the material of an already formed product and into the chamber walls by means of radiation. The heat sink by radiation reaches maximum values at the top of the molten pool, which explains the formation of the CET region. It is also shown in the paper that the predominant orientation of the FCC crystal lattices γ - and γ' -phases, which are the basis of the material of the formed product, along the normal to the substrate surface corresponds to the crystallographic direction of type $\langle 001 \rangle$.

REFERENCES

[1] lM.J.Berminghama, D.H.StJohna, bJ.Krynen, et. al., "Promoting the columnar to equiaxed transition and grain refinement of titanium alloys during additive manufacturing," Acta Materialia, Volume 168, 15 April 2019, Pages 261-274.

[2] Yao-Jian Liang, Jia Li, An Li, Xiao-Tong Pang, Hua-Ming Wang, "Solidification path of single-crystal nickel-base superalloys with minor carbon additions under laser rapid directional solidification conditions," Scripta Materialia 127 (2017) 58–62.

[3] Yao-Jian Liang, Xu Cheng, Jia Li, Hua-Ming Wang, "Microstructural control during laser additive manufacturing of single-crystal nickel-base superalloys: New processing–microstructure maps involving powder feeding," Materials & Design 130 (2017) 197–207.

[4] Yao-Jian Liang, Jia Li, An Li, et. al. "Experimental optimization of laser additive manufacturing process of single-crystal nickel-base superalloys by a statistical experiment design method," Journal of Alloys and Compounds 697 (2017) 174-181.

[i] The work was performed according to the Government research assignment for ISPMS SB RAS, project No. III.23.2.11.

[ii] The reported study was funded by RFBR, project number 19-38-90130.

PREPARATION OF A COPPER SURFACE FOR THE CVD SYNTHESIS OF MONOLAYER GRAPHENE.*

D.V. SMOVZH, I.A. KOSTOGRUD, P.E. MATOCHKIN

Kutateladze institute of thermophysics,Novosibirsk, Russia

Modern CVD methods are developing in two main directions. The first is mass synthesis technologies, which include continuous synthesis systems based on various types of roll technologies, where copper foil is stretched through the hot zone of the reactor. The second direction is the synthesis of a large area graphene single crystal. In this case, it is assumed that the most suitable catalytic substrates are the precious metals like gold or platinum, on which it is possible to obtain large-sized metal grains. However, a number of recent studies have shown that by pre-heat treatment of copper, it is possible to obtain oriented grains on copper foil [1]. Graphene crystals formed on grains with the same crystallographic orientation form a graphene film with properties close to that of a single crystal. Thus, an important task today for the development of large-scale CVD technologies for graphene synthesis, which today are focused only on the use of a copper catalytic substrate, is to develop a method for forming a given copper surface texture.

In this paper, the influence of pretreatment stages of copper foil on the formation of its texture during graphene synthesis is studied. Preparation of the copper foil consisted of washing in water, in water and acetone, processing with acid (30% HNO3), followed by annealing for 0.5-10 hours, after which the graphene layer was grown in a mixture of Ar/H2/C2H2, the synthesis conditions are presented in detail in [2].

As a result of experiments, it is shown that the surface texture of copper is determined mainly by the annealing atmosphere and duration. Annealing regimes are obtained in the atmosphere of hydrogen, in which a surface of copper with an orientation (111) and a grain size of 5-10 mm is formed. The formation of a surface with orientation (111) occurs when the oxide layer is etched, which, as shown in [3], can stabilize the surface (001). Experimentally obtained conditions in which the copper texture is formed with the orientation (001), during annealing in an argon atmosphere and during short-term treatment with hydrogen, while the characteristic scale of copper grains is up to 0.2. Analysis of synthesized graphene on various surfaces showed that under identical conditions, a monolayer with a small number of defects is formed on the surface of 001, and a monolayer coating with inclusions of two and three-layer graphene is formed on the surface of 111.

REFERENCES

[1] *Xiaozhi Xu et al. //* Science Bulletin. – 2017. – 62. – 15. – 1074-1080.
[2] *E. V. Boyko et al. // Materials Research Express.* – 2019. – 12. – 6. – 125628.
[3] *Junxiong Hu et al. // Scientific Reports. – 2017. – 7.* – 45358.

* This work was supported by RFBR / Russian Foundation for Basic Research (Project No. 18-29-19099\18)

ARC-DISCHARGE SYNTHESIS OF COMPOSITE CARBON-TIN NANOMATERIAL FOR LI-ION BATTERY ANODES

A.V. ZAIKOVSKII[1]

[1] *Kutateladze Institute of Thermophysics, SB RAS, Lavrent'ev ave. 1, 630090, Novosibirsk, Russia*

Due to the growth of the portable electronic devices production, interest in Li-ion batteries is increasing. In modern commercial batteries, an anode is made of graphite, which theoretically gives a maximum capacity of 372 mAh/g. The use of tin makes it possible to achieve a greater capacity value: the theoretical maximum capacity is 994 mAh/g. However, the processes of intercalation of lithium ions into the tin material are accompanied by the volume expansion of the anode material, which leads to instability of the solid electrolyte interface layer and the destruction of the anode. An usage of nanoscale tin structures held by a stable matrix helps solve this problem. Moreover, in comparison with bulk tin, the nanoscale tin material has a more expanded surface and shorter diffusion paths for lithium ions, which significantly improves the characteristics of Li-ion batteries.

Arc-discharge synthesis is a promising method for producing composite carbon-metal nanomaterials [1]. This work presents the study results of the electric arc spruttering of composite graphite-tin electrodes, which leads to the formation of the nanomaterial consisting of spherical tin nanoparticles surrounded by a carbon matrix (Fig. 1(a)). The dimensional characteristics of tin nanoparticles, varying from 5 to 30 nm, and the structural characteristics of the carbon matrix, which can be either amorphous or graphene-like, depend on the conditions of electric arc synthesis.

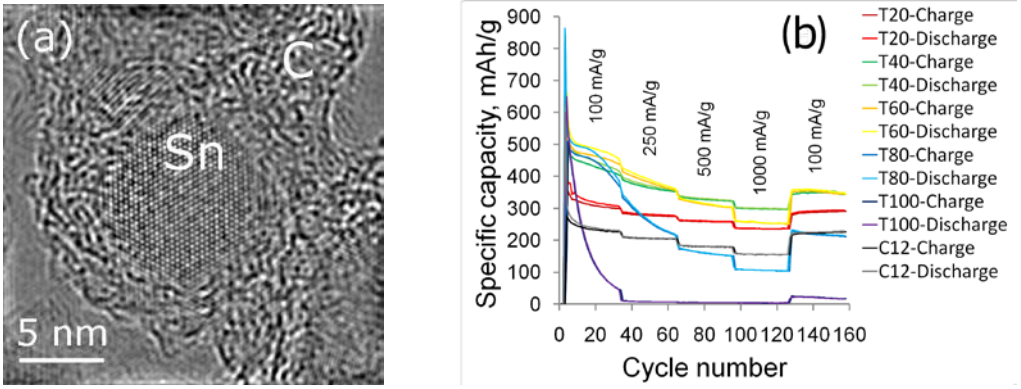

Fig.1. (a) HRTEM of Sn nanoparticle surrounded by carbon matrix, (b) Cycling characteristics of the synthesized C/Sn nanomaterials

The morphological and structural properties of C/Sn nanomaterials affect the capacitive characteristics of the anodes of Li-ion batteries (Fig. 1(b)). A tin content increase leads to an increase in specific capacity, but an tin nanoparticle size increase and an increase in the rigidity of the carbon matrix leads to a decrease in the stability of such materials. As a result, it was found that the optimal material is tin nanoparticles with an average size of 8 nm packed in an amorphous carbon matrix.

REFERENCES

[1] A. Zaikovskii, S. Novopashin, V. Maltsev, T. Kardash, I. Shundrina. "Tin–carbon nanomaterial formation in a helium atmosphere during arcdischarge"/ RSC Adv., V. 9, pp. 36621, 2019,

The work is a continuation of the project RFBR 17-43-540738.

INFLUENCE OF ANODIC SPARK MODE PARAMETERS ON THE PROPERTIES OF MAO-COATINGS

P.I. Butyagin, S.S. Arbuzova, A.V. Bolshanin, A.I. Kondratenko

MANEL JSC Tomsk Russia

It is known that MAO coatings can have a set of properties. The work of many researchers is aimed at studying the properties of MAO coatings [1-4].

By controlling the parameters of the MAO process, materials with new properties are formed. Therefore, it is relevant to study the influence of the parameters of the MAO process — pulse duration, pulse frequency, voltage on the composition, structure of the coatings.

In this study, results of investigation of influence of duration, frequency, voltage on the structure, composition, morphology of MAO coatings are presented

Table 1. MAO parameters and characteristics of the coatings

Number of Sample	Condition of the Coating	Coating thickness, μm	Porosity,%	average size of pores, μm
1	600V, 100Hz, 100μs	30	13,4	16,2
2	600V, 100Hz, 200μs	30	9,8	6,1

It was found that with the same coating thickness of 30 μm, its porosity decreases with increasing pulse duration from 100 μs to 400 μs (Fig. 1). An increase in the pulse frequency from 50 Hz to 100 Hz does not affect the porosity, but changes the size and shape of the pores. Changing the voltage from 350 V to 600 V reduces the porosity from 9% to 4%, while the pore size decreases from 22.5 μm to 10.6 μm.

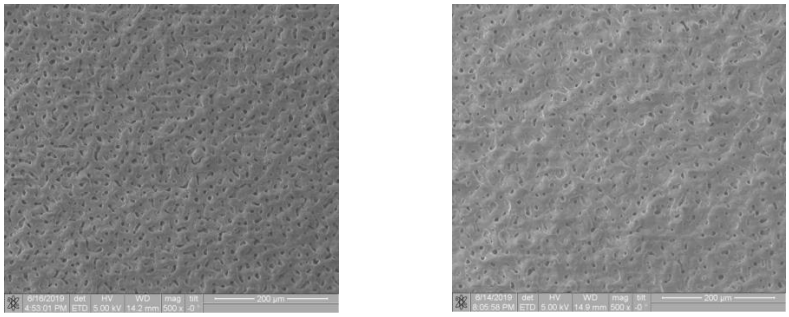

Sample 1 Sample 2

Fig.1 Effect of pulse duration on the morphology of MAO coatings

Thus, it is shown that when we control the parameters of the MAO process, coatings of the required composition and structure are created.

REFERENCES

[1] Gruss L.L. McNeil W.Anodic “Spark Reaction in Aluminate, Tungstate and Silicate Solutions,” Electrochem. Technol. Vol.1. N9, pp.283–287, 1963.

[2] Krysmann W., Kurze P., Dittrich K.-H., Schneider H.G. “Process characteristics and parameters of anodic oxidation by spark discharge (ANOF),” Crystal research and technology. V. 19. № 7, P. 973-979, 1984.

[3] Butyagin P.I., Khokhryakov Ye.V. and Mamaev A.I., Microplasma systems for creating coatings on aluminium alloys, Materials Letters, V.57, iss. 11, p. 1748-1751., 2003,

[4] S.S.Arbuzova, P.I.Butyagin, A.V.Bolshanin et al. “Microarc oxidation of metal surfaces: coating properties and application,” Izvestiya Vysshikh Uchebnykh Zavedenii. Fizika, No. 11. pp. 117–122, 2019.

DEPOSITION IN MICROWAVE PLASMA AND PERFORMANCE OF POLYCRYSTALLINE DIAMOND COATINGS WITH HIGH ADHESION ON SIALON CERAMICS CUTTING TOOLS[i]

E.E ASHKINAZI[1], A.K. MARTYANOV[1], V.S. SEDOV[1], V.G. RALCHENKO[1], D.N. SOVYK[1], S.V. FEDOROV[2], M.A. VOLOSOVA[2], V.I. KONOV[1]

[1]Prokhorov General Physics Institute of the Russian Academy of Sciences, *Moscow, Vavilova 38(1), 117312, Russia*
[2]*Moscow State Technical University "STANKIN", Moscow, Vadkovsky 3a, 127994, Russia*

Applications of new composite materials with high strength for aerospace, automotive, and other industries often meet a problem of their mechanical treatment. The presence of extremely hard components in the composites reduces drastically the lifetime of cutting tools, including ceramic tools. As for tools directly coated with a thin chemical vapor deposition (CVD) diamond film, they can also fail due to insufficient adhesion resulting in the diamond coating peeling. Experimental studies have shown that the surface roughness and its chemical composition are of primary importance for the adhesion of diamond coatings to ceramic base.

Here we describe the process for coating of a group of ceramic (SIALON) substrates (together loaded in reactor) with polycrystalline diamond films in microwave plasma in $H_2/CH_4/SiH_4$ gas mixture. By controlling the configuration of the microwave field in CVD reactor ARDIS–100 (Optosystems Ltd, 2.45 GHz) using a specially designed substrate holder, cutting inserts with uniform diamond layer and high adhesion to the substrate are obtained (Fig.1). Single layer diamond films and multilayer (with diamond grain size varied) films were produced using different diamond growth protocols. The critical load >41 N was measured in adhesion test for the coatings by scratching method.

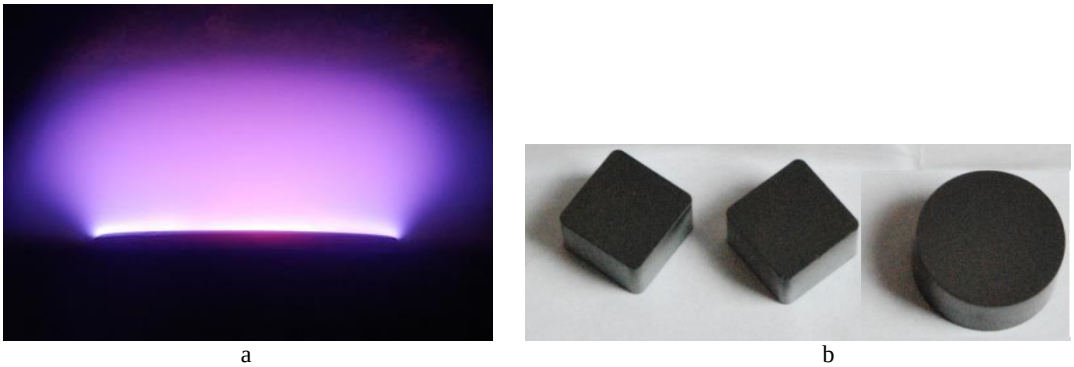

a b

Fig.1. a) Process of diamond coating in microwave discharge; b) SIALON inserts with diamond coating.

Cutting performance of the tools was significantly improved by reducing the friction coefficient. For different samples of bare (uncoated) SIALON ceramics, it varied within 0.33-0.44, while with the coating the friction coefficient decreased by 6-8 times down to 0.04-0.07.

The durability of the diamond coated SIALON inserts has been tested in dry turning of Al-Si alloy. Within the acceptable working parameters of machining the multi-layer coated diamond tools showed better performance compared to those with other types of coatings. Wear of the incisors on the back surface occurs gradually, the worn surfaces had a smooth appearance characteristic for micro-scale abrasive wear mechanism. The criterion wear of 0.4 mm in width, that defines the complete tool-life, still was not achieved with the cutting path of at least 2000 m.

[i] The work was supported by the Ministry of science and higher education of the Russian Federation, agreement No. 14.604.21.0206, unique project ID RFMEFI60418X0206.

THE STUDY OF PHASE FORMATION IN THE SYSTEM OF IRIDIUM - SILICON CARBIDE*

M.A. GOLOSOV, V.V. LOZANOV, N.I. BAKLANOVA

Institute of Solid State Chemistry and Mechanochemistry SB RAS, Novosibirsk, Russia

Silicon carbide has a number of useful properties, such as high hardness, strength, abrasion resistance, high thermal conductivity, thermal shock resistance and high oxidative stability [1,2]. The combination of all these properties makes it an integral component of high-temperature materials. For various applications, for example, such as catalytic substrates, semiconductor and high temperature materials, silicon carbide is used in combination with platinum group metals [3,4]. Due to its high melting point (2466 °C), low oxidation rate, and low oxygen permeability at high temperatures, iridium is a promising component of high-temperature materials [5,6]. That is why the iridium – silicon carbide system is of particular interest. However, information on this system is very limited. Thus, the aim of the work is a physicochemical study of the processes of interaction of iridium with silicon carbide.

To achieve the goal, heat treatment was carried out in the temperature range from 1000 to 1900 ºC with a step of 100ºC of mixtures of iridium powders with three different types of silicon carbide powders. Mixtures were prepared with a molar ratio of the starting components of 3: 1 and 1: 1, respectively. It has been established that the reaction rate is affected not only by the particle size, but also by the presence of oxygen impurities in the starting components. As a result of the interaction, free carbon is released. The process is multi-stage and depends on the processing temperature. At 1000 ° C, the Ir_3Si phase is formed, the content of which increases to a temperature of 1300 ° C. Further heating to 1400 ºC leads to a decrease in the content of this phase and the formation of the IrSi, Ir_3Si_2 and Ir_2Si phases. In the range of 1500–1600 ºC, the formation of a liquid phase occurs, as a result of crystallization of which the phases IrSi, Ir_3Si_2, Ir_2Si are released. At 1800-1900 ° C, in samples obtained from finely dispersed powders of silicon carbide, with a ratio of the starting components 1: 1, the reaction ended with the formation of IrSi. In the samples obtained from finely dispersed SiC powders, with the ratio of the starting components 3: 1, the phases Ir_3Si, Ir_3Si_2 and Ir_2Si are observed. Samples obtained from coarse-grained silicon carbide powder exhibit all the phases listed above. Iridium silicide (Ir_2Si) was discovered that was not previously registered by other researchers. Silicides with a silicon content of more than 50 at. % not found.

Schemes for the interaction of iridium with silicon carbide will be discussed.

REFERENCES

[1] M. Caccia, J. Narciso, SiC manufacture via reactive infiltration, Ceram. Trans. 249, (2014) 15–25.

[2] S. Yoshida, Electric refractory material, in: Y. Kumashiro (Ed.), Marcel Dekker, 2000 New York 437.

[3] Sun, L., Wang, B. & Wang, Y. A Schottky-junction-based platinum nanoclusters@silicon carbide nanosheet as long-term stable hydrogen sensors. Applied Surface Science 473, 641–648 (2019).

[4] Suzuki, S. et al. Improvement in stability of carbon support for platinum catalyst by applying silicon carbide coating. Journal of Power Sources 223, 79–85 (2013).

[5] Strife, J. R. Sheehan, J. E. Ceramic Bulletin, 1988, 67: 369.

[6] Strife, J. R. Smeggil, J. G. Journal of American Ceramic Society, 1990, 73: 838.

* The work was supported by the Russian Science Foundation under grant No. 18-19-00075.

FUNCTIONAL BORATE GLASS-CERAMICS DOPED WITH CR3+ IONS: SYNTHESIS AND CHARACTERIZATIONS*

A. BABKINA[1], *D. VALIEV*[2], *K. ZYRYANOVA*[1]

[1]*ITMO University, Kronverksky Avenue 49, 197101 Saint-Petersburg, Russia*
[2] *National Research Tomsk Polytechnic University, Lenin Avenue 30, 634050 Tomsk, Russia*

Glass-ceramics (GCs) is perspective candidate for functional applications due to the better technological capabilities of transparent GCs compared to single crystals or transparent glasses. The main benefits of such materials are wider possible ranges of operating temperatures, concentrations of dopants, and the possibility of combined use of various transition metal ions (TM); flexibility of varying technological regimes; the best elastic-plastic properties and efficiency of the technology. In the structure of the GC with a certain phase composition, a higher uniformity of the distribution of the activator is provided, the best characteristics of the conversion of UV radiation into visible and IR radiation are achieved [1-4].

Nowadays there is a lack information about systematic comprehensive study of the relationship between the kinetics of crystallization and sintering of oxide matrices of borate composition on the properties of the activation additives, including spectral-kinetic ones. There are unresolved issues also related to the possibility of obtaining and controlling the luminescence characteristics of optical glass-ceramics, such as quantum yield, emission spectrum, and kinetic attenuation parameters of luminescence. These characteristics depend on many factors: methods and modes of synthesis, features of the microstructure of glass ceramics; type, number and distribution of defects (luminescence centers) and dopants.

This work shows the results of the synthesis and study of structural and optical properties of alkali alumina-borate glass-ceramics doped with chromium ions, which possesses high quantum efficiency.

Alkali-alumina-borate GCs doped with Cr^{3+} ions were successfully synthesized by the melt quenching technique. $LiAl_7B_4O_{17}:Cr^{3+}$ nanocrystals were formed in the glass host during the subsequent one- and two-stage isothermal treatments above the crystallization temperature of the nanophase. There are structural, microscopic and optical-luminescent properties of prepared glass-ceramics were characterized.

The differential scanning calorimetry studies exhibited glass transition temperatures to be 411–422 °C and glass crystallization temperatures to locate in the 600–650 °C range. After two-stage heat treatment of glass samples at temperatures 450 °C and 600 °C the chromium-doped borate glass-ceramics was obtained. The two bands of the glass absorption spectra shifted towards small wavelength region after the heat treatment with changing the glass color. The XRD studies revealed the $LiAl_7B_4O_{17}$ nanocrystals nucleation with the mean size of 20–23 nm. The glass-ceramics emission spectra possessed three intense bands in the 685–715 nm spectral region indicating high symmetrical environment around the chromium ions under electron irradiation. The maximum value of the quantum yield corresponding to a chromium concentration of 0.05 wt.% was 30% under excitation of a wavelength of 532.8 nm. The issues of radiation-induced process of prepared borate glass-ceramics are discussed in detail.

REFERENCES

[1] S. Fujita, S. Tanabe, Glass-Ceramics and solid-state lighting, Int. J. Appl. Glas. Sci., vol. 6, pp. 356-363, 2015.

[2] A. Sakamoto, S. YamamotoGlass–Ceramics: Engineering Principles and Applications, Int. J. Appl. Glas.Sci., vol. 1 (3), pp. 237-247, 2010.

[3] G. Delaizir, P. Lucas, X. Zhang, H. Ma, B. Bureau, J. LucasInfrared glass-ceramics with fine porous surfaces for optical sensor applications, J. Am. Ceram. Soc., vol. 90, pp. 2073-2077, 2007.

[4] Y. Teng, K. Sharafudeen, S. Zhou, J. Qiu, Glass-ceramics for photonic devices, J. Ceram. Soc. Japan., vol. 120, pp. 458-466, 2012.

* The work was supported by Russian Science Foundation (No. 19-72-10036).

PULSED ELECTRON-BEAM ASSISTED SYNTHESIS OF A NI-AL SURFACE ALLOY

V.I. PETROV[1], A.B. MARKOV[1], A.V. SOLOVJEV[1], E.V. YAKOVLEV[1,2], D.A. SHEPEL' [1]

[1] Tomsk Scientific Center SB RAS, Laboratory of Advanced Technologies, Tomsk, Russia
[2] Institute of High-Current Electronics, Tomsk, Russia

The Ni-Al multilayer system is an interesting object for research, not only because it is a "storage" of chemical energy, which can be released at high rate in the form of heat during the formation of bonds between atoms of Ni and Al [1], [2]. It also provides a number of intermetallides such as Al_3Ni, Al_3Ni_2, AlNi, $AlNi_3$, which can be synthesized during this reaction. Of greatest important is AlNi intermetallic material, which has the highest melting point of all nickel and aluminum intermetallic compounds. Due to the combination of a high melting point and relatively high thermal and electrical conductivity, NiAl intermetallic have considered as a candidate for use as a matrix material in the manufacture of vacuum interrupter electrodes, i.e. replacements of copper used now in this quality [3], [4].

The results of numerical and experimental studies on the synthesis of Ni-Al surface alloy on a steel substrate are presented. The alloy was formed by preliminary magnetron sputtering of multilayer Ni-Al coatings of two types, consisting of thin (type I) ~ 0.1 and thick (type II) ~ 1 μm films and their subsequent irradiation and mixing by a pulsed electron beam transported to the samples in a plasma-filled diode. In the work, the optimal irradiation mode was determined by the numerical method for the formation of a Ni-Al surface alloy where intensive melting of all deposited films occurs, and there is no evaporation of the surface material. It is experimentally shown that, as a result of pulsed electron-beam melting, a Ni-Al surface alloy is formed, which is represented by NiAl high-temperature intermetallic phase. In the case of Ni-Al multilayer system made up of thin films, the surface alloy formed is homogeneous, but a network of cracks appears on the surface. In the case of Ni-Al multilayer system made up of thick films, the surface alloy formed is heterogeneous, both along the surface and along the depth of the target. Its structure is a composite, combining the alternation of hard (but brittle) and soft (but ductile) components, corresponding to NiAl high-temperature intermetallic phase and (Al, Ni, Fe) solid solution, respectively. It is precisely this structure of the Ni-Al surface alloy that makes it possible to obtain a crack-free surface with high tribological and high-temperature corrosion properties (Fig. 1).

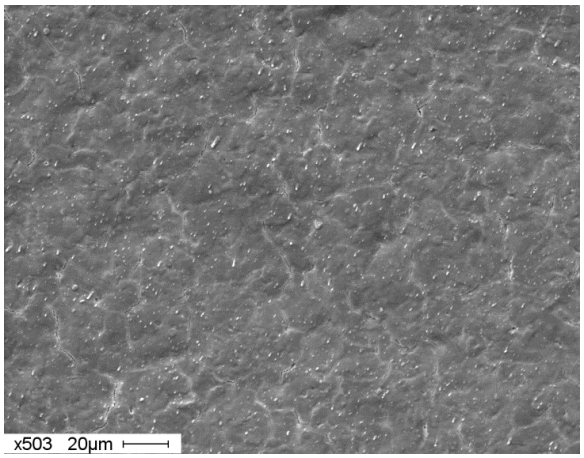

Fig. 1. SEM image of the Ni-Al surface alloy formed from multilayer system of type I.

REFERENCES

[1] Y. Wang, Z. Xing, Y. Qiao, H. Jiang, X. Yu, F. Ye, Y. Li, L. Wang, B. Liu, "Asymmetric atomic diffusion and phase growth at the Al/Ni and Ni/Al interfaces in the Al-Ni multilayers obtained by magnetron deposition," J. Alloys Compd., vol. 789, pp. 887–893, Jun. 2019, DOI. 10.1016/j.jallcom.2019.03.131.

[2] J. Wang, E. Benson, A. Duckham, S. J. Sprey, M. E. Reiss, O. M. Knio, T. P. Weihs, "Joining of stainless-steel specimens with nanostructured Al/Ni foils," J. Appl. Phys., vol. 95, no. 1, pp. 248–256, Jan. 2004, DOI. 10.1063/1.1629390.

[3] R. Watanabe, H. Andoh, K. Iwashita, Y. Kurosawa, "Electrical characteristics of Ni-Al-Cr alloy electrode for vacuum circuit breaker," J. Japan Inst. Metals, vol. 55, no. 3, pp. 337–343, Sep. 1991.

[4] R. D. Noebe, R. R. Bowman, M. V. Nathal, "The physical and mechanical metallurgy of NiAl," in Physical Metallurgy and processing of Intermetallic Compounds. Boston, MA, USA: Springer, 1996, ch. 7, pp. 212–296.

EFFECT OF HEAT LOSES ON THE STRUCTURE OF POROUS SHS MATERIALS*

N.S. Pichugin[1]

[1] *Tomsk Scientific Center SB RAS, Tomsk, Russia*

Self-propagating high temperature synthesis (SHS) is a promising method for manufacturing of porous gas permeable materials. The heat needed for sintering of a porous material is released during the chemical interaction of a mixture of the reactive components, i.e. a green mixture. The sizes of pores and skeleton elements of a synthesized material are significantly differing from the sizes of initial reagents, especially if the maximal temperature in the reaction zone exceed the melting point of any reactive component or a synthesis product. The reason is an existence of capillary effects in the SHS wave. Maznoy et al. [1] have studied the SHS of porous Ni-Al alloys and showed that skeleton elements are formed by up to 10^7 Ni and Al particles, which interacts in melted state during abrupt and superadiabatic temperature impulses.

There is an issue with SHS of coarse-porous materials, namely the formation of a skin-layer with small pores near the outer perimeter of a synthesized material. The skin-layer with small pore channels is dramatically reducing the permeability coefficient of a coarse-porous material. The formation of the skin-layer is favored because of heat loses of reactive media into the walls of a shape-generating molding tool, typically made from a steel or alloys with high thermal conductivity. The heat loses leads to abrupt decrease in temperature of the reactive mixture which significantly hinder the capillary effects, namely Marangony convection. The motivation of this work is a development of an approach for the obtaining of coarse-porous alloys without a small-pores skin-layer. The main approach is an applying of a barrier layer between the green mixture and the wall of a molding tool.

The experiments were conducted on a model SHS-system of Ni+15wt.%Al with the additives of 2 wt.% $Ca(OH)_2$ and 1 wt.% CaF_2. The green mixture was placed in a cylindrical molding tool made of stainless steel with inner diameter of 32 mm, wall thickness 3 mm, height 60 mm. The SHS was performed in the argon atmosphere with the initial preheating of 320 ℃. The following barrier layers were analyzed: office paper, chalk-coated paper, slurry-based coatings of ZrO_2 fine powder and ash-microspheres.

The experimental results as follows: the thicker the barrier layer, the coarser the porous structure of the alloy skin-layer (figure 1).

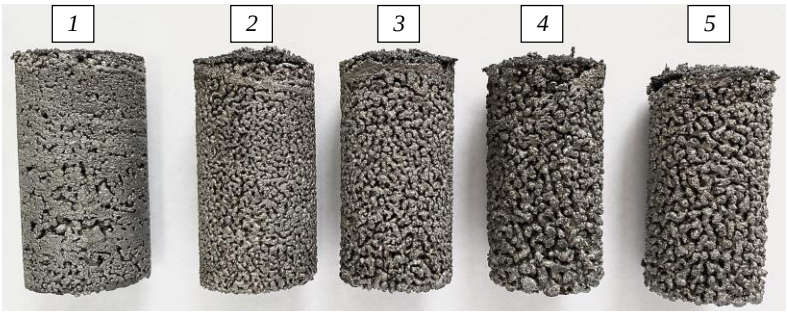

Figure 1. Images of synthesized alloys depending of the thickness of a barrier layer *h* made from the office paper. Part 1 – without barrier layer. Part 2 – *h* = 108 micron, Part 3 – *h* = 216 micron, Part 4 – *h* = 324 micron, Part 5 – *h* = 432 micron.

In the oral presentation the influence of different barrier layers on porous structure and SHS parameters will be presented quantitatively.

REFERENCES

1. A. Maznoy, A. Kirdyashkin, V. Kitler, N. Pichugin, V. Salamatov, and K. Tcoi, "Self-propagating high-temperature synthesis of macroporous B2+$L1_2$ Ni-Al intermetallics used in cylindrical radiant burners," *J. Alloys Compd.*, vol. 792, pp. 561–573, 2019.

* The work was supported by the Russian Science Foundation under grant No. 18-48-700037.

APPLICATION OF THE COLLECTOR PRESSING FOR SPARK PLASMA SINTERING OF THE OPTICAL TRANSPARENT OXIDE CERAMICS *

V.D. PAYGIN, E.S. DVILIS, O.L. KHASANOV., D.T. VALIEV, S.A. STEPANOV

National Research Tomsk Polytechnic University, TPU Nano-Centre, Lenin av.30, Tomsk, 634050, Russia

A large number of studies devoted to the development of transparent ceramics manufacturing technology are discussed in detail in review papers [1-3]. Despite the obvious advantages of transparent polycrystalline materials, their industrial application, until now, is very limited, since the optical quality of these materials is lower than that of their single-crystal and amorphous analogues [1-4]. In this regard, the development and optimization of the production technology of optically transparent polycrystalline materials for various industrial applications remains a very important task of material science. Transparent ceramic has several advantages over its single-crystal counterparts. For example, high mechanical properties, the ability to organize cost-effective large-scale production, the ability to control the shape, size and properties [5].

Promising from the standpoint of improving the quality of transparent ceramics and expanding the product range is the use of rational deformation schemes in the spark plasma sintering (SPS) method. These schemes are deprived the disadvantages of a uniaxial scheme. For example, collector pressing schemes [6]. It provides a uniform distribution of density in the volume of the powder body, which in turn can help to reduce the minimum pressure required to obtain transparent products.

In this work, the mechanical and optical properties of transparent ceramics based on YSZ and Ce:YAG were studied. Ceramics were fabricated by spark plasma sintering (SPS) using various pressing schemes.

Transparent ceramics based on yttrium stabilized zirconia (YSZ) and yttrium-aluminum garnet doped with ceria (Ce:YAG) were consolidated from commercial initial powders using SPS technique combined with method of collector pressing (CP): SPS+CP method.

The use of a collector pressing scheme made it possible to obtain ceramics with acceptable optical and mechanical properties at temperature 1300 ºC and 1600 ºC for YSZ and Ce:YAG respectively, under progressive uniaxial loading at 40 MPa.

The results of measuring the optical (in-line transmittance T and optical density D) and mechanical properties (Young modulus obtained by nanoindentation E_{it}, creep strain at indentation load C_{it} and Vickers microhardness H_{V200}) of obtained ceramics are represented in table 1.

Table 1 – Optical and mechanical properties of spark plasma sintered ceramics

Ceramics		H_{V200}, ГПа	E_{it}, ГПа	C_{it}, %	$T_{\lambda=600nm}$, %	$D_{\lambda=600nm}$, 1/cm	$T_{\lambda=1100nm}$, %	$D_{\lambda=1100nm}$, 1/cm
YSZ	SPS	14,47±0,71	127,7±1,5	1,63±0,24	31,58	9,48	57,68	4,74
YSZ	SPS+CP	15,52±0,41	143,8±7,4	3,03±1,03	34,58	6,01	63,14	3,65
Ce:YAG	SPS	15,01±1,05	171,5±11,7	1,56±0,45	23,54	19,49	28,15	16,01
Ce:YAG	SPS+CP	15,82±0,86	167,1±6,4	1,82±0,56	26,44	18,17	31,7	15,92

Thus, it was found that collector pressing during the SPS improves the optical properties (increase T in visible region by 2,9 – 3 %; in near infrared region by 3,55 - 5,46 %) and does not significantly affect the mechanical properties of transparent ceramics.

REFERENCES

[1] Wang, S. F., et al. "Transparent ceramics: Processing, materials and applications." *Progress in Solid State Chemistry*, vol. 41, no. 1-2, pp. 20-54, 2013.

[2] Shahbazi, H., et al. "Structure-transmittance relationship in transparent ceramics." *Journal of Alloys and Compounds*, vol. 785, pp. 260-285, 2019.

[3] Krell, A., J. Klimke, and T. Hutzler. "Transparent compact ceramics: inherent physical issues." *Optical Materials*, vol. 31, no. 8, pp. 1144-1150, 2009.

[4] Krell, Andreas, Thomas Hutzler, and Jens Klimke. "Transmission physics and consequences for materials selection, manufacturing, and applications." *Journal of the European Ceramic Society*, vol. 29, no. 2, pp. 207-221, 2019.

[5] Pournajaf, Reza, et al. "Polycrystalline infrared-transparent MgO fabricated by spark plasma sintering." *Ceramics International*, vol. 45, no. 15, pp. 18943-18950, 2019.

[6] Dvilis E.S., Khasanov O.L., Sokolov V.M., Pokholkov Yu.P. Method for compacting powder materials into articles and a mold for implementing the method. United States Patent № US 6919041 (19.07.2005)

* The work was supported by the Russian Science Foundation (RSF), project no. 17-13-01233. The authors are grateful to Alishin T.R. for assistance in preparing the collector mold.

HIGH TEMPERATURE SYNTHESIS OF INORGANIC PIGMENTS IN THE ZnO-MgO-CoO-Al(OH)$_3$-Al SYSTEM

N.I. RADISHEVSKAYA, A.Yu. NAZAROVA, O.V. LVOV, N.G. KASATSKY

Tomsk Scientific Center SB RAS, Tomsk, Russia

The self-propagating high-temperature synthesis method based on the velocity of processes and the use of simple equipment is an alternative to available and generally accepted technologies for producing inorganic pigments, in particular, to ceramic and sol-gel methods [1].

Cobalt oxides Co_2O_3, Co_3O_4, oxides ZnO, MgO and aluminum hydroxide $Al(OH)_3$ were used to synthesize medium blue pigments. Aluminum powder (ASD-4) was used as a metal reducing agent. Pigments were obtained in a constant-pressure bomb in air. To provide a layer-by-layer combustion mode, the mixture was heated to temperatures of 300÷500 °C and then the end of the sample was ignited with an electric coil.

The synthesis of SHS pigments with a particle size of ~ 1-2 μm became possible after replacing Al_2O_3 with $Al(OH)_3$. Studies have shown that heating aluminum hydroxide to 500–550 °C leads to the formation of γ-Al_2O_3 particles of the same size (~ 0.6 μm), while long keeping $Al(OH)_3$ in a furnace at a temperature of ~ 500 °C contributes to the coarsening of these particles. The particle size distribution was determined on a DelsaMax PRO analyzer.

High-velocity SHS processes reach high temperatures in a short time. Due to this, the hydroxide structure is rapidly destroyed releasing gaseous reaction products with the formation of submicron and active aluminum oxide, which reacts with cobalt oxide due to high temperatures, forming a fine spinel structure, as confirmed by studying the microstructure of the samples using scanning electron microscopy (Philips SEM 515) (Fig. 1).

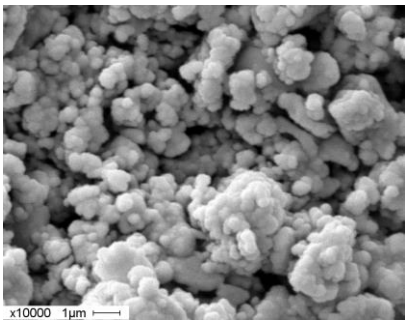

Fig. 1 SEM image of a pigment obtained from the ZnO-MgO-CoO-Al_2O_3 system, (Philips SEM 515).

It is known that aluminum spinels have a high hardness (7÷8 on the Mohs scale), which requires significant costs for their grinding [2]. In this regard, the obtaining of fine spinel SHS-pigments directly in the combustion wave simplifies their flow diagram (only disaggregation is required instead of grinding). Spinels based on zinc, magnesium, cobalt oxides easily form solid substitution solutions, which is favorable for obtaining medium blue pigments in various shades.

Thus, the addition of aluminum hydroxide $Al(OH)_3$ to the reaction mixture provides obtaining blue spinel pigments with a particle size of ~ 1 ÷ 2 μm.

This work was supported by RFBR (Project No. 18-33-00387-mol_a).

REFERENCES

[1] A.P. Amosov, I.P. Borovinskaya, A.G. Merzhanov, "Powder technology of self-propagating high-temperature synthesis of materials," Moscow: Mashinostroenie-1, 2007, 567 p. (in Russian).

[2] L.B. Khoroshavin, "Spineloid nano-refractories," Yekaterinburg: Ural Branch of the Russian Academy of Sciences, 2009. (in Russian).

INORGANIC PIGMENTS BASED ON COMPLEX OXIDES FOR PROTECTIVE-DECORATIVE ALUMINOPHOSPHATE-BONDED COATINGS

N.I. RADISHEVSKAYA, A. Yu. NAZAROVA

Tomsk Scientific Center SB RAS, Tomsk, Russia

Inorganic pigments, which are highly stable when heated and do not react with acids are widely used for colored protective-decorative and fire-resistant coatings based on aluminophosphate binder (APB) obtained by the interaction of aluminum hydroxide with phosphoric acid. Also, inorganic pigments based on complex oxides with the structure of spinel and heteropoly compounds (HPC) deposited on a mineral base, where transition metal cations are used as chromophores, can serve as a colored filler.

Spine pigments were obtained by the SHS method in a constant-pressure bomb in air using transition metal oxides (Co, Ni, Cr, Fe), aluminum oxide, and ASD-4 aluminum powder. HPC pigments (molybdophosphates, molybdosilicates, tungsophosphates and transition metal tungstosilicates) were synthesized by the interaction of a silicate mineral with a heteropolysol precipitated and crystallized on a carier directly in solution according to the procedure described in [1]. Marshalite, wollastonite, and talc were used as carrier minerals.

Pigments were added to the aluminophosphate binder in an amount of 10 -15 wt. % with a small amount of boric acid. Acid aluminum phosphates contained in APB had good binding properties. To obtain a hard ceramic coating, the painted and dried surface of the product was subjected to heat treatment for 1 ÷ 2 minutes by a gas burner (~ 300 °C).

The microstructure of pigments and protective-decorative coatings was studied by optical (Axiovert 200M) and scanning electron microscopy (Fhilips SEM 515) microscopy. The obtained composite decorative material was characterized by X-ray diffraction (DRON-UM1 diffractometer, filtered CuKα radiation) and IR spectroscopy (Nicolet 5700 IR Fourier spectrometer). The reflection spectra of the pigments were recorded with an Evolution-600 spectrophotometer using a reflection attachment. The thermal stability of a ceramic coating consisting of APB and inorganic pigments was determined on an SDT Q600 thermal analyzer. A hard protective-decorative coating was obtained using pigments based on heteropoly compounds deposited on marshalite. Figure 1 shows a thermal analysis of a mixture consisting of APB and an inorganic pigment based on cobalt molybdophosphate and marshallite. The loss of adsorbed and crystallization water is divided into several stages with peaks at 111.1 °C, 168.6 °C and without peaks at ~ 225 °C and ~ 260 °C. A phase transition in marshalite is observed in the range of 566.5-568.8 °C: α-quartz → β-quartz. The coating is stable up to a temperature of 950 °C.

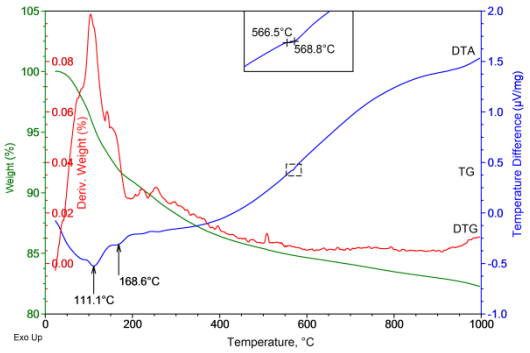

Fig. 1. Thermal analysis of cobalt molybdophosphate sorbed on marshalite and aluminophosphate binder (the maximum mass decrease on the DTG curve is directed upwards).

Similar results were obtained using spinel pigments.

This work was supported by RFBR (Project No. 18-33-00387-mol_a)

REFERENCES

[1] N.I. Radishevskaya Inorganic pigments based on transition metal oxometallates deposited on a silicate base // Technique and Technology of Silicates, vol. 19, no. 1, pp. 18-27, 2012.

NEW MATERIALS AND COATINGS FOR NUCLEAR TECHNOLOGY

V.S. OKUNEV

Bauman Moscow State Technical University, Moscow, Russia

In order to eliminate severe accidents in new generation fast nuclear reactors, it is possible to use pellet fuel based on micrograins of ceramics UO_2-Pu_4O_7 (MOX) or UN-PuN (MN) and depleted (dump) uranium metal nanopowder. The technology for producing such fuel is known. It was developed for VVER in JSC "V.G. Khlopin Radium Institute" (St. Petersburg, Russia, 2011) and involves sintering of micropowder of ceramics and nanopowder of metal hydride. The nature of the emergency conditions in a reactor with MOX-U-fuel (about 20% U by weight) and MN-fuel is almost the same. First of all, emergency modes, accompanied by a failure of emergency protection (ATWS - anticipated transients without scram), and their combinations were considered. The role of the Doppler reactivity coefficient is approximately the same in different emergency conditions. As a result, optimization of the layout of the reactor with restrictions for the functional models simulating the safe termination of ATWS modes is not in conflict.

The most preferred fast reactor fuel (the ATF - Accident Tolerant Fuel) can be considered MN fuel with the addition of U nanopowder (about 20% by weight). MN-U is a high temperature fuel. Emergency behavior is similar to using metallic fuel. The role of the Doppler reactivity coefficient is the same in all emergency conditions. (When using MOX fuel, this role is different.)

To increase the safety of fast reactors, lead coolant is more preferable. The self-protection of the reactor depends on the isotopic composition of lead. By maximizing the content of the twice-magic 208Pb, the neutron balance improves. Additional opportunities are opening up for the disposal of radioactive waste and to increase the breeding ratio, including in the core (BRC). When using MOX-U or MN-U fuel, it is easily achievable BRC = 1, which eliminates large reserves of burnup reactivity: the core operates in self-supplying fuel (the operating and burning rates of fissile nuclides are the same). The use of a coolant based on 208Pb reduces the void effect of reactivity to safe values even in reactors of infinitely high power. Weak absorption of neutrons by 208Pb nuclei contributes to an increase in the lifetime of instantaneous neutrons, which is important to eliminate reactive accidents that pose a potential danger to fast reactors.

Optimization of the composition of lead coolant does not require isotope separation. The maximum content of ^{208}Pb is characteristic of lead of thorium ores (^{208}Pb is the final decay product of ^{232}Th), ^{206}Pb is characteristic of lead of uranium ores (^{206}Pb is the final decay product of ^{238}U).

The use of cladding of tungsten-coated fuel rods on both sides, deposited using low-temperature plasma spraying, can improve the reliability and safety of lead-cooled reactors without impairing (and possibly improving) the economic characteristics of nuclear power plants. The use of tungsten coatings of the claddings will reduce the rate of corrosion and erosion in liquid lead, the void effect of reactivity, will open up the possibility of using cheap lead, which is more contaminated with impurities.

It is possible to adapt new materials for other types of nuclear technology. The problem of ATF search with increased (compared to UO_2) thermal conductivity is relevant for thermal neutron reactors. It can be $UO_{2,1}$, UN, U_2N_3, U_3Si_2 fuel (with a much lower concentration of fissile nuclides) with the addition of a low enriched U nanopowder (to increase the reactor power and increase the density and thermal conductivity of the fuel) or Be (BeO).

Ceramic fuel containing depleted uranium with U nanopowder can be used in the blanket of a thermonuclear reactor. As a neutron multiplier, ^{237}Np, ^{241}Am and ^{243}Am nuclei (long-lived radioactive waste to be disposed of) are more preferable than beryllium. The cross section for their fission in the spectrum of thermonuclear neurons is approximately 10 times higher than the cross section for the (n, 2n) reaction on ^{9}Be nuclei. At neutron energies above 6 MeV, reactions (n, 2n) are realized on Np and Am nuclei. When using a liquid metal coolant containing lead, tungsten coatings of fuel claddings are of interest.

All the proposed innovations can be implemented within the framework of existing technologies.

These studies represent the development of works supported by a grant from the Russian Foundation for Basic Research (grant 94-02-03566).

RANKING OF LMFR COOLANTS BY DEGREE OF PREFERENCE

V.S. OKUNEV

Bauman Moscow State Technical University, Moscow, Russia

The world concepts of liquid metal cooled fast reactors (LMFR) are developed in two main directions: with sodium and lead (based on natural lead) cooling. The development of nuclear technology leads to the need to analyze new materials in nuclear technology. This is necessary in case of unforeseen difficulties in the transition to new generation reactors (including high power). Based on the use of operations research methods, the ranking of potential coolants LMFR was conducted. Traditional and exotic fluids that have never been used in nuclear technology were considered. Not individual coolants or "coolant - structural material" pairs were compared, but the optimal reactor layouts (with different coolants and structural materials compatible with them) obtained in solving mathematical programming problems with restrictions in the same formulation ("DRACON-M" code).

Different designation of reactors requires consideration of different quality criteria. For medium and high power reactors, it is necessary to limit the void effect reactivity (VRE). VRE, implemented during the drainage of the entire reactor was considered as the target functional. VRE, which is realized by draining the central part of the core (which is the most dangerous), was considered among the restrictions: VRE < 0 (or VRE < β, where β is the effective fraction of delayed neutrons). For low power reactors, VRE can be excluded from the optimization problem. Additional requirements are imposed on multipurpose low power reactors and special purpose reactors. For high- and ultra-high-temperature reactors (for example, for the production of hydrogen, liquid fuel from coal, etc.), special attention should be paid to the restrictions for the maximum temperatures of the coolant and structural materials. At the same time, a coolant with a wide range of operating temperature is needed. For space reactors, it is necessary to use a coolant operating in a wide temperature range at a low freezing temperature. In all optimization problems, constraints for the functionalities characterizing the nominal and emergency (anticipated transient without scram - ATWS) reactor operation modes were considered.

Initially, a wide range of potential coolants was considered: almost all stable metals of the periodic system of elements and their alloys. At the first stage of research, the least preferred metals in terms of their physicochemical properties were excluded. Then, metal compounds with different concentrations of components were analyzed, i.e., the multicriteria problem had to be solved on an infinite number of objects (coolants). At the next stage, it was possible to reduce the problem to a discrete finite-dimensional one with a relatively small number of objects (Li, Na, K, Cs, Ga, Pb, Bi, their alloys of a fixed composition). At the final stage, when the ranking was completed, the most preferred options were analyzed and specified. For example, heat carriers based on natural lead, lead of thorium and uranium ores, and lead containing small additives of alkali metals (lowering the freezing temperature and / or minimizing the corrosion rate) were considered as lead coolant. Chemically pure sodium and sodium with small additions of heavy metal (reducing chemical activity) were considered as the sodium coolant. The composition of Na-K-Cs alloys with reduced chemical activity (from the Rosebom triangle) was optimized for reactors for various purposes.

Four groups of criteria were selected: (1) a wide range of operating temperatures, a high boiling point, (2) technological assimilation and possible technological problems, long-term induced activity, (3) self-protection from a combination of severe accidents not ruled out deterministically, (4) prevalence in the earth's crust, etc. The lexicographic method was used to solve the multicriteria tasks.

Lead with a content of ^{208}Pb of more than 75 ... 80% (thorium ores) is preferred for high power reactors (1200 MW-el.), Lead with a high concentration of ^{206}Pb (uranium ores) is preferred for low power (up to 100 MW-el.). For space reactors, Na, K, Cs based alloys are preferred. For ultra-high-temperature small reactors, gallium, lead and alloys based on them are preferable.

These studies represent the development of works supported by a grant from the Russian Foundation for Basic Research (grant 94-02-03566).

STUDY ON THE BIOCOMPATIBILITY OF A-C:H:SIO$_X$ COATINGS ON TI-6AL-4V ALLOY*

A.S. GRENADYOROV[1], *A.A. SOLOVYEV*[1], *K.V. OSKOMOV*[1,2], *M.O. ZHULKOV*[1,2], *A.M. CHERNYAVSKIY*[1,2], *I.A. KHLUSOV*[3], *V.V. MALASHCHENKO*[1,4]

[1]*Institute of High Current Electronics SB RAS, Tomsk, Russia*
[2]*National Medical Research Center named after E.N. Meshalkin, Novosibirsk, Russia*
[3]*Siberian State Medical University, Tomsk, Russia*
[4]*Immanuel Kant Baltic Federal University, Kaliningrad, Russia*

Diamond-like carbon coatings (DLC) are well known for their high hardness, good tribological, optical and biomedical properties [1–6]. The inclusion of the Si or SiO_x in a diamond-like carbon matrix leads to improved biomedical properties while maintaining high mechanical and tribological characteristics [7, 8]. These coatings are called a-C:H:SiO_x, diamond-like nanocomposite (DLN), DLC:SiO_x.

The a-C:H:SiO_x coatings are important in the medical applications for increasing the protection, biocompatibility and wear resistance of medical devices that are implanted in the human body. Most medical devices and implants are made of stainless steel (AISI 304, AISI 316L, AISI 321, et al.) or titanium alloys (Ti-6Al-4V, Ti-6Al-7Nb).

In this work, the properties of a-C:H:SiO_x coatings deposited on the Ti-6Al-4V titanium alloy by plasma chemical deposition in a mixture of argon and polyphenylmethylsiloxane vapors were investigated. Before the coating deposition, samples were treated by a low-energy high-current electron beam to reduce surface roughness. It was shown that after electron beam treatment, the mean-square surface roughness of R_q decreases from 22 to ~ 8 nm. Subsequent deposition of a-C:H:SiO_x films results in an increase in hardness, a decrease in the friction coefficient, and a decrease in the wear rate of the surface.

It has been shown that deposition of a-C:H:SiO_x coatings on the surface of Ti-6Al-4V samples reduces platelet adhesion, which is important from the point of view of thrombosis reducing. *In vitro* investigation of variants of cell death (apoptosis, necrosis) of blood leukocytes at direct 24-hour contact with tested samples by means of flow cytofluorometry was conducted. The fraction of viable cells in the tested samples was more than 75%. According to the international standard ISO 10993-5-2009 it indicates the absence of cytotoxicity of Ti-6Al-4V samples with a-C:H:SiO_x coating with respect to human blood leukocytes.

REFERENCES

[1] Zavaleyev V., Walkowicz J., Kuznetsova T., Zubar T. / The dependence of the structure and mechanical properties of thin ta-C coatings using electromagnetic venetian blind plasma filter on their thickness // Thin Solid Films. – 2017. – V. 638. – P. 153-158.

[2] Fabio Ferreira, Asim Aijaz, Tomas Kubart et al / Hard and dense diamond like carbon coatings deposited by deep oscillations magnetron sputtering // Surface and Coatings Technology. – 2018. – V. 336. – P. 92-98.

[3] Ankit K., Ashish Varade, Niranjan Reddy K. et al / Synthesis of high hardness IR optical coating using diamond-like carbon by PECVD at room temperature // Diamond and Related Materials. – 2017. – V. 78. – P. 39-43.

[4] Niranjan Reddy K., Varade A., Krishna A. et al / Double Side Coating of DLC on Silicon by RF-PECVD for AR Application // Procedia Engineering. – 2014. – V. 97. – P. 1416-1421.

[5] Feng Wen, Jiaqi Liu, Jianlu Xue / The Studies of Diamond-Like Carbon Films as Biomaterials: Review // Colloid and Surface Science. – 2017. – V. 2. – P. 81-95.

[6] Lopes F.S., Oliveira J.R., Milani J. / Biomineralized diamond-like carbon films incorporating titanium dioxide nanoparticles improved bioactivity properties and reduced biofilm formation // Materials Science and Engineering C. – 2017. – V. 81. – P. 373-379.

[7] Barve S.A., Chopade S.S., Kar R., Chand N., Deo M.N., Biswas A., Patel N.N., Rao G.M., Patil D.S., Sinha S. / SiO_x containing diamond like carbon coatings: Effect of substrate bi-as during deposition // Diamond & Related Materials. – 2017. – V. 71. – P. 63-72.

[8] Bociaga D, Sobczyk-Guzenda A, Komorowski P, Balcerzak J, Jastrzebski K, Przybyszewska K, Kaczmarek A. / Surface Characteristics and Biological Evaluation of Si-DLC Coatings Fabricated Using Magnetron Sputtering Method on Ti6Al7Nb Substrate // Nanomaterials. – 2019. – V. 9. – P. 812.

* The work was supported by the Russian Science Foundation under grant No. 19-19-00186 and is a continuation of the work on RFBR grant № 14-08-31164.

EFFECT OF PRESSURE ON THE JOINT REDUCTION OF ZrO_2 AND B_2O_3 WITH CALCIUM*

B.SH. BRAVERMAN, A.N. AVRAMCHIK, O.G. KRYUKOVA, YU.M. MAKSIMOV

Tomsk Scientific Center SB RAS, Tomsk, Russia

Calcium has found application as a reducing agent to obtain f-elements (rare-earth metals, their alloys, uranium, etc.) [1]. Calcium hydride is used [2] to obtain powders of metals, intermetallic compounds, refractory compounds and composite materials from oxides, where calcium is a reducing agent. The obtaining of refractory nitrides from oxides under nitrogen pressure using calcium as a reducing agent was implemented at the Tomsk Scientific Center of SB RAS [3]. The previous studies showed that the pressure of the gaseous medium ambiguously affected the temperature and combustion rate of calciothermal systems [4]. The goal of this work is to study the effect of pressure on the joint reduction of ZrO_2 and B_2O_3 with calcium.

The adiabatic combustion temperature (T_{ad}) and the equilibrium composition of the products were calculated using the TERRA software package [5]. The experiments were conducted in a constant pressure reactor under the argon atmosphere. High-purity titanium TiO_2 and zirconium ZrO_2 oxides, granulated calcium with a diameter of granules of 0.5-2 mm manufactured by Chepetsk Mechanical Plant, calcium iodate $Ca(IO_3)_2$ manufactured by Almerdale Assets Ltd, ultra-high-purity boron oxide B_2O_3, high-purity nitrogen gas (GOST 9293-74, Russia) were used as starting materials. The prepared mixtures were placed in a paper crucible with a diameter of 23 mm. The temperature was measured with thermocouples W-5%Re/W-20%Re welded from Ø 0.2 mm wire. B_2O_3 oxide was added to the mixture, based on the formation of ZrB_2 and Zr in the products. The studies were conducted on 4 samples shown in Table.

Sample #	$Ca(IO_3)_2$, g	ZrO_2, g	B_2O_3, g	Ca, g
1	0	18.48	7.18	28.35
2	1.8	18.48	7.18	29.68
3	3.0	15.4	5.98	25.85
4	5.7	15.4	5.98	27.86

Calculations showed that for P = 0.1 MPa, with an increase in the amount of $Ca(IO_3)_2$ additive, T_{ad} increases from 2283 K (sample 1) to 2703 K (sample 4), which reflects an increase in the thermality of the mixtures. An increase in pressure from 0.1 to 8.1 MPa leads to an increase in the T_{ad} of all compositions to the melting temperature of CaO - 2900 K. Despite the differences in the thermality of these mixtures, the latent heat of CaO melting restricts the growth of T_{ad} to 2900 K. In the pressure range p = 0.1 - 1.5 MPa, the reduction of ZrO_2 is not complete, resulting in the formation of $CaZrO_3$. The composition of condensed products is represented by the phases: CaO, ZrB_2, $CaZrO_3$, Zr. For pressures P> 5 MPa, the oxides are completely reduced. The composition of the products in this case is represented by the phases: CaO, ZrB_2, Zr. An increase in temperature with increasing pressure occurs mainly due to a shift in the equilibrium $CaZrO_3 + Ca \leftrightarrow Zr + CaO$ to the right. The increase in pressure was shown to favorably affect the joint reduction of ZrO_2 and B_2O_3 with calcium.

REFERENCES

1. *The Rare Earths*, Spedding, F.H. and Daane, A.H., Eds., New York–London: Wiley, 1961.
2. A.V. Kasimtsev, Yu.V. Levinsky. Calcium hydride powders of metals, intermetallic compounds, refractory compounds and composite materials, Moscow: MITKhT, 2012. 247 p.
3. A.N. Avramchik, B.Sh. Braverman, Yu.M. Maximov, and L.N. Chukhlomina, "On the possibility of obtaining refractory metal nitrides in a calciothermic process" Combustion, Explosion, and Shock Waves, 2014, vol. 50, no. 5, pp. 532-533. DOI: 10.1134/S0010508214050062
4. A.A. Glazunov, Yu.M. Maksimov, A.N. Avramchik, B.Sh. Braverman. Effect of the Fluid–Vapor Phase Transition in the Combustion of Calcium with Iron Trifluoride // Combustion, Explosion, and Shock Waves, 2020, vol. 56, no. 1, pp. 51-56. DOI: 10.1134/S0010508220010062
5. Trusov B.G. Computer simulation of phase and chemical equilibria, Inzh. Vestn.- 2012, No. 8. - Pp. 1–7. -URL: http://engbul.bmstu.ru/doc/483186.html.

* The work was supported by the Russian Foundation for Basic Research (grant No. 18-03-00875).

PHYSICAL PROPERTIES OF THE NIAL INTERMETALLIC COATING PRODUCED BY IRRADIATION WITH A LOW-ENERGY HIGH-CURRENT ELECTRON BEAM

E.A. PESTEREV, A.B. MARKOV, E.V.YAKOVLEV, D.A. SHEPEL', A.V. SOLOVYOV, V.I. PETROV

Tomsk Scientific Center of the Siberian Branch of the Russian Academy of Sciences , Tomsk, Russia, e-mail: eugenejuk@gmail.com

The widespread use of low-carbon steel in industry in the manufacture of various structures, machine parts and structures is due to the simplicity of processing and the relatively low cost of the material [1]. However, their wear, corrosion and oxidation resistance are weak [2]. One way to improve these properties is to coat in this material. Recently, much attention has been paid to composite coatings of high-temperature intermetallic compounds [1, 2].

A special place among these coatings is occupied by the NiAl intermetallic compound, which combines the properties of both ceramics and metal, having a high melting point, thermal conductivity, oxidation resistance, and high temperature corrosion resistance along with low mass density [3]. All this makes NiAl intermetallic very attractive for coating parts used at high temperatures in aggressive environments, for example, turbine blades of aircraft engines, guide vanes of industrial steam turbines, etc. [4].

Earlier, sources of low-energy high-current electron beam (LEHCEB) and devices for ion-plasma deposition of coatings were separate installations, and during the transfer of processed products from one working chamber to another, they came into contact with the surrounding atmosphere, which is undesirable, and in many cases simply unacceptable. To eliminate this drawback, a combined RITM-SP combined installation, including a source of LEHCEB and a magnetron atomizer, which are mounted on a common vacuum chamber [5].

The aim of this work is to study the physical properties of the synthesis of a surface alloy of Ni-Al using magnetron sputtering of a composite coating on a steel substrate and irradiation with a LEHCEB. The results of a decrease in wear resistance and roughness, as well as an increase in hardness of the formed Ni-Al surface alloy in comparison with an untreated steel substrate, are presented.

REFERENCES

[1] Mohammad Reza Bafandeh, Ali Omidi, Abdullah Irankhah In situ coating of low carbon steel with Ni–Al–Fe powder mixture via mechanical alloying // Surface & Coatings Technology. – 2017. – V. 315. – P. 268–273.

[2] C. Sierra, A.J. Vazquez NiAl coatings on carbon steel by self-propagating high-temperature synthesis assisted with concentrated solar energy: mass influence on adherence and porosity // Solar Energy Materials & Solar Cells. – 2005. – V. 86. – P. 33–42.

[3] Grzegorz Dercz, L. Pająk, B. Formanek Dispersion analysis of NiAl–TiC–Al 2O 3 composite powder ground in a high-energy attritorial mill // Journal of Materials Processing Technology. – 2006. – V. 175 (1). – P. 334-337.

[4] Jing Wen, Hongzhi Cui, Na Wei, Xiaojie Song, Guosong Zhang, Canming Wang, Qiang Song Effect of phase composition and microstructure on the corrosion resistance of Ni-Al intermetallic com-pounds // Journal of Alloys and Compounds. – 2017. – V. 695. – P. 2424 – 2433.

[5] Markov A.B., Mikov A.V., Ozur G.E., Padei A.G. // A РИТМ-СП facility for the surface alloying. Tech. – 2011 – 6 – 122-126.

ACOUSTIC SIGNALS IN NI-AL COATED STEEL INDUCED BY IRRADIATION WITH A LOW-ENERGY HIGH-CURRENT ELECTRON BEAM

E.A. PESTEREV[1], *A.B. MARKOV*[1], *A.V. SOLOVJEV*[1], *E.V. YAKOVLEV*[1,2], *D.A. SHEPEL'*[1], *V.I. PETROV*[1]

[1] *Tomsk Scientific Center SB RAS, Laboratory of Advinced Technologies, Tomsk, Russia*
[2] *Institute of High-Current Electronics, Tomsk, Russia*

The increasing requirements of modern technologies for the formation of new materials and coatings the constant development of scientific methods, techniques of monitoring the characteristics and properties of materials during their modification is required. Exposure by the intense pulsed electron beams is a universal way of modifying the material and forming of various compositions surface alloys. In material or a coating during pulsed exposure by electron beam the thermoelastic stresses is occur. These thermoelastic stresses are sources of acoustic waves. Acoustic waves propagating from the interaction region carry information both on the energy properties and spatial distribution of the particle flux and on the thermodynamic processes during the formation of surface alloys. This acoustic effect can become the basis of a new method for studying the properties of new materials and processes during their formation.

Of particular interest are nickel-aluminide intermetallic compounds such as NiAl and Ni_3Al. The perspective of their use is the necessity to create a new type of high-temperature and high-strength structural materials. The choice of nickel-aluminide intermetallic compounds is justified by high melting points, relatively low densities, good strength and resistance to oxidation. These intermetallic materials have great potential for use in automobile engines, aircraft, as well as in equipment for the production and conversion of energy.

In this work, to form a surface intermetallic compound Ni-Al, an electron-beam machine RITM-SP is used [1]. It operates on the basis of a source of a low-energy high-current electron beam (LEHCEB) created at the Institute of High Current Electronics SB RAS. A distinctive feature of this machine is a wide-aperture electron beam. It provides uniform physical properties over the entire coating area and the absence of problems with coating adhesion. The coatings (surface alloys) formed by this method can be a thickness from fractions to tens of microns.

The action of a pulsed electron beam on a solid creates acoustic waves in it. The amplitude of these waves is proportional to the radiation power density. It is proposed to use radiation-acoustic diagnostics to measure the energy of a pulsed electron beam [2]. Radiation-acoustic diagnostics is based on the registration of acoustic waves in the target during the dissipation of the energy of a pulsed electron beam. This is the so-called radiation-acoustic effect. The object of research is acoustic processes during the formation of surface alloys by LEHCEB.

The study of acoustic signals induced by the action of a LEHCEB of microsecond duration on a Ni-Al coating is presented. The Ni-Al alloy was formed on a steel substrate by sputtering and subsequent single irradiation of the multilayer system Ni(0.5 μm) – Al(1.5 μm) – Ni(0.5 μm). The typical forms of acoustic signals generated during exposure to a multilayer Ni(0.5) / Al(1.5) / Ni(0.5) / Fe multilayer system were experimentally obtained. It has been established that, during the action of an LEHCEB, acoustic signals have groups of characteristic spectral components whose frequencies depend on the type of sample. It has been established that during the influence of the LEHCEB acoustic signals have groups of characteristic spectral components. It was shown that the amplitudes of the characteristic spectral components for Ni-Al coatings depend on the charge voltage of the electron beam.

REFERENCES

[1] A.B. Markov, A.V. Mikov, G.E. Ozur, A.G. Padey. RITM-SP installation for the formation of surface alloys. Instruments and experimental technique. 2011. No 6. S. 122-126.

[2] White R.M. Generation of Elastic Waves by Transient Surface Heating // J. Appl. Phys. 1963. V. 34. pp. 3559-3567.

INFLUENCE OF ENERGY ACTION MODES ON HEAT AND MASS TRANSFER OF SURFACING MATERIAL, FORMATION OF STRUCTURE AND PROPERTIES OF COATINGS*

Yu. N. SARAEV [1], V. P. BEZBORODOV [1], M. V. PEROVSKAYA [1], V. M. SEMENCHUK [1], B. S. BRAVERMAN [2], K. A. BOLGARU [2]

[1] Institute of strength physics and materials science SB RAS, Academichesky Avenue, 2/4, Russia, Tomsk, 634055, phone: 8(3822)286850

[2]Department of structural Macrokinetics of TSC SB RAS

The possibility of influencing the characteristics of heat and mass transfer of the surfacing material and the formation of a dispersed structure in the coatings, increasing their properties when modifying the molten metal is studied.

To solve the problem of controlling droplet formation, transfer of electrode metal, crystallization of the surfacing bath, it is important to control changes in arc voltage, current, instantaneous arc power. New methods of diagnostics of rapidly occurring heat and mass transfer processes accompanying melting, transfer and crystallization of metal from the melt were applied. Steel 09G2S was used to study the influence of surfacing modes at direct current and pulse change of energy parameters of the modes. Surfacing was performed by electrodes T-590-N. Powders of titanium nitrides and carbides were used as a dispersed component. A mixture of powder granules with a liquid glass binder was applied in a thin layer to the electrode coatings. Surfacing by electrodes was carried out by one and two layers. The research complex consisting of the inverter power supply PHOEBUS-315 "MAGMA" with the mode of pulse-arc surfacing, sensors of measurements of the main energy parameters, the Registrar of these parameters AWR-224 MD and the personal computer was applied. The frequency of current modulation was regulated in the range: 1-5 Hz. The analysis of the microstructures of the base metal, the metal of the deposited layer and the zone of thermal influence was carried out with the help of microscopes “Axio Observer D1m” and “Neophot-32”. Measurement of microhardness was carried out on the device Leika. Abrasive wear resistance of the coating surface was determined according to GOST 23.208-79.

Hardening of the deposited coating occurs due to the formation of a new surface layer. The properties of the deposited surface depend on the type of alloying elements that determine the phase composition, the boundaries of phase transitions and mechanical characteristics.

Technological parameters of the surfacing process affect the structure of the deposited metal and its properties. When changing the surfacing mode, the melting process of the material and the chemical homogeneity of the deposited layer change. The coating deposited by T-590 electrodes on the pulse mode has a more uniform structure.

A comprehensive approach to improving the properties of coatings using the method of modifying their materials during surfacing is proposed.

Changing the energy parameters during surfacing allows to reduce the structural heterogeneity of the coating cross-section by reducing the size of the structural components.

Modification allows to increase dispersion of structure and hardness of coatings.

---

* *The work was carried out within the framework of fundamental research Programs of the state academies of Sciences for 2018-2020, project III.23.2.1; according to the RFBR project 18-33-00387*

INFLUENCE OF THE ENERGY IVHFCT ON STRUCTURE FORMATION AND PROPERTIES OF DEPOSITED COATINGS*

Yu. N. SARAEV [1], V. P. BEZBORODOV [1], M. V. PEROVSKAYA [1], V. M. SEMENCHUK [1],B. S.BRAVERMAN [2], K. A. BOLGARU [2]

[1] Institute of strength physics and materials science SB RAS,
Academichesky Avenue, 2/4, Russia, Tomsk, 634055, phone: 8(3822)286850

[2]Department of structural Macrokinetics of TSC SB RAS

To control droplet formation, transfer of electrode metal, crystallization of the surfacing bath, the control of changes in arc voltage, current, instantaneous arc power was used. New methods of diagnostics of fast processes of heat and mass transfer which accompany melting, transfer and crystallization of metal from a melt were applied.

Surfacing was carried out with electrodes EN-60M on plates of steel 09G2C thickness of 6 mm. Surfacing electrodes carried out one and two layers. An experimental complex consisting of a power supply PHOEBUS-315 "MAGMA" with pulse-arc surfacing mode, sensors for measuring energy parameters, a recorder of these parameters AWR-224 MD and a personal computer was used. Current modulation frequency: 1-5 Hz. Analysis of the microstructure was carried out on microscopes “Axio Observer D1m” and “Neophot-32”. Microstructure studies were carried out in the Central part of the coating layers, in the transition zone to the base metal - in the areas of overheating and normalization. The microhardness of the deposited coatings, the ZTV metal and the base metal was measured on the Leika microhardometer.

The structure of the deposited coating metal and its properties are influenced by the technological parameters of the surfacing process, the number and size of alloying elements. When changing the surfacing mode, the melting process of the coating material changes.

The construction of histograms of the average level of microhardness of coatings deposited at DC modes and with pulse changes in energy parameters showed that the application of the second layer leads to an increase in performance. When using pulsed changes in energy parameters, the levels of microhardness of coatings are higher when surfacing both one and two layers. The construction of histograms of the average level of wear resistance of coatings deposited by electrodes in the DC mode showed that this characteristic is higher when surfacing a single layer.

By the directed high-energy influence of the arc on the melt of the deposited coating, its constant reciprocating motion is achieved, thanks to the periodic force action of the arc with the frequency of current modulation. Such surfacing provides cyclical flow of physical and metallurgical processes at the stages of formation of the melt bath and promotes its active mixing. This mixing of the melt under pulsed high-energy action of the arc contributes to the alignment of its heat content and ensures that the required amount of molten metal under the arc to the beginning of the current pulse action, contributing to a decrease in the depth of penetration. The periodic motion of the metal in the melt also contributes to a more uniform distribution of alloying elements in the volume of the molten metal. The use of pulse-arc surfacing technology allows to control the processes of formation of weld metal from the melt through programmable heat input into the surfacing zone and, as a consequence, to grind the structure of the coating metal and improve its properties. When grinding the structure of the deposited coatings, their properties are increased. The use of pulsed energy parameters during surfacing allows to increase the structural homogeneity of the coating cross-section.

Modification of the coating material using pulsed changes in energy parameters allows to increase the dispersion of the structure of the deposited coating, leads to an increase in its hardness and wear resistance.

The use of pulse energy parameters during surfacing allows to increase structural homogeneity in the cross-section of the coating.

** The work was carried out within the framework of fundamental research Programs of the state academies of Sciences for 2018-2020, project III.23.2.1, according to the RFBR project 18-33-00387.*

MATHEMATICAL MODEL FOR LINING THE SURFACE OF THE MECHANOREACTOR DURING GRINDING*

O. V. LAPSHIN

Tomsk Scientific Center SB RAS, 10/4 Akademicheskii Pr., Tomsk, 634021, Russia, ovlap@mail.ru, +7 (3822)492294

Grinding is an important stage not only for mechanochemical synthesis, but also for many manufacturing processes with the use of powder materials [1, 2]. At the same time, despite the relevance of research aimed at reducing energy consumption and optimizing grinding, the problem is far from being solved. The existing concepts revealing the physical features of the process do not allow reliable mathematical models to be constructed to describe the mechanical processing of solids. The equations derived by various researchers to determine the kinetics of grinding are essentially phenomenological, based on experimental data. Such equations contain empirical constants.

One of the problems of efficient using high-energy grinding equipment is associated with the adhesion of the ground material on the internal surface of the mill drum and grinding bodies [3, 4]. This process can lead to the fact that a significant amount of the ground material will be in the layers formed on the working surfaces. This type of self-lining reduces the performance of grinding equipment, creates additional manufacturing difficulties for the extraction of substances and cleaning of working surfaces.

It is necessary to mention the works on the modeling of mechanochemical reactions [5, 6], when the process starts after the complete lining of the working surfaces of the mechanoreactor by the substance.

In this work, a macroscopic mathematical model was constructed for the lining process when a multicomponent mixture was subjected to mechanical processing in the high-energy mill. It was shown that varying the values of the parameters of the mill and mechanical processing time can have a significant effect on the dynamics of lining the internal surface of the mechanoreactor by a ground mixture.

References

1. *Boldyrev V.V.* Mechanochemistry in Siberia // Herald of the Russian Academy of Sciences. 2018. V. 88 No. 3. P. 258-267
2. *Rogachev A.S.* Problems and prospects for the development of mechanochemistry // Russ. Chem. Rev. 2019. V. 88. No. 9. P. 875 - 900.
3. *Shkoda, O.A., Terekhova, O.G.* Single-phase NbSi2 by mechanoactivated SHS . Int. J Self-Propag. High-Temp. Synth. 2017. V. 26. No. 1. P. 83 – 85.
4. *Urakaev F.Kh., Ketegenov T.A., Petrushin E.I., Savintsev Yu.P., Tyumentseva O.A., Chupakhin A.P., Shevchenko V.S., Yusupov T.S., Boldyrev V.V.* A comprehensive study of the abrasive-reactive modification of the surface of quartz particles with amorphous iron compounds in mills with steel fittings // Journal of Mining Science. 2003. No.3. P. 110 – 122.
5. *Urakaev F.Kh., Takach L., Shevchenko V.S. et al.* Modelling of the combustion of termite compositions in mechanochemical reactors using the Zn-Sn-S system // Russian Journal of Physical Chemistry. 2002.V. 76. No. 6. P. 1052-1058.
6. *Urakaev F.Kh., Boldyrev V.V.* Theoretical analysis of the conditions for obtaining nanosized systems in mechanochemical reactors // Russian Journal of Physical Chemistry. 2005. V. 79. No. 4. P. 651 - 661.

* This work was supported by RFBR (Project No. 19-03-00081-a).

SHS OF PIGMENTS BASED ON COBALT AND MAGNESIUM TITANATES

O.V. Lvov, N.I. Radishevskaya, N.G. Kasatsky, A.Yu. Nazarova

Tomsk Scientific Center SB RAS, Tomsk, Russia

At present, titanium dioxide is widely used in the paint industry. Due to its extremely high technical properties such as a whitening ability and heat and light resistance, it is the most popular white pigment. In addition, colored TiO_2-based spinel pigments are widely used in the manufacture of ceramic paints, plastics, chemical fibers, rubber, paper, printing inks, building materials, inorganic glazes and enamels, cosmetical and other products [1].

TiO_2, MgO, Co_3O_4 oxides, $Mg(NO_3)_2 \cdot 6H_2O$ magnesium nitrate and aluminum powder (ASD-4) were mixed to obtain green pigments in the MgO-CoO-ZnO-TiO_2 system by self-propagating high-temperature synthesis (SHS).

Self-propagating high-temperature synthesis was conducted in metal-mesh cups placed into a gradient resistance furnace under an air atmosphere at atmospheric pressure. The bulk density samples were used for the synthesis of spinels. They were ignited beginning from the lateral surface, where the furnace temperature was maximum. The heat transferred from the spiral initiated a chemical reaction, resulting in a combustion wave.

Figs. 1a, b show thermograms of SHS of pigments No.1 and No.2 in the MgO-CoO-ZnO-Al_2O_3 and MgO-CoO-ZnO-TiO_2 systems, respectively.

Fig. 1. Thermograms of SHS of pigment No. 1 with a starting reaction mixture of Al_2O_3, Al, Co_3O_4, MgO, ZnO, $Mg(NO_3)_2 \cdot 6H_2O$ (a), and pigment No. 2 with a starting reaction mixture TiO_2, Al, Co_3O_4, MgO, ZnO, $Mg(NO_3)_2 \cdot 6H_2O$ (b).

A comparative analysis showed that the replacement of Al_2O_3 oxide with TiO_2 in the starting reaction mixture increases the maximum temperature of the synthesis of pigments from 1750 °C to ~ 1900 °C, melting the surface of products and changing the color from blue to green. The thermogram in Fig. 1b is more complex, which is associated, along with the chemical reactions of direct oxidation of aluminum and the thermite reaction with cobalt oxides, with the thermite reaction of aluminum with TiO_2.

X-ray diffraction analysis showed that the main phases of pigment No. 1 were aluminum-cobalt and aluminum-magnesian spinels, and those of pigment No. 2 were $MgTi_2O_5$, $CoTi_2O_5$ and $MgTi_2O_4$, as well as the presence of Mg_2TiO_4 and Co_2TiO_4, $Zn_xMg_yCo_{1-x-y}Al_2O_4$ phases and a perovskite phase. α-Al_2O_3 and Co were found as impurities. No metallic titanium was detected.

The structural features of the synthesized pigments were studied using an Axiovert 200M optical microscope. A micrograph of a pigment based on titanium-containing spinels is shown in Figure 2. Grayish-green sections of the $CoTiO_3$ - based perovskite-like phase as well as blue-green sections related to solid solution spinels of titanates and cobalt and magnesium aluminates were found. Some inclusions of metallic cobalt are observed.

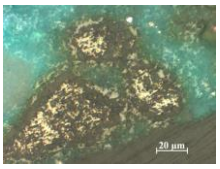

Fig. 2. Micrograph of a section of green spinel pigment based on cobalt and magnesium titanates obtained from the MgO-CoO-ZnO-TiO_2 system (Axiovert 200M).

Thus, titanium-containing pigments obtained by the SHS method can be used as ceramic pigments.

This work was supported by RFBR (Project No. 18-33-00387-mol_a).

REFERENCES

[1] Maslennikova G.N., Pishch I.V. Ceramic pigments. Moscow: RIF «Strojmaterialy». 2009. 224 p.

SYNTHESIS OF INORGANIC PIGMENTS BASED ON VANADIUM COMPOUNDS

O.V. LVOV, N.G. KASATSKY, N.I. RADISHEVSKAYA, A.Yu. NAZAROVA

Tomsk Scientific Center SB RAS, Tomsk, Russia

At present, SHS processes in exothermic organic systems (both powder and liquid) are very promising [1]. Yellow mineral pigments were obtained by the method of low-temperature combustion reactions (LTCR) using bismuth, zinc, and calcium vanadates.

The pigments were synthesized using V_2O_5 oxide, basic salt $BiONO_3 \cdot H_2O$, $Zn(NO_3)_2 \cdot 6H_2O$, $Ca(OH)_2$, and marshalite as the substrate. The starting components were mixed and citric acid was added. The solution was adjusted to pH = 2 with concentrated ammonia NH_4OH and boiled, followed by evaporation and calcination at a temperature of 500 °C. During synthesis, the following reactions occurred:

$$V_2O_5+2(NH_3 \cdot H_2O)=2NH_4VO_3+H_2O \quad (1)$$

$$2NH_4VO_3+BiONO_3=BiVO_4+NH_4NO_3 \quad (2)$$

$$C_6H_8O_7+3NH_4OH=(NH_4)_3C_6H_5O_7+3H_2O \quad (3)$$

$$4NH_4NO_3 \rightarrow 4NH_3\uparrow+4NO_2\uparrow+2H_2O+O_2\uparrow \quad (4)$$

$$(NH_4)_3C_6H_5O_7 \rightarrow 3NH_3\uparrow+4H_2O+CO\uparrow+CO_2\uparrow+4C \quad (5)$$

$$(HOOCCH)_2C(OH)COOH+O_2 \rightarrow 4C+4H_2O+CO\uparrow+CO_2\uparrow \quad (6)$$

$$C+O_2=CO_2 \quad (7)$$

At elevated temperatures, citric acid interacting with hydroxides forms oxalic and acetic acids, which decompose with the formation of carbon oxides and water. In an aqueous solution, citric acid can form chelate complexes with ions of metals that also decompose at high temperatures.

Figure 1 shows the X-ray diffraction patterns of the substrate mineral (marshallite), bismuth vanadate, and yellow pigment deposited on marshalite.

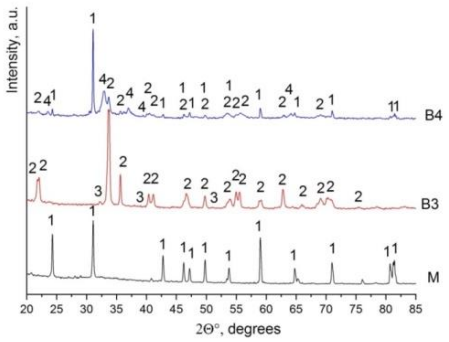

Fig. 1. X-ray diffraction patterns of marshallite and yellow pigment, where M is marshalite, B3 is bismuth vanadate $BiVO_4$, B4 is pigment deposited on marshalite, and used materials are: marshalite (1), $BiVO_4$ (Monoclinic 14-688) (2), VO_2 (Monoclinic 33-1441) (3), 4-$Bi_4V_2O_{11}$ (tetragonal 96-153-3809) (4).

As can be seen, bismuth vanadate contains VO_2 oxide as a microimpurity. 5-valence vanadium oxide subjected to thermal degradation of citric acid and ammonia can be reduced to a four-valence state. In addition to bismuth vanadate $BiVO_4$ and silicon oxide SiO_2, the yellow pigment deposited on marshalite contains complex $Bi_4V_2O_{11}$ oxide belonging to the family of bismuth-containing perovskites with the Aurivillius type of the structure and represented by the general formula $(Bi_2O_2)(A_{m-1}B_mO_{3m+1})$. The color of $Bi_4(V_2O_{11})$ compound is reddish-brown. Its small impurity in the pigment gives the yellow pigment a characteristic beige tone. The addition of Zn^{2+} and Ca^{2+} cations, which are contained in the starting components of the pigment ($Zn(NO_3)_2 \cdot 6H_2O$, $Ca(OH)_2$) brightens the pigment due to the formation of phases of zinc and calcium vanadates.

The use of marshallite as a substrate can reduce the cost of synthesized pigments.

This work was supported by RFBR (Project No. 18-33-00387-mol_a)

REFERENCES

[1] A.G. Merzhanov, The concept of the development of self-propagating high-temperature synthesis as the field of scientific and technical progress, Territoriya, Chernogolovka, (2003).

BIORESORBABLE POLYESTERS AND HYDROXYAPATITE BASED COMPOSITES AS MATERIALS FOR 3D PRINTING OF BONE TISSUE ENGINEERING SCAFFOLDS*

G.E.DUBINENKO[1], *I.O. AKIMCHENKO*[1], *A.L. ZINOVIEV*[1], *E.N. BOLBASOV*[1], *S.I. TVERDOKHLEBOV*[1]

[1]*Tomsk Polytechnic University, Tomsk, Russia*

Despite the downward trend regarding disability prevalence over the last decade statistics of the musculoskeletal system diseases remain at the same high level [1]. Surgical treatment of polytrauma and congenital diseases accompanied by massive bone tissue lose is still one of the most challenging issues for modern orthopedics and traumatology. Consolidation of bone fragments during the treatment of such diseases even with the use of external fixation devices is often accompanied by complications leading to the increase in the time of osteosynthesis and, in some cases, to the additional surgical intervention. There is continuous research for new treatment methods in modern orthopedics, aimed at reducing the time of osteosynthesis.

The designing of new biodegradable polymer composites is one of the most promising areas of modern orthopedics and regenerative surgery. At present, a number of methods have been proposed for designing and processing biodegradable polymer composites via various 3D printing technologies, however, the homogeneity of filler distribution together with mechanical properties of scaffolds made of such composites are far from those required for clinical use [2,3]. In this study, the new method for producing highly filled (up to 60 wt.%) biodegradable composite material based on polylactic acid (PLLA) and polycaprolactone (PCL) solution in organic solvent and hydroxyapatite (HAp) powder by mixing in low-speed ball mill was proposed. Composites were extruded on the horizontal single-screw extruder to obtain filaments for Fused Deposition Modeling (FDM) 3D printing of porous scaffolds. The study of scaffolds morphology showed homogeneous distribution of HAp in the PLLA and PCL matrix and decrease in the scaffolds deformation after additional annealing as the weight fraction of HAp was increasing from 0 to 60 wt.%. Furthermore, XRD results showed that the weight fraction of HAp not only affects the macro deformation of scaffolds but also affects the crystallization process of the polymer matrix. According to the results of Raman spectroscopy, the absence of residual organic solvents in the composite materials was shown. The thermal stability and crystallization kinetics of the polymer matrix was evaluated after each step of the heat treatment using the methods of TGA and DSC. The change in the molecular weight distribution of the polymer matrix was evaluated by GPC. As a result of this study, optimal parameters of highly filled PLLA/HAp and PCL/HAp filament extrusion and 3D printing were proposed which ensure high printing accuracy, the thermal stability of the polymer matrix and its molecular structure. It was shown that porous PLLA/HAp and PCL/HAp composite scaffolds 3D-printed in this study can be potentially employed for bone tissue engineering due to its adjustable physical and mechanical properties.

REFERENCES

[1] *Briggs A.M. et al. Musculoskeletal Health Conditions Represent a Global Threat to Healthy Aging: A Report for the 2015 World Health Organization World Report on Ageing and Health // Gerontologist. 2016. Vol. 56. P. S243–S255.*

[2] *Li X. et al. 3D-printed biopolymers for tissue engineering application // Int. J. Polym. Sci. 2014. Vol. 2014.*

[3] Tappa K., Jammalamadaka U. Novel biomaterials used in medical 3D printing techniques // Journal of Functional Biomaterials. 2018.

* This work was supported the Tomsk Polytechnic University Competitiveness Enhancement Program project VIU-School of Nuclear Science and Engineering-204/2019

BIOMIMETIC SYNTHESIS OF SILICON-SUBSTITUTED HA ON A TITANIUM SUBSTRATE*

O.A. GOLOVANOVA

Department of Inorganic Chemistry Omsk F. M. Dostoevsky State University, Russian Federation

Since silicon plays an important part in physiological processes underlying the growth and transformations of bone tissue and cartilage, the study of the properties of silicon-substituted hydroxyapatite (Si-HA) synthesized under near-physiological conditions is an important and promising physicochemical issue. Analysis of the literature indicates that there is currently great interest in the synthesis of thermally stable ceramic materials based on silicon-containing HA, suggesting that they are of great practical importance for orthopedics and implantology. There is solid evidence that Si-HA has a high affinity for carbonate anions, which compensate for the charge of the silicate anions. Silicon improves the biological activity of materials: in the contact zone between a silicon-stabilized implant and bone, physicochemical processes lead to the formation of Si–OH groups, which activate the functioning of cells: osteoblasts and osteoclasts. Raising the degree of substitution of silicate groups for phosphate ones (to 5 wt %) changes the shape of the particles from equiaxed to needle-like. Such substitutions destabilize the structure, which can be accounted for in terms of the difference in size between the tetrahedral anions: Si–O = 1.66 Å and P– O = 1.55 Å. The surface layer of the particles in singlephase materials is generally thought to account for most of the silicon. Silicon-containing HA has a higher resorption rate and contains a larger amount of active groups to which osteogenic cells attach. The silicon ions in the composition of such materials improve the synthetic capabilities of osteoblasts. An important point in biomimetic synthesis is to optimize conditions for the preparation of fine powders with a high resorption rate, biocompatible with the human body. If calcium phosphates are applied to a titanium substrate, it is necessary to investigate step Si-HA deposition mechanism in order to be able to use such samples in practice. Moreover, an important and highly needed area of modern implantology is in vitro studies of processes that take place on titanium, namely, possible destruction or degradation of ceramics. The purpose of this work was to study the feasibility of producing coatings on titanium substrates by applying silicate-ion-modified calcium orthophosphates synthesized from simulated body fluid (SBF).

Substituted calcium phosphate crystals were grown via room-temperature precipitation from aqueous solution (spontaneous crystallization). The main sources of silicate groups were Na_2SiO_3 and tetraethyl orthosilicate (TEOS), which are most frequently used for the purpose in question. The silicon content of the starting solution was 0.50, 2.50, and 5.00 wt %. The Ca/P ratio chosen, 1.67, corresponded to stoichiometric HA. The synthesis yields amorphous $Ca_3(PO_4)_2$ calcium phosphate as a reaction intermediate, which then gradually converts into HA, the most stable and least soluble compound in the $CaO–P_2O_5–H_2O$ system. They become incorporated into the crystal lattice of the forming phase, namely, silicon-containing HA.

The value pH 7.40, characteristic of extracellular fluid, remained constant throughout the synthesis. The synthesis time was 48 h. After crystallization, the solid phase was filtered off, dried, and characterized by Fourier transform IR spectroscopy and X-ray diffraction. IR spectra were measured on an FT-801 spectrometer (samples were prepared by pressing with KBr). The phase composition of the powders was determined by X-ray diffraction on a D8 Advance powder diffractometer (Bruker, Germany) with monochromatized CuKα radiation. The crystallite size was evaluated from X-ray diffraction data using the Scherrer formula. Quantitative phase analysis was carried out using the TOPAS 3.0 program and Scherrer equation. The detection limit was 0.5–5 wt %.

We have demonstrated that samples synthesized from an SBF solution with different concentrations of silicon ions are single-phase and consist of siliconcontaining HA. The nature of the precursor has no effect on the structure of HA. Analysis of the surface characteristics and morphology of the silicon-modified phosphate coatings obtained indicates that more complete Si-HA deposition on the surface of titanium substrates occurs on etched samples during the first three days of holding in a model solution. After exposure of titanium substrates to an HIB, further crystal growth and surface regeneration are possible. The present results can be useful in producing promising materials for orthopedics and transplantology.

* The presented work is a synthesis of the results of the RFBR project № 15-29-04839 ofi_m

FACILE STRUCTRED SNO_2@PANI NANOTUBE WITH ENHANCED SENSING PERFORMANCE FOR AMMONIA DETECTION AT ROOM TEMPERATURE *

BITAO LIU[1], *QINPING QIANG*[1*], *WENBO CHEN*[1,2], *TAO HAN*[1], *ZEKUN LI*[1], *ZHENGCHUAN ZHAO*[1,2]

[1] *Research Institute for New Materials Technology, Chongqing University of Arts and Sciences, 402160, Chongqing, China.*
[2] *Institute of High Technology Physics, National Research Tomsk Polytechnic University, Tomsk 634050, Russia*

Gas sensor with excellent stability and high response at room temperature has drawn many attentions for the demand of it is huge. Surface design provides an inspiration to make the sensor device more useful. Facile electrosping process are used to fabricate core-shell structured SnO_2 polyaniline (PANI) nanotube. It shows that the surface coated PANI shell can enhance its sensor responsibility through reacting with the target Ammonia (NH_3) gas. It shows that the room temperature for the gas response of NH_3 can reach to 15 at 100 ppm. Finally, its good stability is demonstrated by the response-recovery performances of 3 weeks and multiple cycles. This work indicates that this well designed PANI -SnO_2 is a potential way for design ammonia gas sensors.

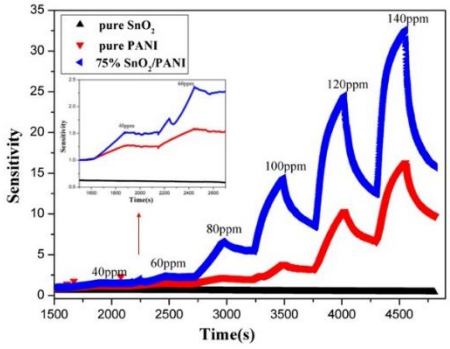

Fig.1. Resistance variation in gas sensing test of different samples.

[1] B. Timmer, W. Olthuis, W, A. Berg, "Ammonia sensors and their applications-a review", Sens. Actuators B, vol. 107, pp. 666-677, 2005.

[2] Y. Li, H. T. Ban, M. J. Yang, "Highly sensitive NH_3 gas sensors based on novel polypyrrole-coated SnO_2 nanosheet nanocomposites", Sens. Actuators B, vol. 224, PP. 449-457, 2016.

[3] H. Y. Li, C. S. Lee, D. H. Kim, J. H. Lee, "Flexible room-temperature NH_3 sensor for ultrasensitive, selective, and humidity-independent gas detection", ACS applied materials & interfaces, vol. 10, PP. 27858-27867,(2018.

[4] O. Lupan, V. Postica, M. Hoppe, N. Wolff, O. Polonskyi, T. Pauporté, B. Viana, O. Majérus, L. Kienle, F. Faupel, R. Adelung, "PdO/PdO_2 nanocluster-functionalized ZnO:Pd films for lower operating temperature hydrogen gas sensing", Nanoscale, vol. 10, pp. 14107-14127, 2018.

[5] Y. F. Chen, C. Li, X. L. Ma, Q. P. Qiang, B. T. Liu, S. X. Cao, L. L. Peng, L. Li, T. C. Lang, "Interface defect engineering induced drastic sensing performance enhancement of $W_{18}O_{49}$@PANI nanowires for ammonia detection at room temperature", Applied Surface Science, vol. 506, pp. 144816, 2020.

[6] Y. D. Wang, Q. Y. Mu, G. F. Wang, Z. L. Zhou, "Sensing characterization to NH_3 of nanocrystalline Sb-doped SnO_2 synthesized by a nonaqueous sol–gel route", Sensors and Actuators B: Chemical, vol. 145, pp. 847-853, 2010.

[7] S. Singkammo, A. Wisitsoraat, C. Sriprachuabwong, A. Tuantranont, S. Phanichphant, C. Liewhiran, "Electrolytically exfoliated graphene-loaded flame-made Ni-doped SnO_2 composite film for acetone sensing". ACS applied materials & interfaces, vol. 7, pp. 3077-3092, 2015.

* The work was supported by Chongqing Natural Science Foundation (cstc2016shmszx20002, cstc2017jcyjAX0259), Scientific and Technological Research Program of Chongqing Municipal Education Commission (KJ1711272), Chongqing university outstanding achievement transformation projects (KJZH17130), Chongqing high school youth backbone teacher funding scheme, National Key Research and Development Project of China (Grant No.2018YFB0407102), Project of Chongqing Science & Technology Commission (cstc2018jszx-cyzdX0137)..

MAGNETIC SORBENTS BASED ON ACTIVATED CARBONS FOR ORGANICS' PRECONCENTRATION*

A.A. ZVEKOV[1], *V.E. TSVETKOV*[1], *O.N. BULGAKOVA*[2], *A.N. EREMENKO*[1], *I.Y. ZYKOV*[1]

[1]*Federal Research Center of Coal and Coal Chemistry SB RAS, Kemerovo, Russia*
[2]*Kemerovo State University, Kemerovo, Russia*

The sorbents for organic substances concentration are widely applied in the field of natural water and soil purification. They are used in the chromatographic analysis of the pollutants in the complex natural objects. Such sorbents should fulfill a number of requirements: high sorption capacity for selected organic substances from aqueous and air medium, high sorption rate, easy desorption, readily separation from the purified medium or analyzed sample. These requirements could be met by magnetic sorbents on the carbonaceous base. The magnetization simplifies the particles' separation from the sample or the desorbing medium. It allows one to decrease the grain size of the sorbent that facilitates the diffusion of the sorbate. In spite of numerous papers and patents in the field of magnetic sorbents few of them are devoted to their preparation on the carbonaceous base. The activated carbons are classical sorbents for the extraction of organic substances from the aqueous and air medium. Thus the research into the possibility of carbonaceous magnetic sorbents preparation for the organic substances concentration is a relevant field of the contemporary chemistry.

The aim of the present work is synthesis of the magnetic sorbents on the carbonaceous base, their complex physical and chemical characterization, and the experimental estimation of their performance in the concentration of organic substances-pollutants from aqueous medium.

The literature survey on the approaches of magnetic carbonaceous sorbents was done. The main methods of magnetic sorbents on the carbon base preparation include:

1. Mixing of the carbon-containing precursor with magnetic particles or their precipitation from the solution followed by carbonization and activation of the material [1];
2. Precipitation of magnetic particles on the high-porous carbon matrix [2];
3. Mechanochemical synthesis using a paste of magnetic particles and carbonaceous sorbent [3].

The main synthetic approaches used in the present work for preparation of magnetite particles were co-precipitation of iron hydroxides II and III or iron hydroxide II oxidation in various conditions. We used commercial samples of the activated carbons as well as selected sorbents prepared from Kuzbass coals activated with potassium hydroxide. The appropriate methods of synthesis were selected and their application range was revised.

The porous structure of the magnetic sorbents obtained was studied with standard methods of low-temperature nitrogen sorption, sorption of methylene blue from aqueous solution, and benzene vapors. We estimated the possibility of prepared magnetic sorbents utilization for concentration of phenol, which is a model organic contaminant of natural water with low maximum permissible concentration.

REFERENCES

[1] Ushakova ES, Sunchugasheva EA, Ushakov AG, "The affect of magnetite nature on magnetic carbon sorbent obtaining process and the properties of product," Bull. KuzSTU, no. 2, pp. 77-86, April 2019.

[2] Kazemi E, Dadfarnia S, Shabani AMH, Hashemi PS, "Synthesis of 2-mercaptobenzothiazole/magnetic nanoparticles modified multi-walled carbon nanotubes for simultaneous solid-phase microextraction of cadmium and lead, International Journal of Environmental Analytical Chemistry," International Journal of Environmental Analytical Chemistry. https://doi.org/10.1080/03067319.2017.1353087.

[3] Zubrik A, Matik M, Lovás M, Danková Z, Kaˇnuchová M, Hredzák S, Brianˇcin J, Šepelák V, "Mechanochemically Synthesised Coal-Based Magnetic Carbon Composites for Removing As(V) and Cd(II) from Aqueous Solutions," Nanomaterials, vol. 9, no. 1, pp. 100, January 2019.

* The work was supported by Russian Foundation for Basic Research (grant 20-43-420012).

OPTICALLY TRANSPARENT Zr(Si)BN HARD FILMS FOR PROTECTION OF SOLAR CELLS*

PH.V. KIRYUKHANTSEV-KORNEEV, N.S. KOZLOVA, E.A.LEVASHOV

National University of Science and Technology "MISIS", Moscow, Russia

Research and development of new protective materials is being conducted in a new direction related to solving the global problem of the impact of space debris particles and micrometeoroids on spacecraft. The use of special maneuvering in orbit, as well as protective systems (Whipple shielding) does not completely avoid the damaging effects of small abrasive particles. The optical devices of spacecraft are particularly vulnerable. Thus, there is an urgent need to find new ways and materials to protect the solar cells. Protection of optical devices (portholes and solar cells of spacecraft, as well as solar power stations, solar collectors, etc.) from abrasive effects can be provided by the use of wear - and erosion-resistant ion-plasma coatings, including those based on oxygen-free ceramics. The use of hard and optically transparent ZrB(Si)N films is promising.

Films were deposited by DC and pulsed DC magnetron sputtering of ZrB_2, ZrB_2+20%Si, and ZrB_2+50%$ZrSi_2$ targets in Ar+N_2 gas mixtures [1-4]. The targets were manufactured by means of self-propagating high-temperature synthesis. The structure, chemical and phase composition of films were studied by HR TEM, XRD, SEM, EDS, XPS, Raman and FTIR spectroscopy, and GDOES. The films were characterized using nanoindentation, sliding pin-on-disk, impact ball-on-plate, abrasive calowear, and scratch tests. The refraction index, coefficients of transmittance (Tr) and reflectance were measured by KFK-3 and Cary 5000 Agilent + UMA attachment for wavelength range from 200 to 2500 nm.

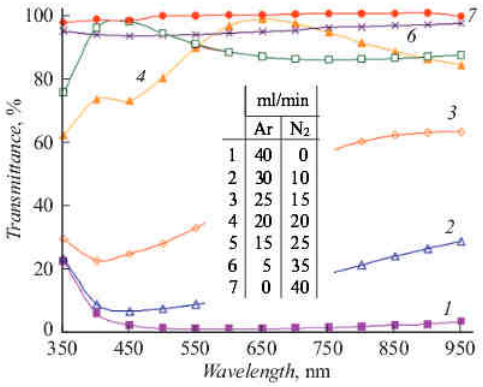

Fig.1. Transmittance vs. wavelength dependence for films deposited at different nitrogen flow rates [1].

Results obtained show that films deposited at low nitrogen partial pressure predominantly consist of nanocrystallites of hexagonal ZrB_2-phase, 1-20 nm in size and amorphous regions. N-rich films exhibit fully amorphous structure. Specific optical properties were observed for these ZrBN and ZrBSiN coatings including Tr=70-100% (Fig.1). The hardness of 15-37 GPa and Young's modulus of 150-470 GPa were determined for films deposited onto alumina substrates. Coatings demonstrated friction coefficient 0.2-0.4. The addition of nitrogen significantly increased wear resistance in sliding and impact conditions.

REFERENCES

[1] Ф.В. Кирюханцев-Корнеев и др. ПЖТФ, 2020, том 46, вып. 4 с. 30-32
[2] F. V. Kiryukhantsev-Korneev et al. Physics of Atomic Nuclei, 2019, V 82, No. 11, pp. 1437–1440
[3] I.V. Iatsyuk et al. IOP Conference Series: Materials Science and Engineering 347 (2018) 012028
[4] F. V. Kiryukhantsev–Korneev et al. Protection of Metals and Physical Chemistry of Surfaces, 2018, Vol. 54, No. 6, pp. 1147–1156

* The work was supported by the Russian Foundation for Basic Research No. 19-08-00187.

CHARACTERIZATION OF BORON CONTAINING COATINGS SYNTHESIZED BY SPRAY PYROLYSIS TECHNIQUE*

A.A. AKULINKIN, KA. BOLGARU, V.D. KITLER

Tomsk Scientific Center SB RAS, 10/4 Akademicheskii Pr., Tomsk, 634055, Russia, akulinkinalex@gmail.com, +7(3822)492294

In last decades, there has been an increasing interest in the use of the spray pyrolysis method to prepare inorganic materials such as powders and coatings [1]. This method involves on forming of aerosol from precursor solution (salts of metal). The aerosol is then very rapidly heated in a tube furnace at different temperatures from 200 to 1300 ºC to produce oxides, oxycarbides, sulfides etc. The spray pyrolysis method is low-cost, because of it does not require to use modern equipment or high-purity materials. Typical spray pyrolysis apparatus contains an atomizer (ultrasonic nebulizer), precursor solution, heater and flow regulator of carrier gas (Fig.1).

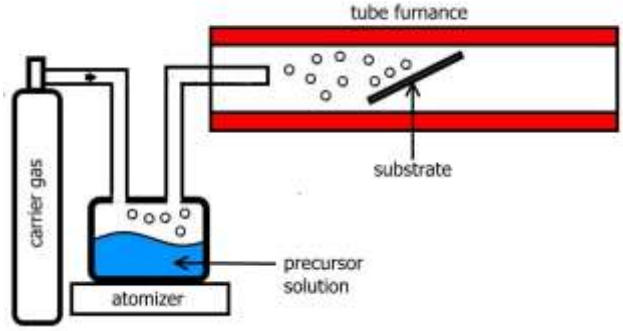

Fig.1. Spray pyrolysis apparatus.

The spray pyrolysis technique was used to deposit boron containing coatings [2]. Glass ceramic were used as substrates. The carrier gas was nitrogen. The starting reagents to deposit films were boric acid. Optical microscopy was used to investigate the microstructure and measure the thickness of the coatings. To understand the structure, phase composition of the coatings SEM and XRD was used. The surface topography evolution of coatings deposited by spray pyrolysis technique were investigated (Fig. 2).

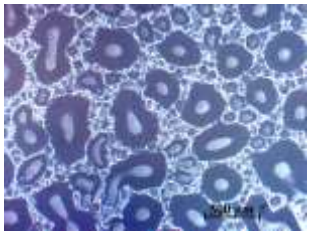

Fig.2. Coating surface topography.

It has been shown that the properties of the coatings depend on their thickness, structure, chemical and phase composition as well as on kinetic parameters used in the process [3].

REFERENCES

[1] D. Perednis, L.J. Gauckler "Thin film deposition using spray pyrolysis" J. Electroceram., 14, pp. 103-111, 2005.

[2] A. Badakhsh, W. Han and all "Preparation of Boron Nitride-Coated Carbon Fibers and Synergistic Improvement of Thermal Conductivity in Their Polypropylene-Matrix Composites" Polymers vol. 11(12), pp. 1-13, 2019.

[3] H.M.Martínez, J.Torres and all "Effect of the substrate temperature on the physical properties of molybdenum tri-oxide thin films obtained through the spray pyrolysis technique" Materials Characterization, vol. 75, pp. 184-193, 2013.

* The work was supported by RFBR (project № 18-33-00387 mol_a).

FORMATION OF A DEFECT STRUCTURE IN ALLOYS OF THE Zr-Nb-H SYSTEM UNDER IRRADIATION WITH A PULSED ELECTRON BEAM*

STEPANOVA E.N.[1], *GRABOVETSKAYA G.P.*[2], *MISHIN I.P.*[2], *LAPTEV R.S.*[1], *TERESOV A.D.*[3]

[1]*National Research Tomsk Polytechnic University, Tomsk, Russia*
[2]*Institute of Strength Physics and Materials Science of Siberian Branch of Russian Academy of Sciences, Tomsk, Russia*
[3]*Institute of High Current Electronics of Siberian Branch of Russian Academy of Sciences, Tomsk, Russia*

In recent years, surface modification by electron beam irradiation has been used to improve the performance of metallic materials and create protective coatings. Under the electron beam exposure in the surface layers of the material, large gradients of temperatures and stresses arise, resulting in the formation of defects. The presence of hydrogen in the material can significantly change the density and type of defects formed during irradiation. It is known [1] that hydrogen can induce the formation of new defects in the material and actively interact with existing structural defects. The resistance of the material to hydrogen embrittlement depends on the type and amount of certain defects in it [2].

In this work, we performed a comparative study of the effect of pulsed electron beam irradiation on the defect structure of zirconium Zr-1 wt.% Nb alloys with a hydrogen content of 0.0014 and 0.25 wt. % (hereinafter Zr-1Nb and Zr-1Nb-H alloys).

In the initial state, the zirconium Zr-1Nb alloy contains two phases: α-Zr and β-Nb. In the Zr-1Nb-H alloy, in addition to the indicated phases, ZrH and ZrH_2 hydrides are observed. The β-Nb phase in the form of particles, ranging in size from several tens of nanometers to several microns, is present in the bulk and at the grain boundaries of the α-Zr phase.

The alloys were irradiated with a pulsed electron beam in the SOLO facility having a pulsed electron source. Two irradiation modes were used: surface melting mode (energy density 12 J/cm^2) and surface non-melting mode (energy density 5 J/cm^2).

It was established that irradiation with a pulsed electron beam without surface melting does not change the average grain size, volume fraction, and distribution of particles of the β-Nb phase in Zr-1Nb and Zr-1Nb-H alloys. At the same time, the dislocation density (ρ) and the crystal lattice microdistortion (Δε) of the α-Zr phase increase in the surface layer of both alloys. In the surface layer of the Zr-1Nb alloy, ρ increases from $1.6\cdot10^{13}$ to $1.5\cdot10^{14}$ m^{-2}, and Δε grows from $3.2\cdot10^{-4}$ to $1.0\cdot10^{-3}$. In the Zr-1Nb-H alloy, the dislocation density increases from $3.0\cdot10^{14}$ m^{-2} to $6.7\cdot10^{14}$ m^{-2}, and the value of the microdistortions of the α-Zr crystal lattice – from $1.4\cdot10^{-3}$ to $2.1\cdot10^{-3}$. In the main bulk of the alloys, the values of the crystal lattice microdistortions and the dislocation density are practically unchanged.

As a result of irradiation with a pulsed electron beam in the melting mode, a lamellar structure is formed in the surface layer of both alloys (8-12 μm in width) with sizes of parallel plate packets of 1-2 μm. The width of the plates in the packets ranges from 20 to 300 nm. The plates are α and α" zirconium phases. There are no precipitates of the β-Nb phase in the modified layer. In the Zr-1Nb-H alloy, no hydrides are observed in the surface layer of ~1 μm width. At the same time, the total concentration of hydrogen in the alloy decreases slightly (by 0.002-0.004 wt.%). The dislocation density in the modified layer of the Zr-1Nb and Zr-1Nb-H alloys increases to $3.2\cdot10^{14}$ and $7.4\cdot10^{14}$ m^{-2}, correspondingly, and the value of the crystal lattice microdistortions rises to $1.3\cdot10^{-3}$ and $2.0\cdot10^{-3}$, respectively. In the main bulk of studied alloys, the indicated structure parameters practically do not differ from the initial values.

Positron annihilation spectroscopy studies have shown that electron beam irradiation in the melting mode results both in growth in the density of defects that increase the free volume (dislocations, vacancies, and vacancy complexes), and the dissolution of β-Nb phase and the formation of defects of "vacancy-impurity" type in the surface layer of alloys. The presence of hydrogen promotes the formation of complex hydrogen-vacancy complexes in the surface layer of the Zr-1Nb-H alloy upon pulsed electron beam exposure in the melting mode. In this case, dislocations remain the main type of defects.

REFERENCES

[1] J. Cizek, O. Melikhova, I. Procházka, "Hydrogen-induced defects and multiplication of dislocations in Palladium", J. Alloys Compd., vol. 645, p. S312–S315, 2015.

[2] B.A. Kolachev, Hydrogen embrittlement of metals, Moscow: Metallurgiya, 1985 [in Russian].

* The work was supported by the Russian Foundation for Basic Research, under grant No. 18-08-00158.

COMBUSTION SYNTHESIS AND PROPERTIES OF SIALON–BASED HETERO-MODULUS CERAMIC COMPOSITES*

K.L. SMIRNOV

Merzhanov Institute of Structural Macrokinetics and Materials Science, Russian Academy of Sciences, Chernogolovka, Russia

Hetero-modulus ceramic composites (HMCCs) represent a ceramic matrix with a high Young's modulus (300–800 GPa) with inclusions of a phase with a markedly lower Young's modulus (15–20 GPa) such as sp^2-structured carbon or h-BN. Generally low fracture toughness and thermal-shock resistance of these materials with high elastic modulus can be greatly improved upon addition of low modulus phases. Unusually high tolerance of HMCCs to impact and thermal shock is caused by their inherent ability to absorb and dissipate the elastic energy released during crack propagation and their capacity to blunt and divert a propagating crack [1, 2]. Another advantage of HMCCs is their remarkable machinability [3]. The HMCCs formed by SiAlON and h-BN are recognized as promising multifunctional materials for high-temperature applications. SiAlON ceramics have high hardness, good strength, and excellent wear/corrosion resistance [4]. The ceramics containing h-BN possess excellent properties such as low wettability with molten metals, low friction coefficient, high thermal shock resistance, high thermal conductivity, low thermal expansion, and high electric resistance [5]. SiAlON–BN composites are capable of combining these properties in desirable proportions. Up to now, the development of new simple and efficient methods for production of SiAlON–BN HMCCs is a hot subject of research. Infiltration-assisted combustion synthesis (CS) under high nitrogen pressure is successfully used for obtaining wide range of nitride-based ceramics [6]. In the present communication, the specific features, potentials, and limitations for combustion synthesis of SiAlON–BN composites are reported.

SiAlON–BN HMCCs were prepared by CS under high pressure of nitrogen gas according to the following reaction scheme:

$$3.45Si + 1.7Al + 0.85SiO_2 + N_2 \rightarrow \beta\text{-}Si_{4.3}Al_{1.7}O_{1.7}N_{6.3} \quad (1)$$

$$B + 0.5\ N_2 \rightarrow BN \quad (2)$$

The diluents like $\beta\text{-}Si_{4.3}Al_{1.7}O_{1.7}N_{6.3}$ or other refractory compounds (SiC, BN, TiN, TiB_2) were added to starting reactive mixture in order to prevent high-temperature dissociation of end product and to suppress coagulation of low-melting combustible components (Si, Al) into large nonreactive formations. Starting mixtures were intermixed in a laboratory-scale attritor with silicon nitride grinding bodies in air, pressed (cold isostatic pressing, 50 MPa) into cylindrical pellets with a relative density of 0.62–0.64, placed first in a special graphite crucible and then installed in a 4-l reaction chamber equipped with water cooling system and double-stage hydraulic gaseous compressor to provide conditions for infiltration-assisted CS under nitrogen pressures up to 150 MPa. The combustion reaction was ignited with an electrically heated tungsten coil.

The main factors that defined structural characteristics (relative density, phase and elemental composition) of SiAlON-based HMCCs obtained by infiltration-assisted CS were revealed experimentally: (a) pressure of gas reagent, (b) amount of combustible components in starting mixture, (c) BN content of product, (d) diluent wettability with low-melting components, and (e) sample diameter. Direct relationships between structural characteristics and such properties of synthesized HMCCs as bending/compressive strength, thermal-shock resistance, corrosion resistance to metallurgical melts, friction and wear behavior, and specific resistance have been studied. The synthesized HMCCs exhibit excellent resistance to thermal shock and metallurgical melts along with good tribological characteristics and machinability.

REFERENCES

[1] D. Hasselman, P. F. Becher, and K.S.Mazdiyasni, "Analysis of the resistance of high-E and low-E brittle composites to failure by thermal shock", Mater.-Wiss. Werkstofftech., vol. 11, no. 3, pp. 82–92, 1980.

[2] I. L. Shabalin, D. M. Tomkinson, and L. I. Shabalin, "High-temperature hot-pressing of titanium carbide–graphite hetero-modulus ceramics", J. Eur. Ceram. Soc., vol. 27, no. 5, pp. 2171–2181, 2007.

[3] R. Shuba, and I.-W. Chen, "Machinable α-SiAlON/BN composites", J. Am. Ceram. Soc., vol. 89, no. 7, pp. 2147–2153, 2006.

[4] T. Ekstrom, and M. Nygren, "Sialon ceramics", J. Am. Ceram. Soc., vol. 75, no. 2, pp. 259–276, 1992.

[5] R. Haubner, M. Wilhelm, R. Weissenbacher, and B. Lux, "Boron nitrides: Properties, synthesis, and applications", Struct. Bonding, vol. 102, no. 1, pp. 1–45, 2002.

[6] I. P. Borovinskaya, V. E. Loryan, and V. V. Zakorzhevsky, "Combustion synthesis of nitrides for development of ceramic materials of new generation", in "Nitride Ceramics: Combustion Synthesis, Properties, and Applications", Weinheim: Wiley-VCH, pp. 1–47, 2015.

* The work was supported by the Russian Foundation for Basic Research (project no. 15-03-01051_a).

SPARK PLASMA SINTERING OF β-SIALON–BN CERAMIC COMPOSITES*

K.L. SMIRNOV, E.G. GRIGORYEV

Merzhanov Institute of Structural Macrokinetics and Materials Science, Russian Academy of Sciences, Chernogolovka, Russia

Solid solutions of β-Si_3N_4 of general formula $Si_{6-z}Al_zO_zN_{8-z}$ (z = 0.0–4.2) are known for their excellent hardness, strength, and wear/corrosion resistance, which explains their wide use in various engineering applications [1]. Hexagonal BN exhibit good dielectric properties combined with high thermal conductivity and corrosion resistance at exceeding law wettability with the melts [2]. Addition of h-BN to ceramic composites greatly improves their thermal shock resistance, machinability, and to decrease friction [3-4]. SiAlON–BN composites are highly promising for metallurgical applications such as nozzles and pipes for metal pouring, annular breakers, crucibles, thermocouple casing, etc. In this context, it seemed interesting to develop of new simple and efficient methods for it's fabrication. In this work, we studied the prospects for combining of two advanced techniques: the combustion synthesis (CS) of raw powders with their subsequent spark plasma sintering (SPS). CS is a convenient technique for production of α- and β-SiAlON powders of varied composition, particle size, and morphology [5]. As compared to conventional hot pressing, SPS ensures higher heating rates and short dwell times (several minutes) and to date has been recognized as an effective tool for consolidation of materials [6].

Infiltration- assisted CS of β-Si_5AlON_7 and h-BN powders in nitrogen gas was carried out by the following schemes:

$$4.5Si + Al + 0.5SiO_2 + 3.5N_2 \rightarrow \beta\text{-}Si_5AlON_7 \quad (1)$$

$$B + 0.5N_2 \rightarrow h\text{-}BN \quad (2)$$

Green mixtures also contained some amount of diluents, β-Si_5AlON_7 and h-BN respectively, in order to improve extent of conversion. Combustion was performed in a 2-L reactor at $P(N_2)$ = 2–4 MPa for synthesis β-Si_5AlON_7 fine powders with a mean particle size of 0.6–1.0 μm and at $P(N_2)$ = 8–10 MPa for synthesis β-Si_5AlON_7 coarse powders with a mean particle size of 3.5–4.0 μm and flaky h-BN particles. Aliquot amounts of combustion synthesized raw powders were intermixed in a high-energy planetary steel-ball mill (800 rpm, ball/mill ratio 10 : 1, τ = 5 min). Then milled powders were sintered in a Labox 625 SPS facility under vacuum (below 10 Pa). The heating rate was 50 deg/min. The sintered compacts were heated from room temperature to 600°C without applied load and then to 1550–1800°C at a compressive stress of 50 MPa. The compacts were held at a desired temperature (T_{max}) for 5 min.

For pure β-Si_5AlON_7 powders, the densification intensified markedly at T > 1400°C. That just corresponded formation of the liquid eutectics caused by surface oxide impurities. The degree of dispersion was main factor determining the shrinkage rate. For fine β-Si_5AlON_7 high-density ceramics was achieved at T_{max} = 1550°C. While relative density (ρ_{rel}) of coarse β-Si_5AlON_7 sintered at same condition was about 0.75–0.77. The addition of h-BN improves the compactibility. Under a compressive stress of 50 MPa at 600°C, the initial value of ρ_{rel} exceeds 0.8 for the compact containing 30 wt % h-BN, and 0.5–0.6 for that of pure β-Si_5AlON_7. As the result, high-density structure of sintered β-Si_5AlON_7-BN composites was achieved at T_{max} = 1550°C for all used raw powders. It is important sintered composites had different structure and strength. The flexural strength (σ_f) of fine-grained composites with homogenous distribution of flaky h-BN particles was in the range 450–600 MPa. A marked decrease in σ_f (200–250 MPa) was registered for coarse-grained composites where small flaky h-BN particles were mainly distributed over the surface of larger β-Si_5AlON_7 ones.

REFERENCES

[1] T. Ekstrom, and M. Nygren, "Sialon ceramics", J. Am. Ceram. Soc., vol. 75, no. 2, pp. 259–276, 1992.

[2] R. Haubner, M. Wilhelm, R. Weissenbacher, and B. Lux, "Boron nitrides: Properties, synthesis, and applications", Struct. Bonding, vol. 102, no. 1, pp. 1–45, 2002.

[3] R. Shuba, and I.-W. Chen, "Machinable α-SiAlON/BN composites", J. Am. Ceram. Soc., vol. 89, no. 7, pp. 2147–2153, 2006.

[4] D. Wei, Q. Meng, and D. Jia, "Mechanical and tribological properties of hot-pressed h-BN/Si_3N_4 ceramic composites", Ceram. Int., vol. 32, no. 5, pp. 549–554, 2006.

[5] G. Liu, K.X. Chen, and J.T. Li, "Combustion synthesis of SiAlON ceramic powders: A review", Mater. Manuf. Processes, vol. 28, no. 2, pp. 113–125, 2013.

[6] M. Tokita, "Recent and future progress on advanced ceramics sintering by spark plasma sintering", Nanotechnol. Russ., vol. 10, nos. 3–4, pp. 261–267, 2015.

* The work was supported by the Russian Foundation for Basic Research (project no. 15-03-01051_a) and the Russian Science Foundation (project no. 16-19-10213).

SYNTHESIS OF MULTICOMPONENT SURFACE ALLOY ON A MAGNESIUM SUBSTRATE PRODUCED BY USING A LOW-ENERGY HIGH-CURRENT ELECTRON BEAM

E.V. YAKOVLEV, A.B. MARKOV, D.A. SHEPEL, V.I. PETROV

Institute of High Current Electronics SB RAS, 2/3 Akademicheskii Pr., Tomsk, 634055, Russia, yakov_e@mail.ru

Magnesium alloys are the lightest metal available for engineering applications and show promise as a structural material in aerospace and automotive industries, because those sectors are seeking increased fuel efficiency through weight reduction. However, due to the low wear resistance and high chemical activity of magnesium alloys, surface treatment of Mg alloy components is usually required in order to increase their durability. It appears that the simplest method of preventing corrosion of the magnesium substrate prohibit contact with the environment by applying the protective coating [1]. Unfortunately, it is still difficult to find a coating technology that can provide good protection of magnesium alloys from corrosion, abrasion and, along with them, satisfactory adhesion of the coating to the substrate. For example, anodizing coatings have excellent wear resistance, but these coatings are not suitable for load-bearing applications. Most wet coating processes are harmful to the environment. Applying a appropriate coating using laser cladding can improve the corrosion resistance of Mg alloys, but it has been found that quality problems such as cracking and porosity cannot be overcome, especially for cladding large surfaces. One of the methods that allow the formation of uniform coatings with good adhesion is the method of forming surface alloys [2,3].

The aim of present work was to synthesize of Ni-Cu-Al surface alloy directly on magnesium substrate using magnetron deposition of multicomponent Ni-Cu-Al films and consequent irradiation with a low-energy, high-current electron beam (LEHCEB).

The electron-beam machine “RITM-SP” with an explosive-emission cathode and a plasma-filled diode generating the LEHCEB was employed in the work [4]. This machine is equipped with a multi-magnetron sputtering system enabling formation of multicomponent surface alloys. Considering that the binary phase diagram of Ni - Cu refers to a system with complete solubility of the components in the liquid and solid phases, a fairly good homogeneous microstructure with good corrosion resistance is expected. Below the copper layer lies an aluminum layer. Aluminum was chosen mainly because its melting point (660 °C) is slightly higher than that of magnesium (649 °C), and about two-thirds of the melting point of copper (1083 °C). In addition, aluminum is a widely used alloying element for casting magnesium alloys.

The surface morphology, phase and elemental composition of the Ni-Cu-Al surface alloys were analyzed, the microhardness and wear resistance were measured. For its characterization different techniques like SEM, XRD and others have been used. The elemental composition of both the surface and cross sections of the samples was analyzed by EDS analysis. The structure and properties of the synthesized Ni-Cu-Al surface alloy was compared with witness-specimens, which is coatings but without LEHCEB treatment.

REFERENCES

[1] *J.E. Gray, B. Luan //* J. Alloy. Compd. – 2002. – 336. – 1-2. – 88-113.
[2] *A.B. Markov, E.V. Yakovlev, V.I. Petrov //* IEEE Transac. on Plasma Science. – 2013. – 41. – №8. 2177-2182.
[3] *A.B. Markov, E.V. Yakovlev, D.A. Shepel', M. Bestetti //* Results in Physics. – 2019. –12. – 1915-1924.
[4] *A.B Markov, A.V. Mikov, G.E. Ozu, A.G. Padei //* Instrum. and Experim. Tech. – 2011 – 54 – 862-866.

ADSORPTION STUDIES OF ARSENIC(III) REMOVAL FROM WATER BY COMPOSITE ION-TRACK MEMBRANES WITH EMBEDDED COPPER AND COPPER(II) OXIDE MICROTUBES *

A.A. MASHENTSEVA[1,2], *T.G. KHASSEN*[2], *A.T. ZHUMAZHANOVA*[1], *D.A. ZHELTOV*[1], *A.N. ZHUMABEKOVA*[1], *A.V. RUSSAKOVA*[3], *S.R. RAKISHEVA*[2], *N.A. AIMANOVA*[2], *D.T.NURPEISOVA*[2]

[1] *The Institute of Nuclear Physics of the Republic of Kazakhstan, Almaty, Kazakhstan*
[2]*L.N. Gumilyov Eurasian National University, Nur-Sultan, Kazakhstan*
[3]*D.Serikbayev East Kazakhstan State Technical University, Ust-Kamenogorsk, Kazakhstan*

Arsenic is one of the most common and dangerous toxic elements for human health and the environment. According to the World Health Organization, the European Union, and the United States Environmental Protection Agency, the maximum permissible concentration for As in drinking water is 10 micrograms/L [2]. In its reports, WHO states that approximately 1 in 100 people who consume water containing more than 0.05 mg/L of arsenic over a long period of time may die from arsenic-related cancer. This rate reaches 10% in cases where As concentrations exceed 0.05 mg/L. Therefore, the removal of arsenic from water sources is one of the most important issues in relation to the protection and preservation of the environment and human health. This work reports the synthesis of copper composite track-etched membranes (fig.1a) using electroless template deposition with sequential temperature annealing at the 140 °C and their application in arsenic(III) sorption. Cu/PET and CuO/PET composites were characterized by using XRD, XPS and SEM techniques. The extent of arsenic(III) removal was studied using batch mode of experiment which was carried out by mixing adsorbent with 15 ml of arsenic(III) solution in 50 ml stopper plastic jar. The effect of contact time on the removal of arsenic(III) was studied in the range of 15 min to 300 min by using 0.26 mg/ml of adsorbent at room temperature (25 °C), at pH=5.0 for initial arsenic(III) concentration of 50 mg/L. The mixture was slow agitated in a mechanical shaker and after a predetermined contact time, the composite sorbents were removed and the arsenic concentration in the filtrate was measured using an ICP-MS. Fig 1b shows the adsorption kinetics of As(II) onto Cu and CuO loaded composites. High adsorption rate for Cu/PET composite membrane was observed within 5 h and the plateau value (i.e. adsorption equilibrium) was found to be 485.1 mg As(III)/g from 50 mg/L initial As(III) solution within 180 min. Composite membrane with loaded copper(II) oxide demonstrate more effective sorption capacity and remove about 61.6% of As(III) ions from feed solution within 5 h.

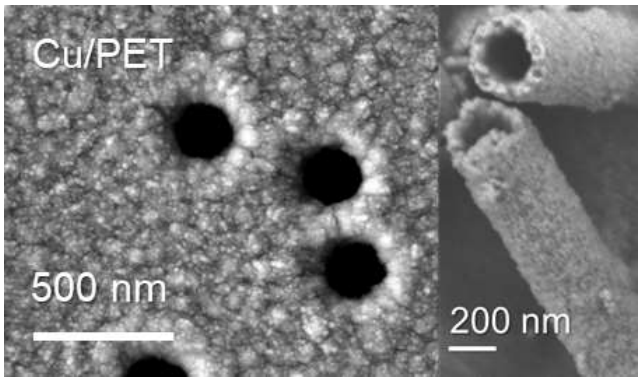

a

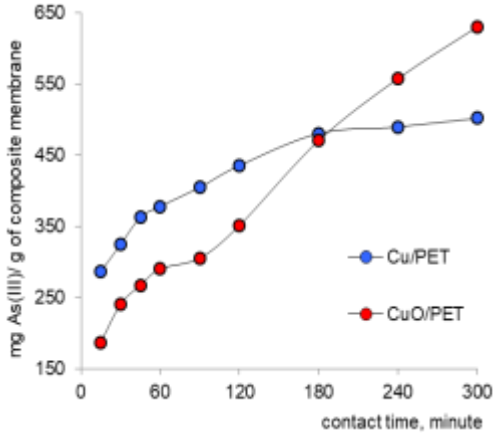

b

Fig.1. – SEM images of Cu/PET composite membrane and released microtubes (a) and effect of contact time on the removal of arsenic(III) by Cu/PET and CuO/PET composite track-etched membranes (b)

REFERENCES

[1] *Shankar S. et al* // Sci. World J. - 2014. - Vol. 2014. -P. 1–18.
[2] *World Health Organization* // Arsenic in drinking-water. - Geneva, 2011.

* This work was supported by the Ministry of Education and Science of the Republic of Kazakhstan (Grant number AP05130797).

Structure modification of Cu-Al system polymetallic materials obtained by electron-beam additive technology

A.V. CHUMAEVSKII, A.V. GUSAROVA, K.N. KALASHNIKOV, T.A. KALASHNIKOVA, E.O. KNJAZHEV

Institute of Strength Physics and Materials Science
of Siberian Branch Russian Academy of Sciences, Tomsk, Russia

At present, additive manufacturing technologies are intensively developed, improved and modified, as evidenced by a large number of reviews and experimental works in scientific literature [1-5]. The technologies based on melting and sintering of powder materials by means of laser beam (SLS, SLM technologies) or electron beam (EBM technology) have received the greatest development in the modern literature. Last years the technologies based on direct material deposition in a printing zone are gaining topicality, the most implementable of which in industrial sphere are technologies of wire-arc 3D-printing (WAAM technologies) and wire-feed electron-beam additive manufacturing (EBAM technologies). One of the advantages of the wire-feed electron-beam additive technology is to obtain large-sized components from different materials, as well as polymetallic ones with a gradient transition zone between materials [6-8]. However, in the process of polymetallic components manufacturing by additive electron-beam technology, in addition to the large-crystalline structure with poor strength there is the formation of building defects as intermetallic interlayers and delaminations along their boundary. Refinement of structural elements and reduction of its distribution heterogeneity can be achieved using friction stir technology [9]. The purpose of this work is to study structural and phase changes in the polymetallic material of Cu-Al system after friction stir processing. Aluminum alloy 5356 and copper C11000 as wire filaments with diameters of 1.2 and 1.0 mm respectively were used as feedstock for additive manufacturing and further processing. Printing was performed in the sequence "copper-aluminum alloy". The obtained structure after electron-beam additive 3D-printing is represented by initial alloy materials with presence of solid solutions and intermetallic phases based on copper and aluminum in the structural gradient zone. There are also a large number of defects such as pores and cracks. After friction stir processing, the originally coarse-crystalline material structure was modified with the formation of fine-grained structure of the stir zone. In addition to reducing structural heterogeneity after processing, no pores or delaminations are detected in the stir zone material, which results in increased mechanical properties in tensile tests.

The work on the additive manufacturing was performed according to the Government research assignment for ISPMS SB RAS, project No. III.23.2.11 The works on obtaining the materials of the Cu-Al system using the friction stir processing method were supported by the Russian Science Foundation (project № 19-79-00136).

References

1. Debroy T., Wei H.L., Zuback J.S., et al. Additive manufacturing of metallic components – Process, structure and properties. *Materials Science and Engineering,* 2018, vol. 92, pp. 112-224. doi: 10.1016/j.pmatsci.2017.10.001.
2. Li N., Huang S., Zhang G., Qin R., Liu W., Xiong H., Shi G., Blackburn J. Progress in additive manufacturing on new materials: A review. Journal of Materials Science & Technology, 2019, vol. 35, iss. 2, pp. 242-269. doi: 10.1016/j.jmst.2018.09.002.
3. Basak A., Das S. Epitaxy and Microstructure Evolution in Metal Additive Manufacturing. *Annual Review of Materials Research,* 2016, vol. 46, pp. 125-149. doi: 10.1146/annurev-matsci-070115-031728.
4. Günther J., Brenne F., Droste M., et al. Design of novel materials for additive manufacturing - Isotropic microstructure and high defect tolerance. *Scientific Reports,* 2018, vol. 8, pp. 1-14. doi: 10.1038/s41598-018-19376-0.
5. Wang Z., Palmer T.A., Beese A.M. Effect of processing parameters on microstructure and tensile properties of austenitic stainless steel 304L made by directed energy deposition additive manufacturing. *Acta Materialia,* 2016, vol. 110, pp. 226–35. doi: 10.1016/j.actamat.2016.03.019.
6. Kalashnikov K.N., Rubtsov V.E., Savchenko N.L., Kalashnikova T.A., Osipovich K.S., Eliseev A.A., Chumaevskii A.V. The effect of wire feed geometry on electron beam freeform 3D printing of complex-shaped samples from Ti-6Al-4V alloy. *International Journal of Advanced Manufacturing Technology,* 2019, vol. 105, iss 7-8, pp. 3147-3156. doi: 10.1007/s00170-019-04589-y.
7. Tarasov S.Y., Filippov A.V., Shamarin N.N., Fortuna S.V., Maier G.G., Kolubaev E.A. Microstructural evolution and chemical corrosion of electron beam wire-feed additively manufactured AISI 304 stainless steel. *Journal of Alloys and Compounds,* 2019, vol. 803, pp. 364-370. doi: 10.1016/j.jallcom.2019.06.246.
8. Kolubaev A.V., Tarasov S.Y., Filippov A.V., Denisova Y.A., Kolubaev E.A., Potekaev A.I. The Features of Structure Formation in Chromium-Nickel Steel Manufactured by a Wire-Feed Electron Beam Additive Process. *Russian Physics Journal*, 2018, vol. 61, iss. 8, pp. 1491-1498. doi: 10.1007/s11182-018-1561-9.
9. Gusarova A.V., Chumaevskii A.V., Osipovich K.S., Kalashnikova T.A., Kalashnikov K.N. Patterns of Structure Formation in Materials obtained by Hybrid Additive-Thermomechanical Method. Obrabotka metallov (tekhnologiya, oborudovanie, instrumenty) = Metal Working and Material Science, 2020, vol. 22, no. 1, pp 114–135. DOI: 10.17212/1994-6309-2020-22.1-114-135.

HARDENING OF ALUMINIUM ALLOY 5556 AND COPPER C11000 OBTAINED BY THE ADDITIVE ELECTRON-BEAM METHOD WITH THE FOLLOWING FRICTION STIR PROCESSING

A.V. GUSAROVA, A.P. ZYKOVA, T.A. KALASHNIKOVA, K.S. OSIPOVICH, A.V. CHUMAEVSKII

Institute of Strength Physics and Materials Science
of Siberian Branch Russian Academy of Sciences, Tomsk, Russia

Wire-feed electron-beam additive technology is currently one of the most effective technologies for obtaining metal components from titanium [1], steel [2], polymetallic ones from copper and aluminum [3] and many other metals and alloys. This technology belongs to a wide class of methods for obtaining metal components through a layer-by-layer additive process [4]. One of the most significant advantages of this technology is the high manufacturing productivity, which allows to build large-sized products without significant restrictions on the material selection for manufacturing. At the same time, in the process of wire-feed electron-beam additive manufacturing, there are inevitably defects of various structural and scale levels, which reduce the mechanical and operational properties of the manufactured product.

Copper and aluminum-magnesium alloys are one of the materials, which most often form defects such as pores, discontinuities or delaminations during the manufacturing process. Defects formed in the structure of these materials may have different origin, size and shape. The presence of defects leads to a reduction in the mechanical or operational properties of materials. One of the possible ways to eliminate defects in the structure of materials obtained by the additive method is friction stir processing, which provides the formation of ultra-fine grain structure with high mechanical properties in the surface layer structure [5]. Moreover, with the use of friction stir processing, it is possible to improve tribological characteristics of materials by introducing hardening particles into the surface layer. Therefore, in the future, the combination of the technologies will allow to obtain complex-shaped components from light aluminum alloys with the presence of wear-resistant surfaces in triboconjugation units. In the present work the modified surface layers of aluminium alloy 5556 and copper grade M1 were used for friction stir processing.

The results of the work show that a hardened layer with almost complete absence of pores and delaminations and increased mechanical properties occurs in the surface layer at the processing depth. The structure of the surface layer is similar to that obtained by friction stir processing of flat rolled products. Mechanical tensile testing of the gradient zone between processed and unprocessed material shows that fracture occurs mainly along the boundary between the processing zone and the additively manufactured material. Thus, the combination of wire-feed electron-beam additive technology and friction stir processing makes it possible to obtain components with a hardened surface layer of the finished product.

The work was performed according to the Government research assignment for ISPMS SB RAS, project No. III.23.2.11.

References

1. Kalashnikov K.N., Rubtsov V.E., Savchenko N.L., Kalashnikova T.A., Osipovich K.S., Eliseev A.A., Chumaevskii A.V. The effect of wire feed geometry on electron beam freeform 3D printing of complex-shaped samples from Ti-6Al-4V alloy. *International Journal of Advanced Manufacturing Technology,* 2019, vol. 105, iss 7-8, pp. 3147-3156. doi: 10.1007/s00170-019-04589-y.
2. Tarasov S.Y., Filippov A.V., Shamarin N.N., Fortuna S.V., Maier G.G., Kolubaev E.A. Microstructural evolution and chemical corrosion of electron beam wire-feed additively manufactured AISI 304 stainless steel. *Journal of Alloys and Compounds,* 2019, vol. 803, pp. 364-370. doi: 10.1016/j.jallcom.2019.06.246.
3. Kalashnikova T.A., Gusarova A.V., Chumaevskii A.V., Knyazhev E.O., Shvedov M.A., Vasilyev P.A. Regularities of composite materials formation using additive electron-beam technology, friction stir welding and friction stir processing. *Obrabotka metallov (tekhnologiya, oborudovanie, instrumenty) = Metal Working and Material Science*, 2019, vol. 21, no. 4, pp. 94–112. doi: 10.17212/1994-6309-2019-21.4-94-112.
4. Debroy T., Wei H.L., Zuback J.S., et al. Additive manufacturing of metallic components – Process, structure and properties. *Materials Science and Engineering,* 2018, vol. 92, pp. 112-224. doi: 10.1016/j.pmatsci.2017.10.001.
5. Kalashnikova, T.A., Chumaevskii, A.V., Rubtsov, V.E., Kalashnikov, K.N., Kolubaev, E.A., Eliseev, A.A. Structural Heredity of the Aluminum Alloy Obtained by the Additive Method and Modified Under Severe Thermomechanical Action on Its Final Structure and Properties (2020) Russian Physics Journal, 62 (9), pp. 1565-1572.

STRUCTURE AND PHASE COMPOSITION OF LEAD-BASED SILICATE GLASSES*

E.A. KRUTSILINA[1], V.I. SHYMANSKI[1], D.A. TASHMUHAMEDOVA[2]

[1]Belarusian State University, Minsk, Belarus
[2]Tashkent State Technical University, Tashkent, Uzbekistan

Recently, materials with improved thermophysical properties are being developed. Lead-based silicate glasses of different composition are perspective in this context. In present work we investigated structure, phase composition and mechanical properties of glasses of following compositions: 33 mass.% SiO_2 + 67 mass.% PbO (marked as C71-K), 29 mass.% SiO_2 + 67 mass.% PbO + 4 mass.% BaO (marked as B34E), 11 mass.% SiO_2 + 58 mass.% PbO + 15 mass.% B_2O_3 +14 mass.% MnO_2 + 2 mass.% CuO (marked as PC5). According to XRD data, C71-K and B34E samples have both amorphous and crystalline structures, while the PC5 sample is represented only by the amorphous phase. The formation of an amorphous phase is indicated by the appearance of an intense first diffuse halo and a weak second diffuse halo with a shoulder in the investigated angular interval. Moreover, X-ray diffraction patterns of partially crystallized C71-K and B34E samples, in addition to diffuse halo from the amorphous phase, contain diffraction reflections from crystalline phases corresponding to lead silicate of the composition $Pb(SiO_3)$ and lead oxide PbO_2. In addition to the indicated phases, diffraction maxima from $BaSi_2O_5$ and BaO were also found on the XRD pattern of B34E sample. The amorphous phase, as can be assumed, corresponds to compounds based on high-siliceous lead-based silicate $PbO{\cdot}2SiO_2$ or silicon oxide SiO_2. The microstructure of the surface layer of the studied samples is not homogeneous. The microstructure of the C71-K sample is characterized by the presence of many particles of spherical shape with a size of less than 50 μm, which, as one can assume, are located in amorphous matrix. B34E sample is characterized by porous structure and consists of individual particles, presumably with an amorphous structure, fused to each other during glass melting. The particles' size varies from 500 μm to 1.5 mm. The amorphous structure formation can be assumed due to the observed "salt – pepper" contrast, which is characteristic of an amorphous state. On the surface of the PC5 sample, pores up to 40 μm in size are observed, which, as can be assumed, were formed during the preparation of the sample. The surface is smooth, without any signs of crystallization. As a result of compression experiments performed for the samples, information concerning of studied lead silicate glasses elastic properties was obtained. So, according to the results, the most elastic sample is C71-K. The substitution of silicon oxide by additional compounds (BaO, B_2O_3, MnO_2, CuO, MgO) leads to a decrease in its elastic properties. Experiments in friction showed the minimum coefficient of friction is characterized by glass of the simplest composition, C71-K. Its initial value was 0.2, and after about 1 m of the friction path reached 0.13.

* The work was supported by Belarusian Republic Fund of Fundamental Researches (project # F019UZBG-013)

DEVELOPMENT OF A GRAPH MODEL OF THE RELATIONSHIP BETWEEN THE PARAMETERS OF THE SYNTHESIS OF TRANSPARENT CONDUCTIVE COATINGS AND PROPERTIES OF OXIDE COATING*

T.O. ZINCHENKO, E.A. PECHERSKAYA., D.V. ARTAMONOV, V.V. ANTIPENKO, S. A. GURIN, Y.V. SHEPELEVA[1]

[1]*Penza State University, Penza, Russia*

Depending on the treatment mode, the spray pyrolysis process allows to obtain various types of powders: magnetic powders of hexaferrite, TiO_2, Al_2O_3, SiO_2 [1-4], while the method is also actively used to produce thin films: transparent conductive oxides, absorbing coatings, protective, etc. Nevertheless, the widespread industrial introduction of spray pyrolysis is constrained by a large number of heterogeneous influencing factors [2], complicating the selection of the optimal technological regime, as well as imperfection of measuring equipment, which is used to control technological parameters during coating [3].

The whole set of factors influencing the properties and quality parameters of TCO coatings can be represented in the form of a directed graph (Figure 1 (a)). In this model, the vertices show the spray pyrolysis parameters, which can act as effects and reactions to these effects, arrows indicate the physical effects that describe the relationship of the parameters-reactions and parameters-effects.

Parameters-effects: T is pyrolysis temperature; χ is the impurity concentration; V is the solution volume ; v is the spraying rate; P is the pressure in the sprayer; t is the spraying time; l is the distance between the substrate and the sprayer, ε is the dielectric constant of the material at high frequencies. Parameters - reactions: R - resistance, D - transmittance.

A number of parameters depend on other factors and, in turn, affect the process parameters. These parameters also act as effects and reactions: J, n, μ, Ef, d, Eg, L, εf, K, p, ρ, η, nk, c, ω, τ. The factors distribution in sets, depending on their influence on other parameters, is shown in Figure 1 (b).

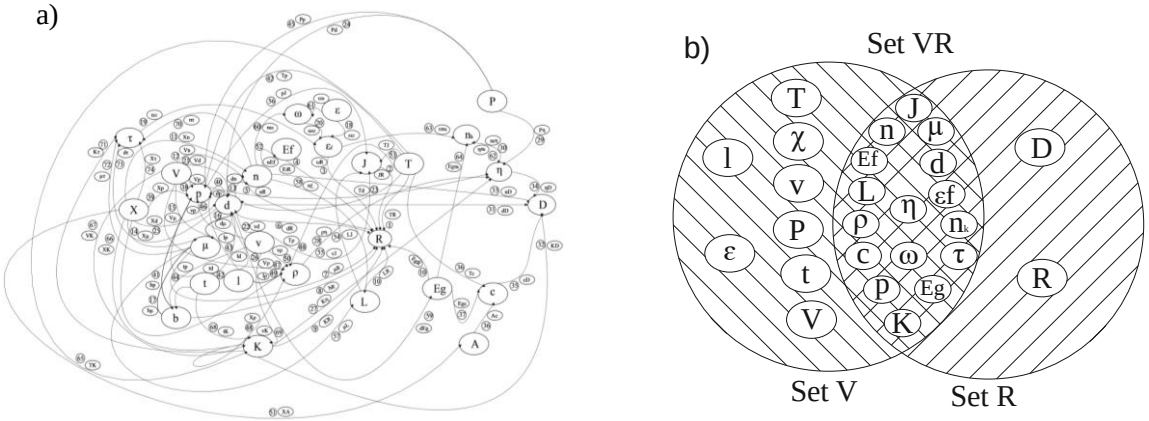

Fig. 1.a) A model of the relationship between the parameters of the synthesis of TCO and the properties of oxide coatings in the form of an oriented graph b) Venn diagram.

The proposed model was used to establish optimal technological conditions for obtaining transparent conductive coatings with desired properties.

REFERENCES

[1] T O Zinchenko, E A Pecherskaya, K O Nikolaev, P E Golubkov, D V Artamonov, Y V Shepeleva. The study of the optical properties of transparent conductive oxides SnO_2:Sb, obtained by spray pyrolysis. Journal of Physics: Conference Series, 2019, 1410: 012090

[2] T Zinchenko, E Pecherskaya, D Artamonov. The properties study of transparent conductive oxides (TCO) of tin dioxide (ATO) doped by antimony obtained by spray pyrolysis. AIMS Materials Science, 2019, 6(2): 276-287.

[3] V.V. Pankov Application of the spray pyrolysis method to obtain functional materials. Bulletin of the Belarusian State University, Ser. 2, Chemistry. Biology. Geography, 2007, 2: 3-13.

[4] Vlasov A. I., Markelov V. V., Zotieva D. E. Management and quality control of electronic equipment. Seven main tools of system analysis in the quality management of electronic products. Sensors and systems, 2014, 8: P. 55-66.

* The work was supported by Scholarship of the President of the Russian Federation to young scientists and graduate students, № SP-2517.2019.1

.

DEVELOPMENT OF A QUALITY CONTROL SYSTEM FOR TRANSPARENT CONDUCTIVE OXIDES *

T.O. ZINCHENKO, E.A. PECHERSKAYA, G.V. KOZLOV, P.E. GOLUBKOV, V.V. ANTIPENKO, A.E. SHEPELEVA[1]

[1]*Penza State University, Penza, Russia*

When controlling the quality parameters of transparent conductive coatings, the problem of analyzing the causes leading to defects arises. The use of the following seven basic tools for quality control of methods with a 95% probability allows to solve the problem [1, 2]:

- control card;
- Pareto diagram;
- a checklist;
- bar graph;
- Ishikawa diagram;
- stratification;
- scatter diagram.

The authors developed the Ishikawa diagram, which systematizes causal relationships between process conditions and the quality parameters of transparent conductive coatings (Fig. 1 (a)). [3]

The Pareto diagram is designed to identify the most significant factors - the causes of defects in transparent conductive oxides. There are two types of Pareto diagrams: according to the results of activities and for reasons [4]. To assess the quality of transparent conductive oxides, the Pareto diagram and the cumulative Pareto curve for reasons are used (Fig. 1 (b))

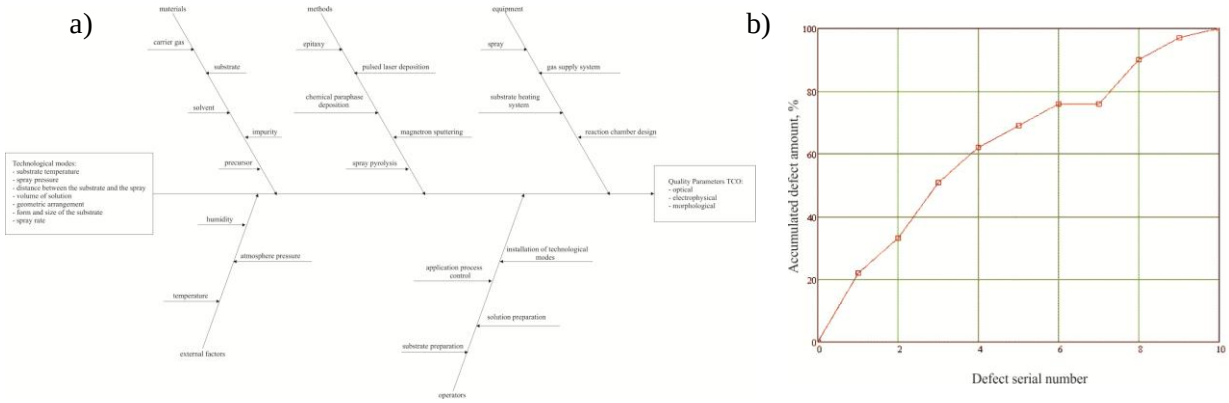

Fig.1. a) Ishikawa diagram for the TCO process b) Pareto cumulative curve.

The obtained results were introduced in the development of a technological process for the synthesis of transparent conductive oxides by spray pyrolysis.

REFERENCES

[1] A. I. Vlasov, V. V. Markelov, D. E. Zotieva Management and quality control of electronic equipment. Seven main tools of system analysis in the quality management of electronic products. Sensors and systems, 2014, 8: 55-66.

[2] E. A. Pecherskaya, A. A. Shamin, , K. O. Nikolaev, T. O. Zinchenko, Y. V. Shepeleva and A. A. Golovyashkin, "Quality Control of Technological Processes of Manufacturing Functional Solar Cells Layers Based on Hybrid Organic-Inorganic Perovskites," *2019 International Seminar on Electron Devices Design and Production (SED)*, Prague, Czech Republic, 2019, pp. 1-5.

[3] E.A. Pecherskaya, V.I. Kondrashin, S.V. Raksha, K.O. Nikolaev. Functional materials for dye-sensitized solar cells, Journal of nano- and electronic physics, 2015, 7(4): 04062.

[4] E. A. Pecherskaya, T. O. Zinchenko, V. I. Kondrashin, A. S. Kozlyakov, K. O. Nikolaev and J. V. Shepeleva. Electrical properties of transparent conductive ATO coatings obtained by spray pyrolysis. IOP Conference Series: Materials Science and Engineering, 225 (2017) 012255.

STUDYING THE PHOTOCATALYTIC ACTIVITY OF IRON OXIDES SYNTHESIZED BY PLASMA DYNAMIC METHOD*

I.I. SHANENKOV[1,2], *A.A. SIVKOV*[1,2], *Y.L. SHANENKOVA*[1,2], *A.S. IVASHUTENKO*[1], *A.I. TSIMMERMAN*[1]

[1]*College of Communication Engineering, Jilin University, 2699 Qianjin St., Changchun, 130012, PR China*
[2]*School of Energy and Power Engineering, Tomsk Polytechnic University, 30 Lenin av., Tomsk, 634050, Russian Federation*

The beginning of the 21st century is characterized by a transition from the use of traditional fuels (mainly carbon raw materials) to more environmentally friendly and energy efficient ones. In this direction, the photoelectrochemical water splitting with the formation of gaseous hydrogen, which can be further used as a fuel, is one of the most interesting researching areas. The obtained hydrogen gas is used not only as a pure energy carrier, but also as a reagent for other chemical reactions, for example, the reduction of carbon dioxide to hydrocarbons.

The photoelectrochemical water splitting includes two half-reactions occurring in an photoelectrochemical cell. Two water molecules are oxidized at the photoanode under the influence of the light to form an oxygen molecule, while hydrogen is generated at the cathode. The water splitting reaction that occurs on the photoanode surface is endothermic under standard conditions and requires the presence of free energy of 1.23 eV. Various metal oxides such as TiO_2 [1], Fe_2O_3 [2, 3], WO_3 [4], ZnO [5] $BiVO_4$ [6] were investigated as possible catalytic material for photoanodes. Among them, the most common and widely spread metal oxide is iron oxide (Fe_2O_3), which exists in four different polymorphic states, namely alpha, betta, gamma and epsilon. Until recently, the most stable α-Fe_2O_3 (hematite) was considered as the most promising candidate for photoelectrochemical cells [2,5], and its theoretically predicted maximum conversion coefficient of solar energy into hydrogen was 15% [7].

On the other hand, there have recently been reports about the possibility of using another metastable polymorph of iron oxide (ε-Fe_2O_3), which is extremely rare, for ethanol photoreforming [8]. Being inherently magnetoelectric and ferroelectric, as well as having a band gap of 1.9 eV, this polymorph can exhibit increased photoabsorption and lower recombination rate that can lead to an improvement in the conversion coefficient of solar energy to hydrogen and increase the overall efficiency of photoelectrochemical cells. However, due to some peculiarities of the synthesis process this phase is difficult to be obtained in the form of ultradispersed powder that limits the possibility of studying its catalytic activity in the photoelectrochemical water splitting.

In this work, both iron oxide phases ε-Fe_2O_3 and α-Fe_2O_3 were successfully synthesized in the ultradispersed form by the plasma dynamic method based on the generation of an iron-containing arc discharge flowing into oxygen atmosphere. By varying the process conditions, the final phase composition of synthesized iron oxide powders can be controlled. Thus, the photocatalytic activity of both phases was studied in the three-electrode photoelectrochemical cell under the influence visible range light, after producing the photoanodes from the initial ultradispersed powders by the electrophoretic deposition.

REFERENCES

[1] T. L. Thompson, J. T. Yates, "Surface science studies of the photoactivation of TiO_2 new photochemical processes", Chem. Rev., vol. 106, no. 10, pp. 4428-4453, 2006.

[2] M. H. Dahan, M. Caspary Toroker, "Water oxidation catalysis with Fe_2O_3 constrained at the nanoscale", J. Phys.Chem. C., vol. 121, no. 11, pp. 6120-6125, 2017.

[3] P. Liao, J. A. Keith, E. A. Carter, "Water oxidation on pure and doped hematite (0001) surfaces: Prediction of Co and Ni as effective dopants for electrocatalysis", J. Am. Chem. Soc., vol. 134, no. 32, pp. 13296-13309, 2012.

[4] C. Santato, M. Ulmann, J. Augustynski, "Photoelectrochemical properties of nanostructured tungsten trioxide films", J. Phys. Chem. B., vol. 105, no. 5, pp. 936-940, 2001.

[5] M. Grätzel, "Photoelectrochemical cells", Nature, vol. 414, no. 6861, p. 338, 2001.

[6] M. Oshikiri, M. Boero, "Water molecule adsorption properties on the $BiVO_4$ (100) surface", J. Phys. Chem. B., vol. 110, no. 18, p. 9188, 2006.

[7] Z. Chen, H. N. Dihn, E. Miller, "Photoelectrochemical water splitting", New York: Springer, 2013.

[8] G. Carraro, A. Gasparotto, C. Maccato, V. Gombac, F. Rossi, T. Montini, D. Peeters, E. Bontempi, C. Sada, D. Barreca, P. Fornasiero, "Solar H_2 generation via ethanol photoreforming on ε-Fe_2O_3 nanorod arrays activated by Ag and Au nanoparticles", RSC Advances, vol. 4, no. 61, pp. 32174-32179, 2014.

* The work was supported by the Russian Foundation for Basic Research (Project No. 19-42-703007).

HIGH VOLTAGE CONSOLIDATION OF TUNGSTEN CARBIDE – COBALT ALLOY AND HAFNIUM CARBIDE

E.G. GRIGORIEV[1], E.L. STRIZHAKOV[2], S.V. NESCOROMNIY[2], V.G. VINOGRADOV[1,2], S.O. AGEEV[1,2]

[1]Merzhanov Institute of Structural Macrokinetics and Materials Science RAS, Chernogolovka, Russia
[2]Don State Technical University, Rostov-on-Don, Russia

The method of high-voltage electric pulse consolidation (HVC) of high-temperature ceramic powder materials based on refractory metal carbides allows you to localize the high energy density of the electromagnetic pulse in the areas of interparticle contacts. Due to intense heating, the material in the zones of interparticle contacts becomes more plastic. This contributes to intense plastic deformation of the material under the influence of external pressure. The combination of a short (duration $\tau \sim 10^{-3} \div 10^{-4}$ s) high-voltage electric pulse (with a current density amplitude $j \sim 10^9$ A/m^2) and simultaneous exposure to mechanical pressure (P ~ 10^8 Pa) causes a high-speed deformation of the powder material localized in the contact region, which leads to the formation of a dense structure of the consolidated material. There is a limitation on the amplitude of the current density in the zone of interparticle contact, the excess of which leads to the effect of "electric explosions contact". A theoretical analysis of the processes occurring in the contact region [1] made it possible to establish the critical value of the current density j_*, for $j \geq j_*$ there occurs an “electric explosion of the contact”:

$$j_* = \sqrt{\frac{2\xi\sigma}{\rho h}} T_b^2 \qquad (1)$$

where: σ is the Stefan – Boltzmann constant; $\xi \leq 1$; T_b is the boiling point (loss of conductivity) of the material, ρ is resistivity, h is the size of the contact region with temperature T_b.

The method of high-voltage electropulse consolidation and the experimental setup are given in [2]. The values of the main technological parameters of electropulse consolidation (applied pressure and amplitude of a high-voltage current pulse) were experimentally determined to obtain dense consolidated samples of tungsten-cobalt carbide and hafnium carbide.

The results of a study of the microstructure of the samples consolidated powder materials by HVC: tungsten carbide–cobalt alloy and hafnium carbide are presented on Fig. 1 and Fig. 2 respectively.

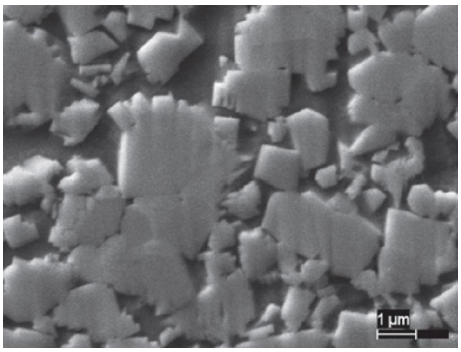

Fig. 1. Microstructure of WC–20%Co obtained by HVC

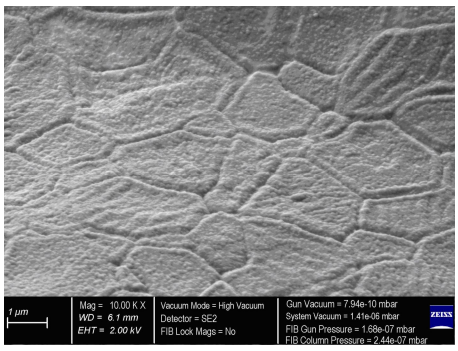

Fig. 2. Microstructure of HfC obtained by HVC.

High-voltage consolidation ensures the preservation of the initial fine-grained structure of the consolidated materials, a uniform distribution of the cobalt binder in the tungsten carbide–cobalt alloy, and an almost complete the absence of porosity in consolidated samples of WC–20%Co and HfC.

The presented work is a generalization of the results of work on the RFBR project No. 12-08-90400-Ukr_a.

REFERENCES

[1] E.G. Grigoryev, E.A. Olevsky, “Thermal processes during high-voltage electric discharge consolidation of powder materials”, Scripta Materialia, vol. 66, Issue 9, p. 662-665, 2012.

[2] E.G. Grigoryev, “High voltage electric discharge consolidation of tungsten carbide-cobalt powder”, In: Nanocomposites with unique properties and applications in medicine and industry, Editor John Cuppoletti, Intech, 372 p., 2011.

SPECTRAL AND X-RAY STUDIES OF INDIUM OXIDE FILMS ON SAPPHIRE SUBSTRATES

A.A. TIKHII[1], *YU.M. NIKOLAENKO*[2], *YU.I. ZHIKHAREVA*[3], *I.V. ZHIKHAREV*[2]

[1] *Lugansk Taras Shevchenko National University, Oboronnaya str., 2, Lugansk 91011, Ukraine*
[2] *Donetsk Institute for Physics and Engineering named after A.A. Galkin, Rozy Lyuksemburg str., 72, Donetsk, 83114 Ukraine*
[3] *Taras Shevchenko National University of Kyiv, Volodymyrska str., 64/13, Kyiv, 01601, Ukraine*

Optical transmission spectra and X-ray diffraction of thin In_2O_3 films deposited by dc-magnetron sputtering on Al_2O_3 (012) substrates are investigated.

The diffraction patterns exhibit the presents of the (222) reflex of cubic In_2O_3 (space group Ia-3). Its position shifts from 30.3 to 30.6°, with a decrease in the film thickness. The half-width of this reflex decreases with decrease of the deposition time, which may indicate an increase in the crystallite size of the film material.

The results of optical transmittance measurements demonstrate its anomalous decrease with decreasing wavelength. Moreover, an interference pattern is observed on the optical transmission curves of thick films, even in the low transmission region. The three layers model of the investigated films was proposed to explain these results. The optical properties of the middle layer correspond to the cubic modification of In_2O_3 according to [1]. The film surface was assumed to be rough, and modeled as a homogeneous layer with optical properties calculated based on the dielectric constant of a cubic modification of In_2O_3 and a fill factor of 0.5. The best fit of the spectral dependence of extinction coefficient of third layer is the law of the fundamental absorption in a semiconductor with band gap of 1.39 eV for direct transitions. The refractive index of this layer was assigned the same spectral dependence of the refractive index as for the film material.

The thicknesses of all layers were choosing manually to agree the calculated transmission spectra with the measured spectra of the films. The calculations are performed using the scattering matrix for a system of plane-parallel homogeneous isotropic layers [2]. A comparison of the optical transmittance calculated within the frame of the proposed model with the measurements shows good agreement.

The total thicknesses of the films were found to be from 97 to 392 nm (deposition time: 15 – 180 min). The thickness of the rough layer on the film surface (~ 60 nm) is practically independent of the deposition time and is mainly determined by the deposition mode. The thickness of the film-substrate transition layer (~ 35 nm) practically does not depend on the deposition time also, and, therefore, its appearance is completely due to the influence of the surface of the substrate. The formation of this layer, presumably, does not require a large violation of the stoichiometry of the film, since it is possibly related to the blurring of the band gap due to the large number of defects in the crystal structure, as well as the formation of impurity levels inside the band gap.

REFERENCES

[1] A. Schleife, M.D. Neumann, N. Esser, Z. Galazka, A. Gottwald, J. Nixdorf, R. Goldhahn, M. Feneberg, Optical properties of In_2O_3 from experiment and first-principles theory: influence of lattice screening, New J. Phys. vol. 20, Article Number 053016, 2018. http://dx.doi.org/10.1088/1367-2630/aabeb0.

[2] H.G. Tompkins, E.A. Irene (Eds), Handbook Of Ellipsometry, William Andrew Publishing, USA, 2005.

INFLUENCE OF SUBSTITUTIONS ON IONIC CONDUCTIVITY AND PHASE TRANSITIONS OF SOLID SOLUTIONS $NA_3SC_{2((1-X)}M_{2X}PO_4)_3$, WHERE M = CR, YB

A. S. NOGAI[1], *A. A. NOGAI*[2], *S. YU. STEFANOVICH*[3], *J. M. SALIKHODZHA*[2], *D.E. USKENBAYEV*[1].

[1] *Kazakh Agro Technical University S. Seifullina, Nur-Sultan, Kazakhstan*

[2] *Eurasian National University named after L.N. Gumilyova, Nur-Sultan, Kazakhstan*

[3] *Federal State Unitary Enterprise "Scientific Research Physicochemical Institute named after L. Ya.Karpova", Moscow, Russia*

The relevance of the study of crystals from the NASICON family is due to the fact that they are already used as structural materials [1]. $Na_3Sc_2(PO_4)$ 3 are the fact that it belongs to the NASICON family, they have low ionic conductivity in the α-phase and high ionic conductivity in high temperature β-, ɣ-phases [2]. Therefore, the further study of the conductive properties and phase transitions occurring in solid solutions of $Na_3Sc_{2((1-x)}M_{2x}PO_4)_3$, where M = Cr, Yb, is relevant.

The aim of this work is to establish the relationship between the appearance, dielectric and superionic states and the laws of change in the temperatures of $T_{\alpha\rightarrow\beta}$ phase transitions in solid solutions $Na_3Sc_{2((1-x)}M_{2x}PO_4)_3$, where M = Cr, Yb during isovalent substitution of scandium atoms by M cations in anionic rhombohedral crystalline framework.

Receiving $Na_3Sc_2(PO_4)_3$ polycrystals and $Na_3Sc_{2((1-x)}M_{2x}PO_4)_3$ solid solutions, where M = Cr, Yb (at x = 0.01 and x = 0.03), were obtained by solid-state ceramic synthesis. Polycrystalline samples of sodium scandium phosphate and solid solutions based on it were tablets with a diameter of 10 mm and a thickness of 2 mm.

The phase affiliation and structural parameters of the synthesized samples of solid solutions were studied by powder X-ray diffraction using a DRON-3 diffractometer (CuK α - radiation). The nonlinear optical properties of sodium-scandium and sodium-chromium phosphates were determined by the method of generating the second optical harmonic from neodymium laser radiation. The conductive and dielectric properties were determined on well sintered polycrystalline samples of $Na_3Sc_{2((1-x)}M_{2x}PO_4)_3$, where M = Cr, Yb. by impedance spectroscopy using a VM – 507 and VM -538 impedance meter in the temperature range 295 - 573 K and in the frequency range 5 – 5 10^7 Hz. To create electrodes, palladium was applied to the samples, which were considered as ideally blocking electrodes. X-ray measurements revealed the single-phase nature of the prepared samples. In work [2], we found that the unit cell of the α-phase polycrystal $Na_3Sc_2(PO_4)_3$ at room temperature has a monoclinic structure with parameters: a = 16.090 Å, b = 9.076 Å, c = 8.956 Å, γ=126.95 0 .

It has been established that substitution of scandium with M cations (where M = Cr, Yb) in the crystal structure of $Na_3Sc_2(PO_4)_3$ narrows the region of the polar dielectric α phase, because at the indicated substitution, the temperatures of the phase transitions α → β decrease.

It has been shown that the temperature dependence of the ionic conductivity of $Na_3Sc_{2(1-x)}M_{2x}(PO_4)_3$ (M = Cr, Yb) solid solutions remains the same as for $Na_3Sc_2(PO_4)_3$, however, the conductivity of the α phase increases and the superionic γ phase declining. In this case, the activation energy of samples with doped atoms decreases both in the dielectric α-phase and in superionic α- and β-phases.

It was established that the conductivity parameters of $Na_3Sc_{2(1-x)}M_{2x}(PO_4)_3$ (M = Cr, Yb) solid solutions are more susceptible to changes when the Sc → M atoms are replaced by ytterbium cations, which has a larger radius than the initial scandium cation, but the phase temperatures transitions α → β less change. When scandium is replaced by ions of a smaller radius (Sc → Cr), the change in the conductivity parameters is less pronounced, and the temperature of the phase transitions α → β is more pronounced.

REFERENCES

[1] Ellis L.B., Linda F.. Sodium and sodium-ion energy storage batteries Current Opinion Solid State Mater. Sci. 2012, V. 16, P. 168 – 177.

[2] Nogai A.S., Nogai A.A., Stefanovich S.Yu., Solikhodzha Zh.M., Uskenbaev D.E. Dipole ordering and ionic conductivity in NASICON-like structures of the $Na_3Sc_2(PO_4)_3$ type. Solid State Physics, 2019, Volume 61, no. 11, S. 2016 — 2023.

OBTAINING A COMPOSITE MATERIAL FOR VARISTOR CERAMICS IN ONE SHORT-TIME OPERATION CYCLE OF A COAXIAL MAGNETOPLASMA ACCELERATOR

Y.L. SHANENKOVA, A.A. SIVKOV, A.S. IVASHUTENKO, I.A. RAHMATULLIN, A.I. TSIMMERMAN, L.V. OSOKINA

National Research Tomsk Polytechnic university, Tomsk, Russia

Zinc oxide is a semiconductor material, which can be used in solar cells, photocatalytic systems, surge arresters, etc [1]. The creation on its basis of varistors (devices for protection against an overvoltage) with improved non-linear current-voltage characteristics is a promising task in science and technology [2-3]. The industrially produced ZnO-based varistors contain additives of other metal oxide phases, for example, bismuth, aluminum, antimony, nickel, cobalt, etc. [3]. However, all existing methods for obtaining varistors are multi-stage and resource consuming [4]. This paper shows the possibility of obtaining a composite material of the Zn-Bi-Ni-Sb-Co-Al-O system in one short-term cycle (about 1 ms) of a coaxial magnetoplasma accelerator operation. The synthesis of such composite product by the proposed method eliminates the preparation, mixing and other stages. The resulting material can be used as the basis for varistor ceramics. Figure 1 shows the XRD pattern of the obtained synthesis product with marked reflections of the main phases, as well as the corresponding SEM-image.

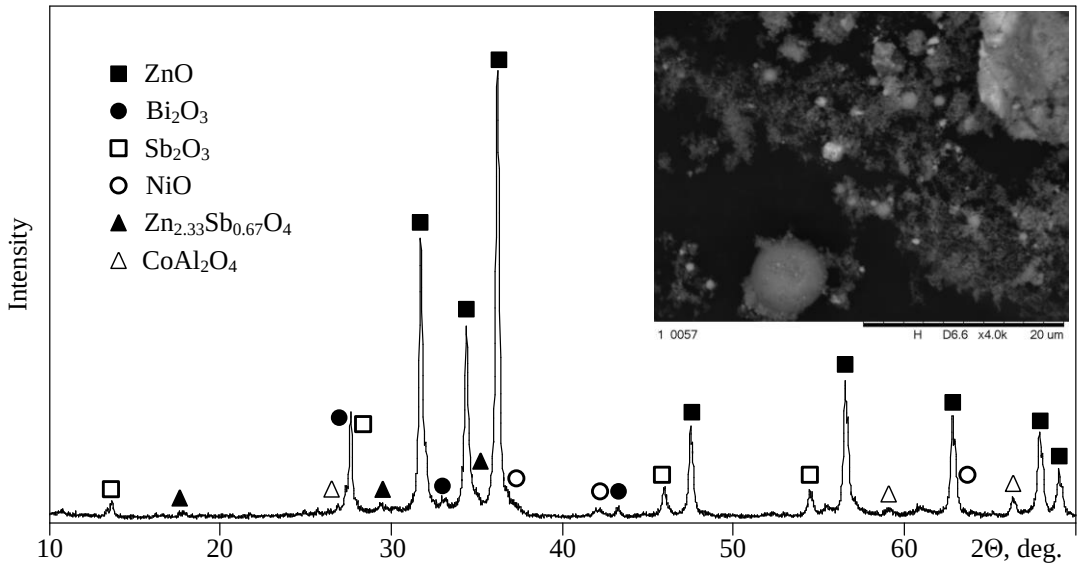

Fig.1. XRD-pattern of the plasma dynamic synthesis product

Earlier in the article [5], the results on the possibility of synthesizing ZnO-Bi_2O_3 composite materials with a core-shell structure by the proposed method were presented. Such a structure of particles improves the characteristics of varistor ceramics (non-linearity coefficient, breakdown voltage, leakage current) and significantly reduces the number of stages for its creation. By analogy with the previous results, analytical studies were carried out to confirm the formation of such a structure for the synthesized multicomponent product. Using this product of plasma dynamic synthesis, ceramic samples were obtained by spark plasma sintering. These samples of varistor ceramics were studied by X-ray diffraction (to find the phase composition) and scanning electron microscopy (to study the structure and density) methods, and their main electrical characteristics were determined by the volt-ampere method.

REFERENCES

[1] Almeida, W. L de., Rodembusch, F. S., Ferreira, N. S., & de Sousa, V. C. (2020). Eco-friendly and cost-effective synthesis of ZnO nanopowders by Tapioca-assisted sol-gel route. *Ceramics International*.

[2] Liu, W., Zhang, L., Kong, F., Wu, K., Li, S., & Li, J. (2020). Enhanced voltage gradient and energy absorption capability in ZnO varistor ceramics by using nano-sized ZnO powders. *Journal of Alloys and Compounds*, *828*, 154252.

[3] Hembram, K., Rao, T. N., Ramakrishna, M., Srinivasa, R. S., & Kulkarni, A. R. (2018). A novel economical grain boundary engineered ultra-high performance ZnO varistor with lesser dopants. *Journal of the European Ceramic Society*, *38*(15), 5021-5029.

[4] Mei, Y., Pandey, S., Long, W., Liu, J., Zhong, S., Zhang, L., ... & Xu, D. (2020). Processing and characterizations of flash sintered ZnO-Bi_2O_3-MnO_2 varistor ceramics under different electric fields. *Journal of the European Ceramic Society*, *40*(4), 1330-1337.

[5] Sivkov, A., Ivashutenko, A., Shanenkova, Y., Shanenkov, I., Rakhmatullin, I., & Osokina, L. (2018). Plasma dynamic synthesis of composite ZnO-Bi_2O_3 material with a core-shell structure for varistor ceramics. *Ceramics International*, *44*(18), 22808-22815.

EFFECT OF THE MULTILAYER STRUCTURE OF THE NI-AL FILM ON THE MELTING THRESHOLD AND MELT THICKNESS WHEN FORMING NI-AL SURFACE ALLOY UNDER THE INFLUENCE OF LOW-ENERGY HIGH-CURRENT ELECTRON BEAM

D.A. SHEPEL'[1], A.B. MARKOV[1], A.V. SOLOVJEV[1], E.V. YAKOVLEV[1,2], V.I. PETROV[1]

[1] Tomsk Scientific Center SB RAS, Laboratory of Advanced Technologies, Tomsk, Russia
[2] Institute of High-Current Electronics, Tomsk, Russia

A surface alloy has a significant advantage over coating since it provides the highest level of adhesion. The process of a surface alloy forming comprises two successive steps. First, one or several layers of surface alloy chemical composition are deposited on treating surface. The proportion of materials in the surface alloy chemical composition determines the thickness and number of layers to be deposited. Second, the deposited multilayer film is then treated with LEHCEB, whereby the layers of film are melted, mixed, and a surface alloy is formed.

It is technically more convenient to deposit thicker layer of material, but for uniform mixing, thinner layer is preferable. The purpose of calculations carried out in this work was to estimate the effect of different film multilayered structure on thermal regime characteristics such as melting threshold, melt thickness and lifetime of melt.

To form the Ni-Al surface alloy, Ni and Al layers were alternately deposited onto the carbon steel substrate. Calculations were made for 5 types of multilayer composition with the number of Ni and Al layers varied from 3 to 19, keeping the total thickness of the multilayer film 2.5 μm.

Dependencies are obtained for melting threshold, melt thickness and melt lifetime versus number of Ni and Al layers included in multilayer film. It was discovered that the melting threshold value for this type of multilayer composition can vary from 4.1 to 4.3 J/cm^2.

STRUCTURAL AND MAGNETIC CHARACTERISTICS OF ANISOTROPIC COMPOSITE MATERIALS BASED ON Y-TYPE HEXAGONAL FERRITES*

V.A. ZHURAVLEV[1], D.V. WAGNER[1], O.A. DOTSENKO[1,2], K.V.DOROZHKIN[1]

[1]*Tomsk State University, Tomsk, Russia*
[2]*Tomsk State University of Control Systems and Radioelectronics, Tomsk, Russia*

Currently, there are many adverse environmental factors in cities. Among them there are electromagnetic emitters, receivers, high-frequency radio equipment, etc. All this entails the development and manufacture of new radio materials that could effectively interact with high-frequency radiation. There are a huge number of articles that are devoted to the study of such materials. The most promising materials for use at high frequencies are composites based on oxide ferrimagnets with hexagonal crystal structures (hexaferrites) [1, 2].

Recently, composites have been widely used instead of solid materials. The reason is that it is possible to change the properties of composite materials without changing their composition.

This report presents the results of a study of composite material based on hexaferrite Y-type.

Hexagonal Y-type ferrite ($Ba_2NiCuFe_{12}O_{22}$) [3] was synthesized using ceramic processing technology. After that the bulk ferrite was crushed. A filler with a particle size of less than 60 microns was taken to make the composite. Epoxy was used as a matrix. The mixture was placed into toroidal mold. After that mixture was treatment by a permanent magnetic field.

Figure 1 are shown the surface morphology of a composite material based on Y-type hexaferrite without/with treatment by an external magnetic field. It can be seen that the sample, which was exposed to a magnetic field, has a layered structure. This leads to the anisotropy of the magnetic properties of the sample.

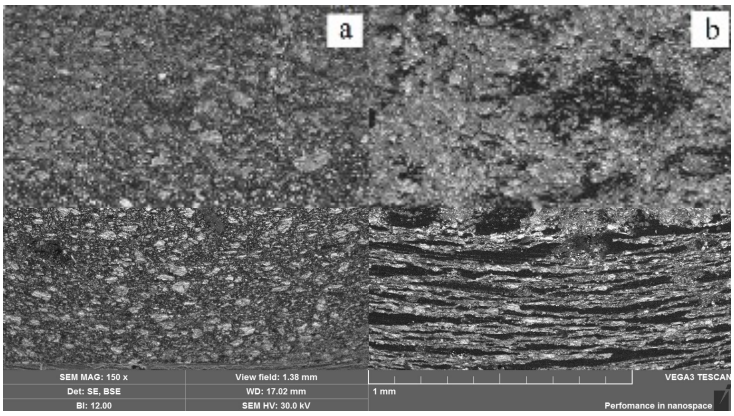

Fig.1. Surface morphology of a composite material based on Y-type hexaferrite manufactured (a) without treatment and (b) with treatment by an external magnetic field.

The results of X-ray diffraction analysis of this sample are shown that structural properties also changed and magnetic texture appeared.

The measurements and calculations by the magnetic permeability spectrum of magnetic composites based on planar hexaferrites in the frequency range 20 MHz - 18 GHz were carried out. The efficiency of magnetic treatment of composites to control the values of magnetic permeability in a wide frequency range is estimated.

REFERENCES

[1] J. Smit and H.P.J. Wijn, Ferrites, London: Cleaver-Hume Press Ltd., 1959.

[2] V.A. Zhuravlev, A.A. Nevmyvaka, V.I. Itin, V.A. Svetlichnyi, D.V. Lapin, D.V. Wagner, “Influence of the reagent types on the characteristics of barium hexaferrites prepared by mechanochemical method,” Mater. Today Commun., vol. 21, pp. 100614-1-100614-9, December 2019.

[3] D.V. Wagner, O.A. Dotsenko, V.A. Zhuravlev, “Structure, magnetic properties and electromagnetic response of Y-type hexaferrites and hexaferrite-based composite materials,” Russ. Phys. J., vol. 62, no. 4, pp. 581–588, April 2019.

* The work was supported by Tomsk State University Improvement Program and supported by the RFBR grant No. 19-32-90150 “Postgraduate students”. Experimental studies were carried out on the equipment of the collective use center of Tomsk State University «Center for Radiophysical Measurements, Diagnostics and Research of Parameters of Natural and Artificial Materials».

FEATURES OF THE PERMEABILITY SPECTRA OF $Co_{2-x}Zn_x$ W HEXAFERRITES IN THE SPIN-REORIENTATION PHASE TRANSITION REGION*

V.A. ZHURAVLEV, V.I. SUSLYAEV, A.A.PAVLOVA

Tomsk State University, Tomsk, Russia

In [1], neutron diffraction studies were carried out, as well as measurements of the anisotropy fields and the initial magnetic permeability of the hexaferrites $Ba(Co_{2-x}Zn_x)Fe_{16}O_{27}$ ($Co_{2-x}Zn_xW$) system. They showed that the spin-reorientation phase transitions (SRPT) such as the easy magnetization axis (EMA) to the easy magnetization plane (EMP) are observed with decreasing temperature from the Curie temperature T_C in the composition range $0 \le x \le 1.6$. This transition is due to a change in the sign of the first magnetocrystilline anisotropy (MCA) constant (k_1=0) with a change in the concentration of Zn^{2+} ions or temperature. The transition is carried out through the phase of the easy magnetization cone (EMC).

According to [2], the main contribution to the permeability of hexaferrites in the microwave frequency range is made by the processes of rotation of the magnetization vector. In this case, the observed dispersion of the permeability spectra $\mu^*(f) = \mu'(f) - \mu''(f)$ is related to the resonance in the internal effective field of the MCA. It is called the natural ferrimagnetic resonance (NFMR). Therefore, the concentration and temperature dependences of the permeability spectra of hexaferrites $Co_{2-x}Zn_xW$ system should also have features in the vicinity of the SRPT.

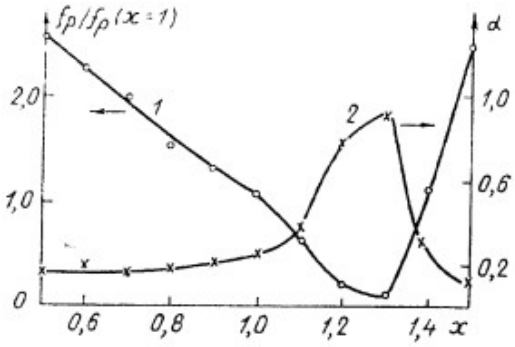

Fig. 1 The concentration dependences of $f_r(x)/f_r(x=1.0)$, determined from the maximum of $\mu''(f_r)$ (curve 1) and the dissipation parameter $\alpha(x)$ (curve2). The measurements were carried out at room temperature.

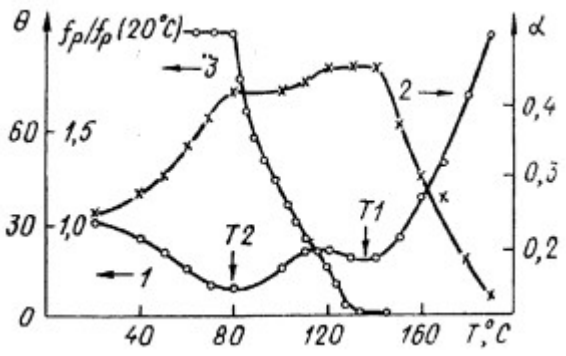

Fig. 2 Temperature dependences the normalized resonance frequency NFMR $f_r(T)/f_r(20\ °C)$ (curve 1) and $\alpha(T)$ (curve 2) of hexaferrite CoZnW (x=1). Curve 3 is the calculated from the neutron diffraction data in [1] temperature dependence of the angle of easy magnetization direction of a given hexaferrite.

An experimental study of the $\mu^*(f)$ spectra was carried out on polycrystalline samples synthesized using a two-stage ceramic technology. The content of the main W phase in the materials was not less than 90 %, the density of the samples was not less than 0.8 of the x-ray density.

Neutron diffraction studies hexaferrites $Co_{2-x}Zn_xW$ system [1] showed that up to concentrations $x \le 1.2$ there is an EMP at room temperature. EMC is realized for ferrite with $x_c = 1.3$. Materials with $x \ge 1.38$ have EMA. Thus, observed in the dependences $f_r(x)/f_r(x=1.0)$, and $\alpha(x)$ anomalies are related to SRPT.

Hexaferrite CoZnW (x=1) up to a temperature T_2 = 80 °C, has EMP phase according to neutron diffraction studies (curve 3 in Fig. 2). Further the easy direction is EMC up to the temperature T_1 = 130 °C, and at higher temperatures phase EMA realized. Fig. 2 shows that the temperatures at which $f_r(T)/f_r(20\ °C)$ passes through the minimum are in good agreement with the temperatures of the SRPT EMP to EMC (T_2) and EMC to EMA (T_1) on the curve 3. The damping constant α is maximum in the interval of the conical phase and rapidly decreases outside the SRPT region. Thus, a change in the concentration of zinc ions allows a wide variation in the frequency of NFMR.

REFERENCES

[1] E.P. Naiden, V.I. Maltsev, G.I. Ryabtsev. "Magnetic Structure and Spin-Orientational Transitions of Hexaferrites of the $BaCo_{2-x}Zn_xFe_{16}O_{27}$ System," phys. status solidi (a)., vol. 120, no. 1, pp. 209–220, February 2006.

[2] J. Smit and H.P.J. Wijn, Ferrites, London: Cleaver-Hume Press Ltd., 1959.

*The work was supported by Tomsk State University Improvement Program and supported by the RFBR grant No. 19-32-90266 "Postgraduate students". Experimental studies were carried out on the equipment of the collective use center of Tomsk State University «Center for Radiophysical Measurements, Diagnostics and Research of Parameters of Natural and Artificial Materials».

SPECTRA AND KINETICS OF LUMINESCENCE OF NATURAL DIAMOND TYPE IIA UNDER OPTICAL INTERZONE EXCITATION *

E.F. MARTYNOVICH[1,2], A.S. EMELIANOVA[1], A.L. RAKEVICH[1], E.I. LIPATOV[3]

[1]Irkutsk Branch of the Institute of Laser Physics, SB RAS, Irkutsk, Russia
[2]Irkutsk Scientific Center SB RAS,
[3]Tomsk State University, Tomsk, Russia

A diamond of type IIa was studied, in the absorption spectrum of which in the region of 200–1000 nm there were no bands and lines of impurity or impurity – vacancy centers. Only intrinsic interband absorption was observed. Interband excitation of luminescence was provided by pulsed radiation of the fifth harmonic of a neodymium laser (213 nm, 7 ns). In addition, to search for the luminescence centers contained in the crystal, intracenter excitation was used with the fourth (266 nm) and second (532 nm) harmonics of this laser. Additionally, a set of picosecond lasers (375, 405, 470, 532 and 640 nm) was used, which were included in the kit of a confocal scanning luminescent microscope with a time resolution of MicroTime 200 from PicoQuant gmbh, which operated in a time-correlated photon counting mode. The luminescence spectra were measured using an Ocean Optics QE65000 spectrofluorimeter coupled to this microscope. The luminescence kinetics in the case of intracenter excitation was measured by means of a microscope, and in the case of interband excitation, by the method of direct oscillography using a photomultiplier and a digital oscilloscope. The sample temperature (78-500 K) was maintained and measured using a Microstat-N cryostat from Oxford Instruments.

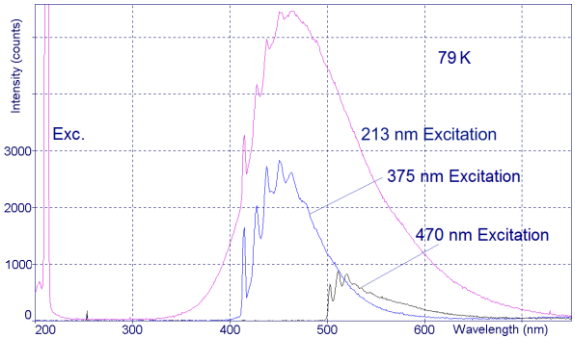

Fig. 1. Luminescence spectra under optical interband and intracenter excitation at 79 K

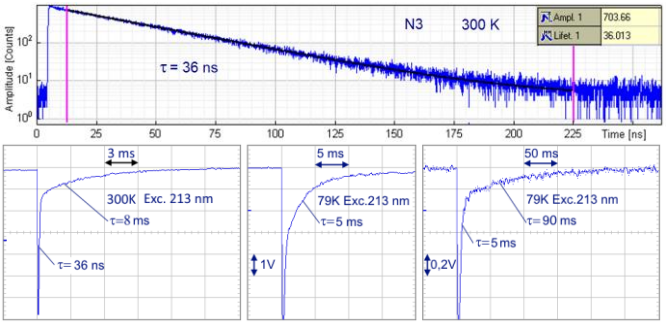

Fig. 2. Kinetics of luminescence during interband and intracenter excitation at 300 and 79 K

Some measurement results are presented in FIG. 1 and FIG. 2. By luminescence, N3, H3, and others centers were detected in the crystal. Upon interband excitation, a glow of N3 centers is observed, as can be seen in Fig. 1 by the characteristic structure of its spectrum. The luminescence spectrum of these centers is superimposed on a wide structureless band. The characteristic luminescence kinetics in this band (8 ms at 300 K, 5 and 90 ms at 79 K) confirms [1-4] that this is the A band of recombination luminescence.

REFERENCES

[1] Martynovich E.F., Morozhnikova L.V., Novikov V.V. X-ray luminescence of diamonds. Luminescence and spectral analysis. Issue 3. Irkutsk, ISU, pp. 146-155, 1974 (In Russian).

[2] Martynovich E.F., Emelianova A.S., Rakevich A.L. XVI International Youth Conference on Luminescence and Laser Physics Devoted to the 100th Anniversary Irkutsk State University, 2 - 7 July 2018. Abstracts. ISU Publishing House, Irkutsk, pp. 60-61, 2018 (In Russian).

[3] E. I. Lipatov, V. M. Lisitsyn, V. I. Oleshko V. F. Tarasenko. Spectral and kinetic characteristics of the pulsed cathodoluminescence of a natural IIa-type diamond. Russian Physics Journal, V. 50, pp. 52–57 (2007).

[4] [4] Martynovich E.F., Mironov V.P. X-ray luminescence of diamonds and its use in the diamond mining industry.Izvestiya vuzov. Physics. T. 52. No. 12-3, pp. 202-210, 2009 (In Russian).

* The work was supported by the Program of fundamental scientific research of the state academies of sciences for 2013–2020, section II.10.1 Project No. 0307-2016-0004, and by the Integration Program "Fundamental Research and Breakthrough Technologies" of the INTs SB RAS No. 0341-2019-0001

NANOWALLS FORMATION ON GLASSY CARBON AND CARBON FIBER SURFACES BY HIGH-FLUENCE ION IRRADIATION

N.N. ANDRIANOVA[1], A.M. BORISOV[1], E.S. MASHKOVA[2], M.A. OVCHINNIKOV[1,2]

[1]Moscow Aviation Institute (National Research University), Moscow, 125993, Russia
[2]Skobeltsyn Institute of Nuclear Physics, Moscow State University, Moscow, 119991, Russia, ov.mikhail@gmail.com

Nanoscale carbon materials are promising materials for creating low-voltage field emission cathodes and electrodes in supercapacitor structures or lithium-ion batteries [1-3]. In addition to the ways of producing isolated nanoscale carbon materials, such as carbon nanotubes, nanofibers, nanoscales, etc., there are the ways of developing and transforming the surface structure and topography of polycrystalline and amorphous carbon materials into nanocrystalline ones with micro or nanoscale relief. Various methods are used to form micro and nanoscale elements on the surface of carbon materials, including high-fluence ion irradiation [4,5]. For example, high-fluence ion irradiation of highly oriented pyrolytic graphite at temperatures $T \approx 250$, 400°C leads to the appearance of low-voltage field emission with the thresholds from 3 to 17 $V/\mu m$ depending on the temperature and geometry of irradiation [2]. Also, to increase specific capacitive and energy characteristics of supercapacitors different methods of electrode surface modification from carbon fibers are used [6]. High-fluence ion irradiation of carbon materials depending on the target temperature T of irradiation leads to the processes of amorphization, recrystallization and development of the surface topography. The surface topography is manifested at temperatures $T \geq T_a$, where the temperature of dynamic annealing of radiation damage T_a in carbon materials is 150 - 200°C depending on the material and type of ion [5].

This work is aimed at studying the structure and development of a relief on the surfaces of carbon fibers from viscose and glassy carbons from the ion irradiation fluence and irradiation temperature. The samples were irradiated by Ar^+ ions with energies of 30 keV using a mass-monochromator of SINP MSU [7] at temperatures from RT to 700°C. Subsequent analysis of samples was carried out using scanning electron microscopy (SEM) and Raman spectroscopy.

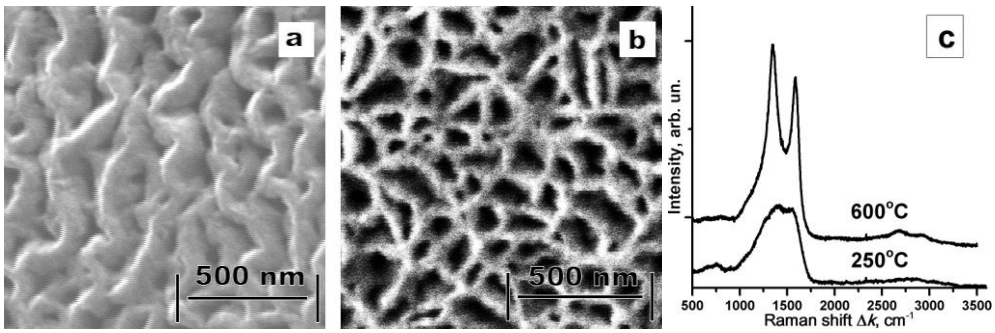

Fig.1. SEM images of nanowall structures formed after 30 keV Ar^+ ion irradiation on the surface of (a) carbon fiber based on viscose and (b) SU-2500 glassy carbon at temperatures of irradiation 200 and 500°C, respectively, and Raman spectra (c) of SU-2500 glassy carbon surface at temperatures of irradiation 250 and 600°C.

The analysis of SEM-images shows that at fluence of irradiation $\varphi t \geq 1 \cdot 10^{18}$ cm^{-2} the formation of nanosize wall structures is observed both on the carbon fibers based on viscose and on the glassy carbon (Fig. 1a,b). The Raman spectra are showed the presence of graphite-like and nanocrystalline structures of a modified layer for glassy carbon SU-2500 at temperatures $T > 200$ and 350°C (Fig.2c), respectively. Changes in the topography of the carbon fiber and glassy carbon surfaces are associated with anisotropic radiation-induced processes of carbon materials and sputtering of fibers under ion irradiation.

REFERENCES

[1] *M. Hiramatsu, M. Hori //* Carbon nanowalls: synthesis and emerging applications. – Springer Science & Business Media, 2010.
[2] *N.N. Andrianova, A.M. Borisov, V.V. Borisov, et. al. //* J. Surf. Invest.–2013. –V.7. –№2. –p.299–302.
[3] *K. Mironovich, S. Evlashin, S. Bocharova //* Journal of Materials Chemistry A. –2017. –V.5, –№34. –p.18095-18100.
[4] *Andrianova N.N., Borisov A.M., Mashkova E.S. et. al. //* Horizons in World Physics. –2013. –V.280. –p.171.
[5] *A. M. Borisov, Yu. S. Virgil'ev, E. S. Mashkova //* J. Surf. Invest.–2008, –V.2. –№1. –p.52–67.
[6] *Hsin-Cheng Hsu, Chen-Hao Wang, S.K. Nataraj, et.al. //* Diam. Rel. Mat. –2012. –V.25. –p.176–179
[7] *Mashkova E.S., Molchanov V.A. //* Medium-Energy Ion Reflection from Solids. Amsterdam. North-Holland, 1985.

PULSE AND FREQUENCY CHARACTERISTICS OF MICROWAVE ANTENNA BASED ON CARBON FIBERS*

V.N. FEDOROV[1,2], N.D. MALYUTIN[2]
[1]*North-Eastern Federal University, Yakutsk, Russia*
[2]*Tomsk State University of Control Systems and Radioelectronics (TUSUR), Tomsk, Russia*

Carbon fibers make it possible to design various microwave elements due to the unique electrical and mechanical characteristics [1, 2]. Strip transmission lines based on carbon fibers were studied in [3] and the experimental results of researching the pulse and frequency characteristics of carbon strip lines were presented. Authors these and others works have shown the applicability of carbon fibers for design of the strip transmission lines.

In this paper, we examined the characteristics of "Ground Plane" type carbon antennas and presented their experimental pulse and frequency characteristics in the near field zone. The view of carbon fiber based antennas is shown in fig. 1a. The antenna itself is placed in a plastic tube. The antennas were excited by a pulse in the form of a voltage step with a front of about 40 ps. The measurements were performed in the time domain on a double-beam stroboscopic memory oscilloscope Tektronix 11801B. Fig. 1b shows the voltage at the input of the emitting carbon antenna with highlighting the reflected signal, and the amplified voltage at the output of the receiving antenna is shown in blue.

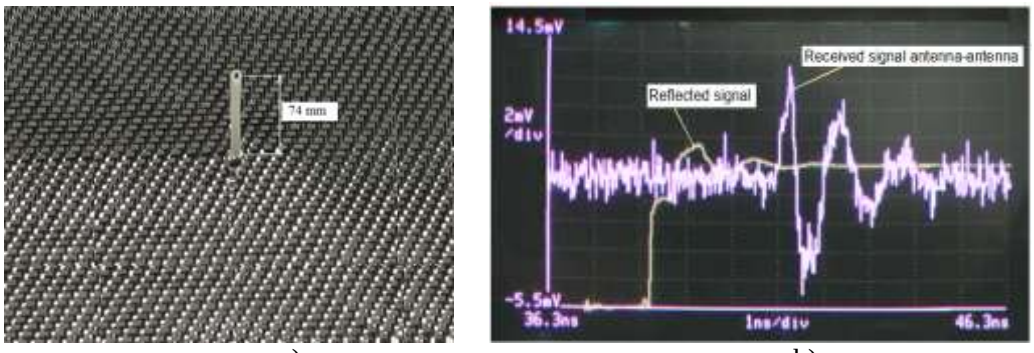

a) b)

Fig.1. Carbon antenna design with carbon base (a), voltages at the input of the receiving carbon antenna (blue color) and at the output of the radiating antenna (b) with highlighting the reflected signal.

The transition to the frequency domain is performed using the Fourier transform. The frequency dependences of the coefficients S_{11}, S_{21} scattering matrix are obtained. The effect on the transfer characteristics of the antennas was studied when replacing a metal base with a carbon base, as well as changing the carbon emitting element to copper. The frequency characteristics are studied by the classical method using a vector network analyzer.

It is shown that the impulse and frequency characteristics of carbon antennas obtained by two methods are well comparable. The placement of antennas above the surface of carbon materials leads to an increase in their broadband and in losses. The obtained results of the antenna's response to pulsed action make it possible to predict the electromagnetic radiation of structural elements from carbon materials, as well as the emission of metal elements over carbon surfaces.

REFERENCES

[1] Aidin Mehdipour; Abdel R. Sebak; Christopher W. Trueman; Iosif. D. Rosca; Suong V. Hoa. Advanced conductive carbon fiber composite materials for antenna and microwave applications. Proceedings of the 2012 IEEE International Symposium on Antennas and Propagation, 8-14 July 2012. DOI:10.1109/APS.2012.6349125.

[2] Mahan Rudd; Thomas C. Baum; Benjamin Mapleback; Kamran Ghorbani; Kelvin J. Nicholson. Reducing the Attenuation in CFRP Waveguide Using Carbon Fiber Veil. IEEE Microwave and Wireless Components Letters, Volume 27, Issue: 12, Dec. 2017. Pp. 1089 – 1091. DOI: 10.1109/LMWC.2017.2762243.

[3] Fedorov, V., Malyutin, N. Nonlinear Properties of a Strip Transmission Line Based on Carbon Fiber. 2016 International Symposium on Fundamentals of Electrical Enginiaring. University Politechnica of Bucharest, Romania, June 30 – Julay 2, 2016. DOI: 10.1109/ISFEE.2016.7803222.

* This work was supported by the Ministry of Science and Higher Education (state assignment). The measurements were carried out using the equipment of the Center of collective using of equipment “Impulse”, project identifier RFMEFI62119X0029/

POLYHEDRAL GRAPHITE PARTICLES AMBIENT AIR DIRECT CURRENT ARC PLASMA SYNTHESIS*

A.Y.PAK[1], KONONENKO P.N.[1], A.I. KOKORINA[1]

[1]Tomsk Polytechnic University, Tomsk, Russia

The arc plasma method is useful to produce carbon nanoparticles for many years [1]. Many papers have discussed the possibility of the carbon nanotubes synthesis by the direct current arcing procedure [2]. Carbon nanotubes, graphene based materials are very popular and have been studied in details, however there are many other morphological types of carbon nanoparticles, for example polyhedral graphite nanoparticles (PGPs). PGPs have the potential for application as an electron field emitter and as a material for electrical energy supercapacitors because of their unique morphology [3]. These particles can be obtained by the direct current arc plasma technique under protective gas medium (helium, hydrogen and helium mixture of hydrogen) [3-4]. In this paper, we present results of the experimental research to discuss the possibility of PDPs synthesis using self-shielding ambient air direct current arc plasma [5] and molybdenum catalyst. This vacuumless method is possible because of the carbon monoxide and carbon dioxide emission during the arcing [5-6]. This approach is very promising due to the potential energy and cost efficiency and simplicity [7]. The PGPs ambient air direct current arc plasma synthesis has never been discussed before.

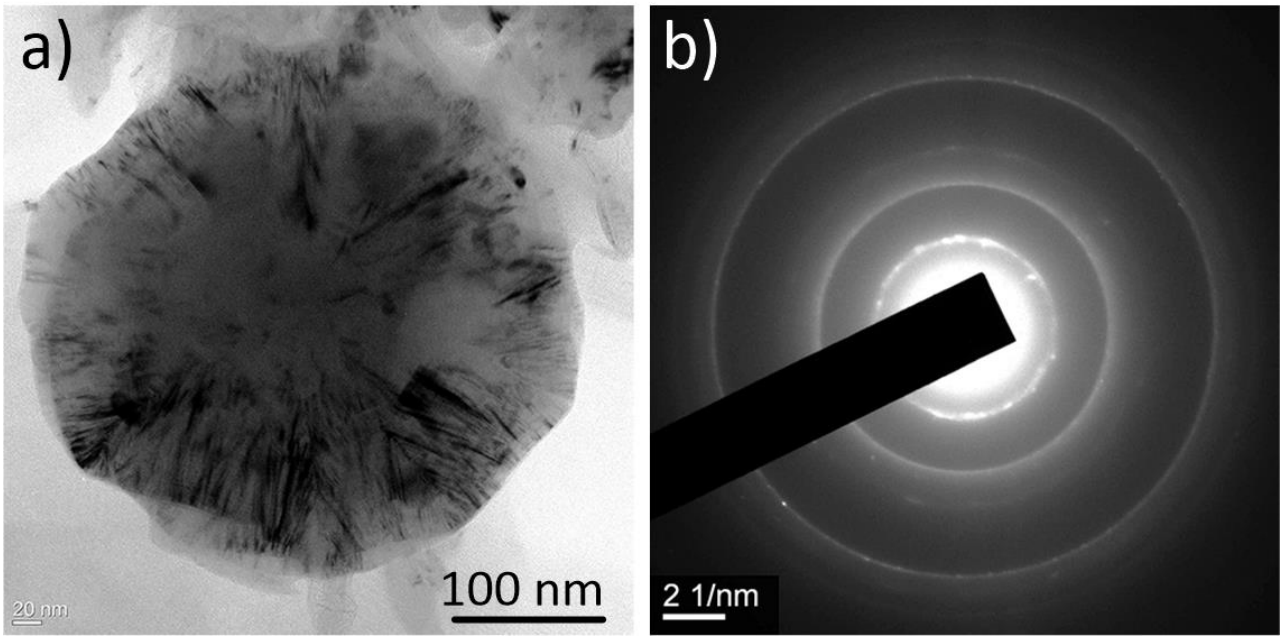

Fig.1. Transmission electron microscopy of the obtained powder product: a) HRTEM image of the PGP; b) selected area electron diffraction pattern.

REFERENCES

[1] Sumbo Lijima. Helical microtubules of graphitic carbon / Lijima Simbo // Letters to Nature.-1991.-№354.-pp.56-58.

[2] Neha Arora. Arc discharge synthesis of carbon nanotubes: Comprehensive review/ Arora Neha, N.N. Sharma // Diamond & Related Materials.-2014.-№50.-pp.135-150.

[3] Feng Liang. Selective preparation of polyhedral graphite particles and multi-wall carbon nanotubes by a transferred arc under atmospheric pressure / Liang Feng [et al.] // Diamond & Related Materials.-2012.-№30.-pp.70-76.

[4] Xiaolong Song. Synthesis of polyhedral graphite in a forced flow arc discharge / Song Xiaolong, Liu Yongning, Zhu Jiewu // Materials letters.-2007.-№61.-pp.4781-4783.

[5] Pak A.Ya. Boron Carbide Synthesis in Low-Voltage DC Electric Arc Initiated in Open Air/ A.Ya.Pak, G.Ya.Mamontov // Technical Physics Letters.-2018.-№7.-pp.615-617.

[6] Yanjie Su. Low-cost synthesis of single-walled carbon nanotubes by low-pressure air arc discharge / Su Yanjie [et al.] // Materials Research Bulletin.-2014.-№50.-pp.23-25.

[7] Joseph Berkmans. Synthesis of thin bundled single walled carbon nanotubes and nanohorn hybrids by arc discharge technique in open air atmosphere / Berkmans Joseph [et al.] // Diamond & Related Materials.-2015.-№55.-pp.12-15.

* This work was supported by the Russia President ‘s grant for young scientists (MK-633.2019.8)

OPTICAL PERFORMANCE OF SILVER-DOPED DIAMOND-LIKE CARBON COMPOSITE FILM*

JIALIN FANG[1], YUWEI LIU[1], XIAOHONG JIANG[1], D.G. PILIPTSOU[2], A.V. ROGACHEV[2]

[1]International Chinese-Belorussian Scientific laboratory on Vacuum-Plasma Technology, Nanjing University of Science and Technology, 200; Xiaolingwei street, Nanjing 210094, China; jiangxh24@njust.edu.cn (X. Jiang)

[2]Francisk Skorina Gomel State University, 104, Sovetskaya Street, Gomel 246019, Belarus

Germanium and silicon substrates has high transparency in IR region and widely used as an window for equipment which a work in IR region, such as thermal and night vision cameras or sensors, and, very important, has an irreplaceable position in the field of infrared optics. However, due to the high refractive index of germanium (n = 4.3), the transmittance of germanium optical elements is only 40%, which seriously affects optical absorbance, especially leading to the destruction of optical elements at high transmitted radiation power. Therefore, it is necessary to prepare an infrared antireflection coating to improve the optical performance in IR region [1]. Diamond-like carbon film (DLC) has excellent light transmission performance in the mid-far infrared, so it can be used as an optical anti-reflection film for infrared optical elements [2,3]. DLC coatings together with excellent abrasion resistance and hardness have a low absorbance in the IR region, therefore it is an ideal coating for germanium windows and has broad application prospects. One way to change the optical characteristics of DLC coatings is to introduce metal into the coating structure. One of the main absorption peak of DLC is carbonyl absorption peak. And oxygen will preferentially combine with silver dropped in DLC [4].

The aim of this work is to study the effect of Ag concentration on the structure, mechanical and optical properties, such as refractive index, absorption coefficient and dielectric constant. Knowing these values will allow us to develop the design of a multilayer coating containing DLC layers and DLC:Ag with a different Ag content. DLC:Ag coatings was deposited on Si and Ge substrates use vacuum pulsed cathode arc deposition method. The concentration of silver in the DLC coatings was changed by using cathodes with different silver-to-carbon ratios.

The concentration of elements in the coating, the chemical composition, and the structure of the resulting coatings were investigated by XPS, XRD, Raman, TEM, SEM with EDS and IR spectroscopy.

The results of RDA studies have shown that with the same thickness of the coating (about 150 nm) with increasing silver concentration, its structure changes from spherical nanoparticles to single crystals with a cubic crystal structure.

At the same time, with the increase of silver content, the infrared transmittance of the DLC:Ag coatings gradually increases, and the area with a high transmission is expands from 500 cm^{-1} to 4000 cm^{-1} . In the sample with the highest silver content, the average transmittance is above 95%. It was found that the increase in silver content changes the interaction mechanism between silver and carbon atoms, and increase destruction of carbonyl and hydroxyl groups, which weaken the diamond-like carbon film's resonance absorbance to infrared light. The silver-doped DLC has good adhesion, and the friction coefficient is about 0.2

REFERENCES

[1] [1] Pan Yongqiang, Zhu Chang, Hang Lingxia. Study on 3~5mkm and 8~12mkm Infrared AR Coatings on Germanium Substrate [J]. Laser & Infrared, 2004, 34 (5): 372-374.

[2] [2] Behranvanda A, Davoudi Darareha M, Jannesaria M, et al. Design and fabrication of PbTe/BaF 2 hydrophobic high-efficiency broadband antireflection coating on Ge substrate in long -wave infrared region [J]. Infrared Physics and Technology, 2018, 92: 163-165.

[3] [3] Gainutdinov I S, Yu N, Shuvalov R S, et al. Antireflection coatings on germanium and silicon substrates in the 3~5 μm and 8~12 μm windows of IR transparency [J]. Journal of Optical Technology, 2009, 76(5): 302-305.[4] F.R.Marciano,L.F. Bonetti et al.. The improvement of DLC film lifetime using silver nanoparticles for use on space devices [J]. Diamond & Related Materials, 2008, 17 (7-10): 1674-1679.

* This study was supported by the Intergovernmental Cooperation Projects in the national key research and development plan of the Ministry of Science and Technology of the People's Republic of China (2016YFE0111800).

THRESHOLD AND SPECTRAL CHARACTERISTICS OF THE ELECTRON-HOLE LIQUID CONDENSATION IN DIAMOND UNDER QUASISTATIONARY PHOTOEXCITATION[1]

D.E.GENIN[1], *E.I. LIPATOV*[1,2]

[1]*Institute of High Current Electronics, Tomsk, Russia*
[2]*Tomsk State University, Tomsk, Russia*

Electron-hole liquid (EHL) is a condensed state of non-equilibrium charge carriers in semiconductors. EHL droplets condensation occurs when the temperature is lower and the charge carriers concentration is higher than some critical value, which is individual for every semiconductor material.

The development of high-power solid-state diamond switches would seem to have stopped due to a fundamental limitation – free excitons (FE) do not take part in electric field drift. However, the condensation of free excitons to the droplets of electron-hole liquid, which was detected in diamond at sufficiently high temperatures (up to 200 K) [1, 2] gives a chance for the use of diamond in high current electronics. EHL droplets have a surface charge and are involved in the drift. The speed of sound in diamond is high ~2*10 6 cm/s. This value is an order of magnitude less than the saturated velocity of the carriers in the diamond.

In our experiments we used UV laser pulses with ns-range pulsewidth for creation of high charge carriers concentration, and liquid nitrogen cooling of the samples. The conditions of EHL droplets formation in diamond samples were determined for that case. Earlier, such like data was obtained mostly for femtosecond laser pulses.

Also we managed to demonstrate the effect of EHL droplets on the sample conductivity: in the presence of EHL the current through the sample was up to 2.5 times higher.

REFERENCES

[1] Thonke K., Schliesing R., Teofilov N., et al. // Diamond and related materials. 2000. V. 9. P. 428.

[2] Shimano R., Nagai M., Horiuchi K., Kuwata-Gonokami M. // Physical review letters. 2002. V. 88. No5. 057404.

1 The work was supported by RFBR, project No 14-02-31132.

CHANGE OF CATHODOLUMINESCENCE SPECTRA OF DIMONDS IRRADIATED BY ELECTRON BEAM[1]

D.E. GENIN[1,2], V.S. RIPENKO[1,2], E.I. LIPATOV[1,2], A.G. BURACHENKO[1,2], M.A. SHULEPOV[1], K.P. ARTYOMOV[1], A.P. ELISEEV[3], V.G. VINS[4]

[1]Institute of High Current Electronics SB RAS, Tomsk, Russia
[2]National Research Tomsk State University, Tomsk, Russia
[3]Institute of Geology and Mineralogy named after V.S. Sobolev, Novosibirsk, Russia
[4]VELMAN Ltd., Novosibirsk, Russia

It is known, that nitrogen-vacancy (NV) centers in diamond are adjective single-photon emitters, with applications in quantum technologies. Two charge states are known for NV centers: NV^0 and NV^- , with the latter being mostly studied due to its long electron spin coherence time. NV centers in diamond are promising elements for quantum optical systems since they are single-photon emitters with high photostability, quantum yield and brightness, even at room temperature [1-3]. Typically, synthetically prepared diamonds with NV centers contain both NV^0 and NV^- states. Therefore, control of NV centers state in diamond is an important scientific problem.

Here we investigate changes in the cathodoluminescence (CL) spectra of HPHT diamonds, irradiated by electron beam at the room temperature (298 K) and liquid nitrogen temperature (77K).

RADAN-220-IMA3-150E accelerator was used as a source of electrons (220 keV). For temperature control we used platinum thermo-resistor. All experiments were conducted in the vacuum chamber (10^{-2} Pa). Optical spectra of diamonds cathodoluminescence were recorded ever 20 K and than compared with each other.

REFERENCES

[1] R. Brouri,A. Beveratos, J.-P.Poizat, P. Grangier, "Photon Antibunching in the Fluorescence of Individual Color Centers in Diamond," Opt. Lett. , vol. 25 (17), 2000.

[2] M. W. Doherty, N. B. Manson, P. Delaney, F. Jelezko, J. Wrachtrup, L. C. L. Hollenberg, "The Nitrogen-Vacancy Colour Centre in Diamond," Phys. Rep. , vol. 528 (1), pp. 1–45, 2013.

[3] A. Gruber, A. Drabenstedt, C. Tietz, L. Fleury, J. Wrachtrup, C. von Borczyskowski, "Scanning Confocal Optical Microscopy and Magnetic Resonance on Single Defect Centers," 2012.

1 This work was performed on state task, project No 0721-2020-0048 and RFBR project No 14-02-31132.

OXIDATIVE RESISTANCE OF IRRADIATED GRAPHITE COATED WITH SILICON CARBIDE

N. ROMANOVA[1], *A. SHAIMERDENOV*[1], *SH. GIZATULIN*[1], *D. DYUSSAMBAYEV*[1], *U.KOZTAYEVA*[1],

S. UETA[2], *T. SHIBATA*[2]

[1]*Institute of Nuclear Physics under the Ministry of Energy,*
1 Ibragimov str., 050032, Almaty, Kazakhstan, romannat@mail.ru, +7 727 3866800(265)
[2] *Japan Atomic Energy Agency, 4002 Narita-cho, Oarai-machi, Higashiibaraki-gun, Ibaraki 311-1393 Japan*

The main characteristics of structural graphite material are stability of linear dimensions, strength, creep, elastic modulus, thermal expansion and thermal conductivity, as well as oxidation resistance [1].

Damage of nuclear reactor materials as a result of its oxidation is one of important items of nuclear safety in case of an accident. In particular, graphite materials are used in internal parts of high-temperature gas-cooled reactor (HTGR) due to its excellent neutron, thermal and mechanical properties. Graphite is used as structural materials in fuel elements, playing also parts of moderator and reflector. In case of an accident with ingress of water or air, oxidation of graphite material would be one of the most serious problems. To avoid this, it is assumed to use graphite covered with oxidation-resistant coating on a base of graphite, coated with silicon carbide (SiC).

At INP (Kazakhstan), jointly with JAEA (Japan), a study of resistance to oxidation of graphite, coated with SiC, after its irradiation in the WWR-K reactor core. Samples of graphite, coated with SiC from four manufacturers from Japan were irradiated in the WWR-K reactor for 200 days. The fast neutron fluency (En>0.18 MeV) comprised $1.1 \cdot 10^{25}$ m^{-2}. After irradiation, the specimens passed through the oxidation test in environment of helium with oxygen (20%) at 1200°C. In course of the test, release of carbon dioxide (CO_2) and concentration of oxygen (O_2) in swept gas were monitored. Only the sample from manufacturer X was found to be resistant to oxidation, there were no detected release of CO_2. Three others oxidized in course of the test.

REFERENCES

[1] *Voevodin V.N., Gribanov Ju.A., Gurin V.A., Gurin I.V., Gujda V.V. //* VANT. – 2015. – №2(96). – p. 52 – 64.

PHOTOLUMINESCENCE OF THE HPHT DIAMOND SAMPLES CONTAINING NV CENTERS UPON EXCITATION BY LASER AND SPONTANEOUS UV AND VISIBLE RADIATION*

E.I. LIPATOV[1,2], *D.E. GENIN*[1,2], *V.S. RIPENKO*[1,2], *VINS V.G.*[3], *ELISEEV A.P.*[4]

[1]*National Researsh Tomsk State University, 36 Lenin ave., Tomsk, 634050, Russian Federation*
[2]*Institute of High Current Electronics SB RAS, 2/3 Akademicheskii ave., Tomsk, 634055, Russian Federation*
[3]*Vellman Ltd., of. 108, 43, Russkaya ave., Novosibirsk, 630058, Russian Federation*
[4]*V.S. Sobolev Institute of Geology and Mineralogy SB RAS, 3 Koptyug ave., Novosibirsk, 630090, Russian Federation*

NV centers in diamond are potentially suitable for quantum information technology applications at room temperature. In this regard, the urgent task of obtaining laser generation in the luminescence band of NV centers. In the future, integrated NV-containing components will be needed when creating photonic integrated circuits, optoelectronic modules for quantum key distribution, and controlling of qubits based on NV centers in solid-state quantum computers.

In this work, we present experimental results on the study of the photoluminescence of diamond samples with a concentration of NV centers about ~ 10^{16} cm^{-3} when excited by optical radiation of excimer lasers and spontaneous emission of excilamps in the range of 222-532 nm. Photoluminescence spectra demonstrate, including intense luminescence of NV centers in a neutral charge state, as well as electron-vibrational centers associated with radiation destruction of the diamond lattice

This study is a continuation of the grant № 14-02-31132 of the Russian Foundation for Basic Research

* The study was carried out as part of the task of the Ministry of Education and Science of Russia, project No. 0721-2020-0048.

VISUALISATION OF MOTION DYNAMICS IN THE ELECTRIC FIELD AND RELAXATION OF PLASMA INDUCED IN A LOCALIZED REGION OF CVD DIAMOND VIA LASER LIGHT TWO-PHOTON ABSORPTION

A.D. SAVVIN[1], *A.E. DORMIDONOV*[1], *V.P. MITROKHIN*[1], *M.A. BUBLIK*[1], *S.A. POTANIN*[2,3]

[1]*All-Russia Research Institute of Automatics (VNIIA), Moscow, Russia*
[2]*Faculty of Physics MSU, Moscow, Russia*
[3]*Sternberg Astronomical Institute M.V. Lomonosov Moscow State University, Moscow, Russia*

The diamond in normal conditions is a dielectric material. However, when exposed to ionizing radiation or irradiated with ultraviolet light, charge carrier pairs are generated. In diamond, these pairs tend to form free excitons (FE), which under certain conditions condensate to droplet of electron-hole liquid (EHL)[1]. To design and to understand the operation of diamond optoelectronic devices, such as radiation detectors, it is important to have an understanding of the properties of charge drift in an external electric field and plasma relaxation..

Two-photon absorption by focusing intense laser radiation allows to form a localized plasma area [2] that can be visualized. In this work, we studied a sample of CVD diamond placed in a thermostat with the possibility of cooling to liquid nitrogen temperature. An electric field of different polarity and intensity can be applied to sample. For excitation, a picosecond Nd:YAG laser was used, the radiation of which was converted into a third harmonic with a wavelength of 355 nm and a duration of 50 ps.

Two visualization methods are explored. In the first, the dynamics of drift and relaxation of the plasma observed by 532 nm second harmonic scattered on it and delayed in time relative to the exciting pulse. In second method blur of spots corresponding to the luminescence of FE and EHL are observed by UV-sensitive CCD camera combined with a slit-free spectrograph.

REFERENCES

[1] Teofilov N., Schliesing R., Thonke K., Zacharias H., Sauer R., Kanda H. “Optical high excitation of diamond: phase diagram of excitons, electron-hole liquid and electron-hole plasma”. Diamond &R elated Materials, vol. 12, pp. 636-641, March 2003.

[2] M. Kozák, F. Trojánek, T. Popelář, P. Malý “Dynamics of electron–hole liquid condensation in CVD diamond studied by femtosecond pump and probe spectroscopy,” Diamond & Related Materials, vol. 34, pp. 13–18, April 2013.

HIGH-TEMPERATURE ELECTRON-HOLE LIQUID IN DIAMOND FILMS*

A.A. VASILCHENKO

Kuban State University, Krasnodar, Russia

The condensation of excitons into an electron-hole liquid (EHL) has been actively investigated since the late 1960s. The properties of three-dimensional EHLs in various semiconductors are rather well studied. EHL has been observed in Si, Ge, CdS, C, SiC, and many other materials. Note that the EHL critical temperature in most semiconductors is several tens of Kelvin.

The properties of EHLs in low-dimensional semiconductor structures are less studied. The formation of a quasi-two-dimensional EHL in $SiO_2/Si/SiO_2$ quantum wells (QWs), Si/SiGe/Si heterostructures, and GaAs/AlAs superlattices was demonstrated fairly recently. In diamond films, the formation of EHL is also possible. We apply density functional theory to calculate the EHL energy and equilibrium density in diamond films with thicknesses of a few nanometers. The exchange and correlation energy is taken into account in the local density approximation.

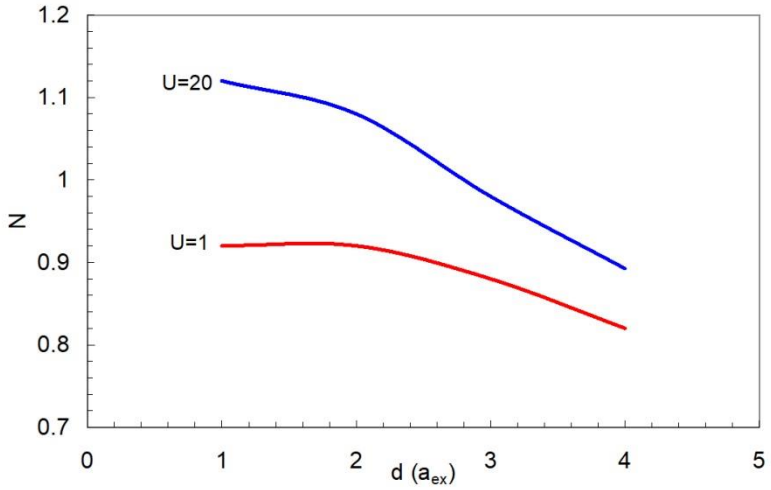

Fig.1. Electron-hole pair density versus the QW width for (111) diamond films.

It is shown that EHL is multicomponent and consists of electrons and heavy, light, and spin-orbit split holes. Figure 1 shows the dependences of the electron-hole pair density on the QW width d for well depths of $U = 1$ and 20 (excitonic units are used). The equilibrium density decreases with increasing d or decreasing U. This behavior is caused by a decrease in the contribution from the exchange-correlation interaction for large d and small U. The EHL is four-component; for example the hole densities for $d = 1$ and $U = 20$ are $N_{hh} \approx 0.73$, $N_{hl} \approx 0.27$, and $N_{so} \approx 0.12$. For a diamond film with a thickness of $d = 1$ and $U = 20$, we obtain a three-dimensional electron-hole pair density of $n \approx N/d = 1.1$ ($4.2 \cdot 10^{20}$ cm^{-3}). This is more than a factor of 4 higher than the density of a three-dimensional EHL. Therefore, following [1], we find that the critical temperature of the EHL in such a film is $T_c = 270$ K. It is noteworthy that the estimate for T_c in [1] is obtained for the three-dimensional case, while the critical temperature of a quasi-two-dimensional EHL can be higher than that of a three-dimensional EHL.

REFERENCES

[1] F.E. Leys, N.H. March, G.G.N. Angilella, M.L. Zhang, "Similarity and contrasts between thermodynamic properties at the critical point of liquid alkali metals and of electron-hole droplets," Phys. Rev. B, vol. 66, Article Number 073314, 2002.

* The work was supported by RFBR and the Administration of Krasnodar Region (project No. 16-42-230280) and the State Assignment of the Ministry of Science and Higher Education of the Russian Federation (project No. 0721-2020-0048).

SYNTHESIS OF CARBON NANOSTRUCTURES BY PLASMA CHEMICAL METHOD

C.M. BEISEBEK[1], M.T. GABDULLIN[2], D.S. KERIMBEKOV[3], D.V. ISMAILOV[3]

[1]Kazakh National University named after al-Farabi, Almaty, Kazakhstan
[2] Kazakh-British Technical University, Almaty, Kazakhstan
[3] National Open Nanotechnological Laboratory at KazNU named after al-Farabi, Almaty, Kazakhstan
+7 778 423 34 48, ismailov_daniyar_v@bk.ru

Annotation

In the work, an installation based on a carbon plasma jet in a helium stream was developed and manufactured. The modernized installation scheme is a compact stand with conveniently located systems for monitoring vacuum, gas and water pressure, and electrode movement devices. An advantage of the installation is also the fact that it does not require reduced pressure for synthesis, which greatly simplifies the production process itself. The content of the obtained fullerene mixture in soot completely depends on the helium flow and power input and ranges from 4% to 20%. The synthesis in our installation is characterized by the high yield of C_{60} and C_{70} - The relative content of the extracted fullerene mixture is 7:3.

Keywords. Carbon nanostructures, fullerenes, Raman spectroscopy, optical microscopy, arc synthesis.

Introduction

Recently, a lot of work in the field of nanotechnology has been held at the development of new materials based on carbon, which have unique properties. Nanotechnology has a broad concept, including the creation, processing, diagnostics and use of materials, devices and systems with the range of size within 0.1-100 nm, which demonstrate new or substantially enhanced physical, chemical and biological properties, functions, phenomena and processes due to their nanoscale features [1]. In the second half of the 80s, a new form of carbon was discovered - fullerene. It turned out that carbon at its option forms the spherical molecules. To create such an object, it is necessary to obtain ionized vapor from carbon atoms and then condense it in the helium atmosphere [2].

The massive use of fullerenes and their derivatives is constrained by the imperfection of synthesis methods. Nowadays, almost all existing fullerenes are synthesized by the thermal evaporation of graphite. The method of thermal evaporation of graphite is based on the formation of fullerenes during thermal spraying of a graphite electrode in an arc discharge plasma burning in a helium atmosphere. This method allows to obtain fullerenes in an amount sufficient for a detailed study of their physical and chemical properties. Fullerenes can be obtained from extended fragments of graphite, which are then purified.

Experiment

The synthesis of fullerenes by the plasma-chemical method proceeded at a higher pressure. Then the pressure used in conventional installations (100-200 torr), which leads to a higher probability of particle collisions, i.e. contributes to increased installation efficiency. The results were analyzed with the use of both Raman spectroscopy, and optical microscopy, which showed the presence of fullerenes. Thus, the results gave a reason to conclude that the plasma-chemical reactor, which can be used for the synthesis of various fullerenes, has rather wider possibilities than it was considered before.

REFERENCES

1. *Matysina Z.A., Zaginaichenko S.Yu., Schur D.V., Gabdullin M.T.* Sorption properties of iron-magnesium and nickel-magnesium hydrides Mg_2FeH_6, Mg_2NiH_4 // News of higher educational institutions, Physics. - 2016. - V.59. - p. 19-29.
2. *Smalley R.E.* Discovering fullerenes // Usp. Fiz. -1998. - V.168.- №3. - p. 324-329.

EXTRACTION OF FULLERENES BY TOLUENE VAPORS

A.G. SADYK [1], M.T. GABDULLIN [2], D.S. KERIMBEKOV[3], D.V. ISMAILOV[3]

[1]Kazakh National University named after al-Farabi, Almaty, Kazakhstan
[2] Kazakh-British Technical University, Almaty, Kazakhstan
[3] National Open Nanotechnological Laboratory at KazNU named after al-Farabi, Almaty, Kazakhstan
+7 778 423 34 48, ismailov_daniyar_v@bk.ru

Annotation

The paper considers the process of fullerene purification and separating into components using the Soxhlet apparatus within 5 cycles. Fullerenes were synthesized using an arc synthesis apparatus in atmosphere of helium.

Keywords. Fullerenes, arc synthesis, toluene, extraction, Raman spectroscopy.

Introduction

To date, two methods are most often used for obtaining the amounts of fullerenes: high-temperature laser evaporation or the “laser furnace” method and the direct-current electric arc discharge method. In these methods, a mixture of empty fullerenes (C_{60}, C_{70}, C_{76}, C_{84}, etc.) with fullerenes are simultaneously formed. The production of fullerenes requires subsequent extraction processes from the carbon soot and the separation / purification of fullerenes from empty fullerenes.

The stage of extraction of fullerenes from fullerene-containing soot with organic solvents is the most responsible at this stage of fullerene production, since the amount of product obtained in the subsequent stages depends on the completeness of extraction of fullerenes. The extraction methods used today differ with the used solvents, the extraction time, the process temperature, as well as laboratory devices. In this work, toluene was taken as a base solvent, and cleaning was carried out on a Soxhlet apparatus.

Experiment

In this experiment the nanostructured soot was obtained. Also, during the synthesis, a “deposit” was obtained, presented from the burnt cathode graphite rod, which varied depending on the pressure of the buffer gas in the reaction zone of the experimental conditions. In such an experiment, it was possible to obtain amorphous carbon, single-walled nanotubes (SWNTs), and multi-walled nanotubes (MWNTs). The main component of the “deposit” is amorphous carbon. Then, after weighing, carbon soot was packaged in filter paper, which passed 5 cleaning cycles on a Soxhlet apparatus. The Soxhlet apparatus is used to evaporate at a low temperature and isolate fullerite crystals, thereby isolating a mixture of fullerenes from carbon soot. The isolated fullerenes from the soot were evaporated, thereby forming solid crystals called fullerites. An optical image of fullerite crystallites were obtained at a change in current, where one can see a change in the geometric shape of fullerite on the dependence of the supplied current to graphite electrodes using a direct current source that served as a welding rectifier. An analysis of Raman spectroscopy showed the presence of the obtained crystals of C_{60} and C_{70}. The position of the peaks in the spectrum of the studied crystals — fullerites — corresponds to the peaks of sample C_{60} and C_{70} presented in the references [1, 2].

REFERENCES

1. Shpak A.P., Kunitsky Yu.A., Karbovsky V.L. // Kiev: "Academic Period." - 2001 .- p. 587.
2. Matysina Z.A., Schur D.V. // - Dnepropetrovsk: Science and education. - 2002 .- p. 420.

ZIRCONIA-BASED COMPOSITES REINFORCED BY CARBON NANOMATERIALS*

A.A. LEONOV[1,2], M.P. KALASHNIKOV[2,3], E.V. ABDULMENOVA[2,3], YU.F. IVANOV[1,2]

[1]Institute of High Current Electronics SB RAS, Tomsk, Russia
[2]National Research Tomsk Polytechnic University, Tomsk, Russia
[3]Institute of Strength Physics and Materials Science SB RAS, Tomsk, Russia

In this work, ZrO_2 composites reinforced by single-walled carbon nanotubes (SWCNT "Tuball", OCSiAl, Russia), multi-walled carbon nanotubes (MWCNT "Taunit", NanoTechCenter, Russia), and graphene nanoplatelets (GNP, NanoTechCenter, Russia) were investigated. The composites were obtained by spark plasma sintering in vacuum in the following mode: sintering temperature – 1500 °C, holding time – 10 min, and uniaxial load – 40 MPa. ZrO_2 nanopowder was mixed with carbon nanomaterials (CNM) in ethanol using an ultrasonic bath and a magnetic stirrer [1, 2]. The concentration of SWCNTs, MWCNTs, and GNPs in composite powders was 1 wt.%. The influence of various CNM on the relative density (ρ_{rel}), microhardness (H_V), and fracture toughness (K_{IC}) of zirconia-based composites was investigated. Individual SWCNTs have an outer diameter of about 2 nm, but there are bundles with a diameter of about 200 nm (Fig. 1a), specific surface area of SWCNTs is 546 m^2/g. MWCNTs have a bamboo-like structure (Fig. 1b), their diameter is 20-50 nm, and their specific surface area is 103 m^2/g. GNPs with n ~ 15-25 layers (Fig. 1c), thickness of the nanoplates 6-8 nm, and their size 2-10 μm, the specific surface area is 25 m^2/g.

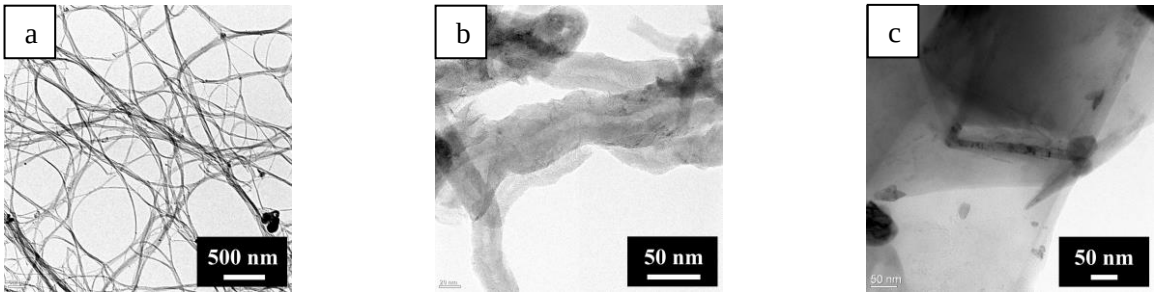

Fig. 1. TEM images showing the morphological features of the SWCNT (a), MWCNT (b) and GNP (c).

The relative density of ZrO_2/SWCNT composite (Table 1) decreases from 98.26 % to 95.50 %, which is associated with the strong agglomeration of SWCNT, which prevents the rearrangement of ZrO_2 particles during compaction/sintering, that increases the free volume. However, in composites with MWCNTs and GPNs, where reinforcing additives are not highly aggregated and have a lower specific surface area, the ρ_{rel} increases, since CNMs can slip during compaction and fill pores. The microhardness of the composites is lower than that of ZrO_2 ceramics (Table 1), because CNMs are a soft phase. The fracture toughness of ZrO_2/SWCNT composite increased by 38 %, ZrO_2/MWCNT composite by 8 % and ZrO_2/GNP by 31 %, compared with ZrO_2 ceramics. Increased fracture toughness of composites is associated with the hardening mechanisms inherent in fibrous/layered composites, which are described in our previous works [3, 4].

Table 1. Properties of the studied samples.

Sample	ρ_{rel}, %	H_V, GPa	K_{IC}, MPa*$m^{1/2}$
ZrO_2	98.26	14.10	3.96
ZrO_2/SWCNT	95.50	11.61	5.48
ZrO_2/MWCNT	99.03	13.47	4.27
ZrO_2/GNP	99.58	13.09	5.19

REFERENCES

[1] A.A. Leonov, E.V. Abdulmenova, "Alumina-based composites reinforced with single-walled carbon nanotubes," IOP Conf. Ser.: Mater. Sci. Eng., vol. 511, pp. 012001, 2019. https://doi.org/10.1088/1757-899X/511/1/012001.

[2] A. Leonov, "Effect of alumina nanofibers content on the microstructure and properties of ATZ composites fabricated by spark plasma sintering," Materials Today: Proceedings, vol. 11, pp. 66–71, 2019. https://doi.org/10.1016/j.matpr.2018.12.108.

[3] A.A. Leonov, et al., "Ceramic composite based on zirconia reinforced by single-walled carbon nanotubes," Nanotechnol. Russia, vol. 14, pp. 118-124, 2019. https://doi.org/10.1134/S1995078019020095

[4] A.A. Leonov, et al., "Effect of electron beam irradiation on structural phase transformations of zirconia-based composite reinforced by alumina nanofibers and carbon nanotubes," J. Phys.: Conf. Ser., vol. 1393, pp. 012106, 2019. https://doi.org/10.1088/1742-6596/1393/1/012106

* The reported study was funded by RFBR according to the research project № 18-33-00763 mol_a.

CARBON MICROWAVE ELEMENTS[1]

E.A. IVANCHIKOVA, I.A. EKIMOVA, V.N. FEDOROV, A.G. LOSCHILOV, N.S. TRUFANOVA, A.S. TRUFANOVA

[1]Tomsk State University y of Control Systems and Radioelectronics, Tomsk, Russia

The expansion of the scope of application of microwave devices not only in special, but also in household electronic equipment has led to the need to manufacture cheaper and lighter devices, including through the use of a technology for creating carbon-containing materials new for microwave technology [1,2]. At the same time, the question of methods and approaches to determining the complex parameters of these microwave devices remained relevant.

The paper reports on the results of a study of the frequency characteristics of microwave elements under pulsed exposure: two-port strip transmission lines based on carbon fiber (Fig. 1); horn antenna manufactured using additive 3D technology with metallization of the structure over the carbon sublayer (Fig. 2). Frequency characteristics were measured on the basis of the TsKP “Impulse” TUCSR and JSC “NPF“ Mikran ”using a nonlinear reflectometer and an automated measuring system using an anechoic chamber.

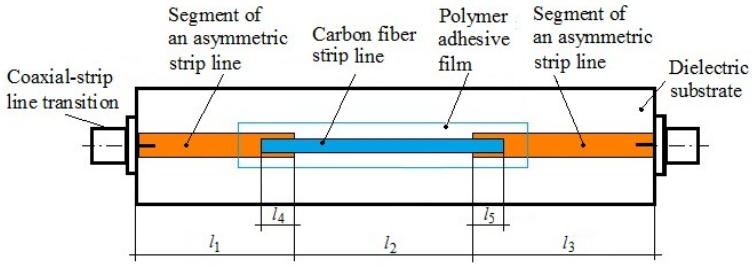

Fig.1. The segment of the strip transmission line based carbon fiber embedded into the interruption of the asymmetric strip line on the dielectric.

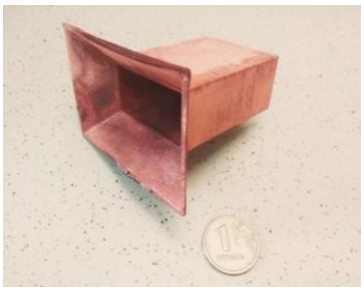

Fig.2. The appearance of carbon antennas

The frequency dependences of the transmission S 21 (f) coefficient of the carbon strip line segment are shown in Fig. 3. The frequency dependence of the SWR antenna measured under the influence of a pulse with a front of 40 ps is shown in Fig. 4. The antenna radiation pattern was measured at frequencies from 4 GHz to 8.5 GHz, in Fig. 5 shows a diagram at a frequency of 8.5 GHz.

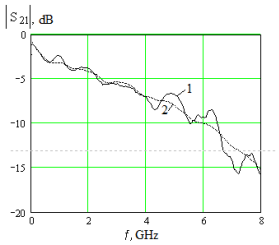

Fig.3.Frequency dependences of the insertion loss of the asymmetric strip line with an insert in the form of a CF-based strip line, with a width of the strip W=1,7 mm and a length l=62 mm: 1 – experimental; 2 – calculated

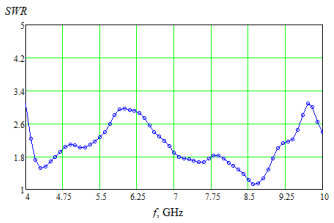

Fig.4.Frequency dependence of the SWR of a horn antenna manufactured using additive 3D technology

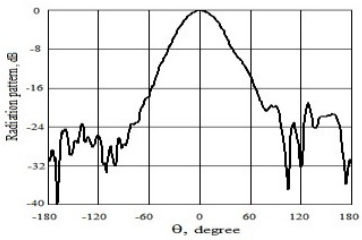

Fig.5.Radiation pattern of 3D printed antenna.

The measurement of the strip line parameters showed a satisfactory agreement between the experimental and theoretically calculated transmission coefficients (Fig. 3). Fig. 4 shows that the operating frequency of the antenna is 8.5 GHz. It is shown that measuring the characteristics of the antenna under pulsed exposure allows us to calculate the frequency characteristics (SWR and transmission coefficient) of elements of microwave devices made with the use of technology for creating composite carbon-containing materials.

REFERENCES

[1] Pantoja, J. P., Savu, R., Canesqui, M. A., Moshkalev, S. A., & Hernandez-Figueroa, H. E. Performance comparison of metallic and graphene buckypaper microstrip transmission lines. 2017 SBMO/IEEE MTT-S International Microwave and Optoelectronics Conference (IMOC).doi:10.1109/imoc.2017.8121104

[2] K. S. Novoselov, A. K. Geim, S. V. Morozov, D. Jiang, Y. Zhang, S. V. Dubonos, I. V. Grigorieva,1 A. A. Firsov. Electric Field Effect in Atomically Thin Carbon Films. Science, 306(5696), 666–669.doi:10.1126/science.1102896.

1 The work was supported by Ministry of Science and Higher Education of Russia. The measurements were carried out using the equipment of the Center of collective using of equipment “Impulse”, project identifier RFMEFI62119X0029.

MEASUREMENT OF THE ELECTRON SPECTRUM BASED ON CHERENKOV RADIATION IN THIN DIAMOND CRYSTALS

K.P. ARTYOMOV[1,2], *V.S. RIPENKO*[1], *M.A. SHULEPOV*[1], *A.G. BURACHENKO*[1]

[1]*Institute of High Current Electronics SB RAS, Tomsk, Russia*
[2]*Tomsk Polytechnic University, Tomsk, Russia*

Nowadays, the great attention is paid to the use of small and ultra-small artificial satellites (CubeSat) for the study of near-Earth space. In particular, they are used to monitor the flows of charged particles captured by the Earth's magnetic field. The dimensions of the CubeSat impose a restriction on the scientific equipment placed in them. We investigated the possibility of creating a compact electron spectrometer based on the Vavilov-Cherenkov effect, in which a thin diamond crystal is used as a radiator.

The efficiency of Vavilov-Cherenkov radiation (VCR) generation in a diamond crystal for electrons in the energy range 0.06–2 MeV we estimated using the numerical simulation. The experimental scheme with the maximum detection efficiency of VCR is proposed. The performed experimental measurements are in good agreement with numerical calculations.

EDGE PHOTOLUMINESCENCE IN DIAMOND: EXPERIMENT AND COMPUTATION[1]

D.V. GRIGORYEV[1], *D.E. GENIN*[1,2]

[1]*Tomsk State University, Tomsk, Russia*

[2]*Institute of High Current Electronics, Tomsk, Russia*

Ultraviolet radiation in the fundamental absorption region of the material causes an internal photoelectric effect, leading to the formation of nonequilibrium electron-hole pairs. Diamond is indirect-gap semiconductor. It is characterized by a high binding energy of a free exciton ~ 80 meV. This energy is two times higher than the energy of thermal lattice vibrations at room temperature. For this reason, in a pure diamond sample, the recombination of nonequilibrium electron-hole pairs occurs through the formation of free excitons. At high excitons concentrations and temperatures below 200 K, in bulk samples, excitons condense into droplets of an electron-hole liquid (EHL). Free excitons and EHL droplets appear in the photoluminescence spectra in the form of one-, two-, and three-phonon components of radiative recombination bands.

In this work, we present the results of experimental studies of the edge photoluminescence of diamond samples excited by laser radiation in the fundamental absorption region ($\lambda<226$ nm) and the calculated decomposition of the measured spectra into phonon components.

[1] The work was supported by the state order of the Ministry of Science and Higher Education of Russia, project No. 0721-2020-0048.

SINGLE-CRYSTAL CVD DIAMOND GROWTH IN AC GLOW DISCHARGE PLASMA *

S.A. LINNIK[1], *S.P. ZENKIN*[1], *A.V. GAYDAYCHUK*[1], *A.V. SUDARIKOV*[1]

[1]*Tomsk Polytechnic University, Tomsk, Russian Federation*

We report the research results of single-crystal diamond CVD growing in a new PACVD reactor with alternating high-current glow discharge plasma. Hydrogen-methane and argon-hydrogen-methane gas mixtures were used as the precursor gases. We found the optimal energy range, working pressure and gas content, temperature and volt-ampere characteristics. In this CVD reactor diamond crystals can be produced at growth rates up to 100 μm/h, which is up to 2 orders of magnitude higher than standard processes for making polycrystalline MPCVD diamond. This high-quality single-crystal MPCVD diamond may find numerous applications in electronic devices as high-strength windows and in a new generation of high-pressure instruments requiring large single-crystal anvils.

* The work was supported by Russian Science Foundation project № 19-72-10057.

OPTICAL DIAGNOSTICS OF REP DD PLASMA*

D.A. SOROKIN, M.I. LOMAEV, D.V. BELOPLOTOV, V.F.TARSENKO, V.A. SHKLYAEV, A.A. GRISHKOV,

Institute of High Current Electronics SB RAS, 2/3 Akademichesky Ave., Tomsk, 634055 Russia, SDmA-70@loi.hcei.tsc.ru

Due to its features, a high-voltage nanosecond discharge in gaps with strongly non-uniform electric field strength distribution is implemented in a diffuse form at high pressures of atomic and molecular gases (runaway electron preionized diffuse discharge – REP DD) [1]. So, REP DD is one of the ways for generating a dense non-equilibrium low-temperature plasma (NLTP) which is able to provide rich gas-phase chemistry at a low gas temperature. The properties of NLTP have led to its extensive use in many technological fields [2]. For a better understanding of the processes occurring in plasma, as well as identification of the areas of its possible application, it is necessary to know its fundamental parameters. These are electron concentration N_e, electron temperature T_e, reduced electric field strength E/N and temperature of heavy particles T_{tr} (gas temperature). Optical techniques, in particular, optical emission spectroscopy (OES), can be considered as diagnostic methods most suitable for determining the parameters of a non-equilibrium low-temperature gas discharge plasma. The study continues a series of works aimed at finding methods and their application for diagnostics of plasma of the pulsed and pulse-periodic REP DD in dense gases. To measure N_e in the discharge plasma, a technique based on measuring the spectral distance S between peaks of the forbidden F (492.07 nm) and allowed A (492.0 nm) components of a He I spectral line (Stark shift method) at a wavelength of 492 nm (Fig. 1a) was tested [5]. N_e measured by this method in the REP DD plasma in pure helium, depending on the pressure, was ~10^{14}–10^{15} cm^{-3} (Fig. 1b). The result obtained correlates well with that obtained earlier by the Stark broadening method [3] and the Stark shift method (He I, 447 nm). Using the technique consisting in measuring the ratio $R_{391/394}$ of peak intensities of the ionic N_2^+ (391.4 nm) and molecular N_2 (394.3 nm) nitrogen bands [4], T_e and E/N in the REP DD plasma in atmospheric-pressure N_2 were measured. The use of an ultrafast streak camera equipped with a spectrometer made it possible to measure the indicated values at the REP DD breakdown stage. The maximum values of these parameters were ~6.5 eV and ~1300 Td, respectively (Fig. 1c). Using the data of measurements of E/N at one of the earliest stages, the average velocity of propagation of the ionization wave (streamer) that breaks down the gap was estimated, which was $V_{IW} \approx 6 \cdot 10^9$ m/s. The values of E/N, as well as V_{IW}, measured in this way are in good agreement with the results of the calculations performed in the model based on the XOOPIC code [5] (Fig. 1d).

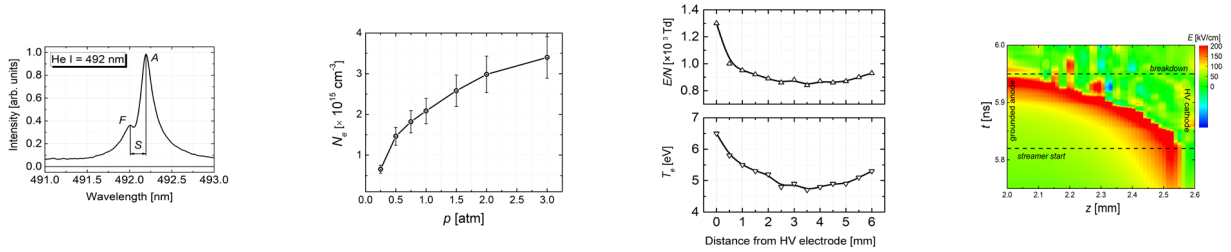

a) b) c) d)

Fig.1. a) He I spectral line (492 nm). b) Dependence of N_e on helium pressure. c) Dependencies of T_e and E/N on the distance ftom an HV electrode. d) The distribution of the electric field strength at the stage of breakdown in nitrogen obtained in the simulation.

REFERENCES

[1] V.F. Tarasenko (ed), Runaway Electrons Preionized Diffuse Discharges, New-York: Nova Science Publishers Inc., 2014.

[2] I. Adamovich, S.D. Baalrud, A. Bogaerts, et al., "The Plasma Roadmap. Low temperature plasma science and technology," J. Phys. D: Appl. Phys., vol. 50, Article number 323001, 2017.

[3] H.G. Adler and A. Piel, "Stark-broadening of the helium lines 447 and 492 nm at low electron densities," J. Quant. Spectrosc. Radiat. Transfer, vol. 45, p. 11, 1991.

[4] D.A. Sorokin, M.I. Lomaev, T.I. Banokina, V.F. Tarasenko, "Determination of the electron concentration and temperature, as well as the reduced electric field strength, in the plasma of high voltage nanosecond discharge initiated in atmospheric pressure nitrogen by runaway electron beam," Tech. Physics,vol. 59, p. 1119, 2014.

[5] S.Ya. Belomyttsev, A.A. Grishkov, V.A. Shklyaev, V.V. and Ryzhov, "Current in a pulsed gas breakdown at a highly inhomogeneous electric field," // J. Appl. Phys., vol. 123. Article number 043309, 2018.

* This work was supported by the State task no. 13.1.4 of Institute of High Current Electronics SB RAS.

Author Index